Proceedings of the Finnish Center of Excellence and Graduate School in "Physics, Chemistry, Biology and Meteorology of Atmospheric Composition and Climate Change" Annual Workshop 27.–29.4.2009

Editors: Markku Kulmala, Jaana Bäck, Tuomo Nieminen, and Antti Lauri

CONTENTS

ABSTRACTS

APPENDICES

Finnish Centre of Excellence in Physics, Chemistry, Biology and Meteorology of Atmospheric Composition and Climate Change: Scientific activities in 2008

Activity report 2006-2007: Graduate School on physics, chemistry, biology and meteorology of atmospheric composition and climate change

FINNISH CENTRE OF EXCELLENCE IN PHYSICS, CHEMISTRY, BIOLOGY AND METEOROLOGY OF ATMOSPHERIC COMPOSITION AND CLIMATE CHANGE: OVERVIEW OF ACTIVITIES IN 2008

M. KULMALA[1], J. BÄCK[2], A. LAURI[1], P. HARI[2], V.-M. KERMINEN[3], A. LAAKSONEN[3,4], E. NIKINMAA[2], M.-L. RIEKKOLA[5], T. VESALA[1] and Y. VIISANEN[3]

[1]Department of Physics, P.O. Box 64, FI-00014, University of Helsinki, Finland
[2]Department of Forest Ecology, P.O. Box 27, FI-00014, University of Helsinki, Finland
[3]Finnish Meteorological Institute, P.O. Box 503, FI-00101, Helsinki, Finland
[4]Department of Physics, P.O. Box 1627, FI-70211, Kuopio, Finland
[5]Department of Chemistry, P.O. Box 55, FI-00014, University of Helsinki, Finland

1. BACKGROUND

Atmospheric aerosol particles and trace gases affect the quality of our life in many different ways. In polluted urban environments, they influence human health and deteriorate visibility (e.g. Stieb *et al.*, 2002). In regional and global scales, aerosol particles and trace gases have a potential to change climate patterns and hydrological cycle (Lohmann and Feichter, 2005; IPCC, 2007). Aerosol particles also influence the radiation intensity distribution that reaches the earth surface having a direct influence on the terrestrial carbon sink (Gu et al. 2003). Better understanding of the various effects in the atmosphere requires detailed information on how different sources (including those of biosphere) and transformation processes modify properties of aerosol particles and trace gases. Trace gases and atmospheric aerosols are tightly connected with each other via physical, chemical, meteorological and biological processes occurring in the atmosphere and at the atmosphere-biosphere interface. An important phenomenon as an example is atmospheric aerosol formation, which involves the production of nanometer-size particles by nucleation and their growth to detectable sizes (Kulmala, 2003). Human actions, such as emission policy, forest management and land use change and various natural feedback mechanisms involving the biosphere and atmosphere have an impact on the coupling between the aerosols and trace gases.

The research in the Finnish Center of Excellence (CoE) aims at reducing the scientific uncertainty related to global climate change. One of the major uncertainties is connected to aerosol particles, and especially on the interactions between aerosols, clouds, climate and terrestrial ecosystems. We aim at creating a deep understanding on the dynamics of aerosol particles and ion and neutral clusters in the lower atmosphere, with the emphasis of biogenic formation mechanisms and their linkage to biosphere-atmosphere interaction processes, biogeochemical cycles and trace gases. The relevance and use of the results in the context of global scale modelling, and the development and utilisation of the newest measurement techniques are addressed. The cores of activities are a) in continuous measurements and databases of atmospheric and ecological mass fluxes and aerosol precursors and CO_2/aerosol/trace gas interactions in SMEAR field stations and GAW station and b) in focused experiments and modelling to understand the observed patterns.

2. METHODS

The work in our CoE is divided into five inter-linked work packages (WP's) that support each other. The necessary requirement for a high quality performance of the WPs is jointly working, truly inter-, multi- and cross disciplinary teams. From each WP we are expecting at least one scientific breakthrough. Our scientific approach starts from basic nucleation theories followed by models of detailed aerosol dynamic/atmospheric chemistry and vegetation – atmosphere exchange

and well-defined laboratory experiments with versatile continuous field measurements in our research stations, and extends to global-scale modelling. Our approach thus covers both experimental (laboratory and field experiments) and theoretical (basic theories, simulations, model development, parametrizations) points of view. The main disciplines used cover aerosol and environmental physics, environmental technology, atmospheric chemistry and physics, analytical chemistry, micrometeorology, forest ecology and ecophysiology. The usage of knowledge on different areas under the common framework creates the added value and synergy benefits of co-operating research teams.

3. MAIN RESULTS

3.1. ATMOSPHERIC NUCLEATION AND CLUSTERS

One of the key issues related to aerosol dynamics is the formation and growth of atmospheric aerosol particles. Although aerosol formation has been observed all over the world (Kulmala et al., 2004) and although it seems to be frequent (see e.g. Dal Maso et al., 2005; 2007), there are still several gaps in our knowledge on this process. The status of current knowledge is that atmospheric aerosol formation is a result of photochemical reactions in the gas phase, particularly the formation of sulphuric acid (Kulmala et al., 2006; Sihto et al., 2006; Riipinen et al., 2007) and other vapours of very low volatility, such as multifunctional organic compounds and iodine oxides (e.g. Allan et al., 2006; O'Dowd et al., 2002a,b; 2005; Laaksonen et al., 2008). Pre-existing aerosol particles, on the other hand, act as a sink for these vapours and nucleated clusters, thus inhibiting atmospheric aerosol formation. Aerosol formation also seems to be affected by several meteorological parameters and phenomena, including the intensity of solar radiation and atmospheric mixing processes such as the evolution of a continental boundary layer or the mixing of stratospheric and tropospheric air near the tropopause.

3.1.1. DEVELOPMENT, TESTING AND OPERATION OF CLUSTER SPECTROMETERS

A new prototype cluster spectrometer, termed NAIS (Neutral cluster and Air Ion Spectrometer, see Kulmala et al., 2007b) was developed and tested under both laboratory and field conditions. The NAIS builds on the Air Ion Spectrometer (AIS, Mirme et al., 2007), following the principle of multi-channel parallel electrical aerosol spectrometry. The NAIS is capable of measuring the concentrations and size distributions of neutral atmospheric clusters well below 3 nm of particle mobility (Millikan) diameter.

The NAIS was developed further in order to extend its operation to variable altitudes, e.g. airborne operation. The development aimed to the improved control and automatic tuning of air flows and other instrument operation parameters following the variations of ambient conditions. The NAIS was tested in airborne measurements during the EUCAARI long-range experiment EUCAARI LONGREX 2008. The NAIS performed very well during the flights.

During January–February, 2008, the first (N)AIS calibration and inter-comparison workshop was organised in Helsinki, Finland (Asmi et al., 2009). Ten cluster spectrometers, including five NAIS instruments, were compared and calibrated in the workshop. Calibrations were made with mobility standards and silver particles by using two high resolution differential mobility analysers (DMA) and a HAUKE-type short DMA. The monomobile mobility standards were measured with the best accuracy. The mobility distribution measured by the (N)AISs broadened to approximately 3 to 5 channels due to the high diffusion of such small ions and wide measurement

channel transfer functions. Results of the HAUKE and the high resolution DMA calibrations were in good agreement in the overlapping size range of 4–10 nm. However, the (N)AISs detected the ions at about 20-50% smaller sizes compared with the DMA selected sizes. Ion concentrations measured by the N(AIS)s were in good agreement with the concentrations measured by the aerosol electrometer and the CPC.

The first field campaign with the NAIS was conducted already in Spring 2007 in Hyytiälä, Finland (Nieminen et al., 2009; Manninen et al., 2009). More comprehensive field measurements, covering 12 field sites in Europe and in a site in Southern Africa, were started during the first half of the year 2008 using different type of cluster spectrometers, including five NAIS instruments. From each site, roughly a year of continuous cluster measurement for detailed studies of atmospheric nucleation mechanisms will be obtained.

Atmospheric clusters can also be detected using different CPCs, particularly with a pulse-height condensation particle counter (PH-CPC) (Sipilä et al., 2008). Recent results show that the cluster concentration measured using PH-CPCs are in the same order of magnitude than concentrations measured with NAIS (Lehtipalo et al., 2008). The instrument has also been tested in laboratory (Sipilä et al., 2009).

3.1.2. ATMOSPHERIC OBSERVATIONS

Atmospheric observations on new particle formation have been conducted since January 1996. The most recent results include studies on natural aerosol over Northern Europe (Tunved et al., 2008), the effect of synoptic situations on new particle formation (Sogacheva et al., 2008), annual and internannual variation of boreal forest aerosol concentrations (Dal Maso et al., 2008) and observations of regional new particle formation in the urban atmosphere (Hussein et al., 2008). The main new insight has been and will be received using new instruments to measure atmospheric nucleation rates around 2 nm (Kulmala et al., 2007a, Nieminen et al., 2009; Manninen et al., 2009) and the composition of newly formed particles (Kulmala et al., 2007b).

3.1.3. LABORATORY EXPERIMENTS

Homogeneous nucleation experiments were conducted in close collaboration between University of Helsinki, Finnish Meteorological Institute, Leibniz Institute for Tropospheric Research and Paul Scherrer Institute using flow tubes and environmental smog chamber. Experiments were made for the sulphuric acid-water system (H_2SO_4–H_2O), sulphuric acid-water-ammonia system (H_2SO_4–H_2O-NH_3) and systems including both sulfuric acid and organic compounds.

Heterogeneous nucleation experiments were conducted in close co-operation with University of Vienna. It was shown experimentally, that organic vapors may condense on molecular ions via initial activation by heterogenous nucleation, with a preference to negative ions, and with significantly lower vapor concentrations than the traditional Kelvin equation predicts (Winkler et al 2008).

3.1.4. QUANTUM CHEMICAL CALCULATIONS

A summary on the use of quantum chemical methods in studies of sulphuric acid-related nucleation mechanisms (mainly, binary sulphuric acid–water and ternary sulphuric acid–water–ammonia nucleation) was written and published (Kurtén and Vehkamäki, 2008).

The role of ammonia in sulphuric acid–water nucleation was revealed by a series of quantum chemical calculations. As indicated by experimental investigations, ammonia significantly assists the growth of clusters in the sulphuric acid - co-ordinate. Our calculations (Kurtén et al., 2007a; Torpo et al., 2007) predict that in atmospheric conditions, this effect becomes important as the number of acid molecules in clusters increases from two to three. On the other hand, small molecular clusters are unlikely to contain more than one ammonia molecule per one sulphuric acid (Kurtén et al., 2007b). This implies that the average $NH_3:H_2SO_4$ mole ratio of small molecular clusters in atmospheric conditions is likely to be between 1:3 and 1:1. Further calculations (Ortega et al., 2008) show that while ammonia enhances the nucleation of neutral sulphuric acid–water clusters moderately effectively, it has little or no effect on ion-induced sulphuric acid–water nucleation. In contrast, short-chain aliphatic amines are likely (Kurtén et al., 2008) to enhance both neutral and ion-induced sulphuric acid–water nucleation very effectively despite their low atmospheric concentrations.

Calculations of thermodynamic and kinetic parameters for the reaction of stabilized Criegee Intermediates with sulphuric acid (Kurtén et al., 2007c) demonstrate that quantum chemistry is a powerful tool for investigating chemically complicated nucleation mechanisms which cannot easily be treated with any other simulation methods. The calculations indicate that if the biogenic Criegee Intermediates have sufficiently long lifetime in atmospheric conditions, the studied reaction may be an important source of nucleation precursors. Organo-sulphates formed from the reaction of a variety of terpene oxidation products with sulphuric acid have also been shown to bind very strongly to both each other and to sulphuric acid molecules, indicating that they would be effective nucleation precursors. Organosulfate ions might possibly also play a role in ion-induced nucleation. Concentration measurements and kinetic data on the formation rates of organo-sulphates in atmospheric conditions is needed before further conclusions can be drawn.

3.2. AEROSOL CLOUD INTERACTIONS

The new aerosol particles formed by atmospheric nucleation events (see e.g. Kulmala et al., 2004) become climatically important only if they grow to sizes larger than about 50-100 nm in diameter. Particles of this size and larger can scatter sunlight back to the space, and they also can act as nuclei for cloud drop formation, having thereby an indirect effect on the albedo of the earth. Furthermore, the health effects of particles are related not only to the toxicity of the particle material, but to the particle size, since the size determines whether the particles are able to penetrate to the lungs and further to the blood circulation. According to our earlier studies on the growth of freshly formed particles both in pristine (Pallas, Finland; Lihavainen et al., 2003, Komppula et al, 2005, Kerminen et al., 2005) and highly polluted (Po Valley, Italy; Laaksonen et al., 2005) environments, nucleation can produce a significant fraction of cloud condensation nuclei regardless of the regional emission strength of primary particulate matter. The recent model calculations (Spracklen et al., 2008) showed, that CCN production due to atmospheric nucleation is very important.

3.2.1. LABORATORY EXPERIMENTS

Cloud drop activation was studied experimentally in collaboration with colleagues from the University of Copenhagen (Prisle et al. 2008). A series CCNC of experiments were conducted for atmospherically relevant surfactants, C8-C14 normal fatty acid sodium salts. It was found, in accordance with earlier studies, that Köhler theory using the reduced surface tension with no account for surfactant partitioning to the droplet surface layer (which reduces the Raoult term) underpredicts experimental critical supersaturations significantly, whereas Köhler theory

modified to account for surfactant partitioning and Köhler theory using the surface tension of pure water reproduced the experimental data well. We are currently analysing datasets for mixed salt-surfactant particles, which brings out the difference between water surface tension and the surface partitioning approach more clearly.

Another set of experiments for which we provided theoretical analysis, was carried out by Swiss colleagues (sse Duplissy et al. 2008). It was demonstrated that in smog chamber, formation of biogenic secondary organic aerosol (SOA) formed during photo-oxidation must be conducted at near atmospheric concentrations to yield atmospherically representative particle composition, hygroscopicity and cloud-forming potential. Currently, we are carrying out similar analysis for plant chamber experiments that were carried out in Kuopio in 2007. We have already shown, that we are able to model well the production of particles from ozone or OH oxidation of pine seedling volatiles, and that the OH oxidation products are more important for particle nucleation whereas the ozonolysis products drive particle growth (Hao et al 2009). As a next step, we will analyze the physicochemical properties (including CCN activity) of the different types of particles.

3.2.2. FIELD OBSERVATIONS

Long term measurements of cloud properties were continued at the Pallas and Puijo stations. First two papers were written on the Puijo measurements. Leskinen et al. (2009) give an overview of the measurement station and the experiments carried out there. Portin et al (2009) provide the first analysis of cloud data recorded during autumns 2006-2008.

3.2.3. CLOUD MICROPHYSICS

The number-to-volume concentration ratio, R, defined as the number concentration of particles larger than a certain cut-off diameter divided by the total particle volume concentration, was used by Kivekäs et al. (2008) to develop a new parameterization for estimating the cloud droplet number concentration (CDNC). The new parameterization demonstrates that if the value of $R(0.1$ μm) can be estimated or parameterized without knowing the whole particle number size distribution, cloud droplet number concentrations can be estimated relatively accurately by using only the four parameters mentioned above. This would reduce significantly the computer resources needed for calculating CDNC in large-scale atmospheric models.

A computational scheme was developed by Anttila et al. (2008) that can be used in connection with in situ measurements of aerosol water uptake and activation of aerosols into cloud droplets to assess the influence of the particle chemical composition and mixing state (in terms of the water uptake) on the cloud nucleating ability of particles. Additionally, it provides an estimate for the peak supersaturation of water vapour reached during the formation of the observed cloud(s). The method was applied in interpreting results of a measurement campaign that focused on aerosol-cloud interactions taking place at a subarctic background site located in northern Finland (second Pallas Cloud Experiment, 2nd PaCE).

Kokkola et al. (2008) showed that an excact solution for the critical supersaturation of particles with insoluble cores can be obtained analytically.

3.2.4. MODEL STUDIES

Romakkaniemi et al. (2009) studied the sensitivity of stratocumulus droplet concentrations on aerosol properties using a Large Eddy Model together either with an adiabatic parcel model or

with a trajectory ensemble model, and compared the results to airborne measurements. It was also found that the sensitivity of cloud droplet number concentration to aerosol properties is much smaller with TEM than expected from the adiabatic air parcel model simulations. As current parameterizations used to estimate cloud droplet number concentration in many large-scale models are based on adiabatic air parcel models, it is possible that the aerosol indirect effect for stratocumulus and stratus clouds with low vertical wind speeds is overestimated unless the sink resulting from ripening process decreasing the cloud droplet number concentration in the air parcels having long in-cloud residence time is taken into account.

In co-operation with the ACPC (Aerosol Cloud Precipitation Climate) project a conceptual model was created to explain the behaviour of cloud condensation nuclei droplets in pristine and polluted clouds, and the formation of precipitation in each case (Rosenfeld et al 2008).

3.3. BIOSPHERE-ATMOSPHERE INTERACTIONS

We study the couplings of biosphere to physical and chemical processes of atmosphere. These couplings include e.g. the factors controlling carbon exchange between forest canopy, soil and the atmosphere. We also analyse the ecosystem carbon, water and nitrogen cycles, the emissions of volatile organic compounds, and how all these are linked to ecosystem biological activity. The used theoretical approaches and measurement tehniques are summarised in Hari and Kulmala (2008).

3.3.1. CO_2 EXCHANGE AND ASSIMILATION

Long records from flux measurement sites show a trend towards increased photosynthesis and respiration during autumn, leading to increased winter-time carbon flux from northern ecosystems under climate change (Piao et al 2008). This trend cannot be explained by changes in atmospheric transport alone and, together with the ecosystem flux data, suggest increasing carbon losses in autumn. We found that both photosynthesis and respiration increase during autumn warming, but that the increase in respiration is greater. In contrast, warming increases photosynthesis more than respiration in spring making the timing of onset of growing season correlated with large ecosystem GPP (Delpierre et al. 2009, Kolari et al. 2009). Our simulations and observations indicated that northern terrestrial ecosystems may currently lose carbon dioxide in response to autumn warming, with a sensitivity of about 0.2 PgC $°C^{-1}$, offsetting 90% of the increased carbon dioxide uptake during spring. Ecosystem carbon sequestration is strongly influenced by atmospheric nitrogen deposition, which affects the net ecosystem productivity by increasing growth and simultaneously decreasing respiration (Magnani et al 2008). Long term modelling analyses show that nitrogen released from accelerated decomposition in warmer climate accelerates the carbon uptake more than decomposition releases (Hari and Kulmala 2008).

Increasing temperature and associated longer growing season increase the probability of droughts especially in the northern regions. The hydrological cycle is intimately linked to carbon cycle and also the distribution of energy in the ecosystem. At SMEAR II station, detailed analysis of factors influencing the water fluxes in the ecosystem has been made (Ilvesniemi et al. 2009). Drought in 2006 at SMEAR II caused a major drop in transpiration (Duursma et al. 2008) which was associated with large (on average about 40%) drop in the photosynthetic productivity (Kolari et al. 2009). Simultaneous clear decrease in soil respiration was observed, but that was not compensating for the decreased production, decreasing the ecosystem carbon sink about 60% during the rainless period of about one month, and turning the forest from sink to carbon neutral during the peak of the drought period (Kolari et al. 2009).

3.3.2 VOC EMISSIONS

Atmospheric concentrations of volatile organic compounds (VOCs) vary diurnally, seasonally and annually, and these variations are regulated by the environment and plant inherent properties. Season affects VOC sources and sinks, e.g. the level of biogenic and photochemical activity, and thus seasonal variation is larger than year to year variation. Boreal evergreen trees undergo pigment composition changes to cope with the stressful winter conditions, in particular late winter, with combination of high light and low temperatures (Porcar Castell et al. 2008a, b). There is evidence that these changes may be linked to variation in VOC synthesis (Porcar Castell et al. 2009). As these changes are also linked to changes in fluoresence signal from leaves (Porcar Castell et al. 2008a, b) new options to follow the seasonality of the biogenic emissions and photochemical activity exist (Porcar-Castell et al 2008c). Labeling experiments with $^{13}CO_2$ have revealed that a significant part of the monoterpenes emitted by coniferous trees originates directly from synthesis, while the rest originates from large monoterpene storage in the trees (Ghirardo et al., 2009). All of the monoterpenes emitted by broadleaved trees, such as birches, originate directly from synthesis (Ghirardo et al., 2009). This will be taken into account in further data analysis and modeling efforts.

The seasonal dynamics of fluxes and concentrations of volatile organic compounds in boreal ecosystems were analyzed and correlated with atmospheric aerosol formation, and with plant biological activity (Rinne et al 2007b, Ruuskanen et al 2009, Hakola et al 2009, Lappalainen et al 2009). Methanol and acetone were the most abundant VOCs in a Scots pine forest in southern Finland, the volume mixing ratio median being in the order of 1 ppbv. Volume mixing ratios of methanol, acetone, isoprene-MBO and monoterpenes were high during summer and low in winter, indicating biogenic or photochemical local or regional origin. Methanol, acetone, isoprene and monoterpene volume mixing ratios had clear diurnal patterns during summer, while other VOC and winter volume mixing ratios were essentially constant. Spring and summer time course of BVOC concentrations followed the photosynthetic capacity. Out of the five studied variables: air temperature, temperature in the humus layer, photosynthetically active photon flux density, gross primary production, and total ecosystem respiration, the day-time mean BVOC concentrations correlated best with air temperature on a daily scale. In addition to canopy processes, forest soil and understorey vegetation seem to be a source of VOCs in frost-free periods, and the emissions peak in early summer and autumn. Work is continued to quantify these emissions both in field and laboratory conditions.

3.3.3. METHANE AND NITROGEN FLUXES

Long term methane flux measurements at a boreal fen ecosystem has revealed methane to be not only an important part of the forcing exerted to the atmospheric radiative balance, but also on the carbon balance of the wetland. About 20 % of the carbon taken up by the wetland as CO_2 is released as methane annually (Rinne et al., 2007a). The methane emission from a fen ecosystem is insensitive to short term water table depth changes but as there is considerable variation between microsites within the fen (Riutta et al., 2007), the long term water table position does effect the methane emission. The ongoing analysis of the multi-year methane flux data set will be also used for modeling the earth system behaviour.

The emissions of N_2O from boreal forest ecosystems are highly variable. A study with the soil gradient and chamber methods revealed that N_2O fluxes ranged from small emissions to small soil uptake with both techniques. The highest soil N_2O fluxes occurred in the late summer and the lowest in the autumn and spring. Overall, the uppermost soil layer was responsible for most of the

N$_2$O production and consumption (Pihlatie et al. 2007). It was also shown that pine needles can act as a source for the nitrogen oxides even under relatively high ambient concentrations (Raivonen 2008).

3.4. EARTH SYSTEM BEHAVIOR

3.4.1 GLOBAL MODELLING: AEROSOL PARTICLES AND CLOUDS

Aerosol dynamics have been simulated using two different global models, namely a) ECHAM5-HAM (Stier et al., 2005; Makkonen et al., 2009) aerosol-climate model with T42 resolution in co-operation with MPI-Hamburg, and b) the GLOMAP aerosol microphysics model (e.g. Spracklen et al., 2008) in co-operation with University of Leeds. The first one is a climate model and the second one is a global chemical transport model. The importance of atmospheric nucleation on global aerosol load and also on global CCN load has been investigated with the models.

3.4.2. SOIL HETEROTROPHIC RESPIRATION

Feedbacks from soils due to heterotrophic respiration are one of the main uncertainties in the coupling of climate and carbon cycling (e.g. Piao et al, 2008). We are currently working on implementing the Yasso07 soil carbon model (www.environment.fi/syke/yasso), into the COSMOS (http://cosmos.enes.org/) Earth System Model framework. The main components of COSMOS are the ECHAM5 atmospheric model (Roeckner et al. 2003), MPIOM (Max Planck Institute Ocean Model), and the land surface scheme JSBACH, which is based on the biosphere model BETHY (Knorr 2000) and the ECHAM5 soil scheme. The work is carried out in co-operation with Finnish Environment Research Institute. Yasso07 model is based on global long-term decomposition data sets on litter bags and soil carbon stocks and is more comprehensive with extensive error analysis than the original model and typical soil schemes in global climate models. The decomposition rate depends on soil moisture and soil temperature but typically it is treated as independent on plant functional types (PFTs). The global model has 14 different PFTs and the new implementation allows for leaf and woody litter production by each PFT. Furthermore, the chemical composition of litter is classified to ethanol (waxes etc.), water (sugars etc.) and acid (celluloses etc.) soluble modes with insoluble class (lignin etc.). Standard models only utilizes two classes, namely, fast and slow carbon pools.

At FMI, the global model was run at 2 degrees spatial resolution for years 1958-2006, first twenty years with fixed carbon dioxide concentration in the atmosphere and since 1977 with freely evolving CO$_2$ concentration. It was revealed that the novel carbon cycle parameterization has greater sensitivity to climate. In addition, different magnitudes and distribution of soil carbon pools are crucial for more realistic understanding of climate change-soil carbon dynamics and feedbacks. The article on this is under preparation and the planning for next 1-2 articles has been started.

3.4.3. VEGETATIVE EMISSIONS OF BIOGENIC VOLATILE ORGANIC COMPOUNDS

Biogenic Volatile Organic Compounds (BVOC) are reactive trace gases emitted by the biosphere, and they can have a substantial role in the chemistry of the atmosphere. Magnitudes of terrestrial BVOC emissions are necessary for reliable estimation of atmospheric ozone and aerosol formation in atmosphere models, as BVOC's affect the atmospheric photochemistry (Atkinson and Arey 2003), and the formation of atmospheric aerosols (Claeys et al. 2004, Kanakidou et al.

2005, Kourtchev et al 2008). Of the wide variety of BVOC's, emissions of isoprene (C_5H_8) typically dominate in broadleaved vegetation (Guenther et al. 1995, 2006, Arneth et al. 2007a,b) and monoterpenes ($C_{10}H_{16}$) typically dominate in coniferous forests (Tarvainen et al. 2007, Schurgers et al. 2009). Biospheric isoprene emissions are widely modelled by a parameterization by Guenther et al. (1995, 2006), based on measured isoprene emissions from plants as a function of light and temperature. Other approaches include process based models by Niinemets et al. (1999, 2002) as applied for isoprene emissions by Arneth et al. (2007a) and for monoterpenes by Schurgers et al. (2009). Emission models based on light and temperature predict increasing BVOC emissions in a warming climate. Recently, modelling efforts have also attempted to include a possible CO_2-inhibition of isoprene and monoterpene production. This process is not yet fully understood, but Arneth et al. (2007b) note that inhibition by CO_2 may offset the strong BVOC emission increase caused by increased temperature (and increased green biomass caused by CO_2 fertilisation of photosynthesis). Models that link BVOC emissions to photosynthesis and dynamic vegetation can account for these interactions in a consistent modelling framework, although (due to lack of process understanding) the CO_2 inhibition still needs to be parameterized empirically.

We are currently working on implementing the process based emission models of isoprene and monoterpenes, by Arneth et al (2007a) and Schurgers et al. (2009), into the COSMOS Earth System Model. In JSBACH, C3-photosynthesis is modelled following Farquhar et al (1980) and C4-photosynthesis following Collatz et al. (1992), and both models directly provide the relevant parameters as needed by the above BVOC emission models. As part of COSMOS/ECHAM5, the BVOC emissions models will also be easily connected to the recent and future work on models of atmospheric chemistry and aerosol formation in the COSMOS framework. As a component of Earth System Model, the BVOC emission models can be applied in fully coupled model run studies of both past and future climate and vegetation and theis interaction.

3.4.4. METHANE EMISSIONS FROM WETLANDS

Wetlands are the largest natural source of methane into the atmosphere. In the current version of the biosphere component JSBACH (Raddatz et al., 2007) of the COSMOS Earth System Model, wetlands and their CH_4 emissions are not included at all, which means that the climate model lacks a realistic description of the behaviour of one of the most important CH_4 sources. Therefore we have recently started the work aiming to the construction of a process-based model on CH_4 production and transport in wetlands to be included as a new wetland-carbon model in the land biosphere part of the COSMOS-ESM. As a starting point, we have the CH_4 model of Wania (2007). The model will be combined with a carbon uptake (photosynthesis), aerobic decomposition and peat accumulation model produced by the Global Vegetation Modelling group at MPI-Hamburg. The first model prototype will be validated using data collected on an ombrotrophic fen, Siikaneva, in southern Finland. We have data sets of meteorological parameters, CH_4 profile in soil, eddy covariance measurements of ecosystem-level CH_4 and CO_2 fluxes above the peatland (Rinne et al., 2007a) and chamber measurements of the spatial variation of the CH_4 and CO_2 fluxes with and without aerenchymatous plants transporting CH_4 (Riutta et al., 2007). More data sets available from Fluxnet (global) and NECC (Scandinavian) will be utilized after the first step.

4. QUANTITATIVE RESULTS

In 2008, the Center of Excellence and the closely connected projects produced altogether 22 MSc theses and 13 PhD theses. Most of them were joint degrees between different units (departments and universities) of the CoE, emphasizing the importance of collaboration within the CoE.

The CoE was organizing or co-organizing 29 workshops and meetings in 2008. These included both national and international workshops and conference sessions, and were co-funded by e.g. IGBP, EU, University of Helsinki, NCAR, Nordforsk, and the Finnish Cultural Foundation, in addition to the CoE. The members of the CoE acted as referees in 40 international journals and as editors in 22 journals. The CoE produced 141 peer-review articles (2 of them in Nature and 2 in Science). Two Special issues in Tellus Ser B, related to the activities within the Nordic Centres of Excellence BACCI and NECC, included 20 articles with contributions by the FCoE scientists. Also 23 other publications (reports, proceedings, special issues etc.) were produced. The results of the CoE were further released in national arena in 24 interviews or articles in national magazines, in 5 television and radio interviews, and in 11 other events. One book on the CoE research (Hari & Kulmala 2008) was published by the Springer Verlag, which will be used as teaching material in the University of Helsinki. The members of CoE were invited in 46 occasions to give a plenary/ invited lecture. Two patents were released.

The annual total funding was 5.4 M€, including the CoE funding. The other funding sources include the Academy of Finland fellowships, several foundations, Ministries, Universities of Helsinki and Kuopio, FMI, EU, Nordforsk, CIMO, Finnish Funding Agency for Technology and Innovation, municipalities and private enterprises. The CoE funding comprised roughly 7 % of the total budget.

5. OUTREACH AND SOCIETAL IMPACT

Climate change is a global problem, and tightly connected to e.g. regional ang global air pollution issues. The CoE yielded new information on the global climatic effects of aerosol particles and trace gases and their interactions with chemical and biological processes, as well as on indirect feedbacks. Particularly, we contributed on the debate regarding artic and boreal environmental changes. The results are relevant to assessments by IPCC, to verification of the Kyoto protocol and to measures on how to control and mitigate emissions of gaseous and particulate pollutants. Long-term flux measurements, as a part of the global community, help to estimate spatio-temporal changes in carbon sinks and hydrological cycles leading to more accurate knowledge for decision-makers to use in multinational negotiations for mitigation of climate change. Our results also support the European policy (e.g. the Vienna Convention on the Protection of the Ozone Layer and the Convention of Long-range transport of Air Pollutants). The CoE results contribute directly to the current debate concerning the National and European Union Strategies for Sustainable Development and the European Strategy for Environment and Health. Our contributions include tackling the role of anthropogenic and natural factors on climate change, air quality, public health, and quality of life. The European implementation of air quality standards and coherency of environmental legislation and related policy initiatives are expected to take place during the next ten years. The basis for this challenging task is the enhanced understanding of emissions and the corresponding atmospheric processes. The non-scientific end-users of the data (such as forestry or public health monitoring bodies) have been informed using distributed written material, press conferences and invitations to project meetings. New aerosol, cloud droplet and trace gas instruments are under development and their commercialization will be promoted.

The University of Helsinki (Physical Sciences) working group 'Gender Equality' was led by Academy fellow Hanna Vehkamäki. The project yielded a leaflet where the problems and solutions associated with gender equality issues in physical sciences were presented. These issues were also discussed during FCoE project meetings.

Many summer workers were recruited from students attending 2nd-3rd year courses, which effectively promotes their further recruitment to the research area.

ACKNOWLEDGEMENTS

REFERENCES

Allan, J.D., Alfarra M.R., Bower K.N., Coe H., Jayne J:T., Worsnop D.R., Aalto P.P., Kulmala M., Hyötyläinen T., Cavalli F. and Laaksonen A. (2006) Size and composition measurements of background aerosol and new particle growth in a Finnish forests during QUEST 2 using an Aerodyne Aerosol Mass Spectrometer, *Atmos. Chem. Phys.* 6: 315-327

Anttila, T., Vaattovaara, P., Komppula, M., Hyvärinen, A.-P., Lihavainen, H., Kerminen, V.-M., and Laaksonen, A. (2008) Size-dependent activation of aerosols into cloud droplets at a subarctic background site during the second Pallas Cloud Experiment (2nd PaCE): method development and data evaluation, , *Atmos. Chem. Phys. Discuss.* 8 14519-14556.

Arneth, A., Niinemets, Ü., Pressley, S., Bäck, J., Hari, P., Karl, T., Noe, S., Prentice, I. C., Serça, D., Hickler, T., Wolf, A. and Smith, B. (2007a). Process-based estimates of terrestrial ecosystem isoprene emissions: incorporating the effects of a direct CO2 -isoprene interaction. *Atmos. Chem. Phys*7: 31–53.

Arneth, A., Miller, P., Scholze, M., Hickler, T., Smith, B. and Prentice, I. C. (2007b). CO_2 inhibition of global terrestrial isoprene emissions: Potential implications for atmospheric chemistry. *Geophys. Res. Lett.* 34: L18813.

Asmi, E., M. Sipilä, H. E. Manninen, J. Vanhanen, K. Lehtipalo, S. Gagné, K. Neitola, A. Mirme, S. Mirme, E. Tamm, J. Uin, K. Komsaare, M. Attoui, and M. Kulmala (2009). Results of the first air ion spectrometer calibration and intercomparison workshop. *Atmos. Chem. Phys.,* 9, 141-154.

Atkinson, R. and Arey, J. (2003). Gas-phase tropospheric chemistry of biogenic volatile organic compounds: a review. *Atmospheric Environment* 37, Supplement 2: 197-219

Claeys, M., Graham, B., Vas, G., Wang, W., Vermeylen, R. et al. (2004). Formation of secondary organic aerosols through photooxidation of isoprene. *Science* 303: 1173–1176.

Collatz, G. J., Ribas-Carbo, M. and Berry, J. A. (1992). Coupled photosynthesis-stomatal conductance model for leaves of C4 plants. *Australian Journal of Plant Physiology* 19: 519-538.

Dal Maso M., Kulmala M., Riipinen I., Wagner R., Hussein T., Aalto P.P. and Lehtinen K.E.J. (2005) Formation and growth of fresh atmospheric aerosols: eight years of aerosol size distribution data from SMEAR II, Hyytiälä, Finland, *Boreal Environ Research* 10: 323-336

Dal Maso, M., Sogacheva, L., Aalto, P.P., Riipinen, I., Komppula, M., Tunved, P., Korhonen, L., Suur-Uski, V., Hirsikko, A., Kurtén, T., Kerminen, V.-M., Lihavainen, H., Viisanen, Y., Hansson, H.-C. and Kulmala, M. (2007) Aerosol size distribution measurements at four Nordic field stations: identification, analysis and trajectory analysis of the new particle formation bursts, *Tellus B*, 59(3), 350-361

Dal Maso, M., A. Hyvärinen, M. Komppula, P. Tunved, V.-M. Kerminen, H. Lihavainen, Y. Viisanen, H.-C. Hansson, and M. Kulmala (2008) Annual and interannual variation in boreal forest aerosol particle number and volume concentration and their connection to particle formation, Tellus 60B, 495-508

Delpierre N., Soudani K., François F., Köstner B., Pontailler JY., Aubinet M., Bernhofer C., Granier A., Grunwald T., Heinesch B., Longdoz B., Misson L., Nikinmaa E., Ourcival JM., Rambal S., Vesala T. & Dufrêne E. (2009) Exceptional carbon uptake in European forests during the warm spring of 2007: a data-model analysis. *Global Change Biology*. doi: 10.1111/j.1365-2486.2008.01835.x

Duplissy, J., M. Gysel, M. R. Alfarra, J. Dommen, A. Metzger, A. S. H. Prevot, E. Weingartner, A. Laaksonen, T. Raatikainen, N. Good, S. F. Turner, G. McFiggans, and U. Baltensperger (2008). Cloud forming potential of secondary organic aerosol under near atmospheric conditions. *Geophys. Res. Lett.*, 35 L03818 doi:10.1029/2007GL031075

Duursma R.A., Kolari P., Perämäki M., Nikinmaa E., Hari P., Delzon S., Loustau D., Ilvesniemi H., Pumpanen J., Mäkelä A. (2008). Predicting the decline in daily maximum transpiration rate of two pine stands during drought based on constant minimum leaf water potential and plant hydraulic conductance. *Tree Physiology* 28: 265-276.

Farquhar, G. D., von Caemmerer, S., & Berry, J. A. (1980). A biochemical model of photosynthetic CO_2 assimilation in leaves of C3 species. *Planta* 149: 78–90.

Ghirardo A., Koch, K., Schnitzler J.-P. & Rinne J. (2009) $^{13}CO_2$ feeding experiment of four common European boreal tree species: ^{13}C incorporation into monoterpenes. 4th International Conference on Proton Transfer Reaction Mass Spectrometry and its applications - Contributions. February 16th – 21st, 2009, Obergurgl, Austria. Conference Series, Innsbruck University Press. 219-220.

Guenther, A., C. N. Hewitt, D. Erickson, R. Fall, C. Geron, T. Graedel, P. Harley, L. Klinger, M. Lerdau, W. A. McKay, T. Pierce, B. Scholes, R. Steinbrecher, R. Tallamraju, J. Taylor, and P. Zimmerman. (1995). A global model of natural organic compound emissions. *Journal of Geophysical Research* D100: 8873–8892.

Guenther, A., Karl, T., Harley, P.,Wiedinmyer, C., Palmer, P. I., Geron, C. (2006). Estimates of global terrestrial isoprene emissions using MEGAN (Model of Emissions of Gases and Aerosols from Nature). *Atmospheric Chemistry and Physics* 6: 3181–3210.

Gu L., Baldocchi D.D. , Wofsy S.C., Munger J.W., Michalsky J.J., Urbanski S.P., Boden T:A. (2003) Response of a Deciduous Forest to the Mount Pinatubo Eruption: Enhanced Photosynthesis. *Science* 299, 2035-2038, 2003

Hakola H., Hellen H., Tarvainen V., Bäck J., Patokoski J. and Rinne J. (2009) Annual variations of atmospheric VOC concentrations in a boreal forest. *Boreal Environment Research*, in press

Hao, L. Q., Yli-Pirilä, P., Tiitta, P., Romakkaniemi, S., Vaattovaara, P., Kajos, M. K., Rinne, J., Heijari, J., Kortelainen, A., Miettinen, P., Kroll, J. H., Holopainen, J.-K., Joutsensaari, J., Kulmala, M., Worsnop, D. R., and Laaksonen, A. (2009). New particle formation from the oxidation of direct emissions of pine seedlings. *Atmos. Chem. Phys. Discuss*. 9 8223-8260

Hari, P. & Kulmala, L. (2008) (eds.) Boreal forest and climate change. Advances in Global Change Research, Vol. 34, Springer Verlag.

Hussein T, Martikainen J, Junninen H, Sogacheva L, Wagner R, Dal Maso M, Riipinen I, Aalto PP, Kulmala M. (2008) Observation of Regional New Particle Formation in the Urban Atmosphere. Tellus 60B: 509-521.

Ilvesniemi H., Pumpanen J., Duursma R., Hari P., Keronen P., Kolari P., Kulmala M., Mammarella I., Nikinmaa E., Rannik U., Siivola E. and Pohja T. (2009) Water balance of two adjacent boreal forest micro-catchments. *Boreal Environment Research*, in print

IPCC (2007). The Scientific Basis. A report of Working Group I of the Intergovernmental Panel on Climate Change. In: *Climate Change 2007: The Physical Science Basis. Contribution of Working Group I to the Fourth Assessment Report of the Intergovernmental Panel on Climate Change*. (ed. by Solomon, S., D.

Qin, M. Manning, Z. Chen, M. Marquis, K.B. Averyt, M.Tignor and H.L. Miller). Cambridge University Press, Cambridge, United Kingdom and New York, NY, USA.

Kanakidou M., Seinfeld J. H., Pandis S. N., Barnes I., Dentener F.J., Facchini M. C., Van Dingenen R., Ervens B., Nenes A., Nielsen C. J. Swietlicki E., Putaud J. P., Balkanski Y., Fuzzi S., Horth J., Moortgat G. K., Winterhalter R., Myhre C. E. L., Tsigaridis K., Vignati E., Stephanou E. G. and Wilson J. (2005). Organic aerosol and global climate modelling: a review. *Atmos. Chem. Phys.* 5: 1053–1123.

Kerminen, V.-M., Lihavainen, H., Komppula, M., Viisanen, Y. and Kulmala, M. (2005) Direct observational evidence linking atmospheric aerosol formation and cloud droplet activation *Geophys. Res. Lett.* 32, L14803, doi:10.1029/2005GL023130

Kivekäs, N., V.-M. Kerminen, T. Anttila, H. Korhonen, H. Lihavainen, M. Komppula, and M. Kulmala (2008) Parameterization of cloud droplet activation using a simplified treatment of the aerosol number size distribution. *J. Geophys. Res*. 113D15207, doi:10.1029/2007JD009485.

Knorr, W. (2000). Annual and interannual CO_2 exchange of the terrestrial biosphere: Process based simulations and uncertainties. *Global Ecology and Biogeography* 9: 225–252.

Kokkola, H., M. Vesterinen, T. Anttila, A. Laaksonen, and K. E. J. Lehtinen (2008) Technical note: Analytical formulae for the critical supersaturations and droplet diameters of CCN containing insoluble material. *Atmos. Chem. Phys*. 8 1989-2005.

Kolari, P., L. Kulmala, J. Pumpanen, S. Launiainen, H. Ilvesniemi, P. Hari and E. Nikinmaa (2009). Carbon balance and component CO_2 fluxes of a boreal Scots pine forest. *Boreal Environment Research* in print

Komppula, M., Lihavainen, H., Kerminen V.-M., Kulmala, M. and Viisanen, Y., (2005) Measurements of cloud droplet activation of aerosol particles at a clean subarctic background site, *J. Geophys. Res*. 110, D06204, doi:10.1029/2004JD005200

Kourtchev I., Ruuskanen T M, Keronen P., Sogacheva L., Dal Maso M., Reissell A., Chi X., Vermeylen R., Kulmala M., Maenhaut W.and Claeys M. (2008) Determination of isoprene and alpha-/beta-pinene oxidation products in boreal forest aerosols from Hyytiälä, Finland: diel variations and possible link with particle formation events, *Plant Biology* 10: 138-149

Kulmala M. (2003) How Particles Nucleate and Grow. *Science* 302, 1000-1001

Kulmala M., Mordas G., Petäjä T., Grönholm T., Aalto P.P, Vehkamäki H., Hienola A.I., Herrmann E., Sipilä M., Riipinen I., Manninen H., Hämeri K., Stratmann F., Bilde M., Winkler P.M., Birmili W. and Wagner P.E. (2007a) The condensation particle counter battery (CPCB): A new tool to investigate the activation properties of nanoparticles. *J. Aerosol Sci.*, 38, 289-304

Kulmala M., Riipinen I., Sipilä M., Manninen H. E., Petäjä T., Junninen H., Dal Maso M., Mordas G., Mirme A., Vana M., Hirsikko A., Laakso L., Harrison R. M., Hanson I., Leung C., Lehtinen K. E. J. and Kerminen V.-M. (2007b) Toward direct measurement of atmospheric nucleation. *Science,* 318, 89-92.

Kulmala, M., Vehkamäki H., Petäjä T., Dal Maso M., Lauri A., Kerminen V.-M., Birmili W., McMurry P.H. (2004) Formation and growth rates of ultrafne atmospheric particles: a review of observations. *J. Aerosol Sci.* 35, 143-176

Kurtén T., Bonn B., Vehkamäki H. and Kulmala M. (2007c) A computational study of the reaction of the reaction between biogenic stabilized Criegee intermediates and sulfuric acid. *J. Phys. Chem. A,* 111, 3394.

Kurtén T., Loukonen V., Vehkamäki H. and Kulmala M. (2008) Amines are likely to enhance neutral and ion-induced sulfuric acid-water nucleation in the atmosphere more effectively than ammonia, *Atmos. Chem. Phys.*, 8, 4095-4103

Kurtén T., Torpo L., Ding C.-G., Vehkamäki H., Sundberg M. R., Laasonen K. and Kulmala M. (2007a). A density functional study on water-sulfuric-acid-ammonia clusters and implications for atmospheric cluster formation, *J. Geophys. Res.,* 112, D04210, doi:10.1029/2006JD007391.

Kurtén T., Torpo L., Sundberg M. R., Kerminen V.-M., Vehkamäki H. and Kulmala M. (2007b). Estimation of the NH_3:H_2SO_4 ratio of nucleating clusters in atmospheric conditions using quantum chemical methods, *Atmos. Chem. Phys.* 7, 2765-2773.

Kurtén T & Vehkamäki, H. (2008) Investigating atmospheric sulfuric acid–water–ammonia particle formation using quantum chemistry, *Advances in Quantum Chemistry: Applications of Theoretical Methods to Atmospheric Science,* 55: 407-427

Laaksonen, A. Hamed A., Joutsensaari J., Hiltunen L:, Cavalli F., Junkermann W., Asmi A., Fuzzi S. and Facchini M.C. (2005) Cloud condensation nucleus production from nucleation events at a highly polluted region, *Geophys. Res. Lett.*, 32, L06812, doi:10.1029/2004GL022092

Laaksonen A., Kulmala M., O'Dowd C.D., Joutsensaari J., Vaattovaara P., Mikkonen S., Lehtinen K.E.J., Sogacheva L., Dal Maso M., Aalto P., Petäjä T., Sogachev A., Jun Yoon Y., Lihavainen H., Nilsson O:, Facchini M.C., Cavalli F., Fuzzi S., Hoffmann T., Arnold F., Hanke M., Sellegri K., Umann B., Junkermann W., Coe H., Allan J:.D., Alfarra M.R., Worsnop D.R., Riekkola M.-L., Hyötyläinen T. and Viisanen Y. (2008) The role of VOC oxidation products in continental new particle formation, *Atmos. Chem. Phys.*, 8, 2657-2665

Lappalainen H. K., Sevanto S., Bäck J., Ruuskanen T., Rinne J., Kolari P., Kulmala M., and Hari P. (2009) Day-time concentrations of biogenic volatile organic compounds in a boreal forest canopy and their relation to environmental and biological factors. Submitted manuscript.

Lehtipalo, K., Sipilä, M., Riipinen, I., Nieminen, T., and Kulmala, M.: (2008) Analysis of atmospheric neutral and charged molecular clusters in boreal forest using pulse-height CPC. *Atmos. Chem. Phys. Discuss.*,8, 20661-20685

Leskinen A., Portin H., Komppula M., Miettinen P., Arola A., Hatakka J., Laaksonen A. and Lehtinen K.E.J. (2009) Overview of the research activities and results at Puijo semi-urban research station. *Boreal Environ. Res.*, in press.

Lihavainen H., Kerminen V.-M., Komppula M., Hatakka J., Aaltonen V., Kulmala M. and Viisanen Y. (2003) Production of 'potential' cloud condensation nuclei associated with atmospheric new-particle formation in Northern Finland, *J. Geophys. Res.* 108 (D24), 4782, doi:10.1029/2003JD003887

Lohmann, U. and Feichter, J. (2005) Global indirect aerosol effects: a review, *Atmos. Chem. Phys.* 5, 715-737

Magnani F., Mencuccini M., Borghetti M., Berninger F., Delzon S., Grelle A., Hari P., Jarvis P.G., Kolari P., Kowalski A.S., Lankreijer H., Law B.E., Lindroth A., Loustau D., Manca G., Moncrieff J.B., Tedeschi V., Valentini R. and Grace J. (2008) Ecologically implausible carbon response? Reply. *Nature* 451, E3-E4.

Makkonen R., Asmi A., Korhonen H., Kokkola H., Järvenoja J., Räisänen P., Lehtinen K.E.J., Laaksonen A., Kerminen V.-M., Järvinen H., Lohmann U., Bennartz R., Feichter J., and Kulmala M. (2009) Sensitivity of aerosol concentrations and cloud properties to nucleation and secondary organic distribution in ECHAM5-HAM global circulation model. *Atmos. Chem. Phys.*, 9, 1747-1766.

Manninen H., Nieminen T., Riipinen I., Yli-Juuti T., Gagne S., Asmi E., Aalto P. P., Petäjä T., Kerminen V.-M. and Kulmala M. (2009) Charged and total particle formation and growth rates during EUCAARI 2007 campaign in Hyytiälä. *Atmos. Chem. Phys. Discuss.* 9, 5119-5151

Mirme A., Tamm E., Mordas G., Vana M., Uin J., Mirme S., Bernotas T., Laakso L., Hirsikko A., and Kulmala M. (2007) A wide-range multi-channel Air Ion Spectrometer. *Boreal Env. Res.*, 12, 247-264

Nieminen T., Manninen H. E., Sihto S.-L., Yli-Juuti T., Mauldin III R. L., Petäjä T., Riipinen I., Kerminen V.-M. and Kulmala M. (2009) Connection of sulphuric acid to atmospheric nucleation in boreal forest. *Environ. Sci. Technol.* in press

Niinemets, Ü., Seufert, G., Steinbrecher, R., and Tenhunen, J. D.(2002). A model coupling foliar monoterpene emissions to leaf photosynthetic characteristics in mediterranean evergreen Quercus species. *New Phytol.* 153: 257–275.

Niinemets, Ü., Tenhunen, J. D., Harley, P. C. and Steinbrecher, R. (1999). A model of isoprene emission based on energetic requirements for isoprene synthesis and leaf photosynthetic properties for Liquidambar and Quercus. *Plant, Cell Environ.* 22: 1319–1335.

O'Dowd, C. D., Aalto, P. P., Hämeri, K., Kulmala, M. and Hoffmann, T. (2002a). Aerosol formation: atmospheric particles from organic vapours. *Nature* 416, 497–498.

O'Dowd, C. D., Jimenez, J. L., Bahreini, R., Flagan, R. C., Seinfeld, J. H., Hämeri K., Pirjola L., Kulmala M., Jennings S.G. and Hoffmann T. (2002b). Marine aerosol formation from biogenic iodide emissions. *Nature* 417, 632–636.

O'Dowd, C. D., Jimenez, J. L., Bahreini, R., Flagan, R. C., Seinfeld, J. H., Hämeri K., Pirjola L., Kulmala M., Jennings S.G. and Hoffmann T. (2005). Marine aerosols and iodine emissions (Reply). *Nature* **433**, E13–E14

Ortega I. K., Kurtén T., Vehkamäki H. and Kulmala M. (2008) The role of ammonia in sulfuric acid ion-induced nucleation. *Atmos. Chem. Phys.*, 8, 2859-2867.

Piao, S., P Ciais, P Friedlingstein, P Peylin, M Reichstein, S Lyussaert, H Margolis, J Fang, A Barr, A Chen, A Grelle, D Y Hollinger, T Laurila, A Lindroth, A D Richardson and T Vesala (2008) , Net carbon dioxide losses of northern ecosystems in response to autumn warming, *Nature* 451 49-52

Pihlatie M., Pumpanen J., Rinne J., Ilvesniemi H., Simojoki A., Hari P. and Vesala T. (2007) Gas concentration driven fluxes of nitrous oxide and carbon dioxide in boreal forest soil. *Tellus*, 59B, 458-469.

Porcar-Castell, A., J. Peñuelas, S. M. Owen, J. Llusià, S. M.Bosch, and J.Bäck. (2009). Leaf carotenoid concentrations and monoterpene emission capacity under acclimation of the light reactions of photosynthesis. *Boreal Environment Research,* in print.

Porcar-Castell, A., E. Juurola, E. Nikinmaa, I. Ensminger, F. Berninger and P. Hari (2008a). Seasonal acclimation of photosystem II in *Pinus sylvestris.* I. Estimating the rate constants of sustained heat dissipation and photochemistry. *Tree Physiology* 28, 1475–1482

Porcar-Castell, A., E. Juurola, I. Ensminger, F. Berninger, P. Hari and E. Nikinmaa (2008b). Seasonal acclimation of photosystem II in *Pinus sylvestris.* II. Using the rate constants of sustained thermal energy dissipation and photochemistry to study the effect of the light environment *Tree Physiology.* 28, 1483–1491

Porcar-Castell A, E. Pfündel, JFJ Korhonen, E Juurola (2008c). A new monitoring PAM fluorometer (*MONI-PAM*) to study the short- and long-term acclimation of photosystem II in field conditions. *Photosynthesis Research* 96: 173-179.

Portin H. J., Komppula M., Leskinen A.P., Romakkaniemi S., Laaksonen A. and Lehtinen K.E.J. (2009) Observations of aerosol-cloud interactions at Puijo semi-urban measurement station. *Boreal Environ.Res.,* in press

Prisle, N., Raatikainen, T., Sorjamaa, R., Svenningsson, B., Laaksonen, A., and Bilde, M. (2008) Surfactant partitioning in cloud droplet activation: a study of C8, C10, C12 and C14 normal fatty acid sodium salts. *Tellus* B 60B 416-431, doi:10.1111/j.1600-0889.2008.00352.x

Raddatz, T. J., Reick, C. H., Knorr, W., Kattge, J., E. Roeckner, E., R. Schnur, R., K.-G. Schnitzler, K.-G., P. Wetzel, P., and Jungclaus, J. (2007). Will the tropical land biosphere dominate the climate–carbon cycle feedback during the twenty-first century? *Clim. Dyn.* 29:565–574

Raivonen M. (2008) UV-induced Noy emissions in gas exchange chambers enclosing Scots pine shoots: an analysis on their origin and significance. *Dissertationes Forestales* 71, 1-50.

Riipinen, I., Sihto, S.-L., Kulmala, M., Arnold, F., Dal Maso, M. , Birmili, W., Saarnio, K., Teinilä, K., Kerminen, V.-M., Laaksonen, A. and Lehtinen, K.E.J. (2007). Connections between atmospheric sulphuric acid and new particle formation during QUEST III - IV campaigns in Hyytiälä and Heidelberg. *Atmos. Chem. Phys.* **7**, 1899–1914, SRef-ID: 1680–7324/acp/2007-7-1899.

Rinne J, Riutta T, Pihlatie M, Aurela M, Haapanala S, Tuovinen J-P, Tuittila E-S, Vesala T. (2007a). Annual cycle of methane emission from a boreal fen measured by the eddy covariance technique. *Tellus* 59B, 449-457

Rinne, R. Taipale, T. Markkanen, T. M. Ruuskanen, H. Hellén, M. K. Kajos, T. Vesala, and M. Kulmala (2007b) Hydrocarbon fluxes above a Scots pine forest canopy: measurements and modeling, *Atmos. Chem. Phys.,* 7, 3361-3372

Riutta T, Laine J, Aurela M, Rinne J, Vesala T, Laurila T, Haapanala S, Pihlatie M, Tuittila E-S. (2007). Spatial variation in plant community functions regulates carbon gas dynamics in a boreal fen ecosystem. *Tellus* 59B: 838-852.

Roeckner, E., Baeuml, G., Bonventura, L., Brokopf, R., Esch, M., Giorgetta, M., Hagemann, S., Kirchner, I., Kornblueh, L., Manzini, E., Rhodin, A., Schlese, U., Schulzweida, U., and Tompkins, A. (2003). The atmospheric general circulation model ECHAM5. PART I: Model description, Report 349, Max Planck Institute for Meteorology, Hamburg, Germany, available from http://www.mpimet.mpg.de

Romakkaniemi, S., G. McFiggans, K. N. Bower, P. Brown, H. Coe, and T. W. Choularton (2009) A comparison between trajectory ensemble and adiabatic parcel modeled cloud properties and evaluation against airborne measurements . *J. Geophys. Res.* 114 D06214. doi:10.1029/2008JD011286.

Rosenfeld, D., U Lohmann, GB Raga, CD O'Dowd, M Kulmala, S Fuzzi, A Reissell and MO Andreae, (2008) Flood or drought: How do aerosols affect precipitation? *Science* 321: 1309-1313

Ruuskanen T.M., Taipale R, Rinne J., Kajos M.K., Hakola H. and Kulmala M. (2009) Quantitative long-term measurements of VOC concentrations by PTR-MS: annual cycle at a boreal forest site. *Atmos. Chem. Phys. Discuss.* 9:81-134.

Schurgers, G., Arneth, A., Holzinger, R. and Goldstein, A.(2009). Process-based modelling of biogenic monoterpene emissions: sensitivity to temperature and light. *Atmos. Chem. Phys. Discussions* 9: 271–307

Sihto, S.-L., M. Kulmala, V.-M. Kerminen, M. Dal Maso, T. Petäjä, H. Korhonen, F. Arnold, R. Janson, M. Boy, A. Laaksonen and K.E.J. Lehtinen, (2006) Atmospheric sulphuric acid and aerosol formation:

implications from atmospheric measurements for nucleation and early growth mechanisms, Atmos Chem Phys 6, 4079-4091

Sipilä, M., Lehtipalo, K., Kulmala, M., Petäjä, T., Junninen, H., Aalto, P. P., Manninen, H. E., Vartiainen, E., Riipinen, I., Kyrö, E.-M., Curtius, J., Kürten, A., Borrmann, S., and O'Dowd, C. D. (2008) Applicability of Condensation Particle Counters to measure Atmospheric clusters, *Atmos. Chem. Phys.* 8, 4049-4060.

Sipilä, M., Lehtipalo, K., Attoui, M., Neitola, K., Petäjä, T., Aalto, P. P., O'Dowd, C. D., and Kulmala, M. (2009) Laboratory verification of PH-CPC's ability to monitor atmospheric sub-3nm clusters. *Aerosol Sci. Tech.* 43, 2:126-135

Sogacheva, L., L Saukkonen, ED Nilsson, M Dal Maso, DM Schultz, G de Leeuw and M Kulmala (2008) New aerosol particle formation in different synoptic situations at Hyytiälä, Southern Finland, Tellus 60B, 485-494

Spracklen, D. V., K. S. Carslaw, M. Kulmala, V.-M. Kerminen, S.-L. Sihto, I. Riipinen, J. Merikanto, G. W. Mann, M. P. Chipperfield, A. Wiedensohler, W. Birmili, and H. Lihavainen, (2008) The contribution of particle formation to global cloud condensation nuclei concentrations, *Geophysical Res. Lett.,* 35, L06808, doi:10.1029/2007GL033038

Stieb, D.M., Judek, S. and Burnett, R.T. (2002) Meta-Analysis of Time-Series Studies of Air Pollution and Mortality: Effects of Gases and Particles and the Influence of Cause of Death, Age, and Season. *J. Air & Manage. Ass.* 52, 470-484

Stier P., Feichter J., Kinne S., Kloster S., Vignati E., Wilson J., Ganzeveld L., Tegen I., Werner M., Schulz M., Balkanski Y., Boucher O., Minikin A., Petzold A. (2005) The aerosol-climate model ECHAM5-HAM. *Atmos. Chem. Phys.*, 5:1125–1156.

Tarvainen V., Hakola H., Rinne J., Hellén H. and Haapanala S. (2007). Towards a comprehensive emission inventory of terpenoids from boreal ecosystems. *Tellus* 59B: 526-534.

Torpo L., Kurtén T., Vehkamäki H., Laasonen K., Sundberg M. R. and Kulmala M. (2007) The significant role of ammonia in atmospheric nanoclusters. *J. Phys. Chem. A,* 111, 10671

Tunved, P., J Ström, M Kulmala, V-M Kerminen, M Dal Maso, B Svenningson, C Lunder and H-C Hansson (2008) The natural aerosol over Northern Europe and its relation to anthropogenic emissions – implications of important climate feedbacks, Tellus 60B, 473-484

Wania R. (2007). Modelling northern peatland land surface processes, vegetation dynamics and methane emissions. PhD thesis, University of Bristol.

Winkler, PM., G Steiner, A Vrtala, H Vehkamäki, M Noppel, KEJ Lehtinen, GP Reischl, PE Wagner and M Kulmala (2008) Heterogeneous nucleation experiments bridging the scale from molecular ion clusters to nanoparticles, *Science* 319, 1374

PAST, PRESENT AND FUTURE OF THE FINNISH GRADUATE SCHOOL ON PHYSICS, CHEMISTRY, BIOLOGY AND METEOROLOGY OF ATMOSPHERIC COMPOSITION AND CLIMATE CHANGE

A. LAURI[1], J. BÄCK[2], T. VESALA[1] and M. KULMALA[1]

[1]Department of Physics, P.O. Box 64, FI-00014, University of Helsinki, Finland
[2]Department of Forest Ecology, P.O. Box 27, FI-00014, University of Helsinki, Finland

INTRODUCTION

The Finnish Graduate School "Physics, Chemistry, Biology and Meteorology of Atmospheric Composition and Climate Change" started in the beginning of 2006 under initial funding of the Ministry of Education for four years. Before that, there was no national Graduate School governing the current topics in aerosol research and technology and ecosystem-atmosphere interactions.

The units participating in the Graduate School organization include six departments of three Finnish Universities:
- University of Helsinki (coordinator)
    o Department of Physics
    o Department of Chemistry
    o Department of Forest Ecology
- University of Kuopio
    o Department of Physics
    o Department of Environmental Sciences
- Tampere University of Technology
    o Department of Physics
Furthermore, the Finnish Meteorological Institute (FMI) units in Helsinki and Kuopio, VTT Technical Research Centre of Finland, and Vaisala Ltd. are strongly involved in the Graduate School activities. The representatives of all the above mentioned organizations form the Steering Committee of the Graduate School. The Graduate School is strongly connected with the National Centre of Excellence, funded by the Academy of Finland and carrying the same name as the Graduate School.

Currently the education in the Graduate School is given mainly on the following topics:
- Atmospheric Sciences
- Aerosol Physics and Technology
- Physics, Chemistry, Biology and Meteorology of Air Pollution, including:
    o Aerosol-Cloud-Climate Interactions
    o Biosphere-Atmosphere Interactions
    o Development of Aerosol and Environmental Technology
    o Aerosol Emissions, Concentrations, Transformation, Deposition, and Effects

The Graduate School received funding from the Ministry of Education for five positions for the period 2006-2009. Three more positions were received for the years 2007-2009.

During the first three years of its operation a total of 27 PhD theses have been completed within the Graduate School. The demand for experts in atmospheric sciences remains high and is increasing, and all the graduated PhD's are employed, hired by both the private and the public sector in Finland, other European countries, South Africa, and the U.S. Also a private enterprise, Helsinki Aerosol Consulting Ltd, has been founded by former Graduate School members.

GRADUATE SCHOOL ACTIVITIES

The activities of the Graduate School include:
- multidisciplinary research training courses;
- inter-university and -institute supervision;
- PhD student mobility;
- students' participation in domestic and international conferences, symposia and workshops;
- training in complementary skills (academic writing, proposal preparation, presentation skills, science philosophy, ethics in science etc.).

Research training courses are typically organized jointly by two or more Graduate School units, either as a one- or two-week intensive course in one of the measurement stations, or as e-learning. During the past three years more than 20 joint graduate student courses have already been given.

Currently there exist over 40 PhD students in the Graduate School having supervisors from at least two participating units. The experience on inter-institution supervision has been extremely positive, providing the Graduate School participants with a broader view on the research problems they are working with.

The mobility of the Graduate School is carried out on three different levels:
- between the universities and institutes;
- between scientific fields (ecology-physics-technology-chemistry-meteorology);
- between the academia and the private sector.
Several Graduate School students have participated in the mobility programme, and the general experience on the mobility is very positive.

The forms of working on the intensive courses include lectures, exercise sessions, seminars, discussion sessions, field work as well as trips to the surrounding areas. Very often the emphasis has been on intensive work in small student groups. The experiences on the courses have been astonishing, both from the teachers' and students' points of view. On all the courses, the students have been very enthusiastic. A number of scientific articles and proposals have been initiated from the work done on these courses (e.g. Vehkamäki et al., 2004; Kulmala et al., 2004).

From the pedagogical point of view, the intensive courses have often represented a form of problem-based learning (PBL; see e.g. Duch et al., 2001). This instructional strategy has been adopted in order to emphasize the students' own responsibility on their learning process, with support from the instructor. The goals for the course have often been set by the students in the beginning of the course, after a few introductory lectures. Teachers have taken the role of facilitators rather than lecturers. Collaborative learning has been carried out throughout the courses. This has allowed social construction, sharing of information and cognition, and finally improved the metacognitive skills of the students which, in turn, enhance self-directed learning skills. It was also noted that motivation and sociability has been blossoming in these small groups, which allows the students to easily adopt the studied issues and open their minds for creative problem-solving.

Another pedagogically interesting fact has been the horizontal learning process on many of the intensive courses. The participants on the courses have been from very different backgrounds, and the students have specialized in very different topics. Thus, traditional "vertical" graduate courses have been out of question. Instead, horizontal learning has taken place, with a broader approach, addressing a cross-section of knowledge from different fields and blending the information to reach new levels of understanding. As the goals of a course are commonly agreed in the beginning, the students working in the small groups have to take the responsibility to find the best ways to reach these goals in a short time. Often the solution has been horizontal: students from different fields gave small lectures to each other in the groups, and several times it has occurred that a student wanted to present her ideas to the whole audience for common discussion.

The success of the intensive courses organized by the Finnish Graduate School is reflected by the fact that the number of applicants to the courses have constantly grown. In fact, during the past couple of years there were several courses where a big fraction of the students willing to participate had to be rejected due to the limited capacity of the teaching or accommodation space.

The internet provides an interesting, flexible and versatile learning environment that at its best motivates and inspires the students. E-learning, i.e. using the internet as a tool of distant learning, frees the student from the requirements of time and space. During the past five years, an increasing number of courses have been given in this format within the Graduate School.

In its own way e-learning may even enhance social interaction, although it is different from face-to-face interaction. Interaction in e-learning is three-fold: it is very much based on the student's own activity, but is still based on the student-instructor-material triangle. An e-learning course demands thorough preparation in order to succeed. The planning consists of at least evaluating the needs for the course, the future students, the learning outcomes, choosing contents and pedagogical approaches, provision of the needed material to the students, arrangement of a personal support for students if they face problems during the course, and last but not least, planning the evaluation of the students after the course.

INTERNATIONAL COLLABORATION

A special advantage for the Finnish Graduate School has been the full utilization of the experiences and best practises of the Nordic Graduate School CBACCI (Biosphere-Carbon-Aerosol-Cloud-Climate Interactions), which was funded by NordForsk during the years 2003-2007. CBACCI partners include universities and research institutes from Finland, Sweden, Norway, Denmark, Iceland, North-West Russia, Estonia and Lithuania. In 2003 the CBACCI Steering Committee set the goals and the framework for the Nordic Graduate School. An important part of the framework was the CBACCI education structure (CBACCI, 2003). Right from the beginning, the education structure was set not only through the postgraduate level, but spanning all the way from master-level studies to the post-doctoral phase.

Based on the CBACCI education structure, a joint Nordic Master's Degree Programme, Atmosphere-Biosphere Studies (ABS) was set up in 2006. The programme is very multidisciplinary, involving a versatile education on atmospheric sciences covering physical phenomena, atmospheric chemistry, meteorology, and ecosystem studies. Part of the content of the programme is related to the interactions between the ecosystems and the atmosphere. All the education of the programme is given in English. The approximate study period is two years and includes 120 ECTS of studies. Currently the ABS network consists of ten universities in four Nordic and Baltic countries. The ABS Programme has trained Masters of Science, some of which are continuing their studies in Finnish, Nordic and European Graduate Schools.

On the senior scientist level, annual workshops intended for teachers became one of the successful traditions of CBACCI. Since 2003, the workshop has been arranged annually, each time in Helsinki. The two-day workshop has always included two parts: training for teachers and discussions on CBACCI and Nordic co-operation. On each time, the training part was different, the themes listed below:
- Self-assessment – tools for understanding and promoting learning
- Experiences on e-lecturing undergraduate chemistry
- Guidelines for writing scientific articles
- Supervising theses work - what is expected?
- Effective presentations skills
- Hands on experience with e-learning
- Aspects of supervising in international education
- International dialogue and collaboration
- Why learning physics is difficult for so many students – Is this a challenge for physics departments or for its students

- Non-verbal communication and body awareness
- Moderated group discussions on Ethics in Science (Intellectual property rights, ego in science, competition, publication issues)

Several times the training part of the workshop has been organized in co-operation with the ACCENT network of excellence. Each time the workshop has attracted some 20-30 university teachers from the Nordic and Baltic countries as well as North-West Russia to share their teaching experiences and to learn new aspects and methods to be utilized in their teaching and supervision processes.

Another significant collaboration partner of the Finnish Graduate School is the global network of iLEAPS/IGBP (Integrated Land Ecosystem Atmosphere Processes Study / International Geosphere-Biosphere Programme). The iLEAPS International Project Office is located at the Kumpula campus, in the immediate vicinity of the Department of Physics of the University of Helsinki and the Finnish Meteorological Institute.

Special attention has been paid in the international networking of the Graduate School participants. Most of the Graduate School students have presented their work on international scientific conferences. Training on complementary skills has often been given as a part of the joint graduate student courses. The teaching forms have included lectures, group discussions, seminars and written tasks.

FUTURE

From the beginning of 2010, all the Graduate Schools in Finland will function under the Academy of Finland. This will enhance possibilities to coordinate the national strategies concerning research and science education in Finland in a more comprehensive way.

In 2008, the Academy of Finland had a call for new Graduate Schools, starting their functioning in the beginning of 2010. The currently working National Graduate School "Physics, Chemistry, Biology and Meteorology of Atmospheric Composition and Climate Change" opted to propose continuation of the Graduate School with an even broader view. The new name of the Graduate School would read as "Atmospheric Composition and Climate Change: From Molecular Processes to Global Observations and Models", and the new research topics would include:
- Aerosol-cloud-climate interactions
- Biosphere-atmosphere interactions
- Global climate modelling
- Land use change quantification methods in relation to climate change and methods for early signalling to adaptation to climate change impacts
- Development of aerosol, remote sensing, radar, and environmental technology
- Linking aerosol and environmental technology to 3D city models and built environment
- Improved positioning to improve in-situ measurements
- Ubiquitous remote sensing
- Snow and ice studies: evolution of sea ice and snow conditions
- Carbon, water, nitrogen and aerosol cycles and balances
- Air quality

The partner list of the new Graduate School is also longer than in the current one:
- University of Helsinki: Department of Physics, Department of Forest Ecology, Department of Chemistry, Department of Geography, Department of Forest Resource Management
- University of Kuopio: Department of Physics, Department of Environmental Sciences
- Tampere University of Technology: Department of Physics
- Helsinki University of Technology: Department of Radio Science and Engineering, Department of Surveying
- Finnish Meteorological Institute: units in Helsinki and Kuopio

- Finnish Geodetic Institute
- VTT Technical Research Centre of Finland
- Finland's Environmental Administration (SYKE)
- Vaisala Oyj
- Beneq Oy
- Space Systems Finland Oy

In the call, the new Graduate School received a total of 12 full-day doctoral student positions for the years 2010-2013. An open call for the positions will be launched in spring 2009, and up to 200 applications are expected. So far no funding has been allocated in order to hire a full-day coordinator. Coordinating the for the new, even more interdisciplinary Graduate School, this massive in size will be a quite a challenge.

Concerning international activities, the Nordic CBACCI Graduate School is currently functioning with short and minimal project funds, but due to the extremely positive experiences the partners have agreed to continue the most important activities such as joint intensive courses and annual teacher workshops. The Nordic Master's Degree Programme in Atmosphere-Biosphere Studies (ABS) is continuing as a permanent activity, funded mainly by the Nordplus Programme funded by the Nordic Council of Ministers. On European level, the Graduate School partners are eagerly looking for new programmes and activities e.g. in the FP7 Marie Curie Initial Training Networks (ITN) and joint Erasmus Mundus Programmes.

CONCLUSIONS

The future of the Finnish Graduate School seems bright. During the first three years of its functioning the Graduate School has been able to integrate the best practices learnt from the previous educational activities fully into the Graduate School. The number of students and graduated doctors has increased firmly. The international activities are a solid part of the Graduate School.

ACKNOWLEDGEMENTS

REFERENCES

CBACCI (2003). CBACCI education structure. Annex of the Steering Committee memorandum of the meeting 5.5.2003 in Oslo.

Duch, B. J., Groh, S. E. and Allen, D. E. (2001). *The Power of Problem-Based Learning*. Stylus Publishing, Sterling, VA, U.S.A.

Hennessy, S. and Murphy, P. (1999). The Potential for Collaborative Problem Solving in Design and Technology, *International Journal of Technology and Design Education* 9(1), 1–36.

Kulmala, M., Boy, M., Suni, T., Gaman, A., Raivonen, M., Aaltonen, V., Adler, H., Anttila, T., Fiedler, V., Grönholm, T., Hellén, H., Herrmann, E., Jalonen, R., Jussila, M., Komppula, M., Kosmale, M., Plauskaite, K., Reis, R., Savola, N., Soini, P., Virtanen, S., Aalto, P., Dal Maso, M., Hakola, H., Keronen, P., Vehkamäki, H., Rannik, Ü., Lehtinen, K. E. J. and Hari, P. (2004). Aerosols in boreal forest: wintertime relations between formation events and bio-geo-chemical activity. *Bor. Environ. Res.*, 9, 63-74.

Vehkamäki, H., Dal Maso, M., Hussein, T., Flanagan, R., Hyvärinen, A., Lauros, J., Merikanto, J., Mönkkönen, P., Pihlatie, M., Salminen, K., Sogacheva, L., Thum, T., Ruuskanen, T. M., Keronen, P., Aalto, P. P., Hari, P., Lehtinen, K. E. J., Rannik, Ü. and Kulmala, M. (2004). Atmospheric particle formation events at Värriö measurement station in Finnish Lapland 1998-2002, *Atm. Chem. Phys.*, 4, 2015-2023.

iLEAPS, THE LAND ECOSYSTEM – ATMOSPHERE PROCESSES STUDY: INTERNATIONAL CUTTING-EDGE RESEARCH

A. REISSELL and M. NYMAN

iLEAPS International Project Office, Department of Physics, P.O. Box 64, FI-00014, University of Helsinki, Finland

INTRODUCTION

iLEAPS, the Integrated Land Ecosystem – Atmosphere Processes Study is a core project of the International Geosphere-Biosphere Programme, IGBP, a research programme that studies the phenomenon of global change and climate change. The iLEAPS project has an international project office (http://www.ileaps.org) at the Kumpula campus of University of Helsinki. iLEAPS coordinates and facilitates international land ecosystem – atmosphere science, and promotes globally interdisciplinary collaboration among physicists, chemists, meteorologists, geo- and bioscientists, particularly involving scientists from the developing countries to participate in iLEAPS activities. The iLEAPS Scientific Steering Committee members are 18 reknown scientists from all over the world, among them Prof. Markku Kulmala from Finland.

iLEAPS is an international interdisciplinary research program aimed at improved understanding of processes, linkages, and feedbacks in the land-atmosphere interface affecting the Earth System. The scientific goal of iLEAPS is to provide understanding how interacting physical, chemical and biological processes transport and transform energy and matter through the land-atmosphere interface. iLEAPS encourages international multi- and interdisciplinary collaboration. The project essentially integrates measurements and modeling at scales from molecular to global, from past through present to future. The scientific foci and implementation plan are described in the iLEAPS Science Plan and Implementation Strategy (2005).

METHODS

iLEAPS initiates and endorses a variety of activities and projects. Currently the project has 12 endorsed projects that span from the research on environmental factors affecting emissions of volatile organic compounds (VOCs) at the leaf level to global scale modelling. The current projects are listed below:

- Aerosols, Clouds, Precipitation, Climate (ACPC, http://www.ileaps.org/acpc/) program
- African Monsoon Multidisciplinary Analyses (AMMA, http://amma.mediasfrance.org/)
- European Integrated project on Aerosol Cloud Climate and Air Quality interactions (EUCAARI, http://www.atm.helsinki.fi/eucaari/)
- IGBP Cross-Project on Fire (Palaeofire working group)
- International Network Measuring Terrestrial Carbon, Water and Energy Fluxes (FLUXNET, http://www.fluxnet.ornl.gov/fluxnet/)
- iLEAPS/GEIA initiative on process-based terrestrial trace gas models
- Isotopes in Project for Intercomparison of Land-surface Parameterization Schemes (iPILPS, http://ipilps.ansto.gov.au/)
- Land-Use and Climate, Identification of robust impacts (LUCID)
- Northern Eurasia Earth Science Partnership Initiative (NEESPI, http://neespi.org/)
- POLar study using Aircraft, Remote sensing, surface measurements and modelling of Climate, chemistry (POLARCAT, http://www.polarcat.no/polarcat)
- Volatile Organic Compounds in the Biosphere - Atmosphere System (VOCBAS, ESF www)
- WATer and climate CHange (WATCH, project www).

iLEAPS International Project Office (IPO) and iLEAPS endorsed projects organize a variety of activities and events, for example modelling intercomparisons, measurement campaigns, sessions in large conferences (EGU, AGU), specific workshops, training workshops, summer schools, and large synthesizing science conferences. The next large scientific event, the iLEAPS Science Conference (http://www.ileaps.org/science_conf_2009/) is organized in parallel with GEWEX, the Global Energy and Water Cycle Experiment, a core project of World Climate Research Programme (WCRP), 24-28 August 2009 in Melbourne, Australia. The parallel conferences have three joint sessions on 1) Land in the Climate System, 2) Aerosol, Cloud, Precipitation and Climate Interactions, and 3) Future Generation of Integrated Observation and Modelling Systems. The projects also organize an Early Career Scientist Workshop (http://www.ileaps.org/ecsw/), 20-22 August 2009, also in Melbourne. Among the most important published products provided by the iLEAPS IPO is the quarterly Newsletter, which contains articles on the latest research carried out by the iLEAPS science community aimed also for wider scientific and related audiences, introductions of researchers, news, activities and meetings reports.

RESULTS

As examples of research results from 2008, four projects' results are highlighted: ACPC, Cross-Project on Fire, LUCID, and VOCBAS.

Aerosol, Cloud, Precipitation, Climate (ACPC)
The concentration of cloud-active particles, especially in the lower troposphere, has a profound influence on the microphysical processes in clouds, and consequently on many aspects of weather and climate. A large number of published and unpublished measurements of cloud condensation nuclei (CCN) concentrations and aerosol optical thickness (AOT) measurements have been analyzed. AOT measurements were obtained mostly from the AERONET network, and selected to be collocated as closely as possible to the CCN investigations. In remote marine regions, CCN0.4 (CCN at a supersaturation of 0.4%) are around 110 cm^{-3} and the mean AOT500 (AOT at 500 nm) is 0.057. Over remote continental areas, CCN are almost twice as abundant, while the mean AOT500 is ca. 0.075. (Sites dominated by desert dust plumes were excluded from this analysis.) Some, or maybe even most of this difference must be because even remote continental sites are in closer proximity to pollution sources than remote marine sites. This suggests that the difference between marine and continental levels must have been smaller before the advent of anthropogenic pollution. Over polluted marine and continental regions, the CCN concentrations are about one magnitude higher than over their remote counterparts, while AOT is about five times higher over polluted than over clean regions. The average CCN concentrations from all studies show a remarkable correlation to the corresponding AOT values, which can be expressed as a power law. This can be very useful for the parameterization of CCN concentrations in modeling studies, as it provides an easily measured proxy for this variable, which is difficult to measure directly. It also implies that, at least at large scales, the radiative and microphysical effects of aerosols on cloud physics are correlated and not free to vary independently. While this strong empirical correlation is remarkable, it must still be noted that that there is about a factor-of-four range of CCN concentrations at a given AOT, and that there remains considerable room for improvement in remote sensing techniques for measuring CCN abundance (Andreae 2008).
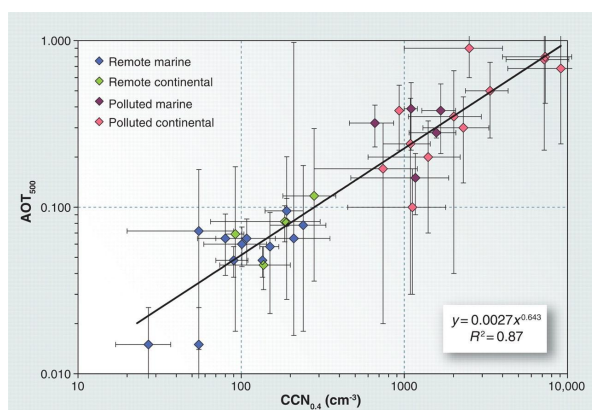
Figure 1. Relationship betweenAOT at 500nm and CCN concentrations at supersaturation of 0.4%. The error bars reflect the variability of measurements within each study (standard deviations or quartiles).
(Modified after Andreae 2008).

Aerosols serve as cloud condensation nuclei (CCN) and thus have a substantial effect on cloud properties and the initiation of precipitation. Large concentrations of human-made aerosols have been reported to both decrease and increase rainfall as a result of their radiative and CCN activities. At one extreme, pristine tropical clouds with low CCN concentrations rain out too quickly to mature into long-lived clouds. On the other hand, heavily polluted clouds evaporate much of their water before precipitation can occur, if they can form at all given the reduced surface heating resulting from the aerosol haze layer. Paper from the ACPC planning team members proposes a conceptual model that explains this apparent dichotomy, the method presented is following the energy flow through the atmosphere and the ways it is influenced by aerosol (airborne) particles. The conclusion is that both can be true, depending on local environmental conditions. The determination of this issue is one with significant consequences in an era of climate change and specifically in areas suffering from manmade pollution and water shortages. This allows the development of more exact predictions of how air pollution affects weather, water resources and future climates (Rosenfeld et al. 2008).
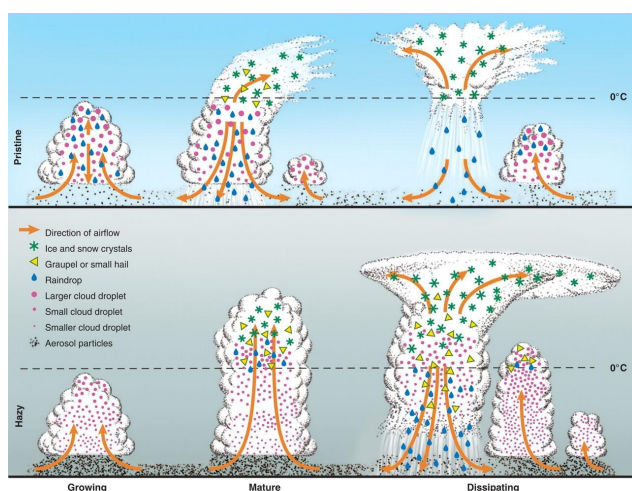
Figure 2. Evolving of deep convective clouds in the pristine (top) and polluted (bottom) atmosphere. Cloud droplets coalesce into raindrops that rain out from the pristine clouds. The smaller drops in the polluted air do not precipitate before reaching the supercooled levels, where they freeze onto ice precipitation that falls and melts at lower levels. The additional release of latent heat of freezing aloft and reabsorbed heat at lower levels by the melting ice implies greater upward heat transport for the same amount of surface precipitation in the more polluted atmosphere. This means consumption of more instability for the same amount of rainfall. The result is invigoration of the convective clouds and additional rainfall (Rosenfeld et al. 2008, with permission).

IGBP Cross-Project on Fire
Fire is the most ubiquitous form of landscape disturbance, and has important effects on climate through the global carbon cycle and changing atmospheric chemistry. There has been a significant increase in large-scale wildfires in all regions of the world during the past decade. This has triggered an interest in knowing how fire has changed in the past, and particularly how fire regimes respond to periods of major warming. The end of the Younger Dryas, about 11,700 years ago, was an interval when the temperature of Greenland warmed by over 5°C in less than a few decades. Marlon et al. used 35 records of charcoal accumulation in lake sediments from sites across North America to see whether fire regimes across the continent showed any response to such rapid warming. They also examined the changes during the major cooling at the beginning of the Younger Dryas, ca 12,900 years ago – because a team of scientists led by an isotope geochemist at Berkeley had suggested that a large comet exploded over North America then, triggering widespread fires as well as the cooling. Marlon et al. found no evidence for continental-scale fires. They did find clear changes in biomass burning and fire frequency whenever climate changed abruptly, but most particularly when temperatures increased at the end of the Younger Dryas cold phase. The Marlon et al. (2009) is the third paper describing important findings stemming from research by the Global Palaeofire Working Group, which is coordinated by Sandy P. Harrison, funded by the QUEST programme lead by Colin Prentice and sponsored by the IGBP Cross-Project Initiative on Fire (Marlona et al. 2009).
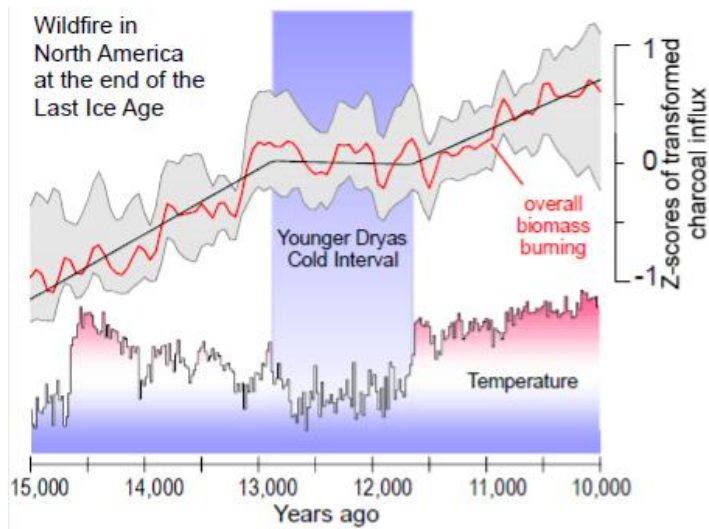
Figure 3. Wildfire in North America at the end of the Last Ice Age (modified after Marlon et al 2009).

Land-use and Climate, Identification of Robust Impacts (LUCID)
Seven climate models, IPSL-ORCHIDEE, SPEEDY-LPJmL, ARPEGE-ISBA, ECEarth-TESSEL, ECHAM5-JSBACH, CCAM-CABLE, CCSM-CLM (with prescribed observed sea-surface temperatures and sea ice extent) were used to explore the biogeophysical impacts of human-induced land cover change (LCC) at regional and global scales. In four of the seven models the imposed perturbation led to statistically significant decreases in northern hemisphere summer latent heat flux and decreases in near-surface temperature over the regions of LCC, but only a few significant changes in precipitation. The results show no common remote impacts of LCC. There was little consistency in the changes simulated by the seven models due to at least four critical factors: 1) the implementation of LCC despite agreed maps of agricultural land, 2) the representation of the phenology of crops, 3) the parameterisation of albedo, and 4) the representation of evapotranspiration (and corresponding parameter choice) for different land cover types. This study highlights a dilemma for both historical hind-casts and future projections; LCC is regionally significant, but it is not feasible within the time frame of the next IPCC (AR5) assessment to implement this change commonly across multiple models (Pitman et al 2009).
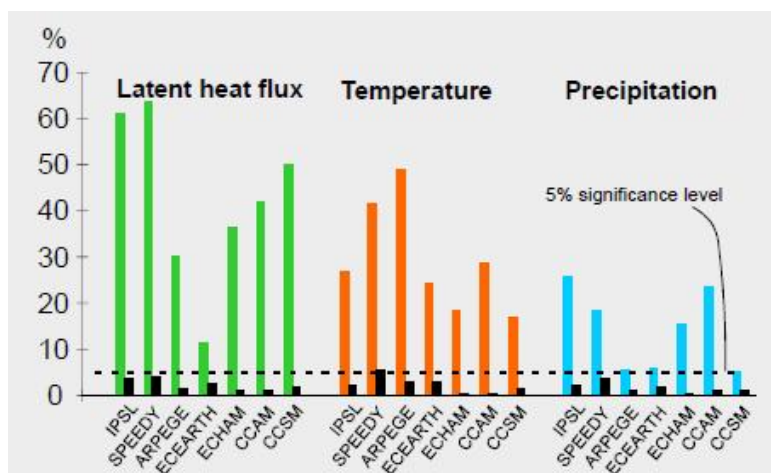
Figure 4. Percent of land area that exhibits statistically significant changes in JJA latent heat flux,
temperature and precipitation. Coloured bars: the percent of grid points with statistically significant changes where land cover changes (change in LAI > 0.5) within each climate model. Black bars: the percent of grid points with statistically significant changes where land cover is not changed (modified after Pitman et al., submitted).

37

Volatile Organic Compounds in the Biosphere-Atmosphere System (VOCBAS)

Isoprene dependence on temperature has been categorized in all published studies and is the cornerstone of all algorithms modelling the emission of this important volatile in the atmosphere. Fortunati et al (2008) for the first time have revealed that a very common stressor (drought) may break this dependency. This work takes into consideration the important fact that drought is a recoverable stress to which most of the plants are transiently and recurrently exposed. They have reported that isoprene emission is resistant to water stress, since sources of carbon alternative to photosynthesis are activated when the drought stress is severe, and rapidly disappear when the stress is relieved. Isoprene emission may transiently increase to levels higher than those observed before stress in leaves that recover from drought. This is an important finding that needs to be incorporated in modelling exercises. Even more importantly, isoprene emission is not dependent on temperature for at least about two weeks after recovering from stress. This is possibly due to the fact that isoprene synthase (the biochemical factor driving isoprene temperature-dependency) reaches its maximum activity immediately after recovering from stress. The discovery of transient yet widespread uncoupling of isoprene emission from temperature should lead to further refining of current algorithms and models of isoprene emission which are based on Guenther's algorithm, especially when applied to areas that are prone to recurrent drought events (Fortunati et al. 2008).
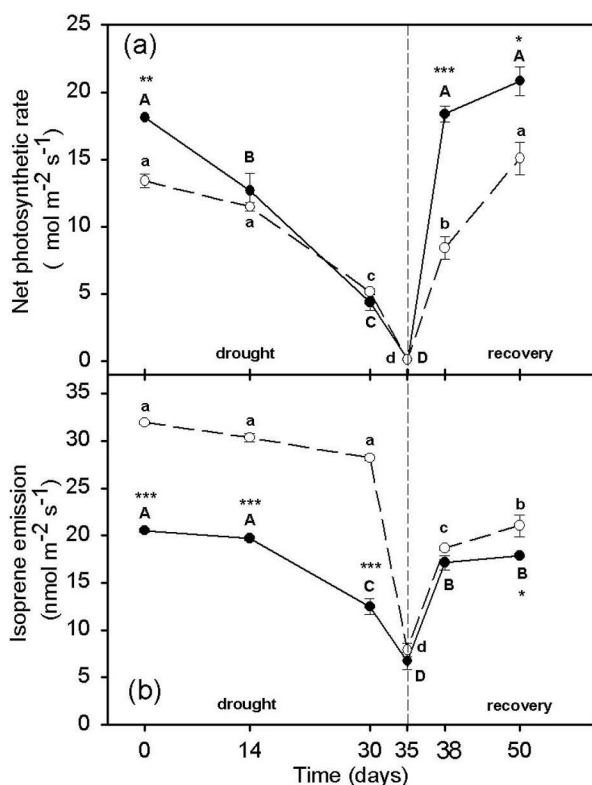
Figure 5. Measurements of photosynthesis and isoprene emission rates during drought stress and re-watering in leaves grown at different temperatures. Measurements of photosynthesis (a) and isoprene emission (b) of black poplar leaves grown at 25°C (black circles) and 35°C (white circles).

CONCLUSIONS

International iLEAPS project is working in a wide field of research on land-atmosphere interactions and the results from the projects represent cutting-edge science. New initiatives and activities are under way and being planned in collaboration with other international research organizations. For example on phenology involving several communities (e.g., phenology networks, palaeo, flux, remote sensing), Arctic project on permafrost, land-atmosphere interactions in China, also collaboration with remote sensing agencies NASA and ESA.

REFERENCES

Andreae, M.O. (2008) Correlation between cloud condensation nuclei concentration and aerosol optical thickness in remote and polluted regions. *Atmos. Chem. Phys. Discuss.* 8, 11293–11320.

Fortunati A., Barta, C., Brilli, F., Centritto, M., Zimmer, I. , Schnitzler, J-P., Loreto, F. (2008) Isoprene emission is not temperature-dependent during and after severe drought-stress: a physiological and biochemical analysis. *Plant Journal* doi: 10.1111/j.1365-313X.2008.03538.x.

iLEAPS Science Plan and Implementation Strategy (2005). IGBP Report 54. IGBP Secretariat, Stockholm. 52pp.

Marlona, J.R., Bartlein, P.J., Walsh, M.K., Harrison, S.P., Brown, K.J., Edwards, M.E., Higuera, P.E., Power, M.J., Anderson, R.S., Briles, C., Brunelle, A., Carcaillet, C., Daniels, M., Hu, F.S., Lavoie, M., Long, C., Minckley, T., Richard, P.J.H., Scott, A.C., Shafer, D.S., Tinner, W., Umbanhowar, C.E. Jr., Whitlock, C. (2009) Wildfire responses to abrupt climate change in North America. *Proceedings of the National Academy of Sciences of the United States of America, PNAS Early Edition*, 10.1073/pnas.0808212106. 6 p.

Pitman, A.J., de Noblet-Ducoudré, N., Cruz, F.T., Davin, E.L., Bonan, G.B., Brovkin, V., Claussen, M., Delire, C., Ganzeveld, L., Gayler, V., van den Hurk, B.J.J.M., Lawrence, P.J., van der Molen, M.K., Müller, C., Reick, C.H., Seneviratne, S.I., Strengers, B. J., Voldoire, A. (2009) Land use and climate via the LUCID intercomparison study: implications for experimental design in AR5, submitted to GRL.

Rosenfeld, D., Lohmann U., Raga, G.B., O'Dowd, C.D., Kulmala, M., Fuzzi, S., Reissell, A., Andreae, M.O. (2008) Flood or Drought: How Do Aerosols Affect Precipitation? *Science* 321, 1309-1313.

Abstracts

EMISSIONS OF BIOGENIC VOLATILE ORGANIC COMPOUNDS FROM BOREAL SCOTS PINE FOREST FLOOR

H. AALTONEN[1], J. PUMPANEN[1], M. PIHLATIE[2], H. HAKOLA[3], H. HELLÉN[3] and J. BÄCK[1]

[1]Department of Forest Ecology, P.O. Box 27, 00014 University of Helsinki, Finland
[2]Department of Physics, P.O. Box 64, 00014 University of Helsinki, Finland
[3]Finnish Meteorological Institute, P.O. Box 503, 00101 Helsinki, Finland

Keywords: Biogenic volatile organic compounds, forest floor, soil, trace gases

INTRODUCTION

Biogenic Volatile Organic Compounds (BVOCs) include a broad spectrum of atmospheric hydrocarbons, emitted by natural sources (Kesselmeier & Staudt, 1999). BVOCs constitute the largest part of volatile chemicals produced and emitted by the biosphere (Guenther et al., 2006). The most common BVOC group, terpenoids, can be divided into three parts: isoprene, monoterpenes and sesquiterpenes.

In the troposphere BVOC compounds take part in the chemical reactions which affect the formation and growth of aerosols (Kulmala et al., 2000). When VOCs react with ozone, and OH and NO_3 radicals, the formed reaction products may have lower volatility and thus condense into aerosol particles. Exact conditions needed for aerosol formation and growth events are not fully understood, however, it has been observed that events peak in early summer and autumn (Dal Maso et al., 2005).

Most of BVOCs are emitted by flowers, fruits and green parts of plants and they can function as inter- and intraspecific messenger compounds, and as repellents or attractants for insects (Kesselmeier & Staudt, 1999). Also decomposing processes, roots (Hayward et al., 2001) and micro-organisms (Leff & Fierer, 2008) have been found to produce and emit these compounds. The lifetime e.g. of terpenoids during the growing season is short, few hours at maximum (Hakola et al., 2003), and therefore the local emission sources determine the atmospheric concentrations at a forest stand scale. This emphasizes the importance to determine emission rates of dominant plant species and soil types for every vegetation zone.

Boreal zone is the second largest forested region in the world, next to tropical forests (FAO, 2000), and the branch- and canopy-level emissions emitted from boreal forests have been rather well characterized (e.g. Hakola et al., 2003, 2006; Ruuskanen et al., 2005). Less is known about the emissions originating from boreal forest soils. Especially understanding on the dynamics of soil processes and the roles of different soil components such as roots, rhizosphere and decomposing organisms to BVOC formation and deposition is limited. In boreal forest soil, BVOC emissions have been observed to be the highest in spring and autumn (Hellén et al., 2006), but the processes behind seasonal variation are still uncertain. Soil temperature and humidity conditions have a direct connection to many physical and biological processes of soil BVOC-formation (Asensio et al. 2007). Due to the heterogeneity of soil as a BVOC source, long lasting and spatially representative sampling series over large areas are needed to assess the temporal and spatial variation in soil BVOC emissions. As a consequence of technically challenging and costly measurements, the soil BVOC emissions are relatively weakly known compared to other trace gases emitted from soils.

The purpose of this study was to identify the BVOC compounds emitted from boreal forest floor as well as to determine the spatial and temporal changes in BVOC fluxes. The aim was also to identify environmental factors controlling soil BVOC fluxes, and to connect BVOC emissions to the emissions of other trace gases (CO_2, CH_4 and N_2O). We concentrated the sampling especially to early and late part of the growing season, which are earlier shown to be the most important in terms of BVOC emissions (Hellén et al., 2006).

METHODS

The BVOC fluxes from Scots pine (*Pinus sylvestris* L.) forest floor were measured at SMEAR II station (61°51´N, 24°17´E, 180 m a.s.l.), located in Hyytiälä Forestry Field Station in southern Finland (Hari and Kulmala, 2005). The measurements were performed between April and November 2008. Samples were collected on permanently installed stainless steel collars using dynamic chamber technique. Five collars (80x40 cm) were installed randomly by pushing the collar edge gently on the ground and by sealing with quartz sand.

Chamber (80x40x25 cm in size) was made of an aluminium frame and its sides were covered inside with polytetrafluoroethylene (PTFE) plate and top with PTFE film. Before the 120 min sampling period the closed chamber was flushed with ambient air for 60 min with a flow rate of 4.5 l min^{-1}. Inlet air ozone was removed with MnO_2 coated copper nets and air was also directed through an active carbon filter to avoid reactions of BVOCs with other air particles. All the tubing was made of PTFE. Samples were taken to Tenax adsorbent tubes using a flow rate of ca. 60 ml min^{-1}. Air temperature inside the chamber and PAR radiation above the chamber were measured during the chamber closure. Summer 2008 was relatively cloudy and cold, so cooling system preventing the temperature rise inside the chamber was not needed.

During the chamber deployment the coverage of ground vegetation in the collar areas was determined twice from photographs. The ground inside the collars was covered with plants by 30-50%, except in one collar where the coverage was less (12%). Field layer consisted only of small shrubs, herbaceous plants did not exist. Lingonberry (*Vaccinium vitis-idaea*) and bilberry (*Vaccinium myrtillus*) were the most predominant species, lingonberry dominating inside three and bilberry inside two collars, and also heather (*Calluna vulgaris*) grown inside of two collars. The ground layers inside the collars were completely covered by three moss species: *Pleurozium schreberi*, *Dicranum sp.* and *Hylocomium splendens*, in the order of abundance. During the growing season plant coverage stayed constant or got higher depending on species composition.

Litter from previous autumn covered 5-35% of the ground inside the collars, and the litter coverage correlated negatively (p: 0.014) with plant coverage. Litter coverage decreased during the growing season, as a consequence of decomposition and plant growth, and increased again rapidly in the autumn.

As the measurements were conducted at SMEAR II station, the station provides ample of supporting data from continuous measurements of physical environmental factors such as humus temperature, below canopy PAR radiation, precipitation and humus water content, which can be used to explain the temporal variation in BVOC emissions. At the station litter fall is collected and weighed monthly on average 20th day of every month. There are also frequent or continuous measurements of trace gas fluxes, such as CO_2, CH_4 and N_2O, measured with automated and manual chambers (Pihlatie et al., 2007).

RESULTS

Temporal variability in emissions

We found 37 VOC compounds with chamber measurements and 19 of them were from natural sources. The most emitted BVOC compound group was monoterpenes (Table 1). α-pinene and Δ^3-carene were clearly the predominant compounds, constituting over 80% of the emissions of all monoterpenes. Isoprene and sesquiterpenes were also detected, but their contributions to the total amount were negligible.

Table 1. Forest floor BVOC emissions between April – November, 2008.

µg m^{-2} h^{-1}	Average	Median	Min	Max
Hemiterpenoids				
isoprene	0.050	0.032	-0.028	0.312
methyl butenol	0.029	0.020	-0.003	0.254
Monoterpenes				
α-pinene	2.975	1.934	-0.695	13.781
β-pinene	0.191	0.134	-0.086	0.991
Δ^3-carene	1.305	1.029	-1.264	6.411
bornylacetate	0.008	0.003	-0.004	0.037
camphene	0.442	0.326	0.032	2.206
limonene	0.012	0.028	-0.297	0.199
linalool	0.026	0.012	0.007	0.074
nopinone	0.012	0.008	0.001	0.059
p-cymene	0.041	0.024	-0.055	0.394
sabinene	0.013	0.005	-0.006	0.066
terpinolene	0.005	0.003	-0.001	0.015
1,8-cineol	0.008	0.007	0.002	0.025
Sesquiterpenes				
aromadendrene	0.013	0.007	0.002	0.030
copaene	0.004	0.002	0.001	0.018
iso-longifolene	0.000	0.001	-0.005	0.003
longicyclene	0.004	0.002	0.001	0.014
longifolene	0.023	0.008	-0.002	0.270

BVOC emissions had a clear seasonal trend (Fig. 1). Monoterpene emissions peaked in early summer and autumn while sesquiterpene emissions peaked only in early summer. Emissions were the highest in late autumn at the sampling date 06/10/2008 while emissions during early summer peaked on 04/06/2008 reaching almost the same level. Two first samplings showed a lowering trend of emissions, which can be a sign of higher emissions in spring before the measurement period had started. During the midsummer emissions were clearly lower, on average 50-70% lower compared to the highest emissions. However, some compounds behaved differently, such as isoprene which peaked in midsummer (0.10 µg m^{-2} h^{-1}), or limonene with no clear emission peak but clear uptake (-0.17 µg m^{-2} h^{-1}) in the autumn. The emission rates varied between the collars, depending on the compound and sampling date.
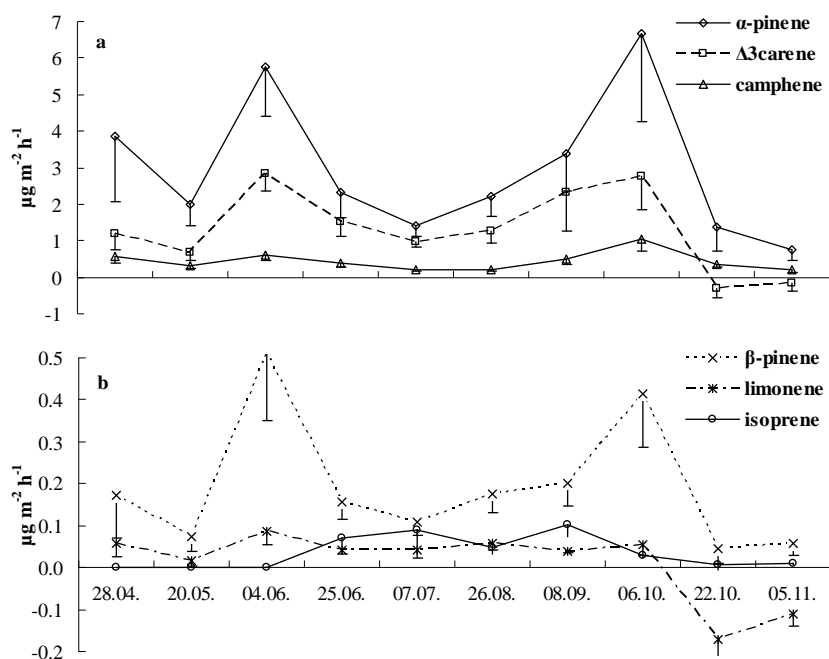
Figure 1. Emissions of the 6 most emitted BVOC compounds between April – November, 2008. **a)** emissions of α-pinene, Δ^3-carene and camphene, **b)** emissions of β-pinene, limonene and isoprene. Error bars represents standard errors of the five collars.

45

Environmental factors controlling BVOC emissions

At SMEAR II station, summer 2008 was cloudy and rainy, and temperatures were relatively low. From the end of May to the beginning of June, there was a two week long warmer period with no precipitation. This period coincided with the peak in forest floor BVOC emissions. At that time the below canopy PAR was the highest of the whole summer and at sampling date 04/06/2008 temperature inside the chamber reached the highest value of 31 °C, being ~6 °C higher than the ambient temperature.

Litterfall at the SMEAR II station was very stable during spring and summer, however, in October the amount of litter deposited increased markedly (app. 5 fold) (Fig. 2). Increase in the litter deposition appeared at the same time as the higher BVOC emissions from forest floor.
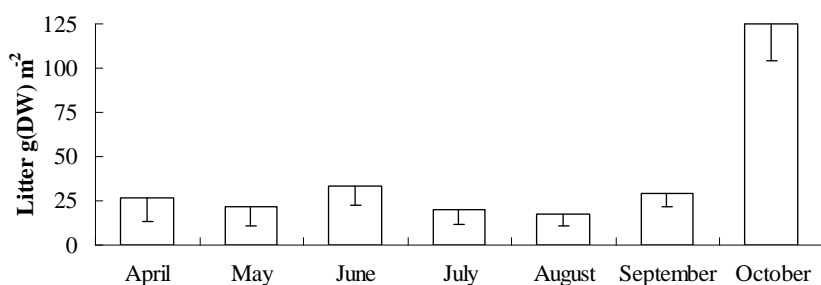
Figure 2. Monthly litterfall at SMEAR II station between April – October, 2008. Error bars represents standard deviations of the 20 litter collectors.

Photosynthesis of ground vegetation started at the end of April, and varied significantly before the summer maximum (3.9 μmol m^{-2} s^{-1}) in the end of July. The largest sub-peak appeared simultaneously with the early summer BVOC emission peak. In the latter half of the year the photosynthesis of the ground vegetation showed no connection to increasing BVOC emissions.

Connection to soil C and N cycling

Soil at SMEAR II station acts as a sink of methane and a small source of nitrous oxide (Pihlatie et al., 2007). During the growing season in 2008 methane uptake was on average 75 μg m^{-2} h^{-1}, while emissions of nitrous oxide were on average 1.2 μg(N) m^{-2} h^{-1} (data not shown). Methane uptake remained relatively stable, except for slightly higher and fluctuating uptake at early summer. Changes in methane uptake took place concurrent with first peak in BVOC emissions. Emissions of nitrous oxide stayed stable in the beginning and at the end of the growing season, but fluctuated greatly during the midsummer, exhibiting high positive and even negative values. Soil CO_2 emissions acted similarly as the ground vegetation photosynthesis, with highest values during the midsummer (data not shown). CO_2 flux got the highest values already mid-July and did not change during the BVOC emission peaks during early summer and autumn.

CONCLUSIONS

Although the synthesis pathways of the main BVOCs; isoprene, monoterpenes and sesquiterpenes; in plants are well known, the purposes of these compounds are still under debate. In the case of soil BVOC emissions also the emission sources and formation processes are practically unknown. Decomposing litter has been found to be the main source of soil BVOC emissions (Hayward et al., 2001; Hellén et al., 2006; Leff & Fierer, 2008), in which both decomposers and decomposing material have a role in the emissions.

The forest at SMEAR II station is dominated by Scots pine, which drops the oldest age class of needles in autumn. Thus in October there is a clearly observable peak in the litter fall. In the needles of conifers there

are cellular storages of monoterpenes, which are released during the decomposition. Thus the peak in BVOC emissions, composed mainly of monoterpenes, in the autumn is most probably caused by decomposition of fallen needles. The high emissions during spring could be related to onset of growth and the active photosynthesis of the forest floor vegetation, and thus follow similar patterns as earlier found in the Scots pine emissions (Ruuskanen et al., 2005).

Dal Maso et al. (2005) have found aerosol formation and growth events at SMEAR II station occurring more often during spring time and autumn. In the spring, the highest number of events appears in May, which is also the highest number of events of the whole year, while in the autumn most of the peaks took place in September. Factors behind the events are still unclear, but one suggested factor is the biogenic emissions of volatile compounds. Although emissions from trees probably are making up the major proportion of these emissions, a possible contributing source may also be the emissions originating from forest floor vegetation and soil, which were shown to peak at approximately the same time as events in the spring and in the autumn. The role of these emissions in the whole stand annual BVOC budget, and their connections with both physical and biological regulating factors will be clarified in the future work.

REFERENCES

Asensio, D., Peñuelas, J., Filella, I. and Llusià, J. (2007). Online screening of soil VOCs exchange responses to moisture, temperature and root presence. *Plant Soil*, 291: 249–261.

Dal Maso, M., Kulmala, M., Riipinen, I., Wagner, R., Hussein, T., Aalto, P.P. and Lehtinen, K.E.J. (2005). Formation and growth of fresh atmospheric aerosols: eight years of aerosol size distribution data from SMEAR II, Hyytiälä, Finland. *Boreal Environ. Res.*, 10: 323–336.

FAO: Global Forest Resources Assessment, 2000.

Guenther, A., Karl, T., Harley, P., Wiedinmyer, C., Palmer, P.I. and Geron, C. (2006). Estimates of global terrestrial isoprene emissions using MEGAN. *Atmos. Chem. Phys.*, 6: 3181–3210.

Hakola, H., Tarvainen, V., Laurila, T., Hiltunen, V., Hellén, H. and Keronen, P. (2003). Seasonal variation of VOC concentrations above a boreal coniferous forest. *Atmos. Environ.*, 37: 1623–1634.

Hakola, H., Tarvainen, V., Bäck, J., Ranta, H., Bonn, B., Rinne, J., and Kulmala, M. (2006). Seasonal variation of mono- and sesquiterpene emission rates of Scots pine. *Biogeosciences*, 3: 93–101.

Hari, P. and Kulmala, M. (2005). Station for Measuring Ecosystem-Atmosphere relations (SMEAR II). *Boreal Environ. Res.*, 10: 315–322.

Hayward, S., Muncey, R.J., James, A.E., Halsall, C.J. and Hewitt, C.N. (2001). Monoterpene emissions from soil in a Sitka spruce forest. *Atmos. Environ.*, 35: 4081–4087.

Hellén, H., Hakola, H., Pystynen, K.H., Rinne, J. and Haapanala, S. (2006). C_2-C_{10} hydrocarbon emissions from a boreal wetland and forest floor. *Biogeosciences*, 3: 167–174.

Kesselmeier, J. and Staudt, M. (1999). Biogenic Volatile Organic Compounds (VOC): An overview on emission, physiology and ecology. *J. Atmos. Chem.*, 33: 23–88.

Kulmala, M., Hämeri, K., Mäkelä, J.M., Aalto, P.P., Pirjola, L., Väkevä, M., Nilsson, E.D., Koponen, I.K., Buzorius, G., Keronen, P., Rannik, Ü., Laakso, L., Vesala, T., Bigg, K., Seidl, W., Forkel, R., Hoffmann, T., Spanke, J., Janson, R., Shimmo, M., Hansson, H.-C., OʹDowd, C., Becker, E., Paatero, J., Teinilä, K., Hillamo, R., Viisanen, Y., Laaksonen, A., Swietlicki, E., Salm, J., Hari, P., Altimir, N. and Weber, R. (2000). Biogenic aerosol formation in the boreal forest. *Boreal. Environ. Res.*, 5: 281–297.

Leff, J.W. and Fierer, N. (2008). Volatile organic compound (VOC) emissions from soil and litter samples. *Soil Biol. Biochem.*, 40: 1629–1636.

Pihlatie, M., Pumpanen, J., Rinne, J., Ilvesniemi, H., Simojoki, A., Hari, P. and Vesala, T. (2007). Gas concentration driven fluxes of nitrous oxide and carbon dioxide in boreal forest soil. *Tellus*, 59B: 458–469.

Ruuskanen, T.M., Kolari, P., Bäck, J., Kulmala, M., Rinne, J., Hakola, H., Taipale, R., Raivonen, M., Altimir, N. and Hari, P. (2005). On-line field measurements of monoterpene emissions from Scots pine by proton-transfer-reaction mass spectrometry. *Boreal Environ. Res.*, 10: 553–567.

EMISSIONS OF VOLATILE ORGANIC COMPOUNDS FROM SELECTED FUNGAL SPECIES OCCURING IN BOREAL FOREST SOILS

H. AALTONEN[1], J. HEINONSALO[2], J. PUMPANEN[1], H. HELLÉN[3], M, KAJOS[4], R. TAIPALE[4] and J. BÄCK[1]

[1]Department of Forest Ecology, P.O. Box 27, 00014 University of Helsinki, Finland
[2]Department of Applied Chemistry and Microbiology, P.O. Box 27, 00014 University of Helsinki, Finland
[3]Finnish Meteorological Institute, P.O. Box 503, 00101 Helsinki, Finland
[4]Department of Physics, P.O. Box 64, 00014 University of Helsinki, Finland

Keyvords: Biogenic volatile organic compounds, fungi, decomposer, boreal soil

INTRODUCTION

Biogenic volatile organic compounds (BVOCs) are produced and emitted by many plants and microbes, and from all plant organs including flowers, leaves, stems and roots. Several studies show that also soil is a source of BVOC in forest ecosystems (Hayward et al., 2001; Hellén et al., 2006; Janson et al., 1999). Soil emissions show strong seasonal variation; the forest floor acted as a significant source of monoterpenes in spring and autumn, but less so in midsummer (Hellen et al., 2006, Aaltonen et al., manuscript). This seasonality may be partially related to changes in biological activity in the soil, which is affected by the plant activity, amount of substrates for decomposing organisms in the soil, soil temperature and water content (Davidson et al., 1998). A large proportion of the carbon bound in the photosynthesis is recycled quickly back to the atmosphere through root exudates (Högberg and Read, 2006), which are rapidly decomposing organic substances leaching out of the roots. They are also used as substrates for root associated mycorrhiza and bacteria. More detailed understanding of the processes underlying these events is needed for predicting the temporal pattern and magnitude of BVOC emissions from forest soils.

Some studies show that most of the soil BVOC emissions originate from decomposing organic matter and plant roots (Hayward et al., 2001; Asensio et al., 2008; Leff and Fierer, 2008). Therefore the amount and quality of soil organic matter plays a crucial role in the formation of BVOCs. Some evidence that monoterpene concentrations are higher in the vicinity of the tree trunk compared to further distance from the tree has been found (Lin et al., 2007; Owen et al., 2007). The high concentrations close to tree trunks can be related either to the amount of leaf and root litter in the soil or to the actual source of volatiles from rhizosphere.

However, soil microbial activity may also contribute significantly to the BVOCs emitted from soil. Soil microbial activity was correlated with net rates of BVOC emissions over a range of different forest soils (Asensio et al., 2007; Leff and Fierer, 2008). By comparing the composition of deciduous leaf litter and intact leaves, Isidorov and Jdanova (2002) suggested that most of the volatile compounds (especially terpenes) found in litter were in fact originating from decomposers. On the other hand, soil microbial community may also act as a sink for many volatile components (e.g. Owen et al., 2007; Smolander et al., 2006), and the gross rates of microbial BVOC production may in fact be considerably higher than the net rates measured.

Multi-trophic interactions mediated by microbially produced BVOCs have proven to be widespread in soils, and the outcome of these interactions is greatly depending on the species composition of the micro-organisms involved (Mackie and Wheatley, 1999). The volatile organic compounds in soil act as info chemicals in plant-insect interactions, between plant individuals and between plants and soil microbial community (Asensio et al., 2008). Small organic volatile compounds emitted from bacterial antagonists can also have allelopathic effects, influencing negatively the mycelial growth of the soil-borne phytopathogenic fungi (Kai et al., 2007). Recently, the production of BVOCs has been studied in relation

to ectomycorrhiza formation and signaling by *Tuber borchii* and other *Tuber* species (Menotta et al., 2004; Zeppa et al., 2004; Splivallo et al., 2007).

We hypothesized that the soil fungi are significant contributors to the BVOCs in the soil. Therefore we aimed at characterizing the blend of volatile organic compounds emitted by decomposing, ectomycorrhizal and endophytic fungi. Moreover, we estimated what are the biomass-specific emissions of BVOCs by these different fungal species in pure cultures under laboratory conditions. This information can be valuable when estimating the contribution of soil biological activity on stand scale emissions of BVOCs.

METHODS

A collection of eight fungal isolates belonging to different functional groups (root-endophytic: *Phialocephala fortinii*, *Meliniomyces variabilis*; wood decomposer: *Ophiostoma abietinum*, *Gymnopilus penetrans*; ectomycorrhiza: *Piloderma olivaceum*, *Cenococcum geophilum*) were used in this study. All fungal isolates were originally isolated from *Pinus sylvestris* L. ectomycorrhizal root tips growing in Finnish podzol soil (see Heinonsalo et al., 2007). For the BVOC analysis, the fungal cultures were grown in 250 mL flasks with 100 mL LN-AS (low-nitrogen AS) media (Hakala et al., 2006) in axenic conditions for one month. During the BVOC measurements, the flasks were closed with glass plugs with lead-ins for ingoing and for outcoming gas flow. Liquid growth media with and without pieces of inoculum agar were used as controls in BVOC measurements.

The measurements were conducted under room temperature in a well ventilated laboratory room. Bottles with fungal cultures were flushed with a room air, which was treated in a zero-air generator to remove all organic components. Zero air concentrations were measured after every three sample measurements and subtracted from the results. The liquid cultures were mixed with a magnetic stirrer and their temperature was kept at 20°C. The outgoing air was diverted into two flows: one was directed into the proton transfer reaction mass spectrometer (PTR-MS), and another one to a stainless steel tube filled with TENAX-TA adsorbent. One bottle was sampled for one hour. The measurements with PTR-MS were done with calibrated masses yielding quantitative emission rate values. Additional measurements were done by scanning all the masses between 30 and 250 amu. Each bottle was sampled three times and the average of these measurements was used for subsequent calculations. The chemical speciation of emissions was done from the adsorbent samples, which were analyzed with GC-MS as described by Hakola et al. (2006).

RESULTS

All fungi were grown in similar conditions, which might have been less optimal for some species. To avoid errors arising from variable growth rates, we grew the fungal cultures between 25 and 40 days, but still their biomasses varied from 0.01 to 0.15 g (DW). Considerably high variations were observed in emission rates, part of which may be due to the variations in growth rates.

All studied fungal species emitted some BVOCs although the emitted spectrum and quantities differed between species. Variation within a functional group was highest in decomposers. The GC-MS measurements showed that most of the fungi emitted limonene (average emission rate 12 ng g^{-1} h^{-1}), but significant quantities of other monoterpenes were emitted only from one species, *M. variabilis* (endophyte). The most abundant sesquiterpene in emissions was α-humulene, which was emitted by four fungal species, on average the emission rate was 2 ng g^{-1} h^{-1}. Large linalool emissions (up to 1.2 µg g^{-1} h^{-1}) were measured from *G. penetrans* (decomposer) and *P. olivaceum* (ectomycorrhiza). Clear emissions of benzene were also detected from all the species except *M. variabilis* and *O. abietinum*, emissions of *P. olivaceum* reaching 700 ng g^{-1} h^{-1}.

In the PTR-MS measurements the M69 (isoprene) and M137 (monoterpene) emission rates varied greatly between species (Fig 1a). Emissions of methyl vinyl ketone/methacrolein (M71) and methyl ethyl ketone

(M73) were also measured in all fungi (Fig 1b). M59 (acetone) was emitted by *G. penetrans*, *P. olivaceum* and *C. geophilum* in much higher quantities than by the other species. The maximum M59 emissions (1883 μg g^{-1} h^{-1}) were measured from *P. olivaceum* cultures. Emissions of M45 (acetaldehyde) were highest in *P. fortinii* cultures (100 μg g^{-1} h^{-1}).
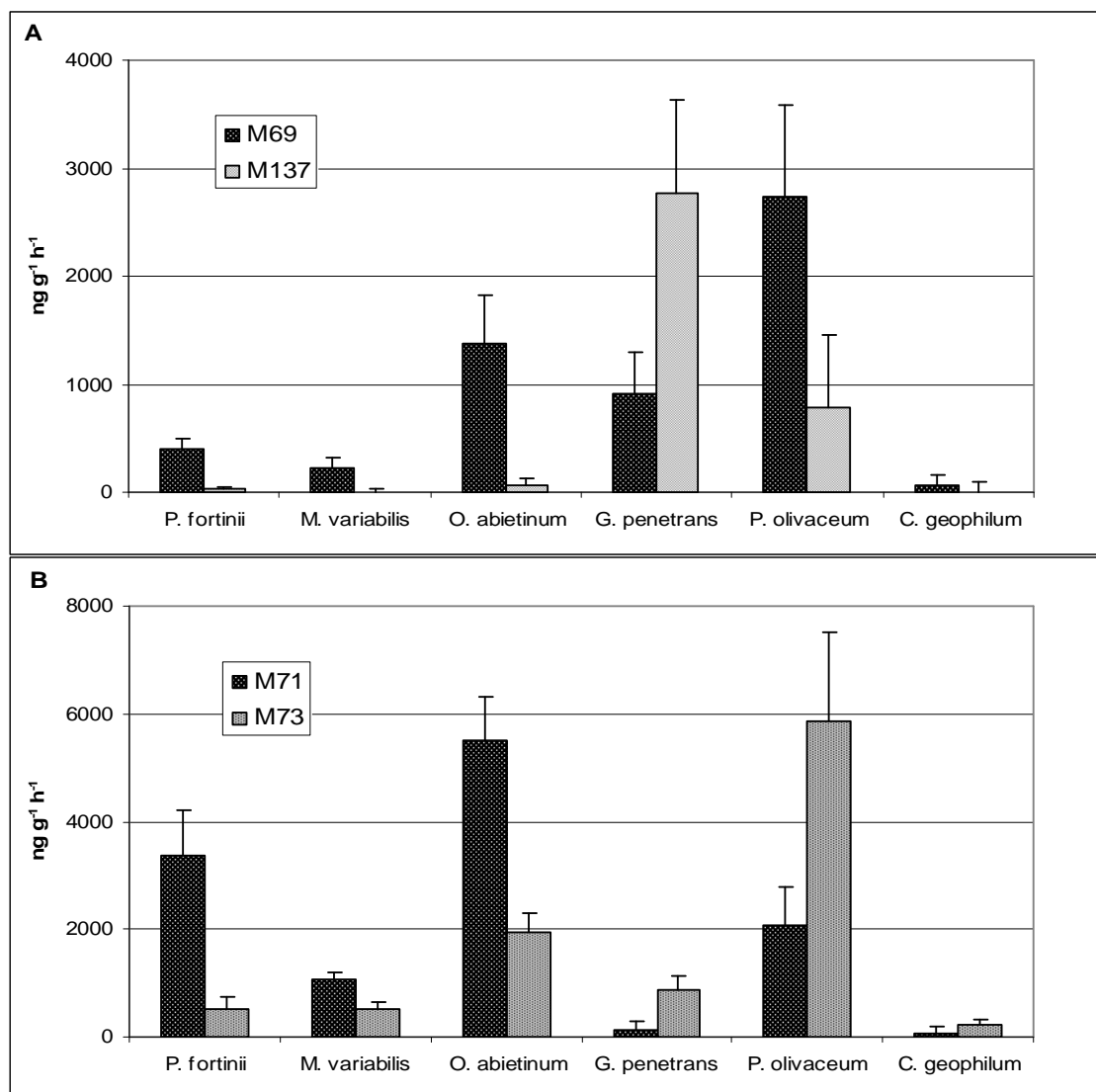
Figure 1. A) Emissions of M69 (isoprene), M137 (monoterpenes), and B) M71 (MACR+MVK) and M73 (MEK) measured with PTR-MS. Error bars show standard error of mean between replicate bottles (n=3).

Significant emissions were also detected in M79 (benzene), M101 (hexanal) (Fig 2.), and M129 (tentatively octanal).
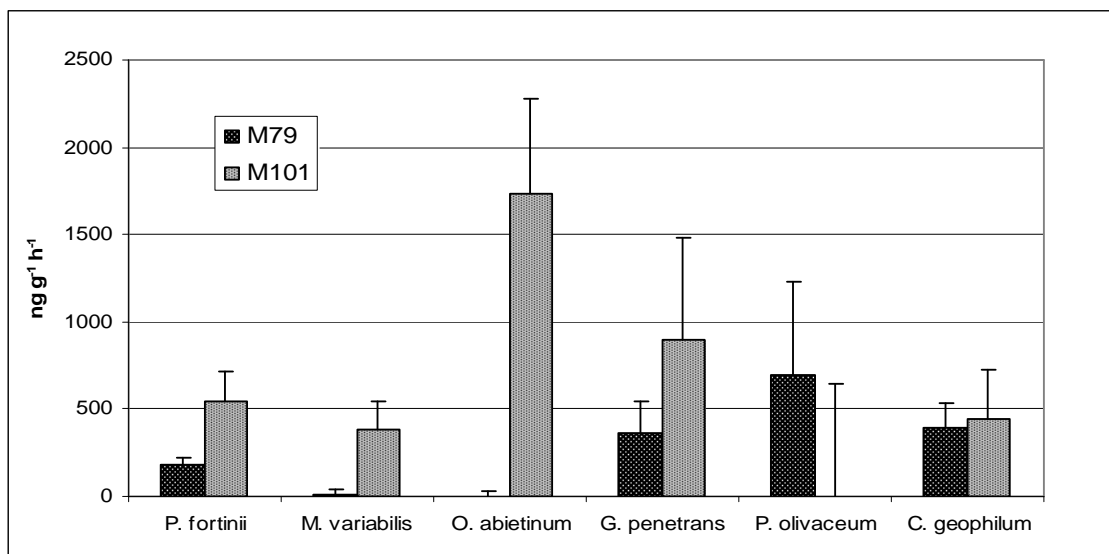
Figure 2. Emissions of M79 (benzene) and M101 (hexanal), measured with PTR-MS. Error bars show standard error of mean between replicate bottles (n=3).

We also measured emissions in all 216 masses between M30-M250, in order to see if some yet unknown compounds would be emitted by the fungi. Results of these measurements are indicative and not comparable with the calibrated masses, even though they usually support the former. Emissions of masses M60, M43, M77, and M65 were the highest, thus containing also unidentified masses.

CONCLUSIONS

Our laboratory measurements showed that soil-originating fungi can produce significant quantities of volatile compounds. The main emissions were carbonyl compounds, but also mono- and sesquiterpene emissions were measured from all studied species. Their emissions can be of similar magnitude or even higher than those from green plants, e.g. from Scots pine branches in boreal areas. Estimates on ecosystem BVOC fluxes have generally concentrated on evaluating the processes above ground, although belowground processes may significantly influence the total quantities and the chemical composition of fluxes (e.g. Asensio et al., 2007). Taking into account the high biomass of fungal hyphae in boreal soils, estimated to be several tens of grams per square metre (Wallander et al., 2001), these emissions can be responsible for a large proportion of the stand scale BVOC budget. However, the contribution of soils to global biogenic BVOC emissions is still poorly known, compared to the knowledge of other atmospheric trace gases such as CO_2 (Guenther et al. 2006).

Emissions of benzene and other aromatic compounds were seen with both PTR-MS and GC-MS. Recently also Leff and Fierer (2008) measured benzene and naphthalene emissions from litter samples. They have earlier been connected only to anthropogenic sources, but these results indicate that at least under some conditions these compounds can be emitted from biogenic sources.

The processes and regulating factors of soil BVOC emissions can differ from those of plants. Mycorrhizal roots show strong stimulation of genes involved in the monoterpene synthesis (Walter et al., 2002). Many agricultural plant roots are known to possess the capability to produce terpenoids as antimicrobials for defense purposes (Bais et al., 2004). Plant growth promoting bacteria emit BVOCs that are involved in induced systemic tolerance of plant roots to abiotic factors such as drought or salt stress (Yang et al., 2008). In addition to the biogenic volatiles, some BVOCs at soil surface layers may be related to abiotic processes such as decay of dead plant material, e.g. perennial litter or senescent annual plants (Warneke et al., 1999). Soil BVOCs may also influence plant growth via nitrification, nitrogen mineralization and

oxidation of methane (Bending & Lincoln, 2000; Paavolainen et al., 1998; Farag et al., 2006), and are thus important in respect of total ecosystem fluxes of several important greenhouse gases.

REFERENCES

Aaltonen, H., Pumpanen, J., Pihlatie, M., Hakola, H., Hellén, H. and Bäck, J. Emissions of biogenic volatile organic compounds from boreal Scots pine forest floor. Manuscript.

Asensio, D., Peñuelas, J., Ogaya, R. and Llusià, J. (2007). Seasonal soil VOC exchange rates in a Mediterranean holm oak forest and their responses to drought conditions. *Atmos. Environ.*, 41: 2456–2466.

Asensio, D., Owen, S.M. Llusià, J. and Peñuelas, J. (2008). The distribution of volatile isoprenoids in the soil horizons around Pinus halepensis trees. *Soil Biol. Biochem.*, 40: 2937–2947.

Bais, H.P., Park, S.-W., Weir, T.L., Callaway, R.M. and Vivanco, J.M. (2004). How plants communicate using the underground information superhighway. *Trends Plant Sci.*, 9: 26–32.

Bending, G.D. and Lincoln, S.D. (2000). Inhibition of soil nitrifying bacteria communities and their activities by glucosinolate hydrolysis products. *Soil Biol. & Biochem.*, 32: 1261–1269.

Davidson, E.A., Belk, E. and Boone. R.D. (1998). Soil water content and temperature as independent or confounded factors controlling soil respiration in a temperate mixed hardwood forest. *Glob. Change Biol.*, 4: 217–227.

Farag, M.A., Ryu, C.M., Sumner, L.W. and Pare, P.W. (2006). GC-MS SPME profiling of rhizobacterial volatiles reveals prospective inducers of growth promotion and induced systemic resistance in plants. *Phytochem.*, 67: 2262–2268.

Guenther, A., Karl, T., Harley, P., Wiedinmyer, C., Palmer, P.I. and Geron, C. (2006). Estimates of global terrestrial isoprene emissions using MEGAN (Model of Emissions of Gases and Aerosols from Nature). *Atmos. Chem. Phys.*, 6: 3181–3210.

Hakala, T.K., Hildén, K., Maijala, P., Olsson, C. and Hatakka, A. (2006). Different regulation of manganese peroxidases and characterization of two variable MnP encoding genes in the white-rot fungus *Physisporinus rivulosus. Appl. Microbiol. Biot.*, 73: 839–849.

Hakola, H., Tarvainen, V., Bäck, J., Ranta, H., Bonn, B., Rinne, J. and Kulmala, M. (2006). Seasonal variation of mono- and sesquiterpene emission rates of Scots pine. *Biogeosciences*, 3: 93–101.

Hayward, S., Muncey, R.J., James, A.E., Halsall, C.J. and Hewitt, C.N. (2001). Monoterpene emissions from soil in a Sitka spruce forest. *Atmos. Environ.*, 35: 4081–4087.

Heinonsalo, J., Koskiahde, I. and Sen, R. (2007). Scots pine bait seedling performance and root colonizing ectomycorrhizal fungal community dynamics before and during the 4 years after forest clear-cut logging. *Can. J. Forest Res.*, 37: 415–429.

Hellén, H., Hakola, H., Pystynen, K.H., Rinne, J. and Haapanala, S. (2006). C_2-C_{10} hydrocarbon emissions from a boreal wetland and forest floor. *Biogeosciences*, 3: 167–174.

Högberg, P. and Read, D.J. (2006). Towards a more plant physiological perspective on soil ecology. *Trends Ecol Evol.*, 21(10): 548–554.

Isidorov, V. and Jdanova, M. (2002). Volatile organic compound from leaves litter. *Chemosphere*, 48: 975–979.

Janson, R., De Serves, C. and Romero, R. (1999). Emission of isoprene and carbonyl compounds from a boreal forest and wetland in Sweden. *Agr. Forest Meteorol.*, 98–99: 671–681.

Kai, M., Effmert, U., Berg, G. and Piechulla, B. (2007). Volatiles of bacterial antagonists inhibit mycelial growth of the plant pathogen Rhizoctonia solani. *Arch. Microbiol.*, 187: 351–360.

Leff, J.W. and Fierer, N. (2008). Volatile organic compound (VOC) emissions from soil and litter samples. *Soil Biol. Biochem.*, 40: 1629–1636.

Lin, C., Owen, S.M. and Peñuelas, J. (2007). Volatile organic compounds in the roots and rhizosphere of Pinus spp. *Soil Biol. Biochem.*, 39: 951–960.

Mackie, A.E. and Wheatley, R.E. (1999). Effects and incidence of volatile organic compound interactions between soil bacterial and fungal isolates. *Soil Biol. Biochem.*, 31: 375–385.

Menotta, M., Gioacchini, A.M., Amicucci, A., Buffalini, M., Sisti, D. and Stocchi, V. (2004). Headspace solid-phase microextraction with gas chromatography and mass spectrometry in the investigation of volatile organic compounds in an ectomycorrhizae synthesis system. *Rapid Commun. Mass Sp.*, 18: 206–210.

Owen, S.M., Clark, S., Pompe, M. and Semple, K.T. (2007). Biogenic volatile organic compounds as potential carbon sources for microbial communities in soil from the rhizosphere of Populus tremula. *FEMS Microbiol. Lett.*, 268: 34–39.

Paavolainen, L., Kitunen, V., Smolander, A., 1998. Inhibition of nitrification in forest soil by monoterpenes. *Plant Soil*, 205: 147–154.

Smolander, A., Ketola, R.A., Kotiaho, T., Kanerva, S., Suominen, K., and Kitunen, V. (2006). Volatile monoterpenes in soil atmosphere under birch and conifers: Effects on soil N transformations. *Soil Biol. Biochem.*, 38: 3436–3442.

Splivallo, R., Novero, M., Bertea, C.M., Bossi, S. and Bonfante, P. (2007). Truffle volatiles inhibit growth and induce an oxidative burst in Arabidopsis thaliana. *New Phytol*, 175: 417–424.

Wallander, H., Nilsson, L.O., Hagerberg, D. and Bååth, E. (2001). Estimation of the biomass and seasonal growth of external mycelium of ectomycorrhizal fungi in the field. *New Phytol*, 151: 753–760.

Walter, M.H., Hans, J. and Strack, D. (2002). Two distantly related genes encoding 1-deoxy-D-xylulose 5-phosphate synthases: differential regulation in shoots and apocarotenoid-accumulating mycorrhizal roots. *Plant J.*, 31(3): 243–254.

Warneke, C., Karl, T., Judmaier, H., Hansel, A., Jordan, A., Lindinger, W. And Crutzen, PJ. (1999). Acetone, methanol, and other partially oxidized volatile organic emissions from dead plant matter by abiological processes: Significance for atmospheric HOx chemistry. *Global Biogeochem. Cy.* 13(1): 9–17.

Yang J., Kloepper J.W. and Ryu C-M. (2008) Rhizosphere bacteria help plants tolerate abiotic stress. Trends in Plant Sci. 14: 1-4.

Zeppa, S., Gioacchini, A.M., Guidi, C., Guescini, M., Pierleoni, R., Zambonelli, A. and Stocchi, V. (2004). Determination of specific volatile organic compounds synthesised during Tuber borchii fruit body development by solid-phase microextraction and gas chromatography/mass spectrometry. *Rapid Commun. Mass Sp.*, 18: 199–205.

DIURNAL VARIATION OF AOD AT AN ANTARCTIC COASTAL SITE

V. AALTONEN[1], G. de LEEUW[1,2], A. AROLA[1], M. GINZBURG[3], M. KULMALA[2]

[1]Finnish Meteorological Institute, P. O. Box 503, 00101 Helsinki, Finland
[2]Department of Physics, P.O. Box 64, FI-00014, University of Helsinki, Finland
[3]Servicio Meteorológico Nacional, 25 de mayo 658, Buenos Aires, Argentina

INTRODUCTION

Aerosol optical depth (AOD) is a columnar measure of aerosol load which combines the effects of scattering and absorption of radiation by aerosols. Governing the direct shortwave radiative forcing, it is an important parameter in air pollution, atmospheric radiation and climatology fields. Ground-based AOD measurements are also important to validate the satellite aerosol retrieval. The diurnal variability of the AOD is usually credible when carried out at dry continental areas (Smirnov et al., 2002a) but become more doubtful when made at maritime environments (Smirnov et al., 2002b), especially at clean Antarctic conditions (Six et al., 2005). The dynamics of the marine boundary layer might affect on the signal of the spectral irradiance measured with the sunphotometer. Secondly, measuring near the lower limit of the instrument detection range may increase the total error. Even small errors made with the instrument calibration remarkably affects on the AOD retrieval. Diffuse irradiance entering the instrument's field of view emerges at low sun elevation angles typical to polar sites (Arola and Koskela, 2004). Measurement set up might also give an artefact on the AOD. All these various factors should be considered when making the analysis based on the AOD data. There have been studies where a convex diurnal AOD pattern has interpreted as a result of overestimated calibration constants, and a correction methods has been presented to smooth the measured AOD pattern (Cachorro et al., 2004; Cachorro et al., 2008). In this study, we will show the diurnal behaviour of the AOD from an Antarctic coastal site and discuss the possible reasons of the measured AOD.

The measurement site is located at Marambio meteorological station (64.24°S, 56.62°W, 205 m asl), in the northern corner of Seamour Island, about 90 km E from the eastern coast of the Antarctic Peninsula and about 900 km SE from Tierra del Fuego. The Marambio base has a permafrost ground. In summer when the sun is high enough for AOD measurements, the surface of the active layer is usually without snow, mostly consisting of clay. The sunphotometer used in this study was a Precision Filter Radiometer (PFR, PMOD/WRC, Switzerland), serial N-29, attached on a Kipp&Zonen 2AP Gear Drive suntracker. The PFR has four separate channels, 368, 412, 500, and 862 nm with 5 nm FWHM bandwidth and a full field of view angle of 2.5°. The instrument is described in detail in Wehrli (2000).

METHODS

The data used in this study was obtained between January 2005 and March 2009. We selected the days with 500 nm irradiance signal indicating clear sky conditions for most of the day to get a clear picture of the behaviour on the both sides of the solar noon. To keep the number of clear sky data as high as possible and thus giving more information for the analysis, automatic cloud screening algorithm was avoided. Instead, a careful manual screening based on visual inspection was performed to remove the remaining cloud contaminated data. The inspected data period had 17 clear sky days (see Table 1). Days with clear sky conditions only either in the morning or afternoon (N=39) were not inspected because there will be a risk for making wrong deductions due to the lack of data at both sides of the solar noon.

Supporting parameters include Ångström alpha calculated using a linear fit over all four AOD channels and data from meteorological measurements as atmospheric pressure, ambient temperature, relative humidity, wind speed and wind direction.

Austral summer period	Number of clear sky days
2004-2005	2
2005-2006	7
2006-2007	(maintenance)
2007-2008	2
2008-2009	6

Table 1. Number of the clear sky days during the austral summer periods.

RESULTS

From the total of 17 cloud free days, there were 13 occurrences with AOD at all four wavelengths having a clear convex pattern. In 9 of these 13 cases, the AOD maximum occurred within half an hour related to the solar noon. The maximum value of the AOD at 500 nm of the days with convex pattern varied between 0.034 and 0.1951. In general, the maximum AOD values at 500 nm were 0.4 – 7 times higher than the minimum values of the corresponding day. The difference between minimum and maximum of AOD is higher in austral summer than soon in spring, although this does not apply later in spring.
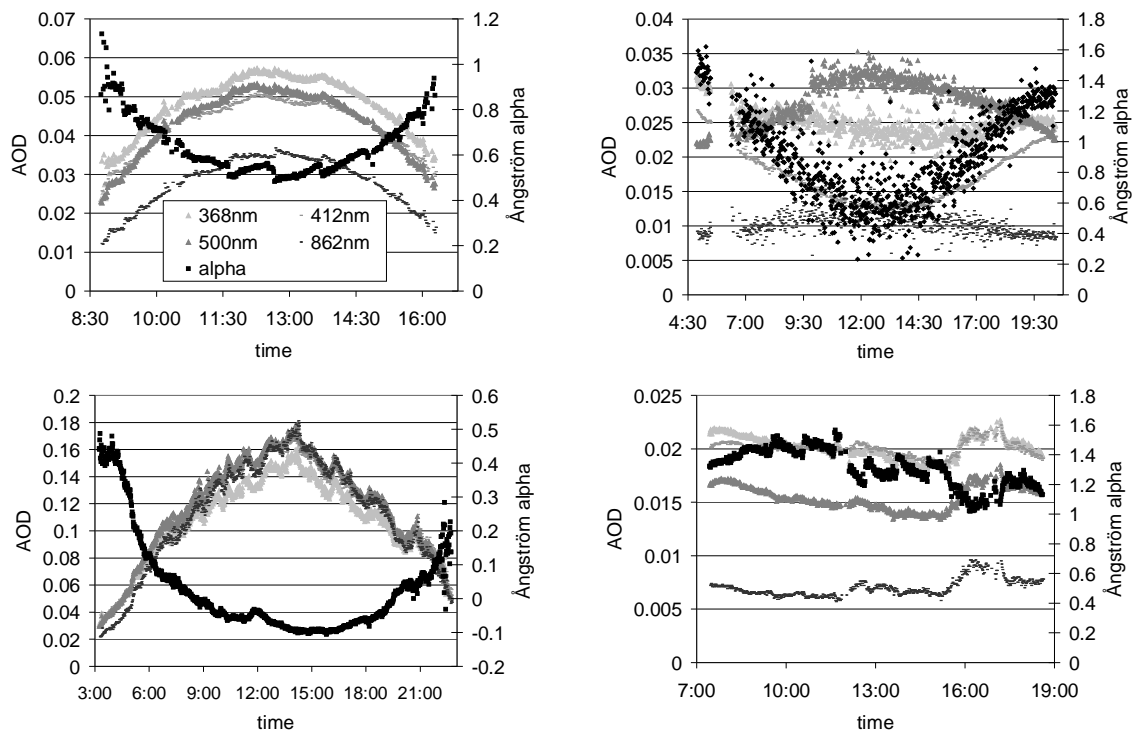
Figure 1. AOD and Ångström alpha obtained on 2005-04-21 (top left), 2007-11-12 (top right), 2008-12-19 (bottom left) and 2009-03-13 (bottom right) at Marambio station. AODs at 368 (light triangles), 412 (light lines), 500 (dark triangles) and 862 nm (dark lines) are shown with Ångström alpha (shown in black squares).

Figure 1 shows examples of the diurnal variation of AOD and the Ångström alpha. Situation on 2005-04-21 was a typical example of the diurnal AOD pattern. The signals of 412 and 500 nm channels are crossing each other both in the morning and afternoon. During that day, both ambient temperature and RH were rising, getting their maximum values afternoon. Since optical properties, especially scattering, is highly sensitive to RH, the convex pattern is likely due to the enhanced scattering. The average particle size is larger at noon and early in the afternoon, which can be seen from the minimum in the Ångström alpha.

2007-11-12 is a rare case where the signals at the wavelengths of 500 and 862 nm are convex whereas the other two wavelengths have a concave pattern. The resulting Ångström alpha is still concave. During that day, the ambient temperature and pressure are increasing. RH in turn is first increasing very rapidly, then decreases towards noon and then increases again.

On 2008-12-19, AOD at wavelengths are very near to each other. Furthermore, AOD at UV and IR channels were strangely crossing each other two times during the day. Contrary to what is expected, highest AOD is obtained at 862 nm channel. Since the Ångström alpha remains below 0.5 during the whole day, with the minimum value being below zero, large particles are prevailing. RH decreases towards noon and increases again after that. On the contrary, ambient temperature is rising with the AOD during the morning.

2009-03-13 is a rare exception with no clear variation in both AOD and Ångström alpha. Large alpha (maximum value 1.57) untypical to this site reveals the presence of fine particles during that day. The ambient temperature increases before sunrise, and starts to decrease after that very rapidly. This likely prevents the humid layer to rise above the station. Atmospheric pressure during that day was untypically low, being around 950 hPa.

CONCLUSIONS

The diurnal AOD patterns of the clear-sky days differ remarkably from those measured at Finnish AOD stations, but are not rare at other Antarctic stations (Virkkula and Vitale, personal communication). Systematic investigation of the meteorological parameters is needed to understand phenomena influencing the daily variation. Particle measurements would give useful support for the analysis but they are not performed at the Marambio station. We are continuing the current study with examining trajectory paths and overall meteorological situation prevailing over the Antarctic Peninsula.

ACKNOWLEDGEMENTS

REFERENCES

Arola, A. and Koskela, T. (2004) On the sources of bias in aerosol optical depth retrieval in the UV range. *J. Geophys. Res.* 109, D08209, doi:10.1029/2003JD004375.

Six., D., Fily, M., Blarel., L., and Goloub., P. (2005) First aerosol optical thickness measurements at Dome C (East Antarctica), summer season 2003-2004, *Atmos. Environ.* 39, 5041-5050.

Smirnov., A., Holben., B. N., Eck, T. F., Slutsker, I., Chatenet., B., and Pinker., R. T. (2002a) Diurnal variability of aerosol optical depth observed at AERONET (Aerosol Robotic Network) sites. *Geophys. Res. Lett.*, 29(23), 2115,, doi:10.1029/2002GL016305, 2002.

Smirnov, A., Holben, B. N., Kaufman, Y. J., Dubovik, Ol, Eck, T. F., Slutsker, I., Pietras, C., and Halthore R. N. (2002b) Optical properties of Atmospheric Aerosol in Maritime Environments, *J. Atmos. Sci.* 59, 501-523.

Cachorro, V. E., Romero, P. M., Toledano, C., Cuevas, E. and de Frutos, A. M. (2004) The fictitious diurnal cycle of aerosol optical depth: A new approach for "in situ" calibration and correction of AOD data series. *Geophys. Res. Lett.* 31, L12106, doi:10.1029/2004GL019651, 2004

Cachorro, V. E., Toledano, C., Sorribas, M., Berjón, A., de Frutos., A. M., and Laulainen, N. (2008) An "in situ" calibration-corrected procedure (KCICLO) based on AOD diurnal cycle: Comparative results between AERONET and reprocessed (KCICLO method) AOD-alpha data series at El Arenosillo, Spain. *J. Geophys. Res.* 113, D02207, doi:10.1029/2007JD009001.

Wehrli, C. (2000) Calibrations of Filter Radiometers for Determination of Atmospheric Optical Depth, Metrologia 37, 419-422.

Carbon sequestration and water-use of agroforestry systems across the Sudanese gum belt

Syed Ashraful Alam, Mike Starr and Eero Nikinmaa

Department of Forest Ecology, University of Helsinki, Finland

Traditional agroforestry systems in drylands[1] are characterized by high levels of biodiversity (Nair, 1993). Agroforestry systems provide various ecosystem services (Fig. 1) to the community, including prevention of excessive erosion and rehabilitation of already degraded lands (Sharawi, 1986). UNEP (1992) classified about 47 % of the earth's surface or about 6.15 billion hectares as drylands. The huge extent of drylands offer considerable potential for C sequestration (FAO, 2004). This potential, however, is largely constrained by water scarcity. Increasing C sequestration can contribute to the mitigation and restoration of degraded drylands through including nutrient and soil water retention, and through promoting infiltration rather than surface runoff generation.

Agro-ecosystems play a central role in the global C cycle and account for approximately 12 % of the world terrestrial C (Dixon, 1995). Soil degradation as a result of land-use change has been one of the major causes of C loss and CO_2 emissions to the atmosphere. Agroforestry may involve practices, including shifting cultivation, pasture management by burning, paddy cultivation, N fertilization and animal production, which favour the emission of GHGs. On the other hand, trees growing in agroforestry systems can capture and store considerable amounts of C in plant biomass and soils (Albrecht and Kandji, 2003; Dixon, 1995). Several studies have revealed that the inclusion of trees in the agricultural systems often improves the land cover and productivity, and makes such systems sinks for atmospheric C (Winjum et al., 1992; Dixon, 1995).

In agroforestry systems, C sequestration is a dynamic process that can be divided into two phases. At the stage of establishment, when the land is prepared for cultivation, many systems are likely to be sources of GHGs (loss of C and N from vegetation and soil). Then follows a quick accumulation phase and a maturation period where C is stored in the boles, stems, roots of trees and in the soil. At the end of the rotation period, when the trees are harvested and the land returned to cropping (sequential systems), part of the C will be released back to the atmosphere (Dixon, 1995). Thus, sequestration can only be considered effective if there is a positive net C balance from an initial stock after a few decades (Feller et al., 2001).

---

[1] Dryland ecosystems are defined as regions in which the ratio of total annual precipitation to potential evapotranspiration (P:PET or the Aridity Index, AI) ranges from 0.05 to 0.65, and include dry sub-humid regions (AI = 0.50-0.65) covering 9.9%; semi-arid regions (AI = 0.20-0.50) covering 17.7%; arid regions (AI = 0.05-0.20) covering 12%; hyperarid regions (AI = < 0.05) covering 7.5% of the earth's land area (Glenn et al., 1993; Lal, 2004).
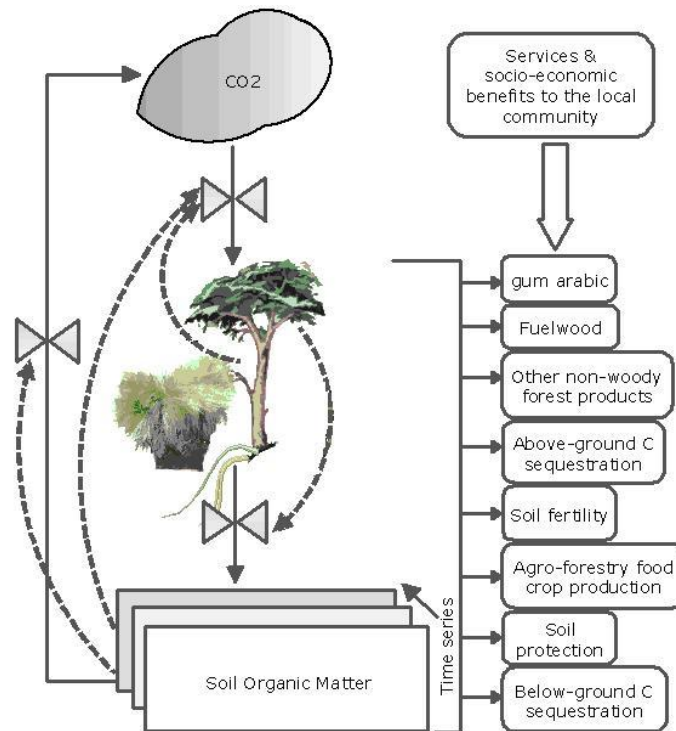
Figure 1: *Acacia senegal* based dryland agroforestry model and its services to the community

In drylands, water scarcity constrains plant productivity severely and hence affects the accumulation of C in biomass and soils. This is partially compensated by the high allocation of plant-accumulated biomass to below ground compared to more moist areas. Low and erratic rainfall exacerbate the C accumulation problem substantially. The soil organic carbon (SOC) pool tends to decrease exponentially with temperature. Dryland soils are also prone to degradation and desertification, which lead to dramatic reductions in the SOC pool. Consequently, soils of drylands contain small amounts of C ($<1\%$). However, there are also some aspects of dryland soils that favour C sequestration. Dry soils are less likely to lose C than wet soils as the lack of water limits mineralization and therefore the flux of C to the atmosphere. Consequently, the residence time of C in drylands soils is long, sometimes even longer than in forest soils. Although the rate of C sequestration is low, there are considerable benefits related to soil improvement and restoration for people living in these areas. Squires (1998) and Lal (2001) estimated the attainable C sink in drylands to be 1.0-1.9 Pg C/yr over the next 25-50 years. In addition to the removal of atmospheric CO_2, increasing SOC in semi-arid environments is socio-economically appropriate and beneficial for food production and erosion control (Ardö and Olsson, 2004). Furthermore, C sequestration in dryland soils would provide financial security for the agro-forestry entrepreneurs under the clean development mechanism (CDM) of the Kyoto protocol.

In order to assess the value of including tree species in agroforestry systems we have studied C sequestration and water use of woodlands across the "gum belt" of Sudan. Agroforestry has been practiced in Sudan for a long time and in various forms. Farmers used to practice traditional bush-fallow systems[2] in sequential phases of crops and trees where land is not a constraint (Elsiddig,

---

[2] Bush-fallow system is Sudan's age-old traditional farming system, in which sequential agricultural cropping and forest regeneration is adopted. At the end of the forest rotation (the bush period), the land is cleared for agricultural cropping.

2002). The *Acacia senegal* based agroforestry system is considered one of the most successful ways of natural forest management in tropical drylands, especially in the Sudan. This agroforestry system is regarded as environmentally sound (restoring soil fertility), economically sustainable (source of income) and socially acceptable (promotes gum arabic production) (Fries, 1990). *A. senegal* is the main source of gum arabic, a worldwide cash crop, and source of fuelwood for household consumption and sale (Sharawi, 1986).

The study follows linked modelling approach (Fig. 2) and will estimate C pools and fluxes in both above- and below-ground biomass and soil. We derived C pools in forest biomass and soil (0-1 m) using spatially distributed aggregated forest inventory data collected by Forest National Corporation of Sudan and soil data from the Harmonized World Soil Database, HWSD (FAO, 2009). Average stem volume per ha values were calculated for 1:250000 Satellite Map Sheet Series of Sudan (Fig. 3) using data from inventory plots on a 10 x 10 km grid. Stem volume per ha values were converted into C pools using a wood density value of 0.65 t dm m^{-3} and C content of 50 %. Soil C pools will be calculated for sandy soils (mainly Arenosols) and clay soils (mainly Vertisols and Regosols) using C %, bulk density and depth values available for HWSD mapped soil units. The spatial pattern of current biomass and soil C pools will be evaluated in relation to location and soil type.

To determine the water use (actual evapotranspiration) and water use efficiency (WUE, mm H_2O used per kg biomass C/ha) we will use a monthly water balance model, WATBAL (Starr, 1999). The required soil hydraulic properties, field capacity and permanent wilting point, will be calculated using soil texture data (HWSD) and published pedotransfer functions. Necessary climate data (rainfall, temperature and sunshine hours) will be derived for each map sheet using the local climate estimator, LocClim (FAO, 2005). Once the WATBAL model has been calibrated, we intend to look at the impacts of a number of climate change scenarios on water use and availability using simulated climate change data.

Depending on the land fertility and crop production; agricultural cropping may continue for 5-7 years before the land has to be abandoned for another rotation of forest cover (Elsiddig, 2002).

Stand data (Sudan NFI, 1998)	Soil data (HWSD)	Meteorological daily data (LocClim)

Stand data (Sudan NFI, 1998)

- Map sheet Coordinates, elevation
- Map sheet area (*.shp file by Gis Analysis) as per GMU
- Land use, land cover types (100 ha), avg. crown closure % (100 ha), Avg. volume (m³/ha)

Soil data (HWSD)

- 0-30 cm, 30-100 cm
  - % C^*, % N
  - Texture, BD

Soil hydraulic properties (PTFs)

- θ_{fc}, θ_{pwp}

Meteorological daily data (LocClim)

- Rainfall
- Temperature
- Cloud cover (1-Sunshine fraction)
- PET (calibration)

Carbon sequestration, g C m⁻²

- Biomass pool (above & below ground)
- Soil pool (0-100 cm)
- http://www.haberlah.com/gras/250741.htm

Water balance (WATBAL)

- Rooting depth, Crop coefficient (K)
- Daily water demand (PET), water use (AET)
- Water use efficiency, mm H₂0 per kg C

Figure 2. Research methods-linked modelling approach
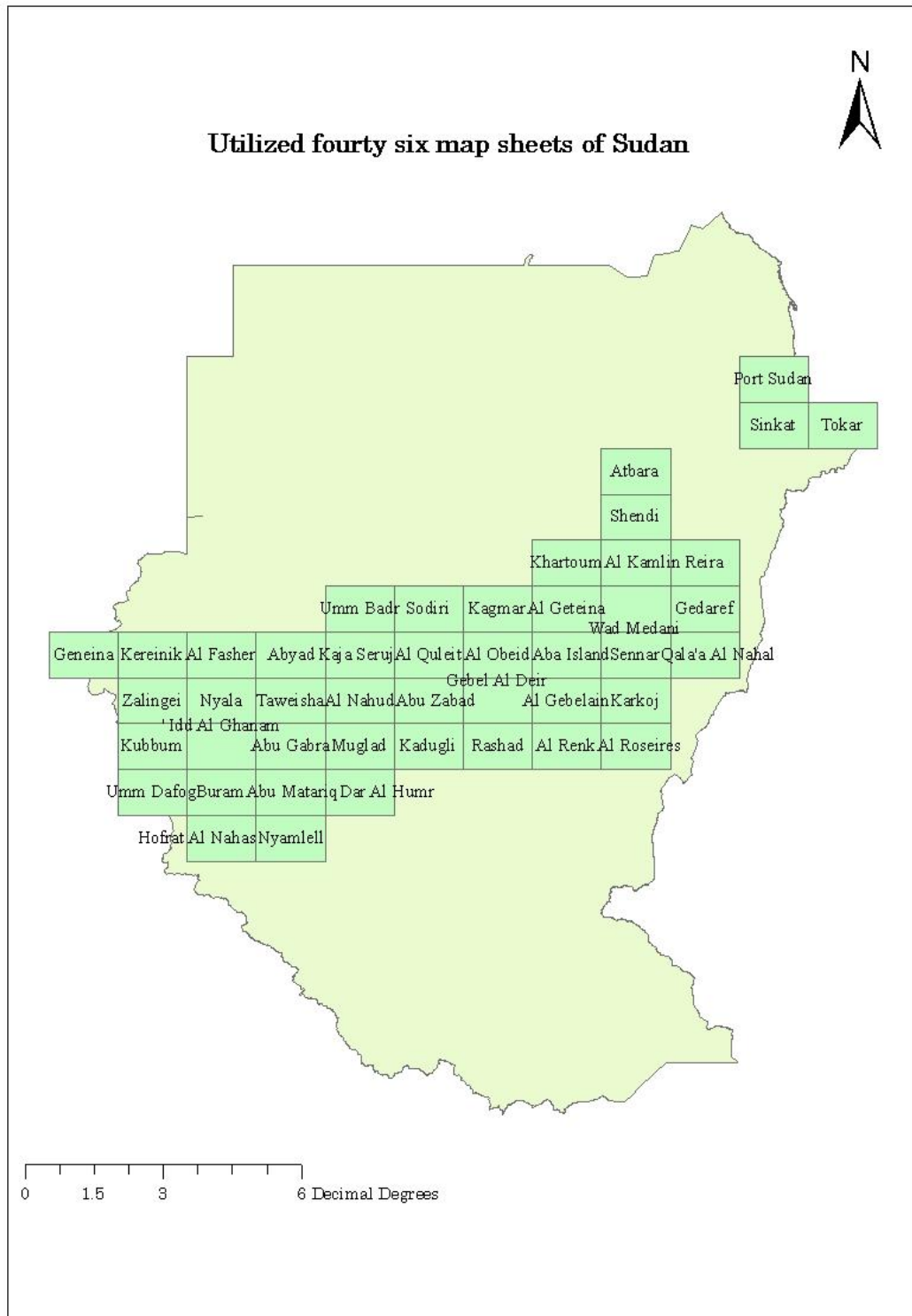
Figure 3.Utilized satellite map sheet areas of Sudan

References

Albrecht, A. and S. T. Kandji. 2003. Carbon sequestration in tropical agroforestry systems. *Agric. Ecosyst. Environ.* 99:15-27.

Ardö, J. and L. Olsson. 2004. Soil carbon sequestration in traditional farming in Sudanese drylands. *Environmental Management* 33(1):S318-S329.

Dixon, R.K. 1995. Agroforestry systems: sources or sinks of greenhouse gases? *Agrofor. Syst.* 31:99–116.

Elsiddig, E. A. 2002. Developments in Forestry Education in the Sudan. Paper presented at VITRI Inauguration Workshop: Tropical Dryland Rehabilitation, 11-14 June, 2002, Hyytiälä Forestry Field Station, University of Helsinki, Finland.

FAO. 2004. Carbon sequestration in dryland soils. World soils resources reports 102. Rome, Italy.

FAO. 2005. New_LocClim: Local Climate Estimator. Environment and natural resources, working paper No. 20 (CD-ROM).

FAO/IIASA/ISRIC/ISSCAS/JRC, 2009. Harmonized World Soil Database (version 1.1). FAO, Rome, Italy and IIASA, Laxenburg, Austria.

Feller, C.; Albrecht, A.; Blanchart, E.; Cabidoche, Y.M.; Chevallier, T.; Hartmann, C.; Eschenbrenner, V.; Larre-Larrouy, M.C.; and Ndandou, J. F. 2001. Soil carbon sequestration in tropical areas: general considerations and analysis of some edaphic determinants for Lesser Antilles soils. *Nutr. Cycl. Agroecosyst.* 61.19–31.

Fries, J. 1990. Management of natural forests in the semi-arid areas of Africa: Present knowledge and research needs. IRDC, Swed. Univ. Agric. Sci., Uppsala. 119p.

Glenn, E.; V. Squires; M. Olson; and R. Frye. 1993. Potential for carbon sequestration in the drylands. *Water, Air and Soil Pollution* 70:341–355.

Lal, R. 2001. Potential of desertification control to sequester carbon and mitigate the greenhouse effect. *Climatic Change* 51:35–72.

Lal, R. 2004. Carbon sequestration in dryland ecosystems. *Environmental Management* 33 (4):528-544.

Nair, P. K. R. 1993. An Introduction to Agroforestry. Kluwer, the Netherlands. 499p.

Sharawi, H. A. 1986. *Acacia senegal* in the gum belt of Western Sudan: A cost benefit analysis. M. Sc. thesis, University College of North Wales, Bangor, UK.

Squires, V. R. 1998. Dryland soils: their potential as a sink for carbon and as an agent to mitigate climate change. *Advances in GeoEcology* 31:209–215.

Starr, M. 1999. WATBAL: A model for estimating monthly water balance components, including soil water fluxes. In: Kleemola, S. Forsius, M. (Eds), 8th Annual Report 1999 UN ECE ICP Integrated Monitoring. Finnish Environment Institute, Helsinki, Finland. The Finnish Environment 325: 31-35.

UNEP. 1992. *World atlas of desertification*. Edward Arnold, Seven Oaks, UK.

Winjum, J.K.; Dixon, R.K.; and P.E. Schroeder. 1992. Estimating the global potential of forest and agroforest management practices to sequester carbon. *Water Air Soil Pollut.* 64:213–228.

MEASURED ULTRAFINE AEROSOL PARTICLE HYGROSCOPIC GROWTH FACTORS DURING PARTICLE FORMATION AND SUBSEQUENT GROWTH IN ANTARCTICA

E. ASMI[1,2], A. VIRKKULA[1,2], M. EHN[1], A. FREY[2], R. HILLAMO[2] and M. KULMALA[1]

[1]Department of Physics, P.O. Box 64, FI-00014, University of Helsinki, Finland
[2]Finnish Meteorological Institute, P.O. Box 503, FI-00560 Helsinki, Finland

INTRODUCTION

Aerosol particles are known to affect the global climate through direct and indirect aerosol effects. However, the actual processes, such as new particle formation and interactions between particles and clouds (Kulmala et al., 2004; Kerminen et al., 2005), are yet uncertain leading to large uncertainties in the magnitude of the aerosol climatic effects. Even less is known on the Antarctic aerosols due to lack of direct measurements. The sensitivity of Antarctic climate to changes in global climate and the role of aerosols in this system are important questions and need intensive research work to be resolved. In addition, Antarctica is a suitable place to study aerosol processes in natural background environment, without significant interference of human influences.

Aerosol hygroscopicity can be used as an indicative of the chemical composition, and further more, the origin of the particles. Together with size, the hygroscopic properties of particles also determine their ability to affect as cloud condensation nuclei (CCN) (Bilde and Svenningsson, 2004). Particles which are able to activate as cloud droplets have an important role in the climate system by influencing the cloud properties, such as their lifetime and scattering characteristics.

Here we study aerosol hygroscopic properties in Antarctica. The results will help to make connections between aerosols, clouds and the complex Antarctic climate system.

METHODS

Aerosol particle number size distributions and hygroscopic properties of the particles were measured in Queen Maud Land, Antarctica. The measurements were conducted at a Finnish research station Aboa (73°03'S, 13°25'W) during the Antarctic summer 2006/2007 from 28 December to 29 January. The station is located about 130 km from the coast on a nunatak Basen in the Vestfjella Mountains. The instruments were located to a separate measurement container, about 250 m from the station main building, at an altitude of about 500 m a.s.l. In the context of the container an automatic weather station (MILOS) recorded the meteorological data at the site.

The hygroscopic growth of 10, 25, 50, and 90 nm particles was measured with a hygroscopicity-tandem differential mobility analyser (H-TMDA). The relative humidity in the second DMA, after the moistening, was $90.0 \pm 0.5\%$. Due to very small particle concentrations, the scanning time of the second DMA was around 15 minutes and thus, the growth factors of all scanned particle sizes were achieved in an hour. Calculation of particle numbers was done with a TSI CPC model 3010. Lognormal modes were fitted for the measured humidified particle size distributions. The growth factors were determined as the size of the peak of the fitted mode divided by the dry particle size.

The size-segregated samples were taken using a 12-stage small-deposit-area low-pressure impactor (SDI). The SDI flow rate was 11 LPM and sample time was around two days. The aerodynamic cut-off diameters (D_{50}) of the SDI stages at 20°C and 1013 mbar are 0.045, 0.086, 0.15, 0.23, 0.34, 0.59, 0.80, 1.06, 1.66, 2.68, 4.08, and 8.5 μm. The analyzed ions were Na^+, NH_4^+, K^+, Mg^{2+}, Ca^{2+}, Cl^-, NO_3^-, SO_4^{2-}, MSA$^-$

($CH_3SO_3^-$), oxalate, acetate, succinate, formate, and malonate. The chemical mass balance was calculated for all impactor stages. Details of the analytical procedure were presented by (Teinilä et al., 2000).

The sector in the direction of the station main building (200 – 270 degrees) was classified as polluted. The impactor samples were collected only at times when the wind blew from the clean sector. Additionally, polluted time periods were excluded from the H-TDMA data.

The aerosol particle number size distributions were measured with a twin-differential mobility particle sizer (DMPS). The twin-DMPS consisted of two Hauke-type differential mobility analysers (DMA) followed by two TSI condensation particle counters (CPC). The two DMPS's operated parallel with a 10-minutes time resolution measuring particle dry size at range 3 – 1000 nm.

RESULTS

The humidified aerosol showed one-modal growth in the H-TMDA, indicating internal mixing and/or similar hygroscopic properties of individual particles. The calculated hygroscopic growth factors (GF) of 90, 50, 25 and 10 nm particles were on average 1.78 ± 0.05, 1.72 ± 0.04, 1.66 ± 0.04 and 1.50 ± 0.06, respectively for the measurement period of 4 weeks in January 2007. Particles were thus very hygroscopic and their GFs indicated existence of sulphur compounds and/or non-neutralized sulphuric acid. Measured growth factors varied slightly during the measurement period. The reasons for this could be different air mass types and aging of the aerosol, leading to different composition, as well as in case of sulphuric acid, small variations of the dry aerosol humidity. The RH of the aerosol line was in a range 1.8 – 4.4%. Even in these low humidity values, the very hygroscopic sulphuric acid particles would not be truly dry. The correlation coefficient between 25 nm particle GF and dry aerosol RH was -0.2. Thus, it seems likely that both the RH of the dry particles and composition affected the determined GF values.

Previous results have shown that typically at Aboa the submicron mode is dominated by the nss-sulphate aerosol (Virkkula et al., 2006). This was similar to what was detected here. In the smallest particles corresponding to two lowest impactor stages, the majority of the particles were sulphate, of which a fraction was neutralized by ammonia. MSA contributed approximately 10% to the small particle mass. The extent of neutralization was higher in Aitken than in the accumulation mode. This is congruent with previous measurements at the site (Virkkula et al., 2004) and also what was presented in the recent study by Biskos et al., 2009 about the hygroscopicity of the sulphuric acid particles and their neutralization probability at different sizes. Hygroscopic growth factors, calculated based on chemical samples, were in the order of the H-TDMA measured growth factors.

The air backward trajectories were calculated with HYSPLIT (Hybrid Single Particle Lagrangian Integrated Trajectory Model). A common feature in January 2007 was that in the beginning and in the end of the month the air masses came from the open sea where as after the first half of the month they came from the inland. The effect of the air mass origin to the measured hygroscopic growth factors is under a study.

New particle formation events had the most pronounced effect on the GF values. The strongest particle formation event was detected on 21 January when the air masses arrived directly from the inland from high altitudes (Fig. 1). As the growing nucleation mode increased to the 25 nm particle size (Fig. 1) the GF of these particles decreased (Fig. 2). After this, as the aerosol aged, the GF again increased slowly. The same applied to the growing nucleation mode, where the GF increased with time. This suggests that less hygroscopic compounds took part to the growth process, possibly some organics or MSA. Nucleation at the site is previously connected with the mixing of the upper air masses with the surface air and marine origin of the air masses (Virkkula et al., 2008; Koponen et al., 2003).
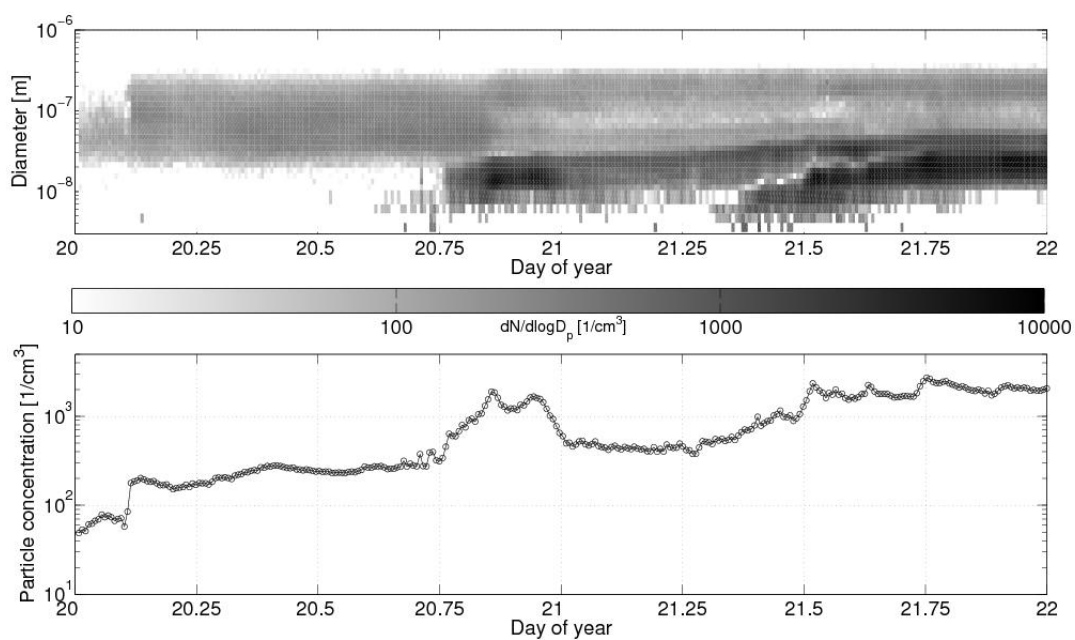
Figure 1. New particle formation events observed on 20-21 January, 2007. Upper panel presents the measured particle number size distributions and lower panel the total particle number.
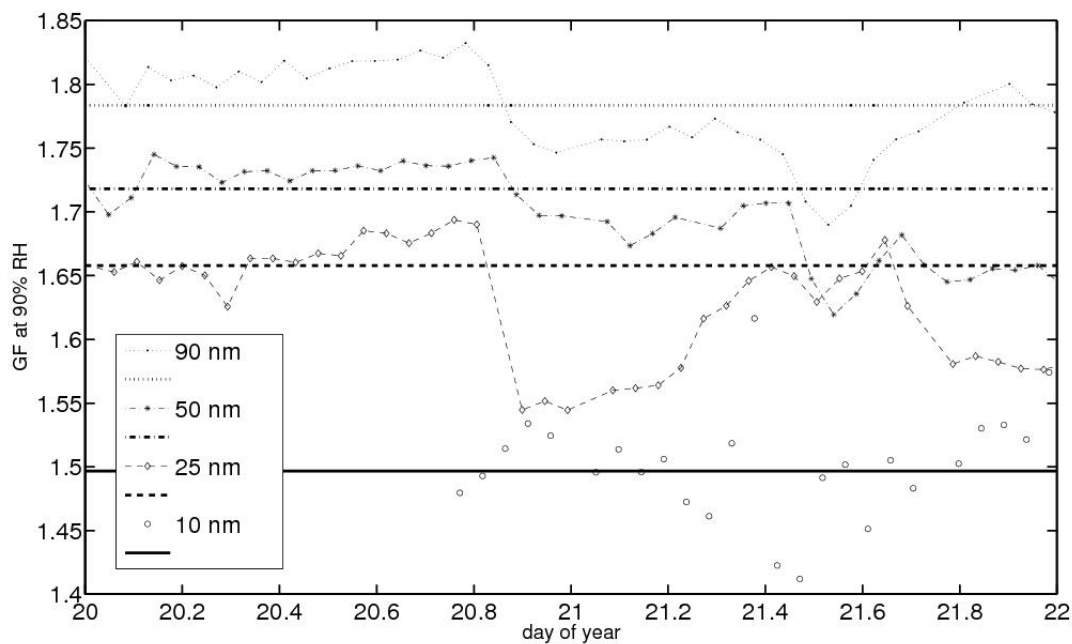
Figure 2. Particle hygroscopic growth factors measured on 20-21 January, 2007. Growth factors for 90, 50 and 25 nm are presented with lines and for 10 nm with dots during times when nucleation mode was existing.

CONCLUSIONS

The hygroscopic growth factors of 10 - 90 nm particles were measured with the H-TDMA for the first time in Antarctica. The measurements suggested that particles are very hygroscopic. This will significantly affect their size, as compared with the measured dry size, and again, increase their potential to act as cloud condensation nuclei (CCN). The measured particles most likely contained sulphur compounds together with extremely hygroscopic sulphuric acid. The results also suggested that less hygroscopic compounds take part to the growth of the newly formed particles. Aging of the aerosol increased the particle hygroscopicity.

ACKNOWLEDGEMENTS

REFERENCES

Bilde, M. and Svenningsson, B. (2004). CCN activation of slightly soluble organics: importance of small amounts of inorganic salt and particle phase. *Tellus 56B*, 128-134.

Biskos, G., Buseck, P.R. and Martin S.T. (2009). Hygroscopic growth of nucleation-mode acidic sulfate particles. *J. Aerosol Sci.* 40, 338-347.

Kerminen, V.-M., Lihavainen, H., Komppula, M., Viisanen, Y. and Kulmala, M. (2005). Direct observational evidence linking atmospheric aerosol formation and cloud droplet activation. *Geophys. Res. Lett.*, 32, L14803, doi:10.1029/2005GL023130.

Koponen, I.K., Virkkula, A., Hillamo, R., Kerminen, V.-M. and Kulmala, M. (2003). Number size distributions and concentrations of the continental summer aerosols in Queen Maud Land, Antarctica. *J. Geophys. Res.*, 108, AAC8.1-AAC8.10.

Kulmala, M., Vehkamäki, H., Petäjä, T., Dal Maso, M., Lauri, A., Kerminen V.-M., Birmili, W. and McMurry, P.H. (2004). Formation and growth rates of ultrafine atmospheric particles: a review of observations. *J. Aerosol Sci.* 35, 143-176.

Teinilä, K., Kerminen, V.-M. and Hillamo, R. (2000). A study of size-segregated aerosol chemistry in the Antarctic atmosphere. *J. Geophys. Res*, 105, 3893–3904.

Virkkula, A., Teinilä, K., Hillamo, R., Kerminen, V.-M., Saarikoski, S., Aurela, M., Koponen, I.K. and Kulmala, M. (2006). Chemical size distributions of boundary layer aerosol over the Atlantic Ocean and at an Antarctic site. *J. Geophys. Res.* 111, D05306, doi:10.1029/2004JD004958.

Virkkula, A., Frey, A., Aurela, M., Timonen, H., Teinila, K., Hillamo, R., Asmi, E., Aalto, P.P. Kulmala, M. and Kirkwood, S. (2008). Atmospheric aerosol and gas measurements at the Finnish Antarctic research station Aboa in summers 2006/2007 and 2007/2008. EAC 2008, Thessaloniki, Abstract T11A002O.

COMPARISON OF TWO MICROPHYSICAL MODELS IN EARTH SYSTEM MODELING FRAMEWORK

T. BERGMAN[1,2], R.. MAKKONEN[2], H. KOKKOLA[3], V.-M. KERMINEN[3]
and M. KULMALA[2]

[1] CSC – IT center for science, P.O. Box 405, FI-02101, Espoo, Finland
[2] Department of Physics, P.O. Box 64, FI-00014, University of Helsinki, Finland
[3] Finnish Meteorological Institute, P. O. Box 503 FI-00101, Helsinki, Finland

INTRODUCTION

Aerosols have an impact on the global radiation budget. They affect both the incoming and outgoing radiation. Therefore the atmospheric aerosols are an important part of atmospheric models from local to global scales. Atmospheric models treat aerosols with differing accuracy. Aerosols are modelled with moment, modal and sectional approaches. Due to high computational demand of the sectional models moment and modal approaches have thus far been more common in general circulation models. The modal and moment approaches, however, have difficulties to represent the processes involved in aerosol formation and growth, cloud processing and aging. Sectional models provide more accurate description of microphysical processes. The novel SALSA (Sectional Aerosol module for a Large Scale Applications)[1] module is designed specifically for usage in regional or global scale models of the atmosphere. Here we present a preliminary evaluation of SALSA module in global circulation modelling framework. We compare the aerosol representation of SALSA to M7[2] modal model implemented to general circulation model. Our comparison focuses on aerosol optical properties and aerosol number concentrations. To assess the accuracy of the representation, comparison to satellite observations is also made.

AEROSOL MICROPHYSICAL MODELS

Microphysical models M7 and SALSA calculate the coagulation of aerosol particles, condensation of gas-phase sulphuric acid on aerosol surface, nucleation and water uptake. The chemical compounds included are sulphate, black carbon, organic carbon, sea salt and dust. Although chemical compounds are the same, composition within size ranges have differences (e.g. SALSA has no carbon in the largest size range while M7 has). The division of different compounds in the size ranges is shown in Fig. 1 for both models.
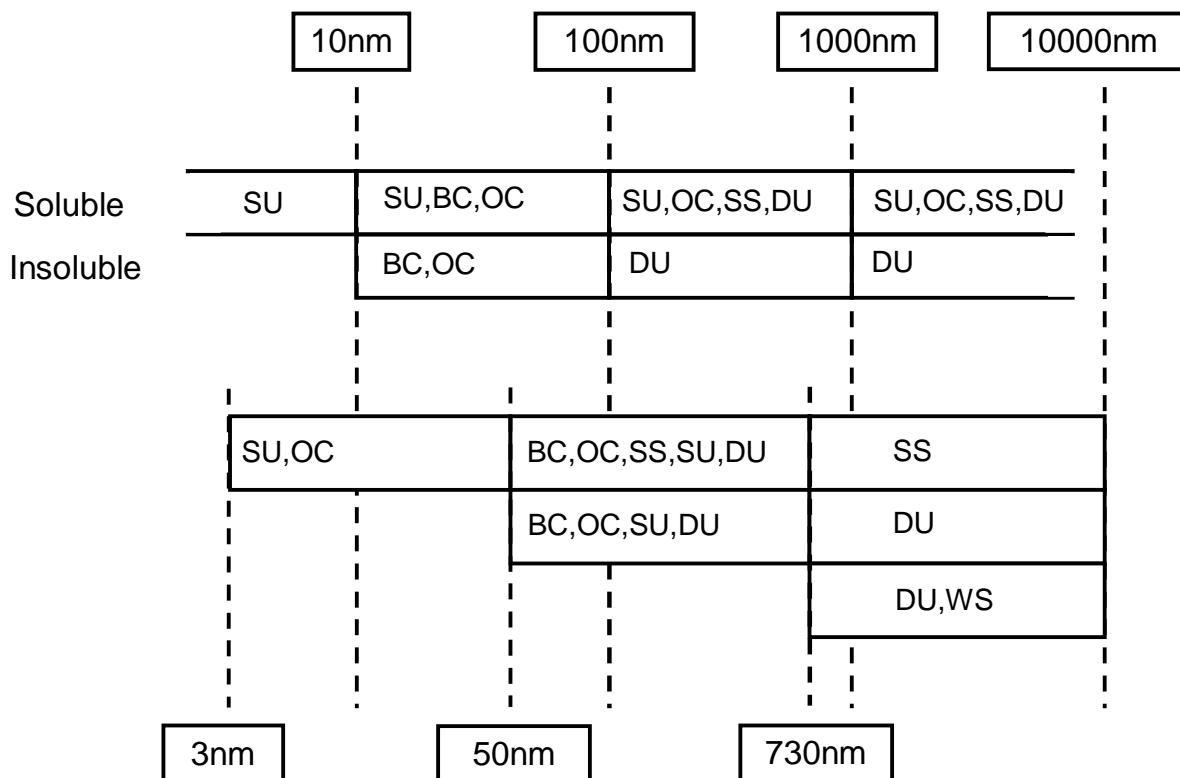
Figure 1. Schematic depicting M7 and SALSA size ranges and compounds therein. Upper boxes are for M7 and lower for SALSA. The acronyms are DU for mineral dust, SS for sea salt, SU for sulfate, OC for organic carbon, WS for water soluble fraction and BC for black carbon.

The SALSA module describes the aerosol population with 20 sections (10 sections in size space with parallel size sections depending on the external mixing of different sizes). Aerosol size distribution is represented with diameters ranging from 3 nm to 10 μm. These sections are both internally and externally mixed. There are three sub ranges of which the first has three sections. The second sub range has two parallel four section sets and the third sub range has three parallel three section sets. The boundary between the first and the second sub range is at 50 nm and the boundary between the second and the third is at 730 nm. These sub ranges and their compounds have been described in Fig. 1. To reduce the computational burden some of the processes have been left out depending on the size range.

M7 describes the aerosol population as seven internally and externally mixed lognormal modes. Four modes are hydrophilic and three modes are hydrophobic. For M7 there are no low or high limits and only mean diameter (radius) boundaries between the modes are defined. The modes are called Nucleation, Aitken, Accumulation and Coarse. The boundaries between these modes are at 10 nm, 100 nm and 1μm.

MODELLING FRAMEWORK IN ECHAM5-HAM

The SALSA module has been implemented to ECHAM5-HAM[3] general circulation model by the Max Planck Institute for Meteorology. Implementation allows the GCM to run simulations with either SALSA or M7 while keeping the rest of the GCM setup untouched.

Study was conducted as a one year nudged model run with half a year spin up for the aerosol fields to develop. With nudged runs atmospheric conditions are relaxed towards large scale meteorology retrieved from ERA-40 database. We have used a horizontal resolution T63 in spectral space which corresponds to

approximately 1.8° x 1.8° on a Gaussian grid. For vertical resolution we used 31 levels up to 10 hPa. The nudging method was chosen to keep the large scale meteorology as similar as possible thereby effectively allowing us to compare the differences caused by the microphysical representation of these models.

Anthropogenic emissions used with both models are based on the AEROCOM project (Aerosol Comparison between Observations and Models). Sea salt, DMS and dust emissions are calculated using prescribed DMS concentrations and wind speeds.

COMPARISON AND PRELIMINARY RESULTS

The annual mean number concentrations of aerosols were compared to evaluate the SALSA model performance. The mean annual particle concentrations were slightly smaller with SALSA as compared with M7. Despite concentrations being slightly lower, in the boundary layer they showed similar behaviour between the two models. The nucleation mode particles, however, showed much higher concentrations with the M7 in the free troposphere. The lower concentrations of SALSA seem possible, as observations do not support such high concentrations higher up in the atmosphere. This might suggest that M7 doesn't reproduce correctly the aerosol growth from nucleation to Aitken mode. Nevertheless, these differences need more thorough investigation.

According to our preliminary investigation, the aerosol optical depth has relatively similar values for both models. The SALSA model showed quite a good agreement with aerosol optical depth observed over remote ocean areas. For large desert areas, however, the aerosol optical depth had much lower values for SALSA than M7. Similar difference in desert areas is visible also in comparisons to the satellite observations. Since this difference is located near desert areas, the discrepancies are probably caused by differences in the treatment of dust production.

ACKNOWLEDGEMENTS

REFERENCES

Kokkola, H., Korhonen, H., Lehtinen, K. E. J., Makkonen, R., Asmi, A., Järvenoja, S., Anttila, T., Partanen, A.-I., Kulmala, M., Järvinen, H., Laaksonen, A., and Kerminen, V.-M.: SALSA – a Sectional Aerosol module for Large Scale Applications, *Atmos. Chem. Phys.,* **8**, pp. 2469-2483 (2008)

Vignati, E., J. Wilson, and P. Stier, M7: An efficient size-resolved aerosol microphysics module for large-scale aerosol transport models, *J. Geophys. Res.*, **109**, (2004) D22202, doi:10.1029/2003JD004485.1.

Stier, P., Feichter, J., Kinne, S., Kloster, S., Vignati, E., Wilson, J., Ganzeveld, L., Tegen, I., Werner, M., Balkanski, Y., Schulz, M., Boucher, O., Minikin, A., and Petzold, A.: The aerosol-climate model ECHAM5-HAM, *Atmos. Chem. Phys.*, **5**, pp. 1125-1156 (2005)

NEW PARTICLE FORMATION IN RURAL AREAS – WHAT WE KNOW AND WHAT'S STILL MYSTERIOUS

MICHAEL BOY[1], ANDREY SOGACHEV[2], SAMPO SMOLANDER[1], JOHANNA, LAUROS[1], HENRI VUOLLEKOSKI[1], SANNA-LIISA SIHTO[1], TANJA SUNI[1], LAURI LAAKSO[3], ALEX GUENTHER[4], MARKKU KULMALA[1]

[1]Department of Physics, University of Helsinki, P.O. Box 64, 00014 Helsinki, Finland
[2]Wind Energy Division, Risø National Laboratory for Sustainable Energy, Technical University of Denmark, P.O. Box 49, DK-4000 Roskilde, Denmark
[3]School of Physical and Chemical Sciences, North-West University, Private Bag x6001, Potchefstroom 2520, Republic of South Africa
[4]ACD, NCAR, 3450 Mitchell Lane, Boulder, CO 80301, USA

Key Words: Atmospheric nucleation; Tropospheric aerosols; Organic vapours; Sulphuric acid

INTRODUCTION

The role of atmospheric aerosols is perhaps the biggest unknown concerning our climate and greenhouse warming (IPCC, 2007). New particle formation has been observed at almost all sites, where particle size distributions have been measured. A comprehensive summary of these studies is given by Kulmala and co-workers (Kulmala et al, 2004). However, many questions remain regarding the extent to which these secondary aerosols influence radiative properties, climate and human health. Most of these issues are linked to the chemical composition of the newly formed particles, which is currently not understood entirely.

 Organic compounds and their reaction products can participate in the formation and growth processes of atmospheric particles (Boy et al., 2003). Mass-balanced-based estimations indicate that approximately 130-910 TgC/yr of the global emitted volatile organic compounds (~1300 TgC/yr) oxidize to low vapour pressure products and transform into secondary organic aerosols (SOA) (Goldstein and Galbally, 2007). Recent research results with a new nucleation parameter including organic vapours explained the seasonal and annual variability of observed nucleation events at different sites (Bonn et al., 2009). Using this parameter it seems very likely that nucleation events will increase in number over the entire boreal regions and several mid-latitude areas, thus impacting both ambient aerosol number concentrations and cloud properties (Spracklen et al, 2006).

Although many field campaigns, laboratory experiments and new modelling approaches have led to increased understanding, detailed mechanisms responsible for the formation of new particles in the troposphere and their influence on health, environment and climate have still not been completely elucidated. In MALTE (Model to predict new Aerosol formation in the Lower Troposphere) individually developed codes from different institutes around the globe are merged into a one-dimensional model including aerosol dynamics, boundary layer meteorology, biology and chemistry in order to investigate the formation and growth processes of SOA under realistic atmospheric conditions.

MODEL DESCRIPTION

MALTE is a one-dimensional model which includes several modules for the simulation of boundary layer dynamics and both chemical and aerosol dynamical processes (Boy et al., 2006 and 2008). For a better description of the Planetary Boundary Layer (PBL) and to improve the vertical transport inside the canopy, a 1-dimensional version of the model SCADIS (plant-atmosphere boundary-layer model) will be implemented (Sogachev and Panferov, 2006). The aerosol dynamics is solved by the size-segregated aerosol model, UHMA (University of Helsinki Multicomponent Aerosol model) and the chemistry is simulated with the Kinetic Pre Processor (KPP) in combination with the Master Chemical Mechanism

from the University of Leeds, England. Emissions of volatile organic compounds are calculated by MEGAN (Model of Emissions of Gases and Aerosols from Nature) with plant specific standard emissions potentials for each ecosystem (Guenther et al., 2006).

Our knowledge concerning the formation of very small particles or clusters (diameter < 2 nm) is still limited. The question of which molecules (sulphuric acid, ammonia, ions and/or organic vapours) are involved in the atmospheric nucleation processes remains controversial within the aerosol community. In MALTE we tested different nucleation theories to investigate which mechanism shows the highest correlation with observed nucleation rates based on calculations using measured particle size distributions.

ENVIRONMENTS

Four background field stations in different ecosystems were selected for our model runs:

- ➢ Boreal forest - SMEAR II in Hyytiälä, Finland
- ➢ Temperate forest - Manitou Forest Station, Colorado, USA
- ➢ Eucalypt forest - Tumbarumba, South-East Australia
- ➢ Savannah – Botsalano game reserve, South Africa

RELEVANCE OF DIFFERENT NUCLEATION THEORIES

It is likely that different nucleation mechanisms are at work in different conditions. In the past the main candidates for nucleation in the lower troposphere have been thought to be binary sulphuric acid – water, ternary sulphuric acid – water – ammonia mixtures or ion induced nucleation of sulphuric acid and water. All of these nucleation theories were implemented in MALTE and tested for different locations with the result that none could satisfactorily explain the observed particle formation events.

Recent laboratory studies reported new particle formation in a nucleation reactor/chamber under the conditions representing those in the lower ambient troposphere (Berndt et al., 2005 and 2008). The H_2SO_4 vapours in those experiments were produced in the same way as that in the real atmosphere (i.e., via the oxidation of SO_2 by OH), which sets them apart from earlier studies in which H_2SO_4 vapours were obtained from the direct vaporization of the liquid H_2SO_4 reservoir. The most interesting result in the work from Berndt and co-workers is that only ~10^7 molecules cm^{-3} of H_2SO_4 were needed to initiate the nucleation if H_2SO_4 vapours were produced in situ via the oxidation of SO_2 while ~10^{10} cm^{-3} of H_2SO_4 were needed if H_2SO_4 vapours were derived from the liquid H_2SO_4 reservoir. It has been suggested that the nucleation, starting via the oxidation of SO_2 (e.g. through the oxidation by peroxy radicals) which eventually leads to H_2SO_4 vapours, may be different from that starting directly from sulphuric acids but it also leaves the opportunity open that other molecules like organic vapours or their reaction products will participate.

Which molecules are the really important key players in atmospheric particle formation processes is still unsure, however limonene which has been highlighted in several publications for the highest nucleation potential of all monoterpenes could inherit this role (e.g. Jonssunn et al., 2006). Until now limonene was never seriously considered in atmospheric nucleation because of its low fraction of the total monoterpenes mass. However, new quantum chemical calculations and chamber experiments with different monoterpenes showed that the reaction products of limonene could be involved in the formation of new particles (see abstract or presentation by Ortega – manuscript in preparation). Including these new findings in MALTE by calculating an organic nucleation rate based on the activation of limononic acid through sulphuric acid resulted in high agreement with the nucleation rates based on measured particle size distributions. These new achievements will help us to understand the role of organic vapours in the nucleation process and will enable us to predict future conditions and possible feedback mechanisms.

CONCLUSION

New available data sets from field campaigns in combination with new hypothetical nucleation theories led to a more optimistically view concerning the understanding of atmospheric nucleation. Up to day we know that ion-induced nucleation often contribute to the new particle formation, but our results and earlier publications showed that its contribution is limited to a few percent in the lower troposphere. Ternary and binary nucleation theories with present understanding underestimate measured atmospheric nucleation rates. The big open question today and for the near future is to what extend organic vapours are involved in the nucleation mechanism and is sulphuric acid still one main steering parameter for the formation of new clusters or only activating the organic compounds.

Acknowledgement

REFERENCES

Berndt, T., Böge, O., Stratmann, F., Heintzenberg, J., and Kulmala, M.: Rapid Formation of Sulfuric Acid Particles at Near-Atmospheric Conditions, Science, 307, 698–700, 2005.

Berndt, T., Stratmann, F., Bräsel, S., Heintzenberg, J., Laaksonen, A. and Kulmala, M.: SO_2 oxidation products other than H_2SO_4 as a trigger of new particle formation. Part 1: Laboratory investigations, Atmos. Chem. Phys., 8, 6365-6374, 2008.

Bonn, B., Boy, M., Kulmala, M., Groth, A., Trawny, K., Borchert, S., and Jacobi, S.: Ambient new particle formation parameter indicates potential rise in future events, Atmos. Chem. Phys. Discuss., 9, 673-691, 2009.

Boy, M., Rannik, U., Lehtinen, K. E. J., Tarvainen, V., Hakola, H., and Kulmala, M.: Nucleation events in the continental PBL – long term statistical analyses of aerosol relevant characteristics, J. Geophys. Res., 108(D21), 4667, doi:10.1029/2003JD003838, 2003.

Boy, M., Hellmuth, O., Korhonen, H., Nillson, D., ReVelle, D., Turnipseed, A., Arnold, F. and Kulmala, M.: MALTE – Model to predict new aerosol formation in the lower troposphere, Atmos. Chem. Phys., 6, 4499–4517, 2006.

Boy, M., J. Kazil, E. R. Lovejoy, H. Korhonen, A. Guenther and M. Kulmala: Relevance of ion-induced nucleation of sulphuric acid and water in the lower troposphere over the boreal forest at northern latitudes, Atmospheric Research, 90, 151-158, 2008.

Goldstein, A.H. and Galbally, I.E.: Known and Unexplored Organic Constituents in the Earth'sAtmosphere Environ. Science and Technology, 41, 5, 1514 - 1521, 2007.

Guenther, A., Karl, T., Harley, P., Wiedinmyer, C., Palmer, P. I., and Geron, C.: Estimates of global terrestrial isoprene emissions using MEGAN (Model of Emissions of Gases and Aerosols from Nature), Atmos. Chem. Phys., 6, 3181–3210, 2006.

IPCC, Intergovernmental Panel on Climate Change (IPCC): Climate Change: The Scientific Basis, Cambridge University Press, UK, 2007.

Jonssunn, A. M., Hallquist, M. and Jungström E.: Impact of humidity on the ozone initiated oxidation of limonene, d3-carene and α-Pinene, Environ. Sci. Technol., 40, 188-194, 2006.

Kulmala, M.,Vehkamäki, H., Petäjä, T., Dal Maso, M., Lauri, A., Kerminen, V.-M., Birmili, W., and McMurry, P.H.: Formation and growth rates of ultrafine atmospheric particles: A review of observations. J. Aerosol Sci. 35, 143-176, 2004.

Sogachev,A. and Panferov, O.: Modification of two-equation models to account for plant drag, Boundary Layer Meteorology, DO 10.1007/s10546-006-9073-5, 2006.

Spracklen, D. V., Carslaw, K.S., Kulmala, M., Kerminen, V.-M., Mann, G. W. and Sihto, S.-L.: The contribution of boundary layer nucleation events to total particle concentrations on regional and global scales, Atmos. Chem. Phys., 6, 5631-5648, 2006.

BINARY HOMOGENEOUS NUCLEATION OF H_2SO_4-H_2O

D. BRUS[1,2], A.-P. HYVÄRINEN[1], H. LIHAVAINEN[1] and M. KULMALA[3]

[1]Finnish Meteorological Institute, Erik Palménin aukio, P.O. Box 503, FI-00101 Helsinki, Finland
[2]Laboratory of Aerosol Chemistry and Physics, Institute of Chemical Process Fundamentals Academy of Sciences of the Czech Republic, Rozvojová 135, CZ-165 02 Prague 6, Czech Republic
[3]Department of Physics, University of Helsinki, P.O. Box 64, FI-00014 Helsinki, Finland

INTRODUCTION

New particle formation in the atmosphere has lately received considerable attention both from atmospheric scientists and aerosol researchers. Atmospheric new particles have been observed to form by self-condensing, or nucleating homogeneously in events lasting few hours nearly all around the world (Kulmala *et al.*, 2004). To understand the mechanism of new particle formation events, considerable work has been done by scientists involving direct field and laboratory measurements, as well as computer simulations both on nucleation itself and the aerosol dynamics observed during the effects. Despite coming closer to drawing conclusions of all available data, exact knowledge of the nucleation event mechanism remains unclear.

Laboratory experiments on binary nucleation of sulfuric acid and water date back to 1976 when Reiss *et al.* measured nucleation rates in a piston cloud chamber. Similar experiments were conducted by Boulaud *et al.* (1977) in a reactor study, Mirabel and Clavelin (1978) in a thermal diffusion cloud chamber, and Friend *et al.* (1980) in a laminar flow reactor. More recent experiments include those made by Wyslouzil *et al.* (1991), Viisanen *et al.* (1997), Ball *et al.* (1999), Zhang *et al.* (2004), Berndt *et al.* (2006), Benson *et al.*, (2008), and Young *et al.*, (2008). All the latter experiments relied on a flow based measurement technique. In general the latter laboratory measurements divide into two main directions, depending on how the gaseous mixture containing sulfur and water molecules is produced. Some experimenters employ photo-oxidation of SO_2, some produce gaseous mixture from liquid H_2SO_4, using saturators or liquid samples. The experiments are generally in fair agreement with each other, but nucleation rates occur at much higher sulfuric acid concentration than those observed at atmospheric conditions.

RESULTS

In this study the laminar flow tube was used to investigate binary homogeneous nucleation of sulphuric acid and water. The laminar flow tube is positioned vertically and it whole length is about three meters. The experimental setup consists of five main parts: an atomizer, a furnace, a mixing unit, a nucleation chamber and a particle detector unit. A liquid solution of known concentration and amount is introduced together with particle free air into the furnace with HPLC Pump through a 20 µm ruby micro-orifice. The dispersion is vaporized in a Pyrex glass tube which is wrapped with resistant heating wires. After the furnace, the vapor is filtered with Teflon filter, the filtered vapor is then introduced into mixing unit where is cooled by turbulent mixing with particle free air. The vapor gas mixture is then cooled to wanted nucleation temperature in nucleating chamber which is kept at constant temperature (298 K) with two liquid circulating baths. The nucleation chamber is made of stainless steel, its ID is 6 cm and whole length is 200 cm. Concentration of water vapor is measured in the middle and at the end of nucleation chamber with a humidity data processor. The aerosol number concentration is measured just after nucleation chamber with an ultrafine condensation particle counter (UCPC TSI 3025A).
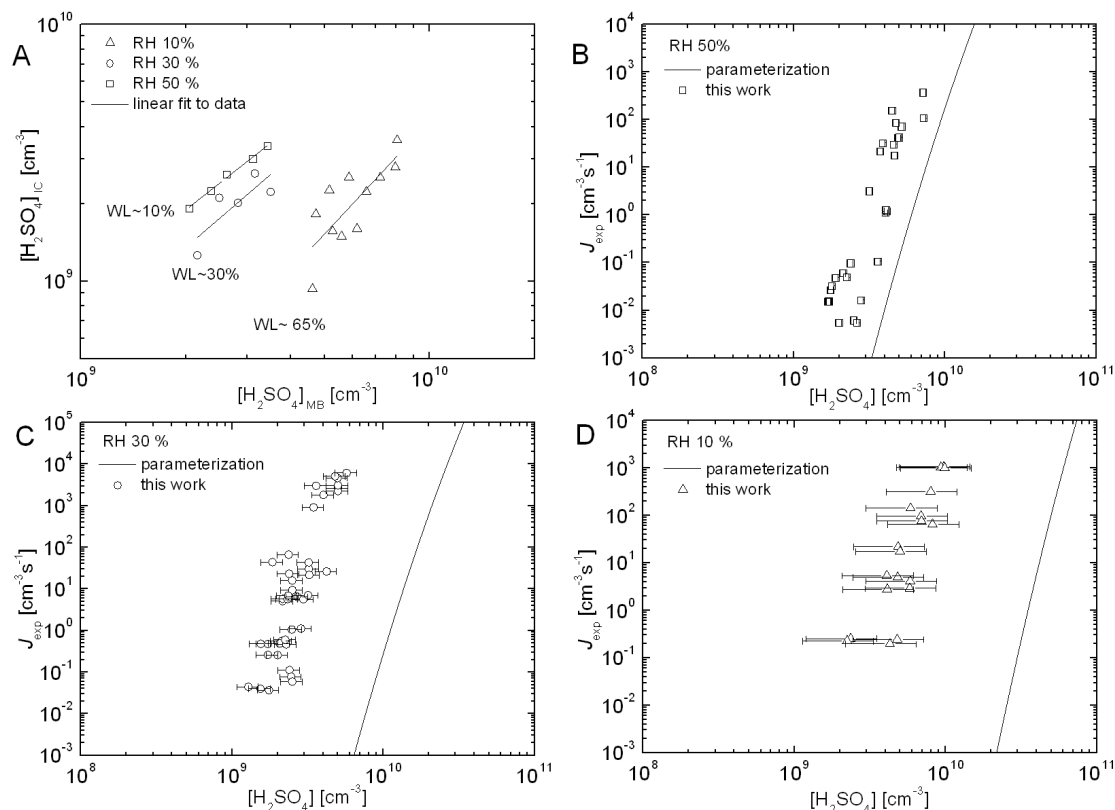
Figure 1 A) Concentration of sulfuric acid determined by Ion Chromatography as a function of concentration of H_2SO_4 calculated by Mass Balance, wall loses "WL" are included for each relative humidity (50, 30 and 10%). B, C and D) Experimental nucleation rates as a function of H_2SO_4 concentration at relative humidities 50, 30 and 10%, left error bar is concentration of H_2SO_4 determined by Ion Chromatography, right error bar is concentration of H_2SO_4 calculated by Mass Balance, theoretical prediction (Vehkamäki et al., 2002) of binary homogeneous nucleation is presented as lines in figures.

The concentration of sulphuric acid was calculated by Mass Balance and also determined experimentally by using several bubblers containing basic solution of NaOH along the nucleation chamber with subsequent Ion Chromatography analysis, see figure 1A. Nucleation rates were determined from a particle number concentration and a residence time that particles have to travel from the nucleation zone to the output of nucleation chamber. Figures 1 B, C, and D show nucleation rates as a function of sulfuric acid concentration at three relative humidities 50, 30, and 10 %.

Figure 2 shows nucleation rates as a function of sulfuric acid concentration, the comparison of experimental results from previous studies at several relative humidities and atmospheric nucleation is presented, (Sihto et al., 2006).
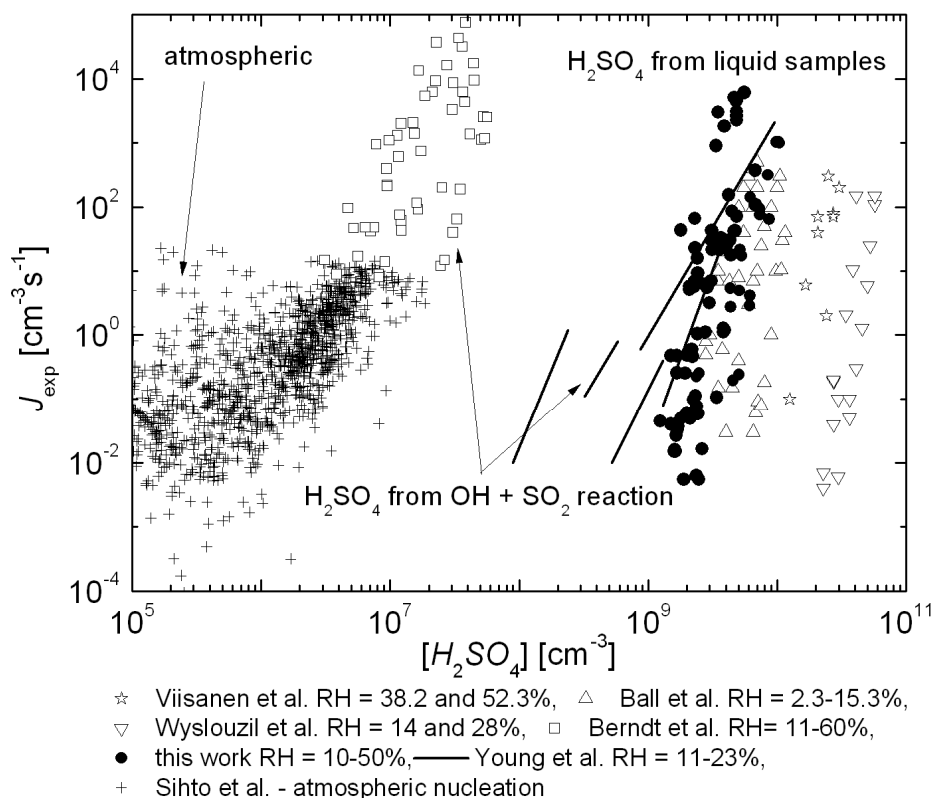
Figure 2 Experimental nucleation rates as a function of H$_2$SO$_4$ concentration, the comparison of laboratory experiments and atmospheric nucleation (Sihto *et al.*, 2006).

CONCLUSIONS

In this study nucleation rates ranging from 10^{-2} to 10^4 particles per cubic centimeter per second of the binary system sulfuric acid and water were measured at three different relative humidities 50, 30 and 10 %. The concentration of sulfuric acid was determined by Mass Balance calculation and also experimentally by Ion Chromatography analysis. The new particle formation was observed at concentrations 1.10^9 to 4.10^9 of sulfuric acid molecules in cubic centimeter. The obtained experimental data are in good agreement with results published earlier. However atmospheric nucleation occurs at much lower concentrations of sulfuric acid which suggests involvement of different species to enhance nucleation process in the atmosphere.

ACKNOWLEDGMENT

REFERENCES

Ball S. M., Hanson D. R., and Eisele F. L., and McMurry P. H., *J. Geophys. Res.* 104, D19, 23.709-23.718, (1999).

Benson, D. R., Young, L. H. Kameel, F. R. and Lee, S. H., *Geophys. Res. Lett.* 35, L11801, (2008).

Berndt, T., Böge, O., and Stratmann, F., *Geophys.Res.Lett.* 33, L15817 (2006).

Boulaud, D., Madelaine, G. and Vigla, D., *J. Chem. Phys.* 66, 4854 (1977).

Friend, J.P., Barnes, R.A., Vasta, R. M., *J. Phys. Chem.* 84, 2423 (1980).

Kulmala, M., Vehkamäki, H., Petäjä, T., Dal Maso, M., Lauri, A., Kerminen, V.-M., Birmili, W., and McMurry, P. H., *J. Aerosol Sci.*, 35, 143 (2004).

Mirabel, P. and Clavelin, J. L., *J. Chem. Phys.* 68, 5020 (1978).

Reiss, H., Margolese, D. I. and Schelling, F. J., *J. Colloid Interface Sci*. 56, 511 (1976).

Sihto, S.-L., Kulmala, M., Kerminen, V.-M., Dal Maso, M., Petäjä, T., Riipinen, I., Korhonen, H., Arnold, F., Janson, R., Boy, M., Laaksonen, A., and Lehtinen, K. E. J., *Atmos. Chem. Phys.* 6, 4079–4091, (2006).

Vehkamäki, H., Kulmala, M., Napari, I., Lehtinen, K. E. J., Timmreck, C., Noppel M., and Laaksonen, A., *J. Geophys. Res.*, 107, 4622, (2002).

Viisanen, Y., Kulmala, M. and Laaksonen, A., *J. Chem. Phys.* 107, 920 (1997).

Wyslouzil, B. E., Seinfeld, J .H., Flagan, R. C., and Okuyama, K., *J. Chem. Phys.* 94, 6842 (1991).

Young, L-H., Benson, D. R., Kameel, F. R., Pierce, J. R., Junninen, H., Kulmala, M., Lee, S-H., *Atmos. Chem. Phys.* 8, 4997-5016, (2008).

Zhang, R., Suh, I., Zhao, J., Zhang, D., Fortner, E. C., Tie, X., Molina, L. T. and Molina, M. J. *Science* 304, 1487 (2004).

COMPARISON OF VOC EMISSIONS FROM
TWO SCOTS PINE SHOOTS WITH A DYNAMIC SHOOT CHAMBER

J. BÄCK[1], P. KOLARI[1], J. AALTO[1], R. TAIPALE[2], M. KAJOS[2], P. HARI[1] and M. KULMALA[2]

[1]Department of Forest Ecology, University of Helsinki, Finland
[2]Department of Physics, University of Helsinki, Finland

Keywords: biogenic volatile organic compounds, Scots pine, PTR-MS

INTRODUCTION

Coniferous forests emit a variety of BVOCs to the atmosphere, the most important ones being carbonyls and isoprenoids; isoprene and monoterpenes. In boreal forested environments, BVOC emissions may have a considerable effect on the ecosystem carbon balance, amounting up to 0.2–10% of the assimilated carbon being re-emitted to the atmosphere, depending on for example the time of year, temperature or water availability (e.g. Guenther, 2002). The reaction products of these emitted compounds participate in atmospheric new particle formation and growth processes, and influence the regional ozone chemistry in troposphere (Atkinson and Arey, 2003).

In the nature, BVOC emissions depend on many interlinked environmental and physiological factors. Emissions vary diurnally and within the season in both quantity and quality of the emitted compounds. The plant phenological development is one of the most important factors influencing emission rates. Although it is known that in many species the photosynthetic processes influence emissions via the supply of energy and substrates for the BVOC biosynthesis, developing leaves may not posses similar emission capacity as the old leaves. This has been shown for example in broad-leaved species where the onset of emissions was correlated with the accumulated temperature sum (Hakola et al 2003). Thus, studies of changes in emission rates at different temporal scales related to changes in environmental variables as well as plant physiology are needed. Here we report preliminary data from field measurements with two dynamic shoot chambers, where a pine branch with mature needles, and a terminal bud of the branch (allowing the branch to grow inside the chamber) have been enclosed.

MATERIAL AND METHODS

The measurements were carried out at the SMEAR II measurement station (Station for Measuring Forest Ecosystem – Atmosphere Relations) in Hyytiälä, Southern Finland (61°N, 24°E, 180 m a.s.l.). The forest around the station is dominated by 45-year-old Scots pine (*Pinus sylvestris* L.) with some Norway spruce (*Picea abies* (L.) Karst.), aspen (*Populus tremula* L.) and birch (*Betula* spp.). The canopy reaches a height of about 16 m. A scaffolding tower permits access to the crowns of three pines and an aspen.

The automatic gas-exchange system consists of 3.5-dm^3 cylindrical shoot chambers, sampling tubing, and analyzers. The chambers are made of acrylic plastic and their internal surfaces coated with Teflon FEP film. The chambers remain open most of the time and close intermittently for 3 minutes, four times per every third hour. While open, the chamber interior is in contact with ambient unfiltered air. During a closure, air is drawn from the chambers to the gas analyzers along the sample lines. Ambient air is allowed to enter the chamber through small holes in the chamber walls to compensate the sample air flow taken from the chamber. VOC sample air is drawn in a separate Teflon PTFE tube of 50 m length and 4 mm internal diameter. One tube with internal diameter of 4 mm is leading the air towards the CO_2 and H_2O analyser at flow rate of 1 dm^3 min^{-1}; the second with i.d. of 6 mm reaches the O_3 and NO_x analysers at 3 dm^3 min^{-1}. Ambient atmospheric concentrations of CO_2, H_2O, O_3, NO_x as well as air temperature and PPFD, are measured during and before chamber closure and the values recorded at 5-s intervals.

The BVOC chamber measurements were started in the end of January, 2009, when the measurement chambers were placed in the uppermost part of the canopy of a Scots pine. The chambers were fastened to the trunk in

order to avoid mechanical damage to the shoot. The axillary buds were carefully removed from one branch and only the terminal bud was left to grow inside the chamber, which was placed upwards so that the new growth will be positioned as naturally as possible and no additional twisting of the branch will be needed. The other shoot had been debudded already previous spring, thus the prevailing needles are now almost two years old. The other chamber was placed horizontally (Figure 1).
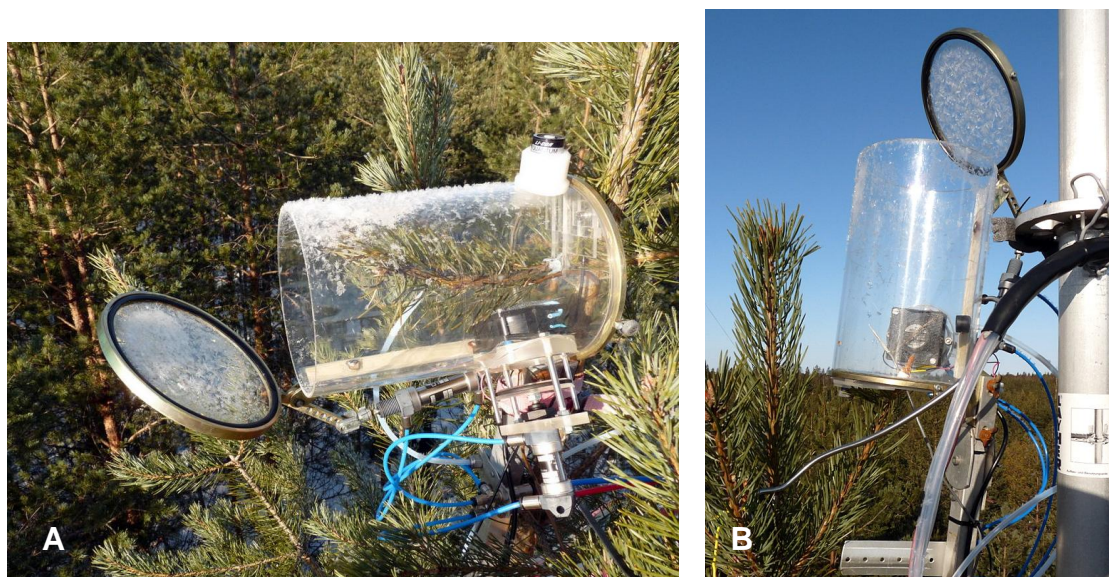
Figure 1. The two cuvettes measuring A) mature shoot and B) terminal bud of a Scots pine tree.

The VOC composition and emission rates were measured using a proton transfer reaction mass spectrometer (PTR-MS, Ionicon GmbH, Innsbruck, Austria). The sample air intake of the PTR-MS, connected to the O_3/NO_x sampling tube, was about 0.1 dm^3 min^{-1}. The measured masses were: M33 (Methanol), M45 (Acetaldehyde), M59 (Acetone), M69 (Isoprene+MBO), M79 (Benzene), M81 (Monoterpene fragment), M99 (Hexenal), M101 (Hexanal, 3-hexenol), M137 (Monoterpene) and M153 (Methylisalicylate). Ambient conditions were obtained from the records when the chamber was open. During chamber closure, gas concentration inside the chamber may change, indicating a net source or sink of that particular gas in the chamber. The change in concentrations, corresponding the incident emission rate for M45, M59 and M81 during closure are reported here.

RESULTS AND DISCUSSION

The two chambers were measured consecutively, and thus the emissions can be compared with each other. In general the VOC emissions from the terminal bud were very small (Fig 2). The concentration increase during the closure remained below 0.2 ppb for M45 (acetaldehyde) and M59 (acetone), whereas the shoot emissions ranged from 3 to 9 ppb and from 1 to 6 ppb for M45 and M59, respectively. These results indicate that the mature needles are a source for oxygenated VOCs such as acetaldehyde and acetone, whereas the dormant buds do not significantly emit these compounds.

For monoterpenes (M81) the concentration change during closure was on the same order of magnitude in both chambers, the range being from 0.1 to 0.7 ppb. The monoterpene emission in the chamber with the bud may be originating from the wound-induced resin leakage due to the recent cutting of the axillary buds, and reflects the large internal monoterpene storage pools in shoots. Monoterpene emissions from Scots pine are extremely sensitive to stresses, and mechanical damage of the shoot was earlier seen to lead to an orders-of-magnitude increase in the monoterpene emissions (Ruuskanen et al., 2005, Hakola et al., 2006). The lack of M45 and M59 emissions from the wounded bud confirms our earlier result (Kolari et al., 2008) that emissions of these compounds may not be induced by wounding.
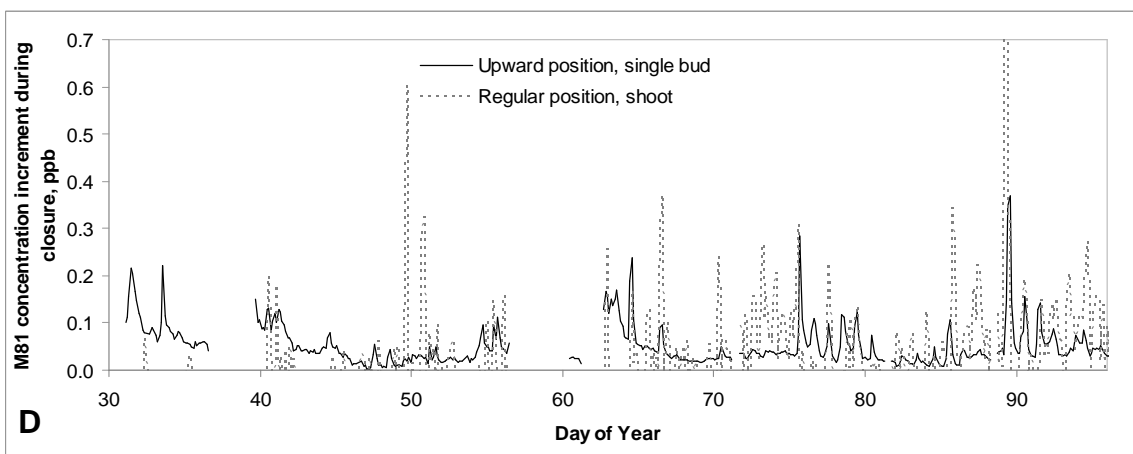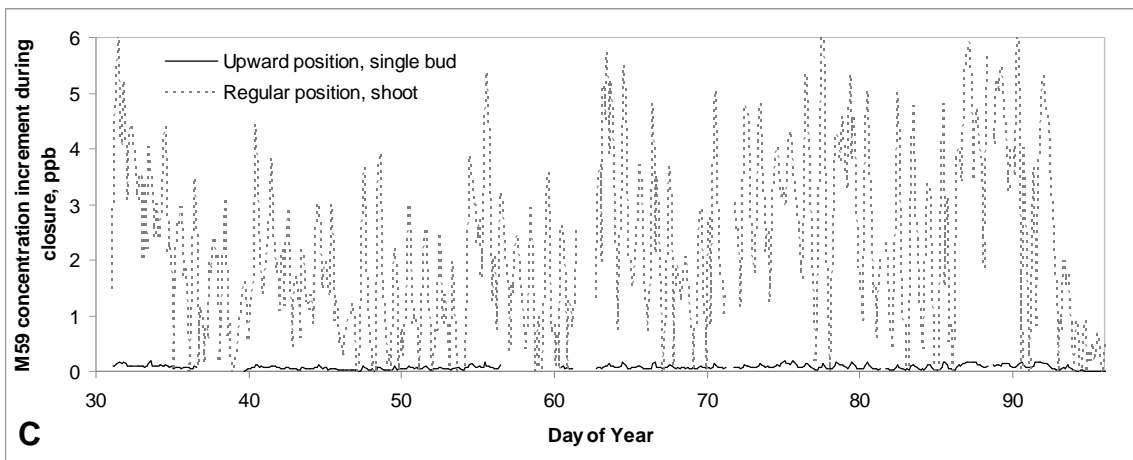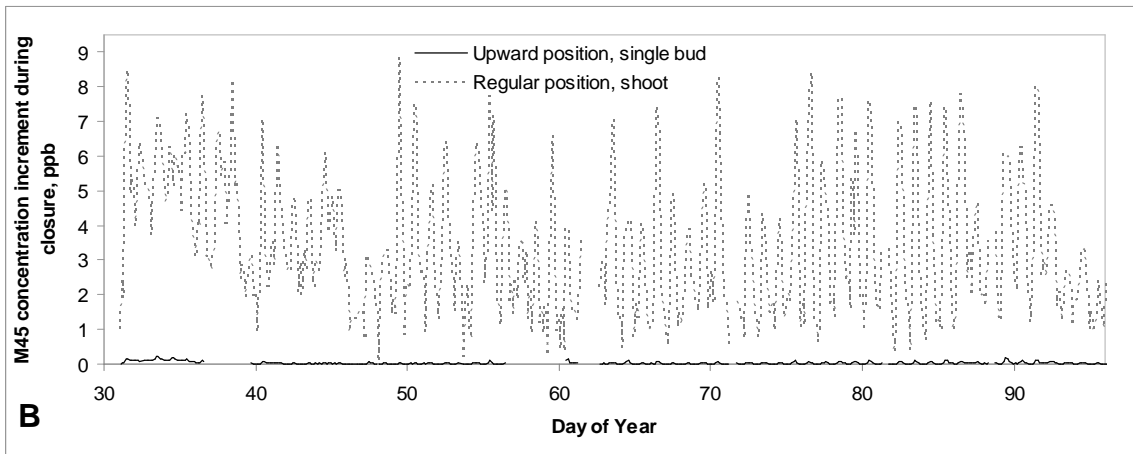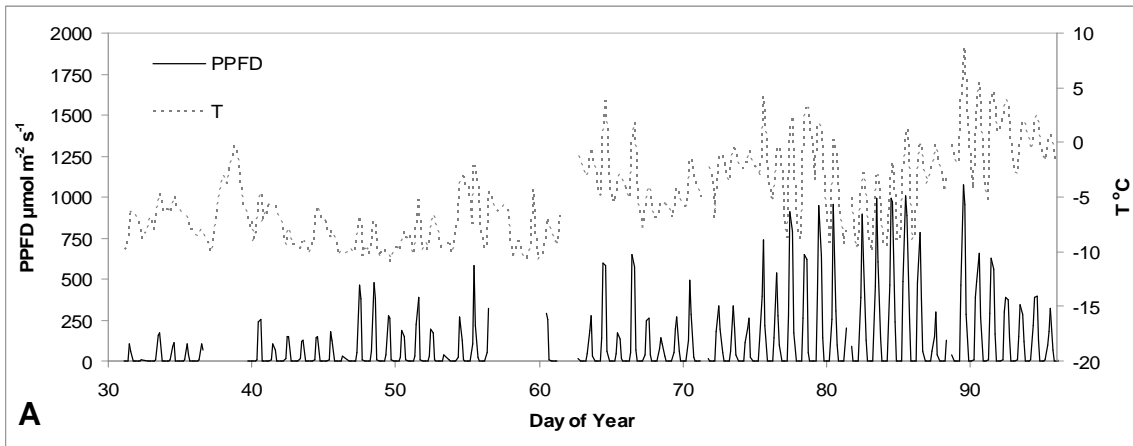
Figure 2. A) Ambient temperature and PPFD (photosynthetically active photon flux), and emissions of B) M45 (acetaldehyde), C) M59 (aceetone), and D) M81 (monoterpenes) from the two chambers between 1st Feb and 7th April, 2009. Values are hourly averages, measured every third hour.

Already in early spring the VOC emissions had a distinct diurnal pattern in both chambers: on most days the emissions exhibited local maximum around midday, and the lowest values were measured during night. The ambient temperatures were rather low during the measured period. Only in the last 10 days the daily maximum temperatures were above zero. The emission peaks generally occurred on sunny and relatively warm days, but the minima seemed to follow more closely the light levels than low temperatures. Based on earlier studies on spring recovery processes at SMEAR II (Porcar-Castell et al., 2008), the evergreen Scots pine needles are in a dormant stage until mid-April, after which a rapid increase in the photochemical efficiency indicates the recovery and onset of active period. The temperature-standardized monoterpene emission in Scots pine has been observed to be highest in the spring and early summer, decline during the summer, and increase again in the autumn (Tarvainen et al., 2005, Hakola et al., 2006). The high emission peaks in early spring have been suggested to serve photoprotective purposes during the inactive periods (Bäck et al 2005). Our measurements will be continued throughout the spring and growing season, and they will be used for further developing a mechanistic model on Scots pine VOC emissions.

REFERENCES

Atkinson, R. and Arey, J. (2003). Gas-phase tropospheric chemistry of biogenic volatile organic compounds: a review. *Atmospheric Environment* 37, Supplement 2: 197-219

Bäck, J., Hari, P., Hakola, H., Juurola, E. and Kulmala, M. (2005) Dynamics of monoterpene emissions in *Pinus sylvestris* during early spring. *Boreal Environment Research*, 10, 409–424.

Guenther, A. (2002) The contribution of reactive carbon emissions from vegetation to the carbon balance of terrestrial ecosystems. *Chemosphere*, 49, 837–844.

Hakola H., Tarvainen V., Laurila L., Hiltunen V., Hellén H. and Keronen P. (2003) Seasonal variation of VOC concentrations above a boreal coniferous forest. *Atmospheric Environment*, 37, 1623–1634.

Hakola, H., Tarvainen V., Bäck J., Ranta H., Bonn B., Rinne J. and Kulmala M. (2006) Seasonal variation of mono- and sesquiterpene emission rates of Scots pine. *Biogeosciences* 3, 93–101.

Kolari, P., Bäck J., Ruuskanen T., Taipale R., Kajos M., Rinne, J., Hari P. & Kulmala M. (2008) Measurements of VOC emissions from mature Scots pine shoots with a duynamic shoot chamber. *Report Series in Aerosol Sciences* 94, 58-64.

Porcar-Castell A., Juurola E., Nikinmaa E., Berninger F. Ensmnger I & Hari P. (2008) Seasonal acclimation of photosystem II in *Pinus sylvestris*. I. Estimating the rate constants of sustained thermal energy dissipation and photochemistry. *Tree Physiology* 28, 1475–1482

Ruuskanen, T.M., Kolari, P., Bäck, J., Kulmala, M., Rinne, J., Hakola, H., Taipale, R., Raivonen, M., Altimir, N. and Hari, P. (2005) On-line field measurements of monoterpene emissions from Scots pine by proton-transfer-reaction mass spectrometry. *Boreal Environment Research*, 10, 553–567.

Tarvainen, V., Hakola, H., Hellén, H., Bäck, J., Hari, P. and Kulmala, M. (2005) Temperature and light dependence of the VOC emissions of Scots pine. *Atmospheric Chemistry and Physics*, 5, 989–998.

SOURCES OF AMBIENT FINE PARTICLES IN HELSINKI DURING WINTER

S. CARBONE[1], M. AURELA[1], S. SAARIKOSKI[1], M. KULMALA[2], D. WORSNOP[2] and R. HILLAMO[1]

[1] Finnish Meteorological Institute, Air Quality Research, P.O. Box 503, FI-00101 Helsinki, Finland
[2] Department of Physical Sciences, FI-00014 University of Helsinki, Finland

INTRODUCTION

Epidemiological studies have reported adverse effects cause by ambient fine particles (diameter < 2.5 μm) to human health (Schwartz et al., 1999; WHO 2003 and Pope et al., 2009). However, of the major constituents of fine particles, sulphate, nitrate, ammonia, organic and elemental carbon and water no single chemical species seem to dominate the health effects (Davidson et al., 2005). In Helsinki the origin of both local and long-range transported fine particles is mostly anthropogenic (Pakkanen et al., 2001; Niemi et al., 2004; Sillanpää et al., 2005 and Saarikoski et al., 2008). In this study, six episodes detected during winter 2008-2009 in Helsinki with different source contribution and chemical composition of fine particles were analyzed.

METHODS

Aerodyne High-Resolution Time-of-Flight Aerosol Mass Spectrometer (HR-ToF-AMS) previously described by DeCarlo et al. (2006) was used to determine major fine particulate matter species such as nitrate, sulphate, ammonium, chloride and organics. HR-ToF-AMS consists of a particle sampling inlet, a particle sizing chamber and a particle composition detection section. The aerosol particles are sampled through aerodynamic lens, forming a narrow particle beam which is transmitted into the detection chamber where non-refractory species are flash vaporized upon impact on a hot surface (~600ºC) under high vacuum and chemically analyzed via electron impact ionization (70 eV) in the high resolution time-of-flight mass spectrometer. Because the AMS is able to analyze non-refractory material only, elemental carbon was determined by thermal-optical transmittance (TOT) method using semi-continuous carbon analyzer (Sunset Laboratory Inc., Portland, OR). The instrumentation operated from December 2008 to March 2009 at an urban background station (SMEARIII, 60°12'N, 24°58'E, 26 m above sea level) in Helsinki, Finland. The site is located 5 km northeast from the centre of Helsinki and 200 m east from a dense traffic road (60 000 vehicles/day).

RESULTS

The six episodes selected for this study are presented in Figures 1 and 2 and numbered from one to six. In the episode number one contribution of organics (31%) and EC (28%) during rush hour (9:00 local time) suggested that aerosol mainly came from the major road close to the station. In addition, meteorological data such as wind speed and direction supports this statement. The following episodes, number two, three and four, according to backward trajectories of air masses were long-range transported either from Central or Eastern Europe. The episode number two came from Holland and Belgium, and particulate matter was most likely formed during transport due to NO_2 and hydrocarbon emissions of intensive traffic. When arrived in Helsinki, the gaseous emissions were oxidized and condensed to organic and ammonium nitrate particles, which corresponds to 39% and 29% of the total mass, respectively. Air masses arriving in Helsinki during episode number three came from Eastern Europe. Chemical composition in relation to total mass was different of the previous episode with mainly sulphate (64%), followed by organics (20%). The high contribution of sulphate which was not neutralized by ammonia, associated with the information of the backward trajectory of air mass, suggested that this highly acidic aerosol came mainly from the Estonian oil shale fuelled power plants in Narva. Similar profile was obtained in the episode number four, where sulphate represented 72% of the total mass followed by organics (18%). During this episode, air

masses were coming straight from Estonia over the Narva power plant. In the episodes number five and six, despite similar chemical composition (mainly organics and EC) and meteorological conditions (thermal inversion), source contribution seems to be quite different. In episode number five there was a high signal at mass-to-charge ratios 60 and 73, which are the main fragments of levoglucosan (Alfarra et al., 2007) indicating the effect of wood combustion probably from nearby residential areas. In episode number six the high contribution of EC (33%) during rush hour (09:00 local time) indicated traffic source and the high mass-to-charge ratio 57 measured by AMS suggested that the major source was diesel particles from the local traffic.
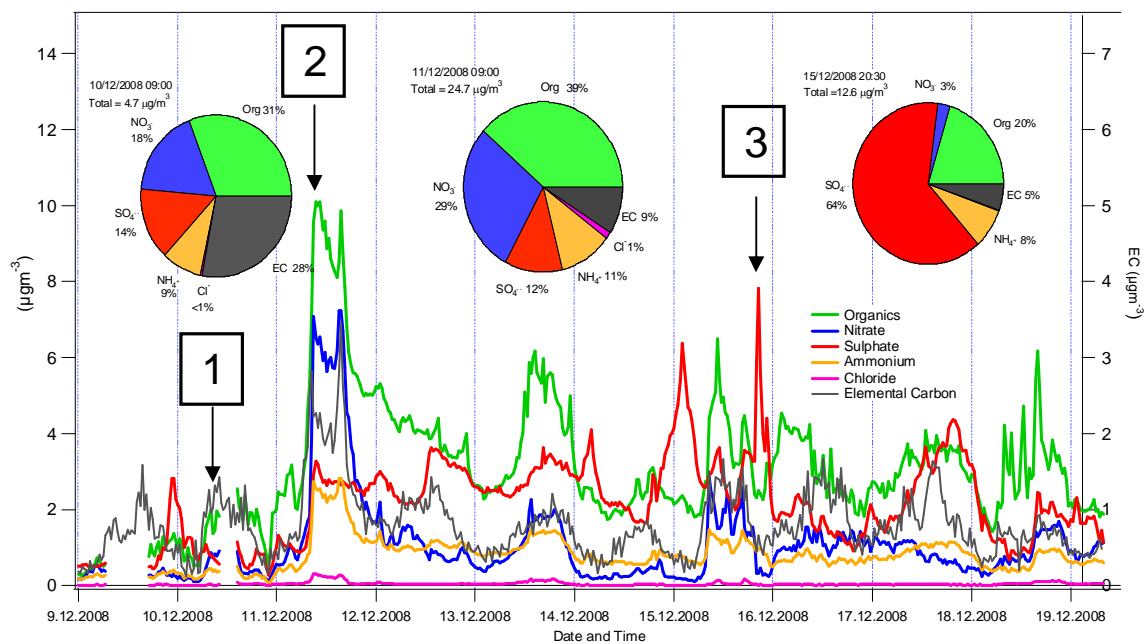
Figure 1. Mass concentration and chemical composition of fine particulate matter during episodes number one, two and three in Helsinki on December 2008.
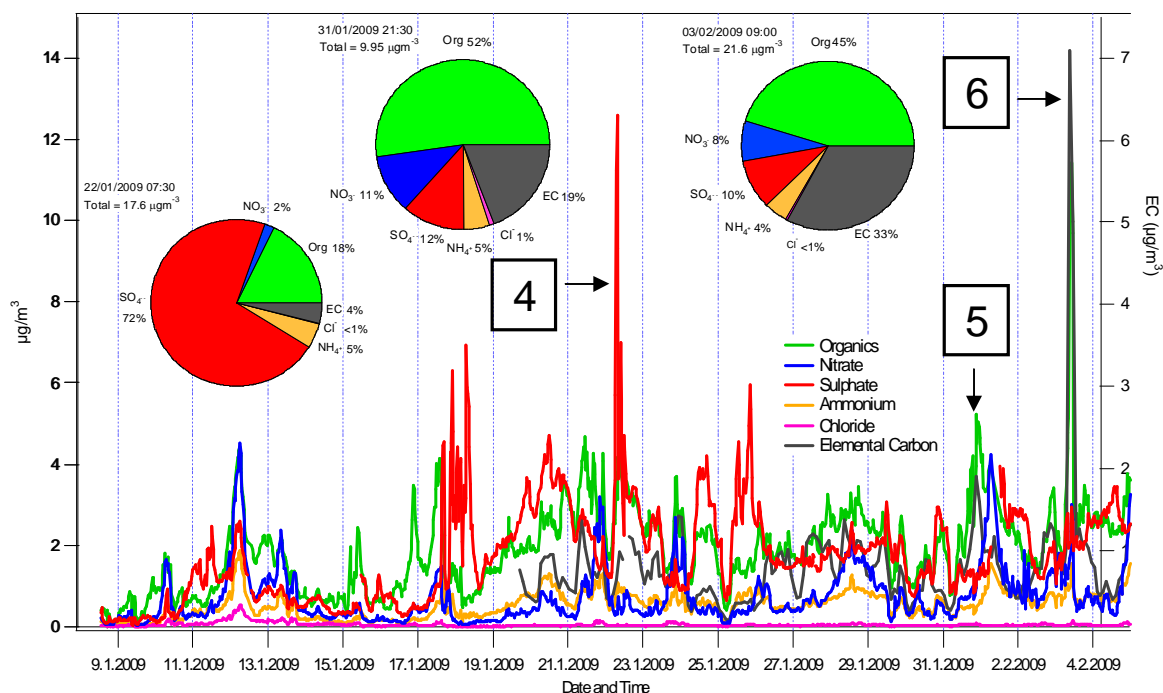
Figure 2. Mass concentration and chemical composition of fine particulate matter during episodes number four, five and six in Helsinki on January and February 2009.

CONCLUSIONS

Six episodes of fine-particulate air pollution were characterized during the intensive field measurement campaign in Helsinki. Using the single unit mass data from the aerosol mass spectrometer and elemental carbon data from the semi-continuous thermal carbon analyzer the episodes could be classified to different sources or source areas. The variable chemical composition shows that the gravimetric mass concentration is not a good indicator of the potential health or climatic effects of aerosols.

ACKNOWLEDGEMENTS

REFERENCES

Alfarra, M. R., Prevot, A. S. H., Szidatt, S., Sandradewi, J.,Weimer, S., Lanz, V. A., Schreiber, D., Mohr, M., and Baltensperger, U. (2007). Identification of the mass spectral signature of organic aerosols from wood burning emissions, Environ. Sci. Technol., 41, 5770–5777.

Davidson, C. I., Phalen, R. F. and Solomon, P. A. (2005). Airborne particulate matter and human health: a review, Aerosol Sci. Technol. 39: 737-749.

DeCarlo, P. F., Kimmel, J. R., Trimborn, A., Northway, M., Jayne, J. T., Aiken, A. C., Gonin, M., Fuhrer, K., Horvath, T., Docherty, K. S., Worsnop, D. R. and Jose L. Jimenez. (2006). Field-Deployable, High-Resolution, Time-of-Flight Aerosol Mass Spectrometer, Anal. Chem., 78: 8281-8289.

Niemi, J. V., Tervahattu, H., Venkamäki, H., Kulmala, M., Koskentalo, T., Sillänpää, M. and Rantamäki, M. (2004). Characterization and source identification of a fine particle episode in Finland, Atmospheric Environment, 38: 5003-5012.

Pakkanen, T. A., Loukkola, K., Korhonen, H., Aurela, M., Mäkelä, T., Hillamo, R. E., Aarnio, P., Koskentalo, T., Kuosa, A. and Maenhaut, W. (2001). Sources and chemical composition of atmospheric fine and coarse particles in the Helsinki area, Atmospheric Environment, 35: 5381-5391.

Pope, C. A., Ezzati, M. amd Worsnop, D. R. (2009). Fine-particulate air pollution and life expectancy in the United States, New England Journal of Medicine, 360: 376-86.

Saarikoski, S., Timonen, H., Saarnio, K., Aurela, M., Järvi, L., Keronen, P., Kerminen, V.-M., & Hillamo, R. (2008). Sources of Organic Carbon in PM_1 in helsinki urban air. Atmos. Chem. Phys. 8, 6281–6295.

Schwarts, J., Norris, G., Larson, T., Sheppard L., Clairbone, C. and Koenig, J. (1999). Episodes of high coarse particle concentrations are not associated with increased mortality. Environ Health Perspect, 107: 339-42.

Sillanpää, M., Saarikoski, S., Hillamo, R., Pennanen, A., Makkonen, U., Spolnik, Z., Grieken, R. V., Koskentalo, T. and Salonen, R. O. (2005). Chemical composition, mass distribution and source analysis of long-range transported wildfire smokes in Helsinki, Science of the Total Environment, 350: 119-135.

World Health Organization (WHO). (2003). Health aspects of air pollution with particulate matter, ozone and nitrogen dioxide. Copenhagen: WHO Regional Office for Europe, Report EUR/03/5042688 of working group, Bonn, Germany.

Anthropogenic aerosol radiative forcing in Asia derived from regional models with atmospheric and aerosol data assimilation

Chul Eddy Chung[1,2], V. Ramanathan[2], Greg Carmichael[3], Youhua Tang[3], Bhupesh Adhikary[3], L. Ruby Leung[4] and Yun Qian[4]

[1]Department of Physics, P.O. Box 64, FI-00014, University of Helsinki, Finland
[2]Scripps Institution of Oceanography, La Jolla, CA. 92093, USA
[3]University of Iowa, Iowa City, IA 52242, USA
[4]Pacific Northwest National Laboratory, Richland, WA 99352, USA

Introduction

A common procedure to estimate direct aerosol radiative forcing is the use of simulated aerosol distributions as input to a radiative transfer model. Simulated aerosol masses are converted into aerosol optical properties by empirical/theoretical algorithms, and then converted into aerosol forcing by radiative transfer models. Kinne et al. (2003) summarized this procedure and also compared various aerosol simulations. As explained in Kinne et al. (2003), uncertainties in aerosol simulations arise from emission sources, meteorology and aerosol/chemistry processing. An independent approach is to use observations of aerosol optical properties such as aerosol optical depth (AOD) and single scattering albedo (SSA) to compute DRF. Aerosol observations are available from field campaigns, aerosol observation networks and satellite retrievals. Recent examples of this approach are Chung et al.'s (2005) and Yu et al.'s (2006).

The present study integrates these two approaches by using simulated aerosols that are nudged towards aerosol observations. This "aerosol observation assimilation" has been conducted before (Collins et al., 2001), and retains advantages of both approaches. Aerosol simulations offer spatially (X-Y-Z) and temporally continuous values, while aerosol observations offer presumably better accuracy. In this study, we attempt to improve Collins et al.'s study by a) employing a high-resolution regional climate model instead of a global climate model and b) using ground and satellite aerosol observations. Giorgi et al. (2002) adopted a regional model to simulate aerosols but did not assimilate aerosol data.

Method

In our study, the regional climate simulation is constrained by global reanalyses throughout the model domain to provide atmospheric forcings for a regional scale chemistry-aerosol model. In turn, the chemistry-aerosol model assimilates ground and satellite aerosol observations to simulate observationally constrained aerosols. The simulated aerosols are incorporated in a radiative transfer model to estimate aerosol radiative forcing. The regional domain for our study is Asia. Regional scale modeling is necessary to capture the spatial heterogeneity associated with orography and emissions in Asia, and to better resolve atmospheric and aerosol processes.

The results in the present study are the products of a NASA-sponsored collaborative project between Scripps Institution of Oceanography (SIO), Pacific Northwest National Laboratory (PNNL), and the University of Iowa. As Fig. 1 illustrates, the PNNL regional climate model simulates meteorological variables that were used by the University of Iowa chemistry transport model STEM-2K1 (Sulfur Transport dEposition Model; version 2001) to simulate aerosols. The regional meteorological variables simulated by the PNNL model as well as the aerosol extinction coefficients simulated by the STEM-2K1 were then used in the SIO Monte-Carlo Aerosol Cloud Radiation (MACR) model to simulate anthropogenic aerosol radiative forcing. Subsequently, the PNNL model was used to produce two simulations, with and without the anthropogenic aerosol radiative forcing, to estimate the impacts of anthropogenic aerosols on the regional hydrological cycle of Asia (Box B in Fig. 1). The first author (Chung) relocated to the University of Helsinki in late 2007 and finished this project with the Finnish Center of Excellence support.
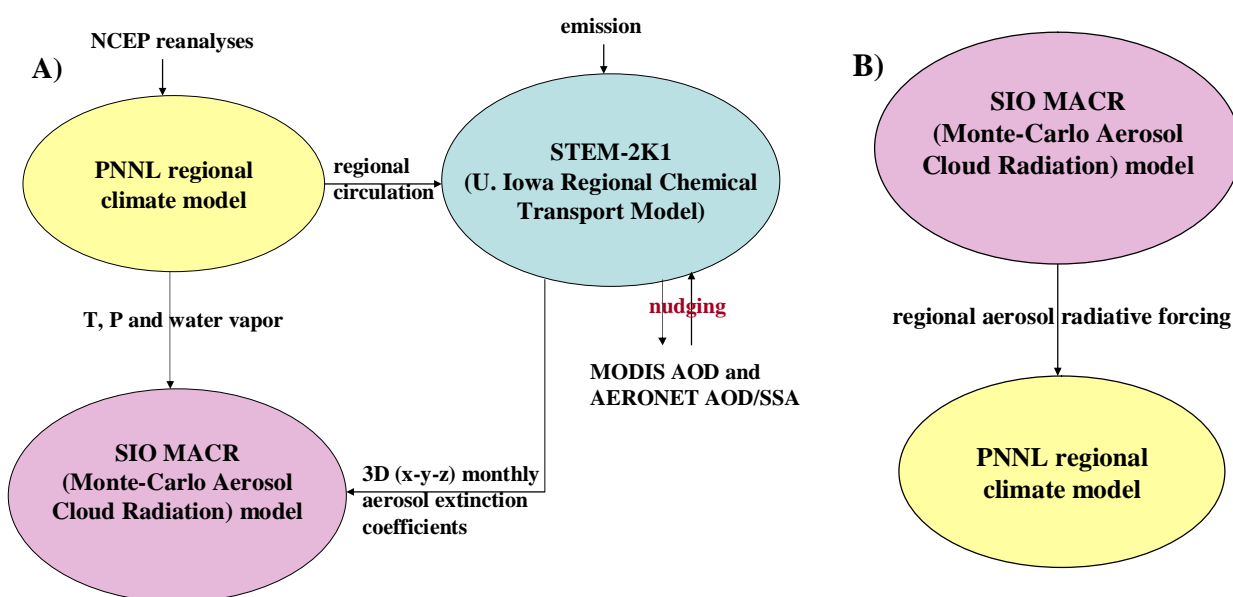
Figure 1. Overview of the Asian aerosol assimilation project. The project has been a joint effort between Scripps Institution of Oceanography (SIO), Pacific Northwest National Laboratory (PNNL) and the University of Iowa. The SIO MACR (Monte-Carlo Aerosol Cloud Radiation) model took aerosol simulations from Iowa STEM (Sulfur Transport dEposition Model), meteorological variables from the PNNL regional model, and cloud from the ISCCP, so as to produce 2001–2004 aerosol radiative forcing.

Results

A. Aerosol data assimilation

MODIS and AERONET observations are assimilated with STEM aerosol calculation here using optimal interpolation technique initially developed for meteorological applications (Lorenc, 1986). The optimal interpolation methodology for assimilating satellite data has also been implemented in other chemical transport models such as ROSE (Research for Ozone in the Stratosphere and Its Evolution) and MOZART2 (Khattatov et al., 2000). We implemented the optimal interpolation technique similar to the methodology described by Collins et al. for INDOEX aerosols using their MATCH model (Collins et al., 2001). There are, however, some differences in our assimilation methodology.
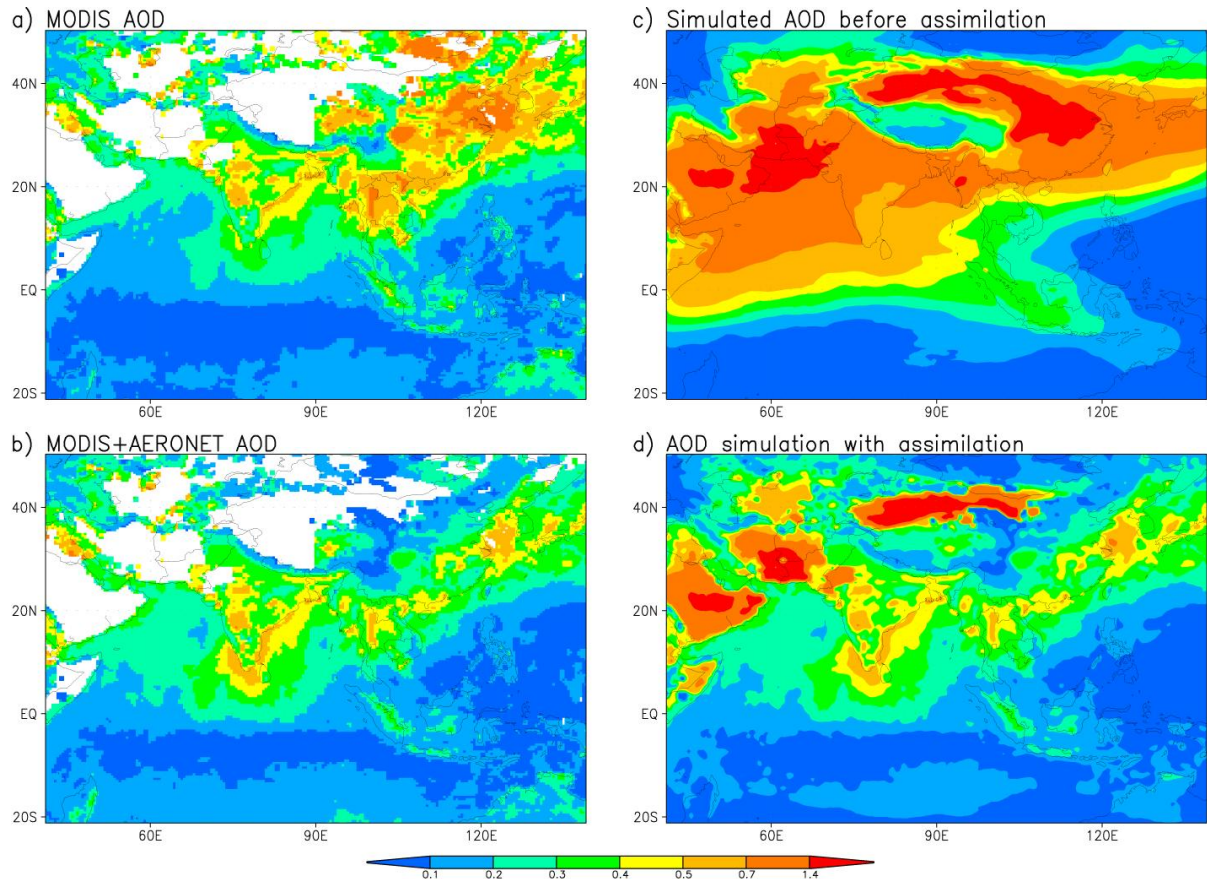
Figure 2. Total (natural + anthropogenic) AOD (Aerosol Optical Depth). A) Monthly AOD observation in March, 2001, from the satellite MODIS instrument. B) March 2001 AOD adjusted with scattered ground observations AERONET. C) Simulated AODs by the STEM-2K1 model (March, 2001). D) AOD simulation after assimilating MODIS+AERONET AOD.

Figure 2 illustrates the overall assimilation procedure for March 2001. Monthly AODs from MODIS are shown in Figure 2a. The MODIS AODs were corrected with AERONET AODs, referred to as "MODIS+AERONET AOD" for brevity here (Figure 2b). Note that the number of AERONET sites in the domain changes from month to month from 4 to 22. The STEM simulated AODs before any aerosol data assimilation are displayed in Figure 2c. After the assimilation, the final AODs are shown in Figure 2d. The final AODs, which are to be converted into aerosol radiative forcing as discussed next, appear similar to the MODIS+AERONET AODs where the latter are available. Where MODIS+AERONET AOD values are missing, the STEM simulated AODs replace the gaps. Our data assimilation technique is in a way a tool for transition from MODIS+AERONET AOD areas to their gaps. Even in areas where MODIS+AERONET AOD exists, our assimilation technique provides additional valuable information such as aerosol vertical profile needed to accurately compute aerosol radiative forcing.

B. Anthropogenic aerosol forcing

Fig. 3 displays the 2001–2004 averaged forcing at the surface, in the atmosphere and at the top of the atmosphere (TOA). F(TOA), i.e., aerosol forcing at the TOA, is negative for the entire domain (Fig. 4a). Negative values are largest in eastern China, South Asia and Southeast Asia. F(S) and F(A) have comparable magnitudes and opposite signs. As a result,

88

F(S) and F(A) are much larger than F(TOA) in magnitude, since F(TOA) = F(S) + F(A). The 4 year mean forcing for each month ranges from −20 Wm^{-2} to +10 Wm^{-2} (TOA), from +2 Wm^{-2} to +50 Wm^{-2} (atmosphere) and from −66 Wm^{-2} to −3 Wm^{-2} (surface). Reverting back to the 2001–2004 annual-mean aerosol forcing (Fig. 4), the largest values in F(S) or F(A) are found in northern Bay of Bengal and along the eastern China coast.
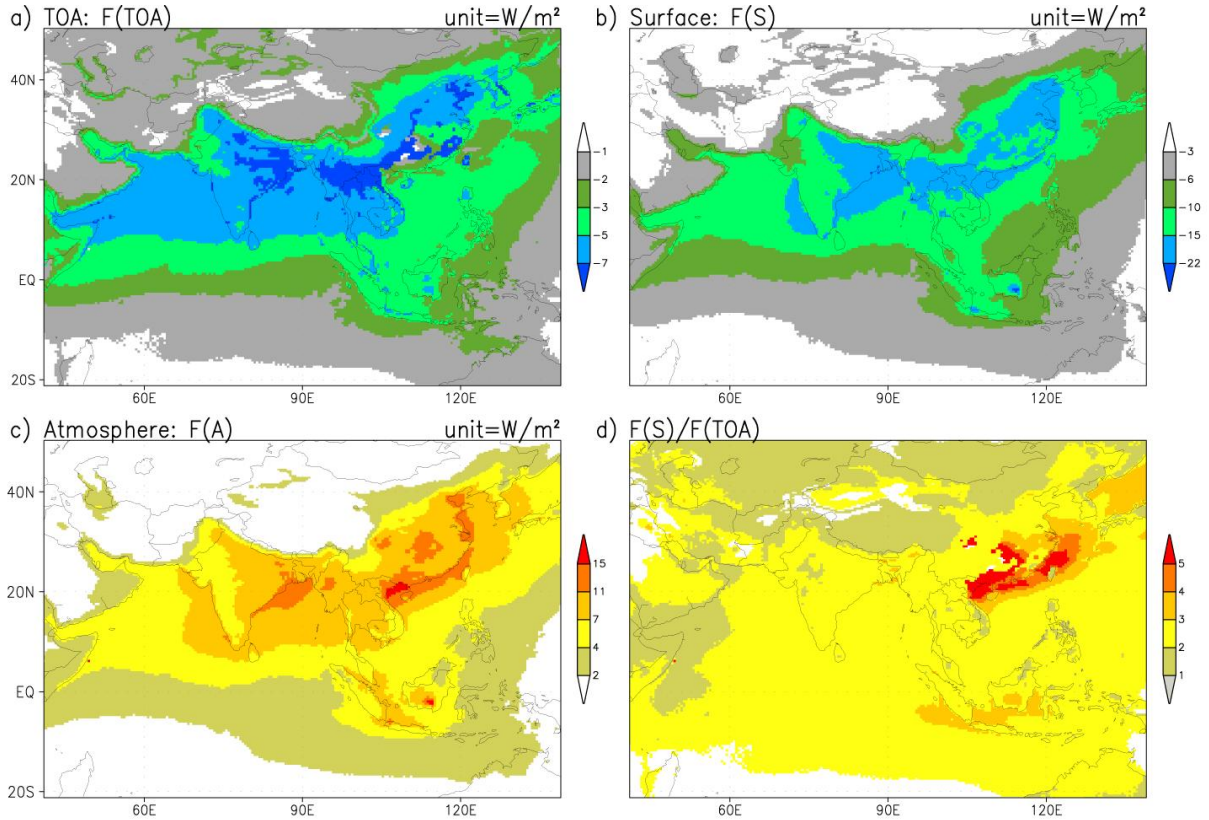
Figure 3. Anthropogenic aerosol radiative forcing averaged over the entire 2001–2004 period. In this and subsequent figures, cloud effects are included.

Conclusion

A high-resolution estimate of monthly 3D aerosol solar heating rates and surface solar fluxes in Asia from 2001 to 2004 is described here. In generating this estimate, a) the PNNL regional model bounded by the NCEP reanalyses was used to provide meteorology, b) MODIS and AERONET data were integrated for aerosol observations, c) the Iowa aerosol/chemistry model STEM-2K1 used the PNNL meteorology and assimilated aerosol observations, and d) 3D aerosol simulations from the STEM-2K1 were used in the Scripps Monte-Carlo Aerosol Cloud Radiation (MACR) model to produce total and anthropogenic aerosol direct solar forcing for average cloudy skies.

The 2001–2004 averaged monthly mean anthropogenic all-sky aerosol forcing ranges from −20 Wm^{-2} to +10 Wm^{-2} (TOA), from +2 Wm^{-2} to +50 Wm^{-2} (atmosphere) and from −66 Wm^{-2} to −3 Wm^{-2} (surface). In the vertical, the forcing is mainly concentrated below 600hPa with maxima near 800hPa. At the 775hPa level, the forcing reaches 1.4 K/day. Seasonally, the low-level forcing is far larger in dry season than in wet season in South Asia, whereas the wet season forcing exceeds the dry season forcing in East Asia.

References

Chung, C. E., V. Ramanathan, D. Kim, and I. A. Podgorny. 2005. Global anthropogenic aerosol direct forcing derived from satellite and ground-based observations. J. Geophys. Res. **110,** doi:10.1029/2005JD006356.

Collins, W. D., et al. 2001. Simulating aerosols using a chemical transport model with assimilation of satellite aerosol retrievals: Methodology for INDOEX. J. Geophys. Res. **106,** 7313-7336.

Khattatov, B. V., et al. 2000. Assimilation of satellite observations of long-lived chemical species in global chemistry transport models. J. Geophys. Res.. **105,** 29135–29144.

Kinne, S., U. Lohmann, J. Feichter, M. Schulz, C. Timmreck, S. Ghan, R. Easter, M. Chin, P. Ginoux, T. Takemura, I. Tegen, D. Koch, M. Herzog, J. Penner, G. Pitari, B. Holben, T. Eck, A. Smirnov, O. Dubovik, I. Slutsker, D. Tanre, O. Torres, M. Mishchenko, I. Geogdzhayev, D. A. Chu, and Y. Kaufman. 2003. Monthly averages of aerosol properties: A global comparison among models, satellite data, and AERONET ground data. J. Geophys. Res. **108,** 4634, doi:10.1029/2001JD001253.

Lorenc, A. C. 1986. Analysis methods for numerical weather prediction. Quart. J. Royal Meteor. Soc. **112,** 1177–1194.

Yu, H., et al. 2006. A review of measurement-based assessments of the aerosol direct radiative effect and forcing. Atmos. Chem. Phys. **6,** 613–666.

FACTORS CHARACTERIZING THE FORMATION EFFICIENCY OF AEROSOLS FROM BIOGENIC VOLATILE ORGANIC COMPOUNDS

M. Dal Maso[1], Th. Hohaus[2], A. Kiendler-Scharr[2], E. Kleist[2], Th. F. Mentel[2], R. Tillmann[2], L. Liao[1], J. Wildt[2]

[1]Division of Atmospheric Sciences, Dept. of Physical Sciences, 00014 University of Helsinki, Finland
[2]Institut für Chemie und Dynamik der Geosphäre, Forschungszentrum Jülich, D-52425 Jülich, Germany

INTRODUCTION

Biogenic Volatile organic compound (VOC) emissions are temperature dependent, with increasing temperatures causing increasing emissions. The ongoing climate change is expected to raise air temperatures; this will have an effect on the vegetation and its emission pattern. Heat stress, which induces changes in plant emissions, is more likely to occur if the global temperature rises. A negative feedback between vegetation and climate has been suggested (Kulmala et al., 2004), with increasing temperatures causing increased aerosol loading, which in turn has a cooling effect.

Most laboratory investigations on the potential to form secondary organic aerosols (SOA) from plant emissions so far have focused on single or a few model VOCs such as for example α-pinene (Saathoff et al., 2003). It has, however, been found that using a single model compound to represent biogenic emissions may lead to biased results: experiments have qualitatively and quantitatively shown that realistic VOC mixtures from real trees produce more particles than α-pinene (Mentel et al., 2009).

In this study we investigated the formation of SOA from the mixture of VOCs emitted by spruce, pine and birch trees by oxidation with ozone and OH.

METHODS

The experiments were performed in the Jülich plant chamber - reaction chamber setup, as described in Mentel et al. (2009), which provides well defined environmental conditions for plants. The setup consisted of two chambers, both approximately 1.5 m3 in volume; the separate volumes are constantly stirred by fans. The plants were put in one of the chambers and fed with CO2. They were also irradiated in a 24-hour cycle to cause emissions of VOCs.

VOC measurements were conducted both in the plant and reaction chamber with a Proton-Transfer-Reaction Mass Spectrometer (PTR-MS, IONICON; Lindinger et al., 1998), to determine the emission kinetics, and an online-GC-MS system for compound identification. VOC mixing ratios were in the lower ppbv to pptv range. Identification by GC-MS was based on mass spectra and retention times of pure chemicals (Fluka / Aldrich, purity > 93 %). The total number of particles formed was measured with an UCPC (TSI3025A). The size distribution of the aerosols in the chamber was measured by a TSI SMPS3936.

The instrumentation enables extensive insights in both the gas phase and aerosol phase characteristics. From the UCPC measurements we could derive the formation rate of particles during the nucleation bursts, while the SMPS measurements allowed the derivation of particle growth rates as well as the determination of volume formation rates. The gas-phase measurements of organics using the PTR-MS could be used to characterize the tree emissions with a good time resolution; using the measured time series of the concentrations of eg. monoterpenes together with ozone data allowed the determination of OH-radical concentrations using a steady state model.

A fraction of the air carrying plant emissions was transferred from the plant chamber to a second camber, the reaction chamber. The reaction chamber was constantly flushed with ozone, and was equipped with a UV-lamp. When the UV lamp was switched on, photolysis of O3 produced OH-radicals and particle formation was initiated. This led to a short nucleation peak, producing a rapid increase in particle number.

After the nucleation peak, no new particles were produced and the condensable vapours condensed on the existing particle surface.

RESULTS

The nucleation rates observed during the particle formation bursts were of the order of 0.1 to 100. The formed particles grew usually with a rate that was of the order of tens of nanometers per hour. The observed rates compare reasonably well with field observations (Kulmala et al., 2004). The air turnover rate in the reaction chamber resulted in an aerosol lifetime of ca one hour; this meant that it was possible to observe events in the chambers with timescales resembling those observed in the field.

The maximum SOA volume produced during VOC oxidation was used as the quantity determining the SOA formation potential. For each of the tree species used, the SOA formation potential showed a first-order linear dependence on the total carbon emission. Plant emissions were more efficient particle producers than α-pinene, with birch the most efficient, then pine and spruce.
The difference in particle formation potential was mainly due to differences in nucleation rates. The particle growth rates were linearly dependent on the total VOC input into the reaction chamber, with pine, spruce and □-pinene not differing significantly from each other, while birch produced slightly more effectively growing particles. The nucleation rates also increased with increasing total carbon, but the dependency varied much more between the species. The species dependence of the nucleation rate seem so be related to the amount of sesquiterpenes or oxidised VOCs in the emission pattern.

Pine trees were subjected to temperatures from 20°C to 35°C and the resulting emissions were fed to a reaction chamber with an ozone concentration of ca. 80 ppb. The temperature in the plant chamber was held constant. Increasing the temperature led to an expected increase in VOC emissions. This caused both increased particle formation and particle growth rates. However, when the CCN activation was measured for two events, one at 25°C and the other at 35°C, it was found that at higher temperatures the CCN activation critical diameter was higher by 10-15 nm, indicating that particles produced from higher-temperature emissions produce particles activate later as CCN.
We investigated the effect of these observations using an aerosol dynamical model. The results indicate that increasing temperatures can have a substantial effect on the CCN production from plant emissions; both the increase in formed number and the reduced losses due to decreased growing time.

Experiments were also performed for alpha-pinene nucleation and varying the intensity of the UV radiation by changing the shading of the UV lamp in the chamber. We also changed the relative humidity (RH) in the reaction chamber. Both increasing the UV irradiation and RH lead to a increase in particle nucleation rate. These effects might be the result of changes in the OH formation process, in which both water vapour and UV radiation participate.

CONCLUSIONS

Although the participation of inorganic vapours in the observed nucleation in the plant chamber is possible, the observation that different plant species show differing particle production efficiencies indicates that the plant emissions play a definite part in the observed nucleation process too. Whether the effect is directly in the nucleation process itself or due to changes in the gaseous precursor chemistry needs to be investigated in more detail. In any case, we show in this study that increased organic emissions not only lead to more aerosol mass, but also increase the number of particles formed.
We also studied the effect of environmental variables such as temperature, relative humidity and UV radiation. Both of the aforementioned parameters increase the nucleation rate observed in the plant chamber. In the case of temperature, this is mostly due to the increase in plant emissions. The reason for the RH effect is more unclear; it is probable that it is mostly due to the OH production enhancement by water.

REFERENCES

Kulmala, M., et al. (2004a). A new feedback mechanism linking forests, aerosols, and climate. Atmos. Chem. Phys. 4, 557-562.

Saathoff, H., et al., Aerosol Science and Technology, 1297-1321, (2003)

Mentel et al., Photochemical production of aerosols from real plant emissions, Atmos. Chem. Phys. Discuss., 9, 3041-3094, 2009

Lindinger, W., Hansel, A., Jordan, A., Int. J. Mass Spec. and Ion Processes, 173, 191-241, (1998)

Kulmala, M., et al.,Formation and growth rates of ultrafine atmospheric particles: A review of observations Aerosol Science 35, 143-176

GROWTH RATES DURING COASTAL NEW PARTICLE FORMATION AT MACE HEAD, IRELAND

M. EHN[1], T. PETÄJÄ[1], P. AALTO[1], M. VANA[1], H. VUOLLEKOSKI[1], D. CEBURNIS[2], G. de LEEUW[1,2], C. O'DOWD[2] and M. KULMALA[1]

[1] Department of Physics, University of Helsinki, Finland
[2] National Univeristy of Ireland, Galway, Ireland
[3] Finnish Meteorological Institute, Helsinki, Finland

INTRODUCTION

Coastal new particle formation was detected already in the 19th century by John Aitken in Scotland. During the last decades this phenomenon has been the focus of numerous studies trying to understand and quantify it (O'Dowd et al., 2000; Dal Maso et al., 2002; McFiggans, 2005). The studies have found particle concentrations exceeding 10^6 cm^{-3} during the particle formation events. The important question concerning the impact of these particles on climate, is whether they will grow large enough to affect cloud condensation nuclei (CCN) concentrations. In this aspect, the important variable is not the nucleation rate, but rather the growth rate (GR).

Growth rates of newly formed coastal particles have been calculated by Dal Maso et al. (2002), who found GR of the order of $15 - 180$ nm per hour for events occurring close to Mace Head. In their data, newly nucleated particles travelled around 100 m before reaching the measurement station. They assumed a constant GR during this short time. O'Dowd et al. (2007) performed measurements on an airplane, following plumes of new particles up to 10 km from the source region. They found GR starting around 120 nm/h after 2 min, decreasing to roughly 50 nm/h after 6 min, and finally after 10 - 20 min the GR were around 20 nm/h. However, these GR were not instantaneous growth rates, but an average GR over the lifetime of the particles, similar to the analysis of Dal Maso et al. (2002). Due to the condensing vapors being depleted, and air mass dilution, the GR is expected to decrease with time. Therefore a more correct way to study the GR, is to express the instantaneous GR as a function of time.

O'Dowd et al. (2007) stated that to provide more accurate estimates than Dal Maso et al. (2002) for GR of new particles in coastal aerosol plumes, airborne measurements are needed. In this study, we have used data from 18 months of stationary measurements at the atmosphperic research station at Mace Head on the west coast of Irelnd, to obtain an estimate of the growth rate of coastal particles during the first hour after nucleation. An air ion spectrometer (AIS) was deployed in January 2006, measuring the ion size distribution from below 1 nm up to 40 nm. The lower half of the measurement range is where the important first steps of the growth take place. As airborne experiments are expensive, require special instrumentation, and only give data for case studies, the approach implemented in this paper gives a statistically better picture of the growth of newly formed coastal particles without the above mentioned complications. The amount of data also allows us to calculate a fit for the size and growth rate of new particles as a function of time.

MEASUREMENTS AND EXPERIMENTAL SETUP

The working principle of an AIS has been described in detail elsewhere (Mirme et al., 2007; Asmi et al., 2009), and the specific instrument measuring in Mace Head was presented by Vana et al. (2008). Thus only a short description will be given here. The AIS measures the mobility distribution of naturally charged positive and negative ions simultaneously with two cylindrical differential mobility analyzers. The mobility range measured by the instrument corresponds to mobility diameters of 0.8-40 nm.
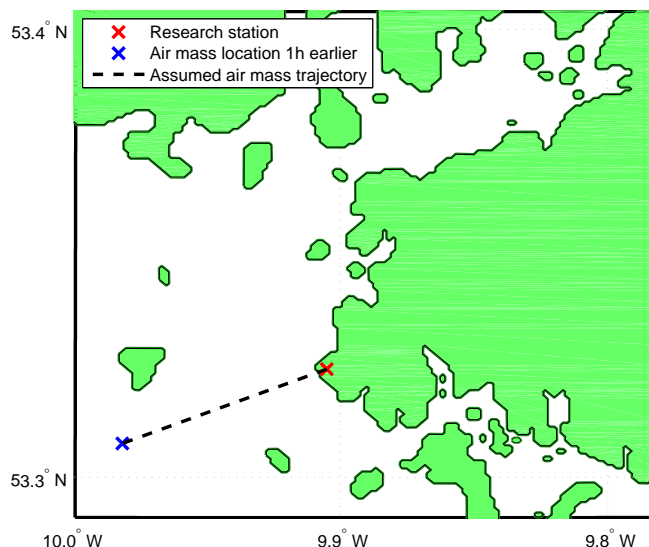
Figure 1: Map of the area around the measurement station (red cross). The dashed line depicts the route the air mass travelled during the last hour prior to reaching the station.

The AIS measured at the Mace Head atmospheric research station on the west coast of Ireland. The station is situated on a peninsula and thus has coast line within a few km in almost all directions except northeast (Fig. 1). The red cross indicates the position of the measurement station. As the coast line has been found to produce large amounts of particles, the station is optimally positioned for analyzing the first steps of the growth of the new particles. Different wind directions and speeds will result in different size distributions reaching the station.

ANALYSIS

The ion number size distributions for each day were inspected visually, and if we observed new particle formation with a clear and stable mode lasting over several scans, the time and position of the mode were recorded. An example of this is shown in Fig. 2; a stable mode of new particles appears at noon and the event last for several hours. We then select a time in the middle of the event (in this example 15:00) and find the particle size at the center of the mode (in this example 6 nm). In this way we collected particle diameter vs. time data for 121 event days.

To be able to calculate growth rates for these days, we needed to know how long ago the particles were formed. The assumption is that these particles are formed on the coast, and the following step
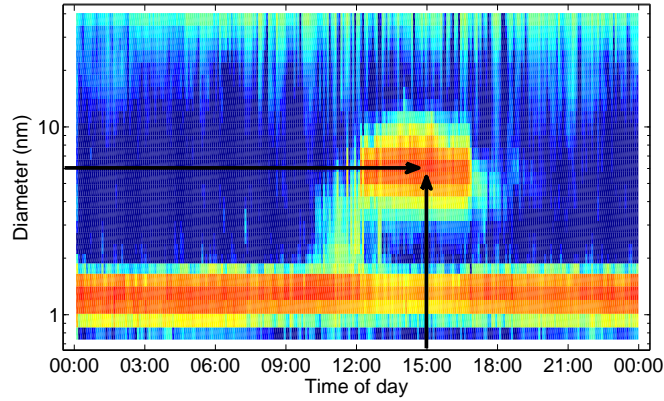
Figure 2: Positive ion size distribution from the AIS. For this example event, 6 nm particles were detected at 15:00.

was to calculate the transport time from the shore line to the station for the times selected above. We calculated HYSPLIT back trajectories and assumed that the air mass followed a straight line during the last hour before reaching the station, as presented in Fig. 1. The blue cross depicts the location of the air mass one hour before reaching the station (red cross). The relative position thus gives us a wind direction, and the relative distance gives us a wind speed (the travel time was always 1 h), making it possible to calculate the time the air mass travelled between the shore line and the station. This time is hereafter referred to as the "growth time". With varying wind speed and direction, we get a distribution of growth times and are able to study the growth rate of the new particles.

The particle size data is taken from air ion measurements. We used the assumption that the particle and ion modes only differ in concentration, not in position. As the smallest particles considered in this study are around 4 nm, this assumption should not be the cause of any large systematic errors. Other possible sources are the uncertainties in HYSPLIT trajectory calculations, and the deviation from the true wind direction to the one calculated by the methods described above. A comparison between this wind direction and the wind directions measured in situ at Mace Head showed a good correlation. The reason for not using the wind direction and the speed measured at the station was that we wanted to study air mass movements up to 1 h backwards, and thus the trajectory was considered more correct although the analysis using measured wind looked very similar. Finally, the exact position of both the coast line and the station itself are crucial. If the relative positions are incorrect, the growth times will appear to be different depending on the wind direction.

RESULTS & DISCUSSION

The result of the growth rate analysis is found in Fig. 3 plotted as particle size versus growth time, and colored by the wind direction (WD). The overall trend is clearly increasing, and we see the strong effect of the wind direction on the transport time with different color groups forming along the x-axis. As the distance to the coast line is different depending on WD, this behavior is expected. However, there is also a WD dependence along the y-axis, with turquoise points (WD≈SSE) forming all the largest particles. Additionally, dark blue and dark red points corresponding to wind roughly from N-NNE have grown to around 10 nm in less than a minute. The explanation for the extremely high growth rates is found in the geography of the stations surroundings, as can be seen in Fig. 1. Air masses coming from NNE or SSE may travel along the coast line for long periods of time
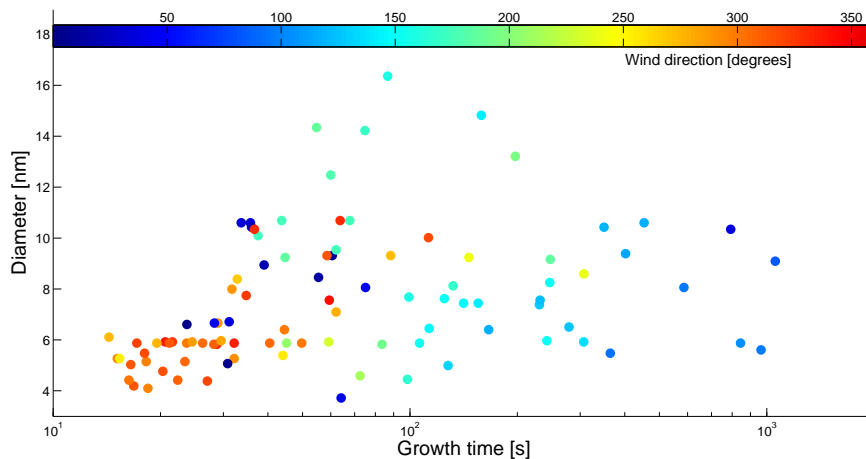
Figure 3: Particle diameter as a function of growth time for all 129 event days, colored by the wind direction.

gathering more precursor vapors than air masses crossing the coast line more perpendicularly. The time spent above a tidal region emitting condensable vapors is directly proportional to the amount of vapor in the air mass. Thus if the trajectory passes the coast line perpendicularly, it will only collect vapors for a few seconds and the particles will not be able to grow as large as particles formed in an air mass that spent tens of seconds above a tidal region.
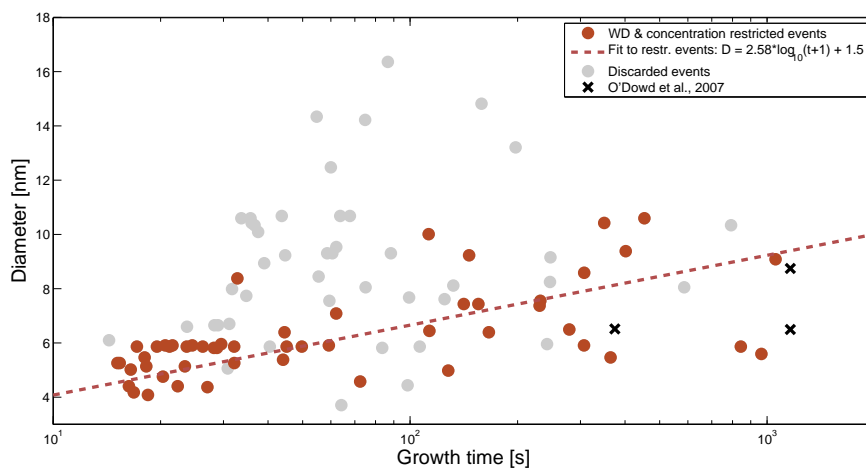
Figure 4: Particle diameter versus growth time for events within a time window of 2 h before to 4 h after low tide. Further restrictions were applied to only consider events when the new particles formed in an air mass that passed over a tidal region roughly perpendicularly (red dots). The black crosses were measured by O'Dowd et al. (2007).

To make sure that we limit our analysis to coastal particle production, events occurring outside a time window starting 2 h before low tide and ending 4 h after were neglected, since these are more likely to be formed somewhere else than on the coast. The resulting 99 events are plotted in fig. 4. In addition to this, we inferred two other selection criteria on the events by neglecting days when the WD was in the range 0-40 or 150-190 degrees, and when the total ion concentration was above 750 cm^{-3}. Events that do not pass these criteria were most likely not formed during the seconds after the last coastal overpass of the air mass. After nucleation takes place, most of the particles are

neutral and it will take some time for them to become charged and reach charge equilibrium, but at the same time the air will be diluting which will decrease the concentration. A high concentration implies that the air mass history is likely more complex and therefore we limited our analysis to events with ion concentrations below 750 cm^{-3}. With the above restrictions, we are left with 55 events corresponding to the red dots in Fig. 4. The dashed red line corresponds to a one parameter least squares fit to the data. The fit assumes a nucleated particle size of 1.5 nm at $t = 0$, and a logarithmic growth curve to account for vapor dilution and depletion. A large part of the events left outside the analysis (grey dots) also fall within the scatter of the red dots, indicating that the fit is representative for a large part of the coastal new particle formation events occurring at Mace Head. The black crosses refer to data from O'Dowd et al. (2007) and all fall below our fit, but also these are within the scatter of our data. The source region for these particles was assumed to be some kilometers NW of Mace Head, and can be found in the northwest corner of Fig. 1.

Table 1: Particle size and growth rates for selected times after nucleation.

Growth time t	Particle size [nm] $2.58 \log_{10}(t+1) + 1.5$	Growth rate [nm/h] $2.58/((t+1)\ln 10)$
1 s	2.3	2020
5 s	3.5	672
10 s	4.2	367
30 s	5.3	130
1 min	6.1	66.1
5 min	7.9	13.4
10 min	8.7	6.71
30 min	9.9	2.24
1 h	10.7	1.12
2 h	11.4	0.56
5 h	12.5	0.22
10 h	13.3	0.11

The fit in Fig. 4 describes the average evolution of new particles forming in air masses passing over a tidal region in the vicinity of Mace Head. The instantaneous growth rates (GR) of these particles is easily calculated by differentiating the particle diameter fit with respect to time. Table 1 gives a summary of size and GR for selected times after nucleation. In the beginning the growth rates are extremely high at a few thousand nm per hour. As the condensing vapors dilute and deplete, the GR quickly decreases, being roughly 3 orders of magnitude lower after 30 min. However, in this short time the particles have already reached 10 nm.

It is important to note that the fit presented here depicts the average growth of coastal particles. Though the fit predicts final particle sizes of 10-15 nm during the first 12 h, some of the events used for the calculations produced larger particles than this in a much shorter time. Additionally, some of grey dots in Fig. 4 not used for calculating the fit showed much higher growth rates within the first few minutes. Thus it is possible that coastal particles become relevant for the climate in situations where air parcels pass along multiple tidal regions. Alternatively, the 10-15 nm particles can function as seeds for other condensing vapors that can continue the growth of these particles up to CCN relevant sizes.

ACKNOWLEDGEMENTS

dispersion model used in this work.

REFERENCES

Asmi, E., Sipilä, M., Manninen, H. E., Vanhanen, J., Lehtipalo, K., GagnÃ©, S., Neitola, K., Mirme, A., Mirme, S., Tamm, E., Komsaare, K., Attouui, M., and Kulmala, M. (2009). Results of the first air ion spectrometer calibration and intercomparison workshop. *Atmos. Chem. Phys.*, 9:141–154.

Dal Maso, M., Kulmala, M., Lehtinen, K., Mäkelä, J., Aalto, P., and O'Dowd, C. (2002). Condensation and coagulation sinks and formation of nucleation mode particles in coastal and boreal forest boundary layers. *J. Geophys. Res.*, 107:10.1029/2001JD001053.

McFiggans, G. (2005). Marine aerosols and iodine emissions. *Nature*, 433:doi:10.1038/nature03.

Mirme, A., Tamm, E., Mordas, G., Vana, M., Uin, J., Mirme, S., Bernotas, T., Laakso, L., Hirsikko, A., and Kulmala, M. (2007). A wide-range multi-channel Air Ion Spectrometer. *Boreal Environ. Res.*, 12:247–264.

O'Dowd, C. D., Becker, E., Mäkelä, J. M., and Kulmala, M. (2000). Aerosol physico-chemical chracteristics over a boreal forest determined by volatility analysis. *Boreal Environ. Res.*, 5:337–348.

O'Dowd, C. D., Yoon, Y. J., Junkerman, W., Aalto, P., Kulmala, M., Lihanvainen, H., and Viisanen, Y. (2007). Airborne measurements of nucleation mode particles i: coastal nucleation and growth rates. *Atmos. Chem. Phys.*, 7:1491–1501.

Vana, M., Ehn, M., Petäjä, T., Vuollekoski, H., Aalto, P., de Leeuw, G., Ceburnis, D., O'Dowd, C. D., and Kulmala, M. (2008). Characteristic features of air ions at mace head on the west coast of ireland. *Atmos. Res.*, 90:278–286.

COMPARISON OF MEASURED AND MODELED BOUNDARY LAYER HEIGHTS IN HELSINKI

N. ERESMAA, J. HÄRKÖNEN, L. KANGAS AND A. KARPPINEN

Finnish Meteorological Institute, P. O. Box 503, FI-00101 Helsinki, Finland

INTRODUCTION

The planetary boundary layer is the lowest part of the troposphere directly influenced by the ground. Substances emitted into this layer disperse gradually horizontally and vertically through the action of turbulence. If sufficient time is given and sinks and sources are absent, these substances become completely mixed. Thus this layer is also called the mixing layer or the mixed layer.

Since the height of the mixing layer, mixing height (MH), determines not only the volume available for pollutants to disperse (Seibert et al., 2000) but also the structure of turbulence in boundary layer (Hashmonay et al., 1991) it is a key parameter in air pollution models. There does not, however, exist any direct way to measure the mixing height. In addition, most of the models and diagnostic formulas for calculating mixing height are based on assumptions not holding in urban areas.

A reliable way for estimating mixing height (MH) is to combine the profile information from any available temperature, wind and pollutant (e.g. particles) measurement. Helsinki Testbed data (http://testbed.fmi.fi) provides enough information for reliably estimating MH, thus making it possible to evaluate the existing MH-models and also to obtain an operative estimate of MH for AQ-forecasting models. In this study we compare MHs evaluated by two computational methods with monitored data based on radio soundings and ceilometer measurements using the data of the Helsinki Testbed campaign.

The emphasis of the study has been on ceilometer method development. Ceilometer measures the atmospheric backscattering profile: the measured backscatter intensity depends mainly on particulate concentration in the air. Since in general aerosol concentrations are lower in free atmosphere than in boundary layer where most of the sources of aerosols are located, the boundary layer height can be distinguished by a strong gradient in the vertical back-scattering profile.

DATA AND MEASUREMENTS

The data used in this study was obtained during the Helsinki Testbed Project (observation period January 2006 – March 2007) in Helsinki Metropolitan area, Finland. Map of the observation sites is shown in figure 1. The observations used in this study have been limited into conditions when the cloud base is above 2000 meters.
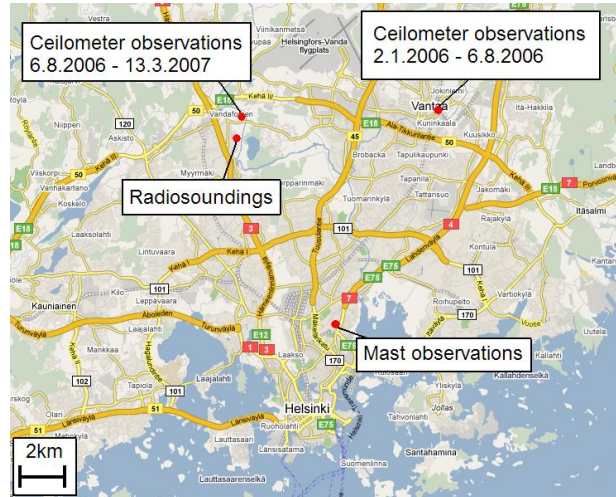
Figure 1. Ceilometer and radiosounding launching sites in the study belonging to the Helsinki Testbed campaign. (Map Google Maps)

Ceilometer observations have been made at two sites. Both of the sites are situated in suburban conditions in Vantaa. The ceilometer used in this study, Vaisala ceilometer CL31, measures the optical backscatter intensity of the air at a wavelength of 910 nm. The main technical properties of the ceilometer CL31 are listed in Table 1. For safety and economic reasons, the laser power used is so low that the noise exceeds the backscattering signal. This can be overcome by summing a large number of return signals, so the desired signal will be multiplied by the number of pulses, whereas the noise, being random, will partially cancel itself. For this study, the raw ceilometer profiles were obtained every 16 seconds. Furthermore, the original ceilometer data were averaged over period of 15 minutes.

Measurement range (m)	0 – 7500
Resolution	10 m (used in this project) or 5 m
Laser system	Indium Gallium Arsenide (InGaAs) MOCVD laser diode
Wavelength (nm)	910 ± 10 at 25°C
Pulse properties	110 ns, 1.2 μJ/pulse
Mean pulse repetition rate (Hz)	8192

Table 1. Technical properties of the ceilometer CL31

Turbulence measurements have been made in 31 meters high mast in Kumpula Campus, Helsinki. Radisoundings have been launched in Vantaanlaakso, Vantaa. The distance between measurement sites is approximately 10 kilometers, therefore we can assume that there is no difference in MH because variable synoptic conditions.

In addition to the measurements we have used the computational MH based on meterological pre-processor of FMI (MPP-FMI). All the methods for MH evaluation are discussed in next section in detail.

METHODS

An idealized 3-step method has been used to obtain the mixing height from ceilometer observations. This method is a revision of the idealized backscattering profile method for one layer described by Steyn et al. (1999). In this 3-step method an idealized profile $B(z)$ is fitted to the measured profile by formula

$$B(z) = \underbrace{\Delta B_{12} - \Delta B_{12} erf\left(\frac{z - MH_1}{\Delta h_1}\right)}_{STEP1} + \underbrace{\Delta B_{23} - \Delta B_{23} erf\left(\frac{z - MH_2}{\Delta h_2}\right)}_{STEP2} + \underbrace{\frac{B_3 + B_4}{2} - \Delta B_{34} erf\left(\frac{z - MH_3}{\Delta h_3}\right)}_{STEP3} \qquad (1)$$

where $\Delta B_{12} = \dfrac{B_1 - B_2}{2}$, $\Delta B_{23} = \dfrac{B_2 - B_3}{2}$ and $\Delta B_{34} = \dfrac{B_3 - B_4}{2}$. B_1 is the backscatter on the ground, B_4 the mean backscatters in free atmosphere above the boundary layer and B_2 and B_3 the mean backscatters between steps. Δh_i is related to the thickness of the entrainment layer (ELT) capping the step. The depth of ELT is typically defined by the mixing ratio of boundary layer and overlying air: the bottom of ELT is defined as a layer in which the mixing ratio is 4-10 %, while the top is defined by ratio of 90-98 %. Ordinates of the error function thus determine the ELT to be $2.77\Delta h_i$ for mixing ratio of 5 – 95 %. The schematic illustration of the idealized profile is shown in figure 1.
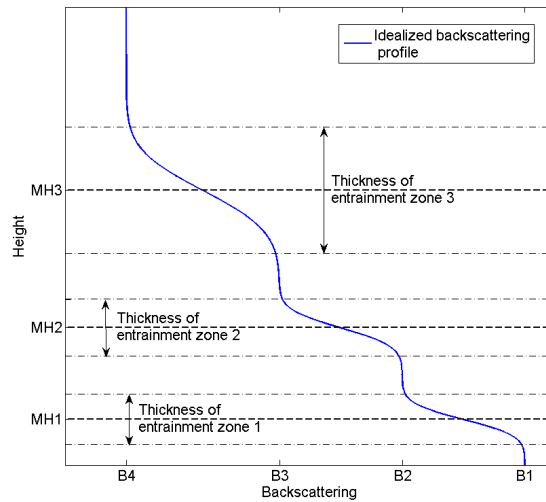
The idealized 3-step method produces three estimates for the mixing layer height. We chose the strongest – i.e. at which the backscatter $B(z)$ faces the biggest decrease – of these steps to mark the MH. However, some exceptions apply to this: the maximum estimate for the MH was set to 2200 meters and the MH may not exceed the height of the cloud.

To estimate the MH based on soundings we divided the soundings into convective and stable cases. This division was based on the temperature profile: if $\partial\theta/\partial z$ between ground and 50 meters above ground is negative, the case was considered convective (13% of investigated cases); otherwise stable (87% of cases). In convective situations, the MH was estimated from radiosoundings by following the dry adiabate starting at the surface up to its intersection with the actual temperature profile (Holzworth 1964, 1967). Thus, this so called "Holzworth-method" estimates the maximum mixing height.

The Richardson number method is traditionally used for MH estimation in stably stratified atmosphere. In this work we followed the Richardson number profile determined by formula of Joffre et al. (2001) with a critical number of 1. This formula aims at smoothing out some of the inherent fluctuations, especially of wind, between adjacent layers:

$$Ri(z_{i+1}) = \frac{g}{T_s} \frac{(\theta_{i+2} - \theta_i)(z_{i+2} - z_i)}{(V_{i+2} - V_i)^2} \qquad (2)$$

T_s is the near-surface air temperature, θ_i the potential temperature and V_i the wind speed at corresponding level z_i. The sub-index i refers to the number of the layer of the profile.

The evaluation of MH in the MPP-FMI is based upon routine radiosounding data (midday and midnight soundings). Under stable and neutral conditions the MH is proportional to the friction velocity and the heat flux integral. Under unstable conditions the MH is determined from the Tennekes (1973) model using the measured temperature profiles and modeled stability parameters. The meteorological preprocessor is discussed in detail in Karppinen et al. (1998)

In stable situations the MH is estimated using a formula (3) discussed by Joffre and Kangas (2001). The Brunt-Väisälä –frequency N above the mixing layer is estimated from radiosoundings; friction velocity u_* and Monin-Obukhov –length L are based on mast observations.

$$MH = C_{st} \left(u_* \middle/ N \right)^{3/4} L^{1/4} \qquad (3)$$

with constant $C_{st} = 7.71 \pm 4.84$.

RESULTS

Examination of Monin-Obukhov –length (based on mast measurements) revealed large uncertainties in turbulence measurements. In some cases the Monin-Obukhov –length obtained from flux measurements was negative even when strong surface temperature inversion indicated extremely stable conditions. Because of this, reliable results could not be gained using the diagnostic formula eq. 3.

The comparison between MHs derived using different methods is shown in figure 2 and table 1.
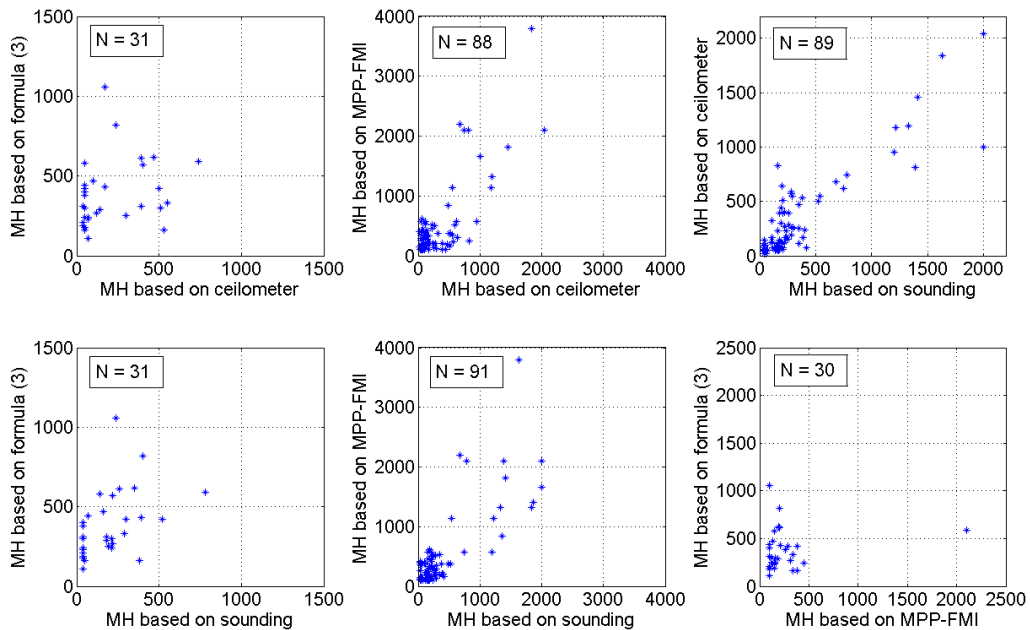
Figure 2. Comparison between MHs estimated using different approaches. The MH is represented in meters.

Correlations between soundings, ceilometer measurements and MPP-FMI (Table 1) are considerably high. Low correlations of formula (3) between the others can be at least partly explained by observed strong temporal fluctuations of friction velocity and Monin-Obukhov –length at Kumpula monitoring site with complex topography and strong dependence of the turbulent fluxes on the wind direction.

	Sounding	Ceilometer	MetPP	Formula (3)
Sounding	-	0.89	0.80	0.45
Ceilometer	0.89	-	0.80	0.25
MetPP	0.80	0.80	-	0.15
Formula (3)	0.45	0.25	0.15	-

Table 1. Correlation coefficients between MH-estimates.

DISCUSSION AND CONCLUSIONS

We observed a very strong correlation between MHs determined by radiosoundings and ceilometer measurements as well as between radiosoundings and MPP-FMI indicating that any of these methods could be used for MH evaluation.

The advantage of the ceilometer method for MH evaluation is its capability to yield continuous information on the boundary layer. Thus this method could be a very useful tool for forecasters. The MH evaluation based on ceilometer could also be used as an input for numerical air quality models.

The threshold of aerosol concentration restricts the ceilometer application for determining MH at regions only moderately polluted However, the investigated 89 cases show that the idealized 3-step method is a suitable method for the estimation of MH in automated use in Helsinki Metropolitan area even if the air is relatively clean compared with most of similar sized cities in Central Europe. In more polluted cities the ceilometer could produce stronger backscattering profiles, and the method would thus produce more reliable results. The current method is also sensitive to atmospheric water droplets limiting the use of it in foggy or cloudy conditions. Also the final criterions for the identification of MH from the three candidate heights is still partly an open question.

REFERENCES

Hashmonay, R., Cohen, A. and Dayan, U. (1991). Lidar observations of atmosphere boundary layer in Jerusalem. *Journal of Applied Meteorology*, 30, 1228-1236

Holzworth, C. G. (1964). Estimates of mean maximum mixing depths in contiguous United States. *Monthly Weather Review*, 92, 235-242

Holzworth, C. G. (1967). Mixing depths, wind speeds and air pollution potential for selected locations in the United States. *Journal of Applied Meteorology*, 6, 1039-1044

Joffre, S. M. and Kangas, M. (2001). Simple diagnostic expressions for the stable and unstable boundary layer height. In Air Pollution IX (eds. Latini, G. and C. A. Brebbia), p, 67-74. WIT Press. Advances in Air Pollution.

Joffre, S. M., Kangas, M. Heikinheimo, M. and Kitaigorodskii, S. A. (2001). Variability of the stable and unstable armospheric boundary-layer height and its scales over a boreal forest. *Boundary-Layer Meteorology*, 99, 429-450

Karppinen, A., Joffre, S. M. and Kukkonen, J. (2000): The refinement of a meteorological preprocessor for the urban environment. *International Journal of Environment and Pollution*, 14, 565-572.

Seibert, P., Beyrich, F., Gryning, S. E., Joffre, S., Rasmussen, A. and Tercier, P. (2000). Review and intercomparison of the mixing height. *Atmospheric Environment*, 34, 1001-1027

Steyn, D. G., Baldi, M. and Hoff, R. M. (1999). The detection of mixed layer depth and entrainment zone thickness from lidar backscatter profiles. *J. Atmos. Ocean. Technol.*, 16, 953-959.

Tennekes, H., 1973. A model for the dynamics of the inversion above a convective boundary layer. *Journal of Atmospheric Sciences*, 30, 558-567

RELATION BETWEEN ^{222}Rn CONCENTRATION AND ION PRODUCTION RATE IN BOREAL FOREST

A. FRANCHIN[1]

[1]Department of Physics, P.O. Box 64, FI-00014, University of Helsinki, Finland

Keywords: Radon, Ion production rate.

INTRODUCTION

Electrically charged aerosol particles (i.e. air ions) are important in the nucleation process because they have been shown to enhance it, but their role is not fully understood and needs further research. Air ions in the troposphere can be generated by galactic cosmic ray and by natural radioactivity (mainly due to radon and uranium content of the soil). Atmospheric ions have two major effects to the earth environment. Firstly air ion induced nucleation plays important role in particle formation, which may lead to the formation of cloud droplets and affect to the weather (Boy et al., 2008). It has been found that the total contribution of ions to nucleation, in Hyytiälä, is about 10% (Kulmala et al., 2007) but it can also be higher and can vary depending on he locations. The ion production rate is one of the key quantity to quantify and to understand the role of small ions in the aerosol formation in atmosphere.

METHODS

In this work the ion production rate has been calculated, using external radiation data and radon concentration measured in Hyytiälä, Finland.
The data of radon activity concentration and the external radiation in atmosphere were used. From those ionization rates were calculated, assuming an average energy of 34 eV per produced ion pair.
The radon activity concentration is measured via its short-lived daughter nuclides ^{214}Pb and ^{214}Bi which are attached to the aerosol particles. The aerosol is collected on a glass fiber filter and a co-axial Geiger-Müller (GM) counter measures the beta activity of the short lived radon daughters.
The experimental setup is made of two identical part each of them consisting of one filter and one GM counter. The air is drawn alternately into one of those two and the flow is switched every four hours to allow to a correction for the ^{220}Rn activity concentration thanks to the difference of the half lives of the two radon isotopes.(Hirsikko et al., 2007).
The external radiation is measured with a scintillation detector Na(Tl). It is maintained in an insulating shelter to avoid a gain drift of the detector due to varying outdoor temperatures.
A computer add-on board containing a high-voltage supply for the photomultiplier tube, a shaping amplifier and a 1024-channel pulse-height analyser records the energy spectra of the ambient gamma radiation field due to uranium content of the soil and cosmic rays.
Energy spectra between100 and 3000 keV were obtained in ten-minutes intervals (Paatero et al., 1998).

RESULTS

The ion production rates in Hyytiälä, were obtained by evaluating the measurements of radiation due to ^{222}Rn decay as well as gamma radiation spectra ("external radiation"). Resulting mean ionization rate is 9.4 ± 1.7 ion pairs per cubic centimeter per second. The average was taken over the whole year of 2008. The absolute value of the ionization rate was found to be governed by external radiation which causes alone a mean ionization rate of 8.7± 1.9 ion pairs cm^{-3} s^{-1} i.e. the 91 % of the total rate. The seasonal variation of the ionization rate due to external radiation and the one due to ^{222}Rnis shown in figure 1(a). The former shows a maximum in August and minimum in March. This is due to snow cover in winter months that decrease external radiation from sources in the soil. The relative seasonal variation of the ionization rate contributed to ^{222}Rn activity is much stronger, though the absolute values are lower: It decreases until September and increases again thereafter. This is due to the change of the height of the mixing boundary layer, which – in average – is located at higher altitudes during summer months. For the same reason, there is a strong diurnal variation of ^{222}Rn activity that can be seen in figure 1(b), while there is no diurnal variation of external radiation at all in the year average.
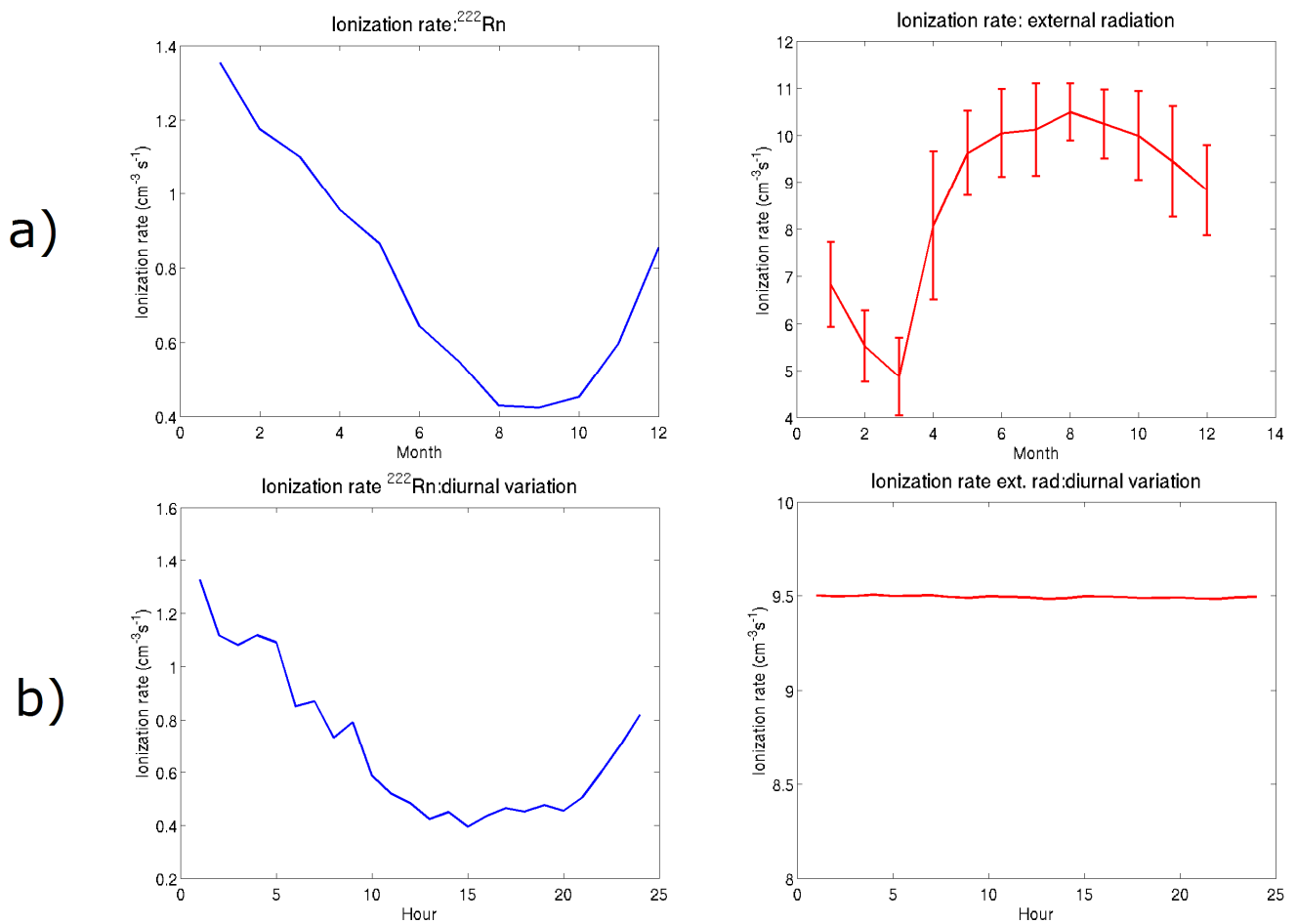
Figure 1: Seasonal (a) and diurnal (b) variations of the ionization rate obtained from measurements of radiation from Rn-222 decay (blue) and from measurements of "external radiation" (red).

	222Rn	external Rad	total Rad	222Rn/ext	222Rn/tot
min	0,40	4,87	5,91	0,04	0,04
median	0,73	9,53	10,12	0,08	0,07
Max	1,35	10,49	10,90	0,22	0,18
mean	0,77	8,67	9,44	0,10	0,09
SD	0,33	1,93	1,67	0,07	0,06
SD/mean	43,42%	22,31%	17,71%	67,39%	61,04%
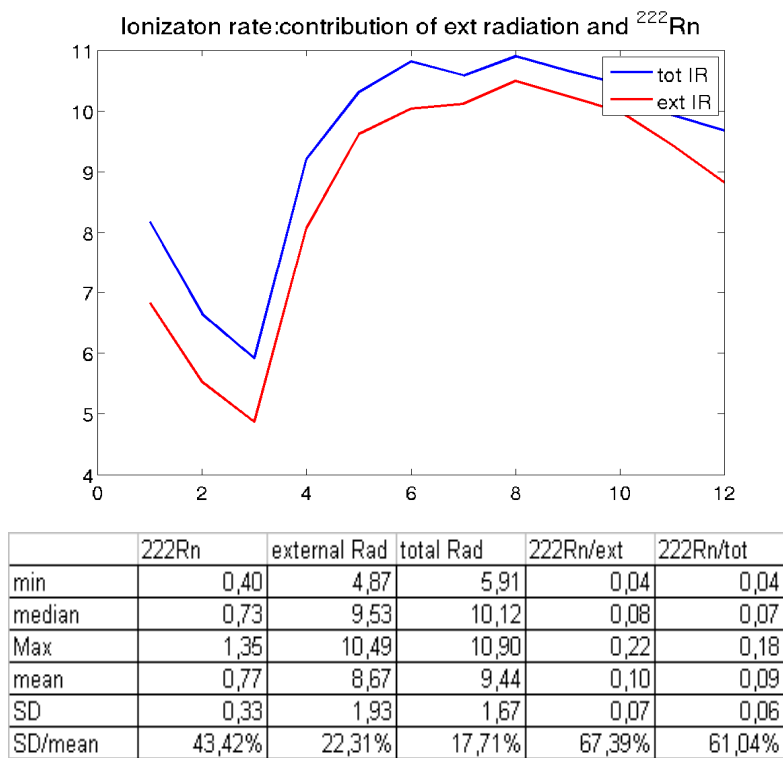
Figure 2. Comparison between the contribution of ^{222}Rn and external radiation to the ion production rate.

The results obtained are similar to (Hirsikko et al. 2007) who used data for the period March 2000 – June 2006.

Both studies results indicate that ion production was typically dominated by the external radiation on this measurement site.

The variation of gamma radiation from the ground is controlled by the water content of the snow cover. The external radiation was at its maximum in late summer and autumn when the surface soil was dry. The minimum occurred in late winter and spring when the water content of the snow cover was at its maximum. The other external radiation component, cosmic radiation has in practice no seasonal cycle. That suggests that cosmic radiation has only a marginal role in the external radiation measurements. Concerning the ^{222}Rn activity concentration, it was found its minimum value during summer and it is not in agreement with the results of (Hirsikko et al 2007) who found the minimum in spring. This may due to meteorological changes from year to year. The diurnal cycle of ^{222}Rn activity concentration was strong, whereas the diurnal cycle of external radiation was practically non–existing throughout the year.

The monthly average ionization rate of about 3.4 ion pairs cm^{-3} s^{-1}, calculated from the small ion balance equation (Schobesberger 2009), is too low compared to the ion production rate found in this work (Fig.3).
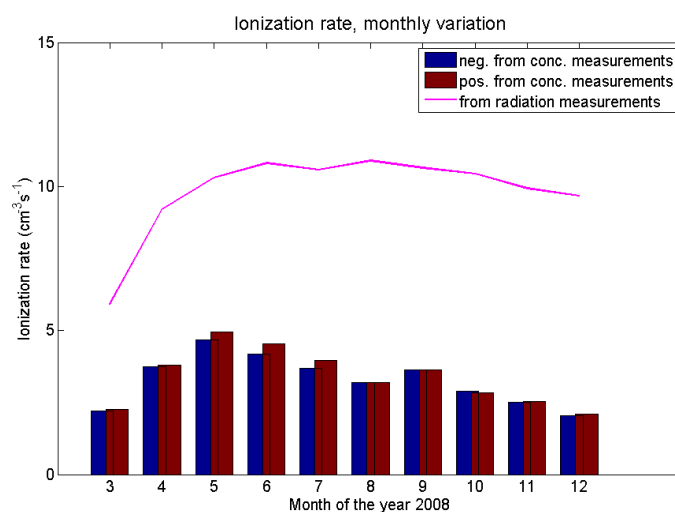
Figure 3. Comparison between the ion production rate calculated in this work (magenta line) and the ion production rate calculated using a balance equation starting from small ion concentration data (blue/red bars) (Schobesberger 2009)

The calculated from small ions and aerosol particle measurements was 3.4 ion pairs cm^{-3} s^{-1}. The method, based on ion and particle measurements, underestimate the ion production rates which means that the sinks of ions and or the recombination are underestimated. That might be due to the chosen range of the small ions (0.4-1.7 nm) in the balance equation. In fact ionization could happen for bigger aerosol particle also, that was not taken into account in the balance equation.

CONCLUSIONS

The ionization rate in Hyytiälä, calculated using external radiation and radon measurements, varied in the range 5.91 – 10.90 ion pairs cm^{-3} s^{-1}. The average and median ion production rate was 9.44 and 10.12 ion pair cm^{-3} s^{-1}, respectively. The contribution of ^{222}Rn to the ion production varied between 4 – 18 %.

This study covers the period between March 2000 and July 2007. The results obtained are similar to (Hirsikko et al., 2007) who used data for the period March 2000 – June 2006.

The monthly average ionization rate of about 3.4 ion pair cm^{-3} s^{-1}, calculated from the small ion balance equation is too low compared to the measured one.

The variation of the ionization rate can be partly explained by the diurnal changes in radon concentration and in aerosol number concentration (ion sink). Ion concentrations are consistent with ion sink and ^{222}Rn concentrations.

In order to understand ionization processes, further studies are necessary.

REFERENCES

Boy, M., Kazil, J., Lovejoy, E.R., Guenther A. and Kulmala M.(2008) Relevance of ion-induced nucleation of sulfuric acid and water in the lower troposphere over the boreal forest at northern latitudes. *Atmos.Res.* 90, 151-158.

Hirsikko, A., Paatero, J., Hatakka, J. & Kulmala (2007) The ^{222}Rn activity concentration, external radiation dose and air ion production rates in a boreal forest in Finland between March 2000 and June 2006. *Boreal Env. Res.* 12: 265–278.

Kulmala, M., Riipinen, I., Sipilä, M., Manninen, H. E., Petäjä, T., Junninen, H., Dal Maso, M.,Mordas, G., Mirme, A., Vana, M., Hirsikko, A., Laakso, L., Harrison, R. M., Hanson, I., Leung, C., Lehtinen, K. E. J. and Kerminen, V-M. (2007) Toward Direct Measurement of Atmospheric Nucleation, *Science* 318: 89 – 92.

Paatero, J., Hatakka, J., Mattsson R., and Lehtinen I..(1994) A comprehensive Station for monitoring atmospheric radioactivity. Rad.Prot. Dos.,54, 1,33-39.

Schobesberger S. (2009) Analysis of the ionization rate at a boreal forest measurement site in Finland in 2008., report series for the joint annual meeting of the Finnish Center of
Excellence and the Finnish Graduate School 2009.

Tammet H. (2006) Continuous scanning of the mobility and size distribution of charged
clusters and nanometer particles in atmospheric air and the Balanced Scanning Mobility Analyzer BSMA. *Atmospheric Research* 82, 523–535.

FACTORS INFLUENCING ON THE CONTRIBUTION OF ION-INDUCED NUCLEATION AS A NUCLEATION MECHANISM IN A BOREAL FOREST SITE, HYYTIÄLÄ, FINLAND

S GAGNÉ[1], T. KURTÉN[1], T. NIEMINEN[1], M. BOY[1], T. PETÄJÄ[1], L. LAAKSO[1,2] and M. KULMALA[1]

[1]Department of Physics, P.O. Box 64, FI-00014, University of Helsinki, Finland
[2]Department of Physics, North-West University, Republic of South Africa

INTRODUCTION

Aerosols have an effect on both the Earth's climate (Chung et al., 2005; Lohmann et al., 2005; Penner et al., 2006) and human health (Pope and Dockery, 2006). Particles nucleated in the boundary layer can contribute to a significant fraction of the cloud condensation nuclei (CCN) population (Spracklen et al., 2008) thus affecting the Earth's climate. Many nucleation mechanisms have been proposed to explain the formation of new atmospheric particles, for example homogeneous, heterogeneous, binary, ternary, activation, kinetic and ion-induced nucleation (IIN). However, the contribution of each mechanism to new particle formation (NPF) remains difficult to assess and may vary both geographically as well as from an event to another. The fraction of nucleated particles produced via IIN is still unclear, and varies significantly depending on the method used in calculations (Laakso et al., 2007; Yu and Turco, 2008). It was also observed that the contribution of IIN to the nucleation mode particle number concentration varies between geographical locations or environments, using similar calculation methods (Iida et al., 2006; Gagné et al., 2008).

NPF events have been observed with an Ion-DMPS (Laakso et al., 2007) since 2005 in SMEAR II (Hyytiälä, Finland, Vesala et al., 1998), in a background boreal forest environment. The Ion-DMPS allows classification of NPF events into overcharged and undercharged days. The overcharged and undercharged classification is based on the charging state of the aerosol population. If there are more charged particles in the sample than there would be in a charge steady-state sample, the sample is said to be overcharged (IIN participates to some extent); if there are fewer charged particles than in a charge steady-state, then the sample is said to be undercharged (IIN participation is ≤ steady-state). In this work, we attempt to understand what conditions are associated with overcharged events compared with undercharged events. At this stage of the work, we have analyzed temperature, relative humidity, water content, sulphuric acid concentration and saturation ratio, cluster and particle concentration (charged and neutral) and condensation sink.

METHODS

The NPF event days were divided into two classes, overcharged and undercharged events, based on a visual inspection of the Ion-DMPS size distribution in its four modes: negative ambient, negative neutralized, positive ambient and positive neutralized. For a given NPF event to be classified as an overcharged event both the negative and positive polarities had to be overcharged; for it to be classified as an undercharged event both polarities had to be either at steady-state or undercharged. We found 164 overcharged events and 42 undercharged events between April 2005 and the end of 2007 (Table 1). The distribution of these events during the year is shown in figure 1.

The supporting data presented in this abstract were retrieved from a measurement mast. The temperature, relative humidity and water concentration were taken from 4.2m height. The charged clusters, as well as ion concentrations were taken from a BSMA (Balance Scanning Mobility Analyzer, Tammet et al., 2006). The total particle number in nucleation, Aitken and accumulation modes and the condensation sink were

taken from a DMPS (Differential Mobility Particle Sizer, Aalto et al., 2001). The sulphuric acid concentration and saturation ratio are calculated by a model (SOSA, Boy et al., in preparation).

Negative	Positive	Classification	Number
Over	Over	Overcharged	164
Over	Under	Discarded	40
Under	Over	Discarded	
Under	Under	Undercharged	42

Table 1. Number of new particle formation event days in each class between April 2005 and the end of 2007. Each class depends on the combination of the negative and positive polarity classification.

Distribution of days over the year
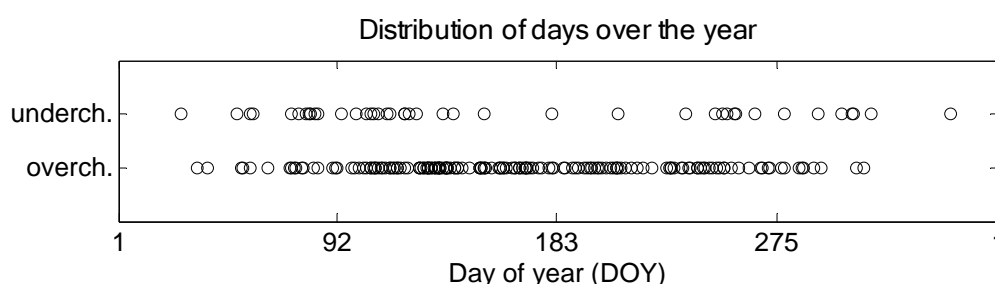
Figure 1. Distribution of overcharged and undercharged days over the year in Hyytiälä, Finland. Overcharged events are centered around summer while undercharged events have a minimum in summer. Generally, there are very few events in winter, hence the rare points before and after day of year 1.

RESULTS

Nearly no undercharged events take place during summer (Figure 1). In order to gauge the role of temperature to the charging state, we separated the summer months (June-July-August, day of year 152 to 243) from the rest of the data. The temperature for non-summer overcharged events was, in average, around 5 degrees Celsius higher than for undercharged events; the relative humidity for overcharged event was 10% lower than for undercharged events. This agrees with the ion production rate measurements by Laakso et al.[13] and the general idea that fog and rain may act as an additional ion sink. The absolute humidity however, was around 35% higher for overcharged events.

The number concentration of nucleation mode particles (DMPS) was higher for undercharged events (figure 2). This behavior is in agreement with observations made in Hyytiälä with different instruments[14]. Other particle modes didn't show any significant difference even though the accumulation mode particle concentration was slightly higher during overcharged events.

The concentration of cluster ions, measured with the BSMA, was about the same during the NPF event itself but was a bit higher before and after the NPF for overcharged events compared to undercharged events. The drop in the concentration of cluster ions was around 20% bigger for overcharged events when compared to undercharged ones in the case of negatively charged particles. A plausible explanation could be activation of a bigger fraction of cluster ions, as it should be with IIN. The difference in the behavior between polarities is consistent with observations that IIN is more frequent for the negative polarity than for the positive polarity. The charged cluster concentration is also higher for overcharged events than for undercharged events, for both polarities.

The sulphuric acid concentration was about the same both for overcharged and undercharged events. The sulphuric acid saturation ratio is 4 times higher for undercharged days that it is for overcharged days (figure 3). The temperature difference can only explain for a factor of 2.

110
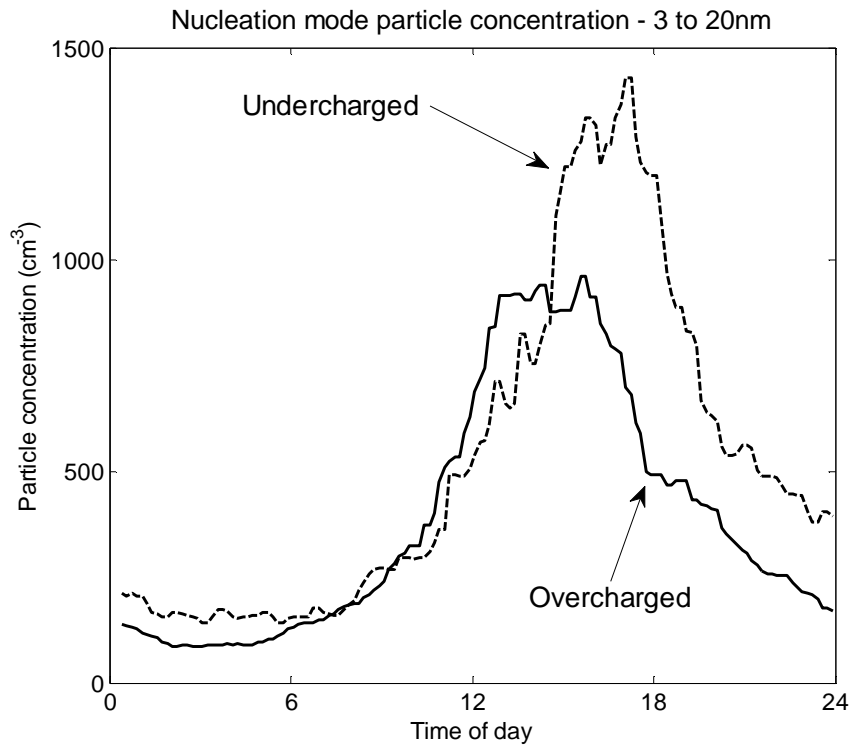
Figure 2. Median nucleation mode particle concentration (3 to 20nm, taken from the DMPS) as a function of time of day during over- and undercharged events. Undercharged events (dashed line) yield higher concentrations than overcharged events (full line).
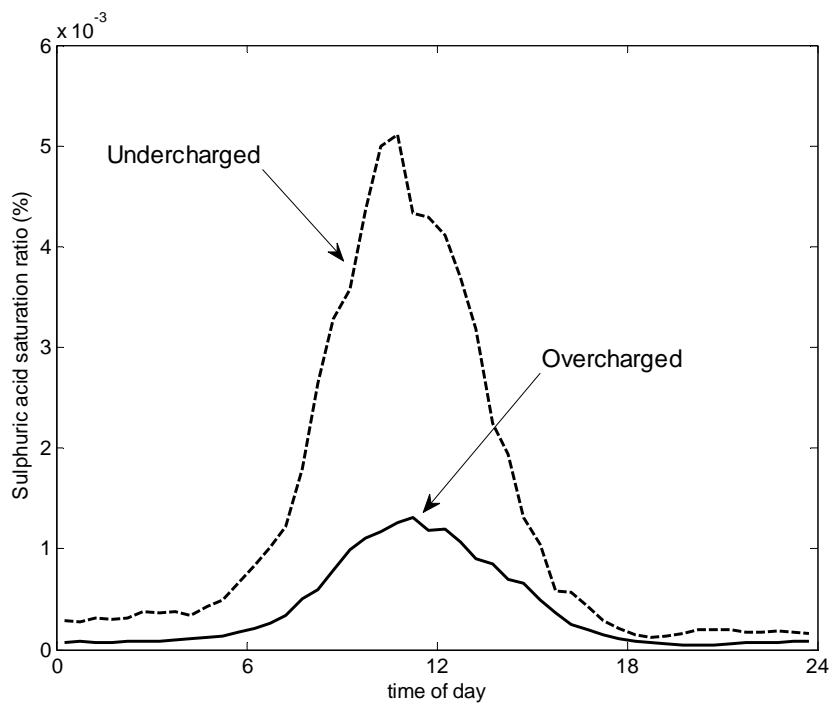
Figure 3. Median sulphuric acid saturation ratio as a function of time of day during over- and undercharged events. Undercharged days (dashed line) take place in a sulphuric acid saturation ratio about 4 times higher than overcharged days (full line).

CONCLUSIONS

The most likely explanation at this point of our analysis is that warmer temperatures are making it more difficult for particles to activate neutrally while it has very little effect on IIN. So assuming that a more or less constant number of particles are nucleated through IIN, the neutrally nucleated particles concentration would be smaller, thus giving a larger ion-induced contribution. This is also in agreement with the result that the concentration of nucleation mode particles is higher for undercharged events.

REFERENCES

Aalto, P., Hameri, K., Becker, E., Weber, R., Salm, J., Makela, J.M., Hoell, C., O'Dowd, C.D., Karlsson, H., Hansson, H.C., Vakeva, M., Koponen, I.K., Buzorius, G. and Kulmala M. (2001) Physical characterization of aerosol particles during nucleation Events. *Tellus,* 53, 344-358.

Chung, C.E., Ramanathan, V., Kim, D. and Podgomy, I.A. (2005) Global anthropogenic aerosol direct forcing derived from satellite and ground-based observations. *J. Geophys. Res.* 110, D24207,doi:10.1029/2005JD006356.

Gagné, S., Laakso, L., Petäjä, T., Kerminen, V.-M. and Kulmala, M. (2008) Analysis of one year of Ion-DMPS data from the SMEAR II station, Finland. *Tellus*, 60, 318-329.

Iida, K., Stolzenburg, M., McMurry, P., Dunn, M. J., Smith, J. N., Eisele, F. and Keady, P. (2006) Contribution of ion-induced nucleation to new particle formation: methodology and its application to atmospheric observations in Boulder, Colorado. *J. Geophys. Res.*, 111, D23201, doi:10.1029/2006JD007167.

Laakso, L., Petäjä, T., Lehtinen, K. E. J., Kulmala1, M., Paatero, J., Hõrrak, U., Tammet, H. and Joutsensaari, J. (2004) Kinetic nucleation and ions in boreal particle formation events. *Atmos. Chem. Phys.,* 4, 1933-1943.

Laakso, L., Gagné, S., Petäjä, T., Hirsikko, A., Aalto, P.P., Kulmala, M. and Kerminen, V.-M. (2007) Detecting charging state of ultra-fine particles: instrumental development and ambient measurements. *Atmos. Chem. Phys.* 7, 1333-1345.

Lohmann, U. and Feichter, J. (2005) Global indirect aerosol effects: a review. *Atmos. Chem. Phys.* 5, 715-737.

Penner, J.E., Quaas, J., Storelvmo, T., Takemura, T., Boucher, O., Guo, H., Kirkevåg, A., Kristjánsson, J.E. and Seland Ø. (2006) Model intercomparison of indirect aerosol effects. *Atmos. Chem. Phys.* 6. 3391-3405.

Pope, C.A.III and Dockery, D.W. (2006) Health effects of fine particulate air pollution: lines that Connect. *J. Air Wast Manage. Assoc.*, 56, 709-742.

Spracklen, D.V., Carslaw, K.S., Kulmala, M., Kerminen, V.-M., Sihto, S.-L., Riipinen, I., Merikanto, J., Mann, G.W., Chipperfield, M.P., Wiedensohler, A., Birmili, W. and Lihavainen H. (2008) The contribution of boundary layer nucleation events to total particle concentrations on regional and global scales. *Geophys. Res. Let.*. 35, L06808, doi:10.1029/2007GL033038.

Tammet, H. (2006) Continuous scanning of the mobility and size distribution of charged clusters and nanometer particles in atmospheric air and the Balanced Scanning Mobility Analyzer BSMA. *Atmos. Res.*, 82 523–535.

Vana, M., Tamm, E., Hõrrak, U, Mirme, A., Tammet, H., Laakso, L., Aalto, P., and Kulmala, M., (2006) Charging state of atmospheric nanoparticles during the nucleation burst events. *Atmos. Res.*, 82, 536-546.

Vesala, T., Haataja, J., Aalto, P., Altimir, N., Buzorius, G., Garam, E., H¨ameri, K., Ilvesniemi, H., Jokinen, V., Keronen, P., Lahti, T., Markkanen, T., M¨akel¨a, J., Nikinmaa, E., Palmroth, S., Palva, L., Pohja, T., Pumpanen, J., Rannik, U., Siivola, E., Ylitalo, H., Hari, P., and Kulmala, M. (1998) Long-term field measurements of atmosphere-surface interactions in boreal forest combining forest ecology, micrometeorology, aerosol physics and atmospheric chemistry *Trends in Heat, Mass & Momentum Transfer*, 4, 17–35.

Yu, F. and Turco, R. (2008) Case study of particle formation events observed in boreal forests: implications for nucleation mechanisms. *Atmos. Chem. Phys.* 8, 6085-6102 (2008).

VOC EMISSIONS OF FOREST FELLING

S. HAAPANALA[1], H. HAKOLA[2], H. HELLÉN[2], M. VESTENIUS[2], and J. RINNE[1]

[1]Department of Physics, P.O. Box 68, FI-00014 University of Helsinki, Finland
[2]Air Chemistry Laboratory, Finnish Meteorological Institute, P.O. Box 503, FI-00101 Helsinki, Finland

INTRODUCTION

Biogenic volatile organic compounds (BVOC) have many important effects on atmosphere and climate. Although the emissions of BVOCs in boreal areas have been studied quite intensively, there are still large gaps remaining. Especially the seasonality of the emission rates is poorly known (Rinne et al., 2008). The emission rates from Scots pine have been measured throughout the growing season (Tarvainen et al., 2005) and there are few measurements from spruces also during dormant period (Hakola et al., 2006). These studies show that little VOCs are emitted also during winter, although these emission rates are quite low due to low temperatures (Tarvainen et al., 2005).

Mechanical damage on trees is known to enhance VOC emission (e.g. Juuti et al., 1990; Hakola et al., 2001). Lots of forestry work is conducted during winter and spring in boreal forests. Cut stumps and logging residue provide a source of BVOCs into the atmosphere (Räisänen et al., 2008), possibly also in biologically inactive periods. Especially the spring period is interesting because the maximum of aerosol particle formation events are observed at that time (Dal Maso et al., 2005), and it is expected to be strongly affected by BVOCs in the atmosphere (Kulmala et al., 2004).

The aim of the present study was to measure the VOC emissions from tree stumps and forest felling areas, and to study their temporal evolution and dependence on environmental parameters. From the results, we can evaluate the share from forestry work in comparison to intact ecosystems.

METHODS

The emission rates and composition were measured from fresh felling areas in the southern Finland during summers 2007 and 2008. In 2007 the measurements were conducted on a clear cut area of about 4.3 ha, felled in November 2006. The emissions from single stumps of Norway spruce, Scots pine and birch were measured using enclosures. The same spruce stump was measured in May, June and August of 2007. Samples were also taken from a birch and a pine stump on one day in June. In 2008 we conducted the measurements on a seeding felling area of about 4.0 ha, felled in the end of April. Beginning in May, the emissions of two Scots pine stumps were measured using enclosures, and in addition to that the ecosystem scale emission was measured using disjunct eddy accumulation.

The enclosure measurements were carried out by placing a Teflon bag around a tree stump. Air was pumped through the bag with a flow rate of about 4 l min^{-1}. The inlet air was passed through a MnO_2 ozone scrubber. The samples were taken from the inlet and the outlet port to Tenax-TA/Carbopack-B adsorbent tubes with a constant flow rate of about 0.1 l min^{-1}. The emission rates were normalized to the cross sectional area of the stump. Temperature inside the enclosure and photosynthetic photon flux density (PPFD) outside the enclosure were recorded at the same time.

The ecosystem scale emission flux was measured using disjunct eddy accumulation (DEA) method (Rinne et al., 2000). During the operation, a large primary sampling valve was opened once a minute for 200 ms. This allowed the pre-evacuated intermediate storage reservoir to fill with sample air. The vertical wind speed, measured by a sonic anemometer (Metek USA-1) placed about 2 m above ground level, was recorded simultaneously. After the sampling, air was drawn through one of the adsorbent tubes reserved

for updraft and downdraft samples. The decision on which tube should be used was based on the direction of the vertical flow at the time of sampling. The duration of the adsorbent flow was proportional to the vertical wind velocity resulting in linearly proportional sample volume, and hence true eddy accumulation. Two similar samplers were operated simultaneously in turns resulting in 30 s sample interval and altogether 120 samples during one hour sampling period.

All adsorbent samples were later analyzed for mono- and sesquiterpenes using an automatic thermodesorption device (Perkin-Elmer ATD-400) connected to a gas chromatograph (HP-5890), with a mass-selective detector (HP-5972).

RESULTS

The birch stump emitted some monoterpenes, mainly α-pinene, β-pinene, limonene and camphene. The average monoterpene emission was 40 μg m^{-2} h^{-1}. Sesquiterpene emission of the birch stump was negligible. It was not possible to indentify whether the stump was silver or downy birch. Both of these birch species are known have variable mono- and sesquiterpene emissions from their leaves (Hakola et al., 2001; Vuorinen et al., 2005). However, the emission from the wooden parts (stem, bark), or their terpenoid content are not well known. As birches don't have resin ducts or other large storage structures for terpenoids, it is easy to understand that the emission was not very strong after the trees were cut down.

Both spruce and pine stump emitted large amounts of monoterpenes and some sesquiterpenes. The average monoterpene emission from spruce and pine stumps, measured in 2007, were 5100 μg m^{-2} h^{-1} and 52000 μg m^{-2} h^{-1}, respectively. The average mono- and sesquiterpene emissions from the pine stumps measured in 2008 were 25000 μg m^{-2} h^{-1} and 600 μg m^{-2} h^{-1}, respectively. These emission rates were significantly higher that those of birch, which is easily understood due to existence of resin ducts in coniferous trees (Table 1).

	Birch, 2007	Spruce, 2007	Pine, 2007	Pine, 2008
Σmonoterpenes	40	5100	52000	25000
Σsesquiterpenes	0	120	140	600

Table 1. A summary of the average emissions [μg m^{-2} h^{-1}] of monoterpenes and sesquiterpenes from stumps of different tree species.

For the spruce stump, the monoterpene emission rates remained quite constant for the whole summer (see Figure 1) and they were not dependent on temperature or on the PPFD. The sesquiterpene emission rates increased in August compared to the measurements earlier in summer. In August the sesquiterpene contribution was about 4 % of the monoterpene emission. Earlier, in May and in June it was only less than 1 %. Hakola et al., (2003) measured the emission rates from living Norwegian spruce and they found out that the contribution of the sesquiterpenes was quite small in comparison with monoterpene emission rates early summer, but in July the emission rates of sesquiterpenes increased contributing more than monoterpenes to the total VOC emission. These high emissions of sesquiterpenes are probably not stored in a tree but released for defensive or other purposes.

In 2008 we measured the emission from a pine stump several times, beginning 3 weeks after logging. The emission rates of both mono- and sesquiterpenes were dependent on temperature. We normalised the measured emissions to temperature following the exponential temperature dependency algorithm of the emissions (Guenther et al., 1993). The resulting temperature dependence coefficients for mono- and sesquiterpene emissions were 0.16 ℃$^{-1}$ and 0.29 ℃$^{-1}$, respectively. Using these values we normalised the

measured emission rates to 30ºC, and plotted their temporal evolution (see Figure 1). During the first month there was some fresh resin on the pine stump surface, probably causing the high emission. In a typical managed forest about 0.5% of the land surface is covered with stumps. This means that the ecosystem scale emission from the stumps alone is around 200 µg m^{-2} h^{-1}.
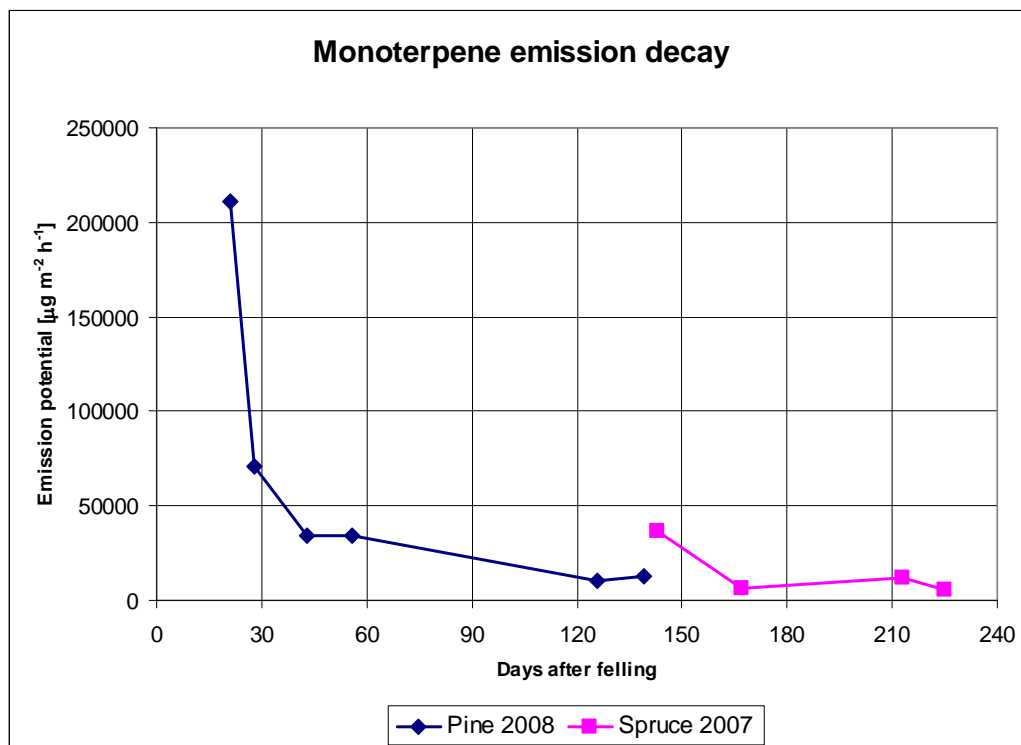
Figure 1. Temporal decay of monoterpene emission potential of two stumps.

The monoterpene emission spectra of the two pine stumps studied in 2008 are plotted in Figure 2. The tree 1 is clearly a strong α-pinene emitter while tree 2 is strong Δ^3-carene emitter. These two genotypes of pine are known to grow in Finland (e.g. Tarvainen et al., 2005 and references therein)
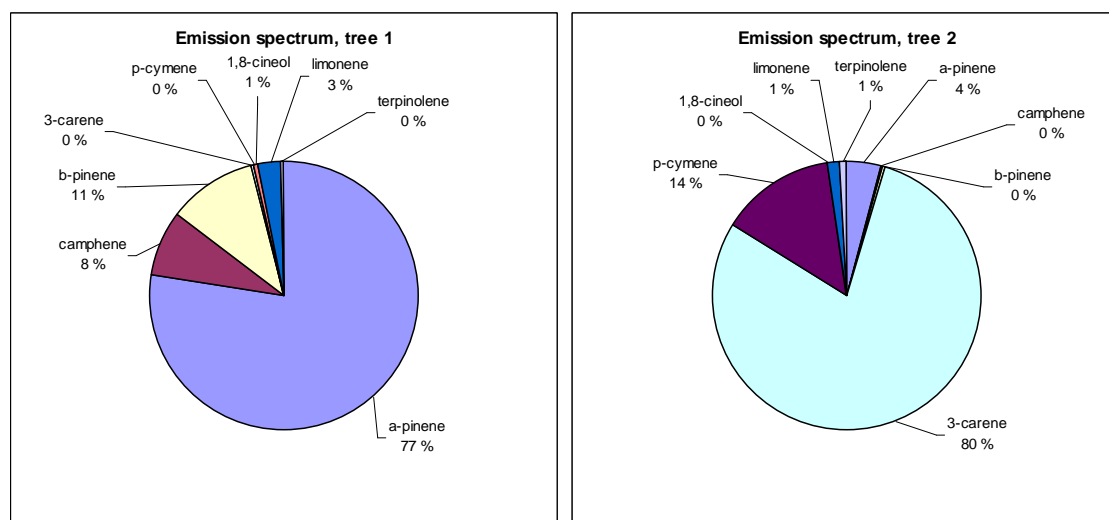
Figure 2. The emission spectra of monoterpenes from two pine stumps studied in 2008.
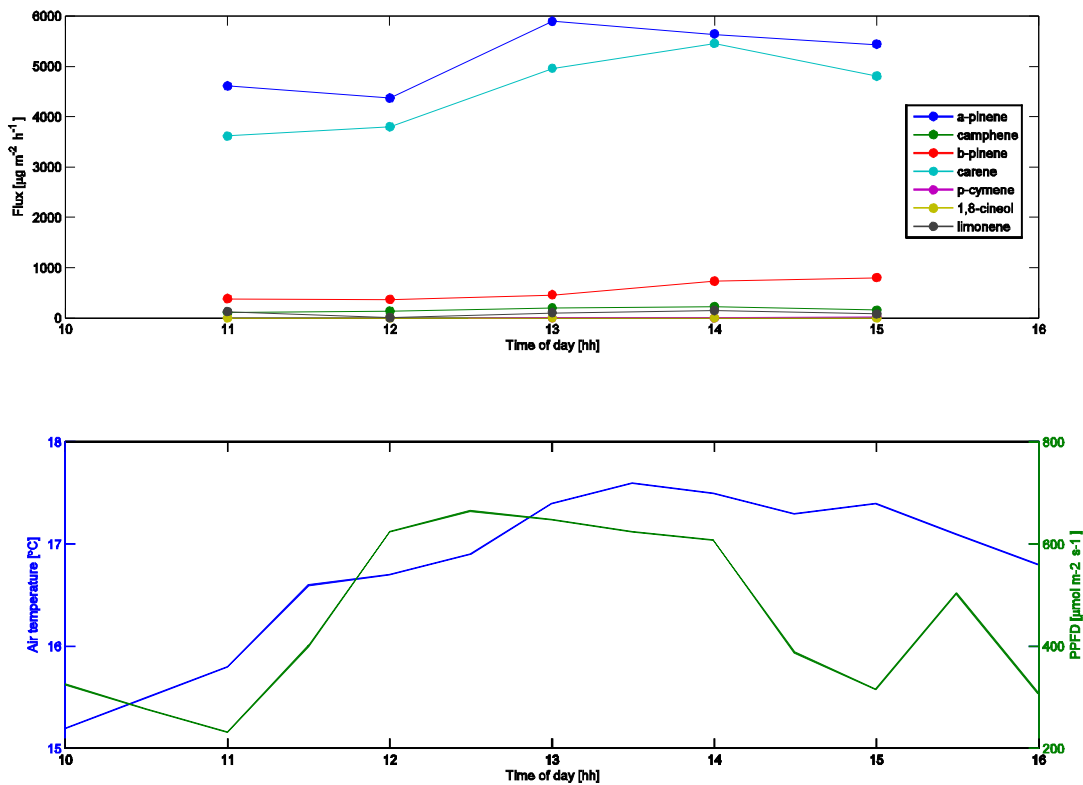
Figure 3. The upper panel show ecosystem scale fluxes of monoterpenes on 26 June 2008. The lower panel show air temperature and incident PPFD at the same time.

The preliminary results from ecosystem scale DEA measurements suggest monoterpene emissions in the scale of 10000 μg m^{-2} h^{-1} (see Figure 3). The emissions of α-pinene and Δ^3-carene are almost equal. The other monoterpenes contribute only a little to the total emission. Normalising the emissions to 30ºC yield to emission potential of about 30000 μg m^{-2} h^{-1}. This is significantly higher than the monoterpene emission potential of intact boreal forests.

CONCLUSIONS

We studied the enhanced VOC emissions caused by forest management. We studied direct stump emissions and ecosystem scale emission including both stumps and logging residual. After felling, the emission from a single stump was about similar than the emission from growing tree. The emission decreased within a couple of months after felling. The ecosystem scale monoterpene emission from a timber felling area was significantly higher than that of intact forest. Roughly 10 to 100 fold emissions depending on the age of the area may be expected. If about 2% of Finnish forests are under management annually, one may expect that forestry operations may contribute as much as 20% to the national monoterpene emission.

REFERENCES

Dal Maso M., Kulmala, M., Riipinen, I., Wagner, R., Hussein,T.,Aalto, P. P., and Lehtinen, K. E. J., (2005). Formation and growth of fresh atmospheric aerosols: eight years of aerosol size distribution data from SMEAR II, Hyytiälä, Finland. *Boreal Env. Res.*, 5, 323–336.

Guenther, A.B., Zimmerman, P.R., Harley, P.C., Monson, R.K. and Fall, R., (1993). Isoprene and Monoterpene Emission Rate Variability: Model Evaluations and Sensitivity Analyses. *J. Geophys. Res.*, 98, 12609-12617.

Hakola, H., Laurila, T., Lindfors, V., Hellén, H., Gaman, A., and Rinne, J., (2001). Variation of the VOC emission rates of birch species during the growing season. *Boreal. Env. Res.*, 6, 237-249.

Hakola, H., Tarvainen, V., Laurila, T., Hiltunen, V., Hellén, H., and Keronen, P., (2003). Seasonal variation of VOC concentrations above a boreal coniferous forest. *Atmos. Environ.*, 37, 1623-1634.

Hakola, H., Tarvainen, V., Bäck, J., Ranta, H., Bonn, B., Rinne, J., and Kulmala, M., (2006). Seasonal variation of mono- and sesquiterpene emission rates of Scots pine. *Biogeos.*, 3, 93-101.

Juuti, S., Arey, J., and Atkinson, R., (1990). Monoterpene emission rate measurements from a Monterey pine. *J. Geophys. Res.*, 95, 7515-7519.

Kulmala, M., Vehkamäki, H., Petäjä, T., Dal Maso, M., Lauri, A., Kerminen, V.-M., Birmili, W., and McMurry, P. H., (2004). Formation and growth rates of ultrafine atmospheric particles: a review of observations, *J. Aerosol Sci.*, 35, 143-176.

Rinne, J., Delany, A., Greenberg, J., and Guenther, A., (2000). A true eddy accumulation system for trace gas fluxes using disjunct eddy sampling method. *J. Geophys. Res.*, 105, 24791-24798.

Rinne J., Bäck J., and Hakola H.., (2008). Volatile organic compound emissions from North European boreal landscape: Progress and key gaps. Proceedings of the Nordic Centers of Excellence BACCI (Biosphere-Atmosphere-Cloud-Climate Interactions) and CBACCI (Carbon-BACCI), Activities in 2003-2007. Report Series in Aerosol Science, 92, 171-181.

Räisänen, T., Ryyppö, A., and Kellomäki, S., (2008). Monoterpene emission of boreal a boreal Scots pine (Pinus sylvestris L.) forest. *Agric. For. Meteorol.*, 149, 808-819.

Tarvainen, V., Hakola, H., Hellén, H., Bäck, J., Hari, P., and Kulmala, M., (2005). Temperature and light dependence of the VOC emissions of Scots pine. *Atmos. Chem. Phys.*, 5, 989-998.

Vuorinen, T., Nerg, A.-M., Vapaavuori, E., and Holopainen, J., (2005). Emission of volatile organic compounds from two silver birch (Betula pendula Roth) clones grown under ambient and elevated CO2 and different O3 concentrations. *Atmos. Environ.*, 39, 1185-1197.

MONITORING THE FORMATION OF SULPHURIC ACID CLUSTERS IN A LAMINAR FLOW TUBE USING AN ATMOSPHERIC PRESSURE INTERFACE TIME OF FLIGHT MASS SPECTROMETER

J. HAKALA[1], T. PETÄJÄ[1], M. EHN[1], M. SIPILÄ[1,2], H. JUNNINEN[1] J. VANHANEN[1], J. MIKKILÄ[1] , D.R. WORSNOP[1,3] and M. KULMALA[1]

[1]Department of Physics, P.O. Box 64, FI-00014, University of Helsinki, Finland
[2]Leibniz Institute for Tropospheric Research, Permoserstrasse 15, D-04318, Leipzig, Germany
[3]Aerodyne Research, Inc., 45 Manning Road, Billerica MA 01821-3976, USA

INTRODUCTION

Atmospheric new particle formation occurs in various environments (Kulmala et al. 2004). Although technical development of the instruments has been pushing the detection efficiency of the instruments closer to the actual sizes where nucleation takes place (Kulmala et al. 2007) there are still open questions related to this phenomenon. Several theories, including binary nucleation of sulphuric acid and water (Mirabel and Katz, 1974), ternary nucleation of H_2SO_4, H_2O and NH_3 (Korhonen et al., 1999), biogenic iodine (O'Dowd et al., 2002), barrierless kinetic nucleation (Weber et al., 1996), activation (Kulmala et al., 2006), organic nucleation (Marti et al. 1997), and ion-induced nucleation (Yu and Turco, 2000) have been put forward and different precursor gases suggested to explain the observed formation and subsequent growth to climatically relevant sizes. Sulphuric acid is considered to be one of the key precursors to new particle formation in the atmosphere (Weber et al. 1996). In laboratory conditions, sulphuric acid readily forms particles (Viisanen et al. 1997) and also the ambient measurements have revealed correlation between the gas phase sulphuric acid and the appearance of atmospheric nanoparticles (Weber et al 1996, Kuang et al. 2008, Nieminen et al. 2009). The initial steps of new particle formation may very well be the formation of sulphuric acid clusters: a sub-nanometer size cluster containing two or more sulphuric acid molecules. To study the formation of new particles containing sulphuric acid, laboratory experiments in stable conditions with reliable sulphuric acid generation and detection methods are needed. In this study an atmospheric pressure interface time of flight mass spectrometer (API-TOF) was used to monitor the formation of sulphuric acid clusters in a laminar flow tube. The formation of larger particles was monitored with a Condensation Particle Counter (CPC).

METHODS

Highly concentrated (fuming) sulphuric acid was used to create a sulphuric acid saturated gas, which was injected into the laminar flow tube. The flow of sulphuric acid saturated gas was controlled by a mass flow controller. At the end of the three meter laminar flow tube, with an inner diameter of 12 cm, was an outlet where the sample was led to the API-TOF and to the Condensation Particle Counter. The CPC was TSI model 3786 ultrafine water CPC, with a calibrated cut off diameter of 3.2 nm for silver particles. A corona charger with negative polarity was used to ionize the sample for the API-TOF, which was set to detect negative ions.

The relative humidity in the flow tube was 21% and the temperature was controlled with a water bath to 26°C. The flow was set to 25 l/min, which gives a plug flow residence time of

82 seconds. The sulphuric acid saturated gas was injected into the flow with 0.5 ml/min increments. The fuming sulphuric acid was cooled to the temperature of 15°C in a water bath.

RESULTS AND DISCUSSION

At the beginning of the experiment sulphuric acid saturated gas with a rate of 0.5 ml/min was injected to the flow tube. Roughly after the residence time, a subsequent increase in the monomer (HSO_4^-), dimer ($H_2SO_4HSO_4^-$), and trimer ($2(H_2SO_4)HSO_4^-$) signals were detected. Subsequent increases in the sulphuric acid flow rate resulted in clearly increased amounts of dimers and trimers roughly 100 seconds after the flow rate was adjusted while the monomer signal increased only marginally. Concurrently the aerosol particle concentration also increased being indicative of formation of particles large enough to be detected with the commercial CPC. The CPC's cut-off diameter was determined with silver particles. Laboratory verification shows that the water-based CPC detects water soluble and hygroscopic particles with a greater efficiency than non-soluble compounds (Petäjä et al. 2005).Thus, due to the high hygroscopic tendency of sulphuric acid, the detected particles in this experiment may have been considerably smaller than that 3.2 nm.

Shortly after four sulphuric acid flow rate increments the CPC data showed the beginning of an intensive nucleation event. The particle concentration rose rapidly, until it reached the detection limit of the CPC at 10^6 particles/cm^3. The API-TOF data showed a collapse in all sulphuric acid concentrations. There are at least two contributing factors for this behaviour: the clusters are scavenged by the larger particles and also the corona charger is not efficient enough to charge the minute sulphuric acid clusters when a high concentration of particles is present acting as a sink for the charges. Further studies are needed to reveal the physical reasons behind these features. Furthermore, more systematic tests have to be performed to explore the reproducibility of the experiments.

REFERENCES

Kulmala, M., Vehkamäki, H., Petäjä, T., Dal Maso, M. Lauri, A., Kerminen, V.-M. Birmili, W. and McMurry, P. H. (2004). Formation and growth rates of ultrafine particles: a review of observations. *J. Aeroso.l Sci.*, 35:143-176.

Kulmala, M., Riipinen, I., Sipilä, M., Manninen H.E., Petäjä, T., Junninen, H., Dal Maso, M., Mordas, G., Mirme, A., Vana, M., Hirsikko, A., Laakso, L., Harrison, R.M., Hanson, I., Leung, C., Lehtinen, K. E. J. and Kerminen V.-M. (2007). Toward direct measurement of atmospheric nucleation. *Science*, 318:89-92.

Mirabel, P. and Kanz, J. L. (1974). Binary homogenous nucleation as a mechanism for the formation of aerosols. *J. Chem. Phys.*, 60:1138-1144.

Korhonen, P., Kulmala, M., Laaksonen, A., Viisanen, Y., McGraw, R. and Seinfeld, J. (1999). Ternary nucleation of H_2SO_4, NH_3 and H_2O in the atmosphere. *J. Geophys. Res.*, 104:26349-26353.

O'Dowd, C. D., Jimenez, J. L., Bahreini, R., Flagan, R. C., Seinfeld, J. H., Hämeri, K., Pirjola, L., Kulmala, M., Jennings, S.G. and Hoffmann, T. (1997). Marine aerosol formation from biogenic iodine emissions. *Nature*, 417:632-636.

Weber, R. J., Marti, J., McMurry, P. H., Eisele, F., Tanner, D. J. and Jefferson, A. (1996). Measured atmospheric new particle formation rates: implications for nucleation mechanisms. *Chem. Eng. Comm.*, 151:53-64.

Kulmala, M., Lehtinen, K. E. J. and Laaksonen, A. (2006). Cluster activation theory as an explanation of the linear dependence between formation rate of 3 nm particles and sulphuric acid concentration. *Atmos. Chem. Phys.*, 6:767-793.

Marti, J., Weber, R., McMurry, P. H., Eisele, F., Tanner, D. and Jefferson A. (1997). New particle formation at the remote continental site: Assessing the contribution on SO2 and organic precursors. *J. Geophys. Res.*, 102:6331-6339.

Yu, F. and Turco, R. P. (2000). Ultrafine aerosol formation via ion-mediated nucleation. *Geophys. Res. Lett.*, 27:883-886.

Viisanen, Y., Kulmala, M., and Laaksonen, A. (1997). Experiments on gas-liquid nucleation of sulphuric acid and water. *J. Chem. Phys.*, 107:920-926.

Kuang C., McMurry P. H., McCormick A. V., Eisele F. L. (2008), Dependence of nucleation rates on sulfuric acid vapor concentration in diverse atmospheric locations, *J. Geophys. Res.*, 113, D10209, doi:10.1029/2007JD009253

Nieminen, T., Manninen, H.E., Sihto, S.-L., Yli-Juuti, T., Mauldin, R.L., III, Petäjä, T., Riipinen, I., Kerminen, V.-M. and Kulmala, M. (2009) Connection of sulphuric acid to nucleation in Boreal forest. *Environ. Sci. Technol.*, doi:10.1021/es803152j (in press).

NUCLEATION EVENTS IN A POLLUTED CONTINENTAL BOUNDARY LAYER AS A SOURCE OF CCN

A. Hamed[1], J. Joutsensaari[1], S. Mikkonen[1], B. Wehner[2], W. Birmili[2], T.Tuch[2], G.Spindler[2], A. Wiedensohler[2], S. Decesari[3], M. Mircea[3], S. Fuzzi[3], M. C. Facchini[3] and A. Laaksonen[1, 4]

[1]Department of Physics, University of Kuopio, P. O. Box 70211 Kuopio, Finland
[2]Institute for Tropospheric Research, Leipzig, Germany
[3]Istituto di Scienze dell'Atmosfera e del Clima Consiglio Nazionale delle Ricerche, Bologna, Italy
[4]Finnish Meteorological Institute, P.O. Box 503, 00101 Helsinki, Finland

INTRODUCTION

Atmospheric nucleation events due to gas-to-particle conversion have received increasing attention as a potentially important global source of new aerosol particles, thereby affecting both climate and human health. After nucleating at diameters of about 1 nm, the new particles may grow by condensation and coagulation, and eventually reach particle sizes where they may act as cloud condensation nuclei (CCN). This growth of particles may take several days, and since many aerosol dynamical as well as meteorological effects interact during such a time span, it has been difficult to determine CCN production rates on the basis of experimental observations.

Here, we study the CCN production due to secondary particle formation based on the characteristics of nucleation events observed in a polluted continental boundary layer. The analysis makes use of continuous particle size distribution measurements at the rural observation site Melpitz (51°32'N, 12°54'E, 87 m a.s.l.). in Eastern Germany. This region is characterized by the presence of diffuse anthropogenic sources, such as vehicular traffic, agricultural and regulated industrial emissions. While particle formation at Melpitz had been studied during an earlier experiment between 1996 and 1997 (Birmili and Wiedensohler, 2000), this study concentrates on the new data, collected continuously between July 2003 and June 2006.
Moreover, we compare the obtained results for Melpitz (moderate rural site) with the earlier presented results in Laaksonen et al (2005) for the polluted rural site (San Pietro Capofiume "SPC" in the Po Valley, (44°3'N, 11°37'E, 10 m a.s.l.).

METHODS

Days studied were classified into different categories, i.e., event and non-event days. For nucleation event days, the particle number concentration in the nucleation mode shows clear growth, accompanied by growth of the newly formed particles for several hours. The classification method of nucleation events we followed here is based on the method described by Hamed et al. (2007).

As a second step after identifying the days into nucleation days and non nucleation days, In order to determine the production rates of CCN resulting from nucleation and growth of new particles, we applied the method of Laaksonen et al. (2005) to the size distribution data. Briefly, we calculated increases of particle number concentrations in the 50-600 nm, 100-600 nm, and 200-600 nm size ranges on nucleation event days. The concentration increases in the given size ranges were simply determined from the differences in particle concentration at the moment when the nucleated mode reaches lower limit of the given size range, and at the moment when the particle concentration in that size range reaches a maximum or, alternatively, at midnight, in case the maximum has not been reached by then. In this way we obtain conservative estimates for the increases of particle concentrations in the different size ranges. We do not believe that the underestimation is too drastic since the nocturnal particle growth usually is not very rapid, and the calculation would in any case have to be stopped in the early morning since very often the

growing mode is disrupted either due to dilution (vertical mixing) or due to aerosols from primary sources, e.g. traffic.   In order to estimate the total CCN production, i.e. the production from nucleation plus production from primary sources, we calculated hypothetical particle source rates that are needed to support the average concentrations of particles in the given size ranges. In the steady state (SS), the particle source rate (P) equals the ratio of particle concentration (C) and the average particle residence time in air (t). Balkanski 1991, gave a value of t = 4 days for particles near the surface which we adopted for our calculations.

Moreover the statistical analysis of significance of CCN differences between SPC and Melpitz stations has been examined. The statistical analyses were carried out with R-software (R Development Core Team, 2008). Figure 2 shows the CCN concentrations for all data for Melpitz (MEL) and for SPC.

RESULTS

The analysis of years 2003-2006 showed that the frequency of nucleation event days in SPC was 32% that was higher than in Melpitz (30%) data while the frequency for non event days was found to be 54 % in Melpitz t and 42% in SPC. 26% of the data in SPC respect to 16% in Melpitz which a clear decision was not possible whether nucleation has taken place or not.

Figure 1 shows the yearly pattern of nucleation event occurrence for Melpitz and SPC. For SPC, events were seen throughout the year, with frequencies peaking at late spring and summertime. From May till August, roughly 65% of the days were event-days. In Melpitz, the overall pattern is similar to SPC. The highest frequencies in Melpitz were also between May and September, with roughly 55% of the days being nucleation event days. In wintertime ~3% of the studied days in Melpitz and ~20% in SPC were nucleation event days. Surprisingly, during November months no particle formation was observed at all in Melpitz measurement station and also very few nucleation days observed for SPC site
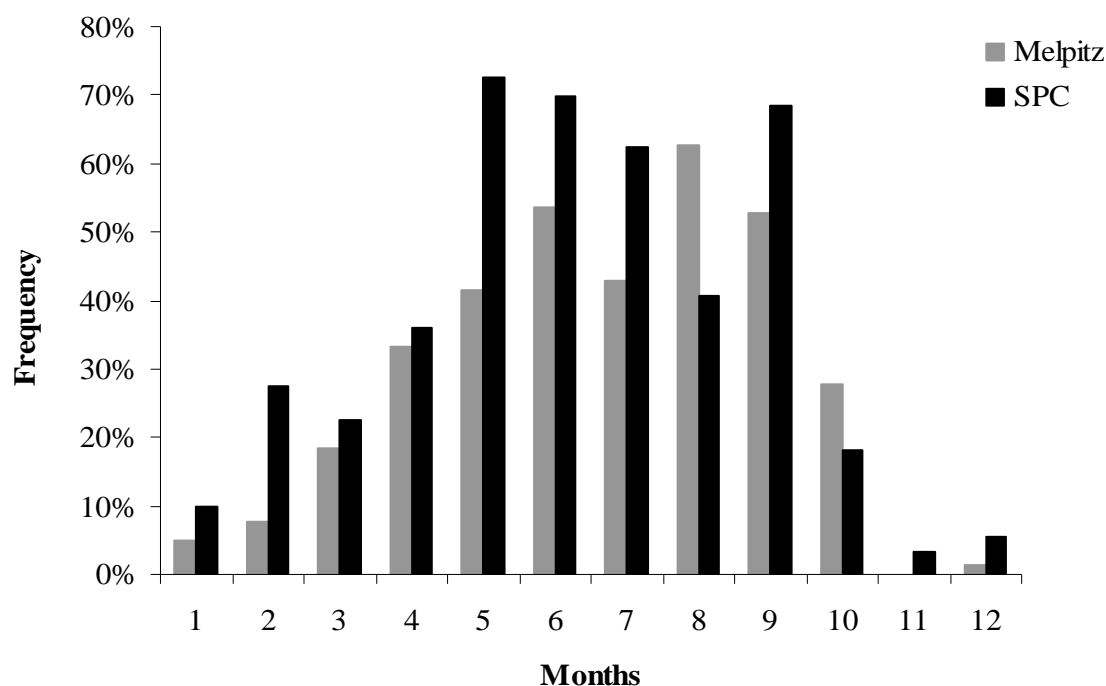
Figure1: Monthly frequency of nucleation events in Melpitz and in SPC stations for 2003-2006.

After nucleating at diameters of about 1 nm in the atmosphere, the newly formed particles may grow by condensation and coagulation, and eventually reach particle sizes where they may act as cloud condensation nuclei (CCN). This growth may take several days, and since many aerosol dynamical as well as meteorological effects interact during such a time span, it has been difficult to determine CCN production rates on the basis of experimental observations. Here, we investigate the significance of the nucleation events as a source of CCN in Melpitz site.

The estimated increase in particle number concentration (size ranges 50-600 nm, 100-600 nm, and 200-600 nm) after nucleation events together with the average concentrations in the respective size ranges are presented in Table 1. For all size ranges the concentration increase per particle formation event was on the same order as the average concentration (see 2nd and 3rd row in Table 1).
The yield of 50-600 nm particles shown in Table 1 corresponds to annual particle production of 1×10^{14} particles per square meter of the Earth's surface.

Table1. The annual yield of particles, the average yield per one nucleation event, the average particle concentrations and hypothetical steady-state particle production rate needed to support the average concentrations for different size ranges presented for Melpitz station.

Size Range (nm)	50-600	100-600	200-600
Annual yield/cc	1.6E+05	7.0E+04	2.2E+04
Average yield/Event	3.1E+03	1.3E+03	4.2E+02
Average Concentration/cc	2.4E+03	1.3E+03	4.4E+02
SS-production/cc/Year	2.2E+05	1.2E+05	3.9E+04

Radke and Hobbs (1976) estimated that globally, the total annual CCN production from primary sources is on the order of 10^{14} m^{-2}, which has same order to the values we calculate for 50-600 nm particles for Melpitz. For further analysis of the importance of the nucleation events, we calculated hypothetical particle source rates (for more details see Laaksonen et al., 2005) that needed to support the average concentrations.

As a result we obtain simple estimates of particle source strengths in the different size ranges the results are shown on the last row of Table 1. The steady state assumption (SS-assumption) is highly simplified, however, it can be seen that the actual annual particle production in the nucleation events is of the same order as the hypothetical steady-state production.

By comparing the ratio of nucleation production to particle source rate (in the steady state), calculated for 100-600 nm particles in Melpitz, (0.7/1.2 = 0.58) to the values obtained before for SPC (0.38) by Laaksonen et al. (2005), we get an estimate of the importance of nucleation as a source of CCN for the two studied regions. We believe that our comparison indicates that nucleation events can be as important source of CCN in the Saxony region, in Germany as in SPC, however it is more significantly pronounced in SPC than in Melpitz due to high amount of anthropogenic contributions in Po Valley area than in Saxony area. Thus, the percentage of CCN produced in Melpitz is somewhat higher than in SPC, however, the absolute yield is higher in SPC than in Melpitz (110 000/year vs. 70 000/year).

Our statistical analysis highlighted the previous conclusion as it was clear that for all size ranges CCN production in higher in SPC than in Melpitz (see figure 2).
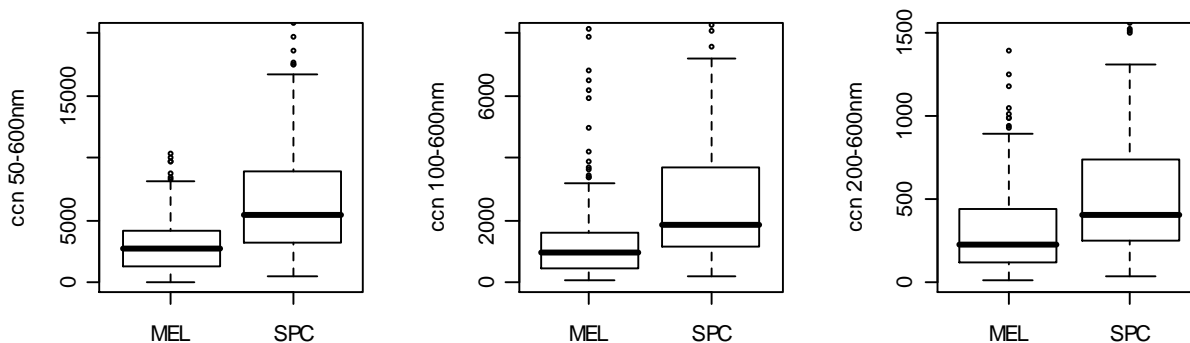
Figure 2. CCN concentrations for Melpitz (MEL) and for SPC. The length of the box represents the difference between the 25th and 75th percentiles, the horizontal line inside the box represents the median, the lengths of the dashed lines (whiskers) correspond to the largest and smallest values that are not outliers, and the outliers, labeled with o, are cases with the values more than 1.5 box-lengths from the 75th percentile or 25th percentile. All outliers not shown.

ACKNOWLEDGMENTS

REFERENCES

Balkanski, Y. J. (1991) Atmospheric residence times of continental aerosols. Ph.D. thesis, Harvard Univ., Cambridge, MA, USA.

Birmili, W. & Wiedensohler, A. (2000) New particle formation in the continental boundary layer: Meteorological and gas phase parameter influence, *Geophys. Res. Lett.*, 27, 3325–3328.

Hamed, A. Joutsensaari, J. , Mikkonen, S., Sogacheva, L., Dal Maso, M., Kulmala, M., Cavalli, F., Fuzzi, S., Facchini, M. C., Decesari, S. , Mircea, M., Lehtinen, K. E. J. , and Laaksonen A. (2007). Nucleation and growth of new particles in Po Valley, Italy, *Atmos. Chem. Phys.*,**7**,355-376.

Laaksonen, A., Hamed, A., Joutsensaari, J., Hiltunen, L., Cavalli, F., Junkermann, W., Asmi, A. Fuzzi, S.,Facchini, M. C. (2005) Cloud condensation nucleus production from nucleation events at a highly polluted region, *Geophys. Res. Lett.*, 32, 1-4.

Radke, L.F. & Hobbs, P.V. (1976). *Science*, 193, 999-1002.

R Development Core Team R. (2008) A language and environment for statistical computing. R Foundation for Statistical Computing, Vienna, Austria. ISBN 3-900051-07-0, URL http://www.R- project.org.

SECONDARY ORGANIC AEROSOL FROM OXIDATION OF REAL PINE EMISSIONS

L.Q. HAO[1], P. YLI-PIRILÄ[2], P. TIITTA[1], S. ROMAKKANIEMI[1], P. VAATTOVAARA[1], M. K. KAJOS[3], J. RINNE[3], J. HEIJARI[2], A. KORTELAINEN[1], P. MIETTINEN[1], J.H. KROLL[4], J.-K. HOLOPAINEN[2], J. JOUTSENSAARI[1], M. KULMALA[3], D.R. WORSNOP[4], and A. LAAKSONEN[1,5]

[1]Department of Physics, University of Kuopio, Kuopio70211, Finland
[2]Department of Environmental Sciences, University of Kuopio, Kuopio70211, Finland
[3]Department of Physics, P.O box 68, University of Helsinki, Helsinki 00014, Finland
[4]Aerodyne Research, Inc., Billerica, MA 08121-3976, USA
[5]Finnish Meteorological Institute, Helsinki 00101, Finland

1 INTRODUCTION

Monoterpenes and isoprene are important classes of globally emitted organic biogenic species. Their oxidation leads to low volatile products (low saturation vapor pressure) which are believed to be able to nucleate once their saturation ratio increased sufficiently. Compounds with higher saturation pressure, known as semi-volatile organic compounds, will partition into the previously formed particle phase, contributing to the growth and mass loadings of atmospheric aerosols. Thus, the secondary organic aerosol (SOA) formation from oxidation of monoterpenes and isoprene by OH, O_3 and NO_3 has been intensively studied in laboratory and field campaign (e.g. Hoffmann et al., 1997; Gao et al., 2004; Ng et al., 2007; Kroll et al., 2006; Presto and Donahue, 2005; Kulmala et al., 2004; Laaksonen et al., 2008, etc.). These studies have demonstrated that atmospheric oxidation of monoterpenes and isoprene represents significant source of SOA. Despite the important advances that have been made in SOA studies, the SOA formation in the atmosphere is still poorly understood. For example, the roles OH and O_3 play in the SOA formation is still partially unknown and the conclusions made to this point in previous studies are somewhat contradictory. Bonn and Moortgat (2002) and Koch et al. (2000) concluded that OH oxidation of monoterpenes in the atmosphere is not an important source of new SOA particles, whereas Burkholder et al. (2007) reported that OH initiated oxidation allows for nucleation.

In this study we concentrate on the aerosol particle nucleation in a laboratory using direct VOCs emissions of living Scots pine seedlings. Scots pine was selected because it is one of the dominant tree species in the European boreal forest (Räisänen et al., 2008). Both O_3 and OH were used as oxidants in the controlled conditions in these experiments. Our motivation is to evaluate the roles that these oxidants play in the formation of new particles and in the subsequent condensational growth.

2. EXPERIMENTAL DESCRIPTION

2.1 CHAMBER EXPERIMENTS

The study was performed in the 6m^3 rectangular chamber made of Neflon^{TM} FEP film in Kuopio University. Prior to experiments, clean air flow took the pine emissions into the chamber. In some experiments, tetramethylethylene (TME) (99+%, Aldrich) was delivered into the chamber to produce hydroxyl radical (OH) radical. After injections of the reactants, ozone was added. The beginning of first ozone injection marked the start of each experiment. In all experiments, temperature was controlled in the range of 25±2°C and relative humidity (R.H.) in 35±5%. No seed aerosols were added and the chamber was shrouded with a black polyethylene tarpaulin from light.

VOC emissions from pine seedlings were measured using gas chromatography-mass spectrometry (GC-MS, Hewlett-Packard GC model 6890, MSD 5973) for off-line analysis and proton transfer reaction mass spectrometer (PTR-MS, Ionicon Analytik GmbH) for on-line analysis. Aerosol chemical composition and mass size distributions were measured by an Aerodyne aerosol mass spectrometer (AMS). Aerosol particle size distributions over a ranger of 5.6-560nm were measured using a fast mobility particle sizer spectrometer (FMPS, TSI model 3091). Besides, O_3 concentration was monitored at the inlet and inside the chamber by two DASIBI 1008-RS O_3 analyzers (Dasibi Environmental Corporation, Glendele, CA, USA).

2.2 MODELING OF VOC OXIDATION

New particle formation is affected by the gas-phase oxidation of VOCs, a kinetic degradation model of VOCs from the oxidation of ozone and OH was built to interpret the new particle nucleation and growth events. In this model, the oxidation of VOCs by O_3 and OH was calculated using the initial measured concentrations of VOCs and known reaction rates. O_3 and OH are assumed to be involved in the oxidation reactions of VOCs and TME with taking into account the second loss processes of OH and O_3. In brief, the chemical model calculate the reaction kinetics for O_3 reactions based on the equations

$$\frac{dO_3}{dt} = \frac{d[O_3]_{inlet}}{dt} - \gamma_i k_{O_3}^{TME}[TME][O_3] - \sum_i \gamma_i' k_{O_3}^{VOC_i}[VOC]_i[O_3] \tag{1}$$

Where k is reaction constants of the chemical reactions and γ_i and γ_i' are the correction factors to take into account the second loss of ozone with the second-generation products. All the parameters are listed in Hao et al (2009).

Similarly, time-dependent OH concentration is

$$\frac{dOH}{dt} = \omega_i k_{O_3}^{TME}[TME][O_3] + \sum_i \omega_i' k_{O_3}^{VOC_i}[VOC]_i[O_3] - \gamma_i'' k_{OH}^{TME}[TME][OH] - \sum_i \gamma_i''' k_{OH}^{VOC_i}[VOC]_i[OH] \tag{2}$$

where ω_i, ω_i' denote the yields of hydroxyl radicals from the O_3 reactions and γ_i'' and γ_i''' are the correction factors to take into account the second loss of OH with the second-generation products.

O_3 and OH oxidation reactivity contributing to the new particle formation are defined as equitation (3) and (4) excluding the contributions from TME

$$r_{O_3} = \sum_i k_{O_3}^{VOC_i}[VOC]_i[O_3] \tag{3}$$

$$r_{OH} = \sum_i k_{OH}^{VOC_i}[VOC]_i[OH] \tag{4}$$

New particle formation rate (F) and growth rate (G) can be constrained directly by the oxidation rates of VOCs

$$F \sim r_{O_3} + r_{OH} \tag{5}$$

$$G \sim r_{O_3} + r_{OH} \tag{6}$$

Similarly, for the loss of other compounds and formation of products, chemical kinetics can be described using the following rate equations

$$\frac{d[VOC]_i}{dt} = -\sum_i k_{O_3}^{VOC_i}[VOC]_i[O_3] - \sum_i k_{OH}^{VOC_i}[VOC]_i[OH] \tag{7}$$

$$\frac{d[TME]}{dt} = -k_{O_3}^{TME}[TME][O_3] - k_{OH}^{TME}[TME][OH] \tag{8}$$

$$\frac{d[AT]}{dt} = \sum_i \beta_i k_{O_3}^{VOC_i}[VOC]_i[O_3] + \sum_i \beta_i' k_{OH}^{VOC_i}[VOC]_i[OH] - k_{OH}^{AT}[AT][OH] \tag{9}$$

$$\frac{d[FAH]}{dt} = \sum_i \alpha_i k_{O_3}^{VOC_i}[VOC]_i[O_3] + \sum_i \alpha_i' k_{OH}^{VOC_i}[VOC]_i[OH] - k_{OH}^{FAH}[FAH][OH] \tag{10}$$

where β_i, β_i' are the yields of acetone (AT) from reactions of O_3 and OH with VOCs and TME and α_i, α_i' are for the formaldehyde (FAH) yield.

2.3 SUMMARY OF EXPERIMENTS PERFORMED

Five experiments were carried out in the present study. The initial conditions are summarized in Table 1. TME was added in E1a-E1c to investigate the role of OH-initiated oxidation in new particle formation. No TME was added in E2 in order to simulate lower OH conditions. Experiment E3 was performed in the presence OH scavenger to investigate the role of ozonolysis alone in new particle formation.

Table 1 Initial conditions of chamber experiments performed and analysis results

Date and year	Experiment No.	VOCs initial (ppb)	TME initial (ppb)	First O_3 addition				Second O_3 addition			
				Inlet (ppb)	time (min)*	Peak O_3 (ppb)**	PeakOH (ppt)***	Inlet (ppb)	time (min)*	Peak O_3 (ppb)**	PeakOH (ppt)***
12.10.2007	E1a	74.1	118	200	25	4.15	0.043	200	25	15.1	0.075
23.10.2007	E1b	28.8	342	200	75	5.17	0.073	0	0	0	0
25.10.2007	E1c	113.8	984	200	75	0	<0.0008	800	30	17.8	0.148
22.10.2007	E2	23.2	0	200	13	20.7	0.0139	0	0	0	0
26.10.2007	E3	100.3	2-butanol, 54ppm	60	30	6.17	0.0001	200	30	37.4	0.0005

* Duration of ozone addition into the chamber.
** Measured maximum O_3 concentration inside the chamber.
***Modeled maximum OH concentration inside the chamber.

3 RESULTS

3.1 REACTION OF EMITTED VOCS
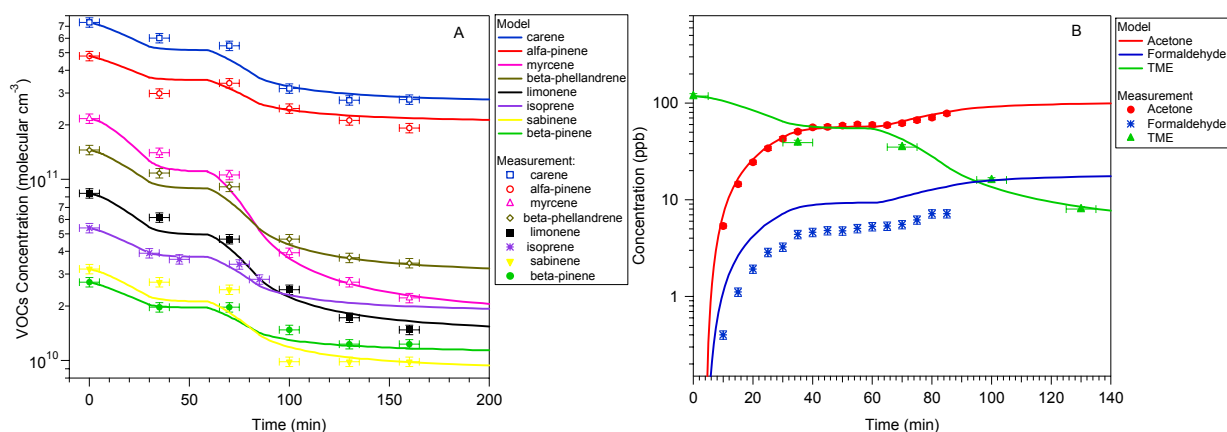
Figure 1. Comparisions of measured and modelled results from experiment E1a: (A) Changes in emitted VOC concentration upon reaction (from GC-MS measurements) (B) TME decay profiles (from GC-MS measurements) and gas-phase product concentration of acetone and formaldehyde (from PTR-MS measurements). Results from other four experiments are similar and so are not be shown here.

Figure 1 shows the decay profiles of ten kinds of VOCs (nine monoterpenes and isoprene) of Scots pine emissions (panel A) and formation curves of gas-phase product of acetone and formaldehyde as functions of time (panel B) in experiment E1a. The modeled concentrations were calculated based on the OH and O_3 induced chemistry of these VOCs as described in Sect. 2.2. Possbile formation sources of acetone and formaldehyde include O_3 and OH induced chemisty of TME and emitted VOCs as shown in Eq. (9) and (10).

Degraded products of these ten VOCs will contribute to new particle formation and will be described in following sections. Good agreement between modelled and modeled VOC and product concentrations provides further confirmation to the validity of the model used in this study.

3.2 NEW PARTICLE FROM OH+O3 INDUCED CHEMISTRY

The contour plots of aerosol particle number size distributions, total number/volume concentrations and gas-phase species concentration are illustrated in Fig. 2. It can be seen that a rapid increase in the particle number concentration occurred and obvious nucleation events took place after the first addition of ozone in all cases. The second ozone injection induced very weak increase of aerosol number concentrations, but an intensive increase in aerosol volume concentrations. In experiment E3, 2-butanol was added into the chamber to remove the OH in the gas phase. It shows that only a very weak nucleation event was observed in this experiment. The maximum number concentration was only 8120 particle cm^{-3}, being much lower than that was found during OH/O_3 initiated cases. On the other hand, a relatively high increase rate in aerosol volume was observed.
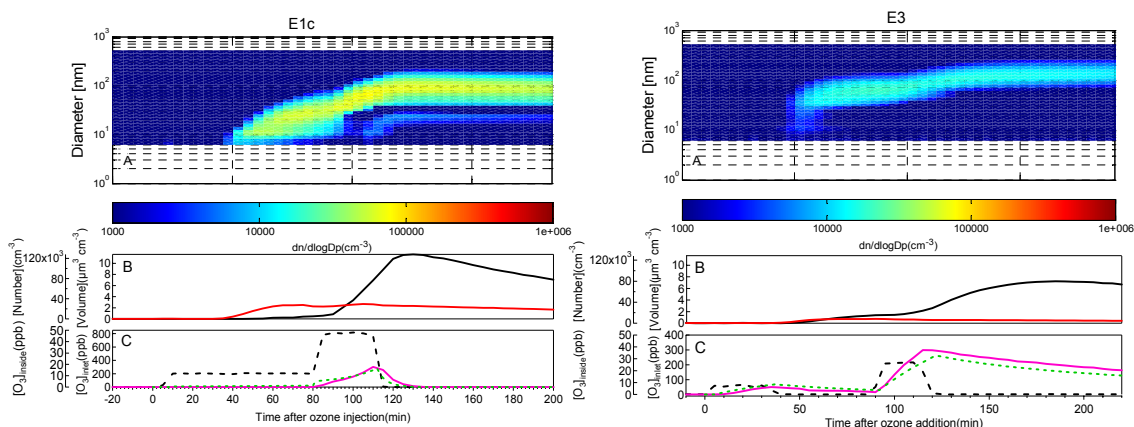
Figure 2. New aerosol formations from OH and O_3-initiated oxidations of pine emissions. The frames contains from top to bottom, in order: (A) new particles size distributions plot, (B) measured aerosol number concentration (red curve) and volume concentration (black curve), and (C) measured ozone concentrations at the inlet (black dashed curve) and inside the chamber (pink curve) and modeled ozone concentration inside the chamber(green dashed curve).

3.4 NUCLEATION AND GROWTH RATES

The correlations of instantaneous nucleation and condensational growth rates with the oxidation reaction rates of monoterpenes with OH and O_3 are shown in Fig. 3. Nucleation events usually ended at the initial stages of reaction in this study (less than 60 minutes after the beginning of experiment) and growth continued as long as there was VOCs and O_3 available. In E1a, very fast aerosol nucleation, with rate as high as 360 $cm^{-3}s^{-1}$, was observed, consistent with the rapid OH oxidation rates calculated with the model. And in the pure ozonolysis experiment (E3, with OH scavenger present), nucleation rate was very low (< 0.5 $cm^{-3}s^{-1}$), despite the very fast O_3 oxidation rate. These results indicate that OH-initiated oxidation reactions play a very important role in the aerosol nucleation stages and ozonolysis of monoterpenes are less effectively involved in the aerosol nucleation process under these experimental conditions.

As can be seen from Fig. 3, the modeled OH and O_3 reaction rates also show good correlations with the condensational growth rates in E1-E3 experiments, suggesting that OH and O_3 reactions both play roles in particle growth process. Furthermore, in E3, the highest aerosol growth rate of 74 $nm\ h^{-1}$ was achieved where the OH reaction rate was slow, suggesting that the ozonolysis of VOCs is more efficient for aerosol growth.
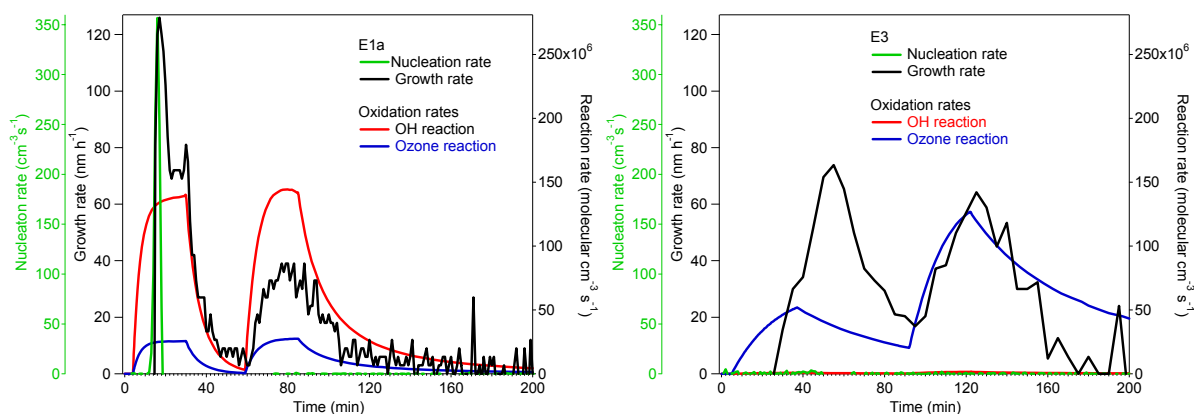
Figure 3. Effects of ozonolysis and OH-initiated oxidation rates with emitted VOCs on new particle nucleation and growth rates. In these panels, nucleation and growth rates were determined from the FMPS size distributions data. OH and O_3 oxidation rates were calculated using the model described in Sect. 2.5.

4 CONCLUSIONS

We have studied freshly formed aerosols following the gas phase oxidation of the direct emissions of Scots pine (*Pinus sylvestris L.*) seedlings in a smog chamber. New particle formation following the ozonolysis and O_3 plus OH initiated oxidation was measured. 2-butanol and TME were used to control the ratios of O_3 and OH concentrations. Emitted species, aerosol nucleation and condensational growth events are measured and investigated in this study.

Ozone plus OH initiated oxidation of these VOCs produced large amounts of new particles. For new aerosol formation, OH-initiated oxidation plays a critical role in a nucleation during the initial stage of new particle formation. Ozonolysis seems to be more efficiently involved in the particle condensational growth, but it does not contribute substantially to nucleation. These results demonstrate that OH oxidation of VOCs could be a source of the new organic particles in the atmosphere.

ACKNOWLEDGEMENTS

REFERENCES

Bonn, B., and Moortgat, G. T. (2000). New particle formation during α- and β-pinene oxidation by O_3, OH and NO_3, and the influence of water vapour: particle size distribution studies. *Atmos. Chem. Phys.,* 2:183-196.

Burkholder, J. B., Baynard, T., Ravishankara, A. R., and Lovejoy, E. R. (2007). Particle nucleation following the O_3 and OH initiated oxidation of α-pinene and β-pinene between 278 and 320K. *J. Geophys. Res.,* 112, D10216, doi: 10.1029/2006JD007783.

Gao, S., Keywood, M., Ng, N. L., Surratt, J., Varutbangkul, V., Bahreini, R., Flagan, R. C., and Seinfeld, J. H.(2004). Low-Molecular-Weight and oligomeric components in secondary organic aerosol from the ozonolysis of cycloalkenes and α-Pinene, *J. Phys. Chem. A,* 108: 10147-10164.

Hao, L. Q., Yli-Pirilä, P., Tiitta, P., Romakkaniemi, S., Vaattovaara, P., Kajos, M. K., Rinne, J., Heijari, J., Kortelainen, A., Miettinen, P., Kroll, J. H., Holopainen, J.-K., Joutsensaari, J., Kulmala, M., Worsnop, D. R., and Laaksonen, A. (2009). New particle formation from the oxidation of direct emissions of pine seedlings. *Atmos. Chem. Phys. Discuss.*, 9: 8223-8260.

Hoffmann, T., Odum, J.R., Bowman, F., Collins, D., Klockow, D., Flagan, R., and Seinfeld, J. H. (1997). Formation of organic aerosols from the oxidation of biogenic hydrocarbons. *J. Atmos. Chem.*, 26:189-222.

Ng, N. L., Chhabra, P. S., Chan, A. W. H., Surratt, J. D., Kroll, J. H., Kwan, A. J., McCabe, D. C., Wennberg, P. O., Sorooshian, A., Murphy, S. M., Dalleska, N. F., Flagan, R. C., and Seinfeld, J. H. (2007). Effect of NO_x level on secondary organic aerosol (SOA) formation from the photooxidation of terpenes. *Atmos. Chem. Phys.*, 7:5159–5174.

Koch, S., Winterhalter, R., Uherek, E., Kolloff, A., Neeb, P., Moortgat, G. K. (2000). Formation of new particles in the gas-phase ozonolysis of monoterpenes. *Atmos. Environ.*, 34: 4031-4042.

Kroll, J.H., Ng, N.L., Murphy, S.M., Flagan, R.C., and Seinfeld, J.H.(2006). Secondary organic aerosol formation from isoprene photooxidation. *Environ. Sci. Technol.*, 40: 1869-1877.

Kulmala, M., Vehkamäki, H., Petäjä, T., Dal Maso, M., Lauria, A., Kerminen, V. -M., Birmili, W., and McMurry, P. H. (2004). Formation and growth rates of ultrafine atmospheric particles: a review of observations. *J. Aerosol Sci.*, 35:143–176.

Laaksonen, A., Kulmala, M., O'Dowd, C. D., Joutsensaari, J., Vaattovaara, P., Mikkonen, S., Lehtinen, K. E. J., Sogacheva, L., Dal Maso, M., Aalto, P., Petäjä, T., Sogachev, A., Yoon, Y. J., Lihavainen, H., Nilsson, D., Facchini, M. C., Cavalli, F., Fuzzi, S., Hoffmann, T., Arnold, F., Hanke, M., Sellegri, K., Umann, B., Junkermann, W., Coe, H., Allan, J. D., Alfarra, M. R., Worsnop, D. R., Riekkola, M. -L., Hyötyläinen, T., and Viisanen, Y.(2008). The role of VOC oxidation products in continental new particle formation. *Atmos. Chem. Phys*, 8: 2657–2665.

Presto, A. A., and Donahue, N. M.(2005). Secondary organic aerosol production from terpene ozonolysis. 2. Effect of NOx concentration. *Environ. Sci. Technol.*, 39: 7046–7054.

Räisänen, T., Ryyppö, A., and Kellomäki, S. (2008). Effects of elevated CO_2 and temperature on monoterpene emission of Scots pine (*Pinus sylvestris* L.). *Atmos. Environ.*, 42: 4160–4171.

UNARY AND BINARY NUCLEATION SIMULATIONS WITH FLUENT-FPM

E. HERRMANN[1], A.-P. HYVÄRINEN[2], D. BRUS[2], and M. KULMALA[1]

[1] Department of Physical Sciences, University of Helsinki, Finland
[2] Finnish Meteorological Institute, Helsinki, Finland

Keywords: nucleation, pressure effect, parametrisation, FLUENT, FPM

INTRODUCTION

Ambient aerosols have a significant impact on climate. They serve as a media for atmospheric heterogeneous chemistry, and affect the earth radiative balance through light scattering (direct effect) and by acting as condensation nuclei in cloud formation (indirect effect). High aerosol concentrations also decrease the air quality thus affecting human health and visibility. New particle formation in the atmosphere has been observed in various locations and conditions all over the world. However, the process is still poorly understood.

To improve our understanding of nucleation on a basic level, the process is studied in laboratory experiments. A typical experimental device to investigate nucleation is the flow chamber in its varying specifications. However, a flow chamber does not give direct information about the actual nucleation rate. To extract this information from the experimental data, a theoretical model of the nucleation process is necessary. We have used FLUENT with the Fine Particle Model (FPM) to simulate and thus analyse the unary nucleation of n-alcohols and now focus on including the binary nucleation of water and sulfuric acid into the FPM.

FLUENT AND THE FINE PARTICLE MODEL

FLUENT (version 6.3.26, Fluent Inc.) is a commercially available CFD (computational fluid dynamics) software to calculate the properties of fluid flows. It models flow based on the Euler equations for mass and momentum conservation. The Fine Particle Model (FPM, version 1.4.2, Particle Dynamics GmbH & Chimera Technologies) is a particle dynamics model which is added to FLUENT in the form of user-defined functions (UDF). The FPM allows to simulate formation, transformation (growth, coagulation), transport and deposition of multicomponent particles in gases and liquids.

UNARY NUCLEATION OF N-ALCOHOLS

The laminar flow diffusion chamber (LFDC) used in the laboratory experiments is described in detail by Hyvärinen et al. (2006). In the experiment, carrier gas is saturated with nucleating vapor in the saturator. The mixture then enters the preheater and is afterwards cooled in the condenser. Since vapor diffusion is slower than heat diffusion in this case, the mixture becomes super-saturated and, at sufficiently high values of S, we observe nucleation. Nucleated particles are counted downstream from the condenser. In the simulation, this setup is reduced to a simple tube with two different wall temperatures to account for preheater and condenser.

We simulated the nucleation of n-butanol, n-pentanol, and n-hexanol with helium and argon as carrier gases and at pressures 50, 100, and 200kPa. Generally speaking, our simulations support the results obtained with the corrected femtube2 model, previously reported by Hyvärinen et al.

(2008) and Brus et al. (2008). This means that also the use of a more accurate mathematical model yielded a pressure effect. Negative and positive pressure effects were found, depending on nucleation temperature and carrier gas. This suggests two competing mechanisms that affect the nucleation process, with the negative effect being amplified by a lighter vapor, a heavier carrier gas, and higher temperatures. According to a recent publication Wedekind et al. (2008), the effect (at low pressures) arises from a competitional effect of nonisothermal nucleation and the extra work that a growing cluster has to do against the pressure of the carrier gas. Beyond this work, more measurements are needed to further investigate the relationship between vapor properties and pressure effect. Additionally, a theoretical analysis of the pressure effect at conditions similar to the ones in the experiment is needed. Figure 1 shows an example of the results. (Herrmann et al. (2009))
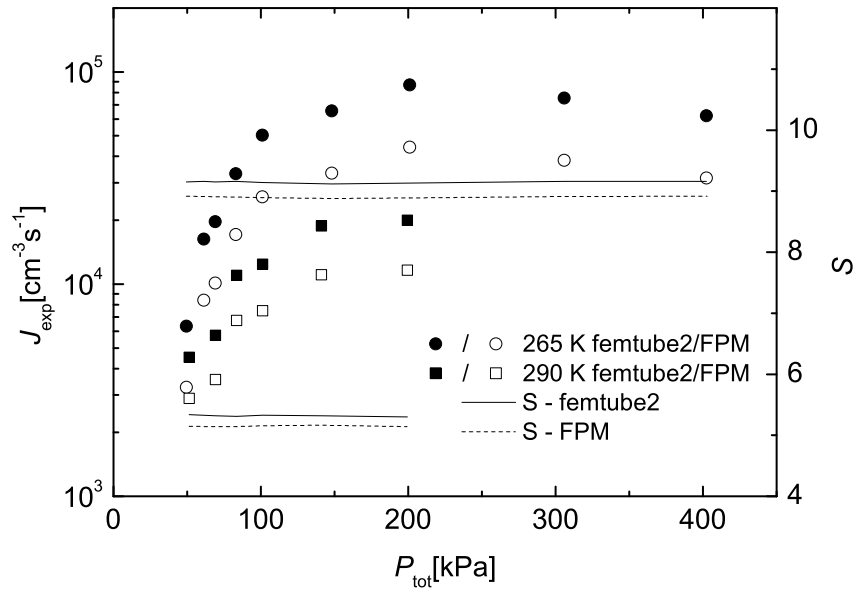
Figure 1: Nucleation rate and saturation ratio as a function of total pressure for the nucleation of n-pentanol in helium. Results are calculated with FLUENT-FPM and the corrected femtube2 model using the same boundary conditions.

NEXT STEP: BINARY NUCLEATION OF WATER AND SULFURIC ACID

Binary nucleation is investigated in the laboratory with a similar setup. A mixture of water vapor, sulfuric acid vapor, and air as the carrier gas is cooled down in a flow tube. Under favorable conditions, nucleation occurs. In the simulation, this turns into a simple tube at constant temperature. The properties of the mixture of nucleating vapors and gas are introduced as boundary conditions. To simulate binary nucleation of water and sulfuric acid, two parametrisations (for high and low temperatures) of the process published in Vehkamäki et al. (2002) and Vehkamäki et al. (2003) are implemented into the FPM code. One of the challenges of this project is finding the right boundary conditions. It is not possible to simulate the exact interactions between water and sulfuric acid at the walls. Instead, the boundary conditions for those vapors have to be adjusted in such a way that vapor profile simulations match the experimental data available. Figure 2 shows the concentration of sulfuric acid molecules along the central axis of the tube as an example. In this simulation, the initial sulfuric acid concentration was set to match the experiment. At the walls, we assumed

zero concentration. With this setup, sulfuric acid concentration at the end of the tube was smaller than measured in the experiment. This suggests that the concentration at the wall must be bigger than zero. The real value can be determined by iterated simulations. Thus found initial boundary conditions will have to be reconsidered once nucleation has been included in the simulation since vapor depletion (Herrmann et al. (2006)) affects vapor concentrations. Results of actual nucleation simulations are not yet available.
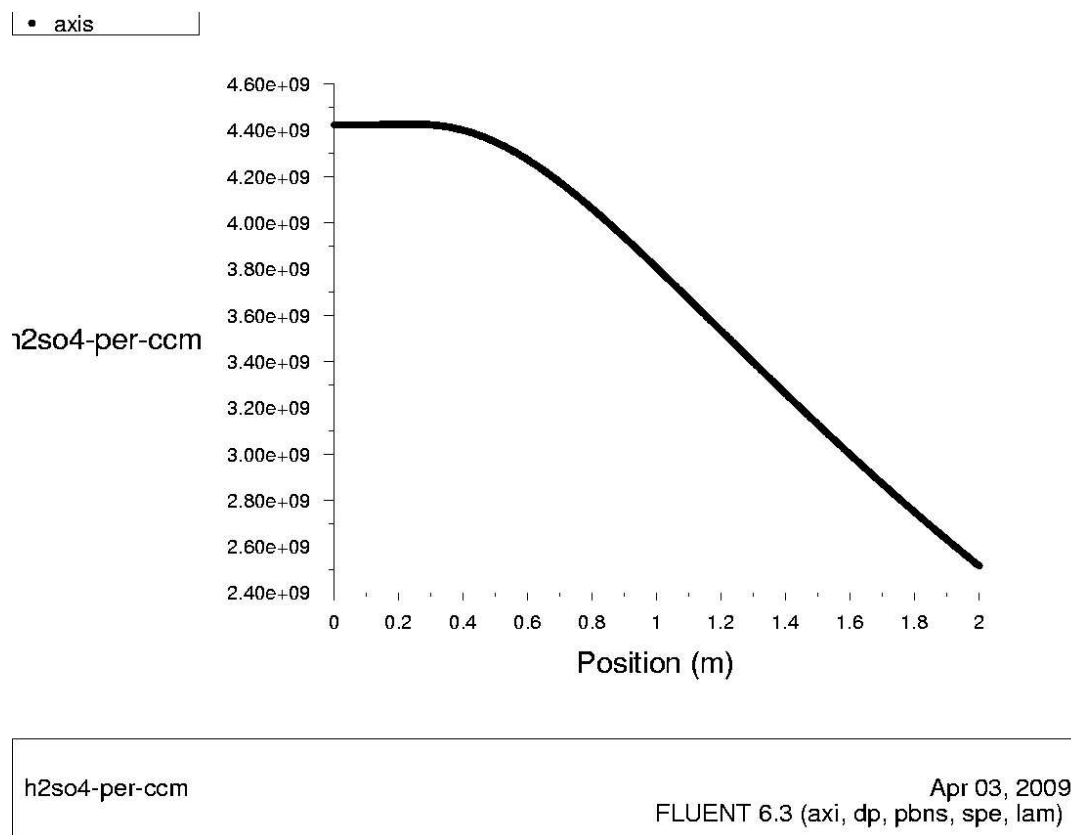
Figure 2: Concentration of sulfuric acid molecules in $1/\text{cm}^3$ along the central axis of the flow tube.

REFERENCES

Brus, D., Hyvärinen, A.-P., Wedekind, J., Viisanen, Y., Kulmala, M., Ždímal, V., Smolík, J., and Lihavainen, H. (2008). The homogeneous nucleation of 1-pentanol in a laminar flow diffusion chamber: The effect of pressure and kind of carrier gas. *J. Chem. Phys.*, 128(13):134312.

Herrmann, E., Hyvärinen, A.-P., Brus, D., Lihavainen, H., and Kulmala, M. (2009). Re-evaluation of the Pressure Effect for Nucleation in Laminar Flow Diffusion Chamber Experiments with Fluent and the Fine Particle Model. *J. Phys. Chem. A*, 113(8):1434–1439.

Herrmann, E., Lihavainen, H., Hyvärinen, A.-P., Riipinen, I., Wilck, M., Stratmann, F., and Kulmala, M. (2006). Nucleation simulations using the fluid dynamics software FLUENT with the fine particle model FPM. *J. Phys. Chem. A*, 110:12448–12455.

Hyvärinen, A.-P., Brus, D., Ždímal, V., Smolík, J., Kulmala, M., Viisanen, Y., and Lihavainen, H. (2006). The carrier gas pressure effect in a laminar flow diffusion chamber, homogeneous nucleation of n-butanol in helium. *J. Chem. Phys.*, 124(22):224304.

Hyvärinen, A.-P., Brus, D., Ždímal, V., Smolík, J., Kulmala, M., Viisanen, Y., and Lihavainen, H. (2008). Erratum: "The carrier gas pressure effect in a laminar flow diffusion chamber, homogeneous nucleation of n-butanol in helium" [J. Chem. Phys. 124. 224304 (2006)]. *J. Chem. Phys.*, 128(16):109901.

Vehkamäki, H., Kulmala, M., Lehtinen, K. E. J., and Noppel, M. (2003). Modelling binary homogeneous nucleation of water-sulfuric acid vapours: Parametrisations for high temperature emissions. *Environ. Sci. Technol.*, 37(15):3392–3398.

Vehkamäki, H., Kulmala, M., Napari, I., Lehtinen, K. E. J., Timmreck, C., Noppel, M., and Laaksonen, A. (2002). An improved parametrization for sufuric acid-water nucleation rates for tropospheric and stratospheric conditions. *J. Geophys. Res.*, 107(D22):4622.

Wedekind, J., Hyvärinen, A.-P., Brus, D., and Reguera, D. (2008). Unraveling the "pressure effect" in nucleation. *Phys. Rev. Lett.*, 101(12):125703.

AEROSOL FORMATION AND SEASONAL VARIATION OF RELATED PARAMETERS IN FIVE EUROPEAN SITES

A.I. HIENOLA[1], A. HAMED[2], T. NIEMINEN[3], P. PAASONEN[3], H. VUOLLEKOSKI[3], S.-L. SIIHTO[3], I. RIIPINEN[3], L. SOGATCHEVA[1], M. KULMALA[3] and A. LAAKSONEN[1,2]

[1] Finnish Meteorological Institute, Helsinki, Finland
[2] Department of Physics, University of Kuopio, Finland
[3] Department of Physical Sciences, University of Helsinki, Finland

Keywords: nucleation, atmospheric aerosols, seasonal variation, sulfur dioxide, global radiation

INTRODUCTION

The commonly accepted opinion is that the nucleation process demands some special conditions concerning a multitude of different factors, such as the chemical composition of the atmosphere which differs according to the location, the pre-existence of aerosol particles serving as condensation sink, divers meteorological parameters (radiation, temperature, relative humidity) and boundary layer dynamics. The high number of variables and their interconnection hinders any straight incursion on the correlation between them and the new particle formation process. Although widely studied, the nucleation mechanism is not well understood, and the condensable vapors involved in this process are not yet identified (Kulmala et al. (2006)). However, water, sulfuric acid and ammonia are presumed to be the main precursors for the new particle formation (Korhonen et al. (1999); Napari et al. (2002); Merikanto et al. (2007)). Because the particle formation events have been observed around the world in various environments (Kulmala et al. (2004)), it is likely that different mechanisms dominate the process, strongly depending on the local/regional atmospheric conditions.

The focus of the present study was to identify similarities and differences of the seasonal distributions of the event and non-event days and to analyze the seasonal distributions of the ambient conditions (meteorological variables and gas concentrations) related to the event and non-event days using long term data sets collected from 5 measurement stations located in in Finland (Hyytiälä and Värriö), Italy (Po Valley) and Germany (Melpitz and Hohenpeissenberg).

RESULTS

The stations are located in different environments and therefore exposed to different levels of pollution, from relatively clean boreal forest to rather polluted areas. The time series range from 2 to 12 years. Measured meteorological parameters and gas phase concentrations (SO_2, O_3, relative humidity, temperature, global radiation) were included in our analysis.

We note several interesting features related to the new particle formation:

1. The occurrence of new particle formation is linked to meteorological conditions characteristic for each station. However, the only common driving factor was global radiation, which was consistently higher during the event days in comparison with non-event days, for all seasons and stations [Figure 1a].

Figure 1: The seasonal variation of the hourly medians event/non-event ratios of the parameters for all five stations: a) global radiation, b)relative humidity, c) temperature, d) sulfur dioxide concentration, e) condensation sink.
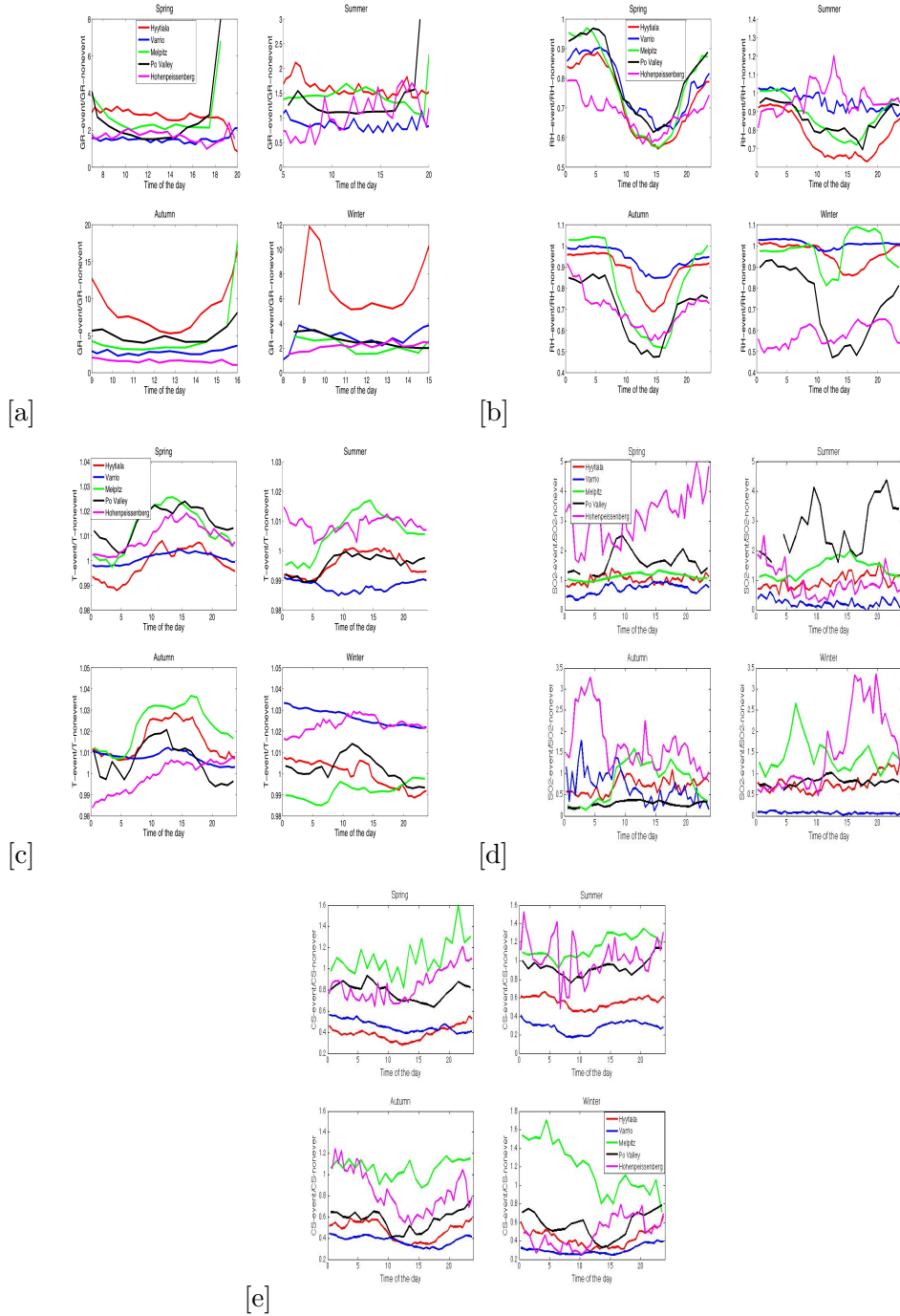
Figure 2: Event (red) and non-event (blue) days in Hyytiälä using the proxy vs condensation sink: a) yearly and b) seasonally .

[a]

[b]
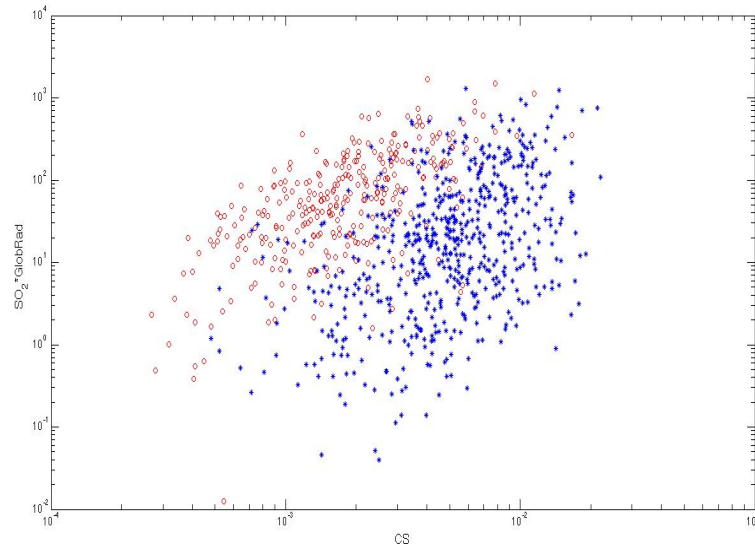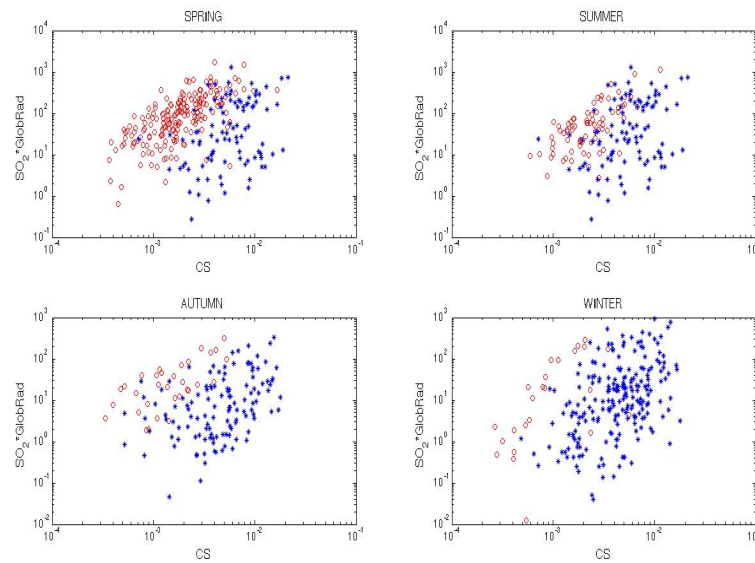
2. The realive humidity is usually negatively correlated to the nucleation events: the relative humidity is lower during the event days and higher during non-event days (Hamed et al. (2007); Laaksonen et al. (2008)). All stations present this trend throughout all seasons, with two exceptions: Hohenpeissenberg, which exhibits a reverse behaviour in the summer, with an obvious increase in RH during the event days, and Värriö, for which the RH ratio between event and non-event is practically unity during the summer and winter. [Figure 1b]

Figure 3: Event (red) and non-event (blue) days in Melpitz using the proxy vs a) condensation sink and b) relative humidity .

[a]

[b]
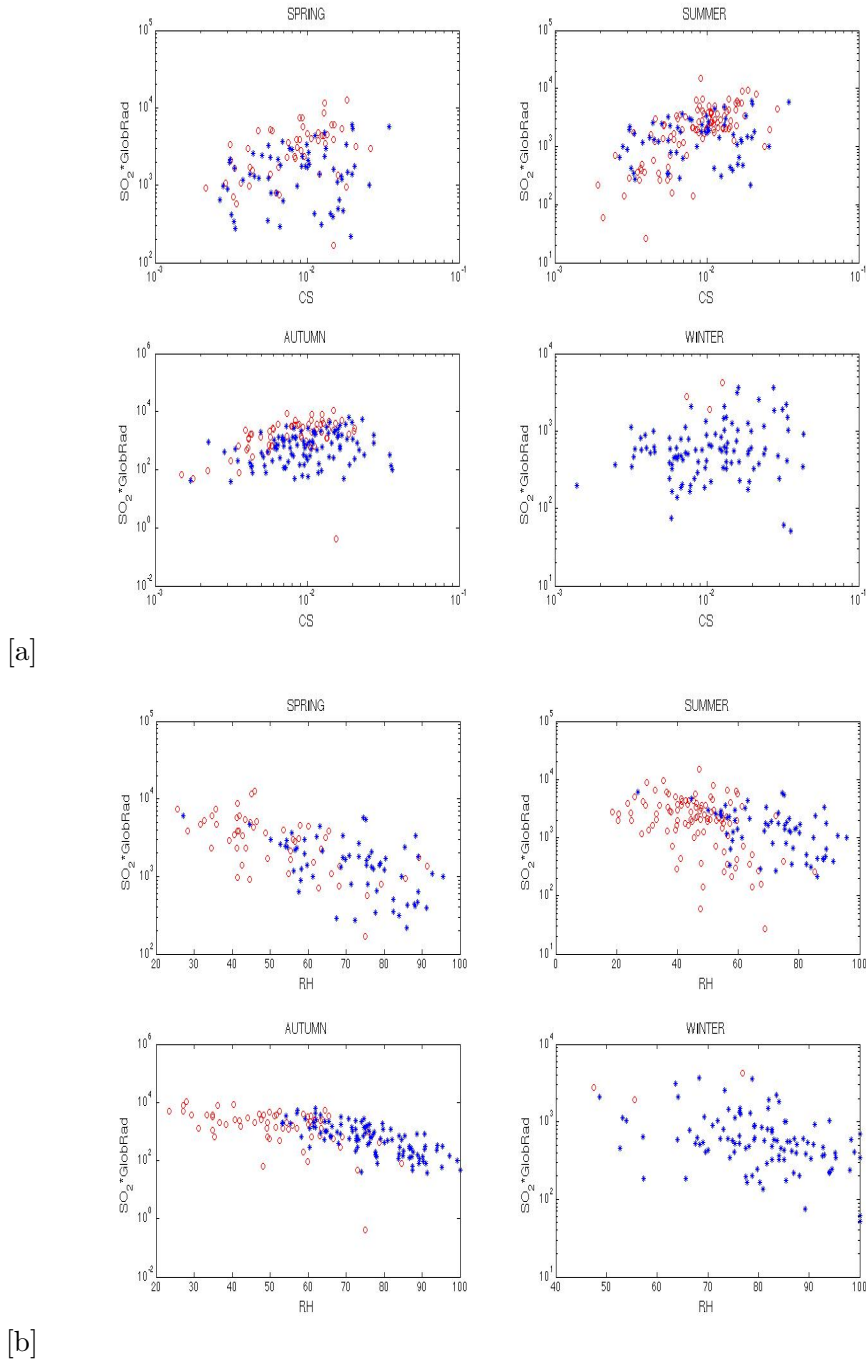
3. As a general rule, the temperature difference between event and non-event days was small for all the stations and seasons. However, a pattern can be observed here as well: the temperature during the event days exceeded the temperature for the non-event days for all stations and seasons, except for Värriö, Hyytiälä and Po Valley during the summer and Melpitz in the winter [Figure 1c].

4. SO_2 is needed for the production of sulfuric acid, which subsequently is involved in the nucleation process (Kerminen and Kulmala (2002)) and therefore a higher concentration of

sulfur dioxide was expected during the event days. However, in Hyytiälä and Värriö, the SO$_2$ concentrations during the non-event days are consistently higher during all seasons. In Po Valley, the SO2 ratio exceeds unity only during the spring and summer, while in Hohenpeissenberg the SO$_2$ ratios range between 1.5 and 5 during spring, autumn and winter [Figure 1d].

5. As the condensation sink (CS) determines the rate at which the molecules in gas phase are condensing onto the surfaces of pre-existing aerosols, it is expected that CS to be lower during the event days. Four of our five stations obey this rule. Only in Melpitz the CS is higher during event days during all seasons.[Figure 1e].

The correlations/anticorrelations can be used to build probability relationships predicting particle formation. Such correlations have been offered before in literature (Boy and Kulmala (2002); Hyvönen et al. (2005)), but it becomes more and more clear that a parameter which plays a strong separative role in one location can be neutral in another location. As such, in order to be able to predict which day can be an event/non-event day, one has to consider the most influencing factors characteristic for a certain environment. In our study, we consider the product between the global radiation and sulfur dioxide concentration (used actually as a proxy for sulfuric acid production) as the main key behind the nucleation events. In our systematic search for the best way of separating the event and non-event days, we found that a seasonal approach gives better results, as the variation of the parameters depends as well on the time of the year.

For instance, Figure 2 shows a possible nucleation day prediction based on global radiation and sulfur dioxide product (hereafter called proxy) plotted against condensation sink. The yearly figure (a) presents already a moderately good separation of the event days, while the seasonal figure (b) gives an even better distinction. However, Figure 3a shows that in Melpitz the condensation sink does not act very well as a separator between event and non-event days, while the relative humidity, shown in Figure 3b gives a relatively better result.

Each station has been examined with respect to all the parameters available and different methods of separation have been used. However, the event predictions developed, although work relatively well in some cases, do not represent a solid method of prognosticating when a nucleation event will occur. At this moment we are still at the stage of understanding the nucleation mechanism and the processes and conditions that trigger it. Future work is focused in developing more reliable tools for predicting the new particle formation events.

References

Boy, M. and Kulmala, M. (2002). Nucleation events in the continental boundary layer: Influence of physical and meteorological parameters. *Atmos. Chem. Phys.*, 2:375–386.

Hamed, A., Joutsensaari, J., Mikkonen, S., Sogacheva, L., Dal Maso, M., Kulmala, M., Cavalli, F., Fuzzi, S., Facchini, M., Decesari, S., Mircea, M., Lehtinen, K., and Laaksonen, A. (2007). Nucleation and growth of new particles in Po Valley, Italy. *Atmos. Chem. Phys.*, 7:355–376.

Hyvönen, S., Junninen, H., Laakso, L., Dal Maso, M., Grönholm, T., Bonn, B., Keronen, P., Aalto, P., Hiltunen, V., Pohja, T., Launiainen, S., Hari, P., Mannila, H., and Kulmala, M. (2005). A look at aerosol formation using data mining techniques. *Atmos. Chem. Phys.*, 5:3345–3356.

Kerminen, V. M. and Kulmala, M. (2002). Analytical formulae connecting the "real" and the "apparent" nucleation rate and the nuclei number concentration for atmospheric nucleation events. *J. of Aerosol Science*, 33:609–622.

Korhonen, P., Kulmala, M., Laaksonen, A., Viisanen, Y., McGraw, R., and Seinfeld, J. H. (1999). Ternary nucleation of H_2SO_4, NH_3 and H_2O in the atmosphere. *J. Geophys. Res.*, 104:26349–26353.

Kulmala, M., Lehtinen, K. E. J., and Laaksonen, A. (2006). Cluster activation theory as an explanation of the linear dependence between formation rate of 3 nm particles and sulphuric acid concentration. *Atmos. Chem. Phys.*, 6:787–793.

Kulmala, M., Vehkamäki, H., Petäjä, T., Dal Maso, M., Lauri, A., Kerminen, V.-M., Birmili, W., and McMurry, P. (2004). Formation and growth rates of ultrafine atmospheric particles: a review of observations. *J. Aerosol Sci.*, 35:143–176.

Laaksonen, A., Kulmala, M., Berndt, T., Stratmann, F., Mikkonen, S., Ruuskanen, A., Lehtinen, K., Dal Maso, M., Aalto, P., PetÃjÃ, T., Riipinen, I., Sihto, S.-L., Janson, R., Arnold, F., Hanke, M., Ücker, J., Umann, B., Sellegri, K., O'Dowd, C., and Viisanen, Y. (2008). SO_2 oxidation products other than H_2SO_4 as a trigger of new particle formation- part 2: comparison of ambient and laboratory measurements and atmospheric implications. *Atmos. Chem. Phys. Discuss*, 8:9673–9695.

Merikanto, J., Zapadinsky, E., Lauri, A., and Vehkamäki, H. (2007). Origin of the failure of classical nucleation theory: incorrect description of the smallest clusters. *Phys. Rev. Lett.*, 98:145702.

Napari, I., Noppel, M., Vehkamäki, H., and Kulmala, M. (2002). Parametrization of ternary nucleation rates for H_2SO_4-NH_3-H_2O vapors. *J. Geophys. Res.*, 107:4381, doi:10.1029/20.

CARBON ISOTOPE FRACTIONATION IN SCOTS PINE PHOTOSYNTHESIS

E. HILASVUORI[1], P. KOLARI[2], M. OINONEN[1] and P. HARI[2]

[1]Dating Laboratory, Finnish Museum of Natural History, P.O. Box 64, FI-00014, University of Helsinki, Finland
[2]Department of Forest Ecology, P.O. Box 27, FI-00014, University of Helsinki, Finland

Keywords: carbon isotopes, photosynthetic discrimination, leaf gas exchange, *Pinus sylvestris*

INTRODUCTION

The abundance of naturally occurring isotope ^{13}C in plant material is less than in atmospheric CO_2. This depletion is caused by discrimination against the heavier isotope during CO_2 assimilation in photosynthesis (Vogel, 1980, Farquhar et al., 1982). The discrimination is a result of differences in diffusion rates of $^{12}CO_2$ and $^{13}CO_2$ into the leaves and to the sites of carboxylation, and especially of differences in reaction rates with photosynthetic enzymes during carboxylation. The magnitude of photosynthetic ^{13}C discrimination is sensitive to environmental variables such as light, water availability and atmospheric humidity.

When environmental conditions change throughout the day or growing season, they create short-term differences in carbon isotope composition in leaf sugars (Brugnoli and Farquhar, 2000). These differences are transferred from leaf sugars to other plant compounds. Therefore carbon isotopic composition measured from plant tissues can be interpreted as a proxy for the environmental effects on photosynthesis integrated throughout the period during which the tissue was synthesized (Keitel *et al*., 2003; Helle and Schleser, 2004, McCarroll and Loader 2004).

Although the basic mechanisms determining isotopic discrimination during photosynthesis are known, direct measurements under field conditions remain scarce (Harwood et al., 1998, Wingate et al., 2007). In this preliminary study we examine momentary carbon isotope discrimination throughout a single day in a shoot of Scots pine (*Pinus sylvestris* L.). We create a method for determining instantaneous carbon isotope discrimination in photosynthesis in association with gas exchange measurements. We develop a model that explains the observed changes in the isotope ratios in gas exchange chamber by stomatal behaviour, diffusion and biochemistry. With this model we further can calculate the isotopic fractionation, using only environmental variables, extending the analysis beyond the direct measurements.

METHODS

A 24-h campaign was carried out in August 2007 at the SMEARII field station. The gas samples for isotope analysis were collected from a gas exchange chamber that comprised a transparent box with a volume of 1 dm^3. It was placed in the upper canopy with one shoot enclosed. The chamber was automatically closed every 10 min for 60 s. During the closure CO_2 concentration, water vapour, air temperature and PAR (photosynthetically active radiation) were monitored at 5-s intervals. The samples for isotope analysis were taken during 40 chamber closings, three samples for each closure. The first sample was taken before the chamber closed the second sample from the replacing air and the third from the chamber air just before the chamber opened again. Three times in a row the samples were taken from a chamber that was protected from light.

$^{13}C/^{12}C$ ratio was analysed from the collected gas samples with an isotope ratio mass spectrometer in Helsinki. The samples were measured against the international VPDB (Vienna Pee Dee Belemnite) isotope standard, and expressed as isotope ratios using delta (δ) notation

The observed variations in $\delta^{13}C$ are compared with those predicted from a gas exchange model. We used a model described in more detail in Hari and Mäkelä (2003) and Hari et al. (2008), where the stomatal action is derived from the optimization hypothesis proposed by Cowan and Farquhar (1977). The model uses PAR, saturation deficit of water vapour and ambient temperature as driving variables.

To simulate the carbon isotope fractionation, we applied the photosynthesis model with different rates of diffusion and carboxylation efficiency specified for $^{13}CO_2$ and $^{12}CO_2$, leading to consumption of two isotopes at different rates from the chamber air. The diffusivity of $^{13}CO_2$ in air is known to be 4.4‰ less than that of $^{12}CO_2$ (Craig, 1954). For discrimination associated with Rubisco carboxylation we used the fractionation factor -28.2‰ given in Brugnoli and Farquhar (2000). The model also includes respiration as an additional source of CO_2 in the stomatal cavity. We set the isotopic composition of the released CO_2 to -24.3‰, which is the photosynthesis-weighted average of assimilated carbon.

Since we wanted to compare the modelled change with the observed change in $\delta^{13}C$ in the gas exchange chamber, we determined the $^{13}CO_2$ and $^{12}CO_2$ fluxes from a mass balance equation of concentration changes in the chamber during the closure and air fluxes. We also applied the model to the measurements of environmental variables from the whole studied day. This made it possible for us to determine the momentary isotopic fractionation for every 10 min and to calculate the isotopic composition of carbon assimilated during the day.

RESULTS

The isotopic composition of the chamber air varied between slight depletion during the dark experiments to an enrichment of several per mill in the δ values. The model explained the changes rather well. R^2 between the measured and modelled values in the chamber was 0.89 (Figure 1). There was however, a small offset between the modelled and observed changes during closure, possibly for several reasons. Our photosynthesis model does not account for the CO_2 transfer in the mesophyll cells. This might cause the model to overestimate the overall fractionation (Farquhar et al. 1989). Also possible uncertainties arising from the experimental setup must be estimated from future control measurements.
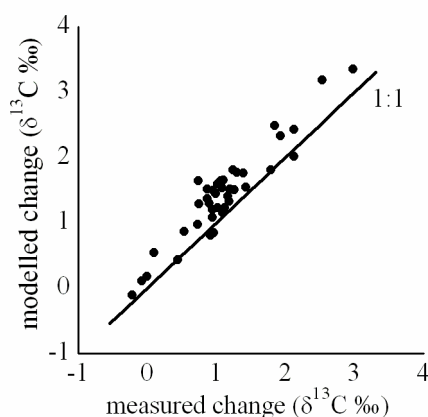
Figure 1. Modelled and observed changes in the isotopic composition of CO_2 inside the gas exchange chamber during closures.

The daily variation in assimilated carbon calculated from the environmental variables exceeded 10‰. The isotope $\delta^{13}C$ values peaked in the afternoon (Figure 2b), unlike the photosynthesis that peaked earlier (Figure 2a). The increasing of light decreased the discrimination against the heavier isotope and thus increased the isotope δ values of assimilated carbon. This discrimination was further decreased by the closure of stomata. The most depleted isotope values were produced in the morning and just before the sun set in the evening. The photosynthesis-weighted average of assimilated carbon for the studied day

calculated from the momentary values was -24.3‰., and is in agreement with other studies. For example Brandes et al. (2006), who studied Scots pines in Germany, determined the water soluble organic matter in pine needles to vary from -27.3% to -25.8%. We calculated the daily time course of $\delta^{13}C$ in assimilated carbon assuming that the isotope value of canopy air CO_2 was constant ($\delta^{13}C$ = -8‰). However, according to our measurements the isotopic composition of the air near the shoot varied from -10.6‰ to -7.3‰ during the studied day. This variation in $\delta^{13}CO_2$ has the potential of further modifying the isotope values of assimilated carbon (Buchmann et al., 2002).
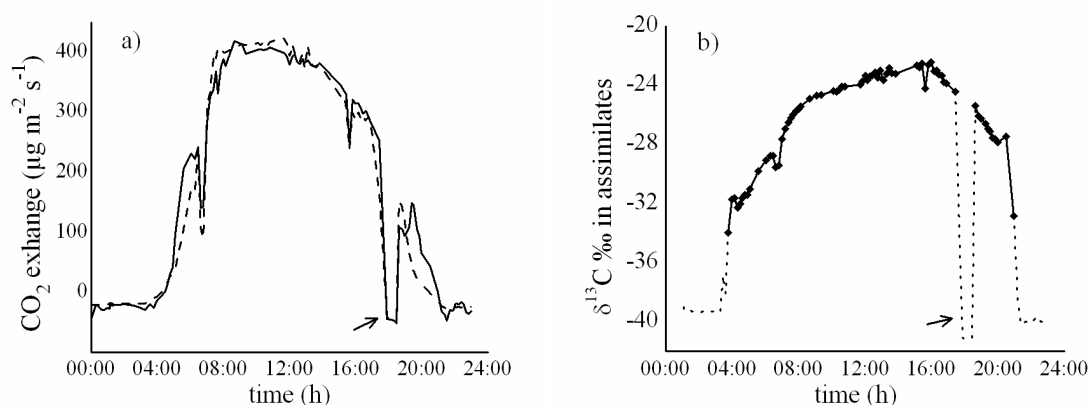
Figure 2. a) Modelled (dashed line) and measured (continuous line) CO_2 exchange of the pine shoot during the studied day. b) Daily time course of $\delta^{13}C$ in assimilated carbon calculated from light, temperature and water vapour saturation deficit. The dotted line represents values when there is insufficient light for photosynthesis. The three closures when the chamber was protected from light are indicated with an arrow.

CONCLUSIONS

We were able to detect changes due to tree processes in CO_2 carbon isotope ratios in gas exchange chamber and to explain the changes with a considerably simplified modelling approach. To our knowledge this is the first time in which daily patterns of isotopic fractionation in Scots pine photosynthesis under field conditions has been directly measured. We used a photosynthetic model that is new within the context of isotopic fractionation. For that reason, this study can also be considered as a test of the photosynthetic model with respect to isotopic fractionation. However, our isotope measurements covered only a warm and sunny summer day and we will need data covering variety of environmental conditions to fully evaluate the capacity of our model.

The results obtained can be used to calculate carbon isotopic composition of photosynthates, using only environmental factors. That provides the possibility to use isotopic composition in plant tissues as time-integrated signals of environmental effects on photosynthesis or to use isotope ratios as tracers in studying ecosystem carbon fluxes. The results can also be applied when interpreting isotopic ratios in tree rings for the purpose of palaeoclimate reconstructions.

REFERENCES

Brandes E., Kodama N., Whittaker K., Weston C., Rennenberg H., Keitel C., Adams M.A., Gessler A. 2006. Short-term variation in the isotopic composition of organic matter allocated from the leaves to the stem of *Pinus sylvestris*: effects of photosynthetic and postphotosynthetic carbon isotope fractionation. *Glob. Chang. Biol.* 12, 1922–1939.

Brugnoli E., Farquhar G.D., 2000. Photosynthetic fractionation of carbon isotopes. In: Leegood R.C., Sharkey T.D., von Caemmerer S. (Ed.) Photosynthesis: physiology and metabolism. Kluwer, Dordrecht, the Netherlands, pp. 399-434.

Buchmann N., Brooks J.R., Ehleringer J.R. 2002. Predicting daytime carbon isotope ratios of atmospheric CO_2 within forest canopies. *Funct. Ecol.* 16, 49-57.

Cowan I.R., Farquhar G.D., 1977. Stomatal function in relation to leaf metabolism and environment. *Soc. Exp. Biol. Symp.* 31, 471-505.

Craig H., 1954. Carbon 13 in plants and the relationship between carbon 13 and carbon 14 variation in nature. *J. Geol.* 62, 115-149.

Farquhar G.D., O'Leary M.H., Berry J.A., 1982. On the relationship between carbon isotope discrimination and the intercellular carbon dioxide concentration in leaves. *Aust J Plant Physiol.* 9, 121-137.

Farquhar G.D., Ehleringer J.R., Hubick K.T., 1989: Carbon isotope discrimination and photosynthesis. *Annu. Rev. Plant Physiol. Plant Mol. Biol.* 40, 503-537.

Hari P., Kolari P., Bäck J., Mäkelä A., Nikinmaa E., 2008. Photosynthesis. In: Hari P., Kulmala L. (Ed.) Boreal Forest and Climate Change. Advances in Global Change Research. Volume 34, Springer, Netherlands, pp. 183-195.

Hari P., Kulmala M., 2005. Station for Measuring Ecosystem-Atmosphere Relations (SMEAR II). *Boreal Environ. Res.* 10, 315-322.

Harwood K.G., Gillon J.S., Griffiths H., Broadmeadow M.S.J., 1998. Diurnal variation of $\Delta^{13}CO_2$, $\Delta C^{18}O^{16}O$ and evaporative site enrichment of $\delta H_2^{18}O$ in Piper aduncum under field conditions in Trinidad. *Plant Cell Environ.* 21, 269-283.

Helle G., Schleser GH., 2004. Beyond CO_2 fixation by Rubisco – an interpretation of $^{13}C/^{12}C$ variations in tree rings from novel intra-seasonal studies on broad-leaf trees. *Plant Cell Environ.* 27, 367-380.

Keitel C., Adams M.A., Holst T., Matzarakis A., Mayer H., Rennenberg H., Geßler A., 2003. Carbon and oxygen isotope composition of organic compounds in the phloem sap provides a short-term measure for stomatal conductance of European beech (*Fagus sylvatica* L.) *Plant Cell Environ.* 26, 1157-1168.

McCarroll D., Loader N. J. 2004: Stable isotopes in tree rings. *Quat. Sci. Rev.* 23, 771-801.

Vogel J.C., 1980. Fractionation of the carbon isotopes during photosynthesis. In: Sitzungsberichte der Heidelberger Akademie der Wissenschaften, matematisch-naturwissen-schaftlichs Klasse Jahrgang, 3 Abhandlung. Springer-Verlag, Berlin/ New York. pp. 111–135.

Wingate L., Seibt U., Moncrieff J.B., Jarvis P.G., Lloyd J., 2007. Variations in ^{13}C discrimination during CO_2 exhange by Picea sitchensis branches in the field. *Plant Cell Environ.* 30, 600-616.

THE "PRESSURE-EFFECT" IN UNARY CONDENSATION OF *N*-ALCOHOLS

A.-P. HYVÄRINEN,[1] J. WEDEKIND,[2] D. BRUS,[1,3] AND H. LIHAVAINEN[1]

[1]Finnish Meteorological Institute, Erik Palménin aukio 1, P.O. Box 503, F1-00101 Helsinki, Finland
[2]Dep. de Física Fonamental, Universitat de Barcelona, Martí i Franquès 1, 08028 Barcelona, Spain
[3]Laboratory of Aerosol Chemistry and Physics, Institute of Chemical Process Fundamentals, Academy of Sciences of the Czech Republic, Rozvojová 135, CZ-16502 Prague 6, Czech Republic

INTRODUCTION

It was generally assumed that the presence of a non-condensable carrier gas does not influence the clustering process. However, experiments since the 1980s have brought forth quite ambiguous results on the influence of the amount and the type of the carrier gas on the observed nucleation rate. During very recent years, interest in the topic was raised again both amongst experimentalists and theorists (Brus, *et al.,* 2006 and 2008; Hyvärinen *et al.*, 2006 and 2008; Barrett, 2007; Merikanto *et al.,* 2006; Tang *et al.,* 2006; Yasuoka *et al.* 2007) The measurements conducted by Brus *et al.*(2006 and 2008) and Hyvärinen *et al.* (2006 and 2008) in diffusion based devices increased the knowledge of the carrier gas effect on *n*-alcohols. Concurrently, Wedekind *et al.* (2008) presented a simple model that explains the pressure effect by a competition of two contributions: non-isothermal effects and pressure-volume work. The theoretical predictions presented in the paper agreed with the corresponding molecular dynamics simulations of Lennard-Jones argon. In this study, we now compare this theory against the available experimental data for *n*-alcohols.

METHODS

The experimental studies were carried out at the Finnish Meteorological Institute in a laminar flow diffusion chamber (LFDC) and at the Laboratory of Aerosol Chemistry and Physics, Institute of Chemical Process Fundamentals, Academy of Sciences of the Czech Republic using a thermal diffusion cloud chamber (TDCC). The detailed experimental setup, design, operation principle and validation of proper operation are discussed in details by Brus *et al.* (2006) and Hyvärinen *et al.* (2006). The measured substances were *n*-propanol in helium (TDCC), *n*-butanol in helium (LFDC), *n*-pentanol in helium (LFDC) and *n*-pentanol in argon (LFDC). The total pressure varied between 50 – 400 kPa depending on the experimental system.

The theoretical framework used in this study was introduced by Wedekind *et al.* (2008). The theory considers the efficiency of thermalization and the additional work that a cluster has to spend for growing in its presence. The "full pressure effect nucleation rate", J_{PE} can be written as

$$J_{PE} = \frac{b^2}{q^2 + b^2} J_{pV} \tag{1}$$

Here, b and q are factors from the thermalization effect. Physically, this is controlled by the competition between the energy increase, q, due to latent heat and the energy removal, b, through elastic collisions with vapor and carrier-gas molecules, given by

$$q = h - \frac{kT}{2} - \gamma \frac{\partial A(n)}{\partial n} \tag{2}$$

and

$$b^2 = 2k^2T^2\left(1 + \frac{N_c}{N}\sqrt{\frac{m}{m_c}}\right)$$

(3)

In equations (2) and (3) γ is the surface tension h is the latent heat per molecule; m, m_c are the molecular mass of the condensable and carrier gas; N, N_c are the number of vapor and carrier gas molecules, respectively. The nucleation rate J_{pV} takes into account the pV work that the growing cluster has to do against the pressure of the carrier gas. J_{pV} can be written as:

$$J_{pV} = K\exp(-\Delta G^*_{pV}/kT)$$

(4)

Here K is the kinetic prefactor and $\Delta G^*_{pV} = (16\pi/3)(v_l^2\gamma^3/\Delta\mu_{eff}^2)$ is the free energy barrier modified with the pressure of the carrier gas through the "effective chemical potential":

$$\Delta\mu_{eff} = kT\ln S - v_l(p + p_c - p_{eq})$$

(5)

Where v_l is the volume per molecule in the bulk liquid, p_c is the carrier gas pressure, $S = p/p_{eq}$ is the supersaturation and p_{eq} the equilibrium vapor pressure.

RESULTS

The desired form of experiments for a thorough investigation of the pressure effect theory would be measurements of nucleation rate as a function of total pressure with constant temperature and saturation ratio. The most extensive data sets are available for n-butanol in helium (Hyvärinen *et al.,* 2006 and 2008) and n-pentanol in helium and argon (Brus *et al.*, 2008).
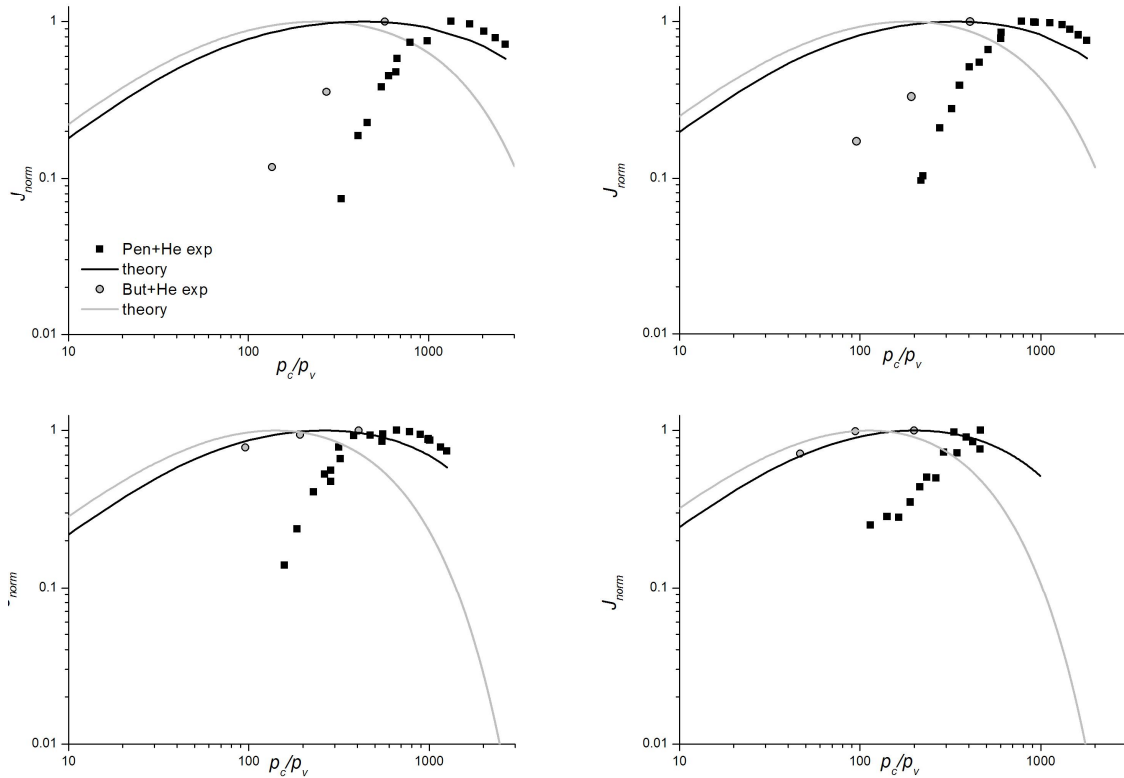
Figure 1. The normalized nucleation rate, J_{norm} as a function of p_c/p_v, the ratio between carrier gas pressure and the partial pressure of the vapor. a) 265 K, b) 270 K, c) 275 K, d) 280 K.

Figure 1 shows a comparison for *n*-butanol and *n*-pentanol in helium. The normalized nucleation rate, J_{norm} is acquired by dividing nucleation rates with the maximum one for each set of rates. The theory catches the correct shape and magnitude of the pressure effect. It also predicts the systematic differences observed between the two different nucleating substances. However, the pressure ratios for theory and experiments are slightly different.

The pressure effect theory suggests that for each system, a maximum nucleation rate exists due to competition of the thermalization effect and pV-work. Figure 2 illustrates how the theoretical p_c/p_v ratio has to be scaled to superimpose this maximum nucleation rates on the experimental ones. For *n*-pentanol + helium and *n*-butanol + helium the correction factors are nearly equal and have the same temperature dependence. However, for *n*-pentanol+argon, the temperature dependence is much steeper. It is possible that this is rather related to the experimental method and transport properties determined in the LFDC. For *n*-propanol in helium, the pressure effect was measured only at 290 K. A correction factor of 0.3 can be applied to the theoretical results to match this data.
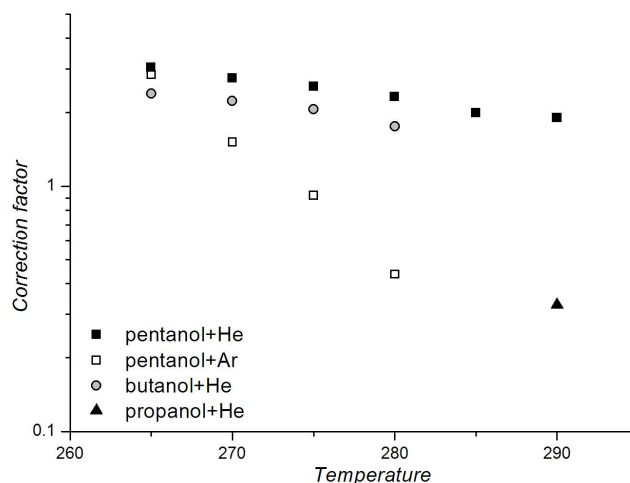
Figure 2. "Correction factor" – the ratio of experimental and theoretical p_c/p_v at nucleation rate maximum – as a function of temperature.

CONCLUSIONS

We have compared experimental pressure dependent nucleation rates of different *n*-alcohols and nucleation rates obtained from a recent theory on pressure effect (Wedekind *et al.*, 2008). A reasonable and promising agreement was found between theory and experiment for *n*-pentanol + helium and *n*-butanol + helium systems. The theory explains both the negative and positive pressure effects observed in the experiments, as well as the magnitude of the effect. However, the p_c/p_v ratios are slightly different between theory and experiment. For *n*-pentanol + helium and *n*-butanol + helium the difference is about a factor of 2.0-3.0 For *n*-pentanol + argon the difference is a strong function of temperature. More measurements are planned to test the pressure effect theory more rigorously. In addition, one of the virtues of the pressure-effect theory is that it is a minimal model with clearly controlled parameters and additional contributions (if applicable) are easily incorporated. For example, we plan to study the influence of nonideality of the vapor and/or carrier gas (Yasuoka *et al*, 2007) as well as basing the theory on a more reliable underlying model than CNT such as the recent Reguera-Reiss theory (Reguera and Reiss, 2004).

REFERENCES

Barrett, J. C., *J. Chem. Phys.* **126**, 074312 (2007).
Brus, D.*et al.*, *J. Chem. Phys.* **128**, 134312 (2008).
Brus, D., Zdimal, V., and Stratmann, F., *J. Chem. Phys.* **124**, 164306-164314 (2006).
Hyvärinen, A.-P. *et al.*, *J. Chem Phys.* **124**, 224304 (2006).
Hyvärinen, A.-P. *et al.*, *J. Chem Phys.* **128**, 109901 (2008).
Kashchiev, D., *J. Chem. Phys.* **104**, 8671-8677 (1996).
Merikanto, J., Zapadinsky, E., and Vehkamäki, H., *J. Chem. Phys.* **125**, 084503 (2006).
Reguera, D., and Reiss, H., *Phys. Rev. Lett.* **93**, 165701 (2004).
Tang, H.Y., and Ford, I. J., *J. Chem. Phys.* **125**, 144316 (2006).
Wedekind, J.*et al.*, *Phys. Rev. Lett.* **101**, 125703 (2008).
Yasuoka, K., and Zeng, X. C., *J. Chem. Phys.* **126**, 124320 (2007).

INTERPRETATION OF STEM CO_2 EFFLUX

T. HÖLTTÄ AND P. KOLARI

Department of Forest Ecology, P.O. Box 24, FIN-00014 University of Helsinki, Finland

INTRODUCTION

CO_2 flux from the stem is frequently taken as an indicator of stem respiration although the two might differ considerably because CO_2 is carried away from the site of production by the xylem sap (Teskey et al. 2008). CO_2 produced by respiration inside the stem diffuses out through the bark where its efflux can be measured, but it is also transported upwards in the xylem by sap flow. The dependence of stem CO_2 efflux on xylem sap flow is well recognized, but still the quantification of actual stem respiration rates from stem CO_2 efflux and sap flow measurements has remained ambiguous. A model of CO_2 transport inside the stem is presented here in order to identify the connection between stem CO_2 production and efflux. The model can then be used for scaling whole tree respiration from stem and branch CO_2 efflux measurements.

METHODS

The model tree was divided radially into the functional components of outer bark, phloem, cambium, sapwood and heartwood. CO_2 diffuses from its site of production following its concentration gradient. In cylindrical coordinates, the coordinate system best suited to describe the tree stem, the diffusion equation is written:

$$\frac{dC^{diff}}{dt} = D\left[\frac{d^2C}{dr^2} + \frac{1}{r}\frac{dC}{dr}\right] \tag{1}$$

where C is CO_2 concentration in the stem (water phase) ($mol\,m^{-3}$), r is the radial distance from the pith (m) and D is the radial diffusion coefficient of CO_2 in the stem ($m^2 s^{-1}$). The model is assumed symmetrical in the tangential direction so there is no net movement of CO_2 tangentially. The diffusion of CO_2 in the axial direction is also neglected due to its insignificance in relation to advection by the xylem sap. Equation for advection of CO_2 in the axial direction along with the xylem sap is written

$$\frac{dC^{adv}}{dt} = v\frac{dC}{dy} + \frac{dv}{dy}C \tag{2}$$

where y is the axial coordinate (m) and v is sap flow velocity ($m s^{-1}$). The second term in the right side of Eq (2) is assumed zero as we assume that the cross-sectional area of the sapwood is preserved at each height and at each branching which leads to the sap flow rate being constant at each height. This is in accordance with the pipe-model theory (Tyree and Zimmermann 2002). The total change in CO_2 concentration was made the sum of (1) and (2). Stem diameter and tapering and the proportionality between bark, phloem, cambium, sapwood and heartwood are taken from actual measurements for Scots Pine trees (Hakkila 1967, Laasasenaho 1983). The model tree is a 16 m Scots pine. The diffusion coefficient of CO2 is taken to be one fourth of the diffusion coefficient of CO_2 in water and the sap flow rate is $1*10^{-4}\,m s^{-1}$.

RESULTS AND CONCLUSIONS

Fig. 1 shows the steady state CO_2 efflux from the stem as a function of tree height. The results show that generally stem CO_2 efflux measurements tend to underestimate stem respiration. The proximity of the site of CO_2 production, low radial diffusion resistance of CO_2 inside the stem and low sap flow velocity were found promote the proximity between CO_2 efflux and the actual respiration rate. High sap flow rates cause marked discrepancy between the two with CO_2 production being higher than CO_2 efflux lower in the stem and the relation turning opposite close to the leaves.
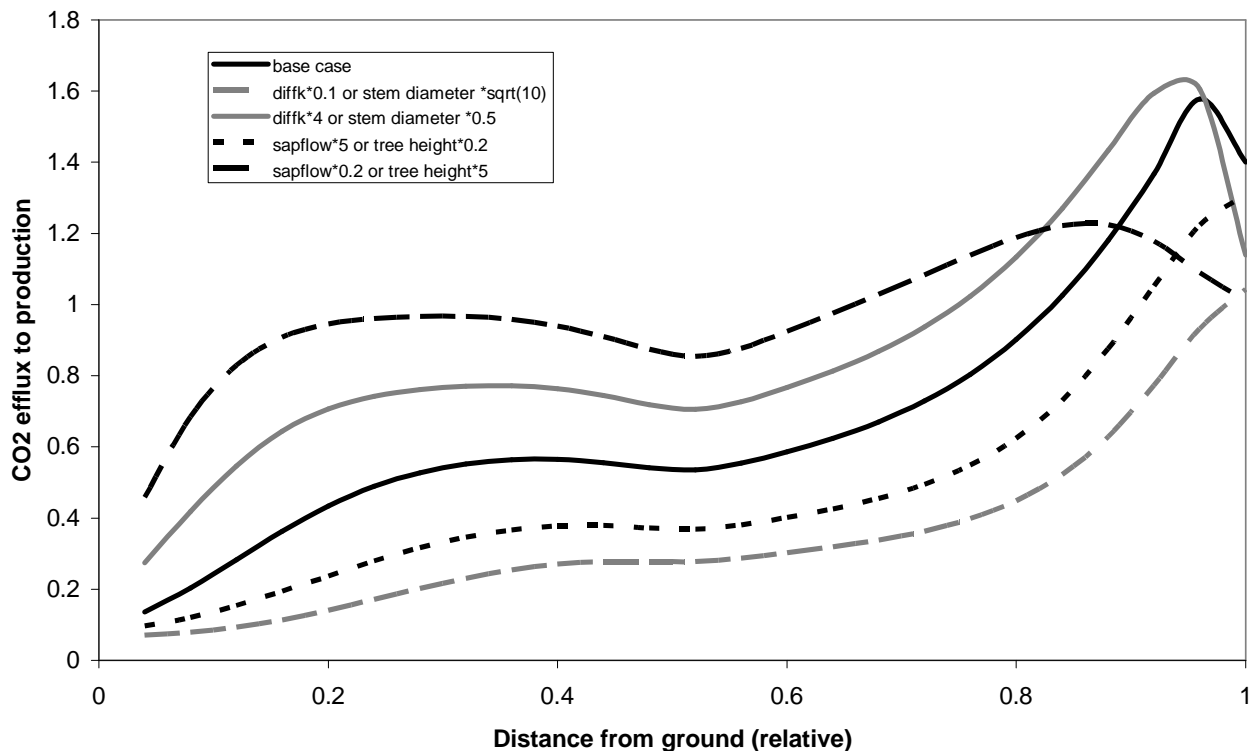
Figure 1. The relationship between CO_2 efflux and CO_2 production at different sites in the stem.

REFERENCES

Hakkila P. 1967. Vaihtelumalleja kuoren painosta ja painoprosentista. "Variation patterns of bark weight and bark percentage by weight". *Communications Instituti Forestalis Fennia* 62: 37 p.

Laasasenaho J. 1982. Taper curve and volume functions for Pine, Spruce and Birch. *Communications Instituti Forestalis Fennia*. 108: 1-74.

Teskey RO, Saveyn A, Steppe K, Mcguire MA. 2008. Origin, fate and significance of CO_2 in tree stems. *New Phytologist* 177: 17-32.

Tyree MT, Zimmermann M. 2002. *Xylem structure and Ascent of Sap*. Berlin: Springer-Verlag.

THE APPLICABILITY OF THREE DIFFERENT NUCLEATION EVENT DAY PREDICTION METHODS AT THREE MEASUREMENT SITES IN EUROPE

A. JAATINEN[1], A. HAMED[1], J. JOUTSENSAARI[1], S. MIKKONEN[1], W. BIRMILI[2], B. WEHNER[2], G. SPINDLER[2], A. WIEDENSOHLER[2], S. DECESARI[3], M. MIRCEA[3], M.C. FACCHINI[3], H. JUNNINEN[4], M. KULMALA[4], K.E.J. LEHTINEN[1,5] and A. LAAKSONEN[1,6]

[1] Department of Physics, University of Kuopio, P.O. Box 1627, FI-70211, Kuopio, Finland
[2] Institute for Tropospheric Research, Permoserstrasse 15, D-04318 Leipzig, Germany
[3] Istituto di Scienze dell'Atmosfera e del Clima Consiglio Nazionale delle Ricerche, I-40129 Bologna, Italy
[4] Department of Physics, P.O. Box 64, FI-00014, University of Helsinki, Finland
[5] Finnish Meteorological Institute, Kuopio unit, P.O. Box 1627, FI-70211 Kuopio, Finland
[6] Finnish Meteorological Institute, P.O. Box 503, FI-00101 Helsinki, Finland

INTRODUCTION

New particle formation is an important source of atmospheric particles and it has been observed to occur almost everywhere in the Earth's atmosphere (Kulmala et al., 2004). Although new particle formation has been studied widely, there still are no nucleation theories reliable enough to unambiguously explain how or why new particle formation events occur in the atmosphere. Hence, it is useful to find correlations between environmental variables which could be used to predict whether a nucleation event occurs or not.

In this study we tested the prediction methods of Boy and Kulmala (2002), Hyvönen et al. (2005) and Stanier et al. (2004) by applying them to the data collected from three European measurement stations located in very different environments: in Central Europe (Melpitz, Eastern Germany, a moderately polluted rural area), in Southern Europe (San Pietro Capofiume "SPC" in the Po Valley, a highly polluted rural area), and in Northern Europe (Hyytiälä station in Finland, a clean forest area). The time period for this study was two years (July 2003-June 2005). All these stations have facilities to measure numerous meteorological and gas phase parameters, such as radiation, relative humidity, temperature and SO_2 concentration. The particle size distribution measurements were performed using a DMPS (Differential Mobility Particle Sizer) system at each site, with measured size ranges of 3-800 nm, 3-600 nm and 3-500 nm at Melpitz, SPC and Hyytiälä, respectively.

METHODS AND RESULTS

The days were classified event or non-event days according to the method described by Hamed et al. (2007). Nucleation event day shows a clear growth in the particle number concentration of the nucleation mode size range which can be observed for several hours. If no new particle formation is observed, day is classified as a non-event day. The analysis of the two year data set showed that in Melpitz $\sim$26 % and $\sim$57% of the days were event and non-event days, respectively. The same numbers for SPC are $\sim$31% and $\sim$40%, and for Hyytiälä $\sim$35% and $\sim$45%. Based on these classifications we compared nucleation event day prediction methods described by Boy and Kulmala (2002), Hyvönen et al. (2005) and Stanier et al. (2004), by applying them to the data

obtained from the three stations.

The "nucleation parameter" (NP) of Boy and Kulmala (2002) is given by the intensity of UV-A radiation, divided by the product of water vapour concentration and temperature. They showed that, for the Hyytiälä data obtained during year 1999, the parameter exceeded a certain threshold on almost all event days, and that on those non-event days the parameter exceeds this threshold, the background aerosol concentration was high. We calculated the NP for event and non-event days for Melpitz, SPC and Hyytiälä as a function of condensation sink (Fig. 1). In this study, condensation sink (CS) was calculated assuming that condensing vapours have a low vapour pressure at particle surfaces and that molecular properties of these vapours are similar to those of sulphuric acid. This method has been described by Pirjola et al. (1998) and Kulmala et al. (2001).
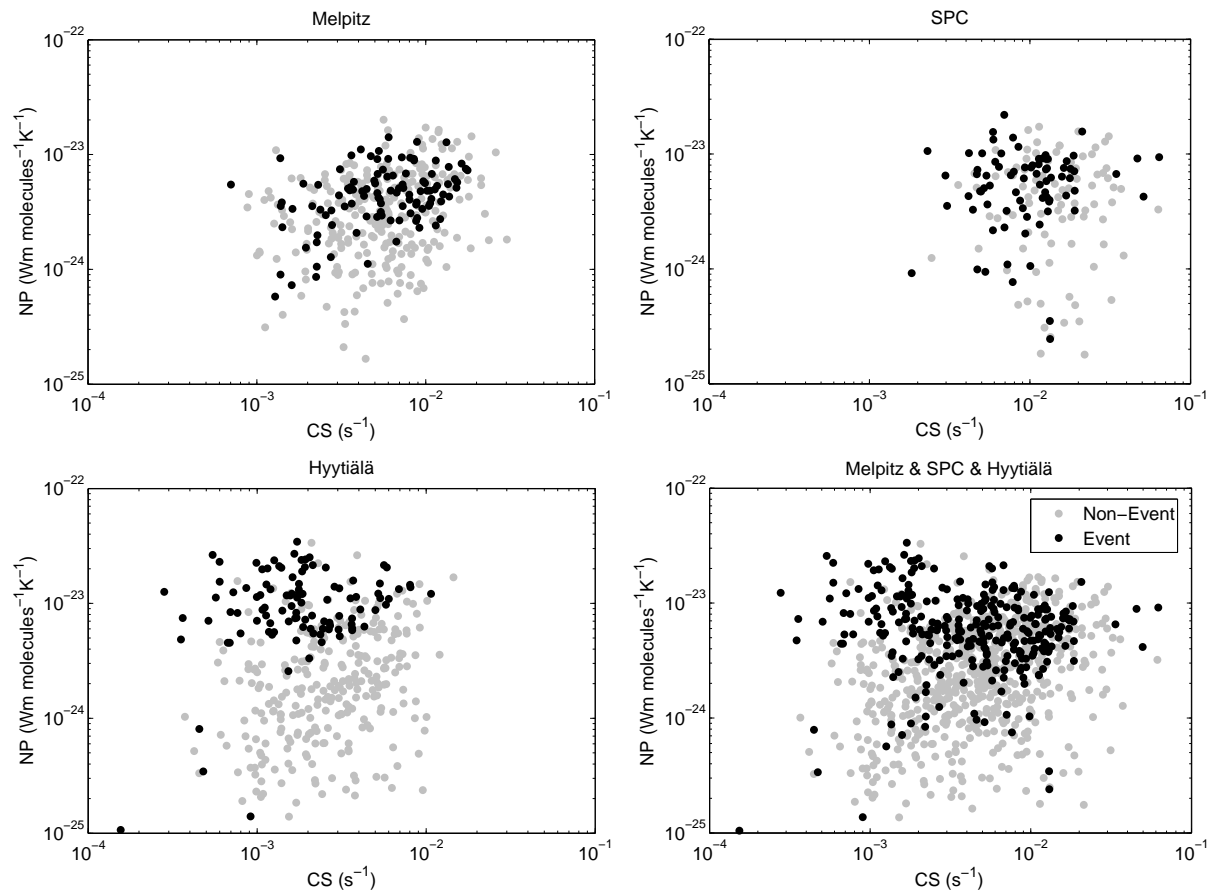
Figure 1: Nucleation parameter of Boy and Kulmala (2002) as a function of condensation sink in Melpitz, SPC and Hyytiälä. The data from the three stations are combined in the lower right panel. Event values for NP and condensation sink (CS) were taken at event start time and non-event values at noon.

The event day values in Fig. 1 were determined at event start time, and the non-event values at noon. Note that we used global radiation instead of UV-A. The lower left panel of Fig. 1 shows that the conclusions of Boy and Kulmala (2002) made based on Hyytiälä 1999 data hold for our Hyytiälä data as well, with the threshold value at about 5×10^{-24} Wm molecules^{-1}K^{-1} (this value is not directly comparable to that given by Boy and Kulmala (2002) because they used UV-A whereas we use global radiation in calculating the NP). However, such a threshold cannot be determined

for Melpitz and SPC (two upper panels of Fig. 1), nor for the combined dataset (lower right panel of Fig. 1).
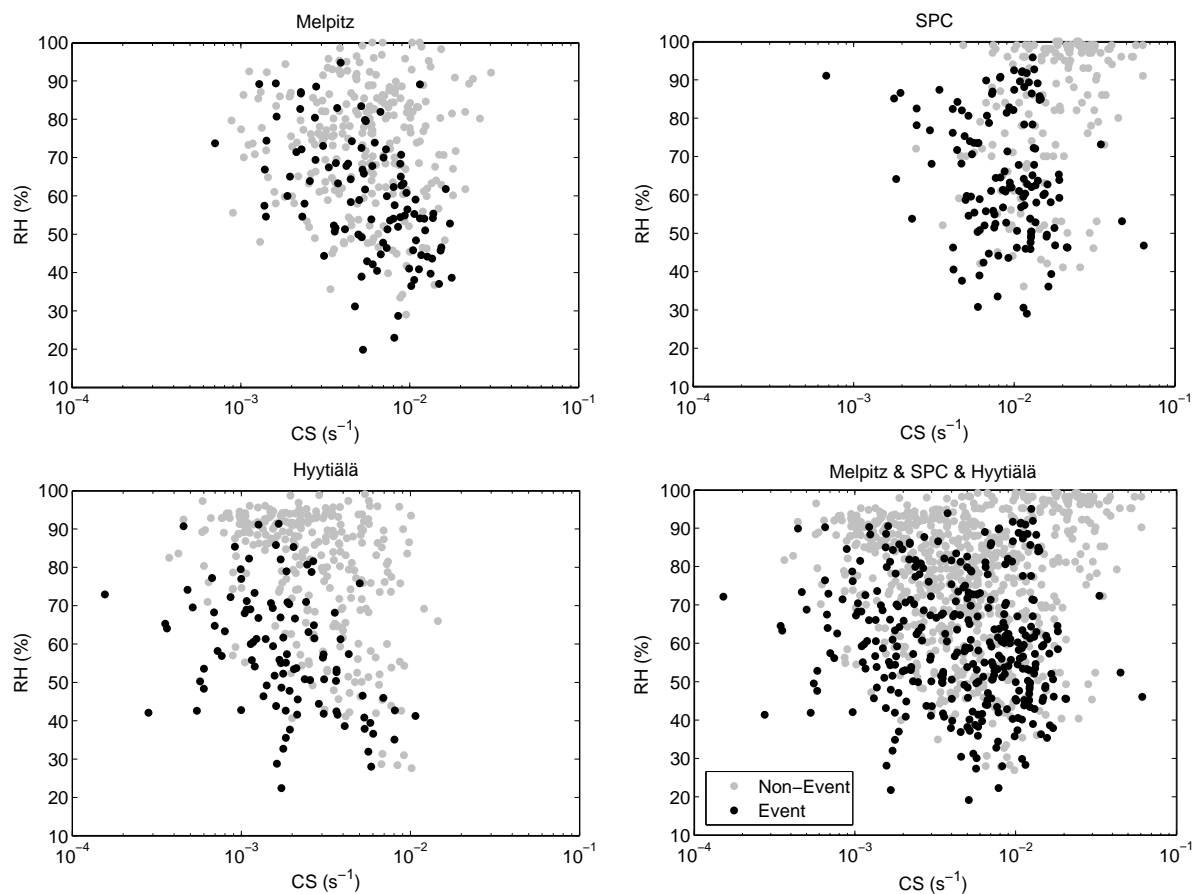
Figure 2: New particle formation event prediction using a method described by Hyvönen et al. (2005) in Melpitz, SPC and Hyytiälä. The data from the three stations are combined in the lower right panel. Event values for relative humidity (RH) and condensation sink (CS) were taken at event start time and non-event values at noon.

Hyvönen et al. (2005) showed that nucleation events in Hyytiälä can be predicted rather successfully using only two parameters, condensation sink and relative humidity. Fig. 2 shows our calculation for Melpitz, SPC and Hyytiälä, and for the combined dataset. (Note that here we took the CS and RH values at event start time, and at noon if the day was a non-event day, whereas Hyvönen et al. (2005) used average daytime values. We have tested that this makes only small difference to the result.) As with the NP, the separation is best for Hyytiälä data. For Melpitz, there is practically no separation of event and non-event data points. The same behaviour can also be seen in the case of SPC.

Stanier et al. (2004) suggested that favourable conditions for new particle formation can be described using a product of SO_2 and incoming UV radiation and condensation sink. Here, we applied the Stanier way of plotting event and non-event data in Fig. 3 (again, we used the global radiation instead of UV). Consistently with Fig. 2, event values for SO_2, radiation and CS were taken at event start time and non-event values were taken at noon. As shown in Fig. 3, the Stanier-type plot works well for Melpitz. In practice, it separates event and non-event days and there is only
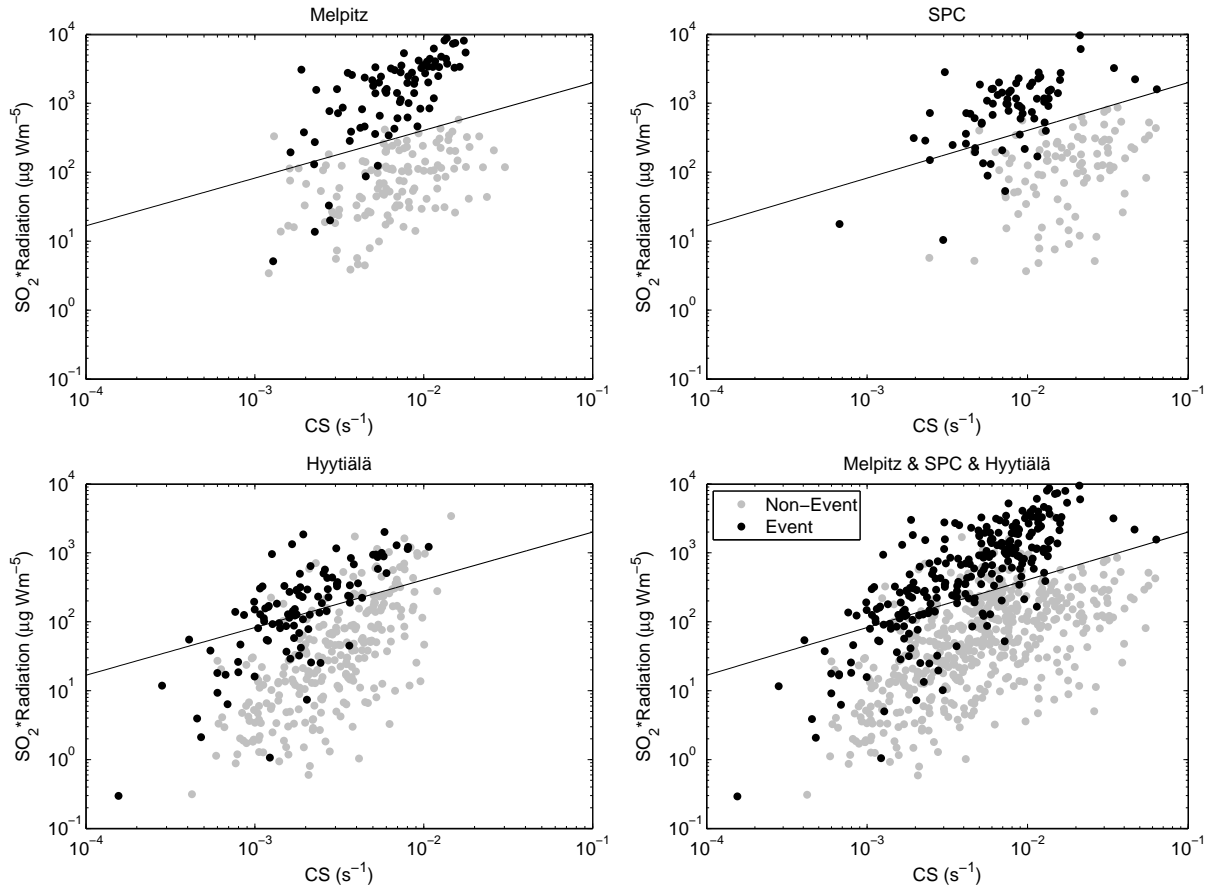
Figure 3: Predicting nucleation event days using a method described by Stanier et al. (2004) in Melpitz, SPC and Hyytiälä. The data from the three stations are combined in the lower right panel. The same separation line, determined by discriminant analysis from the combined data (lower right panel) was reproduced to all four panels. Event values for SO_2, radiation and condensation sink (CS) were taken at event start time and non-event values at noon.

minor overlapping in the event and non-event data points. This suggests that high sulphuric acid together with low condensation sink is a significant factor driving nucleation in Melpitz. Although the same thing can be said for nucleation in SPC, the separation of the data points is not so clear. (Note that we have drawn the same separation line, determined from the combined data (lower right panel of Fig. 3) using discriminant analysis, to all four panels). In Hyytiälä, the correlation between Stanier et al. (2004) parameters with new particle formation is not as good as in the other two stations. There is some kind of a separation between event and non-event day data points, but no unambiguous separation between them can be done; the overlapping is too great for that. Note that most of the SPC and Melpitz data are at CS values above $2\times10^{-3}\text{s}^{-1}$, whereas about half of the Hyytiälä data are below. Interestingly, this "clean" data shows much more event days below the separation line than the more polluted data with higher CS values.

CONCLUSIONS

Out of the three nucleation event day prediction methods studied (Boy and Kulmala (2002), Hyvönen et al. (2005), Stanier et al. (2004)), the Stanier et al. (2004) method gave better re-

sults for Melpitz and SPC than for Hyytiälä, whereas the two other methods worked to some extent for Hyytiälä but did not work at all for Melpitz and SPC. Overall, the Stanier et al. (2004) method was the only one that could be used to make some kind of separation between event and non-event days when the three datasets were combined. Hence, it seems that sulphuric acid plays a key role in the nucleation in Melpitz and SPC, but in Hyytiälä most likely other factors, such as the increased concentration of biogenic condensable vapours together with low condensation sink favours the nucleation process and the growth of the freshly formed particles.

Since atmospheric nucleation can occur in so many different environments and circumstances, methods of predicting nucleation events seem to work only for the environments they are specifically designed for. Thus, further parameterizations are needed to predict nucleation events with greater accuracy in a global scale.

ACKNOWLEDGEMENTS

REFERENCES

Boy, M. and Kulmala, M. (2002). Nucleation events in the continental boundary layer: Influence of physical and meteorological parameters. *Atmos. Chem. Phys.*, 2:1–16.

Hamed, A., Joutsensaari, J., Mikkonen, S., Sogacheva, L., Dal Maso, M., Kulmala, M., Cavalli, F., Fuzzi, S., Facchini, M., Decesari, S., Mircea, M., Lehtinen, K.E.J., and Laaksonen, A. (2007). Nucleation and growth of new particles in Po Valley, Italy. *Atmos. Chem. Phys.*, 7:355–376.

Hyvönen, S., Junninen, H., Laakso, L., Dal Maso, M., Grönholm, T., Bonn, B., Keronen, P., Aalto, P., Hiltunen, V., Pohja, T., Launiainen, S., Hari, P., Mannila, H., and Kulmala, M. (2005). A look at aerosol formation using data mining techniques. *Atmos. Chem. Phys.*, 5:3345–3356.

Kulmala, M., Dal Maso, M., Mäkelä J.M., Pirjola, L., Väkevä, M., Aalto, P., Miikkulainen, P., Hämeri, K., and O'Dowd, C.D. (2001). On the formation, growth and composition of nucleation mode particles. *Tellus*, 53B:479–490.

Kulmala, M., Vehkamäki, H., Petäjä, T., Dal Maso, M., Lauri, A., Kerminen, V.-M., Birmili, W., and McMurry, P.H. (2004). Formation and growth of ultrafine particles: a review of the observations. *J. Aerosol Sci.*, 35:143–176.

Pirjola, L., Laaksonen, A., Aalto, P., and Kulmala, M. (1998). Sulfate aerosol formation in the Arctic boundary layer. *J. Geophys. Res.*, 103:8309–8322.

Stanier, C.O., Khlystov, A.Y, and Pandis, S.N. (2004). Nucleation events during the Pittsburgh air quality study: description and relation to key meteorological, gas phase, and aerosol parameters. *Aerosol Sci. Tech.*, 38:253–264.

A THERMODYNAMICALLY CONSISTENT DETERMINATION OF SURFACE TENSION OF SMALL LENNARD-JONES CLUSTERS FROM SIMULATION AND THEORY

JAN JULIN[1], ISMO NAPARI[1], JOONAS MERIKANTO[2] and HANNA VEHKAMÄKI[1]

[1]Department of Physics, P.O. Box 64, FI-00014, University of Helsinki, Finland
[2]School of Earth and Environment, University of Leeds, Leeds LS2 9JT, United Kingdom

INTRODUCTION

In the usual theoretical description of nucleation, the classical nucleation theory (CNT), the assumption is made that the surface tension of small droplets is the same as the surface tension of a planar interface (this is called the capillary approximation). While the capillary approximation may be reasonable to certain extent, it is clear that in reality a small droplet consisting of only tens or hundreds of particles will have a highly curved surface, with properties that may be quite different from those of a planar surface. It is difficult to experimentally study droplet surface tension, but fortunately different computational and theoretical methods exist that can provide some insight to the problem. In this work we apply three such methods, namely molecular dynamics (MD) and Monte Carlo (MC) simulations and density functional theory (DFT) calculations, with the aim to investigate the surface tension of small Lennard-Jones (LJ) droplets and to find out about possible differences between the results obtained from these different methods.

In a previous study (Julin et al., 2008) we studied the critical sizes and formation energies of Lennard-Jones clusters with the aforementioned three methods. The Lennard-Jones interaction potential was cut and shifted at 5σ and all simulations were performed at the reduced temperature T'=0.662, which corresponds to 80 K with the commonly used parameter values of argon. The systems in the MD simulations consisted of a droplet in equilibrium with the surrounding vapor, at ten different vapor densities, and we combined them with direct simulations of a nucleation event occurring in supersaturated vapor. To complement the MD simulations, MC simulations were performed with the same potential and in the same temperature that were used in the MD simulations. Finally, perturbative DFT calculations were also performed. It was found that there were some differences between MD and MC values of critical size and formation energy, while DFT values agreed quite well with MD. However, the MD and MC bulk equilibrium values, namely surface tension of a planar liquid-vapor interface and the equilibrium vapor density, were in a rather good agreement.

By performing a thermodynamic treatment of a system where a droplet is surrounded by vapor, first presented by Gibbs (Gibbs, 1906), an expression for the surface tension of the droplet is obtained. This expression will depend on the choice of the dividing surface. Calculating the surface tension with respect to the surface of tension one gets

$$\gamma_s = \left(\frac{3W^*(\Delta p)^2}{16\pi} \right)^{1/3}, \tag{1}$$

where W^* is the formation energy of a cluster and Δp is the pressure difference between the liquid and vapor phases at chemical equilibrium. The radius of the cluster corresponding to the surface tension is given by

$$R_s = \left(\frac{3W^*}{2\pi\Delta p} \right)^{1/3}. \tag{2}$$
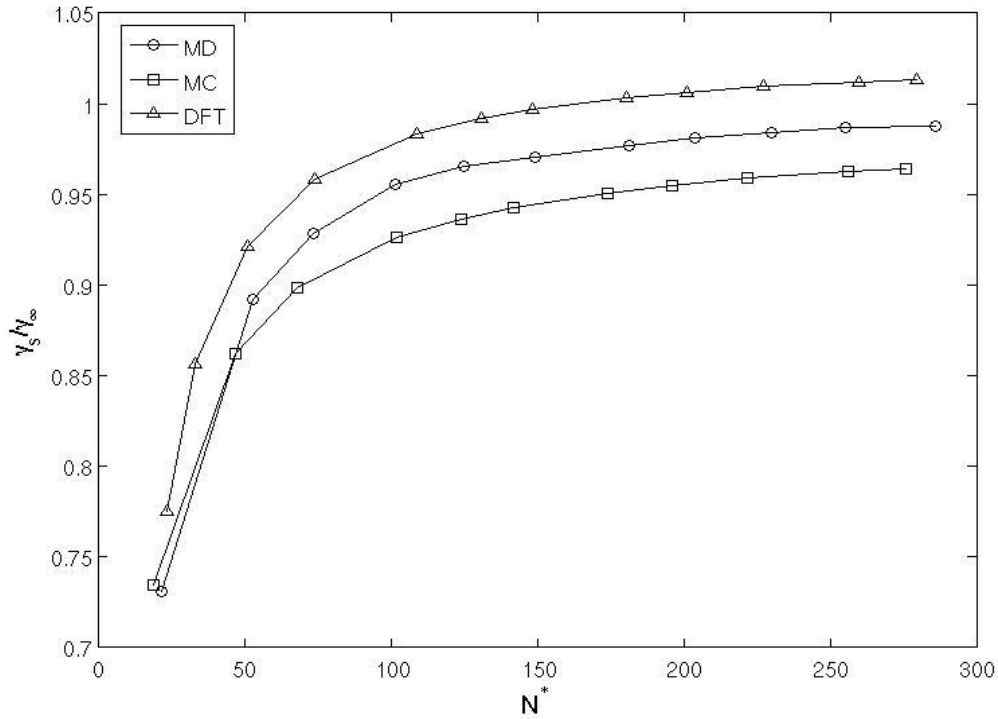
Figure 1. Surface tensions obtained with the different methods.

We already have the formation energies as simulation results (Julin et al., 2008). To calculate the pressure difference we performed MD simulations to obtain an equation of state at both liquid and vapor densities. These were then used to calculate both the MD and MC surface tensions according to Eq. 1.

RESULTS AND DISCUSSION

The ratios γ_s/γ_∞, where γ_∞ is the surface tension of the planar interface, are plotted in Fig. 1 for cluster sizes ranging from approximately 20 to 300 atoms. To be consistent, the MD value for planar surface tension is used to plot the MD points, and the MC points are plotted with the MC planar surface tension. In DFT calculations the parameters of the potential model are fitted so that the MD values for bulk properties are reproduced, and so the MD value of planar surface tension is used to plot the DFT points in Fig. 1.

The surface tension of the MD simulated droplets seems to approach the planar value quite nicely, with a difference of only about 1 % as the cluster size exceeds 250 atoms. The MC values are somewhat further off, with the difference to planar surface tension still at about 4 % for the largest clusters considered here. The DFT surface tensions are larger than the simulated ones, and they actually exceed the planar value at sizes around 150 atoms. This behavior has been found also in previous DFT studies, and at larger sizes than our current range the DFT values approach the planar value again (Koga et al., 1998, Napari and Laaksonen, 2007). All our methods indicate a considerable deviation from the planar surface tension at clusters that have fewer than 50 atoms.

Another way to choose the dividing surface is the equimolar surface. The radius of the equimolar surface is given by

$$R_e = \left(\frac{3N^*}{4\pi\Delta\rho} \right)^{1/3},$$

(3)
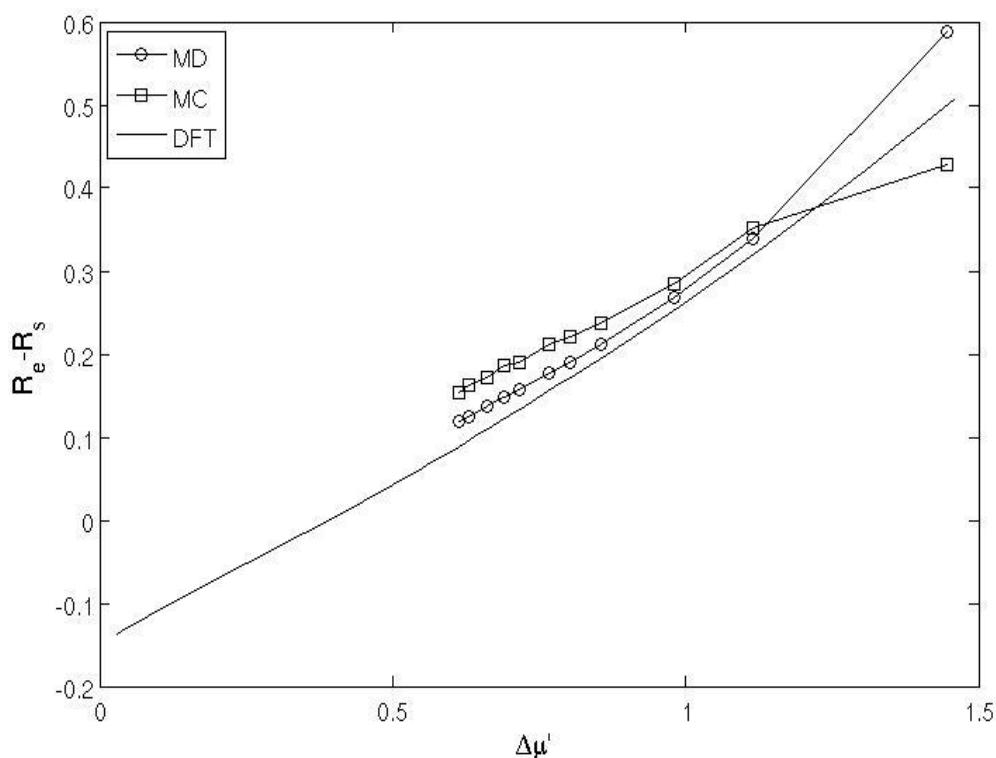
Figure 2. Difference between equimolar radius and the radius of surface of tension.

where N^* is the critical size, which we have as simulation results (Julin et al., 2008), and $\Delta\rho$ is the density difference between the liquid and vapor phases at chemical equilibrium.

In the classical theory the equimolar surface and the surface of tension would coincide, but in practice for our small clusters this is not the case. In Fig. 2 the difference between the equimolar radius R_e and the radius of the surface of tension R_s is plotted as a function of the chemical potential difference between the vapor surrounding the cluster and equilibrium vapor. The different methods produce qualitatively similar behavior for the difference R_e-R_s in the range of supersaturations considered here. It is clear from the DFT calculations seen in Fig. 2 that the difference at the planar interface limit (Tolman's length) will be negative. Assuming that the R_e-R_s lines obtained from simulations follow the same linear trend up to the planar limit, Tolman's length from MD and MC also seems to have a negative value. This is in contradiction with what has been observed in earlier MD simulations (Lei et al., 2005). However, it should be noted that it is impossible to draw any definite conclusions on the behavior of the MD and MC R_e-R_s difference at lower supersaturations based on the relatively small simulated clusters. Larger clusters in equilibrium with a vapor can be simulated, but, unfortunately we were not able to obtain the vapor density accurately enough from those simulations.

In summary, we have applied MD, MC and DFT methods to simple LJ clusters to investigate surface tension and the difference between the radii of equimolar surface and surface of tension. The results from all the methods follow similar trends, but there are notable quantitative differences.

REFERENCES

Julin, J., Napari, I., Merikanto, J., and Vehkamäki, H. (2008). Equilibrium sizes and formation energies of small and large Lennard-Jones clusters from molecular dynamics: A consistent comparison to Monte Carlo and density functional theories. *J. Chem. Phys.* 129, 234506.

Gibbs, J. W. (1906). *Scientific Papers*, London: Longmans Green.

Koga, K., Zeng, X. C., and Shchekin, A. K. (1998). Validity of Tolman's equation: How large should a droplet be? *J. Chem. Phys.* 109, 4063-4070.

Napari, I., and Laaksonen, A. (2007). Surface tension and scaling of critical nuclei in diatomic and triatomic fluids. *J. Chem. Phys.* 126, 134503.

Lei, Y. A., Bykov, T., Yong, S., and Zeng, X. C. (2005). The Tolman Length: Is It Positive or Negative? *J. Am. Chem. Soc.*, 127, 15346-15347.

THE AEROSOL PARTICLE NUMBER FLUXES MEASURED IN HELSINKI, FINLAND

L. JÄRVI[1], Ü. RANNIK[1], I. MAMMARELLA[1], A. SOGACHEV[2], P. AALTO[1], P. KERONEN[1], E. SIIVOLA[1], M. KULMALA[1] and T. VESALA[1,3]

[1]Department of Physics, P.O. Box 64, FI-00014, University of Helsinki, Finland
[2]Risø National Laboratory for Sustainable Energy, Technical University of Denmark, P.O. Box 49, DK-4000, Roskilde, Denmark
[3]Department of Forest Ecology, P.O. Box 27, 00014, University of Helsinki, Finland

Keywords: Eddy covariance, Particle number flux, Urban area, Traffic emissions

INTRODUCTION

Atmospheric aerosols are known to have adverse health effects especially in urban areas (Keeler et al. 2005), where majority of people live and where most of the anthropogenic sources of these particles are located. Aerosols affect also the radiation balance of Earth and local visibility. Despite the effects of these particles there is still lot of uncertainty in the emission strength of different sources, their distribution and effect on particle concentrations. So far the aerosol particle measurements in urban areas have concentrated on particle concentrations including both number and mass, while the measurements of particle emissions itself are scarce as was also reviewed by Pryor et al. (2008). In addition to the above mentioned reasons, measurements of particle exchange yields input parameters on air quality and climate models, and can be used in the validation of emission models.

In Helsinki, Finland, the continuous direct measurement of aerosol particle number flux (F_p) with the eddy covariance (EC) technique was started at the SMEAR III station in July 2007. The complex measurement surrounding enabled us to study the effect of different land use on the particle emissions, and besides the temporal variations on annual and diurnal scales were studied. Also dependencies between F_p and measured traffic rate were studied.

METHODS

The aerosol particle number fluxes were measured at the urban measurement station SMEAR III (*Station for Measuring Ecosystem – Atmosphere relations*) in Helsinki, Finland, between July 2007 and May 2008. The measurements were made on top boom of a 31 metres high measurement tower situated 5 km north-east from the Helsinki Centre. The surroundings of the measurement tower are heterogeneous and can be divided into urban, road and vegetation sector according to the typical land use on the area. Urban sector is mainly covered with University of Helsinki buildings with mean height on 20 metres and paved areas like roads and parking lots. In the road sector, one of the main roads with 40 000 vehicles workday^{-1} (Lilleberg and Hellman 2008) leading to the Helsinki Centre passes the measurement tower with a distance of 150 metres. University Botanical gardens and allotment garden are situated in the vegetation sector where the fraction of vegetated area is 85%. More information about the measurement surroundings can be found from Järvi et al. (2009) and Vesala et al. (2008). The measurement period was divided into three seasons: summer, fall/winter and spring. Summer covered Jul-Aug 2007, fall/winter covered Oct 2007-Mar 2008 and spring covered Apr-May 2008.

The turbulent fluxes of particle number were calculated with the eddy covariance (EC) technique where the flux is defined as co-variance between the vertical wind speed w and particle number. The measurements need to be made with high frequency (typically 10-20 Hz) to get in touch also with the smallest fluctuations. Our EC setup consisted of a Metek ultrasonic anemometer (USA-1, Metek GmbH, Germany) to measure w and a Water-based Condensation Particle Counter (WCPC) (TSI-3781, TSI Incorporated, USA) to measure the aerosol particle number concentration starting from 6 nm. We used 10

Hz as our measurement resolution. In the flux calculation, commonly accepted procedures were used as described by Aubinet *et al.* (2000). Before the flux calculation a linear de-trending and 2-dimensional coordinate rotation were applied on time series.

RESULTS

Particle fluxes showed a clear dependence on wind direction with the highest fluxes measured in the direction of road (60--180°) and lowest in the direction of high vegetation cover (220--340°) (Figure 1 and Table 1). In colder periods, a local flux maximum in northern direction was observed likely due to the residential area behind the University campus where wood burning for heating causes particle emissions. Also the parking lot situated close to the measurement tower in this direction is likely to have some effect. Table 2 lists the median particle fluxes for different land use sectors and seasons. In all land use sectors, the highest concentrations were measured in fall/winter when emissions from stationary combustion sources are high.
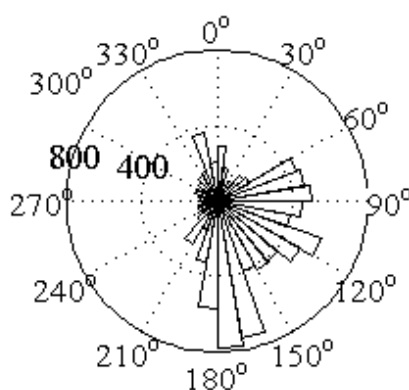
Figure 1. Wind direction dependency of the particle number flux (in 10^6 m^{-2} s^{-1}) in fall/winter.

		Median F_p	5% percentile of F_p	95% percentile of F_p
	Urb	50	7	420
Summer	Road	220	20	970
	Veg	43	7	290
	Urb	92	18	780
Winter/Fall	Road	350	43	1420
	Veg	104	16	500
	Urb	44	9	770
Spring	Road	240	22	1080
	Veg	54	10	370

Table 1. Median, 5% and 95% percentile aerosol particle number fluxes (10^6 m^{-2} s^{-1}) on different seasons and land use sectors.

On weekdays, particle fluxes had a distinguishable diurnal cycle which was most pronounced at the direction of the road reaching 10^9 m^{-2} s^{-1} in daytime (Fig. 2a). The diurnal behaviour followed closely measured traffic patterns excluding the rush hour peaks due to the enhanced mixing conditions in mid-day (not shown). On weekends, the effect of traffic was evident in the road sector while in other land use

sector there was no clear pattern during the day (Fig. 2b). Particle flux normalized with traffic rate was plotted against atmospheric stability to obtain more information about the effect of the mixing conditions on particle fluxes (Fig. 3). Variation of normalized flux was large but clear median dependence on stability could be observed with the particle flux increasing in unstable conditions.

The measured fluxes agree with those reported in other studies, where values have changed between 200 and $1200 \cdot 10^6$ m^{-2} s^{-1} (Nemitz *et al.* 2008, Mårtensson *et al.* 2006, Dorsey *et al.* 2002). Direct comparisons are, however, difficult since other studies have measured particle concentrations of particle larger than 11 nm, and also because particle fluxes are highly dependent on the measurement location, measurement height and the intensity of traffic, which vary strongly between different studies.
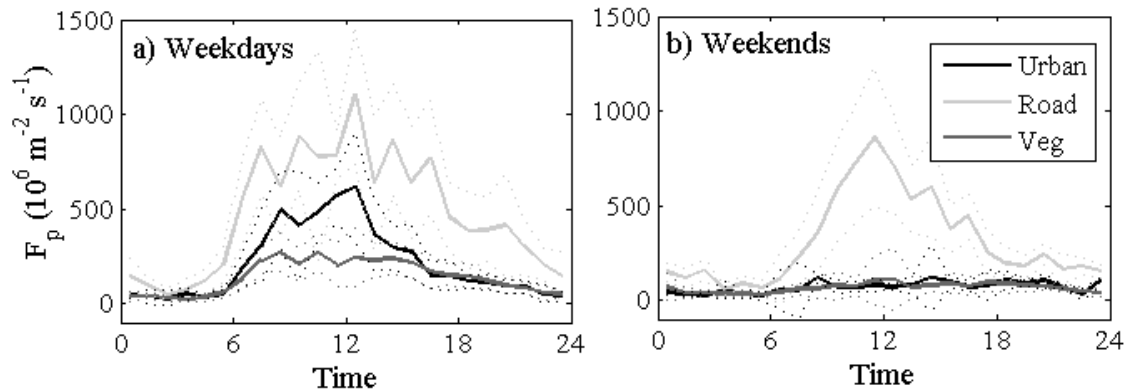
Figure 2. Diurnal behaviour of aerosol particle number fluxes (F_p) for different land use sectors and separately for a) weekdays and b) weekends in fall/winter. Dotted lines show the respective quartile deviations (half of the difference between 25 and 75 percentiles)
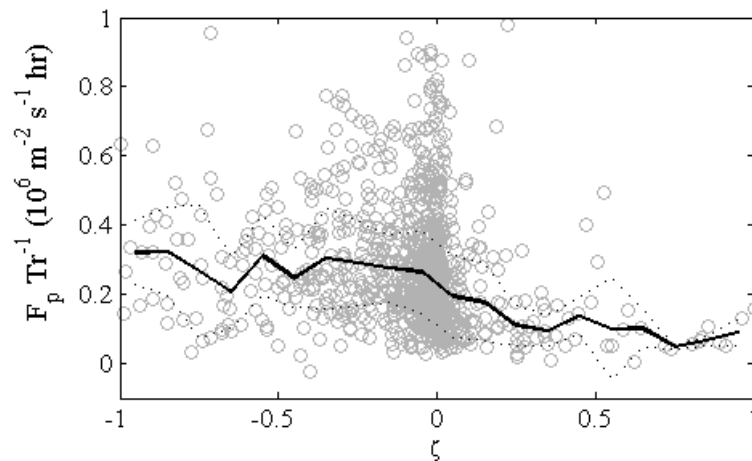
Figure 3. Dependence between particle number flux (F_p) normalized with traffic count (Tr) and atmospheric stability ζ. Circles show the hourly data points, solid line median bin values and dotted lines the quartile deviations.

CONCLUSIONS

The particle number fluxes showed distinguishable dependence on annual and diurnal scale. Higher fluxes were measured in fall/winter when emissions from stationary combustion sources are expected to be higher due to the colder temperatures. The diurnal behaviour followed traffic pattern and this was most pronounced in the direction of the road. Besides traffic, clear dependence on atmospheric stability was observed.

REFERENCES

Aubinet, M., Grelle, A., Ibrom, A., Rannik, Ü., Moncrieff, J., Foken, T., Kowalski, A.S., Martin, P.H., Berbigier, P., Bernhofer, C., Clement, R., Elbers, J., Granier, A., Grünwald, T., Morgenstern, K., Pilegaard, K., Rebmann, C., Snijders, W., Valentini, R. and Vesala T. 2000. Estimates of the annual net carbon and water exchange of forests: The EUROFLUX methodology. Advances in Ecological Research 30, 113–175.

Dorsey, J., Nemitz, E., Gallagher, M., Fowler, D., Williams, P., Bower, K. and Beswick, K. 2002. Direct measurements and parametrisation of aerosol flux, concentration and emission velocity above a city. Atmos. Env. 36, 791-800.

Järvi L., Hannuniemi H., Hussein T., Junninen H., Aalto P.P., Hillamo R., Mäkelä T., Keronen P. Siivola E., Vesala T. and Kulmala M. 2008. The urban measurement station SMEAR III: Continuous monitoring of air pollution and surface-atmosphere interactions in Helsinki, Finland. Bor. Env. Res. 14 (Suppl. A): 86–109.

Keeler G., Morishita M. and Young L.-H. (2005). Characterization of complex mixtures in urban atmospheres for inhalation exposure studies, Experimental and Toxicologic Pathology 57: 19–29.

Lilleberg I. and Hellman T. (2008). Liikenteen kehitys Helsingissä vuonna 2007. Helsingin kaupunkisuunnitteluvirasto, 2008:2.

Mårtensson, E., Nilsson, E., Buzorius, G. and Johansson C. 2006. Eddy covariance measurements and parameterisation of traffic related particle emissions in an urban environment. Atmos. Chem. Phys. 6, 769–785.

Nemitz E., Fowler D., Dorsey J.R., Theobald M.R., McDonald A.D., Bower K.N., Beswick K.M., Williams P.I. and Gallagher M.W. 2000. Direct measurement of size-segregated particle fluxes above a city. *J. Aerosol Sci.* 31, Suppl. 1, 116–117.

Pryor S. C., Gallagher M., Sievering H., Larsen E., Barthelmie R.J., Birsan F., Nemitz E., Rinne J., Kulmala M., Grönholm T., Taipale R. and Vesala T. (2008). A review of measurement and modelling results of particle atmosphere–surface exchange, Tellus 60B: 42–75.

Vesala T., Järvi L., Launiainen S., Sogachev A., Rannik Ü., Mammarella I., Siivola E., Keronen P., Rinne J., Riikonen A. & Nikinmaa E. 2008. Surface-atmosphere interactions over complex urban terrain in Helsinki, Finland. *Tellus B* 60: 188–199.

MONOTERPENE AND OXYGENATED VOC EMISSIONS FROM A SCOTS PINE BRANCH IN FIELD CONDITIONS

M. K. Kajos[1], R. Taipale[1], P. Kolari[2], T. M. Ruuskanen[1], J. Patokoski[1], J. Bäck[2], P. Hari[2] and J. Rinne[1]

[1]Department of Physics, P.O. Box 68, FI-00014, University of Helsinki, Finland
[2]Department of Forest Ecology, P.O. Box 27, FI-00014, University of Helsinki, Finland

Keywords: proton transfer reaction mass spectrometry, shoot chamber

INTRODUCTION

Volatile organic compounds (VOCs) participate in many chemical processes that occur in the atmospheric boundary layer (eg. Atkinson and Arey, 1998; 2003). They also contribute to the formation and growth of atmospheric particles which are an important factor in the climate system (Hoffmann et al., 1997; Tunved et al., 2006). In the ecosystem scale boreal forest is known to emit oxygenated volatile organic compounds (OVOCs) as reported by eg. Rinne et al. (2007). However, the emissions dynamics of individual trees is rather poorly known. To get more information about the branch scale OVOC emissions of Scots pine we constructed a dynamic on-line chamber system.

METHODS

Measurements were carried out at the SMEAR II measurement station (Hari and Kulmala, 2005) in Hyytiälä Southern Finland (61°51´ N, 24°17´ E, 181 m a.s.l.) in summer 2007. The forest around the measurement station was dominated by Scots pine with some Norway spruce, aspen and birch. The canopy height of the forest was about 16 m.

In our automated chamber system a shoot of Scots pine was enclosed into a chamber in the crown part of the canopy to minimize shading. Monoterpenes and some oxygenated VOC (methanol, acetone, and acetaldehyde) concentrations were measured using a proton transfer reaction mass spectrometer (PTR-MS, Ionicon Analytic GmbH; Lindinger et al., 1998). The calibration procedure and volume mixing ratio calculations of the PTR-MS are presented in detail by Taipale et al. (2008). Chamber measurements were done every third hour since the PTR-MS measurements were divided to three cycles each of them lasting an hour. The first hour was allocated to the ambient air volume mixing ratio measurements (Ruuskanen et al., 2009), the second to ecosystem scale flux measurements (Taipale et al., 2009) and the third to chamber measurements.

The dynamic shoot chamber was made of acrylic plastic and coated with Teflon (Fluoro Ethylene Propylene, FEP) film. It remained open most of the time and was closed periodically for a short time four times per hour. Sample air was drawn continuously from the chamber to the PTR-MS via about 60 m long Teflon tubing. Also trace gas (CO_2, H_2O, O_3 and NO_x) concentrations inside the chamber as well as air temperature and photosynthetically active radiation (PAR) were measured continuously (Hari et al., 1998).

During the closure concentration of a gas inside the chamber may change. Increase in the concentration indicates that the shoot is acting as a source of that particular gas, whereas decrease indicates deposition. The changes in the concentrations during the closure can be used to determine the gas fluxes. When we assume that during the chamber closure the VOC concentrations reach steady state, the net flux F (g g_{dw}^{-1} s^{-1}) of a particular VOC can be determined by the mass balance equation

$$F = \frac{q(C_f - C_i)}{m_{biomass}} \, .$$

(1)

In this equation q (m^3 s^{-1}) is the flow rate through the chamber and $m_{biomass}$ (g$_{dw}$) is the dry weight of the branch, C_i (g m^{-3}) is the initial ambient air and C_f (g m^{-3}) the final concentration of the compound inside the chamber.

RESULTS AND DISCUSSION

As an example one of week measurements from June 2007 are presented in Figure 1. Emissions of all the measured four compounds methanol, acetaldehyde, acetone and monoterpenes have a clear diurnal cycle and emission maximum in the noon.
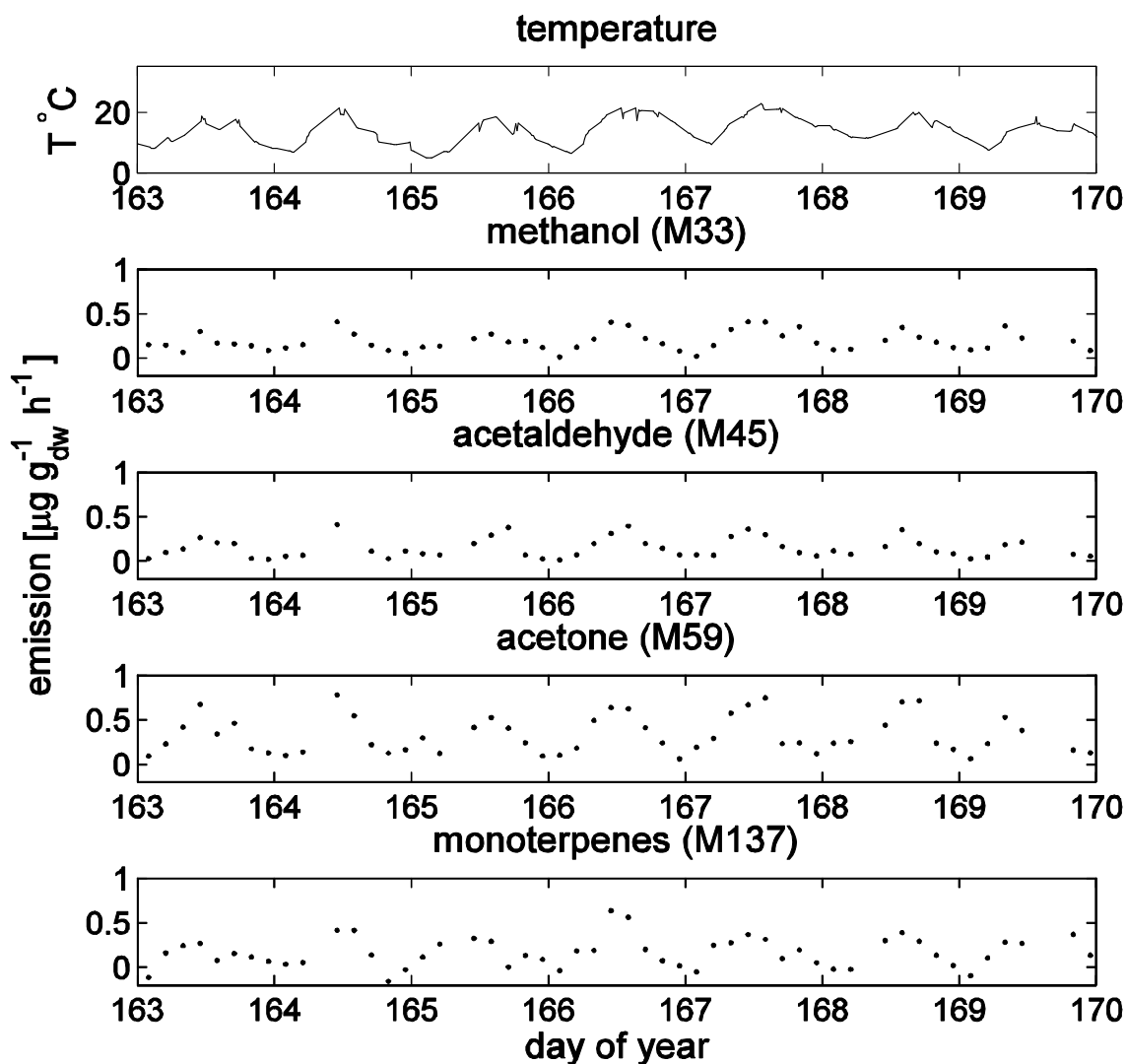
Figure 1. Hourly mean temperature inside the chamber and hourly mean emissions of methanol, acetone, acetaldehyde and monoterpenes measured in Hyytiälä between June 12 and June 19 in 2007.

Measured shoot scale emissions of each of the three OVOCs were of the same order of magnitude as emission of monoterpenes. The emission of OVOCs corresponded to over 80% of the total emission of these four compounds. Previously published results by Rinne et al. (2007) reported that in Hyytiälä the ecosystem scale monoterpene emissions corresponded to about 50 % of the total emission of these compounds.

In mid-June the average emission of monoterpenes from Scots pine branch was about 0.25 μg g_{dw}^{-1} h^{-1}, which corresponds a standard emission rate, normalized to 30˚C, of about 7.5 μg g_{dw}^{-1} h^{-1}. Komeda and Koppmann (2002) reported corresponding standard emission rates of 2.4-3.0 μg g_{dw}^{-1} h^{-1} for Scots pines growing in southern Germany. Thus the estimated standard emissions of the Scots pine growing in Hyytiälä were about three times higher than those reported by Komeda and Koppman (2002).

By using an assumption that all of the monoterpenes emitted from the Hyytiälä forest are from the Scots pine needles, the shoot emissions can be converted from needle mass to areal emissions. The upscaled monoterpene emissions from our measurements were lower than the canopy scale emissions reported by Rinne et al. (2007), indicating that pine needles are not the only source of monoterpenes at the Hyytiälä measurement station.

REFERENCES

Atkinson, R. and Arey, J. (1998). Atmospheric chemistry of biogenic organic compounds. *Accounts of Chemical Research*, 31, 574-583.

Atkinson, R. and Arey, J. (2003). Gas-phase tropospheric chemistry of biogenic volatile organic compounds: a review. *Atmospheric Environment*, 37, 197-219.

Hari, P., Keronen, P., Bäck, J., Altimir, N., Linkosalo, T., Pohja, T., Kulmala, M. and Vesala, T. (1999) An improvement of the method for calibrating measurements of photosynthetic CO_2 flux. *Plant, Cell and Environment*, 22, 1297-1301.

Hari P. and Kulmala, M. (2005). Station for Measuring Ecosystem-Atmosphere Relations (SMEAR II), *Boreal Environment Research*, 10: 315-322.

Komeda, M. and Koppmann, R. (2002). monoterpene emissions from Scots pine (*Pinus sylvestris*): Filed studies of emission rate variabilities. *Journal of Geophysical Research*, 107 (13), 4161, doi 10.1029/2001JD000691.

Lindinger, W., Hansel, A. and Jordan, A. (1998). On-line monitoring of volatile organic compounds by means of Proton-Transfer-Reaction Mass Spectrometry (PTR-MS) Medical applications, food control and environmental research. *International Journal of Mass Spectrometry and Ion Processes*, 173, 191-241.

Rinne, J., Taipale, R., Markkanen, T., Ruuskanen, T.M., Hellén, H., Kajos, M.K., Vesala, T., and Kulmala, M. (2007). Hydrocarbon fluxes above a Scots pine forest canopy: measurements and modelling. *Atmospheric Chemistry and Physics*, 7, 3361-3372.

Ruuskanen, T. M., Taipale, R., Rinne, J., Kajos, M. K., Hakola, H., and Kulmala, M. (2009). Quantitative long-term measurements of VOC concentrations by PTR-MS: annual cycle at a boreal forest site *Atmos. Chem. Phys. Discuss*, 9, 81-134

Taipale, R., Ruuskanen, T. M., Rinne, J., Kajos, M. K., Hakola, H., Pohja, T. and Kulmala, M. (2008). Technical Note: Quantitative long-term measurements of VOC concentrations by PTR-MS - measurement, calibration, and volume mixing ratio calculation methods. *Atmospheric physics and* chemistr*y*, 8, 6681-6698.

Taipale, R., Ruuskanen, T. M., Kajos, M. K., Patokoski, J., Hakola, H. and Rinne, J. (2009). Volatile organic compound emissions from a boreal forest- direct ecosystem scale measurements in 2006-2008. *This issue.*

Tunved, P., Hansson, H.-C., Kerminen, V.-M., Ström, J., Dal Maso, M., Lihavainen, H., Viisanen, Y., Aalto, P. P., Komppula, M., and Kulmala, M. (2006). High Natural Aerosol Loading over Boreal Forests. *Science*, 312, 261-263

DENSITY ANALYZING METHOD OF ATMOSPHERIC PARTICLES: RELIABILITY AND LIMITATIONS USING A NEW ELPI STAGE

J. KANNOSTO, J. YLI-OJANPERÄ, M. MARJAMÄKI, A. VIRTANEN AND J. KESKINEN

Laboratory, Department of Physics, Tampere University of Technology, P. O. Box 692, FIN-33101 Tampere, Finland

INTRODUCTION

The assessment of climatic and health effects of atmospheric aerosol particles requires detailed information on the particle properties. In addition, the particle chemical composition and other chemical and physical properties carry information concerning sources and formation mechanisms of the particles.

Nucleation bursts observed in different environments are producing nucleation mode particles in the atmosphere. There have been intensive and successful efforts to identify different nucleation mechanisms. Regardless of the progress, there are still gaps in the general understanding of the new particle formation, and between the experimental data and models. In the experimental data there are for example long time series available showing particle size evolutions after nucleation event, but the observations of composition and properties are mostly lacking. It is not clear which compounds are responsible of condensational growth process of nucleation mode particles or what kind of shape particles have. A number of different organic species has been linked with the particle growth process in natural forest environment (e.g. O'Dowd, 2002, Laaksonen et al., 2007). As a property complementary to particle composition, the density of the particles is of great interest. We have studied density of boreal forest particles and find density values for nucleation, Aitken and accumulation modes (Kannosto et al. 2008). Measurements in Kannosto et al. 2008 have made using normal ELPI impactor with filter stage. After these measurements, we have developed a new ELPI stage with lower cut point (Yli-Ojanperä et al. 2009). With the new impactor stage, we have been able to lower a detection limit of the density analyzing method down to d_a 10 nm. In this study we have performed calibration measurements in laboratory and simulations to clarify the lowest size limits and reliability of density analyzing method using the old and the new ELPI impactors (Yli-Ojanperä et al. 2009).

DENSITY ANALYZING METHODS

Particle density was estimated using the parallel measurement method developed at Tampere University of Technology, first described by Ristimäki et al. (2002). The method is based on a simultaneous ("parallel") distribution measurement with an electrical low pressure impactor (ELPI) and a scanning mobility particle sizer (SMPS) or a differential mobility particle sizer (DMPS) and, further, on the relationship between particle aerodynamic size, mobility size and effective density. First applied to laboratory aerosols and diesel exhaust particles, the method has been developed further to be suitable for an atmospheric aerosol (Virtanen et al., 2006; Kannosto et al. 2006). The method has been modified to be suitable for large data series and multimodal distributions, which are typical for Boreal forest environment.

The method is based on mathematical model of ELPI. Simulated ELPI currents are produced using mathematical model of ELPI charger and impactor. Modes fitted to SMPS/DMPS distribution and initial guess of density value of each modes are sent through the mathematical model of ELPI and the result is simulated currents. Differences between simulated and measured ELPI currents are minimized altering the density value of each mode. After minimization the result is density values for each mode.

Using the usual ELPI impactor with filter stage we are able to get density values from ~15nm particles and above. To be able to find density value of even smaller particles ELPI impactor must be modified. Now we have developed a new ELPI impactor stage with cut size of ~16 nm. Using ELPI with the new impactor stage and density analyzing method we are able to find density values of ~10nm particles and above.

Density analyzing method has very good time resolution. ELPI measures every 1 s and SMPS and DMPS measure every 2 - 10 minutes. Thus the particle density value can be found from every SMPS/DMPS scan. Therefore the density analyzing method is real-time method and it is very suitable for fast processes as the new particle formation.

MEASUREMENTS

Laboratory tests of density analyzing method were taken in Tampere University of Technology, Aerosol Physics laboratory. We used di-octyl sebacate (DOS, density 0.912 g/cm^3) and evaporation-condensation generator to produce polydisperse aerosol distribution. Geometric mean diameter (GMD) of the particles size distribution varied between 8 nm – 40 nm and distributions were very narrow, geometric standard deviation (GSD) was about 1.2. SMPS was measuring mobility size of particles and aerodynamic size of particles was measured using ELPI with the new impactor stage.

SIMULATIONS

Reliability simulations were calculated using Matlab®. We simulated particle distribution modes with different GMD, GSD and heights. ELPI currents were produced using the simulated modes and specific density values. 5% random error was added to these ELPI currents. This simulates real ELPI measurements allowing 5% error to ELPI currents. We assumed that the 5% is reasonable and the error includes flaws of electrometers zero level, impactor kernel functions and charger efficiency curve. Then the density values of each simulated modes were calculated 50 times using ELPI currents having the random error. The result is 50 density values for each particle mode. By calculating average and standard deviation of density results we could estimate the reliability of the results for each particle mode. Using different particle mode sizes the lowest detection limit could be estimated. Simulations were performed using mathematical model of the new and the old ELPI impactor setup.

RESULTS

Results of reliability simulations show differences between the new and the usual (old) impactors. Average density results and variations as a function of mode GMD can be seen in figure 1. The density values of the initial particle modes were 1.0 g/cm^3. As it can be seen, density analyzing method produces densities closed to the initial value at high GMD values. When size distributions with GMD smaller than 15 nm were used, density analyses produced different values depending on impactor type. However, using the new impactor the density values were equal to the initial values indicating lower size limit for density analysis. Also variation of the density values was much smaller with the new impactor. Lowest detection limit for the new impactor setup is about 10 nm and for the old setup about 15 nm. These limits are in aerodynamic diameters and they are affected by particle density; particle density smaller than 1.0 g/cm^3 changes detection limits higher and particle density higher than 1.0 g/cm^3 changes detection limits lower.

In laboratory measurements only the new impactor setup was used. Results of calibration measurements for the old impactor setup have been presented in Kannosto et al. 2006. Results of the old impactor setup presented in Kannosto et al. 2006 and results measured in this study follow the results of simulations. The density value of DOS particle distributions achieved by the density analyzing method is very close to bulk density of DOS. Due to variation, the density results under the lowest detection limits dispersed.

Results are very promising from the viewpoint of atmospheric particle formation studies and indicate that using the new impactor setup it is possible to find the density result for nucleation mode particle size 10 nm and above.
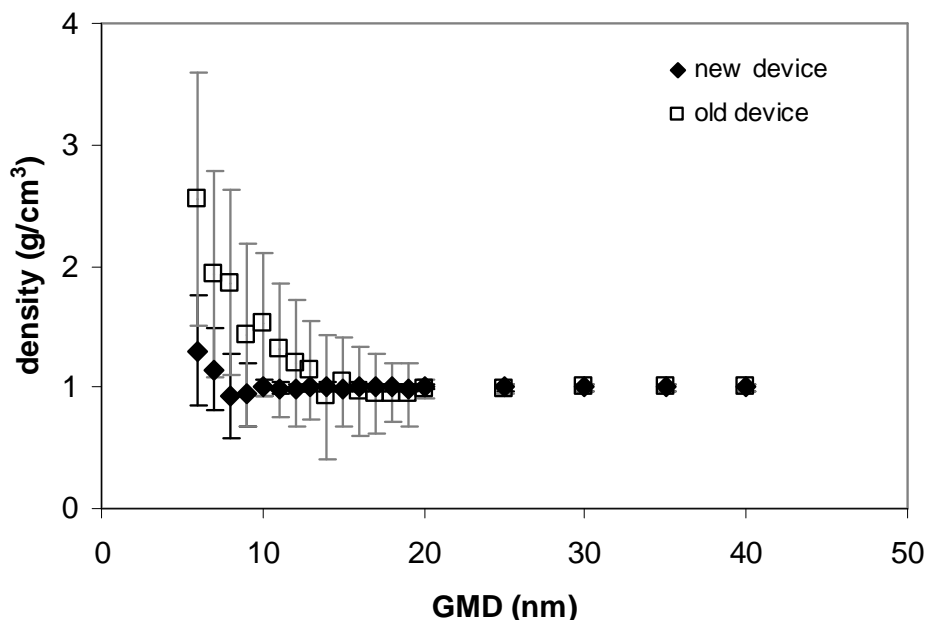
Figure 1. Results of reliable simulations. Average density values of simulations using the new (black diamond) and the old (open square) ELPI impactor. Variation of the density results can be seen in error bars. Density of primary mode particles were 1.0 g/cm³.

REFERENCES

Kannosto J., Virtanen A., Lemmetty M., Mäkelä J.M., Keskinen J., Junninen H., Hussein T., Aalto P., Kulmala M., Mode resolved density of atmospheric aerosol particle, *Atmospheric Chemistry and Physics* 8, 5327-5337, 2008..

Laaksonen, A., Kulmala, M., O'Dowd, C.D. , Joutsensaari, J., Vaattovaara, P., Mikkonen, S., Lehtinen, K.E.J., Sogacheva, L., Dal Maso, M., Aalto, P., Petäjä, T., Sogachev, A., JunYoon, Y., Lihavainen, H., Nilsson, D., Facchini, M.C., Cavalli, F., Fuzzi, S., Hoffmann, T., Arnold, F., Hanke, M., Sellegri, K., Umann, B., Junkermann, W., Coe, H., Allan, J.D., Rami Alfarra, M.,: Worsnop, D.R, Riekkola, M.-L., Hyötyläinen T., and Viisanen Y. The role of VOC oxidation products in continental new particle formation, *Atmos. Chem. Phys. Discuss.*, 7, 7819-7841, 2007.

O'Dowd, C.D., Aalto, P., Hämeri K., Kulmala M., Hoffmann T.: Atmospheric particles from organic Vapours, *Nature*, 416, 497-498, 2002..

Ristimäki, J., Virtanen, A., Marjamäki, M., Rostedt, A., Keskinen J.: On-line measurement of size distribution and effective density of submicron aerosol particles. *J. Aerosol Sci.*, 33, 1541-1557, 2002

Virtanen, A., Rönkkö, T., Kannosto, J., Ristimäki, J., Mäkelä, J. M., Keskinen, J., Pakkanen, T., Hillamo, R., Pirjola, L., Hämeri, K.: Winter and summer time size distributions and densities of traffic related aerosol particles at a busy highway in Helsinki. *Atmos. Chem. Phys.*, 6, 2411-2421, 2006

Yli-Ojanperä J., Kannosto J., Marjamäki M. Keskinen J.: Improving the nanoparticle resolution of the ELPI, Manuscript in preparation/submitted

TECHNIQUE TO ACCURATELY MEASURE ATMOSPHERIC CO_2 CONCENTRATIONS: RESULTS FROM A BOREAL FLUX TOWER SITE

P. KERONEN[1], E. SIIVOLA[1], T. POHJA[2], T. AALTO[3], J. HATAKKA[3] and T. VESALA[1]

[1] Department of Physics, University of Helsinki, Finland
[2] Hyytiälä Forestry Field Station, University of Helsinki, Finland
[3] Finnish Meteorological Institute, Helsinki, Finland

Keywords: NEE, atmospheric CO_2, automatic calibration, IRGA, regional CO_2 flux

INTRODUCTION

Net ecosystem carbon exchange (NEE), i.e. the difference between uptake by photosynthesis and release by respiration of CO_2, at local scale (10-10 000 m) is nowadays routinely assessed using eddy covariance methods (Baldocchi 2003; Helliker et al., 2004). At continental to global scale the NEE can be estimated via inverse modelling with atmospheric tracer transport models, biogeochemical process models, remote sensing based ecosystem models and/or inventory approaches (Potter et al., 1993; Running et al., 1999; Pacala et al., 2001). At regional scale (10-1000 km) methods to assess ecosystem CO_2 exchange are not as established and the coverage of the estimates is limited especially on continents (Gurney et al., 2002; Helliker et al., 2004; Bakwin et al., 2004; Karstens et al., 2006; Desai et al., 2008).

The same techniques that are used to estimate NEE on continental to global scale are used for regional scale estimates also. Integrating local scale eddy covariance data with remote sensing data from satellite appears to be a valuable tool (Running et al., 1999; Yamaji et al., 2007; Wylie et al., 2007). Regional scale NEE estimates can also be obtained with the inverse models (Gurney et al., 2002; Bakwin et al., 2004). The current accuracy of these estimates is unfortunately limited by the sparse observation network especially on continents (Karstens et al., 2006; Xiao et al., 2008). So there is a need for continuous, accurate and consistent data of boundary layer CO_2 concentration to be used in the models estimating global and regional carbon sinks.

This study aims to prove the technical feasibility of an affordable instrumentation that could be routinely operated at tower flux sites for the purpose of obtaining accurate and continuous atmospheric CO_2 concentration data to be used in modelling of regional CO_2 exchange.

MATERIALS AND METHODS

The measurement system (HYDE CO2 set-up) is installed at the SMEAR II site (Kulmala et al., 2001; Hari and Kulmala, 2005; Vesala et al. 2005) at the Hyytiälä Forestry Field Station of the University of Helsinki (61°50'50.69" N, 24°17' 41.17" E, 198 m asl).

Between October 2006 and February 2008 URAS 4 CO_2 and H_2O analysers (Hartmann & Braun, Frankfurt am Main, Germany) were used in the measurements. Since March 2008 an LI-840 $CO_2/H2O$-analyser (Li-Cor Inc., Lincoln, NE, USA) was added to the measurement system. The operation of the analysers is based on infrared absorption (IRGA). Air sample is taken from 67.2 m height in a tower. Sample line outdoors is a 16 mm / 14 mm diameter PTFE tube heated to keep the tube surface temperature above dew point. Sample flow rate is 45 $l·min^{-1}$ and residence time 20 s. Indoors the sample is directed through a PTFE manifold to a 1/8" (outer) diameter SS 316 tube. Flow rate in this line is 0.5 $l·min^{-1}$. Before the analyser the sample flows through a membrane (Nafion™) type drier (12", PD-200T™, Permapure Inc., Toms River, NJ, USA) where the dew point is reduced to about – 38 ° C. The combined residence time in the indoors sample line is less than 3 s. The calibration gases in use at Smear II are manufactured by Deuste Steininger GmbH, Mühlhausen, Germany. The concentrations, covering a range from 350 to 430 ppm, of the calibration gases have been determined to an accuracy of 0.1 ppm by Finnish

Meteorological Institute at their Pallas-Sodankylä Global Atmosphere Watch station against the primary standards (WMO-X2007 CO2-in-air scale). During the time period covered in this study the concentrations were determined twice.

Measurement of the ambient CO_2 concentration and calibration of the analyser is performed automatically twice a day between 01:00 - 01:30 and 13:00 - 13:30 local winter time. The atmospheric concentration is measured both before and after each calibration sequence. The calibration sequence consists of a measurement of bottled natural air, measurements of five calibration gases, and a measurement of the bottled natural air again. Also the calibration gases and the bottled air are fed through the Nafion™ tubes, but they are humidified instead of dried and achieve equal water vapour (H_2O) concentrations with the ambient air sample. The H_2O concentration is measured simultaneously to check the equality. The CO_2 signals are corrected for pressure and temperature dependence. Calibration parameters are calculated by using a 2nd order polynomial fit. The bottled natural air is used to verify calibration stability over the 30 min period and between the days.

After the calibration parameters have been determined the calibrated data, i.e. atmospheric CO_2 concentration and CO_2 concentration in the bottled natural air, is calculated. To ensure that the required 0.5 ppm accuracy is achieved the atmospheric CO_2 concentration data is screened out on the basis of the following criteria:
• if the standard deviation of the measured CO_2 concentration of any calibration gas exceeds 0.5 ppm
• if the root-mean-square of the standard errors of the measured calibration gas CO_2 concentrations exceeds 0.25 ppm (propagation of error estimate for the calibration)
• if the deviation between the measured CO_2 concentration in the bottled natural air before and after the calibration sequence exceeds 0.5 ppm
• if the residual of fit for any calibration gas CO_2 concentration exceeds 0.5 ppm
• if the deviation between the measured CO_2 concentration in the bottled natural air during the night and the afternooon calibration sequence exceeds 0.5 ppm
If any of the mentioned criteria for rejection is met the corresponding atmospheric CO2 concentration data is screened out.

During 28th – 29th August 2007 a comparison experiment, where atmospheric CO_2 concentration was measured simultaneously with a reference instrumentation (MPI CO2 set-up), was performed. The MPI CO2 set-up was provided by BGC-GasLab of Max-Planck-Institute for Biogeochemistry (Jena, Germany). The MPI CO2 set-up consists of a flask sampling instrumentation and a post-collection gas chromatographic analysis (Jordan and Brand, 2003) The CO_2 calibration scale of BGC-GasLab for measurements of atmospheric samples is directly linked to the WMO mole fraction scale (Jordan and Brand, 2003). The analyses were performed about a week after the collection.

The flask sampling instrumentation of the MPI CO2 set-up consisted of a pump, a needle valve, flowmeters, a 3-way valve, pressure gauges, a sample dryer and three sample flasks made of glass (volume 1 l) and equipped with shut off valves. The three sample flasks were installed in series. A chemical dryer (magnesiumperchlorate) was installed in-line in front of the flasks. The air sample was pushed through the flasks with the pump. The flow through the flasks (ca. 2.7 l min^{-1}) was continuous. The pressure inside the flasks was kept at ca. 0.9 bar overpressure with a pressure regulator of the instrumentation. With the chemical dryer installed in the line a dew point of ca. – 70 ºC was presumably achieved.

The flask sampling instrumentation was connected to the 67.2 m main sample line parallel to the instrumentation of the HYDE CO2 set-up. The sample line connecting the MPI CO2 instrumentation to the main sample line was a ca. 1 m long, 6/4 mm diameter (outer/inner) metal tube (seamless, electropolished SS. During this comparison experiment with the MPI CO2 set-up only three of the HYDE CO2 calibration gases (namely 350.87 ppm, 390.55 ppm and 430.37 ppm) were in use for the calibration.

During 8th – 16th July 2008 a comparison experiment where three gas cylinders filled with natural air containing different concentrations of CO_2 were to be analysed with the HYDE CO2 instrumentation was performed. The CO_2 concentrations in the cylinders were unknown beforehand. The ('cucumber') cylinders belong to the CarboEurope-Atmosphere Cucumber Intercomparison programme (see http://cucumbers.webapp2.uea.ac.uk/) as part of the Database quality control activity of the CarboEurope Integrated Project (see http://www.carboeurope.org/). The aim of the inter-comparison programme is to assess and quantify possible offsets in calibration scales between field stations and laboratories. The Smear II station belongs to the loop 'Euro-1' of the programme. Institute of Environmental Physics of the University of Heidelberg (UHEI-IUP), Germany, is the primary laboratory of that loop and provides the reference values for the concentrations in the 'cucumber' cylinders.

The 'cucumber' cylinders were connected to the HYDE CO2 instrumentation by replacing temporarily the natural air cylinder. During the comparison experiment with the 'cucumber' cylinders all the five of the HYDE CO2 calibration gases were in use. During the time period considered in this study one comparison measurement was performed.

RESULTS

The noise (estimated as standard deviation) level of the CO_2 signal of the URAS 4 analyser was observed to fluctuate considerably over time, from 0.04 ppm level to close by 1.4 ppm level, and the noise appeared to depend on the CO_2 concentration of the standard gas. The baseline of the CO_2 signal noise for the URAS 4 analyser was observed to be about 0.04 ppm, and a considerable fraction of this can be assumed to be due to the noise of the sample pressure and temperature signals (data not shown). However, the sample pressure and temperature signal noise levels were stable and so the occasional periods where the CO_2 signal noise of the URAS 4 analyser increased considerably and even exceeded the 0.5 ppm limit could not be related to any increase in the noise of the sample pressure or temperature signal. The periods of an increased CO_2 signal noise also didn't coincide with any disturbances inflicted on the instrumentation. No service or repair measures were performed because no obvious reason for the unstability could be reasoned, but instead the URAS 4 analyser was let to run and the operation of the analyser stabilised in the course of time. The fraction of the URAS 4 atmospheric CO_2 concentration data rejected based on too high noise level was about 6 %. The CO_2 signal noise level of the LI-840 analyser for the standard gases was observed to be stable compared to the URAS 4 analyser. The baseline of the LI-840 CO_2 signal noise was about 0.1 ppm, the noise didn't exceed 0.5 ppm, and the noise was not observed to depend on the concentration of the standard gas.

The calibration of both the CO_2 analysers was observed to be stable, i.e. the difference was less than 0.5 ppm, in the course of the daily calibration sequences. The occasions where the difference exceeded ± 0.5 ppm were related to know malfunction situations pointed out by other indicators also.

The result from the comparison experiment between the HYDE CO2 set-up and the MPI CO2 set-up was that the HYDE CO2 set-up systematically showed lower ambient CO_2 concentrations with an average difference of (-0.32 ± 0.17) ppm.

The CO_2 concentrations of the 'cucumber' cylinders measured with the HYDE CO2 instrumentation were systematically slightly higher than the reference concentrations. On the average the difference was (+ 0.06 ± 0.02) ppm.

The result of these comparison experiments demonstrated that the HYDE CO2 set-up is capable of measuring atmospheric CO_2 concentrations continuosly (Figure. 1) with a better than 0.5 ppm accuracy.
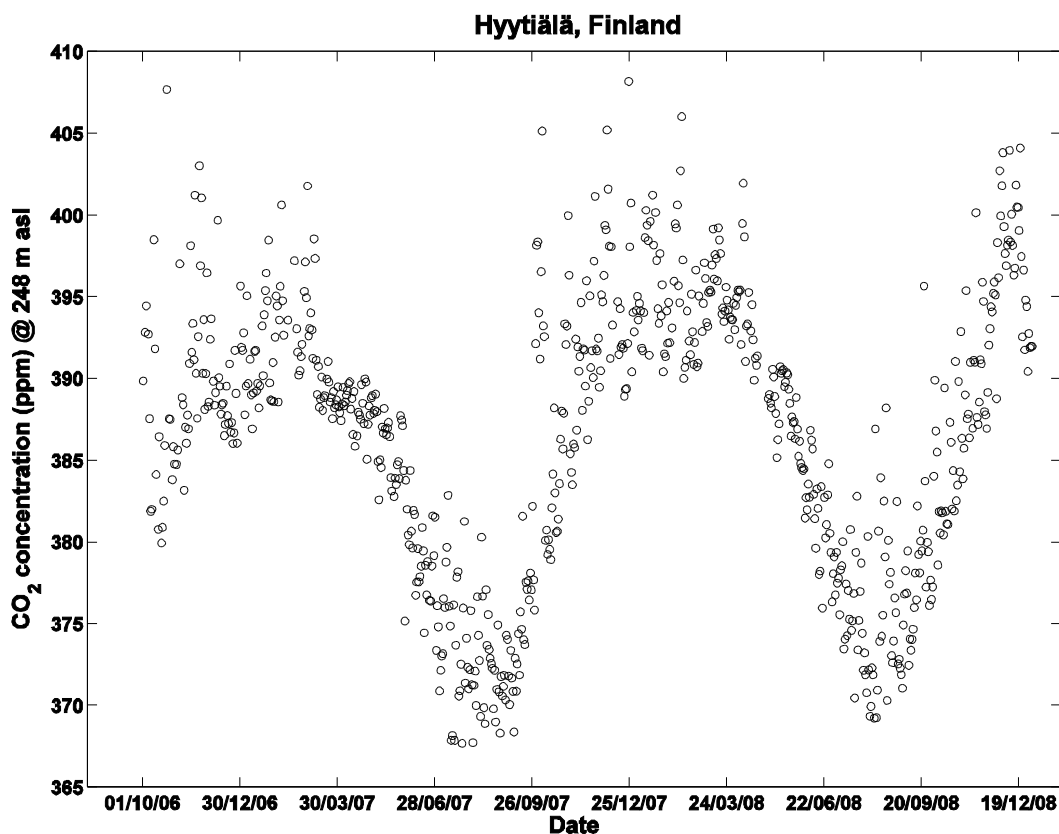
Figure 1. Daily afternoon (between 13:00 – 13:30 local winter time) atmospheric CO_2 concentration at Hyytiälä, Finland, during time period 1st Oct. 2006 – 31st Dec. 2008. The proportion of missing data due to malfunction of the instrumentation is about 5 %.

REFERENCES

Baldocchi D.D. (2003). Assessing the eddy covariance technique for evaluating carbon dioxide exchange rates of ecosystems: past, present and future. Global Change Biol. 9, 479-492.

Potter C.S., Randerson J.T., Field C.B., Matson P.A., Vitousek P.M., Mooney H.A., and Klosster S.A. (1993). Terrestrial Ecosystem Production – a process model based on global satellite and surface data. Global Biogeochem Cycles, 7, 811-841.

S. W. Running, D. D. Baldocchi, D. P. Turner, S. T. Gower, P. S. Bakwin, K. A. Hibbard (1999). A Global Terrestrial Monitoring Network Integrating Tower Fluxes, Flask Sampling, Ecosystem Modeling and EOS Satellite Data. Remote Sensing Environ. 70, 108-127.

S. W. Pacala, G. C. Hurtt, D. Baker, P. Peylin, R. A. Houghton, R. A. Birdsey, L. Heath, E. T. Sundquist, R. F. Stallard, P. Ciais, P. Moorcroft, J. P. Caspersen, E. Shevliakova, B. Moore, G. Kohlmaier, E. Holland, M. Gloor, M. E. Harmon, S.-M. Fan, J. L. Sarmiento, C. L. Goodale, D. Schimel, and C. B. Field (2001). Consistent Land- and Atmosphere-Based U.S. Carbon Sink Estimates. Science 292, 2316-2320.

Kevin Robert Gurney, Rachel M. Law, A. Scott Denning, Peter J. Rayner, David Baker, Philippe Bousquet, Lori Bruhwilerk, Yu-Han Chen, Philippe Ciais, Songmiao Fan, Inez Y. FungI, Manuel Gloor, Martin Heimann, Kaz

Higuchi, Jasmin JohnI, Takashi Maki, Shamil Maksyutov, Ken Masariek, Philippe Peylin, Michael Pratherkk, Bernard C. Pakkk, James Randerson, Jorge Sarmiento, Shoichi Taguchi, Taro Takahashi & Chiu-Wai Yuen (2002). Towards robust regional estimates of CO2 sources and sinks using atmospheric transport models. Nature, 415, 626-630.

Brent R. Helliker, Joseph A. Berry, Alan K. Betts, Peter S. Bakwin, Kenneth J. Davis, A. Scott Denning, James R. Ehleringer, John B. Miller, Martha P. Butler, and Daniel M. Ricciuto (2004). Estimates of net CO2 flux by application of equilibrium boundary layer concepts to CO2 and water vapour measurements from a tall tower. Journal of Geophysical Research, 109, D20106.

P. S. Bakwin, K. J. Davis, C. Yi, S. C. Wofsy, J. W. Munger, L. Haszpra, and Z. Barcza (2004). Regional carbon dioxide fluxes from mixing ratio data. Tellus, 56B, 301–311.

U. Karstens, M. Gloor, M. Heimann, and C. Rödenbeck (2006). Insights from simulations with high-resolution transport and process models on sampling of the atmosphere for constraining midlatitude land carbon sinks. Journal of Geophysical Research, 111, D12301.

Ankur R. Desai, Asko Noormets, Paul V. Bolstad, Jiquan Chen, Bruce D. Cook, Kenneth J. Davis, Eugenie S. Euskirchen, Christopher Gough, Jonathan G. Martin, Daniel M. Ricciuto, Hans Peter Schmid, Jianwu Tang, Weiguo Wang (2008).Influence of vegetation and seasonal forcing on carbon dioxide fluxes across the Upper Midwest, USA: Implications for regional scaling. Agricultural and Forest Meteorology, 148, 288 – 308.

Takehiko Yamaji, Toru Sakai, Takahiro Endo, Pranab J. Baruah, Tsuyoshi Akiyama, Nobuko Saigusa, Yuichiro Nakai, Kenzo Kitamura, Moriyoshi Ishizuka, and Yoshifumi Yasuoka (2008). Scaling-up technique for net ecosystem productivity of deciduous broadleaved forests in Japan using MODIS data. Ecol Res 23, 765–775.

Bruce K. Wylie, Eugene A. Fosnight, Tagir G. Gilmanov, Albert B. Frank, Jack A. Morgan, Marshall R. Haferkamp, Tilden P. Meyers (2007). Adaptive data-driven models for estimating carbon fluxes in the Northern Great Plains. Remote Sensing Environ. 106, 399-413.

Jingfeng Xiao, Qianlai Zhuang, Dennis D. Baldocchi, Beverly E. Law, Andrew D. Richardson, Jiquan Chen, Ram Oren, Gregory Starr, Asko Noormets, Siyan Ma, Shashi B. Verma, Sonia Wharton, Steven C. Wofsy, Paul V. Bolstad, Sean P. Burns, David R. Cook, Peter S. Curtis, Bert G. Drake, Matthias Falk, Marc L. Fischer, David R. Foster, Lianhong Gu, Julian L. Hadley, David Y. Hollinger, Gabriel G. Katul, Marcy Litvak, Timothy A. Martin, Roser Matamala, Steve McNulty, Tilden P. Meyers, Russell K. Monson, J. William Munger, Walter C. Oechel, Kyaw Tha Paw U, Hans Peter Schmid, Russell L. Scott, Ge Sun, Andrew E. Suyker, Margaret S. Torn (2008). Estimation of net ecosystem carbon exchange for the conterminous United States by combining MODIS and AmeriFlux data. Agricultural and Forest Meteorology 148, 1827-1847.

M. Kulmala, K.Hämeri, P. P. Aalto, J. M.Mäkelä, L. Pirjola, E. Douglas Nilsson, G. Buzorius, Ü. Rannik, M. Dal Maso, W. Seidl, T. Hoffman, R. Jansson, H.-C. Hansson, Y. Viisanen, A. Laaksonen, and C. D. O'Dowd (2001). Overview of the international project on biogenic aerosol formation in the boreal forest (BIOFOR). Tellus, 53B, 324–343.

Pertti Hari and Markku Kulmala (2005). Station for Measuring Ecosystem–Atmosphere Relations (SMEAR II). Boreal Environment Research 10, 315–322.

T. Vesala, T. Suni, Ü . Rannik, P. Keronen, T. Markkanen, S. Sevanto, T. Grönholm, S. Smolander, M. Kulmala, H. Ilvesniemi, R. Ojansuu, A. Uotila, J. Levula, A. Mäkelä, J. Pumpanen, P. Kolari, L. Kulmala, N. Altimir, F. Berninger, E. Nikinmaa, and P. Hari (2005). Effect of thinning on surface fluxes in a boreal forest. Global Biogeochem Cycles, 19, GB2001.

Armin Jordan and Willi A. Brand (2003). Technical Report: MPI-BGC, Germany, Proceedings of the 11th IAEA/WMO meeting of CO2 experts, Tokyo, Sept. 2001, WMO-GAW Report 148, pages 149-153, ed. S. Toru. ftp://ftp.wmo.int/Documents/PublicWeb/arep/gaw/gaw148.pdf.

METHANE DYNAMICS IN FORESTED PEAT SOIL DURING GROWING SEASON

A.-J. Kieloaho[1], M. Pihlatie[1], K. Minkkinen[2], K. Butterbach-Bahl[3], R. Kiese[3] and T. Vesala[1]

[1]Department of Physics, P.O. Box 64, FI-00014, University of Helsinki, Finland
[2]Department of Forest Ecology, P.O.Box 27, FI-00014 University of Helsinki, Finland
[3]Institute of Meteorology and Climate Research, Atmospheric Environmental Research, Forschungszentrum Karlsruhe, Garmisch-Partenkirchen, Germany

INTRODUCTION

Methane (CH_4), among carbon dioxide (CO_2) and nitrous oxide (N_2O), is an important trace gas in the atmosphere. It is part of the coupled carbon – oxygen cycle and linked to the nitrogen cycle in ecosystems. These cycles and emissions of greenhouse gases are affected by human activities (IPCC, 2007). Wetlands and land-use practises in wetlands play an important role in carbon cycling on the global scale. The accumulated organic matter, in wetlands, forms one of the greatest carbon stocks in terrestrial ecosystems on the global scale (IPCC, 2007).

The largest wetland areas are in the northern hemisphere above 45° longitude (Gore, 1983). In the boreal region (in Fennoscandia, Russia and Canada) peatlands have been drained for different purposes, such as forestry, agriculture and peat harvesting (Vasander, 1996; Päivänen 2007). In Finland, peatlands cover about one third (10.4 Mha) of the total land area. About half of that, 5.4-5.7 Mha, has been drained for forestry (Minkkinen, 1999).

Peat soils are sources of greenhouse gases CO_2, N_2O and CH_4, because these gases are released into the atmosphere during microbial soil processes such as heterotrophic respiration, denitrification and methanogenesis. Mires also can act as sinks for greenhouse gases. Photosynthetic activity and aerobic processes in soil like methanotrophic activity consumes atmospheric CO_2 and CH_4. The drainage of peatlands changes the sink and source dynamics of greenhouse gases. Peatlands that are well drained usually act as methane sinks (Alm et al., 2007). In natural peatlands CH_4 plays an important role in carbon cycling, whereas CO_2 has the most important role in the carbon cycle in drained peatland. Due to the large variability in methane fluxes between and within measurement sites CH_4 dynamics in drained peat soils are not very well known (Minkkinen and Laine, 1998; Nykänen et al., 1998; Maljanen et al. 2002). Hence, further studies are required in order to model the methane (CH_4) dynamics in peat soils. The aim of the study was to determine methane dynamics and processes during a growing season in a Southern boreal drained peatland using field measurements and a laboratory experiment. The aim of the field measurements was to get more information about concentration gradients and the transport of CH_4 in drained peat soil and between the soil and the atmosphere. The aim of the laboratory study was to determine the importance of microbial CH_4 oxidation in peat soil profile in the CH_4 transport process.

METHODS

We studied CH_4 dynamics during the growing season (April to September) in a nutrient-poor forested peatland in Southern Finland. The research site Kalevansuo is a south boreal drained peatland in Loppi (N/lat 60°38'49'', E/long 24°21'42''). In the Finnish classification scheme, the site is classified as drained a dwarf shrub pine bog (IR) and it was drained in 1971. For drainage, 1-m deep open ditches were dug approximately in 35-m intervals. This caused the water level to drop 40 cm below ground level. Two years after the drainage, the site was fertilised with phosphorus and potassium according to the guideline practises for drained peatland forests in Finland.

The site was dominated by the Scots pine (*Pinus sylvestris* L.) the average height of which was 15-18 m. The forest floor vegetation was mainly hummock dwarf-shrubs and mosses. The most common dwarf-shrub species on the site were the *Vaccinium vitis-idaea*, *Vaccinium myrtillus*, *Empetrum nigrum*, *Vaccinium uliginosum*, *Ledum palustre* and *Betula nana*. The most common moss species is the *Pleurozium schreberi*.

The mean air temperature during the measurement period was 13 °C and the mean soil temperature (15 cm) 8 °C. The soil temperature maximum and minimum were 14 °C and 0 °C, respectively. The minimum value was measured in mid-April and the maximum in mid-August. During the whole measurement period, the sum of precipitation was 370 mm. The highest monthly precipitation occurred in July (97 mm) and the lowest in June (35 mm). The mean water table depth for the measurement period was 32 cm and the water table depth fluctuated between 19 and 49 cm. The lowest water table depth was recorded in late June and the highest in late September.

To determine the components in CH_4 dynamics the following methods were used: static chamber methods and soil CH_4 concentrations in the field, and CH_4 uptake rates in the peat profile in the laboratory. In the measurement site, 16 manual and 9 automatic chambers were used. In manual chamber measurements the gas samples were manually collected from 16 opaque static chambers (Pihlatie et al. 2009). Gas samples stored in glass vials (Labco, Exetainer) and analysed using a gas chromatograph equipped with an electron capture detector (ECD) and a flame ionization detector (FID). In the automatic chamber measurements the transparent rectangular chambers were equipped with a valve driven sampling system connected to a gas chromatograph equipped with an ECD and a FID (Pihlatie et al. 2009).

In the soil gradient method gas concentrations were measured by gas collectors which were installed at different soil depths. Methane concentration in the peat soil profile was measured in two locations at 3 different soil depths and ambient air. Gas samples were manually taken via stainless-steel tubing attached between the gas collector in the soil and the atmosphere. The gas samples were stored in glass vials and analysed for CH_4 using the same gas chromatograph as with the manual chamber gas samples.

Methane uptake in peat profile was studied in a soil incubation experiment. The aim of the experiment was to study CH_4 uptake in natural soil conditions. For the methane peat incubations, 10 replicate soil samples were extracted with a 3-walled core in the vicinity of the soil gas concentration pits. Each core sample was cut into 4 pieces according to the desired sampling depths. The laboratory experiment was done using glass jars with volumes of 1 L and known masses. The CH_4 jar headspace concentration was adjusted to either 5 ppm or 10 ppm, as required. At both starting concentrations the incubation lasted 52 hours and gas samples were collected from the jar headspace 10 times during the incubation. The gas samples were analysed with a gas chromatograph equipped with an FID. CH_4 uptake or emission rates were calculated from the change in CH_4 concentration during the incubation in nmol h^{-1} g^{-1} dry soil.

RESULTS

The Kalevansuo peatland site acted as a net sink for atmospheric methane (-15 µg CH_4-C m^{-2} h^{-1}) during the measurement period from April to September. Methane was produced in the deepest peat layers but almost all the produced methane was consumed in the top soil. Occasionally, the site changed into a net source, but this behaviour was spatially and temporally scarce.

Methane fluxes did not have a clear trend during the growing season. The minimum flux value in the manual chambers was measured at the end of June and the maximum value in mid-July. During the measurement period the mean methane flux for the manual chambers was -14.6 µg CH_4-C m^{-2} h^{-1} and for the automatic chambers -37.1 µg CH_4-C m^{-2} h^{-1}.

During the measurement period methane concentrations in the air and under the litter layer (0 cm) were around 1.9 ppm and there were no clear trends during the measuring period (Figure 1). At the soil depth of

20 cm, methane concentration followed the air concentration in the early measuring period, but the concentration started to increase in early July. Measurements from the deepest depth (40 cm) were available only from July to the end of the measurement period. During this period methane concentration increased rapidly from 197 ppm to over 1400 ppm (Figure 1.).
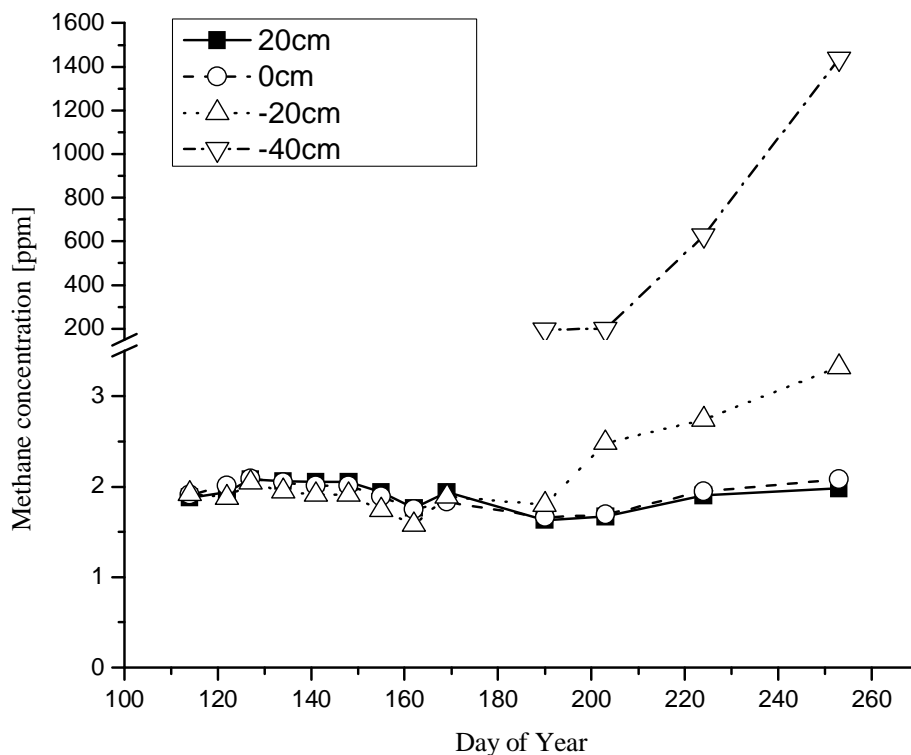
Figure 1. The ambient air (20 cm) and peat concentration gradient for CH_4 at the Kalevansuo peatland site. Methane concentration is given in parts per million.

In the laboratory experiment, the CH4 consumption rate maximum occurred at 25 cm under the soil surface (Figure 2). Consumption occurred also under the litter layer. Microbes consumed both the produced CH_4 from the deep anaerobic layers and the atmospheric CH_4 in top layers. The uptake and release rates in the 5-ppm treatment ranged from -1.3 to 10.8 ng CH_4 g_{dw}^{-1} h^{-1}, and in the 10 ppm treatment from -4.8 to 31.1 ng CH_4 g_{dw}^{-1} h^{-1}. The methane oxidation rates in the peat profile are shown in Figure 2.
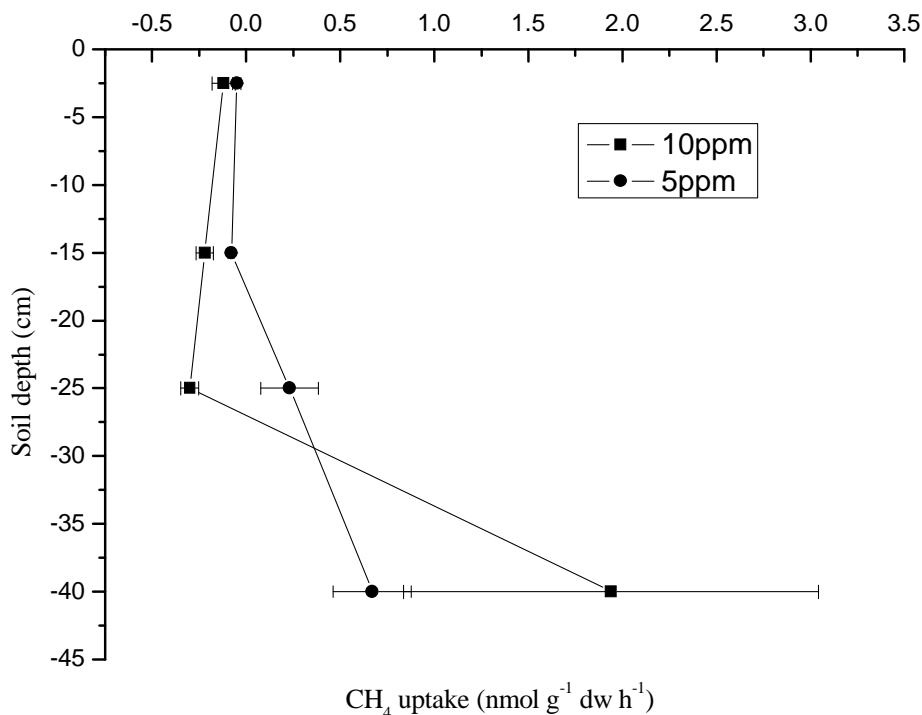
Figure 2. The methane exchange rates in the peat profile of Kalevansuo peat samples. The methane concentrations, 5 and 10 ppm, are the starting concentrations in the headspace of the incubation jars. The positive values in the figure denote the CH_4 release, the negative denote the CH_4 uptake.

Methane uptake pattern was not the same for the both starting concentrations of 5 and 10 ppm. For the 5-ppm starting concentration the methane uptake was weaker than for the 10-ppm concentration. Also, the methane release exceeds the uptake earlier in the peat profile in the 5-ppm concentration.

<div align="center">CONCLUSIONS</div>

The Kalevansuo peat site acted as a net sink for methane during the growing season. The sink behaviour of the site was strong and only on few occasions did the site act as a source of CH_4. However, CH_4 production occurred in the deep peat layers. Therefore drainage did not prevent methane production, but changed the ratio of methane consumption and production in the Kalevansuo peat soil by expanding the depth of the aerobic surface peat layer.

Methane was produced under the water table (around 40 cm below the soil surface), but was oxidised in the oxic part above the water table. Near the soil surface, methane concentrations were close to the atmospheric concentration. Laboratory incubations indicate that most of the methanotrophic bacteria were low-affinity type bacteria that are adapted to high CH_4 concentrations. Also high-affinity bacteria, which are adapted to oxidize atmospheric concentrations of CH_4, were expected to be present near the soil surface.

This study shows that CH_4 is consumed throughout the aerobic peat profile at different rates. This is due to two types of methanotrophic bacteria present in the peat soil. These bacteria are sensitive to different methane concentrations, and hence CH_4 is oxidized at both atmosphere and high concentrations.

REFERENCES

Alm, J., N. J. Shurpali, E.-S. Tuittila, T. Laurila, M. Maljanen, S. Saarnio and K. Minkkinen, 2007: Methods for determining emission factors for the use of peat and peatlands - flux measurements and modelling. *Boreal Environmental Research*, **12**, 85-100.

Gore, A. J. P. (Ed.), 1983: Mires: Swamp, Bog, Fen and Moor. *Ecosystems of the World*, **4**A. Elsevier, Amsterdam, 440 p.

IPCC, 2007: Climate Change 2007: The Physical Science Basis. Contribution of Working Group I to the Fourth Assessment Report of the Intergovernmental Panel on Climate Change [Solomon, S., D. Qin, M. Manning, Z. Chen, M. Marquis, K.B. Averyt, M. Tignor and H.L. Miller (eds.)]. Cambridge University Press, Cambridge, United Kingdom and New York, NY, USA, 996 pp.

Maljanen, M., A. Liikanen, J. Silvola and P. J. Martikainen, 2003: Methane fluxes on agricultural and forested boreal organic soils. *Soil Use and Management*, **19**, 73-79.

Minkkinen, K. and J. Laine, 1998: Vegetation heterogeneity and ditches create spatial variability in methane fluxes from peatlands drained for forestry. *Plant Soil*, **285**, 289-304.

Minkkinen, K, 1999: *Effect of forestry drainage on the carbon balance and radiative forcing of peatlands in Finland*. PhD thesis. Department of Forest Ecology, University of Helsinki. 42 p.

Nykänen, H., J. Alm, J. Silvola, K. Tolonen and P. J. Martikainen, 1998: Methane fluxes on boreal peatlands of different fertility and the effect of long-term experimental lowering of the water table on flux rates. *Global Biogeochemical Cycles*, **12**, 53-69.

Pihlatie, M., R. Kiese, N. Brüggemann, K. Butterbach-Bahl, A.-J. Kieloaho, T. Laurila, A. Lohila, I. Mammarella, K. Minkkinen, T. Penttilä, J. Schönborn and T. Vesala:, Greenhouse gases in a drained peatland forest. Submitted to *Biogeosciences*.

Topp, E., and E. Pattey, 1997: Soils as sources and sinks for atmospheric methane. *Canadian Journal of Soil Science*, **77**, 167-178.

Vasander, H. (ed), 1996: *Peatlands in Finland*. Finnish Peatland Society, Helsinki, Finland, 168 p.

Päivänen, J., 2007*: Suot ja suometsät – järkevän käytön perusteet.* Metsäkustannus, Hämeenlinna, Finland, 368 p.

PHYSICAL AND CHEMICAL CHARACTERISTICS OF THE AEROSOL PARTICLES AND CLOUD DROPLET ACTIVATION DURING THE SECOND PALLAS CLOUD EXPERIMENT (SECOND PaCE)

N. KIVEKÄS[1], V.-M. KERMINEN[1], T. RAATIKAINEN[1], P. VAATTOVAARA[2], A. LAAKSONEN[1,2] and H. LIHAVAINEN[1]

[1] Finnish Meteorological Institute, PO Box 503, FI-00101 Helsinki, Finland
[2] Department of Applied Physics, University of Kuopio, P.O. Box 1627, FIN-70211 Kuopio, Finland

Key Words: Aerosol size distribution; Aerosol chemistry; Cloud microphysics

INTRODUCTION

In global climate modeling, clouds and their interaction with the climate system constitute the largest uncertainty (IPCC, 2007). Yet the number of studies where the influence of aerosols on cloud microphysich has been directly measured (e.g. Lihavainen et al., 2008, Henning et al., 2002). The Pallas-Sodankylä Global Atmospheric Watch (GAW) station (Hatakka et al., 2003), located in a remote continental site in Northern Finland, provides an ideal site to investigate aerosol-cloud interactions via ground-based measurements (Lihavainen et al., 2008; Kerminen et al., 2005; Komppula et al., 2005). Here, we complement our earlier Pallas cloud studies by presenting and analyzing data on an intensive field campaign with simultaneous measurements on cloud microphysics and aerosol physical, chemical and hygroscopic properties (Kivekäs et al., 2009).

METHODS

The Second Pallas Cloud Experiment (Second PaCE), an intensive three-week campaign for measuring aerosol and cloud properties, was conducted by the Finnish Meteorological Institute and by the University of Kuopio at the Pallas-Sodankylä GAW station. The measurements were conducted from September 16th to October 6th 2005. The station is located at the northern limit of the boreal forest zone in a very sparsely populated area. The station consists of several measurement sites, of which only the main site Sammaltunturi (67º58'N, 24º07'E, 560 m above sea level, Muonio Lapland) is considered here. This site is located slightly above the tree line on a top of a fell (Arctic round-topped hill), and was inside cloud (visibility below 200 m) for 25% of the time. During the measurement period the air masses were coming either from North Atlantic or Arctic Ocean or from south or south-west over Central Europe or British Islands and Scandinavia. The ambient temperature was mostly between 0 °C and 10 °C.

The aerosol number concentration and size distribution were measured with two Differential Mobility Particle Sizers (DMPS), one measuring all particles (including cloud droplets) with dry diameter d_p 7-500 nm, the other measuring only the particles with wet diameter below 2500 nm and d_p 7-500 nm. When the station was inside cloud, the number concentration of activated particles (CDNC) can be calculated from the difference between the size distributions (6). The calculated CDNC were compared to ones measured with a FSSP, which was running for two days during the campaign.

The chemical composition of aerosol particles was measured with an Aerosol Mass Spectrometer (AMS). The measured components were sulfate (SO_4), nitrate (NO_3), ammonia (NH_4) and total organic mass. Also the total aerosol mass (m_{tot}) was calculated. The relative contributions of highly oxidized (OOA-1) and less oxidized (OOA-2) organic aerosol were calculated as well.

The hygroscopic growth factor of aerosols at 90 % relative humidity was measured with Hygroscopicity-Tandem Differentia Mobility Analyzer (H-TDMA). The growth factors were measured for monodispersed aerosols with dry diameters 30, 50, 80, 100 and 150 nm.

The main meteorological parameters (temperature, pressure, relative humidity, visibility, rain intensity and type, global solar radiation) were measured at the same site. Air mass back trajectories were also calculated, and air masses were divided into three categories according to their arrival path: marine, mixed and European.

RESULTS

General Aerosol Conditions

The data was converted into one-hour averages. The averaged number concentration varied in the range 56-3900 cm^{-3}, with median value of 710 cm^{-3}. The volume concentration calculated from the DMPS data was in the range 0-11.7 $\square gcm^{-3}$. This concentration was compared to the total mass concentration (m_{tot}) measured with the AMS, and a good correlation ($r^2 = 0.98$) was found. The mass to volume ratio was mostly between 0.5 and 1.5, with a median of 1.07. The ratio was lowest during the high volume peaks. There were peaks in the number concentration in all three air masses, but the low base level was reached mostly in marine air masses. The mass concentration showed peaks as well, but only in European and mixed air masses.

The inorganic fraction (IO) of m_{tot} followed the air mass type as well. In marine air masses the mean IO was 23 %, whereas it was 37 % in mixed and 44 % in European air masses. The inorganic fraction consisted on average of 64 % SO_4, 12 % NO_3 and 25 % NH_4. The contribution of SO_4 was the lowest (60 %) in marine air masses and highest (68 %) in European air masses. The contribution of NO_3 was the opposite, being highest (20 %) in marine air masses and lowest (7 %) in European air masses. The contribution of NH_4 was about the same in all air masses.

The particle hygroscopic growth factors (GF) at 90% relative humidity were measured for particles having dry diameter 30, 50, 80, 100 and 150 nm. The growth factors varied from about 1.1 to 1.5 for all the particle sizes. In each size class the average growth factor increased systematically with increasing dry particle diameter. The GF increased with increasing IO as well. The correlation coefficients (r) between the growth factor and IO were higher that 0.5 for all size fractions. In the two largest size classes ($d_p = 100$ nm and $d_p = 150$ nm) the growth factor depended also on the oxidation state of the organic species in the particles. During periods when the signal from OOA-1 (m/z = 44) was clearly higher than that from OOA-2 (m/z = 43) the growth factor was high, even if the inorganic fraction was low. In the smaller size classes the effect of the oxidation state was not as clear.

Cloud Activation

Particle activation was calculated from the difference between the two DMPS:s. The calculation was done separately for particles with $d_p > 100$ nm (N_{acc}) and for particles with 50 nm $< d_p <$ 100 nm (N_{50}). The fractions of N_{acc} and N_{50} that activated are hereafter called Act_{100} and Act_{50}, respectively. The Act_{100} and Act_{50} were plotted against visibility at the measurement site to check the validity of the method. Visibility (vis) was divided into three ranges: cloud (vis < 200 m), unclear (200 m < vis < 3000m) and no cloud (3000 m < vis < 50000 m). Act_{100} was on average 66 % in cloud cases and decreased towards 0 % as visibility increased. Even in the maximum visibility (50000 m) Act_{100} varied from -20 % to 20 %. Act_{50} varied from -20 % to 20 % quite independent of visibility. As the Act_{50} was below the noise level of the method, no further analysis for Act_{50} was made.

There was activation associated with both high and low IO, as well as with large and small N_{acc}. The cloud cases were clearly different than the no-cloud cases in their N_{acc} vs IO dependency. For any value of IO there was activation only when N_{acc} was on the largest end of N_{acc} values associated with that value of IO (Figure 1).
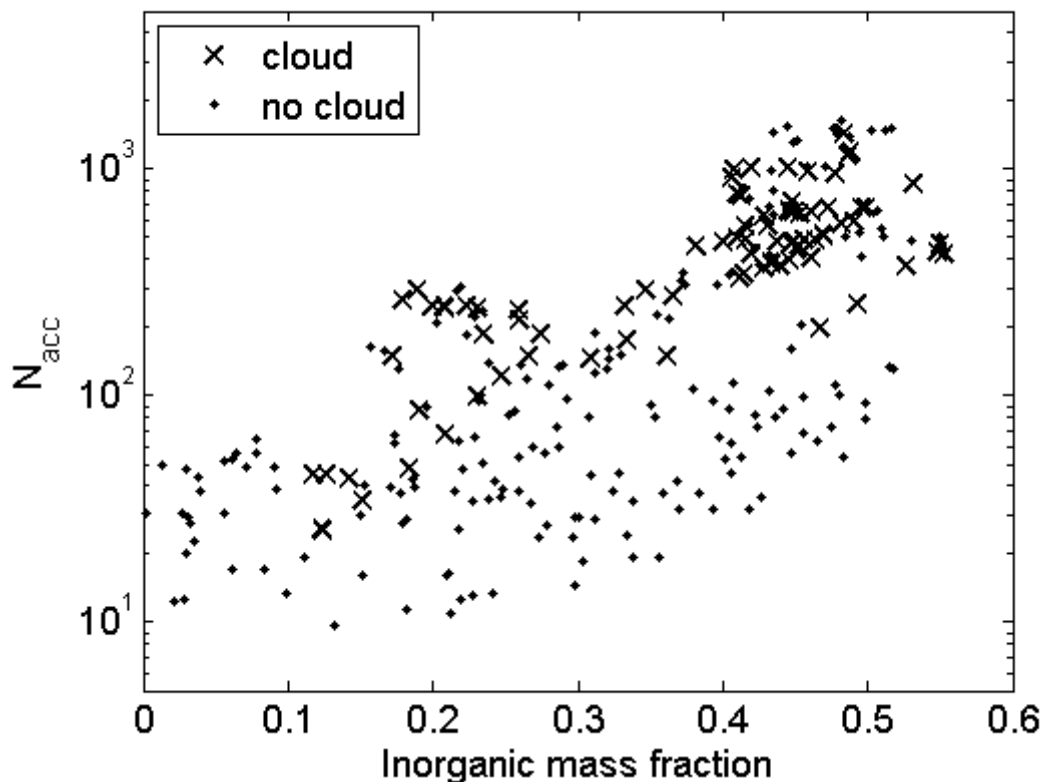
Figure 1. The number concentration of accumulation mode particles, N_{acc} as a function of inorganic fraction of particle mass for both in-cloud and outside cloud cases.

Act_{100} was found to decrease slightly with increasing N_{acc}, and was not found to depend at all on IO. The finding that these dependencies were so weak can be explained N_{acc} and IO being correlated (r = 0.6) and having opposite effect on the activation probability of individual particles. The D_{50} activation diameter (d_p at which 50 % of particles with that d_p activate) did not depend on N_{acc} or IO either, but decreased as Act_{100} increased.

CONCLUSIONS

In conclusion we say that the effects of particle number or mass concentration and chemical composition at Pallas are difficult to separate, as the parameters are highly correlated. The air masses arriving to the site are highly different, but cloud activation was observed in all air mass types, meaning that activation happens in very different aerosol conditions. The connection between the particle activation, number concentration of particles with $d_p > 100$ nm and the inorganic fraction of particle mass is worth studying more.

Acknowledgments

REFERENCES

IPCC. 2007. Summary for Policymakers. [Solomon, S., D. Qin, M. Manning, Z. Chen, M. Marquis, K.B. Averyt, M.Tignor and H.L. Miller (eds.)]. (2007) Cambridge University Press, Cambridge, United Kingdom and New York, NY, USA.

Henning S., Weingartner E., Schmidt S., Wendisch M., Gäggeler H. W. and Baltensperger U. (2002) Size-dependent aerosol activation at the high-alpine site Jungfraujoch (3580 m asl), *Tellus*, 54B, 82-95.

Lihavainen H., Kerminen V.-M., Komppula M., Hyvärinen A.-P., Laakia J., Saarikoski S., Makkonen U., Kivekäs N., Hillamo R., Kulmala M., and Viisanen Y. (2008). Measurements of the relation between aerosol properties and microphysics and chemistry of low level liquid water clouds in Northern Finland, *Atmos. Chem. Phys.* 8: 6925-6938.

Hatakka J., Aalto T., Aaltonen V., Aurela M., Hakola H., Komppula M., Laurila T., Lihavainen H., Paatero J., Salminen K. and Viisanen Y. (2003) Overview of the atmospheric research activities and results at Pallas GAW station, *Boreal Environ. Res.* 8: 365-384.

Kerminen V.-M., Lihavainen H., Komppula M., Viisanen Y. and Kulmala M. (2005). Direct observational evidence linking atmospheric aerosol formation and cloud droplet activation. *Geophys. Res. Lett.* 32: L14803, doi:10.1029/2005GL023130.

Komppula M., Lihavainen H. and Kerminen V.-M. (2005). Measurements of cloud droplet activation of aerosol particles at a clean subarctic background, *J. Geophys. Res.* 110(D0): 6204, doi:10.1029/2004JD005200.

Kivekäs N., Kerminen V.-M., Raatikainen T., Vaattovaara P. Laaksonen A. and Lihavainen H. (2009) Physical and chemical characteristics of the aerosol particles and cloud droplet activation during the Second Pallas Cloud Experiment (Second PaCE) *Boreal Environ. Res.* (submitted)

INTERCOMPARISON OF AEROSOL MODULES IN THE FRAMEWORK OF ECHAM5 CLIMATE MODEL

H. KOKKOLA[1,3], T. BERGMAN[2], J. FEICHTER[3], R. HOMMEL[5], H. JÄRVINEN[6], J. KAZIL[3], V.-M. KERMINEN[6], H. KORHONEN[7], M. KULMALA[4], K.E.J. LEHTINEN[1,7], R. MAKKONEN[4], U. NIEMEIER[3], A.-I. PARTANEN[1,7] and C. TIMMRECK[3]

[1] Finnish Meteorological Institute, Kuopio Unit, Kuopio, Finland
[2] CSC, IT Center for Science Ltd, Espoo, Finland
[3] Max-Planck Institut für Meteorologie, Hamburg, Germany
[4] Department of Physical Sciences, University of Helsinki, Finland
[5] Centre for Atmospheric Science, Cambridge University, Department of Chemistry, UK
[6] Finnish Meteorological Institute, Helsinki, Finland
[7] Department of Physics, University of Kuopio, Finland

Keywords: nucleation, stratospheric aerosols, sulphuric acid, geoengineering, volcano

INTRODUCTION

We present an intercomparison of three different aerosol microphysics modules that are implemented in the climate model ECHAM5. The comparison was done between the modal aerosol microphysics module M7, which is currently the default aerosol microphysical core in ECHAM5, and two sectional aerosol microphysics modules SALSA, and SAM2. A detailed aerosol microphycical model MAIA was used as a reference model to evaluate the results of the aerosol microphysics modules with respect to sulphate aerosol.

The ability of the modules to describe the development of the aerosol size distribution was tested in a zero dimensional framework. We evaluated the strengths and weaknesses of different approaches under different types of stratospheric conditions. Also, we study how the setup of the modal approach in M7 affects the evolution of the aerosol size distribution.

Intercomparison simulations were carried out with varying SO_2 concentrations from background conditions to extreme values arising from stratospheric injections of large volcanic eruptions. Under background conditions, all microphysics modules were in good agreement describing the shape of the size distribution but the scatter between the model results increased with increasing SO_2 concentrations. In particular for the volcanic case, the module setups have to be redefined to be applied in global model simulations capturing respective sulphate particle formation events.

AEROSOL MICROPHYSICS MODULES

In this intercomparison, we compare four different aerosol microphysics modules MAIA, SAM2, SALSA, and M7. Of these, MAIA and SAM2 treat sulphate as the sole aerosol chemical component while SALSA and M7 include also organic compounds, sea salt, black carbon, and mineral dust. The modules describe the processing of aerosol size distribution through the following microphysical processes:

- New particle formation by nucleation.

- Condensation of gas phase compounds to the particle phase.

Table 1: Major characteristics of M7, SALSA, SAM2, and MAIA.

	M7	SALSA	SAM2	MAIA
Method for describing the size distribution	modal	sectional, moving center + fixed center for three largest size sections	sectional, fixed center	hybrid kinetic-sectional, fixed center, first order approximation of size distribution inside geometric size sections
Number of modes or size sections	7	20 (10 in size space)	44	21 kinetic, 99 geometric
Chemical species treated	sulphate, organic carbon, mineral dust, sea salt	sulphate, organic carbon, mineral dust, sea salt	sulphate	sulphate
References	Vignati et al. (2004); Stier et al. (2005)	Kokkola et al. (2008)	Hommel (2008); Timmreck and Graf (2000)	Lovejoy et al. (2004); Kazil et al. (2007)

- Coagulation of the aerosol particles.

- Thermodynamical equilibrium between liquid water and water vapour.

Table 1 summarizes the major features of the aerosol microphysics modules. Three modules of this intercomparison, M7, SALSA, and SAM2 have been designed to be used in large scale climate models and have all been implemented in the climate model ECHAM5 (Roeckner et al., 2003). Since these microphysics modules have been designed for large scale models, they parameterize aerosol microphysical processes and use assumptions to resolve the aerosol size distribution. Binary homogeneous nucleation of sulphate aerosols is treated identically in all the three modules using nucleation scheme by Vehkamäki et al. (2002) extending it for high concentrations of sulphate using collision rate as nucleation rate (H. Vehkamäki, pers. comm.). For other microphysical processes the treatment varies between the modules. To evaluate the results of these modules, the aerosol module MAIA was considered as a reference since it has a highly resolved particle size spectrum and it is based on advanced numerical, thermodynamical and kinetic approaches compared to parametrisations which are currently used in aerosol modules suitable for global climate simulations.

EXPERIMENTAL SETUP

The ability of the microphysics modules to describe the processing of the sulphate aerosol size distribution was investigated by calculating the evolution of the size distribution over a 10 day period assuming typical conditions of the midlatitude stratosphere at 30 hPa ambient pressure and 214.8 K temperature. Initial stratospheric sulphate size distribution was assumed to be unimodal with 0.234 μm geometric mean diameter, 1.59 geometric standard deviation, and a total number concentration of 3 cm^{-3}.

The evolution of the size distribution was affected by varying the initial SO$_2$ concentration which modifies the size distribution through oxidation to H$_2$SO$_4$ and subsequent gas-to-particle partitioning processes. We assume that gaseous H$_2$SO$_4$ is exclusively formed from the oxidation of SO$_2$ by the hydroxyl radical OH. The concentration of the latter is prescribed by an abstracted diurnal cycle with a daytime concentration of 1×10^6 cm^{-3} between 06:00 and 18:00. This value was derived from a time slice experiment conducted with the chemistry-climate model MAECHAM4-CHEM (Timmreck et al., 2003). The initial SO$_2$ mixing ratio was varied between a typical background value of 1.5×10^{-11} kg/kg (~ 10 $pptv$; WMO/SPARC, 2006) and 3.9×10^{-4} kg/kg for the assumed volcanic case and two intermediate mixing ratios of 3.9×10^{-8} kg/kg and 3.9×10^{-6} kg/kg. The extreme case mixing ratio was derived from a 3-D simulation of the Mt. Pinatubo episode with use of the model MAECHAM5 (Niemeier et al., paper in preparation, 2009), initializing 17 Mt SO$_2$ (Read et al., 1993). The sensitivity studies presented here were conducted using integration time step length of $\Delta t = 1$ s, 60 s, and 900 s. The latter corresponds to the default time step of ECHAM5 using the spectral truncation T42.

In M7, the standard deviation σ_g of the individual modes is fixed, so the choice of the value for σ_g affects the module's ability to describe the development of the size distribution especially in conditions, where the shape of the size distribution is heavily modified, for example when high concentrations of sulphuric acid vapor yield to high mass transfer rates into the particle phase. The role of the coarse mode in M7 is to describe primary sea salt and dust particles which are mainly present in the troposphere. Sulphate aerosol can be sufficiently prescribed with three modes as already shown in the M3 model (Wilson and Raes, 1996; Wilson et al., 2001), a predecessor model of M7. Therefore we tested two different mode setups in M7, the default mode setup and a second setup in which the coarse mode was neglected.

- Setup 1, default size distribution of M7; $\sigma_g = 1.59$ for nucleation, aitken and accumulation mode, $\sigma_g = 2.00$ for coarse mode.

- Setup 2, $\sigma_g = 1.59$ for nucleation, aitken and accumulation mode, no coarse mode.

RESULTS

We compared the shapes of aerosol size distributions calculated by individual aerosol microphysics modules when the size distribution is modified by gas-to-particle conversion of sulphur.

In Figure 1, the number size distributions at 12:00, 10 days into the simulations are shown for the given different initial gas phase mixing ratios and different time step lengths. Each row in Figure 1 represents a simulation using a specific initial mixing of SO$_2$ and the columns represent the time step length. The mixing ratios and time step lengths are denoted in the title of each subplot.

From Figure 1, we can see that all microphysics modules reproduce the shape of the size distribution given by the reference model well for background conditions and also when the SO$_2$ load was moderately enhanced (two upper rows). Also in these cases, the time step length has no significant effect on the final size distribution.
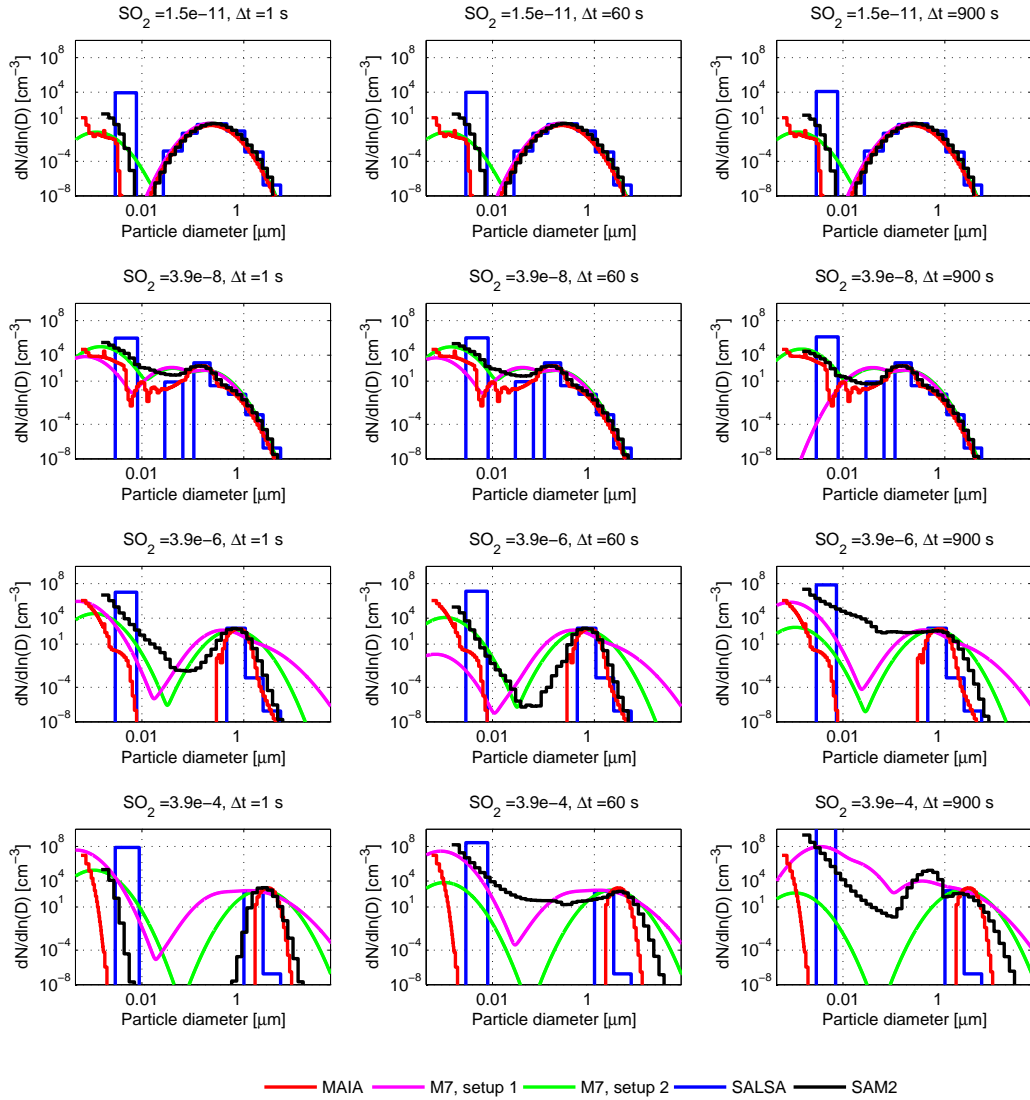
Figure 1: Aerosol number size distributions at noon of the 10th day of the simulations calculated using different aerosol microphysics modules and the reference model. The size distributions were calculated for four different initial gas phase SO_2 mixing ratios and three different time step lengths Δt. The SO_2 mixing ratios ($kg\,kg^{-1}$) and time step lengths are given on the title of each sub-figure.

As the initial SO_2 mixing ratio is increased, the calculated size distributions begin to differ for the individual microphysics modules (two lowest rows). Increased SO_2 mixing ratios yield to a separation of the aerosol size distributions into two narrow modes in the ultrafine regime of the size spectrum and the coarse mode respectively. The feature is pronounced for the case representing conditions in the stratosphere in the course of a large volcanic eruption. Although no direct particle number concentration measurements are known to have been carried out immediately after respective volcanic eruptions in regions were the material was injected into the stratosphere, there is evidence from in situ observations that clearly separated bi-modal particle spectra will evolve under conditions as assumed in this study. Brock et al. (1993) reported aircraft measurements in the subtropical northern hemisphere, starting 10 weeks after the eruption of Mt. Pinatubo in 1991.

During the first days of the campaign, particle size spectrometers registered not continuously but in more than 1/3 of all measurements bi-modal size spectra where a distinct and clearly separated coarse mode appeared beyond particles sizes of 1 μm in diameter. Since the flights were carried out in heights below 40 hPa the authors conclude to measure "fallout" from higher elevations. Due to the fact that these spectrometers were calibrated for sulphuric acid only and volcanic ash fallout terminates after a couple days after it was injected into the stratosphere (Guo et al., 2004), it can be assumed that these ultra large particles contain mainly sulphuric acid.

As can be seen from Figure 1, when the SO_2 mixing ratio is above background levels, M7 with a fixed standard deviation cannot reproduce the shape of the size distribution at the upper end of the spectrum. The sectional approach has advantages to reproduce the narrow band structure of the size distribution in the coarse mode nearly independent on the number of sections used to discretise the aerosol spectrum. Under assumed volcanic conditions the default mode setup of M7 also fails to reproduce the distinct bimodal characteristic of the size distribution in particular when the global model time step length of 900 s is used.

In SALSA, to minimize the amount of tracers, only the number concentration is calculated for the size sections in subregion 3. Also, no coagulation between the particles in subregion 3 is assumed, so these size sections are treated as a sink for smaller particles and condensating gases. In normal atmospheric conditions this assumption is valid, but it fails in the volcanic case.

The sensitivity of the modules to the integration time step length increases as the initial SO_2 mixing ratio increases. Because the evolution of the size distribution become more rapid yielding to steeper gradients in the aerosol concentrations. For example for 3.9×10^{-4} kg/kg, SAM2 describes extremely well the final size distribution when time step length of 1 s is used, whereas for Δt of 60 and 900 s a detached bimodal distribution does not appear at the end of the simulation. The evolution of the size distributions as predicted by M7 and SALSA is less affected by the integration time increment. Notable effects are seen here for fine particles and, in particular for M7 setup 1, also for medium size particles.

ACKNOWLEDGMENTS

REFERENCES

Brock, C., Jonsson, H., Wilson, J., Dye, J., Baumgardner, D., Borrmann, S., Pitts, M., Osborn, M., DeCoursey, R., and Woods, D. (1993). Relationships between optical extinction, backscatter and aerosol surface and volume in the stratosphere following the eruption of mt. pinatubo. *Geophys. Res. Lett.*, 22:2555–2558.

Guo, S., Rose, W. I., Bluth, G. J. S., and Watson, I. M. (2004). Particles in the great pinatubo volcanic cloud of june 1991: The role of ice. *Geochemistry, Geophysics, Geosystems*, 5.

Hommel, R. (2008). *Die Variabilität von stratosphärischem Hintergrund-Aerosol. Eine Untersuchung mit dem globalen sektionalen Aerosolmodell MAECHAM5-SAM2.* PhD thesis, Universität Hamburg.

Kazil, J., Lovejoy, E. R., Jensen, E. J., and Hanson, D. R. (2007). Is aerosol formation in cirrus clouds possible? *Atmos. Chem. Phys.*, 7(5):1407–1413.

Kokkola, H., Korhonen, H., Lehtinen, K. E. J., Makkonen, R., Asmi, A., Järvenoja, S., Anttila, T., Partanen, A.-I., Kulmala, M., Järvinen, H., Laaksonen, A., and Kerminen, V.-M. (2008). SALSA: a sectional aerosol module for large scale applications. *Atmospheric Chemistry and Physics*, 8(9):2469–2483.

Lovejoy, E. R., Curtius, J., and Froyd, K. D. (2004). Atmospheric ion-induced nucleation of sulfuric acid and water. *J. Geophys. Res.*, 109.

Read, W. G., Froidevaux, L., and Waters, J. W. (1993). Microwave limb sounder measurement of stratospheric SO_2 from the Mount Pinatubo volcano. *Geophys. Res. Lett.*, 20:1299–1302.

Roeckner, E., Bäuml, G., Bonaventura, L., Brokopf, R., Esch, M., Giorgetta, M., Hagemann, S., Kirchner, I., Kornblueh, L., Manzini, E., Rhodin, A., Schlese, U., Schulzweida, U., and Tompkins, A. (2003). The atmospheric general circulation model ECHAM5. PART I: Model description. *MPI-Report*, 349:127 pp.

Stier, P., Feichter, J., Kinne, S., Kloster, S., Vignati, E., Wilson, J., Ganzeveld, L., Tegen, I., Werner, M., Balkanski, Y., Schulz, M., Boucher, O., Minikin, A., and Petzold, A. (2005). The aerosol-climate model ECHAM5-HAM. *Atmos. Chem. Phys.*, 5:1125–1156.

Timmreck, C. and Graf, H.-F. (2000). A microphysical model to simulate the development of stratospheric aerosol in a GCM. *Meteorol. Zeitschr.*, 9:263–282.

Timmreck, C., Graf, H.-F., and Steil, B. (2003). volume 139, chapter Aerosol chemistry interactions after the Mt. Pinatubo eruption, pages 214–225. AGU Monograph.

Vehkamäki, H., Kulmala, M., Napari, I., Lehtinen, K. E. J., Timmreck, C., Noppel, M., and Laaksonen, A. (2002). An improved parameterization for sulfuric acid-water nucleation rates for tropospheric and stratospheric conditions. *J. Geophys. Res.*, 107 (D22)(4622).

Vignati, E., Wilson, J., and Stier, P. (2004). M7: An efficient size-resolved aerosol microphysics module for large-scale aerosol transport models. *J. Geophys. Res.*, 109(D22202).

Wilson, J., Cuvelier, C., and Raes, F. (2001). A modeling study of global mixed aerosol fields. *J. Geophys. Res.*, 106:34081–34108.

Wilson, J. and Raes, F. (1996). M3 a multi modal model for aerosol dynamics. *Proceedings of the 14th International Conference on Nucleation and Atmospheric Aerosols*, pages 458–461.

WMO/SPARC (2006). WMO/SPARC scientific assessment of stratospheric aerosol properties (ASAP). Technical report.

SPATIAL DISTRIBUTION AND TEMPORAL PATTERN OF CO$_2$ EFFLUX FROM TREE STEM

P. KOLARI, T. HÖLTTÄ and E. NIKINMAA

Department of Forest Ecology, P.O. Box 27, FI-00014, University of Helsinki, Finland

INTRODUCTION

Woody tissues comprise the majority of the biomass in trees. The rate of respiration in the wood, however, is low. Apart from the low activity, also the proportion of the living cells from the wood biomass is low. Annually the respiration of the stems and branches accounts for approximately 10% of the whole-tree respiration (Kolari et al. 2009). Accurate determination of total respiration of a tree, however, is tedious. First, respiratory activity varies in space according to the amount of active tissue. Vertical profiles of CO$_2$ efflux and local CO$_2$ production are also different because part of the respired CO$_2$ is transported up the stem in xylem sap (e.g. Teskey et al. 2008). In the lower parts of the stem, CO$_2$ efflux out of the bark surface will be lower than local respiration because part of the CO$_2$ released locally is transported upwards the stem by sapflow. When water is transported upwards in the stem, it is enriched in CO$_2$ until an equilibrium concentration gradient is formed. In the upper canopy the efflux is higher than local CO$_2$ production because some of the carbon dissolved lower down in the stem is freed from the water. The concentration gradient and also the efflux will depend on the rate of sapflow through the stem. CO$_2$ efflux from tree stems is monitored continuously in a Scots pine stand at SMEAR II field station. Our aim is to determine and understand the processes behind the seasonal course and the spatial variability in stem CO2 efflux. We present here data on spatial and temporal variability of stem CO$_2$ efflux.

METHODS

The measurements were conducted at SMEAR II field station in Hyytiälä, southern Finland. CO$_2$ efflux from the stems was determined hourly with continuously operating automated chambers (Kolari et al. 2009). Acrylic plastic chambers (height 20 cm, width 3.5 cm) were attached on the bark of one tree. One chamber was normally located in the lower part of the living crown and the other 2–3 m lower, just below the crown. The spatial variability of CO$_2$ efflux per unit stem surface area was determined separately in two measuring campaigns with 4 or 6 chambers installed at different heights in the summer of 2008. The measured CO$_2$ fluxes were analysed using an exponential temperature regression

$$R = R_{10}\, Q_{10}^{(T-10)/10} \tag{1}$$

where R_{10} is the base level of respiration, i.e. respiration at 10°C, and Q_{10} the temperature sensitivity, i.e. the slope of the apparent temperature response of respiration. Q_{10} for each measuring height was first determined from flux measurements pooled over June 2005. The base level of respiration varies during the year due to, for instance, varying proportions of maintenance and growth respiration. This variation in R_{10}, not directly related to temperature, was determined by estimating R_{10} daily in a moving time window of 5 days while keeping the temperature sensitivity Q_{10} fixed. Local CO$_2$ production by respiration inside the stem follows in short term temperature that lags slightly behind air temperature. CO$_2$ efflux from the stems in turn lags behind the actual CO$_2$ production because diffusion out of the stem is slow. The stem CO$_2$ efflux was modelled as a response to temperature T_{stem} that follows air temperature T_{air} with a time constant τ

$$\frac{dT_{\text{stem}}}{dt} = \frac{T_{\text{air}} - T_{\text{stem}}}{\tau} \qquad (2)$$

Note that T_{stem} is not the actual bole temperature; In addition to describing the slowness of heat transfer into the respiring tissues in the stem, the time lag in the diffusion of CO_2 out of the stem is embedded in the time constant.

RESULTS

Figure 1 shows the vertical distribution of CO_2 efflux from the pine stem on three summer days. When integrated to the forest stand, stem respiration was most of the time less than 1 µmol m^{-2}(ground) s^{-1} (Kolari et al. 2009). High up the diurnal variation in stem CO_2 effluxes is larger reflecting the CO_2 released from sapflow in addition to local production. The estimated Q_{10} was relatively high, 2.5. The steep apparent temperature response can be explained by advection of CO_2 in sapflow. The value of the time constant τ that gave the best fit for the exponential temperature response function was on average 4 hours, slightly lower in the upper canopy and higher below the canopy. Smoothing of temperature decreases the temperature range and thus increases the steepness of the temperature response of the CO_2 efflux. We also omitted the radiative heating of the stems which may result in higher daytime bole temperatures than estimation from air temperature.
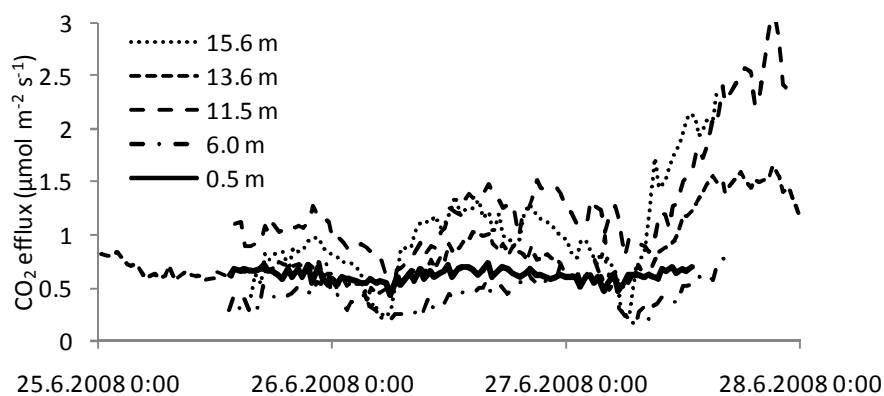
Figure 1. CO_2 efflux from a Scots pine stem at five different heights in June 2008.

The base level of respiration (R_{10}) showed higher values in the early growing season than in late summer and in autumn (Fig. 2). This could reflect the higher respiratory activity in spring when the trees are recovering from winter dormancy and release carbohydrates from the internal storage pools. The higher R_{10} in the early growing season compared to autumn may be explained by cambial activity during xylem development and better availability of sugars as substrate for respiration due to higher photosynthetic production. R_{10} declined considerably during the drought in the late summer of 2006 whereas in a more average summer of 2005 R_{10} varied very little from June through August.
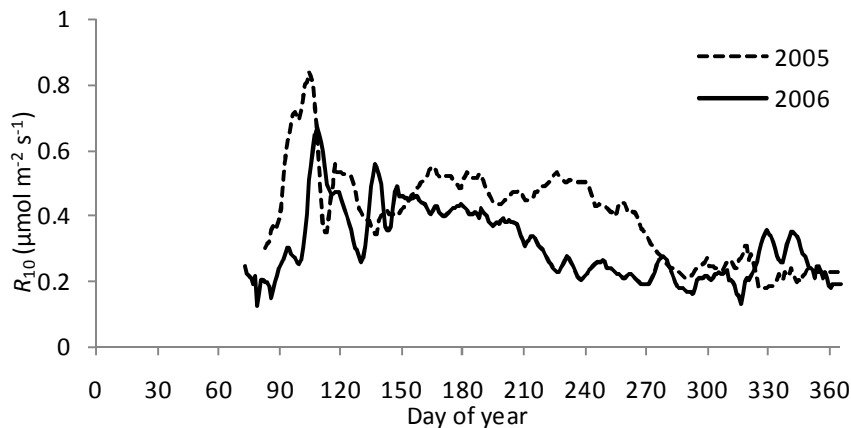
Figure 2. Seasonal course of CO_2 efflux, normalised to 10°C, per unit stem surface area. The flux measurements were done in the lower canopy at a height of 12 m.

CONCLUSIONS

CO_2 effluxes per unit surface area were considerably higher in the upper parts of the stem. Also the temporal variability in the efflux was greater high up. Determining whole tree respiration from stem CO_2 efflux measurements alone would require a vast number of chambers to accurately capture the variation. We have developed a model that links the spatial and temporal variation in the efflux of CO_2 out of the stem surface to axial distribution of CO_2 production in the stem, stem dimensions, and transpiration rate (Hölttä and Kolari, 2009). Acording to the model, CO_2 efflux measurements done on the lower stem are likely underestimate stem respiration while CO_2 efflux measurements very close to the leaves most likely overestimate respiration. These findings will enable an accurate integration of wood respiration over the tree and forest stand.

Like photosynthesis, also the respiratory fluxes have an annual cycle; temperature-normalised respiration varies during a year. The decline of temperature-normalised respiration during the drought and low photosynthetic production suggests that substrate limitation also plays a role in stem respiration. Linking the seasonal variability of respiration to photosynthetic production and to the state of the tree is challenging as the mechanisms behind within-tree carbon allocation are still poorly known. Accurate determination of respiration in stems is one step forward in understanding the function of a forest ecosystem.

REFERENCES

Hölttä, T. and Kolari, P. (2009) Interpretation of stem CO_2 effluxes. *Report Series in Aerosol Science*, this issue.
Kolari, P., Kulmala, L., Pumpanen, J., Launiainen, S., Ilvesniemi, H., Hari, P. and Nikinmaa, E. (2009) CO_2 exchange and component CO_2 fluxes of a boreal Scots pine forest. *Boreal Environment Research*, 14, in press.
Teskey, R.O., Saveyn, A., Steppe, K. and McGuire, M.A. (2008). Origin, fate and significance of CO_2 in tree stems. *New Phytologist*, 177: 17–32.

LARGE INCREASE OF CCN FROM SEA SPRAY DUE TO WIND SPEED CHANGE IN THE SOUTHERN OCEAN

H. KORHONEN[1], K. S. CARSLAW[2], S. MIKKONEN[1], and H. KOKKOLA[3]

[1]Department of Physics, University of Kuopio, P.O. Box 1627, FI-70211 Kuopio, Finland
[2]School of Earth and Environment, University of Leeds, Leeds, LS2 9JT, United Kingdom
[3]Finnish Meteorological Institute, Kuopio Unit, P.O. Box 1627, FI-70211 Kuopio, Finland

INTRODUCTION

Sea spray aerosol, together with DMS-derived particles, is the dominant sources of cloud condensation nuclei (CCN) over remote marine regions (Korhonen et al., 2008). The number flux of sea spray and the flux of DMS into the atmosphere are strongly dependent on the surface level wind speed and thus changes in the local meteorology can be expected to affect the natural marine CCN concentrations.

One region where significant wind speed changes have taken place in the past decades is the Southern Ocean. Figure 1 illustrates the trend in the summer time surface wind speed over the southern hemisphere oceanic regions from 1970 to 2002 (taken from the ERA-40 reanalysis, Uppala et al., 2005). The vertical axis shows the average zonal mean wind speed change in m/s per year and the error bars indicate the 95% confidence interval. Large increases up to about 1.8 m/s in three decades are seen south of 50° S. Here we show that this observed increase in the Southern Ocean surface level wind speeds has enhanced the summer time CCN concentration in the region.

METHODS

The model runs were performed with the global aerosol model GLOMAP, which is an extension to the TOMCAT 3-D chemical transport model (Stockwell and Chipperfield, 1999). A detailed description of GLOMAP is given in Spracklen et al. (2005). The model is run with a T42 spectral resolution (2.8°×2.8°) and with 31 hybrid σ-p levels extending to 10 hPa. Large-scale atmospheric transport is specified from European Centre of Medium-Range Weather Forecasts (ECMWF) analyses at 6-hour intervals. Here, the sectional version of GLOMAP, "GLOMAP-bin" is used, which represents the aerosol size distribution with a sectional moving centre scheme using 20 size sections to cover the size range of 3 nm to 25 μm. In the runs presented here, the aerosol composition is described with three internally mixed components: sulphate, sea spray and carbonaceous aerosol (including both organic and black carbon).

The natural primary sea spray emission flux is simulated according to Mårtensson et al. (2003) for particles smaller than 2 μm in dry diameter and according to Monahan et al. (1986) for sizes larger than 2 μm. Oceanic DMS emissions are calculated using monthly mean seawater concentrations from Kettle and Andreae (2000) and the sea-to-air transfer velocity of Nightingale et al. (2000). DMS is oxidised to form SO_2 and further H_2SO_4 which can both form sulphate aerosol and thus change the marine particle size distribution.

Continental SO_2 emissions are taken from from Cofala et al. (2005) and volcanic SO_2 emissions are based on Andres and Kasgnoc (1998) and Halmer et al. (2002). We assume that 2.5% of SO_2 from these sources is emitted as primary sulfate particles at particle sizes proposed by Stier et al. (2005). Primary carbonaceous emissions are taken from van der Werf et al. (2003) for vegetation fires and from Bond et al. (2004) for fossil and biofuels. BC/OC particles are emitted as lognormal modes at sizes proposed in AEROCOM emissions inventory (http:/nansen.ipsl.jussieu.fr/AEROCOM).
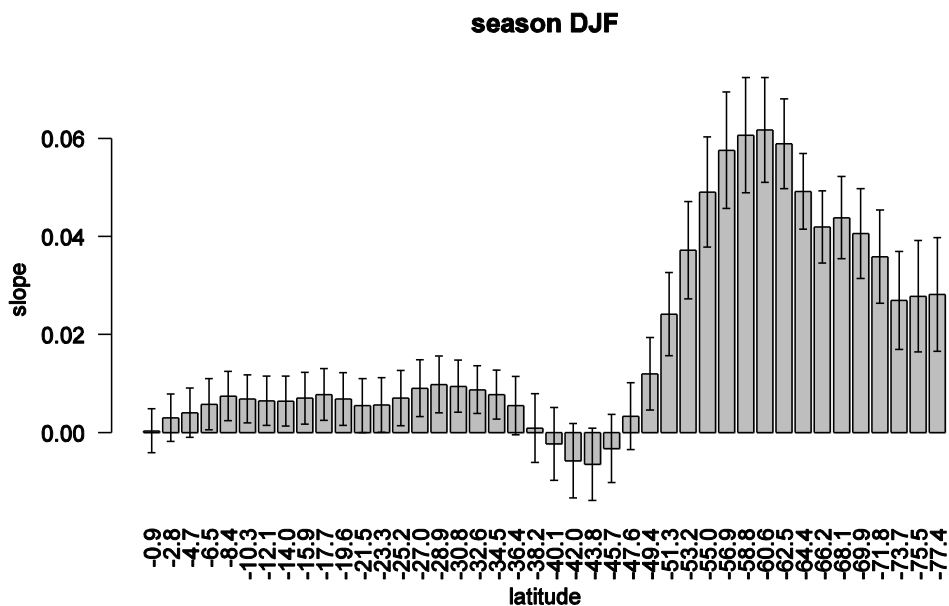
Figure 1. Average zonal mean wind speed change (m/s per year) from 1970 to 2002 in the summer season (December, January, February) over the southern hemisphere oceans.

RESULTS

We present simulations for the summer season (DJF) in 1980-1982 and in 2000-20002. Analysis of the ERA-40 wind data indicates that these three summer periods are representative of their respective decades.

Figure 2 shows a significant increase of the CCN concentration at the cloud base altitude since the 80s. The largest increases in remote marine regions (by up to 60%) are seen along the 60° S latitude band where also the wind speeds have increased the most (Figure 3). Along the 40° S latitude band, on the other hand, the CCN concentration has slightly decreased corresponding well with the small decrease in mean wind speeds in this region.

In principle three reasons can explain the Southern Ocean CCN change between the 1980s and early 21st century: changes in sea spray emission flux due to changed wind speed, changes in DMS emission flux due to the same reason, and changes in continental emissions of aerosol particles. To eliminate the last two possibilities we conducted two sets of sensitivity simulations for Januaries 2000-2002. The results of these simulations are discussed below (no figures shown).

The effect of wind speed change on DMS-derived CCN was investigated with the following set-up: First we calculated the six-hourly DMS ocean-to-atmosphere fluxes for January 1980. Then these fluxes where read in in the simulation of Januaries 2000-2002. In other words, these simulations used real winds for all other atmospheric processes (sea spray emissions, long range transport of pollution, advection, etc.) but forced the DMS emissions to match those in 1980. A comparison of this set of runs with the baseline January 2000-2002 runs showed practically no difference in the cloud-base CCN concentration indicating that the DMS flux change cannot explain the CCN change seen in Figure 2. This result is consistent with our earlier work according to which the effect of enhanced DMS emissions on CCN is spread out over a large region (Korhonen et al., 2008). This is because DMS forms CCN via nucleation in the free

194

troposphere and subsequent growth during entrainment. This process takes several days to a week and thus involves transport over long distances.

The effect of changes in anthropogenic pollution was investigated by rerunning Januaries 2000-2002 using 1980s emission data sets for SO_2, OC and BC. This set of simulations was then compared to the baseline January 2000-2002 runs. While the emission changes have clearly had a large impact on the CCN number in the northern hemisphere industrialised regions, their effect over the Southern Ocean is only up to a few percent. Thus it is clear that anthropogenic emissions do not explain the simulated CCN increase in Figure 2.
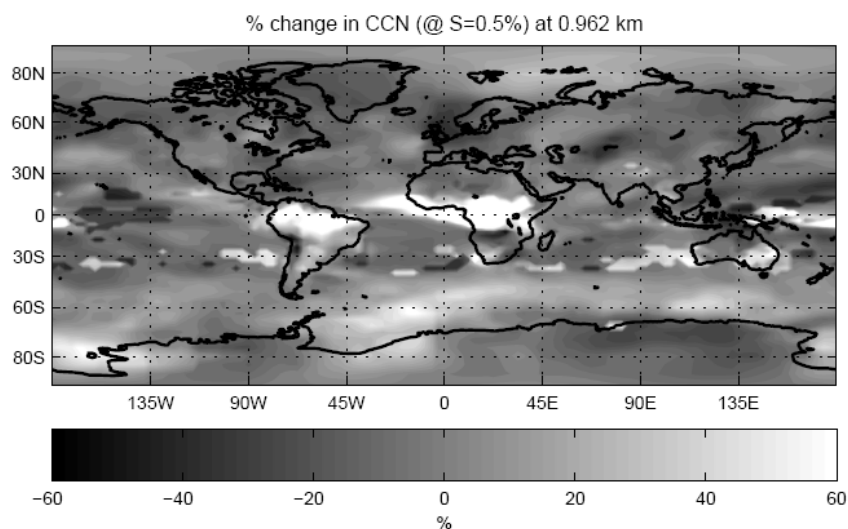
Figure 2. Average change in southern hemisphere summer CCN concentration at 1 km altitude from the early 1980s to the early 21st century.
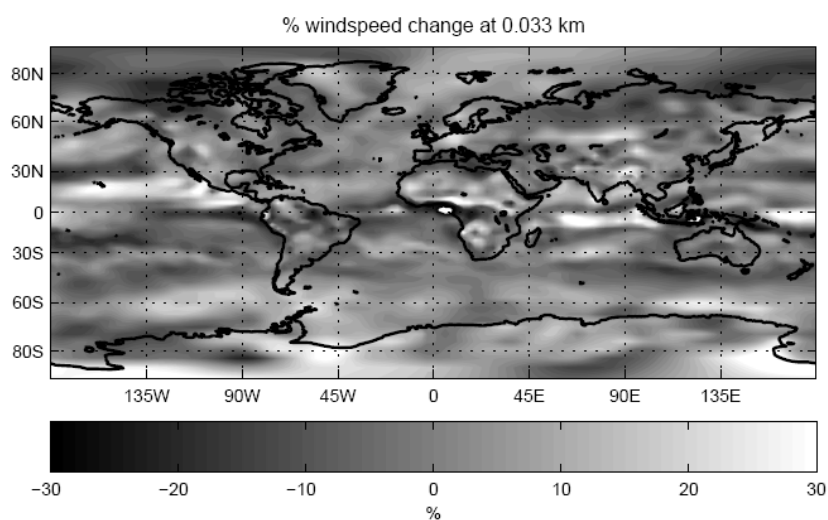
Figure 3. Average change in southern hemisphere summer surface wind speeds from the early 1980s to the early 21st century.

CONCLUSIONS

The surface level wind speeds have increased significantly over the Southern Ocean from 1970s to date. We have shown that this increase has led to a large enhancement of sea spray emission flux and subsequently of CCN in the region. This enhancement is of similar magnitude (but of opposite sign) than the reduction of CCN over Europe and North America as a result SO_2 emission reductions in the 1980s. It is therefore expected to have had a strong climate impact in the southern hemisphere midlatitudes in the past 40 years.

REFERENCES

Bond, T., Streets, D., Yarber, K., Nelson, S., Wo, J.-H, and Klimont, Z. (2004), A technology-based global inventory of black and organic carbon emissions from combustion, *J. Geophys. Res., 109*, D14203, doi:10.1029/2003JD003697.

Andres, R., and Kasgnoc, A. (1998), A time-averaged inventory of sub-aerial volcanic sulfur emissions, *J. Geophys. Res., 103*, 25,251-25,261.

Cofala, J., Amann, M., Klimont, Z. and Schöpp, W. (2005), Scenarios of world anthropogenic emissions of SO_2, NO_x, and CO up to 2030, *Internal report of the Transboundary Air Pollution Programme*, 17 pp., International Institute for Applied Systems Analysis, Laxenburg, Austria.

Halmer, M., Schmincke, H. and Graf, H. (2002). The annual volcanic gas input into the atmosphere, in particular into the stratosphere: A global data-set for the past 100 years. *J. Volca. Geotherm. Res., 115*, 511-528.

Kettle, A. J. and Andreae, M. O. (2000), Flux of dimethylsulfide from the oceans: A comparison of updated data sets and flux models, *J. Geophys. Res., 105*, 26,793-26,808.

Korhonen, H. Carslaw, K., Spracklen, D., Mann G. and Woodhouse, M. (2008), Influence of DMS emissions on CCN concentrations and seasonality over the remote southern hemisphere oceans: A global model study, *J. Geophys. Res.*, 113, D15204, doi:10.1029/2007JD009718.

Mårtensson, M., Nilsson, D., de Leeuw, G., Cohen, L. H., and Hansson, H.-C. (2003), Laboratory simulations and parameterization of the primary marine aerosol production, *J. Geophys. Res., 108*, 4297, doi:10.1029/2002JD002263.

Monahan, E., Spiel, D. and Davidson, K. (1986), A model of marine aerosol generation via whitecaps and wave disruption, in *Oceanic Whitecaps and their role in air-sea exchange processes*, edited by E. C. Monahan and G. MacNiocaill, pp. 167-174, Dordrecht: D. Reidel Publishing.

Spracklen, D., Pringle, K., Carslaw, K., Chipperfield, M., and Mann, G. (2005), A global off-line model of size-resolved aerosol microphysics; I. Model development and prediction of aerosol properties, *Atmos. Chem. Phys., 5*, 2227-2252.

Stier, P., Feichter, J., Kinne, S. et al.(2005), The aerosol-climate model ECHAM5-HAM, *Atmos. Chem. Phys, 5*, 1125-1165.

Stockwell, D., and Chipperfield, M. (1999), A tropospheric chemical-transport model: development and validation of the model transport schemes, *Q. J. R. Meteorol. Soc.*, *125*, 1747-1783.

Uppala, S. M., Kallberg, P. W., Simmons, A. J., et al. (2005), The ERA-40 re-analysis, *Quart. J. Royal Meteor. Soc.*, 131, 2961-3012.

van der Werf, G. R., Randerson, J. T., Collatz, G. J., and Giglio, L. (2003), Carbon emissions from fires in tropical and subtropical ecosystems, *Global Change Biology, 9*, 547-562.

ENVIRONMENTAL RESPONSES OF ROOT AND RHIZOSPHERE RESPIRATION AND RESPIRATION FROM DECOMPOSITION

J. F. J. KORHONEN[1,2], J. PUMPANEN[2], P. KOLARI[2], E. JUUROLA[2] AND E. NIKINMAA[2]

[1]Department of Physics, PO Box 64, FI-00014 University of Helsinki, Finland
[2]Department of Forest Ecology, PO Box 27, FI-00014 University of Helsinki, Finland

INTRODUCTION

Carbon dioxide (CO_2) exchange between the atmosphere and forest ecosystems consists of photosynthesis (gross primary production, GPP) and respiratory processes. In boreal forests GPP is typically higher than total ecosystem respiration (TER), resulting carbon accumulation to the ecosystem. In boreal coniferous forests, aboveground respiration is usually smaller than soil respiration (R_s; Kolari et al. 2009). In general, respiration is observed to respond approximately exponentially to temperature. Globally in soils is stored over two times more carbon than in the atmosphere. Therefore R_s may have a strong positive feedback to global warming making it even stronger. Because of the importance of soils to climate change, R_s has been intensively studied during the past decade.

Only part of the R_s is originating from the decomposition of the actual soil carbon stocks. This is called respiration from decomposition (R_d). Much smaller stocks exist of labile carbon, mainly carbohydrates and starch. This labile carbon, called photosynthates is originating from GPP and is being transported to soil in the phloem of trees. Stocks of photosynthates in the soil can be consumed in respiration in days or weeks. The users of this carbon are the roots and microbes in the rhizosphere, and thus the usage of this carbon is called root and rhizosphere respiration (R_r).

As the variability in the substrate availability for R_r and R_d are different, they respond very differently to the environment. Therefore the environmental response of R_d in the soil is not similar as the environmental response of R_s. Our aim in this study was to determine the environmental responses of R_d and R_r, and quantify how much of GPP is being used in R_r.

METHODS

We used girdling (see Högberg et al. 2000) as a method to separate R_d from R_r. In the procedure we removed the phloem all around the tree, so that phloem flow was stopped. We girdled totally 19 Scots pines (*Pinus sylvestris* L) from an elliptical area of approx. 200 m^2 in the vicinity of the SMEAR II station in Hyytiälä, Southern Finland (61° 51'N, 24° 17'E, 180 m above sea level). Ground vegetation was kept intact. We measured soil CO_2 effluxes with static chambers from 12 collars at the girdled plot and from 14 collars from the SMEAR II continuous measurement plot, which acted as a control plot in our study. Measurements were done in the mornings of consecutive days at the girdled and the control plot every week or every second week at summer and every month at winter. We utilized the comprehensive continuous measurements at the station, including soil water content, soil temperature and GPP, which was calculated from Eddy covariance measurements as described in Mäkelä et al. (2006).

We assumed that after two weeks from the girdling, the measured CO_2 effluxes from the girdled and control plots would represent R_s and R_d, respectively. R_r would be calculated by subtracting R_d from R_s. However, there was a statistically significant ($p > 0.05$) systematic difference in the effluxes before the

girdling at the plots. To get rid of this difference we scaled all the measurements by multiplying the effluxes measured at the girdled plot by 0.82 and after that determined R_r as described above.

We modeled half hour R_d and R_r by Arrhenius type function as a function of soil temperature. Annual respirations were calculated by integrating the half hour values over the year. This value was then compared to a typical annual soil respiration value in SMEAR II (625 g C m^{-2}; Kolari et al. 2009) and all the respirations were scaled using this coefficient (0.61).

RESULTS

After the girdling, the measured CO_2 effluxes ranged from 0.64 to 7.81 µmol m^{-2} s^{-1} at the control plot and from 0.63 to 5.35 µmol m^{-2} s^{-1} on the girdled plot. Before the girdling, control plot showed 22 % lower values than the girdled plot, which is statistically significant ($p<0.05$). The annual CO_2 efflux from the control and girdled plot was 1029 g C m^{-2} and 769 g C m^{-2}, respectively (Fig. 1). The spatial variability of the CO_2 effluxes was significantly lower at the girdled plot. There were no extreme weather events during the period. The measured effluxes were much higher than typical annual soil respirations in SMEAR II.

The annual calculated R_r and R_d were 246 and 379 g C m^{-2}, respectively. We observed very high seasonal variation in both R_d and especially in R_r. 58% and 91% of the annual R_d and R_r, respectively, occurred during the four most active months (from June to September; Fig 2.). We observed small negative values for R_r (very low or not at all R_r) from February to May. During August and September R_r exceeded R_d, R_r:R_d being 1.52 and 1.25 during the respective months. At wintertime R_d was typically about 15 g C m^{-2} and peaked 70 g C m^{-2} during the summer. Annually R_r and R_d were about 22% and 36% of the GPP.
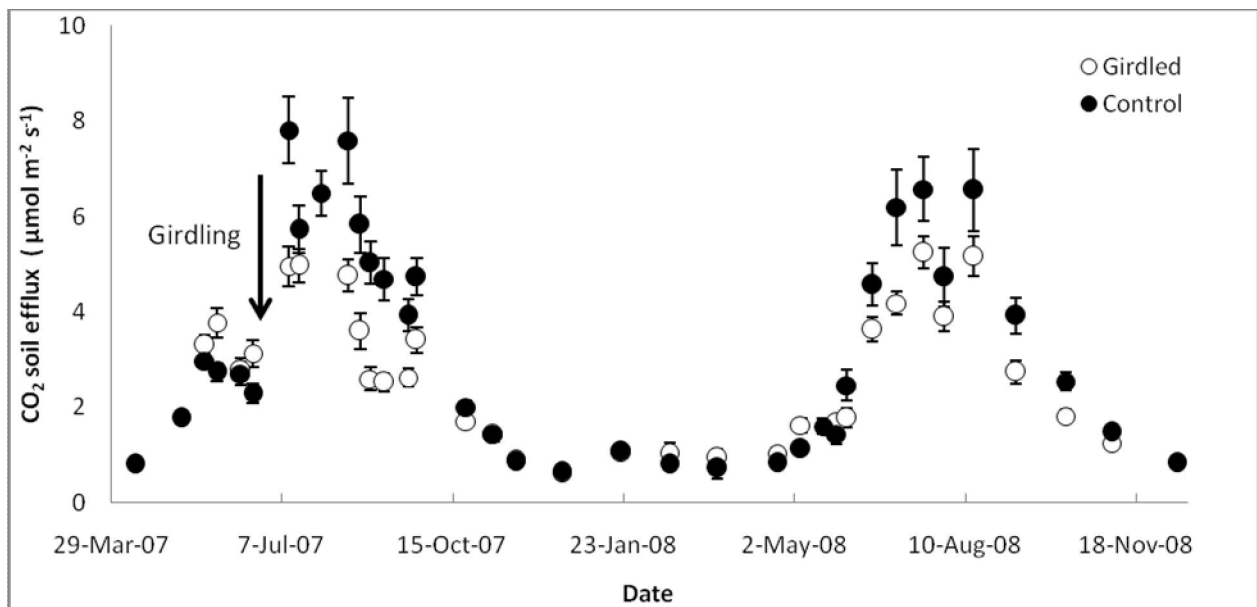
Figure 1. Measured soil CO_2 effluxes from the girdled and control plots from 12 April 2007 to 12 December 2008. Error bars indicate standard errors. The girdled plot was not measured during the first two and the last measurement.
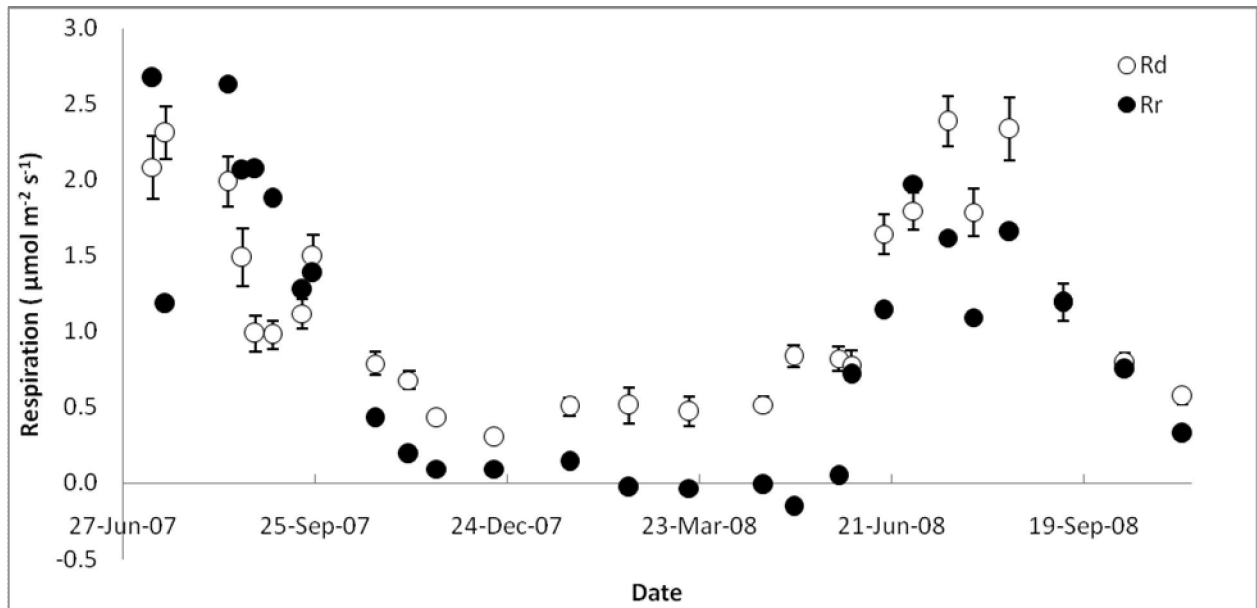
Figure 2. Scaled measured respirations from decomposition (R_d) and from root and rhizosphere (R_r) 10 July 2007 to 31 July 2008. Lines represent modeled half hour respirations using Arrhenius type temperature regression using the scaled measurements. In the scaling initial level of respirations is scaled away. Error bars of R_d indicate standard errors.

The pattern of R_r followed the pattern of R_d with a delay of approximately a month. From February to May when the respirations were low, the calculated R_r:R_d was constantly negative, on average -0.05. R_r:R_d increased very rapidly in June and was from June to July 0.82 From August to September the clearly highest values were observed on average 1.39. R_r:R_d decreased during October to a rather constant value of 0.20 until February.

In agreement with previous studies, GPP followed air temperature with a delay. R_d followed soil temperature, and was more sensitive to temperature during spring than in autumn. We noticed very high temperature sensitivity for R_r, especially in spring. R_r followed GPP with a delay of 1 to 2 months (Fig. 3). In the spring we did not observe R_r at all, though GPP was relatively high and soil temperature had risen and R_d increased. It is known, that foliage can be a very strong sink for photosynthates in the early part of growing season, leaving less carbon available for the root system to respire. During late summer and early autumn R_r remained high, reflecting favourable temperature in soil for biochemical processes and photosyntate availability.

The temperature sensitivity of the soil respiration may be confounded if litter availability changes during the period investigated (Kirschbaum, 2006). The variability of substrate availability is the largest for R_r and it has been reported that in short term R_r is less sensitive to soil temperature than R_d (Bhupinderpal-Singh, 2003). Same kind of response can be seen for R_s, as it includes both R_d and R_r. Therefore the temperature sensitivity data must be interpreted with care and assumption of R_d and R_s responding similarly to soil temperature is doubtful, especially when modelling long term response of soil to climate change.

Also temperature sensitivity of R_d is confounded, as litter availability changes during the year, as most of the litter is produced in autumn. However the properties of needle litter and the hard environment for the decomposition in boreal forests makes the litter rather non-labile and therefore litter availability and temperature response of R_d does not change very much during the year.
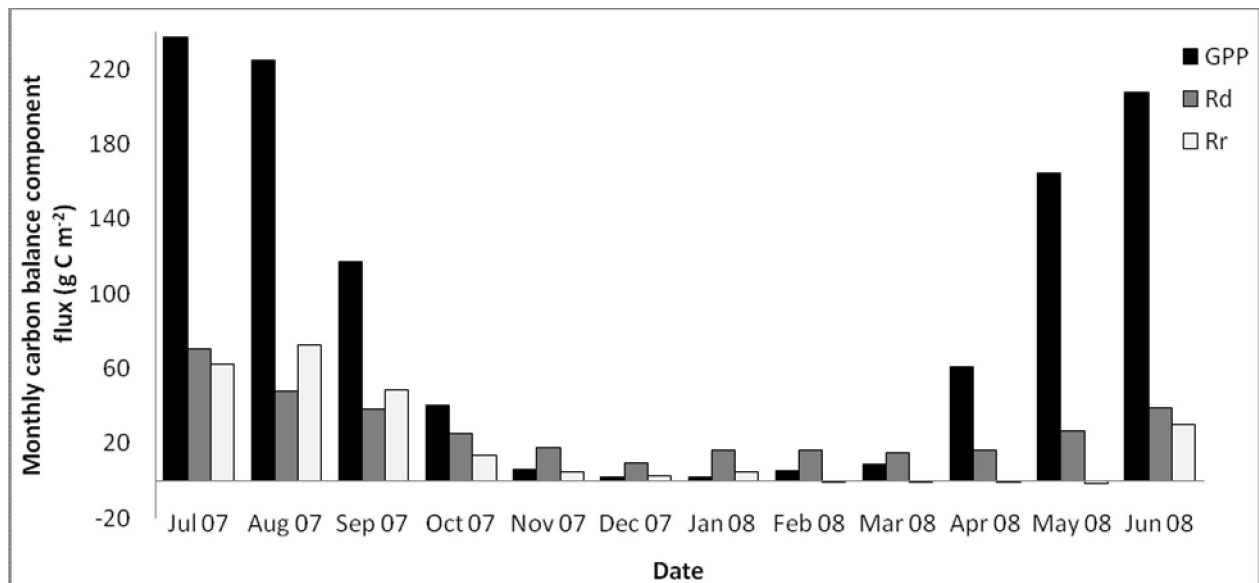
Figure 3. Monthly gross primary production (GPP), respiration from decomposition (R_d) and root and rhizosphere respiration (R_r) for a period of one year from July 2007 to June 2008.

We did not take into account the ground vegetation in our study. It is possible that there were roots of non-girdled trees in the girdled area, though the effect should not be high. Girdling increases the litter availability for R_d as the root system and associated microbes will eventually die. These factors may influence the results.

CONCLUSIONS

We found that significant part of GPP is used in root and rhizosphere respiration (R_r). In summertime (R_r) can be higher than respiration from decomposition (R_d), though annually R_d is significantly higher. It seems probable that during the spring and autumn R_r is responding to plant growth and allocation strategies rather than directly to the environment. Temperature does not explain well R_r, and explaining R_d by soil temperature should be only made with short time periods. Solid modeling of R_r including soil respiration (R_s) requires understanding on photosynthesis and probably on plant growth and allocation strategies.

REFERENCES

Bhupinderpal-Singh, Nordgren, A., Ottosson Löfvenius, M., Högberg, M., Mellander, P. and Högberg, P. (2003). Tree root and soil heterotrophic respiration as revealed by girdling of boreal Scots pine forest: extending observations beyond the first year. Plant, Cell and Environment 26, 1287–1296

Högberg, P., A. Nordgren, N. Buchmann, A.F.S. Taylor, A. Ekblad, M.N. Högberg, G. Nyberg, M. Ottoson-Löfvenius, and D.J. Read. (2001). Large-scale forest girdling shows that current photosynthesis drives soil respiration. Nature 411:789–792

Kirschbaum M. (2006). The temperature dependence of organic-matter decomposition—still a topic of debate. Soil Biology & Biochemistry 38 2510–2518

Kolari, P., Kulmala, L., Pumpanen, J., Launiainen, S., Ilvesniemi, H., Hari, P. and Nikinmaa, E. (2009). CO2 exchange and component CO2 fluxes of a boreal Scots pine forest. Boreal Environment Research, 14, in press.

Mäkelä A, Kolari P, Karimäki J, Nikinmaa E, Perämäki M. and Hari P. (2006). Modelling five years of weather-driven variation of GPP in a boreal forest. Agricultural and Forest Meterology 139, 382-398

NITROGEN BALANCE OF A BOREAL SCOTS PINE FOREST

J. KORHONEN[1,2], M.K. PIHLATIE[1], J. PUMPANEN[2], T. VESALA[1], H. ILVESNIEMI[3], and P. HARI[2]

[1]Department of Physics, P.O. Box 64, FI-00014, University of Helsinki, Finland
[2]Department of Forest Ecology, P.O. Box 27, FI-00014, University of Helsinki, Finland
[3]Finnish Forestry Research Institute, Vantaa Research Center, P.O. Box 18, FI-01301 Vantaa, Finland

Keywords: nitrogen cycling, nitrogen balance, boreal forest, Scots pine

INTRODUCTION

Nitrogen (N) cycling is a key factor controlling the functioning of boreal forest ecosystems. In boreal forest ecosystems nitrogen and carbon cycling are coupled, and the N availability controls the productivity of the ecosystem. Boreal forest ecosystems are nitrogen limited. This means that nitrogen cycling in these ecosystems is closed and the nitrogen coming into the forest is retained there, and cycled internally. Losses of N in the form of N_2O emissions to the atmosphere are very small (Pihlatie et al., 2007). Also, as most of the N released into the soil is taken up immediately into growing vegetation, leaching losses are negligible.

Nitrogen storages and fluxes between the components, and their effect on greenhouse gas emissions are very little studied in boreal ecosystems. The aim of the study was to quantify the nitrogen budget in a boreal forest and to assess changes in the nitrogen pools and fluxes between different years.

METHODS

The measurements were conducted at SMEAR II –station in Hyytiälä, southern Finland (61° 51'N, 24° 17'E). The N pool and flux measurements were started in 1996, and since 2006 the site has been a NitroEurope IP level 3 site. The stand was established in 1962, and it is managed by the current recommendations for forests in economic use. Bedrock under the acidic 0.05 -1.5 m deep soil is solid granite and is sealed with silt containing high portion of clay, enabling water to escape the system only by evapotranspiration or runoff. Measurements related to nitrogen include nitrogen runoff out of the ecosystem via two weirs located at the outlets of two mini catchments (900 m2 and 300 m^2 in size), wet and dry deposition of N, throughfall and stemflow of N. Storages of N in the soil, needles and wood, and in the litterfall are also measured regularly.

During this 10 year period the nitrogen content in the living biomass (trees, understorey and roots) was estimated twice. Soil nitrogen pools were studied by taking soil samples from different soil horizons and analyzing them for total N and total C contents with CN analyzer (LECO). Extractable mineral nitrogen (NO_3-N and NH_4-N) and total nitrogen were determined from the same soil horizons by flow-injection spectrometry.

Fluxes of nitrogen into the ecosystem and out from the ecosystem were studied by measuring the concentrations of N in incoming rainfall and in outgoing runoff. During snow free period water samples were collected from above the forest canopy as wet deposition and below the forest canopy as throughfall and stemflow. Runoff water samples were collected from a damn at the outlet of the forest catchment area. Concentrations of dissolved organic nitrogen (DON), nitrate (NO_3^-) and ammonium (NH_4^+) were measured from frozen water samples by flow-injection spectrometry. Losses of N into the atmosphere were measured as N_2O and NO emissions. N_2O fluxes were measured using static chambers (Pihlatie et al., 2007), and NO_x fluxes using automated dynamic chambers (Pumpanen et al., 2001). Litter fall from

the tree canopy was collected with funnels placed systematically on the measurement site. The funnels were emptied at minimum four times per year or up to every two weeks depending on the year. The litter was dried, and different litter fractions were separated and weighed.

RESULTS

The nitrogen budget at SMEAR II –station is presented in Figure 1. We found that nitrogen accumulates to the forest ecosystem. Soil is the greatest pool of nitrogen. Approximately 99.9% of the N in the soil is bound to organic matter, mostly as humus and proteins, both of which are slowly decomposable. Other important storages of N are wood, needles and fine roots. In the woody tissue N is immobilized from decades to hundreds of years, whereas the N in the needles and fine roots is in constant cycling. Annual uptake of N by plants corresponds 1% of the total N stored in the ecosystem. In the soil the plant available mineral N pool (1 kg N ha^{-2}) was 1-2 orders of magnitude smaller than the pool of dissolved organic nitrogen (DON; 29 kg N ha^{-2}), but both of these were only small fractions of the total N pool of the soil (2000 kg N ha^{-2}). Atmospheric N deposition (5 kg N ha^{-2} yr^{-1}) is around 20% of the N uptake by plants.
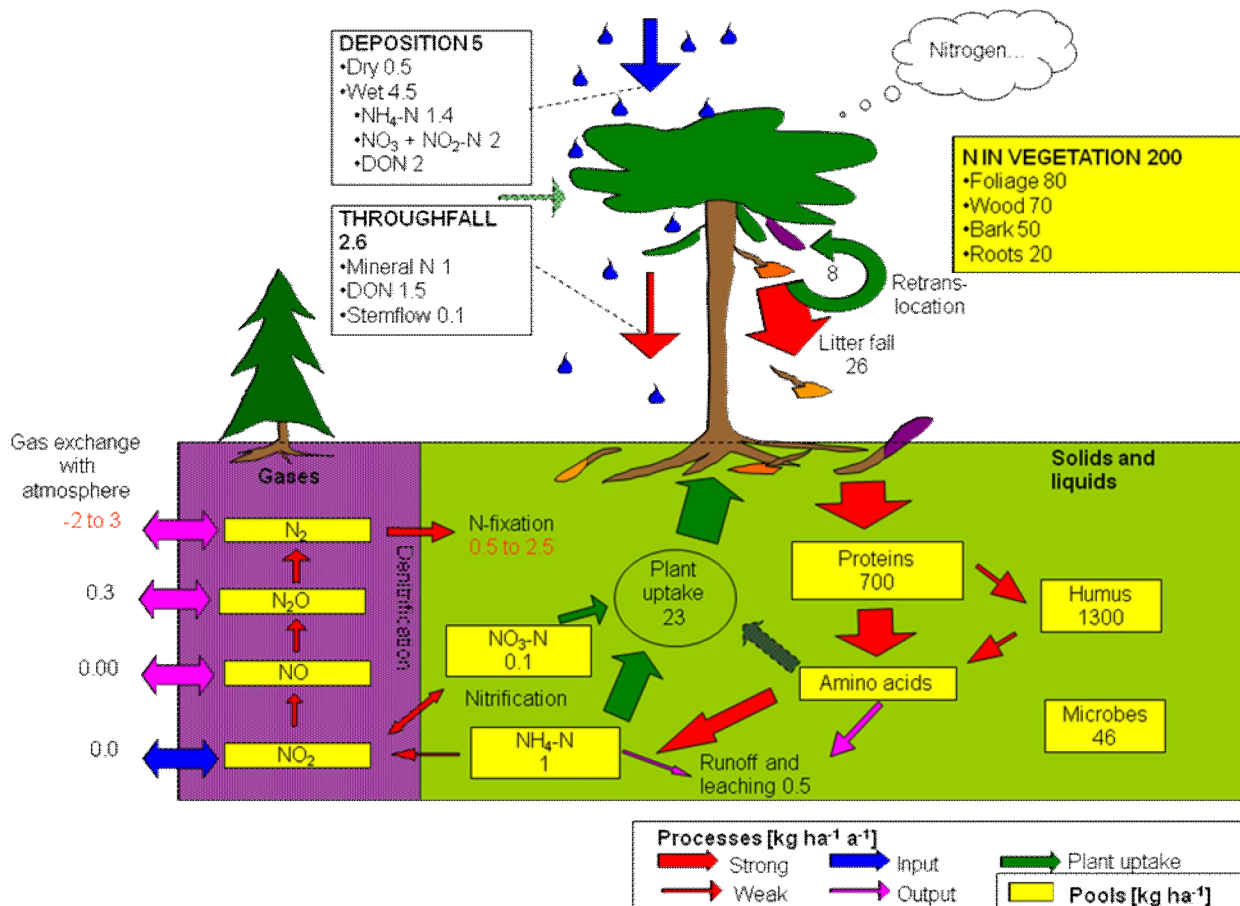
Figure 1. The nitrogen balance of boreal coniferous forest in Hyytiälä, Southern Finland. The non-white boxes represent pools and arrows represent processes and transport. The weight of the arrows represents the strength of the process. Gaseous forms of nitrogen are on the left box in the soil and nitrogen in liquids and solids are presented in the right box. The arrows left represent the gas exchange between soil and the atmosphere. All units are in kg ha^{-1} (yr^{-1}).

Large part of the N deposition from the atmosphere remained in the forest canopy and only small amounts were detected in the throughfall and stemflow waters. Approximately 10% of the atmospheric N inputs are lost in the runoff (0.5 kg N ha^{-2} yr^{-1}), mostly in the form of DON. However, both N deposition and N runoff vary between years. N loss in the form of N_2O emissions from the soil is 0.3 kg N ha^{-2} yr^{-1}, which is around 7% of the N inputs (see Pihlatie *et al.*, 2007). Losses of N into the atmosphere in the form of NO emissions from the soil, or NO_3^- or NH_4^+ leaching into water ways as ions were negligible. Occasionally, small emissions of NO_x from the pine needles were measured. These NO_x emissions occur during periods of high UV-radiation and are assumed to result from chemical reactions not related to the metabolism of trees (Hari et al., 2003).

As part of the internal nitrogen cycling within the forest ecosystem, the largest input of N into the soil was litter. The amount of nitrogen in the litterfall annually entering the soil was 26 kg N ha^{-2} yr^{-1}. The highest uncertainties remaining in the annual nitrogen budget calculations in this boreal forest ecosystem are related to N_2-fluxes from soil via denitrification and N_2-fluxes into the soil via N_2-fixation. Measurements of these components in boreal forest region are very scarce, however, the current estimate is that these two processes counteract each other.

CONCLUSIONS

There are large pools of nitrogen in boreal forests. However, most of the nitrogen is not easily available for the plants, since it has been bound to complex substances. Therefore, plants benefit from any available nitrogen added to the system. The largest pool of nitrogen is in the soil, but also biomass is significant storage. As the biomass increases during the stand development, the more nitrogen that was available to the plants is bound to it. This may influence the productivity of the stand.

The inputs of nitrogen exceed the output and nitrogen is accumulating to boreal forests. Atmospheric deposition from anthropogenic sources is the major input of nitrogen to forests. In areas where atmospheric deposition is near preindustrial level, especially in the north, nitrogen fixation is more important than more polluted areas. The significance of nitrogen fixation, as well N_2 flux from denitrification are, however, somewhat unclear. Development of measurement techniques are needed to quantify these fluxes reliably.

REFERENCES

Hari P., Raivonen M., Vesala T., Munger J. W., Pilegaard K., Kulmala M. (2003). Ultraviolet light and leaf emission of NOX. Nature, 422: 134.
Hari, P., Salkinoja-Salonen, M., Liski, J., Simojoki, A., Kolari, P., Pumpanen, J., Kähkönen, M., Aakala, T., Havimo, M., Kivekäs, R. & Nikinmaa, E. (2008). Growth and Development of Forest Ecosystems: the MicroForest model. In: Hari P. & Kulmala, L. (Eds.) Boreal Forest and Climate Change. Springer Netherlands. p. 433–461.
Hari, P. & Kulmala, M. 2005. Station for Measuring Ecosystem–Atmosphere Relations. Boreal Environmental Research 10: 315–322.
Pihlatie, M., Pumpanen, J., Rinne J., Ilvesniemim H., Simojoki A., Hari P., and Vesala T. (2007). Gas concentration driven fluxes of nitrous oxide and carbon dioxide in boreal forest soil. Tellus, 59B, 458–469.
Pumpanen, J., Kolari, P., Ilvesniemi, H., Minkkinen, K., Vesala, T., Niinisto, S., Lohila, A., Larmola, T., Morero, M., Pihlatie, M., Janssens, I., Yuste, J.C., Grunzweig, J.M., Reth, S., Subke, J.A., Savage, K., Kutsch, W., Ostreng, G., Ziegler, W., Anthoni, P., Lindroth, A., Hari, P., (2004) Comparison of different chamber techniques for measuring soil CO_2 efflux. *Agric. For. Meteorol.* 123: 159-176.

V-TDMA DATA FROM CHAMBER EXPERIMENTS

A. KORTELAINEN[1], P. MIETTINEN[1], S. ROMAKKANIEMI[1] and A. LAAKSONEN[1]

[1] Department of Physics, University of Kuopio, Finland

INTRODUCTION

Secondary organic aerosols (SOA) scatter and absorb incoming solar radiation and thereby directly affect Earth's radiation budget. They affect also indirectly by acting as cloud condensation nucleis (Seinfeld and Pandis, 2006). Thus the formation mechanism and precursors of SOA need to be known when the total effect of aerosol particles on radiation budget is estimated. The number of different precursors in the real atmosphere is very high, and thus the role of different precursors on new particle formation need to be studied in controlled laboratory conditions.

In this study SOA were produced by oxidating volatile organic combounds (VOC) in the chamber. VOCs used were either biogenic (direct plant emission from Scots Pine) or synthetic monoterpenes. Pine mainly emits monoterpenes such as α-pinene, β-pinene, myrcene, limonene and Δ^3-carene (Hao et al., 2009). In the experiments biogenic VOCs were oxidated by reaction with ozone (O_3) and hydroxyl radical (OH). In some experiments SO_2 was used a source of sulfuric acid to increase nucleation rate, and TME (tetramethylethylene) to increase OH concentration (Kulmala et al., 1998; Paulson et al., 1997). We also did some experiments using monodisperse ammonium bisulphate ($(NH_4)_2SO_4$) as seed particles in order to study heterogeneous nucleation.

In this abstract we concentrate on the volatility properties of formed particles. This was done using V-TDMA (Volatility Tandem Differential Mobility Analyzer). In the instrument particles are classified using DMA before and after heating. Upon heating fraction of volatile particles evaporates in a fixed temperature. The instrument was measuring particles having diameter between 10 and 100 nm using three different temperatures of 25, 150 and 280 °C.

It was noticed that in some experiment the particles were volatile even in the room temperature. Also it seem that SO_2 origin particles are not that volatile as the others. OH reactions based SOA seem also to be less volatile than the SOA formed through ozone reactions. Aerosol based on $(NH_4)_2SO_4$ particles appeared to evaporate almost completely at 280°C. Also Bimodal distributions were found in different experiments.

METHODS

The measurements were conducted in laboratory under controlled conditions during three weeks period $23.1 - 11.2.2009$. The experiments were performed in Teflon constructed chamber (volume $6 \ m^3$) which was sustained at 30% relative humidity (RH). Gas phase components were monitored in the chamber by O_3, NO_x and SO_2 analyzers. Ozone concentration was also monitored in the incoming line.

Nucleation and growth of aerosol particles occurred through oxidation of biogenic VOCs and synthetic monoterpenes. Pine seedling used was held in the individual transparent Teflon bag and it was stressed to enhance VOC emission. In the beginning of every experiment the chamber was humidified until the RH reached its desirable value. VOCs were added before SO_2 and TME. OH formed in the chamber through the reactions between ozone and VOCs as well as in the reaction between TME and ozone in some cases. SO_2 concentration were kept under 22 ppbs. Monoterpene concentration changed between $1.5 - 102.6$ ppbs as in the plant experiment cases the emission rates couldn't be prefigured. In order to start nucleation ozone concentration was increased to circa 40 ppbs in the chamber.

The V-TDMA instrument consists of two condensation particle counters (CPC) and three stainless steel volatilisation tubes (length = 50 cm and inner diameter = 6 mm) which were operated at temperatures of 25, 150 and 280 °C. Inside each tube residence time was 0.8 s and heating tube temperature was controlled by thermocouple located inside the tube at 5 cm from the output. Heating column follows an absorber tube, stainless steel mesh (length = 50 cm and inner diameter = 10 mm) inside the cooling section, which reduces nucleation and re-condensation (Burtscher et al., 2001). Sample aerosol particle diameter was classified by the DMA (Vienna type, length = 11 cm) and measured by CPC (TSI 3785) before heating. Change in particle diameter is determined after heating with other DMA (Vienna type, length = 11 cm) and number concentration with CPC (TSI 3010). Comparing number concentrations before and after heating reveals loss of particles during evaporation. Fixed particle diameters were applied to 10, 15, 20, 30, 50 and 100 nm. Time for the total measurement cycle was 30 minutes.

Measurements were divided into six cases according to VOC source and other chemical constituents. Plant emission oxidation reactions were studied by following experiments: pine+O_3, pine+O_3+SO_2 and pine+O_3+SO_2+TME. α-pinene was used in the other experiments: α-pinene+O_3, α-pinene+O_3+SO_2 and α-pinene+$(NH_4)_2SO_4$+O_3. Starting point of each experiment was determined to be the first ozone addition. Measured growth factors were normalised before calculation of average. Growth factors were measured between 0.2 and 1.2.

RESULTS

Initial diameters in the results presented are chosen to be 30 and 50 nm as they were found in all experiments. 10 and 20 nm particles growth factors were not available in any experiments because of rapid growth of particles after ozone addition. 100 nm size was achieved only in one of the experiment, and thus it is not presented. In Figure 1 the comparison of growth factors at 150 °C for five different measurement setup is presented. It can be seen that particles are more volatile (evaporate more, smaller growth factor) when there is no SO_2 included.

The example for particle volatilisation in different temperatures is represented in Figure 2. Almost in all experiments growth factors were circa 1 at room temperature of 25 °C. In experiment α-pinene+O_3 particles were volatile even at room temperature.

Comparison between cases "pine+O_3+SO_2" and "α-pinene+O_3+SO_2" showed that SOA based on synthetic monoterpene oxidation is clearly more volatile than the biogenic one. The same experiments without SO_2 showed entirely different result where pine emissions based SOA were more volatile than α-pinene based SOA. TME seems to clearly decrease the growth factors as can be seen by comparing the cases pine+O_3+SO_2 and pine+O_3+SO_2+TME at the temperature of 150
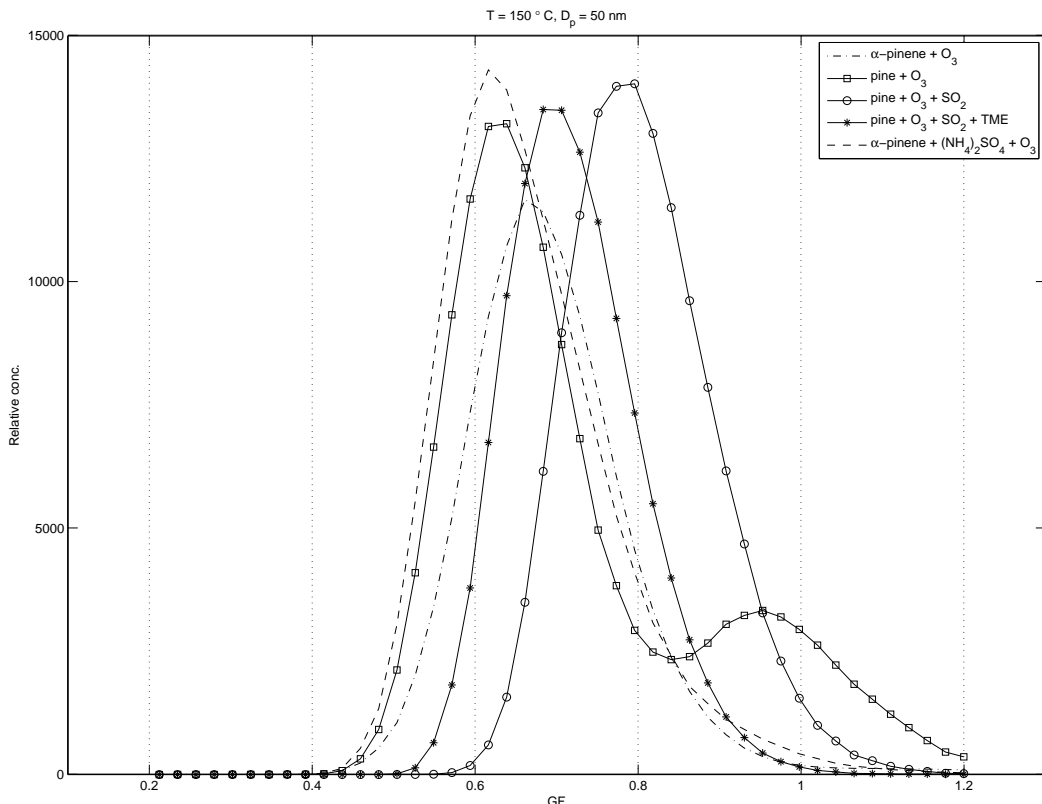
Figure 1: Volatility of 50 nm particles in five experiments at 150 °C temperature. Mean total number concentrations as a function of growth factors (GF).

°C.

CONCLUSIONS

SO_2 concentration was problematic to estimate because of the gas analyzer uncertainty. The instrument showed zero when the real concentration was about 5 ppbs. As can be seen SO_2 makes particles less volatile. TME reactions based SOA seem to be more volatile than the SOA without it. Monoterpene concentration was a bit higher for TME experiments because of OH production uncertainty. That increased the particle number concentration remarkably bigger than in other cases.

Usually measured GF distributions were unimodal. Bimodal distributions can be found in α-pinene+O_3 and pine+O_3 experiments. In pine emission case ozone were added several times and remarkably more than 40 ppbs during one day. That might have caused the bimodal distribution seen at 150 °C temperature during the whole experiment. In α-pinene+O_3 experiment particles were volatile even at the room temperature. At 280 °C particles seem to have multimodal distribution of growth factors. Thus particles were evaporating in different ways and that could be sign of two different densities for SOA.
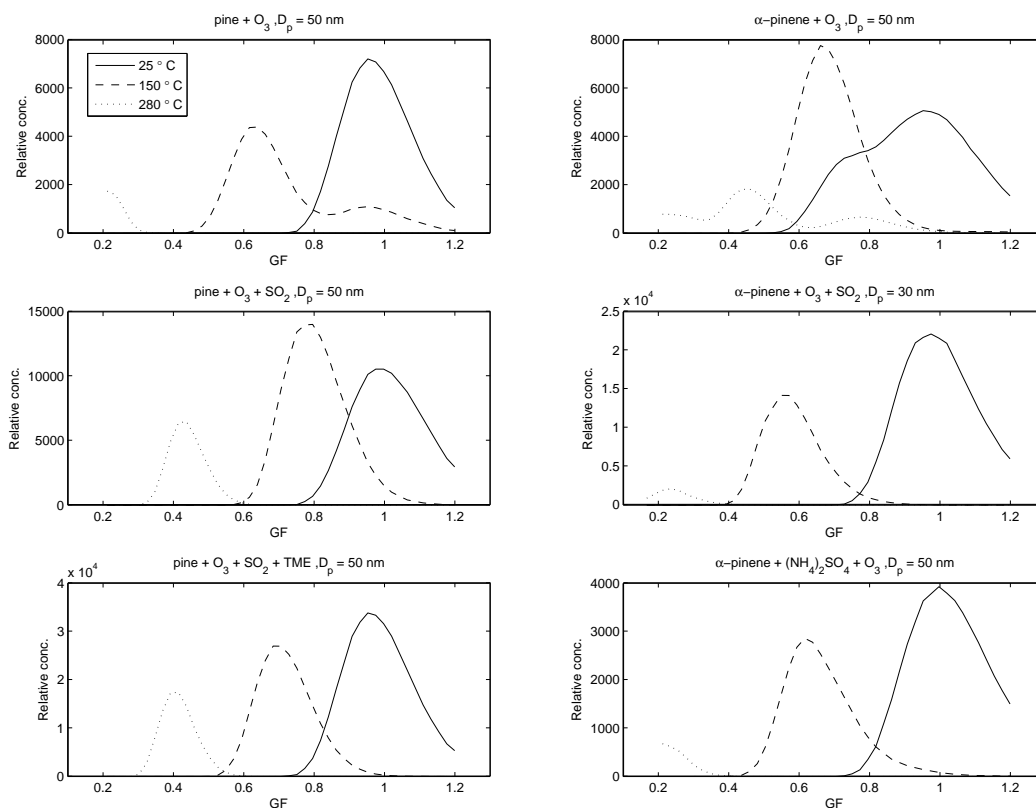
Figure 2: Volatility of 30 and 50 nm particles in all experiments at 25, 150 and 280 °C temperatures. Mean total number concentrations as a function of growth factors (GF).

REFERENCES

Burtscher, H.,Baltensperger, U., Bukowiecki, N., Cohn, P., Hüglin, C., Mohr, M., Matter, U., Nyeki, S., Schmatloch, V., Streit, N. and Weingartner, E. (2001). Separation of volatile and non-volatile aerosol fractions by thermodesorption: instrumental development and applications. *Journal of Aerosol Science*, 32:427-442

Hao, L., Yli-Pirilä, P., Tiitta, P., Romakkaniemi, S., Vaattovaara, P., Kajos, M. K., Heijari, J., Kortelainen, A., Miettinen, P., Kroll, J. H., Holopainen, J.-K., Joutsensaari, J., Kulmala, M., Worsnop, D. R., and Laaksonen, A. (2009). New Particle Formation from the Oxidation of Direct Emissions of Pine Seedlings. *Atmos. Chem. Phys. Discuss*, 9:8223-8260.

Kulmala, M., Laaksonen, A., and Pirjola, L. (1998). Parameterizations for sulfuric acid/water nucleation rates. *J. Geophys. Res.*, 103:8301–8308.

Paulson, S. E., Sen, A. D., Liu, P., Fenske, J. D., and Fox, M. J. (1997). Evidence for Formation of OH Radicals from the Reaction of O3 with Alkenes in the Gas Phase. *Geophys. Res. Lett.*, 24(24):3193-3196.

Seinfeld, J. H. and Pandis, S. N. (2006). Atmospheric chemistry and physics. *John Wiley & sons, inc.*, second edition.

DROUGHT AFFECTS HEAVILY THE RATE OF PHOTOSYNTHESIS OF GROUND VEGETATION IN DIFFERENT PHASES OF SECONDARY SUCCESSION OF A FOREST

L. KULMALA[1], J. PUMPANEN[1], P. HARI[1], T. VESALA[2]

[1] Department of Forest Ecology, P.O. Box 64, FI-00014, University of Helsinki, Finland
[2] Department of Physics, P.O. Box 64, FI-00014, University of Helsinki, Finland

INTRODUCTION

The capacity of forests to bind atmospheric carbon dioxide (CO_2) has been widely researched because increased CO_2 concentration along with other green house gases is predicted to cause severe changes in climate across Earth. However, the research has mainly focused on middle-aged and old trees and the diversity of species and phase of succession have been widely ignored.

Succession describes the natural changes in an ecosystem. Plants affect their own environment and the small changes influence the species and their competitive strength. Therefore dominant species vary in the course of time. In early succession, the dominant species are fast-growing and short-living and responsible for the whole photosynthetic production at a temporarily treeless site. Later, trees start to dominate but the photosynthesis of ground vegetation can still be significant because present silviculture supports low stand density which enables sufficient light intensity for photosynthesis on the ground level. Also small disturbances like thinning, windfall or insect damage generate living space, and locally improve greatly living conditions for the ground vegetation.

Some studies estimate forest floor vegetation to momentarily assimilate as much as 50% (Goulden and Crill, 1997) of the total assimilated carbon in a closed canopy. Kolari et al. (2006) found that the annual gross photosynthesis of forest floor vegetation is 131 g C m^{-2} (13% of the total ecosystem gross photosynthesis). Morén and Lindroth (2000) revealed that the annual gross photosynthesis of forest floor vegetation is 280 g C m^{-2} in a 70-year-old Norway spruce and Scots pine forest. The estimated amount of fixed carbon varies from site to site depending on climate, fertility, canopy structure and vegetation. To clarify the influence of tree age and environmental factors, we studied the species distribution and species-specific annual patterns of CO_2 exchange of ground vegetation and exchange responses to environmental changes in stands of different ages in the growing season of 2006.

METHODS

We measured the CO_2 exchange of the most common forest floor species on five different aged sites located near the station for measuring ecosystem-atmosphere relations (SMEAR II, Hari and Kulmala, 2005) in Hyytiälä, southern Finland (61.52ºN, 24.17ºE). The sites were chosen to be similar with varying dominant tree (stand) age. The ages of the stands were 6, 12, 20, 45 and 120 years. The middle-aged (45-year-old) site was located at the SMEARII station and the 20-year-old site circa 500 m northwest from the SMEARII. The sites of 6, 12, and 120 years are located next to each other app. 3 km south from the SMEARII station. The habitat at all of the sites is rather poor and according to Finnish Forest Classification system (Cajander, 1926) the forests belong to Vaccinium type (VT). The dominant tree species at all of the sites was *Pinus sylvestris*.

We estimated the average biomass of ground vegetation at the sites by systematically collecting samples of the aboveground plant parts. The sample size was 0.0333 m^2 and the number of samples 24 for mosses and 44 for vascular plants. Each sample was separated into different species, and each species into leaves and stem if possible. From the mosses, the green parts were separated from the shoots. These segments were weighed after drying at 60 ºC for 24 h.

We used a manual chamber, based on the closed static chamber technique, for measuring the light response curves of CO_2 exchange of the most common species of ground vegetation. The measurement campaign begun on 2 May and ended on 29 October 2006. We repeated the measurements at app. 2-week intervals. The measured species varied from site to site according to their occurrence. *Vaccinium vitis-idaea* and *Calluna vulgaris* were the only species that were measured at all of the sites. The chamber and the used protocol is introduced in detail in Kulmala et al. (2008).

Photosynthesis is driven by light but the relationship between light and photosynthetic rate is saturating because the availability of CO_2 begins to limit photosynthesis at high light intensities. Respiration accompanies the observable CO_2 exchange during daytimes. Therefore we fitted a simple Michaelis-Menten-type equation (Michaelis and Menten, 1913) for each set of our measurements as follows:

$$NE_i(I) = \frac{NP_i\,I}{b_i + I} - r \qquad\qquad\qquad (1)$$

In the equation, $NE_i(I)$ is the species-specific rate of CO_2 exchange ($\mu mol\ m^{-2}\ s^{-1}$) per full grown leaf mass, I is the light intensity ($\mu mol\ m^{-2}\ s^{-1}$), b is the light intensity ($\mu mol\ m^{-2}\ s^{-1}$) when the assimilation rate is half the rate of light-saturated assimilation, r is the rate of dark respiration and NP_i is the rate of light-saturated assimilation per full grown leaf mass ($\mu mol\ g^{-1}\ s^{-1}$), i.e. photosynthetic activity. In the whole plant measurements as here, the photosynthetic activity indicates both the amounts and catalytic activities of photosynthetic enzymes (Pearcy et al., 1987) and the size and amount of leaves that increases in early summer. The measurement campaign ended for each species before the species-specific senescence of leaves. Then, the aboveground parts of the measured plants were collected, dried for 24 h at 60 ℃ and weighed to obtain the leaf and total biomasses. The single NP_i values were then based on the full-grown leaf biomass.

Air temperature was continuously measured at 30-min interval at app. 1 m height at each site. Soil moisture was measured each week from TDR probes in the topmost horizon of mineral soil with a portable metallic cable tester (Tektronix 1502 B, Tektronix Inc., Redmond, WA). Simultaneously with the TDR-measurements, we measured manually soil water suction using eight tensiometers and a Tensicorder (Soil Measurement Systems, Tuscon, AZ, USA) at a depth of 2 cm in mineral soil.

In Boreal region, there is a clear annual cycle in photosynthesis. To study the changes in the rate of photosynthetic, we used a function called state of development, S (Pelkonen and Hari, 1980; Mäkelä et al. 2004). The estimated daily NP_i values, were assumed to follow the S values. The highest estimated value was set to the highest measured species-specific NP_i value on the measuring date ($t_{max,i}$). Other daily values were estimated by the relationship between the estimated daily $S(t)$ value and the $S(t_{max,i})$. If $S(t)$ was smaller than 0 ℃, it was set to zero. We estimated the species–specific daily NP_i parameters for species that did not follow the S values by interpolating the intermediate values from the measured average NP_i values.

RESULTS

There were patches of snow at SMEARII station still on 24 April but all of the snow had melted by the first of May. In autumn, the first snow fell on 28 October but the snow had melted totally by 27 November. The end of the year was mostly snowless. In general, the night temperatures were coolest and day temperatures highest on the open (youngest) sites during the year. During the summer months, soil moisture was lowest in the 12-year-old site probably due to high occurrence of app. three meters high *Betula* sp that is very common in the particular phase of succession and has relatively high transpiration rate. Overall, the summer was exceptionally dry at the measuring sites. The yearly precipitation was rather typical but the rain fell mostly in the autumn while the precipitation varied between 37 – 40 mm month^{-1} from May to August. Therefore the soil moisture decreased a lot in the summer.

The biomass of the green parts of mosses was highest at the youngest site and decreased substantially during the first phases of succession (Figure 1). After canopy closure, the biomass increased again slowly with stand age. *Pleurozium schreberi* was the most common species with the proportion of 64 – 77 % at all of the sites. The biomass of aboveground parts of vascular plants was highest on the 12-year-old stand. The biomass of grasses and herbs decreased markedly between the stand ages of 6 to 12 years. The occurrence of grasses had fallen to zero in the 120-year-old forest. The total above ground biomass of ground vegetation was at its highest at the 12-year-old site (Figure 1) decreasing thereafter with stand age.
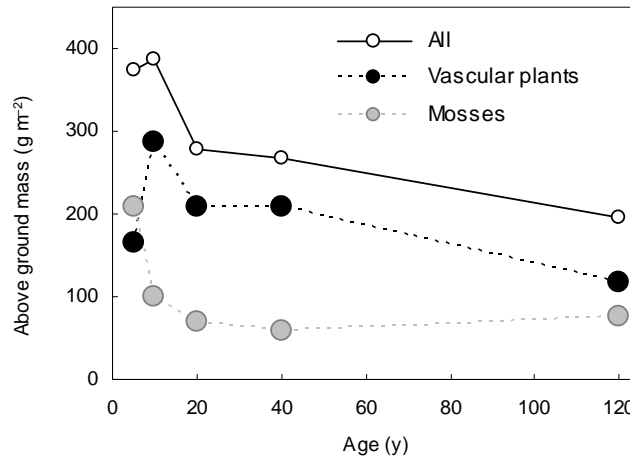
Figure 1. The average biomass (g m^{-2}) of aboveground parts of vascular plants, green parts of mosses and the sum of them at the clear cut sites with stand age.

Figure 2 illustrates the measured *NP* values of *C. vulgaris* at the 6-, 12- and 45-year-old stands in 2006 as an example of the annual cycle of photosynthetic activity. The measured values based on full grown leaf mass are highest at the open (youngest) site but the spring awakening and decrease during mid-summer are rather similar. The measured values start to increase in May and decrease at the youngest sites in October while the activity (NP_i values) stays relatively high at the other sites. This might be at least partly explained by the night temperatures which decreased more at the open young site than in the older stands.
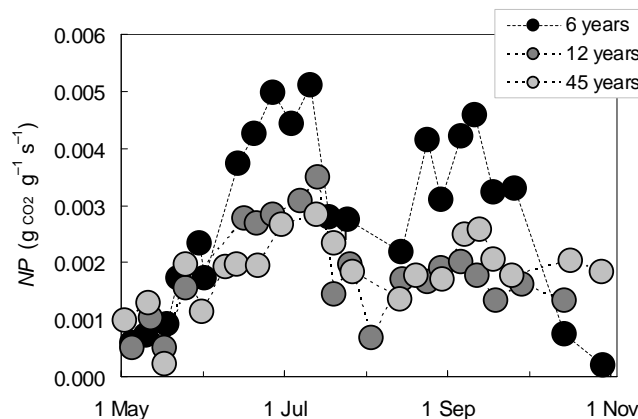
Figure 2. The measured NP_i values (g CO_2 g^{-1} s^{-1}) of *C. vulgaris* at the 6-, 12-, and 45-year-old stands between 1 May – 30 Oct 2006.

Species with perennial leaves had very clear and species-specific annual pattern with maximum around mid-summer while *V. vitis-idaea*, for example, can maintain relatively high photosynthesis as well in early spring as in late autumn. Preliminary results show that measured NP_i values of *C. Vulgaris*, *Deschampsia Flexuosa*, *V. vitis-idaea* and partly also *V. myrtillus* follow the *S* values except for the drought period in

late-summer when *C. vulgaris*, *V. vitis-idaea* and *D. flexuosa* substantially decreased their NP_i values. An example of the drought effect on the NP values of *C. vulgaris* is shown in Figure 3.. The measured values follow very closely to the modelled *NP* values derived from *S* model except for early spring and the prolonged drought in July and August. However, mosses did not have clear annual cycle but the *NP* values were usually increased during and after a rain event.
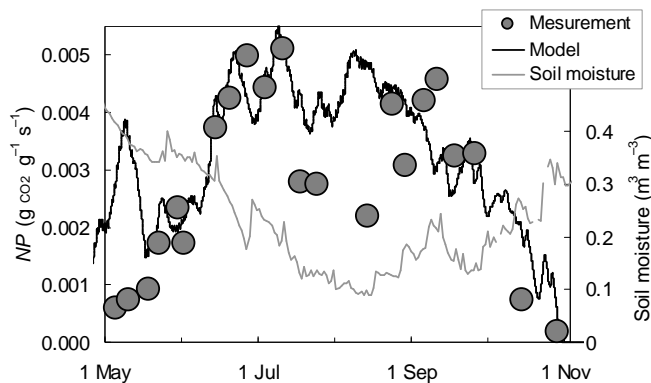
Figure 3. The measured and modelled NP_i values of *C. vulgaris* and the volumetric soil moisture ($m^3 m^{-3}$) at the 6-year-old site between 1 May – 30 Oct 2006. The measurements reveal decreased rates of photosynthesis during prolonged drought in July and August while the model of the state of development predict higher rates of photosynthesis.

These results can be used in quantifying the yearly production by upscaling all the species-specific process rates with species composition and integrating them over the season with environmental factors. Preliminary results indicate that the photosynthetic production of ground vegetation in early succession can be as high as 30 – 75 % of the production of a grown-up forest. Later, the dominant species at the ground level change from fast-growing and short-living to shade-tolerant ones. At this phase, the photosynthetic production of ground vegetation is app. 10 % of the production of the whole forest.

REFERENCES

Cajander, A.K. (1926). The theory of forest types, *Acta For. Fen.* 29: 1–108
Goulden, M.L. & Crill, P.M. (1997). Automated measurements of CO_2 exchange at the moss surface of a black spruce forest. *Tree Physiol.* 17: 537-542.
Hari, P. & Kulmala, M. (2005). Station for measuring Ecosystem-Atmosphere Relations (SMEARII). *Bor. Env. Res.* 10: 315-322
Kolari, P., Pumpanen, J., Kulmala, L., Ilvesniemi, H., Nikinmaa, E., Grönholm T. & Hari, P. (2006). Forest floor vegetation plays an important role in photosynthetic production of boreal forests. *Forest Ecol. Manag.* 221: 241-248
Kulmala, L., Launiainen, S., Pumpanen, J., Lankreijer, H., Lindroth, A., Hari, P. & Vesala, T. (2008). H_2O and CO_2 fluxes at the floor of a boreal pine forest. *Tellus B*, 60: 167–178
Mäkelä, A., Hari, P., Berninger, F., Hänninen, H. & Nikinmaa, E. (2004). Acclimation of photosynthetic capacity in Scots pine to the annual cycle of temperature. *Tree Phys.* 24: 369–376.
Michaelis, L. & Menten, M. (1913). Die Kinetik der Invertinwirkung. *Biochem. Z.*, 49: 333–369
Morén, A.-S. & Lindroth A. (2000). CO2 exchange at the floor of a boreal forest. *Agric. For. Meteorol.* 101: 1-14.
Pearcy, R.W., Björkman, O,. Caldwell, M.M., Keeley, J.E., Monson, R.K., & Strain B.R. (1987). Carbon gain by plants in natural environments. *Bioscience*, 37: 21–29
Pelkonen, P. & Hari, P. 1980. The dependence of the springtime recovery of CO_2 uptake in Scots pine on temperature and internal factors. *Flora* 169: 398–404.

DYNAMICAL ATMOSPHERIC CLUSTER MODEL

M. KULMALA

Department of Physics, P.O.Box 64, FI-00014, University of Helsinki, Finland

INTRODUCTION

The existence of atmospheric ion clusters has been known for decades [1]. Recently the existence of atmospheric neutral clusters have been predicted [2] and also observed [3],[4],[5],[6],[7]. However, the origin and dynamics of those clusters is still unclear. In principle, they could be recombination products of small air ions, but their concentration is typically only several percent of the total cluster concentration. They could also be a) thermodynamically stable clusters [2], b) products of some chemical reactions or c) dynamic clusters, which will continuously form and grow and evaporate. In this study we have developed a dynamical cluster model to evaluate the cluster concentrations and investigate the possible origin of those clusters.

MODEL

The dynamics of molecular clusters can be investigated using dynamical atmospheric cluster model (DACM). The model was developed based a cluster equations typically used in homogeneous nucleation studies [8].

In the model monomers (mass m, volume v) will collide with each other and i-mers. The i-mers will collide with each other and will also be scavenged by pre-existing aerosol particles. They will evaporate and they can activate and after some critical size they will not anymore evaporate (then evaporation coefficient e_i is zero).

The concentration of activating vapor (V) can be described with following differential equation

$$\frac{dV}{dt} = Q_v - CS_v \times V \;.$$
(1)

Here Q_v is source rate and CS_v the condensation sink.

The equation for monomer concentration is

$$\frac{dC_1}{dt} = Q_1 - CS_1 \times C_1 - k_1 \times C_1 \times \sum_{i=1}^{n} C_i + \sum_{i=2}^{n} e_i \times C_i \;\;,$$
(2)

and the equation for dimers is

$$\frac{dC_2}{dt} = k_{1,1} \times C_1 \times C_1 - CS_2 \times C_2 - e_2 \times C_2 - k_{1,2} \times C_1 \times C_2 - C_2 \times \sum_{i=3}^{n} k_{2,i} \times C_i + e_3 \times C_3 - actP_2 \times V \times C_2 \quad (3)$$

Corresponding equations can be written for all i-mers.

CS_i is condensation sink, which for monomer is CS_1 and for i-mers is

$$CS_i = CS_1 \times \sqrt{(1/i)} \; , \tag{4}$$

The coagulation equations are

$$k_{i,j} = aa \times \sqrt{\left(1/(i \times m + 1/(j \times m)\right)} \times ((i \times v)^{1/3} + (j \times v)^{1/3})^2 \; , \tag{5}$$

where

$$aa = \mathrm{sqrt}\sqrt{(6kT)} \left(\frac{3}{4\,\pi} \right)^{1/6} \; .$$

The radius of i-mer is

$$r_i = \left(\frac{3 \times i \times v}{4 \times \pi} \right)^{1/3} \; .$$

The evaporation coefficient for i-mers is

$$e = 4\pi \times r_i^2 \, \frac{C_1}{S} \, \frac{kT}{\sqrt{2\pi \, m \, k \, T}} \exp(2\,\sigma\,v/(r_i\,k\,T)) \; , \tag{6}$$

In this model monomers cannot activate. The activation of dimers and i-mers depends on their size. I-mers, which are bigger than the critical cluster, will not evaporate anymore. Vapor (*V*) will activate the clusters with the coefficient *actP*.

Particle formation can be described by

$$J_{nucl} = \sum_{i=2}^{i^*} actP_i \times V \times C_i \; , \tag{7a}$$

or

$$J_{nucl} = actP_{i^*} \times V \times C_{i^*} \; . \tag{7b}$$

The model can be used in 3 different versions. The above one is based on the concept of virtual monomers [9]. The other possible ways are a) sulphuric acid model i.e. all clusters are sulphuric acid clusters, and b) sulphuric acid and amines (or other vapours, which will cause very small evaporation rate for sulphuric acid dimers.

RESULTS

An example of DACM results is shown in Figure 1. The size of virtual monomers corresponds that of sulphuric acid. The saturation vapour concentration is 1x106 cm-3. The source rate of virtual monomers is $1x10^5$ $s^{-1}cm^{-3}$. The formation of particles can be observed around 100 s.
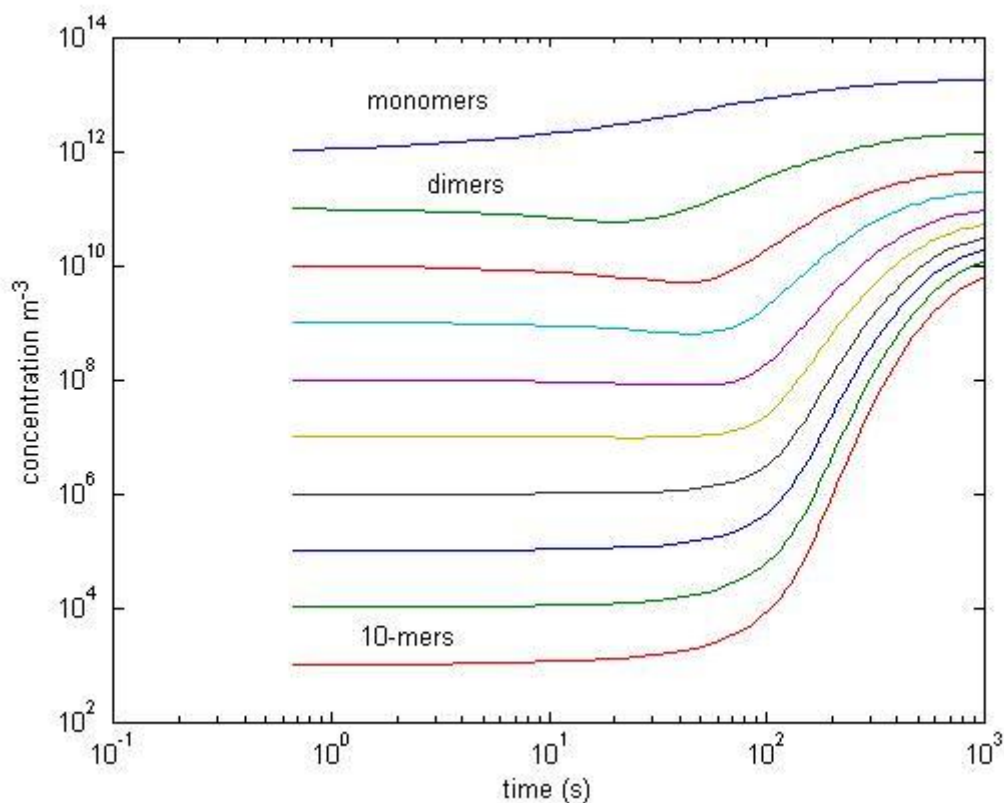
Figure 1. Dynamical evaluation of clusters from monomers to 10-mers.

DISCUSSION AND CONCLUSIONS

A new dynamic model to evaluate atmospheric clusters has been developed. The Dynamic Atmospheric Cluster Model (DACM) is based on vapour production, monomer i-mer coagulation, i-mer j-mer coagulation, i-mer evaporation and scavenging by pre-exiting particles. Fresh atmospheric aerosol particles are formed via activation mechanism [10]. DACM can reproduce the observed cluster concentration and atmospheric nucleation rates.

The model can be used to improve our understanding on cluster dynamics, on atmospheric new particle formation and also to explain laboratory experiments. The preliminary results have already given new insight on so called sulphuric acid mystery in nucleation experiments. According to this mystery sulphuric acid molecules produces in situ via chemical reaction will nucleate easier than sulphuric acid molecules coming from bulk.

ACKNOWLEDGMENTS

REFERENCES

1. Kulmala, M. and Tammet, H., *Boreal Env. Res*. **12**, 237-245 (2007).
2. Kulmala, M., Pirjola, L., and Mäkelä, J. M., *Nature* **404**, 66-69 (2000).
3. Kulmala, M., Riipinen, I., Sipilä, M., Manninen, H., Petäjä, T., Junninen H., Dal Maso, M., Mordas, G., Mirme, A., Vana, M., Hirsikko, A., Laakso, L., Harrison, R. M., Hanson, I., Leung, C., Lehtinen, K. E. J., and Kerminen, V.-M, *Science* **318**, 89-92, (2007).
4. Sipilä, M., Lehtipalo, K., Kulmala, M., Petäjä, T., Junninen, H., Aalto, P. P., Manninen, H. E., Vartiainen, E., Riipinen, I., Kyrö, E.-M., Curtius, J., Kürten, A., Borrmann, S., and O'Dowd, C. D., *Atmos. Chem. Phys*. **8**, 4049-4060 (2008).
5. Sipilä, M., Lehtipalo, K., Attoui, M., Neitola, K., Petäjä, T., Aalto, P. P., O'Dowd, C. D., and Kulmala, M., *Aerosol Sci. Technol*. **43**, 2:126-135 (2009).
6. Lehtipalo, K., Sipilä, M., Riipinen, I., Nieminen, T., and Kulmala, M., *Atmos. Chem. Phys. Discuss*. **8**, 20661-20685 (2008).
7. Lehtipalo, K. et al., This proceedings (2009).
8. Vehkamäki, H., *Classical Nucleation Theory in Multicomponent Systems*, Springer (2006).
9. Kulmala, M. and Viisanen, Y. *J. Aerosol Sci.,* **22**, S97-S100 (1991)
10. Kulmala, M., Lehtinen, K.E.J., and Laaksonen, A., *Atmos. Chem. Phys*. **6**, 787-793 (2006).

THE KINETICS OF ATMOSPHERIC SULFURIC ACID – WATER NUCLEATION

T. KURTÉN[1], H. VEHKAMÄKI[1], C. KUANG[2], P. MCMURRY[2], P. GOMEZ[3], M. NOPPEL[4]
and M. KULMALA[1]

[1]Department of Physics, P.O. Box 64, FI-00014, University of Helsinki, Finland
[2]Department of Mechanical Engineering, University of Minnesota, U.S.A.
[3]Departamento de Química Física I, Universidad Complutense de Madrid, Spain
[4]Institute of Physics, University of Tartu, Estonia

INTRODUCTION

In previous decades, theoretical studies on gas-to-particle nucleation have mainly been based on classical nucleation theory (CNT), which treats molecular clusters as spherical droplets of bulk liquid, and assumes that the growth rates of clusters by monomer addition are given by their hard-sphere collision rates. The thermodynamics predicted by CNT are known to be incorrect for the smallest clusters, and this issue has been extensively investigated using molecular-scale simulations (Merikanto et al., 2007). For one-component nucleation, a combination of quantum-chemical data for smaller clusters with classical thermodynamic results for larger clusters has resulted in good agreement between theoretical and experimental results on e.g. nucleation rates (Du et al., 2007).

In the multicomponent case, moving beyond CNT-type descriptions of nucleation is more difficult due to the large number of different cluster types that have to be accounted for. The time derivative of the concentration of a cluster of any size depends on the concentrations of all other cluster sizes. Furthermore, the large set of non-linear differential equations is numerically stiff. Therefore, even if accurate cluster thermodynamics (e.g. evaporation rates) were available, computing the cluster distribution becomes numerically very demanding, and requires parallelization to be practically feasible. Due to this computational challenge, kinetic nucleation models have so far been limited to quasi-unary schemes (Yu, 2007), where all but one compound are assumed to reach a pseudo-equilibrium for each cluster distribution of the other compound. Typically the amount of water is assumed to equilibrate, and for example the amount sulfuric acid is assumed to be the significant size parameter. In CNT, and thus in all practical atmospheric applications, the nucleation rate is calculated based on the steady-state assumption. This implies that the concentrations of nucleating vapors are constant over the time periods when significant nucleation occurs. The validity of this assumption in atmospheric conditions has never been tested. Atmospheric vapor concentrations are certainly not constant, but this may not be crucial: the key issue is whether in true atmospheric nucleation the integrated number of produced particles, and their properties, are well represented by the steady-state values based on average concentrations (Clement and Ford, 1999).

The number of components participating in a single atmospheric nucleation event may be large, and the dominant species can vary with time over the course of the event. The favored nucleation path depends on cluster thermodynamics, instantaneous vapor concentrations and kinetic factors, and with more than 2-3 components a physicist's intuition is not enough, and a truly multi-component cluster growth model is required to identify the possibly manifold and convoluted particle formation routes.

While developing computationally affordable multicomponent kinetic nucleation models, as a first step we aim to resolve some additional issues required for the nucleation kinetics to be reliably modeled. For example, the assumption of CNT (and most kinetic models to date) that the growth rates of clusters correspond to hard-spheres collision rates may not be well justified. For example for argon, it has been shown (Zahoransky et al., 1995) that the net growth rate of clusters is considerably lower than the collision rate.

In principle, there are three different mechanisms that may lower the net formation rate of molecular clusters below their collision rate. First, there may be a kinetic barrier (associated with a transition state) for the formation of the clusters. The formation rate will then equal the collision rate multiplied by a exponential factor containing the height of this barrier (defined as the activation energy in chemical kinetics). Second, there may be steric effects associated with the structure of the clusters and/or monomers, so that only certain approach geometries will lead to cluster formation. Neither of these mechanisms are likely to play any major roles in atmospheric nucleation, as the cluster formation process does not involve the breaking of any chemical bonds, and as the prime suspects (sulfuric acid and various organic acids) possess multiple hydrogen bond acceptor and donor sites and are thus rather "sticky" in almost all directions. Third, the initially formed clusters may break apart very quickly due to the excess energy liberated in the cluster formation process. If this dissociation occurs more rapidly than the thermalization of the cluster via collisions with inert gas molecules, then only a fraction of the clusters will survive, and the net formation rate will correspondingly decrease.

CALCULATIONS

Energy non-accommodation is known to be important for argon nucleation, and has been claimed to be important for water nucleation (Okada and Hara, 2007). We have qualitatively assessed whether or not energy non-accommodation plays a role in the formation of clusters consisting of sulfuric acid, which is generally thought to be one of the most important molecules participating in atmospheric new-particle formation. Furthermore, we have estimated the effect of hydration on the role of energy non-accommodation. As a test set, we have studied clusters with the stoichiometries $(H_2SO_4)_2$ and $(H_2SO_4)_2(H_2O)_2$. Our calculations are based on bimolecular QRRK (Quantum Rice – Ramsperger – Kassel) theory together with anharmonic quantum chemical vibrational frequencies and couplings computed for sulfuric acid dimers and selected other clusters. QRRK theory treats the excess energy in cluster formation as quantized vibrational energy distributed over a certain number of accessible vibrational modes. We have used quantum chemical data to determine both the appropriate vibrational frequencies and, most importantly, the number of accessible modes required for the QRRK calculations.

First, the harmonic vibrational normal modes for the studied clusters were computed and visualized, and the mode or modes best corresponding to cluster dissociation (of a dimer into two monomers, or a trimer into a monomer and a dimer etc.) were identified. Next, the cubic anharmonic couplings of all other modes to the dissociative mode or modes were computed, and their magnitudes were used to estimate the number of modes into which energy can easily be redistributed from the dissociative mode or modes.

All vibrational calculations were performed at the qualitatively reliable PBE/6-31+G(2d,p) level, using the Gaussian 03 program suite (Frisch et al., 2004). Zero-point corrected dissociation energies for unhydrated sulfuric acid dimers were taken from high-level quantum chemical data by Salonen et al. (2009) and the hydration energies were taken from studies by Ding et al. (2003) and Torpo et al. (2007).

RESULTS AND DISCUSSION

We find that for sulfuric acid dimers, the energy accommodation coefficient (the fraction of dimers that live long enough to be collisionally stabilized by inert gas molecules such as N_2) in atmospheric conditions varies between around 0.1 and 1.0, depending on the assumptions made concerning the vibrational couplings. This shows that while the role of energy non-accommodation in the nucleation of sulfuric acid is significantly smaller than for monatomic vapors such as argon, it is not necessarily negligible, as assumed e.g. by CNT. Thus, at least in the case of unhydrated sulfuric acid clusters, kinetic nucleation models may need to account for energy non-accommodation when calculating the net growth rates.

If energy non-accommodation is a significant effect in sulfuric acid - water nucleation, it will also affect the participation of third compounds in ways not directly related to thermodynamic arguments alone. For example, the thermodynamic enhancement of sulfuric acid – amine – water nucleation compared to sulfuric acid – ammonia – water nucleation might be complemented by a kinetic enhancement due to the greater number of vibrational modes of amine molecules compared to ammonia. Similarly, SO_2 photonucleation - where the recent experimental results are explained by Salonen *et al.* (2009) by the possible involvement of $H_2S_2O_8$ or other molecules with multiple sulfur atoms - might also be kinetically enhanced. We have investigated both these cases using the methodology described above, and find that increased energy accommodation may kinetically enhance the participation of amines rather than ammonia, or $H_2S_2O_8$ in addition to pure H_2SO_4, in sulfuric acid nucleation, but by less than a factor of 5 and 2, respectively. (It should be stressed that these kinetic enhancements are in addition to the thermodynamic enhancements already investigated and reported.)

However, hydration of the clusters – which always occurs in atmospheric conditions – is likely to decrease the overall role of energy non-accommodation, and thus the possible differences between the systems compared above. This is because the presence of water molecules in the cluster increases the total number of vibrational modes, and thus also the number of accessible modes that the excess energy can be redistributed into. Also, hydration introduces new channels for removing excess energy via dissociation of water molecules instead of sulfuric acid molecules from the cluster. Based on preliminary calculations, inclusion of hydration effects is likely to bring all energy accommodation coefficients quite close to 1.0, indicating that energy non-accommodation is only relevant in very dry conditions.

ACKNOWLEDGMENTS

REFERENCES

Berndt, T., Böge, O., and Stratmann, F. (2006) Formation of atmospheric H_2SO_4/H_2O particles in the absence of organics: a laboratory study, Geophys. Res. Lett., 33, L15817.

Clement,C.F. and Ford,I. F. (1999) Gas-to-particle conversion in the atmosphere: II. Analytical models of nucleation bursts, Atmospheric Environment, 33, 489-499.

Dean, A. M. (1985). Prediction of Pressure and Temperature Effects upon Radical Addition and Recombination Reactions, AIChE Journal, 89, 4600 - 4608.

Ding, C.-G.., Laasonen, K., Laaksonen, A. (2003). Two Sulfuric Acids in Small Water Clusters, J. Phys. Chem. A, 107, 8648-8658.

Du, H., Yu, F., and Nadykto, A. B. (2007) "Water Homogeneous Nucleation: Importance of Clustering Thermodynamics" in Nucleation and Atmospheric Aerosols, edited by C. D. O'Dowd and P. Wagner, Springer 2007, pp. 167-171.

Frisch, M. J., *et al.* (2004). Gaussian 03, Gaussian, Inc., Wallingford CT, U.S.A.

Merikanto, J., Zapadinsky, E., Lauri, A., and Vehkamäki, H. (2007), Origin of the failure of classical nucleation theory: incorrect description of the smallest clusters, Phys. Rev. Lett., 98, 145702.

Okada, Y. and Hara, Y. (2007) Calculation of the Sticking Probability of a Water Molecule to a Water Cluster, Earozoru Kenkyu, 22, 147-151.

Salonen, M., Kurtén, T., Vehkamäki, H. and Kulmala, M. (2009) Computational investigation of the possible role of some intermediate products of SO_2 oxidation in sulfuric acid - water nucleation, Atm. Res., 91, 47-52.

Torpo, L., Kurtén, T., Vehkamäki, H., Laasonen, K., Sundberg, M. R., and Kulmala, M. (2007), Significance of ammonia in growth of atmospheric nanoclusters, J. Phys. Chem. A, 111, 10671-10674.

Yu, F. (2007) Improved quasi-unary nucleation model for binary H_2SO_4-H_2O homogeneous nucleation, J. Chem. Phys., 127, 054301.

Zahoransky, R., Hoschele, J., and Steinwandel, J. (1995) Formation of argon clusters by homogeneous nucleation in supersonic shock tube flow, J. Chem. Phys., 103, 9038-9044.

LONG-TERM VARIATION OF AIR POLLUTION IN EASTERN LAPLAND

E.-M. KYRÖ[1], V. VAKKARI[1], K. LEHTIPALO[1], A. VIRKKULA[1], I. RIIPINEN[1,2] and M. KULMALA[1]

[1]Department of Physics, P.O. Box 64, FI-00014, University of Helsinki, Finland
[2]Currently at: Department of Chemical Engineering, Carnegie Mellon University, 5000 Forbes Avenue, Pittsburgh, PA 15213-3890 USA

Keywords: Air pollution, Air Quality, Trace gases, Back-Trajectories

INTRODUCTION

During the mid-80's the changes in the Soviet politics enabled the metal industry at Kola peninsula to announce their pollution emissions. At that time, the yearly sulphur dioxide (SO_2) emissions of Kola Peninsula alone exceeded the total sum of those in Finland, Sweden and Norway (Tuovinen et al., 1993, Hari et al., 1994). It soon became evident that there was not enough of information about the air quality in Lapland and, especially, in the sparsely-populated Eastern Lapland. It was even feared that the acid rains originating from Kola Peninsula emissions would eventually destroy the forests of Eastern Lapland (Hari et al., 1993). Therefore, considerable activities were launched to asses and quantify the effects of Kola Peninsula pollution sources to Finnish Lapland. As part of these activities, the SMEAR I –station (Station for Measuring Ecosystem-Atmosphere Relations) was build in 1991 next to already existing Värriö Research Station in Eastern Lapland, at the northernmost district of the municipality of Salla, close to the Russian border.

Trace gases such as sulphur dioxide, nitrogen oxides and ozone (SO_2, NO_x, O_3) react with water vapour in the atmosphere and form acids (H_2SO_4 and HNO_3) (Finnlayson-Pitts & Pitts, 2000). Ozone acts as an oxidant in these reactions. Of these trace gases the most significant acidifying component is SO_2. Nitrogen oxides are the most important acidifying component in areas with intense traffic. However, in remote areas such as Lapland, SO_2 is more important. High O_3 values are related to long-range transport of traffic emissions from Central Europe.

INSTRUMENTATION AND METHODS

At SMEAR I –station several variables are measured all-year-round. The University of Helsinki is responsible for measuring different type of trace gases (SO_2, NO_x, O_3), the aerosol particle size spectrum and total number concentration, the photosynthesis and growth of Scots pines and meteorology. In addition, the Finnish Meteorological Institute has been measuring both sulphates and heavy metals using filter sampling technique. Of the mentioned trace gases, SO_2 and O_3 have been measured since 1991 but nitrogen oxides since 1997.

Trace gases are measured at four different levels (2, 6.5, 9 and 15 m) above the ground. The sulphur dioxide concentration is measured with a pulsed fluorescence analyzer. The total SO_2 concentration in the air at SMEAR I –station can occasionally be many times higher than the average background level in Helsinki (Fig. 2). Nitrogen oxides (most importantly NO and NO_2) are measured with an analyzer that is based on chemiluminescence. The device differentiates between the total nitrous oxides (NO_x) and NO and by reduction of the NO concentration from NO_x concentration one can get the concentration of NO_2. Ozone is measured with a photometric analyzer.

The total aerosol concentration has been measured since 1991 and the particle size distribution since 1997. The cut-off diameter of the size distribution measurements was changed from 8 nm down to 3 nm in 2003. The total concentration is measured using a Condensation Particle Counter and the size distribution with a DMPS (Differential Mobility Particle Sizer) system (Aalto et al., 2001, Aalto, 2004).

A 16 meter high weather mast is mounted next to SMEAR I –station and it is used to measure a number of different meteorological parameters from different levels, e.g. temperature, humidity, wind speed and direction as well as solar radiation.

RESULTS

The mean and median values for the measured trace gases at SMEAR I –station are low (Table 1). However, occasionally especially the SO_2 and O_3 concentrations can reach very high levels. According to European Union, the hourly and yearly limits for SO_2 are 350 µg m^{-3} and 20 µg m^{-3}, respectively. For NO_2 the same values are 200 µg m^{-3} and 40 µg m^{-3} and for NO_x the yearly limit is 30 µg m^{-3}. The mean and median value for O_3 corresponds to satisfactory air quality (very unlikely health effects / mild environmental impacts) and the 99th percentile to fair air quality (unlikely health effects / clear impacts on vegetation, material impacts). For sulphur dioxide, the 99th percentile corresponds to satisfactory air quality and is two orders of magnitude higher than the median value. The average SO_2 concentration modelled by Tuovinen et al. (1993) in Värriö was at that time 4 µg m^{-3}, which is twice the average concentration during our measurement period.

	SO_2	NO_x	NO_2	O_3
Mean (µg m^{-3})	2.2	0.9	0.8	68.8
Median (µg m^{-3})	0.5	0.5	0.5	69.3
99 % (µg m^{-3})	25.1	5.2	5.1	116.4
Data coverage	86% (1991-)	88% (1995-)	88% (1995-)	80% (1991-)

Table 1. Mean, median and 99th percentile values for trace gases measured at SMEAR I –station 1991-2008.

We have estimated the dry deposition of SO_2(S) using

$$P_X = C_X \cdot t \cdot v_{dep} ,$$

(1)

where C_X is the concentration of a substance X, t is time and v_{dep} the deposition velocity of X. For sulphur dioxide the deposition velocity to snow is 0.2 cm s^{-1} (Virkkula et al., 1999) and hence, the median and mean and maximum fallout for SO_2 are 3.4 and 15.7 µg m^{-2}, respectively. As the highest SO2 concentrations occur during winter in Värriö, it is a good approximation to use the deposition velocity to snow for the whole period.

An example of a pollution episode caused by the Kola emissions is in Fig. 1. SO_2 and particle volume concentration as a function of time are represented together with the 96 h back-trajectories. The SO_2 concentration is given for 10.8. – 19.8.2000 and the trajectories for 15.8. – 18.8.2000. Also the normal background level in Helsinki urban area is shown. The normal background concentration at SMEAR I is close to zero but when the airmass is coming from the Kola Peninsula, the SO_2 concentration rises a couple of magnitudes higher. Also, the total particle volume is higher in the airmasses passing over Kola Peninsula.
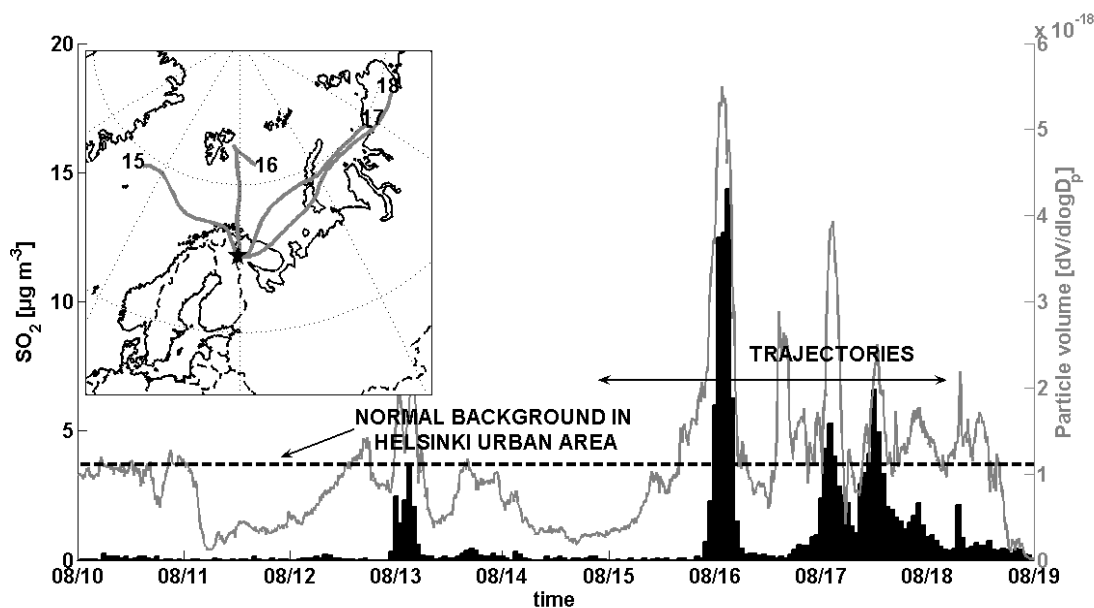
Figure 1. The SO_2 and particle volume concentration at SMEAR I –station 10.8. – 19.8.2000 and 96 hr back-trajectories for 15.8. – 18.8.2000. In addition, the normal background of sulphur dioxide in Helsinki urban area is shown.

The time series of SO_2 concentration is presented in Fig. 2; shaded area encloses the 1st and 3rd quartile. The median is shown in red. There is no visible trend in the median concentration. However, the peak values have been clearly decreasing since the late 1990's. According to Ruoho-Airola (2004) the sulphur dioxide concentration in Ähtäri (central Finland) has been decreasing into one fifth of the value of 1980 and in 1991 when SMEAR I was established, the concentration was roughly twice the concentration in 2000.

The time series of NO_x concentration is presented in Fig. 3. The NO_x 99th percentile in the lower panel shows a slight increase in the peak values. This is very likely due to increased traffic in both Europe and Kola Peninsula. In the median concentration there is no significant trend.

The source areas of trace gases were studied using 96 h back-trajectory analysis. For SO_2, it is evident that the main source areas are Nike and Montchegorsk, in North and East, respectively (Fig. 4). Even though sulphur dioxide concentrations coming from the direction of Nikel are as high as from the direction of Monchegorsk, Monchegorsk dominates the SO_2 deposition. For nitrous oxides, in addition to Montchegorsk, also long-range transport from Central Europe is very clear (Fig. 4). Highest particle volume concentrations are observed with north-easterly and south-westerly winds. The smallest volumes are observed, when the wind direction is northwest. This is when the air is blowing from the Arctic Ocean and the aerosol population is relatively young (Tunved et al., 2006) and hence, the total volume of the particles is small.

The yearly sum of $SO_2(S)$ dry deposition is presented in Fig. 5 together with the percentage of valid data. There is no visible trend in between the years and thus, it is very unlikely that there would be any trend in the sulphate deposition either. This is contrary to the decreasing pan-European trend. The average estimated yearly sum of dry deposition of $SO_2(S)$ is 0.07 g m^{-2}. However, according to the FMI filter sample analysis, the fraction of wet deposition has been decreasing all the time. In Värriö the observed fraction of dry deposition is bigger than that of wet deposition. This is consistent with the model estimations by Tuovinen et al. (1993).
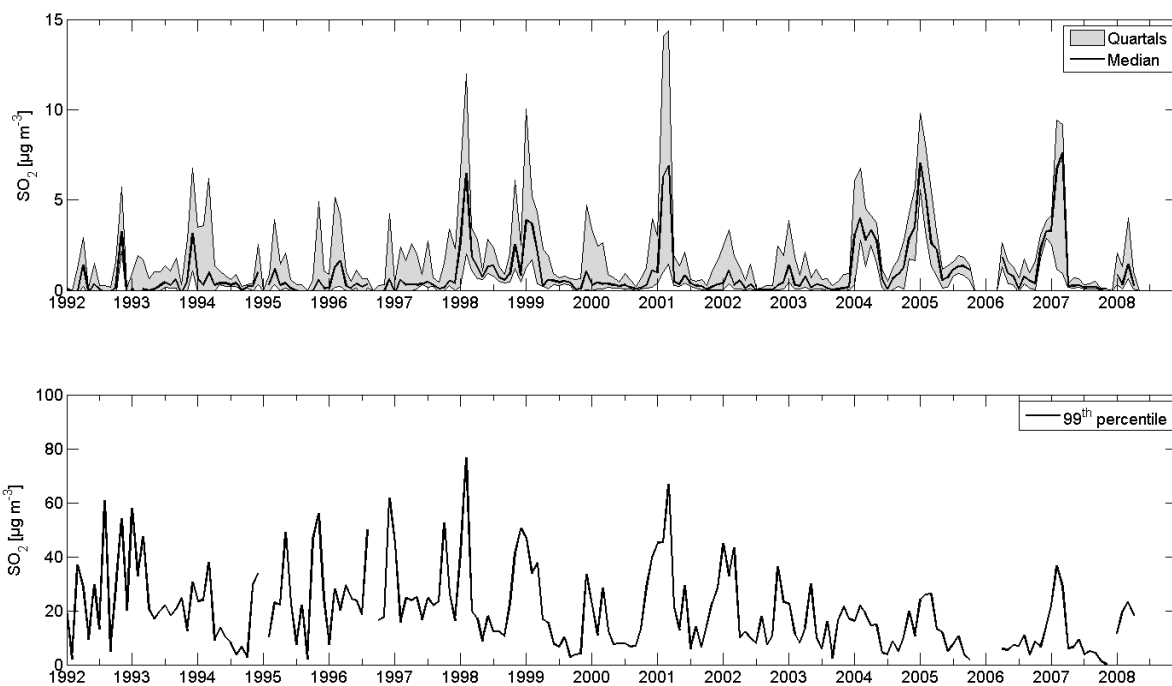
Figure 2. Time series of the 1st and 3rd quartiles and median of SO$_2$ concentration at SMEAR I (Upper figure) and the 99th percentile (lower figure).
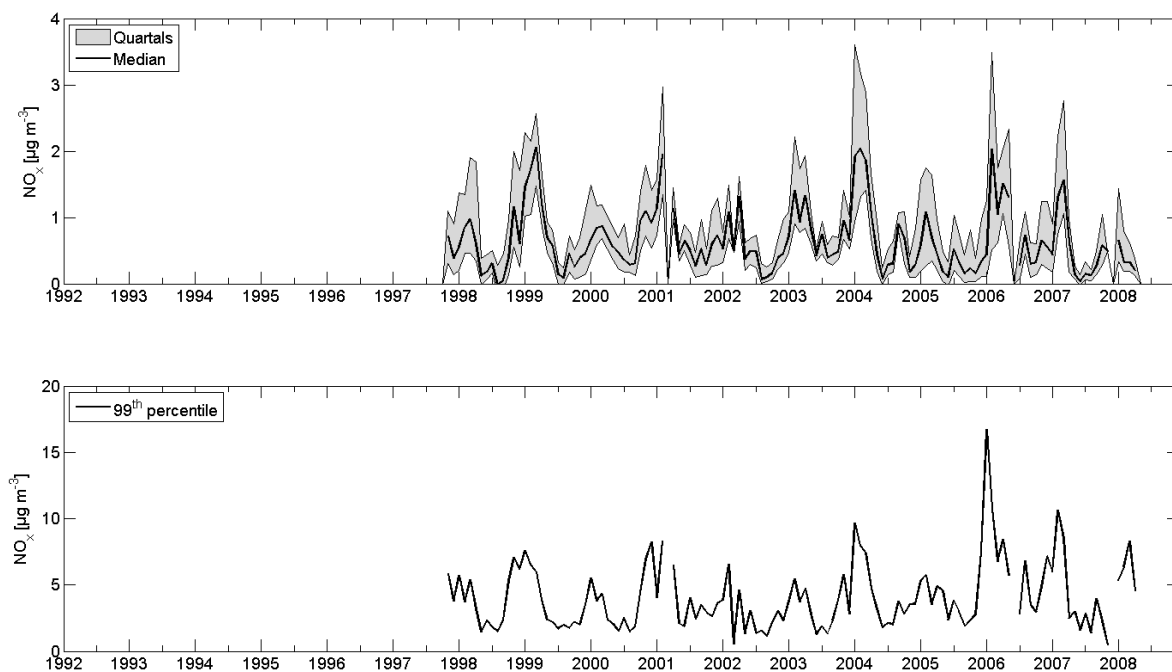
Figure 3. Time series of the 1st and 3rd quartiles and median of NO$_x$ concentration at SMEAR I (Upper figure) and the 99th percentile (lower figure).
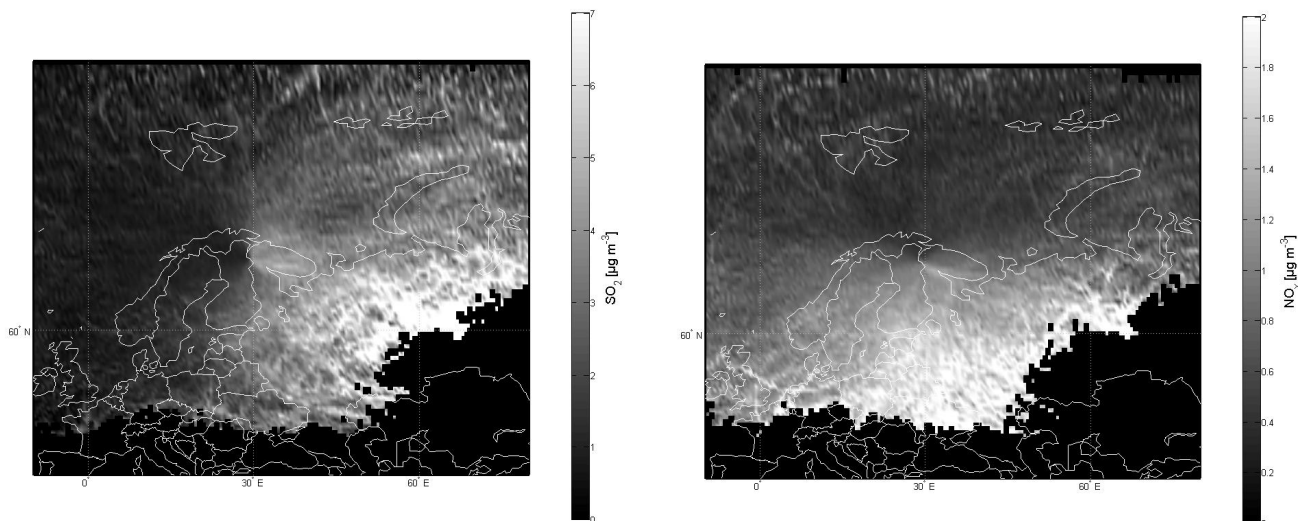
Figure 4. Source areas of SO$_2$ (left figure) and NO$_x$ using 96 h back-trajectory analysis.
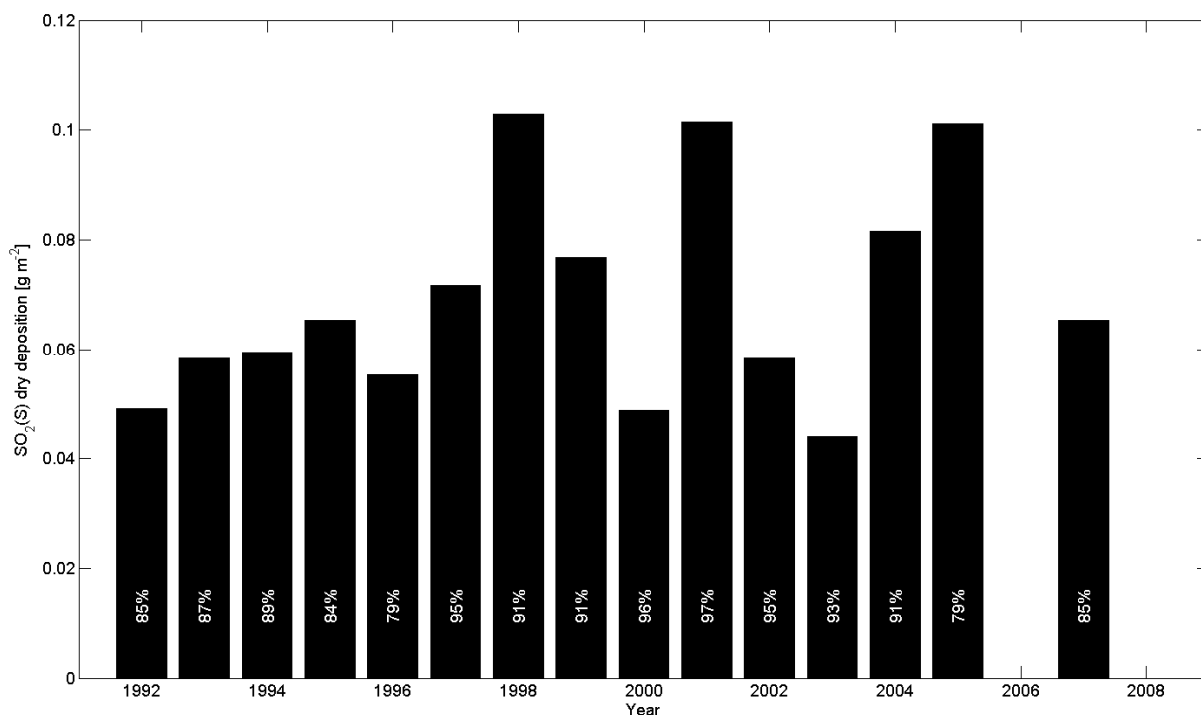
Figure 5. The yearly dry deposition of SO$_2$(S) and the percentage of valid data. Years with less than 70% of valid data are not presented.

CONCLUSIONS

The air quality in the Eastern Lapland is generally clean, characterized with very intense, short-term pollution episodes originating from the Kola Peninsula. Most of the SO$_2$(S) dry deposition is originated from Kola Peninsula smelters with an average yearly sum of 0.07 g m^{-2}. There is no trend in the SO$_2$(S) dry deposition contrary to the decreasing pan-European trend. However, the peak values of SO$_2$ have been decreasing since the late 1990's. The main source areas for SO$_2$ are Nikel and Monchegorsk, whereas for NO$_x$ Monchegorsk and long-range transport from Central Europe.

As it is very likely that a new mine will be opened to Sokli, some 20 km north from Värriö, it is very crucial to continue the monitoring of acidifying components at Värriö. Overall, research should be continued and more extensive measurements are needed to provide a better understanding of the effects of Kola Peninsula smelters into Eastern Lapland.

REFERENCES

Aalto, P., Hämeri, K., Becker, E., Weber, R., Salm, J., Mäkelä, J.M., Hoell, C., O'Dowd, C., Karlsson, H., Hansson, H.-C., Väkevä, M., Koponen, I.K., Buzorius G. and Kulmala, M. (2001) Physical Characterization of Aerosol Particles During Nucleation Events. *Tellus*, 53B, 344-358.

Aalto, P. (2004) Atmospheric Ultrafine Particle Measurements. *Report Series in Aerosol Science*, 64, PhD. Thesis, University of Helsinki.

Finnlayson-Pitts. B.J. and Pitts, J.N. (2000) *Chemistry of the Upper and Lower Atmosphere.* Academic Press, San Diego, California

Hari P., Haavisto., H., Aalto, P. and Vesala, T. (1993) Can Accute Toxic Level Effects of SO_2 Be Detected in Field Data of Photosynthesis. *Proceedings of the 1st Finnish Conference of Environmental Sciences*, Kuopio, 8-9 lokakuuta 1993 ed. J. Tuomisto ja J. Ruuskanen, pp. 139-142.

Hari P. et al. (1994) Air Pollution in Eastern Lapland: Challenge for an Environmental Measurement Station. *Silva Fennica*, 28(1): 29-39.

Ruoho-Airola. T. (2004) Temporal and Regional Patterns of Atmospheric Components Affecting Acidification in Finland. *Finnish Meteorological Institute Contributions*, 44, PhD. Thesis.

Tunved, P., Hansson, H.-C., Kerminen, V.-M., Ström, J., Dal Maso, M., Lihavainen, H., Viisanen, Y., Aalto, P.P., Komppula, M. and Kulmala, M. (2006) High Natural Aerosol Loading over Boreal Forests. *Science*, 312, 261-263.

Tuovinen, J-.P., Laurila, T., Laittila, H., Ryaboshapko, A., Brukhanov, P. and Korolev, S. (1993) Impact of the Sulphur Dioxide Sources in the Kola Peninsula on Air Quality in Northernmost Europe. *Atmos. Env.*, 27, 1379-1395.

Virkkula, A. Aurela, M., Hillamo, R., Makela, T., Pakkanen, T., Kerminen, V. M., Maenhaut, W., Francois, F., and Cafmeyer, J. (1999) Chemical Composition of Atmospheric Aerosol in the European Subarctic: Contribution of the Kola Peninsula Smelter Areas, Central Europe, and the Arctic Ocean. *J. Geo. Res.*, 104, 23 681 – 23 696.

DETERMINATION OF NANOMETER SIZE AEROSOL PARTICLES FROM WOOD PYROLYSIS

T. LAITINEN[1], S. HERRERO-MARTIN[1], J. PARSHINTSEV[1], T. HYÖTYLÄINEN[1], K. HARTONEN[1], M.-L. RIEKKOLA[1], D. WORSNOP[2] AND M. KULMALA[2]

[1]Department of Chemistry, P. O. Box 55, FIN-00014, University of Helsinki, Finland

[2]Department of Physics, P. O. Box 64, FIN-00014, University of Helsinki, Finland

INTRODUCTION

Various techniques exist for the collection and chemical analysis of aerosol particles (McMurry, 2000). Traditionally, aerosol particles have been collected on filters and subjected to an extraction procedure before analysis. The analysis has been done generally with chromatography and/or mass spectrometric techniques. The sampling and analysis should be as short as possible to avoid artifact formation and chemical changes of compounds. In addition, some particles have lifetimes of only a few minutes or hours (Allen et al., 1996). The small mass of ultrafine particles presents an enormous challenge for analytical devices. The biggest issue relates to the time needed to collect a representative sample with sufficient particle mass for the analytical device to detect.

With real-time processes in particular, analysis by modern filter sampling techniques is extremely difficult. Also one chromatographic step does not provide sufficient separation efficiency, but fortunately novel multidimensional chromatographic techniques, such as comprehensive two-dimensional gas chromatography (GCxGC) that combines two chromatographic techniques with different separation mechanisms, offer attractive alternatives for the separation of complex samples (Kallio et al., 2006).

Aerosol mass spectrometry offers a good method to analyze atmospheric aerosols within a short time interval and without sample pretreatment (Johnston, 2000, Nash et al., 2006). Today, the most challenging part in the analysis of ultrafine aerosol particles is to determine the organic fraction of the compounds. The inorganic part is better known. The problem is that many similar and reactive organic compounds may be present in the particles and complicate the analysis (Allan et al., 2006).

Although sophisticated analytical techniques exist already today, the determination of aerosol chemical composition is very difficult task due to a high complexity of atmospheric aerosols and considerable variation of their composition with time and place. Development of new techniques is still crucial for obtaining more reliable results for the analysis of chemical composition of aerosol particles. In this study, one-dimensional GC and GCxGC, both coupled with time-of-flight mass spectrometry (TOFMS) were compared in the characterization of n-alkanes and polyaromatic hydrocarbons (PAH), born in Scots pine burning process. Self-constructed laser aerosol mass spectrometer was also tested with these pyrolysis products and the results obtained were compared to those of GC.

METHODS

In the gas chromatographic analysis, aerosols particles were produced by heating a piece of Scotts pine wood with a butane/propane flame. The particles were charged with a bipolar charger and size separated

with a differential mobility analyzer (DMA). Particle sizes of interest were 30 to 100 nm in diameter. The condensation particle counter (CPC) (3022 A, TSI, MN, USA) was used to count the particles entering the sample syringe filter (0.45 µm, Regenerated cellulose, i.d. 15 mm, Phenomenex, CA, USA). The particle concentrations were generally around 10^5 particles/cm^3 at all particle sizes studied.

The gas chromatographic experiments were carried out on an Agilent t890 gas chromatograph (Agilent Technologies, Santa Clara, USA) equipped with split/splitless injector and time-of-flight mass spectrometer (Leco Pegasus 4D, St. Joseph, MI, USA). Both one-dimensional and comprehensive two-dimensional (GCxGC) modes were employed. A 2 m × 0,53 mm I.D. DPTMDS deactivated retention gap was connected to a HP-5 column (29 m × 0.25 mm I.D., 0.25 um film thickness) which was connected to a RTX-17 column (79 cm × 0.1 mm I.D., 0.1 µm film thickness). 1 µl sample was introduced by splitless injection. Inlet was kept at 250°C and constant flow mode was used for carrier gas (He). Modulation time was 5 s, and the cryogenic modulation was done with liquid nitrogen. The GC oven was temperature programmed as follows: the first column 50°C (5 min)- 5°C/min- 260°C (15 min); and the second column 70°C (5 min)-5°C/min- 280°C (15 min). The interface between the GC × GC and TOF–MS systems was maintained at 300°C and the ionization source at 200 °C. Electron impact ionization (70 eV) was used for ionization and mass spectra from 50 to 500 amu was collected with a rate of 500 spectra/sec.

n-Alkane standard solution in cyclohexane (CERTAN, each 100 µg/ml) was purchased from LGC Promochem GmbH (Wesel, Germany). PAH standard mixture (2.0 mg/ml) was purchased from AccuStandard (New Haven, USA). 4,4'-dibromo-octafluorobiphenyl (98%), used as internal standard, was purchased from Aldrich (Gillingham, UK). Seven point external calibration (50 ppb-5 ppm) was done from the mixture containing both standard solution. Aerosol samples were extracted from the filters with 2 ml of hexane/acetone mixture (50/50). Then 10 µl of internal standard was added, and sample volume was reduced to 150 µl under the gentle stream of nitrogen.

In the aerosol mass spectrometer analysis, the wood combustion particles were sampled similar way as in the GC-analysis. All aerosol particles were first charged with the bipolar charger. Then the particle size of interest was selected with the DMA. The size-selected charged particles were collected by electrostatic deposition onto stainless steel collection surface, which is part of the specially designed sampling valve. The sample flow to the sampling surface was controlled by using of HEPA-filtered pressurized air and a pre-vacuum pump (Edwards RV5, England). The aerosol particles were counted with a condensation particle counter (CPC) (CPC 3023, TSI, MN, USA) before and after the collection. The collected sample was introduced to the high vacuum (10^{-7} torr) of the mass spectrometer (MS) by rotating the sampling valve and after the vacuum was recovered (normally 30 to 60 seconds), desorption was performed. The sample was desorbed with a single laser shot from the IR-laser (New wave research, Polaris II, Fremont, USA), which operates at 1064 nm wavelength. The sample desorption produces a gaseous plume of mostly neutral molecules in the vacuum, which will expand rapidly. Immediately after the desorption pulse, the sample molecules in the plume were ionized with one laser shot from an ArF excimer laser (Neweks, excimer laser PSX-100, Tallinn, Estonia), operating at wavelength 193 nm. The delay between the lasers was generated by a self-made delay circuit and usually it was set to about 10 µs. The produced ions were directed to a time-of-flight mass spectrometer (C-TOF, Tofwerk, Thun, Switzerland). Before a new sample was introduced to the system, the collection surface was cleaned by shooting several shots from the desorption laser with high power. This was done to prevent contamination from a previous sample. A blank sample was run before each new sample.

RESULTS

In the gas chromatographic experiments at GCxGC part, the whole sample is subjected to two-dimensional separation in a single run by using two GC columns with different polarity and a modulating system.

Concentrative modulation in the GCxGC technique offers a high separation efficiency and enhanced sensitivity. In addition, the ordered structure of the GCxGC chromatograms simplifies the identification. In our study, levoglucosan, produced by wood burning process, can be clearly seen as the largest peak in both GC and GCxGC chromatograms (Fig. 1.) it did not interfere with target compounds, n-alkanes and PAHs in the GCxGC-MS, while in the GC-MS the identification of most of the hydrocarbons was not possible. Moreover, it is obvious that for a reliable GC-MS analysis levoglucosan should be carefully removed e.g. by solid phase micro-extraction before the analysis of PAH compounds.
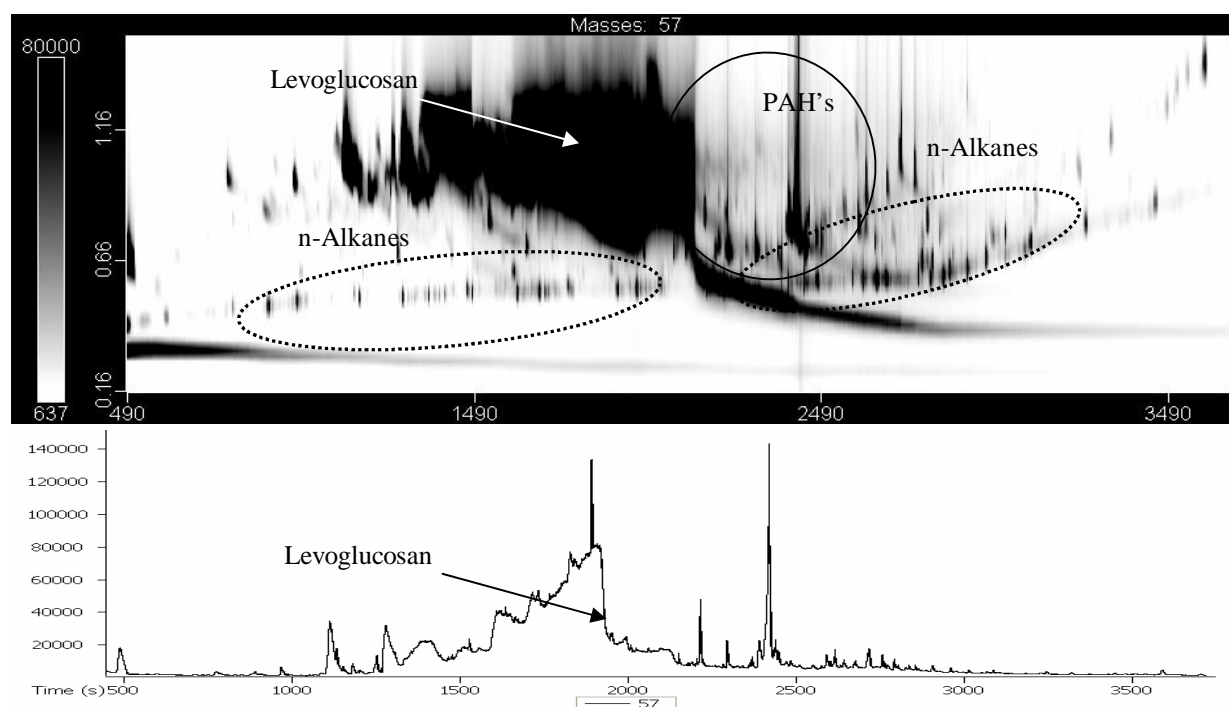
Figure 1. Comparison of GC*GC-TOFMS (upper) and GC-TOFMS chromatograms of 50 nm aerosol particles collected for 60 min. Collected particle mass in this sample was about 3 µg.

In the aerosol mass spectrometer experiments several different samples were analyzed between particle sizes from 30 to 90 nm at collection times of 10 to 30 minutes. Later it was noticed that the sampling time could have been much smaller due to high signals obtained. The same standard solution (containing PAH's and n-alkanes) used in chromatographic experiments was also applied with the aerosol mass spectrometer system. The spectrum obtained from the standard mixture was comparable to that in the GCxGC-MS.

From the analyzed spectra, many n-alkanes and some PAH's were identified. These are the products that are most often detected from wood combustion products. Generally, PAH's were found at smaller concentrations than in GC experiments. The reason for this might be the inaccurate control of the wood burning process. Also the sampling line in the GC experiments was lot shorter, which might have an influence on the results. Many n-alkanes were found and identified from every sample. As an example, Fig. 2 shows a spectrum of 50 nm particles with 10 minutes collection. All the highest peaks were identified, but as can be seen there are many other peaks all over the spectrum, which indicates a higher number of components in this sample.
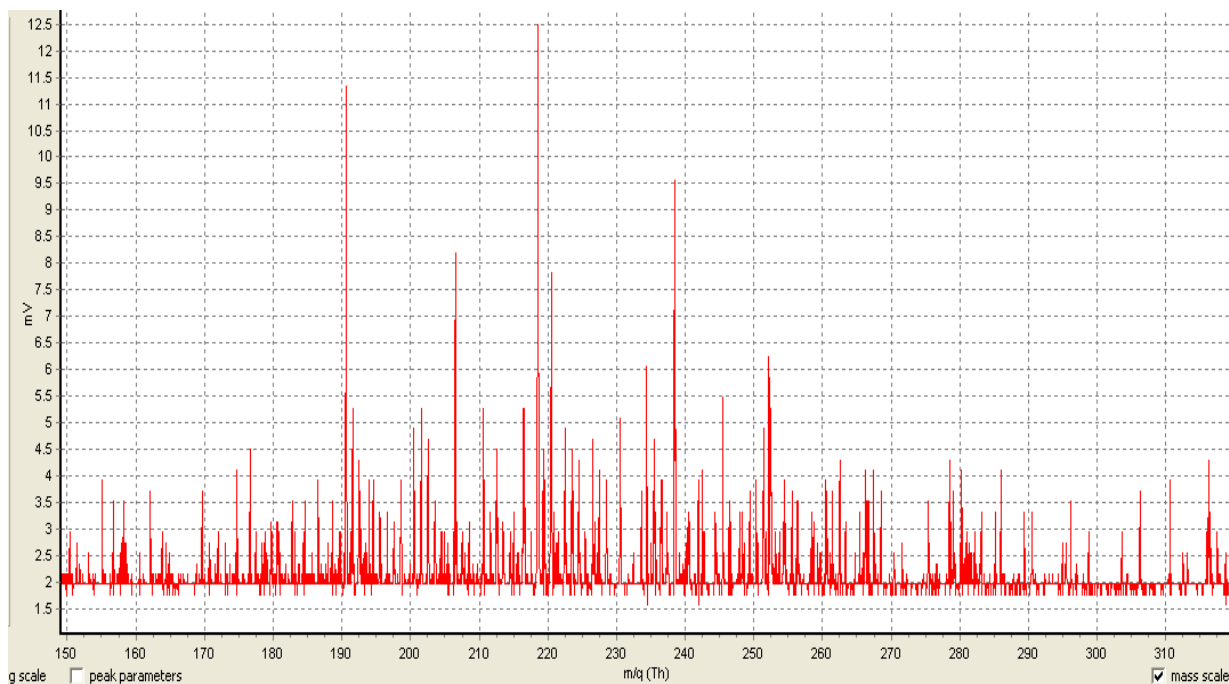
Figure 2. Mass spectra of 50 nm particles from wood burning process by laser aerosol mass spectrometer. The collection time was 10 minutes, particle average number concentration was about $2 \cdot 10^5$ cm^{-3} and particle mass 290 ng.

CONCLUSIONS

The GCxGC system provided a comprehensive picture of compounds in aerosol particles with short time frame. Only a very simple sample pretreatment for the GCxGC was needed. Probably in the study of ambient aerosol particles at this size range, the collection times should be much longer and therefore artifact formation and changes in the chemical composition may occur. The laser aerosol mass spectrometer can be used for the identification of compounds without any sample pretreatment. The concentrations used for aerosol MS were generally too high, since the detection limits of PAH's, for example, are in tens of picograms. The GC experiments gave much clearer picture about burning process and it suits well for this kind of analysis. On the other hand, it is not as good choice for ambient air analysis as the laser aerosol mass spectrometer.

ACKNOWLEDGEMENTS

REFERENCES

Allan J.D., Alfarra M.R., Bower K.N., Coe H., Jayne J.T., Worsnop D.R., Aalto P.P., Kulmala M., Hyötyläinen T., Cavalli F. & Laaksonen A. (2006). Size and composition measurements of background

aerosol and new particle growth in a Finnish forest during QUEST 2 using and aerodyne Aerosol Mass Spectrometer. *Atmospheric Chemistry and Physics*. 6: 315-327.

Allen T.M., Bezabeh D.Z., Smith C.H., McCauley E.M., Jones A.D., Chang D.P.Y., Kennedy I.M. & Kelly P.B. (1996). Speciation of arsenic oxides using laser desorption/ionization time-of-flight mass spectrometry. *Anal. Chem.* 68: 4052-4059.

Johnston M.V. (2000). Sampling and analysis of individual particles by aerosol mass spectrometry. *J. Mass Spectrom*. 35: 585-595.

Kallio M., Jussila M., Rissanen T., Anttila P., Hartonen K., Reissell A., Vreuls R., Adahchour M. and Hyötyläinen T. (2006). Comprehensive two dimensional gas chromatography coupled to time-of-flight mass spectrometry (GC*GC-TOFMS) in the indentification of organic compounds in atmospheric aerosols from coniferous forest. *J. Chromatogr. A*. 1125: 234.

McMurry P.H. (2000). A review of atmospheric aerosol measurements. *Atmospheric Environment*. 34: 1959-1999.

Nash D.G., Baer T. & Johnston M.V. (2006). Aerosol mass spectrometry: An introductory review. *Int. J. Mass Spectrom.* 258: 2-12.

HYDROGEN SOIL DEPOSITION AND MODEL RESULTS

M. LALLO, T. AALTO, J. HATAKKA and T. LAURILA

Finnish Meteorological Institute, Erik Palménin aukio 1, 00560 Helsinki, Finland

Keywords: hydrogen, soil deposition, soil uptake, atmospheric models

INTRODUCTION

The interest to molecular hydrogen is partly promoted by a need for better understanding of atmospheric balance of hydrogen and partly prospect to develop future hydrogen fuel economy (Ehhalt and Rohrer, 2009). The air quality is decreased due to elevated greenhouse gas emissions in many areas in the world, which promotes the research of greenhouse gas emission free energy production methods. The possibility to utilize hydrogen as an energy transport medium in the hydrogen economy deserves more attention. Deposition rates have been studied in field conditions using soil chambers (Conrad and Seiler, 1985; Yonemura *et al.,*1999; Yonemura *et al.*, 2000; Rahn *et al.*, 2002; Lallo *et al. 2008;* Smith-Downey *et al.*2008) and concentration measurements combined with known fluxes of other trace gases (Hammer et al., 2009). In the current work, chamber measurements as well as modeled soil deposition using the radon tracer method and two-dimensional model was applied to find out the magnitude and variation in the hydrogen soil deposition rates. Soil chamber measurements and continuous hydrogen measurements were performed in Pallas region in northern Finland.

METHODS

A chamber campaign was performed on 3–5 Sep 2007 and repeated on 5–7 Aug 2008 in Pallas. Three sites (Sammaltunturi, Kenttärova and Lompolojänkkä) were selected in the northern boreal forest zone according to different soil type properties. Two chambers were fixed to measurement site. Measurements were performed using a chamber with an aluminium cover. Sample collection period was 15–20 minutes. Sample interval was 2 – 5 minutes excluding the first sample which was taken immediately after lowering the cover. Two chambers were fixed into ground about 4–13 cm depth. The experiment was repeated three times. Chamber setup is discussed more detailed in Lallo *et al.* (2008). Hydrogen deposition rates were analyzed using Peak Performer 1 (Peak Laboratories) instrument which uses on HgO reduction gas method (Schmidt and Seiler, 1970). The hydrogen concentration in the mercury bed is proportional to released mercury gas. The detection is based on absorption of UV light into mercury gas.

In the radon tracer method, tropospheric radon observations are used to estimate the surface deposition and emissions rates of other species (Schmidt *et. al.* 2001). The radon increase in the nighttime can be plotted against corresponding hydrogen mixing ratio. The hydrogen flux and deposition velocity can be estimated, if radon flux is known. Also a two-dimensional atmospheric model was applied to model deposition velocities. A three-dimensional model (Aalto *et al.* 2006) was converted to computationally faster algorithm by removing the variation in vegetation and topography, which is not a dominant factor in case of hydrogen, which is mainly taken up by boreal soil. Nocturnal deposition velocities were estimated using this model.

RESULTS

During the campaing period in 2007, air temperature varied between -2 and 10 °C. The coldest night was the one before start of the campaign. Low soil temperature (5 °C) decreased the deposition velocity values at Kenttärova and Sammaltunturi site. At Lompolojänkkä soil surface was saturated with water.and soil uptake was negligible. During the campaign period in 2008, air temperature varied between 4 and 15 °C. At the top of arctic hill Sammaltunturi deposition velocities were higher than in Kenttärova, despite the fact that soil moisture and temperature did not differ significantly. At Lompolojänkkä soil moisture was 95-100% and the surface was saturated with water. Thus, the deposition into the ground was negligible. The deposition velocity values were lower than one measured in southern boreal zone in fall. The radon tracer method and two-dimensional model gave very similar values compared to chamber deposition velocities. Also modeled radon exhalation rate was same than the experimental average for northern Finland (Szegvary *et al.*2007).

CONCLUSIONS

The thin unfrozen soil layer at the top of arctic hill, and the forest floor consumed hydrogen according to results in 2008. Modeled deposition velocity values according to radon tracer method and two-dimensional model were close to experimental deposition velocity values from chamber measurements. The soil temperature and moisture regulate the soil uptake. In this study, variations were minor and the effect to the deposition velocity was not clearly seen in 2008 .Low soil temperature decreased the deposition velocity values in 2007 at Kenttärova and Sammaltunturi. The future research is focused to background levels and transport of atmospheric hydrogen by utilizing observational and modeling tools. Online measurements will also be continued at Sammaltunturi.

ACKNOWLEDGEMENTS

REFERENCES

Aalto T., Hatakka J., Karstens U., Aurela M., Thum T. & Lohila A. (2006), Modeling atmospheric CO2 concentration profiles and fluxes above sloping terrain at a boreal site, *Atmos. Chem. Phys.* **6**, 303–314.

Conrad, R., Seiler, W. (1985), Influence of Temperature, Moisture and Organic Carbon on the Flux of H_2 and CO Between Soil and Atmosphere: Field Studies in Subtropical Regions, *J. Geophys. Res.* **90**, 5699–5709.

Ehhalt,D.H., Rohrer,F.(2009), The tropospheric cycle of H_2: a critical review, *Tellus B* (in press), doi: 10.1111/j.1600-0889.2009.00416.x.

Hammer, S., Vogel, F., Kaul, M., and Levin, I. (2009), The H_2/CO ratio of emissions from combustion sources: Comparison of top-down with bottom-up measurements in south-west Germany, Tellus B (accepted manuscript), doi: 10.1111/j.1600-0889.2009.00418.x.

Lallo M., Aalto T., Laurila T. & Hatakka J. (2008). Seasonal variations in hydrogen deposition to boreal forest soil in Southern Finland. *Geophys. Res. Lett.* **35**, L04402, doi:10.1029/2007GL032357

Rahn T., Eiler, J.M., Kitchen, N. , Fessenden, J.E., Randerson, J.T. (2002), Concentration and δD of molecular hydrogen in boreal forests: Ecosystem-scale systematics of atmospheric H2, *Geophys. Res. Lett.* **29**, 1888 doi:10.1029/2002GL015118.

Schmidt, U., Seiler, W.(1970), A New Method for Recording Molecular Hydrogen in Atmospheric Air, *J. Geophys. Res.* **75,** 713–1716.

Schmidt M., Glatzel-Mattheier H., Sartorius, H., Worthy D.E. & Levin I. (2001), Western European N2O emissions: a top-down approach based on atmospheric observations, *J. Geophys. Res.* **106**, 5507–5516.

Smith-Downey N. V., J. T. Randerson, J. M. Eiler (2008), Molecular hydrogen uptake by soils in forest , desert and marsh ecosystems in California, *J. Geophys. Res.* **113**, G03037, doi:10.1029/2008JG000701.

Yonemura, S., Kawashima,S., Tsuruta, H. (1999), Continuous measurements of CO and H$_2$ deposition velocities onto an andisol: uptake control by soil moisture*, Tellus 51B*, 688–700.

Yonemura, S., Kawashima, S., Tsuruta, H. (2000), Carbon monoxide, hydrogen and methane uptake by soils in a temperate arable field and a forest, *J. Geophys. Res.***105**, 14,347–14,362.

Szegvary T., Leuenberger M.C. & Conen F. (2007), Predicting terrestrial 222Rn f ux using gamma dose rate as a proxy, *Atmos. Chem. Phys.* **7**, 2789–2795.

JARVIS-TYPE MODEL FOR DRY-CANOPY SURFACE CONDUCTANCE: SEASONAL VARIATION

S. LAUNIAINEN[1], S. SEVANTO[1], A. MÄKELÄ[2] AND T. VESALA[1]

[1]Department of Physics, P.O. Box 64, FI-00014, University of Helsinki, Finland
[2]Department of Forest Ecology, P.O. Box 27, FI-00014, University of Helsinki, Finland

Keywords: surface conductance, evaporation, Jarvis-type model, boreal forest

INTRODUCTION

Vegetated ecosystems introduce water vapour into the atmosphere in form of evaporation from wet surfaces and transpiration through the stomata of the plants. When the canopy is dry, the degree of stomatal closure (stomatal conductance) largely regulates the magnitude of transpiration. Thus, the physiological function of the plant strongly influences the partitioning solar energy input (through net radiation, R_n) to latent (LE), sensible (H) and ground heat (G) fluxes at the surface. Therefore, correct description of the response of the stomata to environmental conditions over the entire growing season is essential for unbiased modelling of the energy partitioning and evapotranspiration, for instance in GCM:s (e.g. Noilhan and Mohfouf, 1996). In this study, a Jarvis-type multiplicative model (Jarvis, 1976) for bulk (i.e. big-leaf canopy) surface conductance (G_s) of a boreal Scots pine forest is parameterized using both eddy-covariance and environmental measurements conducted at SMEAR II –station in Hyytiälä, Southern Finland (Hari and Kulmala, 2006). While the seasonal development of leaf area provides a natural way to model the seasonal course of maximum G_s in deciduous vegetation, to our knowledge there are not any similar parameterizations for the seasonality of the conifers. Motivated by this, we set two main questions we aim to answer in this study: 1) Should the seasonal acclimation of boreal coniferous vegetation be taken into account when modelling G_s using Jarvis-type approach and 2) can the seasonal acclimation parameter (S) found to accurately describe the seasonal course of photosynthetic light use efficiency (Mäkelä et al. 2004) be used also in modelling G_s.

METHODS

We utilized the eddy-covariance measurements and the spectrum of environmental measurements conducted in Boreal Scots pine forest (all-sided LAI ~8 m^2m^{-2}, canopy height ~16 m) in Southern Finland. The SMEAR II -site and its measurements are described in detail in Hari and Kulmala (2005) and Markkanen et al. (2001) and are not repeated here.

We calculated the bulk surface conductance for water vapour (G_s, in mm/s) by inverting the Penman-Monteith equation (e.g. Monteith and Unsworth, 1990)

$$\lambda E = \frac{sR_a + \rho c_p D g_a}{s + \gamma(1 + g_a/g_s)},$$ (1)

yielding

$$\frac{1}{G_s} = \frac{1}{g_a}\left\{\frac{\varepsilon R_a + \rho c_p g_a D/\gamma}{LE} - \varepsilon - 1\right\}.$$ (2)

Here R_a is the available energy ($R_a = R_n - G - \sum Q_i$, Wm^{-2}), g_a the aerodynamic conductance (ms^{-1}), s is the slope of saturation vapour pressure curve and γ the psychrometric constant, $\varepsilon = s/\gamma$, ρ the air density, c_p the heat capacity of the air in constant pressure, D (Pa) the vapour pressure deficit and LE the measured

latent heat flux above the forest (in Wm^{-2}). In the above form of the eq. 2 the surface conductance (G_s) is denoted separately from the aerodynamic conductance. The aerodynamic conductance was estimated as $g_a = u_*^2/U$ using values at 23.3 m where the flux measurements were made. T_a and D at 16.8 m height were used to describe the "bulk" conditions at the canopy level. To assure dry-canopy conditions, only periods without precipitation during the previous 24 hours and $G_s > 0$ were qualified for the analysis.

Two Jarvis-type (e.g. Jarvis, 1976) multiplicative models were parameterized using the calculated conductance and environmental data. The model can be written as:

$$G_s = G_{s\max} f(Q) f(D) f(\theta) f(T) f(S),$$

(3)

where G_{smax} (mm/s) is maximum conductance and $f(X_i)$ are the environmental modifier functions which range from 1 (no limitation of G_s by X_i) and 0 (complete stomatal closure as a response to X_i). Both models shared same modifier functions for PAR (Q), vapour pressure deficit (D) and volumetric soil moisture (θ). The Q and D dependencies were described using hyperbolic and exponential functions as in Matsumoto et al. (2005):

$$f(Q) = \frac{Q}{Q + Q_{1/2}}$$

(4)

$$f(D) = \exp(-k_1 D).$$

(5)

The parameters $Q_{1/2}$ represents the value when $f(Q)$ equals ½ and the k_1 is sensitivity of G_s to D. The effect of soil moisture availability to G_s was modeled following Cox et al. (1998) by:

$$f(\theta) = \frac{1 - \exp(-k_2 \beta)}{1 - \exp(-k_2)},$$

$$\beta = \left\{ \theta > \theta_{crit} \to 1; \theta_{wilt} \le \theta \ge \theta_{crit} \to \frac{\theta - \theta_{wilt}}{\theta_{crit} - \theta_{wilt}}; \theta < \theta_{wilt} \to 0 \right\},$$

(6)

where k_2 is a parameter and the characteristic values of wilting point θ_{wilt} and critical soil moisture content (θ_{crit}) for this type of soil (silty glacial till) were set to 0.085 and 0.25 m^{3}m^{-3}.

In addition to above modifiers, the model 1 included a modifier for the state of seasonal acclimation of the photosynthetic capacity (S). According to Mäkelä et al. (2004), the seasonal acclimation of photosynthetic light use efficiency was well described by temperature, in delayed manner, allowing them to postulate a dynamic model for S:

$$\frac{dS}{dt} = \frac{1}{\tau}(T - S),$$

(7)

where τ is a time constant. In this study we calculated S using $\tau = 200$h as in Kolari et al. (2006) for the same site. In model 1, we assumed that the seasonal cycle of G_{smax} could be described by linear but initially saturating function (at threshold value S_0):

$$f(S) = \min(\frac{\sigma}{S_0}, 1),$$

$$\sigma = \left\{ S > 0 \to \sigma = S; S < 0 \to \sigma = 0 \right\}$$

(8)

In model 2, the $f(S)$ was replaced by a modifier for ambient temperature as in Matsumoto et al. (2005):

$$f(T) = \left(\frac{T - T_{min}}{T_{opt} - T_{min}} \right) \times \left(\frac{T_{max} - T}{T_{max} - T_{opt}} \right)^{\left((T_{max} - T_{opt})(T_{opt} - T_{min}) \right)} \quad , \qquad (9)$$

where T_{min}, T_{opt} and T_{max} are the minimum, optimum and maximum temperatures. All free parameters including G_{smax} were solved simultaneously using non-linear least squares optimization in pre-defined (physically reasonable) parameter space. Both models were parameterized using dry-canopy data from the period 16th Apr – 31st Aug 2006. The calibration was done for all data as well as for even and odd days separately. Finally, we verified the models against independent G_s data (even / odd days) and modeled the latent heat flux using Penman-Monteith equation (eq. 1).

RESULTS

The ½ h values of G_s normalized by the estimated maximum value are shown in Figure 1 against the environmental variables. The solid lines represent the respective modifier functions with the parameter values obtained from the whole dataset (Table 1). The model 1 was able to prescribe slightly more of the ½ h variability in the dataset (PEV ~0.58) than the model 2 (PEV ~0.50). Presumably both random nature of turbulence and turbulent fluxes and propagating errors associated to the calculation of G_s from Penman-Monteith equation together with other environmental factors than the modifiers used, were responsible for the relatively low PEV. Because of different construction of the models, the values of G_{smax} and sensitivity to D are markedly higher in model 2. For model 2, T_{min}, T_{opt} and T_{max} were allowed to vary between -5 ˚C and 40 ˚C. The high values of T_{opt} obtained here are presumably caused by almost linear and relatively slow increase of G_s with temperature in spring (not shown). Thus, the temperature modifier describes here rather the seasonal course of temperature and G_s than short-term T response, which is likely to be minor in typical environmental conditions at the site. Moreover, since Q, T and D are strongly correlated in short time scales, the short-term effect of temperature may be partly incorporated in $f(D)$.

Table 1: The parameter values of models 1 & 2 obtained by non-linear least squares optimization.

Model: data	G_{smax} (mm/s)	$Q_{1/2}$ ($\mu molm^{-2}s^{-1}$)	k_1 (kPa^{-1})	k_2	S_0 (˚C)	T_{min} (˚C)	T_{opt} (˚C)	T_{max} (˚C)	PEV
M1:all	18,12	655.6	0,61	4.02	12,28				0.57
M1:odd	17,39	594.1	0,61	4.49	12,10				0.58
M1:even	19,78	776.2	0,62	3.63	12,57				0.57
M2: all	32,14	615.4	0,88	4.89		-5.0	35,9	40.0	0,49
M2: odd	27.88	549,6	0.87	5,00		-5.0	33,3	40.0	0,50
M2 even	32.96	699,3	0.86	4,48		-5.0	35,9	40.0	0,54

Figure 2 shows the evaluation of the models calibrated by odd days against independently measured ½ h G_s (even days). When G_s was below ~6 mm/s both models produced (on average) unbiased estimates. However, neither of the models was able to produce G_s values above 8 mm/s and the underestimation increased approximately linearly with G_s. However, the model 1 was slightly more successful to describe ½ h variability than model 2.
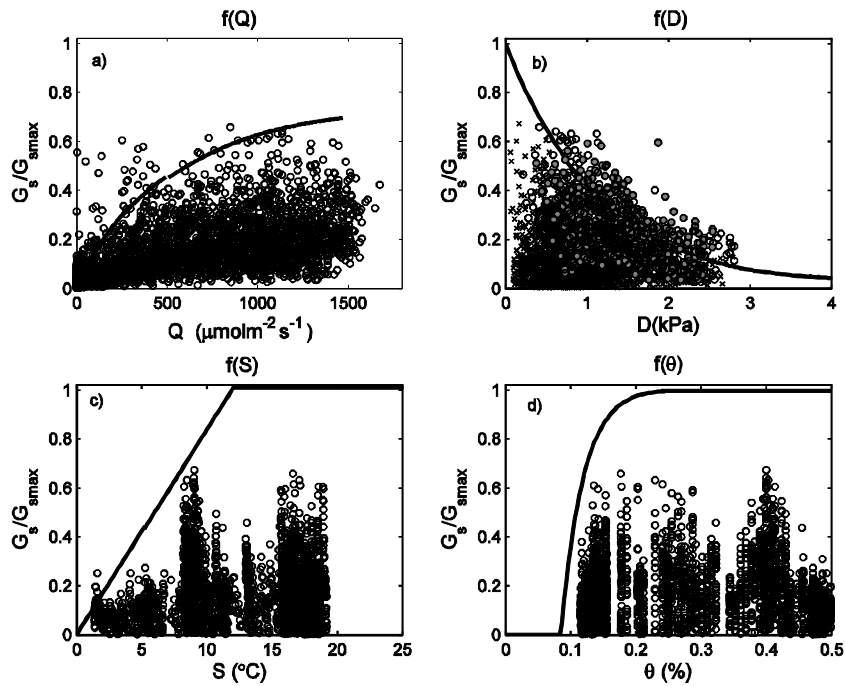
Figure 1. Bulk dry-canopy surface conductance for water vapour (G_s, mm/s) normalized by the maximum value (G_{smax}) against: a) PAR (Q), b) vapour pressure deficit (D), c) seasonal acclimation parameter (S) and volumetric soil moisture content (θ at 9-17 cm depth). The solid lines show the respective response functions with parameter values are in Table 1 (all data).
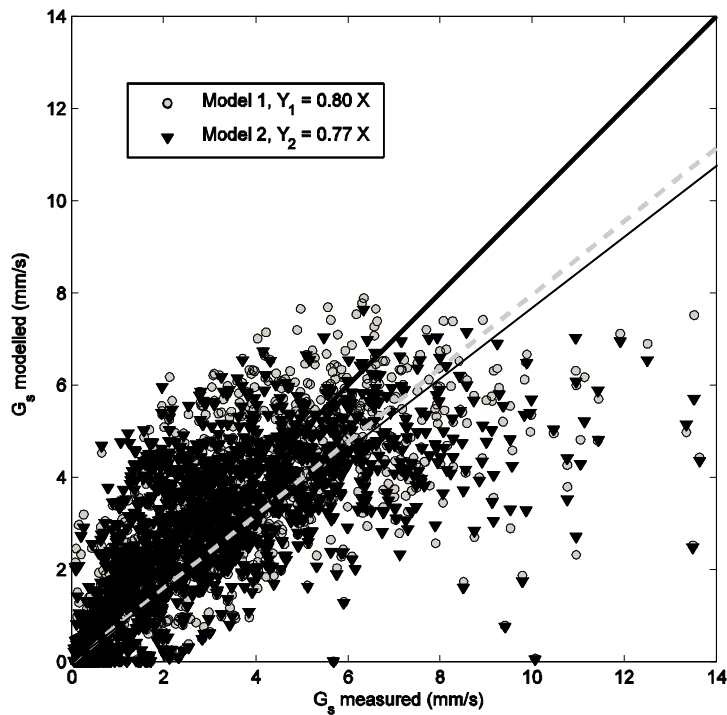
Figure 2. The comparison of modelled 30min conductance in 2006 against observed G_s. The models 1 and 2 were parameterized using odd days (Table 1) and evaluated against independent data (even days). The lines show corresponding linear fits forced through the origin and 1:1 response.

The measured and modelled dry-canopy (evapo)transpiration is shown in Figure 3a for the studied period. Although the modelled and measured LE are not here independent of each other (the measured LE was used to derive G_s that was used to calibrate the model), it is instructive to compare these two in order to study the possible biases and their temporal pattern. Both models were able to describe the seasonal as well as the diurnal cycles (not shown) of the stand scale dry-canopy LE from late April to August reasonably well. Also the intense drought period in August was well prescribed by both models. The model 1 was able to produce the seasonal variability more accurately than model 2 as seen from the bias between the measured and modelled cumulative transpiration (Figure 3b). Model 2 quite strongly overestimated LE in April and May and underestimated it in June-July. Before ~10th of May the overestimation by model 2 corresponds on average to 0.6 mm/d (~30-40% of daily ET) and after that the average underestimation was around 0.3 mm/d (~10% of daily ET). The model 1 slightly underestimated transpiration in April and underestimated thereafter, ~0.25 mm/d. In August there was no significant bias in either of the models. Over the whole period, the cumulative underestimation of the both models was less than 7% of the measured transpiration.
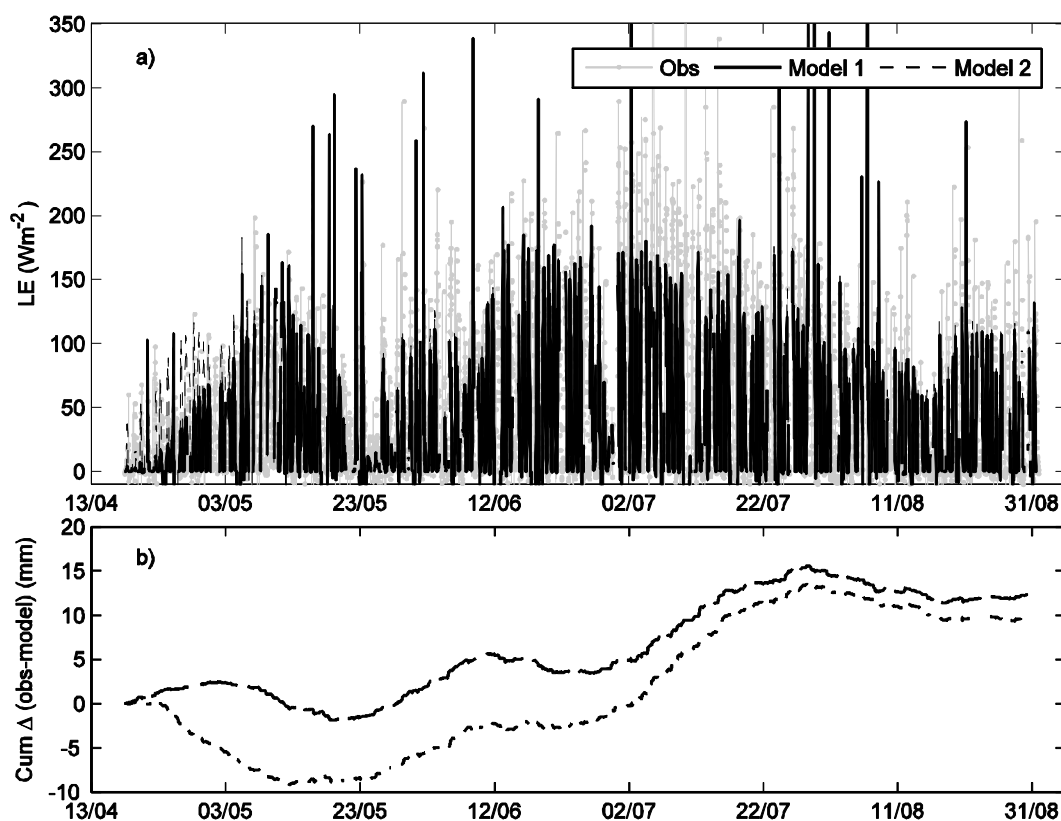
Figure 3. Measured and modelled dry-canopy latent heat flux (LE) in April to August 2006 (a) and the cumulative bias (observed – modelled) of transpiration (in mm) (b).

CONCLUSIONS

Two Jarvis-type models for bulk surface conductance (G_s) were parameterized to describe the diurnal and seasonal cycles of G_s in boreal Scots pine forest. Model 1, which included modifier for the state of acclimation (S) was slightly more successful to describe both ½ h variability and seasonal cycle of G_s than

237

the model 2, which instead of S, had a modifier for the current ambient temperature. The differences between the models were largest in April – early May, when the trees were still recovering from the dormancy. During that period the model 1 produced unbiased estimates of LE while model 2 strongly overestimated the transpiration. The results indicate that some benefits are gained when the seasonal acclimation is taken into account when modelling G_s of a boreal coniferous forest. Whether this can be achieved with even simpler parameter than S, such as the mean of minimum temperature in preceding days motivates further studies. In addition, the validity of combined stomatal conductance – photosynthesis (e.g. Ball et al. (1987); Leuning (1995); Cox et al. (1998)) models over the whole seasonal cycle should be investigated.

REFERENCES

Ball J.T., Woodrow I.E. and Berry J.A. (1987) A model predicting stomatal conductance and its contribution to the control of photosynthesis under different environmental conditions. In: *I. Biggins (Ed.), Progress in photosynthesis research. Martinus Nijhoff, Netherlands*, 221-224.

Cox P.M., Huntingford C. and Harding R.J. (1998) A canopy conductance and photosynthesis model for use in a GCM land surface scheme. *J. Hydrol.* 212-213, 79-94.

Hari P. & Kulmala M. (2005). Stations for Measuring Ecosystem-Atmosphere Relations (SMEAR II). *Bor. Env. Res.* 10, 315–322.

Jarvis P.G. (1976) The interpretation of the variations in leaf water potential and stomatal conductance found in canopies in the field. *Philosophical Transactions of the Royal Society of London, B* 273, 593-610.

Kolari P., Pumpanen J., Kulmala L., Ilvesniemi H., Nikinmaa E., Grönholm T. and Hari P. (2006). Forest floor vegetation plays an important role in photosynthetic production of boreal forests. *Forest Ecology and Management* 221, 241–248.

Leuning R. (1995). A critical appraisal of a combined stomatal-photosynthesis model for C3 plants. *Plant Cell Environ.* 18, 357-364.

Matsumoto K., Ohta T. and Tanaka T. (2005) Dependence of stomatal conductance on leaf chlorophyll concentration and meteorological variables. *Agric. For. Met.* 132, 44-57.

Markkanen T., Rannik Ü., Keronen P., Suni T. and Vesala T. (2001). Eddy covariance fluxes over a boreal Scots pine forest. *Boreal Env. Res.* 6, 65–78.

Monteith J.L. and Unsworth M.H. (1990). Principles of environmental physics, 2nd edn. *Edward Arnold, London.* 291 pp.

Mäkelä A., Hari P., Berninger F., Hänninen H. and Nikinmaa E. (2004) Acclimation of photosynthetic capacity in Scots pine to the annual cycle of temperature. *Three Phys.* 24, 369-376.

Noilhan J. and Mahfouf J.-F. (1996) The ISBA land surface parameterization scheme. *Global and Planetary Change.* 13, 145-159.

CONCENTRATIONS OF NEUTRAL MOLECULAR CLUSTERS: COMPARISION OF PH-CPC MEASUREMENTS IN HYYTIÄLÄ AND MACE HEAD

K. LEHTIPALO[1], M. SIPILÄ[1,2,*], I. RIIPINEN[1,**], D. CEBURNIS[3], R. DUPUY[3], C. O'DOWD[3], and M. KULMALA[1]

[1]Department of Physics, University of Helsinki, Finland
[2]Also at: Helsinki Institute of Physics, Helsinki, Finland
[3]School of Physics & Centre for Climate and Air Pollution Studies, Environmental Change Institute, National University of Ireland, Galway
* Currently at: Leibniz-Institut für Troposphärenforschung, Leipzig, Germany
** Currently at: Department of Chemical Engineering, Carnegie Mellon University, Pittsburgh, PA, USA

INTRODUCTION

The detailed mechanism of secondary new particle formation in the atmosphere is still under debate. It is proposed that particle formation happens via activation of 1–2 nm neutral molecular clusters (e.g. Kulmala et al., 2000; 2006). A reason for the lack of knowledge about the nucleation process has been the incapability to detect neutral particles below about 3 nm. Recent development of measurement techniques has provided us with tools to reach molecular sizes (Mirme et al., 2007; Sipilä et al., 2008).

Different particle formation mechanisms might be prevailing in different conditions. We measured cluster concentrations in two very distinct environments: the boreal forest in Hyytiälä, southern Finland, and the coast of the North Atlantic Ocean, in Mace Head, Ireland. On average new particle formation is observed in Hyytiälä on every fourth day, most frequently in spring time (Dal Maso et al., 2005). Particle formation in Mace Head is usually coinciding low tide and related to biogenic emission of iodine vapors (O'Dowd and Hoffmann, 2005).

MEASUREMENTS AND METHODS

Molecular clusters were measured at SMEAR II station in Hyytiälä 1 – 31 May 2008 and in Mace Head 13 June – 25 August 2008 with a pulse-height condensation particle counter (PH-CPC). Supportive data sets of particle and ion size distributions measured with Differential/Scanning Mobility Particle Sizer (DMPS/SMPS) and Neutral Cluster and Air Ion Spectrometer (NAIS; Mace Head), or Balanced Scanning Mobility Analyzer (BSMA; Hyytiälä) were also available from the stations.

The pulse height analysis technique (e.g. Saros et al., 1996) relies on detecting the intensity of light scattered by particles after their condensational growth in the CPC. Due to supersaturation gradient inside the condenser, particles activate for growth at different axial positions depending on their size. The smaller the particle, the later it will be activated leading to smaller final droplet sizes. The PH-CPC used in this study comprises a TSI-3025A ultrafine CPC with modified optics (Dick et al., 2000) and a multichannel analyzer. For increasing the detection efficiency of small particles, the supersaturation inside the condenser was increased from nominal until homogenous nucleation appeared. The pulse height analysis technique allowed us to distinguish homogenous nucleation from activation of clusters and resolve the size distribution between ~1.3 – 5 nm. Hereafter we refer as cluster concentration to the sum of particles between mobility diameters 1.3 – 3 nm. Detailed description of the performance of the instrument and data inversion is published by Sipilä et al. (2009).

RESULTS

In Hyytiälä the concentration of neutral clusters smaller than 3 nm was almost constantly over 10^3 cm^{-3}, sometimes reaching 10^5 cm^3. The highest concentrations were usually measured shortly after sunset. The results agree with earlier studies (Kulmala et al., 2007; Sipilä et al., 2008), in which a continuous pool of neutral clusters was detected with CPC-applications and Neutral Cluster and Air Ion Spectrometer (NAIS). On average only a few percent of these clusters can be produced by recombination of ion clusters (Lehtipalo et al., 2008). The diurnal behavior of cluster concentrations can be seen in Fig. 1a. The concentrations were on average very similar regardless of whether the day was classified as a new particle formation event day, a non-event day or an undefined day as in Dal Maso et al. (2005).
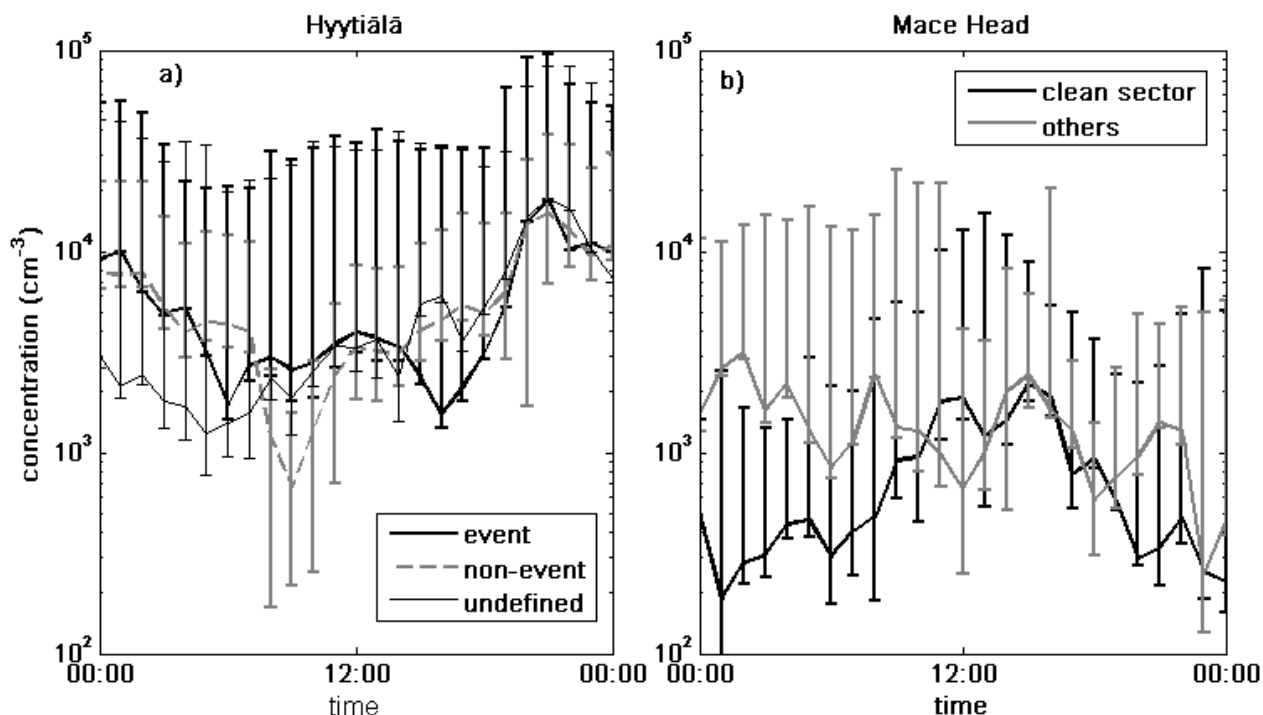
Figure 1. Diurnal variation of neutral cluster concentration. Line is at median value and error bars represent data between 5%- and 95%-percentiles. In Hyytiälä days are classified as 'event', 'non-event' and 'undefined' days regarding new particle formation (Dal Maso et al., 2005). In Mace Head the air mass origin is divided into 'clean sector' (trajectories originating directly from the ocean), and 'other' directions.

In Mace Head the cluster concentrations varied mostly between 10^2 and 10^4 cm^{-3}. In daytime the overall concentration was lower by a factor of two than in Hyytiälä, and in nighttime almost one order of magnitude lower. When the air mass trajectories originated from the ocean, i.e. from the clean sector without anthropogenic influence, the cluster concentration peaked at noon and was at minimum in nighttime (Fig. 1b). When the air mass advecting to the site had travelled over land, no clear diurnal cycle could be distinguished. A few cases of nighttime cluster formation were observed, but not as strong or frequent as in Hyytiälä. The observed cluster concentration had no relation to the tidal cycle. The maximum estimate of recombination products in the size range 1.3–3 nm accounted on average for two thirds of the measured neutral clusters, in nighttime the estimation of recombination products often even exceeded the measured concentration. The fraction of 1.3–3 nm ions from all clusters was also much higher in Mace Head than in Hyytiälä, 22% on average. The ion ratio remained almost constant throughout the day. Table 1 summarizes the characteristics of cluster concentrations in Hyytiälä and Mace Head.

	Hyytiälä	**Mace Head**
Neutral cluster concentration:		
-daytime (cm^{-3})	1000 – 40 000	500 – 20 000
-nighttime (cm^{-3})	1000 – 100 000	100 – 10 000
Recombination ratio	3 %	66 %
Ion ratio	1 %	22 %

Table 1. Characteristics of cluster concentrations. Neutral clusters (1.3-3 nm) are measured with PH-CPC. Recombination ratio is the maximum estimate of recombination products between 1.3-3 nm calculated from ion measurements divided with measured neutral clusters. Ion ratio is the measured 1.3-3 nm ions divided with sum of measured ion and neutral cluster concentrations.

CONCLUSIONS

In Hyytiälä neutral clusters were observed constantly, the highest concentrations being measured in nighttime. The diurnal behavior of cluster concentrations was remarkably similar regardless of whether or not a new particle formation event was observed. This indicates that if clusters participate in the first steps of particle formation, their concentration is not the limiting factor.

In Mace Head the overall cluster concentration was lower than in Hyytiälä, and a much larger fraction of the clusters could be explained by ions. In marine air masses there was a clear diurnal cycle with daytime cluster concentration maximum, which implies that cluster formation requires some photochemical reactions. When air mass has travelled over land area, VOCs emitted from the vegetation or anthropogenic emissions might influence cluster formation and explain the higher and more variable concentrations.

ACKNOWLEDGEMENTS

REFERENCES

Dal Maso, M., Kulmala, M., Riipinen, I., Wagner, R., Hussein, T., Aalto, P.P., and Lehtinen, K.E.J.: Formation and growth of fresh atmospheric aerosols: eight years of aerosol size distribution data from SMEAR II, Hyytiälä, Finland. *Boreal Env. Res.,* 10:323-336, 2005

Dick, W. D., McMurry, P. H., Weber, R. J., and Quant, R.: White-light detection for nanoparticle sizing with the TSI Ultrafine Condensation Particle Counter, J. Nanoparticle Res., 2, 85-90, 2000.

Kulmala, M., Pirjola, L., and Mäkelä, J. M.: Stable sulphate clusters as a source of new atmospheric particles, Nature, 404, 66-69, 2000.

Kulmala, M., Lehtinen, K. E. J. and Laaksonen, A.: Cluster activation theory as an explanation of the linear dependence between formation rate of 3 nm particles and sulphuric acid concentration. Atmos. Chem. Phys., 6, 787–793, 2006.

Kulmala, M., Riipinen, I., Sipilä, M., Manninen, H., Petäjä, T., Junninen H., Dal Maso, M., Mordas, G., Mirme, A., Vana, M., Hirsikko, A., Laakso, L., Harrison, R. M., Hanson, I., Leung, C., Lehtinen, K. E. J., and Kerminen, V.-

M.: Towards direct measurement of atmospheric nucleation, Science, 318, 89-92, 2007a. Supporting online material: www.sciencemag.org/cgi/content/full/1144124/DC1

Lehtipalo, K., Sipilä, M., Riipinen, I., Nieminen, T., and Kulmala, M.: Analysis of atmospheric neutral and charged molecular clusters in boreal forest using pulse-height CPC. Atmos. Chem. Phys. Discuss., 8, 20661-20685, 2008

Mirme, A., Tamm, E., Mordas, G., Vana, M., Uin, J., Mirme, S., Bernotas, T., Laakso, L., Hirsikko, A., Kulmala, M.: A wide-range multi-channel Air Ions Spectrometer. *Boreal Environmental Research*¸ 12, 247-264, 2007

O'Dowd, C. D., and Hoffmann, T.: Coastal new particle formation: a review of the current state-of-the-art. *Environ. Chem.* **2,** 245-255 (2005).

Saros, M., Weber, R. J., Marti, J., and McMurry, P. H.: Ultra fine aerosol measurement using a condensation nucleus counter with pulse height analysis, Aerosol Sci. Technol., 25:200–213, 1996.

Sipilä, M., Lehtipalo, K., Kulmala, M., Petäjä, T., Junninen, H., Aalto, P. P., Manninen, H. E., Vartiainen, E., Riipinen, I., Kyrö, E.-M., Curtius, J., Kürten, A., Borrmann, S., and O'Dowd, C. D.: Applicability of Condensation Particle Counters to measure Atmospheric clusters, Atmos. Chem. Phys. 8, 4049-4060, 2008.

Sipilä, M., Lehtipalo, K., Attoui, M., Neitola, K., Petäjä, T., Aalto, P. P., O'Dowd, C. D., and Kulmala, M.: Laboratory verification of PH-CPC's ability to monitor atmospheric sub-3nm clusters. Aerosol Sci. Technol., 43, 2:126-135, 2009.

REPRODUCING MEASUREMENT DATA USING ION-UHMA MODEL

J. LEPPÄ[1], V.-M. KERMINEN[1], L. LAAKSO[2,3], H. KORHONEN[4], T. YLI-JUUTI[2], H. E. MANNINEN[2], T. NIEMINEN[2] and M. KULMALA[2]

[1]Finnish Meteorological Institute, Climate Change, P.O. Box 503, FI-00101 Helsinki, Finland
[2]Department of Physics, University of Helsinki, P.O. Box 64, FIN-00014 Helsinki, Finland
[3]School of Physical and Chemical Sciences, North-West University, Private Bag x6001, Potchefstroom 2520, Republic of South Africa
[4]Department of Physics, University of Kuopio, P.O. Box 1627, FIN-70211 Kuopio, Finland

INTRODUCTION

The formation of new atmospheric aerosol particles by nucleation and subsequent growth has been found to take place in a variety of environments ranging from clean polar areas to polluted urban centers (Kulmala *et al*., 2004a; Kulmala and Kerminen, 2008). In order to quantify the regional and global effects resulting from atmospheric aerosol formation, we should have better understanding of the initial steps of this phenomenon in different atmospheric environments (Kulmala *et al*., 2004b). Continuous field measurements play a key role in this regard. Unfortunately, the great majority of the conducted measurements are not suitable for investigating the very early steps of aerosol formation, since the used instruments do not usually reach sizes smaller than a few nanometers in particle diameter.

Air ion spectrometers provide a means to measure the number distributions of charged particles and ion clusters down to molecular sizes (Tammet, 2006; Mirme *et al*., 2007). The drawback with these instruments is that they are unable to measure neutral nanometer-size particles which, under most conditions, are expected to dominate over corresponding charged particles. Getting the full advantage of current air ion spectrometer measurements may not be possible without the help of a dynamical model that is able to capture the basic interactions between ion clusters, charged and neutral particles, and condensing vapors. In this study we have used a newly-developed box model Ion-UHMA (Leppä *et al*., 2009). The aim of the study was to test that the model is capable of reproducing the measured time evolution of the particle size distribution and also demonstrate a potential way of using the model in future studies.

METHODS

Ion-UHMA, the model used in this study, is a zero-dimensional box model, which simulates the dynamics of multicomponent tropospheric aerosol particles. The main dynamical processes in the model are condensation, coagulation, nucleation, ion-aerosol attachment and dry deposition. The particles are divided into user specified number of size sections (60 in this study) and three charge classes: neutral, negative and positive. In addition to the growing particles there are pools of charges clusters in the model, and the attachment and recombination of clusters with growing particles are simulated.

In order to test if Ion-UHMA is capable of reproducing the measured time evolution of the particle size distribution, a set of simulations was conducted. In these simulations, the following parameters were taken from measurements and used as inputs for the model: the particle size distribution from 20 to 1000 nm, concentrations and average mobilities of charged clusters, growth rate of particles and the formation rate of neutral and charged particles with diameter of 1.8 nm. The particle size distribution from 20 to 1000 nm was updated every 10 minutes using the measured values. The measured growth rates were obtained as average values over the events for three diameter ranges (1.7-3 nm, 3-7 nm and 7-20 nm). The growth rates as a function of diameter were smoothed for the simulations in order to avoid step-like changes. The measurements were conducted at the SMEAR II station (Hari and Kulmala, 2005) in Hyytiälä, Southern Finland, during the years 2006 and 2007 (Manninen *et al*., 2009; Nieminen *et al*., 2009).

Fourteen days were chosen with the restrictions that all the data listed above were available, that a new particle formation event was observed during the day, and that the measured air masses were sufficiently homogeneous. The last restriction is crucially important, as Ion-UHMA cannot simulate processes associated with changes in air mass transport patterns.

RESULTS AND DISCUSSION

For each of the simulated days, the model reproduced quite well the observed time evolution of the particle number size distribution. An example of such a day is depicted in Fig. 1. The total and charged particle concentrations were measured for the size ranges of 3 – 1000 nm and 0.8 – 40 nm, respectively (Figs 1d, 1e and 1f). In the simulations, the concentrations of particles from 1.8 to 20 nm in diameter were simulated and the concentrations of bigger particles were taken from the measurements. As a result, we may compare simulations and observations over the diameter range 3—20 nm for total particles (Figs 1a and 1d) and over the diameter range 1.8—20 nm for negatively (Figs 1b and 1e) and positively (Figs 1c and 1f) charged particles. Furthermore, we may look at the boundary between simulation and measurement at the diameter of 20 nm (Figs 1a, 1b and 1c). We may see that the evolutions of particle concentrations were very similar and the concentrations at both sides of the boundary between simulation and measurement agreed well with each other.
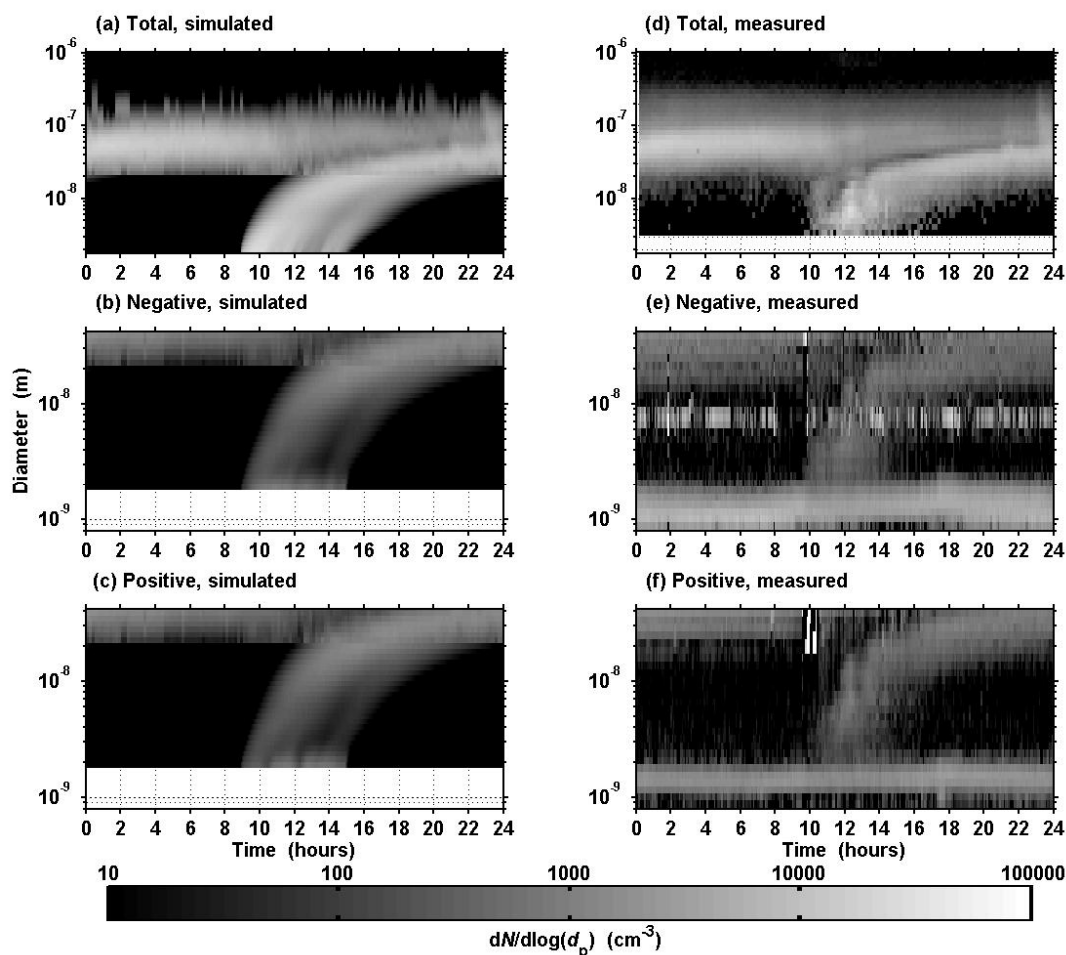
Figure 1. Simulated (panels a, b and c) and measured (panels d, e and f) evolution of the particle number size distribution for 15 September 2006. The evolution is shown for total (panels a and d), negatively charged (panels b and e) and positively charged particles (panels c and f). The shade of grey denotes the particle number concentration ($\mathrm{d}N/\mathrm{dlog}d_p$) as a function of time and diameter.

In order to demonstrate potential ways to use Ion-UHMA in future studies, we conducted eight more simulations for each of the fourteen days mentioned above. In each simulation, we tried to reproduce the measured data of the particular day, with either the formation rate or the growth rate of particles multiplied by a factor of 2, 5, 0.5 or 0.2. The resulting evolution of the particle number size distribution was then visually compared with the measured one, to assess roughly whether a smaller or bigger input growth rate or formation rate resulted in a better agreement between the simulation and measurements. Two examples of such simulations, associated with 15 September 2006, are depicted in Fig. 2. In one of the examples the formation rate of the particles was multiplied by a factor of 0.2 (Figs. 2a, 2b and 2c) and in the other the particle growth rate was multiplied by a factor of 0.5 (Figs. 2d, 2e and 2f). Visual comparison of the evolutions of particle number size distributions depicted in Figs. 1 and 2 shows that in this case, the agreement between the measured and simulated evolutions of the size distributions is worse, if the formation or growth rate of the particles in the model is multiplied by a factor of 0.2 or 0.5, respectively.
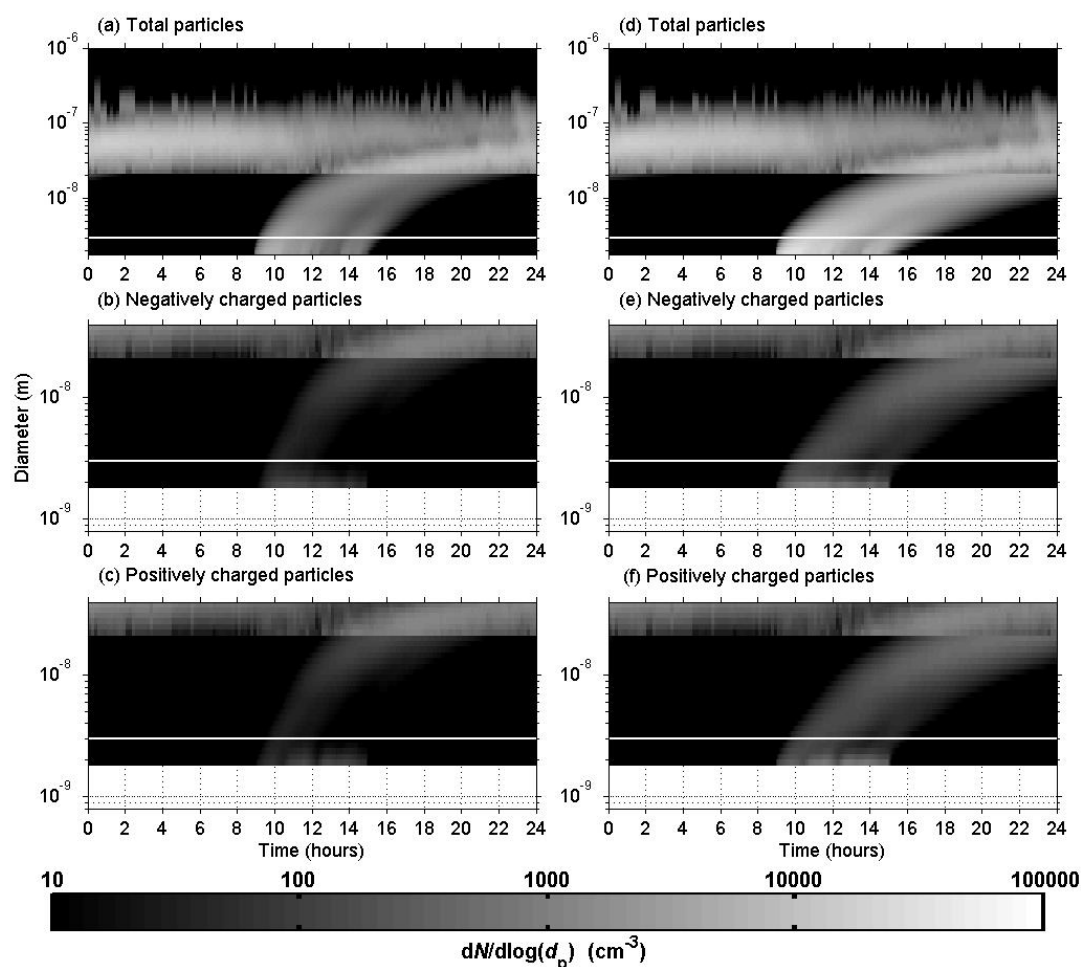
Figure 2. Two simulated evolutions of the particle number size distribution for 15 September 2006. The evolution is shown for total (panels a and d), negatively charged (panels b and e) and positively charged particles (panels c and f). In the simulation shown on the left (panels a, b and c) the measured formation rate of the particles used as input in the model was multiplied by a factor of 0.2, and in the simulation shown on the right (panels d, e and f) the measured growth rate of the particles used as input in the model was multiplied by a factor of 0.5.

For one of the days, the comparison was not reasonable due to significant differences in the diameter dependence of the particle number concentration. For the remaining 13 days, the best agreement between

measurements and simulation was usually obtained by multiplying the particle growth rate by a factor of 1 or 2. Factors above unity would suggest that the growth rate obtained from the observations underestimates the real growth rate of the particles during the particular day. In the case of the particle formation rate, the best multiplier ranged from 0.2 to 5 between the different days. Since the simulated concentrations depend on both formation and growth rate of particles, in principle all the combinations of multipliers should be used to get full understanding on the optimal values. Also the comparison between measured and simulated evolutions of particle size distributions should be quantitative to get more precise results. This procedure was not done in this study, as our aim was only to show potential ways to use the model.

CONCLUSIONS

The Ion-UHMA model is capable of simulating the dynamics of charged and neutral particle populations during atmospheric nucleation events, as seen from the observations. By combining the simulations with ion spectrometer and ion-DMPS data from various locations, we should be able to get new insight into very early steps of atmospheric new-particle formation. As an example, the model may be used to estimate the accuracy of the formation and growth rate of the particles determined from the measurements.

ACKNOWLEDGMENTS

REFERENCES

Hari, P., and Kulmala, M. (2005) Station for Measuring Ecosystem-Atmosphere Relations (SMEAR II), *Boreal Env. Res.* 5: 315–322.

Kulmala, M., Vehkamäki, H., Petäjä, T., Dal Maso, M., Lauri, A., Kerminen, V.-M., Birmili, W. and McMurry, P.H. (2004a) Formation and growth rates of ultrafine atmospheric particles: a review of observations, *J. Aerosol Sci.* 35: 143–176.

Kulmala, M., Laakso, L., Lehtinen, K.E.J., Riipinen, I., Dal Maso, M., Anttila, T., Kerminen, V.-M., Horrak, U., Vana, M. and Tammet, H. (2004b) Initial steps of aerosol growth, *Atmos. Chem. Phys.* 4: 2553–2560.

Kulmala, M., and Kerminen, V.-M. (2008) On the formation and growth of atmospheric nanoparticles. *Atmos. Res.* 90, 132-150.

Leppä, J., Kerminen, V.-M., Laakso, L., Korhonen, H., Lehtinen, K., Gagné, S., Manninen, H., Nieminen, M., and Kulmala, M. (2009) Ion-UHMA: a model for simulating the dynamics of neutral and charged aerosol particles, *Boreal Env. Res.* 14. [In press].

Manninen, H.E., Nieminen, T., Riipinen, I., Yli-Juuti, T., Gagné, S., Petäjä, T., Asmi, E., Aalto, P.P., Kerminen, V.-M. and Kulmala, M. (2009) Charged and total particle formation and growth rates during EUCAARI 2007 campaign in Hyytiälä. *Atmos. Chem. Phys. Discuss.* 9: 5119–5151.

Mirme, A., Tamm, E., Mordas, G., Vana, M., Uin, J., Mirme, S., Bernotas, T., Laakso, L., Hirsikko, A. and Kulmala M. (2007) A wide-range multi-channel Air Ion Spectrometer. *Boreal Env. Res.* 12: 247–264.

Nieminen, T., Manninen, H.E., Sihto, S.-L., Yli-Juuti, T., Mauldin, R.L.III, Petäjä, T., Riipinen, I., Kerminen, V.-M. and Kulmala M. (2009) Connection of sulphuric acid to atmospheric nucleation in boreal forest. *Environ. Sci. Technol.* 43. [In press].

Tammet, H. (2006) Continuous scanning of the mobility and size distribution of charged clusters and nanometer particles in atmospheric air and the Balanced Scanning Mobility Analyzer BSMA. *Atmos. Res.*, 82, 523-535.

RECENT RESEARCH ACTIVITIES AT THE PUIJO SEMI-URBAN MEASUREMENT STATION

A. LESKINEN[1], H. PORTIN[1], M. KOMPPULA[1], P. MIETTINEN[2], H. LIHAVAINEN[3], J. HATAKKA[3]
A. LAAKSONEN[2,3] and K. E. J. LEHTINEN[1,2]

[1]Finnish Meteorological Institute, Kuopio Unit, P.O. Box 1627, FI-70211 Kuopio, Finland
[2]Department of Physics, University of Kuopio, P.O. Box 1627, FI-70211 Kuopio, Finland
[3]Finnish Meteorological Institute, Research and Development, P.O. Box 503, FI-00101 Helsinki, Finland

Keywords: Aerosol-cloud interaction, Measurements, Urban aerosols

INTRODUCTION

Atmospheric aerosol particles are known to affect the climate both directly, by scattering and absorbing energy, and indirectly through cloud formation and cloud optical properties. The effect of aerosols on the climate is cooling but still with a great uncertainty (IPCC, 2007). In order to reduce this uncertainty, better climatic model estimations are needed, and for development of the climatic models, more experimental data are needed.

One important factor in model estimations are the aerosol-cloud interactions, especially activation of the fine particles into cloud droplets. These phenomena can be studied e.g. by carrying out aircraft measurements in clouds. However, aircraft measurements are relatively short-term, complex, and expensive, and they require instruments with very fast time resolution.

For long-term measurements, stationary ground-based measurement are preferred. This can be done at locations, which are at least at times surrounded by clouds. These kinds of locations are, for example, the GAW (Global Atmospheric Watch) stations at Pallas in Finland (Hatakka et al., 2003) and at Jungfraujoch in Switzerland (Baltensperger et al., 1997). Similar aerosol and cloud research was started in Kuopio, Finland, on the top of an observation tower at Puijo, in 2005. The measurements at Puijo produce data from a semi-urban environment for aerosol-cloud interaction studies and e.g. for particle formation studies (Leskinen et al., 2009).

METHODS

The Puijo measurement station (62°54'32" N, 27°39'31" E) is on the top of an observation tower, 306 m above sea level and 224 m above the surrounding lake level. The tower is a 75 m high building on the Puijo hill, approximately 2 km NW of the center of Kuopio. Kuopio (population 92 000) is located 330 km NE from Helsinki, the capital of Finland, on a peninsula surrounded by Lake Kallavesi (82 m above sea level).

The surroundings of Kuopio belong to the southern boreal climatic zone and is characterized by forests with conifer (mostly pine and spruce) and deciduous (mostly birch) trees, an undulating terrain with rocky soil and moderate height hills, and lots of long lakes in the northwest-southeast direction. The vast lake district acts as a heat storage and increases the nightly temperatures in the summers, thus lengthening the growing period.

The most significant local sources are traffic on highways (national/European highway 5/E63 and national highway 17), the local traffic in Kuopio, and point sources, such as a district heating plant 3 km south of Puijo and a pulp mill 5 km NE of Puijo.

Our research groups at the Finnish Meteorological Institute and the University of Kuopio established the station in 2005 and instrumented it for continuous measurements of aerosol particles, cloud droplets, weather parameters and trace gases. We measure the weather parameters (temperature, relative humidity,

atmospheric pressure, wind speed and direction, and present weather including visibility and rain intensity and type), the aerosol size distribution (size ranges of 7–800 nm and 0.25–32 µm) and total number concentration, the aerosol optical properties (light absorbing and scattering coefficient), the cloud droplet size distribution (size range of 3–50 µm), and concentrations of nitrogen oxides (NO_x), ozone (O_3) and sulphur dioxide (SO_2). We also have a weather camera on the roof for verification of cloudy moments.

The instruments for measurement of the meteorological parameters and cloud droplets are located on the top roof of the Puijo observation tower, while the aerosol and trace gas instruments are located inside. We draw the samples to the instruments through two parallel sampling lines, one with a PM10 inlet followed by a PM2.5 cyclone, called an interstitial particle inlet and sampling line, and the other with a heated inlet and heated snow-hood, called a total air inlet and sampling line. We use the total air inlet in order to dry the cloud droplets up to 40 µm in size (Weingartner et al., 1999). We measure the aerosol size distribution from both the interstitial particle and the total air sampling line in 12-minute cycles.

In addition to the continuous measurements at Puijo, we have organized there three intensive measurement campaigns in 2006–2008. In these campaigns we used an aerosol mass spectrometer for aerosol chemical composition studies, a cloud condensation nuclei counter for cloud droplet activation studies and different tandem differential mobility analyzers for aerosol hygroscopicity and organic compound affinity studies, and collected cloud water for ionic analysis.

Closely related to the Puijo measurement station is the automatic weather station (AWS) at the University of Kuopio at Savilahti, 2 km southwest of Puijo and 87 m above sea level. The Kuopio Savilahti AWS belongs to the FMI weather observation network and is used for automatic weather observation including also solar irradiation and flux measurements. The AWS collects data every 10 minutes and the measurements at Savilahti have been continuous since June 2005.

RESULTS

The aerosol number concentration at Puijo has a clear annual variation (Figure 1a), with a long-time average (hourly concentrations) of 2040 cm^{-3} (range 34–26260 cm^{-3}). The seasonal averages were 2870, 2240, 1090, and 1310 cm^{-3} in the spring (March–May), summer (June–August), autumn (September–November), and winter (December–February), respectively. We found that there are peaks in the aerosol concentration with northeasterly and southerly winds (Figure 1b). We suggest that emissions of the pulp mill and the district heating plant northeast and south of Puijo, respectively, increase the average aerosol concentration. For comparison, the long-time average of hourly aerosol number concentrations was 700 cm^{-3} at the Pallas background station (Komppula et al., 2003), and 2220 cm^{-3} and 3210 cm^{-3} at a Boreal forest region in Hyytiälä and at a Baltic background station in Utö, respectively (Dal Maso et al., 2008). The seasonal averages of the aerosol number concentration in Utö were 3315, 2789, 1830 and 1424 cm^{-3} in the spring, summer, autumn, and winter, respectively (Engler et al., 2007). Further overall results, e.g. about meteorology and gas concentrations can be found in Leskinen et al. (2009).

The clouds at Puijo had an average droplet concentration and liquid water content of 138 cm^{-3} and 0.039 g m^{-3}, respectively. The median cloud droplet diameter ranged from 5 to 15 µm. The droplet concentration was highest in the autumn and lowest in the spring. It increased with the aerosol concentration and was inversely proportional to the average droplet diameter, which is similar to some previous studies (Vong and Covert, 1998; Twohy et al., 2005). More about the observations of aerosol-cloud interactions at Puijo is given in Portin et al. (2009).
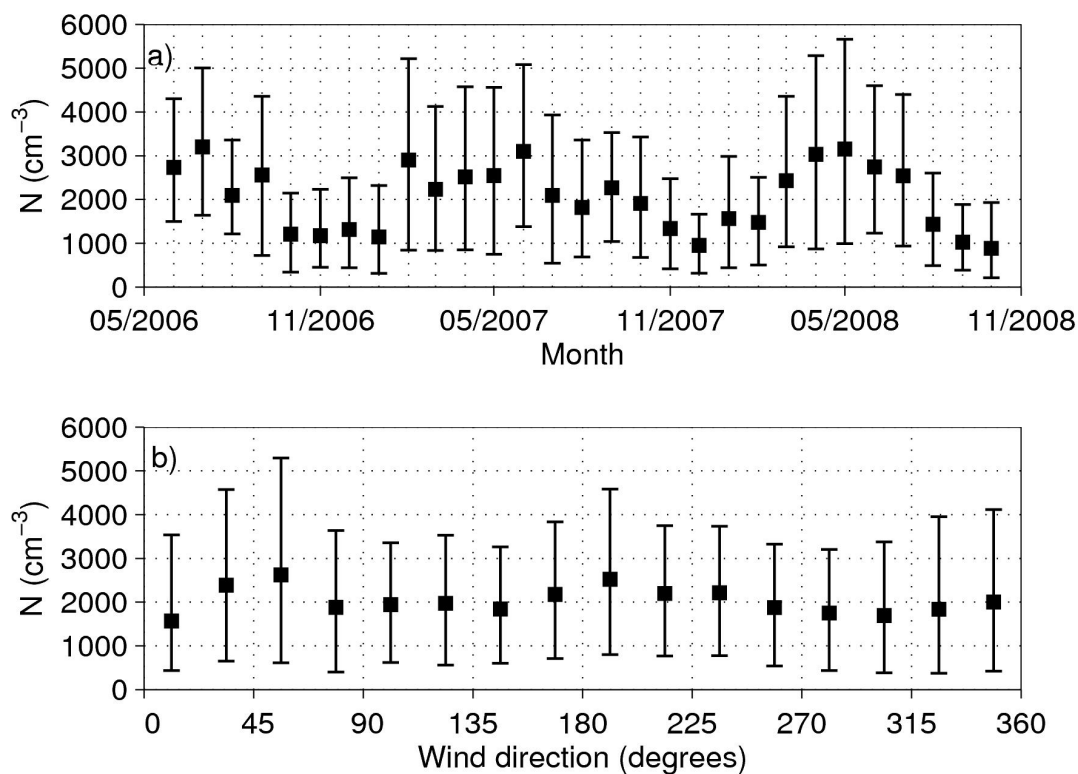
Figure 1. a) The monthly average of aerosol number concentration at Puijo. b) The average aerosol number concentration as a function of wind direction at Puijo. The error bars indicate the concentration range between the 10th and 90th percentiles of the concentration values.

CONCLUSIONS

Even though we have not, so far, been able to distinguish the different cloud types from each other by only looking at the data, we can conclude that Puijo tower is a very good place to gather experimental data on cloud formation. Besides the high enough location, the surroundings are different in each side of the tower. There are distinct sectors for cleaner and more polluted air, which enables us to investigate the effect of local emission sources on aerosol and cloud properties at Puijo. In addition to cloud experiments, we can use the Puijo measurement station for studies of particle formation, which we also observed frequently.

Furthermore, comparison of long-time averages between Puijo and the background measurement sites gives valuable, and so far unique, information on the effect of urban aerosols on cloud formation, as such stationary measurement sites are rare worldwide.

ACKNOWLEDGEMENTS

REFERENCES

Baltensperger, U., Gäggeler, H. W., Jost, D. T., Lugauer, M., Schwikowski, M., Weingartner, E. and Seibert, P. (1997) Aerosol climatology at the high-alpine site Jungfraujoch, Switzerland. *J. Geophys. Res.* 102, 19707-19715.

Dal Maso, M., Hyvärinen, A., Komppula, M., Tunved, P., Kerminen, V.-M., Lihavainen, H., Viisanen, Y., Hansson, H.-C. and Kulmala, M. (2008) Annual and interannual variation in boreal forest aerosol particle number and volume concentration and their connection to particle formation. *Tellus* 60B, 495-508.

Engler, C., Lihavainen, H., Komppula, M., Kerminen, V.-M., Kulmala, M. and Viisanen, Y. (2007) Continuous measurements of aerosol propertiesat the Baltic Sea. *Tellus* 59, 728-741.

Hatakka, J., Aalto, T., Aaltonen, V., Aurela, M., Hakola, H., Komppula, M., Laurila, T., Lihavainen, H., Paatero, J., Salminen, K. and Viisanen, Y. (2003) Overview of the atmospheric research activities and results at Pallas GAW station. *Boreal Env. Res.* 8, 365-383.

IPCC (2007) Summary for Policymakers. In: *Climate Change 2007: The Physical Science Basis. Contribution of Working Group I to the Fourth Assessment Report of the Intergovernmental Panel on Climate Change* [Solomon, S., D. Qin, M. Manning, Z. Chen, M. Marquis, K. B. Averyt, M. Tignor and H.L. Miller (eds.)]. Cambridge University Press, Cambridge, United Kingdom and New York, NY, USA.

Komppula, M., Lihavainen, H., Hatakka, J., Paatero, J., Aalto, P., Kulmala, M. and Viisanen, Y. (2003) Observations of new particle formation and size distributions at two different heights and surroundings in subarctic area in northern Finland. *J. Geophys. Res.* 108(D9), 4295.

Leskinen, A., Portin, H., Komppula, M., Miettinen P., Arola, A., Lihavainen, H., Hatakka, J., Laaksonen, A. and Lehtinen, K. E. J. (2009) Overview of the research activities and results at Puijo semi-urban measurement station. *Boreal Env. Res.*, in press.

Portin, H. J., Komppula, M., Leskinen, A. P., Romakkaniemi, S., Laaksonen, A. and Lehtinen, K. E. J. (2009) Observations of aerosol-cloud interactions at the Puijo semi-urban measurement station. *Boreal Env. Res.*, in press.

Twohy, C. H., Petters, M. D., Snider, J. R., Stevens, B., Tahnk, W., Wetzel, M., Russell, L. and Burnet, F. (2005). Evaluation of the aerosol indirect effect in marine stratocumulus clouds: droplet number, size, liquid water path, and radiative impact. *J. Geophys. Res.* 110, D08203.

Vong, R. J. and Covert, D. S. (1998) Simultaneous observations of aerosol and cloud droplet size spectra in marine stratocumulus. *J. Atmos. Sci.* 55, 2180-2190.

Weingartner, E., Nyeki, S. and Baltensperger, U. (1999) Seasonal and diurnal variation of aerosol size distributions $(10 < D < 750\ nm)$ at a high-alpine site (Jungfraujoch 3580 m asl). *J. Geophys. Res.* 104, 26809-26820.

ATMOSPHERIC SUB-3 NM CLUSTER MEASUREMENTS AND ANALYSIS BASED ON PH-CPC

L. LIAO, M. SIPILÄ, K. LEHTIPALO, I. RIIPINEN and M. KULMALA

Department of Physics, P.O. Box 64, FI-00014, University of Helsinki, Finland

Keywords: Atmospheric cluster; nucleation; monoterpene; PH-CPC

INTRODUCTION

Atmospheric clusters are the embryos of new aerosol particles. However, the sources and formation mechanisms of atmospheric clusters are still poorly understood, because no commercial instrument has the capability to directly detect neutral clusters below 3 nm. Recently, several breakthroughs in instrument development have been progressed in laboratory to monitor atmospheric sub-3 nm clusters. The Pulse Height Condensation Particle Counter (PH-CPC) provides a means to detect these clusters. Sipilä et al. (2008) laboratorial verified the detection ability of a modified PH-CPC to monitor atmospheric sub-3nm clusters.

In this work, to investigate the possible sources and formation mechanisms of atmospheric clusters, we performed a continuous field measurements with the PH-CPC, and then we conducted several comparisons between the sub-3 nm cluster concentrations measured by the PH-CPC and two datasets of atmospheric conditions or gases which may have potential influence on the formation of atmospheric clusters: (1) estimated concentrations of oxidation products of monoterpenes (MT), and (2) sub-3 nm ion cluster concentrations.

METHODS

The field measurements were conducted during 8.3.2007 -- 26.6.2007 at the SMEAR II (Station for Measuring Forest Ecosystem - Atmosphere Relations) station, which is located in the Hyytiälä Forestry Station of the University of Helsinki (61°51'N, 24°17'E). The PH-CPC was placed inside a small cottage. The inlet tube of the PH-CPC was drilled through the wall, which was about 50 cm long outside the wall and about 2 meters above the ground. The PH-CPC worked continuously day and night.

MT concentrations were measured by Proton-Transfer-Reaction Mass Spectrometry (PTR-MS) (see de Gouw and Warneke, 2007). Ion cluster concentrations were measured by Balanced Scanning Mobility Analyzer (BSMA) (see Tammet, 2004).

The estimated oxidation product concentrations of MT were defined by the following method: by assuming a steady state and that the oxidation rate of MT equals to the rate of oxidation products of MT condensing on the aerosol particles, the first order oxidation products of MT by ozone are given by

$$MT_{O_3} = \frac{k[MT][O_3]}{CS}$$

(1)

where k is the chemical reaction constant and its values is $5.83 \cdot 10^{-17}$ s^{-1} (see Rinne et al., 2007); CS is condensation sink (see e.g. Kulmala et al., 2001), which was determined from the data measured by Different Mobility Particle Sizer (DMPS).

RESULTS

Figure 1 (a) illustrates the total sub-3 nm cluster number concentrations versus the estimated concentrations of ozonolysis products of MT in May, 2007, Hyytiälä. It can be seen that the estimated concentrations of oxidized MT are between 10^7 and 10^9 cm^{-3}. From the figure, we can see some correlations between cluster concentrations and oxidized MT concentrations both at daytime and

nighttime. The correlation coefficients are 0.21 during the day and 0.18 during the night, and the p-values are $9.9 \cdot 10^{-9}$ and $7.9 \cdot 10^{-4}$, respectively. The correlations are not strong, but the existent correlations are significant, since the p-values are both small.

Figure 1 (b) depicts the relative frequency of correlation coefficients between sub-3 nm cluster concentrations and estimated concentrations of ozonolysis products of MT from March to June, 2007. In the figure, it is clear that 28% days have the daily correlation coefficient bigger than 0.5, 24% days have the daily correlation coefficient between 0.2 and 0.5, and 21% days show slight correlation having the correlation coefficient between 0 and 0.2. The rest of days show a total anti-correlation, which are 27% of the total 88 days. The white bar representing the correlation coefficients at daytime almost show the same distribution as daily correlation coefficients. However, the black bar illustrating the correlation coefficients at nighttime give a much higher percentage of correlation coefficients bigger than 0.5, which is 50% days. The days showing a correlation coefficient bigger than 0.5 at nighttime have been further checked. These days were randomly distributed and almost equably presented during the whole field measurement period.
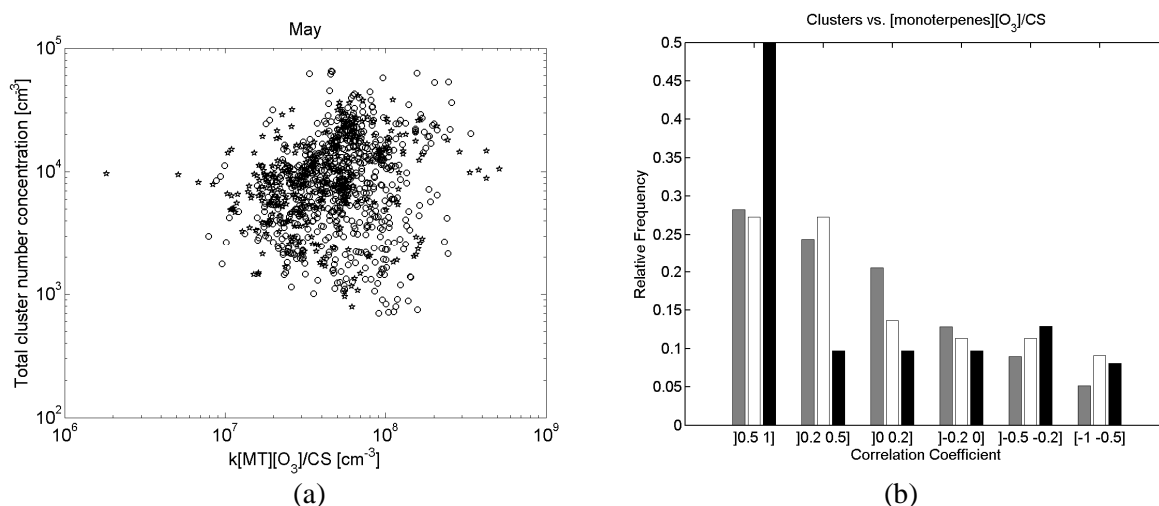
Figure 1. (a) Total cluster number concentration versus the estimated concentration of ozonolysis products of MT in May, 2007, Hyytiälä. The circle marks represents daytime; the star marks indicates nighttime. (b) Relative frequency of correlation coefficients between cluster concentrations and estimated concentrations of ozonolysis products of MT during the whole measurement period. The grey bar represents the whole day, white bar indicates the daytime, and black bar specifies nighttime.

Figure 2 represents the total sub-3 nm cluster number concentrations versus the positive ion cluster concentrations (a) and negative ion cluster concentrations (b) in May, 2007, Hyytiälä. In both figures, the concentrations of positive and negative ion clusters at daytime and at nighttime are almost of the same order of magnitude from several hundreds to thousands cm^{-3}. The total cluster concentration covers much wider order of magnitude. Therefore, the amount of ion clusters only accounts for small percentage of the total cluster concentrations in most of the days. The correlation coefficients between the total sub-3 nm clusters and positive ion clusters are 0.34 at daytime and 0.23 at nighttime in Figure 2 (a), and the correlation coefficients between the total sub-3 nm clusters and negative ion clusters are 0.35 at daytime and 0.24 at nighttime in Figure 2 (b), respectively.
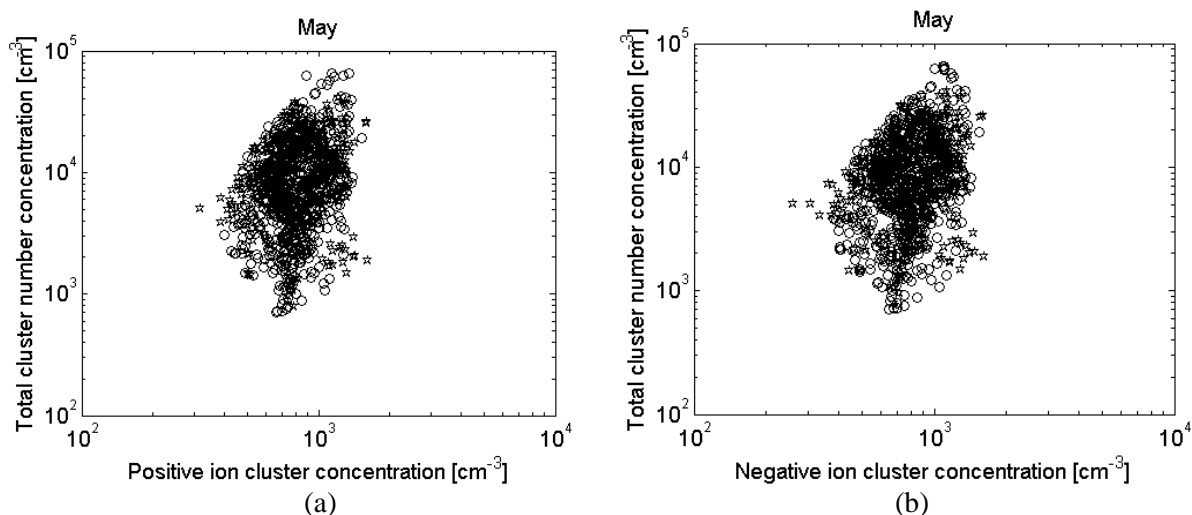
Figure 2. (a) The total cluster number concentration versus the positive ion cluster number concentration and (b) the total cluster number concentration versus the negative ion cluster number concentration during May, 2007, Hyytiälä. The circle marks represents daytime; the star marks indicates nighttime.

CONCLUSIONS

Among the comparisons between the sub-3 nm cluster concentrations and the two datasets, MT oxidized by ozone show some correlations with sub-3 nm clusters; this suggests that the ozonolysis products of MT may influence the formation of clusters, especially during the night time. Ion clusters show some correlations with the total sub-3 nm clusters, which might indicate that ion clusters are partly the sources of atmospheric clusters. The results, however, are not conclusive, and further studies are needed to find the magnitude of these interconnections.

ACKNOWLEDGMENTS

REFERENCES

1. de Gouw, J. and Warneke, C. Measurements of volatile organic compounds in the earth's atmosphere using proton-transfer-reaction mass spectrometry. *Mass Spectrom. Reviews*, 26, 223-257 (2007).
2. Kulmala, M., Dal Maso M., Makela J.M., Pirjola L., Vakeva M., Aalto P., Miikkulainen P., Hameri K., O'Dowd C.D. On the formation, growth and composition of nucleation mode particles. *Tellus B* 53 (4), 479-490 (2001).
3. Rinne, J., Taipale, R., Markkanen, T., Ruuskanen, T. M., Hellen, H., Kajos, M. K., Vesala, T., and Kulmala, M. Hydrocarbon fluxes above a scots pine forest canopy: measurements and modeling. *Atmos. Chem. Phys.*, 7, 3361-3372 (2007).
4. Sipilä, M., Lehtipalo, K., Kulmala, M., Petäjä, T., Junninen, H., Aalto, P. P., Manninen, H. E., Vartiainen, E., Riipinen, I., Kyrö, E.-M., Curtius, J., Kürten, A., Borrmann, S., and O' Dowd, C. D. Applicability of condensation particle counters to measure atmospheric clusters. *Atmos. Chem. Phys. Discussions*, 8, 4373-4405 (2008).
5. Tammet, H. Balanced scanning mobility analyzer, BSMA. In *Nucleation and Atmospheric Aerosols 2004, 16th International Conference*, Japan: Kyoto UniversityPress, 2004, pp. 294-297.

DIRECT AND FIRST INDIRECT RADIATIVE EFFECT BY NATURAL BOREAL FOREST AEROSOLS

H. LIHAVAINEN[1], V.-M. KERMINEN[1], P.TUNVED[2], V. AALTONEN[1], A. HYVÄRINEN[1] AND Y. VIISANEN[1]

[1]Finnish Meteorological Institute P.O. Box 503, FIN_00101, Helsinki, Finland
[2]ITM/Stockholm University, Svante Arrhenius Väg 8c, SE-10691, Sweden

Keywords: Boreal forest; Tropospheric aerosols; Radiative forcing

INTRODUCTION

Despite considerable progress in both atmospheric models and observational systems, large uncertainties in the direct radiative forcing caused by anthropogenic aerosols still exist, (Yu et al., 2006; Bellouin,et al., 2008; Quaas, et al. 2008). A prerequisite for estimating the aerosol radiative forcing is to determine the radiative effects by natural aerosol particles. In this regard, the main emphasis has traditionally been put on sea-salt and dust particles, as well as on sulfate particles of either volcanic or marine origin (Satheesh, et al., 2005). Other potentially important natural aerosol particle types are primary biogenic particles and secondary organic aerosols (SOA) originating from biogenic emissions of volatile organic compounds (Andreae et al., 2008).

Biogenic SOA gives a significant, yet poorly-constrained contribution to the global natural aerosol burden (Hoyle et al., 2007). To our knowledge, however, no observationally-based estimate on the direct radiative effect by biogenic SOA has been made so far. Globally, this is due to the small size of these particles, which makes it very difficult to detect them and to separate them from other submicron particles using satellite retrievals (Kaufman et al., 2005). Regionally, the main difficulty arises from the fact that biogenic SOA is frequently mixed with other aerosol components. In this work, our main objective is to provide an estimate on the direct radiative effect caused biogenic SOA due to boreal forest emissions and to compare it with the corresponding first indirect radiative effect. Our analysis relies on long-term aerosol measurements conducted at a site, in which air masses loaded dominantly by biogenic SOA particles can be confidently isolated from air masses having a significant contribution from other aerosol types.

METHODS

The analysed data is measured at Pallas Global Atmosphere Watch Stations Sammaltunturi measurement site (67°58'N, 24°07'E, 560 m above the sea level). The station is hosted by Finnish Meteorological Institute. Detailed description of the measurement site can be found in Hatakka et al. (2003). The scattering and backscattering coefficients were measured with an integrating nephelometer (model 3563, TSI, Inc., St. Paul, Minnesota). The particle number size distribution in the range 7–500 nm was measured with a Differential Mobility Particle Sizer (DMPS).

The methodology used here is similar to that applied by Tunved et al. (2006). Here, we used air mass back trajectories calculated with FLEXTRA trajectory model (e.g. Stohl and Seibert, 1998) and data from European Center for Medium-Range Weather Forecasts (ECMWF). The trajectories were calculated for every three hours. Since the studied air masses should avoid going through areas with potential anthropogenic influence, we accepted only trajectories coming from the sector ≥ 66 °N and ≤ 30 °E (see Figure 1). This selection should rule out anthropogenic sources in southern Scandinavia and Kola Peninsula in Russia. Only the trajectories spent more than 80 % of their travel time during the last 72 hours in this sector were taken to the analysis. For each trajectory that passed the above criteria, the time spend over land was calculated. The average for each number of hours over land was taken and used in the analyses if there were more than 7 trajectories in specific number of hours. Data from the years 2000–

2006 for the period May-September (corresponding to the days of year in the range 120–270) were analyzed.
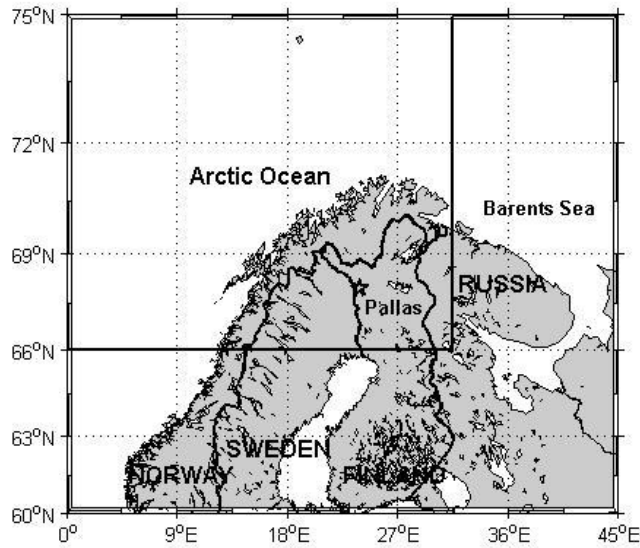
Figure 1. Location of the measurement site and the sector (black lines), from which the trajectories used in the analysis originate.

The cloud fraction was calculated using ceilometer (Vaisala, model CT25K) data. The ceilometer measures the height of cloud layers and determines the cloud fraction over a period of time. The boundary layer height was estimated using the same model as used in the trajectory calculations (ECMWF). The resolution of the model is 1°. We used the boundary layer height estimated at 68 °N and 24°E.

The direct radiative effect (DRF) at the top of the atmosphere (TOA) was calculated from the following formula (Anderson et al, 1999)
:

$$\text{DRE} = S_{rad}\, \tau\, (1 - C_c) T_{at}^2 (1 - R_s)^2 \left[2R_s \frac{1 - \omega}{(1 - R_s)^2} - \beta \omega \right], \tag{1}$$

where S_{rad} (W m^{-2}) is the incident solar radiation, τ is the aerosol optical depth, C_c is the fractional cloud cover, T_{at} (=0.76) is the atmospheric transmissivity, R_s is the surface albedo, ω is the aerosol single scattering albedo, and β is the average upscatter fraction. The corresponding first indirect radiative effect (IRE) can be calculated from the formula (Chameideset al., 2002) $\text{IRE} = - S_{rad} C_c T_{at}^2 \Delta A$, where ΔA is the change in cloud albedo caused by aerosol driven perturbation in the number concentration of cloud droplets.

RESULTS

Figure 2 shows how various aerosol optical properties depend on the time that the measured air masses have spent over land areas. In a broad sense, this figure can be though to represent the typical time evolution of an originally marine aerosol system after it enters the boreal forest region. Visually, the average value of the scattering coefficient, σ_{550}, changes little during the first 15-20 hours of air mass transport time over the land, after which a clear increase with increasing time can be observed. Contrary to this, the Ångström exponent, $å$, first increases significantly and then remains at about a constant level. The backscatter ratio, b, decreases slowly but quite steadily over the time spent over land.
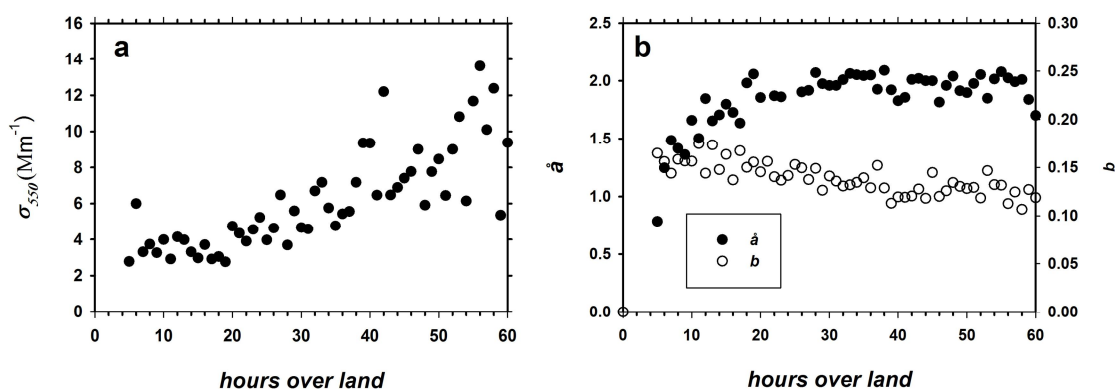
Figure 2: Panel a: Scattering coefficient, σ_{550}, measured at 550 nm. Panel b: Ångström exponent, $\mathring{a}$, calculated based on values of σ at 450 and 550 nm, along with the backscattering fraction, b. The data covers the days of year 120-270 during the period 2000-2006. All quantities have been plotted as function of time the air masses have spent over land prior arriving to the measurement site.

Given the uncertainties in the background value of σ_{550}, we estimate that the increase in σ_{550} due to biogenic SOA lies somewhere in the range 7–12 Mm^{-1} for air masses spent couple of days over the boreal forest region in the northern part of Nordic countries. Using typical values for parameters at Pallas and equation (1), the resulting DRE at TOA is in the range of $-(0.07–0.15)$ W m^{-2}. The above estimate leads to annually-averaged global DRE of $-(0.001–0.003)$ W m^{-2}, when noting that boreal forests comprise between about 3 and 4% of the Earth's surface area

In order to calculate the first indirect radiative effect (IRE) associated with boreal forest emissions, we need to estimate how much the cloud droplet number concentration increases due to these emissions. Komppula et al. (2005) showed that the average minimum "dry" diameter of activating cloud droplets is about 80 nm at our measurement site. Figure 3 depicts how the number concentration of particles larger than 65, 80 and 100 nm increases when air is being transported over the land before entering our measurement site. Over two days of air mass transport time, the average enhancement factor in particle number concentrations is about 7-8 for all these three size categories. The corresponding enhancement factor in cloud droplet number concentrations may slightly lower than this value, since the minimum cloud droplet activation diameters tends to increase with an increasing aerosol load (e.g. Komppula et al., 2005; McFiggans et al., 2006). Anyway, we may calculate that an enhancement in cloud droplet number concentrations by a factor of 4-8 induces an increase in cloud albedo, ΔA, of about 0.08-0.16, depending on how thick the clouds are (Platnick and Twomey, 1994). By noting that boreal forest aerosols are expected to influence boundary-layer clouds only, and by taking into account that the average low cloud cover is about 0.2 or slightly below during the April-September period in our study region, we obtain the value of about $-(1.8-3.6)$ W m^{-2} for the IRE at TOA. A corresponding upper-limit estimate for the global IRE by boreal forest aerosols can be calculated to be equal to -0.07 W m^{-2}.

CONCLUSIONS

We estimated that the direct radiative effect (DRE) due to boreal forest aerosols lies in the range $-(0.07–0.15)$ W m^{-2} over our study region during the summer. Lihavainen et al. (2003) and Kurten et al. (2003) brought up the idea that atmospheric new-particle formation associated with biogenic emissions might increase cloud condensation nuclei (CCN) concentrations over boreal forests and thereby contribute to the indirect radiative effect (IRE). More recently, atmospheric CCN production resulting from biogenic emissions has been studied both regionally and globally (Spracklen et al., 2008; Tunved et al., 2008). Both these studies suggest a potentially large impact by biogenic emissions on the CCN budget. Kerminen et al. (2005) estimated the first indirect radiative effect (IRE) due to boreal forest emissions based on nucleation

event statistics and observed cloud microphysical properties, obtaining a value range of $-(0.2–0.9)$ W m^{-2} over the boreal forest zone. The real value of the first IRE is likely to be somewhere between the estimate of Kerminen et al. (2005) and the upper-limit estimate of $-(1.8–3.6)$ W m^{-2} obtained here, since the traditional way of analyzing atmospheric nucleation events tends to underestimate the frequency of nucleation events (Buenrostro et al., 2009). Taken together, it seems very likely that aerosol particles resulting from boreal forest emissions influence the climate system by a factor or ten or even more via their indirect than direct radiative effects.
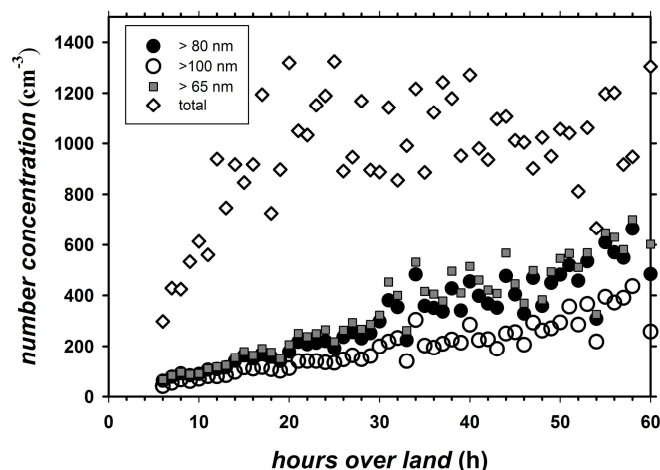
Figure 3: The number concentration of particles >65, 80 and 100 nm in diameter, as well as the total particle number concentration, as function of time that the air masses have spent over land prior arriving to the measurement site. The data covers the days of year 120-270 during the period 2000-2006.

REFERENCES

Anderson, T. L., D. S. Covert, J. D. Wheeler, J. M. Harris, K. D. Perry, B. E. Trost, D. J. Jaffe, and J. A. Ogren (1999), Aerosol backscatter fraction and single scattering albedo: Measured values and uncertainties at a coastal station in the Pacific Northwest, *J. Geophys. Res., 104*, 26,793-26,807.

Anderson, T. L., D. S. Covert, J. D. Wheeler, J. M. Harris, K. D. Perry, B. E. Trost, D. J. Jaffe, and J. A. Ogren (1999), Aerosol backscatter fraction and single scattering albedo: Measured values and uncertainties at a coastal station in the Pacific Northwest, *J. Geophys. Res., 104*, 26,793-26,807.

Andreae, M. O., and D. Rosenfeld (2008), Aerosol-cloud-precipitation interactions. Part 1. The nature and sources of cloud-active aerosols, *Earth-Science Rev., 89*, 13-41.

Bellouin, N., A. Jones, J. Haywood, and S. A. Christopher (2008), Updated estimate of aerosol direct radiative forcing from satellite observations and comparison against the Hadley Centre climate model, *J. Geophys. Res., 113*, D10205, doi:10.1029/2007JD009385.

Buenrostro Mazon, S., I. Riipinen, D. M. Schultz, M. Valtanen, M. Dal Maso, L. Sogacheva, H. Junninen, T. Nieminen, V.-M. Kerminen, and M. Kulmala (2009), Classifying previously undefined days from eleven years of aerosol-particle-size distribution data from the SMEAR II station, Hyytiälä, Finland, *Atmos. Chem. Phys., 9*, 667-676.

Chameides, W. L., C. Luo, R. Saylor, D. Streets, Y. Huang, M. Bergin, and F. Giorgi (2002), Correlation between model-calculated anthropogenic aerosols and satellite-derived cloud optical depths: indication of indirect effect?, *J. Geophys. Res., 107*(D10), 4085, doi:10.1029/2000JD000208.

Hatakka, J., et al. (2003), Overview of the atmospheric research activities and results at Pallas GAW station, *Boreal Env. Res., 8*, 365-384.

Hoyle, C. R., T. Berntsen, G. Myhre, and I. S. A. Isaksen (2007), Secondary organic aerosol in the global aerosol – chemical transport model Oslo CTM2, Atmos. Chem. Phys., 7, 5675-5694

Kaufman, Y. J., O. Boucher, D. Tanre, M. Chin, L. A. Remer, and T. Takemura (2005), Aerosol anthropogenic component estimated from satellite data, *Geophys. Res. Lett., 32*, L17804, doi:10.1029/2005GL023125.

Kerminen, V.-M., H. Lihavainen, M. Komppula, Y. Viisanen, and M. Kulmala (2005), Direct observational evidence linking atmospheric aerosol formation and cloud droplet activation, *Geophys. Res. Lett., 32*, L14803, doi:10.1029/2005GL023130.

Komppula, M., H. Lihavainen, V.-M. Kerminen, M. Kulmala, and Y. Viisanen (2005), Measurements of cloud droplet activation of aerosol particles at a clean subarctic background site, *J. Geophys. Res.,* 110, D06204, doi:10.1029/2004JD005200.

Kurten, T., M. Kulmala, M. Dal Maso, T. Suni, A. Reissell, H. Vehkamäki, P. Hari, A. Laaksonen, Y. Viisanen, and T. Vesala (2003), Estimation of different forest-related contributions to the radiative balance using observations in southern Finland, *Boreal Env. Res., 4*, 275-285.

Lihavainen, H., V.-M. Kerminen, M. Komppula, J. Hatakka, V. Aaltonen, M. Kulmala, and Y. Viisanen (2003), Production of "potential" cloud condensation nuclei associated with atmospheric new-particle formation in northern Finland, *J. Geophys. Res., 108*(D24), 4782, doi:10.1029/2003JD003887.

McFiggans, G. et al. (2006), The effect of physical and chemical aerosol properties on warm cloud droplet activation, *Atmos. Chem. Phys., 6*, 2593-2649.

Platnick, S., and S. Twomey (1994), Determining the susceptibility of cloud albedo changes in droplet concentration with the advanced very high resolution radiometer, *J. Appl. Meteorol., 33*, 334-347.

Quaas, J., O. Boucher, N. Bellouin, and S. Kinne (2008), Satellite-based estimate of the direct and indirect aerosol climate forcing, *J. Geophys. Res., 113*, D05204, doi:10.1029/2007JD008962.

Satheesh, S. K., and K. K. Moorthy (2005) Radiative effects of natural aerosols: A review, *Atmos. Environ., 39*, 2089-2110.

Spracklen, D. V. et al. (2008), Contributions of particle formation to global cloud condensation nuclei concentrations, *Geophys. Res. Lett., 35*, L06808, doi:10.1029/2007GL033038.

Stohl, A., and P. Seibert (1998), Accuracy of trajectories as determined from the conservation of meteorological tracers. *Q. J. R. Meteorol. Soc.*, *125*, 1465-1484.

Tunved, P, H-C. Hansson, V-M. Kerminen, J. Ström, M. Dal Maso, H. Lihavainen, Y. Viisanen, P.P. Aalto, M. Komppula, and M. Kulmala (2006), High natural aerosol loading over boreal forests, *Science, 312*, 261-263

Yu, H. et al. (2006) A review of measurement-based assessments of the aerosol direct radiative

LIGHT SCATTERING BY COATED GAUSSIAN AND AGGREGATE PARTICLES

H. LINDQVIST[1], K. MUINONEN[2], T. NOUSIAINEN[1]

[1] Department of Physics, University of Helsinki, Finland
[2] Observatory, University of Helsinki, Finland

Keywords: light scattering, inhomogeneous, coated particles, discrete-dipole approximation

INTRODUCTION

The rich variety of shapes and structures of natural particles makes the realistic modeling of their optical properties and thus the estimation of their radiative impact very challenging. Atmospheric particles, for instance, are anything but simple: their shapes vary from nearly spherical to faceted and entirely irregular, and the surfaces of the particles are often roughened by ridges and concavities on many scales (Nousiainen (2009)). In addition to nonspherical shapes, the particles often have inhomogeneous compositions. As analytical solutions to light scattering by inhomogeneous, arbitrarily shaped, wavelength-scale particles do not exist, approximate methods must be used and, due to computational considerations, the modeling of natural particles has to be carried out efficiently, yet realistically.

An efficient tool for modifying the shape of an arbitrary particle is introduced by Muinonen and Erkkilä (2007). This concave-hull transformation method is here studied further and applied to the modeling of small-particle inhomogeneity to study light scattering by coated compact and aggregate particles (see also Lindqvist et al. (2009)).

PARTICLE GEOMETRIES

Inhomogeneous small particles are here modeled by the following steps: 1) generating an initial particle which is nonspherical and homogeneous, 2) calculating its concave hull and, 3) choosing a different refractive index for the volume constrained between the concave hull and the surface of the original particle; thus resulting in a coated, inhomogeneous particle.

Two methods are utilized in generating the initial shapes of the particles: ballistic particle-cluster aggregation (BPCA) and the Gaussian random sphere. BPCA is applied to producing clusters of equal-size spheres which, in this study, represent the aggregate particles. Particle shapes generated by this algorithm are random and nonspherical, yet statistically isotropic, but functions of only two parameters: the radius of a single sphere and the number of spheres in the cluster. For the light-scattering studies, we generate 10 and 100-sphere aggregates, ten samples of each to obtain a tentative average over the scattering results.

Compact and nonspherical particle geometries are considered using the Gaussian random sphere method (Muinonen et al. (1996)) for deforming a sphere in a statistically controlled way. This results in a shape where the radial distance of the surface varies as a function of the spherical coordinates θ and φ. The surface is parameterized by a relative standard deviation of the radial distance σ and the power-law index of the covariance function of the logarithmic radial distance ν. Here we adapt a constant value of $\nu = 3.3$ (Muñoz et al. (2007)), while σ is given values 0.05, 0.1, and 0.2.
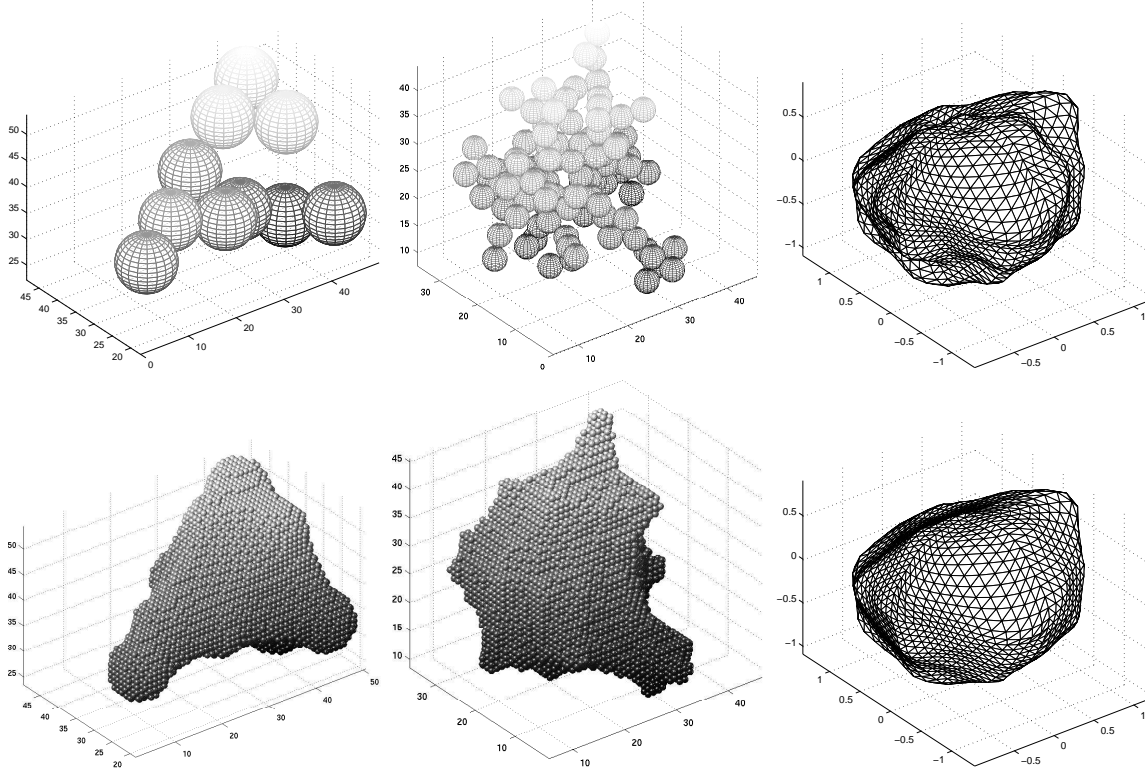
Figure 1: Sample aggregate and Gaussian particles together with their concave-hull transformations. From left to right, the particles are: 10-sphere aggregate, 100-sphere aggregate, and a Gaussian random sphere with $\sigma = 0.2$, $\nu = 3.3$. The initial particle geometries are presented in the upper row, and their concave-hull transformations with scale radius $h = 2$ in the lower row.

For an arbitrary object of equal-volume-sphere radius a_{eq}, the concave hull is obtained by rolling a sphere of radius R over the object: the inner surface formed by the sphere defines the concave hull. A concave coating can then be defined as the volume constrained between the hull and the volume occupied by the original particle. The sole parameter of the transformation is the scale radius $h = R/a_{eq}$. Fig. 1 demonstrates samples of different particle geometries and their concave-hull transformations. In the limits of $h \to 0$ and $h \to \infty$, the concave hull approaches the initial shape of the particle and its convex hull, respectively. The concave hull for an arbitrary object can be computed numerically by volume discretization but, for star-like particles (e.g. Gaussian particles), a faster ballistic approach can also be adapted.

SCATTERING BY GAUSSIAN AND AGGREGATE PARTICLES

Since the small-particle shapes presented above are nonspherical and can be internally inhomogeneous, analytical light-scattering computations cannot be performed. Hence approximate methods must be used, and the discrete-dipole approximation (DDA) is considered the most suitable method for the computations. In DDA, the electromagnetic scattering problem is solved by approximating the volume of the scatterer with small polarizable points, or dipoles, which interact with each other. DDA is an efficient tool in computing scattering by inhomogeneous particles because individual dipoles may have different compositions and, thus, different refractive indices. The scattering computations are here performed using an open-source, Amsterdam implementation of DDA, called ADDA, developed by Yurkin and Hoekstra (2006).

260

The scattered radiation is fully described by a 4×4 scattering matrix $\mathbf{S}$. For unpolarized incident light the matrix element S_{11} describes the intensity of the scattered light and is also known as phase function. We also study the degree of linear polarization for unpolarized incident light, namely the ratio $-S_{12}/S_{11}$, and the depolarization ratio $D = 1 - S_{22}/S_{11}$. For spheres $D = 0$, so depolarization can be used as an indicator of nonsphericity, although the effect is not systematic.

We performed the light-scattering simulations for the coated aggregate and Gaussian particles using volume-equivalent size parameters $(x = 2\pi/\lambda)$ $x = 3.0$, $x = 4.5$, and $x = 6.0$. We studied silicate particles with slightly absorbing ice coatings, and thus used the following complex refractive indices: $m_s = 1.55 + 0.001i$ and $m_i = 1.31 + 0.001i$. The coating volume varied as the scale radius h was given values 0.0, 0.5, and 2.0. The scattering computations were performed in 2080 orientations to approximate random orientation.
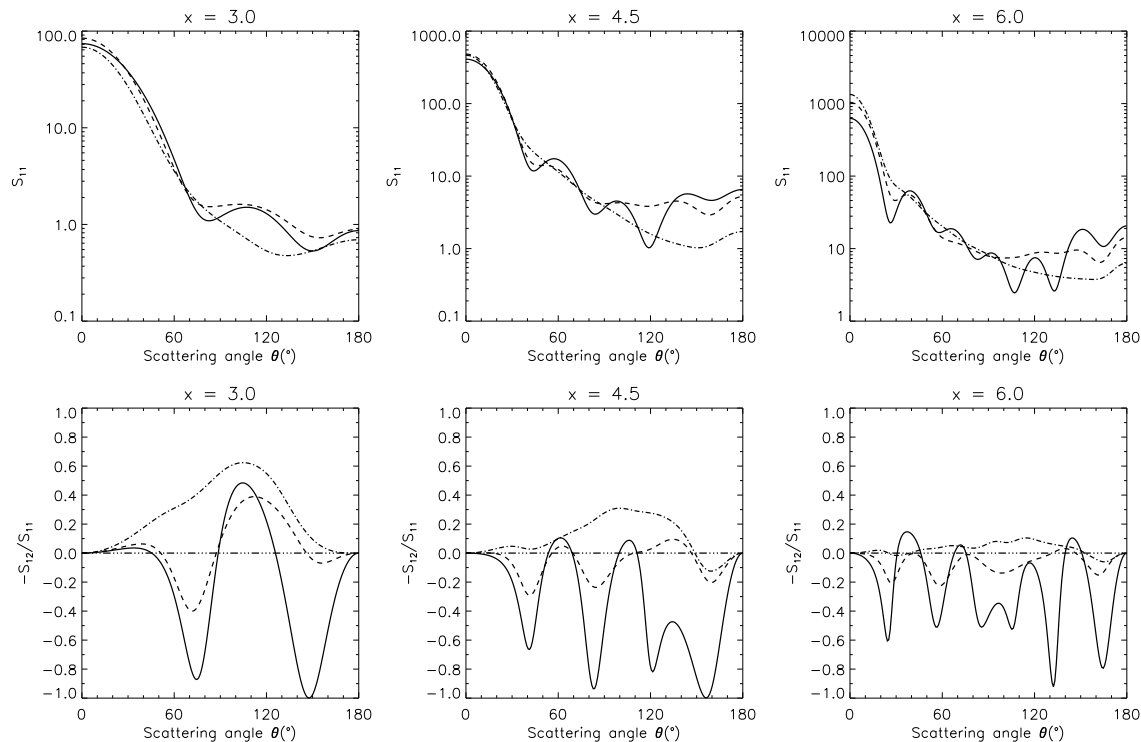
Figure 2: Comparison of the light-scattering results for a coated sphere (solid line), coated Gaussian particle with $\sigma = 0.2$ (dashed line), and coated aggregate of 10 spheres (dash-dotted line).

A comparison of the results for scattering by coated, 10-sphere aggregates and coated Gaussian particles with $\sigma = 0.2$ is presented in Fig. 2. The results of an analytical calculation of scattering by a coated sphere of equal size are also shown. Based on the results, the scattering by coated aggregate particles deviates considerably from scattering by the Gaussian random spheres, especially for the degree of linear polarization of unpolarized incident light. Whereas compact particles generally show net negative polarization, the aggregate particles tend to polarize light positively. An observable similarity between the coated Gaussian particles and coated spheres is that the strong resonant structures characteristic to scattering by spheres in intensity and polarization are visible in scattering by Gaussian random spheres as well, although less pronounced. In the scattering by coated aggregate particles, however, this is not observed. It thus seems that scattering by Gaussian random spheres preserves, to some extent, traces of the spherical original shape of the deformation. The depolarization ratio results for scattering by coated Gaussian particles (Fig. 3), however, show the deviation from the scattering by a sphere.
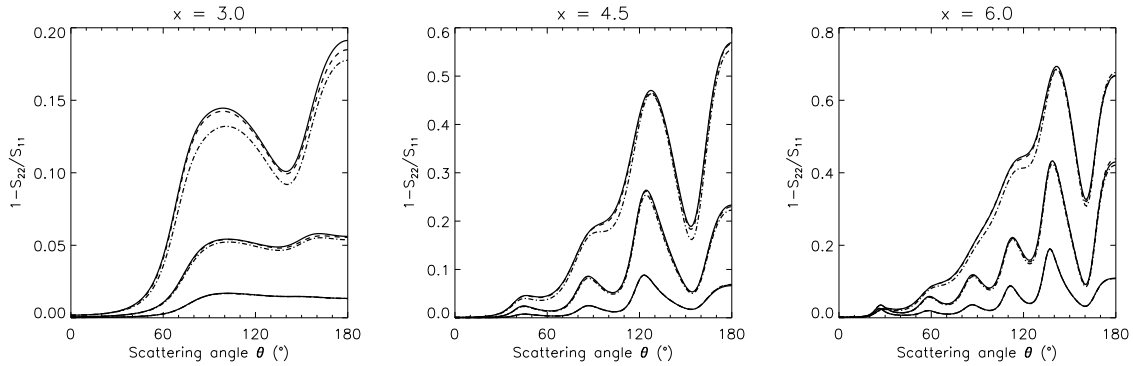
Figure 3: Size and shape dependence of the depolarization ratio of scattering by coated Gaussian particles with varying relative standard deviations σ. The solid, dashed, and dash-dotted lines refer to particles that are uncoated, coated using $h = 0.5$, and coated using $h = 2.0$, respectively. The curves on the top, middle, and bottom in each figure refer to $\sigma = 0.2$, $\sigma = 0.1$, and $\sigma = 0.05$.

One yet unexplained feature is observed in the depolarization results: at large scattering-angle values, depolarization performs systematically a double-lobe feature. This appears regardless of particle size, shape, or coating volume; also for aggregate particles (Lindqvist et al. (2009)). The two maxima and the enclosed minimum move towards the backscattering direction with increasing size parameter. Particle composition affects the height of the maxima and the depth of the minimum, but the phenomenon is, nevertheless, qualitatively similar in all cases studied. The double-lobe feature has been observed previously in light-scattering computations, e.g., by Muinonen and Erkkilä (2007) and Vilaplana et al. (2006), and also in laboratory measurements (Volten et al. (2006)).

CONCLUSION

The concave-hull transformation method for deforming an arbitrary particle has been studied further and applied to Gaussian and aggregate particles, where it has proved to be an efficient tool in adding coatings on the homogeneous particles. The method generally smoothens the surface of the particle but also creates some sharp edges. Moreover, the coatings appear realistic and offer a promising method to study, e.g., light scattering by atmospheric mineral aerosols that easily collect inhomogeneities in their cavities.

In the scattering characteristics, a common feature was observed surprisingly for both the coated Gaussian particles and the coated aggregates of spheres: a double-lobe structure in the depolarization near the backscattering direction. The physical mechanism behind this feature has not yet been uncovered, but it is plausible that it has a connection to the single-scattering mechanisms causing the known backscattering phenomena for intensity and polarization. A profound understanding of the single-scattering mechanisms calls for an in-depth internal-field study in the future.

ACKNOWLEDGMENTS

REFERENCES

Lindqvist, H., Muinonen, K., and Nousiainen, T. (2009). Light scattering by coated Gaussian and aggregate particles. *JQSRT*, in press.

Muinonen, K. and Erkkilä, H. (2007). Scattering of light by concave-hull-transformed Gaussian particles Tenth Conference on Electromagnetic & Light Scattering, Videen, G., Mishchenko, M., Mengüc, M. P. and Zakharova, N. Eds. (Bodrum, Turkey, June 17-22, 2007), 125–128.

Muinonen, K., Nousiainen, T., Fast, P., Lumme, K., and Peltoniemi, J. I. (1996). Light scattering by Gaussian random particles: Ray optics approximation. *JQSRT*, 55:5:577–601.

Muñoz, O., Volten, H., Hovenier, J. W., Nousiainen, T., Muinonen, K., Guirado, D., Moreno, F., and Waters, L. B. F. M. (2007). Scattering matrix of large Saharan dust particles: Experiments and computations. *J. of Geophys. R.*, 112:D13215.

Nousiainen, T. (2009). Optical modeling of mineral dust particles: a review. *JQSRT*, in press.

Vilaplana, R., Moreno, F., and Molina, A. (2006). Study of the sensitivity of size-averaged scattering matrix elements of nonspherical particles to changes in shape, porosity and refractive index. *JQSRT* 100:415–428.

Volten, H., Muñoz, O., Brucato, J. R., Hovenier, J. W., Colangeli, L., Waters, L. B. F. M., and van der Zande, W. J. (2006). Scattering matrices and reflectance spectra of forsterite particles with different size distributions. *JQSRT* 100:429–436.

Yurkin, M. A. and Hoekstra, A. G. (2006). User manual for the discrete dipole approximation code Amsterdam DDA. *http://www.science.uva.nl/research/scs/Software/adda/documentation*

ON THE ROLE OF DIMETHYLAMINE IN SULFURIC ACID-WATER NUCLEATION

VILLE LOUKONEN[1], THEO KURTÉN[1], ISMAEL K. ORTEGA[1], HANNA VEHKAMÄKI[1], AGILIO PADUA[2], KARINE SELLEGRI[3], MARKKU KULMALA[1]

[1]Department of Physics, P.O. Box 64, FI-00014, University of Helsinki, Finland
[2]Department of Chemistry, Université Blaise Pascal, Clermont-Ferrand, 24 avenue des Landais 63177 Aubière, France
[3]Department of Physics, Université Blaise Pascal, Clermont-Ferrand, 24 avenue des Landais 63177 Aubière, France

INTRODUCTION

The key ingredients in new-particle formation through nucleation in tropospheric conditions are currently thought to be sulfuric acid and water. It is also known, based on both experimental and theoretical results, that most of the observed new particle formation events can not be explained by neutral binary sulfuric acid-water nucleation alone. Therefore, atmospheric nucleation mechanisms have been proposed to involve contributions from ions, ammonia or various organic compounds (Korhonen et al., 1999, Kulmala et al., 2000, Anttila et al., 2005). Recent experimental results suggest that neutral pathways dominate over the ion-induced or ion-mediated nucleation channel, at least in boreal forest conditions (Kulmala et al., 2007). The role of ammonia in atmospheric nucleation has also been extensively discussed lately. At the moment, experiments and theoretical calculations are in qualitative agreement, stating that ammonia has an enhancing effect on sulfuric acid-water nucleation (Anttila et al., 2005, Kurtén et al., 2007a, Torpo et al., 2007, Nadykto and Yu, 2007, Ball et al., 1999), but this effect is too small to explain the observed nucleation rates. Clearly, there is a need for some other compounds to explain the experimental observations.

One prominent possibility are amines. Recent studies indicate that amines such as dimethylamine may be more effective than ammonia in enhancing particle formation from nitric acid (Murphy et al., 2007) and organic acids (Barsanti et al., 2008). Dimethlyammonium ($(CH_3)_2NH_2^+$) concentrations in aerosol particles during nucleation event days in boreal forest conditions was observed to be 50 times higher than during non-event days, strongly indicating that dimethylamine was involved in particle formation (Mäkelä et al., 2001). Also, in a recent quantum chemical study involving several different amines possibly present in the atmosphere, it was found that all of them formed significantly more strongly bound structures with sulfuric acid than ammonia. Also, dimethylamine was demonstrated to assist the growth of both neutral and ionic clusters in the H_2SO_4 coordinate, implying that amines are more likely to enhance sulfuric acid-water nucleation than ammonia (Kurtén et al., 2008). In this study we have explicitly investigated the hydration of dimethylamine - containing sulfuric acid clusters using quantum chemical methods, and compared their structures and properties to those of equally hydrated sulfuric acid-ammonia clusters.

METHODS

The calculations were carried out applying a systematic multi-step procedure for quantum chemistry (Ortega et al., 2008) with additional molecular dynamics (MD) simulations. Part of the initial structures were taken from previous studies when available, and using chemical intuition when not. However, as the size of the cluster grows, the number of possible bonding patterns increases rapidly and so the task of finding the most stable conformer for a large cluster becomes very nontrivial. To overcome this inevitable problem of all quantum chemistry cluster studies, we used MD simulations to generate initial guesses for all the structures. This we did with the DL_POLY_2 program (Smith et al., 2002) and a custom-built force field.

Once a fair set of initial guesses (min. 10) for every structure was collected, we optimized the clusters using the SIESTA program (Soler et al., 2002), using the BLYP functional and the DZP basis set with tight convergence criteria to obtain qualitatively reliable structures and vibrational frequencies. For each stoichiometry, several of the most promising (lowest-energy) clusters were then chosen for single-point energy calculations with the TURBOMOLE program (Ahlrichs et al, 1989), using the RI-MP2 method with the aug-cc-pV(T+d)Z basis set. Thermal contributions to the Gibbs free energies were then estimated using the standard harmonic oscillator and rigid rotor approximations, with reference conditions of 298.15 Kelvins and 1 atm. However, as the molecular clusters in nature are far from being rigid and harmonic, we took these physical anharmonicities into account by scaling the calculated vibrational frequencies, since the explicit calculation of anharmonic vibrational frequencies even for a medium size cluster is practically impossible due to extremely high computational cost. The scaling factors were obtained by comparison with the known literature values for the deviation from harmonicity for some of the clusters under study (Kurtén et al., 2007b).

RESULTS AND DISCUSSION

In order to compare the enhancing (nucleation barrier – lowering) roles of dimethylamine and ammonia in sulfuric acid-water nucleation, we have calculated the Gibbs free energies of the addition of one H_2SO_4 molecule to clusters consisting of one sulfuric acid, ammonia or dimethylamine and 0-5 water molecules. These values are also compared to the corresponding free energies for clusters with only sulfuric acid and water. The results are shown in Figure 1.
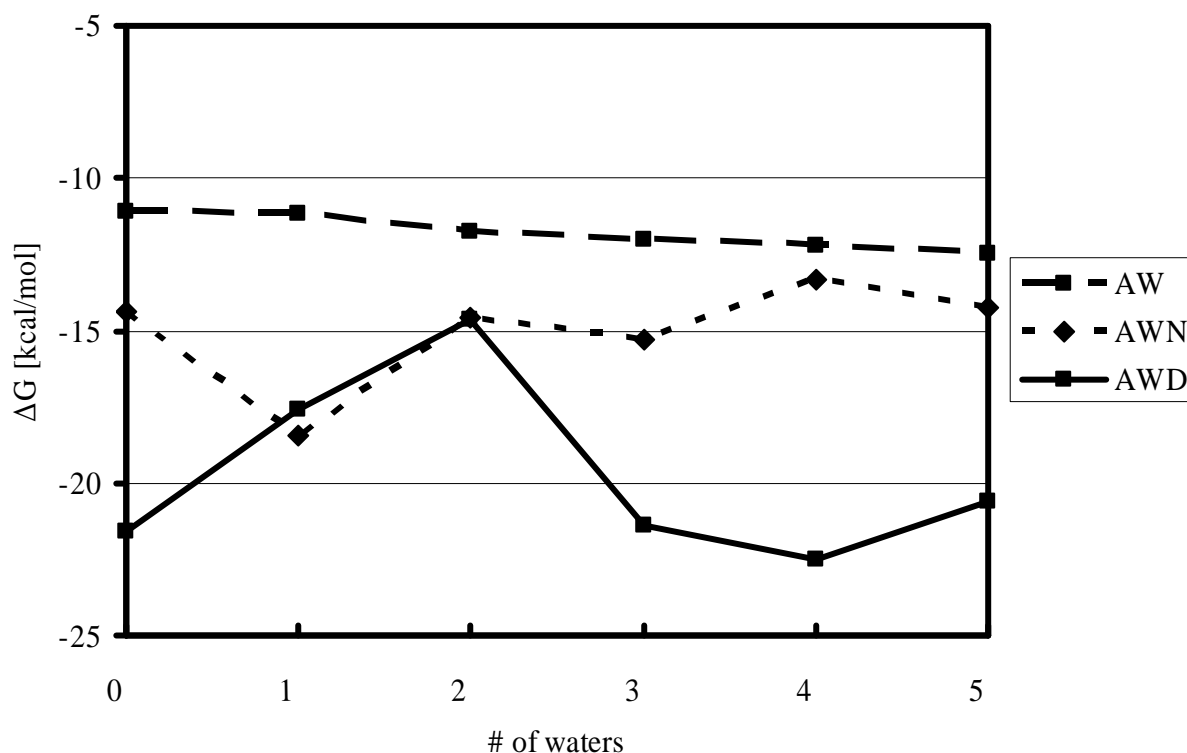
Figure 1. ΔG of addition of one H_2SO_4 molecule to the clusters containing one sulfuric acid and 0-5 water molecules. AW: clusters with only sulfuric acid and water; AWN: clusters containing an ammonia molecule ; AWD: clusters containing a dimethylamine molecule.

As expected from previous studies (Kurtén et al., 2008), in the absence of water molecules dimethylamine enhances the addition of another sulfuric acid to the cluster much more effectively than ammonia. Adding water molecules complicates the picture, as the number of possible bonding patterns in the clusters increases. At first sight, the relative order of the lowest ΔG's for the clusters with one and two water molecules might seem surprising, since the acid addition energies of dimethylamine- and ammonia-containing clusters are predicted to be very similar. The qualitative shape of the curves can, however, be explained by structural factors. The addition of another acid to the cluster containing one sulfuric acid, one ammonia and one water is predicted to promote a proton transfer reaction from one of the acids to ammonia, leading to a much stronger bonding and thus a strongly negative ΔG value. For the clusters containing one water and dimethylamine, a corresponding increase in bonding strength can not take place, as our calculations predict proton transfer to have occurred already for the one-acid case. In addition, since the dimethylammonium ion can only form two hydrogen bonds (whereas the ammonium ion can in principle form four, though in practice usually only three), adding another acid to the dimethylamine - acid - water cluster requires breaking one of the existing amine - water bonds.

In the clusters containing two water molecules, proton transfer already occurs with one sulfuric acid in the presence of both ammonia and dimethylamine, and our calculations predict that addition of another acid does not lead to a second proton transfer, i.e. one of the acids does not dissociate at this hydration level. In contrast, for the two-water clusters without any base molecules, the addition of the second acid causes the first proton transfer reaction, leading to a slight increase in stability for the "plain" sulfuric acid - water clusters, as can be seen from Figure 1. As for the one-water case, acid addition to the dimethylamine clusters is made relatively less favourable by the need to break one of the existing amine - water H-bonds. Thus, all three ΔG values for acid addition to the two-water clusters are relatively similar.

Addition of an acid to the three-water clusters leads to a second proton transfer for the ammonia- and amine-containing structures, again increasing the difference between base-containing and "plain" sulfuric acid clusters. Furthermore, for clusters containing three or more water molecules, the relative advantage (with respect to acid addition) of ammonia-containing clusters due to the greater number of H-bonds formed by NH_4^+ compared to $(CH_3)_2NH_2^+$ has disappeared, as both molecules are fully "saturated" by H-bonds already in the one-acid clusters. Thus, the greater basicity of dimethylamine (which leads to a greater stabilization of the formed ion pairs) is able to dominate the formation energetics, and for extensively hydrated clusters, dimethylamine enhances sulfuric acid addition much more effectively than ammonia.

This pattern is likely to have interesting implications for the relative enhancement of nucleation by amines compared to ammonia as a function of RH. In dry conditions, as well as at high enough RH, enhancement by amines is likely to be important. In contrast, at intermediate-low RH, ammonia can be expected to prevail due to its higher atmospheric concentration.

REFERENCES

Ahlrichs, R., Bär, M., Horn, H., Kölmel, C. (1989) Electronic structure calculations on workstation computers: The program system turbomole, Chem. Phys. Lett. 162, 165-169

Anttila, T., Vehkamäki, H., Napari, I., Kulmala, M. (2005) Effect of ammonium bisulphate formation on atmospheric water-sulphuric acid-ammonia nucleation, Boreal Env. Res. 10, 511-523

Ball, S. M., Hanson, D. R., Eisele, F. L., McMurry, P. H. (1999) Laboratory studies of particle nucleation: Initial results for H2SO4, H2O, and NH3 vapors, J. Geophys. Res. D 104, 23709-23718

Barsanti, K. C., McMurry, P. H., Smith, J. M. (2008) The potential contribution of organic salts to new particle growth, Atmos. Chem. Phys. Discuss .8, 20723-20748

Korhonen, P., Kulmala, M., Laaksonen, A., Viisanen, Y., McGraw, R., Seinfeld, J. H. (1999) Ternary nucleation of H_2SO_4, NH_3, and H_2O in the atmosphere, J. Geophys. Res. 104, 26349-26353

Kulmala, M., Pirjola, L., Mäkelä, J. M. (2000) Stable sulphate clusters as a source of new atmospheric particles, Nature 404, 66-69

Kulmala, M., Riipinen, I., Sipilä, M., Manninen, H., Petäjä, T., Junninen H., Dal Maso, M., Mordas, G., Mirme, A., Vana, M., Hirsikko, A., Laakso, L., Harrison, R. M., Hanson, I., Leung, C., Lehtinen, K. E. J., and Kerminen, V.-M.(2007) Towards direct measurement of atmospheric nucleation, Science, 318, 89-92

Kurtén, T, Torpo, L., Ding, C.-G., Vehkamäki, H., Sundberg, M. R., Laasonen, K., Kulmala, M. (2007a) A density functional study on water-sulfuric acid-ammonia clusters and implications for atmospheric cluster formation, Geophys. Res. 112, D04210

Kurtén, T., Noppel, M., Vehkamäki, H., Salonen, M., Kulmala, M. (2007b) Quantum chemical studies of hydrate formation of H_2SO_4 and HSO_4-, Boreal Environ. Res., 12, 431-453

Kurtén, T., Loukonen, V., Vehkamäki, H., Kulmala, M. (2008) Amines are likely to enhance neutral and ion-induced sulfuric acid-water nucleation in the atmosphere more effectively than ammonia, Atmos. Chem. Phys. 8, 4095-4103

Murphy, S. M., Sorooshian, A., Kroll, J. H., Ng, N. L., Chhabra, P., Tong, C., Surratt, J. D., Knipping, E., Flagan, R. C., Seinfeld, J. H. (2007) Secondary aerosol formation from atmospheric reactions of aliphatic amines, Atmos. Chem. Phys. 7, 2313-2337

Mäkelä, J. M., Yli-Koivisto, S., Hiltunen, V., Seidl, W., Swietlicki, E., Teinilä, K., Sillanpää, M., Koponen, I. K., Paatero, J., Rosman, K., Hämeri, K. (2001) Chemical composition of aerosol during particle formation events in boreal forest, Tellus 53B, 380-393

Nadykto, A. B., Yu, F. (2007) Strong hydrogen bonding between atmospheric nucleation precursors and common organics, Chem. Phys. Lett. 435, 14-18

Ortega, I. K., Kurtén, T., Vehkamäki, H., Kulmala, M. (2008) The role of ammonia in sulfuric acid ion induced nucleation, Atmos. Chem. Phys. 8, 2859-2867

Smith, W., Yong, C. W., Rodger, P. M. (2002) DL_POLY: Application to molecular simulation, Molecular Simulation 28, 385-471

Soler, J. M., Artacho, E., Gale, J. D., Garcia, A., Junquera, J., Ordejon, P., Sanchez-Portal, D. (2002) The SIESTA method for ab initio order-N materials simulation, J. Phys-Condens. Mat. 14, 2745–2779

Torpo, L., Kurtén, T., Vehkamäki, H., Sundberg, M. R., Laasonen, K., Kulmala, M. (2007) Significance of Ammonia in Growth of Atmospheric Nanoclusters, J. Phys. Chem. A 111, 10671-10674

PRE-INDUSTRIAL, PRESENT AND FUTURE NEW PARTICLE FORMATION

R. MAKKONEN[1], A. ASMI[1], V.-M. KERMINEN[2], A. ARNETH[3], P. HARI[4] and M. KULMALA[1]

[1] Department of Physical Sciences, University of Helsinki, Finland
[2] Finnish Meteorological Institute, Helsinki, Finland
[3] Department of Physical Geography and Ecosystems Analysis, Lund University, Sweden
[4] Department of Forest Ecology, University of Helsinki, Finland

Keywords: nucleation, secondary organic aerosol, global model

INTRODUCTION

New particle formation can effectively alter cloud properties by increasing the number of cloud droplets. Clouds with higher cloud droplet number concentration (CDNC) have increased cloud albedo (Twomey, 1977), and high CDNC might even hinder precipitation (Albrecht, 1989). Several observations from various locations show that aerosol nucleation can contribute significantly to cloud condensation nuclei (CCN) concentration (Kerminen et al., 2005; Laaksonen et al., 2005). However, the importance of nucleation on climate on a global scale is difficult to estimate, since precursors for nucleation vary from location to another. Sulphuric acid is known to participate in the initial nucleation process, but for example the roles of ammonia and organic compounds are still rather uncertain.

The role of aerosols on climate has been changing dramatically since the beginning of industrialization (Stier et al., 2006). Emissions of anthropogenic primary particles and sulphur dioxide have been rather steadily increasing. Today, emission regulations and efficient filtering techniques help to reduce these emissions except in rapidly developing countries. But the biosphere can also play a major role in the evolving aerosol-climate system. With the changing geographic patterns and overall anthropogenic emissions the relative role of biogenic vs. anthropogenic aerosol precursors are becoming increasingly important for the overall understanding of the system behaviour. For instance, emission estimates for biogenic VOCs are 702 Tg(C)/yr, 725 Tg(C)/yr and 1251 Tg(C)/yr for preindustrial, present-day and future conditions, respectively, when considering only climate change and the generally more productive vegetation (Lathière et al., 2005). Due to several interacting and changing factors (e.g. the role of atmospheric CO_2 concentration, land use/land cover change) and possible feedback mechanisms, the importance of new particle formation in different conditions is impossible to quantify without a comprehensive global model.

The aim of this study is to explore changes in patterns and magnitude of new particle formation due to industrialization, changes in vegetation and climate change. We focus on the role of biogenic organic compounds on aerosol growth and the actual nucleation process.

METHODS

We use ECHAM5-HAM (Stier et al., 2005) aerosol-climate model with T42 resolution ($\sim 2.8^o$ x 2.8^o) for our simulations. The aerosol model HAM considers the most important aerosol compounds, namely sulfate, black carbon, particulate organic matter, sea salt and dust. The emissions of dust, sea salt and oceanic dimethyl sulfide are calculated online, i.e. the emissions depend on

meteorological situation. The chemistry module of ECHAM5-HAM considers sulfur chemistry with dimethyl sulfide, sulfur dioxide and sulfate as prognostic variables.

Originally, ECHAM5-HAM considers biogenic organic aerosols as part of primary emissions of particulate organic matter. Recently the description of BSOA was improved to account for new particle formation events (Makkonen et al., 2009). Several studies suggest thermodynamic equilibrium partitioning of secondary organic oxidation products. However, the results from such models indicate that equilibrium partitioning increases organic mass only of those particles, which already have a reasonable amount of organic matter. This behavior is not in accordance with observations, which indicate that oxidation products of biogenic organic vapors condense also on newly formed particles and participate in their early growth. In this study we utilize the volatility basis set to describe aging of organic vapours (Donahue, 2009). We consider emissions of biogenic monoterpenes.

ECHAM5-HAM has been previously modified to include boundary layer nucleation with the assumption that the nucleation rate formulation follows a linear form (the so-called activation-type nucleation), according to which the nucleation rate is proportional to the concentration of sulphuric acid (Makkonen et al., 2009). It is assumed that a globally constant coefficient can describe the physics and chemistry behind nucleation. Although the inclusion of boundary layer nucleation mechanism in a global model improves resulting aerosol size distributions (Makkonen et al., 2009; Spracklen et al., 2006), it can be argued that a single constant can not be applied globally. In this study we use an updated formulation for new particle formation. In addition to binary sulphuric acid-water nucleation, we parametrize formation rate of 2 nm particles as a function of sulphuric acid and organic vapour concentrations. We apply a parameterization by Kerminen and Kulmala (2002) to calculate formation rate at 3 nm, which is then given as input for ECHAM5-HAM.

To understand the interactions between new particle formation and climate, the modeled aerosol distributions have to be coupled with cloud droplets. There are several approaches to parametrize the number of activated cloud droplets as a function of aerosol size distribution and meteorological parameters. Lin and Leaitch (1997) use a specific activation radius, above which all particles are assumed to activate as cloud droplets with equal likelihood. In this study we apply a cloud droplet nucleation parameterization by Abdul-Razzak and Ghan (2000), which considers also aerosol composition and size distribution.

Emissions of preindustrial and present-day primary aerosol and precursor gases (other than biogenic organics) are described in Dentener et al. (2006). For future emissions IPCC scenario B2 is used. To account for changes in emissions of biogenic volatile organic compound, we use emission maps of Lathière et al. (2005) as a starting point. Lathière et al. (2005) calculated emissions for the Last Glacial Maximum, the preindustrial (1850s), present-day (1990s) and the future. These are based on climate change and effects of changing atmospheric CO_2 concentration on vegetation.

We run ECHAM5-HAM for three time periods: pre-industrial (1750), present (2000), and future (2100). For each period, we integrate the model for 20 years. The model is run with and without aerosol nucleation in order to distinguish the features produced by atmospheric new particle formation. The atmospheric model is forced with fixed sea-surface temperatures.

RESULTS AND CONCLUSIONS

Due to the low anthropogenic emissions of sulphur dioxide during the pre-industrial period, aerosol nucleation from biogenic organic vapors is relatively significant source of new particles. On the other hand, low condensation sink makes it easy for nucleation sized particles to reach CCN sizes. Since also the concentrations of condensing vapors are low, aerosol growth rates are lower than in present day. In our future scenario, global sulphur dioxide emissions are lower than present-day, but regionally emissions are even higher. Increasing emissions of biogenic volatile organic compounds

stress the role of biosphere in future climate but additional processes (CO_2 inhibition, land cover change) complicate this picture.

REFERENCES

Abdul-Razzak, H. and Ghan, S. J. (2000) A Parameterization of Aerosol Activation. Part 2: Multiple Aerosol Types. *J. Geophys. Res.*, 105:6837–6844.

Albrecht, B. A. (1989) Aerosols, cloud microphysics and fractional cloudiness. *Science*, 245:1227–1230.

Dentener, F., Kinne, S., Bond, T., Boucher, O., Cofala, J., Generoso, S., Ginoux, P., Gong, S., Hoelzemann, J. J., Ito, A., Marelli, L., Penner, J. E., Putaud, J.-P., Textor, C., Schulz, M., van der Werf, G. R., and Wilson, J. (2006) Emissions of primary aerosol and precursor gases in the years 2000 and 1750 prescribed data-sets for AeroCom *Atmos. Chem. Phys.*, 6:4321–4344.

Donahue, N. M., Robinson, A. L. and Pandis, S. N. (2009) Atmospheric organic particulate matter: From smoke to secondary organic aerosol. *Atmos. Environ.*, 43:94–106.

Kerminen, V.-M., Lihavainen, H., Komppula, M., Viisanen, Y., and Kulmala, M. (2005). Direct observational evidence linking atmospheric aerosol formation and cloud droplet activation. *Geophys. Res. Lett.*, 32:L14803.

Kerminen, V.-M. and Kulmala, M. (2002) Analytical formulae connecting the "real" and the "apparent" nucleation rate and the nuclei number concentration for atmospheric nucleation events. *J. Aerosol Sci.*, 33:609–622.

Laaksonen, A., Hamed, A., Joutsensaari, J., Hiltunen, L., Cavalli, F., Junkermann, W., Asmi, A., Fuzzi, S., and Facchini, M. C. (2005) Cloud condensation nucleus production from nucleation events at a highly polluted region. *Geophys. Res. Lett.*, 32:L06812.

Lathière, J., Hauglustaine, D. A., De Noblet-Ducoudré, N., Krinner, G., and Folberth, G. A. (2005) Past and future changes in biogenic volatile organic compound emissions simulated with a global dynamic vegetation model. *Geophys. Res. Lett.*, 32:L20818.

Lin, H. and Leaitch, W. R. (1997) Development of an in-cloud aerosol activation parameterization for climate modeling. *In Proceedings of the WMO workshop on Measurement of Cloud Properties for Forecast of Weather, Air Quality and Climate*, World Meteorol. Organ., Geneva, 328–335.

Makkonen, R., Asmi, A., Korhonen, H., Kokkola, H., Järvenoja, S., Räisänen, P., Lehtinen, K. E. J., Laaksonen, A., Kerminen, V.-M., Järvinen, H., Lohmann, U., Bennartz, R., Feichter, J., and Kulmala, M. (2009) Sensitivity of aerosol concentrations and cloud properties to nucleation and secondary organic distribution in ECHAM5-HAM global circulation model. *Atmos. Chem. Phys.*, 8:10955–10998.

Spracklen, D. V., Carslaw, K. S., Kulmala, M., Kerminen, V.-M., Mann, G. W., and Sihto, S.-L. (2006) The contribution of boundary layer nucleation events to total particle concentrations on regional and global scales. *Atmos. Chem. Phys.*, 6, 5631–5648.

Stier P., Feichter J., Kinne S., Kloster S., Vignati E., Wilson J., Ganzeveld L., Tegen I., Werner M. , Schulz M., Balkanski Y., Boucher O., Minikin A., Petzold A. (2005) The aerosol-climate model ECHAM5-HAM. *Atmos. Chem. Phys.*, 5:1125–1156.

Stier, P., Feichter, J., Roeckner, E., Kloster, S., and Esch, M. (2006) The evolution of the global aerosol system in a transient climate simulation from 1860 to 2100. *Atmos. Chem. Phys.*, 6:3059–3076.

Twomey, S. (1977) The influence of pollution on the shortwave albedo of clouds. *J. Atmos. Sci.*, 34:1149–1152.

DENSITIES OF CRITICAL NUCLEI FROM MEASUREMENTS OF THE PRESSURE DEPENDENCE OF NUCLEATION RATE

J. MALILA[1], I. NAPARI[2] and A. LAAKSONEN[1,3]

[1] Department of Physics, University of Kuopio, Finland
[2] Department of Physical Sciences, University of Helsinki, Finland
[3] Finnish Meteorological Institute, Helsinki, Finland

Keywords: nucleation, density, pressure dependence

INTRODUCTION

Both negative and positive pressure effects, i.e. reduction or increase nucleation rates, are experimentally observed when the pressure of inert carrier providing thermalisation for condensing clusters is varied (cf. Brus et al., 2008). Typically this effect has been viewed either as an artefact due to improper operation of measurement setup or a consequence of some interaction neglected in theoretical treatments of nucleation, and theoretical work has been conducted to estimate this effect. We have recently (Malila et al., 2009) proposed a reverse approach: data on the pressure dependence of nucleation rate J or on-set saturation ratio S_c can be used to extract information on the densities of critical nuclei in a similar fashion than first and second nucleation theorems. In terms of mean molecular volume inside critical nucleus these relations are

$$v = kT \left(\frac{\partial \ln J}{\partial \ln S} \right)_{p_g,T}^{-1} \left(\frac{\partial \ln J}{\partial p_g} \right)_{\Delta\mu,T} + 2B_{gv} \tag{1}$$

and

$$v = kT_c \left(\frac{\partial \ln S_c}{\partial p_g} \right)_{\Delta\mu,T} + 2B_{gv}. \tag{2}$$

Here k is the Boltzmann's constant, T temperature, p_g pressure of the inert carrier gas and B_{gv} the second cross virial coefficient of condensing vapour and carrier gas; subscript c refers to on-set conditions.

Here we discuss on the generality and validity of the obtained results.

DERIVATION

We consider unstable equilibrium between the critical nucleus and surrounding vapour. Slightly imperfect mixture of vapour (v) and inert carried gas (g) is assumed to follow truncated virial equation of state

$$\frac{pv^g}{kT} = 1 + \frac{B}{v^g}, \tag{3}$$

where $B = y_v^2 B_v + 2 y_v y_g B_{gv} + y_g^2 B_g$ is the second virial coefficient, and v^g the mean molecular volume in gas phase. If we assume that carrier gas is ideal ($B_g = 0$) and that $p_g >> p_v > p_e$, where p_e is the saturation vapour pressure, it can be shown (Kashchiev, 1996) that chemical potential difference between nucleus and vapour becomes

$$\Delta\mu = kT \ln S + (2B_{gv} - v)p_g. \tag{4}$$

Since both J and S_c are now some (differentiable) functions of $\Delta\mu$, Eqs. (1) and (2) follow instantaneously after applying the cyclic relation of partial derivatives, the chain rule and $(\partial\Delta\mu/\partial\ln S)_{p_g,T} = kT$. It should be noted that relation corresponding (1) after identification $(\partial\ln J/\partial\ln S)_T \approx -n^*$, where n^* is the number of molecules in the critical nucleus, has been derived earlier under different assumptions (Kashchiev, 1996; Ford, 1992; Oxtoby and Laaksonen, 1995). However, derivation given here proposes that this relation is of general nature, and holds especially independently of the assumed functional form $J(\Delta\mu) = J(S,T,p_g)$.

FIRST APPLICATION AND DISCUSSION

When applying obtained relations (1) and (2) to experimental nucleation rate data, some precaution is necessary, since the given derivation holds only for isothermal unary nucleation and for incompressible nucleus:

– In Eq. (4) it is assumed that no carrier gas molecules are present inside the critical nucleus, which is defined by the equimolar dividing surface (Kashchiev, 1996; Wilemski, 2006). In practice this is only true when molecular interactions between vapour and carrier gas molecules, respectively, are dissimilar enough (cf. Yasuoka and Zeng, 2007). For example, for the homogeneous nucleation of water in nitrogen this might not be the case.

– Since the carrier gas pressure p_g is also a parameter that defines the efficiency of thermalisation of nucleating cluster (e.g. Wedekind et al., 2008), non-isothermality corrections must be applied to measured nucleation rate data before extracting molecular volumes. Unfortunately, the only practical and reasonably model independent formula for this (Feder et al., 1966) also suffers from the same, strict requirement of unary nucleation.

PSfrag replacements
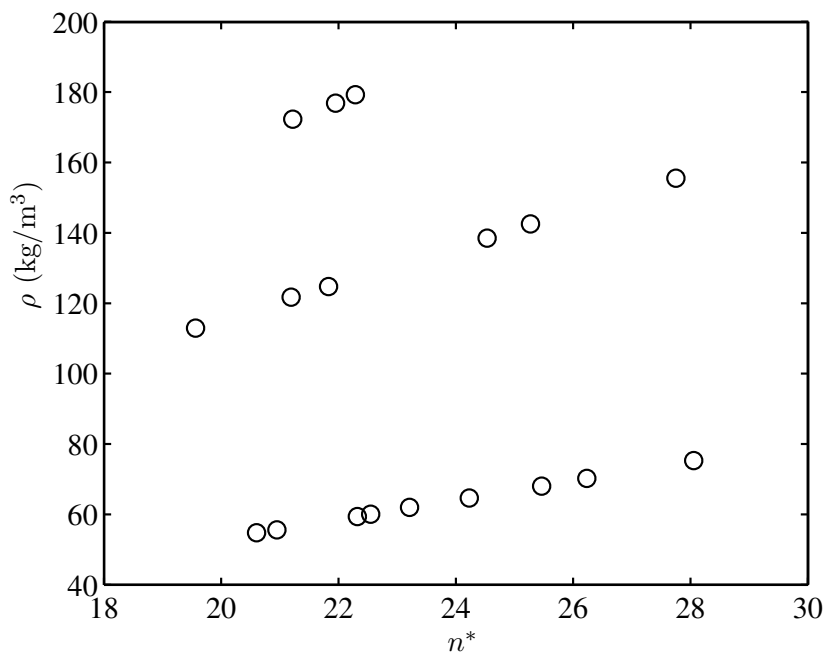
Figure 1: Densities of critical nuclei from Eq. (1) at 240 K. Isobars from top to bottom correspond carrier gas pressures 4.0, 2.5, and 1.0 MPa, respectively.

In Figure 1 first results (Malila et al., 2009) of application of Eq. (1) to nucleation rate data (Luijten, 1999) of water in helium are shown as a function of number of molecules in critical nucleus. It

is clearly seen that the densities of small nuclei are clearly smaller than the corresponding bulk liquid. It should be noted that there is a clear effect of external pressure on the density, though in the derivation of Eq. (4) it is assumed that the effect of external pressure on the compressibility of nucleus is negligible in comparison to Laplace pressure: for small nuclei with no or few interior molecules this assumption can also break down. Also, the non-isothermality correction depends on the surface free energy of critical nucleus, and instead of capillarity approximation used in Fig. 1 this should be obtained from the extension of earlier work (Knott et al., 2000) to binary case. All together, presented results provide a new tool for nucleation studies, allowing model independent extraction of critical nucleus densities from experimental data, but more work should be done to extent the theory to multicomponent mixtures.

ACKNOWLEDGMENTS

REFERENCES

Brus, D., Hyvärinen, A.-P., Wedekind, J., Viisanen, Y., Kulmala, M., Ždímal, V., Smolík, J., and Lihavainen, H. (2008). The homogeneous nucleation of 1-pentanol in a laminar flow diffusion chamber: The effect of pressure and kind of carrier gas. *J. Chem. Phys.*, 128:134312.

Feder, J., Russell, K. C., Lothe, J., and Pound, G. M. (1966). Homogeneous nucleation and growth of droplets in vapours. *Adv. Phys.*, 15:111–178.

Ford, I. J. (1992). Imperfect vapour–gas mixtures and homogeneous nucleation. *J. Aerosol Sci.*, 23:447–455.

Kashchiev, D. (1996). Effect of carrier-gas pressure on nucleation. *J. Chem. Phys.*, 104:8671–8677.

Knott, M., Vehkamäki, H., and Ford, I. J. (2000). Energetics of small n-pentanol clusters from droplet nucleation rate data. *J. Chem. Phys.*, 112:5393–5398.

Luijten, C. C. M., Peeters, P., and van Dongen, M. E. H. (1999). Nucleation at high pressures. II. Wave tube data and analysis. *J. Chem. Phys.*, 111:8535–8544.

Malila, J., Laaksonen, A., and Napari, I. (2009). Densities of critical clusters from nucleation experiments. To be presented in 18th International Conference on Nucleation and Atmospheric Aerosols, Aug. 10–14, 2009, Prague, Czech Republic.

Oxtoby, D. W. and Laaksonen, A. (1995). Some consequenses of the nucleation theorem for binary fluids. *J. Chem. Phys.*, 102:6846–6850.

Wedekind, J., Hyvärinen, A.-P., Brus, D., and Reguera, D. (2008). Unraveling the "pressure effect" in nucleation. *Phys. Rev. Lett.*, 101:125703.

Wilemski, G. (2006). Volumes of critical bubbles from nucleation theorems. *J. Chem. Phys.*, 125:114507.

Yasuoka, K. and Zeng, X. C. (2007). Molecular dynamics of homogeneous nucleation in the vapor phase of Lennard-Jones. III. Effect of carrier gas pressure. *J. Chem. Phys.*, 126:124320.

LONG-TERM AEROSOL PARTICLE FLUX MEASUREMENTS AT SMEAR II FIELD STATION IN HYYTIÄLÄ, FINLAND

I. MAMMARELLA, Ü. RANNIK, P. AALTO, P. KERONEN, T. VESALA and M. KULMALA

Department of Physics, P.O. Box 64, FI-00014, University of Helsinki, Finland

INTRODUCTION

In spite of numerous observational studies particle deposition still lacks thorough understanding. Particle fluxes determined by micrometeorological techniques show large variability in magnitude as well as in sign. Even in remote measurement sites, where in absence of local sources, we would expect mainly deposition (negative) particle fluxes, EC measurements contain significant fraction of upward particle flux (e.g. Pryor et al., 2007). The reason is not yet fully understood and the positive flux values can be due to a combination of large random uncertainty and unknown physical/chemical processes. Pryor et al. (2008) investigates thoroughly the distribution and significance of upward fluxes as well as relevance to several physical mechanisms causing them by taking into account also the error estimates of fluxes. However, flux errors do not scale directly with flux magnitude and therefore selection of fluxes according to relative error criterion leads to systematic selection of observation conditions. Therefore the accuracy of flux error estimates becomes important for interpretation of measurements.

In this study long-term eddy covariance particle flux measurements were performed at a Boreal forest site in Hyytiälä, Southern Finland. The large variability in turbulent flux estimates is inherent to particle flux observations and thus long-term particle flux measurements enable to obtain statistically significant results by suitable averaging. The particle flux random errors were estimated and parameterisation for a time scale relevant to particle flux uncertainty calculation was proposed. Further we demonstrate that in order to obtain reliable average deposition fluxes, the single flux values should not be conditionally classified by using flux error estimates. Finally diurnal, seasonal and annual variability of particle fluxes was analysed and observed that particle deposition rates are higher in winter.

METHODS

For this study the experimental data collected during the period from 2000 to 2007 at SMEAR II field measurement station in Hyytiälä (Finland) have been used. The micrometeorological measurement tower (72 m high) is located within extended forested areas, dominated by a Scots pine trees, whose average height is about 14 m. A detailed description of the site and the measurements can be found in Rannik (1998) and in Hari and Kulmala (2005). The EC fluxes of momentum, heat, and particles were measured at 23 m above the ground. The particle EC system includes an ultrasonic anemometer (Solent Research 1012R2) to measure three wind speed components and a condensational particle counter (CPC) (Model 3010, TSI Inc, USA) for particle number concentration measurements.

Aerosol size distribution (from 3 to 500 nm particles in diameter until 07.12.2004 and up to 1 μm onward) measurements were performed using Differential Mobility Particle Sizer (DMPS) system at 2 m height inside the forest. The geometric mean diameter (GMD) of particle size distribution for each run was calculated from the DMPS size spectrum, after multiplying it with the size transfer function of the EC system.

The eddy covariance (EC) vertical flux $\overline{w'c'}$ is calculated as time averaged product between the fluctuations of the vertical component of wind speed w and of the scalar concentration c.

However, the flux $\overline{w'c'}$ is a random variable estimated over a finite realisation and its average departure from the ensemble average $<w'c'>$ is presented by the random error δF, which is a measure of one

standard deviation of the random uncertainty of turbulent flux observed over an averaging period T (Lumley and Panofsky, 1964, Lenschow et al.,1994). The random error δF associated with EC particle flux is generally due to stochastic nature of turbulence, instrumental noise and counting error due to discrete nature of aerosols (Fairall, 1984).We evaluate the relative flux error $\Delta F = \delta F / |\overline{w'c'}|$ for aerosol particle directly by the instantaneous flux $\varphi = w'c' = (w - \overline{w})(c - \overline{c})$ statistics, according to Wyngaard (1973):

$$\Delta F_{IF} = \sqrt{\frac{2\tau_\varphi}{T} \left[\overline{(w'c')^2} - \overline{w'c'}^2 \right]} \, |\overline{w'c'}|^{-1} . \tag{1}$$

Where τ_φ is the integral time scale relevant for aerosol particle flux uncertainty, defined as

$$\tau_\varphi = \frac{1}{\sigma_\varphi^2} \int_0^\infty R_\varphi(s) ds \tag{2}$$

where $R_\varphi(s) = \overline{(\varphi(t) - \overline{\varphi})(\varphi(t+s) - \overline{\varphi})}$ is the auto-covariance function of φ, s the time delay and σ_φ^2 is the variance of φ.

RESULTS

The time scale τ_φ was numerically evaluated using the Eq. 2 and in order to generalize our result, the time scale τ_φ was converted to a corresponding normalised frequency n_φ by using $n_\varphi = \dfrac{Z}{2\pi\tau_\varphi U}$, where Z is the effective measurement height above the displacement height d and U the mean wind velocity. For particle flux the following parameterization was established

$$\begin{cases} n_\varphi = 0.27 \pm 0.008(s.e.) & \text{for } \dfrac{Z}{L} \leq 0 \\[4mm] n_\varphi = 0.21 \left[1 + 3.4 \left(\dfrac{Z}{L} \right)^{0.26} \right] & \text{for } \dfrac{Z}{L} > 0 \end{cases} \tag{3}$$

where L is the Obukhov length. Similar parameterization was obtained for temperature flux (not shown). The estimated flux timescale is constant in unstable and neutral stratification, and it increases with stability for stable conditions. A reasonable parameterization of τ_φ, based on the surface layer similarity theory, is $\sim Z/U$, corresponding to a normalized frequency $n_\varphi = (2\pi)^{-1} = 0.16$. This theoretical parameterization for τ_φ has been extensively used within the roughness sub-layer above forest canopies (Pryor et al., 2007, 2008a), for calculating the particle flux random error through the Eq. (1). Then the empirically estimated time scale (from Eq. 3) is smaller than the theoretical one, roughly by a factor of 2 in near-neutral and unstable conditions and up to a factor of 6 in stable conditions. For the random uncertainty estimates this implies a difference by the square root of the factor.

The frequency of occurrence of relative flux error $\delta F_{IF} / \overline{w'c'}$ for particle and sensible heat flux is presented in Figure 1. The particle flux errors were several times larger than the sensible heat flux errors. In case of particles fluxes the relative errors are larger for positive flux values. Formally the result indicates statistically less significant values in case of upward fluxes.

In evaluation of average flux statistics classification according to some threshold value of relative flux error is done. For instance, Pryor et al. (2007) used a threshold, $\Delta F_{IF} < 1$, which means that for such subset the fluxes are with probability 68% within one standard deviation from the mean.
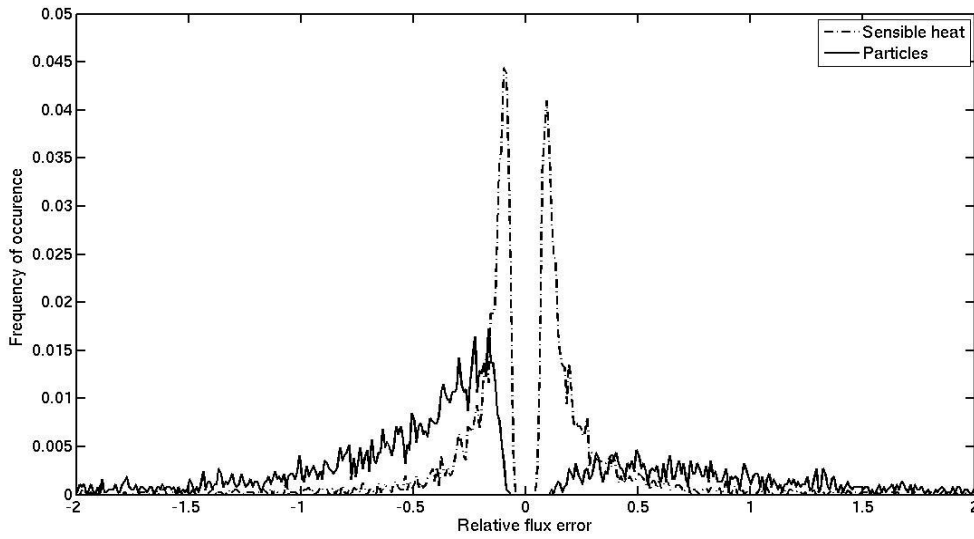
Figure 2. Frequency distribution of relative flux error as estimated by $\delta F_{IF}\big/\overline{w'c'}$. Negative values on x-axis represent downward and positive values upward flux cases.

However, since the relative flux error distribution is not symmetric, the application of such selection criteria leads to selectively systematic bias in average particle deposition statistics and must not be done without good understanding of the relationship between the relative random errors and observation conditions. In remote forest sites (like Hyytiälä station), where, in absence of local sources, we expect to measure mainly deposition (negative) particle fluxes, the occurrence of upward (positive) fluxes cannot be ascribed entirely to high values of random uncertainty (Pryor et al., 2008b). Then as far as the upward fluxes cannot be related to certain physical processes with confidence, the filtering according to flux error must not be done if the purpose is to evaluate unbiased average deposition rates.

Table 1 shows the influence of different relative error thresholds on percent of fluxes passing satisfying it, percentage of downward fluxes in selected subset as well as average normalised deposition velocities. With stronger criterion of relative flux error there is general tendency towards bigger fraction of downward flux estimates and correspondingly higher deposition velocity estimates. An independent error estimates ΔF_{SP} (Lenschow and Kristensen, 1985), which does not include τ_φ, is also displayed as reference. The error estimates ΔF_{IF} and ΔF_{SP} are in relatively good correspondence. As expected, under unstable conditions the error estimate ΔF_{IF} with $\tau_\varphi = Z/\overline{u}$ is somewhat stronger in data filtering than ΔF_{IF} with τ_φ from Eq. 3, but the difference becomes larger in stable conditions.

For further analysis and results presented below we did not apply any threshold value of relative flux error.

L < 0 Unstable	ΔF_{IF} with τ_φ from Eq. (3)			ΔF_{IF} with $\tau_\varphi = Z/\overline{u}$			ΔF_{SP}		
	% passing	% $\overline{w'c'} < 0$	100* v_d/u_*	% passing	% $\overline{w'c'} < 0$	100* v_d/u_*	% passing	% $\overline{w'c'} < 0$	100* v_d/u_*
$\Delta F < 1$	32.3	72.0	0.274	28.1	73.4	0.305	33.9	71.4	0.263
$\Delta F < 0.5$	17.6	82.0	0.596	13.3	85.5	0.821	20.1	80.6	0.494
$\Delta F < 0.3$	7.4	93.2	1.08	4.55	96.6	1.50	10.0	89.8	0.839

$L > 0$ Stable	ΔF_{IF} with τ_φ from Eq. (3)			ΔF_{IF} with $\tau_\varphi = Z / \bar{u}$			ΔF_{SP}		
	% passing	% $\overline{w'c'} < 0$	100* v_d/u_*	% passing	% $\overline{w'c'} < 0$	100* v_d/u_*	% passing	% $\overline{w'c'} < 0$	100* v_d/u_*
$\Delta F < 1$	38.1	76.0	0.247	30.1	78.9	0.300	40.3	74.8	0.240
$\Delta F < 0.5$	26.0	81.6	0.409	15.0	86.6	0.568	29.3	80.1	0.319
$\Delta F < 0.3$	15.6	87.5	0.556	4.8	92.6	0.937	19.2	85.6	0.444

Table 1. Percentages of 60 min average particle fluxes satisfying the test (% passing) for different relative flux error estimates and thresholds values, and percentages of deposition fluxes (negative, % F < 0) of those satisfying the test and the corresponding ensemble average of normalized deposition velocity v_d/u_*. The unstable and stable conditions are selected according to the Obukhov length L and are shown separately. The flux values were selected according to different criteria of ΔF, and the relative flux error ΔF_{IF} is estimated using two different parameterizations of the integral time scale τ_φ.

The long term Hyytiälä dataset give us a statistically robust ground to classify the aerosol particle flux measurements and to study their diurnal, seasonal and annual variability. For the present statistical analysis aerosol particle flux data collected during the period from 2000 to 2007 were used. The diurnal variation of particle fluxes during nucleation days for four different seasons is shown in Figure 2. The lowest deposition flux is measured during the summer, while spring and autumn nucleation events show the largest downward flux. Moreover nucleation events begin later in winter (large downward fluxes start after 12 am) and earlier during the other seasons (approximately around 9 am). This is related to solar radiation increase and boundary layer development, which are strongly correlated (Nilsson et al., 2001). For non-event days such diurnal pattern was not observed (not shown).
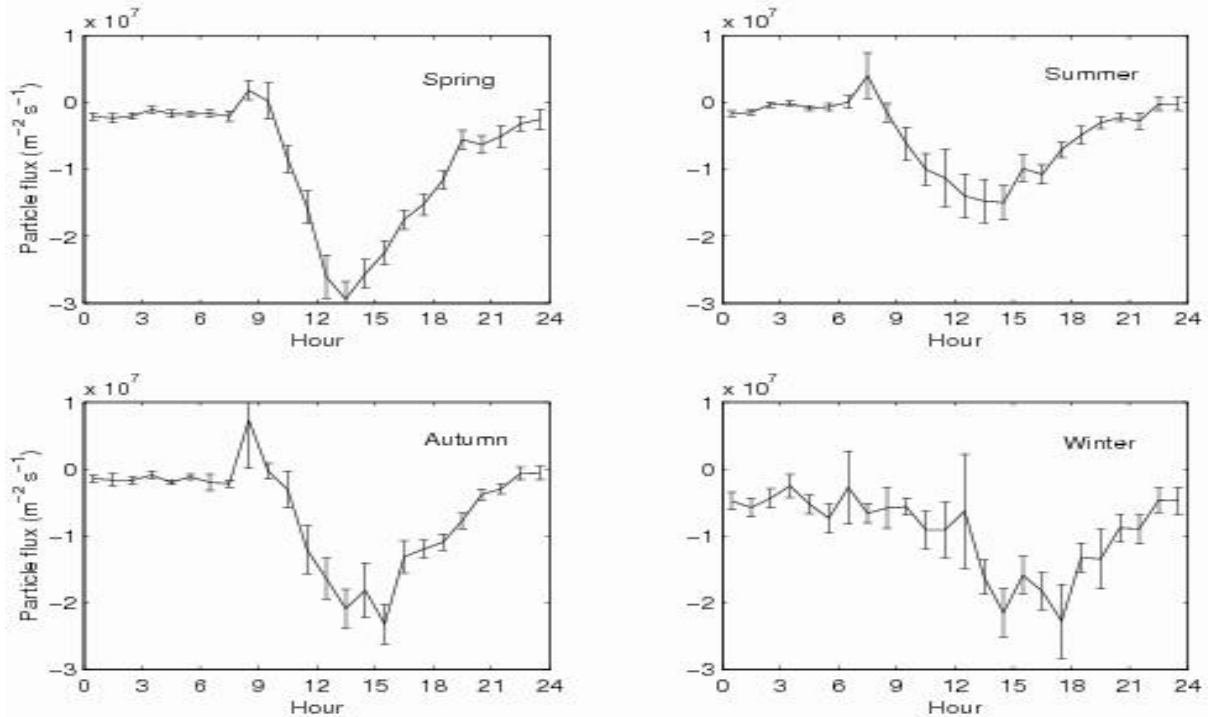
Figure 2. Diurnal variation of aerosol particle flux for different seasons.

Figure 3 shows the annual variation of particle fluxes for all days. To take into account the particle number concentration and turbulence intensity effect, deposition velocity and its ratio to friction velocity are also plotted, respectively. Deposition velocities, including the normalised values with friction velocity,

are highest in winter and lowest in summer. This is in contradiction with the frequency of the occurrence of nucleation event days during different seasons. Nucleation events imply smaller particles and thus higher deposition velocities, which would allow us to expect the largest deposition velocities for spring months. Higher deposition velocities in winter have earlier been observed by Suni et al. (2003), who explained the observation by smaller particles sizes dominating the size spectrum in winter. However the seasonal variability of monthly average GMD values does not clearly support such explanation (not shown).
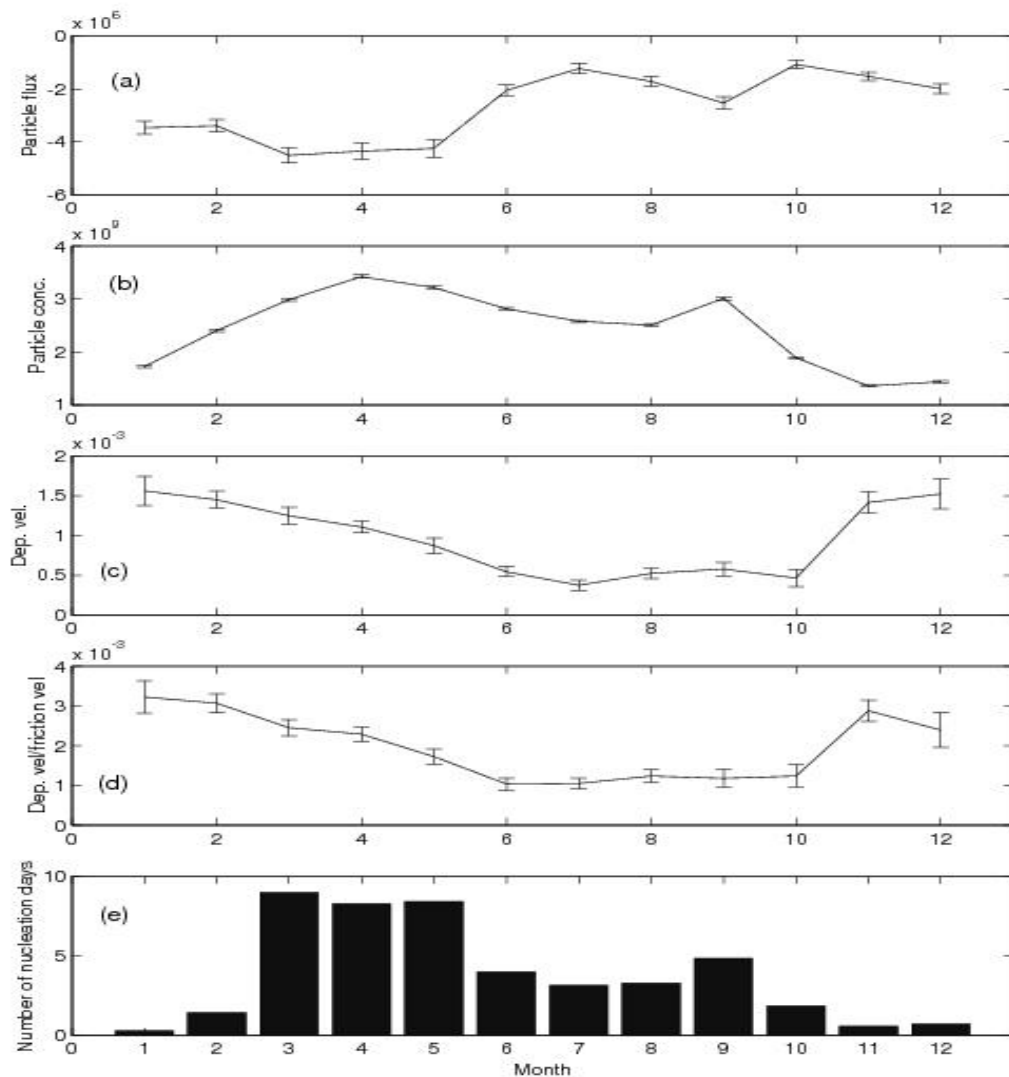
Figure 3. Annual cycle of a) particle flux in $m^{-2}s^{-1}$; b) concentration in m^{-3}; c) deposition velocity in ms^{-1} ; d) deposition velocity normalized with friction velocity (dimensionless); e) number of nucleation days as the average over seven years per month. 30 min flux data measured between 2001-2006 are used.

CONCLUSIONS

In this study we provide a new parameterization of a time scale relevant for flux random error calculation and we noted that simple parameterization commonly used above vegetation canopies (Pryor et al., 2008) leads to an overestimation of random error for aerosol particle flux. We shown that upward fluxes have larger statistical uncertainty and filtering of observations according to some threshold values of the relative flux error produces systematically different ensemble averages. As far as the upward fluxes cannot be related to certain physical processes with confidence, the filtering according to flux error must not be done if the purpose is to evaluate unbiased average deposition rates. Particle fluxes were analysed for the diurnal, seasonal and annual variation by using seven years of measurements. Particle fluxes were normalised with the concentration as well as the friction velocity to remove known dependences. It was observed that the normalised deposition rate was higher in winter than in summer and even in spring period when frequently nucleation events occur and particle concentrations are dominated by small particles. More detailed analysis of functional dependence of particle fluxes on environmental variables (turbulent intensity, stability and solar radiation) is needed.

REFERENCES

Fairall, C.W. (1984) Interpretation of eddy-correlation measurements of particulate deposition and aerosol flux, *Atm. Environ.*, 18, 1329-1337.

Kaimal, J. C. and Finnigan, J. J.,(1994) Atmospheric Boundary Layer Flows. Their Structure and Measurement, Oxford University Press, New York

Lenchow, D.H., and Kristensen, L., (1985) Uncorrelated noise in turbulence measurements. *J. Atmos. Oceanic Technol.*, 2, 68-81.

Lenschow, D. H., Mann J., and Kristensen, L., (1994) How long is long enough when measuring fluxes and other turbulence statistics?. *J. Atmos. Oceanic Technol.,* 11, 661-673.

Lumley, J. L., and H. A. Panofsky, (1964) The structure of Atmospheric Turbulence. John Wiley & Sons, 239 pp.

Nilsson, E.D., Rannik, Ü., Kulmala, M., Buzorius, G., and O'Dowd, C.D. (2001) Effects of continental boundary layer evolution, convection, turbulence and entrainment, on aerosol formation. *Tellus*, 53B, 441-461.

Pryor S. C., Larsen S. E., Sørensen L. L., Barthelmie R. J., Grönholm T., Kulmala M., Launiainen S., Rannik Ü., Vesala T. (2007) Particle fluxes over forests: Analyses of flux methods and functional dependencies. *J. Geophys Res.*, 112, D07205, doi:10.1029/2006JD008066

Pryor S. C., .M., Gallagher, H. Sievering, S. E. Larsen, R. J. Barthelmie, F. Birsan, E. Nemitz, J. Rinne, , M. Kulmala, T. Grönholm, R. Taipale and T. Vesala, (2008a) A review of measurement and modelling results of particle atmosphere-surface exchange. *Tellus B*, 60, 42-75

Pryor, S. C. Barthelmie, R. J. Sørensen, L. L., Larsen, S. E., Sempreviva, A. M., Grönholm, T., Rannik, Ü., Kulmala, M., Vesala, T. (2008b) Upward fluxes of particles over forests: when, where, why? *Tellus B*, Vol 60 (3), 372-380.

Rannik, U. (1998) On the surface layer similarity at a complex forest site. *J. Geophys. Res.* 103, 8685-8697

Suni, T., Rinne, J., Reissell, A., Altimir, N., Keronen, P., Rannik, Ü., Dal Maso, M., Kulmala, M., Vesala, T. (2003) Long-term measurements of surface fluxes above a Scots pine forest in Hyytiälä, Southern Finland, 1996 – 2001. *Boreal Environment Research*, 4, 287-301

Wyngaard, J. C. (1973) On surface layer turbulence, in *Workshop on Micrometeorology*, edited by D. A. Haugen, pp. 101-149, American Meteorological Society, Boston, Mass

COMPARISON OF DIFFERENT METHODS TO DERIVE RELIABLE ESTIMATIONS OF NIGHT-TIME RESPIRATION FROM EDDY COVARIANCE MEASUREMENTS AT SMEAR II FIELD STATION IN HYYTIÄLÄ, FINLAND

I. MAMMARELLA[1], P. KOLARI[2], Ü. RANNIK[1] and T. VESALA[1]

[1]Department of Physics, P.O. Box 64, FI-00014, University of Helsinki, Finland
[2]Department of Forest Ecology, P.O. Box 27, FI-00014 University of Helsinki, Finland

INTRODUCTION

The conservation equation that controls the CO_2 balance in a control volume is

$$NEE = F_{EC} + F_{SC} + F_{VA} + F_{HA} \qquad (1)$$

Where the biological source/sink strength (net ecosystem exchange [NEE]) is the sum of different flux terms: F_{EC} is the turbulent flux measured by eddy covariance (EC) technique, F_{SC} the flux storage, F_{VA} and F_{HA} the vertical and horizontal advection respectively. A detailed estimation of these terms was discussed by several authors (see, for instance, Feigenwinter et al., 2004). In the traditional usage of the EC approach the advective fluxes are assumed negligible and NEE is estimated from the measurements of turbulent fluctuations (F_{EC}) together with measurements of temporal changes of vertical CO_2 concentration profile, on which F_{SC} is calculated.

However it is well known that during night-time stable conditions the sum $F_{EC}+F_{SC}$ frequently underestimates the net ecosystem exchange over tall forest ecosystems (Aubinet et al., 2000). In such condition, beside the systematic and random errors of EC flux measurements, other mechanisms are responsible for carbon dioxide depletion during night-time. With clear sky and strong radiative surface cooling inducing stable thermal stratification, the nocturnal turbulent mixing is suppressed and other non turbulent large scale processes (entrainment, drainage flow, gravity waves) may contribute considerably to the net ecosystem exchange (NEE). It is recognised that, especially in complex topography and/or source-sink heterogeneity, these mechanisms transport the emitted CO_2 in vertical and/or horizontal direction (Finnigan, 2007, 2008) and not considering the advective fluxes leads to a systematic bias in estimated night-time respiration rates. However recent studies (Aubinet et al., 2005, 2008; Feigenwinter et al., 2004, 2008; Leuning et al., 2008; Heinesch et al., 2008) have reported a large uncertainty in the experimental estimation of the advection terms, and Aubinet et al. (2008) conclude that the advection measurements cannot be used directly to correct the night-time NEE. Because of this large uncertainty and the difficult to assess the advection terms on routine basis in most of the micrometeorological sites, NEE estimations under low night-time turbulence conditions are filtered out (filtering approach) and replaced with NEE values modelled as a function of soil/air temperature. The threshold value of a turbulent parameter X (used as indicator of mixing conditions) is defined as the magnitude of X above which the night-time NEE (normalized to a given soil temperature) is constant. Below the threshold value, an apparent increase of NEE with increasing turbulent parameter values is commonly observed.

The first filtering criterion was proposed by Goulden et al.(1996), and is based on the friction velocity ("u_*-filtering approach"). Although this method is commonly used in the Fluxnet community, it is subjected to several drawbacks. First, when the air flows above and below canopy are decoupled, the friction velocity measured above the canopy (at the same level of EC flux) fails to represent the degree of turbulent mixing within the canopy. In fact in some cases, while the turbulence above canopy can still be maintained, the mixing in the subcanopy layer is suppressed. In this situation the gradient Richardson number below the canopy top assumes supercritical values (tends to infinity) and the sub-canopy wind

direction tends to follow the local terrain slope, regardless of the above canopy flow (Marht et al., 2000; Mammarella et al., 2007, and others).

Furthermore, the choice of the u* threshold value is rather subjective and at some sites its determination is impossible. Recently, Acevedo et al. (2008) pointed out another difficult associated with "u*-filtering approach", e. g. the uncertainty in the u* value. Since the friction velocity is a flux itself, it may be subject to large variability due to the mesoscale (low frequency) contribution and/or measurement errors. They proposed to use the standard deviation of vertical velocity σ_w as a proxy to detect periods of low mixing conditions. While this approach needs further experimental validations for above canopy measurements, it is worth to mention that it has been successfully used by Launiainen et al. (2005) for obtaining reliable estimations of CO_2 flux measured in a canopy trunk space.

Finally, van Gorsel et al. (2007, 2008) reported a promising filtering approach, in which they proposed to use the maximum value of $F_{EC}+F_{SC}$ (defined as R_{max}) to derive a temperature response function for the night-time respiration.

In this study we investigate the reliability of a new filtering approach based on a bulk Richardson number RI_c, defined with subcanopy measurements of mean air temperature and wind velocity. We compare the new method with the above mentioned approaches and we used independent respiration measurements based on chamber method to investigate its reliability.

METHODS

For this study the experimental data collected during the summer of 2004 at SMEAR II field measurement station in Hyytiälä (Finland) have been used. The micrometeorological measurement tower (72 m high) is located within extended forested areas, dominated by a Scots pine trees, whose average height is about 14 m. A detailed description of the site in micrometeorological context can be found in Rannik (1998). The EC fluxes of momentum, heat, CO_2 and H_2O were measured at 23 m above the ground. The EC system includes a n ultrasonic anemometer (Solent Research 1012R2) to measure three wind speed components and a closed-path gas analyzer (LI-6262, Licor, USA) which measures CO_2 and H_2O concentrations. Storage change term F_{ST} was calculated using measured concentration profile of CO_2 from 4 levels (4.2 m, 8.4 m, 16.8 m, 33.6 m) according to Mammarella et al. (2007). Air temperature was measured at the same levels with platinum resistance thermometer PT-100.

Independent night-time estimate of NEE was calculated by using chamber measurements, which include forest floor CO_2 efflux, respiration of woody parts of the trees and respiration of foliage (Mammarella et al., 2007).

RESULTS

In this study the reliability of night-time CO_2 EC flux values is assessed by using a canopy Richardson number defined as

$$RI_c = \frac{zg\Delta\theta}{\theta U^2} \tag{1}$$

Where g is the acceleration due to the gravity, θ is the mean potential temperature at 4 m, $\Delta\theta$ is the temperature difference between 16 m and 4 m levels, U is the mean wind velocity measured at 16 m and z = 8.4 m.

Figure 1 shows the relationship between the night-time heat flux wT and RI_c. Three stable boundary layer regimes are distinguishable: 1) a weakly stable regime ($0 < RI_c < 0.02$), where the absolute value of wT increases from the zero neutral value; 2) a transition regime ($0.02 < RI_c < 0.9$), where the heat flux decreases rapidly due to decreasing amplitude of the vertical velocity fluctuations, and 3) a very stable

regime ($RI_c > 0.9$), where the flux are very small. Within the regimes 2) and 3) we can expect that the non-turbulent transport becomes more and more important. In fact when we move in the descending part of the curve in Figure 1 ($RI_c > 0.02$), the thermal decoupling between the boundary layer and the canopy becomes more probable, because the turbulent heat flux cannot oppose the radiative cooling (long-wave radiation), leading to larger temperature difference ($\Delta\theta$) and then larger values of RI_c. Under these regimes the sub-canopy flow was partially or completely decoupled from the flow above the canopy. During some nights while the sub-canopy wind was mainly downslope with a nearly northern direction, the wind direction above the canopy was mainly from south-west / west (not shown).
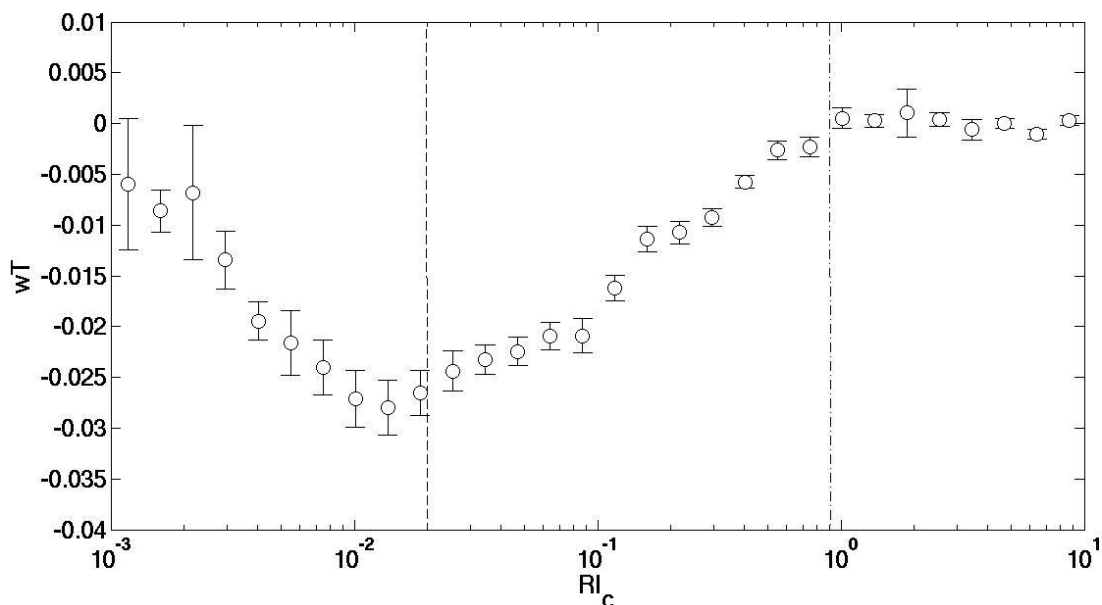
Figure 1. The average values of heat flux in K m s^{-1} conditionally sampled for different classes of canopy Richardson number. The error bars indicate the mean standard errors.

Further the use of RI_c as a filtering criterion of night-time values of $F_{EC}+F_{SC}$ is investigated and a comparison with filtering approaches based on friction velocity u_* (Goulden et al.,1996) and standard deviation of vertical velocity σ_w (Acevedo et al., 2008) is shown in Figure 2. Flux values $F_{EC}+F_{SC}$, normalized by chamber based modelled respiration Re, are conditionally averaged for different classes of explanatory variables (RI_c, u_* and σ_w). The normalization of the EC flux bin averaged values avoids the influence of possible correlations between the EC fluxes and the soil/air temperature. EC fluxes based nocturnal respiration is underestimated for low mixing stable conditions and a threshold value of explanatory variables are observed for all filtering approaches (0.02, 0.35 and 0.55 for RI_c, u_* and σ_w respectively). Although all approaches could be potentially used to filter 30 min EC fluxes according to the estimated threshold values, it can be noted that the u_* conditionally averaged CO_2 flux does not converge to zero for $u_* \to 0$, in contradiction to what we would expect in absence of turbulent mixing, when the total respireted CO_2 from the canopy should be advected by non-turbulent motion (e.g. drainage flow). This means that the friction velocity is not the optimal proxy parameter for identifying CO_2 flux runs which should be rejected and modelled as a function of soil/air temperature.
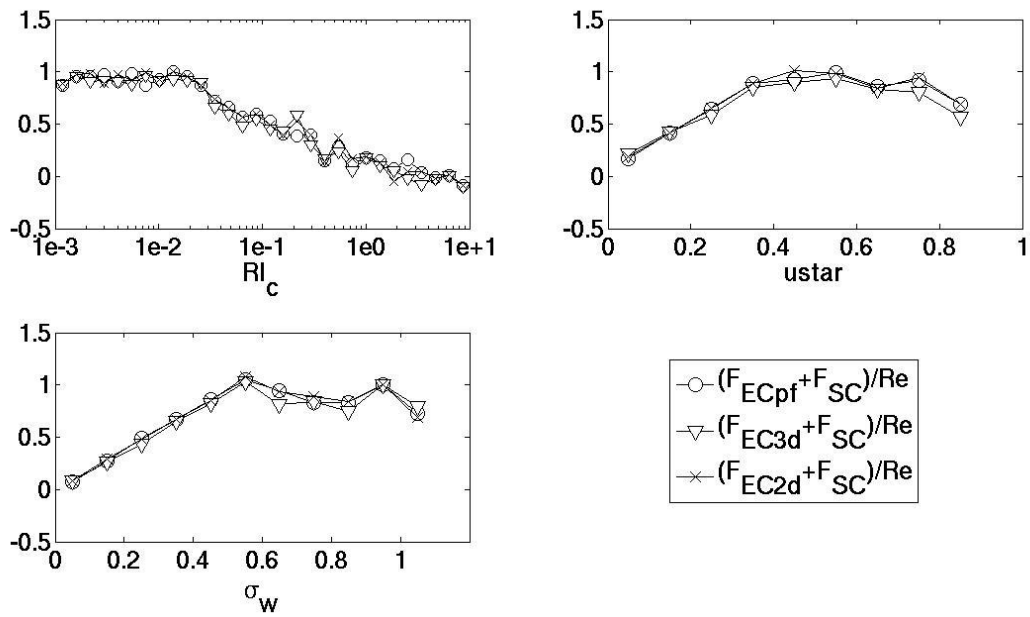
Figure 2. The average values of $F_{EC}+F_{SC}$, normalized by the modelled respiration flux Re, conditionally sampled for different classes of canopy Richardson number RI_c, friction velocity u_* and standard deviation of vertical wind velocity σ_w. The EC flux was calculated by using different rotation methods of wind velocity vectors, e.g. the planar fit (F_{ECpf}), 2d rotation (F_{EC2d}) and 3d rotation (F_{EC3d}).

Different rotation methods give not differences between the estimated CO_2 fluxes, except for high values of u_* and σ_w where F_{EC3d} is slightly smaller than F_{EC} values calculated with 2d and planar fit rotation methods. This results suggests that the 2d and pf methods are superior and the 3d rotation method should not be applied for flux calculation above tall vegetation canopies and in complex terrain, as also it has been suggested by Euroflux methodology (Aubinet et al., 2000).

CONCLUSIONS

In this study we proposed a new method based on a canopy Richardson number RI_c to filter out EC CO_2 flux measured under nighttime low mixing conditions. As RI_c is defined by using temperature profile down to the subcanopy layer, it seems to be a proper proxy parameter for measuring the degree of coupling between the above and below canopy layers. Comparing the EC flux based NEE estimates and the chamber based modelled NEE values, we demonstrate that a threshold value of the filtering method could be obtained also for RI_c. Moreover the analysis shows that the u_* filtering approach could remove periods when the EC CO_2 flux are good estimates of nocturnal NEE.
Further analysis is needed in order to validate the new filtering approach for obtaining reliable gap-filled estimates of long term CO_2 exchange.

REFERENCES

Acevedo, O. C., Moraes, O.L.L., Degrazia, G. A., Fitzjarrald, D.R., Manzi, A.O. and Campos, J. G. (2009) Is the friction velocity the most appropriate scale for correcting nocturnal carbon dioxide fluxes? *Agric. For. Meteorol.,* 149, 1-10.
Aubinet, M., Grelle, A., Ibrom, A., Rannik, Ü., Moncrieff, J., Foken, T., Kowalski, A.S., Martin, P.H., Berbigier, P., Bernhofer, Ch., Clement, R., Elbers, J., Granier, A., Grünwald, T., Morgenstern, K., Pilegaard, K., Rebmann, C.,

Snijders, W., Valentini, R., Vesala, T. (2000) Estimates of the annual net carbon and water exchange of forests: the EUROFLUX methodology. *Adv. Ecol. Res*., 30, 113–175.

Aubinet, M., Berbigier, P., Bernhofer, C.H., Cescatti, A., Feigenwinter, C., Granier, A., Grünwald, T.H., Havrankova, K., Heinesch, B., Longdoz, B., Marcolla, B., Montagnani, L., Sedlak, P. (2005) Comparing CO2 storage and advection conditions at night at different carboeuroflux sites. *Bound.-Lay. Meteorol.*, 116 (1), 63–94.

Aubinet, M. (2008) Eddy covariance CO_2 flux measurements in nocturnal conditions: an analysis of the problem. *Ecological Applications*, 18(6), 1368-1378

Feigenwinter, C., Bernhofer, C. and Vogt, R. (2004) The influence of advection on the short term CO2-budget in and above a forest canopy. *Bound.-Lay. Meteorol.*, 113, 201-224.

Feigenwinter, Ch., Bernhofer, Ch., Eichelmann, U., Heinesch, B., Hertel, M., Janous, D., Kolle, O., Lagergren, F., Lindroth, A., Minerbi, S., Moderow, U., Mölder, M., Montagnani, L., Queck, R., Rebmann, C., Vestin, P., Yernaux, M., Zeri, M., Ziegler, W., Aubinet, M. (2008) Comparison of horizontal and vertical advective CO2 fluxes at three forest sites. *Agric. For. Meteorol.,* 148, 12-24.

Finnigan, J.J. (2007) Turbulent flow in canopies on complex topography and the effects of stable stratification. Flow and Transport Processes with Complex Obstructions. NATO Science Series II: Mathematics, Physics and Chemistry .Vol. 236 Springer, 414 pp.

Finnigan, J.J. (2008) An introduction to flux measurements in difficult conditions. *Ecol. Applic*. 18, 1340-1350

Goulden, M. L., Munger, J.W., Fan, S. M., Daube, B. C. and Wofsy, S. C. (1996) Measurements of carbon sequestration by long term eddy covariance: methods and a critical evaluation of accuracy. *Global Change Biol*. 2, 169–182.

Heinesch, B., Yernaux, Y. and Aubinet, M. (2008) Dependence of CO2 advection patterns on wind direction on a gentle forested slope. *Biogeosciences*, 5, 657-668.

Launiainen, S., Rinne, J, Pumpanen J., Kulmala L., Kolari P., Keronen P., Siivola E., Pohja T., Hari P. & Vesala T., (2005) Eddy-covariance measurements of CO_2 and sensible and latent heat fluxes during a full year in a boreal pine forest trunk-space. *Boreal Environment Research*, 10, 569-588.

Leuning, R., Zegelin, S.J., Jones, K., Keith, H. and Hughes, D. (2008) Measurement of horizontal and vertical advection of CO2 within a forest canopy. *Agric. For. Meteorol.,* 148, 1777-1797.

Mammarella, I., Kolari, P., Rinne, J., Keronen, P., Pumpanen, J. and Vesala T. (2007) Determining the contribution of vertical advection to the net ecosystem exchange at Hyytiälä forest, Finland., *Tellus,* 59B, 900-909.

Rannik, U. (1998) On the surface layer similarity at a complex forest site. *J. Geophys. Res*. 103, 8685-8697

van Gorsel, E., Leuning, R., Cleugh, H.A., Keith, H., Suni, T. (2007) Nocturnal carbon efflux: reconciliation of eddy covariance and chamber measurements using an alternative to the u*-threshold filtering technique. *Tellus* 59B, 397–403.

van Gorsel, E., Leuning, R., Cleugh, H.A., Keith, H., Kirschbaum, M.U.F, Suni, T. (2008) Application of an alternative method to derive reliable estimates of nighttime respiration from eddy covariance measurements in moderately complex topography. *Agric. For. Meteorol.,* 148, 1174-1180.

TOWARDS GLOBAL MAP OF ION CLUSTER PROPERTIES

H. E. MANNINEN[1], E. ASMI[2], M. SIPILÄ[1], S. GAGNÉ[1], T. NIEMINEN[1], M. VANA[1], A. FRANCHIN[1], S. SCHOBESBERGER[1], T. PETÄJÄ[1], V.-M. KERMINEN[2] and M. KULMALA[1]

[1]Department of Physics, P.O. Box 64, FI-00014, University of Helsinki, Finland
[2] Finnish Meteorological Institute, Research and Development, P.O. Box 503, FI-00101 Helsinki, Finland

Keywords: Atmospheric ion clusters, particle formation and growth, nucleation

INTRODUCTION

Number of locations where frequent aerosol particle formation and subsequent growth has been observed is growing (Kulmala et al. 2004, Kulmala and Kerminen 2007). To understand the initial steps of particle formation better in different atmospheric environments, we use continuous measurements at various field sites to quantify the regional and global effects. The detailed formation mechanisms and the chemical composition of the freshly formed particles are still largely uncertain. The activation of existing charged and neutral clusters has been proposed as a possible candidate for aerosol formation. Atmospheric ion clusters can be detected down to the sizes smaller than 1 nm with air ion spectrometers. These cluster spectrometers have already been measuring in various environments like boreal forest (Kulmala et al 2007), Antarctica (Virkkula et al 2007), Nordic Atlantic, eucalyptus forest in Australia (Suni et al 2007), along the Trans-Siperian railroad (Vartainen et al 2007), Estonia (Hõrrak et al 2003), in mountain sites in France (Venzac et al 2007), Switzerland and China.

Here we report results on continuous atmospheric cluster and aerosol measurements within the EUCAARI (European Integrated project on Aerosol Cloud Climate and Air Quality interactions) project. The different types of air ion and cluster spectrometers started measurements in 12 field sites in Europe during the Intensive Observation Period in March 2008. Number size distribution of >0.8 nm ions and >1.8 nm particles was measured with air ion and neutral cluster spectrometers in various environments. The instruments used in this study are Air Ion Spectrometers (AIS), Balanced Scanning Mobility Analyzers (BSMA), Neutral cluster and Air Ion Spectrometers (NAIS) and Airborne-NAIS (A-NAIS). The atmospheric nucleation and cluster activation take place at the size range of 1.5-2 nm. Therefore, the ion spectrometers allow direct measurements at the size where the real atmospheric nucleation occurs.

METHODS

Cluster spectrometers have been operating in a total of 12 field sites around Europe (Table 1). Before the field measurements the cluster spectrometers took part in a calibration and inter-comparison workshop in Helsinki (Asmi et al. 2009). The cluster spectrometer measurements started in March 2008, and they will be completed during April 2009. The AIS (Tammet et al. 2007) and the BSMA (Tammet 2006) measures mobility distributions of charged aerosol particles and clusters in the size range of 0.8-40 nm and 0.8-7.6 nm, respectively, whereas the NAIS is capable of measuring mobility distributions of sub-3 nm neutral and charged aerosol particles and clusters in the size range from 0.8 to 40 nm (Kulmala et al 2007, supporting material). Within EUCAARI project continuous measurements with cluster spectrometers have been conducted in Hyytiälä and Pallas (Finland), Vavihill (Sweden), Mace Head (Ireland), Cabauw (The Netherlands), K-puszta (Hungary), Hohenpeissenberg (Germany), Melpitz (Germany), PoValley (Italy), Jungfraujoch (Schwitzerland), Puy de Dôme (France), Finokalia (Greece) and Rustenberg (South Africa). Each one of these stations has a particular environment. For example, there are stations at marine coastal sites and at continental sites and some have high background concentrations while some have low

background concentrations etc. In addition, the A-NAIS took part in the airborne measurements in an instrumented aircraft over the European field stations.

Field site	Instrument	IOP started
Cabauw, the Netherlands	AIS, NAIS	April 2008
Finokalia, Greece	AIS	April 2008
Hohenpeissenberg, Germany	NAIS	March 2008
Hyytiälä, Finland	BSMA	March 2007
Jungfraujoch, Switzerland	AIS	March 2008
K-puszta, Hungary	AIS	March 2008
Mace Head, Ireland	NAIS	June 2008
Melpitz, Germany	NAIS	March 2008
Puy de Dôme, France	NAIS	March 2008
Pallas, Finland	NAIS	May 2008
San Pietro Capofiume, Italy	BSMA	March 2008
Vavihill, Sweden	AIS	March 2008

Table 1. Continuous field measurements associated with EUCAARI Intensive Observation Period (IOP).

RESULTS

The classification of the days in event, non-event and undefined days was done. Days classified as event day are days on which new particle formation and growth was observed. Non-event days are days on which no formation or growth of aerosol particles is observed. Finally, undefined days are the days that did not fulfill the criteria of event day or those of non-event days. Monthly event distribution varies from one station to another, which was expected because the stations are influenced by different environments and are in different climates. Also some clear seasonal behavior was detected in new particle formation event occurrence. Formation events were observed around the year. New particle formation events have been seen on every one of the 12 EUCAARI sites where cluster spectrometers was measuring, allowing estimations of the contribution of the events on the total aerosol load in the atmosphere as well as their contribution to cloud formation.

Continuous, long-term measurements allowed us, for instance, to investigate the seasonal and diurnal variation of those characteristics and the concentration of charged and neutral cluster. Based on the collected data, we can calculate estimates for atmospheric new particle formation rates and growth rates, and in case of the NAIS, the contribution of ions to particle formation (Kulmala et al 2007). The growth rates show a clear increase with increasing particle/ion size. The growth rates varied from 0.5 to 7.5 nm/h in different environments. Formation rates for positive and negative ions followed each other closely, with negative ions having slightly higher rates.

In EUCAARI field sites, cluster spectrometer measurements are still running. In the future, this database will be integrated to regional and global scale climate models. To estimate regional aerosol source apportionment and long range transport also trajectory analysis will be included into the study.

REFERENCES

Hõrrak, U., J. Salm, and H. Tammet (2003), Diurnal variation in the concentration of air ions of different mobility classes in a rural area, *J. Geophys. Res.*, 108(D20), 4653, doi:10.1029/2002JD003240.

Kulmala, M., Vehkamäki, H., Petäjä, T., Dal Maso, M., Lauri, A., Kerminen, V.-M., Birmili, W. and McMurry, P.H. (2004) Formation and growth rates of ultrafine atmospheric particles: A review of observations. J. Aerosol Sci., 35, 143-176.

Kulmala, M., Riipinen, I., Sipilä, M., Manninen, H., Petäjä, T., Junninen H., Dal Maso, M., Mordas, G., Mirme, A., Vana, M., Hirsikko, A., Laakso, L., Harrison, R. M., Hanson, I., Leung, C., Lehtinen, K. E. J., and Kerminen, V.-M. (2007) Towards direct measurement of atmospheric nucleation, Science, 318, 89-92.

Kulmala, M. and Kerminen, V.-M. (2008) On the growth of atmospheric nanoparticles, Atmos. Res., 90, 132-150.

Mirme, A., Tamm, E., Mordas, G., Vana, M., Uin, J., Mirme, S., Bernotas, T., Laakso, L., Hirsikko, A. & Kulmala, M. (2007) A wide-range multi-channel Air Ion Spectrometer. *Boreal Env. Res.* 12: 247–264.

Suni, T., J. Rinne, A. Reissell, N. Altimir, P. Keronen, Ü. Rannik, M. Dal Maso, M. Kulmala & T. Vesala, (2003) Long -term measurements of surface fluxes above a Scots pine forest in Hyytiälä, southern Finland, 1996-2001. *Boreal Environment Research*, 8, 287-301.

Tammet, H. (2006) Continuous scanning of the mobility and size distribution of charged clusters and nanometer particles in atmospheric air and the Balanced Scanning Mobility Analyzer BSMA, Atmospheric Research, 82: 523–535.

Vartiainen, E., Kulmala, M., Ehn, M., Hirsikko, A., Junninen, H., Petäjä, T., Sogacheva, L., Kuokka, S., Hillamo, R., Skorokhod, A., Belikov, I., Elansky, N. & Kerminen, V.-M. (2007) Ion and particle number concentrations and size distributions along the Trans-Siberian railroad. *Boreal Env. Res.* 12: 375–396.

Venzac, H., Sellegri, K. & Laj, P. 2007: Nucleation events detected at the high altitude site of the Puy de Dôme Research Station, France. *Boreal Env. Res.* 12: 345–359.

Virkkula, A., Hirsikko, A., Vana, M., Aalto, P. P., Hillamo, R. & Kulmala, M. (2007) Charged particle size distributions and analysis of particle formation events at the Finnish Antarctic research station Aboa. *Boreal Env. Res.* 12: 397–408.

COMPARISON OF CALIOP LEVEL 2 AEROSOL SUBTYPES TO AEROSOL TYPES DERIVED FROM AERONET INVERSION DATA

T. MIELONEN[1], A. AROLA[1], M. KOMPPULA[1], J. KUKKONEN[2], J. KOSKINEN[3], G. DE LEEUW[3,4] and K. E. J. LEHTINEN[1,5]

[1] Finnish Meteorological Institute, Kuopio Unit, Kuopio, Finland
[2] Finnish Meteorological Institute, Air Quality, Helsinki, Finland
[3] Finnish Meteorological Institute, Earth Observation, Helsinki, Finland
[4] Department of Physics, University of Helsinki, Helsinki, Finland
[5] Department of Physics, University of Kuopio, Kuopio, Finland

INTRODUCTION

Identification of aerosol types (in terms of their source origin and main composition) is important due to the varying effects of different aerosols on health, visibility and Earth's climate. When aerosol types are known, their sources can be identified more precisely and actions can be better targeted to reduce harmful aerosol emissions. Regarding the ground-based measurements, the origin of particulate matter can be determined by measuring the size distribution and the chemical composition, especially for various tracer constituents, using a sufficiently fine time resolution, in combination with a transport model. Especially for remote sensing, the identification of aerosol types is not easy or straightforward. Measurements and retrieval algorithms have their inherent limitations, and the optical and chemical properties of aerosols can vary tremendously even within one type of aerosol.

The Cloud-Aerosol Lidar and Infrared Pathfinder Satellite Observation (CALIPSO) satellite (Winker et al. (2003); Vaughan et al. (2004)) was launched successfully in April 2006, and measurement data has been available from June 2006 onward. CALIPSO is part of the A-Train constellation, which presently consists of five satellites. CALIPSO carries the Cloud-Aerosol Lidar with Orthogonal Polarization (CALIOP) instrument, which can measure the vertical structure of the atmosphere in three channels using the backscattering signal from the laser pulses. Two orthogonally polarized channels are at 532 nm and one channel measures the total backscattered signal at 1064 nm. The diameter of the laser pulse at ground level is about 70 m. CALIOP has a spatial resolution of 333 m along the orbital path. The satellite repeat cycle is 16 days. (Winker et al. , 2007) Due to the small footprint, CALIPSO covers only 0.2 % of the Earth's surface during the repeat cycle. (Kahn et al. , 2008)

METHODS

The scene classification algorithm of CALIOP can classify features as clouds or aerosols. Both classes have several subtypes. In this study, we investigated the aerosol subtypes and compared them to aerosol types derived from AERONET level 2.0 inversion data. We used CALIOP level 2 V2.01 data from 2006 to 2008. The level 2 V2.01 is the latest version of the data available at the time of writing. The CALIOP data are constructed from the calibrated profiles of attenuated backscatter. They include layer heights and descriptive properties (e.g. integrated attenuated backscatter, layer intergrated depolarization ratio, aerosol optical depth, etc.) with identification
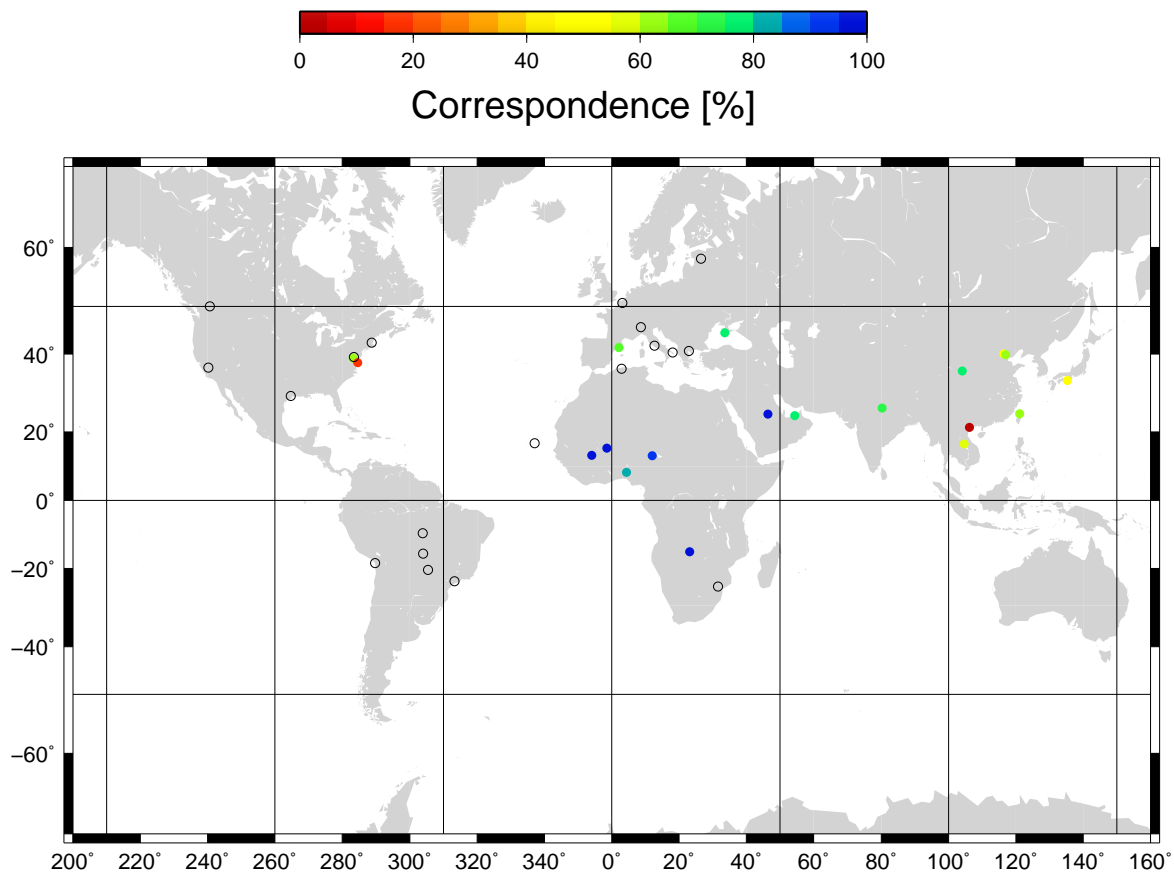
Figure 1: Map of the AERONET sites used in the study. The color coded circles show how well the types agreed at the sites with 5 or more comparison days. The sites with less useful days, are marked with black circles.

and typing (i.e. cloud vs. aerosol, aerosol subtypes, cloud subtypes). (ATBD part 1 , 2006)

CALIOP level 2 data include the following eight aerosol classes: 1) not determined, 2) clean marine, 3) dust, 4) polluted continental, 5) clean continental, 6) polluted dust, 7) smoke, and 8) other. These classes are based on extensive analysis of AERONET observations (Omar et al. , 2005). The subtype 'other' is reserved for an additional aerosol type, while the subtype 'not determined' is for cases where the algorithm fails to find a suitable class. The CALIOP classification of aerosol subtypes utilizes depolarization ratio, integrated attenuated backscatter coefficient, surface type and information on whether the layer is elevated or not. The depolarization ratio is a useful indicator for identifying non-spherical particles, and it can distinguish between dust and spherical aerosols. Multiple scattering has not been taken into account in the algorithms; hence it could introduce some uncertainties when optically thick layers are measured. The integrated attenuated backscatter coefficient is the observed backscatter strength of the layer. (ATBD part 3 , 2005)

AERONET uses Cimel sun photometers which measure AOD at 340, 380, 440, 500, 675, 870 and 1020 nm. Measurements are provided every 15 minutes during the daytime. AERONET also provides angular distribution of sky radiances in four wavelengths (440, 670, 870 and 1020 nm) and aerosol optical properties, such as single scattering albedo (SSA) and complex refractive index. The spectral AOD from AERONET are accurate to within $\pm$ 0.2 (Dubovik et al. (2000); Eck et al. (1999)). Holben et al. (1998) have described AERONET measurements in more detail. We
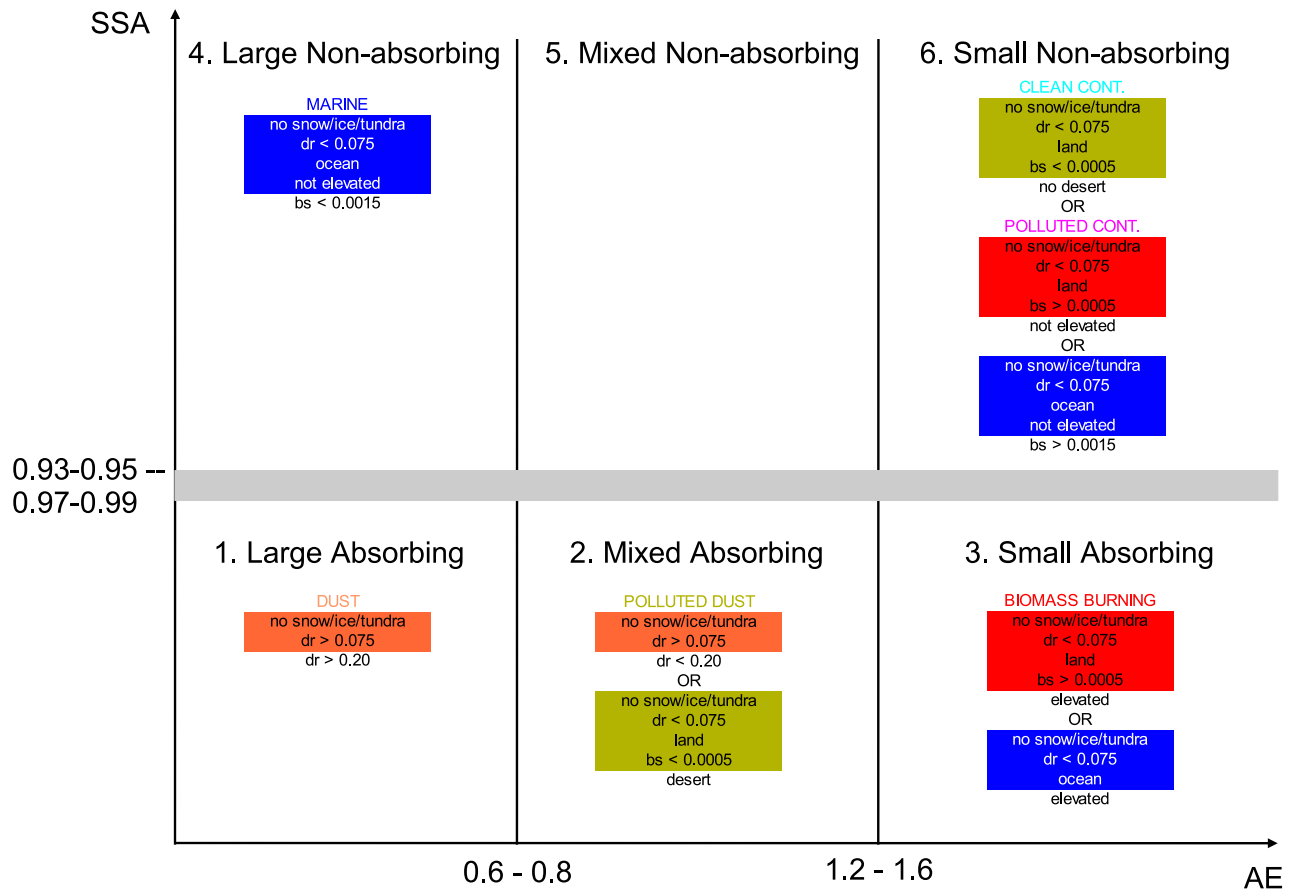
Figure 2: Corresponding CALIOP and AERONET aerosol types. Both AERONET and CALIOP classification criteria are presented for each type. SSA, AE, dr and bs refer to single scattering albedo, Ångström exponent, integrated volume depolarization ratio and integrated attenuated backscatter coefficient, respectively.

used cloud screened and quality assured level 2.0 inversion products with all points in the analysis.

We selected 38 AERONET sites around the world to the comparison based on their location and the amount of SSA measurements. Our attempt was to get as good global coverage as possible. The selected sites are shown in Fig. 1. Unfortunately, we were not able to locate any usable sites from Australia or offshores. We classified the AERONET data into six aerosol types based on daily mean SSA at 440 nm and Ångström exponent at 440-870 nm (AE). Fig. 2 presents the classification criteria for each type. There is some variability in the classification boundaries between the sites, because we checked manually that the aerosol type classes were representative for each site. For the SSA values, we used a "buffer zone" (shown as a gray bar) of 0.02 between the absorbing and non-absorbing types to remove the unclear border cases.

From the CALIOP data, we gathered all aerosol layers inside 1° x 1° box centered on the AERONET sites. Then we selected the most and the second most common aerosol types for each day for the boxes. The second most common subtype was also considered, due to the fact that CALIOP could detect various layers with different types at different altitudes during one overpass. The second most common subtype was taken into account only if the number of layers was more than 40 % of the number of layers in the first mode. This was done to ensure that there actually was a second well represented aerosol type present.

For the comparison, we had to select which CALIOP aerosol subtype corresponds to which AERONET

aerosol type. In our selection, shown in Fig. 2, the CALIOP type "Dust" equals large absorbing aerosols from the AERONET data. "Polluted dust" equals mixed absorbing aerosols, "Biomass burning" small absorbing aerosol, "Marine" Large non-absorbing aerosols and "Clean and Polluted continental" small non-absorbing aerosols. For the mixed non-absorbing type there were no clear CALIOP aerosol subtype, thus we did not attach any CALIOP aerosol subtypes to it.

RESULTS
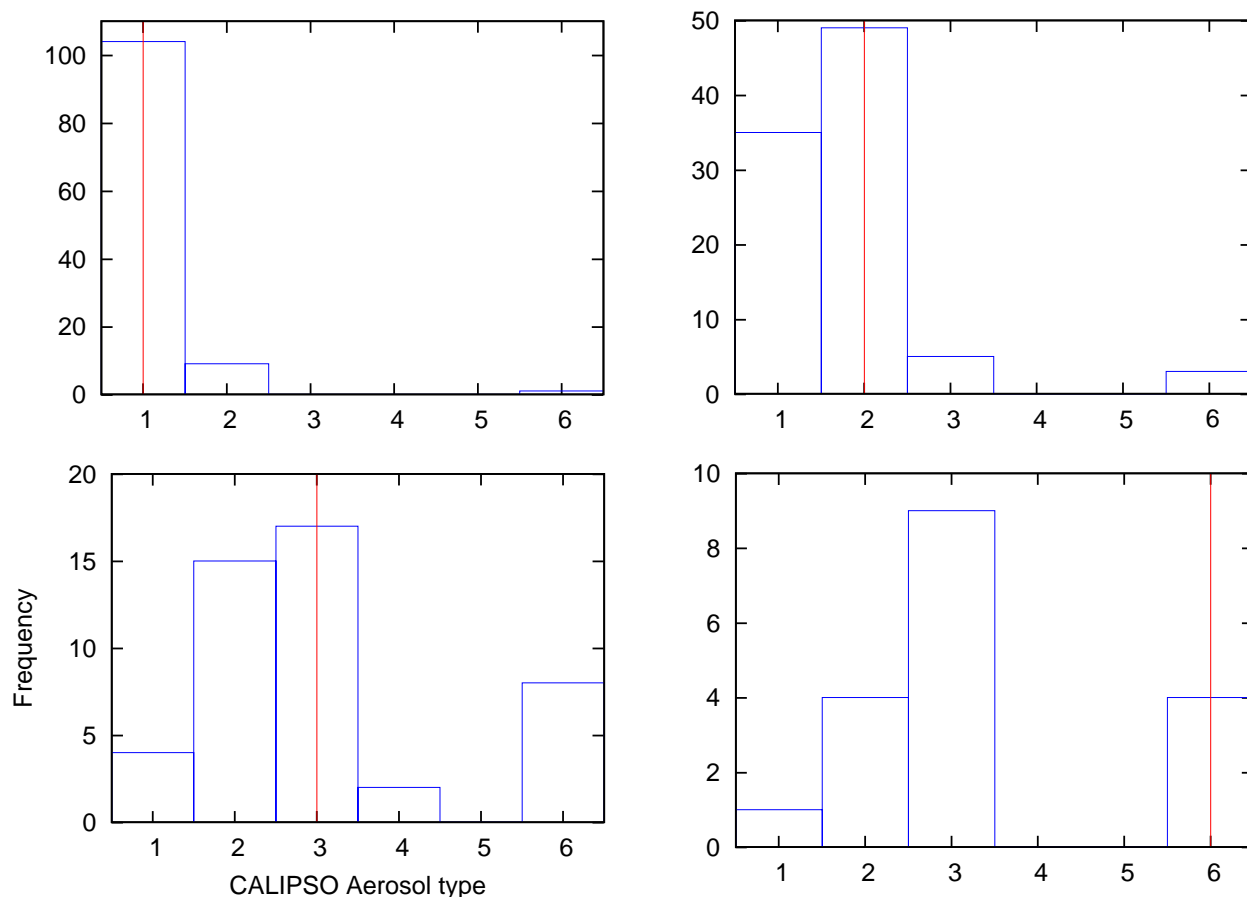
Figure 3: Corresponding aerosol subtypes from CALIOP for each AERONET aerosol type. The red line indicates the AERONET type and the corresponding CALIOP subtypes are on the x-axis. The y-axis denotes the frequency of the different types. Only aerosol types 1 (Large absorbing), 2 (Mixed absorbing), 3 (Small absorbing) and 6 (Small non-absorbing) are shown.

We compared aerosol types from AERONET to the mode of the aerosol subtypes from CALIOP. Overall, we found 277 suitable days for the comparison. The types agreed in 63 % of the cases. When we included the second most common subtype into the comparison, the agreement increased to 71 %.

The color coded circles in Fig. 1 show how well the types agreed at the studied sites. These 19 sites had 5 or more comparison days. The sites with less comparison days, are marked with black circles. The map indicates clearly that the best agreement between the types (91 %) is near desert regions where dust is the most common aerosol type. In the areas dominated by fine aerosols, the level of agreement is lower, albeit still rather good, about 57 %.

We also looked at the corresponding aerosol subtypes CALIOP had detected for each AERONET

aerosol type. The histograms from this comparison are shown in Fig. 3, where the red line indicates the AERONET type and the corresponding CALIOP subtypes are on the x-axis. Aerosol types 4 (large non-absorbing) and 5 (mixed non-absorbing) are not shown due to the small number of corresponding measurements. For the type 1 (large absorbing) and 2 (mixed absorbing) the agreement is very good (91 % and 53 %, respectively) and the mismatches fall to the neighboring aerosol types. For the small aerosols (types 3 and 6, absorbing and non-absorbing, respectively) the agreement percentage is a bit smaller (37 % and 22 %, respectively) and the types detected by CALIOP have more variability.

We also studied the possibility to improve the CALIOP classification scheme for aerosol subtypes by adding color ratio data to the scheme in order to give additional information on the size of the aerosols. We looked at the color ratios for the comparison days and realized that although color ratio anticorrelates to some extent with AE (R = -0.39), the variation of the parameter is large for each aerosol type and the values are all in the same range.

CONCLUSIONS

Our extensive comparison between the aerosol types from CALIOP and AERONET showed that:

1. Both instruments agreed on 70 % of the daily mean aerosol types.

2. Best agreement was achieved with large absorbing (dust) and mixed absorbing (polluted dust) aerosols.

3. Small and non-absorbing aerosols were harder to classify.

4. Color ratio provides some information on the size of the aerosols. However, the variability of the parameter is large, thus utilization of color ratio is not straightforward.

ACKNOWLEDGMENTS

REFERENCES

Dubovik O., A. Smirnov, B. N. Holben, M. D. King, Y. J. Kaufman, T. F. Eck, and I. Slutsker, (2000) Accuracy assessment of aerosol optical properties retrieval from AERONET sun and sky radiance measurements. J. Geophys. Res., 105, 9791–9806.

Eck, T., B. Holben, J. Reid, O. Dubovik, A. Smirnov, N. O'Neill, I. Slutsker, S. Kinne (1999) Wavelength dependence of the optical depth of biomass burning, urban, and desert dust aerosols, J. Geophys. Res., 104, 31,333–31,349.

Holben, B.N, T. F. Eck, I. Slutsker, D. Tanré, J. P. Buis, A. Setzer, E. Vermote, J. A. Reagan, Y. J. Kaufman, T. Nakajima, F. Lavenu, I. Jankowiak and A. Smirnov. (1998). AERONET–A federated instrument network and data archive for aerosol characterization. Rein. Sens. Environ., 66, 1–16.

Kahn, R. A., Chen, Y., Nelson, D. L., Leung, F.-Y., Li, Q., Diner, D., and Logan, J. A., (2008), Wildfire smoke injection heights: Two perspectives from space, Geophys. Res. Letters, 35(04)

Liu, Z., Omar, A. H., Hu, Y., Vaughan, M. A., and Winker, D. M., (2005), CALIOP Algorithm Theoretical Basis Document Part 3: Scene Classification Algorithms, PC-SCI-202 Part 3 Release 1.0.

Omar, A. H., Won, J.-G., Winker, D. M., Yoon, S.-C., Dubovik, O., and McCormick, M. P., (2005), Development of global aerosol models using cluster analysis of Aerosol Robotic Network (AERONET) measurements, J. Geophys. Res., 110, D10S14.

Vaughan, M., S. Young, D. Winker, K. Powell, A. Omar, Z. Liu, Y. Hu and C. Hostetler, (2004), Fully automated analysis of space-based lidar data: an overview of the CALIPSO retrieval algorithms and data products, Proc. SPIE 5575, pp. 16–30.

Winker, D.M., J. Pelon and M.P. McCormick, (2003), The CALIPSO mission: spaceborne lidar for observation of aerosols and clouds, Proc. SPIE 4893, pp. 1–11.

Winker, D. M., W. H. Hunt, and M. J. McGill, (2007), Initial performance assessment of CALIOP. Geophys, Res. Lett., 34, L19803.

Winker, D. M., Hostetler, C. A., Vaughan M. A. and Omar, A. H., (2006), CALIOP Algorithm Theoretical Basis Document Part 1: CALIOP Instrument, and Algorithm Overview. PC-SCI-202 Part 1 Release 1.0.

SIZE RESOLVED AEROSOL PARTICLE FLUX MEASUREMENTS: SAMPLING METHODS AND QUALITY MONITORING

P.MIETTINEN[1], and A. LAAKSONEN[2]

[1]Department of Physics, P.O. Box 1627, FI-70211 Kuopio, University of Kuopio, Finland
[2]Finnish Meteorological Institute, P.O. Box 503, FI-00101 Helsinki, Finland

Keywords: Atmospheric nanoparticles, Vertical flux, Size resolved, Sampling methods

INTRODUCTION

One of the largest uncertainties of earths radiation budget estimation is caused by incomplete understanding of aerosol particle induced cooling effect. Numerous properties of aerosol particle population such as distribution of aerosol particle sizes, aerosol number concentration and particle chemical composition affects interaction characteristics of aerosols and radiative energy. To gain better understanding of aerosol particle impact on atmospheric conditions both theoretical and experimental methods are needed to approximate aerosol particle origin and transport. Aerosol vertical flux measurements can give new information about spatial and temporal evolution of aerosol population. Based on flux measurement data, not only the location and strength of aerosol sinks and sources can be investigated, but analysis can be extended to e.g. estimation of particle deposition velocities. Eddy covariance method provides direct method to estimate vertical aerosol fluxes. Early aerosol particle flux measurements were aimed to study total particle number fluxes and it was not until recent years that size resolved particle flux measurements gained attention and real instrumentation was tested (Schmidt et al.). Major problem prohibiting use of size resolved particle flux techniques have been absence of suitable instrumentation that must be applied. Aerosol particle Eddy covariance measurements involve high speed sampling of 3D wind components and particle information as well. While high sampling frequency 3D anemometers have been at disposal for decades, the high speed particle sizing instruments have been brought to market just few years ago.

In this study we tested flux estimate derived from lower sample frequency size resolved signal and compared it with flux estimate that is derived from higher sampling frequency signal. Furthermore we show that by using total number flux measured by CPC as reference, it is possible to evaluate 1 Hz signal quality and make distinction between good and faulty data.

METHODS

Impact of sampling frequency on size resolved particle flux estimate is studied using experimental methods. Particle flux values is calculated using both low sampling frequency size resolved data and high frequency total number concentration data. It is also shown that by making comparison between higher sampling frequency total particle number flux estimate and accumulated size resolved particle flux estimate at 1 Hz, it is possible to find if 1Hz particle sizing information is adequate to capture all relevant information for size resolved particle flux estimation (Lenschow et al.). Also reference signal provides a tool for detection and removal of artefact of certain type e.g. transient high concentration of 1 Hz signal. Furthermore reference signal can used to derive particle size specific delays in particle sizer.

RESULTS

Experimental testing was done during PuijoCloudExpriment in September 2008. Test system consisted of Metek 3D anemometer, TSI 3772 condensation particle counter and TSI 3091 Fast Mobility Particle Sizer. Anemometer and CPC was sampling at 10 Hz frequency while FMPS had sample rate of 1 Hz. Measurement site was located in tower 2 km North-West from Kuopio city center, tower structure is bulky, causing disturbances in airflow near tower and hence this site is not ideal for long term eddy covariance measurements that involve e.g. annual budget of particle vertical flow estimation.

Figure 1 shows reference 10 Hz signal from CPC and particle total number concentration detected by FMPS at 1 Hz, fairly good agreement between instruments can be seen

Results show that during well developed turbulence conditions 10 Hz cpc data can used for detection of problems of 1 Hz size resolved flux data. Figure 2 shows particle total number flux derived from both 10 Hz CPC signal and 1 Hz FMPS signal. Anemometer signal of 1 Hz sampling frequency is calculated as average of 1 s from 10 Hz anemometer signal. Particle sized signal of FMPS is accumulated over all size channels to get total number concentration for comparison.
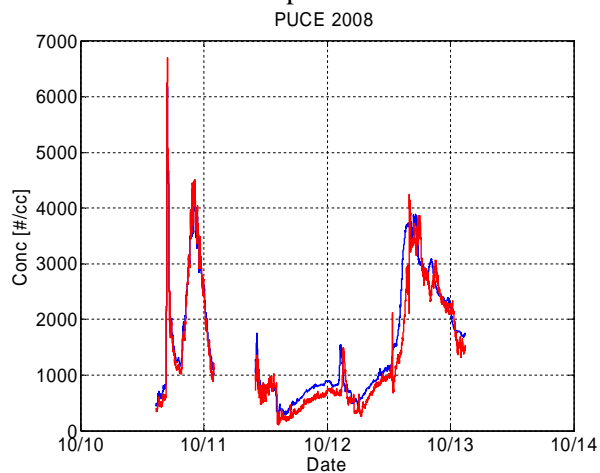
Figure 1. Particle concentration detected by CPC 10Hz signal (TSI3772) blue line and total particle number concentration detected by FMPS (TSI3091) 1 Hz signal (red line).

In figure 2 can be seen that during most of the sample period high and low frequency flux estimates are in agreement hence use of low frequency signal is justified for flux estimation.
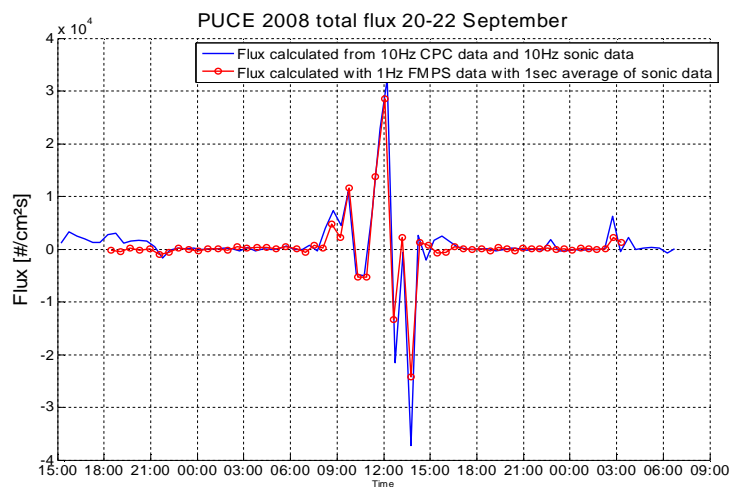
Figure 2. Particle total number fluxes calculated by CPC 10 Hz signal (blue line) and total number flux by FMPS 1 Hz signal (red line).

CONCLUSIONS

Use of low (here 1 Hz FMPS signal) frequency size resolved particle sizing information can used for size resolved vertical flux estimation whenever it can be assured that all relevant information is captured by instruments, here we use high frequency CPC concentration information as reference signal for size-resolved low frequency flux estimate quality monitoring.

REFERENCES

Schmidt, A. and Klemm, O. (2008), Direct determination of highly size-resolved turbulent particle fluxes with the disjunct eddy covariance method and a 12-stage electrical low pressure impactor, Atmos. Chem. Phys. Discuss., 8, 8997-9034.

Lenschow, D.H., Mann, J. and Kristensen, L., (1994). How long is long enough when measuring fluxes and other turbulence statistics. *Journal of atmospheric and oceanic technology*, 11: 661-673.

HYGROSCOPIC AND CCN PROPERTIES OF ATMOSPHERIC AEROSOL PARTICLES AT SMEAR II IN HYYTIÄLÄ

J. MIKKILÄ, J. VANHANEN, M. EHN, T. PETÄJÄ, P. P. AALTO AND M. KULMALA

University of Helsinki, Dept. Physics, P. O. Box 64, 00014 Univ. of Helsinki, Finland

INTRODUCTION

Atmospheric aerosol particles can act as cloud condensation nuclei (CCN) and eventually form clouds. These clouds affect the radiative balance of the atmosphere by scattering and absorbing light. This is called the indirect effect of atmospheric aerosols, and can be either cooling or warming. It is one of the least understood processes affecting climate change (IPCC, 2007). The ability of an aerosol particle to act as a cloud condensation nucleus depends mainly on the size of the particle (Dusek *et al.* 2006), but the chemical composition also plays a part by affecting the hygroscopicity of the particle. In a global change perspective the total amount of CCN active particles affect the climate both by altering the albedo of the clouds as well as affecting the precipitation patterns. In this study, measurements of CCN concentrations at the SMEAR II station in Hyytiälä, Finland are evaluated and compared to hygroscopicity measurements from a hygroscopicity tandem differential mobility analyzer (H-TDMA) and particle size distribution measurements from differential mobility particle sizer (DMPS, Aalto *et al.* 2001).

METHODS

CCN concentrations were measured with a commercial diffusion-type CCN counter (Droplet Measurements Technologies Inc., Roberts and Nenes, 2005). The sample flow surrounded by sheath flow (1/10 flow ratio) is led through a vertical column with walls wetted with water. The column temperature increases along the flow, generating a stable supersaturation. The particles that activate and grow by condensation will be detected by an optical particle counter. The concentration of the cloud condensation nuclei is obtained as a function of the supersaturation. Supersaturations of 0.1, 0.2, 0.4, 0.6 and 1.0 % were used. The CCN counter was calibrated by using ammonium sulphate particles.

The activation of an aerosol particle into a cloud droplet is described by the Köhler equation (Köhler 1936):

$$S = \gamma_w x_w \exp\left(\frac{4 M_w \sigma}{RT\rho D_p} \right), \tag{1}$$

where S is the saturation ratio, γ_w is the activity coefficient, x_w is the mole fraction of water, M_w is the molar mass of water, σ is the surface tension of the solution, R is the universal gas constant, T is temperature, ρ is the density of the solution and D_p is the diameter of the initial dry particle. Atmospheric aerosol particles often have insoluble cores, and for this situation the Köhler equation is described by Laaksonen *et al.* 1998.

The total aerosol particle size distribution is measured by using a differential mobility particle sizer (DMPS, Aalto *et al.* 2001). By comparing the CCN concentration and total particle concentration, the activated fraction is obtained. The DMPS data can also be used to calculate an approximation for the critical particle diameter for all the supersaturations used. In order to acquire this, the activation probability is assumed to behave like a step function, with all particles above the critical size activating. The particle size distribution is summed from the largest particle sizes towards the smallest sizes until the CCN concentration is obtained. At that point the diameter corresponds to the critical diameter.

A HTDMA (Ehn *et al*., 2007) was used to measure the hygroscopicity of aerosol particles. In this instrument, sample aerosol is first brought through a drier and a radioactive charger in order to reach charge equilibrium and a relative humidity below 20%. After this a certain dry particle size, D_{dry}, is selected using a differential mobility analyzer (DMA). Next the particles are passed through a humidifier so that a certain controlled relative humidity is reached. Finally the humidified aerosol passes through another DMA which is used as a DMPS. Thus a humidified size distribution for a certain D_{dry} is measured. The second DMA was located in a temperature controlled box, maintained at a temperature of 19°C and relative humidity of 90%. Four dry sizes (110nm, 75nm, 50nm and 35nm) were used which belong to the standard sizes agreed inside the EUCAARI project. The hygroscopicity of a certain dry size can simply be described as a growth factor

$$g_a = \frac{D_{wet}}{D_{dry}}, \tag{2}$$

where D_{wet} is a mean diameter calculated from the humidified size distribution for a certain D_{dry}. The soluble fractions for different dry sizes were calculated using the equation

$$\varepsilon = \frac{V_{sol}}{V_{tot}} = \frac{g_a^{\,3} - 1}{g_{sol}^{\,3} - 1}, \tag{3}$$

(Swietlicki *et al*., 1999). Here g_{sol} is the known growth factor of the fully soluble reference substance with the same humid particle size as the ambient particle (D_{wet}). In this study ammonium sulphate was used as a reference and ambient aerosol was simply assumed to be a mixture of insoluble material and ammonium sulphate. In most cases the ambient aerosol is a much more complex mixture of different soluble and insoluble compounds. Nevertheless this approach is widely used in H-TDMA studies and can provide comparable information when there is no definite knowledge about the chemical composition of the aerosol.

The critical particle diameter for certain supersaturation can be calculated also from H-TDMA data using so called kappa-Köhler equation (Petters and Kreidenweis, 2007). In this theory the Köhler equation is modified so that all the physico-chemical properties of aerosol are captured into a single kappa parameter thus describing fully the hygroscopic behaviour including cloud droplet activation. The values for kappa are obtained by setting saturation ratio and particle size in the equation according to measured relative humidity, dry size and growth factor. The critical particle diameter with certain kappa is determined by searching the dry size which produces maximum value of Köhler curve equal to corresponding supersaturation. When measuring in constant relative humidity different kappa values might be achieved for different dry sizes. The most valid critical diameter in a size range can be assumed to be the one having the kappa calculated from a dry diameter closest to that size range and probably having similar chemical composition.

<center>RESULTS AND CONCLUSIONS</center>

In figure 2 critical diameters, calculated from CCN and HTDMA data, are presented as a function of supersaturation, together with the corresponding critical diameters of the pure ammonium sulphate particles. The critical diameters for the measured aerosol are larger than for ammonium sulphate, most likely due to insoluble or slightly soluble compounds mixed in the particles. The critical diameter calculations from CCN and HTDMA data give almost the same results, although values from H-TDMA are slightly higher. This indicates that average critical diameters can be calculated also from H-TDMA data.

The insoluble fraction can be calculated by assuming that particles contain only an insoluble compound and ammonium sulphate. We obtained the insoluble fraction by iterating the insoluble fraction in the Köhler equation by Laaksonen *et al*. 1998 to fit the measured data. The results are shown in the figure 3. Also the insoluble fractions calculated from the H-TDMA data (1-ε) are shown in the figure. Soluble fractions ε obtained from the H-TDMA data are in agreement with previous results for the boreal forest aerosol (Hämeri et al., 2001). The Aitken mode (<100 nm) can be seen to differ from the accumulation

mode (>100 nm) for both H-TDMA and CCNC data even though the absolute values obtained with these two methods do not agree completely. In Aitken mode the insoluble fraction is higher than in accumulation mode. This was also detected by Birmili et al. 2009 from number size distribution measurements at different relative humidities. The accumulation mode particles probably contain higher fraction of hygroscopic inorganics, which accumulates to the particles during cloud-processing and ageing. (Swietlicki et al., 2008). The Aitken mode is possibly more influenced by the regional emissions of biogenic organic compounds which might participate to the growth of particles and lower their hygroscopicity. There are several possible error sources which may have lead to the difference between the two approaches mentioned above. In these early considerations only a visual evaluation was used to select which days to use and all calculations were done for the average values. Furthermore, instead of measured ammonium sulphate calibrations, theoretical values for the g_{sol} were used. As the data analysis continues, many of the error sources will be eliminated.
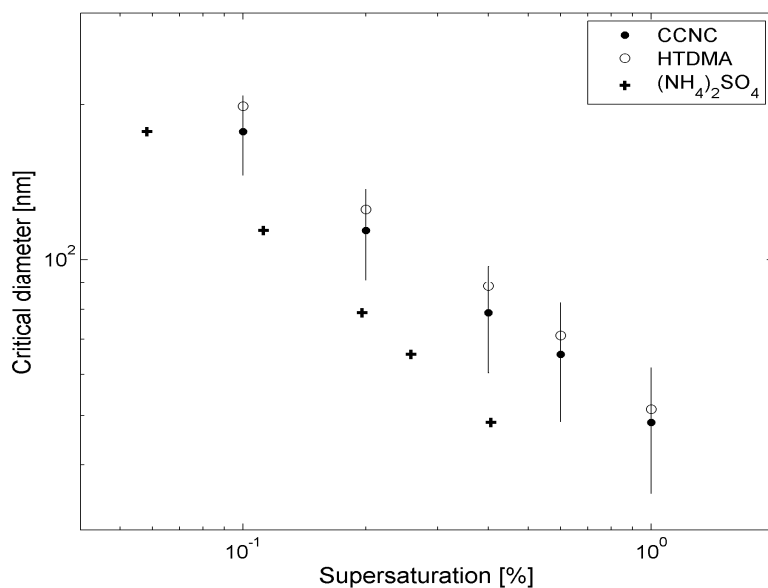
Figure 1. Critical diameter obtained from CCNC and HTDMA data and for ammonium sulphate ((NH$_4$)$_2$SO$_4$) particles as a function of supersaturation.
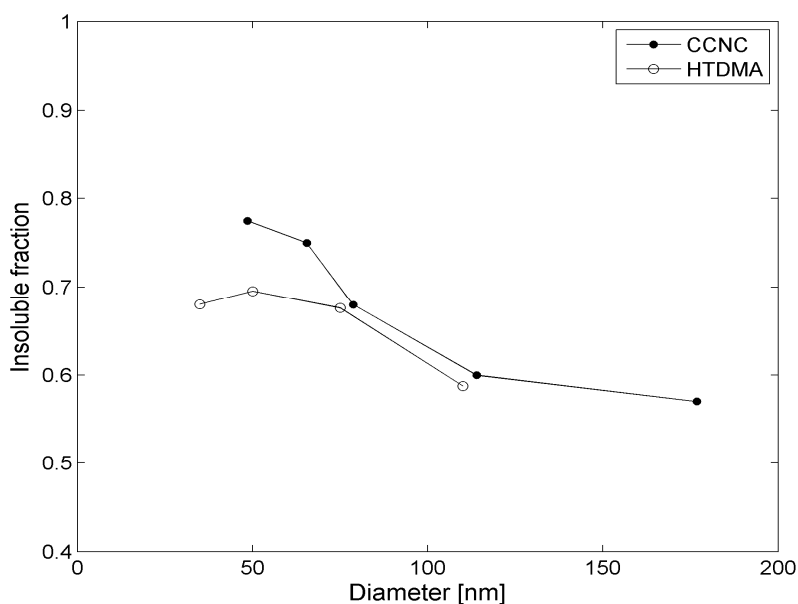
Figure 2. Insoluble fraction as a function of particle diameter calculated from CCNC and HTDMA data.

An example of CCN concentrations compared to DMPS total concentrations and size distributions are presented in figure 3. There is a clear new particle formation event during 2nd of July just before noon. This results a subsequent increase of aerosol number concentration in the Aitken mode. Simultaneously a decrease in the accumulation mode particle number concentration was observed. This change can be seen as a decrease in CCN concentration at supersaturation of 0.1% and 0.2%, while the CCN concentrations at 0.4 to 1.0% increase. This can be explained by the difference in critical diameter, according to figure 1. The formed particles grow toward larger sizes during the next night. This can be seen as an increase in CCN concentration at all saturation ratios. The increase starts at slightly different times for each supersaturation due to the difference in critical diameter. From this we can conclude that new particle formation events affect cloud condensation nuclei concentrations and this way have a contribution to the indirect effect of aerosols on climate.
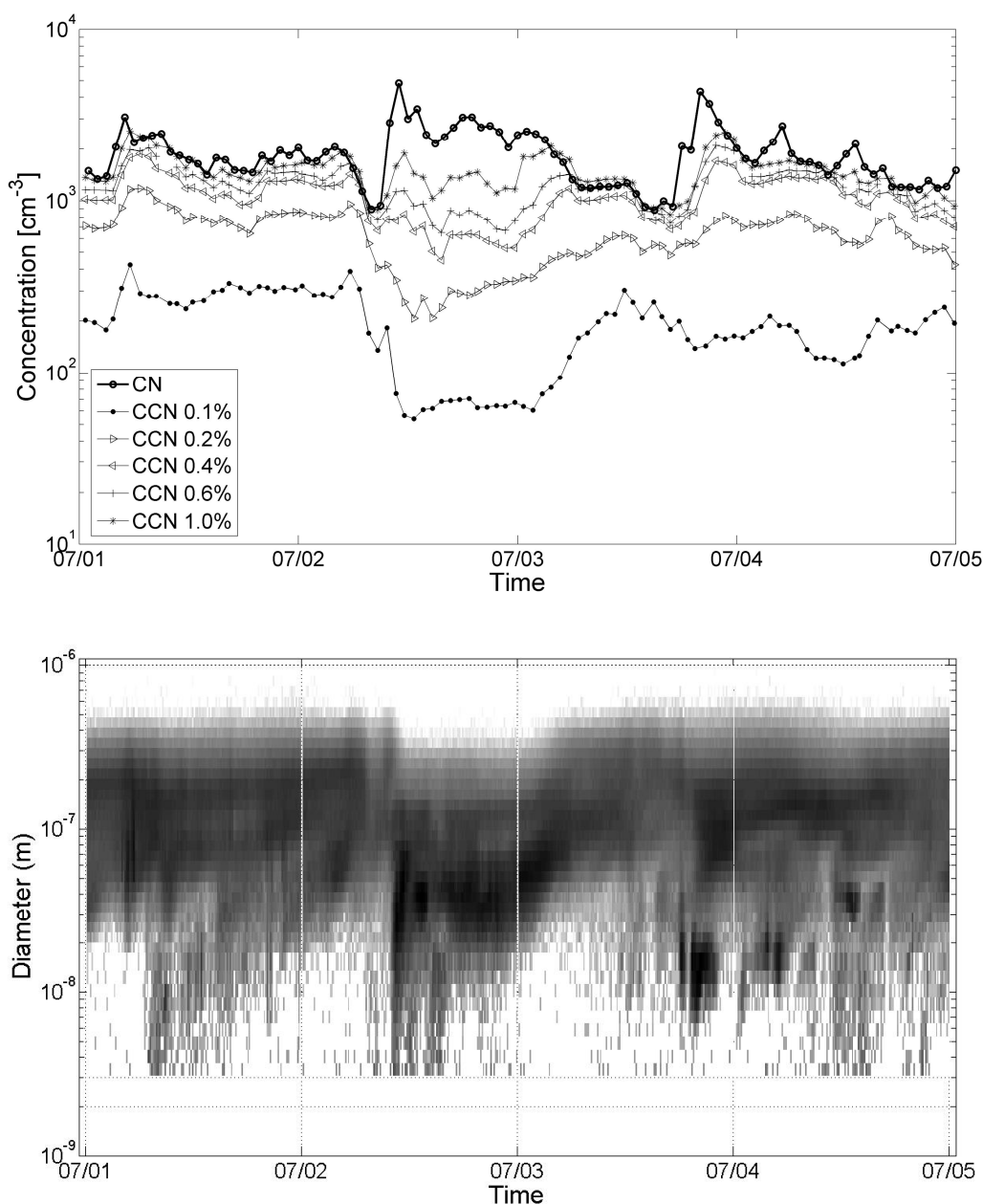
Figure 3. Cloud condensation nucleus concentrations (CCN) in Hyytiälä (1.7.08 - 4.7.08) compared to the total particle concentration (CN) and particle size distribution measured with DMPS.

REFERENCES

Aalto, P. P, Hämeri, K., Becker, E., Weber, R., Salm, J., Mäkelä, J. M., Hoell C., O'Dowd, C. D, Karlsson, H., Hansson H.-C., Väkevä M., Koponen I. K., Buzorius G. and Kulmala M. (2001) Physical characterization of aerosol particles during nucleation events, *Tellus* 53B, 344-358.

Dusek, U., Frank, G. P., Hildebrandt, L., Curtius, J., Schneider, J., Walter, S., Chand, D., Drewnick, F., Hings, S., Jung, D., Borrmann, S., Andreae, O. M. (2006) Size Matters More Than Chemistry for Cloud-Nucleating Ability of Aerosol Particles, *Science*, 312, 1375-1378.

Ehn, M., Petäjä, T., Aufmhoff, H., Aalto, P., Hämeri, K., Arnold, F., Laaksonen, A. and Kulmala, M. (2007) Hygroscopic properties of ultrafine aerosol particles in the boreal forest: diurnal variation, solubility and the influence of sulfuric acid, *Atmos. Chem. Phys.*, 7, 211–222

Hämeri, K., Väkevä, M. Aalto, P. P., Kulmala, M., Swietlicki, E., Zhou, J., Seidl, W., Becker, E. and O'Dowd, C. D. (2001) Hygroscopic and CCN properties of aerosol particles in boreal forests. *Tellus*, 58B, 359-379.

IPCC (Intergovermental panel on climate change), Climate change 2007: The physical science basis, edited by: Solomon, S., Qin, D., Manning, M., Marquis, M., Averyt, K., Tignor, M. M. B., Miller, Jr., H. L. R., and Chen, Z.

Köhler, H. (1936) The nucleus in and the growth of hygroscopic droplets, *T. Faraday Soc.*, 32, 1152–1161.

Laaksonen, A., Korhonen, P., Kulmala, M., Charlson, R. J. (1998) Modification of the Köhler Equation to Include Soluble Trace Gases and Sligthly Soluble Substances, *American Meteorological Society*, 55, 853-862.

Petters, M. D., and Kreidenweis, S. M. (2007) A single parameter representation of hygroscopic growth and cloud condensation nucleus activity, *Atmos. Chem. Phys.*, 7, 1961– 1971.

Roberts, G., and Nenes, A. (2005) A Continuous-Flow Streamwise Thermal-Gradient CCN Chamber for Atmospheric Measurements, *Aerosol Science and Technology*, 39, 206–221

Swietlicki, E., Zhou, J., Berg, O. H., Martinsson, B. G., Frank, G., Cederfelt, S.-I., Dusek, U., Berner, A., Birmili, W., Wiedensohler, A., Yuskiewich, B. and Bower, K. N. (1999) A closure study of sub-micrometer aerosol particle hygroscopic behaviour, *Atm. Res.* 50, 205-240.

Swietlicki, E., Hanson, H.-C., Hämeri, K., Svenningson, B., Massling, A., McFiggans, G., Murry, P., H., Petäjä, T., Tunved, P., Gysel, M., Topping, D., Weingartner, E., Baltensperger, U., Rissler, J., Wiedensohler, A. and Kulmala, M. (2008) Hygroscopic properties of submicrometer atmospheric aerosol particles measured with H-TDMA instruments in various environments - a review, *Tellus*, 60B, 432–469

STATISTICAL ANALYSIS OF FACTORS AFFECTING TO THE NUMBER CONCENTRATION OF ATMOSPHERIC AEROSOLS IN TWO POLLUTED AREAS

S. MIKKONEN[1], K. E. J. LEHTINEN[1,2], S. ROMAKKANIEMI[1], J. JOUTSENSAARI[1], A. HAMED[1] and A. LAAKSONEN[1,3]

[1]Department of Physics, University of Kuopio, P.O.B 1627, FIN-70211 Kuopio, Finland

[2]Finnish Meteorological Institute, P.O.B 1627, FIN-70211 Kuopio, Finland

[3]Finnish Meteorological Institute, P.O.B 503, FIN-00101 Helsinki, Finland

INTRODUCTION

Atmospheric aerosols are known to have a great effect on radiation budget, formation of clouds, on climate change and on human health. Studying the effects of particle mass and number concentration on human health is one of the central topics in aerosol research. Some previous studies suggest that particle number is more responsible for health effects than particle mass (e.g. Woo et al., 2001) - thus we chose it as our variable of interest. The problem in the use of general data analysis methods is that the measurement data is not normally distributed and contains usually different kinds of autocorrelation structures. The purpose of this study is to introduce an advanced statistical data analysis method which takes account the structure of the data and use it to find predictors and indicators for the number concentration of particles in the selected size range in two different measurement sites in central and southern Europe.

METHODS

Our first dataset consists of measurements made between 24.3.2002 - 30.4.2005 at the San Pietro Capofiume (SPC) station in Po Valley, Italy and the second dataset consists of measurements made between 1.7.2003 – 30.6.2006 in Melpitz station in eastern part of Germany. The concentration of particles was measured by using a twin Differential Mobility Particle Sizer (DMPS) system. More details of the measurements at SPC can be found in Hamed et al. (2007) and for Melpitz in Birmili and Wiedensohler (2000).

The aim of our study was to design a model that predicts the number concentration of particles with a set of variables measured continuously at these two different stations. We chose to predict 50nm particles in this study but the same model framework can also be used for any other particle sizes. Most of our models were combinations from hourly averages of gas and meteorological parameters measured at the stations, including temperature, relative humidity, radiation, O_3, SO_2, NO_2, condensation sink, wind speed and - direction and the probability that the day is an event day i.e. a day when significant new particle formation can be seen. The probabilities of event days (PrE) and probabilities of nonevent days (PrNE) were calculated with the discriminant analysis described by Mikkonen et al. (2006). The calculated event probability was used instead of observed event classification because the probabilities of an event day can be estimated also for those days where the event classification has not been made.

Due to the complex structure of processes affecting the concentration of small particles it is not reasonable to use general linear effect models in the analysis. We chose to use generalized linear models with logarithmic link function and combine it with mixed model structure (McCulloch and Searle, 2001). The main idea of a mixed model is to estimate not only the mean of the measured response variable y, but also the variance-covariance structure of the data. Modelling the (co-)variances of the variables reduces the bias of the estimates and prevents autocorrelation of the residuals.

RESULTS

We found out that in SPC relative humidity, PrNE and the concentration of SO_2 had significant additional variance components for different times of year. When the additional variance is taken into account, the model suggests that the effect of RH on the particle number concentration is negative in January and in December and positive for the rest of the year. The decreasing regression effect of PrNE is on its highest in January, June and July, and the effect of SO_2 concentration is negative in winter months (from Nov. to Apr.) and positive for the rest of the year. Condensation sink is suggested to be a preventing factor for nucleation events (e.g. Vehkamäki et al., 2004) but it seemed to have a strong positive effect on the number concentration of 50nm particles. Ozone concentration has been found to affect the oxidation of organic species and thus affect the particle formation and growth. This effect shows also in our data as an increase of the regression effect of ozone concentration during daytime. The model predicts adequately even the highest peaks of the number concentration (Figure 1) but overestimates slightly the smallest observations.
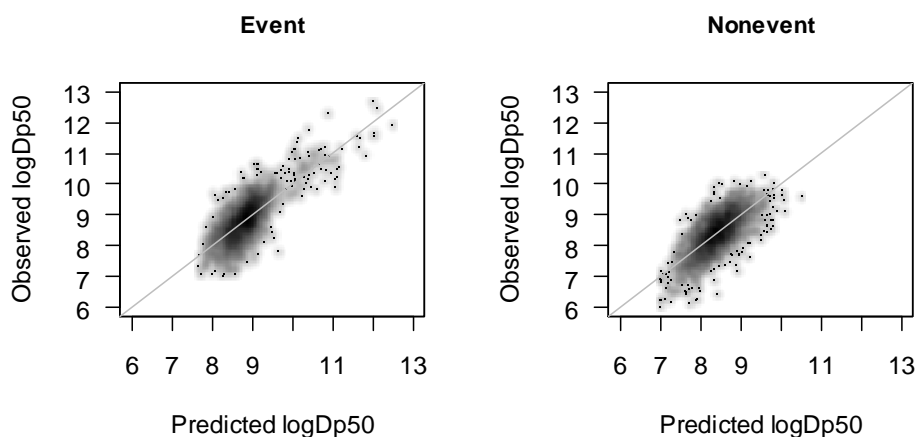
Figure 1. Observed vs. predicted natural logarithms of number concentrations for event and nonevent days in SPC. Diagonal line represents the perfect fit and the tone of the colour shows the density of the datapoints.

In Melpitz the parameterization of the best predictive model was slightly different than in SPC, which indicates that the parameters affecting to the growth of particles are partially site specific. The biggest difference between sites is significant effect of NO_2 in Melpitz. The seasonal variation of the regression effects of RH and SO_2 follow the same pattern than in SPC as well as the effect of condensation sink. The prediction ability of the model is fairly well also in Melpitz (Figure 2), even though it underestimates some of the highest concentration peaks in event days.
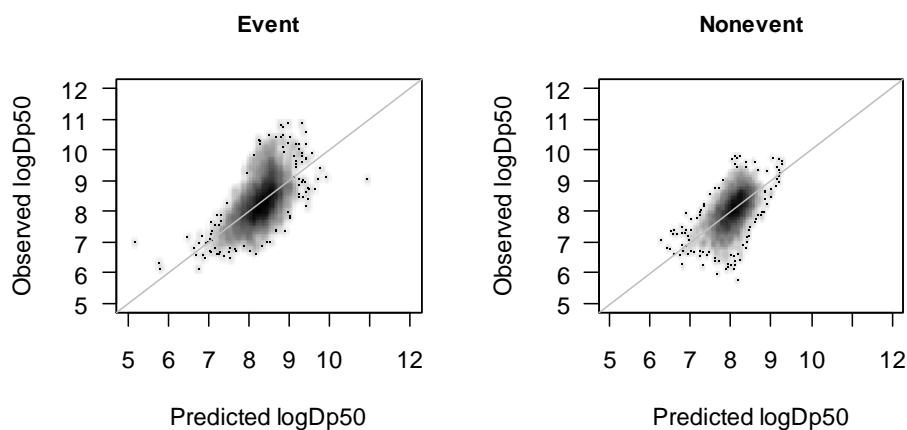
Event

Nonevent

Figure 2. Observed vs. predicted natural logarithms of number concentrations for event and nonevent days in Melpitz. Diagonal line represents the perfect fit and the tone of the colour shows the density of the datapoints.

Figure 3 illustrates how the model predicts the concentration of 50nm particles as a time series. In SPC the predicted values (grey line), follow quite nicely the observed values (dashed line). In Melpitz the agreement of the observations and prediction is not as good as in SPC but still adequate.

SPC
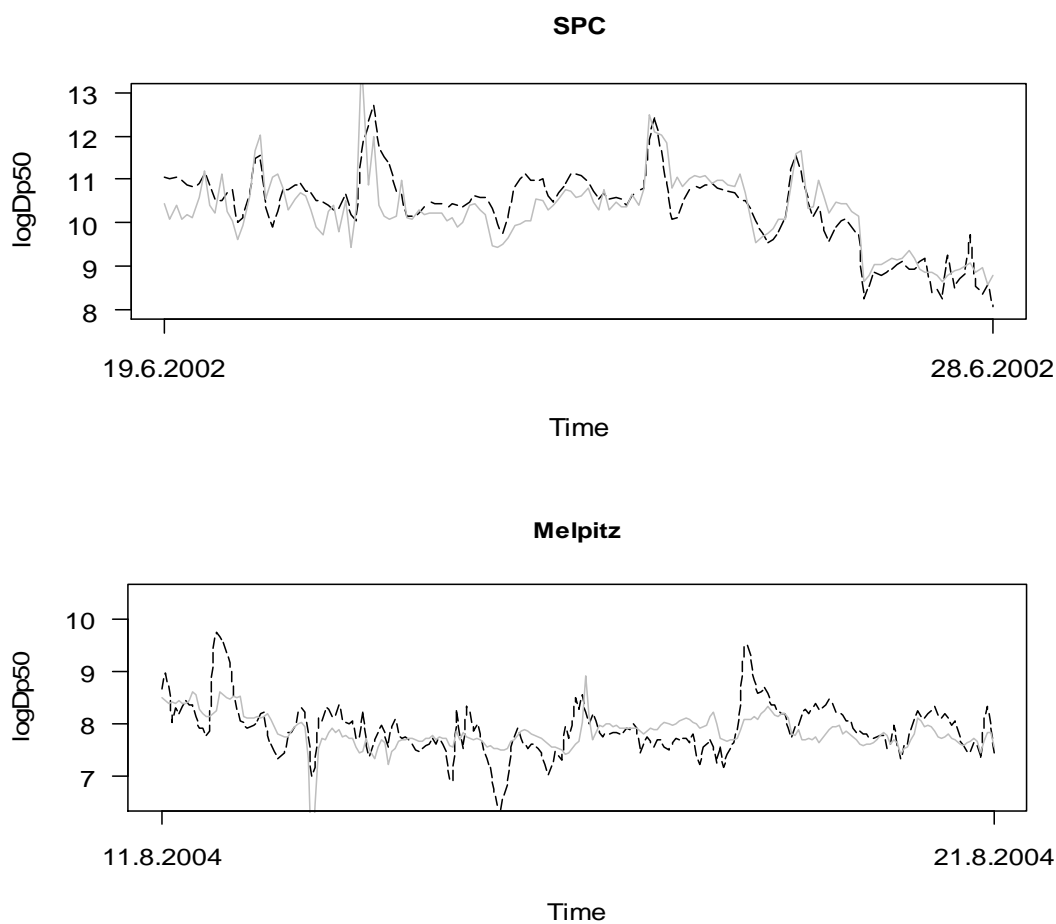
Melpitz

Figure 3. Observed (black dashed line) vs. predicted (grey solid line) natural logarithms of number concentration in SPC station in 19.-28. June 2002 (upper panel) and in Melpitz in 11.8.2004-21.8.2004.

ACKNOWLEDGEMENTS

REFERENCES

Birmili, W. and Wiedensohler, A. (2000): New particle formation in the continental boundary layer: Meteorological and gas phase parameter influence, *Geophys. Res. Lett.*, 27, 3325–3328.

Hamed, A. Joutsensaari, J. , Mikkonen, S., Sogacheva, L., Dal Maso, M., Kulmala, M., Cavalli, F., Fuzzi, S., Facchini, M. C., Decesari, S. , Mircea, M., Lehtinen, K. E. J. , and Laaksonen A. (2007): Nucleation and growth of new particles in Po Valley, Italy, *Atmos. Chem. Phys.*,**7**,355.

McCulloch, C. and Searle, S. R. (2001). *Generalized, Linear, and Mixed Models*, New York: Wiley.

Mikkonen, S., Lehtinen, K. E. J., Hamed, A., Joutsensaari, J., Facchini, M. C. and Laaksonen, A. (2006): Using discriminant analysis as a nucleation event classification method, *Atmos. Chem. Phys.*, 6, 5549-5557.

Vehkamäki, H., Dal Maso, M., Hussein, T., Flanagan, R., Hyvärinen, A., Lauros, J., Merikanto, P., Mönkkönen, M., Pihlatie, K., Salminen, K., Sogacheva, L., Thum, T., Ruuskanen, T. M., Keronen, P., Aalto, P. P., Hari, P., Lehtinen, K. E. J., Rannik, Ü, and Kulmala, M.(2004): Atmospheric particle formation events at Värriö measurement station in Finnish Lapland 1998-2002, *Atmos. Chem. Phys.*, 4, 2015-2023.

Woo, K. S., Chen, D. R., Pui, D. Y. H., and McMurry, P. H.(2001): Measurement of Atlanta aerosol size distributions: Observations of ultrafine particle events, *Aerosol Sci. Technol.*, 34, 75–87.

USER INFLUENCE ON INDOOR MODEL SIMULATION

B. MØLGAARD, T. HUSSEIN

Department of Physical Sciences, University of Helsinki, Finland

Keywords: indoor aerosols, modelling, penetration, deposition

INTRODUCTION

It is well known that inhalation of aerosol particles may have adverse health effects. To reduce the indoor exposure to potentially harmful particles it is important to understand the mechanisms that control the indoor particle number concentration and size distribution. Models are tools to understand the importance of the different mechanisms and to predict the particle number size distribution under given circumstances.

Principles for development of indoor aerosol models are described in Hussein et al. (2005) and Hussein and Kulmala (2008). Some models are very complicated as they include multiple compartments and several of the processes deposition, resuspension, condensation, evaporation, coagulation, nucleation, emission, transport, and filtering mechanisms. In addition models may also include some relevant gas chemistry.

In this study we have made a single compartment model and applied it to data from an office in Viikki. The measurements were done from 15 May to 30 June 2000 with two DMPS systems, that measured indoor and outdoor particle number size distributions. The size range was $7 - 600$ nm. The ventilation rate was kept almost constant around 3 h^{-1}, and there were no indoor sources. A G3-class filter was installed in the ventilation system. The data has already been analyzed by Hussein et al. (2005).

METHODS

The model is a single compartment model. We have assumed that the air is well mixed in the office, and we have ignored coagulation, condensation and evaporation. The following mass-balance equation has been used to calculate the evolution of the number concentration N_i of particles in size section i:

$$\frac{d}{dt}N_i = O_i P_i \lambda - N_i(\lambda + \lambda_{d,i}) \tag{1}$$

Here O_i is the outdoor number concentration of particles in size section i, P_i is the penetration factor for that particles size, λ is the ventilation rate, and $\lambda_{d,i}$ is the deposition rate of particles of that size. Note that it is assumed that the physical properties of particles in a size section are invariant.

The deposition rate depends on particle size and air flow characteristics in the compartment. We have incorporated the model by Lai and Nazaroff (2000) for deposition on smooth surfaces. It requires the input of the friction velocity.

The penetration factor also depends on particle size, so it gives one unknown for each size section. Particles are lost in the filter, mainly, and in the ventilation pipes. Therefore the penetration factor is expected to be a little below the penetration factor of a G3-class filter itself.
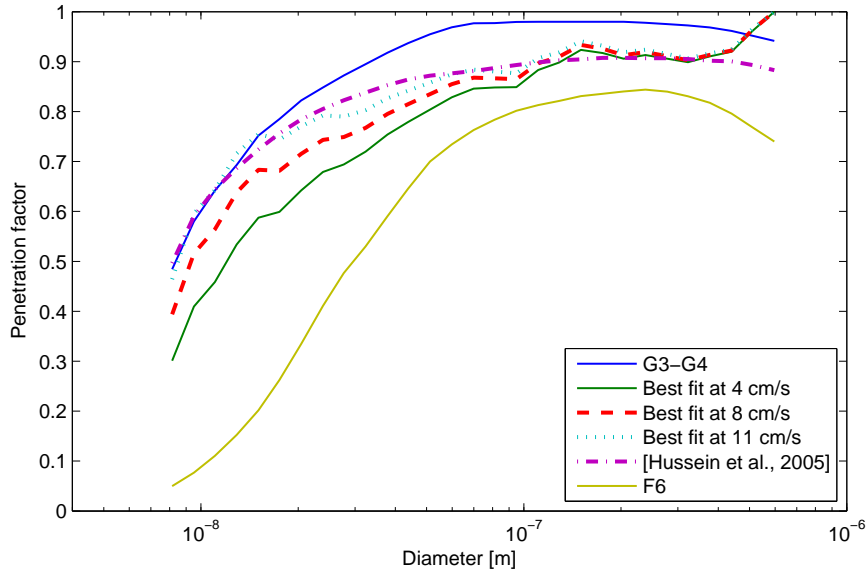
Figure 1: Penetration factors for G3 and F6 filters, penetration factor obtained by Hussein et al. (2005), and best fit penetration factors for friction velocities 4 cm/s, 8 cm/s, and 11 cm/s.

The simulation is done independently for each size section which is possible when ignoring condensation, evaporation and coagulation. The simulation is compared to the measurements by calculating the least square value:

$$S_i = \sum_t \frac{(N_{sim,i,t} - N_{meas,i,t})^2}{N_{meas,i,t} N_{sim,i,t}}.$$

Here i is the size section, t is the time, N_{meas} is measured indoor data, and N_{sim} is the simulated indoor data.

The model first iterates the friction velocity. For each size section S is minimized and a friction velocity is found. The median of these friction velocities is chosen. Then the the model adjusts the penetration factor and the friction velocity in small steps.

The office consists of a main room, a small shower room, and a small bath room. There were no indoor sources, surface to volume ratio $S/V = 3.6 m^{-1}$, and ventilation rate $\lambda = 3h^{-1}$. The ventilation system has a G3-class filter installed so we have used the penetration factor of as the initial penetration factor in most runs. In some runs we assumed a F6-class filter instead to test if the model would approach the same solution.

RESULTS AND DISCUSSION

It turns out that it is in no way trivial to find the right combination of friction velocity and penetration factor. There are many combinations of friction velocity and penetration factor that give similar results for the simulation. The model minimizes the value S that is used to compare data to simulation. The size of the iteration steps affects strongly how close the model gets to the minimum. And there is no guarantee that this minimum actually gives the optimal combination from a physical point of view.

At a friction velocity of 11 cm/s the model suggests a penetration factor that is lower than or equal to the one of a G3-class filter, and it is similar to the one obtained by Hussein et al. (2005) for 19
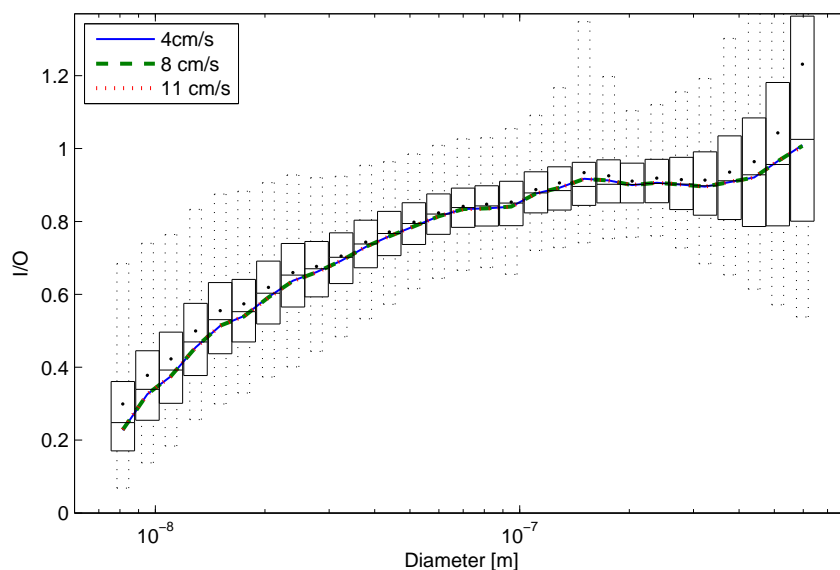
Figure 2: Medians of simulated of I/O ratios for friction velocities 4 cm/s, 8 cm/s, and 11 cm/s combined with their respective best fit penetration factors. Mean (dots), quartiles (boxes), and 5 and 95 percentiles (dashed boxes) of the measured data are also presented.

cm/s. See figure 1. For friction velocities above 11 cm/s my model suggests a penetration factor greater than the one of a G3 filter (for some size classes), which is not realistic. Penetration factors corresponding to friction velocities[1] 4 cm/s and 8 cm/s are also shown in figure 1. The model suggests a solution somewhere between these two. When it comes to predicting I/O ratios, using these friction velocities combined with their best fit penetration ratios give very similar results. The median I/O ratios are shown in figure 2. The agreement between simulation and measurement seems rather good. There seems to be a problem with the measurement of 600 nm particles as the median I/O ratio is above one. Note that a good agreement between the median I/O ratios is a necessary but not sufficient condition for a simulation to be good.

Percentiles of the ratio $\frac{N_{sim}}{N_{meas}}$ between the simulated and measures data are presented in figure 3. The better the model is, the closer these should be to unity. This shows that the three choices of input parameters really give very similar performance of the model. It also show that the model does not predict the concentrations of the smallest and largest particles very well. This is partly due to uncertainty of the measurements though.

It seems impossible to determine the friction velocity and penetration factor based on comparison of simulation results. Let us consider the penetration curves in figure 1. The curves obtained by this model and by Hussein et al. (2005) suggest that the penetration was around 0.9 in the interval $100 - 200$ nm, which is much lower than the 0.98 penetration through the G3-class filter. This can be either due to dirt in the filter or long ventilation pipes that collect particles and thus lower their concentration. Whatever the reason is, it should also cause deposition of particles of other sizes. Therefore the best fit penetration factor corresponding to a friction velocity of 11 cm/s is hardly realistic. The penetration factors corresponding to 4 cm/s and 8 cm/s seem more realistic. But we do not have the knowledge to decide which of them is more realistic. We would guess that the penetration factor is somewhere in between, and that the friction velocity is between 4 cm/s and 8

---

[1]The friction velocity 4 cm/s and the corresponding penetration factor was obtained by starting the iteration from an F6 filter.
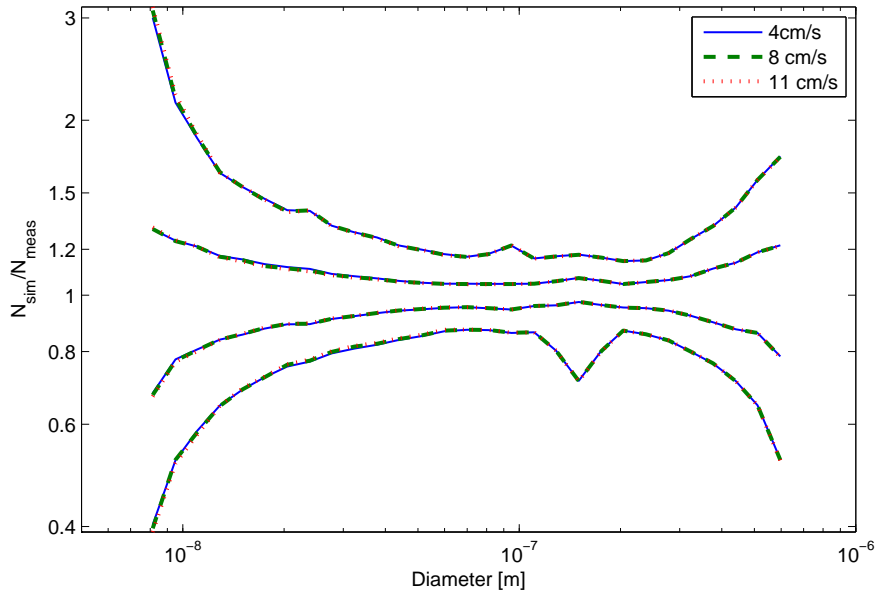
Figure 3: Percentiles (5%, 25%, 75%, and 95%) of the ratio $\frac{N_{sim}}{N_{meas}}$ for simulations using friction velocities 4 cm/s, 8 cm/s, and 11 cm/s combined with their best fit penetration ratios as input parameters.

cm/s. Note that this is less than half of the 19 cm/s estimated by Hussein et al. (2005).

Figure 3 clearly shows that the model could be improved. Even though the office consists of three rooms, we have assumed one well mixed compartment. We would expect a three compartment model to work better. Including coagulation would probably improve the prediction of the concentrations of the smallest particles.

CONCLUSION

Though the model does not work so well for all size sections, the performance seems acceptable considering the simplicity of the model and the uncertainty of the data. Different sets of input parameters gave simulations of very similar quality. One should not rely on the solution that is suggested in the end of the iteration, but use this and intermediate sets of input parameters as suggestions. It is up to the user of the model to select a realistic solution.

REFERENCES

Hussein, T.,Korhonen, H., Herrmann, E., Hämeri, K., Lehtinen, K.E.J., Kulmala, M. (2005) Emission Rates Due to Indoor Activities: Indoor Aerosol Model Development, Evaluation, and Applications, *Aerosol Science and Technology*, $39 : 1111 - 1127$, 2005.

Hussein, T., Kulmala, M. (2008) Indoor Aerosol Modeling: Basic Principles and Practical Applications, *Water Air Soil Pollut: Focus (2008)*, $8 : 23 - 34$.

Lai, A.C.K., Nazaroff W.W. (2000) Modeling indoor particle deposition from turbulent flow onto smooth surfaces, *J. Aerosol Sci.*, Vol.31, No.4, pp. $463 - 476$, 2000.

APPROACHING BULK LIQUID DROP. A THEORETICAL STUDY

ISMO NAPARI

Department of Physics, P.O. Box 64, FI-00014 University of Helsinki,Finland

Keywords: nucleation, liquid drop model, density functional theory

INTRODUCTION

Recent Monte Carlo (MC) simulations (Merikanto et al., 2007b,a; Barrett and Knight, 2008) have shown that, beyond a certain cluster size, the liquid drop (LD) model of classical nucleation theory accurately gives the increase in formation free energy when a single particle (atom or molecule) is added to a cluster at constant vapor conditions. The importance of finding this limit is twofold: on the one hand, it can be used to assess the validity of the LD model; on the other hand, simulating clusters somewhat larger than the limit and plotting the resulting cluster free energies as a function of change in the cluster surface area gives an estimate on the equilibrium vapor pressure and surface tension of bulk fluid. In this study, density functional theory (DFT) is used to calculate the free energies of clusters consisting of atoms and diatomic molecules. The results are used to quantify the deviations from the LD model.

THEORY

The applied molecular models are simple Lennard-Jones (LJ) atoms and molecules composed of two LJ sites. In the latter models the site-site interaction parameters are adjusted to vary the degree of orientation of the molecules on the liquid-vapor surface. The calculations are performed using DFT at the mean-field level. More details are found in Napari (2008). The present application of DFT gives the free energy of a cluster enclosed in a spherical container with perfect non-absorbing walls. This corresponds to the Lee-Barker-Abraham cluster definition used in MC simulations.

The calculations have been done for clusters from $N = 2$ to $N = 1000$. The formation free energy (which in DFT formalism is the grand potential difference $\Delta\Omega_N$) of any of these clusters in a vapor with chemical potential μ_v and pressure P_v is obtained from the grand potential difference (Talanquer and Oxtoby, 1994)

$$\Delta\Omega_N = F_N - \mu_v N - \Omega_u, \tag{1}$$

where F_N is the Helmholtz free energy of the cluster of size N and volume V_N and $\Omega_u = -P_v V_N$ is the grand potential of the uniform vapor. The change in formation energy when a particle is added to the cluster at constant vapor conditions is obtained from (Napari, 2008)

$$\delta\Delta\Omega_N = \delta F_N - \mu_v + P_v v_c, \tag{2}$$

where $\delta F_N \equiv F_N - F_{N-1}$ and v_c is the volume per particle in the cluster.

A similar expression can be written in the LD model. For a cluster in the saturated vapor

$$\delta\Delta\Omega_{N,e}^{\text{LD}} = [N^{2/3} - (N-1)^{2/3}]A_1\gamma, \tag{3}$$

where A_1 is the monomer surface area at bulk liquid density and γ is the surface tension planar interface. Plotting the free energy differences δF_N of DFT clusters on $[N^{2/3} - (N-1)^{2/3}]$ scale
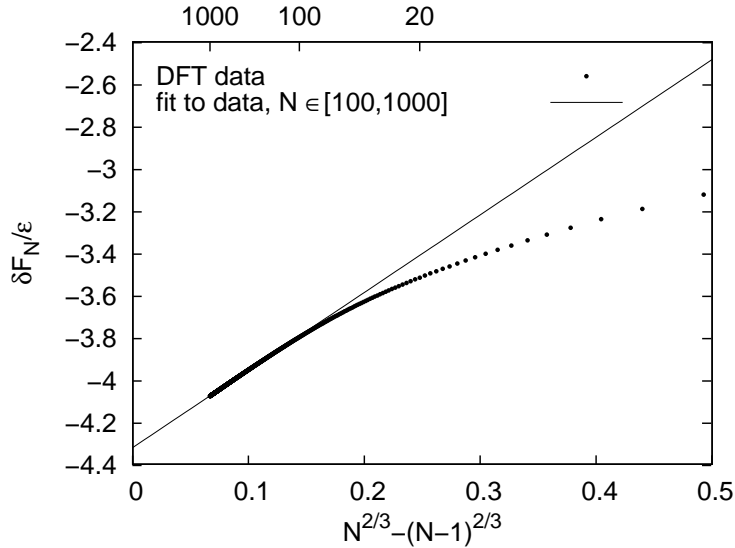
Figure 1: The Helmholtz free energy difference δF_N with respect to area change of a spherical cluster $(N^{2/3} - (N-1)^{2/3})$ for Lennard-Jones clusters at temperature $k_B T/\epsilon = 1$ and constraining volume $V_N/(N\sigma^3) = 5$. (Here σ is the LJ length parameter and ϵ the LJ energy parameter.) The line is a fit to data from $N = 100$ to $N = 1000$. The number of particles in the cluster is indicated on the top of the graph.

immediately shows us where the results deviate from the linear scaling of Eq. (3). (Note that δF_N and $\Delta \Omega_N$ have the same slope in the linear region.)

The bulk equilibrium values of vapor pressure P_e and surface tension are inferred in a simple manner. Fitting the DFT δF_N data to

$$\delta F_N^{\text{fit}} = c[N^{2/3} - (N-1)^{2/3}] + d \tag{4}$$

and comparing

$$\delta \Delta \Omega_{N,e} = \delta F_N^{\text{fit}} - d. \tag{5}$$

with Eqs. (3) and (2), it is immediately seen that $c = A_1 \gamma$ and $d = \mu_e - P_e v_c$.

RESULTS AND DISCUSSION

Figure 1 shows that the DFT calculations of simple LJ clusters at $k_B T/\epsilon = 1$ conform to the LD model when the cluster is larger than about a hundred atoms. At lower temperatures the "bulk" limit of cluster size is reached at smaller sizes, which is in line with the MC simulations (Merikanto et al., 2007b).

The bulk equilibrium vapor pressure and surface tension can be obtained from plots similar to Fig. 1. Results for LJ clusters enclosed in volumes $V_N/(N\sigma^3) = 5$ are shown in Fig. 2, where P_e and γ are shown relative to the exact values obtained from the equation of state and the DFT studies of the planar interface. Figure 2 indicates that the cluster calculations can be used to estimate the bulk fluid values with an accuracy of few percent. The same conclusion was made in MC simulations (Merikanto et al., 2007b,a; Barrett and Knight, 2008). The DFT results are found quite insensitive to the size of the enclosing volume.
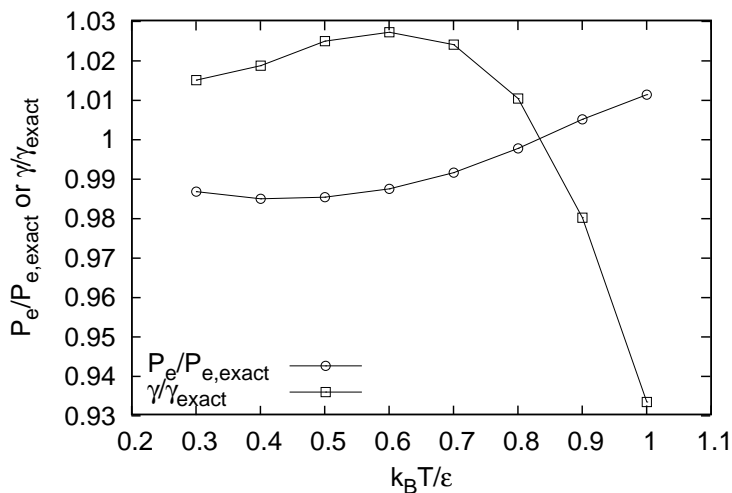
Figure 2: Vapor pressure and surface tension relative to the exact values as a function of temperature. Linear fits to cluster data in the size range $N = 100 - 1000$ are used. The constraining volume is $V_N = 5N\sigma^3$.

Results for diatomic molecules are similar to simple LJ system. This is somewhat surprising, because, in addition to molecules consisting identical sites, molecules with mutual dislike between the atomic sites were also studied. In these systems the molecules orient themselves on the liquid-vapor surface and even show multiple oriented layers. In such systems the cluster surface is expected to be different from the planar surface owing to the finite size of the cluster. Nevertheless, the estimated values of P_e and γ show maximum four percent deviation from the exact values.

CONCLUSIONS

The results of this study support the conclusions from MC simulations that the cluster data can be used to estimate equilibrium vapor pressure and surface tension at wide range of temperatures. This fact is based on the observation that beyond a certain size the energetics of clusters conform to the LD model. In the studied systems the limit of validity of the LD model extends down to clusters of a hundred molecules or, at low temperatures, to somewhat smaller sizes. For some systems this limit may be considerably lower: MC simulations of water show (Merikanto et al., 2007a) that clusters of 10 molecules already exhibit bulk-like behavior. Especially important is the observation that the conclusions hold even for systems with a complex liquid-vapor interface. It may then be assumed that clusters in other systems with a complex interface, for example water-alcohol mixtures, behave in a similar manner as the model systems studied here.

ACKNOWLEDGEMENTS

REFERENCES

Barrett, J. C. and Knight, A. P. (2008). Estimation of bulk liquid properties from monte carlo simulations of lennard-jones clusters. *J. Chem. Phys.*, 128:086101.

Merikanto, J., Zapadinsky, E., Lauri, A., Napari, I., and Vehkamäki, H. (2007a). Connection between the virial equation of state and physical clusters in a low density vapor. *J. Chem. Phys.*, 127:104303.

Merikanto, J., Zapadinsky, E., Lauri, A., and Vehkamäki, H. (2007b). Origin of the failure of classical nucleation theory: incorrect description of the smallest clusters. *Phys. Rev. Lett.*, 98:145702.

Napari, I. (2008). Equilibrium vapor pressure and surface tension from cluster data: Density functional results. *J. Chem. Phys.*, 129:154507.

Talanquer, V. and Oxtoby, D. W. (1994). Dynamical density functional theory of gas-liquid nucleation. *J. Chem. Phys.*, 100:5190–5199.

Particle size dependence on sulphuric acid concentration in binary homogeneous nucleation of H_2SO_4-H_2O system

K. Neitola[2], D. Brus[2,3], M. Sipilä[1,4] and M. Kulmala[1]

[1]*Department of Physics, University of Helsinki, P.O. Box 64, FI-00014 Helsinki, Finland*
[2]*Finnish Meteorological Institute, Erik Palménin aukio, P.O. Box 503, FI-00101 Helsinki, Finland*
[3]*Laboratory of Aerosol Chemistry and Physics, Institute of Chemical Process Fundamentals Academy of Sciences of the Czech Republic, Rozvojová 135, CZ-165 02 Prague 6, Czech Republic*
[4]*Helsinki Institute of Physics, University of Helsinki, P.O. Box 64 FI-00014 Helsinki, Finland*

Abstract. In this experiment we studied water-sulphuric acid binary homogeneous nucleation in laminar flow chamber. Nucleation rates and mean diameter of particles were determined as a function of sulphuric acid concentration in three different relative humidities. Number of sulphuric acid molecules in critical cluster was determined from the experimental data and the results are in fair agreement with previous experiments.

Key Words: Sulfuric acid; water; homogeneous nucleation; laminar flow tube; particle size diameter; condensation particle counter.

INTRODUCTION

Atmospheric new particle formation has been observed almost everywhere in the world[1] and binary homogeneous nucleation of sulphuric acid and water is assumed to be the most important phase involved in this process.[2,3]

Several laboratory studies have been investigating binary nucleation of sulphuric acid and water system earlier.[4-11] The production of sulphuric acid was done either from liquid solution by evaporation or saturating flow with vapour from liquid supply[4-7], or from gas phase by reacting SO_2 with OH radicals.[8-11] In these studies H_2SO_4 concentration has been determined by mass balance calculations,[4,5] organic titration reactions and kinetic model calculations[8,9] or measured by using Chemical Ionization Mass Spectrometers (CIMS).[6,7,10,11] The concentration of H_2SO_4 ranged from $3 \cdot 10^6$ up to $1.5 \cdot 10^{11}$ cm^{-3} and the resulting nucleation rates J from 1.10^{-3} to 1.10^5 $cm^{-3}s^{-1}$. The particle detectors used in earlier studies were all commercial CPCs with the cut-off size (i.e. 50% of this sized particles are detected) ranging from ~10 nm[4,5] to ~2.5 nm[6-11].

In this study a laminar flow tube to study binary homogeneous nucleation of sulphuric acid and water was used. The sulphuric acid vapour was produced from liquid reservoir and evaporated in a furnace before entering the nucleation chamber. We particularly focused on counting efficiency of several different ultrafine CPCs, namely models: TSI 3025A, TSI 3776 (working fluid butanol) and TSI 3786 (working fluid water), all of them were calibrated with silver particles to cut-off = 2.5 nm. The Pulse Height CPC (PH-CPC) was also employed to monitor the particle number concentration. With pulse height technique the particles with diameters below 2 nm can

be detected[12]. To measure size distribution the Differential Mobility Particle Sizer (DMPS) system was used (HAUKE DMA with UCPC TSI 3025A).

The nucleation rates were measured at three different relative humidities (10%, 30% and 50%). The sulphuric acid concentration was calculated by mass balance.

RESULTS

This study covers three independent measurement campaigns. The obtained experimental results are presented separately, because it is very difficult to employ all the instrumentation at the same time. First, the counting efficiency difference between butanol and water based UCPCs is presented, see figure 1. Second, the difference in particles counting efficiency between standard UCPCs TSI 3025, TSI 3776, and the Pulse High CPC is shown, see figure 2. The data are presented only for relative humidity 30 %.

Figure 1 shows measured nucleation rates as a function of sulphuric acid concentration. It is clearly visible that water based UCPC TSI 3786 has better detection efficiency for H_2SO_4 particles due to hygroscopic properties of sulphuric acid than butanol based UCPC TSI 3776. The particle count of TSI 3776 is just one fourth of the count of TSI 3776 at lower concentrations of sulfuric acid. With increasing sulfuric acid concentration the counting efficiency of both becomes comparable. The slope of the linear fit is used to predict the composition of the critical cluster and number of sulphuric acid molecules in critical cluster is predicted and presented in figure 1.
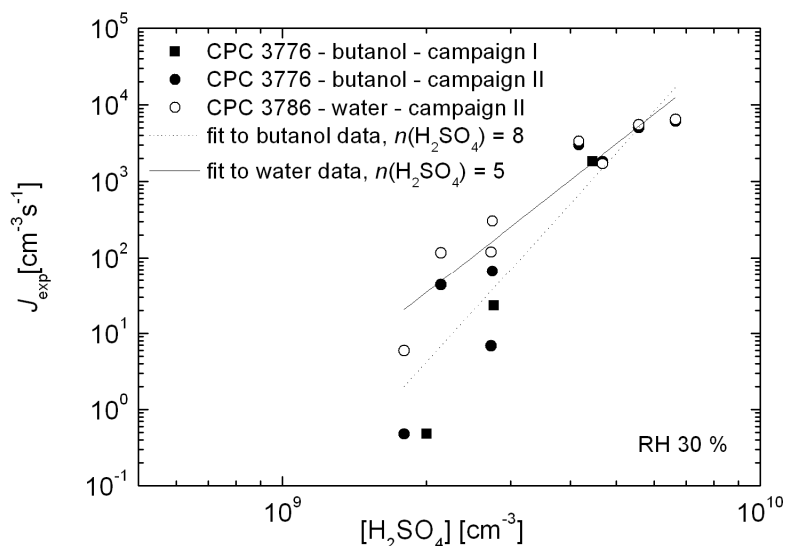
Figure 1 Measured nucleation rate J as a function of sulphuric acid concentration for the two campaigns with linear fits and the prediction of number of H_2SO_4 molecules in critical cluster determined from the slope of the fit.

The comparison of experimental nucleation rates as a function of H_2SO_4 concentration for UCPCs (TSI 3025A and 3776) and PH-CPC measured at two different residence times is presented in figure 2. Both TSI 3025A and 3776 showed similar results and were consistent with each other. The PH-CPC has a different slope due to its better detection efficiency with smaller particles, i.e. at lower sulfuric acid concentrations. Moreover the slope is similar as was found for water based UCPC TSI 3786. When H_2SO_4 concentration increases particles grow and detection efficiency of TSI 3025A and 3776 gets closer to the one of PH-CPC. The increased residence time in the nucleation chamber increases the losses of particles and condensation of H_2SO_4 vapour to the particles and to walls. This can be seen as smaller J for increased t_n.
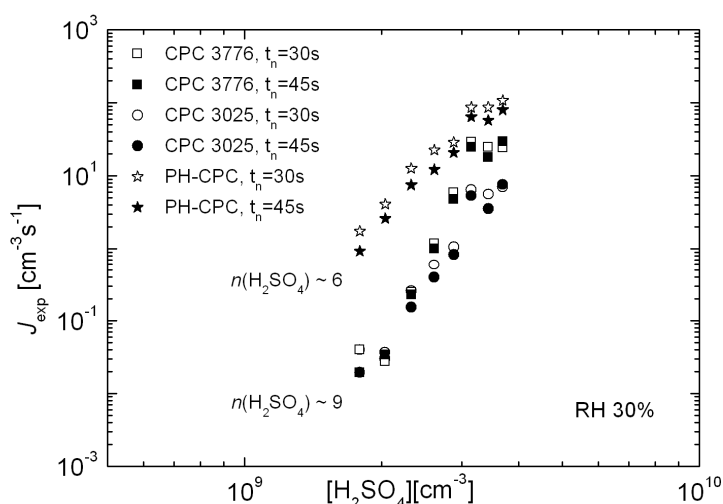
Figure 2 Nucleation rate J as a function of H_2SO_4 concentration measured with three different CPCs at two different residence times t_n.
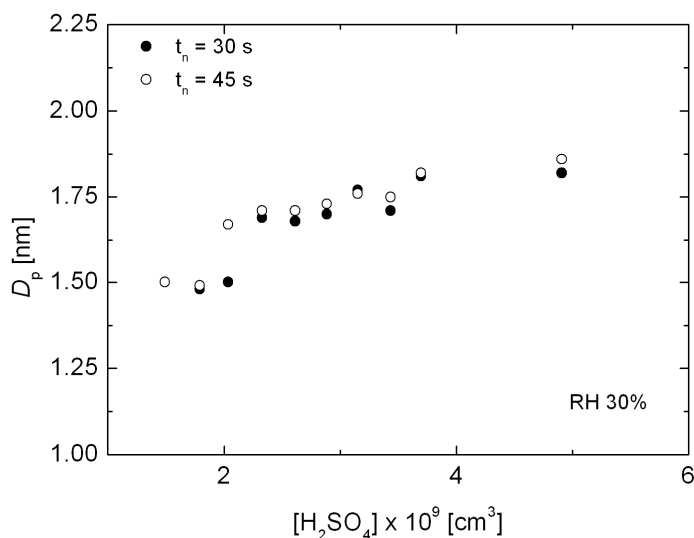
Figure 3 Mean particle diameters D_p as a function of H_2SO_4 concentration, measured with two different residence times.

In figure 3 is presented the mean diameter D_p of the nucleated particles measured with the PH-CPC as a function of sulphuric acid concentration for RH 30% and two different residence times. It can be seen that particles grow with increasing H_2SO_4 concentration from ~1.5 nm to ~1.8 nm. The diameter measured has an error of about 20%, but the trend is still visible.

CONCLUSIONS

Binary homogenous nucleation rates of sulphuric acid water system were measured in laminar flow tube using several different detectors. The counting efficiency was found different for butanol and water based detector. Our results favor the water based UCPC of better sulphuric acid solubility in water. The number of H_2SO_4 molecules in critical cluster was determined from the data for different types of detectors and results from 5 to 9 molecules were obtained. The main advantage in this study compared to others is the use of PH-CPC which can cover particle sizes even down to 1.5 nm. More measurements are still needed to be able to confirm the critical cluster size and the growth rates dependence on sulphuric acid concentration.

Acknowledgments

References

1. Kulmala M., I. Riipinen, M. Sipilä, H. E. Manninen, T. Petäjä, H. Junninen, M. Dal Maso, G. Mordas, A. Mirme, M. Vana, A. Hirsikko, L. Laakso, R. M. Harrison, I. Hanson, C. Leung, K. E. J. Lehtinen & V.-M. Kerminen, *Science* **318**, 89 (2007).
2. Kulmala M., A. Laaksonen & L. Pirjola, *J. Geophys. Res.* **103**, 8301, (1998).
3. Vehkamäki H., M. Kulmala, I. Napari, K. E. J. Lehtinen, C. Timmreck, M. Noppel & A. Laaksonen, *J. Geophys. Res.* **107**, 4622, (2002).
4. Wyslouzil B. E., J. H. Seinfeld, R. C. Flagan & K. Okyama, *J. Chem. Phys.* **94**, 6842, (1991).
5. Viisanen Y., M. Kulmala & A. Laaksonen, *J. Chem. Phys.* **107**, 920, (1997).
6. Ball S. M., D. R. Hanson, F. L. Eisele & P. H. McMurry, *J. Geophys. Res.* **104**, 23709, (1999).
7. Zhang R., I. Zuh, J. Zhao, D. Zhang, E. C. Fortner, X. Tie, L. T. Molina & M. J. Molina, *Science* **304**, 1487, (2004).
8. Berndt T., O. Böge, F. Stratmann, J. Heintzenberg & M. Kulmala, *Science* **307**, 698 (2005).
9. Berndt T., O. Böge & F. Stratmann, *Geophys. Res. Lett.* **33**, L15817, (2006).
10. Benson D. R., L. H. Young, F. R. Kameel & S. H. Lee, *Geophys. Res. Lett.* **35**, L11801, (2008).
11. Young L. H., D. R. Benson, F. R. Kameel, J. R. Pierce, H. Junninen, M. Kulmala & S. H. Lee, *Atm. Chem. Phys.* **8**, 4997, (2008).
12. Sipilä M., K. Lehtipalo, M. Attoui, K. Neitola, T. Petäjä, P. P. Aalto, C. D. O'Dowd & M. Kulmala, *Aerosol Sci. Tech.* **43**, 126, (2009).

CONNECTION OF SULPHURIC ACID TO ATMOSPHERIC NUCLEATION IN BOREAL FOREST

T. NIEMINEN[1], H. E. MANNINEN[1], S.-L. SIHTO[1], T. YLI-JUUTI[1], R. L. MAULDIN, III[2], T. PETÄJÄ[1], I. RIIPINEN[1], V.-M. KERMINEN[3], and M. KULMALA[1]

[1] Department of Physics, University of Helsinki, P.O. Box 64, 00014 Helsinki, Finland
[2] Atmospheric Chemistry Division, Earth and Sun Systems Laboratory, National Center for Atmospheric Research, P.O. Box 3000, Boulder, CO 80307-5000, USA
[3] Finnish Meteorological Institute, P.O. Box 503, 00101 Helsinki, Finland

Key Words: Atmospheric aerosols; Nucleation; Sulphuric acid

INTRODUCTION

New particle formation has been observed to occur in numerous locations around the world (Kulmala et al., 2004). These nucleation events and the subsequent growth of the formed particles may contribute to regional cloud condensation nuclei populations, and can this way have an influence in cloud forming processes. Quantification of the climatic and other potential effects of the aerosol requires a better understanding of nucleation mechanisms and their relation to nucleation precursors in the atmosphere. In many measurements a connection between observed particle formation rate and sulphuric acid concentration to power 1–2 has been observed (Weber et al., 1996; Riipinen et al., 2007). The smallest particles detected in these measurements have been 3 nm in diameter. However, nucleation is expected to occur at sizes closer to 2 nm. In this work, we utilize new neutral cluster and air ion spectrometer measurement data of sub-3 nm total particle concentrations to explore the first steps of atmospheric new particle formation.

MATERIALS AND METHODS

The measurements for this study have been performed at the University of Helsinki SMEAR II in Hyytiälä, Southern Finland. Measurements were performed during the EUCAARI (European integrated project on aerosol, cloud, climate, and air quality interactions) campaign (Kulmala et al., 2008) from 6 March to 30 June 2007. Aerosol particle size distributions in size range 2.0–40 nm were recorded with the Neutral cluster and Air Ion Spectrometer (NAIS) (Kulmala et al., 2007). The lower detection limit of NAIS is set by the requirement to be able to distinguish atmosheric particles from ions generated inside the instrument's corona chargers (Asmi et al., 2009). Sulphuric acid concentration was measured with a chemical ionization mass spectrometer (CIMS) (Petäjä et al., 2008). We also used data from the continuous measurements made at the station.

There were 54 new particle formation events during the measurement campaign. During 30 of these events there is enough sulphuric acid data to enable detailed analysis. Particle formation rates were calculated from NAIS data with the following formula

$$J_2 = \frac{dN_{2-3}}{dt} + CoagS_2 \cdot N_{2-3} + \frac{GR}{1\text{nm}} \cdot N_{2-3}. \quad (1)$$

Here N_{2-3} represents the number concentration of 2–3 nm particles, $CoagS_2$ is the coagulation sink for 2 nm particles and GR is the particle growth rate between 1.8 and 3 nm. First term on the right hand side represents the rate at which concentration of newly formed particles changes, second term takes into account coagulation scavenging by pre-existing particles, and the third term condensational growth of the nucleated particles. Coagulation sink is calculated from DMPS size distribution data between 3–1000 nm.

Sulphuric acid concentrations were compared to particle formation rates J_2 using two proposed nucleation mechanisms:

$$J_{\text{act}} = A \cdot \left[\text{H}_2\text{SO}_4 \right], \quad (2)$$
$$J_{\text{kin}} = K \cdot \left[\text{H}_2\text{SO}_4 \right]^2. \quad (3)$$

The pre-factors A and K were determined for each event by least square fit of the J_{act} and J_{kin} values to observed J_2 values.

RESULTS AND DISCUSSION

There were 54 new particle formation event days during the campaign. On 21 days there was no evidence of new particle formation taking place (non-event days), and 42 days could not be reliably classified as either event or non-event days (undefined days). Sulphuric acid measurement data was available on 30 event days, so that we could use them in our analysis.

The number concentrations and formation rates of newly-formed particles in 2–3 nm size range were clearly correlated during the new particle formation events. Figure 1 shows a comparison between sulphuric acid concentration and particle concentration measured by the DMPS and NAIS on 7 March 2007. With DMPS the smallest detectable particles are 3 nm in diameter, whereas the NAIS can detect particles down to 2 nm. There is a time difference between increase in the sulphuric acid and particle concentration. For 3–6 nm from DMPS this time difference is about 1 hour and for 2–3 nm detected by NAIS it is 10 minutes. This suggests that the new particle formation at 2 nm starts almost at the same time as H_2SO_4 increases, and it takes roughly one hour for the particles to grow to 3 nm. The best correlation between particle and sulphuric acid concentrations is obtained with sulphuric acid concentration to power two.

Variation of the values obtained for the nucleation coefficients A and K are shown in Figure 2 together with similarly determined values during two other springs, 2003 and 2005. It can be seen that the values vary by almost two orders of magnitude. Also values during different years differ from each other. Possible reasons for these differences could be variations in atmospheric conditions between the years, since the nucleation coefficients contain information about the physical and chemical processes related to particle formation. So far we haven't been able to

find out clear dependencies between these coefficients and meteorological variables (such as temperature, RH or condensation sink) or basic ambient gas concentrations (SO_2, NO_x, O_3). Probably also other vapours than sulphuric acid are involved in the first stages of new particle formation. This is supported by the fact that when comparing to the observed growth rates of the newly formed 2–3 nm particles, condensation of sulphuric acid could explain typically only 5–25% of the observed growth rates between 1.8–3 nm during the 2007 campaign.

a) b)
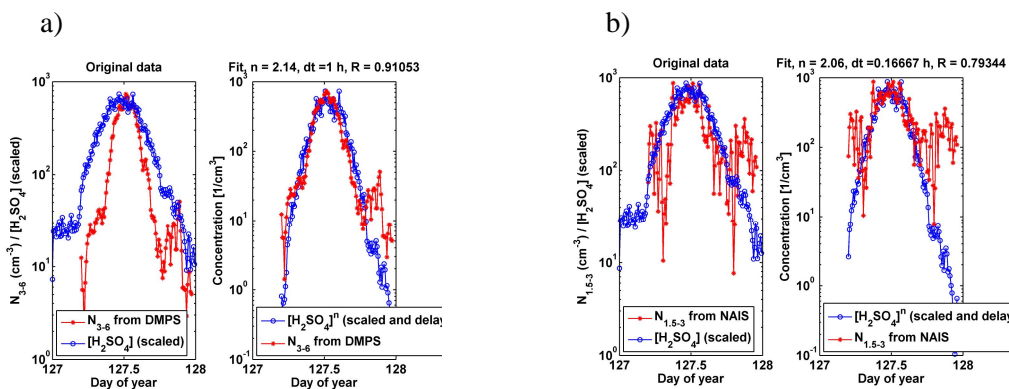
Figure 1. H_2SO_4 concentrations (blue line) and particle concentrations between 3–6 nm (a; measured by DMPS) and 2–3 nm (b; measured by NAIS) on 7 May 2007. The time lag between H_2SO_4 and particle concentrations is 1 h for 3–6 nm particles and 10 min for 2–3 nm particles. In both a) and b) the original measurement data is shown in the left panel. In the right panel sulphuric acid concentration has been delayed by time dt and raised to power n. The value of n is approximately 2 for both DMPS and NAIS data, but the time difference dt between the rise in H_2SO_4 and particle concentration is shorter for NAIS data, i.e. 2–3 nm particles.
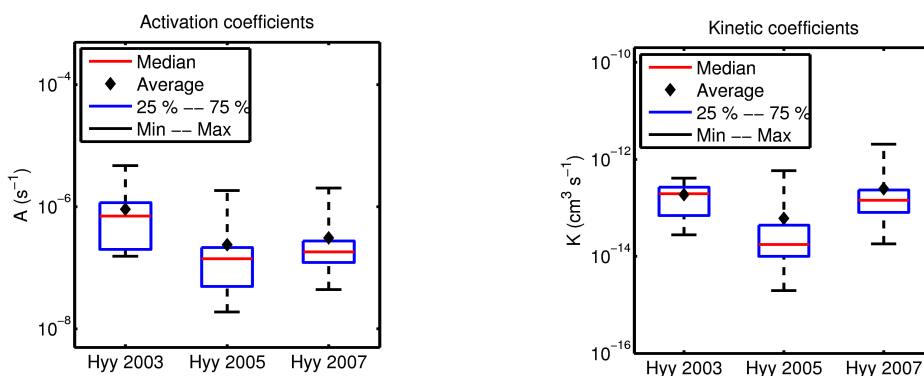
Figure 2. Median, mean, quartile and minimum and maximum values of the activation (a) and kinetic (b) nucleation coefficients during three different measurement campaigns in Hyytiälä in 2003, 2005 and 2007.

REFERENCES

Asmi, E., Sipilä, M., Manninen, H. E., Vanhanen, J., Lehtipalo, K., Gagné, S., Neitola, K., Mirme, A., Mirme, S., Tamm, E., Uin, J., Komsaare, K., Attoui, M., Kulmala, M. Results of the first air ion spectrometer calibration and intercomparison workshop. *Atmos. Chem. Phys.*, 9, 141–154, 2009.

Kulmala, M., Vehkamäki, H., Petäjä, T., Dal Maso, M., Lauri, A., Kerminen, V.-M., Birmili, W. and McMurry, P.H. Formation and growth rates of ultrafine atmospheric particles: a review of observations. *J. Aerosol Sci.* 35, 143-176, 2004.

Kulmala, M., Riipinen, I., Sipilä, M., Manninen, H. E., Petäjä, T., Junninen, H., Dal Maso, M., Mordas, G., Mirme, A., Vana, M., Hirsikko, A., Laakso, L., Harrison R. M., Hanson, I., Leung, C., Lehtinen, K. E. J., Kerminen, V.-M. Toward direct measurement of atmospheric nucleation. *Science* 318, 89–92, 2007.

Kulmala, M., Asmi, A., Lappalainen, H. K., Carslaw, K. S., Pöschl, U., Baltensperger, U., Hov, Ø, Brenquier, J.-L., Pandis, S. N., Facchini, M. C., Hansson, H.-C., Wiedensohler, A., O'Dowd, C. D. Introduction: European Integrated project on Aerosol Cloud Climate and Air Quality interactions (EUCAARI) – integrating aerosol research from nano to global scales. *Atmos. Chem. Phys. Discuss.*, 8, 19415–19455, 2008.

Petäjä, T., Mauldin, R. L., Kosciuch, E., McGrath J., Nieminen, T., Boy, M., Adamov, A., Kotiaho, T., Kulmala, M. Sulfuric acid and OH concentrations in a boreal forest site. In press, *Atmos. Chem. Phys. Discuss.*, 2008.

Riipinen, I., Sihto, S.-L., Kulmala, M., Arnold, F., Dal Maso, M., Birmili, W., Saarnio, K., Teinilä, K., Kerminen, V.-M., Laaksonen, A., Lehtinen, K. E. J. Connections between atmospheric sulphuric acid and new particle formation during QUEST III-IV campaigns in Heidelberg and Hyytiälä. *Atmos. Chem. Phys.* 7, 1899-1914, 2007.

Weber R. J., Marti J. J., McMurry P. H., Eisele F. L., Tanner D. J. and Jefferson A. Measured atmospheric new particle formation rates: implications for nucleation mechanisms. *Chem. Eng. Comm.* 151, 53-64, 1996.

STEADY TEMPERATURE METHOD FOR SAP FLOW MEASUREMENTS IN TREE STEMS

E. NIKINMAA, T. LINKOSALO, T. HÖLTTÄ

Department of Forest Ecology, P.O. Box 24, FIN-00014 University of Helsinki, Finland

INTRODUCTION

Granier method is widely used to measure sap flow in trees. The method uses two temperature sensors inserted into the wood. Thermocouples inside thin metal tubes like IV-needles are often used. The upper needle (trailing in the direction of the flow) is heated by a coil of resistor wire. The heat dissipates to the surrounding wood, and the heat dissipation depends on the sap flow. The temperature difference of the heated needle relative to reference needle is the largest when there is no flow and heat is dissipated only by conduction, while sapflow increases the difference, and consequently the actual flow rate can be estimated with equations suggested by Granier (1988).

The granier method is based on the assumption that the heat flux within the measured trunk is in a steady state. When the flux velocity changes, the assumption does not hold, but there is a delay until a new steady state is achieved. The amount of heat energy storage may also vary between different stages of steady flow, which means that the states may not be comparable. Another drawback of the method is that the heating power of the hot needle is constant, and the power needs to be set for a fairly high level to be able to measure during the high flow conditions. This level of heating is unnecessarily high during no or low flow conditions.

We modified the Granier method to keep the heat distribution closer to steady state at all times. This is done with a thermostat circuitry that keeps the temperature difference between the measurement needles constant, and adjusts the heating power accordingly. The amount of heating energy required to keep the temperature difference relates now to the speed/amount of sap flow. We study how this modification affects the sensor response to changes in the sap flow.

METHODS

The circuitry for the modification is based on a single-chip microcontroller (PIC16F88). This contains program code that reads the temperature from a pair of thermocouples and adjusts the heating power of the unit in order to keep the temperature difference constant. The microcontroller runs in infinite loop where it first measures the temperature difference in the pair of thermistors, compares the measured value to the target value, and determines the desired heating power from the difference of the two. It then heats the resistor coil with a square wave pulse, and loops back for the next measurement. The microcontroller also charges a capacitor with square wave pulses comparable to those used to heat the thermocouple needle. The voltage of the capacitor can be read with an analogue data logger to measure the heating power, as the voltage is directly proportional to the heating power used. If a data logger with digital input is used, the power signal could also be read in digital form, directly from the microcontroller. A microcontroller is a flexible way to build the circuitry, it enables flexible adjustment of all essential parameters of the system, such as the target temperature difference, dampening factor required to prevent oscillations, and scaling the data output. The additional cost that the thermostat circuitry is around 10 to 20 euros per sensor (needle couple).

We used a numerical model (Sevanto et al. 2009) to study the linkages between the power input, sapflow and temperature and their timelags in the traditional Granier type intallation of the sapflow needles and that using the new modification that maintained the temperature difference constant.

The 3-dimensional heat transfer model was based on the energy balance equation for the heated sensor, which can be written as

$$(c_p \rho V)_{sensor} \frac{\partial T_{sensor}}{\partial t} = Q - \bar{v} \cdot \nabla T_{water} - \frac{k_{xylem}}{\rho_{xylem} c_{pxylem}} \nabla^2 T_{xylem} \qquad (1)$$

where the change of the temperature T of the sensor in time (left hand side) is equal to the heating (Q [W]) reduced by the convection and conduction (second and third terms on the right, respectively). $(c_p \rho V)$ is the thermal mass of the sensor (c_p is the heat capacity, ρ the density and V the volume), $\bar{v}$ the sap velocity vector and $\frac{k_{xylem}}{\rho_{xylem} c_{pxylem}}$ is the thermal diffusivity of the xylem tissue [m^{2}s^{-1}], where k_{xylem} is the thermal conductivity, ρ_{xylem} the density and c_{pxylem} the thermal capacity of the tissue. Equation (2) applies at all points in the stem when the thermal mass of the sensor is replaced with the thermal mass of wood.

We constructed a 3-dimensional cylindrical model-grid to represent the xylem and solved eq. (1) for each grid cell numerically using the explicit Euler-scheme. The heat fluxes were calculated at the boundaries of each grid cell and the temperature of that cell was evaluated at the center. We first built a model base case using literature values for the parameters (Sevanto et al. 2009) and then varied the thermal conductivity to see how it influenced the situation.
.

RESULTS AND CONCLUSIONS

Preliminary results with the new sensors showed a fast variation in the sapflow velocity that was similar to simultaneously measured diameter variation of the sapwood xylem at the same height while the tradtional Granier sensors had clear time lag in comparison to the diameter (i.e. stem tension) variation. However, in more thorough tests during this summer similar difference between the traditional and the new method was not observed.

The new method that measures the amount of energy input to the heated needle to maintain the temperature difference between the needles constant seemed to be more stable during the no-flow conditions, in comparison to the traditional granier needles (Fig. 1). It also turned out that during some nights there was a clear sapflow that was detected by both methods but which was easier to see with the new method. Short of that, both the systems measured the sapflow in a very similar fashion (Fig. 2). These test measurements were carried out with both broadleaved trees (aspen or lime), as well conifers (pines).
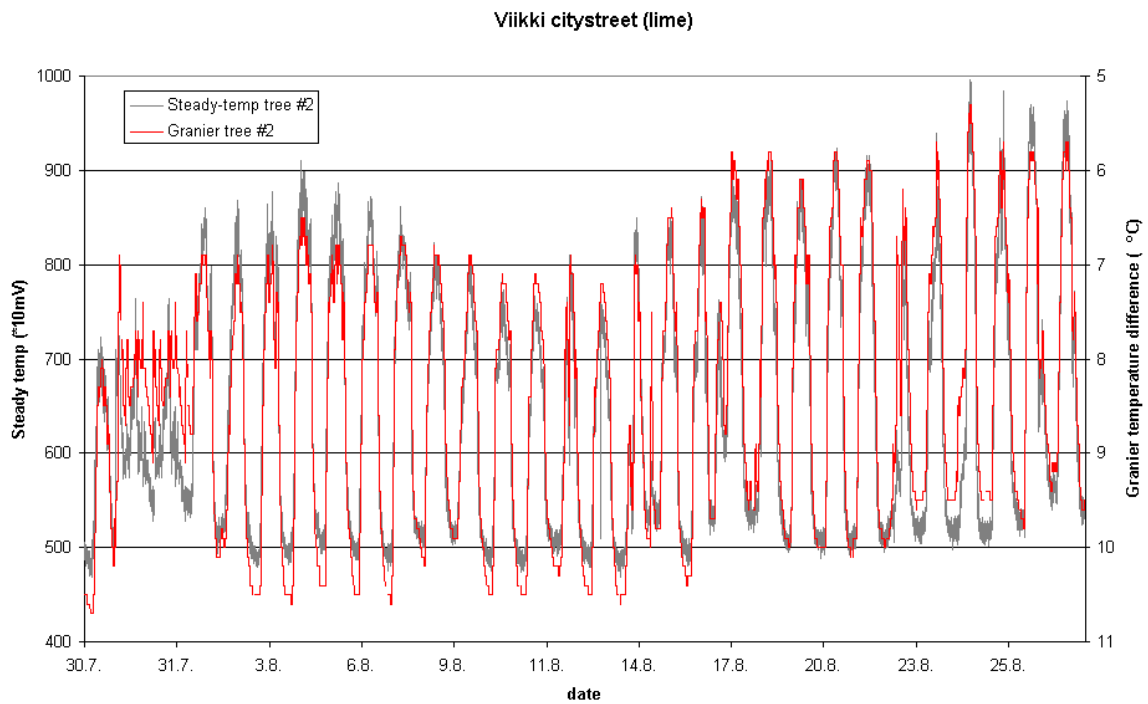
Figure 1. Comparison of daily variation in heating power (new method, measured as capacitor voltage depending on heating pulse ratio) and needle temperature difference (Granier method) in august 2007 at Helsinki urban street laboratory.
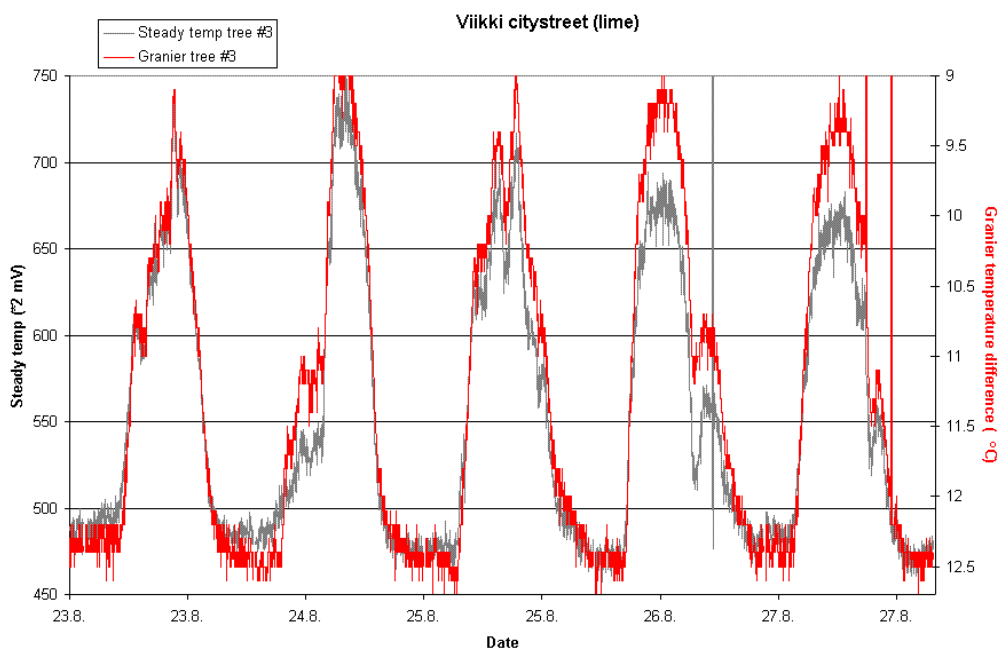
Figure 2. Comparison of daily variation in heating voltage (new method) and needle temperature difference (Granier method) during a week in august 2007 at Helsinki urban street laboratory.

The theoretical calculations showed in the base case situation when the wood heat conduction is about 60% of that of water much faster response to changes to sapflow rate than traditional Granier method. However, when the heat conductivity of the wood was decreased the new method started to approach that of the traditional Granier method. These changes may explain the differences that we observed in the responsiveness of the method to flow rate changes at field. At zero flow conditions the new method should give directly the heat conduction of wood-heated-needle system. That may explain why the night time values of the measurements with the new system were more stable than with traditional Granier method. Nevertheless, a great improvement in the new system is that it is saving quite a lot of energy during low flow condition when the heat supply to the needle is just that conducted away from the needle and no heating of wood takes place.

.

REFERENCES

Granier, A. 1985. A new method of sap flow measurement in tree stems. Ann, Sci. For. 42:193-200.

Sevanto S., Hölttä T., Nikinmaa E. (2009) The effects of heat storage during low flow rates on Granier-type sap flow sensor output. Acta Horticulturae (in print)

MOLECULAR MECHANISMS BEHIND NOCTURNAL NEW PARTICLE FORMATION

H. I. K. ORTEGA[1], T. SUNI[1], M. BOY[1], T. GRÖNHOLM[1], M. KULMALA[1], H. JUNNINEN[1], M. EHN[1], D. WORSNOP[1], H. MANNINEN[1], H. VEHKAMÄKI[1], H. HAKOLA[2], H. HELLÉN[2], T. VALMARI[3] and H. ARVELA[3]

[1]Department of Physics, P.O. Box 64, FI-00014, University of Helsinki, Finland
[2]Finnish meteorology institute, P.O. Box 503, 00 101 Helsinki, Finland
[3] STUK, Radiation and nuclear safety authority, P O Box 14, 00881 Helsinki, Finland

INTRODUCTION

Atmospheric aerosols influence climate directly by scattering and absorbing radiation, and indirectly by acting as cloud condensation nuclei and affecting cloud properties. Unfortunately the role of atmospheric aerosols is still the forcing with the lowest level of scientific understanding, as reported in the newest report by the Intergovernmental Panel on Climate Change (IPCC 2007).

Gas-to-particle nucleation is an important source of new aerosol particles in the Earth's atmosphere. This phenomenon is observed almost every where around the world and has been the subject of intense studies in the last years (Kulmala et al 2004), but the formation mechanism and the participating substances have not been resolved yet.

Nucleation events are in most cases observed during daytime but in some locations they can occur also during the night. In Tumbarumba in New South Wales, Australia, these nocturnal events are very intense and frequently observed (Suni et al. 2008). If we look for differences between Tumbarumba and other sites where the nocturnal events have been observed but where they are much less intense and less frequent, like Hyytiälä in Southern Finland, one of the main one turns out to be the composition of the forest. As a result of this, the volatile organic compounds (VOCs) emitted are different. Another important difference is the observed higher radon concentrations in Tumbarumba.

Recently Ortega et al (2009) have ruled out the participation of radon and eucalyptol (one of the most abundant VOCs in Tumbarumba) leaving the question of what is behind the nocturnal nucleation events open.

The objective of this study is to evaluate the role of different VOCs (other than eucalyptol) in nocturnal nucleation events. The selected VOCs are limonene, alpha-pinene, beta-pinene and 3-carene; these are the most abundant VOCs in Tumbarumba and in Hyytiälä.

We performed a series of chamber experiments with the objective to reproduce the nocturnal events observed in Australia. Additionally we used quantum chemical calculations to study the molecular mechanism behind the nocturnal nucleation events. Finally we have used the quantum chemical results in aerosol formation models to check if the proposed mechanism could explain the observed nucleation events.

METHODS

The experimental set up was similar to that used in Ortega et al. (2009); with the exception that in these experiments we have used a Neutral cluster and Air Ion Spectrometer (NAIS) instead of an Air Ion Spectrometer (AIS) to obtain also the distribution of neutral particles. Additionally an Aerosol Mass Spectrometer (AMS) where use to study the composition of aerosol particles formed during the experiments.

Our quantum chemical calculations were performed using a systematic multi-step method recently developed by our group (Ortega et al. 2008) This multi-step method allows the study of clusters containing a big organic molecule and up to 4 sulfuric acid molecules using a reasonable amount of computing time.

We have focused on the role of different oxidation products of these compounds bearing in mind that the events occur in the dark.

Further we used the 1-dimensional model SOSA (Boy et al., manuscript in preparation) to simulate the nucleation rates of limonene reaction products and compared these results with observed nucleation rates from the SMEAR II in Hyytiälä, Finland.

RESULTS

Table 1 summarizes the formation free energy calculated for complexes formed by sulfuric acid and different VOC oxidation products.

Complex	ΔG (kcal/mol)
Caric acid-Sulfuric acid	-10.5
Caronic acid-Sulfuric acid	-14.4
7- hydroxy caronic acid-Sulfuric acid	-19.3
Pinic acid-Sulfuric acid	-7.2
Pinonic acid-Sulfuric acid	-9.4
7- hydroxy pinonic acid-Sulfuric acid	-11.1
Limonic acid-Sulfuric acid	-4.6
Limononic acid-Sulfuric acid	-10.6
7- hydroxy limononic acid-Sulfuric acid	-6.9

Table 1. ΔG calculated at 1 atm monomer pressure and 298 K

We can see how the hydroxy-caronic, hydroxy-pinonic and limononic acids form the most stable complexes with sulfuric acid while diacids (caric, pinic and limonic acids) form less stable complexes.

However, we need to take into account the different concentration of these compounds in the atmosphere.

Complex	K_{O3} ($\times 10^{18}$) cm^{3}molecules^{-1} s^{-1}
3-Carene	37
Alpha-pinene	86.6
Beta-pinene	15
Limonene	210

Table 2. Ozone oxidation rates(Calogirou et al. 1998)

Limonene has the greatest oxidation rate, thus the oxidation products of limonene will be more relevant for nucleation. Thus, we have chosen limononic acid to extend the calculations to clusters containing up to four sulfuric acid molecules.

Table 3 summarizes the results obtained for limononic acid clusters, and compares it to pure sulfuric acid clusters.

Number of sulfuric acids	Sulfuric acid ΔG (kcal/mol)	Limononic acid ΔG (kcal/mol)
2	-6.3	-17.1
3	-9.3	-19.9
4	-12.9	-23.9

Table 3. Clusters of limononic acid and sulfuric acid

The results show that the presence of limononic acid stabilizes the sulfuric acid clusters, lowering the nucleation barrier and enhancing the nucleation.

During the experiments we were able to produce particles in dark conditions using ozone and different monoterpenes. The results show that the oxidation rate plays a crucial role in the formation of particles, confirming that the oxidation products of monoterpenes rather that the monoterpenes it selves are involved in the formation of new particles.

Model simulations with SOSA show that nucleation rates calculated with the mechanism explained above are in good agreement with nucleation rates based on measured particle size distributions.

CONCLUSIONS

Our results show that the oxidation products of VOCs play an important role in nucleation events. Not all these compounds have the same importance, so characterizing the particle formation potential with, for example, the total concentration of VOCs is probably a unsatisfactory approximation. Taking into account the different emission strengths of VOCs in different environments (like Tumbarumba and Hyytiälä) probably can explain the differences in the observed nucleation events.

This is only a first step in understanding the mechanism behind nocturnal nucleation so further work on this topic is necessary.

REFERENCES

Kulmala, M., Vehkamäki, H., Petäjä, T., Dal Maso, M., Lauri, A., Kerminen V.M., Birmili, W. and McMurry, P. H.,(2004) Formation and growth rates of ultrafine artmospheric particles: a review of observations. *J. Aerosol. Sci.*, 35, 143-146.

Suni T., Kulmala M., Hirsikko A., Bergmaa T., Laakso L., Aalto P.P., Luning R., Cleugh H., Zegelin S., Hughes D., Gorsel E., Kitchen M., Vana M., Hörrak U., Mirme A., Sevanto S., Twining K. & Tadros C. .(2008). Fromation and characteristics of ions and charged aerosol particles in a native Australian eucalypt forest. *Atmos. Chem. Phys.* 8, 129-139.

I. K. Ortega, T. Suni, T. Grönholm, M. Boy, H. Hakola, H. Hellén, T. Valmari, H. Arvela M, H. Vehkamäki and M. Kulmala,(2009) Is eucalyptol the cause of nocturnal events observed in Australia?. *Boreal Env. Res*. Revised manuscript submited

I.K. Ortega, T. Kurtén, H Vehkamäki and M. Kulmala, , (2008). The role of ammonia in sulfuric acid ion induced nucleation. *Atmos. Chem. Phys.*8, 2859-2867

Calogirou A., Larsen B.R., & Kotzias D., (1998), Gas-phase terpene oxidation products: a review, *Atmos. Environ.* 33,1423-1439

SOLID PHASE EXTRACTION OF ORGANIC COMPOUNDS IN ATMOSPHERIC AEROSOLS COLLECTED WITH THE PARTICLE-INTO-LIQUID SAMPLER AND THEIR ANALYSIS BY HPLC-MS

J. PARSHINTSEV[1], T. HYÖTYLÄINEN[1], K. HARTONEN[1], M. KULMALA[2] and M.-L. RIEKKOLA[1*]

[1]Laboratory of Analytical Chemistry, Department of Chemistry, P.O.Box 55, FI-00014, University of Helsinki, Finland
[2]Department of Physics, P.O. Box 64, FI-00014, University of Helsinki, Finland

INTRODUCTION

The particle-into-liquid sampler (PILS) invented by Weber et al. was introduced in 2001 [Weber et al., 2001]. Later, the devise was improved for ground and airborne collection of water soluble aerosols [Orsini et al., 2003]. PILS combines two conventional techniques in aerosol collection: particle growth in oversaturated water vapor and further impaction on quartz impactor. Particles are then washed by water to debubbler and normally introduced to one or two ion chromatograph, for anion or/and cation analysis.

The relevance of oxidation products of sesquiterpenes, especially β-caryophyllene, to aerosol growth has been studied recently [Asa-Awuki et al., 2009]. Presence of β-nocaryophyllone aldehyde in atmospheric aerosols has been proved with the use of authentic standard while β-caryophyllinic acid has been determined tentatively [Jaoui et al., 2007; Parshintsev et al., 2008].

The aim of our research was to collect aerosol samples using PILS for further off-line analysis of organic acids by liquid chromatography-mass spectrometry. Solid phase extraction with anion exchange material was chosen for the sample pretreatment. Based on theory, PILS was expected to be less sensitive for artifacts, because there is no flow through the collected sample. Also, in the set up employed, ozone and organic gas phase compounds were removed, which minimized oxidation and adsorption/absorption of low volatile species. A part of this research was dedicated to the synthesis of β-caryophyllene's acid and its determination in PILS samples.

METHODS

PILS sampling was done in August 2007 at the Station for Measuring Forest Ecosystem Atmosphere Relations (SMEAR II) at Hyytiälä (61°51'N, 24°17'E, 180 m above sea level), which is 230 km north of Helsinki. The forest consists of Scots pines (Pinus sylvestris L.) 30-40 years old, homogeneously spread through 200 m in all directions from the measurement site. A more detailed description of SMEAR II is presented by Kulmala et al. (2001). To remove gas phase compounds, which might affect the aerosol sample during collection and the analysis, three channel annular denuders (242 mm length, Teflon coated, stainless steel sheath, URG, Chapel Hill, USA) with different coating were used. One denuder was coated with equal parts of solutions of potassium iodide (20 g in 10 ml of MilliQ- water) and glycerol (10 % in methanol), to eliminate the oxidation of aerosol compounds during the sampling. Two denuders were coated with XAD-2 resin to remove organic gases, and phosphoric

acid denuder was used for trapping the basic gases. Cyclone (PM2.5, URG, Chapel Hill, USA) was used for the size separation of sampled aerosols and was placed before the denuder line which was connected to the PILS inlet. Samples of two hours were collected to the glass vials (20 ml) and stored in the refrigerator. Anion exchange solid phase extraction cartridges (Oasis MAX 1cc, 30mg, Waters Corp., Milford, USA) were used for the sample pretreatment. Extraction efficiency of MAX-SPE was determined using standard solutions. PILS samples (from 12 to 20 ml) were extracted and eluted with 1ml of 2% formic acid in methanol. Analysis was performed by liquid chromatography (1100 Series, Hewlett Packard, Santa Clara, USA) coupled with Bruker Esquire 300plus ion trap mass spectrometer (Bruker Daltonics, Billerica, USA). LC column was XBridge Shield RP18 (5µm, 2.1*150mm, Water Corp.). MS conditions were 50-370 amu, +4000V capillary, -500V end plate offset, 40psi nebulizer, 8 l/min dry gas, and 300 °C drying temperature. Injection volume for the calibration was 3 µl and for the samples 15 µl. Gradient elution from 10 to 90% of acetonitrile (B) in 40 min was used (A: 1% formic acid in methanol).

β-Caryophyllene (*trans*-(1R,9S)-8-methylene-4,11,11-trimethylbicyclo[7.2.0]undec-4-ene, 80+ %, GC, sum of enantiomers, Sigma-Aldrich Chemie, Steinheim, Germany) solution (10% v/v) was prepared in dichloromethane (HPLC grade, Labscan Ltd., Dublin, Ireland). Aliquots of 10 ml were used for ozonolysis. A test-tube containing the sesquiterpene solution was placed in a beaker filled with cooled ethanol. Pieces of dry carbon dioxide (-78 °C) were added to the ethanol to reduce the temperature to at least -68 °C. Dried, purified, and ozonolyzed air was bubbled through the sesquiterpene solution at a flow rate of 10 L/h (500 M corona discharge ozone generator, Fisher, UK). Temperature was controlled throughout the experiment. Reaction time was 15, 30 and 45 minutes. The reaction mixture was extracted by liquid-liquid extraction two times with 10 ml of 5% ammonia solution in water. Then aqueous fraction were combined and extracted by solid phase extraction with MAX material as explained earlier. Sample obtained was analyzed by HPLC-MS. Ion 253 was used for the MS^2 experiments. To obtain EI spectrum for the β-caryophyllene's acid, ten fraction of HPLC effluent containing target compound were collected to the vial and dried under nitrogen. Then 30 µl of derivatization reagent (BSTFA) was added together with 10 µl of pyridine and the mixture was held in 70 °C for three hours. For GC-MS analysis, mixture was dried and redisolved in 100 µl of hexane. The parameters for the GC-MS analysis and precise explanation of HPLC-MS^2 runs are given elsewhere [Parshintsev et al., 2009].

RESULTS
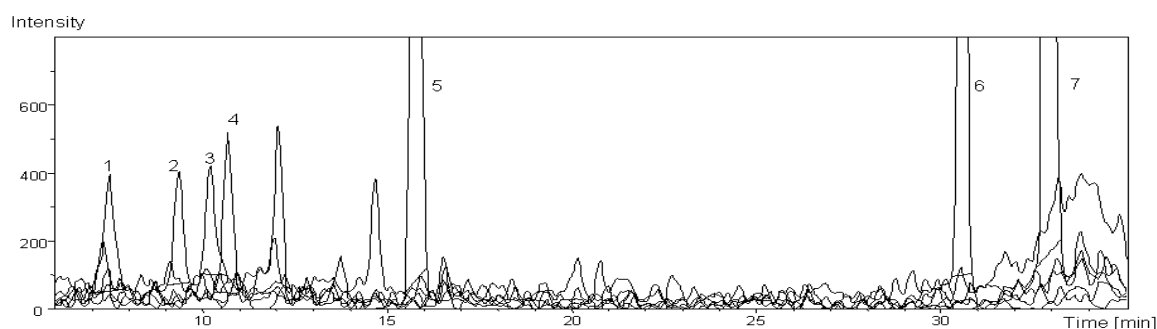
Figure 1. HPLC-MS extracted ion chromatogram of PILS sample (August 13th, 2007). Peaks: 1. cis-pinic acid (185 amu); 2. cis-pinonic acid (183 amu); 3. trans-pinonic acid (183 amu), 4. azelaic acid (187 amu), 5. ISTD (2,4-dichlorobenzoic acid, 189 amu), 6. palmitic acid (255 amu), 7. stearic acid (283 amu).

The extraction efficiency of SPE with anion exchange material was around 100 % with low standard deviation (Table 1). The recoveries of the analytes were not affected by the sample volume, which is important if they are collected by PILS.

Analytical procedure developed during this study proved to be suitable for the determination of selected organic acids in atmospheric aerosols collected by the particle-into-liquid sampler. All the compounds were well separated and limits of detection were exceeded, as can be seen in Fig.1. Beside diurnal variation, changes in aerosol chemical composition could be measured during the day and thus concentrations before, during and after particle formation events could be determined (Figure 2, Table 2). Time resolution of two hours was good enough for the study. Particle-into-liquid sampler together with liquid chromatography-mass spectrometry allowed a reliable analysis of organic acids in aerosol samples. The possibility to couple PILS directly with the instrumental analytical techniques carries a great promise for further method development.
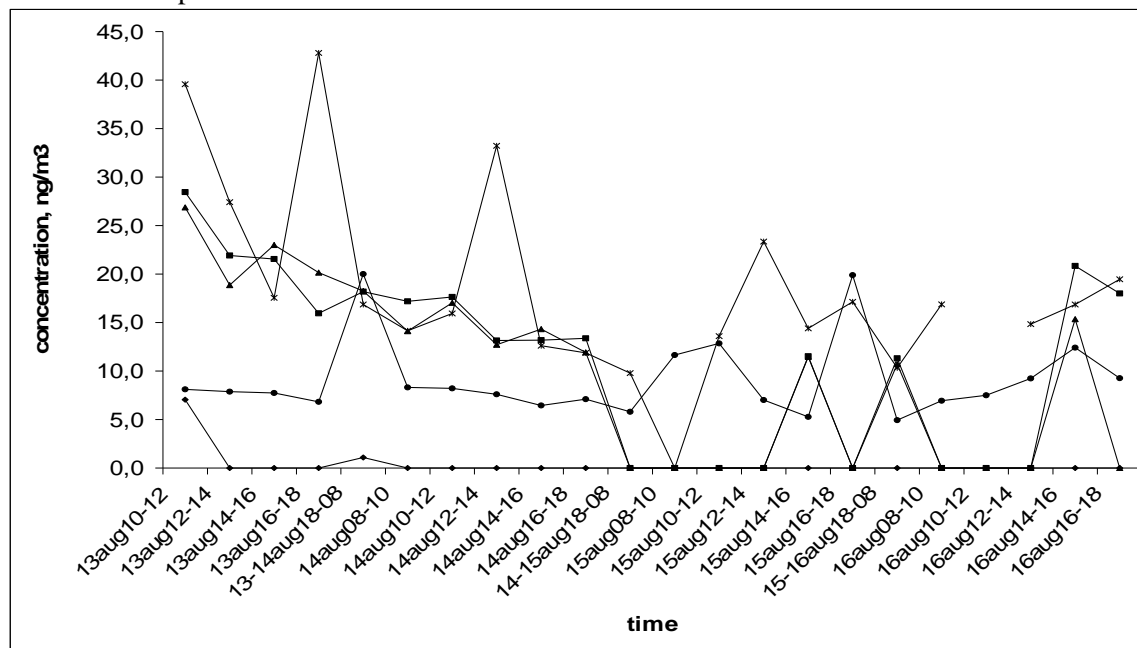
Figure 2. Concentration of studied acids as ng/m^3 of sampled air during the sampling period of 13.8- 16.8. From up line to down: stearic acid, *cis*-pinonic acid, *trans*-pinonic acid, azelaic acid, *cis*-pinic acid.

Table 1. Extraction efficiencies (%±RSD%, n=9) obtained with OasisMAX SPE material with 10 or 20 ml sample size.

conc, µg/L	*cis*-pinic acid, 10 ml	*cis*-pinic acid, 20 ml	*trans*-pinic acid, 10 ml	*trans*-pinic acid, 20ml	*cis*-pinonic acid, 10 ml	*cis*-pinonic acid, 20 ml	azelaic acid, 10 ml	azelaic acid, 20ml
5	64.2±17.0	79.8±19.0	147.9±10.2	114.9±18.0	96.1±14.7	94.6±6.3	106.8±10.0	100.5±7.6
10	74.9±8.3	76.9±9.4	103.7±18.5	70.8±48.4	96.3±4.2	93.8±7.4	116.1±12.4	77.1±30.3
12.5	90.0±2.5	93.1±1.4	110.7±8.2	97.4±2.5	100.0±8.2	98.2±5.1	99.9±2.9	90.1±1.4
25	88.2±7.3	90.8±15.2	88.7±5.5	89.3±6.6	98.9±2.7	99.6±6.5	97.5±7.6	93.3±6.0
50	93.5±7.6	99.4±1.3	82.7±4.9	91.0±12.5	95.7±6.0	99.6±2.1	91.2±4.7	92.8±2.0
100	109.8±6.4	109.8±8.0	94.0±4.9	99.8±9.6	108.5±5.3	111.6±8.4	95.0±3.9	93.5±9.4

Table 2. Concentrations of acids studied in aerosols in ng/m^3 ± RSD% (n=3) of sampled air.

Sample	cis-pinic acid	cis-pinonic acid	trans-pinonic acid	azelaic acid	β-caryophyllinic acid	octadecanoic acid
13aug 10am-12am	7.0±15.0	28.4±36.4	26.9±18.7	8.1±7.5	nd	39.6±10.0
13aug 12am-2pm	-	21.9±27.6	18.9±26.6	7.9±6.5		27.4±13.6
13aug 2pm-4pm	-	21.5±19.4	23.0±11.0	7.7±32.6		17.5±14.9
13aug 4pm-6pm	-	15.9±12.7	20.1±30.6	6.8±10.2		42.8±13.9
13-14aug 6pm-08am	1.1±9.5	18.2±31.3	18.3±24.7	20.0±6.3		16.9±21.1
14aug 08am-10am	-	17.2±1.7	14.1±nd	8.3±19.2		14.1±5.0
14aug 10am-12am	-	17.6±21.1	17.0±18.4	8.2±11.8	56.5±8.3	15.9±2.3
14aug 12am-2pm	-	13.2±14.2	12.7±35.8	7.6±18.9		33.2±5.6
14aug 2pm-4pm	-	13.2±27.3	14.3±14.0	6.5±37.9		12.6±17.5
14aug 4pm-6pm	-	13.4±32.2	11.9±50.9	7.1±7.9		11.9±7.6
14-15aug 6pm-08am	-	-	-	5.8±1.0		9.8±1.0
15aug 08am-10am	-	-	-	11.6±11.7		-
15aug 10am-12am	-	-	-	12.8±9.3	41.6±5.1	13.6±39.7
15aug 12am-2pm	-	-	-	7.0±24.4		23.3±16.4
15aug 2pm-4pm	-	11.5±24.5	11.5±17.8	5.3±16.4		14.4±31.1
15aug 4pm-6pm	-	-	-	19.9±5.5		17.1±72.4
15-16aug 6pm-08am	-	11.3±13.1	10.7±23.6	4.9±24.9		10.3±42.5
16aug 08am-10am	-	-	-	6.9±9.2		16.9±41.5
16aug 10am-12am	-	-	-	7.5±18.9	102.1±10.2	-
16aug 12am-2pm	-	-	-	9.2±16.3		14.8±11.6
16aug 2pm-4pm	-	20.8±33.6	15.4±1.0	12.4±12.8		16.9±21.9
16aug 4pm-6pm	-	18.0±1.0	-	9.3±22.9		19.5±25.1

Ozonolysis experiment of β-caryophyllene lead to the formation of different acids. The main product was determined as β-caryophyllinic acid using LC-MS/MS with ESI and GC-MS with electron impact ionization. β-Caryophyllinic acid was determined in PILS samples by retention time and MS^2 fragmentation. Quantitative analysis was done using cis-pinonic acid as a surrogate (Table 2). Quantitation error of using surrogate (around 50 %) was approximated by comparison the peak areas of cis-pinonic and azelaic acid solution of the same concentration.

CONCLUSIONS

Particle-into-liquid sampler was used for the collection of atmospheric aerosols from the Finnish coniferous forest. Sample pretreatment procedure with the solid phase material for the extraction and concentration of chosen organic acids was optimized and extraction efficiencies were determined. The analytical procedure for the determination of acids was optimized. The amounts of the studied acids in atmospheric aerosols samples were in range from 1 to 40 ng/m^3 that are in the agreement with the previous results. Oxidation product of β-caryophyllene was synthesized and determined in PILS samples by HPLC-MS^2. The amount of β-caryophyllinic acid was in range from 41.6 to 102.1 ng/m^3 with estimated error of 50 %. Reliability of the method as well as the limits of detection and quantitation were satisfactory. Our study proved that PILS is a very promising collection technique for the aerosol samples, and together with the sample pretreatment and analysis method presented here can be successfully used for the determination of acids in atmospheric aerosol particles.

REFERENCES

Asa-Awuku, A., Engelhart, G.J., Lee, B.H., Pandis, S.N., Nenes, A. (2009) Relating CCN activity, volatility, and droplet growth kinetics of β-caryophyllene secondary organic aerosol, *Atmos. Chem. Phys.* **9**, 795-812

Jaoui, M., Lewandowski, M., Kleindienst, T.E., Offenberg, J.H., Edney, E.O. (2007) β-caryophyllinic acid: An atmospheric tracer for β-caryophyllene secondary organic aerosol, *Geophys. Res. Lett.* **34**, L05816, doi:10.1029/2006GL028827

Kulmala, M., Hämeri, K., Aalto, P.P., Mäkelä, J., Pirjola, L., Nilsson, E.D., Buzorius, G., Rannik, U., Dal Maso, M., Seidl, W., Hoffmann, T., Janson, R., Hansson, H.-C., Viisanen, Y., Laaksonen, A., O'Dowd, C. (2001) Overview of the international project on biogenic aerosol formation in the boreal forest (BIOFOR), *Tellus* **53B**, 324-343

Orsini, D.A., Ma, Y., Sullivan, A., Sierau, B., Baumann, K., Weber, R.J. (2003) Refinements to the particle-into-liquid sampler (PILS) for ground and airborne measurements of water soluble aerosol composition, *Atmos. Environ.* **37(9-10)**, 1243-1259

Parshintsev, J., Nurmi, J., Kilpeläinen, I., Hartonen, K., Kulmala, M., Riekkola, M.-L. (2008) Preparation of β-caryophyllene oxidation products and their determination in ambient aerosol samples, *Anal. Bioanal. Chem.* **390**, 913-919

Parshintsev, J., Hyötyläinen, T., Hartonen, K., Kulmala, M., Riekkola, M.-L. manuscript in preparation

Weber, R.J., Orsini, D., Daun, Y., Lee, Y.-N., Klotz, P.J., Brechtel, F. (2001) A particle-into-liquid collector for rapid measurement of aerosol bulk chemical composition, *Aerosol Sci. Technol.* **35(3)**, 718-727

OPTIMIZATION OF GEOENGINEERING BY USING ONE DIMENSIONAL AEROSOL-CLIMATE MODEL

A.-I. PARTANEN[1,2], H: KORHONEN[1], J. KAZIL[3], U. NIEMEIER[3], C. TIMMRECK[3], K.E.J. LEHTINEN [1,2] , J. FEICHTER[3] and H. KOKKOLA[1]

[1] Department of Physics, University of Kuopio, Finland
[2] Finnish Meteorological Institute, Kuopio unit, Finland
[3] Max-Planck Institut für Meteorologie, Hamburg, Germany

Keywords: geoengineering, aerosol modelling, sulfur dioxide, stratospheric aerosols

INTRODUCTION

During the recent years deliberately altering the climate system has been a target of extensive research. Model studies show that injecting sulfur dioxide into the stratosphere could counteract global warming caused by the increased concentrations of green house gases (eg. Robock et al. (2008)). Previous model studies of sulfate geoengineering with climate models have used fairly simple aerosol population description. For example Rasch et al. (2008) and Robock et al. (2008) used a prescribed aerosol size distribution for the generated sulfate aerosol.

MODEL DESCRIPTION AND EXPERIMENT DESIGN

In order to give a more realistic and detailed view on the evolution of the stratospheric aerosol we use single column model (SCM) version of the aerosol-climate model ECHAM5-HAM (Stier et al. (2005)), whose size-segregated microphysical core M7 takes into account nucleation, condensation and coagulation. Computational efficiency of the SCM makes it possible to test a large range of different injection scenarios.

Our goal is to optimize sulfur dioxide injections to create a given radiative forcing with the lowest possible mass flux into the atmosphere. Interesting parameters for injections are for example injection height and interval between injections. We use offline atmospheric dynamics from a preceding full three dimensional model run without additional sulfur dioxide injections. This approach allows us to avoid the interference from the chaotic behavior of the climate system and concentrate fully on the aerosol dynamics.

SIMULATIONS

The difference in meteorological conditions between tropics and the Arctic creates differences in the geoengineered aerosol. Nucleation of new particles is continuous in tropics if sufficient sulfur dioxide injections are provided but in the Arctic there are periods with length of months without nucleation taking place. This makes it harder to maintain constant aerosol population in the arctic stratosphere. Residence times in the Arctic are although longer than in tropics as shown in Figure 1.

Sulfur injections make the stratospheric particles grow and these bigger particles form a coagulation sink for the new particles in the nucleation mode. As a result, concentrations in the nucleation mode are lower compared to the control run in all locations.
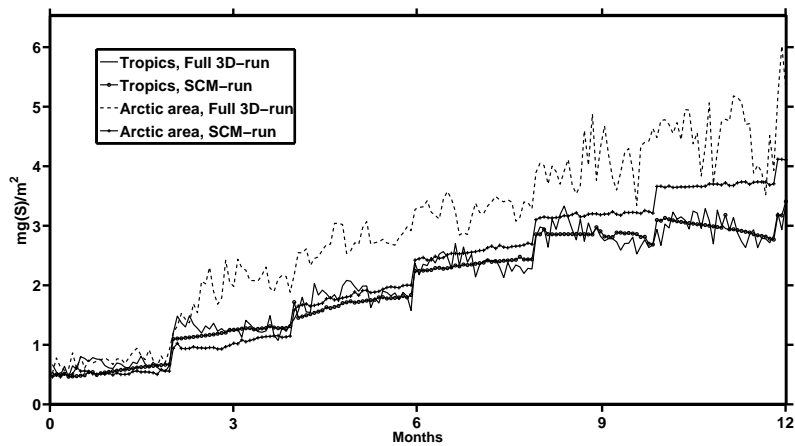
Figure 1: Stratospheric total sulfuric burden in tropics and in an arctic region simulated by the SCM and the full model.

Time-averaged radiative forcing due to the sulfate aerosol is stronger in tropics than in the Arctic. Both have considerable temporal variation. Based on preliminary results a global amount of 2 Tg(S) per year of sulfur dioxide provides a forcing of about -0.4 W/m2 in tropics and about -0.3 W/m2 in the Arctic. These values are based on short simulations where the aerosol population hasn't yet achieved equilibrium and so the forcing is clearly underestimated.

Larger SO_2 injections create larger particles. Simulated effective radii over the North Pole fall between the categories of "small" and "large" particles as defined in Rasch et al. (2008). Figure 2 shows how injected annual mass affects effective the radii and the surface area density of the soluble particles.

The reliability of the SCM is evaluated by comparing results with a full 3-D model run. The SCM can reproduce fairly well the evolution of the aerosol population given by the full model in tropics. It can also be used in other locations to emulate the full model although it underestimates the vertical mixing and the residence time of the sulfate aerosol. The stratospheric sulfur burdens calculated by SCM and the 3-D model are presented in Figure 1.
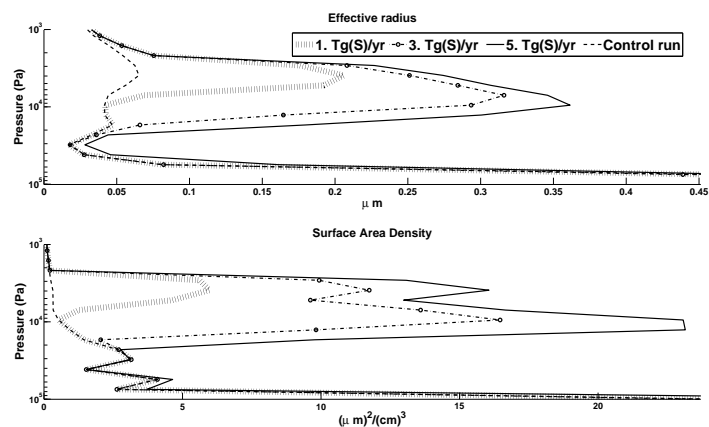
Figure 2: Effective radius and surface area density of the soluble modes with annual injection of SO_2 of 1,3 and 5 Tg(S) over North Pole averaged over the last six months of the simulation. SO_2 was injected continuously at a pressure level of 25 hPa.

Comparison between several model runs with different injection heights shows that for example in

tropics aerosol forcing is strongest if the sulfur dioxide is injected at a level of about 30 hPa, but there are no significant differences in a modest mass flux range. The most effective ratio between aerosol forcing and injected mass is found with a low mass flux.

REFERENCES

Rasch, P. J., Crutzen, P. J. and Coleman D. B. (2008). Exploring the geoengineering of climate using stratospheric sulfate aerosols: The role of particle size. *Geophys. Res. Lett.*, 35:L02809

Robock, A., Oman, L. and Stenchikov, G. L. (2008). Regional Climate Responses to Geoengineering with Tropical and Arctic SO_2 Injections. *J. Geophys. Res* ,113:D16101

Stier, P., Feichter, J., Kinne, S., Kloster, S., Vignati, E., Wilson, J., Ganzeveld, L., Tegen, I., Werner, M., Balkanski, Y., Schulz, M., Boucher, O., Minikin, A., and Petzold, A. (2005). The aerosol-climate model ECHAM5-HAM. *Atmos. Chem. Phys.*, 5:1125–1156.

VOC CONCENTRATION MEASUREMENTS AT NORTH EUROPEAN URBAN SITE

J. PATOKOSKI[1], T. M. RUUSKANEN[1], R. TAIPALE[1], M. K. KAJOS[1] and J. RINNE[1]

[1]Department of Physics, P.O. Box 68, FI-00014, University of Helsinki, Finland

Keywords: VOCs, urban site, anthropogenic, biogenic

INTRODUCTION

Volatile organic compounds were measured online for four and half months continuously at SMEAR III station (Station for Measuring Ecosystem – Atmosphere Relations) which is a high latitude urban measurement station in Helsinki, Finland. The aim of this study was to measure atmospheric concentrations of VOCs, such as methanol and carbonyl compounds. Behaviour of the concentrations of these compounds in high latitude urban areas is not well known and thus one aim is to of these measurements is to observe the possible differences in seasonal and diurnal behaviour of VOC concentrations between SMEAR III and a rural SMEAR II site, previously studied by Ruuskanen et al., (2008). We were especially interested in relative contributions of biogenic and anthropogenic sources of VOCs.

METHODS

VOCs were measured with PTR-MS during 19.12.2005-3.5.2006 at SMEAR III in Helsinki. SMEAR III is an urban measurement site where trace gases, aerosol particles and urban micrometeorology is studied. It is located 5 kilometres northeast from the downtown of Helsinki. In the vicinity of measurement station there are both vegetated areas and major roads (Vesala et al., 2008).

Ambient air was measured with PTR-MS at the fourth floor of a five storey building. Sample air was pulled through few meters of Teflon tubing in to the PTR-MS. In these measurements PTR-MS was calibrated using a gas standard once a week. Measured compounds included methanol, acetonitrile, acetaldehyde, ethanol, acetone, isoprene, methyl ethyl ketone, benzene, toluene, xylenes, monoterpenes, methacrolein, methylvinylketone, hexanal and cis-3-hexenol. Calibrations were done weekly using gas standard. The calibration procedure and volume mixing ratio calculations are presented in detail by Taipale et al (2008).

RESULTS & CONCLUSIONS

Timeseries of whole measurement period for methanol (M33), benzene (M79) and monoterpene (M137) are presented in Figure 1.
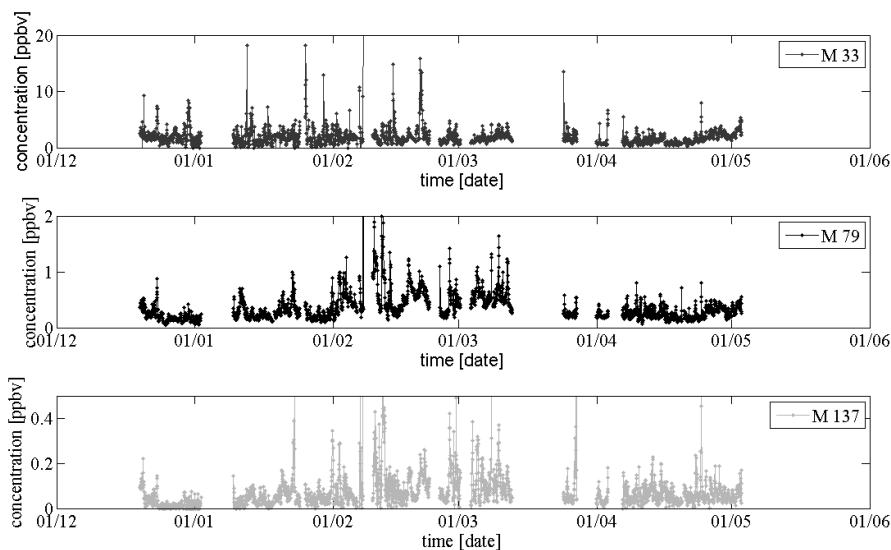
Figure 1. Concentrations of M33, M79 and M137 during whole measurement period.

In wintertime methanol concentrations were higher at the urban site than those measured at a rural site at SMEAR II, southern Finland (Ruuskanen et al., 2009). This is likely due to stronger anthropogenic influence. In winter we could not observe diurnal pattern, however, in spring methanol had a clear diurnal cycle. This behaviour could be indicating biogenic influence (Fig.2).

Benzene concentration was also higher than in rural area because of the stronger anthropogenic influence. Benzene did not have a diurnal pattern during any season in the rural station (Ruuskanen et. al., 2009). In urban site, however, benzene had a clear diurnal variation at the end of the spring (Fig 2).

In rural SMEAR II station monoterpenes originate dominantly from local and regional biogenic sources. Monoterpene concentrations are lower in winter than in summer (Ruuskanen et. al, 2009). In Helsinki monoterpenes are likely to be emitted from patches of vegetation and from anthropogenic sources. In springtime the monoterpene concentration at SMEAR III higher during daytime and low during night, contrary to the diurnal cycle observed at SMEAR II.
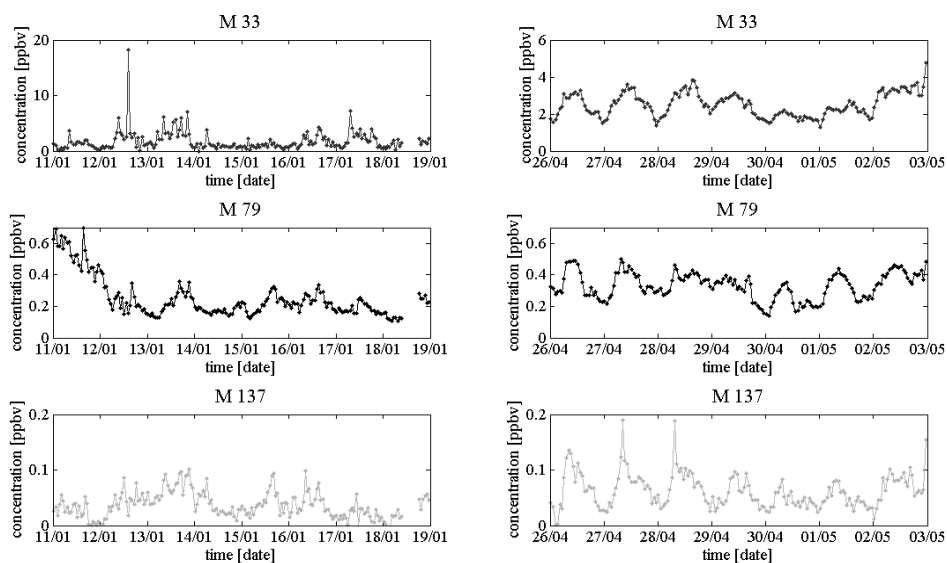
Figure 2. Concentrations of M33, M79 and M137 during one week in winter and in spring measured by PTR-MS at Helsinki.

339

Toluene and benzene are emitted for example from traffic exhaust gases and wood combustion. Ratio of toluene/benzene on the two time periods is presented in figure 3. From figure 3 could be observed also diurnal variation. Lifetime of toluene is shorter than lifetime of benzene. Toluene benzene ratio goes up when emission is fresh at morning and it goes down at the evening when emission was mixed with air (Holzinger et al., 2004).
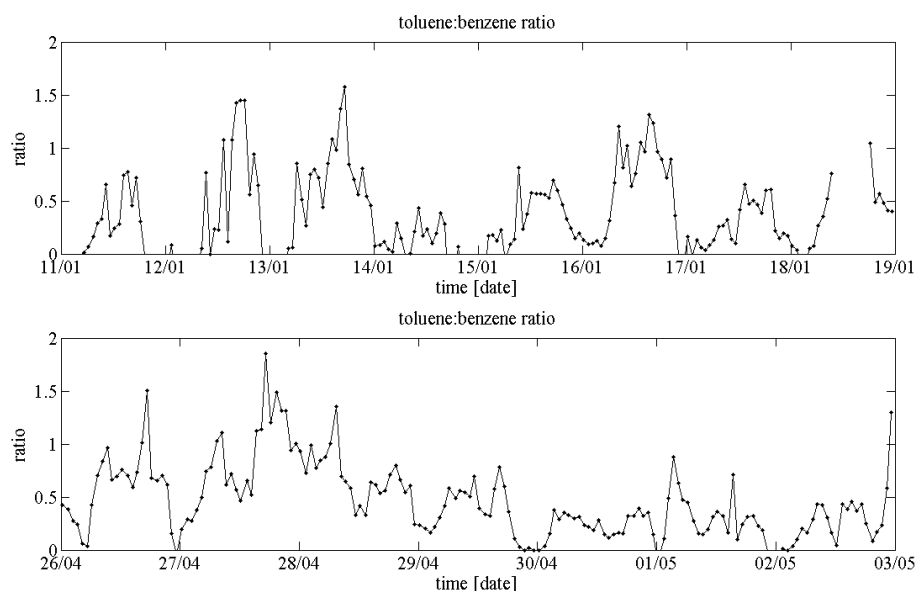
Figure 3. Toluene/benzene ratio during one week in winter and in spring measured by PTR-MS at Helsinki.

REFERENCES

T. Vesala, L. Järvi, S. Launiainen, A. Sogachev, U. Rannik, I. Mammarella, E. Siivola, P. Keronen, J. Rinne, A. Riikonen and E. Nikinmaa, Surface–atmosphere interactions over complex urban terrain in Helsinki, Finland Tellus 60B, 188-199, 2008.

R. Taipale, T.M. Ruuskanen, J. Rinne, M.K. Kajos, H. Hakola, T. Pohja, and M. Kulmala, Technical Note: Quantitative long-term measurements of VOC concentrations by PTR-MS-measurement, calibration and volume mixing ratio calculation methods, Atmospheric Chemistry and Physics, 8, 6681-6698, 2008.

T.M. Ruuskanen, R. Taipale, J. Rinne, M.K. Kajos, H. Hakola and M. Kulmala, Quantitative long-term measurements of VOC concentrations by PTR-MS-measurement: Annual cycle at a boreal forest site, Atmospheric Chemistry and Physics, Discussion, 9, 81-134, 2009.

R. Holzinger, B. Kleiss, L. Donoso and E. Sanhueza, Aromatic hydrocarbons at urban, sub-urban, rural (8°52′N; 67°19′W) and remote sites in Venezuela, International Journal of Mass Spectrometry, 235, 103-110, 2004.

SULFURIC ACID IN A DECIDUOUS FOREST

T. PETÄJÄ[1,2], R.L. MAULDIN, III[2], J. McGRATH[3], E. KOSCIUCH[2], J.N. SMITH[2] and S. PRYOR[4]

[1]Department of Physics, P.O. Box 64, FI-00014, University of Helsinki, Finland
[2]Atmospheric Chemistry Division, National Center for Atmospheric Research, Boulder, CO, USA
[3]Department of Atmospheric and Oceanic Sciences, University of Colorado at Boulder, CO, USA
[4]Atmospheric Science Program, Department of Geography, Indiana University, Bloomington, IN, USA

INTRODUCTION

As demonstrated in a number of investigations (Kulmala et al. 2004), new particle formation occurs readily in the boundary layer, including a deciduous forested region in Denmark (Pryor et al. 2005). Gaseous sulfuric acid is considered to play a central role in atmospheric aerosol formation (Weber et al. 1996). A technique for measuring the gas-phase sulfuric acid concentration even down to about 10^4 molecules cm^{-3} has already been available for more than a decade (Eisele and Tanner, 1993). As a result, a number of field campaigns have been performed that allow us to look at connections between the gas-phase sulfuric acid concentration and aerosol formation or growth rates. Although sulfuric acid seems to be a key component in the formation (Weber et al. 1996, Sihto et al. 2006, Nieminen et al. 2009), there are strong indications that condensing vapors other than sulfuric acid are frequently needed to explain the observed particle growth rates (Kulmala et al. 2001, Fiedler et al. 2005).

The aim of this study is to present measurements of sulfuric acid in the gas phase during a field campaign at Morgan Monroe state forest near Bloomington, IN, USA in May, 2008 and connect them with the aerosol particle number size distribution measurements conducted at the site. We measured gaseous phase sulfuric acid and hydroxyl radical concentrations with a Chemical Ionization Mass Spectrometer (CIMS).

EXPERIMENTAL SETUP

Sulfuric acid in the gas phase was measured with a technique utilizing selected chemical ionization and subsequent detection with a mass spectrometer. The CIMS instrument was operated inside a garden shed at Morgan Monroe State forest. The site is also an AmeriFlux tower site (Pryor et al. 2007). The measurements were performed from May 10 to May 31, 2008.

Measurement of sulfuric acid with the CIMS consists of several steps, including sample transport, chemical ionization, ion reactions, mass filtering and signal detection. Concentration of H_2SO_4 is calculated from the measured ion signals as

$$[H_2SO_4] = C \cdot \frac{HSO_4^-}{NO_3^-},$$

where C is directly measured calibration coefficient (Mauldin et al. 1998). One measurement cycle is completed in 30 seconds. A nominal detection limit of the CIMS instrument (Mauldin et al. 2001) is $5 \cdot 10^4$ molecule cm^{-3} for a 5 minute integration period.

The measurement of hydroxyl radical relies on the detection of isotopically labeled sulfuric acid with the CIMS-technique. More details can be found elsewhere (Eisele and Tanner, 1993, Mauldin et al. 1998, Mauldin et al. 2001).

During a CIMS measurement cycle, H_2SO_4 was measured 10 times followed by 20 measurements of combined OH and H_2SO_4 concentrations each lasting typically 30 s. The concentrations were averaged over 5 minutes.

PRELIMINARY RESULTS AND DISCUSSION

During the field campaign the concentration of sulfuric acid varied almost four orders of magnitude, from 10^4 molec cm^{-3} up to $7 \cdot 10^8$ molec cm^{-3} as a five minute average. Due to the photochemical production, the highest sulfuric acid concentrations were reached around noon as depicted in Figure 1, which represents sulfuric acid data obtained during May 25, 2008. New particle formation was observed during the field campaign on several days. The analysis of the SMPS data from Dec 2006 to Dec 2008 indicates that this site is characterized by a high frequency of nucleation events, where strong new particle formation events are observed to occur on approximately one day in five.

The median diurnal cycle during the whole campaign is presented in Figure 2. The median noon concentration during the whole time period was $1 \cdot 10^7$ molec cm^{-3}, which is clearly higher than for example the corresponding maxima in a boreal forest site Hyytiälä during spring 2007 obtained with a similar CIMS instrument (Petäjä et al. 2008). The NIFTy measurement site is in the Ohio river valley, where there are many coal fired power plants, which emit large amounts of SO_2, when operative. Thus, depending on the backtrajectories, the measurement site is occasionally in their plume, which results in higher sulfuric acid concentrations. On average, the levels are comparable with the values observed in the central Europe (Birmili et al. 2003).
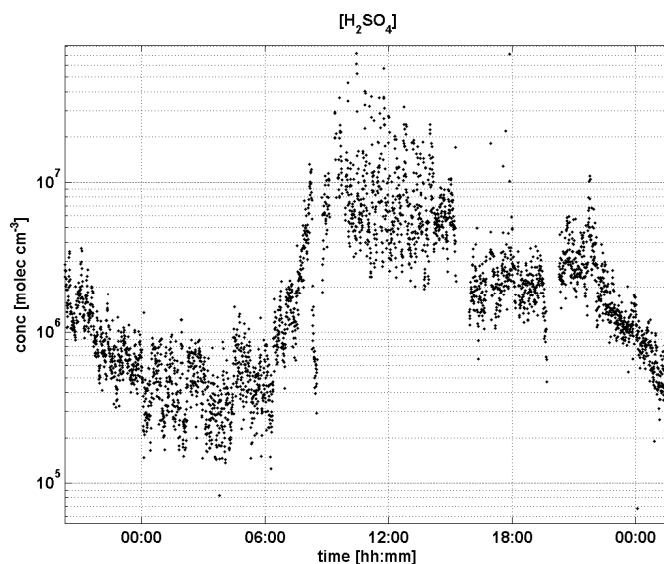
Figure 1. Gas phase sulphuric acid during May 25, 2008 at Morgan Monroe State forest.
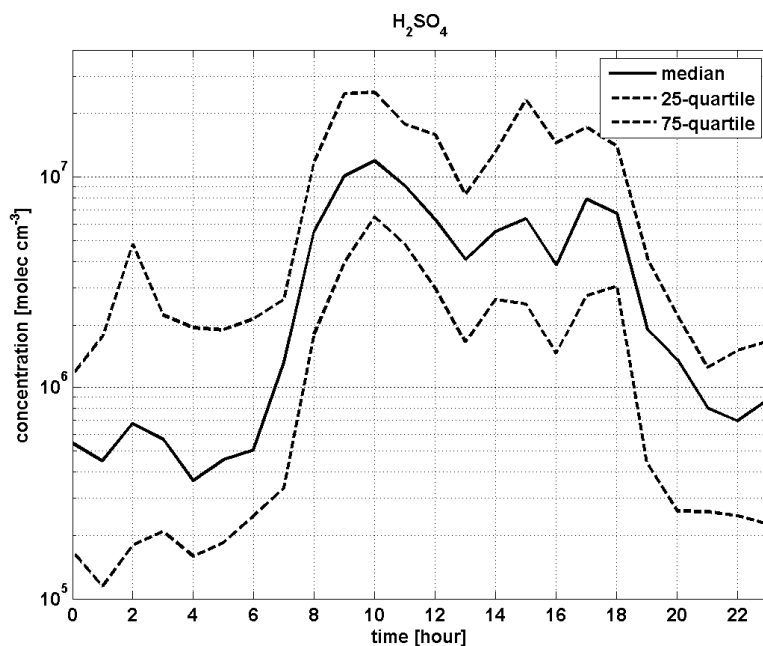
Figure 2. Median diurnal cycle of sulphuric acid during NIFTy.

REFERENCES

Birmili, W., Berresheim, H., Plass-Dülmer, C., Elste, T., Gilge, S., Wiedensohler, A., and Uhrner, U.: The Hohenpeissenberg aerosol formation experiment (HAFEX): A long-term study including size-resolved aerosol, H2SO4, OH, and monoterpenes measurements, *Atmos. Chem. Phys.*, **3**, 361–376, (2003).

Eisele, F. and Tanner, D.: Measurement of the gas phase concentration of H2SO4 and methane sulfonic acid and estimates of H2SO4 production and loss in the atmosphere, *J. Geophys. Res.* **98**, 9001–9010 (1993).

Fiedler, V., Dal Maso, M., Boy, M., Aufmhoff, H., Hoffmann, J., Schuck, T., Birmili, W., Hanke, M., Uecker, J., Arnold, F., and Kulmala, M. The contribution of sulphuric acid to atmospheric particle formation and growth: a comparison between boundary layers in Northern and Central Europe. *Atmos. Chem. Phys.*, **5**, 1773–1785 (2005).

Kulmala, M., Hämeri, K., Aalto, P. P., Mäkelä, J. M., Pirjola, L., Nilsson, E. D., Buzorius, G., Rannik,Ü., Dal Maso, M., Seidl, W., Hoffman, T., Janson, R., Hansson, H.-C., Viisanen, Y., Laaksonen, A., and O'Dowd, C. D.: Overview of the international project on biogenic aerosol 20 formation in the boreal forest (BIOFOR), *Tellus,* **53B**, 324–343, (2001).

Kulmala, M., Vehkamäki, H., Petäjä, T., Dal Maso, M., Lauri, A., Kerminen, V.-M., Birmili, W. and McMurry, P.H.: Formation and growth rates of ultrafine atmospheric particles: A review of observations. *J. Aerosol Sci.,* **35**, 143-176 (2004).

Mauldin III, R., Frost, G., Chen, G., Tanner, D., Prevot, A., Davis, D., and Eisele, F.: OH measurements during the First Aerosol Characterization Experiment (ACE 1): Observations and model comparisons, *J. Geophys. Res.*, **103**, 16 713–16 729, (1998).

Mauldin III, R.L., Eisele, F., Tanner, D., Kosciuch, E., Shetter, R., Lefer, B., Hall, S., Nowak, J., Buhr, M., Chen, G., Wang, P., and Davis, D. Measurements of OH, H2SO4, and MSA at the South Pole during ISCAT, *Geophys. Res. Lett.*, **28**, 3629–3632, (2001).

Nieminen, T., Manninen, H.E., Sihto, S.-L., Yli-Juuti, T., Mauldin, R.L., III, Petäjä, T., Riipinen, I., Kerminen, V.-M. and Kulmala, M. (2009) Connection of sulphuric acid to nucleation in Boreal forest. Environ. Sci. Technol., doi:10.1021/es803152j (in press).

Petäjä, T., Mauldin III, R.L., Kosciuch, E., McGrath, J., Nieminen, T., Adamov, A., Kotiaho, T. and Kulmala, M. Sulfuric acid and OH concentrations in a boreal forest site. *Atmos. Chem. Phys. Discuss.* **8**, 20193-20221 (2008).

Pryor, S., Barthelmie, R., Prip, H., and Sørensen, L. (2005). Observations of ultra-fine particles above a deciduous forest in Denmark. Geophys. Res. Lett., 32:L06804.

Pryor, S.C. and Barthelmie, R.J. Observations of Winter-time Nucleation and Particle Growth over/in a Forest. Nucleation and Atmospheric Aerosols, Proceedings of 17th International Conference, Galway, Ireland, Edited by O'Dowd, C.D. and Wagner, P.E., doi: 10.1007/978-1-4020-6475-3_184, 2007.

Sihto, S.-L., Kulmala, M., Kerminen, V.-M., Dal Maso, M., Petäjä, T., Riipinen, I., Korhonen, H., Arnold, F., Janson, R., Boy, M., Laaksonen, A., Lehtinen, K. E. J. Atmospheric sulphuric acid and aerosol formation: implications from atmospheric measurements for nucleation and early growth mechanisms. *Atmos. Chem. Phys.* **6**, 4079-4091, (2006).

Weber, R. J., Marti, J.J., McMurry, P.H., Eisele, F.L., Tanner and Jefferson, D.J.A.: Measured atmospheric new particle formation rates: Implications for nucleation mechanisms. *Chem. Eng. Comm.* **151**, 53-64 (1996).

COMPARISON OF STATIC CHAMBERS TO MEASURE CH_4, N_2O AND CO_2 FLUXES FROM SOILS

M.K. PIHLATIE[1], J. RIIS CHRISTIANSEN[2], H. AALTONEN[1], J. KORHONEN[1], T. RASILO[3], A.P. ROSA[4], G. BENANTI[5], J. HIRVENSALO[6], M. GIEBELS[7], M. HELMY[5], P. SCHREIBER[8], R. JUSZCZAK[9], R. KLEFOTH[10], S. VICCA[11], S. DOMINIQUE[12], S. JONES[13], R. LOBO DO VALE[14], B. WOLF[15], and J. PUMPANEN[3]

[1]Department of Physics, P.O. Box 64, FI-00014, University of Helsinki, Finland
[2] Department of Forest & Landscape Ecology, University of Copenhagen, Denmark
[3]University of Helsinki, Department of Forest Ecology, FI-00014 University of Helsinki, Finland
[4] Centro de Ecologia e Biologia Vegetal, Departamento de Biologia Vegetal, Lisboa, Portugal
[5] School of Biology and Environmental Science, University College Dublin, Dublin, Ireland
[6] MTT Agrifood Research Finland, Plant Production Research, FI-31600 Jokioinen, Finland
[7] Leibniz-Centre for Agricultural Landscape Research, Institute for Landscape Matter Dynamics, Germany
[8]Ernst Moritz Arndt University Greifswald, Institute for Botany and Landscape Ecology, Germany
[9]Agrometeorology Department, University of Life Sciences in Poznan, Poland
[10]Wageningen University, Soil Science Centre, Wageningen UR, Wageningen, The Netherlands
[11]University of Antwerpen, Department of Biology, Plant and Vegetation Ecology, Belgium
[12]Laboratoire d'Aérologie, FR-31400 Toulouse, France
[13]CEH Edinburgh, Bush Estate, Penicuik, Midlothian, UK
[14]Departamento de Engenharia Florestal, Instituto Superior de Agronomia, Lisboa, Portugal
[15]Forschungszentrum Karlsruhe GmbH, IMK-IFU, Garmisch-Partenkirchen, Germany

INTRODUCTION

Static chamber method is the most commonly used method to measure greenhouse gas (GHG) fluxes from soils. Static chambers, also named as non-steady-state non-flow-through chambers, vary in size, shape and material, as well as in the operation procedure and flux calculation method. Combination of these factors severely affects the measured and the calculated flux, making the comparison of fluxes measured by different chambers problematic (Rochette and Eriksen-Hamel, 2008).

Debate on how to design an optimal chamber and how to calculate the gas fluxes from soils has been under debate since the 1980's (e.g. Matthias et al., 1978; Hutchinson and Mosier 1981; Anthony et al., 1995; Conen and Smith, 2000; Livingston et al., 2005: Kutzbach et al., 2007; Kroon et al., 2008). Recommendations of using a fan to mix the chamber headspace, a vent tube to minimize pressure changes in the chamber (Hutchinson and Mosier 1981; Hutchinson and Livingston, 2001), and a proper insulation to avoid uncontrolled leakage from the chamber (Hutchinson and Livingston, 2001) are still not widely adopted in the field. Also, despite many years of criticism against linear regression method to calculate greenhouse gas fluxes from soils (Livingston et al., 2005; Kutzbach et al., 2007; Kroon et al., 2008), this method is still the most common method.

Inter-comparisons of different chamber designs, sampling protocols in combination with different flux calculation methods are very scarce. Pumpanen et al. (2004) performed a chamber calibration campaign to test different types of chambers used for carbon dioxide (CO_2) flux measurements. As the chamber designs and sampling protocol for methane (CH_4) and nitrous oxide (N_2O) chambers are often very different to the CO_2 chambers, the results obtained from the CO_2 measurement campaign are not directly applicable to CH_4 and N_2O.

Hence, we organized a chamber inter-comparison campaign targeted for static chambers to measure CH_4 and N_2O fluxes from soils. The overall aims of the campaign were to quantitatively assess the uncertainties and errors related to static chamber measurements, and to provide guidelines for chamber designs, sampling procedures, and flux calculation methods.

METHODS

Calibration system

The calibration campaign took place at Hyytiälä Forestry Field station (61°51'N, 24°17' E) southern Finland. Measurements were done between 11th of August and 10th of October 2008. The chamber calibrations were conducted with the same system originally built for CO_2 chamber calibration (Pumpanen et al. 2004).

The principle of the calibration tank is to replicate a diffusive flux of gas through a porous medium (sand) of known density and porosity. This is achieved by injecting gases of known concentrations, higher than in ambient air, into the closed tank. The gas will then diffuse through the sand due to the gas concentration gradient between the inside of the tank and the atmosphere and thus creating a known surface flux. This flux can be compared to the chamber flux measured at the same time on the top of the sand bed.

The calibration system consisted of a cylindrical stainless steel tank (diameter 1130 mm, height 1000 mm) with a 15 cm thick sand bed (diameter 1000 mm). The sand was placed on top of a 20 mm thick perforated high-density polyethylene lid. Dry coarse quarts sand and dry and wet fine quarts sands were used as the soil material. Air inside the tank was mixed with two fans installed at the bottom of the tank. Also, pressure difference between inside and outside the tank, temperatures inside and outside the tank, CO_2 concentration inside and outside the tank, and CH_4 concentration inside the tank, were measured automatically. Concentration of CH_4, N_2O (and CO_2) inside the tank were monitored by sampling gas automatically at 5-minute intervals by a custom made autosampler (MaSa).

During the measurement campaign, each week 1-3 participants calibrated their static chambers. Each week was organized in the same manner, hence making the measurements comparable between the weeks. Five flux levels (FL1-FL5) for the three studied sand types were created by injecting increasing amounts of CH_4, N_2O and CO_2 into the tank. After a stabilization period, the gas concentration change inside the tank was measured and chamber measurements were conducted on the top of the sand bed.

Chambers and gas analysis

In total 16 different chambers and 1 mega-chamber covering the whole surface area of the calibration tank were tested during the measurement campaign. The chambers were from different research groups across Europe. During the campaign all the investigated chambers were treated as similarly as possible with respect to sampling of gas from the chamber headspace and analysis on the gas chromatograph (GC). This was done in order to ensure a uniform protocol throughout the campaign and thus produce comparable results. All chamber enclosures were 35 min during which 4-6 gas samples were taken from the chamber. Samples from the chambers were taken with syringes (BD Plastipak) and transferred immediately to glass vials (12 ml, Labco Exetainer®).

Samples were analyzed on an Agilent Gas Chromatograph model 7890A (Agilent Technologies, USA) with an Electron Caption Detector (ECD) for N_2O, a Flame Ionization Detector (FID) for CH_4 and CO_2 (using a Nickel Catalyst methanizer). Helium was used as a carrier gas, synthetic air and hydrogen for the flame gases and nitrogen as a make-up gas for the FID. Argon-methane was used as a make-up gas for the ECD. The GC was connected to an Autosampler (Gilson GX-271 Liquid Handler) to allow an automatic injection of the samples into the GC.

Flux calculations

The CH_4, N_2O and CO_2 fluxes from the calibration tank were calculated based on the measured concentration changes inside the tank. This flux was called the reference flux, and it was calculated by fitting an exponential equation to concentration versus time as described by Pumpanen et al. (2004).

Fluxes of CH_4, N_2O and CO_2 from the chambers were calculated using a MATLAB-script developed by Kutzbach et al. (2008). The script fits linear, exponential and quadratic (Wagner et al., 1997) functions, and a non-steady-state diffusive flux estimator (NDFE) (Livingston et al., 2006) to the measurement data. The best fitted function for the concentration change inside the chamber, and hence the method of choice was based on the analysis of goodness-of-fit of the functions.

RESULTS

Analysis of the full data set is still ongoing and the results discussed here are based on approximately half of the data. Preliminary results show that most of the static chambers either over- or underestimated the CH_4, N_2O and CO_2 fluxes. This chamber specific over- or underestimation remained near constant with different flux levels. However, the deviation varied greatly with different soil porosities.

Special tests conducted during the campaign studying the effects of air mixing inside the chambers, vent tubes and pressure changes show that air mixing inside the chamber headspace, the way of chamber handling and sampling procedures can have pronounced effect on the trace gas concentration inside a chamber, and as a consequence the calculated chamber fluxes. The moment of chamber enclosure can lead to a rapid increase in the gas (CH_4) concentration due to a pressure effect in the chambers without a vent tube. It was also observed that manual sampling of gas can change the gas concentration in the chamber headspace. When mixing the chamber headspace air by a syringe, the subsequent gas sampling in the syringe may affect the diffusion of gas between the soil and the chamber headspace, and hence affect the flux. It was observed that mixing the chamber headspace with a fan instead of a syringe reduced this effect during the chamber enclosure. Overall, fluxes measured with chamber equipped with a fan always gave higher fluxes (up to 40%) as compared to fluxes measured from chambers without a fan.

CONCLUSIONS

Conclusions of the measurement campaign will be finalized after the full set of data is analyzed. However, the preliminary analysis shows that small chambers tend to be more sensitive to sampling errors, pressure fluctuations and further the calculated fluxes as compared to tall chambers. Underestimations of the CH_4, N_2O and CO_2 fluxes were greater with small chambers as compared with big chambers. There are several simplified models for calculating fluxes by static chambers, like quadratic and linear models. These simplified models tend to regularly underestimate the fluxes, and the amount of underestimation can up to 100%. Using an incorrect flux calculation method leads to a systematic underestimation, which can be very significant even in comparison with the spatial and temporal variability in greenhouse gas production and consumption in soils.

We suggest that static chambers used for greenhouse gas flux measurements should be equipped with at least one fan and a vent tube to increase mixing and reduce pressure propagation in the chamber-soil system, and that special attention should be paid to the handling of the chamber and to the timing of the gas sampling. Non-linear flux calculations methods should be used in order to avoid big underestimations in the flux calculations of greenhouse gas fluxes from soils.

REFERENCES

Anthony, W.H., Hutchinson, G.L., and Livingston, G.P. (1995) Chamber measurement of soil-atmosphere gas exchange: linear vs. diffusion-based flux models. *Soil Sci. Soc. Am. J.*, 59: 1308-1310.

Conen, F., Smith, K.A., (2000) An explanation of linear increases in gas concentration under closed chambers used to measure gas exchange between soil and the atmosphere. *Eur. J. Soil Sci.*, 51: 111-117.

Hutchinson, G.L. and Mosier, A.R. (1981) Improved soil cover method for field measurement of nitrous oxide fluxes. *Soil Soc. Am. J.*, 45: 311-316.

Kroon, P.S., Hensen, A. Van den Bulk, W.C.M., Jongejan, P.A.C. and Vermeulen, A.T., (2008) The importance of reducing the systematic error duet o non-linearity in N_2O flux measurements by static chambers, *Nutr Cycl Agroecosyst*, 82: 175-186.

Kutzbach, L., Schneider, J., Sachs, T., Giebels, M., Nykänen, H., Shurpali, N.J., Martikainen, P.J., Alm, J., Wilmking, M., (2007) CO_2 flux determination by closed-chamber methods can be seriously biased by inappropriate application of linear regression. *Biogeosciences* 4: 1005-1025.

Livingston, G.P., Hutchinson, G.L., and Spartalian, K. (2005) Diffusion theory improves chamber-based measurements of trace gas emissions. *Geophys. Res. Letters* 32: L24817.

Livingston, G.P., Hutchinson, G.L., Spartalian, K., (2006) Trace gas emission in chambers: A non-steady-state diffusion model. *Soil Soc. Am. J.*, 70: 1459-1469.

Matthias, A.R., Yarger, D.N., and Weinbeck, R.S. (1978) A numerical evaluation of chamber method for determining gas fluxes. *Geophys. Res. Lett.*, 5: 765-768.

Pumpanen, J., Kolari, P., Ilvesniemi, H., Minkkinen, K., Vesala, T., Niinisto, S., Lohila, A., Larmola, T., Morero, M., Pihlatie, M., Janssens, I., Yuste, J.C., Grunzweig, J.M., Reth, S., Subke, J.A., Savage, K., Kutsch, W., Ostreng, G., Ziegler, W., Anthoni, P., Lindroth, A., Hari, P., (2004) Comparison of different chamber techniques for measuring soil CO_2 efflux. *Agric. For. Meteorol.* 123: 159-176.

Rochette, P., and Eriksen-Hamel, N.S., (2008) Chamber measurements of soil nitrous oxide flux: Are absolute values reliable? *Soil Soc. Am. J.*, 72: 331-342.

Stolk, P.C., Jacobs, C.M.J., Moors, E.J., Hensen, A.,Velthof, G.L., Kabat, P. (2009) Significant non-linearity in nitrous oxide chamber data and its effect on calculated annual emissions. *Biogeosciences Discussion*, 6: 115-141.

Wagner, S.W., Reicosky, D. C., and Alessi, R. S. (1997) Regression models for calculating gas fluxes measured with a closed chamber, *Agron. J.*, 84: 731–738.

A NEW APPROACH TO REMOTE SENSING OF
PLANT PHYSIOLOGICAL STATUS AND GPP

A. PORCAR-CASTELL

Department of Forest Ecology, P.O. Box 27, FI-00014, University of Helsinki, Finland

INTRODUCTION

Remote sensing of gross primary production (GPP) is a key goal of Earth Observation and Climate Change Research. GPP depends not only on the amount of foliage participating in light interception but also on its physiological status and capacity to convert solar energy into chemical energy through the process of photosynthesis. Photosynthetic performance can be directly followed using optical methods and remote sensing. One approach that has recently received much attention to estimate GPP is the utilization of the light use efficiency term (ε) (Monteith 1972; Hilker et al. 2008), as:

$$GPP = PAR \times f_{PAR} \times \varepsilon, \qquad\qquad (Eq.\ 1)$$

where f_{PAR} is the fraction of photosynthetic active radiation (PAR) absorbed by the foliage and the light use efficiency factor (ε) represents the amount of carbon fixed per unit of absorbed energy.

While determination of PAR and f_{PAR} from remotely sensed data is possible, albeit complex, (Myneni et al. 2002; Hilker et al. 2008), estimation of ε from remotely sensed data yields still very variable results (Nichol et al. 2002; Rahman et al. 2004; Garbulsky et al. 2008). At the present, the state-of-the-art approach to directly estimate ε (Grace et al. 2007, Hilker et al. 2008) is based on reflectance changes induced by the modulation of the fraction of absorbed light dissipated as heat, which is largely controlled by the xanthophyll-cycle mechanism (Adams & Demmig-Adams, 1992). The activity of the xanthophyll-cycle has been associated to changes in leaf reflectance around 531 nm (Bilger et al. 1989). These changes were subsequently employed to derive the photochemical reflectance index (PRI) (Gamon et al. 1992, Peñuelas et al. 1995). PRI has been thenceforth used as a proxy of ε both at the leaf and canopy levels (Gamon et al. 1997; Nichol et al. 2002; Garbulsky et al. 2008). However, the correlation between PRI and ε remains very variable specially in long-term experiments, with periods of low correlation (Rahman et al. 2004; Garbulsky et al. 2008). In particular, PRI might be blind to certain mechanisms of photosynthetic acclimation, for example the photoinhibition of reaction centres.

Similarly, the estimation of sun induced chlorophyll fluorescence (SIF) using hyperspectral reflectance measurements (Moya et al. 2004; Meroni & Colombo, 2006) is also regarded as a potential tool to remotely sense the photosynthetic capacity of vegetation. However, compared to traditional saturating-light-pulse chlorophyll fluorescence analysis, where the yield of photochemistry can be readily estimated and used as a proxy of ε (Porcar-Castell et al 2008), the yield of photochemistry has not yet been solved from the passive fluorescence signal (Grace et al. 2007; Krumov et al. 2008). This is due to the lack of saturating-pulse capabilities in passive fluorescence measurements. The saturating-pulse shuts momentarily down photochemistry and allows solving the yield equation of fluorescence and estimating the quantum yield of photochemistry.

In the same way, I propose that PRI measurements can be combined with SIF, using PRI to estimate the rate constant of thermal energy dissipation (Porcar-Castell et al. 2008a). In this way the yield equation of fluorescence could be solved and allow the estimation of the photochemical yield from the SIF signal.

MODEL

A mechanistic model that integrates reflectance parameters into the yield equation of chlorophyll fluorescence (Kitajima & Butler, 1975) is proposed. The model is conceived as an up-scaled version of a previously described fluorescence model (Porcar-Castell et al. 2006, 2008a). Passive or sun induced chlorophyll fluorescence (SIF) can be expressed as a function of the absorbed photosynthetic active radiation (PAR) by vegetation and the prevailing yield of chlorophyll fluorescence, as:

$$SIF = APAR \frac{k_f}{k_f + k_d + k_P + k_{NPQ}} = f(PAR, NDVI) \frac{k_f}{k_f + k_d + k_P + f(PRI)} \quad \text{(Eq. 2)}$$

where APAR is the absorbed PAR [μmol m^{-2} s^{-1}], and k_f, k_d, k_P, and k_{NPQ} are the rate constants associated to chlorophyll fluorescence, constitutive heat dissipation, photochemistry and regulated thermal energy dissipation, respectively. Subsequently, APAR can be estimated as a function of incident PAR and reflectance indices (e.g. NDVI), and k_{NPQ} as a function of PRI. The result is an equation system from where the photochemical yield can be solved as:

$$\phi P = 1 - \frac{\left[k_f + k_d + f(PRI) \right] SIF}{f(PAR, NDVI) \; k_f} \quad \text{(Eq. 3)}$$

which can be used as a proxy of light-use-efficiency (ε), keeping in mind the number of processes that uncouple electron transport from carbon assimilation.

CONCLUSIONS

The proposed approach is entirely based on parameters that can be remotely sensed, from tower-based, to aircraft and satellite measurements. Previous parameterization from ground measurements, the approach allows for the first time to estimate the yield of photochemistry from passive fluorescence data. This opens up new possibilities in the study of the acclimation of photosynthesis and estimation of GPP at the stand, landscape and regional levels.

REFERENCES

Adams, W.W. and Demmig-Adams, B. (1992) Operation of the xanthophyll cycle in higher plants in response to diurnal changes in incident sunlight. *Planta,* 186: 390-398.

Bilger, W., Bjorkman, O. and Thayer, S.S. (1989) Light-induced spectral absorbance changes in relation to photosynthesis and the epoxidation state of xanthophyll cycle components in cotton leaves. *Plant Physiol.* 91:542-551.

Gamon, J.A., Peñuelas, J. and Field, C.B. (1992) A narrow-waveband spectral index that tracks diurnal changes in photosynthetic efficiency. *Remote Sens. Environ.* 41: 35-44.

Gamon, J.A., Serrano, L. and Surfus, J.S. (1997) The photochemical reflectance index: an optical indicator of photosynthetic radiation use efficiency across species, functional types, and nutrient levels. *Oecologia* 112:492-501.

Garbulsky, M.F., Peñuelas, J., Papale, D. and Filella, I. (2008) Remote estimation of carbon dioxide uptake by a Mediterranean forest. *Glob. Change Biol.* 14:2860-2867.

Grace, J., Nichol, C., Disney, M., Lewis, P. Quaife, T. and Bowyer, P. (2007) Can we measure terrestrial photosyntheis from space directly, using spectral reflectance and fluorescence. *Glob. Change Biol.* 13: 1484-1497.

Hilker, T., Coops, N.C., Wulder, M.A., Black, T.A. and Robert, D.G. (2008) The use of remote sensing in light use efficiency based models of gross primary production: A review of current status and future requirements. *Sci. Tot. Env.* 404: 411-423.

Kitajima, M. and Butler, W.L. (1975) Quenching of chlorophyll fluorescence and primary photochemistry in chloroplasts by dibromothymoquinone. *Biochim. Biophys. Acta* 376:105-115.

Krumov, A., Nikolova, A., Vassilev, V. and Vassilev, N. (2008) Assessment of plant vitality detection through fluorescence and reflectance imagery. *Adv. Space Res.* 41: 1870-1875.

Meroni, M. and Colombo, R. (2006) Leaf level detection of solar induced chlorophyll fluorescence by means of a subnanometer resolution spectroradiometer. *Remote Sens. Environ.* 103: 438-448.

Monteith, J.L. (1972) Solar radiation and production in tropical ecosystems. *J. Appl. Ecol.* 9:747-766.

Moya, I., Camenen, L., Evain, S. Goulas, Y., Cerovic, Z.G., Latouche, G., Flexas, J. and Ounis, A. (2004) A new instrument for passive remote sensing 1. Measurements of sunlight-induced chlorophyll fluorescence. *Remote Sens. Environ.* 91: 186-197.

Myneni, R. B., Hoffman, S., Knyazikhin, Y., Privette, J. L., Glassy, J., Tian, Y., Wang, Y., Song, X., Zhang, Y. and Smith, G. R. (2002) Global products of vegetation leaf area and fraction absorbed PAR from year one of MODIS data. *Remote Sens. Environ.* 83:214-31.

Nichol, C., Lloyd, J., Shibistova, O., Arneth, A., Röser, C., Knohl, A., Matsubara, S. and Grace, J. (2002) Remote sensing of photosynthetic light-use efficiency of a Siberian boreal forest. *Tellus* 54B:677-687.

Peñuelas, J., Filella, I. and Gamon, J.A. (1995) Assessment of photosynthetic radiation-use efficiency with spectral reflectance. *New Phytol.* 131: 291-296.

Porcar-Castell A., Bäck J, Juurola E, Hari P 2006. Dynamics of the energy flow through photosystem II under changing light conditions: a model approach. Funct. Plant Biol. 33:229-239.

Porcar-Castell, A., Juurola, E., Nikinmaa, E., Berninger, F., Ensminger, I. and Hari, P. (2008a) Seasonal acclimation of photosystem II in Pinus sylvestris. I. Estimating the rate constants of sustained heat dissipation and photochemistry. *Tree Physiol.* 28:1475-1482.

Rahman, A.F., Cordova, V.D., Gamon, J.A. Schmid, H.P. and Sims,. D.A. (2004) Potential of MODIS ocean bands for estimating CO2 flux from terrestrial vegetation: A novel approach. *Geophys. Res. Lett.* 31: L10503.

AEROSOL-CLOUD INTERACTIONS AT PUIJO SEMI-URBAN MEASUREMENT STATION

H.J. PORTIN[1], M. KOMPPULA[1], A. LESKINEN[1], S. ROMAKKANIEMI[2], A. LAAKSONEN[3,2]
and K.E..J. LEHTINEN[1,2]

[1]Finnish Meteorological Institute, Kuopio Unit, P.O. Box 1627, FI-70211 Kuopio, Finland
[2]Department of Physics, University of Kuopio, P.O. Box 1627, FI-70211 Kuopio, Finland
[3]Finnish Meteorological Institute, Research and Development, P.O. Box 503, FI-00101 Helsinki, Finland

Keywords: Aerosol-cloud Interaction; Cloud droplet activation; Indirect effect

INTRODUCTION

Anthropogenic aerosol particles have substantially increased the global mean burden of aerosol particles from pre-industrial times to the present-day. Our ability to predict the current and future behaviour of the Earth's climate system is hindered seriously by the uncertainties associated with the indirect effects by atmospheric aerosols (Lohmann and Feichter, 2005). The Intergovernmental Panel on Climate Change considers the indirect effects of aerosols to be the most uncertain components in forcing of climate change over the industrial period (IPCC 2007). This indirect forcing is caused by the ability of aerosol particles to act as cloud condensation nuclei (CCN) or ice nuclei. With increasing CCN concentration, caused by human activity, more and smaller droplets are formed. As a consequence, and under the assumption that liquid water content (LWC) stays constant, the cloud albedo and thus the reflection of solar radiation increase (Twomey, 1977). In addition, the reduction of cloud droplet size weakens precipitation development, resulting in more persistent clouds (Albrecht, 1989). Many of these climatically important cloud properties depend strongly on aerosol particles. Only few measurement stations have been able to provide valuable long-term data on aerosol-cloud interactions, e.g. Global Atmospheric Watch stations at Pallas, Finland (Komppula et al., 2005) and at Jungfraujoch, Switzerland (Henning et al., 2002).

PUIJO MEASUREMENT STATION

The Puijo station was established in 2005 by the Finnish Meteorological Institute and the University of Kuopio (Leskinen et al., 2009). The station resides on the top floor of the Puijo observation tower (306 m a.s.l., 224 m above the surrounding lake level), near the town of Kuopio, in a semi-urban environment. Kuopio is situated in Central Finland, 330 km to the North from Helsinki. The station provides continuous data on particle and cloud droplet size distributions, optical properties of particles, weather parameters and trace gas concentrations. In addition, intensive measurement campaigns have been organized yearly together with the University of Kuopio. During these campaigns, we also measured aerosol chemical composition, particle hygroscopicity, cloud condensation nuclei concentration and collected cloud water samples.

MEASUREMENT DEVICES

We measure the cloud droplet number size distribution in the diameter range of 3-50 µm with a cloud droplet probe (CDP, Droplet Measurement Technologies). The device uses a laser beam to detect the droplets. Size classification is based on the amount of scattered light. From this data, we are able to calculate the cloud droplet number size distribution, average droplet diameter and cloud liquid water content. We are using a twin-DMPS system for particle number size distribution measurement. The measured size range was 10-500 nm until March 2007 and 7-800 nm thereafter. We also have a condensation particle counter (TSI 3010) to measure the total number concentration of particles. The aerosol sample is drawn through a sample line through the roof of the tower. We have a heating in the sample inlet for drying the cloud droplets, so we observe the total (out-of-cloud) particle size distribution.

The first step of our data-analysis was to calculate hourly averages of weather parameters, particle and cloud droplet size distribution data. After this, we classified all hourly averages with visibility below 200 m and rain intensity below 0.2 mm/h as cloud event hours. Besides of the sudden drop in visibility, these events are also characterized by a burst in cloud droplet concentration (Figure 1). We use the limit for rain intensity, since rain drops remove unactivated aerosol particles and would disturb analysis. We also have a weather camera on top of the tower which allows us to check the prevailing weather conditions. With these selection criteria, we have more than 500 hours of cloud event data.

We classify the data into four groups based on the particle number concentration in order to distinguish the correlations between concentration and parameters involved in cloud-particle interaction. To get groups with equal amount of data in each, we use the following concentration limits: < 700 cm^{-3}, 700-1300 cm^{-3}, 1300-2200 cm^{-3} and > 2200 cm^{-3}. For each class we calculate the average cloud droplet concentration N_d, average droplet diameter d_d, accumulation mode particle concentration N_{acc}, ratio of N_d to N_{acc}, ratio of Aitken mode particle concentration to accumulation mode particle concentration N_{ait}/N_{acc} and liquid water content.

We also calculated 120-hour backward trajectories and classified the air masses into marine and continental. The classification between air masses was made visually from the trajectory plots for each event. To avoid any bias, only clear continental cases were selected as "continental" and also for the marine. In the classification, our continental air masses have not touched sea during the last 120 hours. The marine air masses arrive straight from the Atlantic or Arctic Ocean. It should be noted, however, that these air masses spent on average 40 hours over the continent before arriving to our station and thus can not be considered purely marine. For a more detailed description of data evaluation, see Portin et al. (2009).
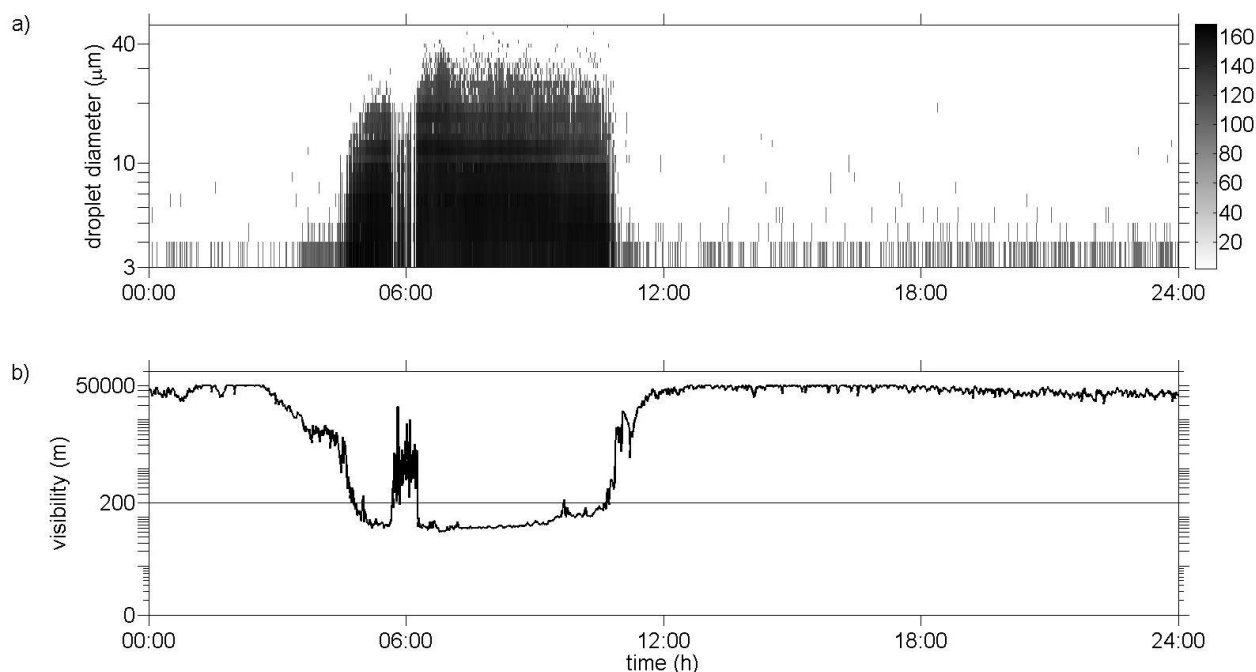
Figure 1. Cloud droplet size distribution and visibility data during a cloud event on 24.9.2008.

RESULTS

Based on the particle concentration classification, we found three indications of the aerosol indirect effects (Table 1): 1) Cloud droplet concentration increased with the increasing particle concentration. 2) Cloud droplet concentration and average droplet diameter were inversely proportional, as previous studies have shown (Komppula et al., 2005; Vong and Covert, 1998; Twohy et al., 2005). 3) ratio of N_d to N_{acc} was smaller when particle concentration is higher. There was a slight tendency to positive correlation between particle concentration and the ratio N_{ait}/N_{acc}.

Statistics of different air masses are given in Table 2. Marine air masses were characterized by the higher particle concentration, higher N_{ait}/N_{acc} ratio, smaller droplet concentration and lower liquid water content compared to continental air masses. The higher N_{ait}/N_{acc} ratio in the marine air masses is consistent with the pronounced Aitken mode of usual marine number size distributions (Anttila et al., 2008; Lihavainen et al., 2008). The lower particle concentration in continental air masses compared to marine was not what one would expect. It seems that during the observed cloud events, the continental air masses were relatively clean, the average particle concentration being below the annual average. But overall the continental air masses have their own characteristics, having different shape of the size distribution (Portin et al., 2009).

N_p (cm^{-3})	N_d (cm^{-3})	d_d (μm)	N_{acc} (cm^{-3})	N_d/N_{acc}	N_{ait}/N_{acc}	LWC (g m^{-3})
< 700	160	7.77	130	1.23	2.41	0.056
700--1300	248	6.16	326	0.76	1.80	0.056
1300--2200	261	5.95	389	0.67	2.72	0.050
> 2200	294	5.37	502	0.59	3.50	0.043
1375	239	6.33	328	0.72	2.47	0.052

Table 1. Cloud droplet concentration N_d, average droplet diameter d_d, total particle concentration N_p, accumulation mode concentration N_{acc}, N_d/N_{acc}, N_{ait}/N_{acc}, and liquid water content LWC during the observed cloud events. Last line shows average values.

class	N_d (cm^{-3})	d_d (μm)	N_p (cm^{-3})	N_{acc} (cm^{-3})	N_d/N_{acc}	N_{ait}/N_{acc}	LWC (g m^{-3})
marine	203	6.82	1313	191	1.06	4.08	0.051
continental	231	6.55	1160	334	0.69	1.90	0.058

Table 2. Average values of cloud droplet concentration N_d, average droplet diameter d_d, total particle concentration N_p, accumulation mode concentration N_{acc}, N_d/N_{acc}, N_{ait}/N_{acc} and liquid water content LWC calculated according to air mass origin.

REFERENCES

Albrecht, B. A. (1989) Aerosols, cloud microphysics, and fractional cloudiness. *Science*, 245, 1227-1230.

Anttila, T., Vaattovaara, P., Komppula, M., Hyvärinen, A.-P., Lihavainen, H., Kerminen, V.-M. and Laaksonen, A. (2008) Size-dependent activation of aerosols into cloud droplets at a subarctic background site during the second Pallas Cloud Experiment (2nd PaCE): method development and data evaluation. *Atmos. Chem. Phys. Discuss.*, 8, 14519-14556.

Henning, S., Weingartner, E., Schmidt, S., Wendisch, M., Gäggeler, H. W. and Baltensberger, U. (2002) Size-dependent aerosol activation at the high-alpine site Jungfraujoch (3580 m a.s.l.). *Tellus*, 54B, 82-95.

Intergovernmental panel on Climate Change (IPCC), Climate change 2007: The physical science basis. Cambridge University Press, New York, 2007.

Komppula, M., Lihavainen, H., Kerminen, V.-M., Kulmala, M. and Viisanen, Y. (2005) Measurements of cloud droplet activation of aerosol particles at a clean subarctic background site. *J. Geophys. Res.*, 110, D06204, doi: 10.1029/2004JD005200.

Leskinen, A. P., Portin, H. J., Komppula, M., Miettinen, P., Arola, A., Lihavainen, H., Hatakka, J., Laaksonen, A. and Lehtinen, K. E. J. (2009) Overview of research activities and results at Puijo semi-urban measurement station. *Boreal Env. Res.*, in press.

Lihavainen, H., Kerminen, V.-M., Komppula, M., Hyvärinen, A.-P., Laakia, J., Saarikoski, S., Makkonen, U., Kivekäs, N., Hillamo, R., Kulmala, M. and Viisanen, Y. (2008) Measurements of the relation between aerosol properties and microphysics and chemistry of low clouds in northern Finland. *Atmos. Chem. Phys.*, 8, 6925-6938.

Lohmann, U. and Feichter (2005) Global indirect aerosol effects: a review. *J., Atmos. Chem. Phys.*, 5, 715-737.

Portin, H. J., Komppula, M., Leskinen, A. P., Romakkaniemi, S., Laaksonen, A. and Lehtinen, K. E. J. (2009) Observations of aerosol–cloud interactions at the Puijo semi-urban measurement station. *Boreal Env. Res.*, in press.

Twohy, C. H., Petters, M. D., Snider, J. R., Stevens, B., Tahnk, W., Wetzel, M., Russell, L. and Burnet, F. (2005) Evaluation of the aerosol indirect effect in marine stratocumulus clouds: droplet number, size, liquid water path, and radiative impact. *J. Geophys. Res.*, 110, D08203, doi:10.1029/2004JD005116.

Twomey, S. (1977) The infl uence of pollution on the shortwave albedo of clouds. *J. Atmos. Sci.*, 34, 1149-1152.

Vong, R. J. and Covert, D. S. (1998) Simultaneous observations of aerosol and cloud droplet size spectra in marine stratocumulus. *J. Atmos. Sci.* 55, 2180-2190.

EFFECT OF CLEAR-CUTTING ON CARBON FLUXES FROM BOREAL FOREST SOIL

J. Pumpanen[1], T. Rasilo[1], L. Kulmala[1], T. Lepistö[2] J. Heinonsalo[3] and H. Ilvesniemi[2]

[1] Department of Forest Ecology, P.O. Box 27, FI-00014 University of Helsinki, Finland
[2] Finnish Forest Research Institute, Vantaa Research Center, P.O. Box 18, FI-01301 Vantaa, Finland
[3] Department of Applied Chemistry and Microbiology, P.O. Box 27, FI-00014 University of Helsinki, Finland

Keywords: Soil CO_2 efflux, clear cutting

INTRODUCTION

Due to their large land area and large carbon pool forests play an important role in the management of soil carbon stocks. Land use, such as forest harvesting affects soil carbon pool, and it has been suggested that carbon stocks can be managed by silvicultural practices. Upon such disturbances as forest fire or clear-cutting, the carbon balance of a forest is profoundly changed. First the carbon assimilation in photosynthesis of trees is ceased and secondly a large amount of fresh litter is released to the soil. When the tree canopy is removed, the solar radiation on the soil surface is increased resulting in higher diurnal temperature fluctuation in the soil. Because the decomposition of soil organic matter is dependent on soil temperature and soil moisture, an increase in these factors can increase the decomposition rate of organic matter. In addition to clear-cutting and residue removal, the site preparation used for promoting the germination of seeds and helping the survival of planted seedlings also affects the decomposition of soil organic matter. There is also a major shift from autotrophic to heterotrophic respiration due to the removal of trees. The aim of this project was to quantify soil CO_2 efflux from boreal forests of different ages and to study how forest clear-cutting and site preparation affect the above and below ground biomass and the CO_2 efflux from soil.

MATERIAL AND METHODS

We studied soil CO_2 efflux and carbon stocks on 5-15 year-old clear-cut sites exposed to site preparation and on adjacent non-cut control forests close to Hyytiälä in Southern Finland (61° 51´N lat., 24° 17´E long.). The sites varied from fertile Norway spruce (*Picea abies*) and Silver Birch (*Betula pendula*) dominated sites on till soil to Scots pine (*Pinus sylvestris*) dominated sites on sedimented sandy soil. The sites were selected from the database of Metsähallitus (the former National Board of Forestry) based on age criteria. Another selection criteria was that the soil had not been exposed to a prescribed burning. The control forest and clear-cut site pairs were located adjacent to each other or within 50 m distance.

Tree biomass was measured in September 2004 in each tree stand and clear-cut site. The height and diameter at breast height (1.3 m) of all trees as well as the diameter of stumps on the plots were measured. The stem, root and leaf biomass of the trees was determined with biomass equations (Marklund 1986, Marklund 1987). The leaf biomass of tree seedlings was based on systematic sampling. Five seedlings of each tree species in size classes of 0-30 cm, 30-60 cm, 60-90 cm, 90-120 cm and 120-150 cm were sampled randomly from the clear-cut site. The seedlings were dried in paper bags in room temperature for 14 days and the leaf mass and length of individual seedlings was measured. A linear regression between the leaf biomass and seedling length was then used to estimate the species specific leaf biomass on the clear-cut site. The biomass of ground vegetation was estimated from ground vegetation samples collected from the clear-cut sites and in the control forests in August 2005. The samples were kept at 5 ℃ until separated by hand. The separated samples were oven dried for 24 h in 70℃ temperature. The dry weight of each plant species as well as root biomass was determined from the dried samples.

Soil C and N content as well as root biomass were determined to 50 cm depth from core samples taken systematically at (1m) distance from the soil collars with a core sampler 5 cm in diameter. The soil cores were frozen immediately after sampling until processed. The soil core samples were separated into their organic and mineral soil horizons and litter, roots and humus were separated into different compartments and weighed after drying in 105 ºC for 24 hours. Finally, the soil samples were milled and analysed for C and N with LECO elemental analyser (LECO Corporation, MI, USA).

We measured soil CO_2 efflux on the clear-cut sites and in the adjacent control forest from 10 PVC collars (220 mm in diameter and 50 mm in height) installed systematically in line at 2 meter distance from each other with manual dynamic closed chambers (diameter 200 mm and height 300 mm) made of polycarbonate and covered with aluminium foil. The chamber has been described in detail in Kolari et al. (2004). A small fan was used to mix the air within the chamber headspace. The CO_2 efflux measurements were conducted during two consecutive years 2005 and 2006. We monitored the increase of CO_2 concentration in the chamber's headspace for 210 seconds at 15-seconds intervals with IRGA (EGM-4, PP-Systems, Hutchinson UK) in 2005 and with a solid state CO_2 sensor (GMP343, Vaisala, Helsinki, Finland) in 2006. The CO_2 flux calculation was conducted using CO_2 values corrected for temperature, RH and air pressure. Soil temperature was monitored at one hour intervals at 5 cm depth in the mineral soil with small temperature loggers (iButton® , Maxim Integrated products Inc., Sunnyvale, CA) installed permanently in the soil next to three collars in each measurement line.

RESULTS AND DISCUSSION

Soil CO_2 efflux at the sites showed a typical seasonal variation following soil temperature the effluxes ranging from 1.3 µmol CO_2 m^{-2} s^{-1} in the beginning of June to 7.6 µmol CO_2 m^{-2} s^{-1} in July. In general the CO_2 effluxes measured from the most recent clear-cut sites were higher compared to the non-cut control forest, but the differences were usually not statistically significant. We studied the differences between treatments with general linear model (GLM). In the first study year 2005, the CO_2 effluxes were statistically higher in the control forest of the 12-year-old Scots pine site (P<0.034) whereas in the other sites the differences between the clear-cut and the control were not significant. The CO_2 efflux from the clear-cut sites remained high even if a major proportion of the actively respiring root biomass was killed upon clear-cutting. In 2006, the CO_2 efflux from control forest was an average higher compared to the 5-year-old Scots pine sites. However, the differences were significant on one site only. At Norway spruce sites, the GLM showed statistically higher CO_2 efflux in the 5-year-old spruce stand (P<0.049) and 10-year-old Silver birch stand (P<0.021) compared to the non-cut control forests. So, the clear-cut seemed to have rather small influence on the soil CO_2 effluxes already after 5 years following the clear-cutting. In previous studies, the contribution of root and rhizosphere respiration to soil CO_2 efflux has been shown to be around 30-70% of the total respiration in forest soils. Here, the lost root and rhizosphere respiration was probably first masked by the decomposition of logging residue remained in the soil and later by the root respiration of the quickly emerging new ground vegetation. Another explanation to the high CO_2 effluxes observed on the clear-cut sites was the soil temperature, which was substantially higher on the clear-cut sites compared to the control forests.

We also determined the amount of branches, leaves, needles and other litter as well as the amount of root biomass and humus on the sites. The amount of branches was higher and the root biomass lower on the clear-cut sites compared to control forests still 12 years after clear-cutting, but no systematic difference in the amount of humus was observed between the clear-cuts and controls.

We will continue studying the carbon stocks and fluxes at the sites with a process based model taking into account the decomposition rates of different fractions of soil organic matter, root and rhizosphere respiration and carbon input from photosynthesis.

ACKNOWLEDGMENTS

REFERENCES

Kolari P., Pumpanen J., Rannik Ü., Ilvesniemi H., Hari P. and Berninger F. 2004. Carbon balance of different aged Scots pine forests in southern Finland. *Global Change Biology* 10:1106-1119

Marklund, L.G. 1987. Biomass functions for Norway spruce (Picea abies (L.) Karst.) in Sweden. Department of Forest Survey. *Report* 43. Swedish University of Agricultural Sciences. 127 p.

Marklund, L.G. 1988. Biomass functions for pine, spruce and birch in Sweden. Department of Forest Survey. *Report* 45. Swedish University of Agricultural Sciences. 73 p.

MODELLING CH₄ EMISSIONS FROM WETLANDS FOR THE COSMOS – EARTH SYSTEM MODEL

M. RAIVONEN[1], S. SEVANTO[1], S. HAAPANALA[1], S. JUUTINEN[2], T. LARMOLA[2], J. PUMPANEN[2], J. RINNE[1], T. RIUTTA[2], E-S. TUITTILA[2], R. GETZIEH[3], V. BROVKIN[3], C. REICK[3], H. JÄRVINEN[4] and T. VESALA[1]

[1]Department of Physics, P.O. Box 64, FI-00014, University of Helsinki, Finland
[2]Department of Forest Ecology, P.O. Box 27, FI-00014, University of Helsinki, Finland
[3]Max Planck Institute for Meteorology, Bundesstraße 55, G-20146 Hamburg, Germany
[4]Finnish Meteorological Institute, P.O. Box 503, FI-00101 Helsinki, Finland

INTRODUCTION

Methane (CH₄) is the second most important greenhouse gas after carbon dioxide (CO₂) and it is about 21 times more powerful at warming the atmosphere than CO₂ (Forster et al., 2007). Atmospheric CH₄ concentration increased steadily throughout the latter part of the twentieth century. The increase levelled off around 1999 until it started again in the beginning of 2007 (Rigby et al., 2008). It is not currently known whether the renewed growth is a consequence of increasing CH₄ emissions or also a decrease in the atmospheric concentration of methane-destroying hydroxyl radicals (OH).

The total global CH₄ source is relatively well known but the strength of each component is not. Most CH₄ (60–70%) is released from anthropogenic sources like energy production and rice cultivation, but also natural sources are significant, above all natural wetlands that are the largest individual source of CH₄ in the atmosphere (20–35%) (Forster et al., 2007). However, the estimates of CH₄ emissions from wetlands also carry the highest uncertainty.

As methane source and carbon sink, wetlands play an important role in the climate system. It would be essential to be able to estimate how the climatic change affects their carbon cycle. The large variation within climate change scenarios and the high structural and functional diversity of wetlands makes it quite impossible question to address empirically. However, this can be achieved via modelling. The already existing process based models for CH₄ fluxes from natural wetlands using different spatial scales — micro site level (e.g. Kettunen, 2003), regional level (Wania, 2007) and global level (Walter et al., 2001) — will facilitate the creation of the wetland model for this purpose.

Earth system models (ESMs) are the only tool we can use for making predictions of the future living conditions on our planet. During the past 10 years, the understanding of the influence of terrestrial biosphere on the climate system has reached the level that nowadays most ESMs contain a sub-model for the terrestrial biosphere. Therefore, they provide means for studying the importance of a specific aspect of the atmosphere-biosphere interaction to the climate as well as the influence of the whole feedback cycle on the Earth system.

The ESM of the Max Plank Institute for Meteorology (MPI-M) is among the top-ranking ESMs extensively referred to in the 4th Assessment Report of the IPCC. It is the core of the COSMOS-ESM that, unlike most other ESMs, is an open-access model. This means that the development is done in open, non-profit collaboration between international research institutes and universities. In the current version of the biosphere component JSBACH (Raddatz et al., 2007) of the COSMOS-ESM, wetlands and their CH₄ emissions are not included at all, which means that the climate model lacks a realistic description of the behaviour of one of the most important CH₄ sources.

OBJECTIVES AND METHODS

The aim of the project is to construct a process-based model on CH_4 production and transport in wetlands to be included as a new wetland-carbon model in the land biosphere part of the COSMOS-ESM. As a starting point, we have the CH_4 model of Wania (2007). We plan to improve this, for instance, we are testing a novel ebullition scheme that bases on the theory of homogenous nucleation. The model will be combined with a carbon uptake (photosynthesis), aerobic decomposition and peat accumulation model produced by the Global Vegetation Modelling group at MPI-Hamburg. The first model prototype will be validated using data collected on an ombrotrophic fen, Siikaneva, in southern Finland. We have data sets of meteorological parameters, CH_4 profile in soil, eddy covariance measurements of ecosystem-level CH_4 and CO_2 fluxes above the peatland (Rinne et al., 2007) and chamber measurements of the spatial variation of the CH_4 and CO_2 fluxes with and without aerenchymatous plants transporting CH_4 (Riutta et al., 2007).

MODEL

The methane production and transport model is still under development. However, a preliminary version exists. As input, it uses water table level, temperature profile in the soil, and the vertical distribution of decomposable organic matter in the soil. The organic matter decomposes anaerobically depending on, e.g., temperature and humidity (according to Wania (2007)), and produces CH_4. This CH_4 is transported to the atmosphere via possible bubbles, aerenchymatous plants and diffusion. The model also calculates diffusion of oxygen from the atmosphere into the soil through the plants and soil layers. Part of the diffused CH_4 and CH_4 bubbles get oxidized on the way up, depending on the available oxygen. As output, we get the CH_4 (and oxygen) fluxes separately for plant transport and diffusion.

REFERENCES

Forster P et al. 2007. Changes in atmospheric constituents and in radiative forcing, in *Climate Change 2007: The Physical Science Basis. Contribution of WG1to the Fourth Assesment Report of the IPCC*. Cambridge University Press, Cambridge, UK.

Kettunen A. 2003. Connecting methane fluxes to vegetation cover and water table fluctuations at microsite level: A modeling study. *Global Biogeochemical Cycles* Vol. 17(2), doi: 10.1029/2002GB001958.

Raddatz TJ, Reick CH, Knorr W, Kattge J, Roeckner E, Schnur R, Schnitzler KG, Wetzel P, Jungclaus J. 2007. Will the tropical land biosphere dominate the climate-carbon cycle feedback during the twenty-first century? *Climate Dynamics* 29(6): 565-574.

Rigby M, Prinn RG, Fraser PJ, Simmonds PG, Langenfelds RL, Huang J, Cunnold DM, Steele LP, Krummel PB, Weiss RF, O'Doherty S, Salameh PK, Wang HJ, Harth CM, Mühle J, Porter LW. 2008. Renewed growth of atmospheric methane. *Geophys. Res. Lett.* Vol 35 L22805, doi:10.1029/2008GL036037.

Rinne J, Riutta T, Pihlatie M, Aurela M, Haapanala S, Tuovinen J-P, Tuittila E-S, Vesala T. 2007. Annual cycle of methane emission from a boreal fen measured by the eddy covariance technique. *Tellus* 59B, 449-457.

Riutta T, Laine J, Aurela M, Rinne J, Vesala T, Laurila T, Haapanala S, Pihlatie M, Tuittila E-S. 2007. Spatial variation in plant community functions regulates carbon gas dynamics in a boreal fen ecosystem. *Tellus* 59B: 838-852.

Walter BP, Heimann M, Matthews E. 2001. Modeling modern methane emissions from natural wetlands 1. Model description and results. *J Geophys. Res.* Vol 106(D24), 34207-34219.

Wania R. 2007. Modelling northern peatland land surface processes, vegetation dynamics and methane emissions. PhD thesis, University of Bristol.

CARBON FLOW THROUGH AN OLD-GROWTH FOREST CATCHMENT INTO A LAKE IN SOUTHERN BOREAL ZONE IN FINLAND

T. RASILO[1], J. HUOTARI[2], A. OJALA[3] and J. PUMPANEN[1]

[1]Department of Forest Ecology, P.O. Box 27, FI-00014, University of Helsinki, Finland
[2]Lammi biological station, Pääjärventie 320, FI-16900 Lammi, University of Helsinki, Finland
[3]Department of Ecological and Environmental Sciences, Niemenkatu 73, FI-15140 Lahti, University of Helsinki, Finland

Keywords: Carbon flux, dissolved organic carbon (DOC), dissolved inorganic carbon (DIC), old-growth forest

INTRODUCTION

Studies from tropical and temperate regions (e.g. Richey *et al*,. 2002,. 2005, Billett *et al*,. 2004) have shown that for proper estimates of carbon sink/source role of ecosystems on landscape level the aquatic components cannot be ignored and besides organic carbon components, the pool of inorganic carbon must be included in studies. CO_2 which can escape from aquatic ecosystems to the atmosphere originates from the surrounding soils and wetlands, and from in-stream mineralization of organic carbon (Jones and Mulholland, 1998). Although dissolved organic matter (DOM) exported from terrestrial to aquatic ecosystems is partly refractory and becomes buried in sediments, a considerable part of it can be mineralised to CO_2 (Hanson *et al*., 2004, Kortelainen *et al*., 2004). However, traditionally streams and rivers are considered as systems exporting dissolved organic carbon (DOC). Thus, the release of carbon as DOC has been studied quite extensively, whereas inorganic carbon export and the release of carbon as dissolved CO_2 has often been ignored in studies. For example in boreal zone there are plenty of studies on the transport of organic carbon in streams and rivers (e.g. Hope *et al*., 1994), but the role of running waters in transfer of inorganic carbon has been neglected. Inorganic carbon in comparison with organic carbon is a highly dynamic variable (e.g. Hope *et al*., 2001, Striegl *et al*., 2005) and can originate from respiration in terrestrial soil.

Boreal forests contain large amounts of carbon both in living biomass and in soil (e.g. Kauppi *et al*. 1997). The amount of carbon leaching from forest ecosystems to surface water is also important (Kortelainen and Saukkonen, 1998). Seasonality of rainfall and snowmelt inputs determines the annual flow regime, whereas, within each season, short-term variations in transport along hydrologic pathways occur during storms (Burt and Arkell, 1986). The effect of a rain event can vary significantly depending on the state of catchment area before the rain. The magnitude of the hydrologic and chemical response is highly correlated with soil moisture status and rainfall intensity in the catchment. For example, water yield for a given storm size (magnitude and intensity) is greater when a catchment is wet than when it is dry (Moldan & Černý 1994).

The aim of this study is to quantify the carbon fluxes through a tree stand and soil into a lacustrine ecosystem. We will study the way of water through the catchment area of Valkea-Kotinen and to examine how the dissolved carbon is transported with water. Even though water has many ways through a catchment area, here we will concentrate to its way through canopy to the soil and to the lake and the brook. To have a holistic picture of carbon flow, we will also calculate inorganic carbon flux from photosynthesis to respiration of trees and soil, and amount of dissolved inorganic carbon (DIC) in soil water, lake and brook.

METHODS

DOC concentrations of various water compartments from Valkea-Kotinen catchment were analysed. The study site is situated in southern boreal zone in Finland (61°14' N, 25°04' E) and belongs to Evo nature

reserve area. It consists of a head-water lake Valkea-Kotinen (surface area 4.1 ha), small brook running out from it and the catchment area (30 ha). 79 % of the catchment area is natural state old-growth forest dominated by Norway spruce with some Scots pine, Birch and Aspen and the rest is covered by peatland. The dominant forest vegetation site types are mesic and rich heath forest. Also the riparian zone forest has a thick peat layer.

Water samples were analysed from precipitation, throughfall, soil water at 10 and 30 cm depth and ground water, the lake water and brook at a weekly interval. Precipitation and throughfall water were collected with 20 cm diameter funnels at 1.3 m heights. For precipitation three funnels were placed to an open fen and water was pooled for analysis. Throughfall gauges were placed systematically at three lines starting perpendicularly 2 m from the shore line, 4 gauges in each line at 3 m distance. The pooled throughfall of each was analysed. Soil waters were collected with suction cup lysimeters (model 653X01-B02M2; Soil moisture Corporation, California, USA). Lysimetres at 10 and 30 cm depth were installed in soil next to each other, three pairs at 2 m from shore line and three pairs at 12 m from the shore line. Groundwater samples were taken from perforated plastic tubes (20 mm in diameter) placed in soil. There were three lines and three tubes in every line, at 2 m, 7 m and 12 m from the shore line. A groundwater sample of 30 ml was taken carefully with a plastic tube and a syringe avoiding air bubbles and the samples were taken to the laboratory in ice. A sample of lake water was taken at pelagial (in the middle of the lake). The brook water sample was taken 10 m from the lake (2007) or at the beginning of the brook and at 50 m distances.

Water samples were transported to the laboratory in ice and analysed during 24 hours for pH and conductivity (except for groundwater and sometimes soil water because of too small, less than 80 ml, sample size). For DOC analysis samples were filtered (GF/C Whatman, Millex-HA 0.45 µm Millipore). If the DOC concentration were not analysed immediately, the filtered samples were frozen (-20 °C). The DOC concentration of water samples was analysed with total organic carbon analyser (TOC-5000A, Shimadzu Corporation, Australia).

Ground water and water form brook was analysed for DIC concentration. 30 ml of N_2 gas was added to 30 ml water sample taken with a syringe, and the syringe was shaken to ensure the equilibrium state between water and gas phase. CO_2 and CH_4 concentrations in gas phase were measured with gas chromatograph (6890N Agilent Technologies) and corresponding concentration in water was calculated.

Soil CO_2 flux was measured at weekly interval with a manual closed non-through flow chamber (height 0.24 m, diam. 0.19 m). The opaque chamber was equipped with CO_2 probe and temperature and RH sensors (GMP343, HM70, respectively, Vaisala Oyj, Finland) and for measurements it was placed on a collar for five minutes and CO_2 concentration and RH and temperature values were registered at 5 second intervals. Soil CO_2 flux was calculated using linear regression. There were all together 18 collars placed systematically in three lines running perpendicularly from the shore line.

Trees were measured from the study site in November 2008 and the biomass of different compartments was calculated with Marklund's function (1988). The biomass of ground vegetations was estimated based on twelve samples of 0.05 m^2 collected systematically at three lines in mid August 2008. Photosynthesis and respiration of the tree stand was modelled with Stand Photosynthesis Program (SPP) (Mäkelä et al. 2006). The model was parameterized with sites biomass values and weather data.

RESULTS

In the riparian zone of the catchment area of the lake Valkea-Kotinen, the density of standing trees was over 2000 stems (> 5 cm) per hectare and the average height was 11 m. 56 % of trees were Norway spruce, 28 % Scots pine and 16 % silver birch. The carbon storage of trunks is 25 kg C m^{-2}. In the foliage there is approximately 1.5 kg C m^{-2} and in branches 3.7 kg C m^{-2}. The carbon storage of ground vegetation is 134 g C m^{-2} and dwarf shrubs (bilberry, lingonberry) form 78 % of it. Carbon pool of the soil is big in

Valkea-Kotinen catchment area, because of large amount of peat. There is over 100 t of carbon per hectare in the soil (humus+0-20 cm) (Starr and Ukonmaanaho 2004).

Cumulative precipitation and runoff for year 2007 are presented in Fig 1. The canopy interception was approximately 25 % of precipitation and 422 mm of water reach the forest floor. The calculated annual transpiration of the catchment area was 239 mm.
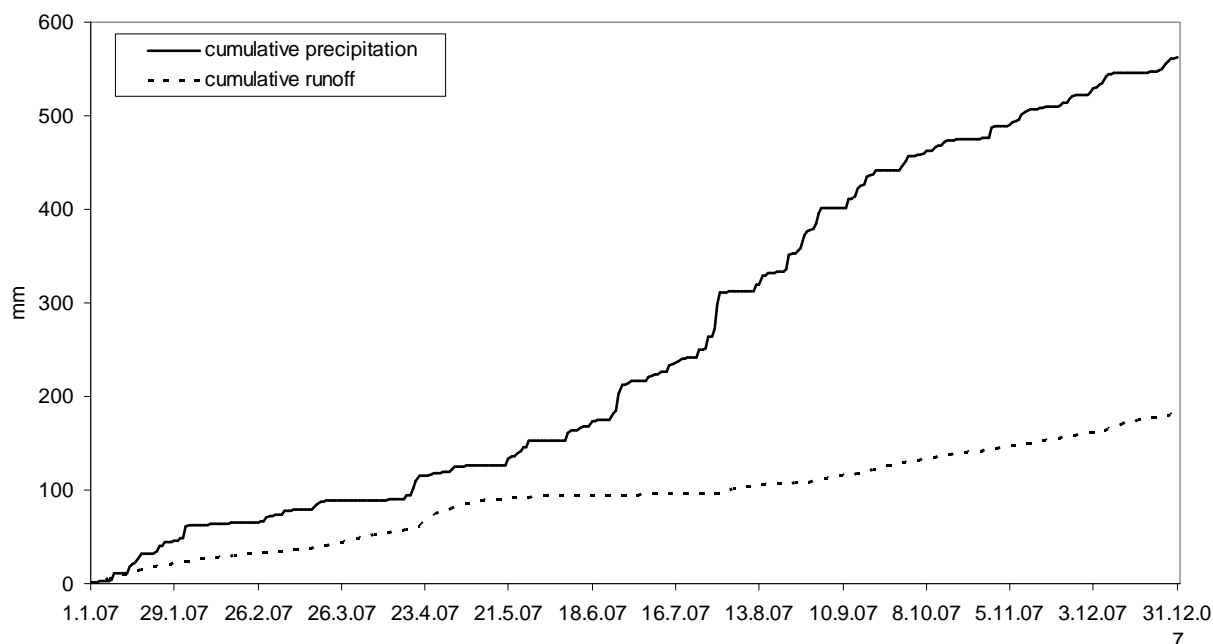
Figure 1. Cumulative precipitation (mm, solid line) and runoff (mm, dashed line) from Valkea-Kotinen catchment in Evo, Finland 2007. The precipitation is averaged from the measurements of Finnish meteorological institute in Iso-Evo, Lammi and Syrjäntaka, Padasjoki.

Dissolved organic carbon concentration from water samples of the study site are presented in table 1. DOC concentration of the lake water, groundwater and rainwater were more or less stable during the ice free period. DOC concentration of throughfall varied a lot. High concentrations followed dry periods, when dry deposition (e.g. pollen) was accumulating on branches. The influence of rain can be seen also in DOC concentrations of the brook. Heavy rains are flushing carbon from the soil to the brook. Concentration of DOC in soil water seems to increase during growing season.

	2007	2008	mean
Precipitation	3.2	3.0	3.1
Throughfall	14.5	20.4	17.5
Soil water 10 cm	107.9	98.3	103.4
Soil water 30 cm	121.5	84.0	104.1
Ground water	57.7	54.3	55.9
Lake	12.2	11.9	12.0
Brook	18.0	18.9	18.5

Table 1. Mean ice free period DOC concentration (mg C L^{-1}) of different water compartments at Valkea-Kotinen catchment, Evo, Finland for years 2007 and 2008 and the mean of them.

Photosynthesis turns inorganic carbon to organic form and respiration can return organic carbon in the biomass, soil and water back to inorganic form. There is a little amount of organic carbon coming to the study site with precipitation (Fig. 2), but photosynthesis is the main input of organic carbon. Rainwater is

leaching DOC from the canopy. Hence, the amount of DOC reaching forest floor is several times larger than DOC input of precipitation (Fig 2.). Soil gains carbon also through litterfall, root turnover and root exudates originating from photosynthesis. Soil respiration releases 1550 g C m^{-1} yearly and approximately half of it is autotrophic respiration by plant roots and half heterotrophic respiration on microbes decaying organic matter in the soil (Pumpanen et al. 2008).
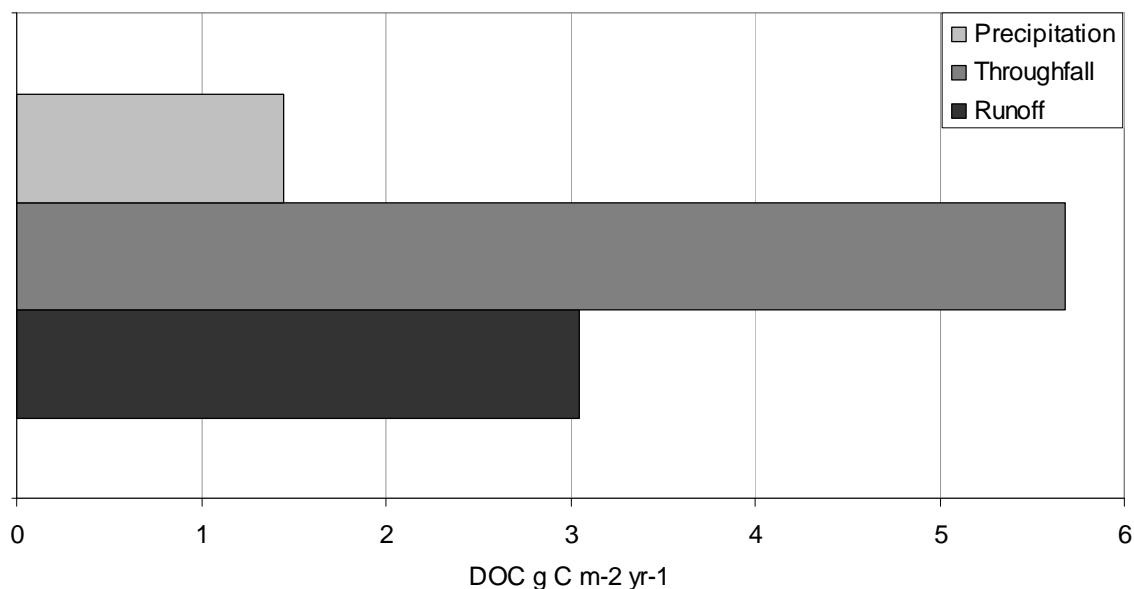
Figure 2. Annual (2007) amount of dissolved organic carbon (DOC) coming to the catchment area of Lake Valkea-Kotinen with precipitation, entering the forest floor in throughfall and running out from the catchment in the brook.

CONCLUSIONS

In the study of Starr and Ukonmaanaho (2004) the average throughfall TOC concentration ranged from 4.2 to 18.6 mg L^{-1}. In Valkea-Kotinen the mean throughfall TOC concentration was 16.3 mg L^{-1}, and bulk deposition 3.7 mg L^{-1}. These values as well values from temperate forests (Michalzik et al. 2001, review of 42 case studies) are in similar range as our values. When passing through the canopy the rainwater is dissolving slightly soluble and soluble organic acids both from the foliage and from dry deposition accumulated on the canopy surfaces (Thurman 1985). It seems also that Norway spruce canopy is more susceptible for carbon leaching than other species in boreal zone (Starr and Ukonmaanaho 2004). In our study as well as in the study of Starr and Ukonmaanaho (2004) carbon concentrations in throughfall are peaking during growing season and are lower in spring and in autumn.

As well as in our measurements, also Starr and Ukonmaanaho (2004) found out that the dissolved carbon concentrations were higher deeper in the soil than near the soil surface. This indicates the removal of carbon from soil solution as it moves downwards and may be due to microbial decay, coagulation and precipitation (Thurman et al. 1985, Riise et al. 2000). Local soil factors are more important in controlling soil solution TOC concentrations than climate factors (Starr and Ukonmaanaho 2004).

Final conclusions can not yet be drawn because the calculations are still under processing. In general boreal forests and forest soils forms important storages of carbon also globally and the carbon flux through them is considerable.

REFERENCES

Billett, M. F., S. M. Palmer, D. Hope, C. Deacon, R. Storeton-West, K.J. Hargreaves, C. Flechard and D. Fowler (2004). Linking land-atmosphere-stream carbon fluxes in a lowland peatland system. *Global Biogeochemical Cycles* 18, GB1024, doi:10.1029/2003GB002058.

Burt, T.P. and Arkell, B.P. (1986) Variable source areas of stream discharge and their relationship to point and non-point sources in nitrate *pollution.IAHS Pub!*. 157: 155-164.

Hanson. P. C., A.I. Pollard, D.L. Bade, K. Predick, S.R. Carpenter, and J.A. Foley (2004). A model of carbon evasion and sedimentation in temperate lakes. *Global Change Biology* 10: 1285-1298.

Hope, D, M.F. Billet and M.S. Cresser (1994). A review of the export of carbon in river water — fluxes and processes. *Environmental pollution* 81: 301–324.

Hope, D., S. M. Palmer, M.F. Billet. and J.C. Dawson (2001). Carbon dioxide and methane oxidation evasion from a temperate peatland stream. *Limnology and Oceanography* 46: 847-857.

Jones, J. B. and P.J. Mulholland (1998). Carbon dioxide variation in a hardwood forest stream: an integrative measure of whole catchment soil respiration. *Ecosystems* 1: 183-196.

Kauppi, P., Posch, M., Hänninen, P., Henttonen, H.M., Ihalainen, A., Lappalainen, E., Starr, M., Tamminen, P. (1997). Carbon reservoirs in peatlands and forests in the boreal regions of Finland. *Silva Fenn.* 31:13-25.

Kortelainen, P., Saukkonen, S. (1998). Leaching of nutrients organic carbon and iron from Finnish forestry land. *Water, Air, Soil Pollut.* 105:239-250.

Kortelainen, P., H. Pajunen, M. Rantakari, and M. Saarnisto (2004). A large carbon pool and small sink in boreal Holocene lake sediments. *Global Change Biology* 10: 1648-1653.

Marklund, L.G. (1988). Biomassafunktioner för tall, gran och björk i Sverige. Summary: Biomass functions for pine, spruce and birch in Sweden, Swedish Univ.Agric.Sci., *Dept.For.Survey*, Report 45.

Michalzik, B., Kalbitz, K., Park, J.-H., Solinger, S., Matzner, E. (2001). Fluxes and concentrations of dissolved organic carbon and nitrogen - Asynthesis for temeprature forests. *Biogeochemistry* 52:173-205.

Moldan & J. Cerný. (Editors) (1994). Biogeochemistry of Small Catchments A –Tool for Environmental Research. B. Scientific Committee On Problems of the Environment (SCOPE) SCOPE 51. Wiley.

Mäkelä A., Kolari P., Karimäki J., Nikinmaa E., Perämäki M. and Hari P. (2006). Modelling five years of weather-driven variation of GPP in a boreal forest. *Agriculture and Forest Meteorology.* 139: 382-398.

Pumpanen J., Ilvesniemi H., Kulmala L., Siivola E., Laakso H., Helenelund C., Laakso M., Uusimaa M., Iisakkala P., Räisänen J. and Hari P. (2008). Respiration in boreal forest soil as determined from carbon dioxide concentration profile. Soil Science Society of America Journal. 72(5): 1187-1196.

Richey, J. E., J.M. Melack, A.K. Aufdenkampe, V.M. Ballester and L.L. Hess (2002). Outgassing from Amazonian rivers and wetlands as a large tropical source of atmospheric CO_2. *Nature* 416: 617-620.

Riise, G., Van Hees, P.A.W., Lundström, U.S., Strand, L.T. (2000). Mobility of different size fractions of organic carbon, Al, Fe Mn and Si in podzol. *Geoderma* 94:237-247.

Starr, M., Ukonmaanaho, L. (2004). Levels and characteristics of TOC in throughfall, forest floor leachate and soil solution in undisturbed boreal forest ecosystems. *Water, Air, Soil Poll:Focus*. 4:715-729.

Striegl, R. G., G.R. Aiken, M.M. Dornblaser, P.A. Raymond and K.P. Wickland (2005). A decrease in discharge-normalized DOC export by the Yukon River during summer through autumn. *Geophysical Research Letters* 32, L21413, doi:10.1029/2005GL024413.

Thurman, E.M. (1985). Organic chemistry of Natural Waters. Nijhoff/Dr. W. junk Publishers, Dordrecht, The Neatherlands.

INTEGRATED MEASUREMENTS OF BRANCH AND CANOPY SCALE BVOC EMISSIONS FROM SCOTS PINE FOREST AND ATMOSPHERIC BVOC CONCENTRATIONS

J. RINNE[1], T.M. RUUSKANEN[1], R. TAIPALE[1], M. K. KAJOS[1], J. PATOKOSKI[1], P. KOLARI[2], J. BÄCK[2] and P. HARI[2]

[1]Department of Physics, P.O. Box 68, FI-00014, University of Helsinki, Finland

[2]Department of Forest Ecology, University of Helsinki, Finland

Keywords: biogenic VOCs, eddy covariance, chamber, Scots pine

INTRODUCTION

Biogenic volatile organic compound (BVOC) emissions from vegetation can be determined using various techniques in different spatial and temporal scales. Reconciling the results of the measurements conducted using different techniques is not always straightforward. At SMEAR II station in Hyytiälä integrated measurements of branch and ecosystem scale BVOC emissions and their atmospheric concentrations have been conducted using an automated system. A four-day period of measurements is presented in this paper. We will introduce and compare simultaneously-measured 1) emissions from a Scots pine shoot, 2) above-canopy fluxes and 3) ambient volume mixing-ratios below, within and above the canopy in the Scots-pine-dominated forest for two VOCs, monoterpenes and methanol.

METHODS

The measurements were carried out at the SMEAR II measurement station (Station for Measuring Forest Ecosystem-Atmosphere Relations (Hari & Kulmala, 2005) at Hyytiälä in southern Finland (61°51´N, 24°17´E, 180 m above sea level). The Scots pine dominated forest at the SMEAR II site was sown in 1962 after a controlled burning and during these studies the height of the trees was about 16 m. Chamber measurements of VOC emissions with automated chambers were conducted at the top of the crown of the trees to minimize shading effects (Ruuskanen et al., 2005). The ecosystem scale emissions were measured using disjuct eddy covariance technique (Rinne et al., 2007). The chamber, disjunct eddy covariance, and ambient concentration measurements were conducted subsequently one hour at time during a three hour measurement cycle. In all measurements VOCs were analysed by on-line proton transfer reaction – mass spectrometer (PTR-MS) with regular calibrations and background checks (Taipale et al., 2008). The chamber measurements of a Scots pine shoot were up-scaled to canopy-scale by assuming that all emissions originated from the needles and that the needle mass per ground area ratio was 540 g_{dw} m^{-2}.

RESULTS & CONCLUSIONS

The monoterpene emissions from the shoot exhibited a clear diurnal pattern with daily maximum in the afternoon (Figure 1). The DEC method is based on turbulent transport of the emissions, and measurement become unreliable at night when turbulent mixing is weak; the typical diurnal emission pattern is thus less distinct for the above-canopy fluxes than for the branch scale measurements. The diurnal afternoon emission maximum is typical for Scots pine, and is related to the variation of temperature and possibly light (e.g. Janson, 1993; Tarvainen et al., 2005; Hakola et al., 2006; Ghirardo et al., 2009). The majority of the Scots pine monoterpene emissions have been assumed to originate from evaporating storage pools in mature needles. However it seems likely that a significant part of the monoterpene emissions have been

observed to depend on irradiation (Shao et al., 2001; Ghirardo et al., 2009). However, separating the influences of irradiation and temperature on emissions is problematic in field measurements. That was also the case, during the four-day period when the air temperature clearly followed the solar radiation measured as the photosynthetic photon flux density.

The monoterpene emission rates measured with the DEC method above the canopy and by the automated online chamber method were between 10 and 270 $\mu g \ m^{-2} \ h^{-1}$ and between -30 and 360 $\mu g \ m^{-2} \ h^{-1}$, respectively.

The ambient air volume mixing-ratios are affected by the emission rate, loss due to photochemistry and dilution by turbulent mixing. The ambient monoterpene volume mixing-ratio median was 0.2 ppbv during these four days. High momentary peaks in the monoterpene mixing-ratio are seen in Figure 1. Night-time maximum is typical for the diurnal pattern of the summer-time monoterpene volume mixing-ratio in a conifer boreal forest, due to emissions from storage pools during night and low turbulent mixing at this time.

Methanol emissions between 10 and 200 $\mu g \ m^{-2} \ h^{-1}$ were determined from canopy-scale measurements with the DEC and automated online chamber method (Figure 2). The methanol emissions from shoot-level and above-canopy measurements showed a clear diurnal pattern following that of solar radiation and evapo-transpiration. The lowest emissions were measured by night and the highest before noon.

The methanol volume mixing-ratio was between 0.4 and 5 ppbv during the four-day measurement period. The diurnal cycle of the methanol volume mixing-ratio, with afternoon maximum, can be explained by the emission pattern of methanol. Although the monoterpene emissions peak only a few hours later, their mixing-ratio is highest at night-time. The differences are mainly due to the different emission processes leading to different diurnal patterns: methanol emissions are both light and temperature-controlled, and emissions diminish at sunset, while part of the monoterpene emission is governed solely by temperature, and continue through the night. The methanol and monoterpene emissions were of the same order of magnitude. However, the ambient volume mixing-ratios of methanol were almost an order of magnitude larger than those of the monoterpenes. This is due to their different atmospheric lifetimes of these compounds. Many monoterpenes are oxidized in less than an hour; the lifetime of methanol, however, is several days.

Integrated measurements of BVOC emissions in different scales and their atmospheric concentrations can be very useful in studies of the effect of biosphere on atmospheric chemistry. In order to fully exploit the data numerical models of boundary layer chemistry and mixing will be used to quantitatively interpret the data.
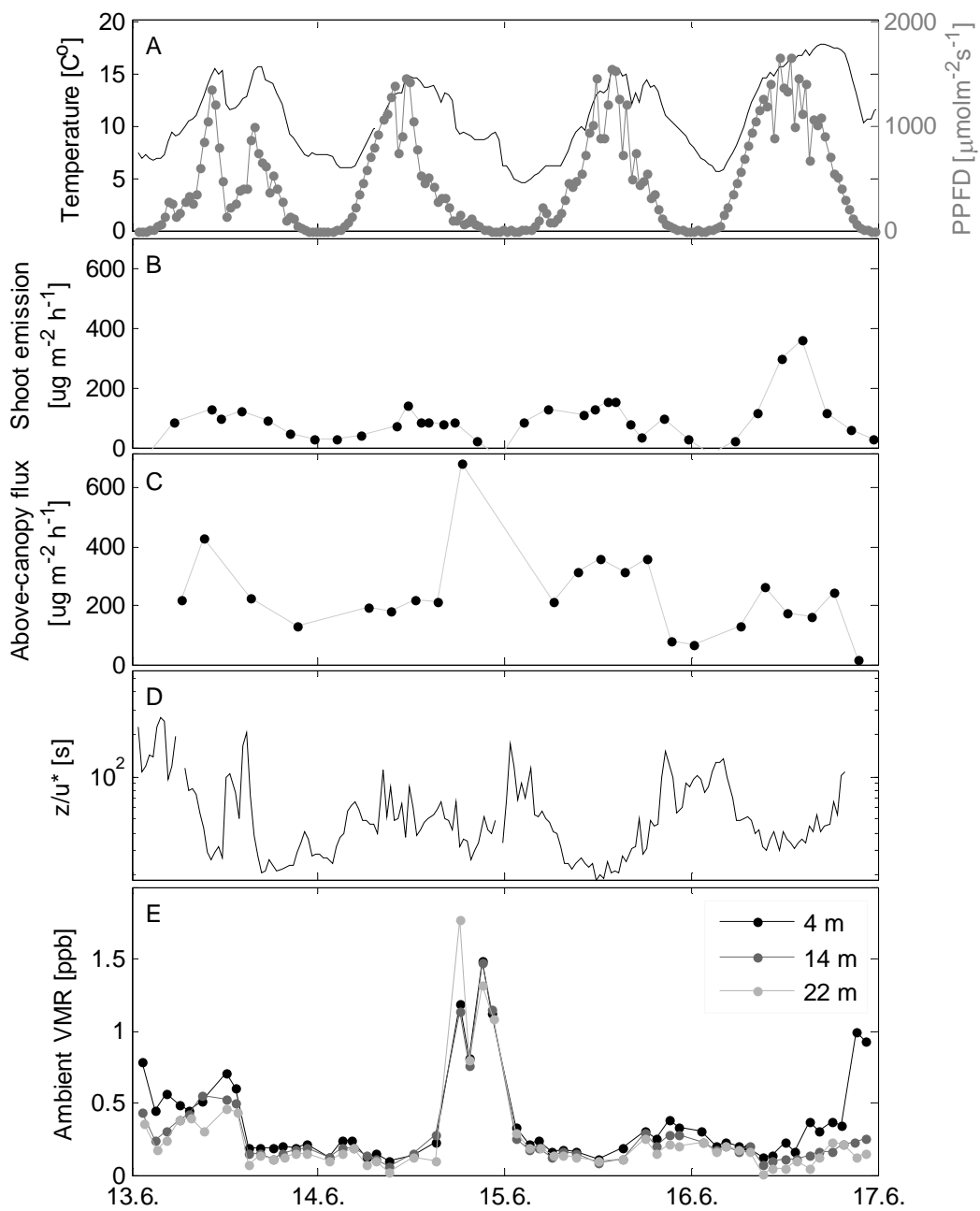
Figure 1. Results of online monoterpene measurements at SMEAR II from summer 2007. A) air temperature and photosynthetic photon flux density (PPFD), B), monoterpene emission measured from a shoot in an automated online chamber and up-scaled to canopy level using a biomass of 540 $g_{dw}m^{-2}$, C) monoterpene flux above the canopy determined with the DEC method, D) turbulent mixing time-scale at above-canopy height z=22 m (t = z/u*), and E) monoterpene volume mixing-ration in ambient air at three heights.

Figure 2. Results of online methanol measurements at SMEAR II from summer 2007. A) air temperature and photosynthetic photon flux density (PPFD), B), shoot water flux, from evaporation and transpiration in the automated online chamber C) methanol emission measured from a shoot in the automated online chamber and up-scaled to canopy level using a biomass of 540 $g_{dw}m^{-2}$, D) methanol flux above the canopy determined with the DEC method, and E) methanol volume mixing-ratio in ambient air at three heights.

REFERENCES

Ghirardo, A., K. Koch, J.-P. Schnitzler & J. Rinne, 2009: 13CO2 feeding experiment of four common European boreal tree species: 13C incorporation into monoterpenes. 4th International Conference on Proton Transfer Reaction Mass Spectrometry and its applications - Contributions. February 16th – 21st, 2009, Obergurgl, Austria. Conference Series, Innsbruck University Press. 219-220.

Hakola, H., Tarvainen, V., Bäck, J., Ranta, H., Bonn, B., Rinne, J., & Kulmala, M., 2006b: Seasonal variation of mono- and sesquiterpene emission rates of Scots pine. Biogeosci., 3, 93-101.

Hari P. and Kulmala M. 2005. Station for Measuring Ecosystem–Atmosphere Relations (SMEAR II). Boreal Env. Res. 10, 315–322.

Janson, R., 1993: Monoterpene emissions from Scots pine and Norwegian spruce. J. Geophys. Res., 98, 2839-2850.

Rinne, J., Taipale, R., Markkanen, T., Ruuskanen, T.M., Hellén, H., Kajos, M.K., Vesala T., & Kulmala, M., 2007: Hydrocarbon fluxes above a Scots pine forest canopy: measurements and modeling. Atmos. Chem. Phys., 7, 3361-3372.

Ruuskanen, T.M., Kolari, P., Bäck, J., Kulmala, M., Rinne, J., Hakola, H., Taipale, R., Raivonen, M., Altimir, N., & Hari, P., 2005: On-line field measurements of monoterpene emissions from Scots pine by proton transfer reaction - mass spectrometry. Boreal Environ. Res., 10, 553–567.

Shao, M., Czapiewski, K.V., Heiden, A.C., Kobel, K., Komenda, M., Koppman, R., & Wildt, J., 2001: Volatile organic compound emissions from Scots pine: Mechanisms and description by algorithms. J. Geophys. Res., 106, 20483-20491.

Taipale, R., Ruuskanen, T.M., Rinne, J., Kajos, M.K., Hakola, H., Pohja, T., & Kulmala, M., 2008: Technical Note: Quantitative long-term measurements of VOC concentrations by PTR-MS – measurement, calibration, and volume mixing ratio calculation methods. Atmos. Chem. Phys., 8, 6681-6698.

Tarvainen, V., Hakola, H., Hellén, H., Bäck, J., Hari, P., & Kulmala, M., 2005: Temperature and light dependence of the VOC emissions of Scots pine. Atmos. Chem. Phys., 5, 989-998.

ANALYSIS OF THE EFFECT OF BIOMASS BURNING SMOKE EPISODES ON ATMOSPHERIC COMPOSITION IN FINLAND IN 2006

L. RIUTTANEN[1], M. DAL MASO[1], G. DE LEEUW[1,2], I. RIIPINEN[1], L. SOGACHEVA[2], V. VAKKARI[1] and M. KULMALA[1]

[1] Department of Physics, University of Helsinki, Finland
[2] Finnish Meteorological Institute, Finland

Keywords: biomass burning emissions, trace gases, atmospheric aerosols

INTRODUCTION

There were exceptionally extensive wild fires in Eastern Europe and Russia in spring and summer 2006. Smoke was transported thousands of kilometres, and unusually high air pollution levels were measured even in Spitsbergen (Stohl et al., 2006) and the United Kingdom (Witham and Manning, 2006). Smoke episodes were recorded also in all parts of Finland in April–May and in Southern Finland in August 2006.

Continuous measurements are run at three atmospheric measurement stations (SMEAR, Station for Measuring Forest Ecosystem – Atmosphere Relations) in Finland: SMEAR II is a remote background station in Hyytiälä, Southern Finland, SMEAR III is an urban background station in Helsinki, Southern shore of Finland, and SMEAR I is a remote background station in Värriö, Lapland.

MATERIALS AND METHODS

MODIS Terra thermal anomalies MOD14A1.5 data was used together with HYSPLIT 4 trajectories. For hourly four-days-backward trajectories we studied if the air arriving to the station had been over active fires, how long it had been over fire areas and when it had last been over an active fire. The inaccuracy of the trajectories was expected to be ten percent of the travelling distance (Draxler and Hess, 1998).

Figure 1 represents a backward trajectory that arrived to Hyytiälä on 2 May 2006 at 18 local time. There were several active fires (red points) during the path of the trajectory.

Trace gas concentration and particle number size distribution data from the SMEAR stations were used to define the characteristics of the smoke. Trace gases were measured from a tower, 67 meters above the ground.

RESULTS

The episodes were defined based on the trajectories, as described in the previous chapter. The spring episode lasted almost continuously from 25 April to 7 May. A spring reference period was selected to be 12 days before and after the smoke period. During August there were several shorter episodes at the two southern stations.

Trace gas and particle concentrations were highly elevated especially during the spring episode. Distributions of the gas concentration data during the spring and summer episodes and the reference
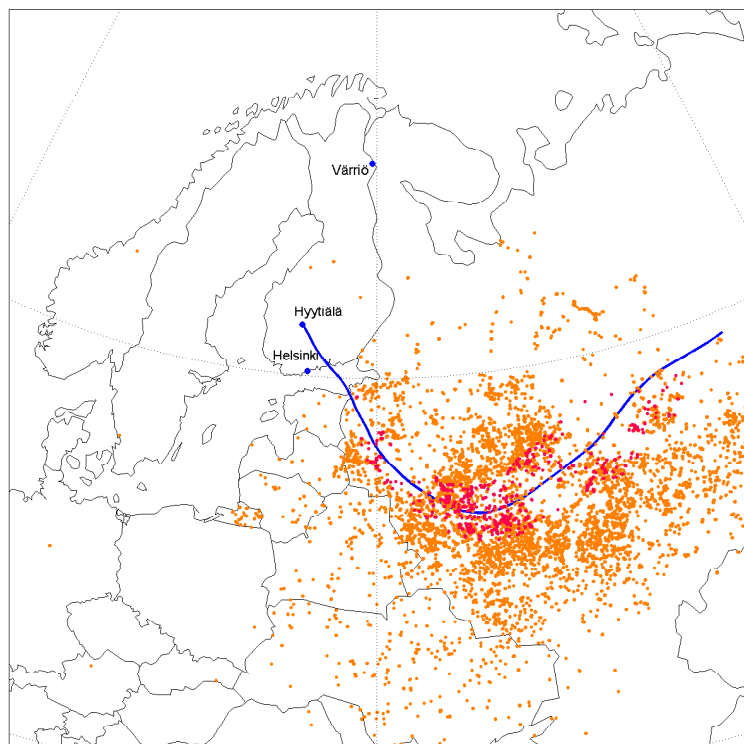
Figure 1: MODIS fire detections and a four-days-backward trajectory arriving to Hyytiälä on 2 May 2006 at 18 local time. Active fire pixels during the four-days-backward trajectory are marked with orange and fire pixels that were active when the trajectory was above them are marked with red colour.

period are presented in figure 2. Concentrations in Hyytiälä are generally much lower in summer than in spring (Lyubovtseva et al., 2005).

Particle mean number and size during the spring 2006 smoke episode and the reference period are presented in table 1. There were more particles during the smoke episode and they were significantly larger at all of the three stations.

Positive correlations were found between time air had been over fires along a trajectory (fire sum) and NO_x, SO_2, CO_2 and CO concentrations (table 2). There were negative correlations for time air last was over an active fire (back time) and these gases. There are many other sources of these gases in Eastern Europe, but according to these data, we can confirm, that we measured these gases because of wild fires.

During the spring smoke episode in Hyytiälä we noticed 20 exceptionally high particle concentration plumes, lasting from half an hour to some hours. Plume times were defined from the particle number size distribution data. Trace gas concentrations were quite similar during the plumes than during the smoke period in general. However, there were 20% more NO, NO_x and SO_2 than during the spring smoke episode on average. SO_2 concentration was even seven times higher than during the reference period. During the plumes, wind was always from the sector of 114–152 degrees, which means from the South-East. According to the MODIS fire detections and HYSPLIT trajectories, we conclude that these plumes came from certain very extensive fires at the Eastern shore of the
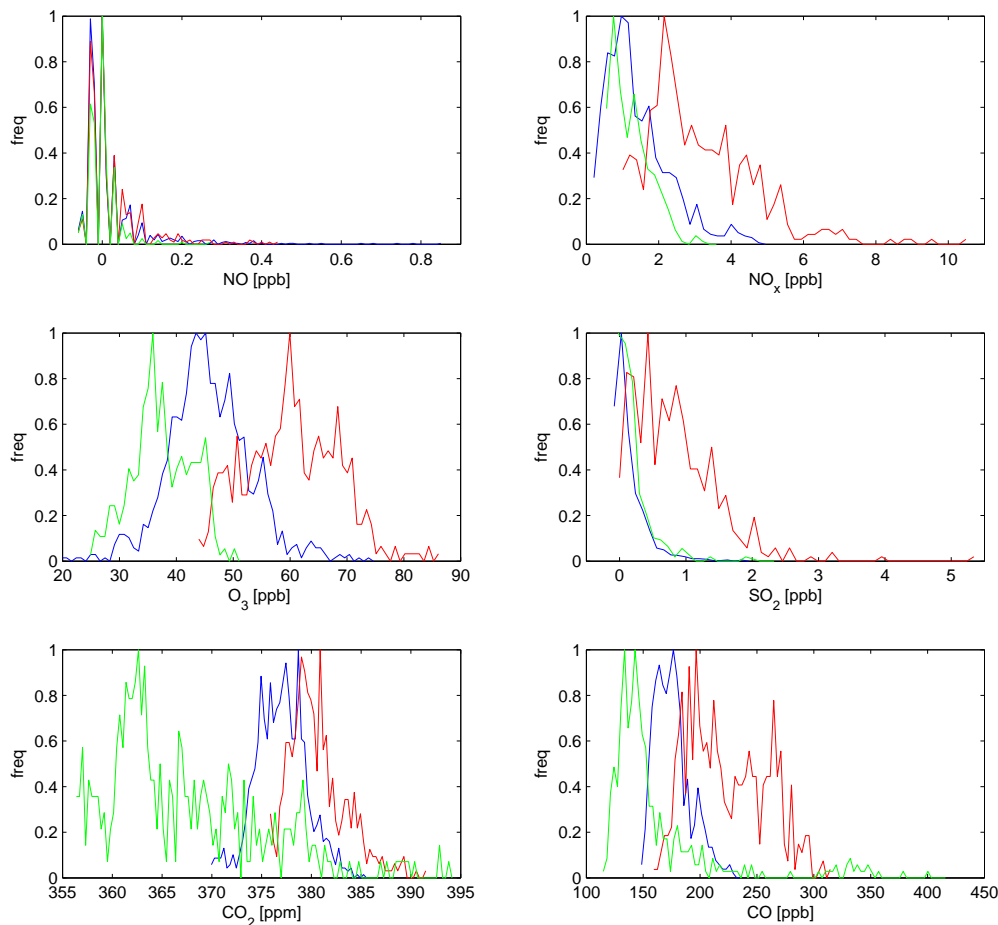
Figure 2: Frequency distributions of trace gas concentrations in Hyytiälä. Red represents spring smoke episodes, blue the reference period and green summer smoke episodes.

Gulf of Finland, less than 300 kilometres from Hyytiälä.

Particle number size distributions for Hyytiälä, Helsinki and Värriö, and particle volume distribution for Hyytiälä are presented in figure 3. Differences between reference and smoke periods are obvious. There were more particles in the air and they were significantly larger. The summer smoke episodes were not that extensive than the spring episode, but the shape of particle number size distribution is similar.

A very similar shape of the smoke size distribution was seen at all of the three stations. The distribution peaked between 0.1 and 0.2 μm. The peak was narrowest in Helsinki, broader in Hyytiälä and broadest in Värriö. The relative amount of particles smaller than 50 nm was the biggest in Helsinki, second biggest in Hyytiälä and the smallest in Värriö. The relative amount of particles smaller than 10 nm was the largest in Helsinki, smaller in Hyytiälä and minor in Värriö.

During the very extensive plumes in Hyytiälä, as described earlier, the particle number size distribution revealed a very interesting pattern. There were two clear peaks: a nucleation mode (close to the Aitken mode size range) at around $2 \cdot 10^{-8}$ m and 3500 particles cm^{-3} and an accumulation mode close to $2 \cdot 10^{-7}$ m and 5700 particles cm^{-3}. The larger peak was almost the same as the

Table 1: Particle concentration and size at the three stations in spring and summer 2006.

	Spring episode	Spring reference	Ratio
Hyytiälä			
Ntot [cm$^-$3]	4748	3403	1.40
NmedianDp [μm]	0.1129	0.0525	2.15
Helsinki			
Ntot [cm$^-$3]	15870	13544	1.17
NmedianDp [μm]	0.0604	0.0313	1.93
Värriö			
Ntot [cm$^-$3]	2081	805	2.59
NmedianDp [μm]	0.1128	0.0748	1.51

Table 2: Correlations for fire parameters and trace gases in Hyytiälä in spring 2006.

	fire sum	back time
NO_x [ppb]	0.37	-0.30
SO_2 [ppb]	0.40	-0.48
CO_2 [ppm]	0.45	-0.40
CO [ppb]	0.41	-0.30

peak during the smoke hours and the smaller peak was a new one. We concluded that the smaller mode came from the fires only some hundreds of kilometres from the station and the larger mode consisted of old fire particle on the background, that had travelled many hundreds to thousands of kilometres to the station.

According to the number size distribution data we can confirm, that we measured the same smoke at all of the three stations. The air travelled from South to North and small particles grew to bigger sizes. Particles were removed from the air during its path.

No new particle formation events were seen during the smoke days. However, in Helsinki the number of particles smaller than 5 nm was large.

CONCLUSIONS

Trace gas concentrations and particle size distributions were studied at three atmospheric measurement stations in Finland in 2006. MODIS Terra thermal anomalies data was used together with HYSPLIT 4 trajectories to identify smoke episodes at the stations. Spring smoke episode was compared to a reference period.

High NO_x, SO_2, CO_2 and CO concentrations were measured due to biomass burning smoke emissions from Eastern Europe and Russia in 2006. Atmospheric particle concentrations were elevated and the smoke particles had a median size of (100 ± 10) nm. There was a suppression of small particles.

ACKNOWLEDGMENTS
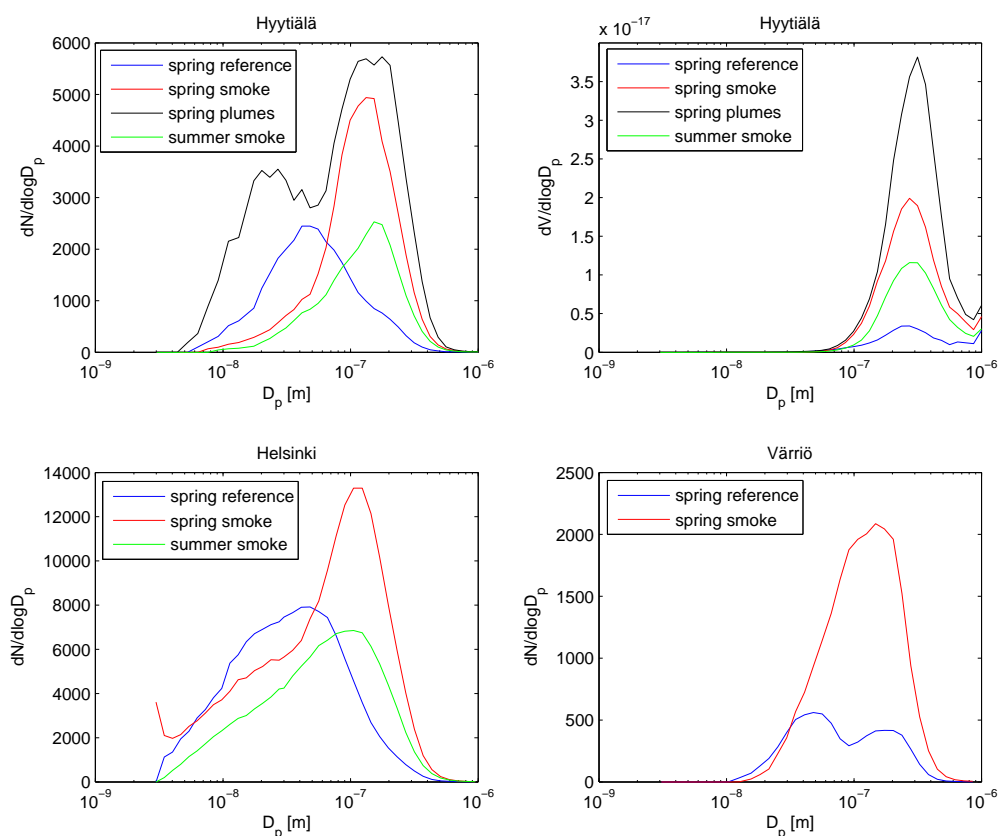
Figure 3: Particle size distributions at the three stations and particle volume distribution in Hyytiälä. Red represents spring smoke episodes, blue the reference period and green summer smoke episodes. Black represents the most intensive plumes during the spring smoke episode.

REFERENCES

Draxler, H. H. and Hess, G. D. (1998). An Overview of the HYSPLIT 4 Modelling System for Trajectories, Dispersion and Deposition. *Austr. Met. Mag.*, 47:295–308.

Lyubovtseva, Y. S., Sogacheva, L., Dal Maso, M., Bonn, B., Keronen, P. and Kulmala, M. (2005). Seasonal variations of trace gases, meteorological parameters, and formation of aerosols in boreal forest. *Boreal. Env. Res.*, 10:493–510.

Stohl, A., Berg, T., Burkhart, J. F., Fjæraa, A. M., Forster, C., Herber, A., Hov, Ø., Lunder, C., McMillan, W. W., Oltmans, S., Shiobara, M., Simpson, D., Solberg, S., Stebel, K., Ström, J., Tørseth, K., Treffeisen, R., Virkkunen, K. and Yttri, K. E. (2006). Arctic smoke - record high air pollution levels in the European Arctic due to agricultural fires in Eastern Europe in spring 2006. *Atmos. Chem. Phys.*, 7:511–534.

Witham, C. and Manning, A. (2006). Impacts of Russian biomass burning on UK air quality. *Atmos. Env.*, 41:8075–8090.

EFFECT OF DROPLET NUMBER CONCENTRATION ON THE RADIATIVE FOG

S. ROMAKKANIEMI[1], A. LAAKSONEN[1,2], and B. STEVENS[3]

[1] University of Kuopio, Department of Physics, P.O.Box 1627 Kuopio, Finland
[2]Finnish Meteorological Institute, Research and Development, P.O. Box 503, 00101 Helsinki, Finland.
[3]Max Planck Institute for Meteorology, Bundesstrasse 53, 20146 Hamburg, Germany

Keywords: Aerosol, cloud, fog, large eddy model

INTRODUCTION

The role of aerosol-cloud interactions on Earth's radiative balance is recognised to be substantial, but still poorly constrained on its many aspects. This is due to very complicated interactions between aerosol particles, cloud droplets, and cloud systems both on microphysical and meteorological levels. Beyond clouds, aerosol particles will also affect the formation and dissipation of fogs. In the previous studies it has been shown that increase in the number concentration of fog droplets will make fogs denser and delay their evaporation in the morning (Bott et al. 1990, Bott 1993). Although it can be expected that the role of fogs on atmospheric radiative balance is smaller than the role of clouds, there are many other reasons like heterophase chemistry, interactions between fog and vegetation, traffic safety and aviation to study fogs (Gultepe et al. 2007).

One of the most studied types of fog is the radiative fog, which is formed during clear sky nights when air above ground is cooled after sunset. Strong inversion in the potential temperature profile can be observed soon after sunset, and the actual formation time of fog is dependent on the properties of gas phase moisture content, aerosols and land surface (Bott et al. 1990, Bott 1993). During the night radiative fog will develop and increase in height due to the radiative heat loss from the top of fog layer. Surface is no longer cooled substantially as fog layer above it will absorb the longwave radiation. After sunrise shortwave radiation warms the surface and droplets, and this will cause more turbulence leading to evaporation fog. The altitude fog reaches before evaporation is dependent both on the aerosol and surface properties (Bott et al. 1990, Bott 1993).

MODEL

Radiative fogs have been previously studied with many modeling setups, but as far as we know this is the first time to use Large Eddy Model (LEM) in this kind of study. In this study we use previously developed LEM code UCLALES, which has been modified to take account surface heat and moisture budget Stevens 2004, Stevens and Seifert 2008, Acs et al. 1991). Model uses delta four stream code to calculate radiative transport in the atmosphere (including clouds) and cloud microphysics is calculated with a two moment scheme (Fu and Liou 1993, Seifert and Beheng 2001). In the simulations model is used with 1.5m vertical resolution for the lowest 50 meters, stretching by 1.05 above that for each grid level. Horizontal grid is 40m by 40m, with the total number of grid points being 26x26x110. Surface albedo has been set to 0.1, and initially both potential temperature and total water content profiles are set to the constant (283 K, and 5.8 g/kg, respectively) from surface up to 450 meters where temperature inversion is set. Model is run for 30 hours in order to study fog formation and evaporation.

In the following we show an example of radiative fog formed in October at the latitude of 45 degrees north. With these values the sunset is around 5:30 pm and sunrise at 6:30 am. We start our simulation before sunset, and in our case fog is formed after midnight, when surface temperature has dropped approximately to 275 Kelvins. Results from the simulation can be seen in Figure 1 where liquid water content (LWC) is presented as a function of time and altitude. As expected, fog is first formed few meters above ground, reaching ground during the first hour. In the current study we are studying only the effect of increased fog droplet number concentration, and neglect the effect of aerosol particles on radiative transport, and thus there is no difference on the formation time of radiative fog between different cases. As can be seen from the Figure 1 LWC is higher with higher droplet concentration. This is simply due to the smaller mean size and less efficient gravitational settling of fog droplets.
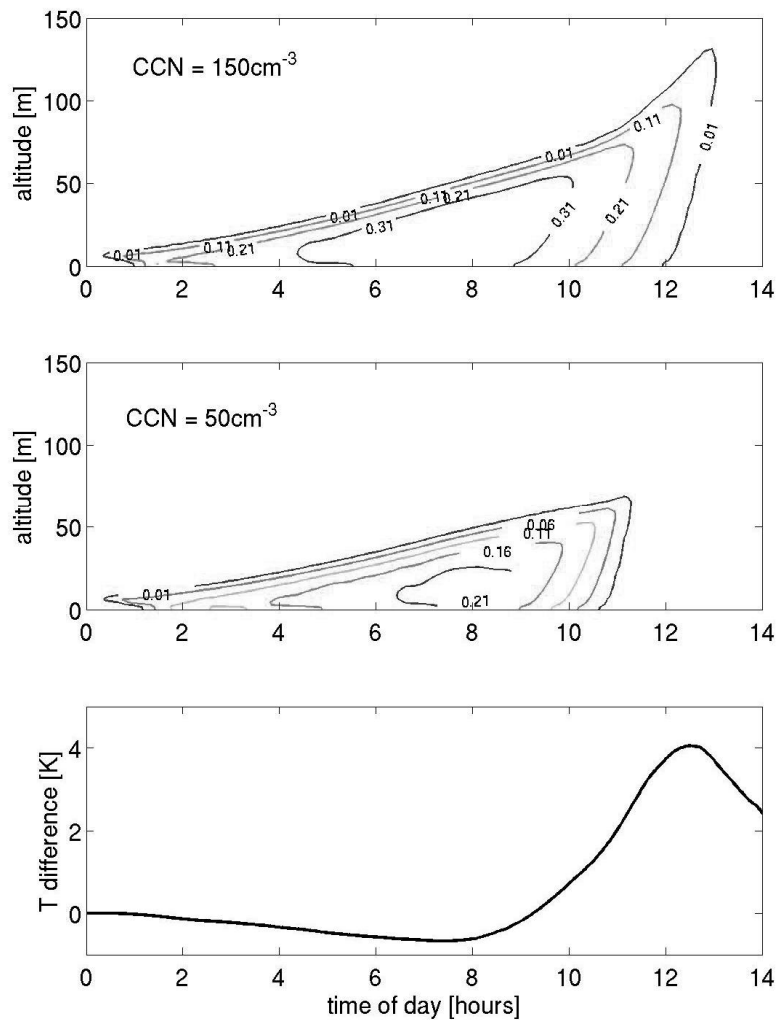
Figure 1. Liquid water content in radiative fog simulations having fog droplet number concentrations of 50 cm^{-3} (middle panel) and 150 cm^{-3} (upper panel). In the figure liquid water content is presented as a function of time and altitude. In the lowest panel we show the surface temperature difference between two cases so that during the day 50 particle case is warmer

Higher droplet number concentration affects the radiative properties of fog. During night land surface is cooler in the 50 droplet case, but the difference is not substantial. The largest difference can be seen after the sunrise. In the 150 droplet case fog is optically thicker, and more shortwave radiation is reflected back to the space. This will reduce surface heating compared to the 50 droplet case, and consequently increase fog lifetime. In the example presented lifetime is increased by two hours. Due to the increased lifetime, droplet concentration, and LWC, the average (taken for day) albedo increases from 0.15 in the 50 droplet case to 0.2 in the 150 droplet case. Correspondingly, the mean short wave radiation flux to surface during daylight is decreased from $232W/m^2$ to $191W/m^2$ during the one day simulation. This can naturally be seen in the surface temperature, which is shown as a difference between two cases in the lowest panel of Figure 1.

CONCLUSIONS

As can be seen, depression in the surface heating due to the increased fog droplet number concentration can lead to prolonged lifetime of radiate fog. Thus our results are in the agreement with the results previously published by Bott and coworkers using 1-D model (Bott et al. 1990, Bott 1993). However, at the moment our study takes only account the effect of fog droplet concentration, and do not include radiative properties of aerosols. Depending on the aerosol properties it can be expected that surface heating in the morning is delayed as aerosol particles scatter and absorb radiation. However, at the same time evaporation of fog might start from the top as fog is heated more efficiently. To study the total effect both on fogs and low level stratus clouds is the topic our future work.

REFERENCES

Bott, A., U. Sievers, and Zdunkowski W., (1990) A radiation fog model with a detailed treatment of the interaction between radiative transfer and fog microphysics. *J. Atmos. Sci.*, **47**, 2153-2166.

Bott, A., On the influence of the physico-chemical properties of aerosols on the life cycle of radiation fogs. *Boundary layer Met.* **56**, 1-31,

Gultepe, I.; Tardif, R.; Michaelides, S. C.; Cermak, J.; Bott, A.; Bendix, J.; Müller, M. D.; Pagowski, M.; Hansen, B.; Ellrod, G.; Jacobs, W.; Toth, G.; Cober, S. G. (2007) Fog Research: A Review of Past Achievements and Future Perspectives. *Pure appl geophys*, **164**, 1121.1159

Stevens, B., C.-H. Moeng, A.S. Ackerman, C.S. Bretherton, A. Chlond, S. de Roode, J. Edwards, J.-C. Golaz, H. Jiang, M. Khairoutdinov, M.P. Kirkpatrick, D.C. Lewellen, A. Lock, F. Müller, D.E. Stevens, E. Whelan, and P. Zhu, (2005): Evaluation of large-eddy simulations via observations of nocturnal marine stratocumulus. *M. Weather Rev.*, **133**, 1443-1462

Stevens B. and A. Seifert, (2008) Understanding macrophysical outcomes of microphysical choices in simulations of shallow cumulus convection, *J. Met. Soc. Japan*, **86A**, 143−162

Acs, F. T. Mihailovic, and B. Rajkovic (1991) A Coupled soil moisture and surface temperature prediction model, *J. Appl. Meteo.,* **30**, 812-822, (1991)

Fu, Q., and K.-N. Liou (1993). Parameterization of the radiative properties of cirrus clouds, J. Atmos. Sci., **50**, 2008–2025. (1993)

Seifert A., and K. D. Beheng. (2001) A double-moment parameterization for simulating autoconversion, accretion and selfcollection, *Atmos. Res.*, 59-60, 265—281

DETERMINATION OF *D*-MANNOSE AND LEVOGLUSAN AS MARKER COMPOUNDS IN AEROSOL PARTICLES BY GAS CHROMATOGRAPHY - MASS SPECTROMETRY

J. RUIZ-JIMÉNEZ, J. PARCHINTSEV and M.-L. RIEKKOLA

Laboratory of Analytical Chemistry, Department of Chemistry, P.O. Box 55, FI-00014 University of Helsinki, Finland

INTRODUCTION

Atmospheric aerosol particles consist of a complex mixture of inorganic and organic compounds. It has been reported that 10–70% of the total dry fine particle mass comprises organic compounds (Turpin B.J. *et al.* 2000; Saxena *et al.* 1996). Despite the significant abundance of organic compounds in aerosol particles, very little is known about their chemical composition. The number of organic compounds in aerosol particles can easily be several hundreds (Oros D.R. *et al.* 2001 a,b). These organic species are often present at trace levels (less than ng m^{-3}), and vary significantly in polarity and volatility.

Levoglucosan, a primary organic aerosol component and a molecular marker for wood combustion (Simoneit B.R.T. *et al.* 1999), is associated with the fine size fraction, consistent with formation by a high-temperature combustion process. In contrast, the sugar mannose, is enriched in the coarse size fraction, as could be expected for compounds typical of fungal spores and plant pollen (Graham B. *et al.*2003).

One of the most widely used techniques for the analysis of these compounds is gas chromatography–mass spectrometry (GC–MS). However, natural samples often cannot be analysed directly by GC. Disturbing compounds such as water and inorganic or nonvolatile compounds must be removed from the sample before the GC analysis, or nonvolatile compounds, if important, can be transferred to volatile ones by exploiting the derivatisation. Sample pretreatment for analysis of organic compounds in atmospheric aerosol particles frequently involves at least two steps. First, the analytes are extracted from the sample matrix with an organic solvent (e.g. ultrasonic or Soxhlet extraction). Second, excess solvent is removed and derivatisation is performed if necessary (Abas B.M.R. *et al.* 1996; Nolte C.G. *et al.* 2001; Fraser M.P. *et al.* 2002).

The aim of this study was to develop a well-optimised technique for the determination of some sugars taken from our list of marker compounds employed in aerosolomics profiling.

METHODS

Aerosol samples were collected from 27 March to 10 April in 2003 using a high-volume sampler fitted with quartz filters (240 mm diameter). On total, 10 aerosol samples were collected. The air-flow through the filter was 80–90 m^{-3} h^{-1}, and the sampling time was 4 h. Before use, the quartz filters were preheated at 880 ºC for 5 h to remove organic impurities. After sampling and until analysis, each filter was kept in a cleaned glass jar in a freezer at –25 ºC.

The leaching procedure was similar to those provided by Rissanen T. *et al.* 2006. Dynamic sonication assisted extraction method (DSAE) was used. Six pieces (2.5 × 2.5 cm) —cut the previous day from the filter, placed in a clean desiccator, and dried at 4ºC overnight— were folded and place in an extraction vessel column with 10µl of recovery standard (4,4 dibromooctafluorobiphenyl). The internal volume of the column was 2.2 ml. A mixture of acetone and hexane (1:1) was used as leaching solvent and pumped through the vessel by means of a HPLC pump. The flow rate was 3 ml min^{-1} until the vessel was full and the extract started to run to the glass collecting tube. At this point the vessel was placed in an ultrasonic bath and the flow rate was set to 0.5 ml min^{-1} for 40 min. Once the leaching was completed the extract was filtered and the filtered solution was concentrated to 1 ml under a gentle stream of nitrogen, and 10µl of injection standard (binaphthyl) and derivatisation standard (2,4 dichlorobenzoic acid) were added.

The target analytes —*D*–mannose and levoglucosan—were derivatised in order to be suitable for gas chromatographic separation. The derivatisation method was similar to that proposed by Medeiros P.M. *et al.* 2007. Briefly, aliquots of the total extracts (200 µl) were evaporated completely using a gentle stream of nitrogen, and then converted to their trimethylsilyl derivatives using BSTFA containing 2% TMCS (100 µl) and pyridine (100 µl) for 3 h at 70 ºC. Immediately before GC–MS analysis, derivatised extracts were evaporated to dryness using nitrogen gas and redissolved in 200 µl of hexane for injection.

Aliquots of 1 µL of silylated total extracts of the aerosol samples, as well as standard sugar solutions, were analyzed within 24 h.

A DB5-MS capillary column (30m × 0.25mm I.D. and film thickness of 0.25 µm) was used with helium as the carrier gas at a constant flow rate of 1.3ml min^{-1}. The injector and MS source temperatures were maintained at 280 and 230 ºC, respectively. The column temperature program consisted of injection at 65 ºC and hold for 2 min, temperature increase of 6 ºC min^{-1} to 300 ºC, followed by an isothermal hold at 300 ºC for 15 min. The MS was operated in the electron impact mode with an ionisation energy of 70 eV. The samples were analysed in the splitless mode with splitless time of 30 s. Single ion monitoring was used in the detection step. The retention time and the selected masses for each compound and standard are shown in Table 1.

Table 1. Retention times and isolated masses for the compounds employed in the study.

Compound	Retention time	Isolated masses (m/z)
Binaphthyl (injection standard)	27.42	126, 252, 253, 254
2,4 dichlorobenzoic acid (derivatisation standard)	14.68	247, 249, 173
Decafluorbenzophenon (extraction standard)	10.41	362, 195,167,117
Levoglucosan	17.96	204, 217, 333
D-mannose	α : 20.48; β : 21.06	204, 191, 217, 147

RESULTS

Characterisation of the method. Calibration plots were run for all the analytes using as response the peak area of the most intense mass, 204 m/z in both analytes, as a function of the standard concentration for each compound.

The limit of detection, LOD is expressed as the concentration of the given analyte which gives a signal 3σ above the mean blank signal (where σ is the standard deviation of the blank signal). The LOD is 20 ng l^{-1} for both analytes. The limits of quantification, LOQ is expressed as the concentration of analyte which gives a signal 10 σ the mean blank signal 70 ng l^{-1} for both analytes.

Application of the method. To assess the applicability of the method developed to aerosol samples, it was used to the determination of the target analytes in samples of the days when nucleation events were not occured (NN) and of the days with nucleation events (N).

The precision in the analysis of natural samples ranged from 4.5 to 9%. The precision of the determination step, expressed as relative standard deviation of the injection standard was under 3%. The precision of the derivatisation step expressed as relative standard deviation of the derivation standard was under 5%. The recovery obtained from the study of the results provided by the extraction standard was ranged from 95 to 104%.

ACKNOWLEDEGEMENTS

REFERENCES

Medeiros, P.M., Simoneit, B.R.T. (2007) Analysis of sugars in environmental samples by gas chromatography–mass spectrometry, Journal of Chromatography A, 1141, 271-278.

Rissanen, T., Hyötyläinen, T, Kallio, M., Kronholm, J., Kulmala, M., Riekkola, M.L. (2006) Characterization of organic compounds in aerosol articles from a coniferous forest by GC-MS, Chemosphere 64 1185-1195.

Abas B.M.R., Simoneit, B.R.T. (1996) Composition of extractable organic mater of air particles from Malaysia: Initial studies, Atmospheric Environment 30 2779-2793.

Nolte C.G., Schauer J.J., Cass G.R., Simoneit B.R.T. (2001) Highly polar organic compounds present in wood smoke and in the ambient atmosphere Environmental Science Technology 35 1912–1919.

Fraser M.P., Yue Z.W., Tropp R.J., Kohl S.D., Chow J.C. (2002) Molecular composition of organic fine particulate matter in Houston, TX Atmospheric Environment 36 5751–5758.

Graham, B., Mayol-Bracero, O.L., Guyon, P., Roberts, G.C., Decesari, S., Facchini, M.C., Artaxo, P., Maenhaut, W., Köll, P., Andreae, M.O. (2002) Water-soluble organic compounds in biomass burning aerosols over Amazonia: 1. Characterization by NMR and GC-MS. Journal of Geophysical Research, 107 8047.

Simoneit B.R.T., Schauer, J.J., Nolte, C.G., Oros, D.R., Elias, V.O., Fraser, M.P., Rogge, W.F., Cass, G.R.(1999) Levoglucosan, a tracer for cellulose in biomass burning and atmospheric particles *Atmos. Environ.* 33, 173-182.

Oros D.R., Simoneit B.R.T. (2001) Identification and emission factors of molecular tracers in organic aerosols from biomass burning: Part 1. Temperate climate conifers. Applied Geochemistry, 16 1513-1544.

Oros D.R., Simoneit B.R.T. (2001) Identification and emission factors of molecular tracers in organic aerosols from biomass burning: Part 2. Deciduous trees. Applied Geochemistry, 16 1545-1565.

Turpin B.J., Saxena P., Andrews E. (2000) Measuring and Simulating Particulate Organics in the Atmosphere: Problems and Prospects. Atmospheric Environment 34 2983–3013.

Saxena P., Hildemann L.M. (1996) Water-soluble organics in atmospheric particles: A critical review of the literature and application of thermodynamics to identify candidate compounds. Journal of Atmospheric Chemistry 24:57–109.

SIGN PREFERENCE AND ATMOSPHERIC NUCLEATION

K. RUUSUVUORI[1], T. KURTÉN[1], H. VEHKAMÄKI[1], I.K. ORTEGA[1], M. TOIVOLA[1]
and M. KULMALA[1]

[1]Department of Physics, P.O. Box 64, FI-00014, University of Helsinki, Finland

Keywords: Heterogeneous nucleation, Sign preference, Quantum chemistry, Modelling, Sulphuric Acid

INTRODUCTION

Understanding of the processes involving atmospheric aerosols is essential if we are to understand the Earth's atmosphere, climate change or the health effects of air impurities. Aerosols are, by definition, solid or liquid particles (or combinations of these) uniformly distributed in a finely divided state in a gas, usually air. Their size ranges from nanometers to tens of micrometers. Unfortunately, both the birth and interaction mechanisms of atmospheric aerosols are varied and often also poorly understood.

Nucleation on ions is an important process in the atmosphere. Ions of opposite sign were observed to exhibit different nucleation rates as early as 1897 (Wilson, 1897) but the reason for this sign preference remained a mystery for more than a century. In a recent paper by Nadykto et al. (2006) it was demonstrated that the sign effect can be predicted by carrying out relatively simple quantum chemical calculations. This means we can use quantum chemical methods to help us understand the role of ion-induced nucleation in atmospheric nucleation reactions. Since the role of sulfuric acid in atmospheric new-particle formation is thought to be very important, this negative sign preference can be chemically rationalized by assuming that sulfuric acid is the molecule responsible for the first steps of nucleation and showing that sulfuric acid exhibits a negative sign preference.

However, the computational methods in use today are generally iterative methods that employ a variety of approximations in order to keep the cost in computational resources reasonable. Because of this, we must also do comparisons between theoretical predictions and high quality experimental results in order to gain reliable insight on the initial steps of ion-induced nucleation.

COMPUTATIONAL DETAILS

Our calculations have been performed using the Gaussian 03 (Frisch et al., 2004), Siesta (Soler et al., 2002) and Turbomole (Ahlrichs et al., 1989; versions 5.9, 5.10 & 6.0) quantum chemistry programs.

RESULTS

The binding of sulfuric acid to a series of anions and cations of varying chemical complexity was studied (see Table 1 for some representative results). Sulfuric acid is always bound more strongly to anions than to cations. This can be qualitatively explained using two rather simple structural and chemical concepts. First, the three-member S-O-H groups which form hydrogen bonds to anions are much more flexible than the two-member S=O groups which bond to cations. In effect, the S-O-H groups act as "claws", grabbing and holding on tightly to the anions (see Figure 1). Second, sulfuric acid is a strong acid, and thus prefers to bind to anions, which usually have some degree of basic character. In some extreme cases (*e.g.* dimethylamine vs dimethylammonium), sulfuric acid is actually more strongly bonded to the neutral molecule than to the corresponding cation, indicating that specific chemical interactions may, in some cases, be far more important for ion-induced nucleation than general electrostatic effects. For more information, see Kurtén et al. (2009).

Reaction	ΔE_0	$\Delta G°$
$H_2SO_4 + Na^+ \Rightarrow H_2SO_4 \bullet Na^+$	-27.2^b	-20.2^b
$H_2SO_4 + Cl^- \Rightarrow H_2SO_4 \bullet Cl^-$	-46.8^b	-39.9^b
$H_2SO_4 + (CH_3)_2NH_2^+ \Rightarrow H_2SO_4 + (CH_3)_2NH_2^+$	-19.8^c	-10.0^c
$H_2SO_4 + C_{10}O_3H_{15}^- \Rightarrow H_2SO_4 \bullet C_{10}O_3H_{15}^-$ ^{a}	-59.9^c	-43.9^c

a)The conjugate base anion corresponding to limononic acid. b)MP2(full)/6-311++G(3df,3pd) values. c)RI-MP2/aug-cc-pV(T+d)Z//BLYP/DZP values.

Table 1. Electronic energies (ΔE_0) and standard Gibbs free energies ($\Delta G°$), in kcal/mol, for the binding of sulfuric acid to some representative simple and complex anions and cations.
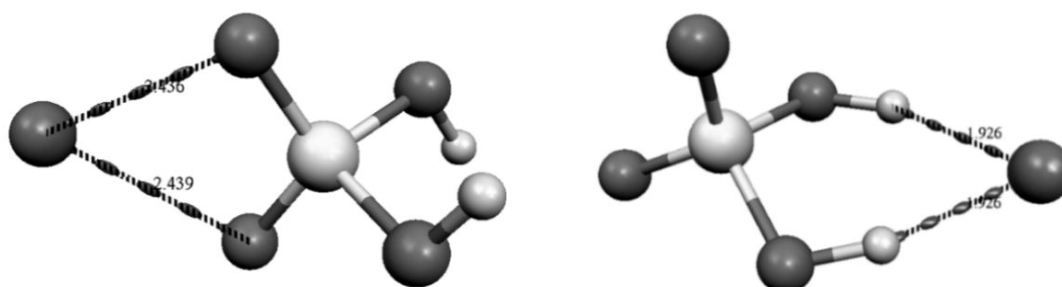
Figure 1. Structure of $H_2SO_4 \bullet Na^+$ (left) and $H_2SO_4 \bullet Cl^-$ (right) clusters. Note the greater flexibility of the SOH groups.

We also studied the binding energies of small charged and neutral n-propanol – tungsten oxide and n-propanol - silver clusters. The objective of our study was to reproduce the experimental results obtained by Winkler et. al. (2008), which indicated a negative sign preference for the case of tungsten oxide. This was done to get quantitative results which could be used to explain the experimental data and to test the limits and reliability of the used quantum chemical methods. The silver clusters observed in the experiment were so large that no sign preference was observed. Nevetheless, calculations for silver were done for comparison.

Silver and tungsten atoms are relatively large, so out of computational considerations we began our studies by considering very small, neutral or singly charged seed molecules (WO_3, W_3O_9, Ag_2 and Ag_3) and a single n-propanol molecule. This choice was also supported by the fact that the experimentally observed sign effect was stronger for smaller seed particles. One larger silver cluster (Ag_{20}) was also studied to see how the results would behave when approaching the cluster sizes observed in the experiment, and due to difficulties encountered in modelling the tungsten oxide, we also considered the case where the tungsten in WO_3 was replaced by a chromium atom.

We started by optimizing the geometries of the seed molecules and n-propanol both alone and together (one seed molecule paired with one n-propanol molecule). Initial guesses were gotten from Spartan, except for the larger silver cluster, which was constructed by manually. For the seed molecules, the geometry optimization was performed for neutral and both positively and negatively charged cases. The geometries were optimized using the Siesta program with two different convergence criteria and the Gaussian 03 employing both Hartree-Fock and density functional methods. Several optimization runs in the Gaussian 03 failed to converge, which lead us to try several different functionals and basis sets for the calculations. We also tried using the geometries optimized by the Siesta program as initial guesses for the optimizations done with Gaussian 03. Despite these steps, WO_3 is the only case where all structures have been successfully optimized using Gaussian 03 so far. An MP2-level optimization of the case of WO_3

done using Turbomole is currently underway and has also proved challenging. No problems were encountered in the optimization with the Siesta program. Finally, we proceeded to calculate the binding energies for each optimized geometry with the Turbomole program employing the Møller-Plesset perturbation method to second order.

However, even in these simple cases and with the several approaches and levels of accuracy employed we were unable to reproduce the sign preference on a qualitative level. The absolute values of the electronic energies for the positively charged tungsten oxide clusters were not only larger than for the negatively charged clusters (which would imply a positive sign preference), but the difference was also as much as one order of magnitude in the worst cases. Since the geometries didn't differ radically between the three charge states, the energies for the positively charged case can be said to be unphysical. We also noted that cations proved to be computationally more demanding than anions in all cases. Comparison between the energies calculated with the Turbomole program and the energies calculated during the optimization procedure has not resolved the issue. The basis set superposition error has also been studied as a possible source for the results, but so far it has not proved significant. For silver and chromium oxide, the intermediate results imply a positive sign preference as well. However, for both cases the binding energies are still plausible and when moving to larger silver clusters, the difference between negatively and positively charged cases gets smaller, as could be expected.
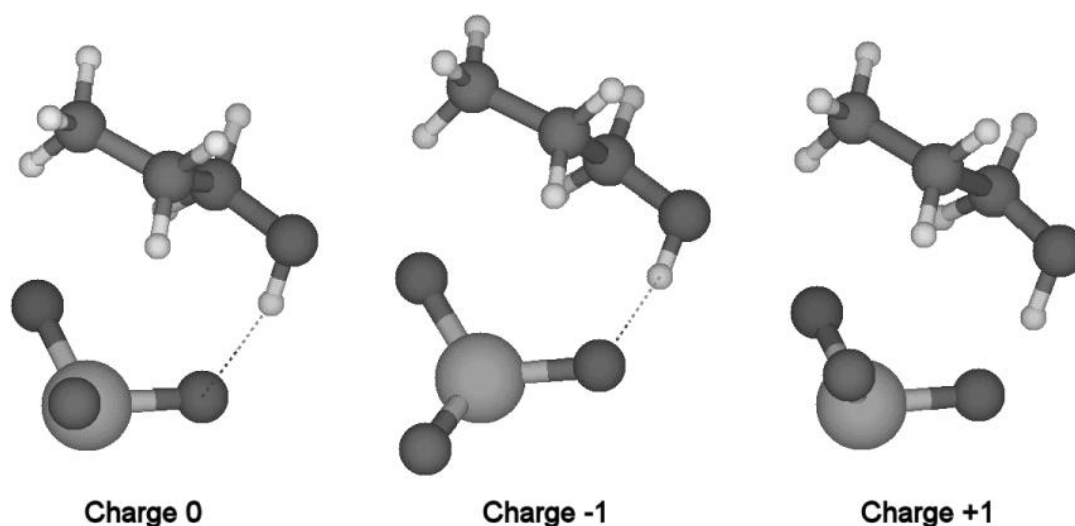
Figure 2. The optimized geometries, calculated with the Siesta program at the BLYP/DZP level using norm-conserving relativistic pseudopotentials for all atom types, for the neutral and singly charged cases of WO_3 seed particle and n-propanol. The binding energies related to these cases, calculated using the Turbomole program at the RI-MP2/def2-QZVPP level, are given in Table 2.

Cluster	ΔE_0 [kcal/mol]
$WO_3 \bullet C_3H_8O$	-3.9
$WO_3^- \bullet C_3H_8O$	-15.1
$WO_3^+ \bullet C_3H_8O$	-144.8

Table 2. Binding energies for the geometries presented in Figure 2.

CONCLUSIONS

As expected from structural and general chemical considerations, and previous computational studies on charged sulfuric acid – water clusters, sulfuric acid is bound much more strongly to anions than cations. This result helps explain the sign effect observed in atmospheric nucleation phenomena, and indicates that the first steps of ion-induced nucleation are controlled by the specific chemical interactions between the core ion and the condensing molecules rather than by electrostatic effects.

For the case of reproducing the experimental results of Winkler et al. the situation is more complex. While the exact reasons for both the computational problems and the results remain at this time unknown, we suspect that for the case of tungsten oxide the problem is of a technical nature and can be caused by the fact that tungsten has such a large amount of electrons (74). If this is true, profound method development might be necessary to resolve the issue. This is also the reason for modelling chromium, which belongs to the same group as tungsten and thus can be assumed to have at least approximately similar chemical properties, but has 50 electrons less. Results for the chromium oxide may thus provide helpful insight on both the technical difficulties and what the sign effect for tungsten oxide should be like. However, different methods and levels of accuracy are not equally suitable even for all the cases tested here, so further studies are still required.

REFERENCES

Wilson, C.T.R. (1897) Condensation of Water Vapour in the Presence of Dust-free Air and other Gases, *Phil. Trans. R. Soc. A*, 189, 265

Nadykto, A.B., Natsheh, A.A., Yu, F., Mikkelsen, K.V. and Ruuskanen, J. (2006) Quantum Nature of the Sign Preference in Ion-Induced Nucleation, *Phys. Rev. Lett.*, 96, 125701

Frisch, M.J. et al. (2004) Gaussian 03, Revision C.02, Gaussian, Inc., Wallingford CT

Soler, J.M., Artacho, E., Gale, J.D., García, A., Junquera, J., Ordejón, P. and Sánchez-Portal, D. (2002) The Siesta method for *ab initio* order-N materials simulation, *J. Phys. Condens. Matt.*, 14, 2745

Ahlrichs, R., Bär, M., Häser, M., Horn, H. and Kölmel, C. (1989) Electronic structure calculations on workstation computers: The program system Turbomole, *Chem. Phys. Lett,,* 162, 165

Kurtén, T., Ortega, I.K., Vehkamäki, H. (2009) The sign preference in sulfuric acid nucleation, *Journal of Molecular Structure: THEOCHEM,* 901: 169–173

Winkler, P.M., Steiner, G., Vrtala, A., Vehkamäki, H., Noppel, M., Lehtinen, K.E.J., Reischl, G.P., Wagner, P.E. and Kulmala, M. (2008) Heterogeneous Nucleation Experiments Bridging the Scale from Molecular Ion Clusters to Nanoparticles, *Science,* 319, 1374

ANALYSIS OF THE IONIZATION RATE AT A BOREAL FOREST MEASUREMENT SITE IN FINLAND IN 2008

S. SCHOBESBERGER, A. FRANCHIN, M. VANA, and M. KULMALA

Department of Physics, P.O. Box 64, FI-00014, University of Helsinki, Finland

INTRODUCTION

The presented work is based on investigations made on new particle formation events as they were observed on several of locations across Europe. The investigated data was gathered within the framework of the EUCAARI (European Integrated project on Aerosol Cloud Climate and Air Quality Interactions) project from spring 2008 on until spring of 2009. The purpose of the EUCAARI project is to investigate the production of small charged and neutral aerosol particles (i.e. down to less than 1 nm and up to 40 nm in mobility equivalent diameter) by means of measurements performed in different regions in Europe using various ion mobility spectrometers. (More details on the EUCAARI project can be found in Manninen, 2009.)

Particular emphasis was put on air ions (i.e. on electrically charged molecules, molecular clusters, and larger aerosol particles). Ion-induced nucleation was shown to play an important role in new particle formation (Boy et al., 2008). It has been found that the total contribution of ions to atmospheric nucleation processes is about 10% in Hyytiälä (Kulmala et al., 2007), but this number varies according to location. The ion production rate (also "ionization rate") is one of the key quantities that is sought to be analyzed in order to understand the role of small ions (mobility diameters up to 1.7 nm) in new aerosol particle formation in the atmosphere.

This report presents the calculation and analysis of ionization rates in a measurement site located in a boreal forest in Hyytiälä, Finland, for the time period from March to December 2008.

METHODS

The main producers of small positive and negative ions in the atmosphere are cosmic rays, as well as high-energetic radiation stemming from natural radioactive sources, such as ^{222}Rn nuclides and various sources in the soil. At the same time, small ions are lost due to ion-ion recombination and coagulation with aerosol particles. The balance equation can be written as

$$\frac{dn_\pm}{dt} = Q - \alpha\, n_\pm\, n_\mp - \beta_{eff}\, N_{tot}\, n_\pm \tag{1}$$

$n_\pm$ is the concentration of small ions ($\pm$ denotes the polarity), Q is the ionization rate, α the recombination coefficient, β_{eff} the effective ion-aerosol attachment coefficient for polydisperse aerosols, and N_{tot} the total concentration of aerosol particles. $\beta_{eff}\, N_{tot}$ is also called the "ion sink" and was calculated according to Hõrrak et al. (2008), while using the number size distribution of aerosol particles as measured by a Differential Mobility Paricle Sizer (DMPS; see Mäkelä et al., 2000) between 3 and 520 nm mobility equivalent diameters. The recombination coefficient α was chosen as 1.5×10^{-6} cm^3 cs^{-1} in accordance with Hõrrak et al. (2008). The ion concentrations were measured by a Balanced Scanning Mobility Analyzer (BSMA; see Tammet, 2004) that scans the ion mobility distribution range corresponding to 0.4 to 6.5 nm in mobility equivalent diameter. Because of the lower limit size of the BSMA, "small ions" is defined in this study as those ions with mobility diameters from 0.4 to 1.7 nm.

Being able to measure or calculate all other variables, equation 1 can now be used to calculate the ionization rate Q.

Applying equation 1 to BSMA and DMPS ion and particle size distribution measurements, results in a mean ionization rate of 3.38 positive ions per cubic centimeter and second, and 3.28 negative ions cm^{-3} s^{-1}. The average was taken over ten months of 2008 (March through December). Note that in the month July more than 50% of the data is missing, which was ignored in the data evaluation. The monthly variations of the ionization rate can be seen from figure 1.
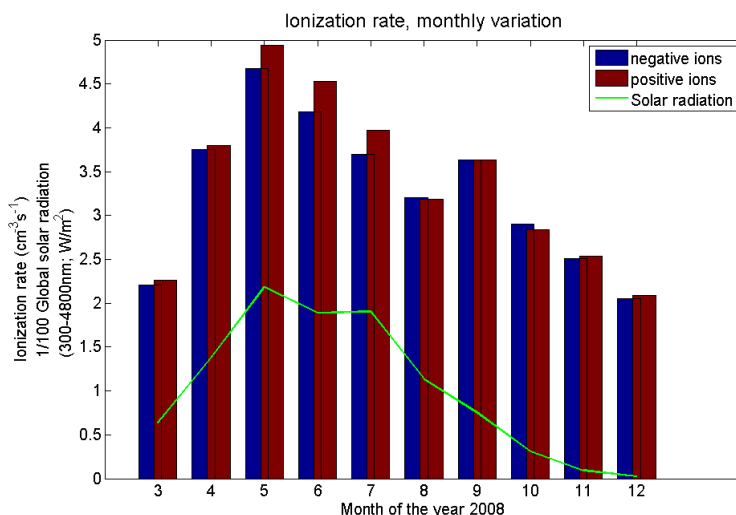
Figure 1. Monthly variation of ionization rate as obtained from concentration measurements (blue bars for the formation rate of negative ions, red bars for the formation rate of positive ions) plus monthly variation of global solar radiation during same times.

Interpolating between December and March, there seems to be a minimum in the ionization rate during winter months. This can be attributed to highly probable snow cover in this period that decreases the amount of ionizing radiation from sources in the soil.

The results shown in figure 1 were also compared to the results on the ion production rate as they were obtained by evaluating measurements of radiation due to ^{222}Rn radioactive decay and gamma radiation spectra (Franchin, 2009). The monthly variations of the ionization rates obtained from both methods were found to be similar. However, the absolute values obtained from radiation measurements are around 9 ion pairs cm^{-3} s^{-1}. As of yet, these discrepancies of almost a factor of three cannot be explained. Notably, Hõrrak et al. (2008) reported similar calculated ionization rates as presented in this report by applying the same method (i.e. using concentration measurements and a balance equation similar to equation 1). Possible explanations for underestimating the ionization rate with this method are insufficiently accurate coefficients α and β_{eff} or concentration measurements. However, wrong assumptions about the actual ionization processes in the atmosphere as well as misinterpretation of radiation measurement data might lead to deviations when determining the ionization rate from this data.

As there apparently is a summer maximum in the calculated ionization rates, the results were compared with the results of solar radiation measurements that are performed continuously the Hyytiälä measurement station, which shows some correlation (figure 1). However, solar radiation is absorbed relatively effectively by higher layers of the atmosphere, so practically none of the solar radiation reaching the surface is energetic enough to ionize molecules or molecular clusters. Of course, however, a big part of all natural processes is modulated by solar radiation. So the correlation between the monthly averages of solar radiation and ionization rate does not indicate a direct physical connection between them two.

The diurnal variation of the obtained ionization rates – averaged over the period from March to December 2008 – is presented in figure 2 along with calculated ion sinks and measured radon concentrations.
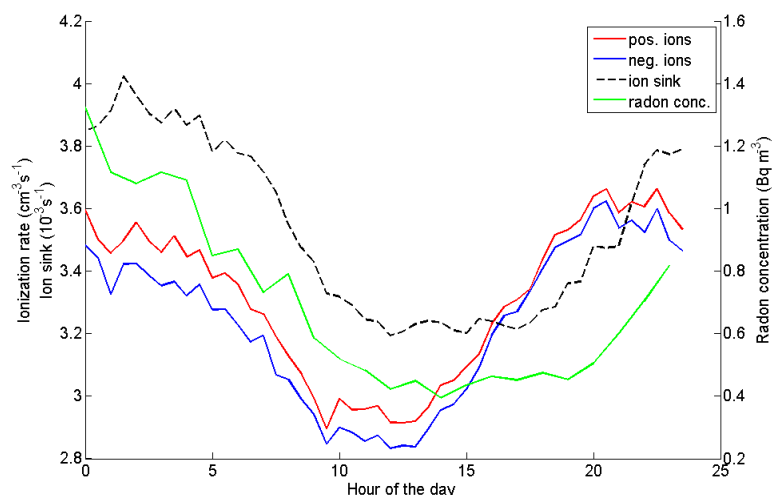
Figure 2: Diurnal variation of calculated ionization rates (red and blue), radon concentration (green), and ion sink as calculated according to Hõrrak et al. (2008). Averages were taken over the full period from March 2008 to December 2008. Except for the radon concentration, times when no DMPS data was available have been ignored.

According to theoretical expectations (i.e. the assumption the ^{222}Rn activity and other sources that should not show any diurnal variation, e.g. cosmic rays, are the cause of ion production in the lower troposphere) the diurnal variation of the ionization rates should be well correlated with radon concentration. However, the correlation is (in average) only very good until around 13:00. Then the ionization rates already start to climb back to their nightly values, while radon concentration stays at the daily low until around 20:00. No explanation has been found yet for this discrepancy. It is interesting to note (see figure 2) that the diurnal variation of radon concentration correlates very well with the calculated ion sink. This is due to the mixing boundary layer height being the primary diurnal modulation for the both of them.

CONCLUSIONS

Ionization rates for Hyytiälä, Finland, were calculated for most of the year of 2008 using a well-known method. An average ion production rate of 3.3 ion pairs cm^{-3} s^{-1} was found, along with a significant monthly variation showing a maximum in summer and a minimum in winter. While similar monthly variations were found using a different method of obtaining the ionization rate – confirming the opinion that natural radiation is the main producer of ions –, the total values from both methods do not agree quantitatively.

The obtained diurnal variation of the ionization rate shows a very good correlation with the diurnal variation of the ^{222}Rn concentration, which is expected to be the primary diurnal modulator of the ionization rate, until the early afternoon.

The discrepancies in the presented results show that our understanding of the ionization processes in the atmosphere is probably not complete and that further investigations are necessary. In particular, new particle formation event days should be looked at, and more parameters should be considered in the analyses.

REFERENCES

Boy, M., Kazil, J., Lovejoy, E.R., Guenther A., and Kulmala, M. (2008). Relevance of ion-induced nucleation of sulfuric acid and water in the lower troposphere over the boreal forest at northern latitudes. *Atmos. Res.*, 90, 151-158.

Franchin, A. et al. (2009). Relation between ^{222}Rn concentration and ion production rate in boreal forest. *Report Series for the joint annual meeting of the Finnish Center of Excellence & the Finnish Graduate School 2009.*

Hirsikko, A., Bergman, T., Laakso, L., Dal Maso, M., Riipinen, I., Hõrrak, U., and Kulmala, M. (2007). Identification and classification of the formation of intermediate ions measured in boreal forest. *Atmos. Chem. Phys.*, 7: 201-210.

Hõrrak, U., Aalto, P.P., Salm, J., Komsaare, K., Tammet, H., Mäkelä, J.M., Laakso, L., and Kulmala, M. (2008). Variation and balance of positive air ion concentrations in a boreal forest. *Atmos. Chem. Phys.*, 8, 655-675.

Kulmala, M., Riipinen, I., Sipilä, M., Manninen, H.E., Petäjä, T., Junninen, H., Dal Maso, M., Mordas, G., Mirme, A., Vana, M., Hirsikko, A., Laakso, L., Harrison, R.M., Hanson, I., Leung, C., Lehtinen, K.E.J., and Kerminen, V-M. (2007). Toward direct measurement of atmospheric nucleation, *Science*, 318: 89-92.

Mäkelä, J.M., Koponen, K.I., Aalto, P., and Kulmala, M. (2000). One-year data of submicron size modes of tropospheric background aerosol in southern Finland. *J. Aerosol Sci.*, 31(5), 595–611.

Manninen, H.E. et al. (2009). *Report Series for the joint annual meeting of the Finnish Center of Excellence & the Finnish Graduate School 2009.*

Tammet, H. (2004). Balanced scanning mobility analyzer, BSMA. *Nucleation and Atmospheric Aerosols 2004, 16th International Conference*, 294-297, Kyoto University Press, Japan.

DROUGHT RESPONSES OF CABRON UPTAKE AND WATER USE IN A BOREAL FOREST

S. SEVANTO[1], T. HÖLTTÄ[2], S. LAUNIAINEN[1], P. KOLARI[2], J. KORHONEN[1], J. PUMPANEN[2], P. KASKI[3], H. MANNILA[3], E. UKKONEN[3], T. VESALA[1] and E. NIKINMAA[2]

[1]Department of Physics, P.O. Box 64, FI-00014, University of Helsinki, Finland
[2]Department of Forest Ecology, P.O. Box 27, FI-00014, University of Helsinki, Finland
[3]Department of Computer Science, P.O. Box 68, FI-00014, University of Helsinki, Finland

Keywords: Carbon balance, Eddy-covariance, Sap flow, xylem conductivity

INTRODUCTION

Atmospheric carbon balance is controlled by emissions and absorption at the surface-atmosphere boundary. In global scale oceans and forests are the main absorbing surfaces of CO_2. However, a forest ecosystem may act as a sink or a source of carbon dioxide depending on the relative magnitudes of two components: the total ecosystem respiration (TER) and gross primary production (GPP). The former consists primarily of heterotrophic soil respiration, and autotrophic and maintenance respiration of the plants, and the latter approximately equals the CO_2 assimilation in photosynthesis (GPP). The sum of these two, the net ecosystem exchange of CO_2 (NEE), describes the balance of CO_2 exchange, negative NEE indicating CO_2 uptake and positive NEE CO_2 release by the forest. If water availability is not limiting, respiration processes are mainly temperature controlled (Tuomi et al. 2009). On the other hand, in well-watered conditions GPP is strongly driven by the radiation, but in seasonal scale it depends also on the temperature via the physiological state of the plant (Hänninen et al. 2008). Water availability can, however, inhibit both respiration and photosynthesis.

When the soil dries, the organic matter decomposition processes that result in heterotrophic respiration slow down. The plants have to close the stomata to prevent extensive water loss that might lead to air-filling of the water conduits in the xylem and fatal dysfunction of the whole water transport system of the plants (Kolari *et al.* 2008). Closing the stomata prevents CO_2 from entering the photosynthetic apparatus and plant production decreases. On the other hand, autotrophic respiration may increase during drought, because refilling the air-filled xylem conduits with water requires active use of energy that enhances respiration. Each of these processes responds to the environmental conditions and reduction in water availability separately. This makes the net effect of drought on the NEE strongly controlled by the environment. Currently, water is seldom a limiting factor for plant activity in the boreal zone. Melting snow in the spring loads soil water reservoirs and during the short summertime the amount of precipitation usually is enough to prevent the ecosystems from drought. In Finland, for example, the three summer months (June, July and August) account for more than 30% of the annual precipitation (700 mm/year). Today, boreal forests are sinks of carbon on annual basis, but it is not known whether this may be the case in the future. According to the climate scenarios, the mean annual air temperature in Northern Europe is expected to increase between 2 - 6 °C in this century and the increase is likely be strongest during winter months (Christensen et al. 2007). The annual amount of precipitation is also expected to increase, but also during the winter months. Therefore, summertime drought may become more frequent despite the increased annual precipitation.

In this study we used an 11-year dataset (1997-2007) of eddy-covariance measurements above a Scots pine (*Pinus sylvestris* L.) forest in Hyytiälä, Southern Finland to analyse the changes in ecosystem CO_2 fluxes during occasional summer drought. Our aim was to analyse under what conditions the forest becomes a CO_2 source at summer and how this change is linked with changes in plant water uptake and stem conductivity. Here we present preliminary results of the study.

METHODS

The forest at the measurement site (SMEAR II station in Hyytiälä, Southern Finland (61°51'N, 24°17'E)) is located in a homogenous Scot pine stand that was established through direct sowing in 1962. Other species than Scots pine contribute 1% to the stand. The height of the dominant trees is 16m and the tree density is 1200-1200 ha^{-1}. The LAI changes from 6 in winter to 8 right after the maturation of new growth in June. The wood biomass is about 41 t ha^{-1} and the forest represents Finnish forests half through the rotation cycle (see e.g. Suni et al. 2003). The annual mean temperature at the site is 3.5°C and annual precipitation 700 mm. The soil material is coarse, silty glacial till and the soil type is haplic podzol. The homogenous pine forest extends some 250 m in all directions from the measurement site and some 1 km to the north. Between January and March 2002, an area of 4.33 ha was manually thinned mainly to the south of the measurement tower. In the thinning about 26% of the basal wood area was removed. The effect of the thinning could not be seen in the ecosystem conductance even in summer 2002 (Vesala et al. 2005).

The ecosystem exchange of CO_2 (NEE) was measured using the standard eddy-covariance system at 23 m above the ground. The system consists of an ultrasonic fast-response anemometer (Gill Solent 1012R) and a fast-response gas analyser (Li-Cor LI-6262). In-coming photosynthetically active photon flux density (PPFD) and was measured above the canopy with LI-190SZ quantum sensor (LiCor, Lincoln, NE, USA). Air temperature was detected above (33 m) and inside the canopy (8.4 m) with radiation-shielded pt-100 sensors. Soil water content was measured at three depths (humus-layer, A- and B- horizons) using the time-domain reflectometry (TDR)-method (Tetronix) at several pits around the site. The measurement systems are descried in more detail in Vesala et al. 1998. TER was estimated from night time NEE and extrapolated to day time using a temperature regression. GPP was calculated by subtracting TER from NEE.

We also measured the sap flow rate and the diurnal diameter variation on three dominant trees during summer 2006. Sap flow rate was measured with Granier-type heat dissipation sensors and stem diameter variations with LVDTs (linear displacement transducers; Solartron Inc). Each tree had two sets of diameter variation sensors: one measuring at 1.5-2.5 m well below the first living branch (found at about 6m) and the other at the upper canopy (10-12 m). Using these measurements we calculated the apparent xylem water conductance, apparent soil-root water conductance and apparent leaf conductance during moist and dry periods. The conductance was calculated from the linear relationship between sap flow rate and xylem diameter variation (see Sevanto et al. 2008). To obtain the root conductance we assumed soil water potential to be constant and compared the sap flow rate to xylem tension at the lowest measurement height. Similarly, the leaf conductance was evaluated by comparing xylem tension at the top most measurement with sap flow rate and assuming constant leaf water potential. Xylem conductance was calculated with xylem pressure difference between the two measurement heights.

RESULTS

Summers (1999, 2002 and 2006) were the driest during the measurement period. In those years, the soil water content was exceptionally low during June, July and August although the annual precipitation was average (Fig 1). The volumetric soil water content dropped below 0.2 m^3 m^{-3}, which represents soil water potential of -2 MPa at the B-horizon. This has been observed to be the limiting leaf water potential for stomatal closure at our site (Duursma et al. 2008). During each of these summers there was a clear ecosystem-scale reduction in CO_2 uptake during the drought. Interestingly, however, the ecosystem did not turn to a source of CO_2 until right after the first rain fall event after the drought (Fig 2.). This indicates that either the release of CO_2 accumulation in the soil was triggered by precipitation or the soil decomposition processes recovered much faster than photosynthesis.
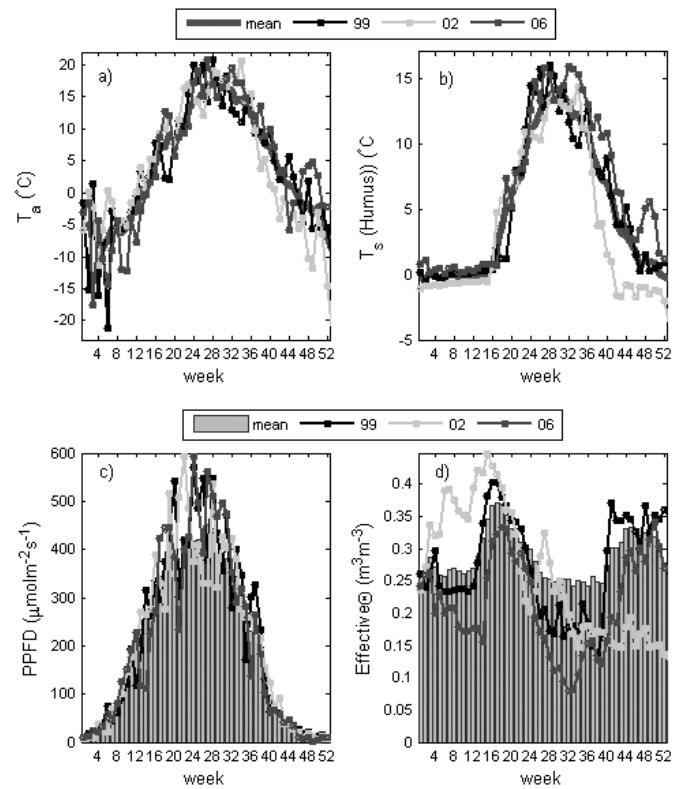
Figure 1. Weekly average air temperature a) soil temperature (humus layer)b) photosynthetically active photon flux (PPFD) density c) and effective soil water content (weighed by pine fine root distribution see e.g. Helmisaari et al. 2007) for years 1999, 2002 and 2006. The average is calculated for years 1996-2006.
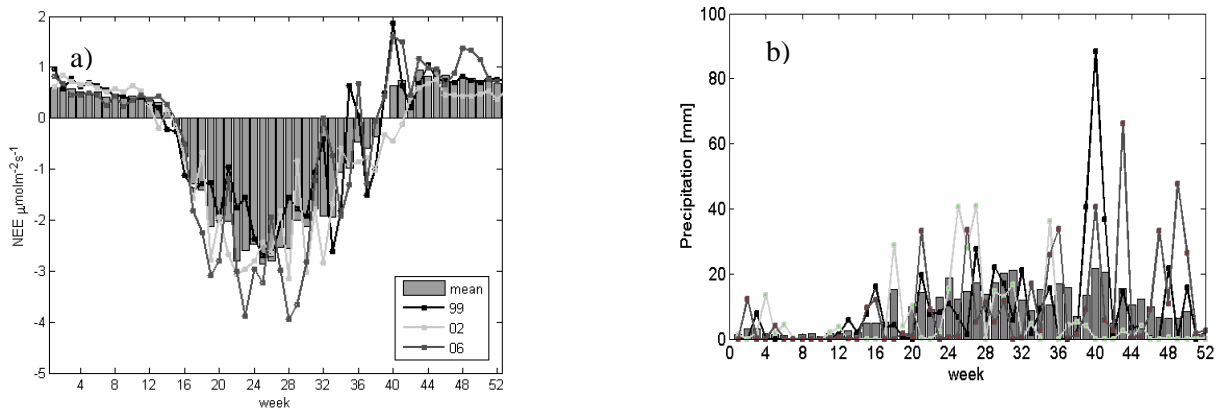
Figure 2. Weekly average of NEE a) and precipitation b) for years 1999, 2002 and 2006. The average of 1996-2006 is marked with bars.

To estimate the strength and thresholds of TER drought response we parameterized an exponential function of soil temperature (average of humus-layer and A-horizon) to estimate nighttime NEE for the whole dataset (data not shown). This model could explain ~80% of the variation. Interestingly, omitting any other year except 2006 from the parameterization data had no effect on the parameter values. Omitting 2006, on the other hand made the function steeper at high temperatures. The drought in 2006 seemed to be sever enough to reduce the nighttime NEE considerably compared to other years. Interestingly, the model

residuals also increased significantly when soil water content dropped below 0.2 $m^3 m^{-3}$. This indicated that when the soil water potential was <-2MPa, soil moisture started limiting respiration.

During the dry period in 2006 (Aug 1 – Aug 20), the daily sap flow rate dropped to about half compared to the moist period (June 29 – July 28) (data not shown). At the same time, the apparent xylem conductivity in the mornings decreased about the same amount (Fig 3), but the apparent xylem conductivity in the afternoon did not change. The apparent root conductance was slightly higher than the apparent leaf conductance during the moist period and did not change from the morning to the afternoon. During the dry period, however, they both dropped in the morning, but, interestingly, increased in the afternoon.
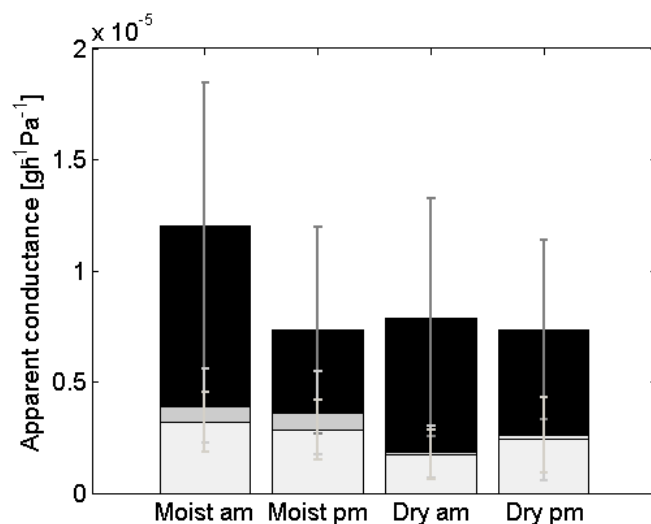
Figure 3. The apparent xylem conductance (black bars), soil-to-root –conductance (dark grey) and leaf conductance (light grey) during moist and dry periods in summer 2006. For the moist period started on June 29th and lasted for 30 days preceding the drought. The dry period started on Aug 1st and lasted for 19 days, until the first rain fall event.

The decrease of the apparent xylem conductance between morning and afternoon can be interpreted as change in the capacitance of the stem. The afternoon conductance would represent the value when all the conduits, the tree is willing to let embolize and air-filled. This could explain the similar afternoon conductance during the dry and moist periods. During the moist period there is water available for refilling embolized conduits at night and the capacitance stays high in the morning. When the soil is dry, the refilling capacity is limited and only few conduits can cavitate in the morning releasing water for the transpiration stream. The apparent root and leaf conductance increasing in the afternoon during the dry period is difficult to explain and the dynamics of the response of the Granier sap flow sensor at dry conditions should be analysed more carefully before further conclusions (see e.g. Sevanto et al. 2008 and 2009).

CONCLUSIONS

The carbon uptake of the Hyytiälä forest responded to drought during summers 1999, 2002 and 2006. The reduction in CO_2 uptake was clear, but drought also reduced respiration so that during drought, the ecosystem was a small carbon sink. After drought, the change to carbon source occurred right after the first rainfall when the respiration rate increased rapidly while photosynthesis remained inhibited. Interestingly, the drought response limit of water potential for the respiration seemed to coincide with the limiting leaf water potential for photosynthesis. The apparent xylem conductance in the morning decreased significantly during drought, indicating a reduction in xylem capacitance and refilling capacity. In the future, we would like to compare the response functions of respiration and photosynthesis to changing soil water content and analyse the connection of these with reducing xylem conductivity.

REFERENCES

Christensen, J.H. et al. (2007) In: Climate Change 2007: The Physical Science Basis. Contribution of Working Group I to the Fourth Assessment Report of the IPCC University Press, Cambridge, United Kingdom and New York, NY, US.

Duursma, R. A., Kolari, P., Perämäki, M., Nikinmaa, E., Hari, P., Delzon, S., Loustau, D., Ilvesniemi, H., Pumpanen, J. and Mäkelä A. (2008) Predicting the decline in daily maximum transpiration rate of two pine stands during drought based on constant minimum leaf water potential and plant hydraulic conductance. *Tree Physiol*. 28:265-276.

Helmisaari, H. S., Derome, J., Nöjd, P. and Kukkola M. (2007) Fine root biomass in relation to site and stand characteristics in Norway spruce and Scots pine stands. Tree Physiol. 27:1493-1504.

Hänninen, H., Linkosalo, T., Häkkinen, R. and Hari, P. (2008) Bud burst phenology. In: Kulmala, L. and Hari, P. (eds.) Boreal Forests and Climate Change. Springer p.225-228.

Kolari, P., Nikinmaa, E. and Hari, P. (2008) Photosynthesis and Drought. In: Kulmala, L. and Hari, P. (eds.) Boreal Forests and Climate Change. Springer p.256-262.

Petäjä, T., Mordas, G., Manninen, H., Aalto, P.P., Hämeri, K. and Kulmala, M. (2006) Detection efficiency of a water-based TSI Condensation Particle Counter 3785. *Aerosol Sci. Technol.* 40: 1090-1097.

Sevanto, S., Hölttä, T. and Nikinmaa, E. (2009) The effects of heat storage during low flow rates on Granier –type sap flow sensors output. In press *Acta Horticulturae*.

Sevanto, S., Nikinmaa, E., Riikonen, A., Daley, M., Pettijohn, J. C., Phillips, N. and Holbrook N. M. (2008) Linking xylem diameter variations with sap flow measurements. *Plant and Soil* 305:77−90.

Suni, T., Berninger, F., Markkanen, T., Keronen, P., Rannik, Ü. and Vesala, T. (2003) Interannual variability and timing of growing-season CO_2 exchange in a boreal forest. *J. Geophys. Res*. 108(D9), 4265, doi:10.1029/2002JD002381.

Tuomi, M., Thum, T., Järvinen, H., Fronzek, S., Berg, B., Harmon, M., Trofymow, J. A,, Sevanto, S. and Liski, J. (2008) Global patterns of leaf litter decomposition. Submitted to *Ecological Modeling*.

Vesala. T., Haataja, J., Aalto, P., Altimir, N., Buzorius, G., Garam, E., Hämeri, K., Ilvesniemi, H., Jokinen, V., Keronen, P., Lahti, T., Markkanen, T., Mäkelä, J. M., Nikinmaa, E., Palmroth, S., Palva, L., Pohja, T., Pumpanen, J., Rannik, U., Siivola, E., Ylitalo, H., Hari, P. and Kulmala, M. (1998) Long-term field measurements of atmosphere- surface interactions in boreal forest combining forest ecology, micrometeorology, aerosol physics and atmospheric chemistry. *Trends in Heat, Mass, Momentum Transfer* 4: 17–35.

Vesala, T., Suni, T., Rannik, Ü., Keronen, P., Markkanen, T., Sevanto, S., Grönholm, T., Smolander, S., Kulmala, M., Ilvesniemi, H., Ojansuu, R., Uotila, A., Levula, J., Mäkelä, A., Pumpanen, J., Kolari, P., Kulmala, L., Altimir, N., Berninger, F., Nikinmaa E. and Hari, P. (2005) The effect of thinning on surface fluxes in a boreal forest. *Global Biogeochemical Cycles* Vol. 19, GB2001 doi:10.1029/2004GB002316.

STUDIES ON THE VERTICAL DISTRIBUTION OF NEW PARTICLE FORMATION IN LOWER TROPOSPHERE: SIMULATIONS WITH MALTE

S.-L. SIHTO[1], M. BOY[1], T. GRÖNHOLM[1], L. LAAKSO[1,2], and M. KULMALA[1]

[1] Department of Physics, University of Helsinki, Finland
[2] Department of Physics, North-West University, Mmabatho, South Africa

Keywords: new particle formation, modelling, turbulent mixing, boundary layer

INTRODUCTION

MALTE (Model to predict new Aerosol formation in the Lower TropospherE) is a 1-dimensional model that is designed to simulate aerosol formation and mixing in a vertical column of atmosphere (Boy et al., 2006). The leading idea of MALTE has been to include all essential phenomena that are related to new particle formation: aerosol dynamics, gas phase chemistry, and vertical mixing. A great advantage compared to 0-dimensional box models is, that in MALTE turbulent vertical mixing can be modelled. Still MALTE is computationally efficient enough to be used in detailed process modelling, which is not possible with 3-dimensional global or regional models.

Mixing between the atmospheric boundary layer (BL) and the free atmosphere favours new particle formation as it leads to dilution of background aerosol concentration (*e.g.* Nilsson et al., 2001). In addition, temperature and thereby saturation ratio of *e.g.* sulphuric acid may differ significantly between the surface and the upper part of BL. This may have an effect on the vertical distribution of the nucleation and particle growth rates.

MALTE offers a tool to investigate how vertical mixing and vertical profiles of different quantities affect the new particle formation. We utilize MALTE to model new particle formation and aerosol dynamics on days when measurements from a hot-air balloon were carried out during springs 2006 and 2007 in Hyytiälä.

SIMULATIONS

As an input for the simulation, we give trace gas concentrations (SO_2, CO, NO, NO_x, O_3) and initial particle concentrations from the measurements in Hyytiälä, SMEAR II station. The model is initialised with these data. Soundings for temperature, RH and potential temperature from Jokioinen, a meteoroliogical station about 100 km from Hyytiälä, are used to validate the modelling of the vertical distribution of meteorological quantities.

From the hot-air balloon flights the following measurement data is available: total particle concentration and ion concentrations in different size ranges, as well as meteorological parameters such as temperature and relative humidity (Laakso et al., 2007). The quantities were measured during both the ascent and descent phases of the hot-air balloon flight. The profiles extend upto about 2 km, depending on the conditions during the flight. In addition, volatile organic compounds were measured from air samples collected during the flight.

We test different nucleation mechanisms (cluster activation nucleation, ion-induced nucleation and organic nucleation), and examine the relevant importance of these mechanisms and their ability to explain the observed particle and ion concentrations. The vertical distribution of the nucleation is investigated by comparing different assumptions for the location where nucleation takes place (e.g.

on the surface or in the whole boundary layer). Aircraft measurements from Hyytiälä indicate that nucleation would take place in the whole boundary layer (O'Dowd et al., 2009), and previous model simulations support that (Laakso et al., 2007). We study the effect of the vertical temperature profile on nucleation and particle growth by implementing a temperature dependent saturation vapour pressure for sulphuric acid, which has been previously treated in the model as totally non-volatile, *i.e.* with $p_{sat} = 0$. The simulated profiles of particle number concentration and ion concentrations across the boundary layer are compared with the measured concentrations.

ACKNOWLEDGEMENTS

REFERENCES

Boy, M., Hellmuth, O., Korhonen, H., Nilsson, E. D., ReVelle, D., Turnipseed, A., Arnold, F., and Kulmala, M. (2006). MALTE – model to predict new aerosol formation in the lower troposphere. *Atmos. Chem. Phys.*, 6, 4499–4517.

Laakso, L., Grönholm, T., Kulmala, L., Haapanala, S., Hirsikko, A., Lovejoy, E. R., Kazil, J., Kurtén, T., Boy, M., Nilsson, E. D., Sogachev, A., Riipinen, I., Stratmann, F. and Kulmala, M. (2007). Hot-air balloon as a platform for boundary layer profile measurements during particle formation. *Boreal Env. Res.*, 12, 279–294.

E. D. Nilsson, Ü. Rannik, M. Kulmala, G. Buzorius, C. D. O'Dowd (2001). Effects of continental boundary layer evolution, convection, turbulence and entrainment, on aerosol formation. *Tellus*, 53B, 441–461.

O'Dowd, C. D. and Yoon, Y. J. and Junkermann, W. and Aalto, P. and Kulmala, M. and Lihavainen, H. and Viisanen, Y. (2009). Airborne measurements of nucleation mode particles II: boreal forest nucleation events. *Atmos. Chem. Phys.*, 9, 937–944.

IMPLEMENTING VEGETATION ISOPRENE AND MONOTERPENE EMISSIONS IN THE JSBACH ECOSYSTEM MODEL

S. SMOLANDER[1]

[1] Department of Physics, University of Helsinki, Finland

Keywords: BVOC, isoprene, JSBACH, monoterpenes

INTRODUCTION

Biogenic Volatile Organic Compounds (BVOC) are reactive trace gases emitted by the biosphere, and they can have a substantial role in the chemistry of the atmosphere. Magnitudes of terrestrial BVOC emissions are necessary for reliable estimation of atmospheric ozone and aerosol formation in atmosphere models, as BVOC's affect the atmospheric photochemistry, and the formation of atmospheric aerosols. Of the wide variety of BVOC's, emissions of isoprene (C_5H_8) typically dominate in broadleaved vegetation and monoterpenes ($C_{10}H_{16}$) typically dominate in coniferous forests.

This documents serves the work on implementing process based emission models of isoprene and monoterpenes into JSBACH, which is the ecosystem and land surface model of the the COSMOS (http://cosmos.enes.org/) Earth System Model framework. The isoprene emssion model is based on Niinemets et al. (1999) and Arneth et al. (2007), and the monoterpene emission model is based on Schurgers et al. (2007) and Niinemets et al. (2002). The models are slightly refined, according to recent work in cooperation with the Lund group.

ISOPRENE EMISSIONS

Leaf isoprene emission rate, E_I, is the same as isoprene production rate. The leaf isoprene emission rate E_I is modelled as:

$$E_I(J, C_i, \Gamma^*, T, \mathrm{day}) = \epsilon_I\, J\, \frac{C_i - \Gamma^*}{6\,(4.67 C_i + 9.33 \Gamma^*)}\, e^{a(T - T_{\mathrm{ref}})}\, \frac{C_{i370}}{C_i}\, \mathrm{Phenology(day)} \tag{1}$$

with:

$$\mathrm{Phenology(day)} = \begin{cases} \min\left(1, \frac{\mathrm{gdd5}}{2\,\mathrm{gdd5full}}\right) & ,\text{for spring and summer} \\ 0.95^{n_{\mathrm{autumn}}} & ,\text{after } T_{\min}(\mathrm{day}) < 5\ ^{\circ}\mathrm{C} \text{ and daylength} < 11\text{ h} \end{cases} \tag{2}$$

where n_{autumn} is the difference between current day number, and the day when the autumn conditions were triggered. The Phenology term is applied only to the landcover class of temperate broadleaf decidous trees.

The input variables are:

J	Electron transfer rate
C_i	Leaf internal CO_2 concentration
Γ^*	CO_2 compensation point
T	Leaf temperature
gdd5	Growth degree days above 5 °C, from beginning of year

This model, as originally developed by Niinemets et al. (1999), is defined at leaf level. In JSBACH, the canopy consists of 3 layers, so the light-dependent variables can have different values in different layers.

The parameters are:

ϵ_I Emission factor. In principle, ϵ is the fraction of electrons available for isoprene synthesis, but we don't directly know the value of ϵ. In practice, ϵ is used as a scaling factor, to fit the model to measured E_I at a point of some known input variables.

a Scaling parameter for temperature dependency.

T_{ref} Reference temperature for temperature dependency.

C_{i370} Leaf internal CO_2 with no water stress, and when ambient CO_2 is 370 ppm. In JSBACH this is $0.87 \times$ ambient. Arneth et al. (2007) may have used 0.7. The purpose of this term is to decrease the emissions in the long term, when atmospheric CO_2 levels increase.

gdd5full   Growth degree day sum (over 5 °C) required for full leaf cover

The emissions factors ϵ_I (and ϵ_M similarly) are solved, so that at standard conditions, Eq. 1 (Eq. 3) gives the standard emissions listed in Table 2. The standard conditions are: pfd (photon flux density) 1000 μmol m^{-2} s^{-1}, temperature 30 °C, and ignoring the C_{i370} and phenology terms.

<div align="center">MONOTERPENE EMISSIONS</div>

The production of monoterpenes, P_M, is modelled in the same manner as the production of isoprene:

$$P_M(J, C_i, \Gamma^*, T, \text{day}) = \epsilon_M J \frac{C_i - \Gamma^*}{6\,(4.67C_i + 9.33\Gamma^*)} \, e^{a(T - T_{ref})} \frac{C_{i370}}{C_i} \, \text{Phenology(day)} \qquad (3)$$

The only difference is the monoterpene emission factor ϵ_M instead of ϵ_I.

However, in some vegetation types (see Table 2), monoterpenes are produced into storage, and then are released from the storage according to emission rate:

$$E_M(m, T) = \frac{m}{\tau(T)} \qquad (4)$$

The variables are:

m Size of monoterpenes storage pool

τ The average residence time in storage (in days)

Further, τ depends on the temperature as:

$$\tau(T) = \frac{\tau_s}{Q_{10}^{(T - T_{ref})/10}} \qquad (5)$$

The parameters are:

τ_s Standard residence time at $T = T_{ref}$. Schurgers et al. (2007) test different values from 0 to 160 days.

Q_{10} Coefficient for increase, when temperature increases 10 degrees.

Finally, the size of the monoterpenes storage pool changes according to:

$$\frac{dm}{dt} = P_M - E_M \qquad (6)$$

Table 1: Parameters constant for all landcover classes

a	0.1
T_{ref}	30 °C
C_{i370}	30 0.87×370 ppm
τ_{s}	(to be determined)
Q_{10}	1.9

Table 2: Parameters related to JSBACH ladcover classes[1]

Landcover class	E_{I} (μgCg^{-1}h^{-1})	E_{M} (μgCg^{-1}h^{-1})	M storage?
Tropical broadleaf evergreen trees	24	0.4	no
Tropical broadleaf deciduous trees	45	1.2	no
Temperate broadleaf evergreen trees	24	0.8	no
Temperate broadleaf deciduous trees	45	0.8	no
Coniferous evergreen trees	8 (16?)	2.4	yes
Coniferous deciduous trees	8	2.4	?
Raingreen shrubs	?[2]	?	?
Deciduous shrubs	?	?	?
C3 grass	8	0.8(?)	yes(?)
C4 grass	8	1.2(?)	yes(?)
Tundra	?	?	?
Swamp (not used)	x	x	x
Crops	?	?	?
Glacier	x	x	x

[1]This is the 14 class scheme. JSBACH also contains an optional 11 class scheme.
[2]Values yet to be determined.

ACKNOWLEDGMENTS

REFERENCES

Arneth, A., Niinemets, Ü., Pressley, S., Bäck, J., Hari, P., Karl, T., Noe, S., Prentice, I. C., Serça, D., Hickler, T., Wolf, A. and Smith, B. (2007). Process-based estimates of terrestrial ecosystem isoprene emissions: incorporating the effects of a direct CO2–isoprene interaction. *Atmos. Chem. Phys.*, 7: 31–53.

Niinemets, Ü., Tenhunen, J. D., Harley, P. C. and Steinbrecher, R. (1999). A model of isoprene emission based on energetic requirements for isoprene synthesis and leaf photosynthetic properties for *Liquidambar* and *Quercus*. *Plant. Cell. Eviron.*, 22:1319–1335.

Niinemets, Ü., Seufert, G., Steinbrecher, R. and Tenhunen, J. D. (2002). A model coupling foliar monoterpene emissions to leaf photosynthetic characteristics in Mediterranean evergreen *Quercus* species. *New Phytol.*, 153:257–275.

Schurgers, G., Arneth, A., Holzinger, R. and Goldstein, A. (2009). Process-based modelling of bio-

genic monoterpene emissions: sensitivity to temperature and light. *Atmos. Chem. Phys. Discuss.*, 9:271–307.

Case studies on satellite based and in situ measured cloud microphysical properties

R. SORJAMAA[1], S. ROMAKKANIEMI[1], and A. LAAKSONEN[1],[2]

[1] Department of Applied Physics, University of Kuopio, Finland
[2] Finnish Meteorological Institute, Helsinki, Finland

INTRODUCTION

Atmospheric aerosols affect climate not only directly by absorbing and scattering radiation energy but also in an indirect manner by acting as cloud condensation nuclei (CCN) in cloud formation processes. According to the Intergovernmental Panel on Climate Change the uncertainty related to the indirect effects of aerosols is clearly the largest among the components of radiative forcing (IPCC, 2007). In order to diminish this uncertainty long term measurement data on aerosol-cloud interactions are required. It is also vitally important that results obtained with models and satellite measurements agree with the in situ measurements. In a newly started case study cloud microphysical properties, a key factor in determining the effect of clouds on radiation, are being analyzed and compared by using all three methods: long term measurements from Puijo measurement station, cloud microphysical model and remotely sensed data from two MODIS (Moderate Resolution Imaging Spectroradiometer) sensors aboard NASA's Terra and Aqua satellites.

CLOUD EVENTS AT PUIJO

The Puijo measurement station is situated on top of the Puijo observation tower (62º54'32" N, 27º39'31"E, 306 m asl, 224 m above surrounding lake level) in a semi-urban environment. The cloud events at the station have been recorded daily since 2006 with roughly 160 cloud events occurred by October 2008 (Portin et al., 2009). A sudden drop in visibility (Vaisala FD12P), onset of cloud droplets (DMT, 2-50 μm) as well as changes in scattering coefficient (TSI 3563 Nephelometer) and in cloud interstitial particle size distribution (DMPS, 10-500 nm) characterize a cloud event. The event is omitted if precipitation intensity exceeds 0.2 mm/h (Vaisala FD12P). A weather camera at the top of the observation tower confirms the cloud event with still images. Cloud droplet size distribution, required for determining the cloud properties like liquid water content (LWC), optical depth and effective particle radius (R_{eff}), is measured with a cloud droplet probe (CDP) (DMT, 2-50 μm). CDP is fairly sensitive to weather conditions and it needs to be turned off during the summer and winter months to prevent damage caused by heat and coldness, respectively.

SATELLITE DATA

Satellite data are obtained from NASA's two satellites, Aqua and Terra. MODIS instruments on board of these two satellites gather information on physical and radiative cloud properties by combining infrared and visible techniques. Cloud properties such as cloud-particle phase, effective cloud-particle radius, cloud optical depth, cloud-top height and temperature are retrieved once or twice a day with spatial resolution of 1 by 1 or 5 by 5 kilometers (cloud optical parameters and cloud top parameters, respectively).

Table 1: R_{eff} and liquid water path (LWP) retrieved from MODIS data together with R_{eff} and LWC calculated from the CDP data

date	MODIS R_{eff} (μm)	MODIS LWP (gm^{-2})	Measured R_{eff} (μm)	Measured LWC (gm^{-3})
28.9.2007	12.00	151	4.07	0.018
29.9.2007	21.65	767	6.83	0.229
16.10.2007	20.50	88	5.39	0.140
7.5.2008	17.67	271	11.66	0.054
20.10.2008	26.24	105	8.3	0.240

DATA ACQUISITION AND COMPARISON

There are several things that restrict the use of all 160 cloud event days in this study. The first restriction was that the cloud event needed to take place approximately at the same time as either of the satellites scanned over Puijo area. There were also days when the satellite scanned the right area at the right time but the data were either missing or corrupted. Furthermore, the event days when the CDP has shown unreliable results or the data are missing had to be omitted. Since in situ measurements take place only 224 m above the surrounding lake level and 75 meters above the ground as the Puijo tower is built on a hill there is reason to suspect that what is actually measured is many times the droplet concentration at the base of the cloud. While the MODIS instruments scan the clouds from space there is a strong possibility that there are several levels of clouds and the cloud detected around the measurement station is not the same cloud as detected by the satellite. Therefore we have also used ceilometer (Vaisala CT25K) to measure the height of the cloud base and to see if there were several levels of clouds. This restricted the amount of available data even more as in many cases there were two or more levels of clouds. Finally only five cloud event days from the total of 160 was left for closer investigation.

Preliminary results from the MODIS and measurements on top of the tower are presented in Table 1. As can be seen R_{eff} is much smaller from the measurement level than estimated using MODIS. This can be expected as most of the time measurements are conducted close to the base of the cloud. We have used adiabatic air parcel model to estimate what would R_{eff} be at the top of cloud with similar LWP as measured with MODIS. It turns out that such an approach will give us R_{eff} in the order of ten micrometer, being clearly smaller than the values presented in Table 1 from the MODIS. We are currently estimating cloud droplet number concentrations from the MODIS data and the results will be compared to measured concentrations (Boers et al., 2006).

ACKNOWLEDGMENTS

REFERENCES

S. Solomon, D. Qin, M. Manning, Z. Chen, M. Marquis, K. B. Averyt, M. Tignor and H.L. Miller (edit.) (2007). IPCC. "Summary for Policymakers", in Climate Change 2007: The Physical Science Basis. Contribution of Working Group I to the Fourth Assessment Report of the In-

tergovernmental Panel on Climate Change. Cambridge University Press, Cambridge, United Kingdom and New York, NY, USA, 2007.

Portin, H., Komppula, M., Leskinen, A., Romakkaniemi, S., Laaksonen, A., and Lehtinen, K. (2009). Observation on aerosol-cloud interactions at the Puijo semi-urban measurement station. *Boreal Env. Res.*, accepted for publication.

Boers, R., Acarreta, J. R., and Gras, J. L. (2006). Satellite monitoring of the first indirect aerosol effect: Retrieval of the droplet concentration of water clouds. *J. Geophys. Res.*, 111, D22208, doi:10.1029/2005JD006838.

MEASURED VERTICAL PROFILES OF AEROSOL NUMBER CONCENTRATIONS INSIDE THE PLANETARY BOUNDARY LAYER (PBL) OVER THE BOREAL FOREST IN FINLAND

A. S. STAROVEROVA[1], M. BOY[1], T. GRÖNHOLM[1], L. LAAKSO[1], A. GUENTHER[2], A. SOGACHEV[1], A. VIRKKULA[1] and M. KULMALA[1]

[1]Department of Physics, P.O. Box 64, FI-00014, University of Helsinki, Finland
[2]ACD, NCAR, P.O. Box 3000, 80307 Boulder, Colorado, USA

Keywords: Atmospheric aerosols, Aerosol measurements, Boundary layer, Vertical distribution.

INTRODUCTION

Atmospheric aerosols affect climate directly by scattering and absorbing the solar radiation and indirectly by modifying radiative properties, amount and lifetime of clouds (IPCC, 2007). Measured concentration of aerosols in the boundary layer can be used in chemical and aerosol models. In addition, these measurements can give information about formation or growth of new aerosol particles. Unfortunately, measurements of aerosols in the boundary layer are not taken continuously and there is lack of knowledge about it.

In this study, we present aerosol particle concentration measured through the boundary layer (up to 1400 meters above the ground) using a tethered balloon as a platform. The soundings were made above boreal ecosystem in Hyytiälä, Finland, in August 2001, October 2004, and in February and April 2005. We compare the measurements with corresponding ground based measurements obtained at the nearby Smear II station, and discuss characteristics of boundary layer measurements and the utilization of ground measurements as input values for boundary layer chemical and aerosol models. The experiments covered days with new particle formation as well as days when no formation was registered at SMEAR II station.

MATERIALS AND METHODS

The aerosol particle concentrations were measured with a TSI Hand-held Condensation Particle Counter (CPC) Model 3007. This device is capable for particle counting at concentrations up to 100,000 particles cm^{-3} with particle size range from 10 nm to larger than 1μm and accuracy of ± 10 %. For more information about the TSI-3007, see Hämeri et al. 2002. In addition, temperature, relative humidity and pressure were measured.

The aerosol particle number size distribution was measured at the ground by DMPS system (Aalto et al. 2001). Concentrations of SO_2, NO_x and wind direction at the height of 33.6 were used to investigate their influence to aerosol particle concentration. Back trajectories were calculated by using HYSPLIT 4 model (Draxler and Hess, 1998). The mixed layer height (MLH) was predicted by the model SCADIS (Sogachev et al., 2002).

RESULTS AND CONCLUSIONS

The vertical structure of the aerosol particles depended on MLH. We found that the measurements at the ground are good estimates for the whole mixed and even boundary layer. In our experiment aerosol particles were evenly distributed with height inside and outside the mixed layer, and vertical gradients were negligibly small in each layer. On the top of mixed layer concentrations sharply decreased with height (see Fig. 1). When atmosphere was not mixed, concentration showed the same vertical distribution in stable and residual layers, with large gradient between them.
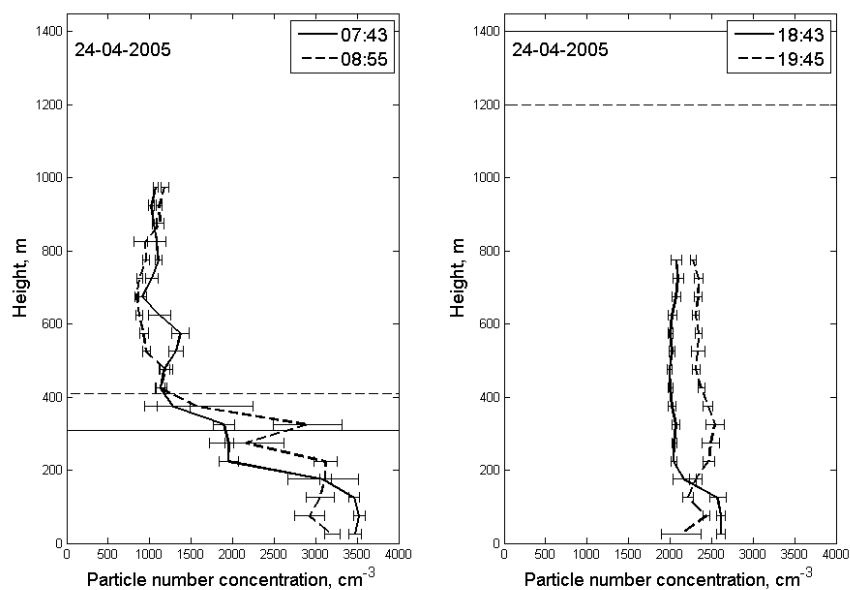
Figure 1. Aerosol particle concentration measured during soundings on the 24th April 2005. Short horizontal lines are error bars. Long horizontal lines through whole pictures show MLH.

Aerosol concentrations distinctly increased within all measurement height when air mass changed from clean northern or western to polluted southern or eastern origin. We also noticed that the aerosol particle concentration measurements from the evening were a good estimate for the next morning's concentration in the residual layer, in conditions where no change of air mass and no rainfall was observed.

During several days with sounding measurements in April 2005 new particle formation and growth were observed. Some soundings were performed during time when growth of aerosol particles was registered by the DMPS at SMEAR II station. We took into account the intensity of the growth of aerosol particles near the size of 10 nm. (see DMPS plot on Fig. 2). This size is important since this is the lower detection limit of the CPC 3010, which was used in the soundings. When the growth of aerosol particles near this size occurs, a certain fraction of particles reached the lower detection limit of the device, and the CPC measurements showed increased concentrations on the height where this growth happens.

In the afternoon, when the newly formed particles reached a size near 10 nm (registered by DMPS) increased aerosol concentration near the surface and up to about 100 m was visible in the vertical profile. This could be seen during the sounding at 18:43 in Figures 1 and 2. During the next sounding, at 19.45, when most of these particles already based 10 nm, aerosol particles were homogeneously distributed inside the MLH due to their mixing in the atmosphere. This dependence was clearly seen during two event days in April 2005. During the next days, it was difficult to register this behaviour. Probable reason is a strong pollution prevailed over the site.

These results can enable the use of ground-based measurements to represent the concentration within the boundary layer. They can be important for initializing aerosol background concentration vertical profiles in chemical and aerosol models. To achieve a better understanding of aerosol particle vertical distribution in the PBL, more measurements for different cut sizes particle diameters are needed.
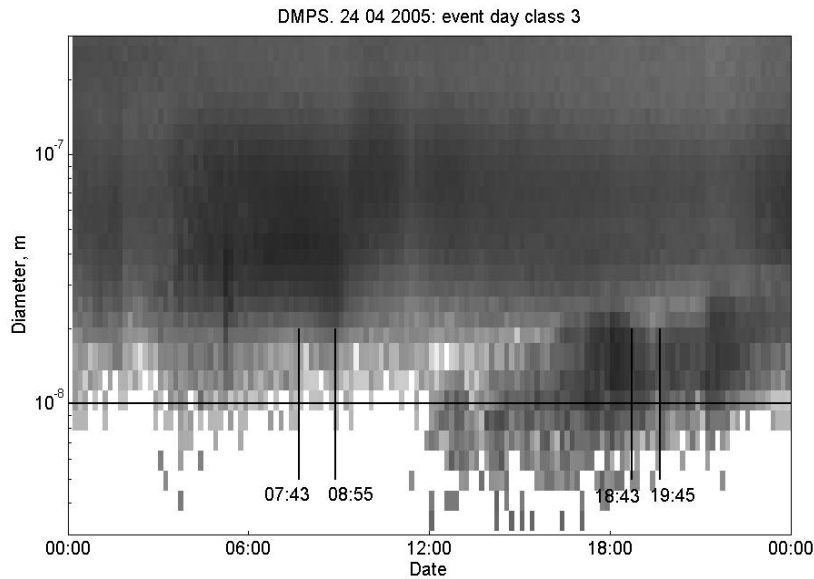
Figure 2. Particle number size distribution measured by the DMPS. Horizontal line is at 10 nm particle diameter. Vertical lines show time of soundings presented in figure 1.

ACKNOWLEDGEMENTS

REFERENCES

Aalto, P., Hämeri, K., Becker, E., Weber, R., Salm, J., Mäkelä, J., Hoell, C., O'Dowd, C., Karlsson, H., Hansson, H.-C., Väkevä, M., Koponen, I., Buzorius, G., and Kulmala, M. (2001) Aerosol physical properties of aerosol particles during nucleation events. *Tellus* 53B, 344-358.

Intergovernmental Panel on Climate Change (2007) Climate Change 2007: The Physical Science Basis - Summary for Policymakers.

Draxler, R. R. & Hess, G. D. (1998) An overview of the HYSPLIT_4 modeling system for trajectories, dispersion and deposition. Australian Meteorological Magazine 47: 295-308.

Hämeri, K., Koponen, I.K., Aalto, P.P., and Kulmala, M. (2002) The particle detection efficiency of the TSI- 3007 condensation particle counter. *Technical Note, J. Aerosol Sci.* 33, 1463-1469.

Sogachev, A., Menzhulin, G., Heimann, M. , and Lloyd J. (2002) *Tellus* 54B (5), 784-819.

VOLATILE ORGANIC COMPOUND EMISSIONS FROM A BOREAL FOREST – DIRECT ECOSYSTEM SCALE MEASUREMENTS IN 2006–2008

R. TAIPALE[1], T. M. RUUSKANEN[1], M. K. KAJOS[1], J. PATOKOSKI[1], H. HAKOLA[2], and J. RINNE[1]

[1]University of Helsinki, Department of Physics, Helsinki, Finland
[2]Finnish Meteorological Institute, Air Quality Research, Helsinki, Finland

Keywords: disjunct eddy covariance method, proton transfer reaction mass spectrometry

INTRODUCTION

Volatile organic compound emissions from the boreal vegetation zone contribute to the formation and growth of atmospheric aerosol particles (Tunved et al., 2006), which are an important factor in the climate system. Boreal vegetation emits large amounts of terpenoids (isoprene, monoterpenes, and sesquiterpenes; Tarvainen et al., 2007) and oxygenated volatile organic compounds (OVOCs). To quantify OVOC emissions in the ecosystem scale and to assess their importance in comparison with monoterpene emissions, we carried out micrometeorological flux measurements above a boreal forest in southern Finland in 2006–2008. We also measured emissions in the shoot scale (Kajos et al., 2009) as well as ambient concentrations (Taipale et al., 2008; Ruuskanen et al., 2009) at the same time.

METHODS

The disjunct eddy covariance method enables direct trace gas flux measurements in the ecosystem scale (Rinne et al., 2001). We applied it to VOCs above a Scots pine (*Pinus sylvestris*) dominated forest at the SMEAR II station (Station for Measuring Ecosystem–Atmosphere Relations II; Hari and Kulmala, 2005). The flux measurement height was 22 m, about 6 m above the top of the forest canopy, and the flux averaging time was 45 min. The wind velocity was measured with a three-dimensional sonic anemometer (Gill Instruments Ltd., Solent HS1199) using a sampling frequency of 10 Hz. The VOC concentrations were measured with a proton transfer reaction mass spectrometer (PTR-MS; Ionicon Analytik GmbH; Lindinger et al., 1998), which was calibrated with a gas standard (Apel–Riemer Environmental, Inc.) approximately once a week. Depending on the measurement period, the PTR-MS measurement cycle contained 11–13 masses which were measured successively within 5.6–6.6 s. The measured VOC-related masses were M31 (formaldehyde, protonated mass 31 amu), M33 (methanol), M45 (acetaldehyde), M59 (acetone), M69 (isoprene and fragments of methylbutenol), M81 (fragments of monoterpenes), M87 (methylbutenol), M99 (hexenal), M101 (*cis*-3-hexenol and hexanal), M113 (?), and M137 (monoterpenes). A sampling time of 0.5 s was used for these masses.

RESULTS AND DISCUSSION

OVOC emissions consisted of methanol, acetaldehyde, and acetone. They were of the same order of magnitude as monoterpene emissions (Fig. 1). The median flux for the measurement period 13 June–15 August 2006 and 28 March–25 June 2007 was 142 $\mu g\ m^{-2}\ h^{-1}$ for methanol, 38 $\mu g\ m^{-2}\ h^{-1}$ for acetaldehyde, 86 $\mu g\ m^{-2}\ h^{-1}$ for acetone, and 217 $\mu g\ m^{-2}\ h^{-1}$ for monoterpenes.

The compatibility of the measured monoterpene emissions with the traditional temperature dependent emission algorithm $E = E_{30}\exp\{\beta(T - 30\ °C)\}$ (Guenther et al., 1993) was reasonable (Fig. 2). A fixed temperature coefficient $\beta = 0.09\ °C^{-1}$, commonly used in emission inventory models, yielded an emission potential $E_{30} = 744\ \mu g\ m^{-2}\ h^{-1}$. This value agrees well with the ones derived from micrometeorological flux measurements with the gradient method (648 $\mu g\ m^{-2}\ h^{-1}$; Rinne et al., 2000) and from shoot scale

measurements with the dynamic chamber method (626 μg m^{-2} h^{-1}; Hakola et al., 2006). To determine the dependence of OVOC emissions on environmental variables, further micrometeorological flux measurements as well as shoot scale experiments in a controlled environment are required.
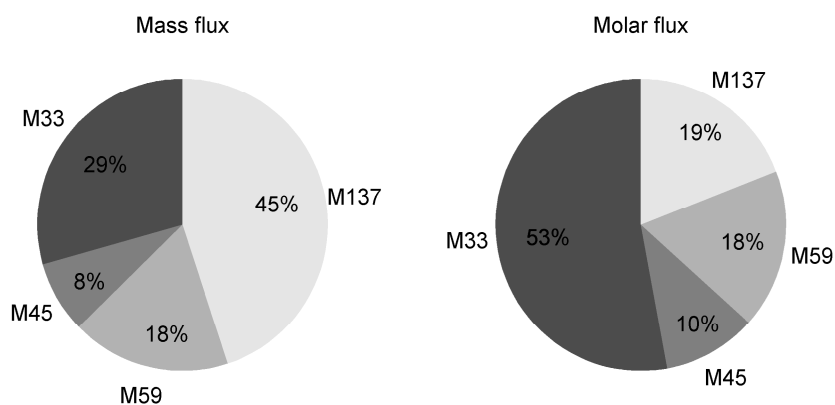
Fig. 1. Relative magnitudes of the median VOC fluxes (M33 methanol, M45 acetaldehyde, M59 acetone, and M137 monoterpenes).
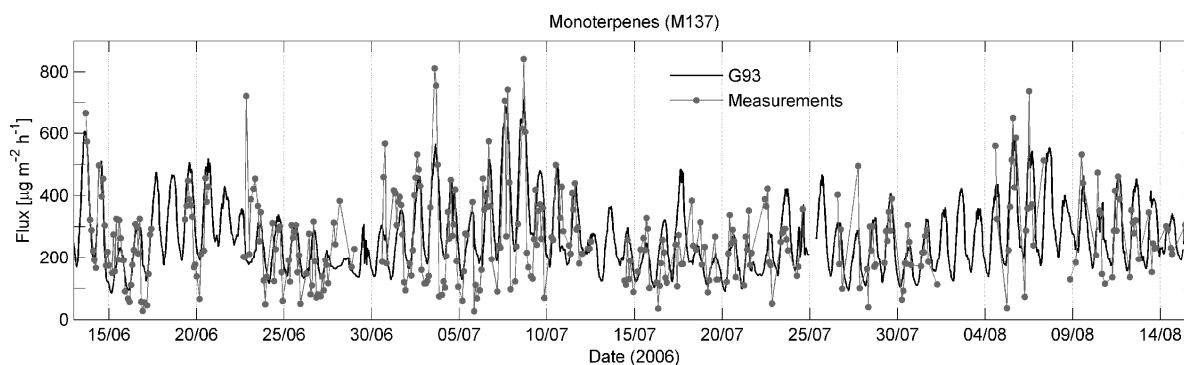
Fig. 2. Monoterpene emissions in the summer 2006. The black line shows the emissions derived from the temperature dependent emission algorithm (G93).

ACKNOWLEDGEMENTS

REFERENCES

Guenther, A. B., Zimmerman, P. R., Harley, P. C., Monson, R. K., and Fall, R.: Isoprene and monoterpene emission rate variability: Model evaluations and sensitivity analyses, J. Geophys. Res., 98(D7), 12609–12617, 1993.

Hakola, H., Tarvainen, V., Bäck, J., Ranta, H., Bonn, B., Rinne, J., and Kulmala, M.: Seasonal variation of mono- and sesquiterpene emission rates of Scots pine, Biogeosciences, 3, 93–101, 2006.

Hari, P. and Kulmala, M.: Station for Measuring Ecosystem–Atmosphere Relations (SMEAR II), Boreal Environ. Res., 10, 315–322, 2005.

Kajos, M. K., Taipale, R., Kolari, P., Ruuskanen, T. M., Patokoski, J., Bäck, J., Hari, P., and Rinne, J.: Monoterpene and oxygenated VOC emissions from a Scots pine branch in field conditions, this issue, 2009.

Lindinger, W., Hansel, A., and Jordan, A.: On-line monitoring of volatile organic compounds at pptv levels by means of Proton-Transfer-Reaction Mass Spectrometry (PTR-MS) – Medical applications, food control and environmental research, Int. J. Mass Spectrom., 173, 191–241, 1998.

Rinne, J., Hakola, H., Laurila, T., and Rannik, Ü.: Canopy scale monoterpene emissions of *Pinus sylvestris* dominated forests, Atmos. Environ., 34, 1099–1107, 2000.

Rinne, H. J. I., Guenther, A. B., Warneke, C., de Gouw, J. A., and Luxembourg, S. L.: Disjunct eddy covariance technique for trace gas flux measurements, Geophys. Res. Lett., 28(16), 3139–3142, 2001.

Ruuskanen, T. M., Taipale, R., Rinne, J., Kajos, M. K., Hakola, H., and Kulmala, M.: Quantitative long-term measurements of VOC concentrations by PTR-MS: annual cycle at a boreal forest site, Atmos. Chem. Phys. Discuss., 9, 81–134, 2009.

Taipale, R., Ruuskanen, T. M., Rinne, J., Kajos, M. K., Hakola, H., Pohja, T., and Kulmala, M.: Technical Note: Quantitative long-term measurements of VOC concentrations by PTR-MS – measurement, calibration, and volume mixing ratio calculation methods, Atmos. Chem. Phys., 8, 6681–6698, 2008.

Tarvainen, V., Hakola, H., Rinne, J., Hellén, H., and Haapanala, S.: Towards a comprehensive emission inventory of terpenoids from boreal ecosystems, Tellus, 59B, 526–534, 2007.

Tunved, P., Hansson, H.-C., Kerminen, V.-M., Ström, J., Dal Maso, M., Lihavainen, H., Viisanen, Y., Aalto, P. P., Komppula, M., and Kulmala, M.: High natural aerosol loading over boreal forests, Science, 312, 261–263, 2006.

ROADSIDE UFP STUDY USING HYGROSCOPIC, ORGANIC AND VOLATILITY TDMAS

PETRI TIITTA[1], PASI MIETTINEN[1], PETRI VAATTOVAARA[1], JORMA JOUTSENSAARI[1], TUUKKA PETÄJÄ[4], ANNELE VIRTANEN[5], PASI AALTO[4], HARRI PORTIN[2], KARI E.J. LEHTINEN[1,2], MARKKU KULMALA[4] AND ARI LAAKSONEN[1,3]

[1]Department of Physics, University of Kuopio, P.O.Box 1627, FIN-70211, Finland
[2]Finnish Meteorological Institute, Kuopio Unit, P.O.Box 1627, FIN-70211, Finland
[3]Finnish Meteorological Institute, Helsinki Unit, P.O.Box 503, FIN-00101, Finland
[4]Department of Physics, University of Helsinki, P.O.Box 64, FI-00014, Finland
[5]Tampere University of Technology, Institute of Physics, P.O. Box 692, FIN-33101, Finland

INTRODUCTION

Investigating of particle hygroscopicity, volatility and ethanol uptake in parallel will give insights into the particle mixing state and composition indirectly. The growth of particles in elevated relative humidity inside a hygroscopicity TDMA (H-TDMA) will reveal typically an inorganic contribution, whereas growth in ethanol vapor implies the involvement of organic compounds. Heating the sampled particles adds a temperature-dependent volatility of the particles, which separates the contribution of elemental carbon, non-volatile organics and metal particles in the particulate phase. To characterize traffic related UFP composition and properties, different types of tandem differential mobility analyzer (TDMA) techniques are adapted. These include hygroscopicity, volatility and organic TDMAs (Hämeri et al., 2000, Joutsensaari et al., 2001; Vaattovaara et al., 2005b).

By using a Zdanovskii-Stokes-Robinson (ZSR) mixing rule, the measured growth factors of particles of mixed composition can be expressed as a linear interpolation of the water or ethanol uptake of the pure components (see e.g. Stokes and Robinson, 1966). In a general form, the growth factors of the mixed particles (GF_{mix}) can be written as (see e.g. Gysel et al., 2007):

$$GF_{mix}^3(\alpha) \approx \sum_i \varepsilon_i GF_i(\alpha)^3 \qquad (1)$$

where α is water or ethanol activity, ε_i represents volume fraction of the compound i in dry particles, and GF_i the growth factor of the pure substance i. The observed growth factor is then obtained by summing over all the components i.

Let's assume a three component system, which consists of a non-volatile (ε_{nv}), organic (ε_{org}) and ammonium sulphate fraction (ε_{as}). The observed growth factors are thus

$$GF_{obs}^3 \approx \varepsilon_{nv} GF_{nv}^3 + \varepsilon_{org} GF_{org}^3 + \varepsilon_{as} GF_{as}^3 \qquad (2)$$

where GF_{nv}, GF_{org} and GF_{as} are growth factors for the non-volatile, organic and ammonium sulphate particles at a fixed activity, respectively.

A three-week measurement campaign was conducted in Kuopio, Finland, from 15 June to 5 July, 2004. The instruments were located in the immediate vicinity of traffic lanes in order to investigate the composition, properties and mixing state of traffic-related fresh UFP with low disturbing background aerosol concentration.. In the volatility TDMA, the selected sample was exposed to three different temperatures (50°C, 150°C and 280°C) in sequence and the evaporation from the particle phase was monitored. The hygroscopic TDMA exposed the quasi-monodisperse sample to around 89% RH and monitored subsequent hygroscopic growth. In the organic TDMA, the sample was treated with ethanol vapor in a saturation ratio (S%) of 82. More detailed information see Tiitta et al. (2007) and Tiitta et al. (2009).

Figure 1. A layout of the Savilahti measuring site approximately 2 km from Kuopio city center between Savilahdentie road and Motorway E63. X denotes the location of the measurement site next to Savilahdentie road. Traffic flow was between 14 000 and 16 000 vehicles per weekday (Monday to Friday) corresponding to daytime traffic flow between 800–1200 vehicles h^{-1} on the Savilahdentie road.

RESULTS

The results show that the non-volatile fraction was highest when the direct traffic emissions were the main source of the sampled particles (SR, Figure 2). When the temperature increased to 150°C, a major fraction of nucleation mode particles already evaporated, but there was still a clear non-volatile fraction of 10 nm particles even at 280°C. When wind blows from the Savilahdentie road, the non-volatile fraction was about 2 times higher than at MW or BG conditions. This indicates that also the non-volatile fraction of 10 nm particles was related to traffic emissions.

At relative humidity of 90%, the HGFs of pure ammonium sulphate particles are 1.38, 1.52 and 1.66 for 10, 20 and 50 nm particles, respectively (Hämeri et al., 2000). Highly ethanol-soluble material has growth factors of 1.11, 1.31 and 1.45, for 10, 20 and 50 nm particles, respectively and estimates for moderately ethanol-soluble material, on the other hand, has GFs of 1.06, 1.16 and 1.23 and slightly soluble GFs of 1.03, 1.08 and 1.11 for 10, 20 and 50 nm particles, respectively (Vaattovaara et al., 2005, S% = 82).
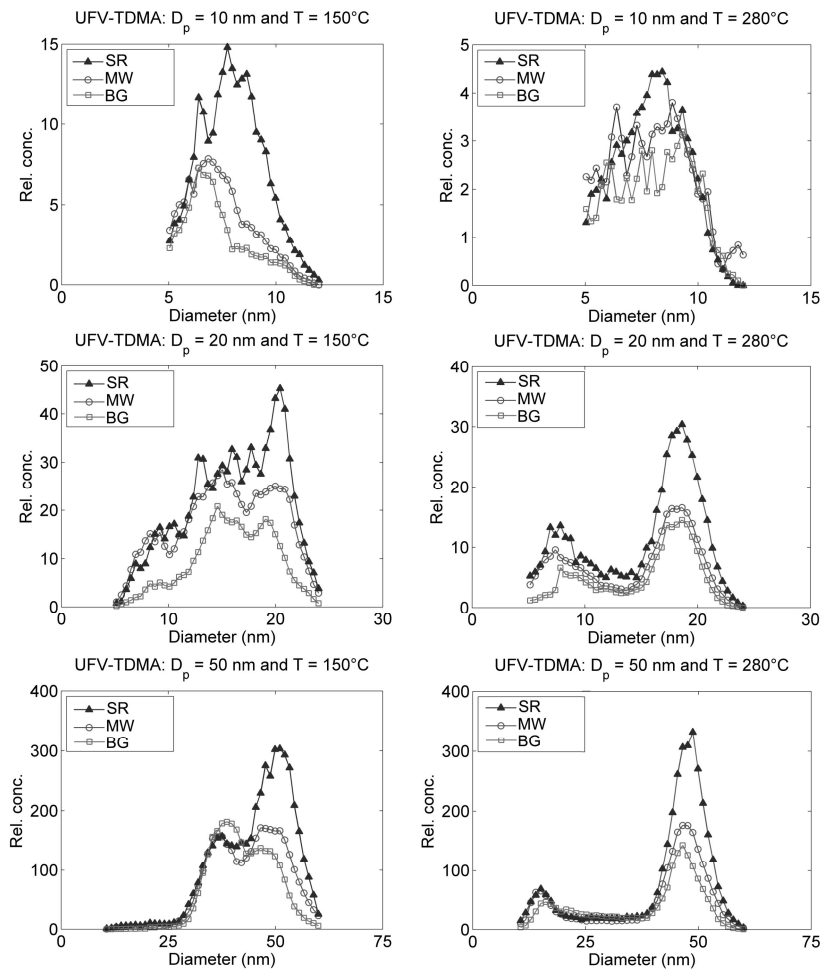
Figure 2. Median volatility spectra conditioned to 150°C and 280°C for 10 nm, 20 nm and 50 nm particles when 1) the wind blew from the Savilahti road (SR) to the measurements site, 2) the wind blew from the motorway E63 (MW) to the measurements site, 3) urban background (BG).

The maximum ammonium sulphate fraction can be estimated roughly by assuming that both the non-volatile and organic fractions do not uptake water at all. Also in the case of organic volume fraction, the other fractions are considered not to participate in the growth observed in the sub-saturated ethanol concentration. The non-volatile material can be considered as a proxy for black carbon in the particles which is insoluble both in water and ethanol (insoluble fraction). Also, since a variety of the organic compounds are only slightly hygroscopic (McFiggans et al., 2005), these assumptions are well justified if we keep in mind that this method only gives a crude estimate the maximum ammonium sulphate volume fraction in the particulate phase. If chosen a different model compound with a lower affinity to water vapor, the resulting water-soluble fraction would have been larger.

The volume fractions estimated based on equation (2) in Fig.3. The descriptive growth factors in water and ethanol in each case are taken from Table 1. Thus, these results describe the average composition inferred by the TDMA method.
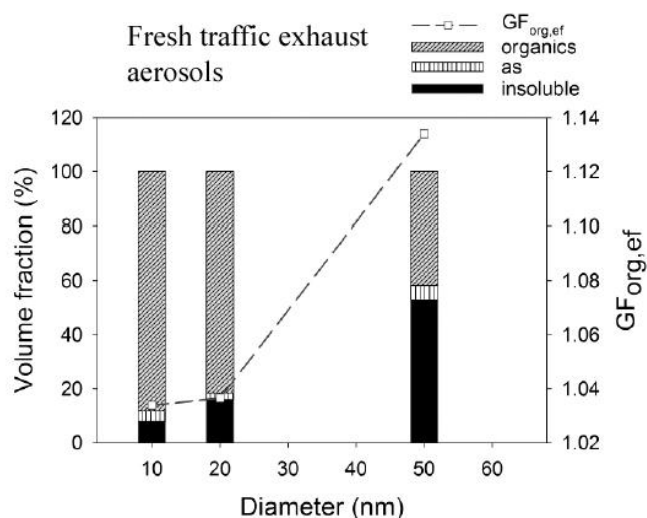
Figure 3: The organic, ammonium sulphate (as) and insoluble volume fractions as a function of particle size. The calculations were conducted using effective organic growth factor (GF$_{org,ef}$) meaning GF$_{org}$, with 100% total closure ($\sum \varepsilon_i = 1$ in Equation 2).

The contribution of the insoluble material increases as a function of size, being typically less than 10% at 10 nm and about 50% at 50 nm, in contrast to the organic fraction, which decreased from about 80% at nucleation modes to 40% at 50 nm (Fig. 1). The average ammonium sulphate fraction, on the other hand, was low, owing to the low measured growth factors in water. During DW traffic conditions, the population was mainly internally mixed in terms of hygroscopicity. As the transport time from the traffic sources is longer, the particle population is more heterogeneous and externally mixed than during a shorter residence times after the emission from the tail pipe. Disregarding the external mixing, the average water-soluble fraction of traffic related particles was less than 10% assuming that the water-soluble material acted as ammonium sulphate. The best closure estimation was obtained assuming the organic volume to consist of slightly ethanol-soluble species.

Particles size (nm)	HGF at RH = 89%	OGF at S% = 82	Insoluble volume fraction at temperature of 280 °C
10	1.02	1.03	8 %
20	1.02	1.03	16 %
50	1.06	1.06	53 %

Table 1: Characteristics of the variation of hygroscopic (HGF), organic (OGF) growth factors and insoluble volume fraction for 10, 20 and 50 nm particles measured in the vicinity of the road when the wind blew from the nearest road at distance of 10 m towards the measurements site.

CONCLUSIONS

A suite of Tandem Differential Mobility Analyzers was applied to detect the hygroscopicity, ethanol solubility and volatility of nucleation and Aitken mode particles. With these measurements we inferred the chemically resolved size distribution of the UFP in vicinity of the road.

This work has shown that, a combination of three TDMA gives more detailed information about particle composition than traditional H-TDMA measurements, which gives information about aerosols water-soluble/insoluble fraction.

REFERENCES

Gysel, M., Crosier, J., Topping, D.O., Whitehead, J.D., Bower, K.N., Cubison, M.J., Williams, P.I., Flynn, M.J., McFiggans, G.B., Coe, H., 2007. Closure study between chemical composition and hygroscopic growth of aerosol particles during TORCH2. *Atmospheric Chemistry and Physics* 7, 6131–6144.

Hämeri, K., Väkevä, M., Hansson, H.-C., Laaksonen, A., 2000. Hygroscopic growth of ultrafine ammonium sulphate aerosol measured using an ultrafine tandem differential mobility analyser. *Journal of Geophysical Research* 105, 22231–22242.

Joutsensaari, J., Vaattovaara, P., Vesterinen, M., Hämeri, K., Laaksonen, A., 2001. A novel tandem differential mobility analyzer with organic vapor treatment of aerosol particles. *Atmospheric Chemistry and Physics* 1, 51–60.

McFiggans, G., Alfarra, M.R., Allan, J., Bower, K., Coe, H., Cubison, M., Topping, D., Williams, P., Descari, S., Faccini, C., Fuzzi, S., 2005. Simplification of the representation of the organics component of atmospheric particulates. *Faraday Discuss* 130, 341–362.

Stokes, R. H., Robinson, R. A., 1966. Interactions in aqueous nonelectrolyte solutions. I. Solute-solvent equilibria, *Journal of Physical Chemistry* 70, 2126–2130.

Tiitta P., Miettinen P., Vaattovaara P., Laaksonen A., Joutsensaari J., Hirsikko A., Aalto P., Kulmala M., 2007. Road-side measurements of aerosol and ion number size distributions: A comparison with remote site measurements. *Boreal Environmental Research* 12, 311–321.

Vaattovaara, P., Räsänen, M., Kühn, T., Joutsensaari, J., Laaksonen, A., 2005b. A method for detecting the presence of organic fraction in nucleation mode sized particles. Atmospheric Chemistry and Physics 5, 3277–3287.

HIGH-TIME-RESOLUTION MEASUREMENTS OF WATER-SOLUBLE ORGANIC CARBON AT AN URBAN SITE IN HELSINKI, FINLAND

H. Timonen[1], M. Aurela[1], S. Carbone[1], K. Saarnio[1], T. Mäkelä[1], M. Kulmala[2], D. Worsnop[1,2], R. Hillamo[1]

1 Finnish Meteorological Institute, Air Quality Research, P.O. Box 503, FI-00101 Helsinki, Finland
2 Department of Physical Sciences, FI-00014 University of Helsinki, Finland

INTRODUCTION

The thorough knowledge on chemistry of atmospheric aerosol particles is needed to understand the effect of multiphase and multi-component aerosol particles on the earth's radiative budget and climate. During the last few years increasing attention has been focused to the carbonaceous fraction (organic carbon, OC and elemental carbon, EC) of atmospheric aerosols. The organic compounds in atmospheric aerosols can be further divided to water-soluble compounds (WSOC) and water-insoluble compounds (WISOC). Large fraction of WSOC is assumed to be SOA formed by condensation of atmospheric oxidation products of VOCs or via gas-to-particle conversion (e.g. Kondo et al., 2007, Pio et al., 2007). Both processes are generally dependent on the atmospheric conditions like temperature, radiation, photo-oxidants, amount of water vapor and other condensable gases (Fuzzi et al., 2006). WSOC comprises typically 20-70% of OC (Pio et al., 2007). The identified sources or formation mechanisms of WSOC are e.g. biomass burning, soil particles, aged sea salt and in-cloud processing (Huang et al., 2007). Particulate water-soluble organic matter is expected to affect the chemical and physical properties of aerosols e.g. hygroscopic behaviour (the ability of particles to act as CCN), acidity, and radiative properties (Jacobson et al., 2000). Despite the evident significance of OC and WSOC in atmospheric chemistry and physics, information concerning their concentration, size distribution and seasonal variation is limited. Also the sources and formation mechanisms of water-soluble organic compounds are not well known.

The aim of this work was to improve the online PILS-WSOC-method and to use it in measuring WSOC concentrations of atmospheric aerosols with a time resolution comparable with other online instruments, e.g. aerosol mass spectrometer. The first field campaign was carried out during winter.

METHODS

The measurements were conducted in Helsinki, Finland at an urban background station (SMEARIII, 60°12'N, 24°58'E, 26 m above sea level). The site is located 5 km northeast from the centre of Helsinki. The most important local source of fine particulate matter is traffic since a densely trafficked major road (60 000 vehicles/day) is situated at a distance of 200 m to the east. However, the contribution of regional residential wood combustion may be substantial during winter.

During the winter campaign the chemical composition of aerosol particles in the submicron size range was measured with an aerosol mass spectrometer (HR-ToF-AMS, Aerodyne Research Inc.; Jayne et al., 2000), a semi-continuous organic and elemental carbon analyzer (OC/EC; Bae et al., 2004), and two Particle-Into-Liquid-Samplers (PILS, Orsini et al., 2003) one coupled with two ion chromatographs (IC) (for cation and anion analysis) and the other coupled with a total organic carbon analyzer (TOC analyzer, Shimadzu, Model TOC-V$_{CPH}$). In the online PILS-WSOC-method the PILS is used to feed the sample directly to the TOC-V$_{CPH}$ analyzer. The time-resolution of the WSOC measurement was about 6 minutes. The WSOC data was averaged over one hour to enable the comparison with the slower measurements.

The online WSOC measurements were conducted for three weeks, from the January 20th to February 10th., 2009. The measured WSOC concentrations were typically between 0.1 and 3.6 μg m-[3] (Fig 1). The measured carbon concentration (WSOC) has to be multiplied by the assumed organic-matter to organic carbon ratio to achieve the amount of water-soluble particulate organic matter (WSPOM). In this study a preliminary multiplier of 1.6 has been used following a recommendation of Turpin et al. (2001), but the exact multiplier can be extracted later from the AMS data. The AMS measures directly the particulate organic matter. Measured water-soluble particulate organic matter (WSPOM) concentrations show clearly similar general trend with particulate organic matter (POM) concentrations measured by the AMS. The WSOC/OC –ratio was typically between 0.35 and 0.75, on average the measured WSOC contributed 55% to the measured OC concentration.
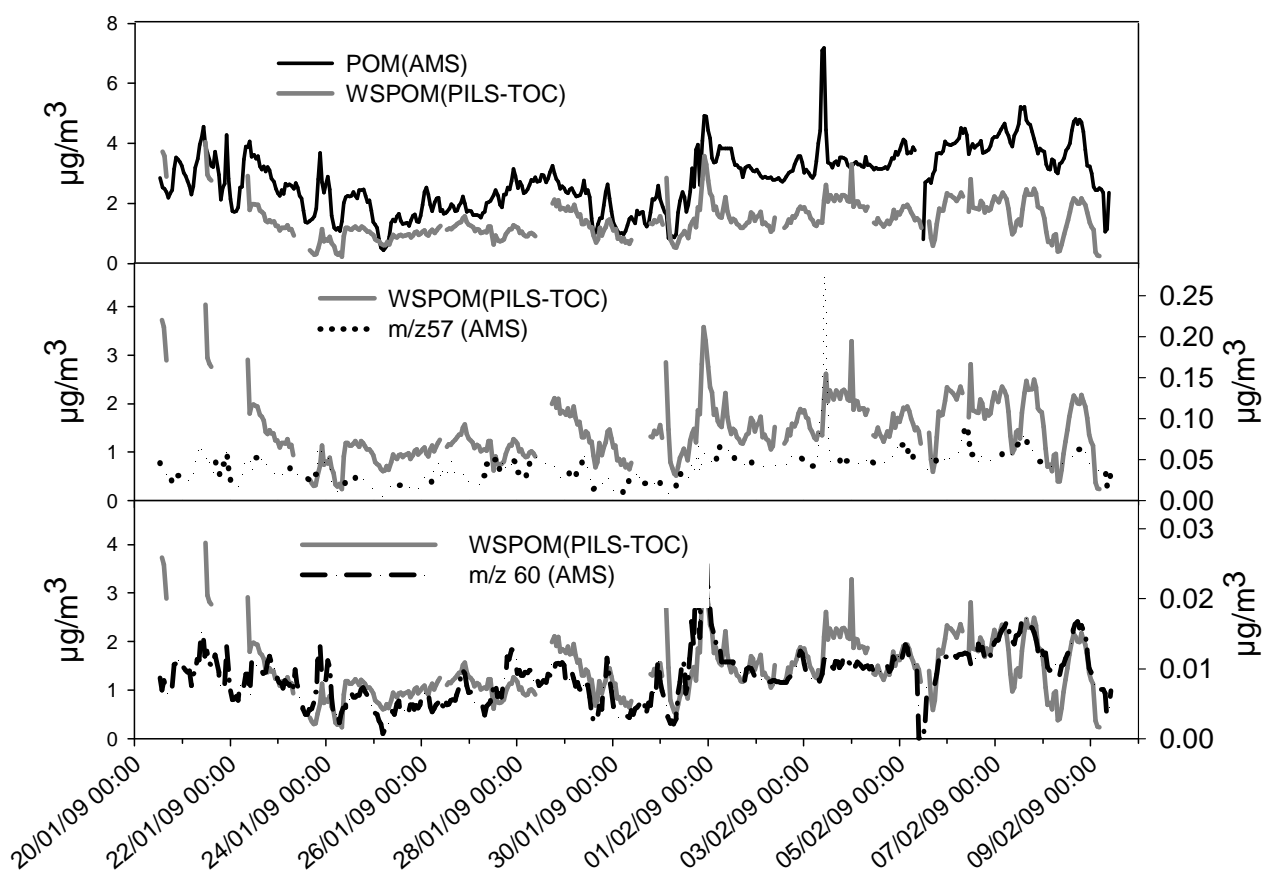
Fig 1. The measured water-soluble particulate organic matter (PILS-TOC, 1-hour average) and particulate organic matter concentration, m/z 57 and m/z 60 results (AMS, 1-hour average) from January 20th to February 10th, 2009.

To to assess the source of WSPOM, the results were compared to m/z 57 and m/z 60 data measured by the AMS. Previous studies have shown that signal at m/z 57 is dominated by hydrocarbon-like combustion aerosols (e.g. diesel exhausts) and the signal at m/z 60 is a tracer for wood combustion (Lanz et al. 2007). The m/z 60 shows clearly similar trend with WSPOM, indicating that in winter wood combustion is clearly the major source of WSPOM.

CONCLUSIONS

WSOC concentrations were successfully measured for three weeks with the PILS-WSOC method with 6 minutes time-resolution. The changes in WSOC concentrations in the urban polluted atmosphere are rapid (Fig 1) and clearly there is a need for on-line measurements in order to detect these changes and connect them to distinct sources of organic carbon.

ACKNOWLEDGEMENTS

REFERENCES

Bae, M., Schauer, J., DeMinter, J., Smith, D., & Carry, R. (2004). Validation of a semi-continuous instrument for elemental carbon and organic carbon using a thermal-optical method. Atmos. Environ. 38, 2885-2893.

Jayne, J.T., Leard, D.C., Zhang, X., Davidovits, P.,Smith, K.A., Kolb, C.E. & Worsnop, D.R. (2000). Development of an Aerosol Mass Spectrometer for Size and Composition Analysis of Submicron Particles, Aerosol Sci. Technol. 33, 49-70.

Orsini, D., My, Y., Sullivan, A., Sierau, B., Baumann, K., & Weber, R. (2003). Refinements to the particle-into-liquid sampler (PILS) for ground and airborne measurements of water-soluble aerosol composition. Atmos. Environ. 37, 1243-1259.

Fuzzi, S., Andreae, M.O., Huebert, B.J., Kulmala, M., Bond, T.C., Boy, M., Doherty, S.J, Guenther, A., Kanakidou, M., Kawamura, K., Kerminen, V.-M., Lohmann, U., Russell, L.M., and Pöschl, U. (2006). Critical assessment of the current state of scientific knowledge terminology, and research needs concerning the role of organic aerosols in the atmosphere, climate, and global change, Atmos. Chem. Phys. 6, 2017-2038.

Huang, X.-F., Yu, J.Z., He, L.-Y., and Yuan, Z. (2006). Water-soluble organic carbon and oxalate in aerosols at a coastal urban site in China: Size distribution characteristics, sources, and formation mechanisms, J. Geophys. Res. 111, D22212,doi:10.1029/2006JD007408.

Jacobson, M.C., Hansson, H.-C., Noone, K.L., and Charlson, R.J.(2000) Organic atmospheric aerosols: Review and state of the science, Rev. Geophys. 38, 267–294.

Kondo, Y., Miyazaki, Y., Takegawa, N., Miyakawa, T., Weber, R.J., Jimenez, J.L., Zhang, Q., and Worsnop, D.R. (2007): Oxygenated and water-soluble organic aerosols in Tokyo, J. Geophys. Res., 112, D011203, doi:10.1029/2006JD007056.

Lanz, V.A., Alfarra, M.R., Baltensberger, U., Buchmann, B., Hueglin, C., Prévôt, A.S.H. (2007). Source apportionment of submicron organic aerosols at an urban site by factor analytical modelling of aerosol mass spectra, Atmos. Chem. Phys. 7, 1503-1522.

Pio, C. A., Legrand, M., Oliveira,T., Afonso, J., Santos, C., Caseiro, A., Fialho, P.,Barata, F., Puxbaum, H., Sanchez-Ochoa, A., Kasper-Giebl, A., Gelencse´r, A.,Preunkert, S., and Schock, M. (2007). Climatology of aerosol composition (organic versus inorganic) at nonurban sites on a west-east transect across Europe, J. Geophys. Res., 112, D23S02, doi:10.1029/2006JD008038.

Turpin, B.J. and Lim, H.-J. (2001). Species contributions to PM2.5 mass concentrations: revisiting common assumptions for estimating organic mass, Aerosol Sci. Technol., 35, 602-610.

HYDRATION OF HSO$_5$ AND PARTICIPATION OF H$_2$S$_2$O$_8$ IN NUCLEATION

M. TOIVOLA[1], T. KURTÉN[1], T. BERNDT[2], I. K. ORTEGA[1],
V. LOUKONEN[1], H. VEHKAMÄKI[1], M. KULMALA[1]

[1]Department of Physics, P.O. Box 64, FI-00014, University of Helsinki, Finland
[2]Institute for Tropospheric Research, Permoserstrasse 15, D-04318 Leipzig, Germany

INTRODUCTION

Sulfuric acid is a key component in atmospheric aerosol formation. Recently, Berndt et al. (2005, 2008) have experimentally observed the formation of new particles in the H$_2$SO$_4$/H$_2$O system. They found that sulfuric acid produced in situ via the reaction of OH radicals with SO$_2$ in the presence of water vapor nucleates much more effectively than sulfuric acid evaporated from a liquid reservoir. The experimental results (Laaksonen et al. 2008) give reason to expect that reaction intermediates of sulfuric acid formation and their alternative reaction products could be involved in particle formation.

A necessary but not sufficient condition for some molecule to enhance H$_2$SO$_4$ nucleation by complexation is that it binds to H$_2$SO$_4$ more strongly than another H$_2$SO$_4$ molecule. According to calculations by Salonen et al. (2009), the sulfuric acid-peroxodisulfuric acid (H$_2$S$_2$O$_8$) dimer is more stable than the sulfuric acid dimer with respect to the electronic energy, while none of the postulated intermediate or alternate reaction products containing only one sulfur atom were able to fulfill the minimum condition mentioned above. This indicates that the experimental results are likely to be explained by the participation in nucleation of compounds containing two or more sulfur atoms, such as, but not necessarily limited to, H$_2$S$_2$O$_8$.

Experimental results (Berndt et al. 2008) indicate that the nucleation rate from the SO$_2$ + OH mixture is independent of whether OH is produced from ozone, water vapor and UV light, or from chemical reactions in the absence of ultraviolet light. Also, a SO$_3$ + H$_2$O mixture nucleates no better than the corresponding amount of sulfuric acid. These observations indicate, on one hand, that no direct photochemistry of sulfur – containing molecules is likely explain the observed nucleation rate, and on the other hand that the key steps must involve reactants that lie before SO$_3$ on the SO$_2$ oxidation chain. Based on the known mechanism of SO$_2$ oxidation (Wayne 2000) there are thus only two alternatives: the HSO$_3$ and HSO$_5$ radicals. Since the concentration of HSO$_3$ is almost certainly very low due to its efficient reaction with O$_2$ to form HSO$_5$, the observed nucleation mechanism is thus very likely to involve as a key step the reaction of HSO$_5$ with some other molecule, leading (either directly or via more steps) to the formation of efficiently nucleating products. For example, self-reaction of HSO$_5$ would form H$_2$S$_2$O$_8$ (plus an oxygen molecule).

A central uncertainty in any nucleation mechanism involving HSO$_5$ is the lifetime of this metastable intermediate radical. Previous modeling studies have predicted the dissociation of HSO$_5$ into SO$_3$ and HO$_2$ to be very rapid, leading to a short lifetime of HSO$_5$, and a low net yield for the pathways forming alternative reaction products such as H$_2$S$_2$O$_8$. However, these studies have not accounted for the effect of hydration on the stability of HSO$_5$.
In this study, we have investigated both the growth energetics of H$_2$SO$_4$-H$_2$S$_2$O$_8$ clusters, and studied the effect of hydration on the stability (and thus, lifetime) of HSO$_5$.

METHODS

Calculations on larger clusters have been performed using a systematic multi-step method. The initial molecule and cluster geometries are taken from earlier computational studies (Ortega et al. 2008, Salonen et al. 2009) or generated with the DL_POLY_2 (Smith et al. 2002) molecular dynamics program. The structures are optimized (and the vibrational frequencies calculated) with the SIESTA (Soler et al. 2002)

program, using the BLYP functional with a DZP basis set and corresponding pseudopotentials. Finally, we calculated single point energies using the TURBOMOL (Ahlrich et al. 1989) program suite. Energies were computed at the RI-MP2/aug-cc-pV(T+d)Z level (Dunning et al. 2001)

Hydrates of HSO_3, HSO_5, HO_2 and SO_3 have been studied at the G3B3 (mono- and dihydrates) and UCCSD(T)/aug-cc-pV(T+d)Z//UB3LYP/6-311++G(3d,3p) level (monohydrates only) using the Molpro 2006.1 program (Werner et al. 2006) for the coupled-cluster energy calculations and the Gaussian 03 program suite (Frisch 2004) for all other steps.

Reaction		ΔE
$(H_2SO_4)_3 + H_2SO_4$	$(H_2SO_4)_4$	-18,7
$(H_2S_2O_8)\bullet(H_2SO_4)_2 + H_2SO_4$	$(H_2S_2O_8)\bullet(H_2SO_4)_3$	-19,7
$(H_2S_2O_8)_2\bullet(H_2SO_4) +$	$(H_2S_2O_8)_2\bullet(H_2SO_4)_2$	
H_2SO_4		-20,9

Table 1. Electronic energies of sulfuric acid addition reaction in units of kcal mol-1

RESULTS

The electronic energies for the addition of sulfuric acid to various cluster types is shown in Table 1. It can be seen from the Table that the energy of the sulfuric acid addition reaction decreases (becomes more negative) when we replace one or two sulfuric acids with peroxodisulfuric acid molecules. Thus, the addition of sulfuric acid to a cluster containing peroxodisulfuric acid is more favorable than the addition to a pure sulfuric acid cluster. The cluster structures studied here are shown in Fig. 1. To obtain a realistic picture of the stability of clusters in the atmosphere we also need to consider the free energies. We are in the process of calculating the Gibbs free energy values for the addition reactions.
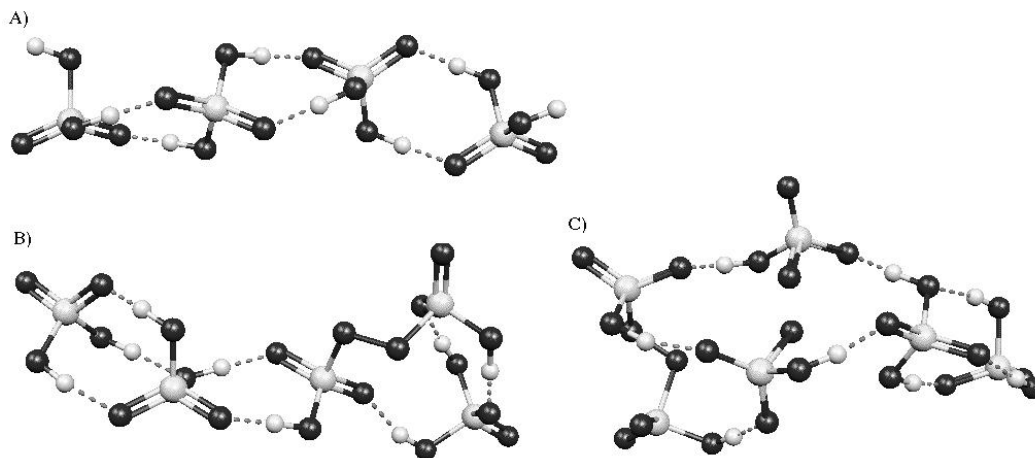
Figure 1. Schematic structure of the most stabile clusters: A) $(H_2SO_4)_4$ B)$(H_2S_2O_8)\bullet(H_2SO_4)_3$ C) $(H_2S_2O_8)_2\bullet(H_2SO_4)_2$

High-level quantum chemical calculations (Kurten et al. 2009) demonstrate that HSO_5 is much more strongly hydrated than SO_3 and HO_2, leading to a significant increase in its lifetime with respect to dissociation. Due to hydration, the stability of HSO5 with respect to dissociation is increased by several kcal/mol in ambient conditions. At least partial proton transfer from HSO_5 to H_2O is predicted to occur in the $HSO_5(H_2O)_2$ cluster, which may have important implications for the reactivity of hydrated HSO_5. Kinetic modeling assuming an efficient self-reaction for $HSO_5(H_2O)_2$ (and using the computed evaporation rates for various hydrates) indicates that this mechanism could, in principle, explain the experimentally observed particle formation rate.

REFERENCES

Ahlrichs, R., Bär, M., Häser, M., Horn, H., and Kölmel, C. (1989) electronic-structure calculations on workstation computers - the program system turbomole, Chem. Phys. Lett. 162, 165-169.

Berndt, T., Böge, O., Stratmann, F., Heintzenberg, J., & Kulmala, M. (2005) Rapid formation of sulfuric acid particles at near-atmospheric conditions, Science. 307(5710), 698-700.

Berndt, T., Stratmann, F., Bräsel, S., Heintzenberg, J., Laaksonen, A., and Kulmala M. (2008) SO_2 oxidation products other than H_2SO_4 as a trigger of new particle formation. Part 1: Laboratory investigations, Atmos. Chem. Phys., 8, 6365-6374.

Dunning Jr., T. H., Peterson, K. A., and Wilson, A. K. (2001) Gaussian basis sets for use in correlated molecular calculations. X. The atoms aluminum through argon revisited ,J. Chem. Phys. 114, 9244-9253.

Frisch, M. J., et al. (2004) Gaussian 03, Gaussian, Inc., Wallingford CT, U.S.A.

Kurtén, T., Berndt, T., and Stratmann, F. (2009) Hydration increases the lifetime of HSO5 and enhances its ability to act as a nucleation precursor – a computational study, Atmos. Chem. Phys. Discuss. 9, 2823-2853.

Laaksonen, A., Kulmala, M., Berndt, T., Stratmann, F., Mikkonen, S., Ruuskanen, A, Lehtinen, K. E. J., Dal Maso, M., Aalto, P., Petäjä, T., Riipinen, R., Sihto, S.-L., Janson, R., Arnold, F., Hanke, M., Ücker, J., Umann, B., Sellegri, K., O'Dowd, C. D. , and Viisanen, Y. (2008) SO2 oxidation products other than H2SO4 as a trigger of new particle formation. Part 2: Comparison of ambient and laboratory measurements, and atmospheric implications, Atmos. Chem. Phys., 8, 7255-7264.

Ortega, I. K., Kurtén, T., Vehkamäki, H., and Kulmala, M (2008) The role of ammonia in sulfuric acid ion induced nucleation, Atmos. Chem. Phys. Discuss. 8, 5413-5436.

Salonen, M., Kurten, T., Vehkamaki, H., Berndt, T., and Kulmala, M., (2009) Computational investigation of the possible role of some intermediate products of SO2 oxidation in sulfuric acid-water nucleation, Atmospheric Research 91 (1), 47-52.

Smith, W., Yong, C. W., Rodger, P.M. (2002) DL_POLY: Application to molecular simulation, Molecular Simulations 28 385-471

Soler, J. M., Artacho, E., Gale, J. D., Garcia, A., Junquera, J., Ordejon, P., and Sanchez-Portal, D. (2002) The SIESTA method for ab initio order-N materials simulation, J. Phys. Condens. Mat. 14, 2745-2779.

Wayne, R. P. (2000) Chemistry of atmospheres: an introduction to the chemistry of the atmospheres of earth, the planets and their satellites, Oxford: Oxford University Press.

Werner, H.-J., et al. (2006) MOLPRO, version 2006.1, a package of ab initio programs, see http://www.molpro.net.

COMPARISON BETWEEN INVENTORY BASED AND TERRESTRIAL BIOSPHERE MODELLING OF EUROPEAN FOREST CARBON BALANCE

B. ŤUPEK[12], H. VERKERK[2], G. ZANCHI[3], G. CHURKINA[4], N. VIOVY[5], J. HUGHES[6], and M. LINDNER[2]

[1] Department of Forest Ecology, Latokartanonkaari 7, FI-00014University of Helsinki, Finland
[2] European Forest Institute, Torikatu 34, 80100 Joensuu, Finland
[3] Joanneum research Forschungsgesellschaft mbH, Steyrergasse 17-19, 8010 Graz, Austria
[4] Max-Planck Institut für Biogeochemie, Hans-Knoell-Strasse 10, 07745 Jena, Germany
[5] Laboratoire des Sciences du Climat et de l'Environnement, CEA CNRS UVSQ, 91191 Gif sur Yvette, Franc
[6] Met Office Hadley Centre, FitzRoy Road, Exeter, Devon, EX1 3PB, United Kingdom

Keywords: EFISCEN, BIOME - BGC, ORCHIDEE, JULES

ABREVIATIONS

Europe: Austria, Belgium, Bulgaria, Czech Republic, Denmark, Estonia, Finland, France, Germany, Hungary, Ireland, Italy, Latvia, Lithuania, Luxemburg, Malta, Netherlands, Poland, Portugal, Romania, Slovakia, Slovenia, Spain, Sweden, United Kingdom, Norway, and Switzerland

NPP: net primary production ($gC/m^2/y$)
NEP: net ecosystem production ($gC/m^2/y$)
NBP: net biome production ($gC/m^2/y$)

EFISCEN - European Forest Information SCENario model, a forest inventory based carbon model
BIOME-BGS - a terrestrial ecosystem model describing the carbon, nitrogen and water
ORCHIDEE - a process-oriented integrated global terrestrial carbon cycle and water model
JULES - Joint UK Land Environment Simulator; a process-based terrestrial carbon cycle model

INTRODUCTION

The atmosphere-biosphere carbon balance has been intensively studied to quantify individual fluxes with the aim to reduce the ambient level of CO_2 in the atmosphere (Kyoto protocol 2009, IPCC 2007). The forest have a natural ability to utilize CO_2 from the atmosphere and generally to sequester C in the organic material (Schulze et al., 1999; Nabuurs et al., 2003, Janssens et al., 2003). The European forest C balance has been studied in various projects over Europe. Some studies used ground measurements particularly forest inventory data to reconstruct the biomass growth; others used continuous measurements of meteorological factors to reconstruct CO_2 fluxes.

The comparison of two approaches can help to find the plausible European forest estimate of C balance. On the one hand side, the modelling approach based on the forest inventory data represented model Efiscen (Nabuurs et al., 2000; Schelhaas et al., 2007). On the other hand side, the terrestrial modelling approach based on meteorological data represented BGC-Biome (Running and Gower, 1991; Thornton, 1998), Orchidee (Krinner et al., 2005), and Jules (http://www.jchmr.org/jules/). The main difference between the inventory based and terrestrial bio-geo-chemistry models are the data used for modelling and the validation of C fluxes (dense network of ground level forest biomass measurements used in Efiscen, and scarcer measurements of ecosystem level CO_2 fluxes with meteorological data used in BGC-Biome, Orchidee, and Jules).

The atmospheric CO_2 sink of forests makes them act as 'coolers' in the battle of redeeming the increasing global temperature. Though, higher temperature in boreal zone increases the possibility of forest to lose more carbon by respiration than to gain the carbon by photosynthesis (Lindroth et al., 1998).

We aim to provide the components of C balance and investigate the effect of management across countries and regions of Europe, by using Efiscen, because the forest management and measurements of forest increment are included only in Efiscen. Further we aim to provide comparison between inventory based and biosphere modelling approaches of C balance estimation.

In Efiscen, the measured net forest increment is providing ground reference for the modelling of heterotrophic respiration (HR). The HR values in global scale models of BGC-Biome, Orchidee, and Jules contains the C flux components of various ecosystems together making uncertain separation between forest, grassland, or mire at the regional and local level. The HR aggregation over the large area is propagating into larger difference of NEP estimates between two modelling approaches. In order to compare the modelling approaches, we use NPP as the flux without HR suitable for the minimizing the effect of aggregation of ecosystems.

METHODS

The focus of this study is on the components of the forest carbon cycle (NPP, NEP, and NBP) for 26 European countries and regions (Table 1). Especially, we studied the effect of increasing and lowering the intensity of forest management, and comparison between an inventory based model Efiscen and the process-based terrestrial models BGC-Biome, Orchidee, and Jules.

Country	Forest area (1000 ha)	Regions	Country	Forest area (1000 ha)	Regions
Austria	3354	8	Lithuania	1757	1
Belgium	673	2	Luxembourg	86	1
Bulgaria	2257	1	Netherlands	286	1
Czech	2560	14	Norway	6644	17
Denmark	344	1	Poland	8334	17
Estonia	2103	1	Portugal	949	1
Finland	21846	2	Romania	5615	1
France	14275	22	Slovakia	1770	1
Germany	10648	13	Slovenia	1159	1
Hungary	1576	1	Spain	10476	1
Ireland	432	1	Sweden	22472	6
Italy	7495	1	Switzerland	1140	5
Latvia	2807	1	United Kingdom	2202	4

Table 1. The number of regions of 26 European countries used by Efiscen, BGC-Biome, Orchidee, and Jules. The total forest area used by Efiscen.

Fluxes of the carbon cycle

From the components of forest C balance, the most common forest C flux is the net primary production (NPP) calculated by all models. The NPP values are including the gross primary production (GPP) and the autotrophic respiration (AR), which is a sum of maintenance (MR) and growth (GR) respiration. Once NPP has been calculated, the litterfall provides input to the soil carbon pools and soil respiration. The amount of heterotrophic respiration (HR) efflux from NPP determines the net ecosystem production (NEP). The remaining C flux after harvesting forest biomass (removals) in forests available for wood supply is net biome production (NBP). Natural disturbance of vegetation and soil C storage determines NBP in natural forests.

Description of models

EFISCEN (The European Forest Information SCENario model) (Schelhaas et al., 2007) projects forest resource development on a given forest area and for a given demand for wood and management regime at European, national or regional scale (Karjalainen et al., 2003). The forest area is derived from national

forest inventories along with the average growing stock and the annual increment. The forest area is divided into forest types that are defined by region, owner class, site class and/or tree species. The number of forest types differs per country and the detail level of the forest inventory data determines how many forest types can be distinguished. European wide data are gathered in the EFISCEN European Forest Resource Database (Schelhaas et al., 2006).

EFISCEN projects stem wood volume, increment, age-class distribution, removals, forest area, natural mortality and dead wood for every five year time-step. With the help of biomass expansion factors, stem wood volume is converted into whole-tree biomass and subsequently to whole tree carbon stocks. Information on litterfall rates, felling residues and natural mortality is used as input into the soil module YASSO (Liski et al., 2005), which is dynamically linked to EFISCEN and delivers information on forest soil carbon stocks.

BIOME-BGC is a terrestrial ecosystem model describing the carbon, nitrogen and water cycles (Thornton, 1998; Running and Gower, 1991). It has been corroborated for a number of hydrological and carbon cycle components as well as for forest management (Churkina et al. 2003; Hasenauer 1999; Vetter et. al., 2005). The model can be parameterized for seven biomes including evergreen needleleaf, evergreen broadleaf, deciduous needleleaf, deciduous broadleaf, shrubs, and grass (C3 and C4 type photosynthesis) as well as fertilized grasses. For this study model we used version model 4.1.1 with carbon and nitrogen allocation routine from 4.1. Parameters for evergreen needleaf and deciduous broadleaf forests were optimized from field measurements of net carbon fluxes (Trusilova et al. 2009). Forest management was not included in the simulations due to lack of regional inventories of forest age structure.

ORCHIDEE (Krinner et al., 2005) is a process-oriented integrated global land-surface model consisting of three submodules: a global land surface scheme (Ducoudré et al., 1993), a global continental carbon cycle model and a dynamic model of long-term vegetation dynamics including competition and disturbances based on LPJ (the latter module being switched off in the present study). The model simulates the turbulent fluxes of CO2, water and energy at a half-hourly time step, while the ecosystem carbon and water dynamics (allocation, plant respiration, growth, mortality, soil organic matter decomposition, water infiltration and runoff) are calculated at a daily time step.

JULES (Joint UK Land Environment Simulator; http://www.jchmr.org/jules/) is a process-based surface exchange scheme, including a dynamic representation of vegetation and the terrestrial carbon cycle. Its predecessor, MOSES 2.1 (Cox et al, 1999) was the land surface exchange scheme in the Met Office climate model but JULES has been released as a separate community model. JULES also includes an improved representation of radiative transfer through vegetation canopy (Mercado et al, 2007).

JULES calculates the surface energy balance and hydrological cycle and as such only requires near surface meteorology data (shortwave and longwave radiation fluxes, air temperature, precipitation, wind speed, humidity and air pressure), the atmospheric CO2 concentration and soil hydraulic properties. From these JULES produces estimates of carbon storage (vegetation PFTs and soil pools), LAI, NPP, GPP, litter fall and soil respiration. Photosynthesis rates are predicted based on the Collatz et al, 1991, 1992 relationships (Cox et al, 1998).

RESULTS

The preliminary results of regional NPP values (all in $gC/m^2/y$) in year 2005 for total, broadleaved and coniferous forest showed an East-West belt of higher levels in central Europe. According to forest inventory based model Efiscen, especially regions of Germany, Austria, and Czech Republic had the highest rates of total annual NPP (from 754 to 914 on averages). Highest of all forests, the NPP values of Efiscen coniferous forest (top NPP in Belgium, Flamande 1569) stretched further from central Europe to west towards regions of France 761±173, and also to east towards Hungary 831, Romania 902, and Bulgaria 1183. The total, broadleaved and coniferous forest NPP values of terrestrial models are lower than the estimates from the forest inventory model. For total forests was the maximum NPP of Biome-BGC 793 found in France, region of Haute-Normandie, the maximum NPP of Orchidee was 658 in Czech,

Jihlavsky region, and Jules showed maximum NPP 597 also in France, Aquitaine region. The regional NPP values for total, broadleaved and coniferous forest of Biome-BGC were at the similar level from 500 to 750 with an increase for broadleaved forest to a higher level until 1000 at the Atlantic coast of middle Europe. The band of higher NPP values modelled by Orchidee was shifted Northward in comparison to the location of higher levels of Biome-BGC, and Jules. Especially for broadleaved forests, Jules showed the concentration of larger NPP from 500 to 750 only in western EU regions of France, Germany, and Benelux, while eastern European regions were at the lower level from 250 to 500. In contrary to Efiscen, Jules did not show increased NPP belt across the middle Europe. The apparent difference between forest inventory and terrestrial models was the level of saturation for the regional NPP (Figure 1). The maximum regional NPP of Efiscen was 1256 for total, 1171 broadleaved, and 1569 coniferous forests, whereas the maximum regional NPP of terrestrial models did not surpasses the maximum level of 683±100, 669±157, and 595±85 respectively. While average regional NPP of terrestrial models showed similar values for coniferous 467±105 and broadleaved forest 468±136, the Efiscen average regional NPP was 83 higher for coniferous than for broadleaved forest. Therefore, for broadleaved forest the lower regional NPP values of Efiscen fit better with the regional NPP values of Biome-BGC, Orchidee, and Jules. The level of Biome-BGC regional NPP for broadleaved forest was on average 611±171, what was closer to Efiscen 623±187, than to other terrestrial models 395±118. The modelled NPP for broadleaved and for coniferous forests was correlated best between Efiscen and Biome-BGC (R^2 = 0.4 and 0.57), for Orchidee the correlation was better for broadleaved forest R^2 = 0.61), and for Jules better correlation was for coniferous (R^2 = 0.59). For the regions of total forests was the R^2 between Efiscen and Biome-BGC 0.59, between Efiscen and Orchidee 0.27, and between Efiscen and Jules 0.44.
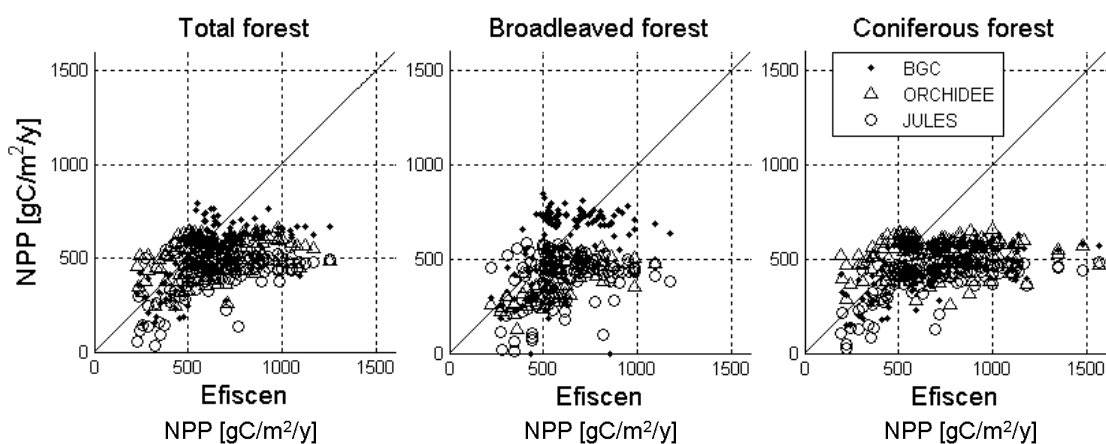
Figure 1. Scatter plot of modelled NPP between Efiscen versus Biome-BGC, Orchidee, and Jules for coniferous, broadleaved and total forest of European regions in year 2005.

The preliminary results of national NPP values (all in gC/m²/y) in year 2005 for total forests modelled by the Biome-BGC, Orchidee, and Jules - terrestrial models were generally lower than those modelled by the Efiscen - forest inventory based model (Figure 2). On the average of all models of European countries (EU25 including Norway and Switzerland, and excluding Greece) showed the NPP level 532±154 (Efiscen 664±197, Biome-BGC 534±110, Orchidee 505±91, and Jules 425±92). Efiscen NPP values were larger than others especially for Switzerland 933, while the average of Biome-BGC, Orchidee, and Jules was 423±53. The only case, when the Efiscen NPP value 237 was less then the others, 335 on average, was Spain. Spain had lowest NPP value 310 on average of all models of European countries. The highest NPP 703 was associated with Luxembourg instead, though Czech Republic, Germany, and Austria had high levels of NPP too (636, 627 and 625). Models did not identify the same country with lowest and highest NPP. The country of Efiscen with lowest NPP was 236 of Spain and the highest one was 988 of

Austria. Minimum and maximum NPP of all countries for Biome-BGC were Norway 267 versus Belgium 672, Italy 331 versus Luxemburg 656 for Orchidee, and Finland 198 versus Belgium 552 for Jules.
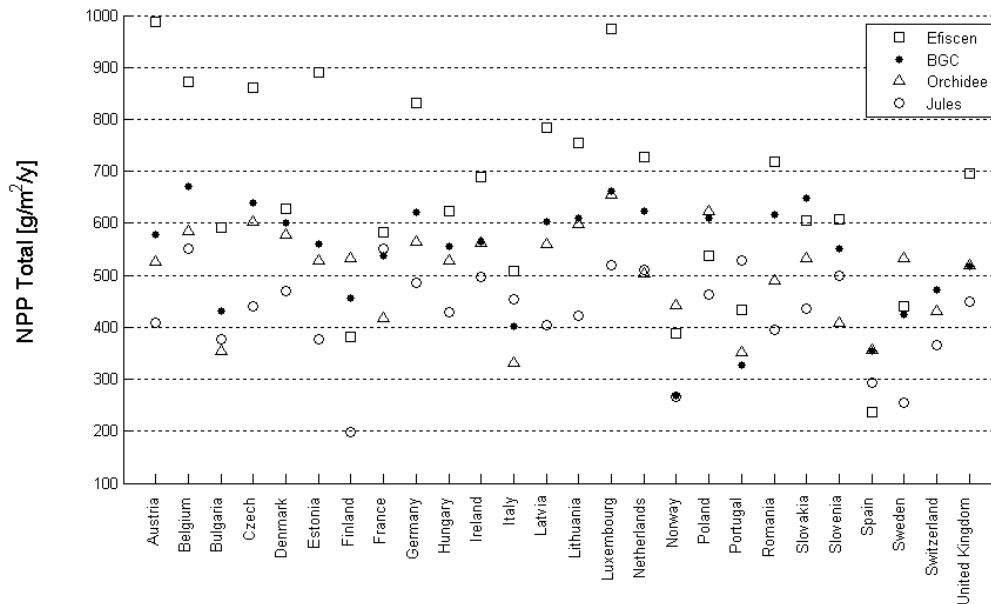
Figure 2. The comparison of modelled NPP [gC/m^2/y] between Efiscen, Biome-BGC, Orchidee, and Jules for the total forest of European countries in year 2005.

REFERENCES

Cox, P.M., Huntingford, C., and Harding, R.J. (1998): A canopy conductance and photosynthesis model for use in a GCM land surface scheme, *J. Hydrology*, 212-213, pp 79-94

Cox, P.M., Betts, R.A., Bunton, C.B., Essery, R.L.H., Rowntree, P.R., and Smith, J. (1999): The impact of new land surface physics on the GCM simulation of climate and climate sensitivity, *Climate Dynamics*, 15, pp 183-203

Churkina, G., Tenhunen, J., Thornton, P.E. (2003) Analyzing the ecosystem carbon dynamics of four European coniferous forest using a biogeochemistry model. *Ecosystems*, 6, 168-184.

Ducoudre, N. I., K. Laval, and A. Perrier, 1993: SECHIBA, a new set of parameterizations of the hydrologic exchanges at the land/atmosphere interface within the LMD atmospheric general circulation model. J. *Climate*, 6, 248–273.

Hasenauer H, Nemani RR, Schadauer K, Running SW (1999) Forest growth response to changing climate between 1961 and 1990 in Austria. *Forest Ecology and Management*, 122, 209-219.

IPCC (2007). IPCC Fourth assessment report: Climate Change 2007 Synthesis Report <http://www.ipcc.ch/pdf/assessment-report/ar4/syr/ar4_syr.pdf> (1/4/2009).

Janssens, I. A., A. Freibauer, P. Ciais, P. Smith, G. J. Nabuurs, G. Folberth, B. Schlamadinger, R. W. A. Hutjes, R. Ceulemans, E. D. Schulze, R. Valentini, and A. J. Dolman. (2003). Europe's terrestrial Biosphere Absorbs 7 to 12 % of European anthropogenic CO2 emissions. *Science* 300: 1438-1541.

Karjalainen, T., Pussinen, A., Liski, J., Nabuurs, G.J., Eggers, T., Lapvetelainen, T., Kaipainen, T. (2003). Scenario analysis of the impacts of forest management and climate change on the European forest sector carbon budget. *Forest Policy and Economics* 5: 141-155. doi:10.1016/S1389-9341(03)00021-2

Krinner, G., Viovy N. , deNoblet-Ducoudr´ e, N., Og´ee, J., Polcher, J., Friedlingstein, P., Ciais, P., Sitch, S., and Prentice, I. (2005) A dynamic global vegetation model for studies of the coupled atmosphere-biosphere system, *Glob. Biogeochem. Cyc.,* 19(1), GB1015, 20 doi:10.1029/2003GB002199.

Lindroth A., Grelle A. and Morén A.S., (1998). Long-term measurements of boreal forest carbon balance reveal large temperature sensitivity. *Global Change Biology*, 4:443-450.

Mercado, L.M., Huntingford, C., Gash, J.H.C., Cox, P.M., Jogireddy, V. (2007). Improving the representation of radiation interception and photosynthesis for climate model applications, *Tellus*, 59B, 553-565.

Nabuurs G-J, Schelhaas M-J, Pussinen A (2000) Validation of the European Forest Information Scenario Model (EFISCEN) and a projection of Finnish forests. *Silva Fennica*, 34, 167–179.

Nabuurs, G.J., Schelhaas, M.J., Mohren, G.M.J., Field, C.B. (2003). Temporal evolution of the European forest sector carbon sink from 1950 to 1999. *Global Change Biol.* 9, p. 152–160.

Running, S.W., Gower, S.T. (1991) FOREST-BGC, A general model of forest ecosystem processes for regional applications. II Dynamic carbon allocation and nitrogen budgets. *Tree Physiology*, 9, 147-160.

Thornton, P.E. (1998) Regional Ecosystem Simulation: Combining Surface- and Satellite-Based Observations to Study Linkages between Terrestrial Energy and Mass Budgets. University of Montana, Missoula.

Schelhaas, M.J., Eggers, J., Lindner, M., Nabuurs, G.J., Pussinen, A., Päivinen, R., Schuck, A., Verkerk, P.J., van der Werf, D.C., Zudin, S. (2007) Model documentation for the European Forest Information Scenario model (EFISCEN 3.1.3). Alterra-rapport 1559/EFI Technical Report 26, Alterra, Wageningen, 118 pp.

Schelhaas, M.J., van Brusselen, J., Pussinen, A., Pesonen, E., Schuck, A., Nabuurs, G.J., Sasse, V. (2006). Outlook for the development of European forest resources. A study prepared for the European Forest Sector Outlook Study (EFSOS). Geneva Timber and Forest Discussion Paper ECE/TIM/DP/41. UN-ECE, Geneva.

Schulze, E.-D., Lloyd, J., Kelliher, F.M., Wirth, C., Rebmann, C., Lähker, B., Mund, M., Knohl, A., Milyukova, I., Schulze, W., Ziegler, W., Varlagin, A., Valentini, R., Dore, S., Grigoriev, S., Kolle, O., and Vygodskaya, N.N. (1999): Productivity of forests in the Eurosiberian boreal region and their potential to act as a carbon sink - A synthesis. *Global Change Biology*, 5(6):703-722

Trusilova K, Trembath J, Churkina G (2009) Parameter estimation for the terrestrial ecosystem model BIOME-BGC using eddy-covariance flux measurements. Max-Planck Institute for Biogeochemistry, Jena.

Vetter M, Wirth C, Böttcher H, Churkina G, Schulze ED, Wutzler T, Weber G (2005) Partitioning direct and indirect human-induced effects on carbon sequestration of managed coniferous forests using model simulations and forest inventories. *Global Change Biology*, 11, 810-827.

UN FCCC (2009). Kyoto protocol, Official web-site of the Climate Change Secretariat. <http://unfccc.int/kyoto_protocol/items/2830.php> (1/4/2009).

TROPOSPHERIC OZONE UPTAKE INTO FORESTS OF SLOVAKIAN MOUNTAINS IN RELATION TO SYNOPTIC WEATHER PATTERNS

B. ŤUPEK[12], P. FLEISCHER[3], J. ŠKVARENINA[2], and L. TUŽINSKÝ[2]

[1] Department of Forest Ecology, Latokartanonkaari 7, FI-00014 University of Helsinki, Finland
[2] Department of Natural Environment, T. G. Masaryka 24, Technical University of Zvolen, 96053 Zvolen, Slovakia
[3] Research station of Tanap state forests, 05960 Tatranska Lomnica, Slovakia

INTRODUCTION

Naturally, tropospheric ozone (O_3) in lower atmosphere originates mainly from the photochemical reactions of the volatile organic compounds (VOC), or by the direct deposition of ozone form the stratosphere. The human origin of ozone also requires photochemical reactions of CH4, NOx, VOC, NOC - non methane organic compounds emitted especially by the fuel consumption (Závodská a Závodský 1992). The tropospheric O_3 is one of the major air pollutants of West- and Mid- European forests. The ambient levels typically show spatial and temporal variability. Winter concentrations occur from 41 to 58 ugO_3/m^3, higher in Western Europe, while during summer ozone level increases to levels typically from 84 to 120 ugO_3/m^3 (Scheel et al., 1997). The recent studies showed the reduction of the photosynthetic production and biomass accumulation, when the ambient levels of ozone were high (Emberson et. al., 2000; Wieser et. al., 2000; Matyssek et al., 2004). The experiments of ozone related reduction of photosynthesis resulted into establishing levels of ozone protection. For example, in Europe was the exposure expressed as the index AOT40, which is the ozone accumulated exposure over the threshold of 40 ppb (85.7 ugO_3/m^3) (Furher et al. 1997). The critical level for forest ecosystem is 10 ppm/h (21420 ugO_3/m^3) accumulated over the summer season during the daylight hours (Nabel, 1999). The index AOT40 has a good biological application because of a time duration and focus on the higher ozone concentrations. Though, in the conditions of elevated O_3 concentrations the forest ecosystems undergo a physiological stress and O_3 is via stomata deposited and accumulated into the plant tissues. If the tropospheric ozone would degrade the plant depends both on the ammount of O_3 entering stomata, on the O_3 uptake, and on the leaf detoxication mechanism (Heath, 1994; Wieser, 1997). Degradation is caused by the unbalance between the O_3 uptake from the atmosphere and the subsequent O_3 detoxication in the leaf mesophyl, if the ozone uptake is larger than the leaf O_3 detoxication by ascorbates. The ozone uptake (UO_3) is controlled by the opening - closing of the stomata, stomatal conductance for O_3. In this study we aimed to estimate ozone uptake levels into the mountainous coniferous forest on the elevation transect. The ozone uptake was studied in relation to the meteorological data of temperature, solar radiation and relative humidity. The modelled ozone uptake was also evaluated for differences of repeating weather patterns, based on the assumption that synoptic types show characteristic meteorological conditions (Konček et al., 1974; Comrie, 1994; Blandford et. al, 2008).

METHODS

The study sites forms the elevation transect in Slovakian High Tatra Mountains (Stará Lesná, Tatranská Lomnica, Štart, Deviatka, Skalnaté pleso, Lomnický Štít) (Figure 1). During the period of 2001-2003 were continuously measuring daily ambient O3 concentrations based on the system of UV absorption by the automatic O_3 analyzers (Thermoelectron, MLU, Horiba). Simultaneously with ozone, we recorded the meteorological weather characteristics (air temperature and moisture, global radiation). Beside the weather records, we kept the track on the synoptic movements and the pressure formations of the air masses over the Europe.

The ozone uptake for the coniferous forests was modelled based on the reconstructed stomatal conductance of the water vapour by using the stand photosynthesis program (Mäkelä et al., 2006). The stomatal conductance for O_3 (GO_3) equals to 0.613 of stomatal conductance for H_2O (Nobel, 1983). By the Fick law the multiplication of the O_3 and GO_3 values gives ozone uptake (UO_3) (Wieser et al., 2000).
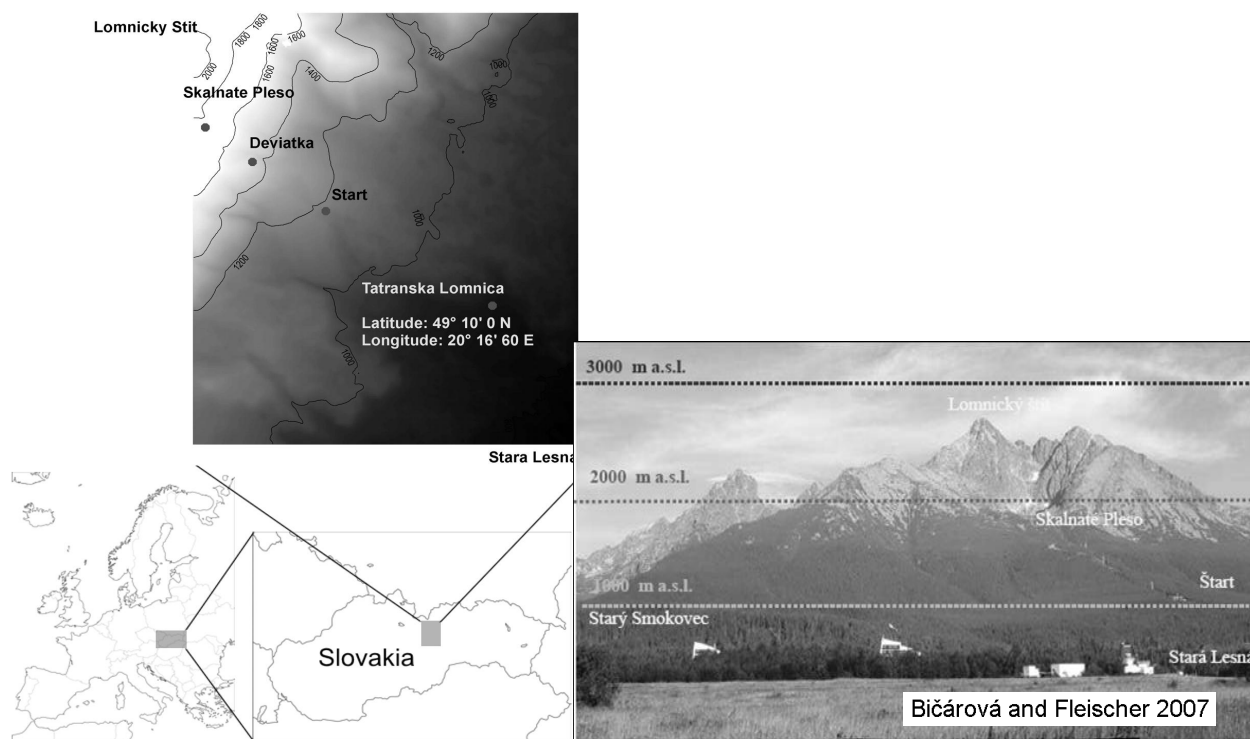
Fig. 1. Geographical location and photo of study sites (Stará Lesná, Tatranská Lomnica, Štart, Deviatka, Skalnaté pleso, Lomnický Štít) in the High Tatra mountains with the elevation gain of 1824 meters.

Calculated UO_3 values were used for non-linear regression fitting by the air temperature (equation 1):

$$UO_3 = uo_{3\,max} EXP\left[-0.5\left(\frac{T - T_{opt}}{T_{tol}}\right)^2\right] \qquad (1)$$

where, uo_{3max} is the max UO_3 value reached by the optimal air temperature (T_{opt}). The parameter T_{tol} is the temperature tolerance, the deviation from the maximum where are 60% of UO_3 values.

To analyse the relation between the synoptic weather patterns and the ozone uptake, we used the daily records of weather classification for Slovakia during the period of 2001 - 2003. Synoptic types were grouped into 13 types according to the prevailing wind direction (Fig 2). We recognise Anticyclonic situations (A (central, Ap1, Ap2, Ap3), Ea (East, NEa, Ea), Sa (South, SEa, Sa), SWa (South-West, Swa), Wa (West, Wa,Wac), NWa (North-West, NWa)), Cyclonic situations (Bc (C - central, B, Bc), Nc (North, Nc, NWc), Ec (East, NEc, Ec, Cv), Sc (South, SEc, SWc1,WCs), SWc (South-West, SWc2, SWc3), Wc (West, Wc)), and Baric saddle V (Vfz). The effect of synoptic types on the ozone uptake, we analysed from the residuals of recontructed UO_3 values by O_3 concentrations and stomatal conductance, and modelled UO_3 values by the nonlinear air temperature model.

RESULTS

On the elevation transect the air temperatures typically decrease with elevation gain. Between the lowest station Tatranska Lomnica, and the highest one Lomnicky Stit was the elevation gain 1824 meter, and mean temperature lapse rate 0.59 degree Celsius on 100 meters ($R^2 = 0.69$) was during summer (April-

September) stable, decreasing towards winter lapse rate (0.17 degree Celsius on 100 meters, R^2 =0.205). The temperature inversion was common in January and February. January was the coldest month of the year with average temperature -3.5 degree Celsius along the elevation transect. The hottest air temperature was 29.6 degree Celsius measured in August 2003 in Tatranska Lomnica. August was the warmest month for all stations on average from 13.9 to 19.0 degree Celsius (Fig. 1). In the station Start were the annual temperature maximum around 8.9 degrees Celsius and the minimum was around 1.7 degree Celsius. The difference of approximately 7 degree Celsius between temperature maximum and minimum was observed constantly every day during a year. Typically, seasonality was shown on air temperatures and also on the time of the temperature min and max occurrences. In winter, daily maximum occurred around 10 am (4 degrees Celsius) in comparison to 1pm for summer (16 degree Celsius). Daily minimum fluctuated between 4 am in winter (- 4 degree Celsius) and 7 am in summer (8 degree Celsius).
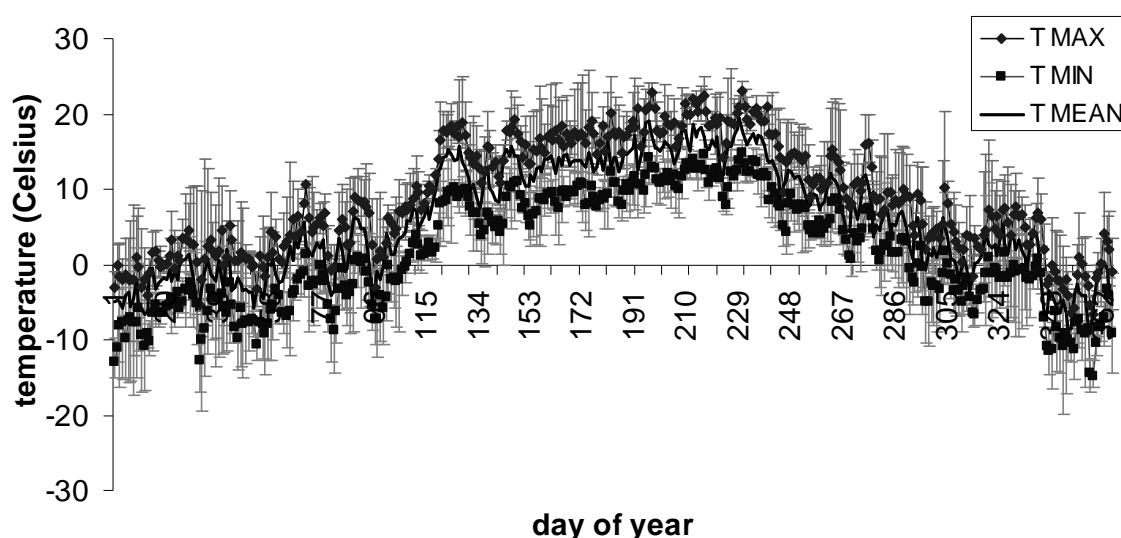
Fig. 1. The average daily trends of the minimum (Tmin) , maximum (Tmax), and average (Tmean) air temperature on the station Štart. The error bars of values show the range of recorded values of Tmin and Tmax.

The measured O_3 concentrations on the High Tatra mountains remained regurarly higher than tha daily limit for protection of vegetation (96%) (Fig. 2). Typically, ambient O_3 values increased with higher elevation, and also showed typical winter minimum and summer maximimum. Winter O_3 concetrations were mostly in range from 60 to 100 ugO_3/m³, while summer values increased to the level from 100 to 140 ugO_3/m³. During mid-summer O_3 concentrations slightly fell before small rise towards the end of summer and steep lowering in fall. Exeptionally, in the station Start the summer values of 2002 droped from the May ozone maximum 136 ug/m3 below the level of 60 ugO_3/m³ to the July minimum 32 ug/m3 during the period of low temperatures. Mid - summer decrease of O_3 levels had the least effect on one of the top mountainous station Skalante pleso (from max 133 ug/m³ to min 80 ug/m³). The average O_3 levels on the same stations Bičárová a Fleisher (2007) measured during summer 2003 at station Stará lesná (65 ug/m³), Štart (90 ug/m³), a Skalnaté pleso (93 ug/m³) correspond with our study (Stará lesná (77 ug/m³), Štart (95 ug/m³), a Skalnaté pleso (105 ug/m³)). The lapse rate of ozone 2.31 ug/m³ on 100 meters of elevation gain was close to the summer Alpine value of 2.5 ug/m³/100m Sanz et. al. (2005). Subsequently, due to very high daily summer O_3 concentrations the index AOT40 was over the limit 3 times for the station at the tree line Skalnate pleso, and 5 times for top station above the tree line Lomincky Stit. Therefore, summer O_3 exposure was alike to high concentrations of central Alps in Switzerland (Lattecaldo 32473 ppb/h) or in Italy (Leonessa 45659 ppb/h (Gerosa et. al, 2007).
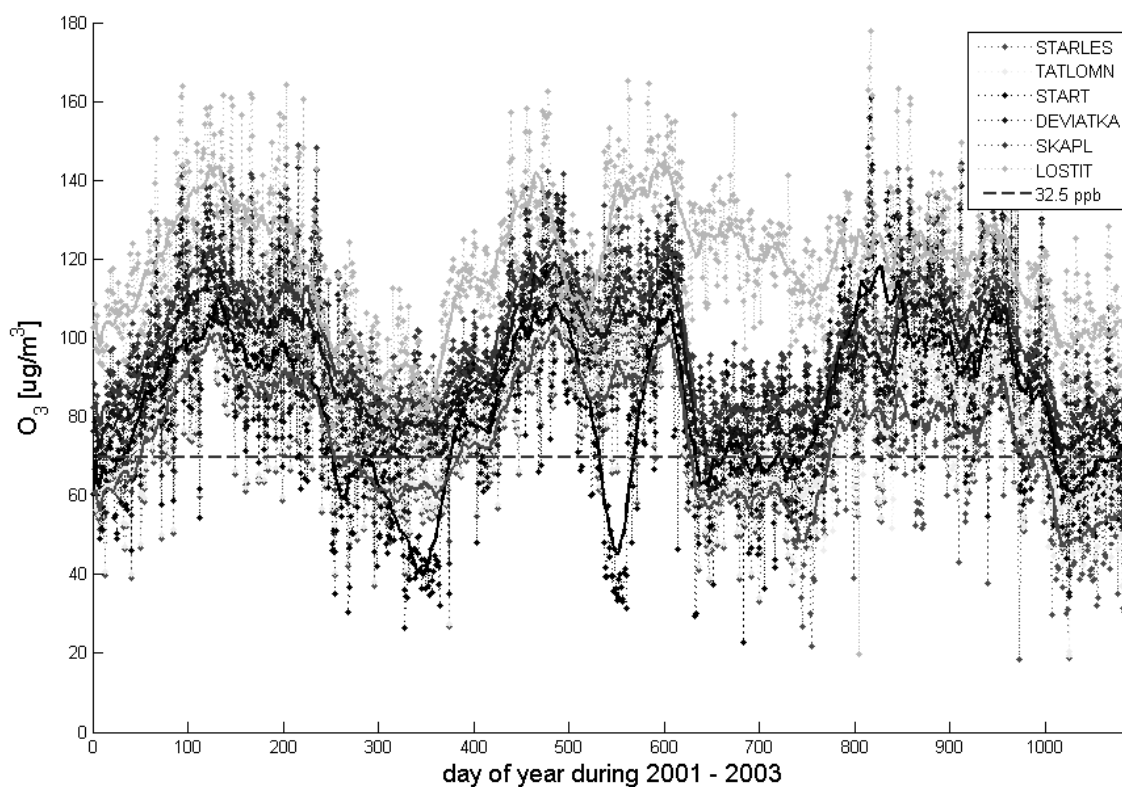
Figure 2. Daily tropospheric ozone concentrations in the High Tatra mountains elevation transect during the period 2001 - 2003. Lines show the 30 days average. The level 32.5 ppb is the daily limit to protect vegetation.

Comrie (1994) found for Pelsylvania, that the highest ambient O_3 concentrations were associated with conditions of South - West transport of anticyclonic weather type, and lowest ambient O_3 concentrations were typical for post-frontal and cyclonic situations. In our study, during summer we found the O_3 concentrations of Ea and Sa to be at the same level as the ozone concentrations of Sc and Swc. However, the cyclonic situation clearly showed higher ozone uptake over the anticyclonic types.

The difference of the daily ozone uptake between the coldest and warmest synoptic type, between Nc and Wa was through a year 900 ug/m²/d. The synoptic types (Ec, Bc, NWa, A, Sa, SWa) close to the annual temperature average 5 ±7 degree Celsius showed UO_3 average 1000 ±1000 ug/m²/d. During the vegetation period was the average higher at 11 ±5 degrees Celsius and UO_3 average at 1800 ±800 ug/m²/d. The warmest weather types of the summer (Sa, SWa with average 13 degree Celsius) had least favourable conditions for the ozone uptake (only 1600 ug/m²/d). These synoptic types were typical by the O3 concentrations over 100 ug/m³, though the high temperature inhibited the stomatal conductance and limited the ozone uptake. Southern cyclone in summer radically increased the ozone uptake from 900 ug/m²/d up to the value of 2200 ug/m²/d. Weather type specific non-linear regression is show on the figure 3. The average maximum UO_3 for all synoptic types was 1700 ug/m2/d reached by the optimal temperature 19 degree Celsius. The typically warmer anticyclonic situations shown on average 500 ug/m²/d UO_3 maximum at the lower optimal temperature 18 degrees Celsius. The overall highest maximum UO_3 2300 and 1900 ug/m²/d corresponded with the Sc and V, very rare synoptic types with occurrence less then 5%. However, the most common synoptic types Bc 17%, and A 13% favoured the ozone uptake, the UO_3 values 1650 and 1750 ug/m²/d was above the average.

The reduction of net primary production found by Wieser (1997) on 1-year shoots of Spruce and Pine in Alps was from 10% to 40% with UO_3 values from 15 to 40 mmol/m². However, when we used the same

model for High Tatras, for the ozone uptake of less then 10 mmol/m^2 of O$_3$ per vegetative season, the photosynthetic reduction was less than 5%.
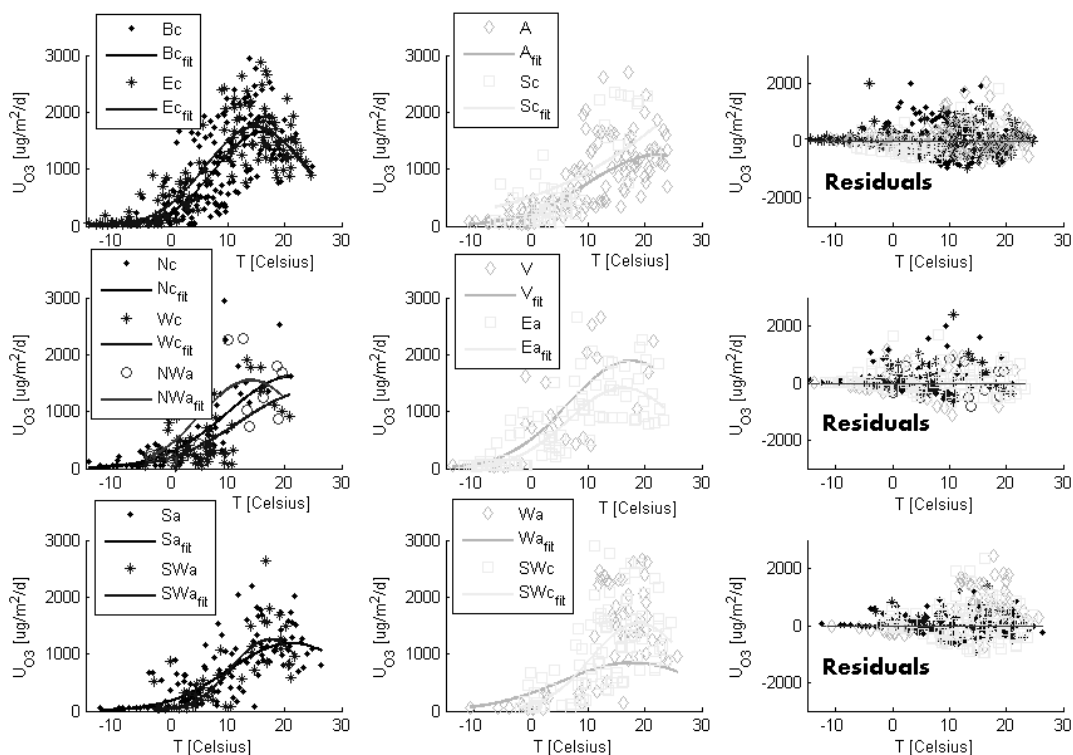
Fig. 3. Daily sums of ozone uptake versus the air temperature, fitted models, and residuals on average for all stations for single days of synoptic weather patterns.

CONCLUSIONS

The ambient levels of tropospheric ozone in High Tatra mountains in Slovakia were similar to those of central Alps. The cumulative exposure of ozone during the growing season index AOT40 3 times exceeded the level for forest protection for the station situated at the tree line. However, the calculated reduction of the photosynthetic production based on the cumulative ozone uptake over the growing season in High Tatras was less than 5 %. The estimated reduction of the photosynthesis might be low, though forest may be prone to physiological damage due to the high instantaneous ozone uptake often occurring under cyclonic weather situations.

REFERENCES

Bičárová, S., Fleischer, P. (2007) Changes of ground level ozone concentration after the 19 November 2004 windstorm in the High Tatras. *Zborník Pokalamitný výskum v TANAP-e 2007*, Tatranská Lomnica, 25. - 26. október 2007, Geofyzikálny ústav SAV, ISBN: 978-80-85754-17-9

Blandford, T., Humes, K., Harshburger, B., Moore, B., Walden, V., & Ye, H. (2008) Seasonal and Synoptic Variations in Near-Surface Air Temperature Lapse Rates in a Mountainous Basin. *Journal of Applied Meteorology & Climatology*, 47(1), 249-261. doi:10.1175/2007JAMC1565.1

Comrie A.C. (1994) A synoptic climatology of rural ozone pollution at three forest sites in Pennsylvania. *Atmospheric Environment*, 28 (9), pp. 1601-1614.

Emberson L.D., Wieser G., Ashmore M.R. (2000): Modelling of stomatal conductance and ozone flux of Norway spruce: Comparison with field data. *Environmental Pollution*, 109 (3), pp. 393-402.

Fuhrer, J., Skärby, L., Ashmore, M.R. (1997) Critical levels of ozone effects in Europe. *Environmental Pollution* 97, 18–29.

Gerosa G., Ferretti M., Bussotti F., Rocchini D. (2007) Estimates of ozone AOT40 from passive sampling in forest sites in South-Western Europe, *Environmental Pollution*, 145 (3), pp. 629-635

Heath, R.L. (1994). Alteration in plant metabolism by ozone exposure. In: Alscher, R., Wellburn, A.R. (Eds.), Plant Response to the Gaseous Environment. Chapman and Hall, London, pp. 121-145.

Konček M., Bohuš I., Briedoň V., Chomicz K., Intribus R., Kňazovický L., Kolodziejek M., Kurpelová M., Murínová G., Myczkowski S., Orlicz M., Orliczowa J., Otruba J., Pacl J., Peterka V., Petrovič Š., Plesník P., Pulina M., Smolen F., Sokolowska J., Šamaj F., Tomlain J., Volfová E., Wiszniewski W., Wit-Jozwikowa K., Zych S., Žák B. (1974) Klíma Tatier. *Veda, vydavateľstvo Slovenskej akadémie vied*, Bratislava. 750s.

Mäkela A., Kolari P., Karimäki J., Nikinmaa E., Peramäki M., Hari P. (2006). Modelling five years of weather-driven variation of GPP in a boreal forest. *Agricultural and Forest Meteorology*, 139 (3-4), pp. 382-398.

Matyssek, R., Wieser, G., Nunn, A. J., Kozovits, A. R., Reiter, I. M., Heerdt, C., Winkler, J. B., Baumgarten, M., Haberle, K. -H., Grams, T. E. E., Werner, H., Fabian, P., Havranek, W. M. (2004) Comparison between AOT40 and ozone uptake in forest trees of different species, age and site conditions, *Atmospheric Environment* 38: 2271-2281, DOI: 10.1016/j.atmosenv.2003.09.078.

Nabel, (1999). Luftbelastung 1998. Herausgegeben vom Bundesamt fur Umwelt, Wald und Landschaft (BUWAL), Bern.

Nobel, P.S. (1983) Biochemical Plant Physiology and Ecology. *Free-man and Co*, New York

Scheel, H.E., Areskoug, H., Geiss, H., Gomiscek, B., Granby, K., Haszpra, L., Klasinc, L., Kley, D., Laurila, T., Lindskog, A., Roemer, M., Schmitt, R., Simmonds, P., Solberg, S., Toupance, G., (1997) On the spatial distribution and Seasonal Variation of Lower-Troposphere Ozone over Europe. *Journal of Atmospheric Chemistry* 28, no. 1-3,11-28.

Závodský, D., Závodská, E. (1992) Kvalita ovzdušia a zmeny klímy. NKP ČSFR 7, Praha 1992, 4 – 50

Wieser, G., 1997. Ozone impact on photosynthetic capacity of mature and young Norway spruce (Picea abies (L.) Karst.): external versus internal exposure. *Phyton* 37, pp. 279–302

Wieser, G., 1999. Evaluation of the impact of ozone on conifers in the Alps: a case study on spruce, pine and larch in the Austrian Alps. *Phyton* 39: 241–252

Wieser G., Hasler R., Gotz B., Koch W., Havranek W.M. (2000) Role of climate, crown position, tree age and altitude in calculated ozone flux into needles of Picea abies and Pinus cembra: A synthesis. *Environmental Pollution,* 109 (3), pp. 415-422

ULTRAFINE PARTICLE OBSERVATION ON THE OPEN WATER ARCTIC OCEAN CLOSE TO ICE EDGE: SECONDARY ORGANIC CONTRIBUTION

P. Vaattovaara[1], Z.D. Ristovski[2], M. Graus[3], M. Müller[3], E. Asmi[8], L. Di Liberto[4], S. Sjögren[5], D. Orsini[6], C. Leck[7] and A. Laaksonen[1,8]

[1]University of Kuopio, Department of Physics, Finland
[2]ILAQH, Queensland University of Technology, Brisbane, Australia
[3]Institute of Ion Physics and Applied Physics, Innsbruck University, Austria
[4]Instituto of Atmospheric Sciences and Climate of the Italian National Research Council
[5]University of Lund, Department of Physics, Sweden
[6]Leibniz Institute for Tropospheric Research, Leipzig, Germany
[7]University of Stockholm, Department of Meteorology, Sweden
[8]Finnish Meteorological Institute, Helsinki, Finland

Key Words: Arctic Ocean; ice melting; nucleation; SOA; clouds; climate

INTRODUCTION

Newly-formed nanometer-sized particles have been observed at coastal and remote marine environments worldwide (see references within Kulmala et al. 2004). Such nanoparticles can grow into larger sizes (O'Dowd et al., 2001), being able to scatter incoming radiation and contribute to direct and indirect (via clouds) cooling effects to the Earth's radiation budget (Slingo et al., 1990). Marine coastal nucleation events are frequently observed and the size and composition of newly-formed particles has been intensively studied especially at Mace Head in Irish coast (O'Dowd and de Leeuw, 2007). Observation of nucleation events in open oceans are much more rare (e.g., Katoshevski et al., 1999) and the composition of observed particles is still unknown. A common feature of the coastal and open water nucleation events is that they have occurred on highly biologically active waters (Vaattovaara et al., 2006).

It is important to note that the surface of these biologically active open waters has expanded especially in the Arctic Ocean region during the last decades due to climate warming and consequent ice melting (Arrigo et al., 2008). Arctic Ocean open waters have been reported to contribute to new particle production (e.g., Wiedensohler et al., 1996) during the nightless polar summer season. More generally, the solar radiation is known to play an important role in the presence of nucleation mode sized particles in the Arctic Ocean region (Ström et al., 2003). However, the formation, composition and growth of those newly-formed particles should be better understood in order to better understand also the effects of ice melting Arctic Ocean on the connections between Arctic biota, clouds and climate.

We carried out this Arctic Ocean open water study of nucleation mode and Aitken mode sized particles growth and organic fraction as a part International Polar Year (IPY) 2007-2009 related "Arctic Summer Cloud Ocean Study (ASCOS)" project on the board of Swedish Icebreaker Oden during solar radiation intensive and the biologically active polar summer time in August 2008. The chosen measurement route and time opened up a good opportunity to study

the processes of ultrafine particles (d < 100 nm) on the Arctic Ocean conditions expected to dominate also in the near Arctic future.

METHODS

Measurements were carried out on the ice melted part of Greenland Sea, covering a highly biologically active surface region (about 78° N – 79° N and 9° E – 5° E, to the west from the Spitzbergen) close the ice edge, during the nightless polar summer time period (3th August 3 p.m. – 4th August 12 a.m.). The air was drawn for sampling of atmospheric aerosol and trace gases from about 25 meters above the sea surface into the measurement containers fixed on the 4th deck of Oden. The inlet system extended at an angle of 45° to about 3 meter above the roof of the containers. In order to avoid the emissions from the ships diesel motors the ship was moving continuously heading against the wind direction. The wind speed onboard was about 2 m/s that is generally typical for polar summers. Typically, the ice coverage, the ice thickness and the antropogenic transportation from continents to the ice melting Arctic Ocean are in minima whereas photosynthetically important solar radiation affect on the marine biota is high during this time of polar summer.

In this study, the measurement systems used to characterize the newly-formed particles consisted of the UFO-TDMA (ultrafine organic tandem differential mobility analyzer; Vaattovaara et al., 2005), measuring the 10-50 nm (in mobility diameter) particles, the VH-TDMA (volatile and hygroscopicity tandem differential mobility analyzer; Johnson et al., 2005), measuring particles with 16 nm mobility diameter and H-TDMA (hygroscopicity tandem differential mobility analyzer) measuring the Aitken mode sized particles. CIMS (chemical ionisation mass spectrometry) and the HR PTR-ToFMS (high resolution proton transfer reaction time of flight mass spectrometer) were used to measure the gaseous particle precursors as well as to check for anthropogenic traces in the air masses. The particle size distribution from 3-800 nm (in mobility diameter) was measured by a twin DMPS (differential mobility particles sizer). The particles relative vertical concentration was followed using LIDAR (light detection and ranging). The marine origin of the air masses were followed using 96 hours HYSPLIT (Hybrid Single-Particle Lagrangian Integrated Trajectory) model (Draxler and Rolph, 2003; Rolph, 2003) backward trajectories and marine biological activity using Sea-WiFs (Sea viewing Wide Field-of-view Sensor) and MODIS (Moderate Resolution Imaging Spectroradiometer) Aqua and Terra satellite data (NASA/Goddard Space Flight Center and ORBIMAGE).

RESULTS AND CONCLUSIONS

The nucleation mode sized particles, included to a mode from 10 nm to 40 nm, were observed starting around 3 p.m. (see Fig. 1 for particle size distribution) on the Greenland Sea, at about 78° N and 9° E, when local wind and ship direction were western and air mass arrived from East Greenland Sea. The VH-TDMA data reveal the hygroscopicity of 16 nm particles with the GF about 1.3-1.35 in the start of event. The particle concentration increased from below 100 up to 1500 #/cm^3.
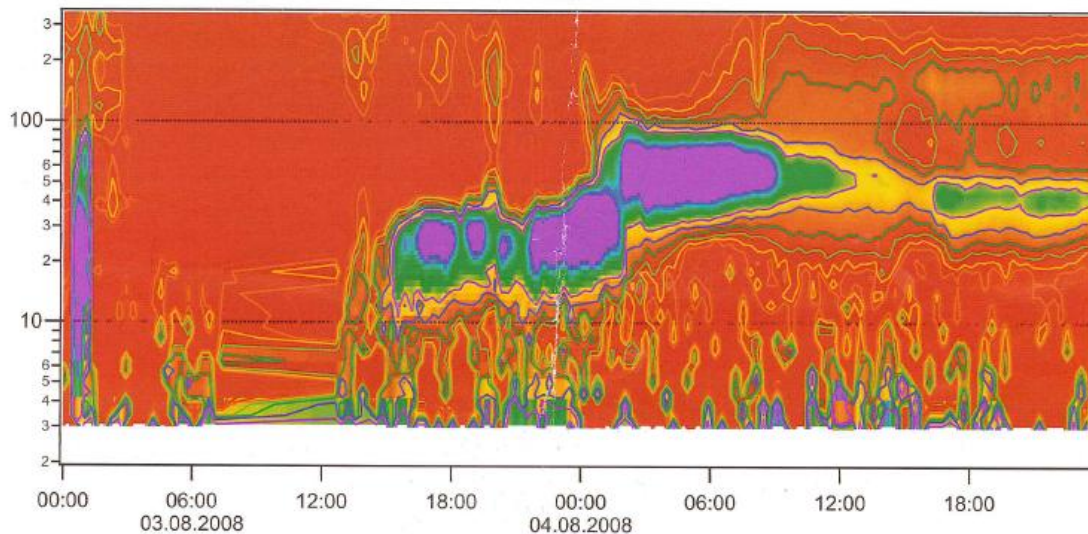
Figure 1. Particle size distributions measured on the Greenland Sea during 3.8-4.8.2008 ultrafine particle event

Potential reasons for the observed biogenic nucleation mode sized particles close to sea level could be related to free troposphere transport (e.g., Clarke, 1993), cloud induced nucleation (Raes and Van Dingenen, 1992) and marine biota (e.g., O'Dowd and De Leeuw, 2007, Leck and Bigg, 1999). LIDAR polarized aerosol backscattering data reveal that the particles did not arrived downwards at the moment of observation of nucleation mode sized particles. When the local wind direction and ship turned to more northern direction after 6 p.m. and the lowest air masses still travelled from East Greenland Sea, a new 15-40 nm particles mode was observed and particle concentration increased from about 500 up to 3500 #/cm^3 until midnight during particles growth with the mode median growth rate (GR) 1.6 nm/h. After midnight the local wind direction and ship turned to north-westerly direction and new particles arrived upwards from few hundred meters (LIDAR data) and particle concentration was about 2000 particles cm^{-3}. Since that, the particles size was 30-100 nm and thus the upper end of these Aitken mode sized particles being potentially cloud condensation nuclei (CCN). The hygroscopicity of 72 nm (in mobility diameter) Aitken mode sized particles was measured by HTDMA, the growth factor (GF) around 1.4 at 90% RH (relative humidity, corrected to 90%) supporting the CCN potential of the particles. The GR of the mode median was about 1.2 nm/h after midgnight.

The lowest 100 m air masses were travelled several days from the biologically active East Greenland coast and the island of Jan Mayen directions close the biologically active coastal regions and ice edges with blankton blooms. The observation day was more or less cloudy. However, the Sun was able to shine through the cloud cover about at the moment of the first nucleation mode sized particles observation. The preliminary results of the UFO-TDMA and VH-TDMA show that the 15-30 nm particles consisted of at least 20-50 percent organics (see Fig. 2) during the first few hours after the nucleation mode sized particles was observed. Since 6 p.m. until midnight, the organic volume fraction (OVF; for OVF calculation method, see Vaattovaara et al., 2006) of the UFO-TDMA measured 15-30 nm particles increased to an minimum estimate of about 55-65 % (Fig. 3). After midnight, an organic volume fraction estimate of the UFO-TDMA measurements was about 55-60 % for 50 nm particles until 3 a.m. of August 4 (Fig. 4) when the upper end of Aitken mode reached 100 nm size. After 3 a.m. air mass changed again, now arriving from western direction, and the OVF of 50 nm particles

consequently dropped down to 25 % until 6 a.m., meanwhile particle concentration dropped from 2000 to 500 #/cm^3.
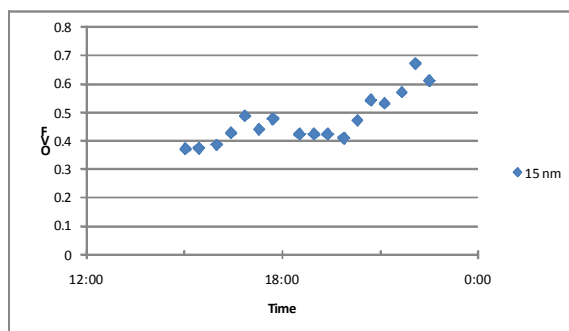
Figure 2. OVF estimated for 15 nm particles based on the UFO-TDMA measurements 3.8.2008 on the open water Arctic Ocean.
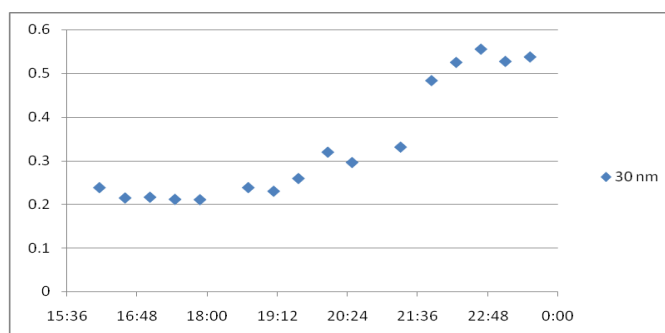
Figure 3. OVF estimated for 30 nm particles based on the UFO-TDMA measurements 3.8.2008 on the open water Arctic Ocean.
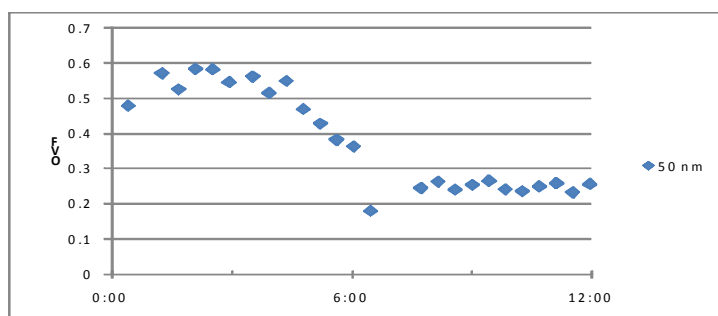
Figure 4. OVF estimated for 50 nm particles based on the UFO-TDMA measurements 4.8.2008 on the open water Arctic Ocean.

In addition to the organic fraction, the growth of the observed particles may be related to the presence of DMS (Dimethyl Sulfide) and its elevated levels from 50 ppt (3 p.m. on August 3th) up to 130 ppt (5 a.m. on August 4th), as measured by CIMS. When the air mass turned to ice covered region after midnight, DMS concentration dropped down, being about 1-2 ppt. Those support the important role that marine biota played in the origin of the precursor gases. Potential candidates for the precursors of the secondary organic contribution could be atmospherically very reactive phytoplankton biosynthesis products such as isoprene (Glatt, 2009), monoterpenes

(Yassaa et al., 2009), chlorobenzenes (Colomb et al., 2008), and their derivates and organic derivates of DMS. A growth (even though disturbed by local wind direction and ship direction change) in particle size distribution as a function of time indicates that the particles production was a large area phenomena, further supporting also the role of biologically active sea surface as an origin for the observed particles. The observations also support the importance of biologically active marine areas for secondary organic contribution to the properties of atmospheric particles.

Due to climate warming and consequently due to ice and snow melting of the Arctic Ocean, the highly biologically active ocean surface area has been expanding quickly making possible longer marine biota growth seasons during polar summers. This increase the probability of the remote marine environment contribution to particle production and particle growth events and particle properties consequently effecting on the open ocean, pack ice and ground based regions radiation budget and thus on the feedbacks between arctic biota, particles, clouds, and climate.

ACKNOWLEDGEMENTS

REFERENCES

Arrigo, K., van Dijken, G., and Padi, S. (2008). Impact of a shrinking Arctic ice cover on marine primary production. *Geophys. Res. Lett.*, 35, LI9603.

Clarke, A.D. (1993) Atmospheric nuclei in the Pacific midtroposphere: Their nature, concentration, and evolution. *J. Geophys. Res.*, 98, 20633-20647.

Colomb, A., Yassaa, N., Williams, J., Peeken, I., and Lochte, K. (2008). Screening volatile organic compounds (VOCs) emissions from five marine phytoplankton species by head space gas chromatography/mass spectrometry (HS-GC/MS). *J. Environ. Mon.*, 10, 325-330.

Draxler, R.R. and Rolph, G.D. (2003). HYSPLIT (HYbrid Single-Particle Lagrangian Integrated Trajectory). Model access via NOAA ARL READY Website (http://www.arl.noaa.gov/ready/hysplit4.html), Silver Spring, MD: NOAA Air Resources Laboratory.

Gantt, B., Meskhidze, N., Kamykovski, D. (2009). A new physically-based quantification of isoprene and primary organic aerosol emissions from the world's oceans. *Atmos .Chem. Phys. Discuss.*, 9, 2933-2965.

Johnson, G.R., Ristovski, Z.D., D'Anna, B., Morawska, L. (2005) Hygroscopic behavior of partially volatilized coastal marine aerosols using the volatilization and humidification tandem differential mobility analyzer technique. *J. Geophys. Res.*, 110, D20203.

Katoshevski, D., Nenes, A., and Seinfeld, J.H. (1999). A study of Processes that Govern the Maintenance of Aerosols in the Marine Boundary Layer. *J. Aerosol Sci.*, 30, 503-532.

Kulmala, M., Vehkamäki, H., Petäjä, T., Dal Maso, M., Lauri, A., Kerminen, V.-M., Birmili, W., and McMurry, P.H. (2004). Formation and growth rates of ultrafine atmospheric particles: a review of observations. *J. Aerosol Sci.,* 35, 143-176.

Leck, C. and Bigg, K. (1999). Aerosol production over remote marine areas – A new route. Geophys. Res. Lett., 23, 3577-3581.

O'Dowd, C.D. Biogenic coastal aerosol production and its influence on aerosol radiative properties. (2001). *J. Geophys. Res.*, 106, 1545-1550.

O'Dowd, C.D. and de Leeuw, G. (2007). Marine aerosol production: a review of the current knowledge. *Phil. Trans. R. Soc. A*, 365, 1753-1774.

Raes, F., and Van Dingenen. Simulations of condensation and cloud condensation nuclei from dimethyl sulphide in the natural marine boundary layer. (1992). J. Geophys. Res., 97, 12901-12912.

Rolph, G.D. (2003). Real-time Environmental Applications and Display sYstem (READY) Website, Silver Spring, MD: NOAA Air Resources Laboratory.

Slingo, A. (1990). Sensitivity of the Earth's radiation budget to changes in low clouds. *Nature*, 343, 49-51.

Ström, J., Umegård, J., Torseth, K., Tunved, P., H.-C. Hansson, Holmén, K., Wismann, V., Herber, A., König-Langlo, G. (2003). One year of particle size distribution and aerosol chemical composition measurements at the Zeppelin Station, Svalbard, March 2000-March 2001. *Phys. Chem. Earth*, 28, 1181-1190.

Vaattovaara, P., Räsänen, M., Kühn, T., Joutsensaari, J., Laaksonen, A. (2005). A method for detecting the presence of organic fraction in nucleation mode sized particles. *Atmos. Chem. Phys.*, 5, 3277-3287.

Vaattovaara, P., Huttunen, P.E., Yoon, Y.J., Joutsensaari, J., Lehtinen, K.E.J., O'Dowd, C.D., and Laaksonen, A. (2006). The composition of nucleation and Aitken modes particles during coastal nucleation events: evidence for marine secondary organic contribution. Atmos. Chem. Phys. 6., 4601-4616.

Wiedensohler, A, Covert, D.S., Swietlicki, E., Aalto, P., Heintzenberg, J., and Leck, C. (1996). Occurrence of an ultrafine particle mode less than 20 nm in diameter in the marine boundary layer during Arctic summer and autumn. *Tellus*, 48B, 213-222.

Yassaa, N., Peeken, I., Zöllner, E., Bluhm, K., Arnold, S., Sparclen, D., Williams, J. (2008). Evidence for marine production of monoterpenes. *Environ. Chem.*, 5, 391-401.

BACK-TRAJECTORY ANALYSIS OF NEW PARTICLE FORMATION IN A SEMI-CLEAN SAVANNAH ENVIRONMENT

Ville Vakkari[1], Heikki Laakso[1], Desmond Mabaso[2], Moses Molefe[2], Nnenesi Kgabi[2], Markku Kulmala[1] and Lauri Laakso[1]

[1]University of Helsinki, Dept. Physics, P. O. Box 64, 00014 Univ. of Helsinki, Finland
[2]Department of Physics, North-West University, Private Bag X 2046, Mmabatho, South Africa

Keywords: new particle formation, Southern Africa, savannah, Hysplit.

Combined long-term measurements of trace gas concentrations, aerosol particle mass concentrations and number size distributions (especially in ultrafine size range), air ion number size distributions and meteorological variables are extremely few in Southern Africa (Piketh et al., 2005; Laakso et al., 2008). We will describe here first results of back trajectory analysis of new particle formation observed during the first 1.5 years of measurements with a transportable measurement trailer (Petäjä et al., 2007) in a relatively clean savannah environment in Botsalano game reserve from the period 20 July 2006 to 30 January 2008.

The aerosol particle size distribution from 10 to 840 nm was measured using a DMPS system and air ion and charged particle distribution from 0.4 to 40 nm using an Air Ion Spectrometer (AIS, Airel Ltd, Estonia, Mirme et al.2007). In addition to the measurements in the trailer 96-hour back-trajectories were calculated for each hour during the measurement period using HYSPLIT 4.8 model (Draxler and Hess, 2004). The back-trajectory arrival height was 100m.

A one to three-modal log-normal size distribution was fitted on the aerosol particle size spectra from the DMPS system for the whole measurement period. For a description on the fitting method used see Vartiainen et al. (2007). New particle formation events were classified and formation and growth rates calculated according to Dal Maso et al. (2005). From the ion spectra the growth rates for 1.5-3nm, 3-7nm and 7-20nm ions were calculated using the method described in Hirsikko et al. (2005). The 2-3nm ion formation rate $J_2^{\pm}$ was calculated as in Kulmala et al. (2007). For the calculation of ion J_2 we assumed the number of neutral 2-3nm particles to be twice the sum of the total 2-3nm ion concentration.

RESULTS

Clear new particle formation and growth was observed on 69% of the days during the measurement period. In addition to this, on 14% of the days non-growing ion formation was observed. The average particle growth rate for particle size range 10-30 nm was 9.2 nm h^{-1} and average formation rate of 10nm particles, J_{10}, 4.7 cm^{-3}s^{-1}. The average ion (or charged particle) growth rates for size ranges 1.5-3 nm, 3-7 nm and 7-20 nm were 7.6 nm h^{-1}, 10.1 nm h^{-1}, and 8.6 nm h^{-1}, respectively. The average ion J_2 was 0.6 cm^{-3}s^{-1}.

Both DMPS (Figure 1) and AIS (Figure 2) growth rates show a weak minimum during winter and maximum at spring and summer, as do observations from other sites (Kulmala et al., 2004). The levels of growth rates and formation rates are among the highest observed in continental areas (Kulmala et al., 2004; Hamed et al., 2007).
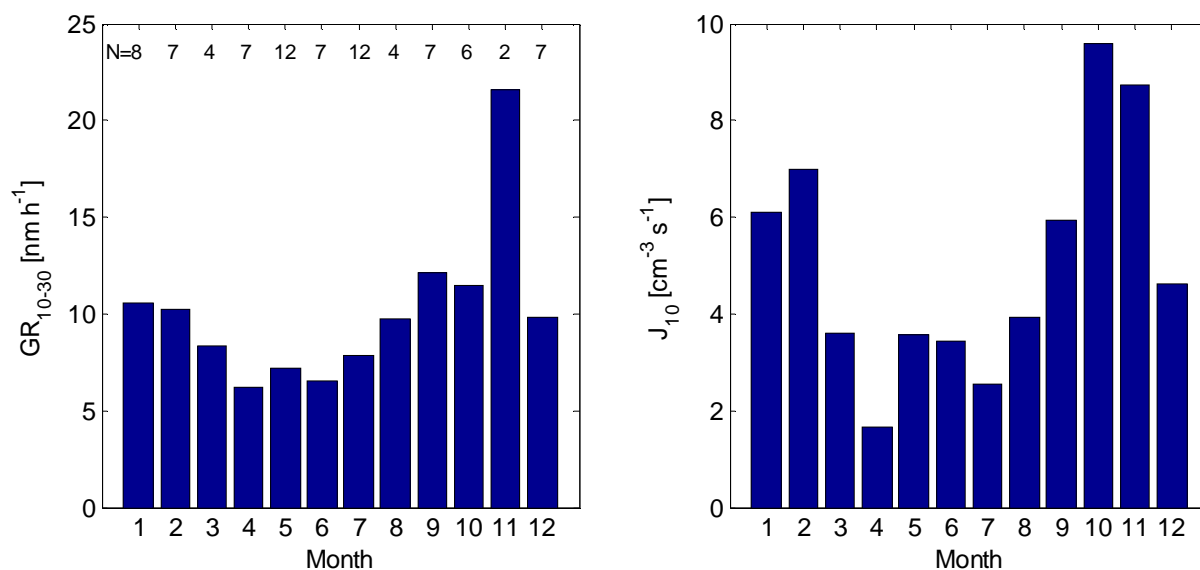
Figure 1 Monthly averaged 10-30nm growth rate and 10nm formation rate from DMPS data. November GR is based on only two well-behaving nucleation events due to poor data coverage in November 2006 and 2007.
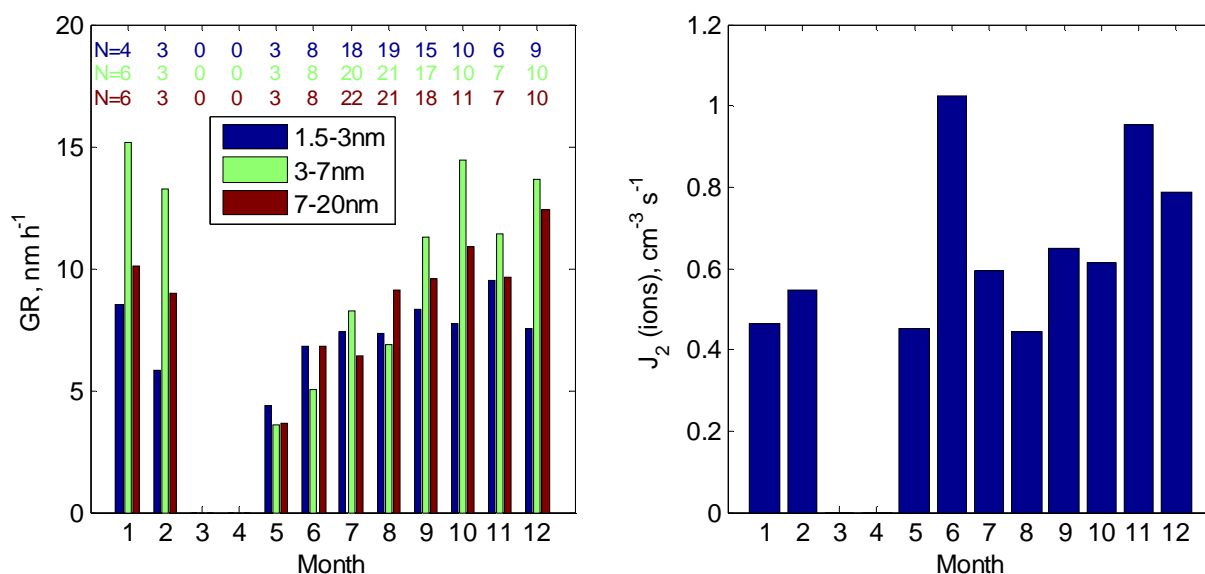
Figure 2 Monthly averaged growth and formation rates for ions on different size ranges. Data from March-April 2007 is missing as the device was under maintenance in Estonia.

In order to deepen the understanding of the source area on the observed new particle formation and growth the world was divided to a 0.5° x 0.5° grid. Each of the calculated back-trajectories was associated with the growth rate observed when the trajectory landed in Botsalano. The grid cells were then assigned the average value of growth rate based on which trajectories passed by each grid cell. Only 24 hours of the back trajectories were taken into account on determining the source regions. The source area maps for AIS negative and positive polarity growth rates are presented in Figure 3 and 4, respectively.

The growth rate for the smallest size range 1.5 – 3nm negative particles (Figure 3) has a maximum south-east from the Johannesburg metropolitan area. For the positive ion growth rate the pattern of 1.5 – 3nm

440

growth rate is not as clear. For both negative and positive particles in the larger sizess the peak growth rates seem to originate north-east from Botsalano. The DMPS 10 – 30nm growth rate behaves similarly as the largest size range ion growth rate with maximum north-east of Botsalano.

We conducted similar back-trajectory analysis as for growth rate also for observed SO_2, Figure 5. As expected, the highest SO_2 concentrations originate in the Johannesburg metropolitan area and in the High Veldt region east of Johannesburg. The negative 1.5 – 3nm growth rate maximum coincides with the area where we obtain the highest SO_2 concentrations.

The northernmost part of the Republic of South Africa was found to have the highest monoterpene emissions from the vegetation in the volatile organic compound inventory by Otter et al. (2003), which is the direction where we obtain highest growth rates of larger particles in both AIS and DMPS.
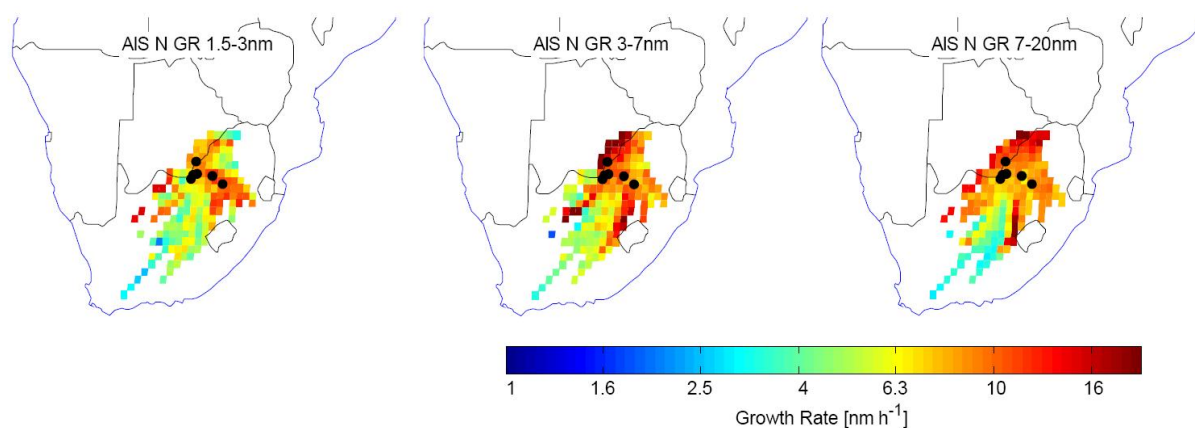
Figure 3 AIS negative polarity growth rate source areas.
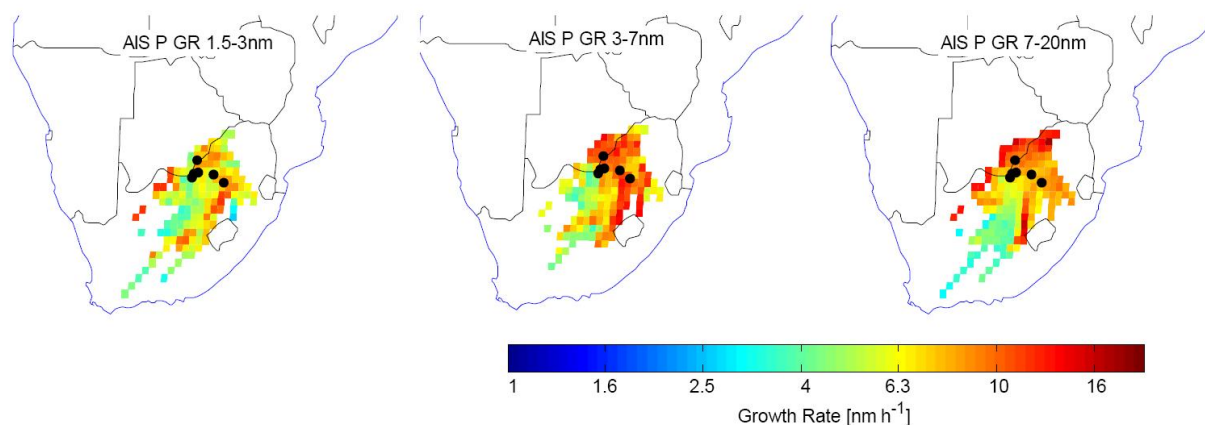
Figure 4 AIS positive polarity growth rate source areas.
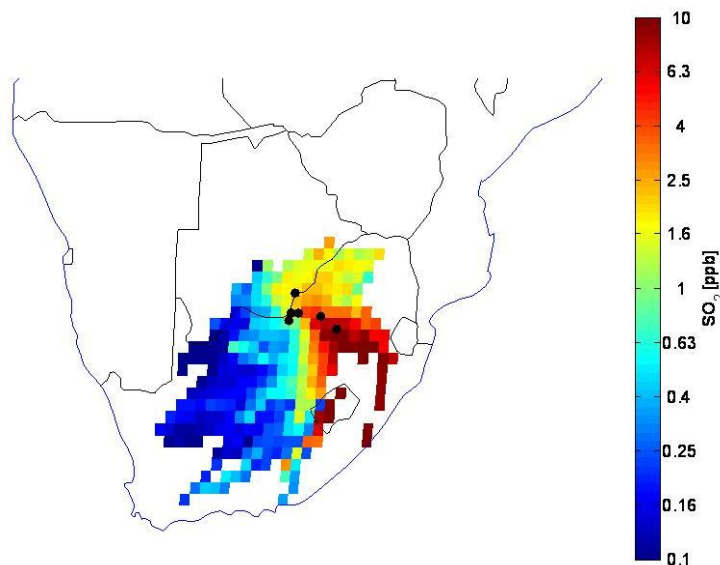
Figure 5 SO$_2$ source areas.

CONCLUSIONS

The observed formation and growth rates, as well as the new particle formation frequency, are among the highest reported in the literature, and thus the particle formation may significantly modulate the clouds and their properties. The source areas of growth rates and SO$_2$ suggest that sulphur-containing compounds or some other anthropogenic emissions would contribute most to the growth of ions in the size range of 1.5 – 3nm, whereas higher emissions of volatile organic compounds would contribute more to the growth of 7 – 20nm ions and 10 – 30nm neutral particles.

REFERENCES

Dal Maso, M., Kulmala, M., Riipinen, I., Wagner, R., Hussein, T., Aalto, P. P., and Lehtinen, K. E. J. (2005) Formation and growth of fresh atmospheric aerosols: Eight years of aerosol size distribution data from SMEAR II, Hyytiälä, Finland, Boreal Environ. Res., 10, 323–336.

Draxler R.R., and Hess, G.D. (2004) Description of the HYSPLIT_4 Modeling System, NOAA Technical Memorandum ERL ARL-224.

Hamed, A., Joutsensaari, J., Mikkonen, S., Sogacheva, L., Dal Maso, M., Kulmala, M., Cavalli, F., Fuzzi, S., Facchini, M. C., Decesari, S., Mircea, M., Lehtinen, K. E. J. and Laaksonen, A. (2007) Nucleation and growth of new particles in Po Valley, Italy, Atmos. Chem. Phys., 7, 355-376.

Hirsikko A., Laakso L, Hõrrak U., Aalto P.P., Kerminen V.-M. & Kulmala M. (2005) Annual and size dependent variation of growth rates and ion concentrations in boreal forest, Boreal Env. Res. 10: 357–369.

Kulmala, M., Riipinen, I., Sipilä, M., Manninen, H. E., Petäjä, T., Junninen, H., Dal Maso, M., Mordas, G., Mirme, A., Vana, M., Hirsikko, A., Laakso, L., Harrison, M.M., Hanson, I., Leung, C., Lehtinen, K.E.J. & Kerminen, V-M. (2007) Toward direct measurement of atmospheric nucleation. Science 318:89-92.

Kulmala, M., Vehkamäki, H., Petäjä, T., Dal Maso, M., Lauri, A., Kerminen, V.-M., Birmili, W., and McMurry, P. H. (2004) Formation and growth rates of ultrafine atmospheric particles: A review of observations, J. Aerosol Sci., 35, 143-176.

Mirme, A., Tamm, E., Mordas, G., Vana, M., Uin, J., Mirme, S., Bernotas, T., Laakso, L., Hirsikko, A., Kulmala, M. (2007) A wide-range multi-channel Air Ion Spectrometer. Boreal Environ. Res., 12, 247 – 264.

Laakso, L., Laakso, H., Aalto, P. P., Keronen, P., Petäjä, T., Nieminen, T., Pohja, T., Siivola, E., Kulmala, M., Kgabi, N., Molefe, M., Mabaso, D., Phalatse, D., Pienaar, K. and Kerminen, V.-M. (2008) Basic characteristics of atmospheric particles, trace gases and meteorology in a relatively clean Southern African Savannah environment, Atmos Chem Phys 8, 4823-4839.

Laakso, L., Koponen, I.K., Mönkkönen, P., Kulmala, M., Kerminen, V.-M., Wehner, B., Wiedensohler, A., Wu, Z., Hu, M. (2006) Aerosol particles in the developing world; a comparison between New Delhi in India and Beijing in China, Water, Air and Soil Pollution, 1 - 16, doi:10.1007/s11270-005-9018-5.

Otter, L., Güenther, A., Wiedinmyer, C., Fleming, G., Harley, P., Greenberg, J.: Spatial and temporal variations in biegenic volatile organic compound emissions for Africa South of equator, J. Geophys. Res., 108, doi:10.1029/2002JD002609, 2003

Petäjä, T., Laakso, L., Pohja, T., Siivola, E., Laakso, H., Aalto, P.P., Keronen, P., Kgabi, N.A. and Kulmala, M. (2007) Mobile air quality monitoring trailer for developing countries, Proceedings of International Conference on Nucleation and Atmospheric Aerosols 2007, Galway, Ireland, August.

Piketh, S., van Nierop, M., Rautenbach, C., Walton, N., Ross, K., Holmes, S., Richards, T. (2005) Rustenburg Local Muncipality Air Quality Management Plan, Palace consulting engineers ltd., Republic of South Africa.

Vartiainen, E., Kulmala, M., Ehn, M., Hirsikko, A., Junninen, H. and co-authors. (2007) Ion and particle number concentrations and size distributions along the Trans-Siberian railroad. Bor. Env. Res. 12, 375–396.

MEASUREMENTS OF CHARGED AND NEUTRAL NANOMETER-SIZED PARTICLES AT MACE HEAD

M.VANA[1,2], H.E. MANNINEN[1], T. NIEMINEN[1], K. LEHTIPALO[1], M. SIPILÄ[1], D. CEBURNIS[3], C.D. O'DOWD[3] and M. KULMALA[1]

[1]Department of Physics, P.O. Box 64, FI-00014, University of Helsinki, Finland
[2]Institute of Physics, University of Tartu, Ülikooli 18, 50090 Tartu, Estonia
[3]School of Physics and Centre for Climate and Air Pollution Studies, Environmental Change Institute, National University of Ireland, Galway, Ireland

Keywords: Atmospheric nanoparticles, Nucleation, Particle formation and growth, Marine aerosols

INTRODUCTION

Atmospheric nanoparticles are the product of various gas-to-particle transformation processes: homogeneous and heterogeneous nucleation of the gaseous ingredients and the growth of the newborn nuclei by condensation, coagulation and/or chemical reactions on their surface. Observations and theory suggest that the initial nucleation in the atmosphere produces particles with diameters of the order of 1 – 2 nm (Kulmala et al., 2000). Hence, in order to understand formation mechanisms of atmospheric aerosol particles direct measurements of the sub-3 nm particles are needed. Air ions have been measured at different sites around the world (Kulmala and Tammet, 2007). Some experimental evidence on the existence of a pool of neutral clusters in the sub-3 nanometer size range has also been reported (Kulmala et al., 2007; Sipilä et al., 2008). Cluster formation mechanisms can vary in different locations. Therefore, more continuous long-term measurements of sub-3 nm particles at different locations will be required.

Coastal regions are places where new particle formation takes place frequently, typically during exposure of shore biota during low tide conditions (O'Dowd and Hoffmann, 2005). Therefore, coastal aerosols can significantly contribute to the natural background aerosol population. Coastal nucleation events can be driven by emissions of iodine vapours that undergo rapid chemical reactions to produce condensable iodine oxides. Recent studies have shown that the bursts of intermediate air ions are common phenomenon at coastal regions (Vana et al., 2008).

In this work we utilized three different instruments to measure the size (mobility) distribution of charged and neutral particles at the Mace Head research station. Sub-3 nm particles were measured with two different instruments. One of our aims was to obtain more information on the behavior of neutral and charged particles with diameter < 3 nm and also to detect possible seasonal variation in the particle formation. We characterize coastal nucleation events and behavior of neutral and charged clusters at the Mace Head research station on the west coast of Ireland.

METHODS

We measured particle size distribution with a Neutral cluster and Air Ion Spectrometer (NAIS), designed by the University of Tartu, and built by Airel Ltd., Estonia. The NAIS is a further development of the Air Ion Spectrometer (AIS) (Mirme et al., 2007) and measures mobility distributions of neutral and charged aerosol particles and clusters in the mobility range from 0.0013 to 3.2 cm^{2}V^{-1}s^{-1}, which corresponds to the diameter range from 0.8 to 41 nm. The NAIS was calibrated during a special calibration and intercomparison workshop (Asmi et al., 2009). As a supporting data sets, we also measured particle size distribution with a Pulse-Height Condensation Particle Counter (PH-CPC) (Sipilä et al., 2008; Sipilä et al., 2009) and Scanning Mobility Particle Sizer (SMPS).

As a part of the European Commission 6th Framework program project EUCAARI (European Integrated project on Aerosol Cloud Climate and Air Quality interactions), we deployed a NAIS at the Mace Head Atmospheric Research Station (53°19'N, 9°54'W) on the west coast of Ireland from 13 June 2008, and continuing in 2009. The PH-CPC measured at Mace Head from 13 June to 25 August 2008. The SMPS measures continuously at the research station.

Supporting basic meteorological data (temperature, pressure, relative humidity, precipitation, wind speed and direction), solar radiation, air mass trajectories and modelled data of the tidal height for the measurement location were included in the data analysis.

RESULTS

Our dataset enables to compare the concentrations of freshly nucleated aerosol particles measured with three different instruments. In diameter range below 3 nm we can use only data from the NAIS and PH-CPC, since the SMPS has the cutoff diameter of about 3.5 nm. Data analysis showed that all three different instruments can detect nanometer-sized particle formation and give similar results. The concentrations of 1.8 – 3 nm particles measured during nucleation events varied between 10^3 and 10^6 cm^{-3} having higher values in autumn. Figure 1 shows scatterplots of the fraction number concentration of nanometer-sized particles measured by the NAIS and PH-CPC. Data points in Figure 1 are from time period 21 – 23 June, 2008. All three days were nucleation event days. Correlation between the PH-CPC and the NAIS is better for 3 – 5 nm particles size range and during nucleation events when concentration is considerably higher compared to background conditions. In background conditions the NAIS tends to show higher concentration than the PH-CPC, especially in size range 1.8 – 3 nm.
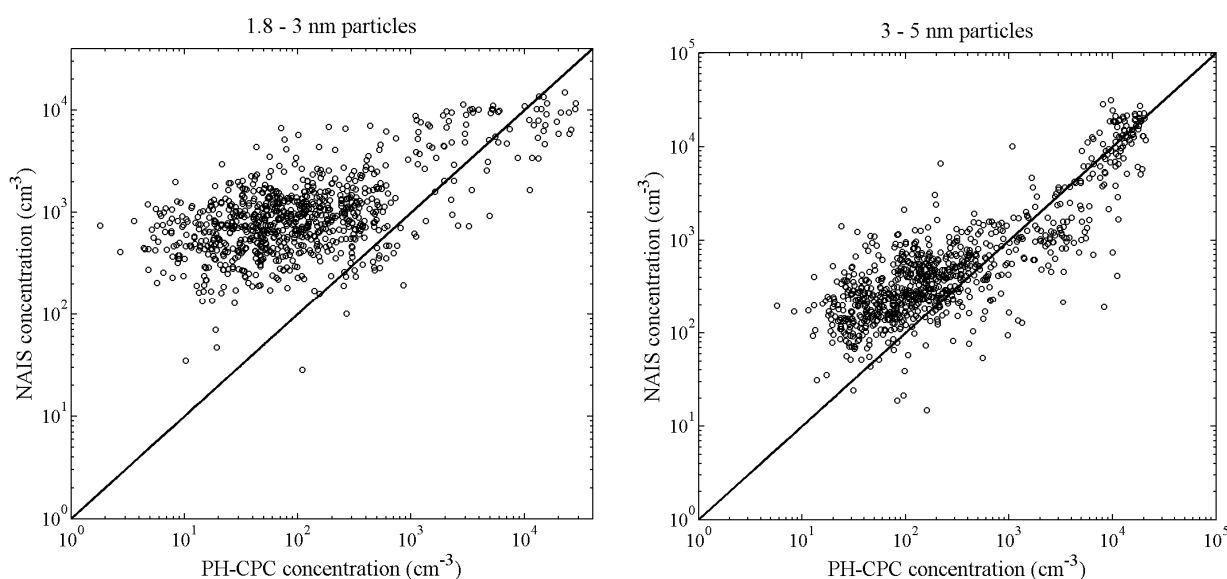
Figure 1. Scatterplots of the fraction number concentration of nanometer-sized particles measured by the NAIS and PH-CPC.

The analysis shows that bursts of intermediate ions and neutral clusters are a frequent phenomenon in the marine coastal environment. Nucleation events occurred during most of the measurement days. Particle formation and growth events mostly coincided with the presence of low tide. We calculated the formation rate (J_2) values for charged and neutral clusters using calculation scheme described by Kulmala et al., 2007. Figure 2 shows typical "apple"-type event which coincided with low tide occurrence and the wind

direction was from the sector where air was advected over sparsely populated land in the northwest-to-north direction (Vana et al., 2008). We can see that J_2 can be more than 200 cm^{-3}s^{-1} during the nucleation event. Coastal areas are somewhat different from other places around the world from the point of view of new particle formation and therefore this result differs from that observed over the boreal forest where values of J_2 are typically in the range 1 to 2 cm^{-3}s^{-1} (Kulmala et al., 2007). For positive and negative ions, values of J_2 calculated from the NAIS data varied between 1 – 3 cm^{-3}s^{-1} during the same coastal nucleation event. In calculations of J_2 for ions we have not taken into account ion attachment by neutral particles.
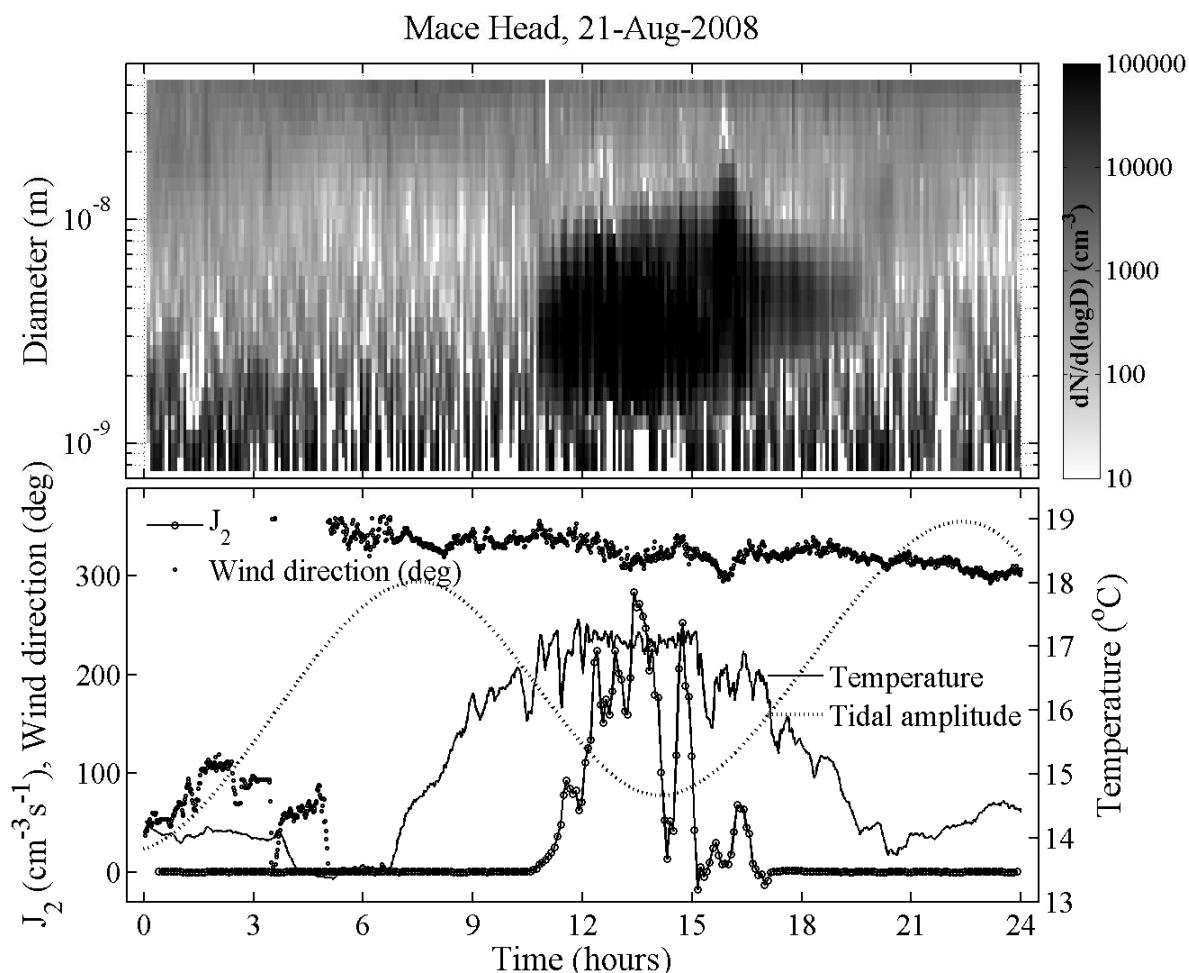
Figure 2. The time variations of the particle size distribution measured by the NAIS, the formation rate of 1.8-nm clusters (J_2), wind direction, temperature, and tidal amplitude during a coastal nucleation event day.

The NAIS can measure in several different modes which enable to estimate charging state of freshly nucleated particles. Also the size distributions measured with the PH-CPC and the SMPS in combination with the size distribution of air ions measured by the NAIS can be used to estimate the percentage of charged particles. Figure 3 illustrates the variation of total cluster concentration in the diameter range 1.8 – 3 nm and the charging probability for negatively and positively charged particles in the same size range. The charging probability for negatively charged particles has maximum values about 0.04 – 0.05 during 1 hour before the concentration burst of neutral particles and decreases drastically during nucleation event being sometimes less than 0.005. This is a typical feature for the nucleation events detected at Mace Head, and shows that negatively charged clusters activate easier than positively charged and neutral particles.
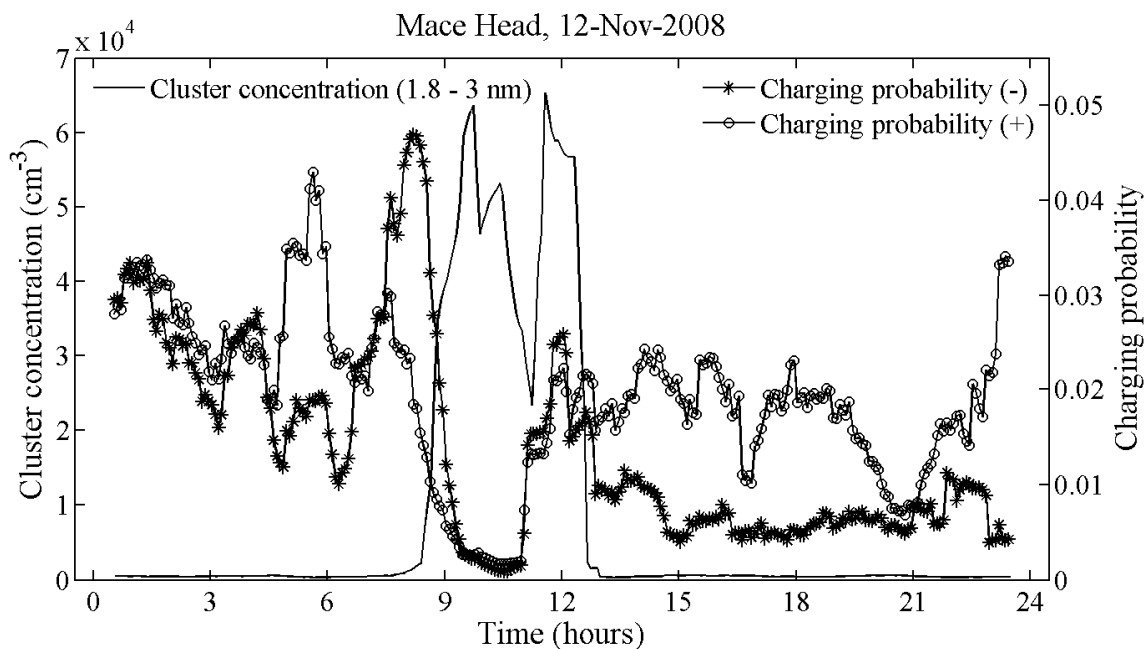
Figure 3. The time variations of the cluster concentration measured by the NAIS, and the charging probability for negatively and positively charged particles in the diameter range of 1.8 – 3 nm during a coastal nucleation event day.

CONCLUSIONS

We measured particle size distributions in the diameter range of 0.8 – 41 nm. Nucleation events occurred during most of the measurement days. We can conclude that the NAIS and the PH-CPC can be used for observation of sub-3 nm particles in the atmosphere. The two instruments give better results then they measure high concentrations during nucleation events. The concentration of 1.8 – 3 nm particles varied between 10^3 to 10^6 cm^{-3} during nucleation events.

Formation rates of 2 nm particles are high during coastal nucleation events. J_2 can be 100 – 1000 cm^{-3}s^{-1}, which differ from observations over the boreal forest where values of J_2 are typically 1 – 2 cm^{-3}s^{-1}. We calculated charging probabilities for > 1.8 nm particles. Time variation of charged fraction of 1.8 – 3 nm particles show that negatively charged clusters seem to activate easier than positively charged and neutral particles. During nucleation event 1.8 – 3 nm particles seem to be highly undercharged.

To get more information about sub-3 nm charged and neutral particles more field measurements should be performed in different kind of atmospheric environments.

ACKNOWLEDGMENTS

REFERENCES

Asmi, E., Sipilä, M., Manninen, H. E., Vanhanen, J., Lehtipalo, K., Gagné, S., Neitola, K., Mirme, A., Mirme, S., Tamm, E., Uin, J., Komsaare, K., Attoui, M. and Kulmala, M. (2009). Results of the first air ion spectrometer calibration and intercomparison workshop. Atmos. Chem. Phys., 9, 141-154.

Kulmala, M., Pirjola, L., Mäkelä, J. M. (2000). Stable sulphate clusters as a source of new atmospheric particles. Nature, 404, 66-69.

Kulmala, M., Riipinen, I., Sipilä, M., Manninen, H. E., Petäjä, T., Junninen, H., Dal Maso, M., Mordas, G., Mirme, A., Vana, M., Hirsikko, A., Laakso, L., Harrison, R. M., Hanson, I., Leung, C., Lehtinen, K. E. J. and Kerminen, V.-M. (2007) Towards direct measurement of atmospheric nucleation. Science, 318, 89-92.

Kulmala, M. and Tammet, H. (2007). Finnish-Estonian air ion and aerosol workshop. Boreal Env. Res., 12, 237-245.

Mirme, A., Tamm, E., Mordas, G., Vana, M., Uin, J., Mirme, S., Bernotas, T., Laakso, L., Hirsikko, A. and Kulmala, M. (2007). A wide-range multi-channel Air Ion Spectrometer. Boreal Env. Res., 12, 247-264.

O'Dowd, C. D. and Hoffmann, T. (2005). Coastal new particle formation: a review of the current state-of-the-art. Environ. Chem., 2, 245-255.

Sipilä, M., Lehtipalo, K., Kulmala, M., Petäjä, T., Junninen, H., Aalto, P. P., Manninen, H. E., Vartiainen, E., Riipinen, I., Kyrö, E.-M., Curtius, J., Kürten, A., Borrmann, S. and O'Dowd, C. D. (2008). Applicability of condensation particle counters to measure atmospheric clusters. Atmos. Chem. Phys., 8, 4049-4060.

Sipilä, M., Lehtipalo, K., Attoui, M., Neitola, K., Petäjä, T., Aalto, P. P., O'Dowd, C. D. and Kulmala, M. (2009). Laboratory verification of PH-CPC's ability to monitor atmospheric sub-3 nm clusters. Aerosol Sci. Technol., 43, 126-135.

Vana, M., Ehn, M., Petäjä, T., Vuollekoski, H., Aalto, P., de Leeuw, G., Ceburnis, D., O'Dowd, C. D. and Kulmala, M. (2008). Characteristic features of air ions at Mace Head on the west coast of Ireland. Atmos. Res., 90, 278-286.

MIXING-TYPE CONDENSATION PARTICLE COUNTER DETECTING CHARGED CLUSTERS DOWN TO 1.05 nm

J. VANHANEN[1], M. SIPILÄ[1,2], J. MIKKILÄ[1], T. PETÄJÄ[1] and M. KULMALA[1]

[1]Department of Physics, P.O. Box 64, FI-00014, University of Helsinki, Finland
[2]Institute for Tropospheric Research, Permoserstrasse 15, D-04318 Leipzig, Germany

Keywords: CPC, Cluster, Heterogeneous nucleation

INTRODUCTION

Atmospheric new particle formation is an important source of aerosol particles in the atmosphere (Kulmala, 2003). These particles affect the climate system by scattering and absorbing light and acting as cloud condensation nuclei. It has been suggested that new particle formation initiates from a stable pool of neutral and charged clusters (Kulmala et al., 2007). Measurements show that in boreal forest there is a constant cluster pool with median diameter of 1.5 to 1.8 nm (Kulmala et al., 2007). These clusters can activate and grow to larger sizes. For detection of particles down to nanometer sizes, condensation particle counters (CPC) are widely used (McMurry, 2000; Sipilä et al., 2008).Current state of the art commercial particle counters are able to detect neutral particles having diameter larger than 3 nm. In the CPC the particles are grown to optical sizes via vapor condensation. There has been a few attempts to improve current commercially available CPCs but the detection efficiency of particles having diameter smaller than 2 nm is usually less than 10% and only few percents for the particles smaller than 1.5 nm (Sipilä et al., 2008; Iida et al., 2009), depending on the composition and on the condensable vapors. In this study a new portable mixing type condensation particle counter (MCPC) was developed and tested. The main benefit of a mixing type CPC is smaller diffusion losses due to higher sample flow rate. This makes it suitable for detection of the smallest particles. Previous laboratory studies have shown that MCPCs are able to activate and count particles down to 1.2 nm (Sgro et al., 2004)

DESIGN OF THE MIXING-TYPE CPC

The figure 1 shows a block diagram of the portable mixing-type CPC developed in this study. The basic idea is to mix turbulently clean filtrated air, which is saturated with the working fluid, with cooled aerosol flow inside a mixing T-part. The mixing section had dimensions similar to the design by Sgro and de la Mora (Sgro et al. 2004). A high supersaturation of the working fluid is achieved and the particles larger than a certain critical size are activated. These particles grow inside the growth section, and a TSI 3010 CPC is used to count the activated particles.

Physical characteristics of the working fluid, such as saturation vapor pressure and surface tension, affect the size-dependent activation efficiency of the CPC (Iida et al. 2009). In this study diethylene glycol was used as the working fluid. It has relatively high surface tension and low saturation vapor pressure. Because of these properties a high saturation ratio is acquired without homogeneous nucleation. This choice of working fluid was due to modelling results presented in Iida et al. (2009). The particles, however, can not be easily grown to optical sizes (>~1μm in diameter) using diethylene glycol because of its low vapor pressure. This is why an external CPC (TSI 3010) is used for detecting the activated particles in this preliminary design.
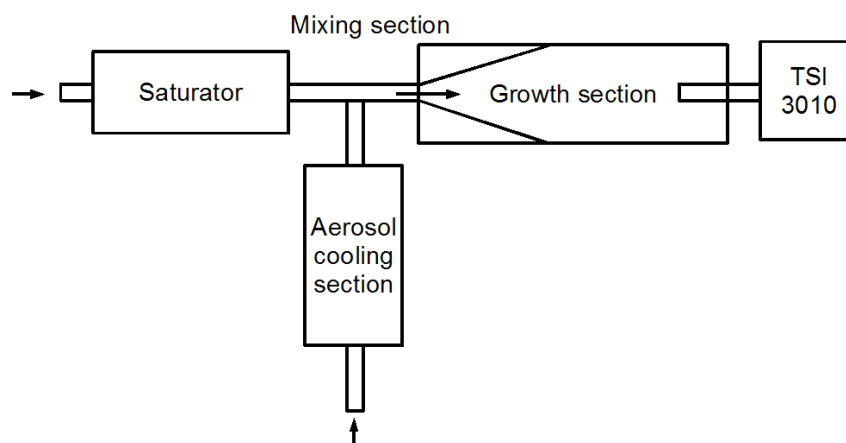
Figure 1. A block diagram of the mixing-type condensation particle counter.

FIRST MEASUREMENTS AND RESULTS

The first measurements were conducted with mobility standards (Ude. et al., 2005), and silver nanoparticles. Mobility standard particles were produced with electrospray and the correct size was selected with a high resolution and high flow differential mobility analyzer (HDMA (Herrmann et al., 2000)). By using this setup a highly monodisperse aerosol is achieved. An electrometer (TSI 3068B) was used as a reference instrument. Tetra-heptyl ammonium bromide (THAB) and Tetra-methyl ammonium iodine (TMAI) were used as the mobility standards. Silver nanoparticles were generated with tube furnace and a correct size was selected by using a short Hauke-type DMA. Flow through the saturator of the MCPC was chosen to be 0.6 l min^{-1}, and the sample flow was 2.5 l min^{-1}. The external CPC (TSI 3010) had a sample flow of 1.0 l min^{-1}. This results a mixing ratio of 0.19 and a saturation ratio of 17 with chosen temperatures (Okuyama et al., 1984). We assumed that the flow was fully saturated after the saturator. By using this saturation ratio a background of <10cm^{-3} caused by homogenous nucleation was measured when placing a filter in front of the inlet.

In figure 2 the detection efficiency is presented as a function of particle mobility diameter. The detection efficiency for THAB monomer (mobility of 0.971 cm^2 Vs^{-1} and mobility diameter of 1.47 nm) is 55% and for the TMAI monomer (mobility of 2.179 cm^2 Vs^{-1} and mobility diameter of 1.05 nm) 23%. From these preliminary measurements the cut-off size of the CPC for positively charged particles of ~1.4nm can be determined.

If the mixing ratio is changed also the saturation ratio changes (Okuyama et al., 1984). By changing the saturation ratio the cut-off of the MCPC can be changed. In figure 3 the detection efficiency of the MCPC (scaled to 1) is presented as a function of the mixing ratio for TMAI monomer, THAB monomer and THAB dimer. Detection efficiency increases steeply as the mixing ratio is increased. The 50% cut-off is different for different mobility diameters. This indicates that by scanning over the mixing ratio the particle size can be distinguished, and eventually the MCPC can be used as a mobility size spectrometer for the smallest clusters.
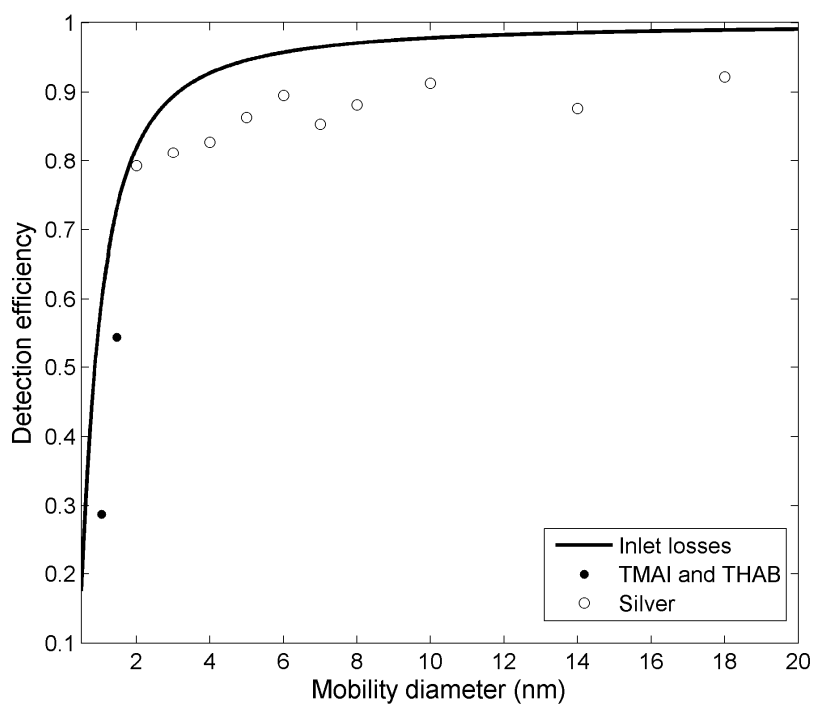
Figure 2. Detection efficiency measured using THAB monomer (mobility of 0.971 cm^2 Vs^{-1} and mobility diameter of 1.47 nm) and TMAI monomers (mobility of 2.179 cm^2 Vs^{-1} and mobility diameter of 1.05 nm) and silver nanoparticles.
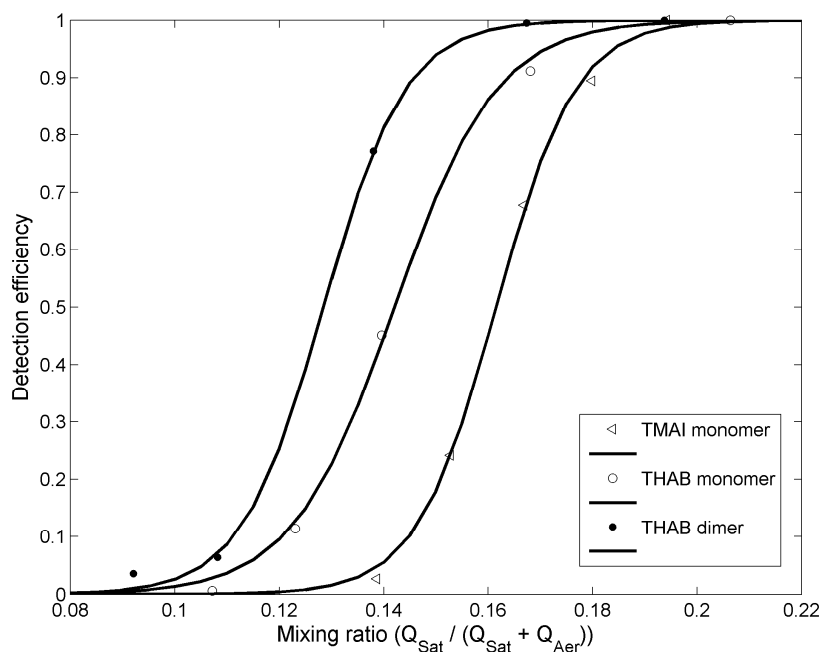
Figure 3. Detection efficiency of the MCPC as a function of mixing ratio for TMAI monomer (mobility of 2.179 cm^2 Vs^{-1} and mobility diameter of 1.05 nm), THAB monomer (mobility of 0.971 cm^2 Vs^{-1} and mobility diameter of 1.47 nm) and THAB dimer (mobility of 0.654 cm^2 Vs^{-1} and mobility diameter of 1.78 nm). Solid lines are fits to the measured values. Detection efficiency is scaled to 1.

CONCLUSIONS

A new mixing-type CPC using diethylene glycol as a working fluid was developed and tested. The first measurements showed that the MCPC was able to activate charged particles down to 1.05 nm in diameter with detection efficiency of 23%, which is at least order of magnitude higher than e.g. reported by Iida et al. (2009) and Sipilä et al. (2008) for improved TSI ultrafine CPC's (TSI 3025 (Stolzenburg and McMurry, 1991)). Also measurements by scanning the mixing ratio were conducted. These measurements showed clearly that after a proper calibration the MCPC can also be used as a mobility size spectrometer. Future plans include measurements of neutral particles down to the cluster sizes, and atmospheric measurements.

REFERENCES

Hermann, W., Eicher, T., Bernardo, N., and de la Mora, J. F., Abstract to the annual conference of the *AAAR,* St. Louis, MO, 6-10 October 2000.

Iida, K., Stolzenburg, M. R. and McMurry, P. H. (2009) Effect of Working Fluid on Sub-2 nm Particle Detection with a Laminar Flow Ultrafine Condensation Particle Counter, *Aerosol Science and Technology*, 43:81-96.

Kulmala, M. (2003) How particles nucleate and grow?, *Science*, 302, 1000-1001.

Kulmala, M., Riipinen, I., Sipilä, M., Manninen, H., Petäjä, T., Junninen H., Dal Maso, M., Mordas, G., Mirme, A., Vana, M., Hirsikko, A., Laakso, L., Harrison, R. M., Hanson, I., Leung, C., Lehtinen, K. E. J., and Kerminen, V.-M.(2007) Towards direct measurement of atmospheric nucleation, *Science*, 318, 89-92.

McMurry, P. H. (2000) A review of atmospheric measurements, *Atmospheric Environment*, 34, 1959-1999.

Okuyama, K., Kousaka, Y., and Motouchi, T. (1984) Condensation Growth of Ultrafine Aerosol Particles in a New Particle Size Magnifier, *Aerosol Science and Technology*, 3:4, 353-366.

Sgro, L. A., de la Mora, J. F. (2004) A Simple Turbulent Mixing CNC for Cherged Particle Detection Down to 1.2 nm, *Aerosol Science and Technology*, 38:1-11.

Sipilä, M., Lehtipalo, K., Kulmala, M., Petäjä, T., Junninen, H., Aalto, P. P., Manninen, H., Kyrö, E.-M. Asmi, E., Riipinen, I., Curtius, J., Kürten, A., Borrmamm, S., and O'Dowd, C. D. (2008) Applicability of condensation particle counters to measure atmospheric clusters, *Atmospheric Chemistry and Physics*, 8, 4049-4060.

Stoltzenburg, M. R. & McMurry, P.H. (1991) An ultrafine aerosol condensation nucleus counter. *Aerosol Sci. Technol,*. 14, 48-65.

Ude. S., and de la Mora, J. F. (2004) Molecular monodisperse mobility and mass standards from electrospray of tetra-alkyl ammonium halides, *Journal of Aerosol Science*, 36, 1224-1237.

NON-LINEARITY IN CHAMBER FLUX MEASUREMENTS REVISITED AND POTENTIAL BENEFITS OF MEASURING SIMULTANEOUSLY SEVERAL GASES

T. VESALA[1], A. NORDBO[1], M. PIHLATIE[1], H. AALTONEN[1], J. KORHONEN[1], P. KOLARI[2], L. KULMALA[2], E. NIKINMAA[2], P. HARI[2], J. PUMPANEN[2] and P. KROON[3]

[1]Department of Physics, P.O. Box 64, FI-00014, University of Helsinki, Finland
[2]Deparrtment of Forest Ecology, P.O. Box 27, FI-00014, University of Helsinki, Finland
[3]Department of Air Quality and Climate Change, Energy Research Centre of the Netherlands, Westerduinweg 3, 1755 LE Petten, The Netherlands

Keywords: gas fluxes, static chambers, photosynthesis, soil respiration

INTRODUCTION

Biosphere-atmosphere gas exchange can be measured by various techniques. The most common methods are micrometeorological ones (like eddy covariance) and those based on chambers. Several types of chamber designs exist and there is no single ideal universal chamber for all purposes, since the item to be measured (soil efflux, leaf/shoot, ground vegetation exchange), the compound, its possible chemical reactivity and the typical magnitude of the flux all affect the decision on the measurement configuration. Systematic comparisons of different chamber types are scarce. Pumpanen et al. (2004) utilized the known source of CO_2 for testing and comparing different chambers. Beside plain technical details (size of the chamber, ventilation, leakage etc.) the differences in the flux estimates may rise also on different calculation methods. Namely, the chamber does not detect the flux itself but the concentration change in the chamber is monitored, and the flux is estimated from the concentration change. This concerns especially the closed, non-steady-state chamber, which is probably the most widely used type, and which is considered in this study. The chamber is typically in the non-measurement state, that is open and minimally disturbing the measured object, for extended periods, and then it is closed for a measurement. During the closure the concentration tends to increase in the case of the source and decrease for the sink and one crucial point is the significance of non-linearity in the concentration change (see e.g. Livingston et al., 2005; Kutzbach et al., 2007; Kroon et al., 2008; Stolk et al., 2009). In this study we formulate the mass balance equation for the closed chamber and give the general mathematical solution for it. This is not the novel feature and can be found, possibly in somewhat different forms, for example in the studies mentioned above. The point is in the interpretation of the result in the case of simultaneous measurements of two compounds and potential benefits of the approach.

THEORY

The formulation of the mass balance equation for the closed chamber includes I) exchange with the environment (leakage or controlled feed of the air), II) exchange due to leaf/shoot or soil enclosed by the chamber and III) first-order chemical reaction on chamber walls. The equation is

$$V\frac{dC}{dt} = q\left(C_a - C(t)\right) + Ag(C_i - C(t)) - A'kC(t) \qquad (1)$$

where V is the chamber volume, C is the concentration in chamber headspace, q is the flow between ambient and chamber (leakage or controlled flow), C_a is the ambient concentration or the concentration in the controlled inflow, A is the soil surface area enclosed by the chamber or the leaf/shoot area, g is the mass transfer coefficient for soil-air gas transport or the stomatal conductance [m/s], C_i is the compensation point in the soil (effective driving variable) or compensation point for stomatal gas

exchange (concentration in the sub-stomatal cavity), A' is the chamber wall surface and k is the first-order rate of chemical reactions on the chamber wall.

Note that only the concentration itself is time-dependent and all other factors are assumed to be constant (for a single closure). Thus the equation includes only constant and linear terms in respect of the solvable C(t) and the general solution is always exponential (shown below). In addition, the physical transport phenomena are generally proportional to concentration (differences) and as long as the chemical reactions are the first–order the exponential time-dependence of the concentration is the fundamental feature. However, as an example, for a soil chamber the compensation point in the soil may also change in time especially for long closure times. If this is taken into account the simple solution given below is not valid anymore.

If the concentration at t = 0 (at the beginning of the closure) is fixed, i.e. known, the general solution is

$$C = -\frac{\beta}{\alpha} + (C_0 + \frac{\beta}{\alpha})e^{\alpha t} \tag{2}$$

where

$$\alpha = -(\frac{q}{V} + \frac{Ag}{V} + \frac{A'k}{V})$$

$$\beta = \frac{qC_a}{V} + \frac{AgC_i}{V} \tag{3}$$

and

$$C_0 = C(0)$$

Since the argument of the exponent is always negative the concentration saturates in time and the concentration change follows

$$\frac{dC}{dt} = (\alpha C_0 + \beta)e^{\alpha t} \tag{4}$$

For curiosity, let us assume maybe the most simplified case setting q = 0 and k = 0 and assuming that t is small, then, for the soil chamber, when the height of the chamber h is equal to $\frac{A}{V}$, the above equation is

reduced to

$$\frac{dC}{dt} = \frac{q}{h}(C_i - C_0) \tag{5}$$

This formula is often used for soil chambers in flux calculations although it includes several simplifying assumptions.

RESULTS AND CONCLUSIONS

The flux calculation is based on the solving of the unknown parameters by fitting to the measured concentration changes. Eq. (2) includes two parameters α and β, of which values can be deduced by fitting. However, in general there are altogether 5 unknowns, on which α and β depend: q, C_a, g, C_i and k,

and their values cannot be obtained by knowing only α and β. Let us consider some special cases of soil chambers.

If the gas is inert then $k = 0$ or if k is determined by means of, for example, the reference chamber then k is known, If in addition the ambient exchange is controlled (and leakages are small compared to controlled exchange), then q and C_a are also known, In this case there are only two unknowns, g and C_i, and their values can be calculated from the known, fitted α and β according to Eq. (3).

However, the controlled ambient exchange is not always feasible and the leakages are not known. Then, although we assume that $k = 0$ (or k is known), we have 4 unknowns: q, C_a, C_i and g. Let us consider two gases measured simultaneously (referred by subscripts 1 and 2). Then we have 8 unknowns: q_j, $C_{a,j}$, g_j, $C_{i,j}$ where j refers to 1 or 2, and 4 fittings parameters α_j and β_j. However, the parameters related to the physical transport are coupled, which can be utilized in reducing the number of unknowns. If the soil-air transport is governed by diffusion, the transport rates are scaled by diffusion coefficients D_i according to

$$g_1 = \frac{D_1}{D_2} g_2 \qquad \text{(diffusion governed)} \tag{6}$$

or if the transport is convection (bulk flow) then

$$g_1 = g_2 \qquad \text{(convection governed)} \tag{7}$$

One of these assumptions reduces the number of unknowns to 7.

The same assumptions, either diffusion or convection controlled modes, can be similarly applied also to the leakage. This reduces the number of unknowns to 6.

If C_a is measured for both gases, then the number of unknowns is reduced to 4, which is exactly the amount of the fitting parameters, that is α_1, β_1, α_2 and β_2. Now using Eq. (3) for both compounds together with relationships (6) or (7), the unknown physico-biological quantities, i.e. q_1, g_1, $C_{i,1}$, $C_{i,2}$ and q_2, g_2, can be solved. Note that if only one compound was measured, the number of fitting parameters would be 2 and the number of unknowns, when C_a has been measured, would be 3. Thus the simultaneous measurement of two gases makes the problem solvable and facilitates the determination of transport rates and compensation points, which are difficult to measure/determine directly.

REFERENCES

Kroon, PS, Hensen, A. Van den Bulk, WCM, Jongejan, PAC, Vermeulen, AT, 2008. The importance of reducing the systematic error duet o non-linearity in N_2O flux measurements by static chambers, Nutr Cycl Agroecosyst, 82, 175-186.

Kutzbach,L., Schneider,J., Sachs,T., Giebels,M., Nykanen,H., Shurpali,N.J., Martikainen,P.J., Alm,J., Wilmking,M., 2007. CO_2 flux determination by closed-chamber methods can be seriously biased by inappropriate application of linear regression. Biogeosciences 4, 1005-1025.

Livingston, G.P., Hutchinson, G.L., and Spartalian, K. 2005. Diffusion theory improves chamber-based measurements of trace gas emissions. Geophysical Research Letters 32, L24817.

Pumpanen, J., Kolari, P., Ilvesniemi, H., Minkkinen, K., Vesala, T., Niinisto, S., Lohila, A., Larmola, T., Morero, M., Pihlatie, M., Janssens, I., Yuste, J.C., Grunzweig, J.M., Reth, S., Subke, J.A., Savage, K., Kutsch, W., Ostreng, G., Ziegler, W., Anthoni, P., Lindroth, A., Hari, P., 2004. Comparison of different chamber techniques for measuring soil CO_2 efflux. Agricultural and Forest Meteorology 123, 159-176.

Stolk,P.C., Jacobs,C.M.J., Moors,E.J., Hensen,A.,Velthof,G.L., Kabat,P. 2009. Significant non-linearity in nitrous oxide chamber data and its effect on calculated annual emissions. Biogeosciences Discussion, 6, 115-141.

MEASURING POLYCYCLIC AROMATIC HYDROCARBONS AND TRACE ELEMENTS IN PARTICULATE MATTER IN ARCTIC AIR

M. VESTENIUS, U. MAKKONEN, J. PAATERO and H. HAKOLA

Finnish Meteorological Institute, P.O. BOX 503 FI-00101 HELSINKI, FINLAND

INTRODUCTION

Polycyclic aromatic hydrocarbons (PAH-compounds) and trace elements (Al, As, Cd, Co, Cu, Pb, Mn, Ni, Fe, Zn and V) were measured at the Arctic Ocean during ASCOS campaign in August-September 2008.

PAH compounds are formed during the incomplete burning of organic material. They have several natural (volcanic activities, forest fires) and anthropogenic (burning of different fuels in energy production, biomass burning and traffic) emission sources (Ravindra *et al.*, 2008). For example wood combustion in house warming is one remarkable PAH-source in Northern countries in Europe (Hellen *et al*, 2008).

Main sources of heavy metals are fossil fuel combustion in industrial, residential and commercial boilers and energy-consuming industries, for example steel, iron and other metal production. Also waste incineration, cement production and traffic product heavy metal emissions. The main air pollution sources in Arctic area are Norilsk mining and metallurgical industry and Kola Peninsula. Typically, largest PAH- and heavy metal concentrations in air are measured near emission sources. In Northern Europe long-distance pollution is also remarkable source (EMEP 2008). In Arctic Ocean the measured concentrations were generally very low, as expected.

EXPERIMENTAL

PAH-measurements

Low-volume samplers were used to collect aerosol samples onto 3 µm Millipore Teflon-coated filters, using flow rate 38 lmin^{-1}. Between 47 to 55 cubic meters of air was collected for each sample. PAH-compounds analyzed here were phenantrene, anthracene, fluoranthene, pyrene, benz(a)anthracene, chrycene, benzo(k+b+j)fluoranthene, benzo(a)pyrene, benzo(ghi)perylene, indeno(1,2,3-cd)pyrene and dibenz(a,h+a,c)anthracene. Masses of those compounds varies from 178 (phenantrene) to 278 gmol^{-1} (dibenzo(a,h+a,c)anthracene). Benzo(a)pyrene (BaP) shall be used as a marker for the carcinogenic risk of PAH-compounds in ambient air and the limit values are set for benzo(a)pyrene.

Samples from filters were first extracted 16 hours in dichloromethane using Soxhlet extractor, then concentrated to 0,8-1,0 ml. Concentrated samples were analyzed with gas chromatographic-mass spectrometric method (Agilent 6890N GC and Agilent 5973 MS). Deuterated PAH-compounds (phenantrene-d12, chrysene-d12, perylene-d12 and dibenzo(a,h)anthracene-d14, Dr Ehrenstorfer) were used as internal standards. External standards with five different concentration levels were used for quantification.

LOD:s (limits of detection) and LOQ:s (limits of quantification) of the analysis were estimated from the standard deviation of field blank samples (3xSTDEV and 10xSTDEV, respectively).

The uncertainties of the analysis were calculated according to the method described in the standard (prEN 15549 (2006) using standard reference material "Urban Dust" (NIST 1649a).

Table 1 presents measuring uncertainties and detection and quantification limits for analyzed compounds.

Table 1. Limits of detection (LOD), limits of quantitation (LOQ) and measuring uncertainties (MU) of analyzed PAH-compounds

	LOD	LOQ	LOD	LOQ	MU
	ng/ml	ng/ml	pg/m3	pg/m3	k=2
Phenantrene	0,14	0,46	2,5	8,4	90 %
Anthracene	0,11	0,38	2,1	6,9	90 %
Fluoranthene	0,10	0,34	1,8	6,1	40 %
Pyrene	0,27	0,90	4,9	16,3	80 %
benz(a)anthracene	0,08	0,25	1,4	4,6	40 %
chrycene/trifenyleeni?	0,02	0,06	0,3	1,1	40 %
benzo(k+b+)fluoranthene	0,42	1,41	7,7	25,6	30 %
benzo(a)pyrene	0,67	2,23	12,1	40,5	30 %
benzo(ghi)perylene	0,04	0,14	0,8	2,5	50 %
Indeno(1,2,3-cd)pyrene	0,02	0,06	0,3	1,2	60 %
Dibenz(a,h+a,c)anthracene	0,05	0,15	0,8	2,8	40 %

Trace elements

For measuring trace element concentrations in airborne particulate matter daily air samples were collected with a flow rate of 35 l min^{-1} on Teflon filters (PTFE, Millipore, 3 µm). The samples were collected between 3 August and 7 September 2008. Trace elements (Al, As, Cd, Co, Cu, Pb, Mn, Ni, Fe, Zn and V) were detected from the samples with an ICP-MS (Perkin Elmer Sciex Elan 6000) after the digestion with a solution of HF and HNO_3 in an ultrasonic bath. The detection limits are presented with the mean concentrations measured on Oden in Table 2.

Table 2. The limits of detection (LOD) for components analyzed from the filter samples and the daily average and maximum concentrations measured at Oden.

Component	Average	Max	LOD	Number of values
	Ng/m^3	ng/m^3	ng/m^3	(above LOD/Total)
Aluminum	4.80	31.1	0.24	25/30
Arsenic	0.01	0.05	0.01	5/30
Cadmium	<0.005	0.01	0.005	2/30
Cobalt	0.008	0.10	0.005	11/30
Copper	1.01	14.2	0.13	22/30
Iron	4.70	23.2	0.60	30/30
Manganese	0.08	0.55	0.01	30/30
Nickel	0.38	3.0	0.08	30/30
Lead	0.96	13.3	0.01	30/30
Vanadium	0.25	5.0	0.01	27/30
Zinc	0.58	4.4	0.08	22/30

LODs were calculated as three times the standard deviation of blanks.

RESULTS AND DISCUSSION

At first, we analyzed few selected daily samples to realize overall PAH-levels PAH-concentrations of these samples were generally very low, as expected, and in order to get results above detection limits we decided to combine selected samples into fractions. Sample combining were made according the simultaneously measured radon (Rn^{222}) concentrations, which is useful way to differentiate marine and continental air masses. PAH concentration levels for Benzo(a)pyrene and total PAH sum in ASCOS samples are presented in figure 1 and 2. In Table 2, measured PAH-compounds are arranged according their reactivity in air.
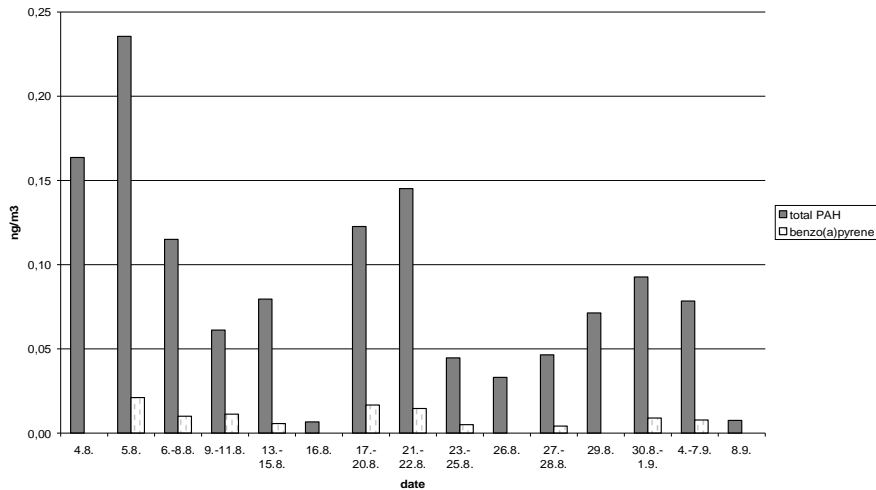
Figure 1: total PAH- and Benzo(a)Pyrene concentration levels in ASCOS samples.
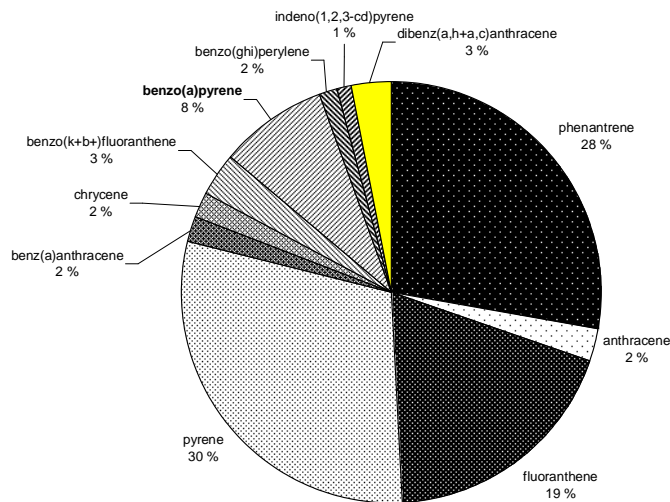
Figure 2: fractions of different PAH-compounds in ASCOS samples.

459

Table 3. Reactivities of analyzed compounds (Finlayson-Pitts and Pitts).

Anthracene

benzo(a)pyrene

dibenz(a,h+a,c)anthracene

benzo(ghi)perylene

benz(a)anthracene

Pyrene

Fluoranthene

phenantrene

indeno(1,2,3-cd)pyrene

Chrycene

benzo(k+b+)fluoranthene

increasing reactivity (vertical arrow)

PAH-levels in the Arctic sea for total PAH and single components are generally very low, between 0.07-0.5 and 0.003-0.03 ng/m3 respectively. When comparing data from Virolahti rural background station from the same time (figure 3), PAH-concentrations in ASCOS samples were generally 5-20 times smaller. PAH-compounds react in air with OH and NO_3-radicals and ozone. These reactions and photo-oxidation are significant decay processes for some of these compounds (table 3). Because of differences in reactivities, we can estimate that concentrations of the more reactive compounds, Anthracene, for example, have decreased remarkably during the transport. Compounds existence in the vapour or particulate phase depends mainly on compound volatility. In this study we analyzed only compounds from particulate phase. Another uncertainty is that part of the most volatile collected PAH-compounds may have been evaporated from the filter.
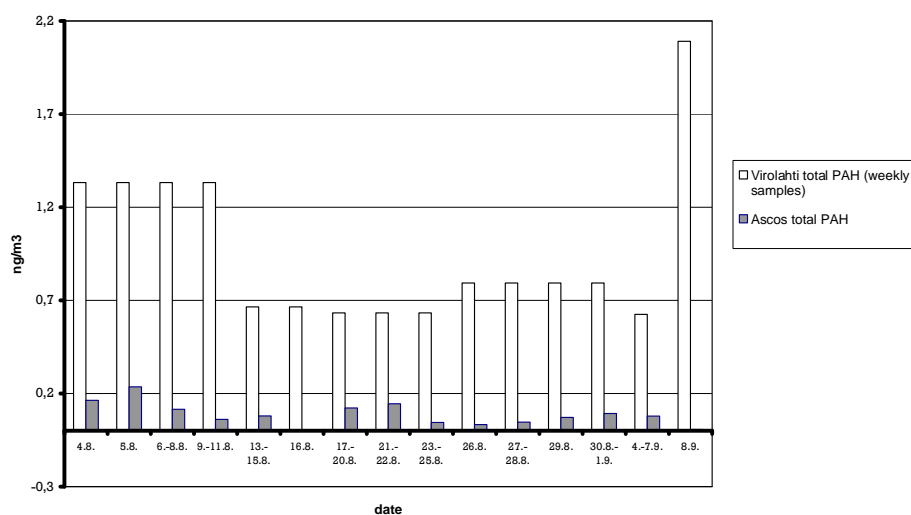
Figure 3. ASCOS total PAH vs. Virolahti total PAH data.

The trace element levels measured on Oden were compared to the concentrations measured at the arctic atmospheric monitoring station at Pallas in the northwestern Finland (Figure 3) during the same time period. All the cadmium, arsenic and cobalt concentrations measured onboard were extremely low, occasionally even below the detection limit. Furthermore, the concentrations of iron and manganese were lower than those measured at Pallas.

The total trace element concentrations were highest on the first day of the measurements onboard. During a slight period with elevated lead, aluminum and zinc concentrations

between 10 – 15 August concentrations were higher than those detected at Pallas. On 6 August there was a peak of nickel, cobalt and vanadium, which might be caused by the emissions of the ship itself (Figure 2).
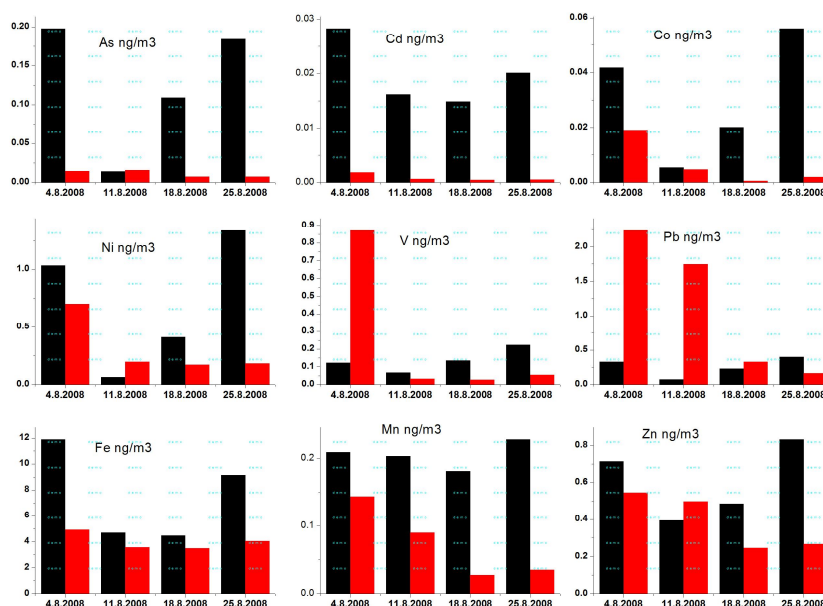
Figure 4. Trace element concentrations measured at Pallas GAW-station in Northern Finland (black) and on Oden (red).

REFERENCES

EMEP Status Report 3/08 *"Persistent Organic Pollutants in the Environment"* Joint MSC-E & CCC Report.

Finlayson-Pitts, B. and Pitts, J.,(2000) *Chemistry of the upper and lower atmosphere* (Academic Press, London), p. 507.

Hellen, H., Hakola, H., Haaparanta, S., Pietarila, S. and Kauhaniemi, M., Influence of residential wood combustion on local air quality, Science of the total environment 393(2008), p.283-290.

Pacyna, J. M., Pacyna E. G., Aas W., 2009. Changes of emissions and atmospheric deposition of mercury, lead, and cadmium. Atmospheric Environment 43, 117-127.

Ravindra, K., Sokhi, R., Van Grieken, R., Review: Atmospheric polycyclic aromatic hydrocarbons: Source attribution, emission factors and regulation,/ Atmospheric Environment 42 (2008), p.2895-2921.

Stebel, K., Christensen, G., Derome, J. and Grekelä I. (editors), 2007. State of the Environment in the Norwegian, Finnish and Russian Border Area, The Finnish Environment 6, 2007. ISBN 978-952-11-2591-1.

THE PLANT FLOW CHAMBER SIMULATION USING
A CONDENSATIONAL GROWTH MODEL

M. VESTERINEN[1], K.E.J. LEHTINEN[2], H. KORHONEN[1] and J. JOUTSENSAARI[1]

[1]Department of Physics, P.O.Box 1627, FIN-70211, University of Kuopio, Finland
[2]The Finnish Meteorological Institute, Kuopio Unit, P.O.Box 1627, FIN-70211, University of Kuopio, Finland

INTRODUCTION

Aerosol flow chambers (a.k.a. reactors) have been used to study the aerosol dynamics both in laboratory experiments and in studies induced by industry needs. Modern research is concentrated mostly in closed chamber measurements, where the system's environment is sealed after gas – phase chemistry initialization. These measurements are used to parameterize the SOA mass concentration for different reactive species as a function of environmental parameters and to give an insight into the chemistry that remains as a large uncertainty in modeling work. Usually, in these measurements the mass concentration of formed SOA is described time – independently and plotted against the reacted VOC concentration. However, the research of flow chambers has increased recently due to some interesting physical phenomena observed from the measurements, for example, the oscillation of particle number concentration during the measurements.

The oscillatory behavior of aerosol number concentration was first noticed by Badger and Dryden (1939), back in the late 1930's. They made a qualitative conclusion that the oscillation was a result of nucleation and flow processes in the chamber. Later other scientists have reported similar results, for example, Reiss et al. (1977). Pratsinis et al. (1986) conducted a theoretical study to investigate the stability characteristics of an aerosol reactor, and in their model the aerosol particles were formed by homogeneous nucleation from molecules and via a chemical reaction of zero-order. They investigated specially the effect of small perturbations to the steady state equilibrium. The work was based on the research by Friedlander (1982, 1983), who presented a theoretical framework that was used to describe the dynamic behavior of a set of four coupled differential equations describing the system.

In this work we investigate a so called plant flow chamber using suitable modeling tools. The measurement data and equipment is described in Joutsensaari (2008) and the modeling work is performed using a recently developed aerosol model called ACDC (**a**erosol **c**ondensation/**d**eposition/**c**oagulation model). The model does not include a mechanism for nucleation, so a simple method for nucleation and a mechanism for aerosol particle removal from the gas phase by wall loss process and a loss by carrier gas (air) exchange were required. The model is applied to the case of only one non-volatile condensing gas (CG), which was supposed to be formed in the oxidation process between one typical hydrocarbon compound and ozone. At this point, the nucleation was presumed to have a simple coupling for gas – phase concentration of the semi-volatile compound formed in the oxidation process.

DESCRIPTION OF THE MODEL

The computer model constructed for this work is suitable for the problems of aerosol dynamics arising from the flow chamber studies. The basic aerosol processes that are included automatically in the model are coagulation, deposition and the condensational growth. The aerosol size distribution is handled using fixed sectional method. The description of the aerosol dynamics in case of these processes induces non-

stiff, ordinary differential equations of first degree that are solved using Euler forward method. At the each time step, each physically essential subroutine is executed and each time - dependent variable updated.

Therefore, the total number concentration of the particles is affected by nucleation, coagulation and the particle loss due to wall processes and the carrier gas flow. The nucleation model is presented as a simple exponential function of the CG concentration so that the effect of the nucleation can be tested in the simulations using different exponent factors (in this work, factor = 2). Coagulation kernel used follows the standard calculation routines introduced by Seinfeld et al. (1998). The particle wall loss process and the loss due to the flowing air are presumed to be processes of the first order. However, we study the effect of the size - dependency of the wall loss coefficient by performing a model fit for an additional measured data set using the same chamber as in the main measurement of the work. After successful fit, the obtained size-dependent wall loss function was applied to the actual simulations (see Figure 2).

In the case of one condensing compound, the gas-phase chemistry can be described using one adjustable parameter that includes both chemical rate constant and molar yield term. The magnitude of this constant can be approximated using quantitative information of growth rates of the particles during nucleation burst and the terpene concentration measurements in the chamber. The time-dependent terpene concentration inside the chamber was determined using measured terpene concentrations at the inlet and outlet of the chamber and by taking into account the oxidation of hydrocarbons.

RESULTS

In first part of the study, we searched a somewhat optimal function for wall loss size-dependency by investigating the aerosol size distribution under steady – state conditions. In this measurement, the only aerosol processes affecting to the created particle population were coagulation, losses to the walls and the air exchange. The size distribution was monitored inside the chamber.
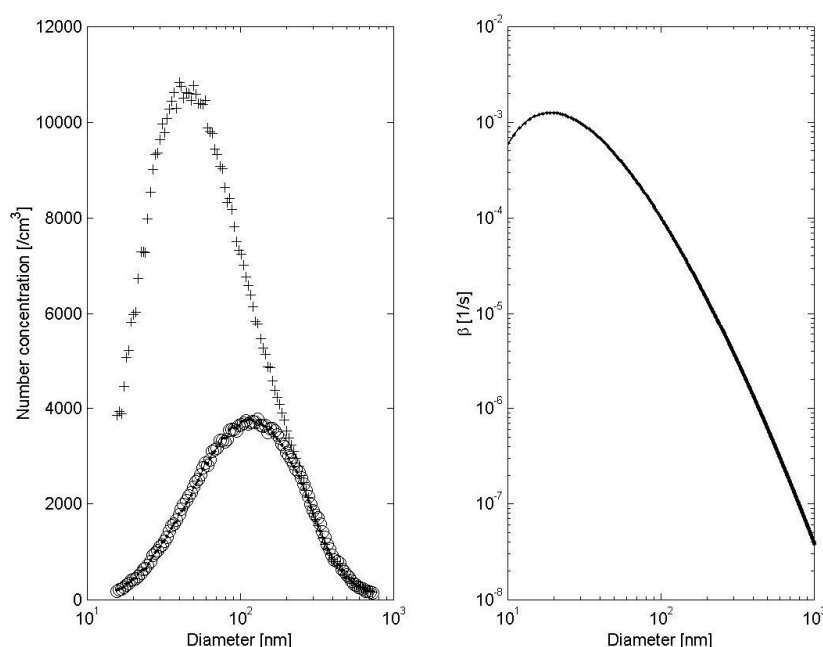
Figure 1 a) Particle number size distribution measured at the inlet (+) and the distribution (o) after 3 hours inside the chamber (particle population in steady-state). The modelled distribution (in steady – state, as well) is plotted using solid line. Figure 1 b) The wall loss coefficient as a function of diameter obtained after the fit.

Using these presumptions in the model, a steady-state condition was found to be formed after 3 hours simulation, as observed in the size distribution measurement inside the chamber. The inlet particle size distribution and the average size distribution after 3 hours can be seen in Figure 1a. The measured inlet size distribution was used as the "continuous aerosol source" in ACDC (aerosols in one unit volume that were fed to each size class continuously). During the fit, ACDC was used as an external program whereas the actual fit procedure was performed using Nelder - Mead (1965) algorithm.

After the first phase, the wall loss function as well as the molar yield of CG (obtained from growth rate measurements) was inserted to ACDC. Presuming that the CG concentration in the chamber can be estimated, then by using the growth rate data, a scarce estimation for the molar yield of the CG can be obtained (here ca. 0.1 – 0.15). The nucleation model was tested using trial – and – error method so that the total average absolute errors between measured aerosol number concentration and sink (calculated from the data) and the modelled ones would be as small as possible. Finally, the modelled aerosol sink and aerosol number concentration for one measurement period (26 hours) can be presented in Figure 2:
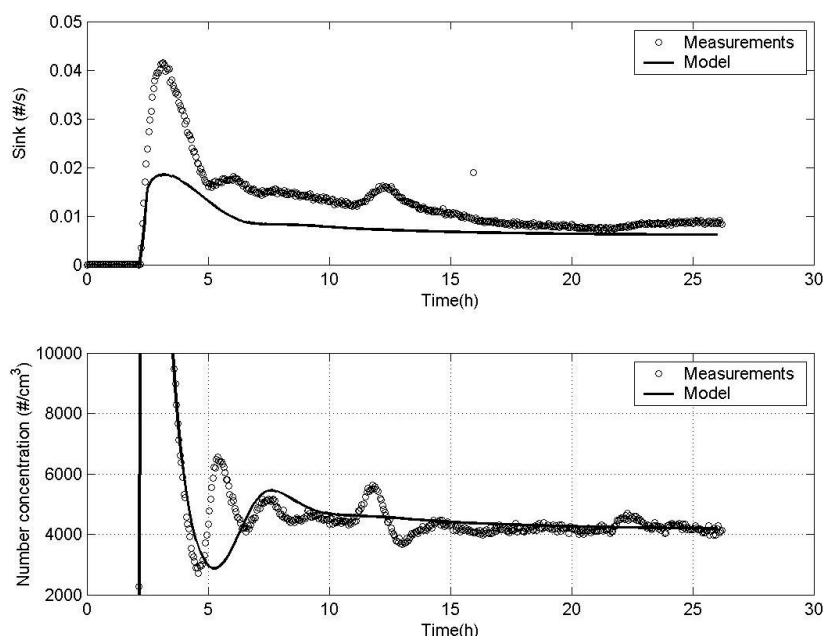
Figure 2 a) Aerosol particle sink calculated from the measurement (o) and the modelled sink (solid line) and 2b) aerosol particle number concentration as a function of time. The results in Fig. 2a and 2b were calculated using approximated molar yield and a nucleation model, where nucleation rate was presumed to be of form $J = \alpha[CG]^2$. Here α is an adjustable parameter and [CG] is the gas – phase concentration of CG.

CONCLUSIONS

According to our preliminary simulation results, it seems difficult to obtain an unambiguous model response for chosen modelling parameters. Furthermore, it is possible that other parameter choices could lead to better results, but we were unable to obtain such group of parameters at this moment. In this work we have not attempted to identify the chemical composition of SOA precursor and SOA formed and the exact chemical processes in the particle phase. Instead, the essential physical parameters of the SOA formation are considered as adjustable variables, thus turning the problem basically to a curve fitting problem.

Analysis of the measurement data revealed the oscillatory behavior in the aerosol number concentration data as a function of time, and as the model response to the chosen group of independent variables was investigated, cyclic behavior was observed in the simulations, too. The coagulation only is not sufficient to maintain the oscillatory behavior and the modeling required other processes that removed particles from the gas - phase. Of certain values of the controllable parameters of the system, it is even possible to sustain oscillations without noticeable damped behavior (not presented here). It was also noted that the modeled results were highly dependent on the used model parameters and a clear linear coupling between model response and adjustable variables as model input could not be obtained yet. Nevertheless, using the constructed model, we believe that some of the essential features of the physical properties of the aerosol population can still be captured and investigated without the exact details of the processes underlying the problem. The size-dependent wall loss coefficient function was noted (when applied to fit) to produce the modeled steady-state size distribution well. However, the comparison of the wall loss function to those found in the literature [ex. (Hussein et al., 2009), (Park et al., 2001)], there's a reason to believe that the carrier gas flow in the chamber is not fully laminar.

REFERENCES

Badger, E.H.M. and Dryden, I.G.C. (1939). The formation of gum particles in coal gas. *Trans. Farday Soc.* 35: 607.

Friedlander, S.K. (1982). The behaviour of constant rate aerosol reactors. *Aerosol Sci. and Tech.* 1: 3.

Friedlander, S.K. (1983). Dynamics of aerosol formation by chemical reaction. *Annals NY Acad. Sci.* 404: 354.

Hussein. T. et al. (2009). Deposition rates on smooth surfaces and coagulation of aerosol particles inside the test chamber. *Atmospheric Environment* 43: 905 – 914.

Joutsensaari J. et al. (2008). Formation of secondary organic aerosols by ozonolysis of plant-released volatiles. *Report Series in Aerosol Science* 93: 61-66.

Nelder, J.A. and Mead, R. (1965). A simplex method for function minimization. *Computer Journal* 7: 308 – 313.

Park,S.H. et al. (2001). Wall loss rate of polydispersed aerosols. *Aerosol Sci. and Tech.* 35: 710 – 717..

Pratsinis, S.E. and Friedlander, S.K. (1986). Aerosol reactor theory: stability and dynamics of a continuous stirred tank aerosol reactor. *AIChE Journal*, 32, 2:177—185.

Reiss.H. et al. (1977). The use of nucleation and growth as a tool in chemical physics. *J. Colloid Interface Sci.* 58: 125.

Seinfeld, J. H. & Pandis, S.N. (1998) Atmospheric chemistry and physics. *John Wiley & Sons, Inc.*

AEROSOL NUCLEATION AND HIGH OZONE CONCENTRATION ASSOCIATED WITH TURBULENT TRANSPORT OF HIGHER LEVEL AIR MASSES AT AN ANTARCTIC SITE

A.VIRKKULA[1], E. ASMI[2], S. KIRKWOOD[3], R. HILLAMO[2], M. KULMALA[1]

[1]Department of Physics, P.O. Box 64, FI-00014, University of Helsinki, Finland
[2] Finnish Meteorological Institute, Research and Development, FIN-00560 Helsinki, Finland
[3]Swedish Institute of Space Physics, Kiruna, Sweden

Keywords: Atmospheric nucleation; Tropospheric aerosols; Antarctic aerosols; Ozone intrusions

INTRODUCTION

Aerosol measurements have been conducted at the Finnish Antarctic research station Aboa (73°03'S, 13°25'W, 490 m.a.s.l) mainly during austral summers since the first campaign in December 1997 - Aboa (73°03'S, 13°25'W, 490 m.a.s.l) mainly during austral summers since the first campaign in December 1997 - February 1998 (Kerminen et al., 2000; Teinilä et al. 2000). Aerosol formation and growth were studied during the following campaigns and several nucleation episodes have been observed (Koponen et al., 2003; Virkkula et al, 2006; Virkkula et al. 2007). Trajectory analyses of these episodes have shown that they occur most often when air masses have flown along the coast – neither directly from the Weddell sea nor directly from inland. These analyses have not suggested that vertical transport would play a significant role in explaining the source region of the freshly nucleated particles. The trajectory calculations, however, are based on meteorological data with a rather coarse grid and especially the vertical transport in these is inaccurate. To study the contribution of upper level aerosols to those observed at the surface other means but coarse trajectories are necessary, for instance a combination of in situ trace gas measurements and fast 3D measurements of wind speed and direction.

The composition of stratospheric air differs substantially from tropospheric air - for example it has high levels of ozone, low levels of methane and anomalous isotope distributions due to photochemical processing. If stratospheric air reaches the surface at polar latitudes it can lead to unexpected air quality problems (high ozone) and it can potentially affect the gases trapped in ice-cores, leading to problems in interpreting the climate record. Ozone plays an important role both in snow-photochemisty. Intrusions of stratospheric ozone into the boundary layer have been observed in several areas, for instance in the Alps reaching even the valleys (Stohl et al., 2000), in Greenland (Helmig et al. 2007a) , and in Antarctica (Gruzdev et al., 1993; Taalas et al. 1993; Helmig et al., 2007b).

In the austral summer 2006 – 2007 a new radar that provides 3-dimensional wind data was installed in the vicinity of the aerosol container at Aboa. In the following summer season both aerosols and surface ozone concentrations were measured in the aerosol laboratory. The data are presented in this work.

INSTRUMENTATION

In the Aboa aerosol laboratory following measurements were conducted: aerosol number size distributions and volatility in the size range 10 - 700 nm were measured with a custom-made Hauke-type DMA connected to a TSI Model 3010 CPC. An oven was installed in the sample line to heat the sample stepwise between temperatures 50 – 280 °C. Light scattering was measured with a TSI 3-wl nephelometer and absorption coefficient with a Radiance Research 3-wl Particle Soot Absorption Photometer. Aerosol chemical composition was determined from samples taken by a 12-stage low pressure impactor and two high-volume samplers. In this work only the data provided by the in situ instruments are discussed. An Environnement S.A. model O_3 42M monitor was used for measuring surface ozone concentrations.

The Movable Atmospheric Radar for Antarctica (MARA) of the Swedish Institute for Space Physics, Kiruna, was installed approximately at a 100 m distance from the aerosol sampling site. MARA measures spectral characteristics of echoes from dusty plasma close to the summer mesopause (80 – 90 km heights), and from small-scale structure in the air in the troposphere and lowermost stratosphere (~1000 m to 12 000 m heights). Tropospheric wind profiles, and the derivation of temperature gradients were validated by radiosondes launched from the site. Basic meteorological data: wind, humidity, temperature, pressure and solar radiation are measured at the automatic weather station at the aerosol container.

The aerosol and ozone measurements were operational from 14 December, 2007 through 31 January, 2008; MARA from 4 December, 2007 to 1 February, 2008; and the basic meteorological measurements continuously. The contaminated wind sector 210–270° was determined during an earlier campaign (Virkkula et al. 2007).

<center>RESULTS AND DISCUSSION</center>

Several particle formation episodes were observed analogous to those observed in earlier campaigns (Koponen et al., 2003; Virkkula et al, 2006; Virkkula et al. 2007). Here the one with the clearest association with an intrusion from higher atmospheric layers is analyzed in detail. On 10 and 11 January wind was blowing from the clean sector, ozone concentration decreased steadily (Figure 1). Scattering coefficient and correspondingly the accumulation coefficient varied clearly and they followed each other as they should. No clear nucleation mode was observed. On 12 January wind speed increased from < 10 close to 20 m/s. At the peak wind speed close to noon a clear step in ozone concentration and scattering coefficient as well as a clear Aitken mode were observed.

The highest ozone concentration was observed approximately 12 hours later at the same time as a clear nucleation mode appeared and started growing. The MARA produces, among other data, information on turbulence and vertical wind speed. These were averaged over the lowest 4 km. It is obvious that the peak ozone concentration and the nucleation mode appear when the downward wind was highest suggesting of an intrusion of air from upper atmospheric levels. An interesting and peculiar observation is that the peak turbulence and downward wind did not occur simultaneously with the highest wind speed. The explanation of this may only be obtained through a detailed meteorological analysis which is out of the scope of the present paper.
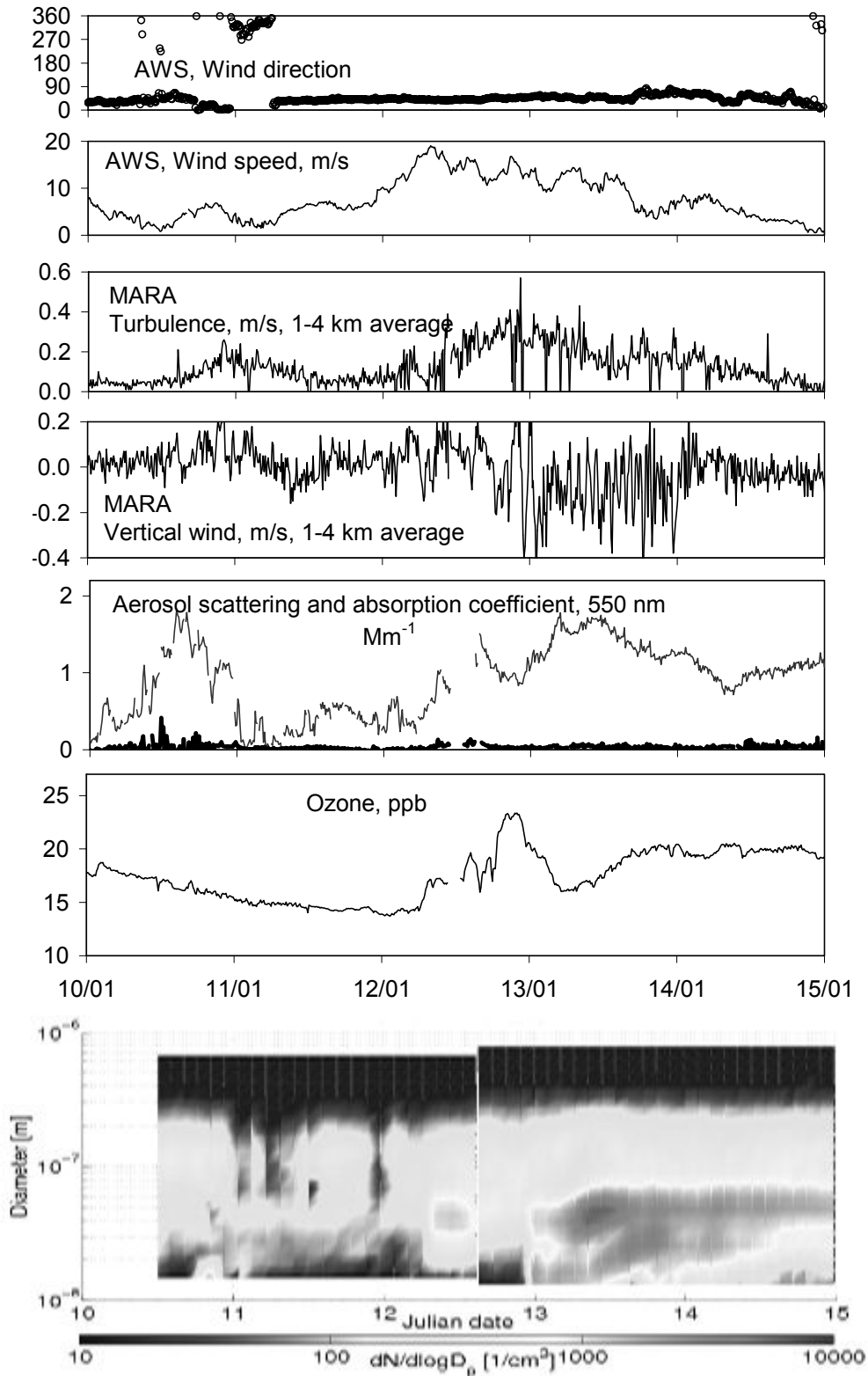
Figure 1. Surface wind direction and speed measured at the Automatic Weather Station, MARA turbulence and vertical wind, averaged over the lowest 4 kilometers, aerosol scattering and absorption coefficient, surface ozone concentration, and aerosol size distributions in January 10 – 14, 2008.

CONCLUSIONS

The 3-dimensional wind measurements of the MARA have proven to be very valuable in explaining both trace gas and aerosol concentration variations observed in the surface layer. The episode analyzed above shows that at Aboa nucleation may often be associated with an intrusion of air from higher levels to the surface layer, possibly even from the stratosphere. In earlier campaigns it was observed that often the nucleation episodes occur during high wind speeds, without even a possible explanatory guess. The analysis of this episode showed that high surface wind speed at the nunatak Basen where the station is located generates turbulence that may well reach several kilometers above ground. The turbulence also contains clear downward wind. A rigorous meteorological analysis is needed in order to understand the extent of this phenomenon, both vertically and horizontally. The Basen mountain is not a unique one, there are several mountain ranges in Antarctica, so the results obtained from the present analysis and especially the future rigorous meteorological analyses may well be generalized to a larger area.

ACKNOWLEDGEMENT

REFERENCES

Kerminen V.-M., Teinilä K. and Hillamo R. (2000) Chemistry of sea-salt particles in the summer Antarctic atmosphere. *Atmos. Environ.* **34,** 2817-2825..

Teinilä K., Kerminen V.-M. and Hillamo R. (2000) A study of size-segregated aerosol chemistry in the Antarctic atmosphere. *J. Geophys. Res.* **105**, 3893-3904.

Koponen I. K., Virkkula A., Hillamo R., Kerminen V-M, Kulmala M. (2003) Number size distributions and concentrations of the continental summer aerosols in Queen Maud Land, Antarctica. *J. Geophys. Res.* **108**(D18), 4587, DOI:10.1029/2003JD003614.

Virkkula A., Koponen I. K., Teinilä K., Hillamo R., Kerminen V-M., and Kulmala M. (2006) Effective real refractive index of dry aerosols in the Antarctic boundary layer, *Geophys. Res. Lett.* **33***, No. 6, L06805, 10.1029/2005GL024602*

Virkkula A., Hirsikko A., Vana M., Aalto P.P., Hillamo R., and Kulmala M. (2007) Charged particle size distributions and analysis of particle formation events at the Finnish Antarctic research station Aboa. *Boreal Environ. Res.*, **12**: 397 – 408.

Stohl, et al., The influence of stratospheric intrusions on alpine ozone concentrations, Atmos. Environ., 34, 1323–1354, 2000.

Helmig, D., Oltmans S.J., Morse T.O, and Dibb J.E, What is causing high ozone at Summit, Greenland? Atmos. Environ. 41, 5031-5043, 2007a.

Gruzdev, A. N. and Sitnov, S. A., Tropospheric ozone annual variation and possible troposphere-stratosphere coupling in the Arctic and Antarctic as derived from ozone soundings at Resolute and Amundsen-Scott stations, Tellus 45(B), 89 – 98, 1993.

Taalas, P., Kyrö E., Supperi A., Tafuri M., and Ginzburg M. Vertical distribution of tropospheric ozone in Antarctica and in the European Arctic, Tellus 45(B), 106 - 119, 1993.

Helmig, D., Oltmans, S. J., Carlson, D., Lamarque, J.-F., Jones, A., Labuschagne, C., Anlauf, K., and Hayden, K.: A review of surface ozone in the polar regions, Atmos. Environ., 41, 5138– 5161, 2007b.

NEW PARTICLE FORMATION DURING THE EUCAARI 2007 CAMPAIGN: A MODELING STUDY

H.VUOLLEKOSKI[1], T. NIEMINEN[1], S.-L. SIHTO[1], H. KORHONEN[2]
and M. KULMALA[1]

[1]Department of Physics, P.O. Box 64, FI-00014, University of Helsinki, Finland
[2]Department of Physics, P. O. Box 1627, FI-70211, University of Kuopio, Finland

INTRODUCTION

Aerosols are ubiquitous. In addition to having both verse and adverse health effects in human respiratory system, they have a say in climate change. They provide a negative radiative forcing through direct and indirect cooling phenomena. Particles act as condensation nuclei for clouds that reflect light emitted by the sun back into space, but also reflect light by themselves. On the other hand, for an example soot particles absorb heat and thereby have a positive radiative forcing. According to IPCC (2007), the overall radiative forcing of the aerosols is negative, but with an uncertainty equal to the positive radiative forcing credited to carbon dioxide. To better predict the global changes on the door, one must first try to resolve some of the uncertainties related to fine particles.

One of the greatest unknowns related to aerosols is the formation mechanism of new particles. Classically, binary nucleation of sulphuric acid and water (Vehkamäki et al., 2002), and more recently, ternary nucleation of sulphuric acid, ammonia and water (Napari et al., 2002), have been believed to be responsible for new particle formation. However, several studies have shown that the ambient conditions of the lower troposphere simply cannot provide the observed numbers of fine particles via these nucleation mechanisms (Mäkelä et al., 1997; Ball et al, 1999). A recently proposed explanation for new particle formation is spontaneous activation of clusters (Kulmala et al., 2006): the ever-present 1.5—2 nm pool of clusters is somehow activated for growth to bigger sizes. Several studies suggest that sulphuric acid is at least one of the key elements in the process.

In this study we focus on the identity and properties of the activating and condensing vapors. We compare different activation schemes with other generally known nucleation theories. We also investigate the effect of background aerosol by comparing new particle formation events on clean and polluted air masses. Comparison with experimental observations is easy to make for the EUCAARI campaign from March to June in 2007 (Kulmala et al., 2008). The results will reduce the burden of global climate modelers by limiting the number of possible nucleation implementations.

MODEL DESCRIPTION

The modeling studies are conducted with a modified version of the UHMA model (University of Helsinki Multicomponent Aerosol model (Korhonen et al., 2004)). The model is an aerosol dynamics box model that simulates the evolution of particle distribution in clear sky conditions. All the basic aerosol dynamics processes are included: nucleation, condensation, coagulation and dry deposition, which are solved with the 4th order Runge-Kutta method.

METHODS

Box model input is taken from and results are compared with experimental observations made during the EUCAARI 2007 spring (6 May – 30 June) campaign at the SMEAR II (Station for Measuring Ecosystem--Atmosphere Relations (Hari and Kulmala, 2005)) forest research station in Hyytiälä, Finland. From the measurements we get the background aerosol distribution, sulphuric acid concentration and also some

estimates for the concentrations and other properties of the different organic vapors that participate in early growth of the newly formed particles.

In this study we use several nucleation mechanisms depending on different vapors. The campaign consisted of several new particle formation event days, which occurred in different air mass types. This provides us with a means to test the effect of clean versus polluted air masses in a process model with a reference point in the measurements.

<div align="center">RESULTS</div>

Tentative results suggest good agreement between the model and the measurements. An example of a DMPS (Aalto et al., 2001) measurement of a new particle formation event is presented in Figure 1. Clear period of new particle formation with fast growth to the background aerosol can be seen. We performed several test runs on the model against this day, taking the background aerosol and sulphuric acid concentrations from the measurements, and estimating profiles for two differently behaving organic vapors. An example particle distribution from one of these runs is presented in Figure 2. By visual inspection alone, the new particle formation events appears to closely resemble one another. However, the models seems to underestimate the formation rate of particles, and also the growth of over 10 nm particles is somewhat slower than during the actual measurement, whereas the background particles seem to grow more than they should.
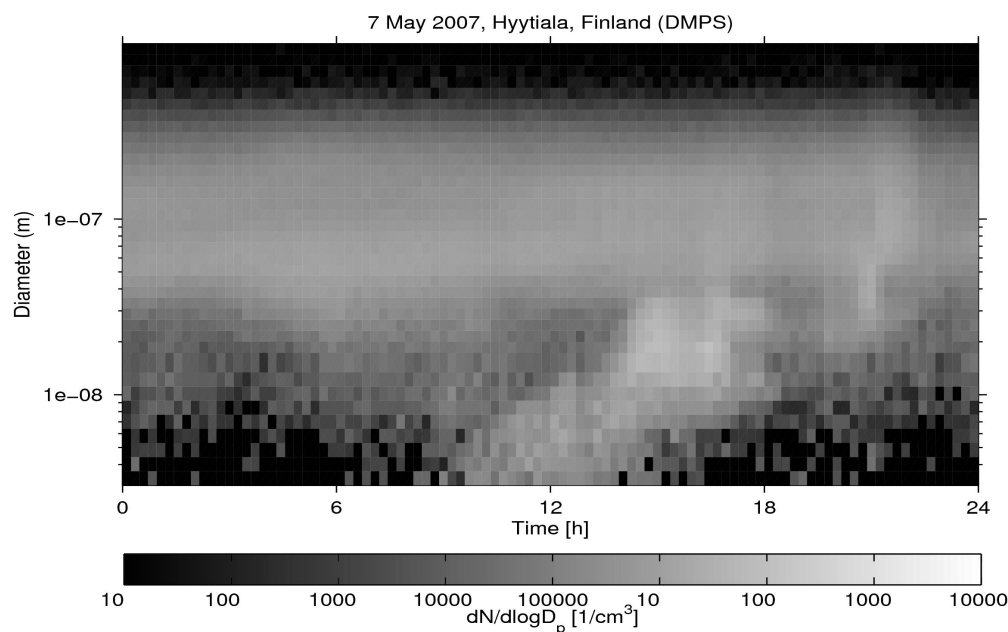
Figure 1: Particle number--size distribution as a function of time on 7 May 2007 from a DMPS measurement.

<div align="center">CONCLUSIONS AND FUTURE WORK</div>

A process model study on new particle formation events from a field campaign in Hyytiälä, Finland is conducted. Preliminary results suggest good agreement between the model and the measurements. We intend to test different kinds of cluster activation type nucleation mechanism by changing the identity and physical properties of the activating vapor or vapors, and study the effect of clean versus polluted air masses on new particle formation potential. The eventual results will hopefully pave way for more accurate climate models in the future.
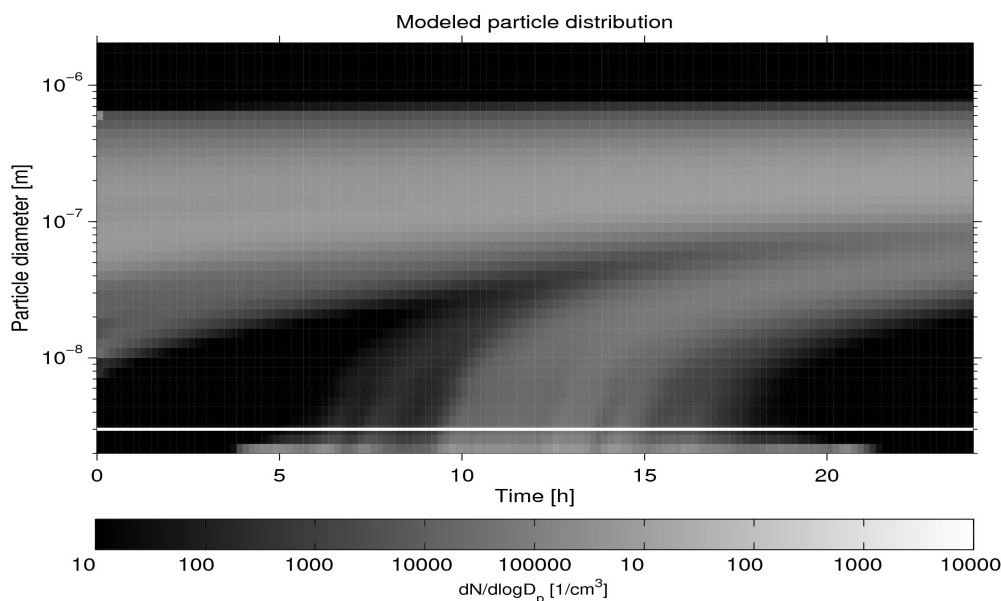
Figure 2: Modeled particle number--size distribution as a function of time in ambient conditions representing those during the day in Figure 1.

ACKNOWLEDGEMENTS

REFERENCES

IPCC, Intergovernmental Panel on Climate Change (IPCC), (2007) Climate Change: The Scientific Basis, Cambridge University Press, UK.

Vehkamäki, H., Kulmala, M., Napari, I., Lehtinen, K. E. J., Timmreck, C., Noppel, M., and Laaksonen, A., J. (2002) An improved parameterization for sulfuric acid-water nucleation rates for tropospheric and stratospheric conditions. *Geophys. Res.*, 107: 4622.

Napari, I., Noppel, M., Vehkamäki, H., and Kulmala, M. (2002) An improved model for ternary nucleation of sulfuric acid-ammonia-water. *J. Chem. Phys.* 116: 4221.

Mäkelä, J., Aalto, P., Jokinen, V., Pohja, T., Nissinen, A., Palmroth, S., Markkanen, T., Seitsonen, K., Lihavainen, H. and Kulmala, M. (1997) Observations of ultrafine aerosol particle formation and growth in boreal forest. *Geophys. Res. Lett.*, 24(10): 1219-1222.

Ball, S. M.. Hanson, D. R., Eisele, F. L. and McMurry, P. H. (1999) Laboratory studies of particle nucleation: Initial results for H2SO4, H2O, and NH3 vapors. *J. Geophys. Res.*, 104: 23709-23718.

Kulmala, M., Lehtinen, K. E. J. and Laaksonen, A. (2006) Cluster activation theory as an explanation of the linear dependence between formation rate of 3nm particles and sulphuric acid concentration. *Atmos. Chem. Phys.*, 6: 787-793.

Kulmala, M., Asmi, A., Lappalainen, H. K., Carslaw, K. S., Pöschl, U., Baltensperger, U., Hov, Ø., Brenquier, J.-L., Pandis, S. N., Facchini, M. C., Hansson, H.-C., Wiedensohler, A. and O'Dowd, C. D. (2008) Introduction: European Integrated project on Aerosol Cloud Climate and Air Quality interactions (EUCAARI) – integrating aerosol research from nano to global scales. *Atmos. Chem. Phys. Discuss.*, 8: 19415-19455.

Korhonen, H., Lehtinen, K. E. J. and Kulmala, M. (2004) Multicomponent aerosol dynamics model UHMA: model development and validation. *Atmos. Chem. Phys.*, 4: 757-771.

Hari, P. and Kulmala, M. (2005) Station for Measuring Ecosystem–Atmosphere Relations (SMEAR II). *Boreal Env. Res.*, 10: 315-322.

Aalto, P. P., Hämeri, K., Becker, E., Weber, R., Salm, J., Mäkelä, J. M., Hoell, C., O'Dowd, C. D., Karlsson, H., Hansson, H.-C., Väkevä, M., Koponen, I., Buzorius, G., and Kulmala, M. (2001) Physical characteristics of aerosol particles during nucleation events. *Tellus B*, 53: 344-345.

MASS SPECTROMETRY OF ATMOSPHERIC AEROSOL:
1 NANOMETER TO 1 MICRON

Douglas R. Worsnop
Department of Physics, University of Helsinki
University of Kuopio, FMI
Aerodyne Research

INTRODUCTION

The role of aerosol particles in the atmosphere represents the largest uncertainty in anthropogenic perturbation of climate forcing – direct scattering (global dimming) and indirect (cloud) effects *(IPCC, 2007)*. In urban and regional environments, aerosols show the strongest correlations of any pollutant with adverse health effects. Despite much effort in the past decade, uncertainties in both climate impacts and health effects of atmospheric aerosols are still significant. This reflects both the complexity of suspended aerosols – size, composition and morphology – and the lack of fundamental understanding of many chemical and physical details of the atmospheric aerosol system.

Much of this uncertainty is associated with lack of detailed knowledge of aerosol chemistry, particularly as a function of size. During the last ten years, the development of a unique aerosol mass spectrometer (AMS) has enabled routine measurement of sub-micron chemical composition worldwide *(Canagaratna et al, 2007)*. Particular examples include contrasting inorganic and organic composition of ultrafine (<100nm) particles in polluted and forest environments *(Zhang et al, 2004; Allan et al, 2006)*. Most recently the incorporation of a high resolution time-of-flight mass spectrometer (TOFMS) has enabled the determination the aerosol elemental chemical composition *(Aiken et al, 2008)*.

AMS observations have shown that highly oxygenated organic aerosol (OOA) compose roughly half the global aerosol *(Zhang et al, 2007)*. Secondary OOA is produced faster and in larger yields than predicted by models *(Volkamer et al, 2006)*. Recent work has shown that about a third of this OOA has lower volatility than inorganic sulphate *(Huffman et al, 2009)*. This low volatility OOA has been characterized only with mass spectrometry (*Lanz et al, 2007*). For example, comparison of continuous gas chromatography (GC) analysis of collected aerosol showed the GC analysis detected only ~10% of the total organic, missing the dominant highly oxygenated components *(Williams et al,2007)*.

CHEMISTRY OF AEROSOL NUCLEATION AND GROWTH

Another fundamental uncertainty in the atmospheric aerosol system is chemistry the formation of new aerosol particles via nucleation and growth of small molecular clusters *(Kulmala and Kerminen, 2008)*. Much of this uncertainty again reflects lack of knowledge of the chemistry of the molecular clusters believed to participate in aerosol formation and growth. For example, there is strong evidence that sulfuric acid is a critical player in this process *(Weber et al, 1997; Riipinen et al, 2007)*. Yet neither observed nucleation nor growth rates can be explained by sulphuric acid vapor concentrations *(Benson et al, 2008; Boy et al, 2008)*. At the same time, laboratory studies show that organic species can be involved in the nucleation and growth of molecular clusters and nano-particles *(Zhang et al, 2004; Veheggen et al, 2007; Wehner et al, 2005)*.

AMS observation of low volatility OOA is relevant to nucleation and growth of nano-particles, which depend on condensation of very low volatility species. For example, observations in Hyytiala show that the evolution of "biogenic" OOA *(Allan et al, 2005)* correlates with particle formation *(Laaksonen et al, 2008)* and with observed organic and hygroscopic growth factors of 50nm particles

in Hyytiala (*Raatikainen et al, 2009*). Moreover, the observation of low volatility residuals and high organic growth factors both suggest at least particle organic composition of growing 10nm particles observed in nucleation events (*Ehn et al, 2007; Vaattovaara et al, 2005*). Thermal desorption mass spectrometry of 10-20nm particles suggest complex inorganic/organinc composition *(Smith et al, 2004; 2005; 2008).*

AEROSOL MASS SPECTROMETRY

This talk will discuss aerosol mass spectrometry (AMS) results obtained under various COE activities. This includes AMS deployments at SMEAR stations in Hyytiälä and Helsinki, plant chamber experiments in Kuopio, aerosol evaporation laboratory experiments in Copenhagen and, most recently, atmospheric pressure ion time-of-flight mass spectrometric (API-TOFMS) analysis of cluster ions. The goal is to connect global measurements of aerosol chemistry (*Zhang et al, 2007*) to observations of growth of nanoparticles observed with air ion and neutral ion spectrometers (AIS and NAIS, *Kulmala et al, 2007*). Of particular interest is understanding the role of oxygenated organic species in aerosol growth across the size range of nano-, ultrafine and fine particles that determine the lifecycle of atmospheric aerosol. Full characterization of that lifecycle is required ion order to reduce uncertainties in aerosol impact on climate change.

REFERENCES

Aiken *et al* (2008), *Environ. Sci. and Tech*, doi: 10.1021/es703009q.

Allan et al (2006) *Atmos. Chem. Phys*., 6, 315-327.

Benson *et al* (2008), *Geophys. Res Lett.* 35

Boy *et al.* (2008), *Atmos. Chem. Physs* 8, 1577.

Canagaratna *et al* (2007) *Mass Spectrometry Reviews*, 26, 185-222.

DeCarlo *et al* (2006), *Anal. Chem.*, 78: 8281.

Ehn *et al* (2007), *Atmos. Chem. Phys*., 7, 677-684.

Huffman *et al* (2009), *Atmos Chem. and Phys. Discus.*, 9, 2645-2697.

IPCC (2007), The Intergovernmental Panel on Climate Change: Climate Change 2007: The Physical Science Basis. Cambridge University Press, New York.

Kulmala *et al* (2007). *Science* 318, 89.

Kulmala and Kerminen (2008, *Atmos Res*., 90, 132.

Laaksonen *et al* (2008), *Atmos. Chem. Phys*., in press.

Lanz *et al* (2007), *Atmos Chem. and Phys*, 7, 1503–1522.

Mäkelä et al (1996). *J. Aerosol Sci* 27, 175 - 190

Raatikainen *et al* (2009), in preparation.

Riipinen *et al* (2007)., *Atmos. Chem. Phys.* 7, 1899 (2007)

Smith *et al*, (2004) *Aerosol Sci. Technol.*, 38, 100-110.

Smith *et al* (2005). *J. Geophys. Res.*, 110, d22S03, doi:10.1029/2005JD005912.

Smith *et al* (2008) *Geophy. Res. Lett.* 35 (2008).

Ude *et al* (2005), *J. Aerosol Sci.*, 36, 1224.

Vaattovaara *et al* (2005). *Atmos. Chem. Phys.*, 5, 3277-3287

Verheggen *et al.* (2007) *Environ. Sci. Technol* 41, 6046.

Volkamer et al (2006(, *Geophys Res. Let.* 33(17), L17811.

Weber *et al* (1997) *J. Geophys. Res.*, 102, 4375-4385.

Wehner *et al* (2005) *Geophys. Res. Lett.,* 32, L17810, doi:10.1029/2005GL023827.

Williams *et al* (2007), *J. Geophys. Res*, 112, D10S26,doi:10.1029/2006JD007601.

Zhang *et al* (2004),. *Environ. Sci. Technol.,* 38, 4797-4809.

Zhang *et al* (2007), *Geophys. Res. Lett*, 34, L13801, doi:10.1029/2007GL029979.

Zhang, R. *et al* (2004). *Science* 304, 1487.

GROWTH RATES OF ATMOSPHERIC AEROSOL PARTICLES AT SMEAR II: SEASONAL VARIATION AND SIZE DEPENDENCY

T. YLI-JUUTI[1], I. RIIPINEN[1] and M. KULMALA[1]

[1]Department of Physics, P.O. Box 64, FI-00014, University of Helsinki, Finland

Keywords: Atmospheric aerosols, Atmospheric ions, Particle formation and growth

INTRODUCTION

Formation of new nanometer-sized aerosol particles is observed to take place frequently (Kulmala et al. 2004). These particles are likely to have an important impact on the climate if they grow to sizes sufficiently large to act as cloud condensation nuclei. Therefore it is important to investigate the growth of the freshly formed particles. In this study we present growth rates of particles in size ranges below 20 nm in diameter during nucleation events. The data is obtained from measurements performed at SMEAR II (Station for Measuring Forest Ecosystem-Atmosphere Relations), Hyytiälä, Finland (Hari and Kulmala 2005), during a 51 month long period. The method that is used here to calculate the growth rates has previously been utilized for a 13 month long data set from SMEAR II by Hirsikko et al. (2005). In the present study the dataset extends over a longer time period, therefore providing better statistics.

MATERIALS AND METHODS

The dataset used in this study contains atmospheric aerosol particle and ion size distribution data measured with a Differential Mobility Particle Sizer (DMPS) (Aalto et al. 2001), an Air Ion Spectrometer (AIS) (Mirme et al. 2007) and a Balanced Scanning Mobility Analyzer (BSMA) (Tammet 2006). The DMPS measures concentrations of neutral and naturally charged aerosol particles in the size range 3–517 nm whereas the AIS and the BSMA measure naturally charged aerosol particles, i.e. air ions, in the size ranges 0.3–40 nm and 0.4–7.5 nm, respectively. The measurements were done at the boreal forest site SMEAR II during April 2003-June 2007 but the AIS had long measurement breaks during 15.4.–10.8.2003, 17.5.-9.8.2006 and 16.9.2006-9.1.2007.

The change of average diameter of nucleation mode particles, i.e. the particle growth rate (GR), was determined with the method that has previously been utilized for 13 month long dataset from SMEAR II by Hirsikko et al. (2005). The method is based on comparing the moments of maximum concentrations of different sized particles. When a new particle formation event starts, a peak in the concentration of particles of few nanometers in diameter is seen. The peak is later detected in concentrations of larger particles as the particles grow. The moment of the maximum concentration of particles in a size bin was taken to be the moment when a normal distribution function fitted in the concentration of particles in the size bin in question as a function of time reached its maximum. The growth rate was calculated by least-square-fitting of a straight line in the size of particles as a function of moment of maximum concentration. To obtain the growth rates of particles in three size ranges, a straight line was fitted in three size ranges separately: 1.3–3 nm, 3–7 nm and 7–20 nm. These are the same size ranges as used by Hirsikko et al. (2005) and the smallest size range is not used for DMPS data whereas the largest size range is not used for BSMA date due to the detection limits of these instruments.

RESULTS

To increase accuracy, daily values for GR in each size range were calculated as mean of the growth rates obtained from the three instruments. The median (mean) values of daily GRs in size ranges 1.3–3 nm, 3–7 nm and 7–20 nm were 1.9 (2.2) nm/h, 3.4 (3.9) nm/h and 3.9 (5.6) nm/h, respectively. This means that, on

average, the growth rates increased as a function of the size of the particles. The size-dependency in growth rates found here is similar to that found by Hirsikko et al. (2005).

The growth rates of particles larger than 3 nm showed an annual pattern, reaching higher values during summer than during the rest of the year (Fig. 1). Especially, GR of particles in size range 7-20 nm were clearly higher during summer months (June-August) than during rest of the year. The summertime median GR in the size ranges 3–7 nm and 7–20 nm were 3.8 nm/h and 7.4 nm/h, respectively. However, growth rates in the size range 1.3-3 nm did not show any clear annual variation. Also these annual patterns in GRs are in accordance with previous results (Hirsikko el al. 2005), where it was found that the seasonal variation of growth rates of particles larger than 3 nm resembled the variation of temperature and photosynthetically active radiation.
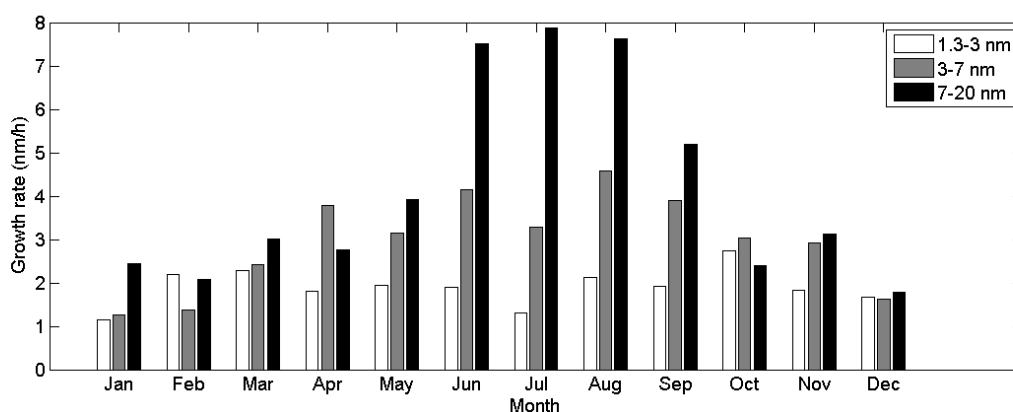
Figure 1. Monthly medians of daily growth rates of particles in size ranges 1.3-3 nm, 3-7 nm and 7-20 nm at SMEAR II in April 2003–June 2007.

As stated before, daily mean GR in each size range was calculated based on the data from the three instruments. To estimate the accuracy of the values of GR, the standard deviation of GRs were calculated for each day. The mean daily standard deviations of GRs in size ranges 1.3–3 nm, 3–7 nm and 7–20 nm during the whole measurement period were 0.6 nm/h, 0.8 nm/h and 0.5 nm/h. These can be used as a rough estimate of the accuracy of the method. When these error estimates are compared to the values in Fig. 1 it can be concluded that the seasonal variation of growth rates of particles larger than 3 nm is not within the uncertainty of the values.

CONCLUSIONS

It was found that particle growth rates increased as a function of size. This suggests that there are different factors affecting the growth of different sized particles. This might be interpreted as a size dependence in growth rates. On the other hand, as the larger particles are detected later than the smaller ones, the larger particles may be growing in different ambient conditions than the smaller ones. Therefore growth rates increasing as a function of size might actually point to the time-dependency in growth rates.

Particularly, at summertime the difference in growth rates of different sized particles was notable. Also, growth rates of particles larger than 3 nm, especially in size range 7–20 nm, were found to be substantially larger during the summer months than during rest of the year, whereas growth rates of particles smaller than 3 nm did not have such annual pattern. This would point to the direction of different vapours participating on the growth of different size particles and to the important role of solar radiation and organic vapours emitted from the plants on the growth of particles larger than 3 nm.

476

REFERENCES

Aalto, P., Hämeri, K., Bercker E., Weber, R., Salm, J., Mäkelä, J.M., Hoell, C., O'Dowd, C.D., Karlsson, H., Hansson, H.-C., Väkevä, M., Koponen, I.K., Buzorius, G., and Kulmala, M., (2001). Physical characterization of aerosol particles during nucleation events. *Tellus* 53B, 344–358.

Hari, P., and Kulmala, M., (2005). Station for Measuring Ecosystem-Atmosphere Relations (SMEAR II). *Boreal Env. Res.* 10, 315–322.

Hirsikko, A., Laakso, L., Hõrrak, U., Aalto, P.P., Keminen, V.-M., and Kulmala, M., (2005). Annual and size dependent variation of growth rates and ion concentration in Boreal forest. *Boreal Env. Res.* 10, 357–369.

Kulmala, M., Vehkamäki, H., Petäjä, T., Dal Maso, M., Lauri, A., Kerminen, V.-M., Birmili, W., and McMurry, P.H., (2004). Formation and growth rates of ultrafine atmospheric particles: a review of observations. J. of Aerosol Science 35:143–176.

Mirme, A., Temm, E., Mordas, G., Vana, M., Uin, J., Mirme, S., Bernotas, T., Laakso L., Hirsikko, A., and Kulmala, M., (2007). A wide-range multi-channel Air Ion Spectrometer. *Boreal Env. Res.* 12, 247–264.

Tammet, H., (2006). Continuous scanning of the mobility and size distribution of charged clusters and nanometer particles in atmospheric air and the Balanced Scanning Mobility Analyzer BSMA. *Atmospheric Research* 82, 523–535.

Appendices

Finnish Centre of Excellence in
Physics, Chemistry, Biology and Meteorology of Atmospheric Composition and Climate Change

SCIENTIFIC ACTIVITIES in 2008

ACADEMIC DEGREES

Master's theses

1. Buenrostro Mazon, Stephany, Classification scheme for previously undefined days. Department of Physics, supervisor: I. Riipinen
2. Hannuniemi, Hanna, Pienhiukkaset ja meteorologia kaupunkiympäristössä. Department of Physics, supervisors: T. Vesala, T. Hussein, M. Kulmala
3. Jaatinen, Antti. Atmospheric nucleation in Italy, Germany and Finland: A comparative study.University of Kuopio, Department of Physics, A. Laaksonen, A. Hamed,
4. Järvenpää, Leo, Ilmakehän kemiaa ympäristökasvatuksen näkökulmasta (Atmospheric chemistry from environmental education perspectives), Department of Chemistry, supervisor Tuulia Hyötyläinen
5. Kajos, Maija, Mono- ja seskviterpeenien fragmentoituminen PTR-MS-mittauksissa. Department of Physics, supervisor J. Rinne
6. Kaltio, Laura, Kaksivaiheiset kromatografiset tekniikat ympäristöanalytiikassa (Two-dimensional chromatographic techniques in environmental analysis), Department of Chemistry, supervisors Tuulia Hyötyläinen and Marja-Liisa Riekkola
7. Korhonen Janne: Transpiraation mittaaminen IR-lämpömittaria ja energiataseyhtälöä hyödyntäen, Department of Forest cology, supervisor: Eero Nikinmaa
8. Koskinen, Katja: Kuusen uudistamistulos MONTA-kokeen pienaukkohakkuin käsitellyissä metsiköissä Etelä-Suomessa; Department of Forest Ecology, supervisors E.Nikinmaa, S.Valkonen (METLA)
9. Kyrö, Ella-Maria, Alle mikrometrin kokoisten aerosolihiukkasten lumipesukerroin, Department Physics, supervisors: Lauri Laakso, Aki Virkkula, Tiia Grönholm
10. Lehtonen, Mervi, Typpeä, happea ja rikkiä sisältävien aromaattisten monirengasyhdisteiden määrittäminen ympäristönäytteistä (Determination of nitrogen, oxygen and sulphur containing aromatic hydrocarbons in environmental samples), Department of Chemistry, supervisors Kari Hartonen and Marja-Liisa Riekkola
11. Lepistö Tanja. Kasvillisuuden vaikutus maahengitykseen sekä juuri- ja ritsosfäärihengityksen osuus maan kokonaishengityksestä, University of Helsinki, Department of Forest Ecology, Supervisors Jukka Pumpanen, Hannu Koponen and Hannu Ilvesniemi
12. Liao, Li, Atmospheric sub-3 nm cluster measurements and analysis based on the application of PH-CPC, Department of Physics, supervisors: Markku Kulmala, Mikko Sipilä, Ilona Riipinen, Katrianne Lehtipalo
13. Malila Jussi: Klassisen nukleaatioteorian muunnelmia binäärisille vesi-alkoholiseoksille. (Modifications of the classical nucleation theory into binary water-alcohol mixtures), University of Kuopio, Department of Physics, A. Laaksonen, I. Napari

14. Nieminen, Tuomo, Rikkihapon vaikutus aerosolihiukkasten muodostumiseen ja kasvuun Hyytiälässä 1.4.2003 - 31.5.2005. Department of Physics, supervisors: L. Laakso, I. Riipinen, M. Kulmala
15. Paasonen, Pauli, Liikkuvalla laboratoriolla mitattujen vilkasliikenteisen tien hiukkas- ja kaasupäästöjen laimeneminen kaupunki-ilmaan. Department of Physics, supervisors: K. Hämeri, L. Pirjola
16. Pessala, Suvi: Männyn, Kuusen ja Koivun fotosynteesikapasiteetti sekä ilmarakojontavuus suhteessa lehden latvusasemaan ja vesitilanteeseen, Department of Forest Ecology, supervisor: E.Nikinmaa
17. Rasilo Terhi. Maahengitys metsänrajaseudulla Itä-Lapissa, University of Helsinki, Department of Biological and Environmental Sciences, supervisors Jukka Pumpanen, Sirkku Manninen
18. Riuttanen, Laura, Effect of biomass burning emissions on atmospheric composition in Finland, Department of Physics, supervisors Gerrit de Leeuw and Ilona Riipinen
19. Tamminen, Lauri: Alueellinen Metsäsuunnittelu UPM:n Metsissä-Tapaustutkimus Harvialan Metsätilalla Department of Forest Ecology, supervisors: E.Nikinmaa, T. Lehesvirta (UPM)
20. Tiitta Jaakko, Katupuiden fotosynteesikoneiston kehitys; tutkimus katupuiden fotosynteettisen koneiston kehityksesta yhden kasvukauden aikana erityispiirteisessä kasvuympäristössä, Department of Forest Ecology, supervisors E.Nikinmaa, Albert Porcar-Castell
21. Tollman, Niko, Characterizing rimed versus aggregated snow when analyzing the shape of hydrometeor size distributions. Department of Physics, supervisor: S. Göke
22. Vestenius, Mika, Orgaanisten yhdisteiden ja joidenkin hivenkaasujen jatkuvatoimiset määritykset ilmasta (On-line monitoring of atmospheric organic compounds and some trace gases), Department of Chemistry, supervisors Kari Hartonen and Marja-Liisa Riekkola

Academic dissertations

1. Chung Chul, ENSO variability and Asian summer monsoon, Dept. Meteorology (University of Maryland, USA), supervised by Sumant Nigam
2. Hienola Anca, On the homogeneous and heterogeneous nucleation of some organic compounds, Department of Physics, supervisors:M. Kulmala, H. Vehkamäki
3. Kallio Minna, Comprehensive two-dimensional gas chromatography: Instrumental and methodological development, Laboratory of Analytical Chemistry, supervisor Tuulia Hyötyläinen
4. Lohila Annalea, Carbon dioxide exchange on cultivated and afforested boreal peatlands. Department of Environmental Sciences, University of Kuopio (supervised by Mika Aurela, Pertti Martikainen and Timo Vesala)
5. Pikkarainen Anna-Liisa, Organic contaminants – Occurrence and Biological Effects in the Baltic Sea, Laboratory of Analytical Chemistry, supervisors Eeva-Liisa Poutanen ja Marja-Liisa Riekkola

6. Porcar-Castell Albert, Studying the diurnal and seasonal acclimation of photosystem II using chlorophyll-a fluorescence. Supervisors: P. Hari, E. Nikinmaa, E. Juurola
7. Raivonen Maarit, 2008. UV-induced NOy emissions in gas-exchange chambers enclosing Scots pine shoots: an analysis on their origin and significance. Department of Forest Ecology. Supervisors: P. Hari, Vesala and M. Kulmala
8. Riipinen Ilona, Observations of the first steps of atmospheric particle formation and growth, Department of Physics, supervisors:M. Kulmala, K. E. J. Lehtinen
9. Riutta Terhi, Fen ecosystem carbon gas dynamics in changing hydrological conditions. supervisors T. Vesala, E-S. Tuittila, J. Laine, J. Rinne
10. Saarikoski Sanna, Chemical mass closure and source-specific composition of atmospheric particles, Laboratory of Analytical Chemistry, supervisors Risto Hillamo, FMI and Marja-Liisa Riekkola from Department of Chemistry
11. Sogacheva Larisa, Aerosol particle formation: Meteorological and synoptic processes behind the event, Department of Physics
12. Sorjamaa Riikka, Cloud drop activation of surface active and insoluble aerosols. University of Kuopio, Department of Physics. supervisors: A. Laaksonen, M. Kulmala.
13. Tarvainen Virpi, Development of biogenic VOC emission inventories for the boreal forest, Finnish Meteorological Institute, supervisors:

WORKSHOPS AND TRAINING COURSES ORGANIZED BY THE CoE

II Plant Biophysics Day: Photosynthesis, Plant Function and Environment. University of Helsinki, 7.1.2008, National

First ISSI TEAM Meeting & iLEAPS, ACPC Management Committee Meeting, ISSI, Bern, Switzerland, 28-30 January 2008. Participants: Andi Andreae, Sandro Fuzzi, Markku Kulmala, Ulrike Lohmann, Colin O'Dowd, Graciela Raga, Anni Reissell, Danny Rosenfeld, Pier Siebesma.

Training course Marie Curie-iLEAPS – Model-data assimilation: "Physics and chemistry of air pollution and their effects" University of Helsinki, Hyytiälä Forestry Field Station, 9.-19.3.2008, International. Participants (total number 91): 1 from Belgium, 9 from Estonia, 52 from Finland, 1 from France, 6 from Germany, 1 from Ghana, 4 from India, 4 from Italy, 1 from Mozambique, 2 from Poland, 3 from Russia, 2 from Spain, 2 from Sweden, 2 from the Netherlands,1 from U.S.A.

iLEAPS-ICOS-NitroEurope Workshop on "Eddy covariance flux measurements of methane and nitrous oxide exchanges" , April 8-11, 2008, Hyytiälä Forestry Field Station, Finland.70 particip.

European Geosciences Union General Assembly 2008, Vienna, Austria, 13 – 18 April. iLEAPS organised/co-organised scientific sessions:
1. iLEAPS session BG2.1 "Interactions of land cover and climate" Convener: A. Reissell, Co-Convener: M.O. Andreae, P. Kabat
2. MAIRS-iLEAPS session BG2.7 "Land - atmosphere interactions and human activity in Monsoon Asia" Convener: C. Fu, Co-Convener: P. Kabat, A. Reissell

3. NEESPI session BG2.8 "Land-atmosphere interactions in Northern Eurasia" Convener: P. Groisman, Co-Convener: P. Kabat, K. Hibbard and K. van Huissteden. organized by NEESPI in collaboration with AIMES and iLEAPS.
4. Session BG2.11 "Synthesis Efforts From the Global Network of Ecosystem-Atmosphere CO2, Water and Energy Exchange" (FLUXNET) Convener: Reichstein, M. , Co-Convener: Papale, D. organized in collaboration with iLEAPS
5. Session AS3.21 "The dry deposition process at the substrate- to global scale. Convener: Ganzeveld, L. , Co-Convener: Altimir, N. organized in collaboration with iLEAPS
6. Session CL22 "Land-climate interactions from models and observations: Implications from past to future climate" Convener: Seneviratne, S., Co-Convener: van den Hurk, B., Ciais, P. organized in collaboration with iLEAPS and GLASS.

Kickoff-Workshop of the Finnish Centre of Excellence and the Finnish Graduate School. FMI, Helsinki, 22.-23.4. 2008. Participants: total number 135, including the SAB members, others from Finland. National

HERC-iLEAPS seminar on "Interactions between land use and climate: multidisciplinary perspective from local land use to global climate", seminar held in Viikki Info Center, 24 April 2008, 4 international invited speakers, approx 100 Finnish participants

Workshop with teachers from Stavanger secondary school, Norway, University of Helsinki, Hyytiälä Forestry Field Station, 24.-25.4.2008, International. Participants (total number 11): 2 from Finland, 9 from Norway

4th IGBP Congress, Cape Town, South Africa, 4 – 10 May 2008. iLEAPS organised/co-organised scientific sessions:

1. Intercomparison of modeling components under modern and palaeo-conditions, organised by iLEAPS and AIMES
2. Global Change in the Arctic, organised by IGAC, PAGES, iLEAPS and AIMES
3. Methane in the Earth System: sources, sinks and concentrations, organised by iLEAPS, AIMES, PAGES, SOLAS and IGAC
4. Nitrogen in the Earth System: from Fundamental Research to Application Is it time for an Earth System N model, organised by IGBP SC, INI, AIMES and iLEAPS
5. Fire in the Landscape, organised by iLEAPS, AIMES and PAGES
6. Aerosol-cloud-precipitation-climate interactions (ACPC), organised by iLEAPS, IGAC, GEWEX/WCRP and SOLAS.
7. Water cycle, water resources, floods and drought, organised by iLEAPS, WATCH, GEWEX, GWSP, AMMA, AfricanNESS, PAGES
8. Monsoon Systems: Interactions with and Implications for the Earth System, organised by IGAC, MAIRS, GLP, PAGES, iLEAPS

Course on Measurements of Atmospheric Aerosols: Aerosol Physics, Sampling and Measurement Techniques, University of Helsinki, Hyytiälä Forestry Field Station 10.-16.5.2008, International. Participants (total number 32): 1 from Brazil,2 from Czech Republic, 8 from Finland, 2 from France, 3 from Germany, 2 from Greece, 2

from Italy, 1 from Jordan, 1 from Latvia, 1 from Lithuania, 1 from Poland, 2 from Spain, 2 from Sweden,1 from Switzerland, 3 from U.K.

NEESPI Science Team Meeting, 2-6 June 2008, Helsinki, Finland, 51 participants (15 from Finland, 11 Russia, 19 USA, 1 Japan, 1 Netherlands, 2 Austria, 1 Germany, 1 Italy), international

Summer School on Formation and Growth of Atmospheric Aerosols, University of Helsinki, Hyytiälä Forestry Field Station, 4.-14.8.2008, International. Participants (total number 34): 3 from Austria, 18 from Finland, 1 from France, 1 from Germany,1 from Greece, 2 from Italy, 6 from Russia, 1 from Sweden, 1 from the Netherlands

Chamber calibration campaign, Hyytiälä forestry field station, August-October 2008, 16 participants, 12 nationalities

Biogenic SOA, observations to global modelling, Tovetorp Zoological Research Station, Sweden, 11-15 August 2008. Participants: 14 US, 14 Northern Europe Countries, International

Nordforsk course on Analytical methods for environmental and bioanalytical studies, Laboratory, Department of Chemistry, University of Helsinki, August 18-22, 2008, 35 participants, international

Course: Introduction to Atmosphere-Biosphere Studies, University of Helsinki, Department of Physics and Hyytiälä Forestry Field Station, 18.-22.8.2008, International. Participants (total number 21): 1 from Australia, 14 from Finland, 6 from Russia

Field course in micrometeorology and hydrology, University of Helsinki, Hyytiälä Forestry Field Station 25.-29.8.2008, International. Participants (total number 27): 18 from Finland, 1 from Jordan, 6 from Russia, 2 from Sweden

CBACCI Views, workshop in Värriö Biological Station, University of Helsinki and Värriö Biological Station, Sept 22-25, 2008, 19 participants, national

EC-China Workshop, 12-14 October 2008, University of Helsinki, Helsinki, Finland, 49 participants (18 from Finland, 12 China, 5 Italy, 5 Netherlands, 4 Germany, 1 Austria, 1 Denmark, 1 Spain, 1 Sweden, 1 USA), international

EUCAARI IOP workshop and EUCAARI IMPACT-LONGREX join workshop MeteoFrance, Toulouse. 6-8.10.2008, Participants: Germany 14, Finland 2, France 2, UK 8, Netherlands 8, Poland 2, Sweden 2, Estonia 2, Norway 2, TOTAL 42

Second ISSI TEAM Meeting & ACPC Management Committee Meeting, ISSI, Bern, Switzerland, 7-9 October 2008. Participants: Andi Andreae, Sandro Fuzzi, Ulrike Lohmann, Graciela Raga, Anni Reissell, Danny Rosenfeld, Bjorn Stevens, Henri Vuollekoski, Ella-Maria Kyrö

Helsinki Climate Workshop – Workshop on Past, Present and Future Climate, 10 – 12 November 2008, Hotel Arthur, Helsinki, Finland, 44 participants (26 from Finland, 4 Sweden, 4 USA, 2 Germany, 2 Netherlands, 2 Italy, 1 Switzerland, 2 UK, 1 France), international (organised together with Dept. Bio- and Environmental Sciences, Univ. Helsinki)

Marie Curie - iLEAPS Conference on Feedbacks-Land-Climate Dynamics - Key Gaps, 17-20 November 2008, Hyeres, France

EUCAARI Annual meeting 17-21.11.2008, university of Helsinki. Participants: Austria 1, Brazil1, China 1,Crete 3, Czech Republic 2, Denmark 1, Estonia 3, EU 3, Finland

43, France 9, Germany 14, Hungary 1, Israel 2, Italy 2, Netherlands 4, Norway 9, Poland 1, Portugal 1, Switzerland 6, South-Africa 1, Sweden 4, UK 11, total 123

New opportunities for Finnish – Japanese cooperation in Urban land-atmosphere and air quality research, 24-26 November 2008, Helsinki, Finland. 39 Participants (34 from Finland, 4 Japan, 1 UK), bilateral

Chamber calibration workshop, Copenhagen, 15-17 December 2008, 28 participants, 14 nationalities

CBACCI/ABS workshop for teachers, University of Helsinki, 8.-9.12. 2008 Participants: 20 from Finland, 2 from Sweden, 1 from Estonia,1 from Russia, International

10th Anniversary Euroflux workshop, 10-12 December, 2008, Hyytiälä, 50 participants from Italy,Sweden, Denmark, France, China, Poland, Germany, USA, Finland. International

TASKS OF AN EXPERT

In international scientific journals

Referee work

Aalto Tuula: Tellus

Aurela Mika: Agricultural and Forest Meteorology

Boy Michael: Atmospheric Chemistry and Physics, Journal of Geophysical Research, Boreal Environment Research

Brus David: J. Chem. Phys.

Bäck Jaana: Silva Fennica, Boreal Environment Research

Ehn Mikael: Atmospheric Chemistry and Physics, Journal of Aerosol Science, Atmospheric Environment

Hyvärinen Antti-Pekka: J.Chem., Eng. Data, J. Chem. Phys., Atmos. Res., Atmos. Chem. Phys. International Journal of Applied Chemistry

Juurola Eija: Silva Fennica, Plant and Cell Physiology

Kerminen Veli-Matti: J. Geophys. Res., Geophys. Res. Lett. Atmos. Chem. Phys. Atmos. Res., Boreal Env. Res., Environ. Sci. Technol., Aerosol Sci. Technol., Atmos. Environ., Energy & Fuels, International Journal of Environment and Pollution

Kolari Pasi: Tree Physiology

Kulmala Markku: Aerosol Science and Technology, Atmospheric Chemistry and Physics,Atmospheric Environment, Atmospheric Research, Boreal Environment Research, Chemical Engineering Science, Environmental Monitoring and Assessment, Geophysical Research Letters, Journal of Aerosol Science, Journal of Geophysical Research, Quarterly Journal, Royal Meteorological society, Science, Tellus B, The Science of The Total Environment

Kurten Theo: Journal of Physical Chemistry, International Journal of Molecular Sciences, Atmospheric Chemistry and Physics

Laakso Lauri: Journal of Geophysical Research, Aerosol Science and Technology, Space Science Reviews, Atmospheric Environment, Atmospheric Chemistry and Physics

Lauri Antti: Journal of Chemical Physics

Laurila Tuomas: Biogeosciences
Lihavainen Heikki: Atmospheric Research, J. Geophys. Res.
Makkonen Risto: Atmospheric Chemistry and Physics, Journal of Geophysical Research-Atmospheres
Nikinmaa Eero: Boreal Environment Research, Silva Fennica, International Journal of Forestry Research, JGR, Functional Plant Biology, Annals of Botany, Plant Cell Environment, Ecological Modelling
Porcar-Castell Albert: Functional Plant Biology, Plant Growth Regulation, Forest Ecology and Management
Pumpanen Jukka: Silva Fennica, Canadian Journal of Forest Research, Agricultural and Forest Meteorology
Riipinen Ilona: Journal of Aerosol Science, Chemical Physics Letters,International Journal of Thermal Sciences, Journal of Geophysical Research, Atmospheric Chemistry and Physics, Environmental Science and Technology
Ruuskanen Taina: Atmospheric Research, Atmospheric Chemistry and Physics
Sevanto Sanna: Plant Biology, Tree Physiology, Trees, Plant, Cell and Environment
Tuovinen Juha-Pekka: Agricultural and Forest Meteorology, Atmospheric Chemistry and Physics, Atmospheric Environment, Biogeosciences, Boreal Environment Research, Monthly Weather Review
Vehkamäki Hanna: Journal of Chemical Physics
Vesala Timo: Ecological Monographs, Nature, Biogeosciences, Journal of Experimental Botany, Boundary Layer Meteorology, Boreal Environment Research

Editorial work

Bäck Jaana:
-- Boreal Environment Research; Subject editor (Forests)
Hyötyläinen Tuulia:
-- LCGC Europe; Chromedia- learning webpages; Member of Advisory editorial board
-- Eclipse publications; Member of Scientific Advisory Council
Hämeri Kaarle:
-- Atmospheric Research, editor
-- Atmospheric Chemistry and Physics, editor
-- Report Series in Aerosol Sciences, Member of Board
Juurola Eija:
-- Metsätieteen aikakauskirja; assisting scientific editor
-- Silva Fennica; assisting scientific editor
Kerminen Veli-Matti:
-- Boreal Environment Research; Subject editor (Atmosphere and climate)
-- Atmospheric Chemistry and Physics
Kulmala Markku:
-- Boreal Environment Research, member of Editorial Board, 2002-
-- Report Series in Aerosol Science, member of Editorial Board, 1986 -
Kolari Pasi:
-- iForest - Biogeosciences and Forestry; member of Advisory Review Board
Laurila Tuomas:
-- Biogeosciences; editor

Nikinmaa Eero:
-- Tree Physiology, member of Editorial Board
Pumpanen Jukka:
-- Silva Fennica; assisting scientific editor
Riekkola Marja-Liisa:
-- J. Chromatography A (Elsevier); Editor
-- Chromatographia (Vieweg Publishing); Electrophoresis (Wiley-VCH); J. Chromatographic Science (Preston Publications); J. Separation Science (Wiley-VCH); Analyst (Royal Society); Member of Advisory editorial board
Rinne Janne:
-- Atmospheric Chemistry and Physics; Editor
-- Ilmansuojelu-Uutiset, member of editorial board
Sorvari Sanna:
--iLEAPS Newsletter, special issue on Aerosols-clouds-Precipitation-Climate, issue no 5, April 2008, Editor
Toivola Martta:
-- Report Series in Aerosol Science; Editor-in-chief
Vehkamäki Hanna:
-- Boreal Environment Research, member of Editorial Board, 2006-
--Arkhimedes, Finnish magazine on Physics and Mathematics, member of Editorial Board, 2008 –
Vesala Timo:
-- Agricultural and Forest Meteorology, Editor
-- Journal of Geophysical Research, Editor

In scientific organizations

Hämeri Kaarle:
-- 2010 International Aerosol Conference, Helsinki, conference co-chair, 2008
-- Finnish Association for Aerosol Research FAAR, Chair
-- International Aerosol Research Assembly, vice chairman, 2006-
-- Formas – Forskningsrådet för miljö, areella näringar och samhällsbyggande, Sweden, expert member
-- Professoriliitto, member of Board
Kulmala Markku
-- iLEAPS Scientific Steering Committee member
-- Finnish Association for Aerosol Research FAAR, member of the board, 1984 –
--European Aerosol Conference 24-29 August 2008, Thessaloniki, Greece, member of the scientific committee
-- Greenhouse gases and aerosols: Interactions between northern ecosystems and climate, International conference given by the NECC and BACCI Nordic Centres of Excellence, Reykjavik, Iceland, June 16–18, 2008, member of the scientific committee
-- EUCAARI X[nd] Annual Meeting, 17-21.11.2008, chairman of the organizing committee
-- New opportunities for Finnish-Japanese cooperation in urban land-atmosphere and air quality research, seminar held in Kumpula 24.-25.11.2008, member of the scientific committee

-- 2010 International Aerosol Conference, Helsinki, conference co-chair, 2008

Laakso Lauri

--APSA (Aerosol Particles in Southern Africa) project betw. Univ. Helsinki, North-West Univ. (Rep. South Africa) & Finnish Environment Inst., Project Manager & member of steering group, 2005 - 2009

Nikinmaa, Eero:

-- Member of Board, The Finnish Society of Forest Science

-- Chairman of the Board of the Hyytiälä Forestry Field Station

-- Coordinator of the Global Industrial Forestry Network (University of Helsinki, University of Sao Paulo, Stellenbosch University)

-- Trans-national access coordinator in the EU FP6 project IMECC (Infrastructure for measurements of the European Carbon Cycle)

-- PI of the Long term ecological research station of Northern - Häme

-- Member of the coordination committee of the Finnish Long Term Socio Ecological Research Network (Fin LTSER)

Reissell Anni:

-- Monsoon Asia Integrated Regional Study (MAIRS), member of the scientific committee

--New opportunities for Finnish-Japanese cooperation in urban land-atmosphere and air quality research, seminar held in Kumpula 24.-25.11.2008, member of the organizing committee

-- Chairman of the iLEAPS session in the EGU General Assembly, co-convener in the MAIRS-iLEAPS session and co-organizer of four other session, Vienna, Austria, 13 – 18 April 2008

Riekkola Marja-Liisa:

-- TEKES DC-member of COST in the domain "Chemistry and Molecular Sciences and Technologies"

-- Vice-dean (Research) Faculty of Science, University of Helsinki

-- Vice--Chairman of Board of Directors of CSC - Scientific Computing Ltd, Finland

-- Member of the Senate, University of Helsinki

-- Board Member of Palmenia Centre for Continuing Education University of Helsinki

-- Committee Member for Public Information, Ministry of Education, Finland

-- Council Member of Faculty of Science, University of Helsinki

-- Scientific Council Member of Kumpula Campus

-- Deputy Board Member of Helsinki Institute of Physics

-- Deputy Advisory Board Member of Helsinki City and University of Helsinki

-- Member of Evaluation Board of the Komppa Award in Chemistry

-- Board Member of the Finnish National Graduate School in Nanoscience (NGS--NANO)

-- Board Member of Graduate School of Chemical Sensors and Microanalytical Systems (CHEMSEM)

--Board Member of the Graduate School "Physics, Chemistry, Biology and Meteorology of Atmospheric Composition and Climate Change"

Sorvari Sanna:

--New opportunities for Finnish-Japanese cooperation in urban land-atmosphere and air quality research, seminar held in Kumpula 24.-25.11.2008, member of the organizing committee

--HERC-iLEAPS seminar on "Interactions between land use and climate: multidisciplinary perspective from local land use to global climate", seminar held in Viikki Info Center, 24 April 2008, member of the organising committee

--Science workshop on past, present and future climate change –project 2007-2008, funded by Finnish Cultural Foundation, member of the project committee

--AVARA/Ilmaston muutoshanke, University of Helsinki, member of the project committee

Suni Tanja:

-- Finnish Association for Aerosol Research FAAR, secretary

Vehkamäki Hanna:

--Finnish Association for Aerosol Research FAAR – vice chair 2008-

--Nordic Society for Aerosol Research, 2003 -, member of Board

--Expert member of the Committee on Nucleation and Atmospheric Aerosols 2004-

-- NOSA representative in the Junge Award committee 2004-

--Finnish/Nordic representative in the European Aerosol Assembly (EAA) 2004-

--Finnish Physical Society, working group Female Physicists in Finland, national, member of Board

--NOSA Aerosol Symposium 2008, Oslo, 6.-7.11.2008, member of the organizing committee

--Leader of the working group 'Gender Equality' at Department of Physics, University of Helsinki and Finnish Physical Society (product: 'What you should know about women and Physics- Gender equality at the Department of Physics', 2008).

--Chair of the session "Fundamental aerosol physics – Aerosol formation" in the NOSA 2008 Conference, Oslo, Norway, 6.-7.11.2008

Vesala Timo:

--ICOS, member of the Core Team

--Workshop Eddy Covariance 2008, Hyytiälä, April 8–11, chairman of the organizing committee

--Greenhouse gases and aerosols: Interactions between northern ecosystems and climate, International conference given by the NECC and BACCI Nordic Centres of Excellence, Reykjavik, Iceland, June 16–18, 2008, member of the scientific committee

--New opportunities for Finnish-Japanese cooperation in urban land-atmosphere and air quality research, seminar held in Kumpula 24.-25.11.2008, member of the scientific committee

--Suomalainen Tiedeakatemia 100 vuotta 2008, Symposium Maan ytimestä avaruuteen, member of the program committee

--10th Anniversary Euroflux workshop 10.-12.12.2008, Hyytiälä, chairman of the organizing committee

Other

Aalto Tuula:
--Evaluation of research application: European Center for Arctic Environmental
   Research, Norway
Nikinmaa Eero:
-- Member of the expert panel of the Faculty of Agriculture and Forestry on evaluating
   the National strategic plan on the development of urban greening
-- Member of the expert panel of the Faculty of Agriculture and Forestry on evaluating
   the National Action Plan for proteccion of biodiversity in Southern Finland
Riipinen Ilona:
--member of evaluation panel, Academy of Sciences of the Czech Republic (2008)
--member of evaluation panel, National Oceanic and Atmospheric Administration
   (NOAA), USA (2008-)
Rinne Janne:
-- External evaluator, docentship in University of Kuopio, November 2008, Kuopio,
   Finland
Vehkamäki Hanna:
--The Faculty of Science at Göteborg University. Sweden: strategic project
   developments, mid-term review for the project */Nanoparticles in interactive
   environments/.*
--evaluator in professorship, The Faculty of Science, Gothenburg University, Sweden
Vesala Timo:
-- External evaluator, professorship in Lund University, May 2008, Lund, Sweden
-- External evaluator, docentship in University of Kuopio, November 2008, Kuopio,
   Finland

Opponents and reviews of academic dissertations

Anttila Tatu:
-- Reviewer of PhD thesis by MSc Larisa Sogacheva (University of Helsinki, Department
   of Physics)
--Reviewer of PhD thesis by MSc Taina Ruuskanen (University of Helsinki, Department
   of Physics)
Bäck Jaana:
--Reviewer of PhD thesis by Delia M. Pinto, University of Kuopio, Jan 2008.
Hyötyläinen Tuulia :
--Faculty opponent of the doctoral thesis by Erik Spinnel, "PLE with integrated clean up
   followed by alternative detection steps for cost-effective analysis of dixons and
   dioxin-like compounds", Umeå University, Umeå, June 13, 2008, Sweden
Kerminen Veli-Matti:
--Reviewer of the dissertation of MSc Riikka Sorjamaa (University of Kuopio,
   Department of Applied Physics)
--Reviewer of the dissertation of MSc Ari Leskinen (University of Kuopio, Department
   of Applied Physics)

--Reviewer of the dissertation of MSc Anca Hienola (University of Helsinki, Department of Physics)

Korhonen, Hannele:

--Review of PhD thesis by Larisa Sogacheva "Aerosol Particle Formation: Meteorological and Synoptic Processes behind the Event"

Laakso Lauri:

--Referee of MSc-thesis of Elne Kleynhans, "Spatial and temporal distribution of trace elements in aerosols in the Vaal Triangle", The North-West University, Republic of South Africa, 2008

Laaksonen, Ari:

-- Opponent for Mikko Lemmetty in dissertation titled as "Computational studies of aerosol growth, formation and measurement in diesel exhaust"

Lihavainen Heikki:

--Ann-Christine Engvall, University of Stockholm, 30.5.2008

Nikinmaa, Eero:

-- Reviewer of the dissertation of MSc Taina Ruuskanen (University of Helsinki, Department of Physics)

Riekkola Marja-Liisa:

--Faculty opponent of the doctoral thesis by Anna Lundquist: "Nanosized Bilayer Disks as Model Membranes for Interaction Studies", Uppsala University, Uppsala, March 28, 2008, Sweden

Vehkamäki Hanna:

--Examiner (opponent) in the Ph. D. defence of Martin Enghoff (University of Copenhagen) 7.5.2008

--Examiner (opponent) in the Ph. D. defence of Topi Rönkkö (Tampere University of Technology) 21.11.2008

OTHER ACTIVITIES

Tasks in organizations

Hämeri Kaarle:

-- chair in 'Tieteellinen ja yhteiskunnallinen näkökulma', Hiukkasfoorumin syysseminaari: Ympäristön monitorointi, Innopoli 31.10.2008

-- Acatiimi, Professoriliiton, Tieteentekijöiden liiton ja Yiopistonlehtorien liiton lehti, toimitusneuvosto, member of editorial board

Kerminen Veli-Matti:

--Member of FAAR board

Laakso Lauri:

-- HELAC Helsinki Aerosol Consulting Ltd, Research manager Manager, 2008

Lauri Antti:

--Expert member in steering committee and consortium, Innovaatioputkesta yritystoimintaa - Cleantech innovaatioiden kaupallistaminen, national

--Secretary, Luonnontieteiden foorumi (matemaattis-luonnontieteellisten järjestöjen epävirallinen neuvotteluelin), national

--FAAR board, Treasurer

Lihavainen Heikki:

--Member of FAAR board
Nikinmaa Eero:
--Member of the board of the Mustila arboretum
--Member of the board of the NGO for water quality improvement of the Lakes
　　Poikkipuoliainen, Tervalampi, and Huhmarjärvi
Riipinen Ilona:
-- HELAC Helsinki Aerosol Consulting Ltd, Executive Manager, 2008
Vesala Timo:
-- Chair: Geoscience symposium session 'Ilmastonmuutos eilen ja tänään' in University of
　　Helsinki, Physicum 11.1.2008, Finland

Public presentations in radio, TV and other media

Kulmala Markku:
-- "Saved by pollution?", Helsinki University Bulletin 1/2008, report about the
　　EUCAARI project, April 2008, Finland
-- "Mittaamatonta mittaamassa", Yliopisto-lehti 4/2008, 25.4.2008, Finland
-- "Kaksi astetta katastrofiin", Helsingin Sanomat, Anniversary interview, s. C 6,
　　toimittaja Tuomas Kaseva, 29.10.2008, Finland
-- "Chasing the origins of aerosol particles in the air", cscnews 3/2008, interview by Ari
　　Turunen, p. 18-21, November 2008, Finland
-- "Chasing the origins of aerosol particles in the air", cscnews 3/2008, interview by Ari
　　Turunen, p. 18-21, November 2008, Finland
-- "IT-based science is the microscope of today", cscnews 3/2008, interview by Anni
　　Jakobsson, p. 22-23, November 2008, Finland
Kurten Theo:
--Interview in Radio Vega 29.1.2008, about diesel car exhausts, in swedish
Lauri Antti:
--Karjalainen-lehti: Ulkomaiset eurot yhä harvassa (interview) 22.9.2008
Lihavainen Heikki:
--Luoteis-Lapin sanomat, Ilmastonmuutoksen juurilla, March 2008
Riipinen Ilona:
--"Bright eyes and cloudlets", Helsinki University Bulletin HUB, Science illustrated pp.
　　44-45, interview by Heli Perttula, October 2008, Finland
--"Physicumin katolla", Yliopisto-lehti 11/2008, haastattelu, s. 24-25, toimittaja Heli
　　Perttula, November 2008, Finland
Vesala Timo:
--"Trees absorbing less CO_2 as world warms, study finds. This means potentially a bigger
　　warming effect", The Guardian's netpage, interview by science correspondent James
　　Randerson, 3.1.2007
--"Tutkimus: Metsät ovat luultua heikompi jarru ilmastonmuutokselle", Helsingin
　　Sanomat, STT Science news, 3.1.2008, Finland
--"Lämpimät syksyt pienentävät metsien hiilinieluja", TV 4, News, interview based on an
　　article in Nature, 2.1.2007 klo 23, Finland
--"Lämpimät syksyt lisäävät luontoperäisiä hiilidioksidipäästöjä", Helsingin yliopisto,
　　kotisivut, http://www.helsinki.fi/ajankohtaista/uutisarkisto/1-2008/3-08-54-09.html,
　　3.1.2008, Finland

--"Varm höst ökar uppvärmningen", Hufvudstadsbladet, intervju, redaktör Erik Wahlström, s. 33, 6.1.2008, Finland
--"Trees absorbing less CO_2", Online edition of India's National Newspaper, The Hindu, http://www.hindu.com/seta/2008/01/10/stories/2008011050191400.htm, 10.1.2008, India
--"Lämmin syksy tukkii metsän hiilinielun", Etelä-Suomen Sanomat, science news, toimittaja Sammeli Heikkinen, 3.1.2008, Finland
--"Lämmin syksy tukkii metsän hiilinielun", Aamulehtiscience news, 3.1.2008, Finland
--"Lämmin syksy tukkii metsän hiilinielun", Savon Sanomat, science news, 3.1.2008, Finland
--"Pohjoiset metsät saattavat pahentaa ilmastonmuutosta", YLE TV1, News Boradcast 20:30, 2.1.2008, Finland
--"Metsät eivät hillitse ilmaston lämpenemistä niin paljon kuin on luultu", Kaleva, Science news, 3.1.2008, Finland
--"Lämmin syksy tukkii metsän hiilinielun", Länsi-Uusimaa, Science news, 3.1.2008, Finland
--"Metsien hiilinielu uhattuna", Yliopisto-lehti, Science news, 25.1.2008, Finland
--Hiilinielua ja hakkuita ei voi maksimoida yhtä aikaa", Helsingin Sanomat. Science news and interview, toimittaja Irina Vähäsarja, 27.1.2008, Finland
--"Kuuma vaara. Ilmastonmuutos on tullut jäädäkseen. Vain aikataulu on epävarma.", Yliopisto-lehti, interview, toimittaja Meri Siippainen, 20.3.2008, Finland
--"Ilmastonmuutos ja havumetsät", TV1 Prisma-science broadcast, 2.4.2008, Finland
--"Too much to take in – About climate change", Helsinki University Bulletin 1/2008, interview by Meri Siippainen, April 2008, Finland

Public presentations related to own scientific field

Asmi Eija:
--Ilmasto ja sen muutos – uusinta tutkimustietoa Etelämantereelta. 27.11.2008, Vihreän puiston kulttuurikeskus, Helsinki, Suomi.
Bäck Jaana:
-- "Ilmakehän koostumuksen ja ilmastonmuutoksen fysiikka, kemia, biologia ja meteorologia". Helsingin Luonnontiedelukio, 13.11.2008
Kulmala Markku:
-- "Aerosolit ja ilmastonmuutos", Geotieteellinen symposium, Physicum, 11.1. 2008, Finland
-- "Ilmakehätiede ja tietotekniikka", eScience - uusi tapa tehdä tiedettä, OPM:n tiedepoliittinen seminaari, Säätytalo, 15.5.2008, Finland
Kurten Theo:
-- Esitelmä: Ilmastonmuutoksen luonnontieteelliset perusteet. Polttavan Kysymyksen kampanjakoulutus (Maan Ystävät r.y.), Nuorten Luontotalo, Helsinki, 26.1.2008
-- Helsingin Suomalaisen Yhteiskoulun (SYK) lukion Ilmastonmuutos – erikoiskurssilla luennoimassa 11.03.2008 ja 18.4.-19.4.2008.
Nikinmaa Eero:
--Puun kunto selville lehdestä mittaamalla eli fluoresenssimenetelmän hyödyntäminen puiden kunnon arvioinnissa, Tampereen Viherpäivät, 12-13.2.2008, Tampere

--Metsäammattikunta muotoutuu. 100 year anniversary of Forest Education in Evo
   Forestry School 11.3.2008 Evo
Riekkola Marja-Liisa:
--"Mitä kuuluu, Marja-Liisa?", Luova-verkkolehti, Tutkimus@Tutkijat, published May 3,
   2008 (http://www.helsinki.fi/luova/2008/05/03/mita-kuuluu-marja-liisa)
Riipinen Ilona:
--Esitelmä: Minäkin kävin Tammerkoskea ja minusta tuli ilmakehäfyysikko,
   Tammerkosken koulut 100 vuotta, 7.11. 2008
Sorjamaa, Riikka:
-- Interview, Yle local news 4.4.2008
-- Interview, Yle national news 6.4.2008
Vesala Timo:
--"Ilmakehän ja biosfäärin vuorovaikutukset", Jyväskylän Kesän Uusiutuva energia -
   seminaari, Jyväskylä, 8.7.2008

Other activities in society

Markku Kulmala:
-- Hosting, together with Rector Ilkka Niiniluoto, the visit of Indian Minister for Science
   & Technology and Earth Sciences Shri Kapil Sibal to the Department of Physics and
   the Division of Atmospheric Sciences and Geophysics on 26 March 2008.
-- Chairman of the book release seminar due to the publication of "Boreal Forest and
   Climate Change", Infokeskus Korona, Viikki, 21.10.2008.

Awards and recognitions

Kulmala Markku:
-- Honorary doctorate, University of Tartu, 30.5.2008
-- European Research Council ERC Advanced Scientist Grant
-- nomination for the King Carl XVI Gustaf Visiting Professorship in Environmental
   Science, 1.9.2009-30.6.2010
-- nomination for the 2007 Descartes Prize for Transnational Collaborative Research (the
   BACCI project)

Riekkola Marja-Liisa:
-- Magnus Ehrnrooth Prize in Chemistry in 2008, the Finnish Society of Science and
   Letters

VISITS AND VISITORS

To the FCoE

Guest scientists
iLEAPS IPO guest scientist - Dr. Garik Gutman, NASA LCLUC programme manager,
22 May – 31.10 October 2008.
Visitors:
Host: Finnish Meteorological Institute:

--Noenne Prisle (1), University of Copenhagen, FMI Aerosols&Climate, 18th May - 1st June, laboratory measurements on surface tension.

--Noenne Prisle (2), University of Copenhagen, FMI Aerosols&Climate, 6th October - 20th October, laboratory measurements on surface tension.

--Alexandra Manka, University of Cologne, Aerosols&Climate, 8th September - 5th October, laboratory measurements on homogeneous nucleation.

Host: Eija Juurola:

--Ingo Ensminger, (Institut für Forstbotanik und Baumphysiologie, Universität Freiburg and Forstliche Versuchsanstalt Baden-Württemberg, Freiburg, Germany): Department of Forest Ecology, 16.-21.11.2008, purpose: Guest lecturer, research collaboration

Host: iLEAPS

1. Congbin Fu, Prof., Institute of Atmospheric Physics, Chinese Academy of Sciences, Beijing, China, 11 April, 2008, 1 day
2. Zhiwei Han, Prof., Key Laboratory of Regional Climate-Environment for East Asia Institute of Atmospheric Physics, Chinese Academy of Sciences, Beijing, China, 1 day
3. Kapil Sibal, Minister of Science and Technology of India, 26 March, 2008, 1 day
4. Y.P. Kumar, Head of International Division, Department of Science & Technology, India, 26 March, 2008, 1 day
5. Rajiv Sharma, Advisor, Department of Science & Technology, India, 26 March, 2008, 1 day
6. A.J. Kurian, PS to the Minister, Department of Science & Technology, India, 26 March, 2008, 1 day
7. H.E. Pradeep Singh, Ambassador of India, 26 March, 2008, 1 day
8. R.K. Kalra, Counsellor, Indian Embassy, 26 March, 2008, 1 day
9. Wolfgang Lucht, Prof., Postdam Institute for Climate Impact Research, Univ. Postdam, Germany, 24-26 April, 2008, 3 days
10. David Demeritt, Prof., King's College, London, UK, 24 April 2008, 1 day
11. Günther Fischer, Prof., IIASA, Luxemburg, Austria, 24 April 2008, 1 day
12. Ryan Teuling, Dr., ETH Zurich, Institute for Atmospheric and Climate, Switzerland, 24 April 2008, 1 day
13. Diego Fernandez Prieto, EO Science, Applications and Future Technologies Department European Space Agency (ESA) ESA-ESRIN, Frascati, Italy, 28 August, 1 day
14. Stephen Plummer, IGBP-ESA Joint Projects Office, Frascati, Italy, 28 August, 1 day
15. Rudich Yinon, Prof., Weizmann Institute, Rehovot, Israel, 6 June 2008, 1 day
16. Paul Wagner, Prof., Dept. Physics, Univ. Vienna, Austria, 30 October 2008, 1 day
17. Hans-Christen Hansson, Prof., Dept. Applied Environmental Science, Stockholm University, Sweden, 30 October 2008, 1 day
18. Ken Carslaw, Prof., School of Earth and Environment, Univ. Leeds, UK, 30 October 2008, 1 day
19. Sue Grimmond, Prof., Environmental Monitoring and Modelling Group, Department of Geography, King's College London, UK, 24-25 November 2008, 2 days
20. Toshio Koike, Prof., Department of Civil Engineering, School of Engineering, The University of Tokyo, Japan, 24-26 November 2008, 3 days
21. Yutaka Kondo, Prof., Research Center for Advanced Science and Technology,

University of Tokyo, Japan, 24-26 November 2008, 3 days
22. Ryo Moriwaki, Prof., Ehime University, Department of Civil and Environmental Engineering, Japan, 24-26 November 2008, 3 day
23. Koji Tamai, Prof., Forestry & Forest Products Research Institute, Ibaraki, Japan, 24-26 November 2008, 3 days
24. Adnan Abu-Surrah, Prof., The Hashemite University, Zarqa, Jordan, 5 December, half day

Host: Lauri Laakso:
--Van Zyl, Pieter, PhD, lecturer, North-West University, South Africa, 14 days, research
-- Ferguson, Kirsten, BSc, student, Univ. Witwatersrand, South Africa, 14 days, research
-- Chiloane, Kgaugelo, MSc, Project chief, ESKOM Ltd, South Africa, 14 days, research

Host: Antti Lauri /Graduate School, ABS program:
1. Aan de Brugh, Joost, MSc, Wageningen University and Research Centre, the Netherlands, 9.-19.3.2008, research
2. Aarflot, Asbjørn, MSc, Stavanger katedralskole, Norway, 24.-26.4.2008, teaching visit
3. Abouabdillah, Aziz, MSc, Water Research Institute (IRSA-CNR), Bari,, 9.-19.3.2008, research
4. Abu Al-Ruz, Rasha, MSc, University of Jordan, Italy, 10.-16.5.2008, research
5. Alexeychik, Pavel, BSc, Russian State Hydrometeorological University, St. Petersburg, Russia, 15.-18.12.2008, teaching visit
6. Alexeychik, Pavel, BSc, Russian State Hydrometeorological University, St. Petersburg, Russia, 4.-13.8.2008, research
7. Ambade, Balram, MSc, Pandit Ravishankar Shukla University, Raipur, India, 9.-19.3.2008, research
8. Appiah - Gyapong, Joseph Yaw, MSc, Ghana Forestry Commission, Ghana, 9.-19.3.2008, research
9. Arabas, Sylwester, MSc, University of Warsaw, Poland, 9.-19.3.2008, research
10. Arneth, Almut, PhD, Lund University, Sweden, 17.-19.3.2008, research
11. Baduel, Christine, MSc, Westfälische Wilhelms-Universität Münster, Germany, 10.-16.5.2008, research
12. Bandeeva, Angelina, MSc, Russian State Hydrometeorological University, St. Petersburg, Russia, 18.-22.8.2008, research
13. Baneschi, Ilaria, PhD, Geosciences and Earth Resources Institute, CNR, Pisa, Italy, 9.-19.3.2008, research
14. Bougiatioti , Katerina, MSc, University of Crete, Crete, 10.-16.5.2008, research
15. Butterbach-Bahl, Klaus, PhD, Institute for Meteorology and Climate Research, Atmospheric Environmental Research (IMK-IFU), Germany, 10.-12.3.2008, teaching visit
16. Bycenkiene, Svetlana, MSc, Institute of Physics, Lithuania, 10.-16.5.2008, research
17. Capon, Elisabet, MSc, Universidad Politécnica de Catalunya, Barcelona, Spain, 9.-19.3.2008, research
18. Čech, Jan, MSc, Czech Hydrometeorological Institute; Czech Republic, 10.-16.5.2008, research
19. Chumak, Ekaterina, MSc, Russian State Hydrometeorological University, St. Petersburg, Russia, 18.-22.8.2008, research

20. Costabile, Francesca, MSc, IFT, Germany, 10.-16.5.2008, research
21. Crumeyrolle, Suzanne, PhD, Metéo-France/CNRM/GMEI/MNPCA, France, 4.-13.8.2008, research
22. Curtius, Joachim, PhD, Goethe-Universität Frankfurt am Main, Germany, 10.-11.8.2008, research
23. Cusack, Michael, MSc, Instituto de Ciencias de le Tierra "Jaume Almera" CSIC, Spain, 10.-16.5.2008, research
24. del Mar Sorribas Panero, María, MSc, University of Valladolid (Spain), 10.-16.5.2008, research
25. Donají González Cantú, Nélida Jocelyn, MSc, Stockholm University, Sweden, 10.-16.5.2008, research
26. Duchi, Rocco, MSc, CNR-ISAC Bologna, Italy, 10.-16.5.2008, research
27. Eller, Margus, PhD, University of Tartu, Estonia, 17.-19.3.2008, research
28. Engström, Erik, MSc, University of Stockholm, Sweden, 4.-13.8.2008, research
29. Filippenko, Anna, MSc, Russian State Hydrometeorological University, St. Petersburg, Russia, 18.-22.8.2008, research
30. Forbrich, Inke, MSc, University of Greifswald, Germany, 9.-19.3.2008, research
31. Franchin, Alessandro, MSc, University of Milan, Italy, 4.-13.8.2008, research
32. Gallet, Jean-Charles, MSc, University Joseph Fourrier, France, 10.-16.5.2008, research
33. Ganbat, Gantuya, MSc, Russian State Hydrometeorological University, St. Petersburg, Russia, 9.-19.3.2008, research
34. Gupta, Shilpy, MSc, Physical Research Laboratory (PRL), Ahmedabad, India, 9.-19.3.2008, research
35. Helen Faloon, Kate, MSc, University of Birmingham, UK, 10.-16.5.2008, research
36. Hesemann, Jonas, MSc, IFT, Germany, 10.-16.5.2008, research
37. Hõrrak, Urmas, PhD, University of Tartu, Estonia, 17.-19.3.2008, research
38. Janson, Robert, PhD, Stockholm University, Sweden, 8.-9.12.2008, teaching visit
39. Janssen, Ruud, MSc, Wageningen University, The Netherlands, 4.-13.8.2008, research
40. Kanepi, Andrey, MSc, Russian State Hydrometeorological University, St. Petersburg, Russia, 18.-22.8.2008, research
41. Kanukhina, Anna, PhD, Russian State Hydrometeorological University, St. Petersburg, Russia, 8.-9.12.2008, teaching visit
42. Kononova, Ekaterina, MSc, Russian State Hydrometeorological University, St. Petersburg, Russia, 4.-13.8.2008, research
43. Kuang, Chongai, MSc, University of Minnesota, USA, 9.-19.3.2008, research
44. Kumar, Ashwini, MSc, Physical Research Laboratory (PRL), Ahmedabad, India, 9.-19.3.2008, research
45. Lankreijer, Harry, PhD, Lund University, Sweden, 8.-9.12.2008, teaching visit
46. Lebedev, Dmitry, MSc, Russian State Hydrometeorological University, St. Petersburg, Russia, 4.-13.8.2008, research
47. Markakis, Konstantinos, MSc, Aristotle University of Thessaloniki, Greece, 4.-13.8.2008, research
48. Matisāns, Modris, MSc, Latvian Environment, Geology and Meteorology Agency, Latvia, 10.-16.5.2008, research

49. Mazaheri, Mandana, MSc, Queensland University of Technology, Australia, 17.-23.8.2008, research
50. Meyer, Astrid, MSc, Karlsruhe Research Centre, Garmisch-Partenkirchen, Germany, 9.-19.3.2008, research
51. Mirme, Aadu, PhD, University of Tartu, Estonia, 17.-19.3.2008, research
52. Mirme, Sander, MSc, University of Tartu, Estonia, 17.-19.3.2008, research
53. Nazarova, Elena, MSc, Russian State Hydrometeorological University, St. Petersburg, Russia, 4.-13.8.2008, research
54. Niall Hamilton, Robinson, MSc, University of Manchester, UK, 10.-16.5.2008, research
55. Nikolaeva, Vera, MSc, Russian State Hydrometeorological University, St. Petersburg, Russia, 18.-22.8.2008, research
56. NN, NN, MSc, Stavanger katedralskole, Norway, 24.-26.4.2008, teaching visit
57. NN, NN, MSc, Stavanger katedralskole, Norway, 24.-26.4.2008, teaching visit
58. NN, NN, MSc, Stavanger katedralskole, Norway, 24.-26.4.2008, teaching visit
59. NN, NN, MSc, Stavanger katedralskole, Norway, 24.-26.4.2008, teaching visit
60. NN, NN, MSc, Stavanger katedralskole, Norway, 24.-26.4.2008, teaching visit
61. NN, NN, MSc, Stavanger katedralskole, Norway, 24.-26.4.2008, teaching visit
62. NN, NN, MSc, Stavanger katedralskole, Norway, 24.-26.4.2008, teaching visit
63. NN, NN, MSc, Stavanger katedralskole, Norway, 24.-26.4.2008, teaching visit
64. Noe, Steffen M., PhD, Estonian University of Life Sciences, Tartu, Estonia, 18.-19.10.2008, teaching visit
65. Noe, Steffen M., PhD, Estonian University of Life Sciences, Tartu, Estonia, 9.-19.3.2008, research
66. Noppel, Madis, PhD, University of Tartu, Estonia, 17.-19.3.2008, research
67. Noppel, Madis, PhD, University of Tartu, Estonia, 8.-9.12.2008, teaching visit
68. Ondracek, Jakub, MSc, Laboratory of Aerosol Chemistry and Physics, Czech Academy of Sciences, Czech Republic, 10.-16.5.2008, research
69. Oueslati, Ons, MSc, Water Research Institute (IRSA-CNR), Bari, Italy, 9.-19.3.2008, research
70. Paixão, Melina, MSc, University of São Paulo; Brazil, 10.-16.5.2008, research
71. Pandey, Praveen, MSc, Flemish Institute for Technological Research (VITO), Mol, Belgium, 9.-19.3.2008, research
72. Parts, Tiia-Ene, MSc, University of Tartu, Estonia, 17.-19.3.2008, research
73. Perez-Fortes, Mar, MSc, Universidad Politécnica de Catalunya, Barcelona, Spain, 9.-19.3.2008, research
74. Persson, Lars, MSc, University of Gothenburg, Sweden, 9.-19.3.2008, research
75. Podgaisky, Edward, PhD, Russian State Hydrometeorological University, St. Petersburg, Russia, 4.-13.8.2008, teaching visit
76. Pridacha, Vladislava Borisovna, PhD, Forest Research Institute, Petrozavodsk, Russia, 9.-19.3.2008, research
77. Pryputniewicz, Dorota, PhD, University of Gdańsk, Poland, 10.-16.5.2008, research
78. Queface, Antonio Joaquim, MSc, Eduardo Mondlane University, Maputo, Mozambique, 9.-19.3.2008, research
79. Raventos Duran, Teresa, MSc, University of Birmingham, UK, 10.-16.5.2008, research

80. Rayner, Peter, PhD, Laboratoire des Sciences du Climat et de l'Environnement (LSCE), France, 10.-12.3.2008, teaching visit
81. Sachs, Torsten, MSc, Alfred Wegener Institute for Polar and Marine Research, Potsdam, Germany, 9.-19.3.2008, research
82. Sapart, Celia Julia, MSc, Institute for Marine and Atmospheric Research Utrecht, The Netherlands, 9.-19.3.2008, research
83. Schobesberger, Siegfried, MSc, University of Vienna, Austria, 4.-13.8.2008, research
84. Siluch, Marcin, MSc, Maria Curie Skłodowska University, Lublin, Poland, 9.-19.3.2008, research
85. Tang, Pei-Yun, MSc, National Taiwan University, Taiwan, 4.-13.8.2008, research
86. Theodosi , Christina, MSc, University of Crete, Crete, 10.-16.5.2008, research
87. Tritscher, Torsten, PhD, Paul Scherrer Institut, Switzerland, 10.-16.5.2008, research
88. Uin, Janek, PhD, University of Tartu, Estonia, 17.-19.3.2008, research
89. Wagner, Robert, MSc, University of Vienna, Austria, 4.-13.8.2008, research
90. Verma, Santosh Kumar, MSc, Pandit Ravishankar Shukla University, Raipur, India, 9.-19.3.2008, research
91. Virdiano, Giovanni Andrea, MSc, Institute of Agro-environmental and Forest Biology, Italy, 9.-19.3.2008, research
92. Vogt, Matthias, MSc, Stockholm University, Sweden, 10.-16.5.2008, research
93. Voulkoudis, Stephan Christos, MSc, Westfälische Wilhelms-Universität Münster, Germany, 9.-19.3.2008, research
94. Yakovleva, Ekaterina, PhD, Voeikov Main Geophysical Observatory, St. Petersburg, Russia, 9.-19.3.2008, research
95. Zabanova, Viktoria, MSc, Russian State Hydrometeorological University, St. Petersburg, Russia, 4.-13.8.2008, research
96. Zecha, Gudrun, MSc, University of Vienna, Austria, 4.-13.8.2008, research

Host: Markku Kulmala:
1. McMurry, P. H., Prof., Univ. Minnesota, USA, 24.-26.3.2008, 3 days, research
2. Janson, Robert, Assoc. prof., Univ. Stockholm, Sweden, 13.-15.5.2008, 3 days, research
3. Lazaridis, Mihalis, Assoc. prof., Technical Univ. of Crete, Greece, 3.-5.6.2008, 3 days, research
4. Gómez, Pedro, Dr., Dept. Química Física I, Universidad Complutense de Madrid , Spain, 5.3.2008, 1 day, research
5. Hansel, Armin, Univ. Innsbruck, Austria, 6.6.2008, 1 day, research
6. Koike, Toshio, Prof., Univ. Tokyo, Japan, 24.-25.11.2008, 2 days, research
7. Kondo, Yutaka, Prof., Univ. Tokyo, Japan, 24.-25.11.2008, 2 days, research
8. Moriwaki, Ryo, Prof., Ehime Univ., Japan, 24.-25.11.2008, 2 days, research
9. Grimmons, Sue, Prof., King's College London, Great Britain, 24.-25.11.2008, 2 days, research
10. Tamai, Koji, Dr., FFPRI, Japan, 24.-25.11.2008, 2 days, research
11. Birmili, Wolfram, PhD, senior scientist, Leibniz Institute for Tropospheric Research, Leipzig, Germany, 14.-16.12.2008, 3 days, research

Host: Hanna Manninen :
-- Attoui, Michel, Prof., Université de Paris XII, France, 24.4.-8.5.2008, 14 days, research

Host: Eero Nikinmaa:
-- Prof. Ulo Niinemets, Tartu Maaylikool, 28-29.8. 2008, 2 days, research
Host: Jukka Pumpanen:
--Benjamin Wolf, Forschungszentrum Karlsruhe GmbH, Bereich Atmosphärische Umweltforschung (IMK-IFU) 5.10.-14.10.2008, Research
--Prof. Peter Murdoch and Rob Striegl USGS, 18.-19.10. 2008, excursion to SMEARII-station and Siikaneva site
Host: Marja-Liisa Riekkola:
--Sara Herrero-Martin, Departamento de Química Analítica, Nutrición y Bromatología, Facultad de Ciencias Químicas, Universidad de Salamanca, Salamanca, Spain, September – November 2008, research cooperation
--Laura Núñez, INIA, Madrid, Spain, September – November 2008, research cooperation
--Prof. Torgny Fornstedt, Uppsala University, Uppsala, Sweden, August 17-22, 2008 and November 17-20, 2008, research cooperation
Host: Ilona Riipinen:
--Yu, Fangqun, Dr. State University of New York at Albany, Atmospheric Sciences Research Center,19.-27.5.2008, research
Host: Mikko Sipilä:
--Gerhard Steiner, University of Vienna, Austria, visited Dept. Physics Feb 2008 ca 2 weeks. Purpose: Joint laboratory experiments on nanoparticles and ions.
--Michel Attoui, University of Paris XII, visited Dept. Physics Feb (4 weeks) and Apr (2 weeks), 2008. Purpose: Joint laboratory experiments on nanoparticles and ions.
Host: Timo Vesala:
1. Abouabdillah, Aziz, MSc, Water Research Institute, Bari, Italy, 10.-19.3.2008, 10 days, research
2. Ambade, Balram, PhD, India, 10.-19.3.2008, 10 days, research
3. Appiah-Gyapong, Josph Yaw, Ghana Forestry Commission, Ghana, 10.-19.3.2008, 10 days, research
4. Arabas, Sylwester, Univ. Warsaw, Poladn, 10.-19.3.2008, 10 days, research
5. Baneschi, Ilaria, MSc, Dipartimento di Scienze Ambientali, Università Ca'Foscari Venezia, Italy, 10.-19.3.2008, 10 days, research
6. de Brugh, Joost Aan, Wageningen Institute for Environment and Climate Research, the Netherlands, 10.-19.3.2008, 10 days, research
7. Capon Garcia, Elisabet, Dept. of Chemical Engineering, Univ. Politècnica de Catalunya, Spain, 10.-19.3.2008, 10 days, research
8. Forbrich, Inke, Univ. Greifswald, germany, 10.-19.3.2008, 10 days, research
9. Gupta, Shilpy, Ahmedabad, India, 10.-19.3.2008, 10 days, research
10. Kumar, Ashwini, Physical Research Laboratory, Ahmedabad, India, 10.-19.3.2008, 10 days, research
11. Meyer, Astrid, Karlsruhe Research Centre, Garmisch-Partenkirchen, Germany, 10.-19.3.2008, 10 days, research
12. Oueslati, Ons, Università Ca'Foscari Venezia, Italy, 10.-19.3.2008, 10 days, research
13. Pandey, Praveen, Belgium, 10.-19.3.2008, 10 days, research
14. Perez Fortes, Maria, Dept. of Chemical Engineering, Univ. Politècnica de Catalunya, Spain, 10.-19.3.2008, 10 days, research

15. Queface, António Joaquim, PhD, Eduardo Mondiane Univ., Maputo, Mosambique, 10.-19.3.2008, 10 days, research
16. Sapart, Célia-Julia, Univ. Utrecht, The Netherlands, 10.-19.3.2008, 10 days, research
17. Sachs, Torsten, Alfred Wegener Institute for Polar and Marine Research, Potsdam, Germany, 10.-19.3.2008, 10 days, research
18. Shaltout, Nayrah, Alexandria Univ., Egypt, 10.-19.3.2008, 10 days, research
19. Siluch, Marcin, Marie Curie Sklodowska Univ.; Lublin, Poland, 10.-19.3.2008, 10 days, research
20. Kumar Verma, Santosh, Pandit Ravishankar Shukla Univ., Raipur, India, 10.-19.3.2008, 10 days, research
21. Virdiano, Giovanni Andrea, Inst. of Agro-Environmental and Forest Biology, Italy, 10.-19.3.2008, 10 days, research
22. Voulkoudis, Stephan Christos, Westfalische Wilhelms-Universität Münster, Germany, 10.-19.3.2008, 10 days, research
23. Rudich, Yinon, Weizmann Inst., Israel, 6.6.2008, 1 day, research
24. Acosta, Manuel, Czech Academy of Sciences, Czech republic, 8.-11.4.2008, 4 days, research
25. Ambus, Per, Risø, Denmark, 8.-11.4.2008, 4 days, research
26. Bonal, Damien, Francen Guyana, 8.-11.4.2008, 4 days, research
27. Carrara, Arnaud, Spain, 8.-11.4.2008, 4 days, research
28. Chojnicki, Bogdan, Akademia Rolnicza im. Augusta Cieszkowskiego w Poznaniu, Poland, 8.-11.4.2008, 4 days, research
29. Di Marco, Chiara, Center for Ecology & Hydrology, Great Britain, 8.-11.4.2008, 4 days, research
30. Denmead, Owen, CSIRO, Australia, 8.-11.4.2008, 4 days, research
31. Di Tommasi, Paul, CNR, Italy, 8.-11.4.2008, 4 days, research
32. Drewer, Julia, Center for Ecology & Hydrology, Great Britain, 8.-11.4.2008, 4 days, research
33. Dusek, Jiri, Inst. of Systems Biology and Ecology, Czech republic, 8.-11.4.2008, 4 days, research
34. Elbers, Jan, Wageningen University and Research Centre, The Netherlands, 8.-11.4.2008, 4 days, research
35. Eugster, Werner, ETH – Inst. of Plant Science, Switzerland, 8.-11.4.2008, 4 days, research
36. Falcimagne, Robert, INRA, Clermont-Ferrand, France, 8.-11.4.2008, 4 days, research
37. Famulari, Daniela, Center for Ecology & Hydrology, Great Britain, 8.-11.4.2008, 4 days, research
38. Forbrich, Inke, Ernst-Moritz-Arndt-Univ. Greifswald, Germany, 8.-11.4.2008, 4 days, research
39. Grace, John, University of Edinburgh, Great Britain, 8.-11.4.2008, 4 days, research
40. Grover, Samantha, Charles Darwin University, Australia, 8.-11.4.2008, 4 days, research
41. Gupta, Sapana, Intia, 8.-11.4.2008, 4 days, research
42. Hansen, Georg, NILU, Oslo, Norja, 8.-11.4.2008, 4 days, research
43. Hendriks, Dimmie, Vrije Universiteit Amsterdam, The Netherlands, 8.-11.4.2008, 4 days, research

44. Hensen, Arjan, Energy Research Centre of the Netherlands, The Netherlands, 8.-11.4.2008, 4 days, research
45. Herbst, Mathias, Univ. Copenhagen, Dept. of Geography & Geology, Denmark, 8.-11.4.2008, 4 days, research
46. Jackowicz-Korczynski, Marcin, Univ. Lund, Sweden, 8.-11.4.2008, 4 days, research
47. Johansson, Torbjörn, Univ. Copenhagen, Dept. of Geography & Geology, Denmark, 8.-11.4.2008, 4 days, research
48. Juszczak, Radoslaw, Akademia Rolnicza im. Augusta Cieszkowskiego w Poznaniu, Poland, 8.-11.4.2008, 4 days, research
49. Kiese, Ralf, Germany, 8.-11.4.2008, 4 days, research
50. Klemedtsson, Leif, Sweden, 8.-11.4.2008, 4 days, research
51. Klumpp, First, INRA, Clermont-Ferrand, France, 8.-11.4.2008, 4 days, research
52. Kroon, Petra, Energy Research Centre of the Netherlands, The Netherlands, 8.-11.4.2008, 4 days, research
53. Lindroth, Anders, Lund University, Sweden, 8.-11.4.2008, 4 days, research
54. McDermitt, Dayle, LI-COR Biosciences, USA, 8.-11.4.2008, 4 days, research
55. Michalak, Maria, Poland, 8.-11.4.2008, days, research
56. Neftel, Albrecht, Forschungsanstalt Agroscope Reckenholz-Tänikon ART, Switzerland, 8.-11.4.2008, 4 days, research
57. Nordstroem, Claus, Aarhus University, Denmark, 8.-11.4.2008, 4 days, research
58. Olejnik, Janusz, Postdam Institute for Climate Impact Research, Univ. Postdam, Poland, 8.-11.4.2008, 4 days, research
59. Papale, Dario, Università della Tuscia, Italy, 8.-11.4.2008, 4 days, research
60. Siedlecki, Pawel, Poland, 8.-11.4.2008, 4 days, research
61. Taufarova, Klara, Inst. of Systems Biology and Ecology, Czechk Republic, 8.-11.4.2008, 4 days, research
62. Tsuang, Ben, National Chung Hsing University, Taiwan, 8.-11.4.2008, 4 days, research
63. Urbaniak, Marek, Poznan University of Life Sciences, Poland, 8.-11.4.2008, 4 days, research
64. Weidman, Damien, Rutherford Appleton Laboratory, Great Britain, 8.-11.4.2008 , 4 days, research
65. Werle, Peter, Inst. für Meteorologie und Klimaforschung, Germany, 8.-11.4.2008, 4 days, research
66. Xu, Liukang, LI-COR Biosciences, USA, 8.-11.4.2008, 4 days, research
67. Yamulki, Sirwan, Forestry Commission – National Inventory of Woodland and Trees, Great Britain, 8.-11.4.2008, 4 days, research
68. Zahniser, Mark, Aerodyne, Billerica, USA, 8.-11.4.2008, 4 days, research
69. Zawitowska-Blacha, Olga, Poznan University of Life Sciences, Poland, 8.-11.4.2008, 4 days, research
70. Arneth, Almuth, MCT-ELSA, Lund Univ., Sweden, 10.-12.12.2008, 2 days, research
71. Bernhofer, Christian, Dept. of Meteorology, Techn. Univ. of Dresden, Germany, 10.-12.12.2008, 3 days, research
72. Cescatti, Alessandro, Climate Change Unit, JRC, Italy, 10.-12.12.2008, 3 days, research

73. Chojnicki, Bogdan, Agrometeorology Dept., Agricultural Univ. of Poznan, Poland, 10.-12.12.2008, 3 days, research
74. Grünwald, Thomas, Dept. of Meteorology, Techn. Univ. of Dresden, Germany, 10.-12.12.2008, 3 days, research
75. Ibrom, Andreas, Risø National Laboratory, Denmark, 10.-12.12.2008, 3 days, research
76. Jung, Martin, Max-Planck-Institute for Biogeochemistry Jena, Germany, 10.-12.12.2008, 3 days, research
77. Lassiop, Gitta, Max-Planck-Institute for Biogeochemistry Jena, Germany, 10.-12.12.2008, 3 days, research
78. Lindroth, Anders, Dept. of Physical Geography and Ecosystems Analysis, Lund Univ., Sweden, 10.-12.12.2008, 3 days, research
79. Loustau, Denis, INRA, France, 10.-12.12.2008, 3 days, research
80. Matteucci, Girogio, Inst. for Mediterranean National research Council, Italy, 10.-12.12.2008, 3 days, research
81. Papale, Dario, Forest Ecology Laboratory, Univ. Tuscia, Italy, 10.-12.12.2008, 3 days, research
82. Piao, Shilong, Dept. of Ecology, Peking Univ., Kiina, 10.-12.12.2008, 3 days, research
83. Pilegaard, Kim, Risø National Laboratory, Denmark, 10.-12.12.2008, 3 days, research
84. Reichstein, Markus, Max-Planck-Institute for Biogeochemistry Jena, Germany, 10.-12.12.2008, 3 days, research
85. Shurpali, Narasinha, Dept. of Environmental Science, Univ. Helsinki, Suomi, 10.-12.12.2008, 3 days, research
86. Valentini, Riccardo, Forest Ecology Laboratory, Univ. Tuscia, Italy, 10.-12.12.2008, 3 days, research

From the FCoE

Aalto Pasi:
-- Max Planck Institute, Leipzig, Germany, 5.3.2008, 1 day, research visit
Aalto Tuula:
--JSBach-biosphere model meeting, Hamburg, Germany, 10 June 2008
--Methane and regional modelling meeting, Hamburg, Germany, 9–10 Sept
Aurela Mika:
--Veolia Environmental Services (Emerald Park landfill) and Waste Management (Metro landfill), Franklin, Wisconsin, USA, 29 Sept. – 10 Oct. 2008, US Fugitive emissions campaign.
Boy Michael:
--NCAR, Boulder, CO, USA, 17.11.-11.12.2008, 25 days, research
-- Tovetorp Research Station, NorUsBa Workshop, Sweden, 11.-15.8.2008, 5 days, research
Bäck Jaana:
-- Tovetorp Research Station, NorUsBa Workshop, Sweden, 11.-15.8.2008, 5 days, research
-- Tartu Maaylikool, Estonia (Steffen Noe, Kalev Jögiste and Kajar Köster), May 21-22. research

Chung Chul:
-- Seoul National University, 30 Sep.- 28 Oct., 2008; research
Ehn Mikael:
-- Woods Hole Oceanographic Institution, Research vessel Knorr, Measurement campaign from Boston to Tromssa, , March – April 2008, 37 days, research
-- AMS users' meeting, Manchester, Great Britain 5.-7.9.2008, 3 days, research
-- Tofwerk Ag, Thun, Switzerland   10.-14.11.2008, 5 days, research
-- Univ. Galway, MAP (Marine Aerosol Production) project meeting, Dublin, Ireland, 1.-4.12.2008, 4 days, research
Hellen Heidi:
--Paul Scherrer Institute Zurich, Switzerland, Feb. 2007-Feb. 2008, post doc visit
Hussein Tareq:
-- Academy of Sciences of the Czech Republic, Prague, Czech Republic, 1.-11.7.2008, 11 days, research
--Institute of Chemical Process Fundamentals, Czech Republic,July – August 2008, 8 weeks; research
Hämeri Kaarle:
-- Univ. Galway, Ireland, 11.-14.2.2008, 4 days, research
--Leibniz Institute for Tropospheric Research, Leipzig, Germany, 14.-18.4.2008, 5 days, research
Kulmala Markku:
-- ISSI meeting, Bern, Switzerlandi, 28.-30.1.2008, 3 days, research
-- CLOUD consortium meeting, Frankfurt, Germany, 7.-8.2.2008, 2 days, research
-- Nordic Centre of Excellence meeting, Denmark, 3.4.2008, 1 day, research
-- Cabauw Experimental Site for Atmospheric Research, The Netherlands, 19.5.2008, 1 day, research
-- Univ. Vienna, Austria, 17.-18.4.2008, 2 days, research
-- Univ. Tartu, Estonia, 19.6.2008, 1 day, research
-- Univ. Stockholm, Sweden, 14.-16.8.2008, 3 days, research
-- Univ. Tartu, Estonia, 30.11.-3.12.2008, 4 days, research
-- Max-Planck-Institut für Chemie, Mainz, Germany, 12.12.2008, 1 day, research
Kurten Theo:
--Univ. Frankfurt, Saksa, 7.-11.4.2008, 5 days, research
--Instituto de tecnologia química e biológica, Universidade nova de Lisboa, Portugali, 5.5-10.5.2008, 5 days, research
--Université Blaise-Pascal, France, 12.5.-5.6.2008, 26 days, research
--University of Copenhagen, Denmark, 10.11.-14.11.2008, 5 days, research and teaching
Laakso Lauri:
-- North-West University, South Africa, January, May, September-December, 180 days, teaching and research
Lauri, Antti:
--Univ. Tartu, Estonia, 20.-23.1.2008, 4 days, research
--NordForsk, Oslo, Norway, 12.-13.3.2008, research
-- Univ. Stockholm, Department of Applied Environmental Science ITM, Sweden, 5.-8.4.2008, 4 days, research

-- Russian State Hydrometeorological University RSHU, St. Petersburg, Russia 4.-8.5.2008, 5 days, research
-- TEMPUS JEP-26005-2005 NetFAM summer school, St. Petersburg, Russia, 7.-11.7.2008, 5 days, teaching
--University of Thessaloniki; Greece, 24.-30.8.2008, research
--Norwegian Institute for Air Research, Oslo, Norway, 5.-7.11.2008, 3 days, research
-- Kungliga Tekniska Högskolan och Stockholms universitet, Stockholm, Sweden, 10.-12.12.2008, 3 days, teaching

Laurila Tuomas:
--Veolia Environmental Services (Emerald Park landfill) and Waste Management (Metro landfill), Franklin, Wisconsin, USA, 29 Sept. – 10 Oct. 2008, US Fugitive emissions campaign.

Lihavainen, Heikki:
--NASA, USA, March-October 2008, Scientific collaboration.

Manninen Hanna:
-- K-puszta Measurement Station, Hungary, 10.-14.3.2008, 5 days, research
-- Hohenpeissenberg Measurement Station, Germany, 23.-25.6.2008, 3 days
-- Cabauw Experimental Site for Atmospheric Research, the Netherlands, 18.-20.8.2008 , 3 days, research
--San Pietro Capofiume Experimental Field Site for Atmospheric Research, ISAC-CNR, Italy 18.-21.11.2008, 4 days, research
--Cabauw Experimental Site for Atmospheric Research, the Netherlands, 15.-16.12.2008, 2 days, research
--K-puszta Measurement Station, Hungary, 15.-17.10.2008, 3 days, research

Neitola Kimmo:
-- Univ. Crete, Heraklion, EUCAARI project AIS service, Greece, 10.-14.8.2008, 5 days, research

Nieminen Tuomo:
--CLOUD consortium meeting, Frankfurt, Germany, 7.2.2008, 1 day, research

Petäjä Tuukka:
-- Tovetorp Research Station, NorUsBa Workshop, Sweden, 11.-15.8.2008, 5 days, research

Pumpanen Jukka:
--site visit with Dr. Mike Billet, CEH (Centre for Ecology and Hydrology, Edinburgh) in Nurmes, Finland, 14.05.08. together with Pirkko Kortelainen and Anne Ojala.
--University of Tartu at Kalev Jögiste and Kajar Köster; windfall site, 23.7.-24.7. 2008, planning of soil respiration measurements

Reissell Anni:
--International Space Science Institute ISSI, Bern, Switzerland, 26.-30.1.2008, 5 days, research
-- Univ. Wageningen, the Netherlands, 1.-3.4.2008, 3 days, research
-- Nanjing Univ. of Information Science & Technology, Nanjing, China, 21.-24.4.2008, 3 days, research

Riekkola Marja-Liisa:
-- Toyohashi University of Technology, Toyohashi, Japan, February 4, 2008.
-- JASCO Ltd, Tokyo, Japan, February 5, 2008.

-- CSIC-Institute Madrid, Spain, June 4, 2008.

Riipinen Ilona:

-- Univ. Leeds, UK, 20.4.2008, 1 days, research

-- Univ. Copenhagen, Denmark, 27.-29.10.2008, 3 days, research

-- Univ. Leeds, UK, 20.5.2008, 1 days, research

-- Univ. Stockholm, Intensive course on nucleation, Sweden, 1.-2.6.2008, 2 days, teaching

-- Carnegie Mellon University, PA, and Aerodyne Research Inc., MA, USA, 16.-24.8.2008, 9 days, research

Rinne Janne:

-- EUSOR planning meeting, Oslo, Norway 21.-23.1.2008, 3 days, research

-- ICOS Meeting, Nice, France 28.1.-2.2.2008, 6 days,research

--Agricultural University of Tartu, Estonia, 21.-23.5.2008, 3 days,research

--Univ. Ghent, IMPECVOC project meeting, Belgium, 6.-8.7.2008, 3 days, research

-- Tovetorp Research Station, NorUsBa Workshop, Sweden, 11.-15.8.2008, 5 days, research

-- Research Centre Karlsruhe, Institute for Meteorology and Climate Research, Garmisch-Partenkirchen, Germany, 18.-21.8.2008, 4 days , research

-- Research Centre Karlsruhe, Institute for Meteorology and Climate Research, Garmisch-Partenkirchen, Germany, 3.-13.9.2008, 10 days, research

-- Tartu Maaülikool, Estonia, 21.-23.6.2008, 3 days, research

-- CNPq – Akatemia yhteishaun laadinta, Brazil, 28.6.-4.7.2008, 5 days, research

-- National Center for Atmospheric Research, Boulder, CO, USA, 11.-18.10.2008, 7 days, research

Ruuskanen Taina:

--Univ. Innsbruck, Austria, 25.-28.6.2008, 4 days, research

Sevanto Sanna:

--Australia National University, Apr 25-30, research

--University of Western Australia, May 1-5, research

--Harvard University, Jun 21- Jul 17, research

Sipilä Mikko:

-- Finokalia-station/Univ. Crete, Greece. EUCAARI measurements 2.-6.4. 2008 research

-- IfT, Leipzig, Germany. ,Nucleation Experiments 14.-18.4. 2008 research

--Mace Head/NUI Galway, Ireland. , EUCAARI measurements 19.-22.8. 2008 research

-- Univ. Vienna, Austria, CLOUD-meeting. 29.-30.9. 2008 research

--IfT, Leipzig, Germany, 2.-6.10. 2008, research

--Tofwerk GmbH, Thun, Switzerland, Research and Development. 10.-14.11. 2008, research

Sorvari Sanna:

--EINAR 1st Planning Meeting, Vienna, Itävalta, 17.4.2008, 1 day, research

--EINAR 2nd Planning Meeting, Frankfurt, Germany, 16.9.2008, 1 day, research

Tuovinen Juha-Pekka:

-- Barnsdale, UK, 27–29 Oct. 2008, ACCENT Synthesis & Integration Meeting

Vehkamäki Hanna:

-- Lecturing intensive course "Atmospheric particle formation" with Ilona Riipinen, Stockholm University 2.-3.6. 2008, teaching

Vesala Timo:
--Greenhouse Gas Meeting, Nice, France, 29.1.-1.2.2008, 4 days, research
-- Russian State Hydrometeorological University, RSHU, St. Petersburg, Russia, 5.-7.5.2008, 3 days, teaching and research
--ICOS Stakeholders Conference Agenda, Amsterdam, the Netherlands, 18.-21.5.2008, 4 days, research
--Univ. Vienna, Austria, 17.-18.4.2008, 2 days, research
--Nitrogen cycling workshop (Nitroeurope), Utrecht, the Netherlands, 22.-23.9.2008, 2 days, research
--Max Planck Institute for Biogeochemistry, Jena, Germany, 29.9.-2.10.2008, 4 days, research
--Institute of Atmospheric Physics, Beijing, China, 13.-17.10.2008, 5 days, research
--Scandinavian Research Infrastructure conference, Stockholm, Sweden, 12.-13.11.2008, 2 days, research

PUBLISHED RESEARCH

Nature and Science

1. Magnani F, Mencuccini M, Borghetti M, Berninger F, Delzon S, Grelle A, Hari P, Jarvis PG, Kolari P, Kowalski AS, Lankreijer H, Law BE, Lindroth A, Loustau D, Manca G, Moncrieff JB, Tedeschi V, Valentini R, Grace J 2008. Ecologically implausible carbon response? Reply. Nature 451, E3-E4.
2. Piao,S., P Ciais, P Friedlingstein, P Peylin, M Reichstein, S Lyussaert, H Margolis, J Fang, A Barr, A Chen, A Grelle, D Y Hollinger, T Laurila, A Lindroth, A D Richardson and T Vesala, Net carbon dioxide losses of northern ecosystems in response to autumn warming, Nature 451 (2008) 49-52
3. Rosenfeld, D., U Lohmann, GB Raga, CD O'Dowd, M Kulmala, S Fuzzi, A Reissell and MO Andreae, Flood or drought: How do aerosols affect precipitation? Science 321 (2008) 1309-1313
4. Winkler, PM., G Steiner, A Vrtala, H Vehkamäki, M Noppel, KEJ Lehtinen, GP Reischl, PE Wagner and M Kulmala, Heterogeneous nucleation experiments bridging the scale from molecular ion clusters to nanoparticles, Science 319 (2008) 1374-1377

Other peer-reviewed articles

5. Aarnio P, Martikainen J, Valkama I, Hussein T, Vehkamäki H, Sogacheva L, Härkönen J, Karppinen A, Koskentalo T, Kukkonen J, Kulmala M. Analysis and evaluation of selected PM10 pollution episodes in the Helsinki Metropolitan Area in 2002. Atmospheric Environment 2008, 42: 3992-4005.
6. Altimir N., Vesala T., Aalto T., Bäck J. & Hari P. (2008) Competition between ozone sinks at the air-leaf interface. Tellus 60B, 381–391.
7. Anttila P., Makkonen U., Hellen H., Pyy K., Leppänen S., Saari H., Hakola H., 2008. Impact of the open biomass fires in spring and summer of 2006 on the chemical composition of background air in south-eastern Finland. Atmospheric Environment 42, 6472-6486

8.   Anttila, T., and Kerminen, V.-M. (2008). Modeling study on aerosol dynamical processes regulating new particle and CCN formation at clean continental areas. Geophysical Research Letters, 35, L07813, doi:10.1029/2008GL033371.

9.   Anttila, T., P. Vaattovaara, M. Komppula, A.-P. Hyvärinen, H. Lihavainen, V.-M. Kerminen, and A. Laaksonen (2008). Size-dependent activation of aerosols into cloud droplets at a subarctic background site during the second Pallas Cloud Experiment (2nd PaCE): method development and data evaluation. Atmospheric Chemistry and Physics Discussions, 8, 14519-14556.

10.   Asmi, E., M. Sipilä, H. E. Manninen, J. Vanhanen, K. Lehtipalo, S. Gagné, K. Neitola, A. Mirme, S. Mirme, E. Tamm, J. Uin, K. Komsaare, M. Attoui, and M. Kulmala (2008). Results of the first air ion spectrometer calibration and intercomparison workshop. *Atmospheric Chemistry and Physics Discussions* 8: 17257-17295.

11.   Baklanov, A., PG Mestayer, A Clappier, S Zilitinkevich, S Joffre, A Mahura and NW Nielsen, Towards improving the simulation of meteorological fields in urban areas through updated/advanced surface fluxes description, Atmos Chem Phys 8 (2008) 523-543

12.   Berndt, T., Stratmann, F., Bräsel, S., Heintzenberg, J., Laaksonen, A., and Kulmala, M. (2008) SO2 oxidation products other than H2SO4 as a trigger of new particle formation – Part 1: Laboratory investigations, Atmos. Chem. Phys. 8 6365-6374.

13.   Bonn, B., Kulmala, M., Riipinen, I., Sihto, S.-L. and Ruuskanen, T., 2008. How biogenic terpenes govern the correlation between sulfuric acid concentrations and new particle formation, J. Geophys. Res., 113, D12209, doi:10.1029/2007JD009327

14.   Boy M., et al. with M Kulmala, New particle formation in the Front Range of the Colorado Rocky Mountains, Atmos Chem Phys 8 (2008) 1577-1590

15.   Boy, M., J Kazil, E R Lovejoy, A Günther and M Kulmala, Relevance of ion-induced nucleation of sulfuric acid and water in the lower troposphere over the boreal forest at northern latitudes, Atmos Res 90 (2008) 151-158

16.   Brinksma E.J., et al. with G de Leeuw, The 2005 and 2006 DANDELIONS NO$_2$ and aerosol intercomparison campaigns, J Geophys Res 113 (2008) D16S46

17.   Brus, D., A.-P. Hyvärinen, V. Ždímal, and H. Lihavainen, Erratum: "Homogeneous nucleation rate measurements of n-butanol in helium: A comparative study of a thermal diffusion cloud chamber and a laminar flow diffusion chamber", Journal of Chemical Physics, 128 (7), (2008).

18.   Brus, D., A.-P. Hyvärinen, J. Wedekind, Y. Viisanen, M. Kulmala, V. Ždímal, J. Smolík and H. Lihavainen, The homogeneous nucleation of 1-pentanol: The effect of carrier gas pressure and kind in a laminar flow diffusion chamber, J. Chem. Phys. 128 (13) (2008).

19.   Brus D., Ždímal V., and Smolík J.: Homogeneous nucleation rate measurements in supersaturated water vapor, J. Chem. Phys. 129, 174501 (2008).

20.   Curier, R.L., JP Veefkind, R Braak, B Veihelmann, O Torres and G de Leeuw, Retrieval of aerosol optical properties from OMI radiances using a multiwavelength algorithm: Application to western Europe, J Geophys Res 113 (2008) D17S90

21.   Dal Maso, M., A. Hyvärinen, M. Komppula, P. Tunved, V.-M. Kerminen, H. Lihavainen, Y. Viisanen, H.-C. Hansson, and M. Kulmala, Annual and interannual

variation in boreal forest aerosol particle number and volume concentration and their connection to particle formation, Tellus 60B (2008) 495-508

22.   Dal Maso, M., L Sogacheva, MP Anisimov, M Arshinov, A Baklanov, B Belan, TV Khodzher, VA Obolkin, A Staroverova, A Vlasov, VA Zagaynov, A Lushnikov, YuS Lyubovtseva, I Riipinen, V-M Kerminen and M Kulmala, Aerosol particle formation events at two Siberian stations inside the boreal forest, Boreal Env Res 13 (2008) 81-92

23.   Dinar, E., Anttila, T., and Rudich, Y. (2008). CCN activity and hygroscopic growth of organic aerosols following reactive uptake of ammonia. Environmental Science and Technology, 42, 793–799.

24.   Duplissy, J., M. Gysel, M. R. Alfarra, J. Dommen, A. Metzger, A. S. H. Prevot, E. Weingartner, A. Laaksonen, T. Raatikainen, N. Good, S. F. Turner, G. McFiggans and U. Baltensperger. "Cloud forming potential of secondary organic aerosol under near atmospheric conditions", Geophys. Res. Lett., Vol. 35, L03818, doi:10.1029/2007GL031075, (2008)

25.   Duursma R.A., Kolari P., Perämäki M., Nikinmaa E., Hari P., Delzon S., Loustau D., Ilvesniemi H., Pumpanen J. and Mäkelä A. 2008. Predicting the decline in daily maximum transpiration rate of two pine stands during drought based on constant minimum leaf water potential and plant hydraulic conductance. Tree Physiology 28: 265-276.

26.   Ekberg A., Arneth A., Hakola H., Hayward S., Holst T., 2008. Leaf isoprene emission in a subarctic wetland sedge community. Biogeosciences Discuss.5, 5061-5091.

27.   Facchini M.C., et al. with G de Leeuw, Primiray submicron marine aerosol dominated by insoluble organic colloids and aggregates, Geophys Res Lett 35 (2008) L17814

28.   Frey A., Rose D., Wehner B., Müller T., Cheng Y. , Wiedensohler A., Virkkula A. (2008) Application of the volatility-TDMA technique to determine the number size distribution and mass concentration of less volatile particles, Aerosol Sci. Technol., 42, 817 — 828.

29.   Gagné, S., L Laakso, T Petäjä, V-M Kerminen and M Kulmala, Analysis of one year of Ion-DMPS data from the SMEAR II station, Finland, Tellus 60B (2008) 318-329

30.   Grönholm, T., S Haapanala, S Launiainen, J Rinne, T Vesala and Ü Rannik, The dependence of the beta coefficient of REA system with dynamic deadband on atmospheric conditions, Environ Pollut 152 (2008) 597-603

31.   Göckede, M., Foken, T., Aubinet, M., Aurela, M, Banza, J., Bernhofer, C., Bonnefond, J. M., Brunet, Y., Carrara, A., Clement, R., Dellwik, E., Elbers, J., Eugster, W., Fuhrer, J., Granier, A., Grünwald, T., Heinesch, B., Janssens, I. A., Knohl, A., Koeble, R., Laurila, T., Longdoz, B., Manca, G., Marek, M., Markkanen, T., Mateus, J., Matteucci, G., Mauder, M., Migliavacca, M., Minerbi, S., Moncrieff, J., Montagnani, L., Moors, E., Ourcival, J.-M., Papale, D., Pereira, J., Pilegaard, K., Pita, G., Rambal, S., Rebmann, C., Rodrigues, A., Rotenberg, E., Sanz, M. J., Sedlak, P., Seufert, G., Siebicke, L., Soussana, J. F., Valentini, R., Vesala, T., Verbeeck, H. & Yakir, D., 2008. Quality control of CarboEurope flux data – Part I: Footprint analyses to evaluate sites in forest ecosystems, *Biogeosciences* 5, 433–450.

32.	Halonen, J.I., T Lanki, T Yli-Tuomi, M Kulmala, P Tiittanen and J Pekkanen, Urban air pollution, and asthma and COPD hospital emergency room visits, Thorax 63 (2008) 635-641

33.	Hari P, Pumpanen J, Huotari J, Kolari P, Grace J, Vesala T, Ojala A 2008. High-frequency measurements of productivity of planktonic algae using rugged nondispersive infrared carbon dioxide probes. Limnology and Oceanography: Methods 6, 347-354.

34.	Hellén H., Hakola H., Haaparanta S., Pietarila H. and Kauhaniemi M., 2008. Influence of residential wood combustion on local air quality. Science of the Total Environment 393, 283– 290.

35.	Hellén H., Dommen J., Metzger A., Gascho A., Duplissy J., Tritscer T., Prevot A.S.H. and Baltensperger U., 2008. Using Proton Transfer Reaction Mass Spectrometry for Online Analysis of Secondary Organic Aerosols. Environmental Science and Technology, 42, 7247-7353.

36.	Hienola, A., Riipinen, I., Vehkamäki, H. and Kulmala, M., 2008. Homogeneous vs. heterogeneous nucleation in water-dicarboxylic acid systems, Atmos. Chem. Phys. Discuss., 8, 18295-18321

37.	G Hoek, et al. with M Kulmala, A Puustinen and K Hämeri, Indoor-outdoor relationships of particle number and mass in four European cities, Atmos Environ 42 (2008) 156-169

38.	Hussein T, Karlsson H, Johansson C, Hansson H-C. Factors affecting particle emissions from paved roads: on road measurements in Stockholm, Sweden. Atmospheric Environment 2008, 42: 688-702.

39.	Hussein T, Kulmala, M. Indoor aerosol modeling: basic principles and practical applications. Water, Air, and Soil Pollution: Focus 2008, 8: 23-34.

40.	Hussein T, Martikainen J, Junninen H, Sogacheva L, Wagner R, Dal Maso M, Riipinen I, Aalto PP, Kulmala M. Observation of Regional New Particle Formation in the Urban Atmosphere. Tellus 2008, 60B: 509-521.

41.	Hyvärinen, A.-P., M. Komppula, C. Engler, N. Kivekäs, V.-M. Kerminen, M. Dal Maso, Y. Viisanen and H. Lihavainen, Atmospheric new particle formation at Utö, Baltic Sea 2003-2005, *Tellus B*, 60 (3), DOI: 10.1111/j.1600-0889.2008.00343.x (2008).

42.	Hyvärinen, A.-P., D. Brus, V. Ždímal, J. Smolík, M. Kulmala, Y. Viisanen and H. Lihavainen, Erratum: "The carrier gas pressure effect in a laminar flow diffusion chamber, homogeneous nucleation of *n*-butanol in helium", *Journal of Chemical Physics*, 128 (10), (2008).

43.	Hyötyläinen, T. On-line coupling of extraction with gas chromatography, *J. Chromatogr. A,* 1186 (2008) 39-50.

44.	Hyötyläinen T. and M.-L. Riekkola, Sorbent- and liquid phase microextraction techniques and membrane-assisted extraction in combination with gas chromatographic analysis. *Analytical Chimica Acta* 614 (2008) 27-37

45.	Hörrak, U., PP Aalto, J Salm, K Komsaare, H Tammet, JM Mäkelä, L Laakso and M Kulmala, Variation and balance of positive air ion concentrations in a boreal forest, Atmos Chem Phys 8 (2008) 655-675

46.	Julin, J., Ismo Napari, Joonas Merikanto, and Hanna Vehkamäki: Equilibrium sizes and formation energies of small and large Lennard-Jones clusters from molecular

dynamics. A consistent comparison to Monte Carlo simulations and density functional theories. Journal of Chemical Physics, Vol 129, 234506, 2008.

47.   Junninen, H., Hulkkonen, M., Riipinen, I., Nieminen, T., Hirsikko, A., Suni, T., Boy, M., Lee, S.-H., Vana, M., Tammet, H., Kerminen, V.-M. and Kulmala, M., 2008. Observations on nocturnal growth of atmospheric clusters, Tellus, B60, 365-371

48.   Järvi, L. H Junninen, A Karppinen, R Hillamo, A Virkkula, T Mäkelä, T Pakkanen and M Kulmala, Temporal variations in black carbon concentrations with different time scales in Helsinki during 1996-2005, Atmos Chem Phys 8 (2008) 1017-1027

49.   Kallio M. & Hyötyläinen, T. Simple Calibration Method for Comprehensive Two-Dimensional Gas Chromatography, *Journal of Chromatography A* 1200 (2008) 264-267

50.   Kallio M. Matti Jussila, Päivi Raimi, Tuulia Hyötyläinen, Modified Semi-Rotating Cryogenic Modulator for Comprehensive Two-Dimensional Gas Chromatography, *Analytical and Bioanalytical Chemistry* 391 (2008) 2357-2363

51.   Kanak, KM ., JM Straka and DM Schultz, Numerical simulation of mammatus, J Atmos Sci 65 (2008) 1606-1621

52.   Kannosto J, Lemmetty M, Virtanen A, Mäkelä JM, Keskinen J, Junninen H, Hussein T, Aalto P, Kulmala M. Mode resolved density of atmospheric aerosol particles. Atmospheric Chemistry and Physics 2008 8: 5327-5337.

53.   Kannosto, J., A Virtanen, M Lemmetty, JM Mäkelä, J Keskinen, H Junninen, T Hussein, P Aalto and M Kulmala, Mode resolved density of atmospheric aerosol particles, Atmos Chem Phys 8 (2008) 5327-5337

54.   Kivekäs, N., Kerminen, V-M., Anttila, T., Korhonen, H., Lihavainen, H., Komppula, M., and Kulmala, M. (2008). Parameterization of cloud droplet activation using a simplified treatment of the aerosol number size distribution. Journal of Geophysical Research – Atmospheres, 113, D15207, doi:10.1029/2007JD009485

55.   Kokkola, H., Vesterinen, M., Anttila, T., Laaksonen, A., and Lehtinen, K. E. J. (2008). Technical Note: Analytical formulae for the critical supersaturations and droplet diameters of CCN containing insoluble material. *Atmospheric Chemistry and Physics,* 8, 1985–1988.

56.   Kokkola, H., H. Korhonen, K. E. J. Lehtinen, R. Makkonen, A. Asmi, S. Järvenoja, T. Anttila, A.-I. Partanen, M. Kulmala, H. Järvinen, A. Laaksonen, and V.-M. Kerminen (2008). SALSA - a Sectional Aerosol module for Large Scale Applications. Atmospheric Chemistry and Physics, 8, 2469-2483. SRef-ID: 1680-7324/acp/2008-8-2469

57.   Korhonen, H., K.S. Carslaw, D. V. Spracklen, G. W. Mann and M. T. Woodhouse (2008): Influence of DMS emissions on CCN concentrations and seasonality over the remote southern hemisphere oceans: A global model study. J. Geophys. Res. 113 D15204, doi:10.1029/2007JD009718.

58.   Kourtchev, I., T M Ruuskanen, P Keronen, L Sogacheva, M Dal Maso, A Reissell, X Chi, R Vermeylen, M Kulmala, W Maenhaut and M Claeys, Determination of isoprene and alpha-/beta-pinene oxidation products in boreal forest aerosols from Hyytiälä, Finland: diel variations and possible link with particle formation events, Plant Biology 10 (2008) 138-149

59. Kristensson A, Dal Maso M, Swietlicki E, Hussein T, Zhou J, Kerminen V-M, Kulmala M. Characterization of New Particle Formation Events at a Background Site in Southern Sweden: Relation to Air Mass History. Tellus 2008, 60B: 330-344.

60. Kuglitsch, F. G., Reichstein, M., Beer, C., Carrara, A., Ceulemans, R., Granier, A., Janssens, I. A., Koestner, B., Lindroth, A., Loustau, D., Matteucci, G., Montagnani, L., Moors, E. J., Papale, D., Pilegaard, K., Rambal, S., Rebmann, C., Schulze, E. D., Seufert, G., Verbeeck, H., Vesala, T., Aubinet, M., Bernhofer, C., Foken, T., Grünwald, T., Heinesch, B., Kutsch, W., Laurila, T., Longdoz, B., Miglietta, F., Sanz, M. J. & Valentini, R., 2008. Characterisation of ecosystem water-use efficiency of European forests from eddy covariance measurements. *Biogeosciences Discussions* 5, 4481–4519

61. Kulmala L., Launiainen S., Pumpanen J., Lankreijer H., Lindroth A., Hari P. and Vesala T. 2008. H_2O and CO_2 fluxes at the floor of a boreal Pine forest. Tellus 60B:167-178.

62. Kulmala M. and V-M Kerminen, On the formation and growth of atmospheric nanoparticles, Atmos Res 90 (2008) 132-150

63. Kulmala M., Kerminen V.-M., Laaksonen A., Riipinen I., Sipilä M., Ruuskanen T.M., Sogacheva L., Hari P., Bäck J., Lehtinen K.E.J., Viisanen Y., Bilde M., Svenningsson B., Lazaridis M., Tørseth K., Tunved P., Nilsson D. Pryor S., Sorensen L.-L., Hõrrak U., Winkler P.M., Swietlicki E., Riekkola M.-L., Krejci R., Hoyle C., Hov Ø., Myhre G. & Hansson H.-C. (2008). Studies on Biosphere-Aerosol-Cloud-Climate Interactions within BACCI. Tellus 60B, 300–317

64. Kurtén, T., V Loukonen, H Vehkamäki and M Kulmala, Amines are likely to enhance neutral and ion-induced sulfuric acid-water nucleation in the atmosphere more effectively than ammonia, Atmos Chem Phys 8 (2008) 4095-4103

65. Kurtén T & Vehkamäki, H., Investigating atmospheric sulfuric acid–water–ammonia particle formation using quantum chemistry, Advances in Quantum Chemistry: Applications of Theoretical Methods to Atmospheric Science, Vol. 55 (2008) 407-427

66. Laakso, L., H Laakso, PP Aalto, P Keronen, T Petäjä, T Nieminen, T Pohja, E Siivola, M Kulmala, N Kgabi, M Molefe, D Mabaso, D Phalatse, K Pienaar and V-M Kerminen, Basic characteristics of atmospheric particles, trace gases and meteorology in a relatively clean Southern African Savannah environment, Atmos Chem Phys 8 (2008) 4823-4839

67. Laaksonen, A., Kulmala, M., Berndt, T., Stratmann, F., Mikkonen, S., Ruuskanen, A., Lehtinen, K. E. J., Dal Maso, M., Aalto, P., Petäjä, T., Riipinen, I., Sihto, S.-L., Janson, R., Arnold, F., Hanke, M., Ücker, J., Umann, B., Sellegri, K., O'Dowd, C. D., and Viisanen, Y (2008) SO2 oxidation products other than H2SO4 as a trigger of new particle formation. Part 2: Comparison of ambient and laboratory measurements, and atmospheric implications, Atmos. Chem. Phys. 8 7255-7264.

68. Laaksonen, A., M. Kulmala, C. D. O'Dowd, J. Joutsensaari, P. Vaattovaara, S. Mikkonen, K. E. J. Lehtinen, L. Sogacheva, M. Dal Maso, P. Aalto, T. Petäjä, A. Sogachev, Y. Jun Yoon, H. Lihavainen, D. Nilsson, M. Cristina Facchini, F. Cavalli, S. Fuzzi, T. Hoffmann, F. Arnold, M. Hanke, K. Sellegri, B. Umann, W. Junkermann, H. Coe, J. D. Allan, M. Rami Alfarra, D. R. Worsnop, M.-L. Riekkola, T.

Hyötyläinen, and Y. Viisanen, The role of VOC oxidation products in continental new particle formation, *Atmos. Chem. Phys.*, 8, 2657-2665, 2008

69.   Lagergren F, Lindroth A, Dellwik E, Ibrom A, Lankreijer H, Launiainen S, Mölder M, Kolari P, Pilegaard K, Vesala T 2008. Biophysical controls on CO2 fluxes of three Northern forest based on long-term eddy covariance data. Tellus 60B, 143–152.

70.   Lallo, M., Aalto, T., Laurila, T. & Hatakka, J., 2008. Seasonal variations in hydrogen deposition to boreal forest soil in southern Finland. *Geophysical Research Letters* 35, L04402, doi:10.1029/2007GL032357

71.   Lee, S-H., L-H Young, DR Benson, T Suni, M Kulmala, H Junninen, TL Campos, DC Rogers and J Jensen, Observations of nighttime new particle formation in the troposphere, J Geophys Res 113 (2008) D10210

72.   Lehtipalo, K., Sipilä, M., Riipinen, I., Nieminen, T. and Kulmala, M., 2008. Analysis of atmospheric neutral and charged molecular clusters in boreal forest using pulse-height CPC, Atmos. Chem. Phys. Discuss., 8, 20661-20685.

73.   Leskinen, A.P., M Kulmala and KEJ Lehtinen, Growth of nucleation mode particles: Source rates of condensable vapour in a smog chamber, Atmos Environ 42 (2008) 7405-7411

74.   Lihavainen, H., V.-M. Kerminen, M. Komppula, A.-P. Hyvärinen, J. Laakia, S. Saarikoski, U. Makkonen, N. Kivekäs, R. Hillamo, M. Kulmala, and Y. Viisanen (2008), Measurements of the relation between aerosol properties and microphysics and chemistry of low level liquid water clouds in Northern Finland, Atmos. Chem. Phys., 8, 6925-6938.

75.   Lihavainen, H., Y. Viisanen and M. Kulmala, Erratum: Homogeneous nucleation of n-pentanol in a laminar flow diffusion chamber [JCP 114, 10031-10038 (2001)], *J. Chem. Phys.,*128, 139902 , 2008

76.   Lindroth, A., Lagergren, F., Aurela, M., Bjarnadottir, B., Christensen, T., Dellwik, E., Grelle, A., Ibrom, A., Johansson, T., Lankreijer, H., Launiainen, S., Laurila, T., Mölder, M., Nikinmaa, E., Pilegaard, K., Sigurdsson, B. D. & Vesala, T., 2008. Leaf area index is the principal scaling parameter for both gross photosynthesis and ecosystem respiration of Northern deciduous and coniferous forests. *Tellus* B60, 129–142

77.   Lushnikov, A.A. Exact post-critical behavior of a source-enhanced gelling system, J Phys A: Math Theor 41 (2008) 072001

78.   Makkonen, R., Asmi, A., Korhonen, H., Kokkola, H., Järvenoja, S., Räisänen, P., Lehtinen, K. E. J., Laaksonen, A., Kerminen, V.-M., Järvinen, H., Lohmann, U., Feichter, J., and Kulmala, M.: Sensitivity of aerosol concentrations and cloud properties to nucleation and secondary organic distribution in ECHAM5-HAM global circulation model, Atmos. Chem. Phys. Discuss., 8, 10955-10998, 2008.

79.   Malila, J., Hyvärinen, A.-P., Viisanen, Y., and Laaksonen, A. (2008), Displacement barrier heights from experimental nucleation rate data, Atmospheric Research 90 303-312, doi:10.1016/j.atmosres.2008.07.002

80.   Mammarella, I., E Dellwik and N O Jensen, Turbulence spectra, shear stress and turbulent kinetic energy budgets above two beech forest sites in Denmark, Tellus 60B (2008) 179-187

81. Mazon, S., Riipinen, I., Valtanen, M., Schultz, D., Junninen, H., Nieminen, T., Dal Maso, M., Sogacheva, L., Kerminen, V.-M. and Kulmala, M., 2008. Classifying previously undefined days from eleven years of particle size distribution data from SMEAR II station, Hyytiälä, Finland, Atmos. Chem. Phys. Discuss., 8, 12665-12693.

82. Mikkonen, S., Rahikainen, M., Virtanen, J., Lehtonen, R., Kuikka, S., and Ahvonen, A. (2008), A linear mixed model with temporal covariance structures in modelling catch per unit effort of Baltic herring, ICES Journal of Marine Science 65 1645-1654. doi:10.1093/icesjms/fsn135

83. Mitrakos D., Ždímal V., Brus D., Housiadas C.: Data evaluation of laminar flow diffusion chamber nucleation experiments with different computational methods, J. Chem. Phys. 129(5), 054503-1 - 7 (2008).

84. Mordas, G., HE Manninen, T Petäjä, PP Aalto, K Hämeri and M Kulmala, On operation of the ultra-fine water-based CPC TSI3786 and comparison with other TSI models (TSI3776, TSI3772, TSI3025, TSI3010, TSI3007), Aerosol Sci Technol 42 (2008) 152-158

85. Mordas, G., M Sipilä and M Kulmala, Nanometer particle detection by the condensation particle counter UF-02proto, Aerosol Sci Technol 42 (2008) 521-527

86. Müller, J-F., T Stavrakou, S Wallens, I De Smedt, M Van Roozendael, MJ Potosnak, J Rinne, B Munger, A Goldstein and AB Günther, Global isoprene emissions estimated using MEGAN, ECMWF analyses and a detailed canopy environmental model, Atmos Chem Phys 8 (2008) 1329-1341

87. Mäkelä A, Pulkkinen M, Kolari P, Lagergren F, Lindroth A, Loustau D, Nikinmaa E, Vesala T, Hari P 2008. Developing an empirical model of stand GPP with LUE approach: results from an analysis of eddy covariance data at five contrasting conifer sites in Europe. Global Change Biology 14, 92–108.

88. Napari, I., Equilibrium vapor pressure and surface tension from cluster data: Density functional results, J Chem Phys 129 (2008) 154507

89. Norris, SJ., IM Brooks, G de Leeuw, MH Smith, M Moerman and JJN Lingard, Eddy covariance measurements of sea spray particles over the Atlantic Ocean, Atmos Chem Phys 8 (2008) 555-563

90. O'Dowd, C. D., Y. J. Yoon, W. Junkerman, P. Aalto, M. Kulmala, H. Lihavainen, and Y. Viisanen.: Airborne measurements of nucleation mode particles II: boreal forest nucleation events. *Atmos. Chem. Phys. Discuss.*, 8, 2821-2848, 2008

91. Ortega, I.K., T Kurtén, H Vehkamäki and M Kulmala, The role of ammonia in sulfuric acid ion induced nucleation, Atmos Chem Phys 8 (2008) 2859-2867

92. Paatero P., and PK Hopke, Rotational tools for factor analytic models, J Chemometr 22 (2008), *Online First* October 6, doi: 10.1002/cem.1197

93. Parshintsev, J., Nurmi, J., Kilpeläinen, I., Hartonen, K., Kulmala, M., Riekkola, M.-L, Preparation of β-caryophyllene oxidation products and their determination in ambient aerosol samples. *Anal. Bioanal. Chem.* 390 (2008) 913-919.

94. Pol Jaroslav and Hyötyläinen Tuulia, "Comprehensive two-dimensional liquid chromatography-mass spectrometry", *Analytical and Bioanalytical Chemistry* 391 (2008) 21-31.

95. Porcar-Castell A, Juurola E, Nikinmaa E, Berninger F, Ensminger I, Hari P. 2008. Seasonal acclimation of photosystem II in Pinus sylvestris. I. Estimating the rate

constants of sustained thermal dissipation and photochemistry. Tree Physiology 28:1475-1482.

96.   Porcar-Castell A, Juurola E, Ensminger I, Berninger F, Hari P, Nikinmaa E. 2008. Seasonal acclimation of photosystem II in Pinus sylvestris. II. Studying the effect of light environment through the rate constants of sustained thermal dissipation and photochemistry. Tree Physiology 28:1483-1491.

97.   Porcar-Castell A, Pfündel E, Korhonen JFJ, Juurola E, 2008.A new monitoring PAM fluorometer (MONI-PAM) to study the short- and long-term acclimation of photosystem II in field conditions. Photosynthesis Research 96:173-179.

98.   Prisle, N.L., T. Raatikainen, R. Sorjamaa, B. Svenningsson, A. Laaksonen and M. Bilde. "Surfactant partitioning in cloud droplet activation: a study of C8, C10, C12 and C14 normal fatty acid sodium salts", Tellus B, 60(3), 416-431, doi:10.1111/j.1600-0889.2008.00352.x, (2008)

99.   Pryor,S.C., RJ Barthelmie, LL Sørensen, SE Larsen, AM Sempreviva, T Grönholm, Ü Rannik, M Kulmala and T Vesala, Upward fluxes of particles over forests: when, where, why? Tellus 60B (2008) 372-380

100.   Pryor, S.C., M Callagher, H Sievering, S E Larsen, R J Barthelmie, F Birsan, E Nemitz, J Rinne, M Kulmala, T Grönholm, R Taipale and T Vesala, A Review of measurement and modelling results of particle atmosphere-surface exchange, Tellus 60B (2008) 42-75

101.   Pumpanen J, Ilvesniemi H, Kulmala L, Siivola E, Laakso H, Kolari P, Helenelund C, Laakso M, Uusimaa M, Hari P 2008. Respiration in boreal forest soil as determined from carbon dioxide concentration profile. Soil Sci. Soc. Am. J. 72: 1187–1196.

102.   Raatikainen, T., A. Laaksonen, A.-P. Hyvärinen, J. Vanhanen, K. Hautio, H. Lihavainen, Y. Viisanen and I. Napari. "Surface Tensions of Multicomponent Aqueous Electrolyte Solutions: Predictive Models Based on Binary Limits", J. Phys. Chem. C., 112(28), 10428-10434, doi:10.1021/jp7117136, (2008)

103.   Riipinen, I., I. K. Koponen, G. P. Frank, A.-P. Hyvärinen, J. Vanhanen, H. Lihavainen, K. E. J. Lehtinen, M. Bilde and M. Kulmala, Adipic and malonic acid aqueous solutions: surface tensions and saturation vapor pressures, J. Chem. Phys., 111 (50), pp. 12995-13002, 2008

104.   Riipinen, I., Manninen, H., Yli-Juuti, T., Boy, M., Sipilä, M., Ehn, M., Junninen, H., Petäjä, T. and Kulmala, M., 2008. Applying the CPCB setup to study the hygroscopicity and composition of freshly-formed 2 – 9 nm particles in boreal forest, Atmos. Chem. Phys. Discuss., 8, 14893-14925

105.   Rinne, J., T Douffet, Y Prigent and P Durand, Field comparison of disjunct and conventional eddy covariance techniques for trace gas flux measurements, Environ Pollut 152 (2008) 630-635

106.   Robles-Gonzalez C. and G de Leeuw, Aerosol properties over the SAFARI-2000 area retrieved from ATSR-2, J Geophys Res 113 (2008) D05206

107.   Räisänen J., and Ruokolainen,L. Estimating present climate in a warming world: a model-based approach, Clim Dyn 3 (2008) 573-585

108.   Räisänen J. & Ruokolainen, L., Ongoing global warming and local warm extremes: a case study of winter 2006–2007 in Helsinki, Finland, Geophysica 44 (2008) 45-65

109.   S Saarikoski, H Timonen, K Saarnio, M Aurela, L Järvi, P Keronen, V-M

Kerminen and R Hillamo, Sources of organic carbon in fine particulate matter in northern European urban air, Atmos Chem Phys 8 (2008) 6281-6295

110.   Salonen, M., Kurtén, T., Vehkamäki, H. and Kulmala, M. Computational investigation of the possible role of some intermediate products of SO_2 oxidation in sulfuric acid – water nucleation. Atmospheric Research, Vol 91, pp. 47-52, 2009.

111.   Schultz, D.M., AJ Durant, JM Straka and TJ Garrett, Comments on "The mysteries of mammatus clouds: Observations and formation mechanisms" – Reply, Notes and Correspondence, J Atmos Sci 65 (2008) 1095-1097

112.   Sears-Collins A.L. and DM Schultz, Corrigendum,The spatial and temporal variability of drizzle in the United States and Canada, J Climate 21 (2008) 1447-1448

113.   Sevanto, S. E. Nikinmaa, A. Riikonen, M. Daley, J. C. Pettijohn, T. N. Mikkelsen, N. Phillips, N. M. Holbrook 2008. Linking xylem diameter variations with sap flow measurements. Plant and Soil 305(1-2), 77-90.

114.   Sievänen, R., Perttunen, J., Nikinmaa, E. and P. Kaitaniemi. 2008. Towards extension of a single tree functional- structural model of Scots pine to stand level: effect of the canopy of randomly distributed, identical trees on development of tree structure. Functional Plant Biology 35(9/10):964-975.

115.   Sihto, S.-L., H. Vuollekoski, J. Leppä, I. Riipinen, V.-M. Kerminen, H. Korhonen, K. E. J. Lehtinen, M. Boy, M. Kulmala, "Aerosol dynamics simulations on the connection of sulphuric acid and new particle formation", Atmos. Chem. Phys. Discuss., 8, 11363–11394 (2008).

116.   Sipilä M., K. Lehtipalo, M. Kulmala, T. Petäjä, H. Junninen, P. P. Aalto, H. E. Manninen, E. Vartiainen, I. Riipinen, E.-M. Kyrö, J. Curtius, A. Kürten, S. Borrmann, and C. D. O'Dowd (2008). Applicability of condensation particle counters to measure atmospheric clusters. Atmos. Chem. Phys., 8, 4049-4060, 2008

117.   Sipilä, M., Lehtipalo, K., Attoui, M., Neitola, K., Petäjä, T., Aalto, P. P., O'Dowd, C. D., and Kulmala, M.: Laboratory verification of PH-CPC's ability to monitor atmospheric sub-3nm clusters. Aerosol Sci. Tech. 43, 2:126-135, 2009

118.   Sogachev, A., Monique Y. Leclerc, Gengsheng Zhang, Üllar Rannik, Timo Vesala (2008). CO2 fluxes near a forest edge: a numerical study, Ecological Applications, Volume 18, Issue 6 pp 1454-1469

119.   Sogacheva,L., L Saukkonen, ED Nilsson, M Dal Maso, DM Schultz, G de Leeuw and M Kulmala, New aerosol particle formation in different synoptic situations at Hyytiälä, Southern Finland, Tellus 60B (2008) 485-494

120.   Spracklen, D. V., K. S. Carslaw, M. Kulmala, V.-M. Kerminen,S.-L. Sihto, I. Riipinen, J. Merikanto, G. W. Mann, M. P. Chipperfield, A. Wiedensohler, W. Birmili, and H. Lihavainen, The contribution of particle formation to global cloud condensation nuclei concentrations, *Geophysical Research Letters,* 35, L06808, doi:10.1029/2007GL033038, 2008

121.   Suni, T., M Kulmala, A Hirsikko, T Bergman, L Laakso, P P Aalto, R Leuning, H Cleugh, S Zegelin, D Hughes, E van Gorsel, M Kitchen, M Vana, U Hörrak, S Mirme, A Mirme, S Sevanto, J Twining and C Tadros, Formation and characteristics of ions and charged aerosol particles in a native Australian Eucalypt forest, Atmos Chem Phys 8 (2008) 129-139

122. Susiluoto S., Rasilo T., Pumpanen J. and Berninger F. 2008. Effects of grazing on the vegetation structure and carbon dioxide exchange of a Fennoscandian fell ecosystem. Arctic, Antarctic and Alpine Research. 40(2): 422-431.

123. Svenningsson B, Arneth A, Hayward S, Holst T, Massling A, Swietlicki E, Hirsikko A, Junninen H, Riipinen I, Vana M, Dal Maso M, Hussein T, Kulmala M. Aerosol particle formation events and analysis of high growth rates observed above a subarctic wetland-forest mosaic. Tellus 2008, 60B: 353-364.

124. Swietlicki, E., H-C Hansson, K Hämeri, B Svenningsson, A Massling, G McFiggans, PH McMurry, T Petäjä, P Tunved, M Gysel, D Topping, E Weingartner, U Baltensperger, J Rissler, A Wiedensohler and M Kulmala, Hygroscopic properties of submicrometer atmospheric aerosol particles measured with H-TDMA instruments in various environments – a review, Tellus 60B (2008) 432-469

125. Taipale, R., TM Ruuskanen, J Rinne, MK Kajos, H Hakola, T Pohja and M Kulmala, Technical Note: Quantitative long-term measurements of VOC concentrations by PTR-MS – measurement, calibration, and volume mixing ratio calculation methods, Atmos Chem Phys 8 (2008) 6681-6698

126. Thum, T., Aalto, T., Laurila, T., Aurela, M., Lindroth, A. & Vesala, T., 2008. Assessing seasonality of boreal coniferous forest CO_2 exchange by estimating biochemical model parameters from micrometeorological flux observations. *Biogeosciences* 5,1625–1639

127. Timonen, H., S Saarikoski, O Tolonen-Kivimäki, M Aurela, K Saarnio, T Petäjä, PP Aalto, M Kulmala, T Pakkanen and R Hillamo, Size distributions, sources and source areas of water-soluble organic carbon in urban background air, Atmos Chem Phys 8 (2008) 5635-5647

128. Tunved,P., J Ström, M Kulmala, V-M Kerminen, M Dal Maso, B Svenningson, C Lunder and H-C Hansson, The natural aerosol over Northern Europe and its relation to anthropogenic emissions – implications of important climate feedbacks, Tellus 60B (2008) 473-484

129. Tuovinen, J.-P. & Simpson, D., 2008. An aerodynamic correction for the European ozone risk assessment methodology. *Atmospheric Environment* 42, 8371–8381.

130. Ťupek, B., Minkkinen, K., Starr, M., Kolari, P., M., Chan, T., Vesala, T., Alm, J., Laine, J. and Nikinmaa, E. 2008. Forest floor versus ecosystem CO2 exchange along boreal ecotone between upland forest and lowland mire. Tellus B, 60(2):153-166.doi:10.1111/j.1600-0889.2007.00328.x

131. Vana, M., M. Ehn, T. Petäjä, H. Vuollekoski, P. Aalto, G. de Leeuw, D. Ceburnis, C. D. O'Dowd and M. Kulmala: Characteristic features of air ions at Mace Head on the west coast of Ireland, Atmos. Res., 90, 278-286, 2008.

132. van Gorsel, E., R Leuning, HA Cleugh, H Keith, MUF Kirschbaum and T Suni, Application of an alternative method to derive reliable estimates of nighttime respiration from eddy covariance measurements in moderately complex topography, Agr Forest Meteorol 148 (2008) 1174-1180

133. Vanhanen, J., A.-P. Hyvärinen, T. Anttila, Y. Viisanen, and H. Lihavainen, Ternary solution of sodium chloride, succinic acid and water; surface tension and its influence on cloud droplet activation, *Atmos. Chem. Phys.*, 8, 4595-4604, 2008.

134.	Wedekind, J., A.-P. Hyvarinen, D. Brus, D. Reguera, Unraveling the "pressure effect" in nucleation, *Physical Review Letters*, *Phys. Rev. Lett.* 101, 125703 (2008).
135.	Vesala, T. L. Järvi, S. Launiainen, A. Sogachev, Ü. Rannik, I. Mammarella, E. Siivola, P. Keronen, J. Rinne, A. Riikonen & E. Nikinmaa 2008. Surface-atmosphere interactions over complex urban terrain in Helsinki, Finland. Tellus 60B, 188-199.
136.	Vesala, T., N Kljun, Ü Rannik, J Rinne, A Sogachev, T Markkanen, K Sabelfeld, Th Foken and M Y Leclerc, Flux and concentration footprint modelling: State of the art, Environ Pollut 152 (2008) 653-666
137.	Winkler P.M., A Hienola, G Steiner, G Hill, A Vrtala, GP Reischl, M Kulmala and PE Wagner, Effects of seed particle size and composition on heterogenous nucleation of n-nonane, Atmos Res 90 (2008) 187-194
138.	Viskari, T., Järvinen, H., Anttila, T., Kerminen, V.-M., Lehtinen, K. E. J., Korhonen, H., Sihto, S.-L. and Kulmala, M. (2008) Duration of the tangent-linear regime in sectional multi-component aerosol dynamics. Journal of Aerosol Science, 39, 726-736.
139.	Young, L.H., DR Benson, FR Kameel, JR Pierce, H Junninen, M Kulmala and S-H Lee, Laboratory studies of H_2SO_4/H_2O binary homogeneous nucleation from the SO_2+OH reaction: evaluation of the experimental setup and preliminary results, Atmos Chem Phys 8 (2008) 4997-5016
140.	Zilitinkevich, S.S. T Elperin, N Kleeorin, I Rogachevskii, I Esau, T Mauritsen and MW Miles, Turbulence energetics in stably stratified geophysical flows: Strong and weak mixing regimes, Q J Roy Meteor Soc 134 (2008) 793-799
141.	Zilitinkevich, S.S. I Mammarella, AA Baklanov and SM Joffre, The effect of stratifications on the aerodynamic roughness length and displacement height, Bound-Lay Meteorol 129 (2008) 179-190

Articles in press

142.	Delpierre N., Soudani K., François F., Köstner B., Pontailler JY., Aubinet M., Bernhofer C., Granier A., Grunwald T., Heinesch B., Longdoz B., Misson L., Nikinmaa E., Ourcival JM., Rambal S., Vesala I. & Dufrêne E. 2009 - Exceptional carbon uptake in European forests during the warm spring of 2007: a data-model analysis. *Global Change Biology.* in press
143.	Filella I, Porcar-Castell A, Munné-Bosch S, Bäck J, Garbulsky M, Peñuelas J, 2008. PRI assessment of long-term changes in carotenoids/chlorophyll ratio and short-term changes in de-epoxidation state of the xanthophyll cycle. International Journal of Remote Sensing (In Press).
144.	Hari P & Nöjd P. (2008). The effect of temperature and PAR on the annual photosynthetic production of Scots pine in northern Finland during 1906-2002. Boreal Environment Research, accepted
145.	Herrmann, E., A.-P. Hyvärinen, D. Brus, H. Lihavainen and M. Kulmala: Re-evaluation of the pressure effect in nucleation with the CFD software Fluent and the fine particle model FPM, *J. Phys. Chem. A, (accepted),* 2008
146.	Huotari J., Ojala A., Peltomaa E., Pumpanen J., Hari P. and Vesala T. 2008. Temporal variations in surface water CO2 concentration in a boreal humic lake based on high frequency measurements. Boreal Environment Research (in press).

147. Hussein T, Hruška A, Dohányosová P, Džumbová P, Hemerka J, Kulmala M, Smolik M. Evaluation of deposition rates of aerosol particles on smooth surfaces inside a test chamber. Atmospheric Environment (Accepted 2008).

148. Hyvärinen, A.-P., H. Lihavainen, Y. Viisanen, and M. Kulmala: Erratum: "Homogeneous nucleation rates of higher *n* -alcohols measured in a laminar flow diffusion chamber", *Journal of Chemical Physics*, *(in press)* 2008

149. Hölttä, T., Cochard, H., Nikinmaa, E. and M. Mencuccini. 2009. Capacitive effect of cavitation in xylem conduits: results from a dynamic model. PCE 32(1):10-21.

150. Järvi L, Hannuniemi H, Hussein T, Junninen H, Aalto PP, Hillamo R, Mäkelä T, Keronen P, Siivola E, Vesala T, Kulmala M. The urban measurement station SMEAR III: continuous monitoring of air pollution and surface-atmosphere interactions in Helsinki, Finland. Boreal Environment Research (in press 2008).

151. Kallio, Minna , Matti Jussila, Sami Varjo, Sari Järvimäki, Tuulia Hyötyläinen, "Data Analysis Programs for Comprehensive Two-Dimensional Gas Chromatography", *J. Chromatogr A,* available on-line

152. Komppula, M., H. Lihavainen, A.-P. Hyvärinen, V.-M. Kerminen, T.S. Panwar, V.P. Sharma and Y. Viisanen, Physical properties of aerosol particles at a Himalayan background site in India, *Journal of Geophysical Research Letters,* (*accepted*) (2008).

153. Kyllönen, K., Karlsson, V. and Ruoho-Airola, T. (2008) Trace element deposition and trends during a ten year period in Finland. Accepted for publication in Science of the Total Environment 17.11.2008.

154. Malila, J., A.-P. Hyvärinen, and A. Laaksonen, Displacement barrier heights from experimental nucleation rate data: Scaling and universality, *Atmospheric Research (accepted)*, (2008).

155. Parshintsev, J., Räsänen, R., Hartonen, K., Kulmala, M., Riekkola, M.-L., "Analysis of Organic Compounds in Ambient Aerosols Collected with the Particle-into-Liquid Sampler", *Boreal Environmental Research* (2009) in press

156. Pumpanen J., Heinonsalo J., Rasilo T., Hurme Kaj-Roger and Ilvesniemi H. Carbon balance and allocation of assimilated CO_2 in Scots pine, Norway spruce and Silver birch seedlings determined with gas exchange measurements and 14C pulse labelling. Trees-Structure and Function. (in press)

157. Ruuskanen T.M., Taipale R, Rinne J., Kajos M.K., Hakola H. and Kulmala M. Quantitative long-term measurements of VOC concentrations by PTR-MS: annual cycle at a boreal forest site. *Atmos. Chem. Phys. Discuss.* 9:81-134.

158. Tuovinen, J.-P., Emberson, L. and Simpson, D. Modelling ozone fluxes to forests for risk assessment: status and prospects. Annals of Forest Science, in press.

159. Vuollekoski, H., V.-M. Kerminen, T. Anttila, S.-L. Sihto, M. Vana, M. Ehn, H. Korhonen, G. McFiggans, C. D. O'Dowd, and M. Kulmala (2008), Iodine dioxide nucleation simulations in coastal and remote marine environments, J. Geophys. Res., doi:10.1029/2008JD010713, in press.

Monographs

Lohila, A., 2008. Carbon dioxide exchange on cultivated and afforested boreal peatlands. Finnish Meteorological Institute Contributions 73, Finnish Meteorological Institute, Helsinki, 110 pp.

Other publications (Abstracts, reports)

1. Ballesta P.P., Brinc R., Brorström-Lunden E., Cao N., Dumitrean P., Fernandez P. R., Fröhlich M., Gohy M., Grenfell R., Hakola H., Hellen H., Leeb C., Locoge N., Mabilia R., Milton M., Novak J., O'Dwyer J., O'Leary B., Potter A., Quincey P., Reimann S., Rogge A., Schinerl A., Telling S., Wauters E., Woods P. and Yau L., 2008. EC Intercomparison of VOC measurements between National Reference Laboratories (AQUILA network). JRC Scientific and Technical Reports, European Communities.

2. Hakola H., Laurila T. and Hellén H., 2008. Trends in light hydrocarbon (C_2-C_6) concentration measurements in background air in Finland. In: The second Ny-Ålesund-Pallas Sodankylä Atmospheric Research Workshop, Ny Ålesund, Svalbard, Norway, 16-18 April, 2007, abstracts, 43-46. Brief report series 08, Norsk Polarinstitutt.

3. Hakola H., Laurila T., and Hellén H., 2008. VOC trends in northern Europe. In: Steinbrecher R. and Reimann S. (eds.) Abstracts of the meeting: 2008 GAW-VOC/CCQM-GAWG Workshop, Dübendorf, Switzerland, 7-9.7 2008

4. Hakola H., Vestenius M., Hellén H. and Paatero J., 2008. Polycyclic aromatic hydrocarbons in air and in precipitation in Kainuu border area. In: Várkonyi G., Heikkilä R. and Heikkilä J. (eds.). The impact of Kostomuksha mining plant on human environment on the Finnish-Russian border. EUREGIO Karelia Neighbourhood Programme. Final Report. Reports of Kainuu Regional Environment Centre 2, 14-19, 2008.

5. Kyllönen, K., Karlsson, V. and Ruoho-Airola, T. (2008) Trends of trace elements in wet deposition in Finland during 1998-2007. Extended abstract in Proceedings of 14th International Conference on Heavy Metals in the Environment 16.-23.11.2008, Taipei, Taiwan. Eds. Zueng-Sang Chen, Dar-Yuan Lee, Tser-Sheng Lin., Department of Agricultural Chemistry and National Taiwan University, ISBN 978-986-01-5851-9, p. 485–488

6. Lauri, A.E. Zapadinsky, A.I. Hienola, H. Vehkamäki,M. Kulmala: Monte Carlo simulations on heterogeneous nucleation II :line tension. In: Nucleation and Atmospheric Aerosols, Part I, Eds. C O'Dowd and P Wagner, ISBN 978-1-4020-6474-6, Springer Netherlands 2008, pp. 302-305

7. Lauri, A., E. Zapadinsky, J. Merikanto,H. Vehkamäki, M. Kulmala: Monte Carlo simulations on heterogeneous nucleation I: The point where the classical theory fails, In: Nucleation and Atmospheric Aerosols, Part I, Eds. C O'Dowd and P Wagner, ISBN 978-1-4020-6474-6, Springer Netherlands 2008, pp. 317-321

8. Laurila, T., Hatakka, J., Tuovinen, J.-P., , Aurela, M., Lohila, A., Karhu, K., Kopalainen, S., Ettala, M. & Samuelsson, J., 2008. Ämmässuon kaatopaikan metaanin ja hiilidioksidin mikrometeorologiset päästömittaukset tammikuu 2007 – huhtikuu 2008, raportti YTV Jätehuollolle. Ilmatieteen laitos, Helsinki, 57 pp.

9. Laurila, T., Hatakka, J., Tuovinen, J.-P., Aurela, M., Lohila, A. & Ettala, M., 2008. Mikrometeorologinen mittausmenetelmä kaatopaikkojen päästöjen mittaamisessa, liite päästöraporttiin Päijät-Hämeen Jätehuollolle. Ilmatieteen laitos, Helsinki, 32 pp.

10. Laurila, T., Aurela, M., Hatakka, J., Lohila, A., Tuovinen, J.-P., Ettala, M., Leiskallio, A. & Lilleberg, H., 2008. Mikrometeorologiset metaanin ja hiilidioksidin

päästömittaukset Päijät-Hämeen Jätehuolto Oy:n Pikijärven kaatopaikalla 2008. Ilmatieteen laitos, Helsinki, 15 pp.

11. Laurila, T., Aurela, M., Hatakka, J., Lohila, A., Tuovinen, J.-P., Ettala, M., Leiskallio, A. & Lilleberg, H., 2008. Mikrometeorologiset metaanin ja hiilidioksidin päästömittaukset Päijät-Hämeen Jätehuolto Oy:n Aikkalan kaatopaikalla 2008. Ilmatieteen laitos, Helsinki, 20 pp.

12. Nikinmaa, E., A. Riikonen, P. Peurasuo 2008. Viikki urban tree laboratory. COST action C15: Improving relations between technical infrastructure and vegetation. Final scientific report. COST office, 2008.

13. Paatero, Jussi , Ulla Makkonen, Hannele Hakola, Jukka Lehto, Gergely Varkonyi and Raimo Heikkilä, 2008. Metals and aerosol particles in the atmosphere in Kainuu province, Finland. In: Várkonyi G., Heikkilä R. and Heikkilä J. (eds.). The impact of Kostomuksha mining plant on human environment on the Finnish-Russian border. EUREGIO Karelia Neighbourhood Programme. Final Report. Reports of Kainuu Regional Environment Centre 2, 7-13, 2008.

14. Pumpanen J., Ilvesniemi H., Heinonsalo J. and Rasilo T. 2008. Effect of clear-cutting on soil carbon pool and CO_2 fluxes from forest soil. In Blum W.H. and Gerzabek M.H. (Eds.) EUROSOIL 2008 Book of Abstracts. University of Natural Resources and Applied Life Sciences, Vienna, Austria, August 2008-09-04. pp. 366

15. Pyy K., Paatero J. and Hakola H., 2008. Total gaseous mercury in the air in south-eastern Finland - First results. In: The second Ny-Ålesund-Pallas Sodankylä Atmospheric Research Workshop, Ny Ålesund, Svalbard, Norway, 16-18 April, 2007, abstracts, 47-50. Brief report series 08, Norsl Polarinstitutt.

16. Riikonen, A., E. Nikinmaa, and P. Peurasuo 2008. Shoot growth of street trees on structural soils in Helsinki. Proceedings of The European Congress of Arboriculture 2008.

17. Special issue on flux measurement in difficult conditions from the Boulder workshop 2006 (ed. John Finnigan), *Ecological Applications*, Volume 18, Issue 6 (September 2008).

18. iLEAPS Newsletter, special issue on Aerosols-Clouds-Precipitation-Climate, issue no 5, April 2008

Scientific textbook chapters

1. Hari, P. (2008) Introduction. In: Hari, P. & Kulmala, L. (eds.) Boreal forest and climate change. Advances in Global Change Research, Vol. 34, Springer Verlag. pp. 1–11.

2. Hari, P. (2008) Background. In: Hari, P. & Kulmala, L. (eds.) Boreal forest and climate change. Advances in Global Change Research, Vol. 34, Springer Verlag. pp. 13–14.

3. Hari, P., Mäkelä A. (2008) Dynamic modelling. In: Hari, P. & Kulmala, L. (eds.) Boreal forest and climate change. Advances in Global Change Research, Vol. 34, Springer Verlag. pp. 14–15.

4. Hari, P., Rita H. (2008) Statistical methods. In: Hari, P. & Kulmala, L. (eds.) Boreal forest and climate change. Advances in Global Change Research, Vol. 34, Springer Verlag. pp. 16–19.

5. Petäjä, T., Siivola, E., Pohja, T., Palva, L., Hari, P. (2008) On Field Measurements. In: Hari, P. & Kulmala, L. (eds.) Boreal forest and climate change. Advances in Global Change Research, Vol. 34, Springer Verlag. pp. 20–46.

6. Hari, P., Nikinmaa, E., Vesala, T., Pohja, T., Siivola, E., Lahti, T., Aalto, P., Hiltunen, V., Ilvesniemi, H., Keronen, P., Kolari, P., Grönholm, T., Palva, L., Pumpanen, J., Petäjä, T., Rannik, Ü., Kulmala, M. (2008) SMEAR network. In: Hari, P. & Kulmala, L. (eds.) Boreal forest and climate change. Advances in Global Change Research, Vol. 34, Springer Verlag. pp. 46–56.

7. Rannik, Ü., Vesala, T., Sogacheva, L., Hari, P. (2008) Annual cycle of environmental factors. In: Hari, P. & Kulmala, L. (eds.) Boreal forest and climate change. Advances in Global Change Research, Vol. 34, Springer Verlag. pp. 57–65.

8. Rannik, Ü. (2008) Temporal and spatial variation: atmosphere. In: Hari, P. & Kulmala, L. (eds.) Boreal forest and climate change. Advances in Global Change Research, Vol. 34, Springer Verlag. pp. 65–72.

9. Pumpanen, J. (2008) Temporal and spatial variation: soil. In: Hari, P. & Kulmala, L. (eds.) Boreal forest and climate change. Advances in Global Change Research, Vol. 34, Springer Verlag. pp. 72–74.

10.   Vesala, T., Rannik, Ü., Hari., P. (2008) Transport. In: Hari, P. & Kulmala, L. (eds.) Boreal forest and climate change. Advances in Global Change Research, Vol. 34, Springer Verlag. pp. 75–88.

11.   Hari, P., Bäck, J., Nikinmaa, E. (2008) Hierarchy of structure. In: Hari, P. & Kulmala, L. (eds.) Boreal forest and climate change. Advances in Global Change Research, Vol. 34, Springer Verlag. pp. 89–90.

12.   Bäck, J., Hari, P. (2008) Chemical structure. In: Hari, P. & Kulmala, L. (eds.) Boreal forest and climate change. Advances in Global Change Research, Vol. 34, Springer Verlag. pp. 90–102.

13.   Bäck, J. (2008) Cellular level. In: Hari, P. & Kulmala, L. (eds.) Boreal forest and climate change. Advances in Global Change Research, Vol. 34, Springer Verlag. pp. 103–106.

14.   Bäck, J., Nikinmaa, E. (2008) Tissue. In: Hari, P. & Kulmala, L. (eds.) Boreal forest and climate change. Advances in Global Change Research, Vol. 34, Springer Verlag. pp. 106–111.

15.   Bäck, J., Nikinmaa, E., Simojoki, A. (2008) Organs. In: Hari, P. & Kulmala, L. (eds.) Boreal forest and climate change. Advances in Global Change Research, Vol. 34, Springer Verlag. pp. 111–117.

16.   Nikinmaa, E., Bäck, J. (2008) Individual. In: Hari, P. & Kulmala, L. (eds.) Boreal forest and climate change. Advances in Global Change Research, Vol. 34, Springer Verlag. pp. 117–120.

17.   Nikinmaa, E., Hari, P., Kulmala., L. (2008) Stand. In: Hari, P. & Kulmala, L. (eds.) Boreal forest and climate change. Advances in Global Change Research, Vol. 34, Springer Verlag. pp. 121–123.

18.   Jögiste, K., Kulmala, L., Bäck, J., Hari, P. (2008) Boreal zone. In: Hari, P. & Kulmala, L. (eds.) Boreal forest and climate change. Advances in Global Change Research, Vol. 34, Springer Verlag. pp. 124–126.

19.   Hari P., Mäkelä A. (2008) Quantitative description of vegetation structure. In: Hari, P. & Kulmala, L. (eds.) Boreal forest and climate change. Advances in Global Change Research, Vol. 34, Springer Verlag. pp. 126–127.
20.   Rannik, Ü., Nilsson D., Hari P., Vesala, T. (2008) Structure of the atmosphere. In: Hari, P. & Kulmala, L. (eds.) Boreal forest and climate change. Advances in Global Change Research, Vol. 34, Springer Verlag. pp. 127–132.
21.   Simojoki, A., Garcia, H., Pihlatie, M., Pumpanen, J., Kurola, J., Salkinoja-Salonen, M., Hari P. (2008) Soil. In: Hari, P. & Kulmala, L. (eds.) Boreal forest and climate change. Advances in Global Change Research, Vol. 34, Springer Verlag. pp. 132–142.
22.   Hari, P., Mäkelä, A. (2008) Temporal and spatial scale of processes and fluxes. In: Hari, P. & Kulmala, L. (eds.) Boreal forest and climate change. Advances in Global Change Research, Vol. 34, Springer Verlag. pp. 143–144.
23.   Vesala, T., Kolari, P., Petäjä, T., Siivola, E., Hari, P. (2008) Temporal Phase transitions and energy exchange. In: Hari, P. & Kulmala, L. (eds.) Boreal forest and climate change. Advances in Global Change Research, Vol. 34, Springer Verlag. pp. 144–156.
24.   Boy, M., Bonn, B. (2008) Chemical reactions in the air. In: Hari, P. & Kulmala, L. (eds.) Boreal forest and climate change. Advances in Global Change Research, Vol. 34, Springer Verlag. pp. 156–167.
25.   Dal Maso, M., Riipinen I., Petäjä, T., Kulmala, M. (2008) Aerosol formation and growth. In: Hari, P. & Kulmala, L. (eds.) Boreal forest and climate change. Advances in Global Change Research, Vol. 34, Springer Verlag. pp. 167–171.
26.   Simojoki, M. (2008) Ion exchange and retention. In: Hari, P. & Kulmala, L. (eds.) Boreal forest and climate change. Advances in Global Change Research, Vol. 34, Springer Verlag. pp. 171–172.
27.   Hari, P., Bäck, J. (2008) General. In: Hari, P. & Kulmala, L. (eds.) Boreal forest and climate change. Advances in Global Change Research, Vol. 34, Springer Verlag. pp. 172–176.
28.   Bäck, J., Kolari, P., Hari, P. (2008) Respiration. In: Hari, P. & Kulmala, L. (eds.) Boreal forest and climate change. Advances in Global Change Research, Vol. 34, Springer Verlag. pp. 176–180.
29.   Kolari, P., Bäck, J., Perämäki, M., Hari, P. (2008) Transpiration. In: Hari, P. & Kulmala, L. (eds.) Boreal forest and climate change. Advances in Global Change Research, Vol. 34, Springer Verlag. pp. 180–183.
30.   Hari, P., Kolari, P., Bäck, J., Mäkelä, A., Nikinmaa, E. (2008) Photosynthesis. In: Hari, P. & Kulmala, L. (eds.) Boreal forest and climate change. Advances in Global Change Research, Vol. 34, Springer Verlag. pp. 183–195.
31.   Bäck, J., Nikinmaa, E., Simojoki, A. (2008) Carbon and nitrogen metabolism and senescence. In: Hari, P. & Kulmala, L. (eds.) Boreal forest and climate change. Advances in Global Change Research, Vol. 34, Springer Verlag. pp. 195–199.
32.   Bäck, J., Hari, P. (2008) BVOC emission. In: Hari, P. & Kulmala, L. (eds.) Boreal forest and climate change. Advances in Global Change Research, Vol. 34, Springer Verlag. pp. 199–205.

33. Altimir, N., Hari, P. (2008) Ozone deposition. In: Hari, P. & Kulmala, L. (eds.) Boreal forest and climate change. Advances in Global Change Research, Vol. 34, Springer Verlag. pp. 206–210.

34. Raivonen, M., Hari, P. (2008) NO_x exchange of needles. In: Hari, P. & Kulmala, L. (eds.) Boreal forest and climate change. Advances in Global Change Research, Vol. 34, Springer Verlag. pp. 210–214.

35. Simojoki, A. (2008) Uptake of water and nutrients by roots. In: Hari, P. & Kulmala, L. (eds.) Boreal forest and climate change. Advances in Global Change Research, Vol. 34, Springer Verlag. pp. 214–221.

36. Hänninen, H., Hari, P., Häkkinen, R., Linkosalo, T. (2008) Annual cycle of processes. In: Hari, P. & Kulmala, L. (eds.) Boreal forest and climate change. Advances in Global Change Research, Vol. 34, Springer Verlag. pp. 222–224.

37. Hänninen, H., Linkosalo, T., Häkkinen, R., Hari, P. (2008) Bud burst phenology. In: Hari, P. & Kulmala, L. (eds.) Boreal forest and climate change. Advances in Global Change Research, Vol. 34, Springer Verlag. pp. 225–228.

38. Kolari, P., Bäck, J., Hari, P. (2008) Seasonality of respiration. In: Hari, P. & Kulmala, L. (eds.) Boreal forest and climate change. Advances in Global Change Research, Vol. 34, Springer Verlag. pp. 228–231.

39. Hari, P., Kolari, P., Bäck, J., Mäkelä, A., Nikinmaa, E. (2008) Photosynthesis. In: Hari, P. & Kulmala, L. (eds.) Boreal forest and climate change. Advances in Global Change Research, Vol. 34, Springer Verlag. pp. 231–242.

40. Hari, P., Väänänen, P., Nikinmaa, E. (2008) Shoot elongation. In: Hari, P. & Kulmala, L. (eds.) Boreal forest and climate change. Advances in Global Change Research, Vol. 34, Springer Verlag. pp. 242–247.

41. Porcar-Castell, A., Bäck, J., Juurola, J., Hari, P. (2008) Short-term acclimation of photosynthetic light reactions to light. In: Hari, P. & Kulmala, L. (eds.) Boreal forest and climate change. Advances in Global Change Research, Vol. 34, Springer Verlag. pp. 248–255.

42. Kolari, P., Nikinmaa, E., Hari, P. (2008) Photosynthesis and drought. In: Hari, P. & Kulmala, L. (eds.) Boreal forest and climate change. Advances in Global Change Research, Vol. 34, Springer Verlag. pp. 256–262.

43. Juurola, E., Hari, P. (2008) Increasing CO_2 and photosynthesis. In: Hari, P. & Kulmala, L. (eds.) Boreal forest and climate change. Advances in Global Change Research, Vol. 34, Springer Verlag. pp. 262–267.

44. Bäck, J. (2008) VOC emissions under changing climate. In: Hari, P. & Kulmala, L. (eds.) Boreal forest and climate change. Advances in Global Change Research, Vol. 34, Springer Verlag. pp. 267–269.

45. Simojoki, A., Kurola, J., Pihlatie, M., Pumpanen, J., Kähkönen, M., Salkinoja-Salonen, M. (2008) Decomposition of soil organic matter. In: Hari, P. & Kulmala, L. (eds.) Boreal forest and climate change. Advances in Global Change Research, Vol. 34, Springer Verlag. pp. 269–271.

46. Pihlatie, M., Simojoki, A., Kurola, J., Pumpanen, J., Salkinoja-Salonen, M. (2008) Nitrogen processes in soil. In: Hari, P. & Kulmala, L. (eds.) Boreal forest and climate change. Advances in Global Change Research, Vol. 34, Springer Verlag. pp. 271–277.

47.   Pihlatie, M., Kurola, J., Simojoki, A., Pumpanen, J., Salkinoja-Salonen, M. (2008) Methane processes in soil. In: Hari, P. & Kulmala, L. (eds.) Boreal forest and climate change. Advances in Global Change Research, Vol. 34, Springer Verlag. pp. 277–280.

48.   Hari, P., Mäkelä, A. (2008) Mathematical tools. In: Hari, P. & Kulmala, L. (eds.) Boreal forest and climate change. Advances in Global Change Research, Vol. 34, Springer Verlag. pp. 281–284.

49.   Vesala, T., Hari, P., Räisänen, J. (2008) Atmospheric Processes and Transport. In: Hari, P. & Kulmala, L. (eds.) Boreal forest and climate change. Advances in Global Change Research, Vol. 34, Springer Verlag. pp. 284–297.

50.   Rannik, Ü., Kolari, P., Launiainen, S. (2008) Environmental factors in the canopy. In: Hari, P. & Kulmala, L. (eds.) Boreal forest and climate change. Advances in Global Change Research, Vol. 34, Springer Verlag. pp. 298–306.

51.   Simojoki, A., Garcia, H., Pihlatie, M., Pumpanen, J., Kurola, J., Salkinoja-Salonen, M. (2008) Environmental factors in soil. In: Hari, P. & Kulmala, L. (eds.) Boreal forest and climate change. Advances in Global Change Research, Vol. 34, Springer Verlag. pp. 306–313.

52.   Kolari, P., Hari, P. (2008) Photosynthetic production of a tree. In: Hari, P. & Kulmala, L. (eds.) Boreal forest and climate change. Advances in Global Change Research, Vol. 34, Springer Verlag. pp. 313–325.

53.   Nikinmaa, E., Perämäki, M., Hölttä, T., Vesala, T. (2008) Long-distance transport of water and solutes in trees. In: Hari, P. & Kulmala, L. (eds.) Boreal forest and climate change. Advances in Global Change Research, Vol. 34, Springer Verlag. pp. 325–343.

54.   Pumpanen, J., Ilvesniemi, H., Hari., P. (2008) CO_2 in soil. In: Hari, P. & Kulmala, L. (eds.) Boreal forest and climate change. Advances in Global Change Research, Vol. 34, Springer Verlag. pp. 343–351.

55.   Kolari, P., Pulkkinen, M., Kulmala, L., Pumpanen, J., Nikinmaa, E., Mäkelä, A., Vesala, T., Hari., P. (2008) Forest ecosystem CO_2 exchange. In: Hari, P. & Kulmala, L. (eds.) Boreal forest and climate change. Advances in Global Change Research, Vol. 34, Springer Verlag. pp. 351–382.

56.   Duursma, R., Kolari, P., Perämäki, M., Hari., P. (2008) Maximum transpiration rate and water tension during drought. In: Hari, P. & Kulmala, L. (eds.) Boreal forest and climate change. Advances in Global Change Research, Vol. 34, Springer Verlag. pp. 382–387.

57.   Pihlatie, M., Pumpanen, J., Simojoki, A., Hari., P. (2008) Fluxes and concentrations of N_2O in boreal forest soil. In: Hari, P. & Kulmala, L. (eds.) Boreal forest and climate change. Advances in Global Change Research, Vol. 34, Springer Verlag. pp. 387–393.

58.   Pihlatie, M., Simojoki, A., Pumpanen, J., Hari., P. (2008) Methane fluxes in boreal forest soil. In: Hari, P. & Kulmala, L. (eds.) Boreal forest and climate change. Advances in Global Change Research, Vol. 34, Springer Verlag. pp. 393–398.

59.   Bonn, B., Boy, M., Hellén, H. (2008) Reactive gases in the air. In: Hari, P. & Kulmala, L. (eds.) Boreal forest and climate change. Advances in Global Change Research, Vol. 34, Springer Verlag. pp. 398–409.

60.   Riipinen, I., Dal Maso, M., Petäjä, T., Laakso, L., Grönholm, T., Kulmala, M. (2008) Aerosol particles in the air. In: Hari, P. & Kulmala, L. (eds.) Boreal forest and climate change. Advances in Global Change Research, Vol. 34, Springer Verlag. pp. 409–415.

61.   Hari, P., Kolari, P., Nikinmaa, E., Pihlatie, M., Pumpanen, J., Kulmala, L., Simojoki, A., Vesala, T., Kulmala, M. (2008) Annual energy, carbon, nitrogen and water fluxes and amounts at SMEAR II. In: Hari, P. & Kulmala, L. (eds.) Boreal forest and climate change. Advances in Global Change Research, Vol. 34, Springer Verlag. pp. 416–423.

62.   Nikinmaa, E., Hari, P., Mäkelä, A. (2008) Connections between processes, transport and structure. In: Hari, P. & Kulmala, L. (eds.) Boreal forest and climate change. Advances in Global Change Research, Vol. 34, Springer Verlag. pp. 425–432.

63.   Hari, P., Salkinoja-Salonen, M., Liski, J., Simojoki, A., Kolari, P., Pumpanen, E., Kähkönen, M., Aakala, T., Havimo, M., Kivekäs, R., Nikinmaa, E. (2008) Growth and development of forest ecosystems; The MicroForest Model. In: Hari, P. & Kulmala, L. (eds.) Boreal forest and climate change. Advances in Global Change Research, Vol. 34, Springer Verlag. pp. 433–461.

64.   Kivekäs, R., Havimo, M., Hari, P. (2008) Need for rigorous testing. In: Hari, P. & Kulmala, L. (eds.) Boreal forest and climate change. Advances in Global Change Research, Vol. 34, Springer Verlag. pp. 461–462.

65.   Havimo, M., Kivekäs, R., Aalto, J., Schiestl, P., Hari, P. (2008) Test with six stands near SMEAR II. In: Hari, P. & Kulmala, L. (eds.) Boreal forest and climate change. Advances in Global Change Research, Vol. 34, Springer Verlag. pp. 461–467.

66.   Köster, K., Kangur, A., Hari, P., Jögiste, K. (2008) Test in Estonia at the southern border of the boreal zone. In: Hari, P. & Kulmala, L. (eds.) Boreal forest and climate change. Advances in Global Change Research, Vol. 34, Springer Verlag. pp. 468–472.

67.   Pohjonen, V., Mönkkönen, P., Hari, P. (2008) Test at northern timber line. In: Hari, P. & Kulmala, L. (eds.) Boreal forest and climate change. Advances in Global Change Research, Vol. 34, Springer Verlag. pp. 472–475.

68.   Hari, P., Havimo, M., Kivekäs, Nikinmaa, E. (2008) Evaluation of the performance of MicroForest. In: Hari, P. & Kulmala, L. (eds.) Boreal forest and climate change. Advances in Global Change Research, Vol. 34, Springer Verlag. pp. 476–478.

69.   Räisänen, J., Tuomenvirta, H. (2008) Climate change. In: Hari, P. & Kulmala, L. (eds.) Boreal forest and climate change. Advances in Global Change Research, Vol. 34, Springer Verlag. pp. 479–493.

70.   Hari, P. (2008) The approach. In: Hari, P. & Kulmala, L. (eds.) Boreal forest and climate change. Advances in Global Change Research, Vol. 34, Springer Verlag. pp. 493–494.

71.   Hari, P., Bäck, J., Nikinmaa, E. (2008) Process responses to climate change. In: Hari, P. & Kulmala, L. (eds.) Boreal forest and climate change. Advances in Global Change Research, Vol. 34, Springer Verlag. pp. 494–495.

72.   Hari, P., Nikinmaa, E. (2008) Ecosystem responses to climate change. In: Hari, P. & Kulmala, L. (eds.) Boreal forest and climate change. Advances in Global Change Research, Vol. 34, Springer Verlag. pp. 496–499.

73. Hari, P., Nikinmaa, E. (2008) Response of boreal forests to climate change. In: Hari, P. & Kulmala, L. (eds.) Boreal forest and climate change. Advances in Global Change Research, Vol. 34, Springer Verlag. pp. 499–503.

74. Hari, P., Nikinmaa, E. (2008) Carbon sequestration. In: Hari, P. & Kulmala, L. (eds.) Boreal forest and climate change. Advances in Global Change Research, Vol. 34, Springer Verlag. pp. 503–504.

75. Pihlatie, M., Pumpanen, J., Hari, P. (2008) N_2O emissions from boreal forests. In: Hari, P. & Kulmala, L. (eds.) Boreal forest and climate change. Advances in Global Change Research, Vol. 34, Springer Verlag. pp. 504–506.

76. Pihlatie, M. (2008) CH_4 fluxes in changing climate. In: Hari, P. & Kulmala, L. (eds.) Boreal forest and climate change. Advances in Global Change Research, Vol. 34, Springer Verlag. pp. 506–507.

77. Räisänen, J., Smolander, S. (2008) Climatic effects of increased leaf area: reduced surface albedo and increased transpiration. In: Hari, P. & Kulmala, L. (eds.) Boreal forest and climate change. Advances in Global Change Research, Vol. 34, Springer Verlag. pp. 508–516.

78. Bäck, J., Hari, P. (2008) BVOC emissions from boreal forests. In: Hari, P. & Kulmala, L. (eds.) Boreal forest and climate change. Advances in Global Change Research, Vol. 34, Springer Verlag. pp. 516–517.

79. Kulmala, M., Riipinen, I., Dal Maso, M., Petäjä, T. (2008) Climatic effects of increasing aerosols. In: Hari, P. & Kulmala, L. (eds.) Boreal forest and climate change. Advances in Global Change Research, Vol. 34, Springer Verlag. pp. 517–519.

80. Hari, P., Räisänen, J., Nikinmaa, E., Vesala, T. (2008) Evaluation of the connections between boreal forests and climate change. In: Hari, P. & Kulmala, L. (eds.) Boreal forest and climate change. Advances in Global Change Research, Vol. 34, Springer Verlag. pp. 519–528.

81. Hari, P., Nikinmaa, E., Kulmala, M. (2008) Concluding remarks. In: Hari, P. & Kulmala, L. (eds.) Boreal forest and climate change. Advances in Global Change Research, Vol. 34, Springer Verlag. pp. 529–532.

82. Hyötyläinen T. and Kallio, M. "Air and aerosols" in Comprehensive two dimensional gas chromatography, edited by L. Ramos, Comprehensive Analytical Chemistry series, Elsevier, 2008

Published proceedings

1. Report Series in Aerosol Science vol 92. Proceedings of the Nordic Centers of Excellence BACCI (Biosphere-Atmosphere-Cloud-Climate Interactions) and CBACCI (Carbon-BACCI) Activities in 2003-2007, Editors: Markku Kulmala, Jaana Bäck and Martta Salonen

2. Report Series in Aerosol Science vol 93. Proceedings of the Nordic Center of Excellence BACCI (Biosphere-Atmosphere-Cloud-Climate Interactions) and the Finnish Center of Excellence 'Research Unit on Physics, Chemistry and Biology of Atmospheric Composition and Climate Change' Activities in 2002-2007, Editors: Markku Kulmala, Jaana Bäck and Martta Salonen

3. Report Series in Aerosol Science vol 94. Proceedings of the Finnish Center of Excellence 'Research Unit on Physics, Chemistry and Biology of Atmospheric

Composition and Climate Change' Activities in 2002-2007, Editors: Markku Kulmala, Jaana Bäck and Martta Salonen

4. Report Series in Aerosol Science vol 97. Proceedings of the Finnish Graduate School "Physics, Chemistry, Biology and Meteorology of Atmospheric Composition and Climate Change" workshop 22.-23.4.2008, Editors: Markku Kulmala and Antti Lauri

5. Report Series in Aerosol Science vol 99. Proceedings of 2008 EUCAARI Annual Meeting Helsinki 17.-21.11.2008, , Editors Hanna K. Lappalainen, Ari Asmi, Tuomo Nieminen, and Markku Kulmala

CONFERENCE PRESENTATIONS

Invited lectures

Hussein, Tareq:
-- Urban Aerosol Particles: Characteristics of the Particle Number Size Distribution in Helsinki. New opportunities for Finnish – Japanese cooperation in Urban land-atmosphere and air quality research, 24-26 November 2008, Helsinki, Finland

Hyvärinen Antti-Pekka:
--Ilmatieteen laitoksen aerosolimittaukset kenttäasemilla, Particle Measurement from Science to Industry, 29th April, Helsinki

Hämeri Kaarle:
-- Facing the key workplace challenge: assessing and preventing exposure to nanoparticles", 11th International Inhalation Symposium INIS, 11.-15.6.2008, Hannover, Germany

Junninen Heikki:
--Aerosol chemistry in boreal forest station, SMEAR I. New opportunities for Finnish – Japanese cooperation in Urban land-atmosphere and air quality research, 24-26 November 2008, Helsinki, Finland

Korhonen Hannele:
--How well do we understand the processes that determine atmospheric CCN concentrations? NOSA aerosol Symposium 2008, Oslo, 6.-7.11.2008

Kulmala Markku:
--"Aerosolit ja ilmastonmuutos", Geotieteellinen symposiumi "Maan ytimestä avaruuteen" Suomalaisen Tiedeakatemian 100-vuotisjuhlavuoden seminaarii, 10.-11.1.2008, Helsinki, Finland

-- "Aerosol-cloud-precipitation-climate: The interlinked formation processes", 4th IGBP Congress, 1.-9.5.2008, Cape Town International Convention Centre, Cape Town, South Africa

-- "Introduction to land – atmosphere interactions", Helsinki University Environmental Research Centre HERC seminar, 24.4.2008, Univ. Helsinki, Viikki Info Center, Helsinki, Finland

-- "Generation of nanoparticles from vapors in case of exhaust filtration", Environmental and Medical Aerosol Nanoparticles and their Interaction with the Respiratory System, 29.-30.5.2008, Jablonna, Poland

-- "EUCAARI project status overview", EUCAARI 2008, 17.-21.11.2008, Finnish Meteorological Institute, Helsinki. Finland

-- "Concluding remarks", EUCAARI 2008, 17.-21.11.2008, Finnish Meteorological Institute, Helsinki. Finland
-- "Invited talk", New opportunities for Finnish-Japanese cooperation in urban land-atmosphere and air quality research, 24.-25.11.2008, Kumpula, Helsinki, Finland
-- "The role of atmospheric aerosols in climate change", Congregation, Early December 2008, Univ. Tartu, Estonia

Kurten Theo:
--Using Quantum Chemistry to Study Atmospheric Nucleation Mechanisms. 9th informal conference on atmospheric chemistry and molecular science. 6.6-8.6.2008, Helsingör, Denmark
--Recent quantum chemical calculations on sulfuric acid - water nucleation: the role of ammonia, amines, ions and SO2 oxidation intermediates", 9.4.2008, J. W. Goethe Universitet, Frankfurt, Germany
--Recent quantum chemical calculations on sulfuric acid - water nucleation: the role of ammonia, amines, ions and SO2 oxidation intermediate", 9.5.2008, Instituto de tecnologia química e biológica, Universidade nova de Lisboa, Portugal
--Using molecular simulations to study tropospheric nucleation mechanisms involving sulfuric acid, 4.6.2008, Université Blaise-Pascal, France
--Selecting appropriate methods for computational studies on clusters relevant to atmospheric nucleation (and some typical problems), 13.11.2008, University of Copenhagen, Denmark
--Recent quantum chemical studies of atmospheric nucleation processes, 14.11.2008, University of Copenhagen, Denmark

Laakso Lauri:
--L Laakso et al.: Atmospheric measurements", October 2008, North-West University, South Africa

Lauri, Antti:
--What activities have been done and what could have been done given more time or funding? What activities have been priorized and why? Exit strategy and length of programme – BACCI (Biosphere-aerosol-cloud-climate interactions), NORFA Symposium on NCoE Experiences, Oslo, Norway, 12.-13.3.2008
--Atmospheric new particle formation, Collaboration meeting between the Russian State Hydrometeorological University and the University of Helsinki, St. Petersburg, Russia, 6.5.2008
--Cloud formation and aerosol dynamic processes, NetFAM School and Workshop on Integrated Modelling of Meteorological and Chemical Transport Processes / Impact of Chemical Weather on Numerical Weather Prediction and Climate Modelling, Zelenogorsk, Russia, 7.-11.7.2008
--Atmosphere-Biosphere Studies - Nordic Master's Degree Programme in Atmospheric Sciences and Biogeochemical Cycles, Nordic-Russian University Network for Successful Cooperation in Higher Environmental Education, Stockholm, Sweden, 10.-12.12.2008

Lohila, A:
--Turvemaat kasvihuonekaasujen lähteinä ja nieluina – mitä mikrometeorologiset vuomittaukset kertovat?" Suomen IPCC-ryhmän seminaari "Turpeen ilmastovaikutusten arviointi", 31.10.2008, Ilmatieteen laitos, Helsinki

Nikinmaa, Eero:

-- Land use changes in Finland: impacts of forest management changes to carbon balance, Helsinki University Environment Research Centre Seminar on Climate Change 24.4.2008, Viikki, University of Helsinki

-- SMEARII: Station for measuring ecosystem atmosphere interactions, ANAEE (ANalysis and Experimentation on Ecosystems) workshop: Scientific stakes in continental biosphere sciences. Which research infrastructures do we need to face them? Paris 2-4.9.2008

Pumpanen Jukka:

--Measuring soil respiration in the field – different chamber designs, Workshop on Comparison of static chambers to measure N_2O, CH_4 and CO_2 fluxes from soils, 15 - 17 December 2008, University of Copenhagen, Denmark

Riipinen Ilona:

-- Riipinen, I., Manninen, H.E., Nieminen, T., Sipilä, M., Petäjä, T., Ehn, M., Junninen, H., Sihto, S.-L., Yli-Juuti, T., Dal Maso, M., Lehtinen, K.E.J., Laaksonen, A., Kerminen, V.-M and Kulmala, M.: Observations on the first steps of atmospheric particle formation and growth in boreal forest. Seminar series of the School of Earth and Environment, Leeds University, 23.4.2008.

--Observations on the first steps of atmospheric particle formation and growth in boreal forest. Carnegie Mellon University, Pittsburgh, USA, 18.8.2008

--Observations on the first steps of atmospheric particle formation and growth in boreal forest, Aerodyne Research, Ltd., Billerica, USA,21.8.2008

--Biogenic aerosol formation. 10th anniversary EUROFLUX workshop, Hyytiälä, Finland, 10.12.2008

-- Primary versus secondary, natural versus anthropogenic particle number concentration", EUCAARI 2008, II Work Package Session Global/Regional Scale - Particle Number, 17.-21.11.2008, Finnish Meteorological Institute, Finland

Rinne Janne:

--Biogenic VOCs in North European boreal coniferous forest site, IMPECVOC project meeting, 6.-8.7.2008, Ghent, Belgium

Sevanto Sanna:

--Invited participant and speaker in Vegetation Network workshop on Leaf Temperature. Apr 19-24 Sydney, Australia 2008.

--"Carbon balance in boreal ecosystems" Seminar series of terrestrial ecosystem studies at Max-Plank-Institute, Hamburg, Sept, 8th

--"Data-driven approach to modeling total ecosystem respiration" EUROFLUX 10th anniversary workshop, Hyytiälä, Finland Dec 10, 2008.

-- "Soil carbon dynamics in global climate models -a comparison of two approaches" Climate Change workshop in Helsinki, Nov 12th, 2008

Tuovinen, J.-P.:

--Ozone flux modelling for risk assessment: status and future needs, Cost Strategic Workshop "Forest ecosystems in a changing environment: identifying future monitoring and research needs", 11–13 March, Istanbul, Turkey

Vehkamäki Hanna:
--Sulphuric acid containg clusters in the atmosphere' at a workshop on Nucleation of inorganic atmospheric clusters and particles. Gothenburg University, Sweden 13.-15.8.2008.
--Molecular modelling of atmospheric particle formation, Nanopartiklar i aktiva miljöer, 12.-15.8.2008, Gothenburg University, Sweden
--Sulphuric acid containg clusters in the atmosphere", Nucleation of inorganic atmospheric clusters and particles, 13.-15.8.2008, Gothenburg University, Sweden

Vesala Timo:
--Micrometeorology and environmental physics: From Karman vortex streets to phloem mass transport, Colloquium, 16.5.2008, Univ. Jyväskylä, Dept. of Physics, Finland
--Kasvihuonekaasut ja biosfäärivuorovaikutukset, Sodankylän observatorion 100-vuotisjuhlaseminaari, 7.10.2008, Finland
--Ympäristön ja ilmastonmuutoksen reunaehdot Suomen talouden ja työllisyyden kehitykselle, OP-Pohjola -ryhmän palkansaajafoorumi, Kuusankoski, 23.10.2008
--How to translate physics to forest ecologists?, Book release seminar due to the publication of "Boreal Forest and Climate Change", Infokeskus Korona, Viikki, 21.10.2008, Finland

Oral and Poster Presentations

Ion workshop, Hyytiälä, Finland, 17.-19.3.2008.

--Asmi Eija: Calibration of Air Ion Spectrometers (AIS) for the EUCAARI Intensive --operation period (IOP) – preliminary results. Oral Presentation
--Kurtén T.: Quantum chemical studies on charged sulfuric – acid containing clusters possibly relevant to ion-induced nucleation in the atmosphere
--Laakso L., et al.: Particle, gas and ion measurements in Marikana mining

Finnish Graduate School 'Physics, Chemistry, Biology and Meteorology of Atmospheric Composition and Climate Change' workshop, 22–23 Apr. 2008, Helsinki, Finland

--Asmi Eija. Analysis of particle formation events in Hohenpeissenberg, Poster
--Keronen, P., Siivola, E., Pohja, T., Aalto, T., Hatakka, J. & Vesala, T.: Virtual tall tower measurement of background CO_2 concentration in Southern Finland. Poster
--Kulmala Liisa: CO_2 exchange of ground vegetation, poster
--Laitinen, T., K. Hartonen, M.-L. Riekkola and M. Kulmala, Aerosol mass spectrometer for the analysis of ultrafine aerosols. poster
--Lallo, M., Aalto, T., Hatakka, J. & Laurila, T.: Hydrogen mixing ratio measurements in Finland. Poster
--Parshintsev, J., Räsänen, R., Hartonen, K., Kulmala, M., Riekkola, M.-L. Utilization of particle-into-liquid sampler (PILS) in the analysis of organic compounds in ambient aerosols. oral
--Pyy, K., Karlsson, V. and Ruoho-Airola, T. Wet Deposition of Trace Elements in Finland during 1998-2007.
--Thum, T., Aalto, T., Laurila, T., Aurela, M., Hatakka, J., Vesala, T. & Lindroth, A.: Seasonality of carbon cycle in northern boreal forests.

European Geosciences Union General Assembly 2008, Vienna, Austria, 13 – 18 April.

--Aurela, M., Laurila, T., Lohila, A., Hatakka, J., Tuovinen, J.-P., Riutta, T., Penttilä, T. & Viisanen, Y.: Carbon dioxide and methane exchange on a northern boreal aapa mire.

-- B Bonn, M Kulmala, D Spracklen, I Riipinen, S-L Sihto, K Carslaw, M Boy and TM Ruuskanen: Nucleation in a boreal ecosystem: The link to terpenes and sulphuric acid. poster

-- Bonn, B. , Ü. Rannik, H. Hakola, J. Bäck, E. Nikinmaa, Ü. Niinemets, S. M. Noe, T. Vesala, P. Hari and M. Kulmala, Sesquiterpenes at a Boreal Forest Site: Emission and ambient Concentration.

-- Chung, Chul: Land precipitation, temperature and aerosols, oral

--Coyle, M., Altimir, N., Gruenhage, L., Gerosa, G., Tuovinen, J.-P., Loubet, B., Ammann, C., Cieslik, S. Paoletti, E., Fowler, D., Mikkelsen, T., Ro-Poulsen, H. & Cellier, P.: Non-stomatal ozone deposition to vegetation: new insights and models.

-- Dommen, J., H. Hellen, M. Saurer, R. Siegwolf, M. Jaeggi, A. Metzger, J. Duplissy, M. Fierz, U. Baltensperger. Determination of isoprene aerosol yields in an organic seed by carbon isotope analysis.

--Ekberg A., Arneth A., Bäckstrand K., Crill P.M., Hakola H., Holst T., Stark H., BVOC emission from high-latitude peatlands: Isoprene and monoterpene fluxes in plant communities defined by differences in surface hydrology.

--Haapanala S., Hakola H., Vestenius M. and Rinne J., VOC Emissions from Tree Stumps. poster

-- Järvi, I Mammarella, S Launiainen, J Rinne, E Siivola, A Sogachev, A Riikonen, E Nikinmaa and T Vesala: The surface flux measurements of volatile organic compound emissions from a boreal forest, oral

-- Korhola, A., M Kulmala, T Vesala and M Nyman: Science Workshop on past, present and future climate change, poster

--Ortega, I.K.T Suni, H Vehkamäki and M Kulmala: The role of Eucalyptol in new particle formation. oral

--Korhola, A., M Kulmala, T Vesala and M Nyman: Science Workshop on past, present and future climate change, poster

--Lallo, M., Aalto, T., Hatakka, J. & Laurila, T.: Hydrogen mixing ratio measurements in Finland.

--Makkonen R., S Romakkaniemi, P Stier, J Feichter, S Rast, M Kulmala and A Laaksonen: Global evaluation of nitric acid effect on cloud droplet number concentrations, Poster

--Ortega, I.K., T Suni, H Vehkamäki and M Kulmala: The role of Eucalyptol in new particle formation, oral

--Ruuskanen T.M., R Taipale, J Rinne, MK Kajos, H Hakola and M Kulmala: Seasonal to daily patterns of VOC concentrations in boreal forest, over a year of continuous measurements, oral

--Taipale, R., J Rinne, TM Ruuskanen, MK Kajos, H Hakola, T Vesala and M Kulmala: Direct ecosystem scale measurements of volatile organic compound emissions from a boreal forest, poster

--Thum, T., Aalto, T., Laurila, T., Aurela, M., Lindroth, A. & Vesala, T.: Assessing seasonality with air temperature, CO_2 eddy covariance measurements and CO_2 mixing ratio in northern boreal coniferous forests. poster
--Tuovinen, J.-P., Simpson, D. & Altimir, N.: Modelling the stomatal and non-stomatal ozone fluxes to coniferous forests in Northern Europe.
-- Zardini A.A., IK Koponen, I Riipinen, M Kulmala and M Bilde: Evaporation of organic and inorganic/organic particles, poster

The NECC-BACCI conference: Greenhouse gases and aerosols: Interactions between northern ecosystems and climate, 16-18.6 2008. Reykjavik, Iceland.

-- Boy et al.: Field study on new particle formation at the Front Range of the Colorado Rocky Mountains, oral
-- Bäck, J., Rinne, J. & Hakola, H.: 'Volatile organic compound emissions from North European boreal landscape: progress and key gaps' Oral
--Haapanala, S., H Hakola, M Vestenius and J Rinne: VOC emission measurements from tree stumps, poster
--Kulmala L., Pumpanen J., Hari P. and Vesala T. Carbon balance of ground vegetation in early succession. Oral
--Kulmala M. and BACCI team: Biosphere-Aerosol-Cloud-Climate Interactions: atmospheric new particle formation, oral
--Lindroth A. et al with T Vesala: Strength of sources and sinks for atmospheric CO_2 in different ecosystems within the Nordic countries, oral
-- Lund, M., A Lindroth, MB Nilsson, M Aurela, J Rinne and N Roulet: Environmental controls on gross primary production and ecosystem respiration in wetlands: a synthesis based on FLUXNET data, poster
--Pihlatie, M., R Kiese, M Aurela, N Brüggemann, K Buttercah-Bah, A-J Kieloaho, T Laurila, A Lohila, I Mammarella, K Minkkinen, T Penttilä, J Schönborn, S Zechmeister-Boltenstern and T Vesala: Greenhouse gas fluxes in a drained peatland forest, oral
-- Ruuskanen, T., R Taipale, MK Kajos, J Rinne, H Hakola, H Hellén, A Reissell, P Kolari, J Bäck, P Hari and M Kulmala: Volatile organic compound measurements in boreal forest with Proton-Transfer-Reaction-Mass-Spetrometry, poster
--Sogachev A., E Dellwik, J Mann and T Vesala: Fetch requirements for CO_2 fluxes measured behind a forest edge: a modelling study, oral
--Thum, T., Aalto, T., Laurila, T., Aurela, M., Lindroth, A. & Vesala, T.; Modelling seasonality of the boreal forest CO_2 exchange. Oral
-- Vesala, T., S Launiainen, S Sevanto, P Kolari, J Pumpanen and P Hari: Warming of autumns and carbon exchange of a boreal pine forest, oral
-- Zardini, A.A., IK Koponen, I Riipinen, M Kulmala and M Bilde: Evaporation of organic and inorganic/organic particles, oral

European Aerosol Conference 24.-29.8.2008 Thessaloniki, Greece:

--Asmi Eija, , M Sipilä, S Gagne, HE Manninen, K Lehtipalo, K Neitola, J Vanhanen, A Mirme, S Mirme, E Tamm, M Attoui and M Kulmala: :Results of air ion spectrometer (AIS) calibration and intercomparison workshop. Oral

--Asmi Eija: Atmospheric aerosol and gas measurements at the Finnish Antarctic research station Aboa in summers 2006/2007 and 2007/2008. Oral

-- Attoui, M.,HE Manninen, M Sipilä, G Steiner and M Kulmala: Characterization of three commercialised 'equivalent' CPCs in the sub 10 nm range, poster

-- Attoui, M., M Sipilä, K Lehtipalo, K Neitola, G Steiner and M Kulmala: Generation of monodisperse and multicharged sub 10 nm PEGs particles, oral

-- Boy, M.: Field study on new particle formation at the front range of the Colorado Rocky Mountains. oral

-- Boy, M., S-L Sihto, B Bonn, A Guenther, J Kazil, ER Lovejoy and M Kulmala: New particle formation in rural areas - what are the relevant processes, oral

--Brus, D., AP Hyvärinen, H Lihavainen, Y Viisanen and M Kulmala: Binary homogeneous nucleation of sulfuric acid and water mixture. poster

-- Ehn, T Petäjä, P Aalto, G de Leeuw, C O'Dowd and M Kulmala: Growth rates during marine and coastal new particle formation, oral

-- Gagné, S., L Laakso, VM Kerminen, T Petäjä and M Kulmala: Ion-DMPS: Ion-induced nucleation contribution and cluster activation, poster

--Hamed, A., J. Joutsensaari, B. Wehner, W.Birmili, A.Wiedensohler, K. E.J. Lehtinen and A. Laaksonen: Sulphur Dioxide Emission Reduction Leads to Decreased SOA Particle Formation, oral

-- Hienola, H Vehkamäki and M Kulmala: Binary heterogeneous nucleation of two dicarboxylic acids and water: Can it happen in atmosphere? poster

-- Hussein, J Martikainen, H Junninen, L Sogacheva, R Wagner, M Dal Maso, I Riipinen, PP Aalto and M Kulmala: Observation of regional new particle formation in the urban atmosphere, poster

--Hyvärinen Antti-Pekka: Continuous measurements of optical properties of atmospheric aerosols in Mukteshwar, Northern India, poster

--Hämeri K.: Facing the key workplace challenge: Assessing and preventing exposure to nanoparticles at source, oral

--Julin, J., I Napari, J Merikanto and H Vehkamäki: Molecular dynamics and Monte Carlo studies of equilibrium cluster porperties, poster

--JunninenH. et al.: Physically constrained receptor modelling of PM10 from winter time in Krakow, oral

-- Junninen, H., M Hulkkonen, I Riipinen, T Nieminen, A Hirsikko, T Suni, M Boy, SH Lee, M Vana, H Tammet, VM Kerminen and M Kulmala: Nocturnal formation of atmospheric clusters, oral

-- Junninen, S Rantanen, K Rosman, HC Hansson, VM Kerminen and M Kulmala: Long term measurements of low levels of ammonia in rural environment, oral

--Järvi, L., H Hannuniemi, T Hussein, H Junninen, PP Aalto, R Hillamo, T Mäkelä, P Keronen, E Siivola, T Vesala and M Kulmala: Continuous air pollution and surface-atmosphere interaction measurements at the SMEAR III station in Helsinki, Finland. Oral

--Kivekäs Niku: DMPS measurements at Mount Waliguan, inland China, poster

--Korhonen, H., K. S. Carslaw, D. V. Spracklen, G. W. Mann, M. T. Woodhouse and K. E . J. Lehtinen: Primary and secondary oceanic sources of CCN over the Southern Ocean: a global model study, Oral

-- Kulmala M., A Asmi, HK Lappalainen and the whole EUCAARI team: EUCAARI Integrated Project - Aerosol, cloud, climate and air-quality interactions - Progress overview 2007 – 2008, poster

--Kurtén, T., V. Loukonen, H. Vehkamäki and M. Kulmala: Amines enhance neutral and ion-induced sulfuric acid nucleation more than ammonia. Poster

-- Laakso,L., H Laakso, M Kulmala, N Kgabi, M Molefe, D Mabaso, K Pienaar and M Jokinen: New particle formation in a clean and polluted Southern African savannah, poster

-- Lauros, J., T Nieminen, I Riipinen and M Kulmala: The role of atmospheric boundary layer growth in new particle formation, poster

-- Lehtipalo, K., M Sipilä, E Asmi, I Riipinen and M Kulmala: Indoor air concentrations of neutral and charged clusters, poster

-- Leppä, J., V.-M. Kerminen, L. Laakso, H. Korhonen, K.E.J. Lehtinen, H. Junninen and M. Kulmala: A model study on growth rates of neutral and charged particles : A model study on growth rates of neutral and charged particles, poster

--Leskinen, A., H. Portin, M. Komppula, H. Lihavainen, P. Miettinen, Y. Viisanen, A. Laaksonen and K.E.J. Lehtinen: Two years of measurements at the Puijo semi-urban aerosol-cloud interaction station. Poster

-- Lähde,T., T Rönkkö, A Virtanen, T Schuck, L Pirjola, K Hämeri, M Kulmala, F Arnold, D Rothe and J Keskinen: Heavy duty diesel engine exhaust ion measurements down to cluster size scale, Oral

--Maenhaut W., X Chi, P Aalto and M Kulmala: Mass size distribution of organic carbon and the particulate mass during a 2007 summer field campaign at SMEAR II in Finland, presentation

- Makkonen R., S Romakkaniemi, P Stier, J Feichter, S Rast, M Kulmala and A Laaksonen: Global evaluation of nitric acid effect on cloud droplet number concentrations , poster

-- Manninen, V Hiltunen, H Laakso, H Ranta and M Kulmala: Annual cycle of airborne pollen, fungal spores and particle mass in boreal forest, oral

--Merikanto, J., A Lauri, H Vehkamäki, I Napari and E Zapadinsky: The virial equation of state as a tool for calculating the formation energy of small molecular clusters, poster

--Mikkonen, S., K. E. J. Lehtinen, A. Hamed, J. Joutsensaari and A. Laaksonen: Predicting aerosol particle concentrations with mixed effects regression model, Oral

-- Modini, R.L., ZD Ristovski, GR Johnson, C He, L Morawska and T Suni: Physicochemical characterisation of nucleation mode particles observed at a remote coastal site (Agnes Water) on the east coast of Australia, poster

-- Neitola, D Brus, M Sipilä and M Kulmala: Binary homogeneus nucleation of sulfuric acid-water: Particle size distribution and effect of detector on total count and determination of critical cluster size, oral

-- Nieminen, T., HE Manninen, I Riipinen, T Yli-Juuti and M Kulmala: Analysis of nucleation events during spring 2006 and 2007 in Hyytiälä, Finland, poster

-- Ortega, I.K., T Kurtén, A Määttänen, H Vehkamäki and M Kulmala: CO_2 and water clusters in Mars, poster

-- Parts, T.E., A Luts, E Tamm, M Vana, A Hirsikko and M Kulmala: On the role of iodine in the new charged water clusters formation, poster

-- Petäjä, T., RL Mauldin III, E Kosciuh, J McGrath, poster, T Nieminen, M Boy, A Adamov, T Kotiaho and M Kulmala: Sulfuric acid and OH concentrations at a boreal forest site

--Prisle, N.L., T. Raatikainen, R. Sorjamaa, B. Svenningsson, A. Laaksonen and M. Bilde: Surfactant partitioning in cloud droplet activation. Oral

-- Raatikainen Tomi: Estimating critical droplet size using experimental critical saturation ratios, oral

-- Riipinen, I., M Kulmala, HE Manninen, T Yli-Juuti, M Boy, M Sipilä, M Ehn, H Junninen and T Petäjä: On the water-solubility of freshly-formed 2-9 nm particles in boreal forest, oral

--Saarnio, S Saarikoski, M Aurela, K Teinilä, T Mäkelä, PP Aalto, M Kulmala and R Hillamo: On-line aerosol measurements during the short-term biomass smoke plumes, oral

--Salonen, M., T. Kurten, H. Vehkamäki and M. Kulmala: Quantum chemical calculations on nucleation of sulfur containing molecules. oral

--Sihto, S-L., I Riipinen, P Paasonen, H Vuollekoski, T Nieminen et al. with M Kulmala: Connection of sulfuric acid and new particle formation: Analysis of field data from Finnish and German stations, oral

--Sipilä, M., M. Attoui, K. Lehtipalo, K. Neitola, G. Steiner, and M. Kulmala: Effect of charge (up to +8e) on activation probabilities of sub-10 nm aerosol particles, oral

-- Steiner, G.W., M Attoui, GP Reischl, D Wimmer, M Sipilä and M Kulmala: High resolution mobility measurement of ionic molecular clusters, oral

-- Steiner, G.W., M Attoui, M Sipilä, GP Reischl, D Wimmer and M Kulmala: Performance evaluation of the Grimm 7.860 WOx generator, poster

--Tiitta, P., Pasi Miettinen, Petri Vaattovaara, Jorma Joutsensaari, Ari Laaksonen, Pasi Aalto and Markku Kulmala: Roadside aerosol characteristics measured with TDMAs, Oral

-- Tunved, HC Hansson and M Kulmala: The mixed natural-anthropogenic aerosol of northern Europe - Changing emissions and their possible relation to climate change, oral

--Uhrner, U., H. Vehkamäki, M. Zallinger, F. Stratmann, S. von Löwis, B. Wehner and A. Wiedensohler: Nucleation and growth simulations within a diluting Diesel car exhaust plume. Poster

--Vaattovaara, P., T. Petäjä, J. Joutsensaari, P. Miettinen, D.R. Worsnop and A. Laaksonen. The composition of nucleation mode sized particles during nucleation events at a boreal forest environment, Poster

--Vana, M., M Ehn, T Petäjä, H Vuollekoski, P Aalto, G de Leeuw, M Kulmala, D Ceburnis, T Neary and CD O'Dowd: The role of air ions in coastal new particle formation, poster

--Vehkamäki, H, J. Merikanto, A. Lauri and E. Zapadinsky: Correction to the classical description of the smallest clusters, oral

--Virkkula A., A. Frey, M. Aurela, H. Timonen, K. Teinila, R. Hillamo, E. Asmi, P.P. Aalto, M. Kulmala, S. Kirkwood, Atmospheric aerosol and gas measurements at the Finnish Antarctic research station Aboa in summers 2006/2007 and 2007/2008 , Oral

-- Vrtala, A., PM Winkler, H Vehkamäki, M Kulmala and PE Wagner: A physically consistent heterogeneous nucleation probability (PCHNP) function for determination of critical cluster size using the heterogeneous nucleation theorem, poster

-- Vuollekoski, H., V.-M. Kerminen, T. Anttila, S.-L. Sihto, I. Riipinen, H. Korhonen, G. McFiggans, C. D. O'Dowd and M. Kulmala: Simulating iodine dioxide nucleation in coastal and remote marine environments, poster
--Winkler, P.M., A. Vrtala, H. Vehkamäki, M. Kulmala and P.E. Wagner: Seed diameter and cluster size in heterogeneous nucleation processes, oral presentation
--Wimmer, D., M Attoui, GW Steiner, M Sipilä and GP Reischl: Performance of different Faraday cup electrometers with high resolution electro mobility spectrometers, poster
-- Yli-Juuti, I Riipinen, PP Aalto, T Nieminen, W Maenhaut, I Salma and M Kulmala: Characteristics of aerosol particle formation events at K-Puszta, Hungary, Poster
--Yli-Pirilä, P., J. Heijari, J. Holopainen, J. Kroll, D. Worsnop, A. Laaksonen and J. Joutsensaari: Formation of secondary organic aerosols by ozonolysis of biogenic VOCs, Poster
-- Zardini, A.A., IK Koponen, I Riipinen, M Kulmala and M Bilde: Evaporation of organic and inorganic/organic particles, poster

NOSA Aerosol Symposium, 6-7.11, 2008 Oslo, Norway

--Chung, Chul: Land precipitation, temperature and aerosols, oral presentation
--Dal Maso, M. et al.: Temperature dependence of natural aerosol production: Insights from the Jülich plant chamber experiment, poster
--Hamed A., Jaatinen A., Joutsensaari J., Birmili W., Wehner B., Wiedensohler A., Facchini M.C., Decesari S., Mircea M., Junninen H., Kulmala M., Lehtinen K.E.J. and Laaksonen A. Nucleation events in Italy, Germany and Finland: A comparative study, poster
--Hussein T.: Aerosol dynamics in the continental boundary layer in Southern Sweden: A study of the aging of the urban plume from Malmö. Poster
-- Hussein, H Junninen, I Riipinen, M Dal Maso, PP Aalto, P Tunved, A Kristensson, E Swietlicki, H-C Hansson and M Kulmala: Time-span, spatial-scale, and features of identical new particle formation events, poster
-- Hämeri, K., J Koivisto and T Hussein: Facing the key workplace challenge: assessing and preventing exposure to nanoparticles, oral
--Kannosto, J., A Virtanen, M Lemmetty, JM Mäkelä, H Junninen, T Hussein, P Aalto, M Kulmala and J Keskinen: Online density measurements of aerosol particles in boreal forest, poster
--Kivekäs N., Kerminen V.-M., Anttila T., Korhonen H., Lihavainen H., Komppula M., Viisanen Y. and Kulmala M: Cloud droplet parameterization based on number-to-volume concentration ratio, poster
--Korhonen Hannele: How well do we understand the processes that determine atmospheric CCN concentrations?
--Kurtén T., Kuang C., Gomez P., McMurry P. and Vehkamäki H. The role of energy non-accommodation in sulfuric acid nucleation. Poster
--Laitinen, T., S. Herrero-Martin, J. Parshintsev, T. Hyötyläinen, K. Hartonen and M.-L. Riekkola. Collection and chemical characterization of nanometer size aerosol particles from wood pyrolysis. poster
-- Laitinen, T., K. Hartonen, M. Kulmala and M.-L. Riekkola. Aerosol mass spectrometer for ultrafine aerosol particles. poster

--Lauri A., Merikanto J., Vehkamäki H., Napari I. and Zapadinsky E. Formation energy in homogeneous nucleation applying the virial equation of state. Poster
--Mikkonen S., Lehtinen K.E.J., Hamed A., Joutsensaari J. and Laaksonen A. Finding factors affecting to the number concentration of atmospheric aerosols with advanced statistical methods, Poster
-- Paasonen, P., S-L Sihto, T Nieminen, H Vuollekoski, I Riipinen, C Plass-Dulmer, H Berresheim, W Birmili and M Kulmala: Contribution of sulphuric acid and volatile organic compounds to new particle formation in Hohenpeissenberg (Germany)" oral
--Parshintsev, J., Hyötyläinen, T., Hartonen, K., Kulmala, M., Riekkola, M.-L. Organic acids in atmospheric aerosols collected by particle-into-liquid sampler. Their extraction with anion exchange material and determination by liquid chromatography-mass spectrometry. Poster.
--Portin H.J., Leskinen A.P., Komppula M. and Lehtinen K.E.J. Puijo semi-urban station for measuring aerosol-cloud interactions, Poster
--Prisle N.L., Raatikainen T., Laaksonen A. and Bilde M. Measuring cloud droplet activation of surfactant-salt particles , Poster
--Raatikainen T., Prisle N.L., Sorjamaa R., Svenningsson B., Laaksonen A. and Bilde M. Modeling of cloud droplet activation of surfactant-salt particles, poster
--Roldin, P., E Swietlicki, J Löndahl, A Massling, A Kristensson, E Nilsson and T Hussein: Aerosol dynamics in the continental boundary layer in southern Sweden. a study of the aging of the urban plume from Malmö, poster
--Ruusuvuori K., Kurtén T., Vehkamäki H and Ortega I.K. Sign preference and nucleation. Poster
--Vehkamäki H., Julin J., Napari I. and Merikanto J. Molecular dynamics, Monte Carlo and density functional studies of equilibrium cluster properties. Poster

EUCAARI annual meeting 2008, November 17th - 21st, Helsinki

--Decesari S. et al. with E Asmi, D Worsnop and M Kulmala: New particle formation and organic aerosol evolution during the 2008 EUCAARI experiment in the Po valley, oral
-- Hamed A., H Korhonen, S-L Sihto, K Lehtinen, M Kulmala and A Laaksonen: The role of relative humidity in new particle formation, oral
-- Lehtipalo, K., M Sipilä and M Kulmala: Atmospheric molecular clusters in boreal forest, poster
-- Leppä, J., V-M Kerminen, L Laakso, H Korhonen, KEJ Lehtinen, H Junninen and M Kulmala: A model study on growth rates of neutral and charged particles, oral
-- Manninen, H., S Gagné, E Asmi, M Sipilä, I Riipinen, L Laakso, M Vana et al. with M Kulmala: Cluster and ion spectrometers measuring in 13 selected EUCAARI field sites, poster
-- Nieminen, T., S-L Sihto, H Manninen, I Riipinen, T Petäjä and M Kulmala: Connections between new particle formation and sulphuric acid in Hyytiälä, Finland, oral
-- Petäjä, T., RL Mauldin, E Kosciuch, J McGrath, T Nieminen, M Boy, A Adamov, T Kotiaho and M Kulmala: Sulfuric acid and OH concentrations in Hyytiälä, poster
-- Sihto, S-L., J Lauros, M Boy, A Sogachev and M Kulmala: Modelling the turbulent mixing and atmospheric particle formation in boundary layer with MALTE, oral

-- Sihto, S-L., I Riipinen, P Paasonen, H Vuollekoski, T Nieminen et al. with M Kulmala: Connection of sulfuric acid and new particle formation: Analysis of field data from Finnish and German stations, oral
--Staroverova Anna: Comparison of MODIS and AERONET derived aerosol optical properties for selected oceanic locations, poster
-- Staroverova, A., L Sogacheva, G de Leeuw, A-M Sundström and M Kulmala: Validation of MODIS aerosol algorithm, poster
-- Vakkari Ville: New particle formation and aerosol particle characteristics in a semi-clean savanna environment, oral presentation
-- Vanhanen, J., J Mikkilä, M Ehn, P Aalto and M Kulmala: CCN properties of aerosol particles at SMEAR II in Hyytiälä, poster
-- Worsnop D., Aerosol Mass Spectrometer
-- Zardini, A., I Koponen, I Riipinen, M Kulmala and M Bilde: Evaporation of mixed inorganic/organic aerosol particles, poster

New opportunities for Finnish – Japanese cooperation in Urban land-atmosphere and air quality research, 24-26 November 2008, Helsinki, Finland

-- Hussein Tareq: Urban Aerosol Particles: Characteristics of the Particle Number Size Distribution in Helsinki, Oral
--Nikinmaa Eero: Long term measurement of performance of street trees, Oral
--Riekkola, Marja-Liisa "Possibilities and challenges of analytical instrumental techniques in aerosol particle studies" Oral

The 10th Anniversary of Hyytiälä EUROFLUX workshop, 10–12 Dec. 2008, Hyytiälä, Finland.

--Laurila, T., Aurela, M., Thum, T., Tuovinen, J.-P., Aalto, T. & Hatakka, J.: On the carbon balances of a Scots pine forest site of Sodankylä
--Pumpanen Jukka. Presentation of SMEARII station.

Other

Aalto, T.:
--Updating the status of virtual tall tower measurements. Carboeurope Trend & Atmosphere meeting, 30 Jun. – 2 Jul., Schoorl, Netherlands.
--Variation in H_2 at an urban site in Helsinki, Finland. Eurohydros Second Annual Meeting, 14–16 Sept. 2008, Bologna, Italy.
--Comparison of short tower CO_2 mixing ratio observations to model results. Annual CarboEurope-IP Project Meeting, 29 Sept. – 3 Oct. 2008, Jena, Germany.
--Spring initiation and autumn cessation of boreal coniferous forest CO_2 exchange assessed by meteorological and biological variables tracking the active vegetation period. Annual CarboEurope-IP Project Meeting, 29 Sept. – 3 Oct. 2008, Jena, Germany.

Anttila T.:

-- Oral Presentation: On the contribution of Aitken mode particles to cloud droplet populations at clean continental areas - a parametric sensivity study, 15th International Conference on Clouds and Precipitation, July 7-11, Cancun, Mexico.

Asmi Eija:

--Air ion spectrometer calibration workshop results – discussion and questions. Ion workshop, Pühajärve, Estonia, 8.-10.9.2008, Oral Presentation

Aurela, M.:

-- Aurela, M., Lohila, A., Tuovinen, J.-P., Hatakka, J., Viisanen, Y. & Laurila, T.: Methane exchange of a northern fen measured by the eddy covariance technique. Workshop on eddy covariance flux measurements of CH_4 and N_2O exchanges, 8–11 Apr. 2008, Hyytiälä, Finland.

Boy Michael:

--Report on the progress of the activity on NA6", 3rd EUSAAR General Assembly Meeting, 4.-5.3.2008, Sofia, Bulgaria, oral

Ehn Mikael:

--Open ocean nucleation & growth rates during coastal new particle formation ", MAP Project meeting, 3.12.2008, Dublin, Ireland, oral

--Formation of atmospheric nanoparticles", AGU (American Geophysical Union) Meeting, 15.-19.12.2008, San Francisco, CA, USA, oral

--Volatility-resolved Measurements of the Chemical Composition of Arctic Aerosol Particles", AGU (American Geophysical Union) Meeting, 15.-19.12.2008, San Francisco, CA, USA, oral

-- Hygroscopic Properties of Aerosol Particles in the Arctic", AGU (American Geophysical Union) Meeting, 15.-19,12.2008, San Francisco, CA, USA, oral

Göke Sabine:

--Tyynelä, J., T Nousiainen, S Göke and K Muinonen: Modeling polarization radar echoes of hydrometeors using Discrete Dipole Approximation", ERAD 2008 - The 5th European Conference on Radar in Meteorology and Hydrology, 30.6.-4.7.2008, Helsinki, Finland, Poster

--Lautaportti,S., T Puhakka and S Göke: Raindrop size distributions and updraft determination by combining a Doppler radar and a dual polarization radar ", ERAD 2008 - The 5th European Conference on Radar in Meteorology and Hydrology , 30.6.-4.7.2008 Helsinki, Finland, oral

--Tollman, N., S Göke, M Leskinen and E Siivola: Characterizing rimed versus aggregated snow when analyzing the shape of hydrometeor size distributions", ERAD 2008 - The 5th European Conference on Radar in Meteorology and Hydrology, 30.6.- 4.7.2008, Helsinki, Finland, oral

--Göke S. and L Konkola: Interpretation of polarization radar measurements of the melting layer", International Conference on Clouds and Precipitation ICCP, 7.- 11.7.2008, Cancun, Mexico, poster

Hyötyläinen Tuulia:

--"Qualitative and quantitative data-analysis methodologies for comprehensive two-dimensional chromatographic techniques"**,** the 32nd International Symposium on Capillary Chromatography and 5th GC·GC Symposium, Riva del Garda, May 26-30, 2008, Italy.

Julin Jan:

--Molecular dynamics studies of nucleation and equilibrium properties of clusters",
Kumpula Computational Chemistry and Physics KCCP, 28.3.2008, Univ. Helsinki,
Finland, oral

Juurola, Eija:

--Juurola E., Nikinmaa E., Bäck J., Pumpanen J., Porcar-Castell A., Korhonen JFK,
Pihlatie M., Aaltonen H., Hölttä T., Hakola H. 2008. Impacts of blocking phloem
transport on photosynthesis, VOC emissions, sapflow and soil carbon fluxes in Scots
pine. Poster presentation, Abstracts of the XVI Congress of FESPB. Physiologia
Plantarum 133, Abstract P09-080. FESPB, XVI Congress of the Federation of
European Societies of Plant Biology, 17-22 August 2008, Tampere, Finland

Järvi Leena:

--Continuous air pollution and surface atmosphere interaction measurements at the
SMEAR III stations in Helsinki, Ubicasting Workshop, 10.9.2008

Kivekäs Niku:

-- Aerosol and cloud droplet properties during Pallas Cloud Experiment 2005, IGAC,
9.9.2008, Annecy, France, poster

Kurten Theo:

--Quantum chemical studies on charged sulfuric – acid containing clusters possibly
relevant to ion-induced nucleation in the atmosphere. Finnish-Estonian Ion Workshop
17.3-19.3.2008, Hyytiälä, Finland, oral presentation

Laakso Lauri:

--Laakso, L., H Laakso, M Kulmala, N Kgabi, M Molefe, D Mabaso, K Pienaar and M
Jokinen: New particle formation in a clean and polluted Southern African savannah",
IGBP meeting, May 2008, Cape Town International Convention Centre, South
Africa, oral

Lallo, Marko:

--Seasonal variations in hydrogen deposition to boreal forest soil. Eurohydros Second
Annual Meeting, 15–16 Sept. 2008, Bologna, Italy.

Laurila, Tuomas:

--Laurila, T., Tuovinen, J.-P., Hatakka, J., Aurela, M., Lohila, A., Ettala, M., Samuelsson,
J. & Karhu, K.: Micrometeorological eddy-covariance method as a tool to observe
landfill methane and carbon dioxide emissions and landfill processes. Intercontinental
Landfill Research Symposium, 10–12 Sept. 2008, Copper Mountain, Colorado, USA.

Leppä Johannes:

--On particle growth rates. Ion workshop, Pühajärve, Estonia, 8.-10.9.2008. Oral

Lohila, Annalea:

--Greenhouse gas balances of natural and drained peatlands - micrometeorological studies
in the boreal zone. NECC workshop on assessing the potential for GHG mitigation in
the Nordic region: Land use options on drained peatlands and upland afforestation.
28–29 Feb. 2008, Kuopio, Finland.

--Greenhouse gas flux measurements on Lompolojänkkä wetland in northern Finland.
First NitroEuropeIP Wetland-Shrubland Modeling Workshop, 8–10 Oct. 2008,
Stockholm, Sweden.

--Lohila, A., Aurela, M., Hatakka, J., Minkkinen K., Penttilä T. & Laurila T.: Chamber
and eddy-covariance measurements of greenhouse gas fluxes on a sedge fen in

northern Finland. NitroEurope IP Open Science Conference 'Reactive Nitrogen and the European Greenhouse Gas Balance', 20–21 Feb. 2008, Ghent, Belgium.

--Lohila, A., Minkkinen, K., Penttilä, T., Aurela, M. & Laurila, T.: CO_2 balance of a drained peatland forest in Finland. NitroEurope IP Open Science Conference 'Reactive Nitrogen and the European Greenhouse Gas Balance', 20–21 Feb. 2008, Ghent, Belgium.

--Lohila, A., Aurela, M., Laurila, T., Hatakka, J., Tuovinen, J.-P., Aalto, T. & Viisanen, Y.: Radiative forcing of northern ecosystems - effect of earlier snow melt through changes in CO_2 balance and albedo. Annual CarboEurope-IP Project Meeting, 29 Sept. – 3 Oct. 2008, Jena, Germany

Malila, Jussi:

--Malila, J. and Laaksonen, Properties of Supercooled Water Clusters from Nucleation Rate Data with the Effect of Non-Ideal Vapour Phase. Proceedings of the 15th International Conference on the Properties of Water and Steam, September 7-11, 2008, Berlin/Germany, (oral)

Manninen Hanna:

-- Manninen, H.E., E Asmi, M Sipilä, S Gagne, K Neitola, K Lehtipalo, T Niemenen, M Vana, S Mirme, A Mirme and M Kulmala: EUCAARI cluster spectrometer measurements. 11th Air Ion and Aerosol Workshop, 8.-10.9.2008, Pühajärve, Estonia, oral

Neitola Kimmo:

--"Binary homogeneous nucleation of sulfuric acid-water: Particle size distribution and effect of detector on total count and determination of critical cluster size." European Aerosol Conference. Thessaloniki, Greece 25.8.2008 Poster presentation

Nikinmaa Eero:

-- Whole tree interactions control carbon and water fluxes between ecosystems and atmosphere? Helsinki Climate workshop, 10-12 Nov 2008, Hotel Arthur, Helsinki, Finland, Oral

Parshintsev Jevgeni:

--Parshintsev, J., Hartonen, K., Kulmala, M., Riekkola, M.-L., Hyötyläinen, T. Determination of organic acids in atmospheric aerosols collected by particle-into-liquid sampler using comprehensive two-dimensional gas chromatography coupled with electron capture detector, the 32nd International Symposium on Capillary Chromatography and 5th GC·GC Symposium, Riva del Garda, May 26-30, 2008, Italy**.**

Pihlatie Mari:

--Pihlatie,M., T Vesala, I Mammarella, A-J Kieloaho, T Laurila, M Aurela, K Minkkinen, T Penttilä, S Zechmeister-Boltenstern et al.: Results on a flux measurements campaign at a drained peatland pine forest", Reactive Nitrogen and the European Greenhouse Gas Balance, 20.-21.2.2008, Ghent, Belgium, oral

Porcar-Castell Albert:

--Porcar-Castell A, Vesala T, Nikinmaa E. On the linkage between remotely sensed data and plant physiological processes. SpecNet Meeting 2008. 30 June- 4 July 2008, Trento, Italy. oral presentation

Pumpanen Jukka:

--Effect of clear-cutting on soil carbon pool and CO_2 fluxes from forest soil Pumpanen J, Ilvesniemi H, Heinonsalo J., Rasilo T. , EUROSOIL 2008 conference, 25-29 August 2008, Vienna, Austria, Poster

Reissell Anni:

-- iLEAPS ↔ GEWEX collaborative activities, GEWEX SSG meeting, 4-8 February 2008, Buenos Aires, Argentina. Oral presentation

-- iLEAPS, Integrated Land Ecosystem - Atmosphere Processes Study. International Workshop on Anthropogenic Impacts on Asian Monsoon (MAIRS, NUIS). 21-23 April 2008, Nanjing University of Information Science & Technology, Nanjing, China.

-- Reissell A and Sorvari S.: iLEAPS – Integrated Land Ecosystem – Atmosphere Processes Study, HERC-iLEAPS seminar on Interaction Between land use and climate. Multidisciplinary perspectives from local land use to global climate, 24 April 2008, Helsinki, Finland, national, poster

-- Reissell A. and S Sorvari: Interactions and feedbacks between land ecosystem and atmospheric processes", 4th IGBP Congress, 5.-9.5.2008, Cape Town International Convention Centre, South Africa

-- Cross-disciplinary international research on land-atmosphere interactions. ESF-FMSH Entre-Sciences Conference in Interdisciplinary Sciences. New Methodologies and Interdisciplinary Approach: Global Change Research. 5-10 November 2008, Porquerolles, France. Oral presentation

--Cross-disciplinary international research on land-atmosphere interactions – MENA perspective. IGBP Regional Workshop - Middle East and North Africa (MENA), Sustainable Water and Land Management in Semi-Arid Regions, 20-21 November, Cairo, Egypt. Oral

Riekkola, **Marja-Liisa**

--"Pressurized hot water and supercritical water as alternative, green solvents", JASCO Ltd, Tokyo, Japan, February 5, 2008.

--"Three versatile techniques: Comprehensive two-dimensional gas chromatography and liquid chromatography as well as capillary electrochromatography" CSIC Madrid, Spain, June 4, 2008.

Riikonen Anu:

-- Annual shoot growth of trees on structural soils in Helsinki, European Congress of Arboriculture, 16.-18.6.2008, Turin, Italy. Poster

--Viikki Urban Tree Laboratory, The Landscape Below Ground III, 6.-8.10.2008, Lisle, Illinois, USA. Poster

Riipinen Ilona:

--Observations on the first steps of particle formation and growth", Aerosols in the Amazon – Changes and their Consequences from Past and Future Human Activities, 18.-22.2.2008, Manaus, Amazonia, Brazil

-- Riipinen, I., HE Manninen, K Lehtipalo, S Häkkinen, T Nieminen, M Sipilä, H Junninen, M Ehn, S-L Sihto, T Petäjä, M Dal Maso, T Yli-Juuti et al. and Kulmala, M.: On the role of sulfuric acid and organics in the first steps of particle formation and growth", American Association for Aerosol Research (AAAR) conference, 19.-25.10.2008, Orlando, FL, USA

Rinne, Janne:

--Rinne, J., Pihlatie, M., Aurela, M., Tuovinen, J.-P., Hatakka, J., Riutta, T., Laurila, T. & Vesala. T.: Methane flux measurements using Campbell TGA-100 tunable diode laser absorption spectrometer. Workshop on eddy covariance flux measurements of CH_4 and N_2O exchanges, 8–11 Apr. 2008, Hyytiälä, Finland

--Modeling the effect of within canopy chemistry on fluxes of chemically reactive trace gases in a tropical rainforest, Biogenic Secondary Organic Aerosol in Amazon, 18.-22.2.2008, Ariau Towers, Amazonas, Brazil

--Methane flux measurements by eddy covariance method at a boreal wetland site, AMERIFLUX Science Meeting 2008, 15.-17.10.2008, Boulder, CO, USA,

Sevanto Sanna:

--The effects of heat storage during low flow rates on Granier-type sap flow sensor output, Oral presentation at 7th International Workshop on sap flow in Sevilla, Spain. Oct 21-24,2008.

Sorvari Sanna:

-- European Institute for Atmospheric Research, EINAR", CBACCI/ABS workshop for teachers, 8.12.2008, University of Helsinki, Finland

Thum Tea:

--Modelling seasonality of the boreal forest CO_2 exchange, JSBach-biosphere model meeting , 10 Jun. 2008, Hamburg, Germany.

Vehkamäki Hanna:

-- Tala, S., J Lauros and H Vehkamäki: Gender issues in physics education at the University of Helsinki", Annual Meeting of the European Meteorological Society, 29.9.-3.10.2008, Amsterdam, Netherlands, oral

Vesala Timo:

--Kiese, R., T Vesala, M Pihlatie, I Mammarella, A-J Kieloaho, T Laurila et al.: Quantification of C and N trace gas fluxes from a drained peatland forest in Finland using different measuring techniques", Reactive Nitrogen and the European Greenhouse Gas Balance, 20.-21.2.2008, Ghent, Belgium, poster

--Nemitz, S.U., T Vesala, P Ambus et al.: Biosphere atmosphere exchange of reactive N and greenhouse gases at the NitroEurope core measurement siten: A synthesis of the first annual data set", Reactive Nitrogen and the European Greenhouse Gas Balance, 20.-21.2.2008, Ghent, Belgium, oral

--Pihlatie, M., T Vesala, I Mammarella, A-J Kieloaho, T Laurila, M Aurela, K Minkkinen, T Penttilä, S Zechmeister-Boltenstern et al.: Results on a flux measurements campaign at a drained peatland pine forest", Reactive Nitrogen and the European Greenhouse Gas Balance, 20.-21.2.2008, Ghent, Belgium, oral

--Vesala T. & E Nikinmaa: Case III, Land use changes in Finland: Impacts of forest management changes to carbon balance", Helsinki University Environmental Research Centre HERC seminar, 24.4.2008, Univ. Helsinki, Viikki Info Center, Finland, oral

--Sogachev A., O Panferov and T Vesala: Simple modification of two-equation models for non-neutral flow", American Meteorological Society Conference on Boundary Layers and Turbulence, 9.-13.6.2008, Univ. Stockholm, Sweden, oral

Virkkula, A:
-- Satheesan K., Kirkwood S., and Virkkula A. (2008) A study of the transport of ozone into the surface over Antarctica, Abstracts of the SPARC 4th General Assembly 31 August - 5 September 2008 Bologna, Italy.
--Virkkula A., Teinilä K., Frey A., Aurela M., Timonen H., Mäkelä T., Hillamo R., Aalto P.P., Asmi E., Koponen I.K., and Kulmala M. (2008) Atmospheric aerosol research in Aboa and the surroundings. In Ojala A.E.K. (Editor) Congress of the International Polar Year 2007/08: IPY 07/08 celebration of Finnish geoscientific studies in Polar areas November 12-13, 2008, GTK, Espoo, Finland. Abstracts, p. 59.

Vuollekoski Henry:
-- Iodine dioxide nucleation simulations in coastal and remote marine environments. Marine Aerosol Production –project meeting, Dublin, Ireland, 3.-4.12.2008

Worsnop Douglas:
--Advanced field measurement techniques for sampling ambient atmospheric particles", Hiukkasfoorumin syysseminaari: Ympäristön monitorointi, 31.10.2008, Innopoli 2, Espoo, Finland

PATENTS

1. K. Hartonen, K. Kuuspalo, H. Lihavainen, P. Aalto, M. Rasilainen, M.-L. Riekkola, M. Kulmala and Y. Viisanen, US Patent application A1, 20070275474 (US 11/438689), Notice of allowance issued 12.9.2008. "Sampling device for introduction of samples into analysis system"
2. Hartonen, K., Kuuspalo, K., Lihavainen, H., Aalto, P., Rasilainen M., Riekkola, M.-L., Kulmala M. and Viisanen, Y. US patent application A1, 20070275474 (US 11/438689), International patent application, PCT/IB2007/001340, Chinese patent application 200780018681.2, European patent application 07734646.8-1226. "Sampling device for introduction of samples into analysis system".

ACTIVITY REPORT 2006-2007:
GRADUATE SCHOOL ON PHYSICS, CHEMISTRY, BIOLOGY AND METEOROLOGY OF ATMOSPHERIC COMPOSITION AND CLIMATE CHANGE

BASIC FACTS

The Graduate School started in the beginning of 2006. The education in the Graduate School is given mainly on the following topics:
- Atmospheric Sciences
- Aerosol Physics and Technology
- Physics, Chemistry, Biology and Meteorology of Air Pollution, including:
    o Aerosol-Cloud-Climate Interactions
    o Biosphere-Atmosphere Interactions
    o Development of Aerosol and Environmental Technology
    o Aerosol Emissions, Concentrations, Transformation, Deposition, and Effects

The units participating in the Graduate School organization include six departments of three Finnish universities (University of Helsinki, University of Kuopio, and Tampere University of Technology), two research institutes (Finnish Meteorological Institute and VTT Technical Research Centre of Finland) and two private enterprises (Vaisala Ltd. and Dekati Ltd.).

RESEARCH STUDENTS DURING 2006-2007

The Ministry of Education provided funding for the Graduate School for five full-day positions for the period 2006-2009. In 2006, three more positions were received for the years 2007-2009. The Steering Committee of the Graduate School announced an open call both in 2005 and 2006 for these positions. The call was announced through universities, research institutes, in the World Wide Web and using the partners' own channels of communication.

On both calls, more than 90 applications were received. When selecting the students for the positions, the following aspects were taken into account:
- number and quality of publications (peer reviewed journals, peer reviewed conference papers)
- grades in master's degree studies
- other scientific and technological merits
- supervisors' statements

Special attention was paid to gender equality and balance between different fields and research units. Each of the selected students got an employment contract until the end of 2009.

All the applicants were accepted as members of the Graduate School. An email list including all the members was formed in order to efficiently disseminate information about forthcoming graduate courses, workshops, seminars as well as other issues potentially interesting for the Graduate School students.

One of the students selected for the Graduate School positions finished his PhD degree in 2007. The Steering Committee decided to select another student amongst the applicants to the position from the beginning of 2008.

In the end of 2007 the Graduate School had a total of 105 students, 48 of which were female. The total number of students during 2006-2007 was 130, including the 17 persons that finished their PhD degree during 2006-2007 and those who changed to another Graduate School or left for other reasons. The average age of getting the PhD degree was 31 years, and the average time spent for PhD studies was 4.8 years. Each PhD graduated from the Graduate School was employed immediately after graduation:

- 5 employed by Finnish universities
- 3 employed by foreign universities
- 3 employed by Finnish research institutes
- 3 employed by foreign research institutes
- 3 employed by the private sector.

Distribution of the Graduate School students in the end of 2007 is shown in Figure 1.
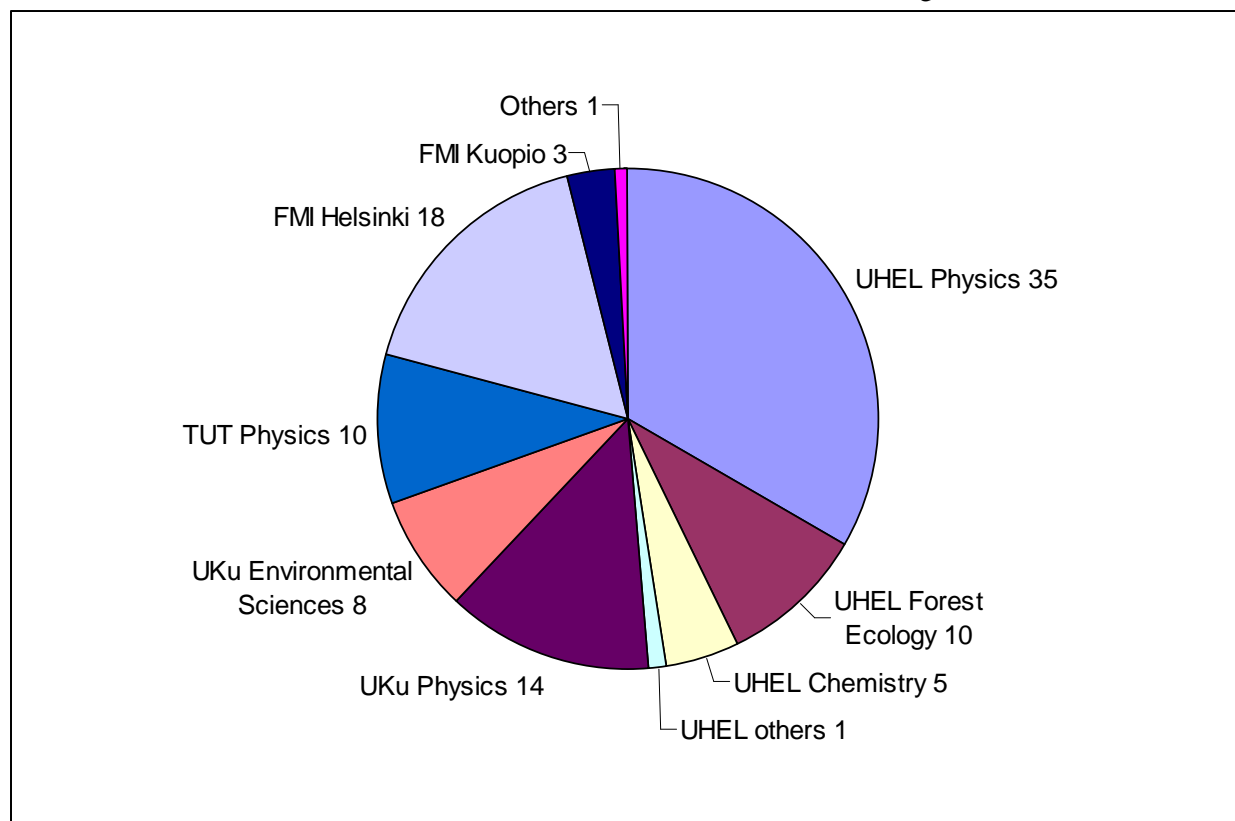
Figure 1. Distribution of the Graduate School students in December 2007. UHEL = University of Helsinki; UKu = University of Kuopio; TUT = Tampere University of Technology; FMI = Finnish Meteorological Institute.

COORDINATION OF THE GRADUATE SCHOOL

Academy Professor Markku Kulmala was the leader of the Graduate School during the period 2006-2007. The Graduate School did not receive funds to hire a coordinator. Thus, the general coordination was carried out by several persons. Major part of the coordination was done by Dr. Antti Lauri, whose main work was to coordinate a Nordic Master's Degree Programme in Atmosphere-Biosphere Studies, and Dr. Jaana Bäck, who was the scientific secretary of the National Centre of Excellence "Physics, Chemistry, Biology and Meteorology of Atmospheric Composition and Climate Change".

TEACHING AND SUPERVISION ARRANGEMENTS

The teaching and supervision arrangements of the Graduate School are based on long-term solid collaboration within Atmospheric Sciences and Aerosol Physics and Technology. In the end of 2007, approximately 40% of the Graduate School students had supervisors from at least two partner units. Several students were also supervised by professors and senior scientists of foreign universities. Part of the thesis works were made in collaboration with private enterprises (e.g. Vaisala, Nokia, Dekati).

The essential research topics have included:
- Formation and growth of atmospheric aerosol particles: theory, measurements and modelling
- Measurements of neutral and charged clusters
- Fluxes of greenhouse gases
- Biogenic VOC emissions
- Development of measurement devices and technologies
- Air quality
- Traffic emissions
- Global modelling

During 2006-2007, the following people have supervised the Graduate School students:

University of Helsinki, Department of Physics
Markku Kulmala, PhD, Academy Professor, Aerosol and Environmental Physics, Aerosol and Ion Dynamics
Timo Vesala, PhD, Professor, Micrometeorology, Forest-Atmosphere Interactions
Kaarle Hämeri, PhD, Professor, Aerosol Physics, Occupational Aerosols
Hannu Savijärvi, PhD, Professor, Dynamic Meteorology, Numerical Models
Timo Puhakka, PhD, Laboratory Head, Radar Meteorology (-2007)
Sabine Göke, PhD, Laboratory Head, Radar Meteorology (2007-)
Jouni Räisänen, PhD, University Lecturer, Dynamic Meteorology, Climate Change
Marja Bister, PhD, University Lecturer, Dynamic Meteorology, Cloud Dynamics
Janne Rinne, PhD, Postdoctoral Fellow, Micrometeorology
Hanna Vehkamäki, PhD, Academy Fellow, Aerosol Physics, Simulation Methods
Ismo Napari, PhD, University Lecturer, Aerosol Physics, Nucleation Research
Anni Reissell, PhD, iLEAPS executive coordinator, Atmospheric Chemistry
Pasi Aalto, PhD, Laboratory Engineer, Aerosol Physics, Measurement Technique
Boris Bonn, Ph.D., Scientist, Atmospheric Chemistry
Alex Lushnikov, Ph.D., Visiting Professor, Theoretical Aerosol Dynamics
Michael Boy, PhD, Doc., Atmospheric Chemistry, Aerosol Models
Lauri Laakso, PhD, Doc., Atmospheric Aerosols
Chul Eddy Chung, PhD, Global Modelling

University of Helsinki, Department of Forest Ecology
Pertti Hari, PhD, Professor, Forest Ecology, Cycles and Flows in Ecosystems
Eero Nikinmaa, PhD, Professor, Ecophysiology of Trees
Annikki Mäkelä, PhD, Doc., Forest Ecological System Analysis
Jaana Bäck, PhD, Doc., Physiology of Trees
Jukka Pumpanen, PhD, Physiology of Trees

University of Helsinki, Department of Chemistry
Marja-Liisa Riekkola, PhD, Professor, Analytical Chemistry

University of Kuopio
Ari Laaksonen, PhD, Professor, Aerosol Physics, Aerosol-Cloud-Climate Interactions
Kari Lehtinen, PhD, Professor, Aerosol Physics, Aerosol Dynamic Models
Jorma Jokiniemi, PhD, Professor, Aerosol Technology, Aerosol Dynamic Models, Aerosol Sources
Jorma Joutsensaari, DSc (Tech.), Research Director, Aerosol Technology, Experimental Aerosol Research
Hannele Korhonen, PhD, Doc., Global Models
Harri Kokkola, PhD, Cloud Models

Tampere University of Technology
Jorma Keskinen, DSc (Tech.), Aerosol Technology, Sources

Jyrki Mäkelä, PhD, lehtori, Aerosol Physics, Measurements of Nanoparticles
Kauko Janka, Doc., Aerosol Technology
Matti Lehtimäki, Doc., Measurement Technology

Finnish Meteorological Institute
Yrjö Viisanen, PhD, Research Director, Professor, Atmospheric Research
Veli-Matti Kerminen, PhD, Professor, Aerosol Physics, Climate Change
Kari Lehtinen, PhD, Professor, Aerosol Physics, Aerosol Dynamic Models
Risto Hillamo, PhD, Doc., Group Leader, Aerosol Chemistry, Measurement Technology
Aki Virkkula, PhD, Doc., Aerosol Physics, Radiation Transfer in the Atmosphere
Tuula Aalto, PhD, Doc., Concentrations and Fluxes of GHGs
Hannele Hakola, PhD, Organic Atmospheric Chemistry
Heikki Lihavainen, PhD, Aerosol Technology, Laboratory Measurements
Jussi Paatero, PhD, Doc., Radio Chemistry
Juhani Damski, PhD, Atmospheric Modelling
Antti-Pekka Hyvärinen, PhD, Aerosol Measurements
Ari Karppinen, PhD, Doc., Atmospheric Modelling
Mikhail Sofiev, PhD, Atmospheric Modelling

VTT
Jorma Jokiniemi, PhD, Research Professor, Fine Particles, Aerosol Technology, Synthesis and Characterization of Nanoparticles
Jouni Pyykönen, DSc (Tech.), Modelling of Fluid and Aerosol Dynamics

Foreign supervisors:
Hans-Christen Hansson, Professor, ITM/Stockholm University, Laboratory Head, Air Pollution
Paul E. Wagner, Professor, Experimental Physics/University of Vienna, Aerosol Physics, Laboratory Measurements
Merete Bilde, Professor, Chemistry/University of Copenhagen, Atmospheric Chemistry
Ken Carslaw, Professor, Atmospheric Sciences/University of Leeds, Global Modelling
Zissis Samaras, Professor, Aristotle University Thessaloniki, Sources
Christodoulos Pilinis, Professor Department of Environmental Studies, University of Aegean, Mytilene, Greece, Pollution Modelling
Frank Stratmann, PhD, Doc., IfT, Leipzig, Aerosol and Fluid Dynamics
Bo Larsen, PhD, EU Joint Research Centre Ispra, Air Pollution
Douglas Nilsson, PhD, Stockholm University, Atmospheric Sciences

The demand for experts in atmospheric sciences remains high and is increasing, and all the graduated PhD's are employed, hired by both the private and the public sector in Finland, other European countries, South Africa, and the U.S. Also a private enterprise, Helsinki Aerosol Consulting Ltd, has been founded by former Graduate School members.

GRADUATE SCHOOL COURSES DURING 2006-2007

The two foundation pillars of the Graduate School have been the education programme following the strategies and quality systems of the partner universities, and the education structure built in the context of the Nordic CBACCI Graduate School (Biosphere - Carbon - Aerosol - Cloud - Climate Interactions), spanning all the way from MSc level education to postdoctoral training.

During 2006 and 2007 a total of 11 joint intensive courses, each of 1-2 weeks' length, were organized in the context of the Graduate School. Each of these courses involved organizers, lecturers and students from at least two participating units. Each course attracted a number of foreign graduate students. Furthermore, internationally well-known top researchers gave several lectures on these courses. The topics of the

courses included aerosol physical theories, field measurements, modelling and data analysis of environmental field data. The topics were selected to represent the most recent research trends and results. The courses always involved sections related to general skills: communication, networking, science philosophy, scientific career planning, and scientific writing. According to the feedback from the students this kind of courses have been very motivating. Table 1 includes the courses, which were organized together by at least two partners of the Graduate School.

Course name	ECTS	Time	Number of students
Physics and chemistry of air pollution and their effects: field course and data analysis	5	Spring 2006	23
Measurements of atmospheric aerosols: Aerosol physics, sampling and measurement techniques	3	Spring 2006	15
Summer School on Air-Sea Interaction	3	Summer 2006	30
Environmental physics	5	Autumn 2006	10
Forest-atmosphere interactions	5	Autumn 2006	24
Cloud microphysics	5	Spring 2007	15
Arctic air pollution	4	Spring 2007	12
Integrated measurements over land ecosystem atmosphere boundaries	3	Spring 2007	34
Measurements of atmospheric aerosols: Aerosol physics, sampling and measurement techniques	3	Spring 2007	19
Physics and chemistry of air pollution and their effects: field course and data analysis	5	Spring 2007	33
Formation and growth of atmospheric aerosols	5	Summer 2007	33
Summer Course on Mesoscale Meteorology and Predictability	4	Summer 2007	35
Statistical analysis of environmental field observations	3	Autumn 2007	30
Introduction to atmospheric chemistry and aerosol physics	3	Autumn 2007	7

Table 1. A summary of the joint courses of the Graduate School organized in 2006 and 2007.

As a pilot project in the Graduate School, a total of four e-learning courses were organized. When implemented carefully, e-learning makes it possible to take challenging graduate courses remotely using the Internet. The e-learning courses included lecture and supporting material, exercises, web quizzes, and a weekly chat session with the other course participants, assistants, and teachers.

FUNDING OF THE GRADUATE SCHOOL STUDENTS

Concerning funding, the Graduate School collaborated and interacted very strongly with the Finnish Centre of Excellence "Physics, Chemistry, Biology and Meteorology of Atmospheric Composition and Climate Change". 26.9% of the Graduate School students received their main funding by the Centre of Excellence programme.

During 2006-2007, 78.5% of the Graduate School students had an employment contract with a Finnish university. The participating research institutes employed 19.2% of the students. The main funding sources were EU projects (29 students), Centre of Excellence programme (35 students), and industry and commerce (including TEKES projects; 17 students). The main funding source of 10 students was private foundations.

INTERNATIONAL COOPERATION

International collaboration has been a solid part of the research and study plans of each Graduate School student. The Graduate School has had several supervisors from Nordic, Baltic and other European countries. Several EU projects involve PhD training, and the EU networks are very strong within the Graduate School. Through the EU projects (e.g. EUCAARI, EUSAAR, NITROEUROPE, CARBOEUROPE), a large number of foreign students and lecturers have participated in the Graduate School activities. Furthermore, also the Graduate School students have been able to participate in international courses organized in different countries. On global scale, iLEAPS (Integrated Land Ecosystem Atmosphere Processes Study) has been an essential collaboration network.

The possibility of joint and double degrees has been investigated within the Nordic CBACCI Graduate School. So far the differences in national legislation and the lack of practical experience have been the barrier in the practical implementation of joint degrees.

International mobility within the Graduate School has included the following elements:
- conference visits including oral and/or poster presentations
- laboratory visits
- measurement campaigns
- long-term visits involving research work in a foreign laboratory

The Graduate School has been reasonably successful in recruiting foreign students. In the end of 2007, there were a total of 14 foreign students.

In 2006, the Graduate School students made a total of 20 long (>2 weeks) and 27 short visits (excluding conferences). In 2007, the numbers were 11 and 41, respectively.

The Graduate School students gave 66 oral presentations in international conferences and workshops, and 7 in domestic workshops. The total number of poster presentations was 120 in international conferences, 5 in domestic workshops. In 2007, the total number of conference presentations given by the Graduate School students was 167.

The total number of graduate students from foreign universities participating in the Graduate School courses and visiting the partner institutions was 101 during 2006-2007.

SELF-ASSESSMENT

The Graduate School has given a more assertive structure to the planning and implementation of PhD training in the fields of Atmospheric and Environmental Sciences in Finland. The determined

collaboration has increased the quality of education and the scientific level. The network with its diversified national and international connections, both on public and private sectors, has given the students a better view of academic career opportunities. Moreover, recruitment of students has become possible in a broader community on national level.

The Graduate School has already relieved the constantly increasing need for PhD's in Atmospheric Sciences. The doctors graduated from the School have been nationally and internationally desired labour force, working as experts both on public and private sector in research and development as well as education.

The Graduate School has increased cooperation between universities and research institutes, both of which have been very committed in organizing and developing the Graduate School activities. The national Graduate School, together with the existing international networks, has increased international collaboration very strongly. The courses and workshops organized in the context of the national Graduate School have become very popular amongst graduate students in foreign universities.

The classroom education went through both the required university-level quality control and the quality criteria set by the Steering Committee, which considered the education from two points of view: high-quality international research, and industry and commerce.

Concerning PhD theses, the following methods were applied to assure high quality:
- Versatile supervision
- Published articles in premium international peer-reviewed journals
- External pre-reviewers of PhD theses
- External, mostly foreign opponents.

The teaching and supervision arrangements have worked excellently. The good practices learnt during the first years of operation of the Nordic Graduate School CBACCI were immediately available to be utilized in the national Graduate School. The supervisors, lecturers and students have been very satisfied with inter-institutional supervision and the course studies within the Graduate School.

The connections to industry and commerce have become closer and more diversified. Both the students and collaborative enterprises have digested a model, in which the research work needed by the company can be carried out within the Graduate School so that the cooperation makes up a reasonable part of the PhD work.

The Graduate School has also structurized international education cooperation, offering new ways to approach potential international collaborators and increasing existing cooperation. The Graduate School has also increased the opportunities to recruit talented foreign students to Finland.